ABSORPTION AND STRIPPING

P. Chattopadhyay

Absorption
&
Stripping

P. Chattopadhyay

Senior Faculty
Dept. of Mechanical Engineering
Techno India College of Technology,
Rajarhat, New Town,
Kolkata-700156

Preface

Absorption & Stripping are essentially two very important unit operations frequently encountered in both CPIs (Chemical Process Industries) and PCIs (Petrochemical Industries). In many plants, absorption & stripping operate in conjunction with distillation —the oldest unit operation that emerged from alchemists' laboratory centuries back. Yet surprisingly there is quite a few titles exist in the market. Of course, I must admit that there are some excellent texts still available on *absorption and stripping.* They're old ones but very good ones. They provide sound theoretical backup to these unit operations. It is here that this present title bears good similarities to them.

However, there is a basic difference between those erstwhile texts and the present one: It is the *industrial approach.* This one banks heavily on industry & focuses its major concern on the industrial application of absorption and stripping inasmuch as *all unit operations must find their ultimate application in industries.* It gives a detail survey of Tower Internals, Design of Absorbers & Strippers, Typical Industrial Absorbers & Strippers, Revamping of Absorbers & Strippers, Cost Estimation of Absorption Towers. Author's two-&-a-half decades of cumulative experience as Assistant Process Engineer & as Senior Process Engineer involved in the operation & troubleshooting of Mass Transfer Equipment (particularly, fractionators, absorbers, strippers, reactors and heat exchangers) has provided the book industrial design concept & many practical tips. Proprietary design data of tower internals have been planted into the book to expand its coverage. As such the book *may* reward the reader with a sense that the book is a complete one —from sound theoretical base to concrete industrial design.

Obviously, the theoretical bases for these design procedures had been developed many years ago. These theories are available in most academic texts the reader may encounter in chemical engineering courses on mass transfer. Unfortunately, the direct application of these theoretical concepts in many practical situations ends up with inaccurate sizing of absorbers & strippers of industrial scale. This is due to lack of physical & chemical constants and mostly because the data in academic texts are based on laboratory columns and pilot plants operating near atmospheric pressure. In sharp contrast, some large-dia industrial columns must operate at high pressures or with foaming systems that are dirty.

Very often than not industrial absorption & stripping columns are fretted with the nagging problems of corrosion, side reactions, foaming, packing degradation, and the like. And that renders actual plant (or pilot-plant) operating data invaluable adjuncts to a theoretical design. As such operating data have been given due emphasis and inducted wherever possible.

The first two chapters provide the necessary fundamentals & theoretical development of absorbers & strippers. Adequate numerical examples have been dished out to enable the reader to get a good grip of the topics.

Design of all gas-liquid contacting columns begins with the hydraulics of operation. So is this one. **Hydraulics** of all the three basic tray-columns as well as of packed towers have been explained to the minutest details. Discussed also are the factors & parameters that influence the hydraulics of packed towers. This is followed by basic concepts of design of **Tray Towers** and **Packed Towers**. Adequate numerical examples have been plugged in. Two chapters (CH-4 & CH-5) deal exclusively with **design**.

Packings come almost inevitably with Absorption & Stripping. So little wonder why they'll occupy a special position in this book. So the author has devoted one whole chapter (CH-6) on packing.

Equally important are tower internals without which the packing's functions are seriously impaired. Each & every such tower internals has been discussed in comprehensive detail (CH-7).

Finally, the last three chapters on absorption & stripping of **industrial importance, revamping of absorbers & strippers & cost estimation of absorption towers** are a pleasant excursion to the domain of large commercial absorbers & strippers. Design consideration, design guidelines & operation of important industrial absorption have been discussed at length. The author believes that the title will come in good stead to the students of Chemical Engineering and Applied Chemistry as well as Process Engineers and Designers of CPIs and PCIs. Any shortcoming of the book lies entirely on the shoulder of the author.

2nd January, 2007   **P. Chattopadhyay**

Content

NOTATIONS USED IN THE BOOK

BDF	Bottom Driving Force	mtc	mass transfer coefficient
BTEX	Benzene, Toluene, Ethylbenzene & Xylene	NCH	Non-condensable Hydrocarbon
		NG	Natural Gas
BTMS	Bottoms	NTU	Number of Transfer Units
⑤ d	Circulated	OL	Operating Line
⑤ ng	Circulating	Op. line	Operating Line
⑤ n	Circulation	OVHD	Overhead
Col	Column	Press	Pressure
CPI	Chemical Process Industries	qty	quantity
CTC	Carbon Tetra Chloride	scm	Standard cubic meter
DCA	1:2-Dichloroethane	SG	Sour Gas
DCE	1:1-Dichloroethylene	sol^n	solution
DEP	Diethanolpiperazine	TCA	1:1:1-Trichloroethane
DIPA	Di-isopropanolamine	TCE	Trichloroethylene
EPA	Environmental Protection Agency	TDF	Top Driving Force
HAP	Hazardous Air Pollutants	TEG	Triethylene Glycol
HC	Hydrocarbon	Temp	Temperature
HCB	Hexachlorobenzene	THEED	Trihydroxyethylethylene diamine
HE	Heat Exchanger	VLE	Vapor Liquid Equilibrium
htc	heat transfer coefficient	VOCs	Volatile Organic Compounds
HTU	Height of a Transfer Unit		
h/up	hold up		
k$	kilo-dollar [1k$ = US$1000]		
l/up	lined up		
MDF	Mean Driving Force (usually log-mean-driving force)		
MGD	Million Gallons per Day		
MMBtu	Million Btu		
MMs.ft^3	Million Standard Cubic foot required referred to 15°C/100kPa		

1

Absorption

Absorption is a gas-liq mass transfer operation in which a component is transferred from the gas phase to the liquid. And the rate of absorption is determined by the rate of molecular diffusion that largely controls this interphase mass transfer.

The component which is absorbed is called **solute** and in which it is absorbed is called **solvent.**

Generally, the solute enters the column in a gas introduced at the bottom of a column while the solvent is fed to the top as liquid. The solute is more or less soluble in the solvent while the carrier gas is either insoluble or slightly soluble in the liquid phase. The absorbed gas and solvent leave at the bottom and the unabsorbed components plus some of the liquid vaporized into the gas phase leave as gas from the top.

The absorbed solute may form a simple solution in the liquid phase or it may react chemically with a component in the liquid phase. Therefore, the absorption processes are conveniently divided into two main groups :

- **Physical Absorption** – in which the process is solely physical and is limited to the formation of solution of the gas in the liquid, *e.g.*, absorption of ammonia by water from an air-ammonia mixture; similarly liquid methanol at low temperature absorbs CO_2 and H_2S at high pressure and forms their solution.

- **Chemical Absorption** — in which absorption follows incipient chemical reaction, *e.g.*, absorption of CO_2 in hot alkali and absorption of NO_x in water.

Gas absorption is a major unit operation for the selective removal of one or more components from a gas mixture by a suitable liquid forming a solutions of the gases upon absorption. The solvent is regenerated from the solution by a process called **Desorption.**

Desorption (or **Stripping**) is the just reverse of gas absorption. The rich solution, *i.e.*, the solvent loaded with absorbed solute (or solutes) is charged to the regeneration tower (*i.e.*, stripping column) at the top and the stripping stream (usually saturated steam) is introduced at the bottom. Upon gas-liq contact, mass transfer occurs in the opposite direction, *i.e.*, physical transfer of solute from the liq phase to the gas phase. The lean solution (*i.e.*, the solution stripped off much of its gas load) recovered from the bottom of the column is recycled to the absorption tower to ensure continuous operation.

This is incidental to the absorption operation

Absorption and desorption are traditional thermal separation processes. A complete absorption process comprises an absorber and a desorber **Figure 1.1.**

In the absorber the scrubbing liquor (solvent) is charged with the gaseous component (components) to the removed, and in the desorber (regenerator) it is regenerated or freed from the substances dissolved in it. The stripped solvent is pumped back to the absorption tower to complete the cycle.

Absorption plant with absorption and regeneration column.
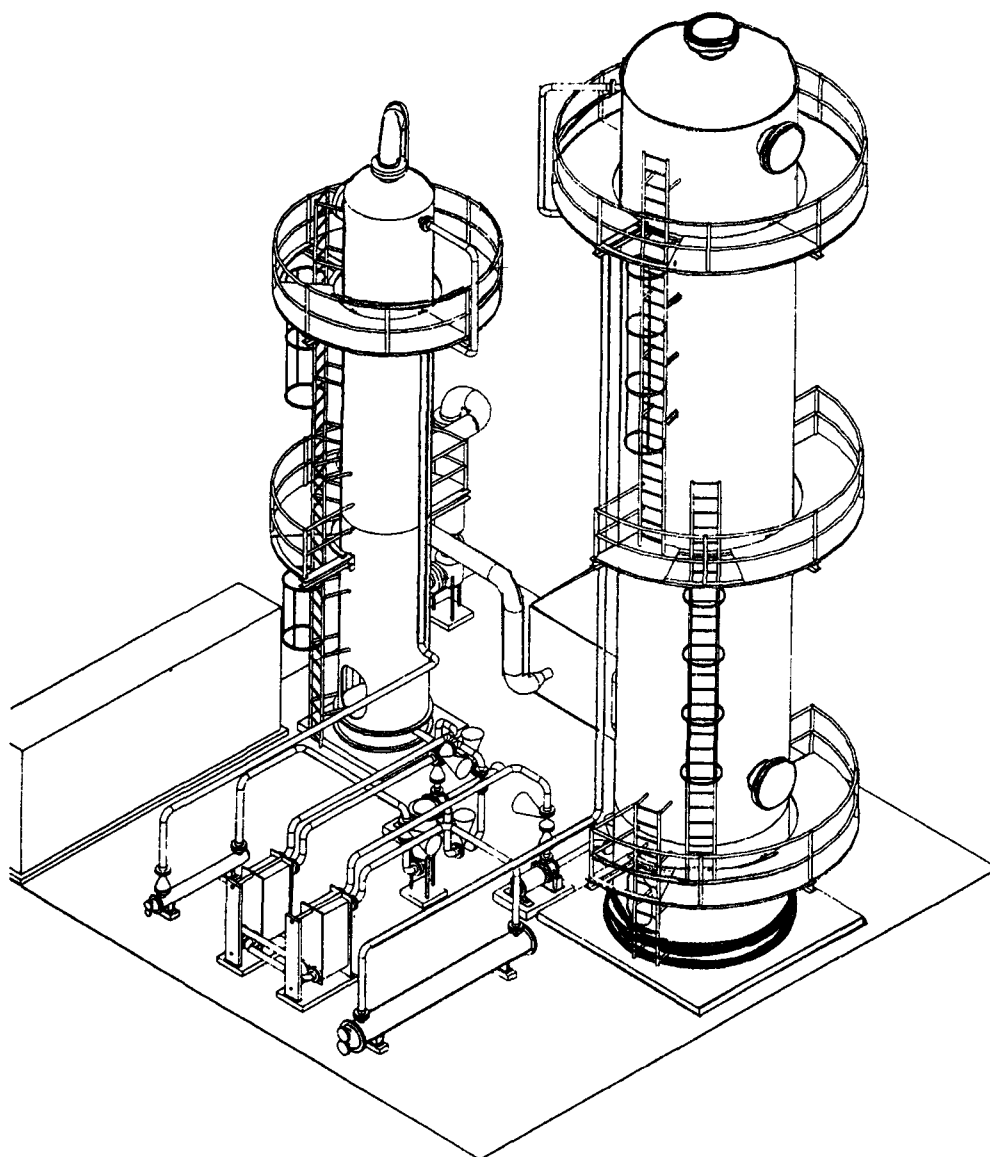
© Sulzer Brothers Limited. Reproduced with kind permission of Sulzer Brothers Limited/Winterthur/Switzerland

Fig. 1.1. *Absorption Tower Hooked up with a Regeneration Column completes A Commercial Absorption Process.*

Source : **Absorption Technology** — Sulzer Chemtech

Be it absorption or desorption—the intimate gas-liq contact is essential in both cases and as such the effectiveness of the equipment is, by and large, determined by the success with which it promotes contact between the two phases.

Absorption differs from distillation in the following aspects :

- Stripping vapor is generated in the distillation column by the partial evaporation of the liquid which is therefore at its boiling point, whereas in absorption the liquid is always well below its boiling point.

- Distillation is characterized by simultaneous molecular diffusion in both directions and in ideal systems equimolar counter-diffusion occurs across the gas-liq phase boundaries of these two contacting streams. But in gas absorption, diffusion is chiefly unidirectional — the solute molecules are diffusing into the liquid while the movement in the reverse direction is practically very small.

- The ratio of the liq flowrate to the gas flowrate is considerably greater in absorption than in distillation with the effect that the layout of trays is different in these two cases.

- The primary objective of absorption is only solute recovery or solute removal while distillation involves separation of solutes from each other to any important extent.

1.1. APPLICATIONS

Gas absorption technology finds its commercial application in the following fields :

The Gas Industry

- Gas dehydration
- Removal of CO_2 and H_2S
- Selective absorption of H_2S

Refineries

- Hydrocarbon absorbers for lean oil etc.)
- H_2S absorbers (MEA, DSA, etc.)
- Various types of stripping columns
- Sour water strippers

The Petrochemical Industry

- Synthesis gas processing
- Gas saturation
- Ethylene oxide absorption
- Acrylonitrile absorption

The Chemical Industry

- Synthesis gas processing (CO_2 removal, Saturation)
- Chlorine drying
- HCl and ammonia absorption
- Absorption of nitrous gases

The Cellulose Industry

- Sulfur dioxide absorption
- Chlorine dioxide absorption
- Flue gas scrubbing with sulfur recovery.

Food Processing

- Stripping various components producing odours (*i.e.*, deodorization)
- Processing fatty acids
- Hexane absorption and stripping

The Metal & Packaging Industries

- Absorption of triethylamine (in foundries)
- Absorption of lube & cooling oils
- Absorption of nitrous gases
- Absorption and recovery of solvent vapors

Exhaust Air Scrubbing

- Removal of acid components (wet-and dry-scrubbing of SO_x & NO_x)
- Removal of base components
- Removal & recovery of organic solvents

Wastewater/sewage Treatment and Pollution Control

- Airstripping of chlorinated hydrocarbons
- Desorption & recovery of ammonia
- Effluent neutralization
- Deaeration of seawater.

1.2. GAS-LIQ EQUILIBRIUM : CONDITIONS OF

The liq and the gas phases, when brought into contact, tend to reach equilibrium. The rate at which a gaseous component from a feed gas mixture will dissolve is an absorbent liquid depends upon the departure from equilibrium which exists.

The solubility of any gas in a liquid [defined as the resulting concentration of the dissolved gas in the liquid at the prevailing pressure and temperature when the equilibrium is established] is influenced by the temperature and pressure in a manner described by van't Hoff's law of dynamic equilibrium :

— *at a fixed temperature, the solubility concentration will increase with pressure*

— *if, on the other hand, temperature of a gas-liq system in equilibrium is raised, that change will occur which will absorb heat.* Frequently, the dissolution of a gas in a liq results in an evolution of heat and it follows, therefore, that in most cases the solubility of a gas decreases with increasing temperature.

If the concentration of solute (dissolved gas) in the liquid phase is small and the solute forms a simple solution, Henry's Law applies :

$$p^* = H.x \qquad \qquad ...(1.1)$$

where, **p*** = partial pressure of solute in the gas phase over the liquid in equilibrium with the gas, Pa.

It is also the vapor pressure of solute as the latter is very little soluble in liquid phase & resides mostly in gas phase.

H = Henry's Law constant, Pa/mol fraction

x = mol fraction of solution in liq phase.

This equilibrium relationship is valid for dilute solutions of most gases and over a wide range for some gases.

The partial pressure of solute in the gas phase is a function of the gas composition :

$$p = y.P \qquad \qquad ...(1.2)$$

where, **p** = partial pressure of solute in gas phase, Pa

y = mol fraction of solute in gas phase

P = total system pressure, Pa

Combining these Equations (1.1) and (1.2) we get :

$$y^* = \frac{H.x}{P} \qquad \qquad ...(1.3)$$

where, **y*** = equilibrium mol fraction of solute in gas phase.

Since, Partial Pressure = Mol Fraction × Total Pressure
$$p^* = y^* \cdot P$$

Eqn. (1.3) is the expression for the vap-phase concentration of solute in equilibrium with the liq phase.

Now, the physical transfer of solute from the gas phase to the liquid (*i.e.*, absorption process) will occur whenever the partial pressure of solute in gas phase (Eqn. 1.2) exceeds the vapor pressure of solute above liq phase (Eqn. 1.1).

If the temperature of the liq phase is gradually increased to its boiling point, its vapor pressure will approach the system pressure. Thus, at the solvent (liq phase) boiling temperature, the solubility of the solute is reduced to zero*. The vapor pressure of the solute gas also increases with increasing temperature. Therefore, the Henry's Law constant increases with the rising of liq-phase temperature [Eqn. 1.1). Now, as per Eqn. 1.3, the solubility of a gaseous solute in the liquid phase, at constant gas composition and pressure, is inversely proportional to the Henry's Law constant. Therefore, with the rise of liq-phase temperature, the concentration of solute in liquid phase decreases.

Eqn. 1.1 enables us to calculate the vapor pressure of the solute only for low concentrations of the solute in the liquid phase. Should this equation be applied at higher concentrations of the solute in the liquid phase, the value of Henry's Law constant, **H,** must be modified. In case the system pressure exceeds 1000 kPa, a correction factor to account for the pressure effect may be introduced.

---

*This is the basic principle of desorption. Also it explains why the temperature of absorbent (liq solvent) is kept well below its boiling temperature in the absorption tower.

1.3. DRIVING FORCE

Absorption is the physical transfer of solute from the gas phase to the liquid phase. It is a diffusional mass transfer operation that occurs across the gas-liq interface. Since the solute is diffusing from the gas phase into the liquid, there must be a concentration gradient in the direction of mass transfer within each phase. Of course, it is the difference of chemical potential of solute in the gas phase and in the liquid phase that acts as the real driving force of absorption and determines the rate of this interphase mass transfer.

For any mass transfer operation between two gases in contact, it is the departure from the state of dynamic equilibrium of the two phases that generates the driving force. This driving force is measured by the difference between the chemical potentials ($\mu_y - \mu_x$) of the transferring component (solute) at equal temperature and pressure of the phases. When the phases are in equilibrium, the driving force is nil, so

$$\mu_y - \mu_x = 0$$

i.e., $\mu_y = \mu_x$

For Absorption : $\mu_y > \mu_x$

For Desorption : $\mu_x > \mu_y$

Now substituting for μ_x the potential of the equilibrium gaseous phase μ_y^* equal to it, the driving force becomes :

$$\mu_y - \mu_x = \mu_y - \mu_y^* \qquad\qquad \dots(1.3)$$
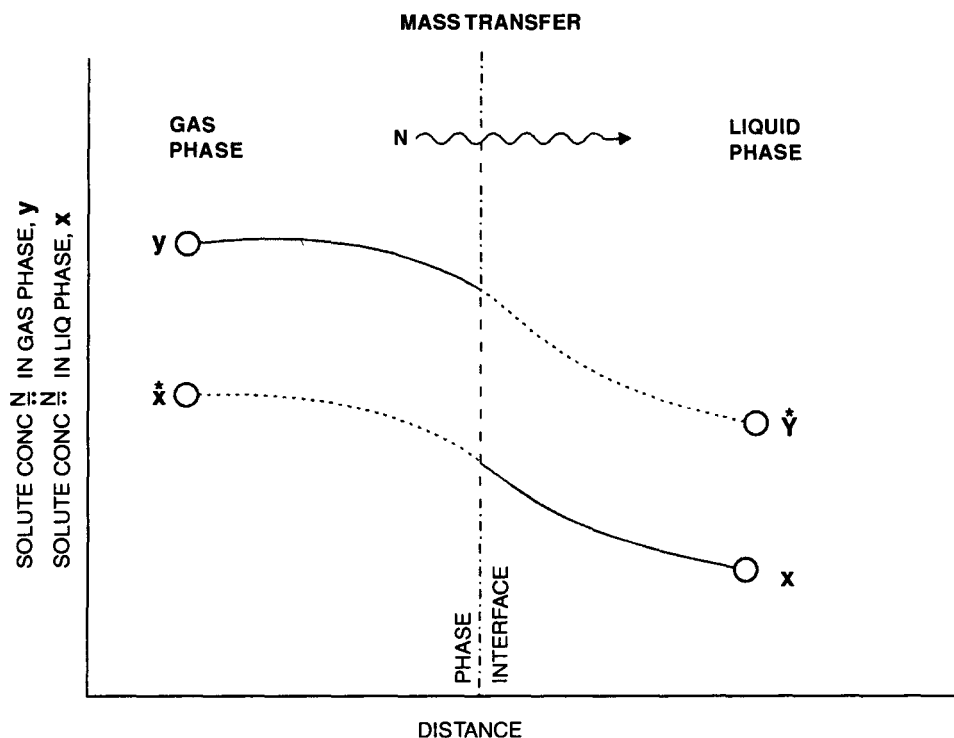
MASS TRANSFER

Fig. 1.3.1. *Mass Transfer Mechanism.*

Similarly, substituting for the chemical potential μ_y the potential of the equilibrium liquid phase μ_x^* equal to it, we get :

$$\mu_y - \mu_x = \mu_x^* - \mu_x \qquad \qquad ...(1.4)$$

The pair of Eqns. 1.3 and 1.4 lends us two different ways to express the difference between the chemical potentials $\mu_y - \mu_x$:

— with respect to gas phase

— with respect to gas phase

It must be remembered that the gas phase with chemical potential μ_y^* and solute concentration

y^* is a hypothetical phase, so is the liquid phase with the chemical potential μ_x^* and solute concentration x^* — in a real process of mass transfer they are absent *(Figure 1.3.1)*

In practical calculations, the chemical potentials are not used : instead they are replaced by the concentration terms (x, y etc.,) which are simpler quantities and they are easy to determine. They can also be used to characterize the deviation of the gas and liquid phases from equilibrium. However, unlike $(\mu_y - \mu_x)$, the difference between the concentration (y – x) never equal zero upon equilibrium and hence it cannot be the measure of the deviation of the phases from the equilibrium state, *i.e.*, cannot be the driving force of a mass transfer process. Therefore, for the sake of practical calculation, the driving force of any mass transfer process — the deviation of the system from the state of equilibrium — is expressed as the difference :

ABSORPTION PROCESS

y – y* = the driving force with respect to the gas phase

x* – x = the driving force with respect to the liquid phase

Forasmuch as the concentration can be expressed in different units, the driving force of any mass transfer process, accordingly, can have different units **(Table 1.1)**

<div align="center">

Table 1.1. Driving Force of Absorption

</div>

Phase	*The Driving Force*	
	Expression	*Unit*
Gas	$\Delta p = p - p^*$	mm Hg or Pa
Gas	$\Delta y = y - y^*$	mol fraction
Gas	$\Delta Y = Y - Y^*$ $= \dfrac{y}{1-y} - \dfrac{y^*}{1-y^*}$	mol ratio
Liquid	$\Delta x = x^* - x$	mol fractions
Liquid	$\Delta X = X^* - X$ $= \dfrac{x^*}{1-x^*} - \dfrac{x}{1-x}$	mol ratio

1.3.1. Mean Driving Force

The general equation of absorption when the driving force is expressed with respect to gaseous phase as $\Delta y = y - y^*$ is

$$N = K_{G,y} \cdot A \cdot \Delta y_m \qquad \qquad ...(1.5)$$

and when the driving force is expressed with respect to liquid phase as $\Delta x = x^* - x$, it becomes

$$N = K_{L,x} \cdot A \cdot \Delta x_m \qquad \qquad ...(1.6)$$

These two general expressions of mass transfer results from its complete analogy to heat transfer.

N = molar flowrate of solute from gas phase to liquid phase, kmol/h

A = area of mass transfer surface, m^2

$K_{G,y}$ = overall liq phase mass transfer coefficient related to the driving force Δy, kmol/$(m^2.h)$ or, kmol/$(m^2.h.kmol/kmol)$

$K_{G,y}$ = overall gas phase mass transfer coefficient related to the driving force Δy, kmol/$(m^2.h)$ or, kmol/$(m^2.h.kmol/kmol)$

Δy_m & Δx_m = mean driving forces of the entire process with respect to gas phase and liquid phase respectively

The Equation 1.5 can be expressed with Δy_m replaced by ΔY_m, Δc_{y_m} and Δp_m :

$$N = K_{G,y} \cdot A \cdot \Delta Y_m \qquad \qquad ...(1.5A)$$

$$N = K_{G,c} \cdot A \cdot \Delta c_{y_m} \qquad \qquad ...(1.5B)$$

$$N = K_{G,p} \cdot A \cdot \Delta p_m \qquad \qquad ...(1.5C)$$

Likewise, Eqn. 1.6 can be expressed with Δx_m replaced by ΔX_m and Δc_{x_m} :

$$N = K_{L,x} \cdot A \cdot \Delta X_m \qquad \qquad ...(1.6A)$$

$$N = K_{L,c} \cdot A \cdot \Delta c_{x_m} \qquad \qquad ...(1.6B)$$

If the rate of flow of the component being absorbed is expressed in kg/h, the general equation of mass transfer becomes :

$$M' = K_{G,\bar{y}} \cdot A \cdot \Delta \bar{Y}_m \qquad \qquad ...(1.7)$$

where, M' = mass flowrate of diffusing solute, kg/h

$K_{G,\bar{y}}$ = overall gas phase mass transfer coefficient, kg/$(m^2.h)$

A = surface area of mass transfer in the absorber, m^2

$\Delta \bar{Y}_m$ = mean driving force

$$= \frac{\Delta \bar{Y}_b - \Delta \bar{Y}_t}{\ln \left[\dfrac{\Delta \bar{Y}_b}{\Delta \bar{Y}_t} \right]} \qquad \qquad ...(1.8)$$

$\Delta \bar{Y}_b = \bar{Y}_b - \bar{Y}_b^*$ = terminal driving force at the bottom of the absorber when $\bar{X} = \bar{X}_b$

$\Delta \bar{Y}_t = \bar{Y}_t - \bar{Y}_t^*$ = terminal driving force at the top of the absorber when $\bar{X} = \bar{X}_t$

where $\bar{X}$ = mass ratio of solute in liq phase

$$= \left[\frac{kg \text{ of Solute}}{kg \text{ of Remaining Components}} \right] \text{in liq phase}$$

$\bar{Y}$ = mass ratio of solute in gas phase

$$= \left[\frac{\text{kg of Solute}}{\text{kg of Remaining Components}} \right] \text{in gas phase}$$

Case – (I) In case

$$\frac{1}{2} \le \left[\frac{\Delta \overline{Y}_b}{\Delta \overline{Y}_t} \right] \le 2$$

use the simpler formula :

$$\Delta \overline{Y}_m = \frac{1}{2} \left[\Delta \overline{Y}_b + \Delta \overline{Y}_t \right] \qquad \qquad ...(1.9)$$

to calculate the mean driving force in an absorber.

Case – (II) In case the **VLE** (vapor-liq equilibrium) line is not straight, then

$$\Delta \overline{Y}_m = \frac{\Delta \overline{Y}_b - \overline{Y}_t}{\displaystyle\int_{\overline{Y}_t}^{\overline{Y}_b} \frac{d\overline{Y}}{\overline{Y} - \overline{Y}*}} \qquad \qquad ...(1.10)$$

The value of the integral $\displaystyle\int_{\overline{Y}_t}^{\overline{Y}_b} \frac{d\overline{Y}}{\overline{Y} - \overline{Y}*}$ can be obtained either by the method of graphical integration or by graphical construction.

Frequently the driving force is expressed in units of pressure while calculating absorbers. The pressure driving force (*i.e.*, pressure difference) must be determined at the bottom (Δp_b) as well as at the top (Δp_t) of the absorber.

For a gas stream containing a low concentration of solute, the ratio of liq to vapor flowrate **(L/ G)** is almost constant and the operating line of the absorber is straight. Now if absorption accompanies negligible heat of solution, the pressure driving force, under these conditions, is the logarithmic mean of the driving forces at the bottom and top of the column :

$$\Delta p_{lm} = \frac{\Delta p_b - \Delta p_t}{\ln \left[\dfrac{\Delta p_b}{\Delta p_t} \right]} \qquad \qquad ...(1.11)$$

and the mass transfer equation becomes :

$$N = K_{G,p} \cdot A \cdot \Delta p_{lm} \qquad \qquad ...(1.12)$$

where, N = rate of solute transfer from gas to liq phase, kmol/h

$K_{G,p}$ = overall gas phase mass transfer coefficient in terms of partial pressure, kmol/(m². h. Pa)

1.4. ABSORPTION MECHANISM

The most widely accepted theory to explain gas-liq mass transfer operations is the **double-film theory** of Lewis and Whitman (W. K. Lewis and W. G. Whitman — *Industrial and Engineering Chemistry, Vol. 16 (1924)* :

The boundary between the gas phase and liquid phase in contact is presumed to be composed of two films — a gas film and a liq film — separated by an interface **Figure 1.4.1.** The gas film is adjacent to the main bulk of gas and the liq film to the main bulk of liq.
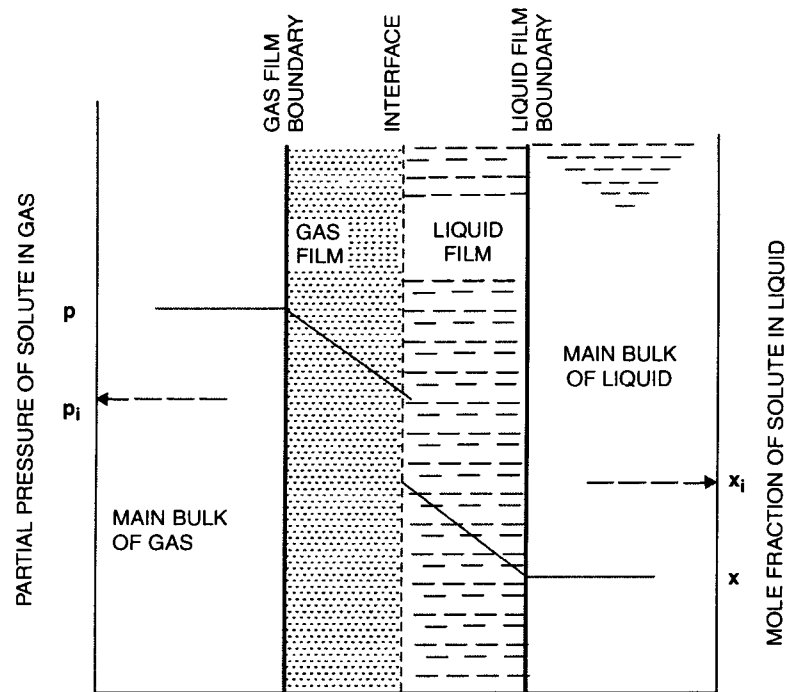
Fig. 1.4.1. *Double-Film Theory of Mass Transfer Mechanism in Absorption.*

Diffusional resistances reside only in the fluids themselves and there is no resistance to solute transfer across the interface separating the phases. Therefore, the solute concentration in the gas film at the interface is assumed to the in equilibrium with the solute concentration in the liquid film at the interface.

Concentration gradient exists in both films and the flow in both these films is assumed to the laminar or stagnant. However, no concentration gradient exists in the main body of both the gas and liq phases because of prevailing turbulences that thoroughly mix up either phase.

The driving force causing solute transfer in the gas phase :

$$p - p_i \equiv DE \qquad \boxed{\textbf{Fig. 1.4}}$$

and the driving force causing solute transfer in the liquid phase :

$$x_i - x \equiv BE \qquad \boxed{\textbf{Fig. 1.4}}$$

In complete analogy to heat transfer wherein the flow of heat is equal to the product of a heat transfer coefficient, a transfer surface area and a driving force, the rate of mass transfer from the main body of gas phase thru the gas film in absorption is given by the Eqn.

$$N = k_{G,P} \bullet A \bullet (p - p_i) \qquad \qquad \text{...(1.13)}$$

where, $k_{G,P}$ = gas film transfer coefficient in terms of partial pressure, $kmol/(h.m^2.Pa)$

$p - p_i$ = difference between the partial pressure of solute in the main-body gas phase and that in the gas film at the interface. It is the driving force for mass transfer across the gas film.

A = area of mass transfer surface. In absorber design calculations it is taken equal to column cross-sectional area, m^2.
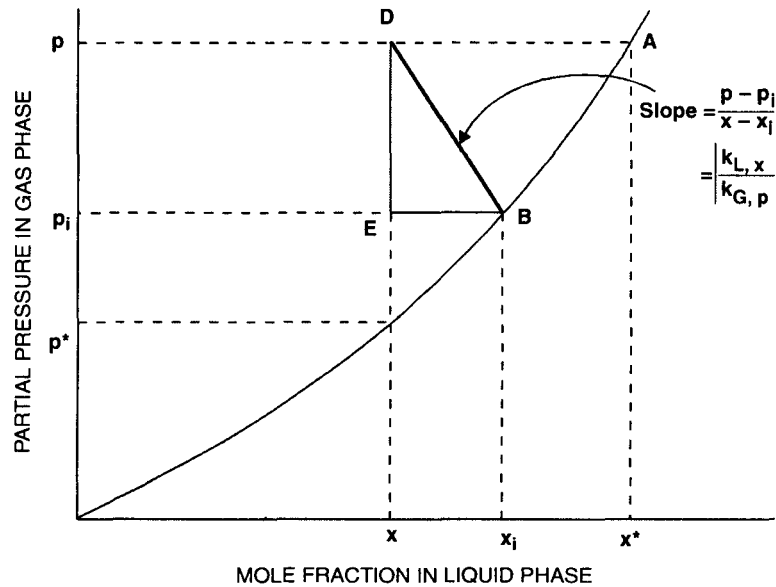
Fig. 1.4.2. *Driving Forces in Gas & Liq Phases in the Course of Absorption.*

Similarly the rate of solute transfer across the liq film to the main bulk of liq phase is given by the expression :

$$N = k_{L,X} \cdot A \cdot (x_i - x) \qquad \qquad ...(1.14)$$

where, $k_{L,X}$ = liq film transfer coefficient in terms of mol fraction, kmol/(h.m^2.kmol/kmol)

$x_i - x$ = concentration difference across the liq film. It is the driving force across the liq film.

In the steady-state process of absorption, the rate of transfer of material thru the gas film equals the rate of transfer of the material thru the liq film and with that the general equation of mass transfer may be represented as :

$$N = k_{G,P} \cdot A \cdot (p - p_i) = k_{L,X} \cdot A \cdot (x_i - x)$$

$$\frac{k_{L,X}}{k_{G,P}} = \frac{p - p_i}{x_i - x} = \text{ratio of driving forces in gas phase to liquid phase} \qquad ...(1.15)$$

The value of x_i and p_i are difficult to determine in practical cases. Hence overall terms have been adopted for calculative purposes.

For absorption involving highly soluble solutes, the driving force usually is the partial pressure of the solute in the gas phase minus the vapor pressure of the solute above the liquid phase, *i.e.*, the driving force is $p - p^*$ [or $p - H.x$ where Henry's Law is applicable]. The greater this driving force, the faster will be the rate of mass transfer. Thus the overall mass transfer analogous equation for the gas phase is :

$$N = K_{G,P} \cdot A \cdot (p - p^*) \qquad \qquad ...(1.16)$$

where, $K_{G,P}$ = overall gas-phase mass transfer coefficient in terms of partial pressure, kmol/(h.m^2.Pa)

Likewise the driving force in liquid phase for the diffusion of highly soluble solutes during absorption is **x* − x** [Or, **p/H − x** where Henry's Law applies]. Therefore, for practical purposes the rate of mass transfer in liquid phase in absorption process is :

$$N = K_{L,X} \cdot A \cdot (x^* - x) \qquad \qquad ...(1.17)$$

where, $K_{L,X}$ = overall liq-phase mass transfer coefficient in terms of mol fraction, $kmol/(h.m^2.mol/mol)$

For steady-state absorption,

$$N = K_{G,P} \cdot A \cdot (p - p^*) = K_{L,X} \cdot A \cdot (x^* - x)$$

or,
$$\frac{K_{G,P}}{K_{L,X}} = \frac{x^* - x}{p - p^*} \qquad \qquad ...(1.18)$$

If the partial pressure terms are replaced by concentration terms **c**, the Eqn. 1.16 would become

$$N = K_{G,C} \cdot A \cdot (c - c^*) \qquad \qquad ...(1.19)$$

whereupon the Eqn. 1.18 would take the shape of :

$$\frac{K_{G,C}}{K_{L,X}} = \frac{x^* - x}{c - c^*} \qquad \qquad ...(1.20)$$

1.4.1. Overall and Film Transfer Coefficients : Interrelationships

The rate of mass transfer of solute in gas phase :

Film Transfer	$N = K_{G,Y} \cdot A \cdot (y - y_i)$	...(1.21)
Overall Transfer	$N = K_{G,Y} \cdot A \cdot (y - y^*)$	...(1.22)

The rate of mass transfer of solute in liq phase :

Film Transfer	$N = k_{L,X} \cdot A \cdot (x_i - x)$	...(1.14)
Overall Transfer	$N = K_{L,X} \cdot A \cdot (x^* - x)$	...(1.17)

For steady-state absorption :

$$\frac{N}{A} = k_{G,Y}(y - y_i) = K_{G,Y}(y - y^*) = k_{L,X}(x_i - x) = K_{L,X}(x^* - x) \qquad ...(1.23)$$

Now, combining Eqns. 1.21 & 1.22 we get :

$$\frac{1}{K_{G,Y}} = \frac{1}{k_{G,Y}} \cdot \left[\frac{y - y^*}{y - y_i} \right] \qquad \qquad ...(1.24)$$

And combining Eqns. (1.14) and (1.7) we get :

$$\frac{1}{K_{L,X}} = \frac{1}{k_{L,X}} \cdot \left[\frac{x^* - x}{x_i - x} \right] \qquad \qquad ...(1.25)$$

Expanding Eqn. 1.24 results :

$$\frac{1}{K_{G,Y}} = \frac{1}{k_{G,Y}} \cdot \left[\frac{y - y_i}{y - y_i} \right] + \frac{1}{k_{G,Y}} \cdot \left[\frac{y_i - y^*}{y - y_i} \right] = \frac{1}{k_{G,Y}} + \frac{1}{k_{G,Y}} \cdot \left[\frac{y_i - y^*}{y - y_i} \right]$$

But from Eqn. 1.23 :

$$\frac{1}{k_{G,Y}} = \frac{1}{k_{L,X}} \cdot \left[\frac{y - y_i}{x_i - x} \right]$$

$$\therefore \qquad \frac{1}{K_{G,Y}} = \frac{1}{k_{G,Y}} + \frac{1}{k_{L,X}} \cdot \left[\frac{y_i - \overset{*}{y}}{x_i - x} \right] \qquad \qquad ...(1.26)$$

From the geometry of **Figure 1.5**, slope of the chord *CM*
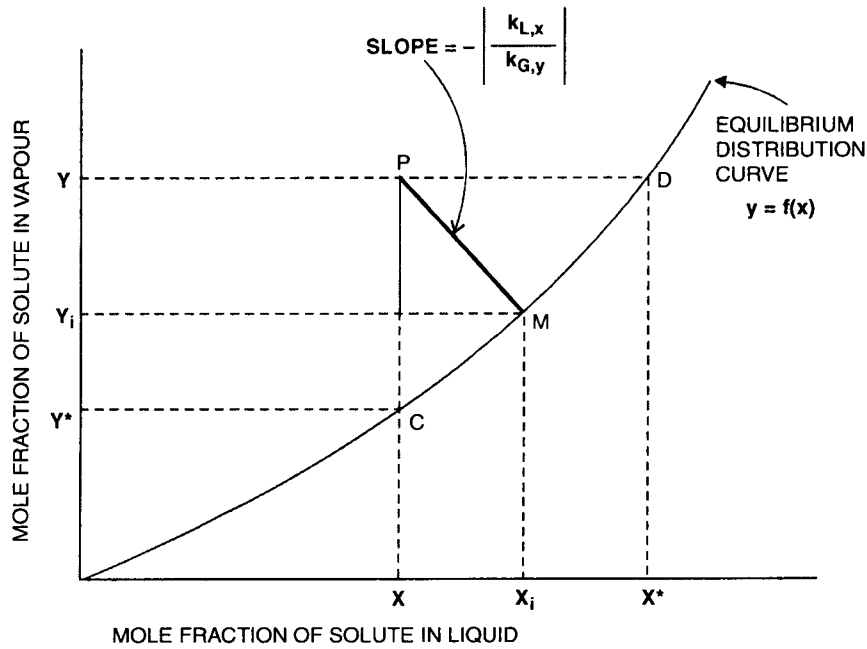
Fig. 1.5. *Equilibrium Distribution Curve*

$$m = \left[\frac{y_i - y_*}{x_i - x} \right]$$

Therefore, Eqn. 1.26 reduces to

$$\frac{1}{K_{G,y}} = \frac{1}{k_{G,y}} + \frac{m}{k_{L,x}} \qquad \qquad ...(1.27)$$

Similarly, from Eqn. 1.25 we get :

$$\frac{1}{K_{L,X}} = \frac{1}{k_{L,X}} \cdot \left[\frac{x^* - x_i}{x_i - x} \right] + \frac{1}{k_{L,X}} \cdot \left[\frac{x_i - x}{x_i - x} \right]$$

$$= \frac{1}{k_{L,X}} \cdot \left[\frac{x^* - x_i}{x_i - x} \right] + \frac{1}{k_{L,X}}$$

$$= \frac{1}{k_{G,Y}} \cdot \left[\frac{x^* - x_i}{y - y_i} \right] + \frac{1}{k_{L,X}} \qquad ...(1.29)$$

From Fig. 1.5, slope of the chord DM

$$m' = \left[\frac{y - y_i}{x^* - x_i} \right]$$

Therefore Eqn. 1.28 reduces to

$$\frac{1}{K_{L,X}} = \frac{1}{k_{G,Y} \cdot m'} + \frac{1}{k_{L,X}} \qquad ...(1.30)$$

When the solution obeys Henry's Law,

$$m' = H$$

Likewise, it can be shown for solutions obeying Henry's Law :

$$\frac{1}{K_{G,P}} = \frac{1}{k_{G,P}} + \frac{H}{k_{L,X}} \qquad ...(1.31)$$

and

$$\frac{1}{K_{L,X}} = \frac{1}{k_{G,P} \cdot H} + \frac{1}{k_{L,X}} \qquad ...(1.32)$$

1.5. MASS TRANSFER RESISTANCE

In analogy to heat transfer wherein the resistance to heat transfer

$$= 1/h$$

$$= 1/\text{heat transfer coefficient}$$

the reciprocal of individual film transfer coefficient is the resistance to mass transfer exhibited by that film :

$$1/k_{G,Y} = \text{resistance in gas film}$$

$$1/k_{L,X} = \text{resistance in liq film}$$

Therefore, it follows :

$$\frac{\text{Resistance in gas film}}{\text{Overall resistance (of both phases)}} = \frac{1/k_{G,Y}}{1/K_{G,Y}} \qquad ...(1.33)$$

$$\frac{\text{Resistance in liq film}}{\text{Overall resistance (of both phases)}} = \frac{1/k_{L,X}}{1/K_{L,X}} \qquad ...(1.34)$$

The absorption is said to be gas-film controlled, *i.e.*, the major resistance to mass transfer resides within the gas when $1/k_{G,Y}$ is very large compared to $1/k_{L,X}$, *i.e.*, when the gas-film mass transfer coefficient is $(k_{G,y})$ small compared to liq-film mass transfer coefficient $(k_{L,X})$ or when m is small. Under these circumstances the equilibrium distribution curve is very flat so that at equilibrium only a small concentration of solute in the gas will create a very large concentration in the liq, the term $m/k_{L,X}$ becomes minor whereupon Eqn. 1.27 transforms to :

$$\frac{1}{K_{G,Y}} \approx \frac{1}{k_{G,Y}}$$

...(1.35)

Or, $[y - y^*] \approx [y - y_i]$ ...(1.36)

In systems which are gas-film controlled **Table 1.2,** the solute either will be highly soluble in the liquid phase or will react rapidly with a component in the liq phase. In such cases, even fairly large percentage change in $k_{L,X}$ will not significantly affect $K_{G,Y}$ and in order to increase the rate of absorption efforts should best be directed toward decreasing gas-phase resistance.

Table 1.2. Gas-Film Controlled Absorptions

Solute	*Absorbent (Liq Solvent)*	*Remarks*
Sulfur trioxide (SO_3)	98% H_2SO_4	**Chemical Absorption.** Oleum is produced : $SO_3 + H_2SO_4 \rightarrow H_2S_2O_7$
Sulfur dioxide (SO_2)	4% NaOH	Chemical reaction : $SO_2 + NaOH \rightarrow NaHSO_3$ follows absorption
Chlorine (Cl_2)	5% NaOH	**Chemical Absorption.** Chemical reaction : $Cl_2 + 2NaOH \rightarrow NaCl + NaOCl + H_2O$ follows absorption
Hydrogen chloride (HCl)	Water	**Chemical Absorption.** Covalent hydrogen gets converted to ionic hydrochloric acid upon reaction with water : $HCl + H_2O \rightarrow H^+ + Cl^-$ (Vap)
Ammonia (NH_3)	10% H_2SO_4	**Chemical Absorption.** Ammonia is chemically abosorbed in sulfuric acid solution: $NH_3 + H_2SO_4 \rightarrow NH_4HSO_4 + (NH_4)_2 SO_4$
Ammonia (NH_3)	Water	**Physical Absorption.** $NH_3 + H_2O \rightarrow NH_3 \cdot H_2O$
Water vapor	93% H_2SO_4	**Physical Absorption.**
Water vapor	Water (liq)	**Physical Absorption.**

The absorption is considered to be liq-film controlled if the major resistance to mass transfer resides within the liquid, *i.e.*, when liq-film mass transfer coefficient ($k_{L,X}$) is small compared to the gas-film mass transfer coefficient ($k_{G,X}$) or when m' is large. Under these circumstances, the equilibrium distribution curve is nearly vertical so that at equilibrium only a small concentration of solute in the liquid phase will provide a large concentration in the gas, the term $1/(k_{G,Y} \cdot m')$ becomes very small whereupon Eqn. 1.30 transforms to :

$$\frac{1}{K_{L,X}} \approx \frac{1}{k_{L,X}} \qquad \qquad ...(1.37)$$

Or, $\qquad \qquad (x^* - x) \approx [x_i - x] \qquad \qquad$ ...(1.38)

In systems which are liq-film controlled **Table 1.3,** the solute either has a low solubility in the liq phase or reacts with a component in the liquid phase at a slow rate. In such cases, in order to increase the rate of mass transfer from gas phase to liq phase efforts should be directed to reduce the liq-film mass transfer resistance.

Table 1.3. Liq-Film Controlled Absorptions

Solute	*Absorbent (Liq Solvent)*	*Remarks*
Oxygen	Water	**Physical Absorption**
Chlorine	Water	**Chemical Absorption** $Cl_2 + H_2O \rightarrow HCl + O_2$
Carbondioxide	Water	**Chemical Absorption.** $CO_2 + H_2O \rightarrow H_2CO_3$
Carbondioxide	4% NaOH	**Chemical Absorption.** $CO_2 + NaOH \rightarrow NaHCO_3$
Carbondioxide	12% MEA	**Physical Absorption.**

1.6. ABSORBER

The process of absorption is carried out in a tower called **Absorption Tower** or simply **Absorber.**

An absorber may be either a packed column [packed bed absorber) or a trayed column or a spray tower.

Packed Bed Absorbers are vertical columns filled with randomly dumped packing or structured packing to expose a large surface area for gas-liq contact **[Figure 1.6.1].**

These packed towers lend themselves for continuous contact of liq and gas in both countercurrent and cocurrent flow.

The solvent liq is distributed, thru a distributor, over the packed bed, and spreads over along the packing profile to come in contact with the upflowing gas stream. The gas-liq contact over extended surfaces enhances mass transfer.

The packings are of two types :

— random packing (Figure 1.6.2)
— structured packing (Figure 1.6.3)

The packing should
• provide for large interfacial area between gas an liq.
• permit passage of large volumes of gas and liq thru small tower cross-sections with loading or flooding.
• ensure low gas pressure drop.
• be chemically inert to contacting gas and liq streams.

- be economically available.
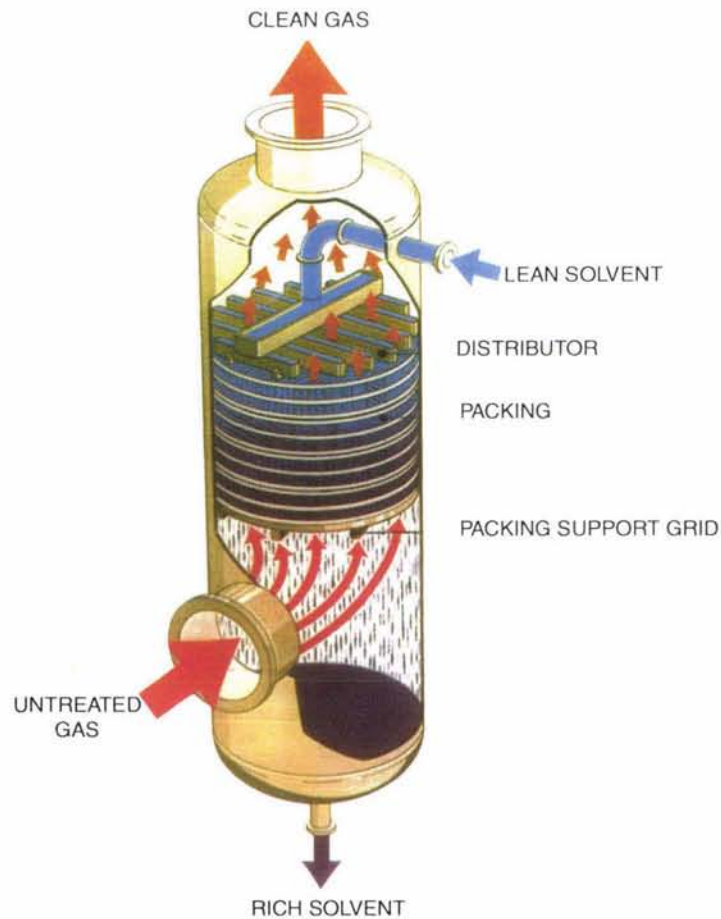
Fig. 1.6.1. *Sectional arrangement of a Sulzer countercurrent Absorption column.*
Courtesy : Sulzer Brothers Ltd., Winterthur, Switzerland
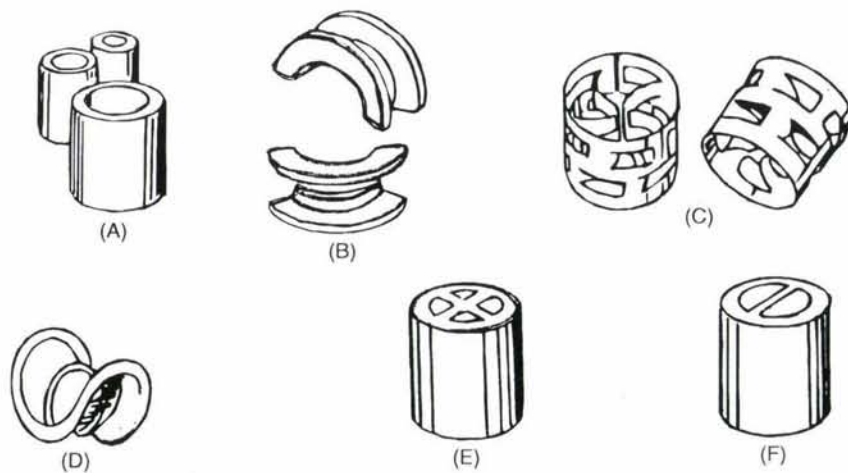
(A) Raschig rings; (B) Intalox saddles; (C) Pall rings (D) Berl saddle; (E) Cross-partition ring; (F) Lessing ring
Fig. 1.6.2. *Random Packings* *(Courtesy : GLITSCH Inc.)*

Fig. 1.6.3. *Structured Packings.*

Courtesy : Sulzer Brothers Ltd., Winterthur, Switzerland
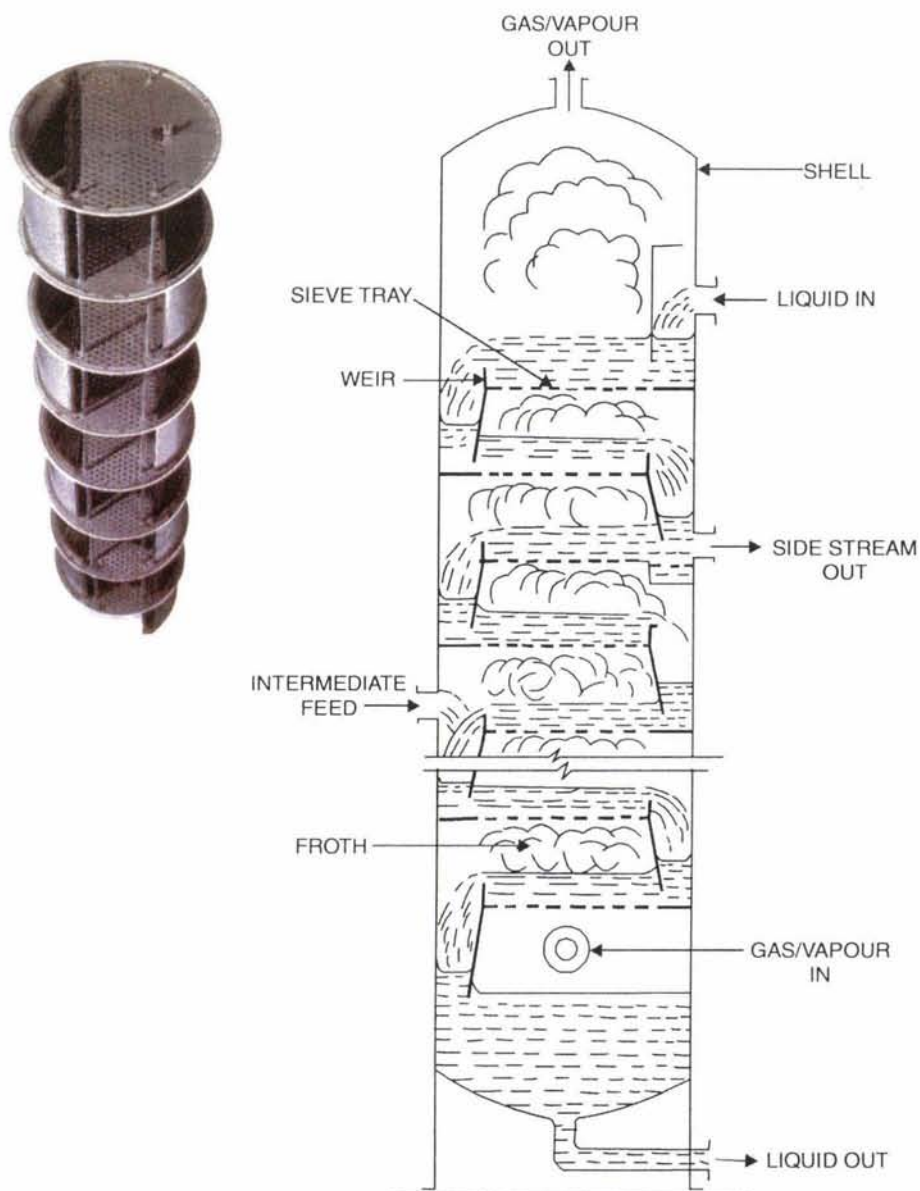
Fig. 1.6.4. *A Tray Tower consists of a Number of Trays (also called plates) set at specific interval.*

Fig. 1.6.5. *Bubblecap Tray.*

Courtesy : Norton Chemical Process Products Corpn. Akron, Ohio, USA

Fig. 1.6.6. *Valve Tray*   Fig. 1.6.7. *Sieve Tray*

Courtesy : Norton Chemical Process Products Corpn. Akron, Ohio, USA.

Tray Towers are vertical cylinders in which gas and liq are contacted in stepwise fashion on trays or plates **(Fig. 1.6.4).**

The trays come in the form of :

— bubblecap tray **(Figure 1.6.5)**

— valve tray **(Figure 1.6.6)**

— sieve tray **(Figure 1.6.7)**

The solvent liquid is introduced to the column at the top and it flows downward by gravity. On the way, it comes across each tray, overflows the weir and comes down to the tray below thru a downspout (also called downcomer).

On its way up, the gas passes thru the tray openings and bubbles thru the liq-on-tray to form froth and then it disengages from the froth & passes on to the next tray above.

Each tray acts as a stage, forasmuch as on each tray the counterflowing gas & liq streams are brought into intimate contact, solute diffusion occurs across the interphase and the fluids are then separated.

Spray Towers are vertical columns in which the solvent liquid is sprayed into the upflowing gas stream by means of a nozzle dispersing the liq into a fine spray of drops. The flow is countercurrent and interphase mass transfer takes place during droplets suspension.

These equipment have the advantage of lowest gas pressure drop amongst different types of absorbers. But they're fretted with disadvantages too :

- Relatively high pumping cost for the liquid owing to the large pressure drop thru the spray nozzle

- High tendency for entrainment of liquid rendering the installation of mist eliminators all but necessary

- Gas-liq thorough mixing gets hampered until or unless column dia : column length ratio is very small. However, this ratio cannot be made very small since the spray would quickly reach the tower walls, come down as wetted film rendering the spray ineffective.

1.7. MATERIAL BALANCE OF A COUNTERCURRENT ABSORBER

Certain basic parameters such as specific flowrate of absorbent, the number of theoretical stages of contact (*i.e.*, the number of theoretical plates) are required in calculating the processes of absorption. These parameters are determined by simultaneous solution of the material-balance equation (equation of **OL**) and the equation of equilibrium line (**VLE-line**).

A countercurrent tower may be either a packed tower or tray-tower fitted with bubblecap or valve or sieve trays to bring about intimate gas-liq contact.

The general expression of a material-balance equation in an absorber is :

$$- G_s \cdot dy = L_s \cdot dx \qquad \qquad ...(1.39)$$

where,

G_s = gas (vapor) flowrate on solute-free basis kmol/(h.m^2)

L_s = liq flowrate on solute-free basis kmol/(h.m^2)

y = mol fraction of solute in gas phase

x = mol fraction of solute in liq phase.

The negative sign accounts for the depletion of solute in the gas phase.

If the molar (or mass) flowrates of gas and liquid phases are constant all along the height of the absorber, integration of Eqn. 1.39 between the limits (x_t, y_t) and (x_b, y_b), [see **Figure 1.7.1**]

yields :

Fig. 1.7.1. *Material Balance in a Countercurrent Absorber.*

$$\frac{L_S}{G_S} = -\frac{|y|_{y_b}^{y_t}}{|x|_{x_t}^{x_b}}$$

$$= \frac{y_b - y_t}{x_b - x_t} \qquad \qquad ...(1.40)$$

Eqn. 1.40 is a straightline passing thru the points (x_t, y_t) and (x_b, y_b) and of slope L_s/G_s. (**Figure 1.7.2**). This straightline is the *operating line* (**OL**) of the absorption process.
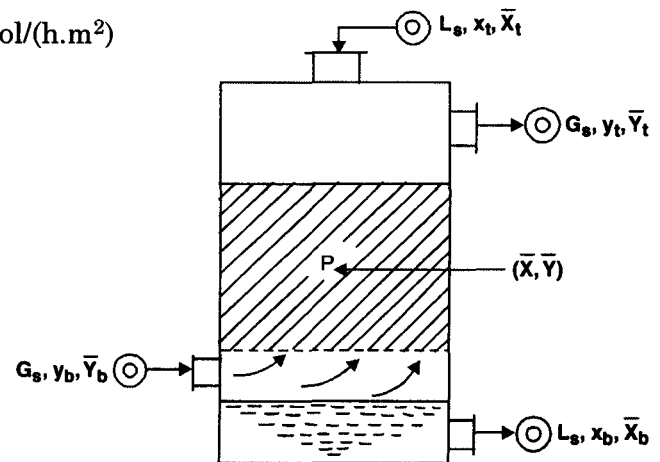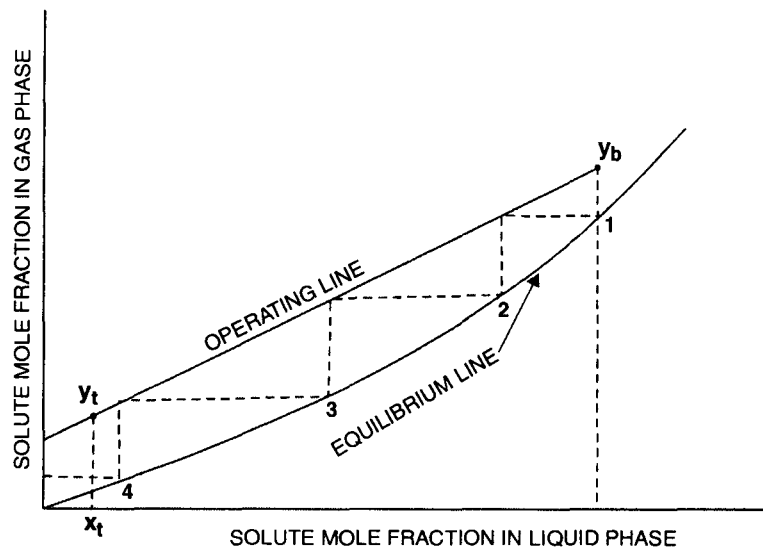
Fig. 1.7.2. *Operating and Equilibrium Lines of Absorption Process.*

Also plotted in the **Figure 1.7.2** is the **VLE**-line (vapor-liq equilibrium line) of the solute. It lies below the **OL** since during the process of absorption transfer of solute takes place from gas phase to the liquid due to higher concentration of solute in the gas phase than in liquid phase [$y_t > x_t$ and $y_b > x_b$].

The slope of the **OL** is the ratio **L/G** which is called **specific consumption of an absorbent.**

The greater the specific consumption of the absorbent, the greater the distance between the **OL** and **VLE** line and so larger will be the concentration difference $\Delta y = y - y^*$, *i.e.* greater will be the driving force of mass transfer from gas (vapor) phase to the liq phase. As the **OL** shifts away from the **VLE**-line, the liq-phase driving force $\Delta x = x^* - x$ will also increase favouring mass transfer from the gas-liq interface to the bulk of the liq. That means the driving force in both phases will simultaneously increase bringing about higher mass transfer rate of solute from gas to liq phase. This concurrent change in a given concentration to the equilibrium one in both gas and liq phases is called one THEORETICAL STAGE OF CONTACT or the THEORETICAL PLATE.

The number of such contact stages or theoretical plates can be determined by two ways :

• *Graphically* : constructing step by step the number of theoretical stages using OL and VLE-line simultaneously to accomplish a definite concentration difference in the absorber (**Fig. 1.7.3**).

• *Analytically* : solving together the equations of the **OL** and **VLE**-line.

With an increase in the specific consumption of the absorbent **(L/G)**, the slope of **OL** increases shifting the **OL** away from **VLE** curve with the effect that the driving force of the absorption process **(Δy, Δx)** increases and the required number of theoretical plates diminishes.

If we express the solute concentration in mole ratio, the material balance equation (in molar units) becomes :

$$\frac{L_s}{G_s} = \frac{Y_b - Y_t}{X_b - X_t}$$

...(1.41)

If we express the solute concentration in mass ratio, the material balance equation in molar units :

$$\frac{\mathbf{L_s}}{\mathbf{G_s}} = \frac{\overline{Y}_b - \overline{Y}_t}{\overline{X}_b - \overline{X}_t}$$

...(1.42)
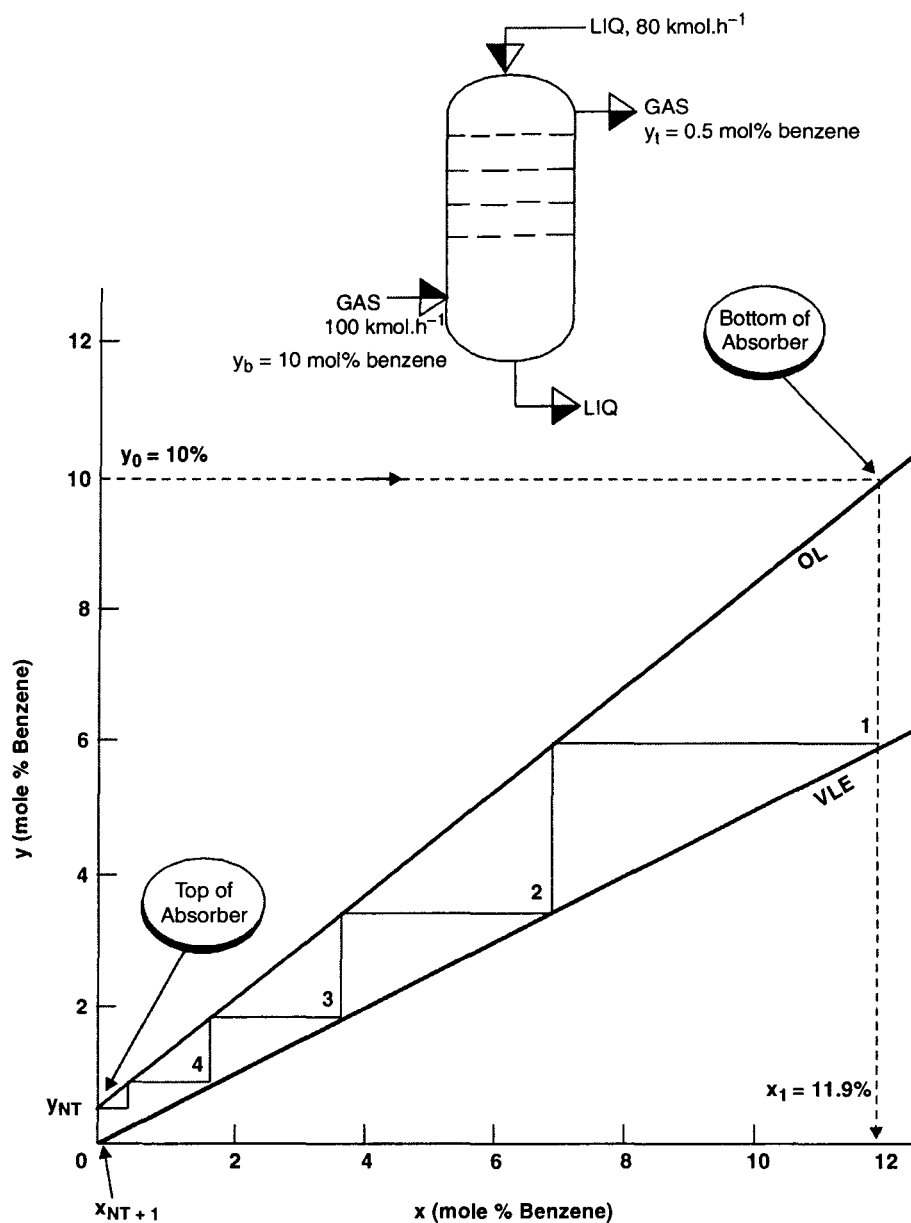
Fig. 1.7.3. *Graphical Construction of Theoretical Plates in a typical Absorber.*

and in mass units :

$$\frac{\mathbf{L'_s}}{\mathbf{G'_s}} = \frac{\overline{Y}_b - \overline{Y}_t}{\overline{X}_b - \overline{X}_t}$$

...(1.43)

where $\mathbf{L_s}$ = liq molar flux on solute-free basis, kmol/(h.m^2)

$\mathbf{L_s'}$ = liq mass flux on solute-free basis, kg/(h.m^2)

$\mathbf{G_s}$ = gas molar flux on solute-free basis, kmol/(h.m^2)

G'_s = gas mass flux on solute-free basis, kg/(h.m^2)

X = mol ratio of solute in the liq phase

$$= \left(\frac{\text{kmol of solute}}{\text{kmol of remaining components}}\right) \text{in liq phase}$$

$\overline{X}$ = mass ratio of solute in liq phase

$$= \left(\frac{\text{kg of solute}}{\text{kg of remaining components}}\right) \text{in liq phase}$$

X_b, X_t = mol ratio of solute in the liq phase at the absorber bottom and top respectively

$\overline{X}_b, \overline{X}_t$ = mass ratio of solute in the liq phase at the absorber bottom and top respectively

Y = mol ratio of solute in the gas (vapor) phase

$$= \left(\frac{\text{kmol of solute}}{\text{kmol of remaining components}}\right) \text{in the gas}$$

$\overline{Y}$ = mass ratio of solute in the gas (vapor) phase

$$= \left(\frac{\text{kg of solute}}{\text{kg of remaining components}}\right) \text{in the gas}$$

Y_b, Y_t = mol ratio of solute in the gas phase at the absorber bottom and top respectively

$\overline{Y}_b, \overline{Y}_t$ = mass ratio of solute in the gas phase at the absorber bottom and top respectively.

Eqns. 1.41, 1.42, 1.43 are the equations of straight line and they all represent the **OL** of the same absorber but in different units.

If $(\overline{X}, \overline{Y})$ be the coordinate of a point *P* in the packed bed **Figure 1.7.1**, it will lie on the operating line *AB* generated upon plotting $\overline{Y}$ against $\overline{X}$ [**Figure 1.7.4**]

Since the point $(\overline{X}, \overline{Y})$ lies on the st. line AB :

$$\overline{Y}_b - \overline{Y}_t = \frac{L_s}{G_s}\left[\overline{X}_b - \overline{X}_t\right]$$

we can also express the **OL** *(AB)* as :

$$\overline{Y} = \overline{Y}_b + \frac{L_s}{G_s}\left[\overline{X} - \overline{X}_b\right] \qquad \text{...(1.44)}$$

$$\text{or, } \overline{Y} = \overline{Y}_t + \frac{L_s}{G_s}\left[\overline{X} - \overline{X}_t\right] \qquad \text{...(1.45)}$$

Fig. 1.7.4. *OL and VLE Curve of an Absorber*

It is important to note that the **OL** is straight only when plotted in terms of the mol-ratio units. When expressed in terms of mol fractions or partial pressure, the line gets curved as shown in **Figure 1.7.5**. The eqn. of **OL** under these circumstances is :

$$G_s \left[\frac{y_t}{1-y_t} - \frac{y}{1-y} \right] = G_s \left[\frac{p_t}{P-p_t} - \frac{p}{P-p} \right] = L_s \left[\frac{x_t}{1-x_t} - \frac{x}{1-x} \right] \qquad \ldots (1.46)$$
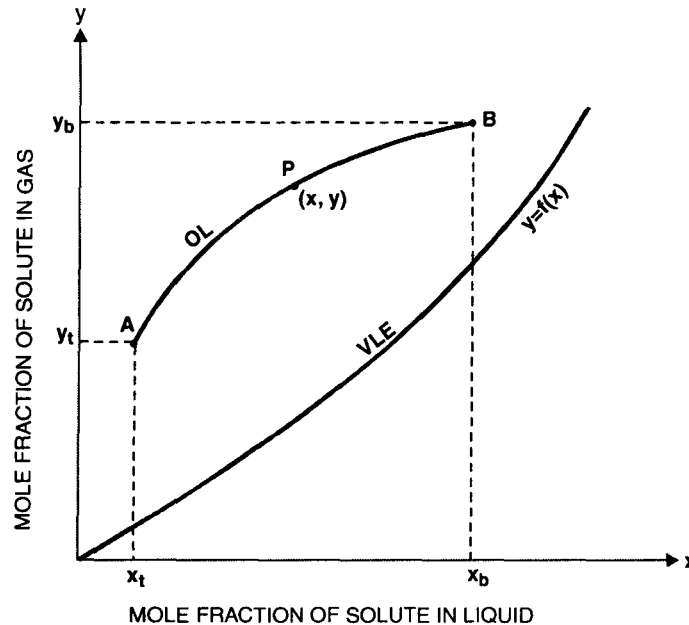
Fig. 1.7.5. *OL (AB) of an Absorber becomes Curved when it is expressed in Mol-Fraction Terms.*

For primary absorber design calculation, the total pressure P at any point may be taken constant thruout the tower.

1.8. MINIMUM LIQ-GAS RATIO

In the design of absorbers, usually the following quantities are fixed :

* Gas rate, G_s
* Terminal concentration in gas phase Y_t, Y_b
* Terminal concentration in liq phase X_t

So we have the point A (X_t, Y_t) of OL fixed (**Figure 1.8.1**).

Also we have the ordinate (Y_b) of the end point of the operating line fixed. A horizontal thru Y_b marks this limit. Therefore, between the pt.-A and the limit of Y_b we can have infinite number of OLs of varying slope L_s/G_s. Since G is preset we're to vary the liq flowrate to obtain these OLs — AB_1, AB_2, AB_3....etc.

With the increase of liq rate the slope of OL increases and with that the mol ratio of the solute in liq phase decreases, *i.e.*, the quantity of solute transferred to solvent progressively dwindles. Conversely, if less liq is used, the solute content in the exit liq will clearly be greater. However, the driving forces for diffusion wane, and the absorption becomes progressively difficult as the liq rate is gradually reduced. Therefore, in order to maintain the specified absorption, the contact time between the gas and liq phases must be raised and as such the absorber must be correspondingly *taller*. When the liq rate reaches its lower limit, *i.e.*, at $L_s = L_{s, min}$, the operating line (AB_3) touches the

VLE-curve at a point P. At this point, the **OL** is tangent to the equilibrium line and the diffusional driving force is zero with the effect that infinite time of contact is required to produce the desired concentration change. And as such the absorption tower must be infinitely large. The slope of the **OL** at which the **OL** touches the **VLE**-line represents the limiting liq-gas ratio. Since G is fixed, L_s becomes $L_{s\,min}$ when **OL** touches the **VLE**-line.
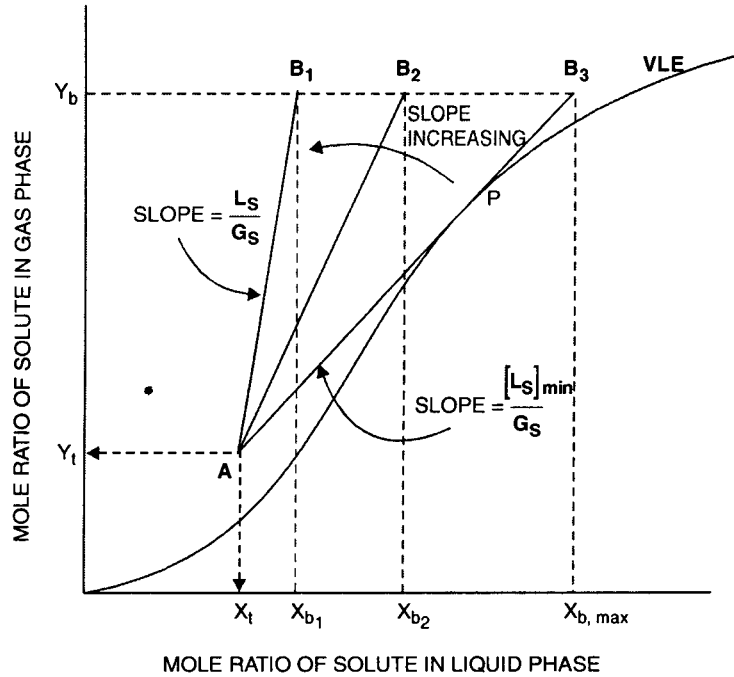
Fig. 1.8.1. *Minimum Liq-Gas Ratio in Absorption.*

Limiting liq-gas ratio, $\left[\dfrac{L_s}{G_s}\right]_{lim} = \dfrac{L_{smin}}{G_s}$

The **VLE**-curve is frequently concave upward [**Figure 1.8.2**]. The liq-gas ratio for such systems is the slope of the operating line (*AC*) passing thru the point *C* that corresponds to an exit-liq concentration in equilibrium with the entering gas.

The rate of flow of absorbent is :

$$L_s = \varphi \cdot L_{s\,min} \qquad ...(1.47)$$

where, φ = excess absorbent coefficient.

The theoretically minimum flowrate of absorbent $L_{s\,min}$ can be determined either graphically [**Figure 1.8.2**] or analytically by the equation :

$$L_{s\,min} = \dfrac{M}{\overline{X}_b^* - \overline{X}_t} \qquad ...(1.48)$$

where, M = molar rate of solute, kmol/(h.m^2)
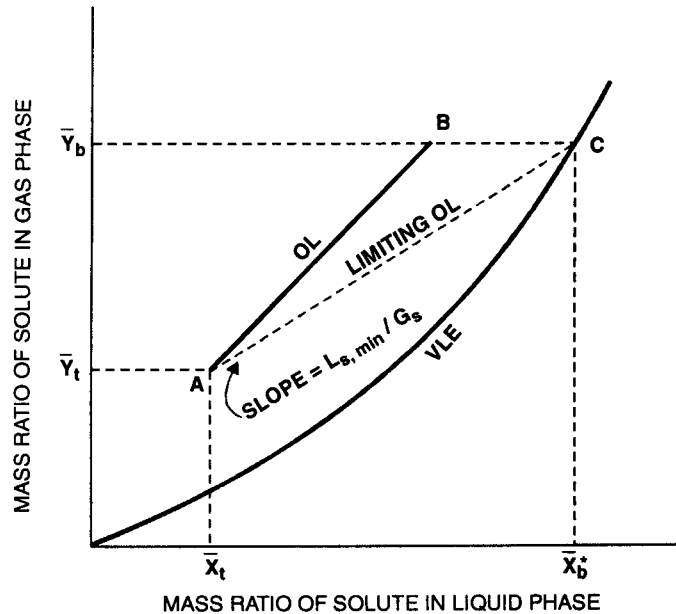
Fig. 1.8.2. *VLE and OLs of A Countercurrent Absorber.*
AB = OL
AC = Limiting OL.

1.9. MATERIAL BALANCE : COCURRENT PROCESS

A **cocurrent absorber**, shown schematically in **Figure 1.9.1** is usually a packed bed absorption tower in which physical transfer of solute takes place from the gas (vap) stream to the liq stream as both the streams flow cocurrently, *i.e.*, in the same direction thru the column.
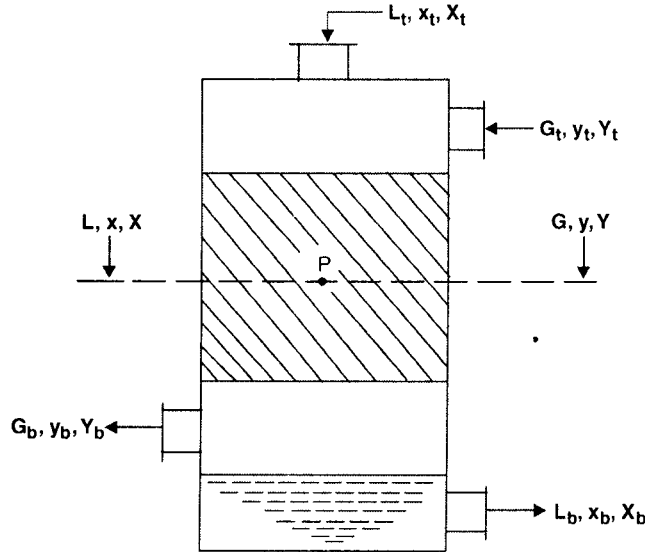
Fig. 1.9.1. *Cocurrent Absorber.*

Overall material balance of the column results :

$$L_t \cdot X_t + G_t \cdot Y_t = L_b \cdot X_b + G_b \cdot Y_b \qquad \qquad ...(1.49)$$

For constant liq and gas flowrates

$$L_s (X_t - X_b) = G_s (Y_b - Y_t) \qquad \qquad ...(1.50)$$

$$\therefore \qquad \qquad \frac{Y_b - Y_t}{X_b - X_t} = -\frac{L_s}{G_s} \qquad \qquad ...(1.51)$$

which represents the **OL** of the cocurrent absorber. Thus when gas and liq streams flow cocurrently, the **OL** has a negative slope $\left[-\dfrac{L_s}{G_s} \right]$.

Since P **(X, Y)** is a point in the packed bed, it will lie on the same operating line which therefore, can be represented as :

$$Y = Y_b - \frac{L_s}{G_s} [X - X_t] \qquad \qquad ...(1.52)$$

Or, $\qquad \qquad Y = Y_t - \dfrac{L_s}{G_s} [X - X_t] \qquad \qquad ...(1.53)$

Cocurrent absorption is used where there is no advantage of countercurrent operation — *i.e.*, if the gas to be absorbed in a scrubbing liquid is a pure substance.

Also it is practised if the physical absorption is followed by a rapid, irreversible chemical reaction of the dissolved solute in the absorbent where only the equivalent of one theoretical stage is required.

Cocurrent flow may be used in those cases where an exceptionally tall tower is built into two sections **[Figure 1.9.2]**—first section is operated in countercurrent flow and the second in cocurrent flow to save on the large-diameter gas pipeline connecting the two columns.
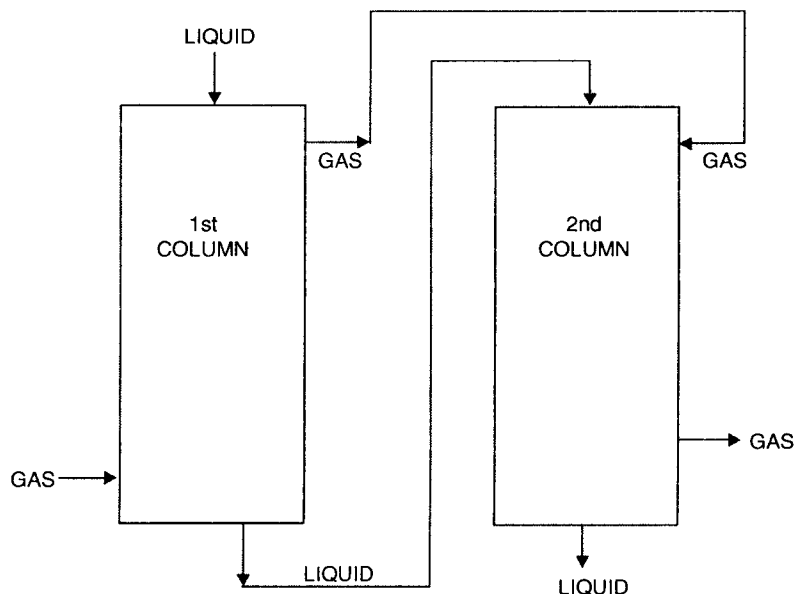
Fig. 1.9.2. *Countercurrent-Cocurrent Arrangement For Very Tall Towers.*

1.10. TRAY TOWERS

Bubblecap trays, valve trays and sieve trays are sometimes used for gas absorption. They are preferred particularly when the load is more than can be handled in packed tower of about 1m dia and when there is any likelihood of plugging of packing due to solids deposition.

Also the plate columns are particulary useful when the liq rate is sufficient to flood a packed tower.

Though the tray towers for absorption are similar in construction to those used in distillation, but they are not same in tray layouts. The ratio of liq/gas flowrates (L_s/G_s) being much greater in the case of absorption than in distillation, the slot area is rather less and the downcomers rather larger for absorption columns.

Tray efficiency ranks lower than that in distillation and usually ranges from 20% to 80%.

1.10.1. Countercurrent Multistage Operation

Tray towers bring about stepwise contact of gas (vap) and liq phases moving countercurrently thru the tower. Hence absorption process conducted in such a system is essentially a countercurrent multistage operation—each tray constitutes a stage, because the gas and liq are brought into intimate contact and separated on each tray.

Though the overall flow schemes of gas and liq phases are countercurrent, they're at crossflow on each individual tray where the exit gas is seldom in equilibrium with liq leaving the tray. Hence for the sake of design and measurement of actual tray performance, regardless of their method of

operation, a **Theoretical (Ideal) Tray** is defined. It is the tray on which the average composition of all the gas leaving the tray is in equilibrium with the average composition of all the liq leaving the tray.
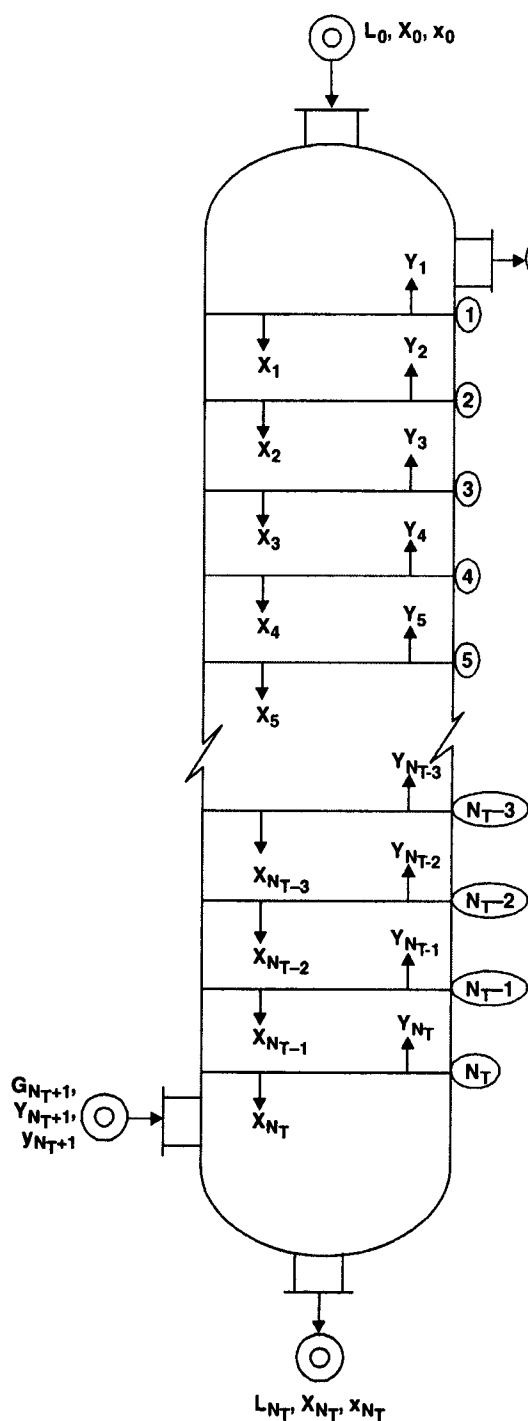
Fig. 1.10.1.1. *Multistage Absorber.*
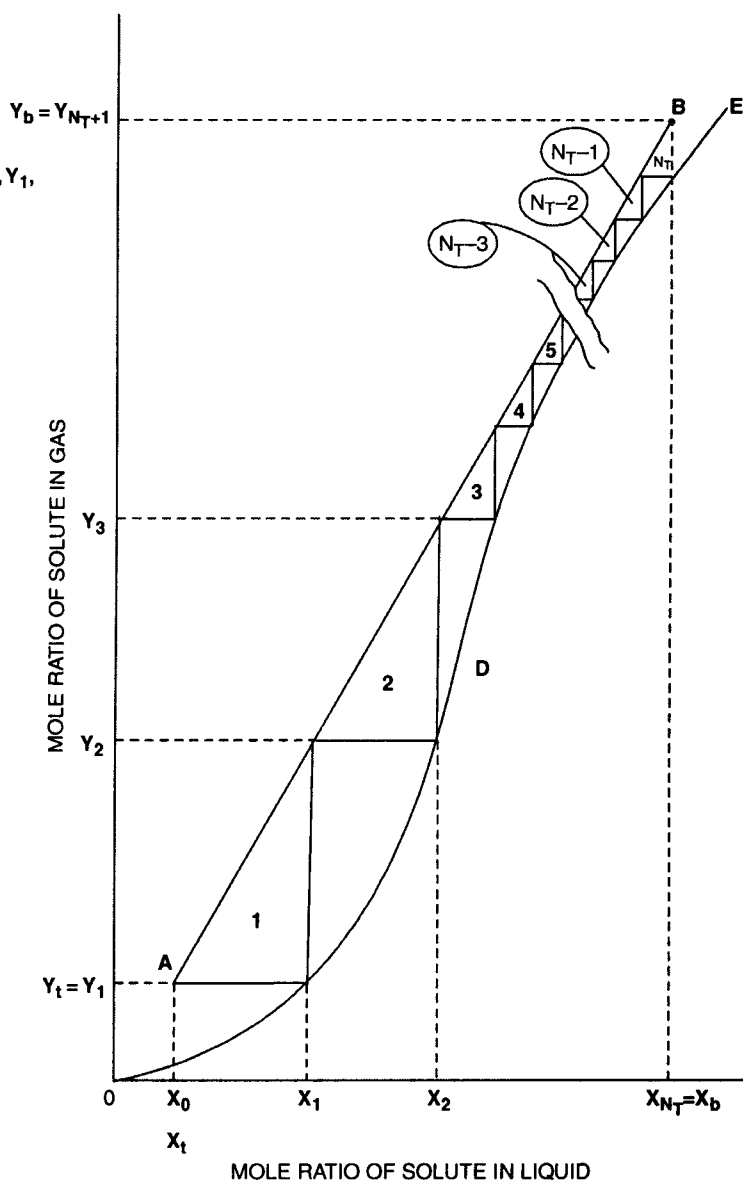
Fig. 1.10.1.2. *Graphical Construction of Theoretical Stages in a Countercurrent Multistage Absorber.*

Figure 1.10.1.1 presents the schematic illustration of an absorber fitted with N_T number of ideal trays.

Figure 1.10.1.2. illustrates how the number of ideal trays required to bring about a specified change in composition of the liq and the gas phase can then be determined graphically.

AB is the **OL** and **ODE** is the **VLE**-line.

A marks the composition of gas and liq streams at absorber top and *B* marks those at the absorber bottom.

A horizontal from *A* upto **VLE**-line and a perpendicular from thereof upto **OL** complete a triangle with the OL-segment. This is the 1st theoretical stage or **ideal stage No. 1** which brings about a change in liq composition from X_0 to X_1 and gas composition from Y_1 to Y_2.

Similarly the ideal stages **2, 3, 4, ...N_T –3, N_T –2, N_T –1, N_T** are constructed

The nearer the **OL** to the **VLE** curve, the more such steps or stages will be required and should the **OL** touch **VLE**-line at any point corresponding to a minimum L_s/G_s ratio, the number of steps will be infinite.

The number of steps can equally be constructed on diagrams plotted in terms of any concentration units viz. mole fractions, partial pressure etc.

1.10.2. Non-Isothermal Operation

Isothermal absorption is rarely met. Absorption dealing with dilute gas mixtures and liquids may approach isothermal condition ; however, in large majority of cases as practically encountered in commercial processes, absorption operations are usually exothermic.

Heat generation in absorption towers is counter-productive :

- The equilibrium solubility of the solute will go down.

- The capacity of the absorber falls and will require larger liq flowrates to compensate and that may invite flooding.

- In case the heat evolution is excessive, cooling coils may be installed in the absorber or the liq is to be removed at intervals, cooled and returned to the absorber.

Therefore, when large quantities of solute gas are absorbed, the thermal factor cannot be ignored.

We can draw up a heat balance for the entire tower **Figure 1.10. 2.1** :
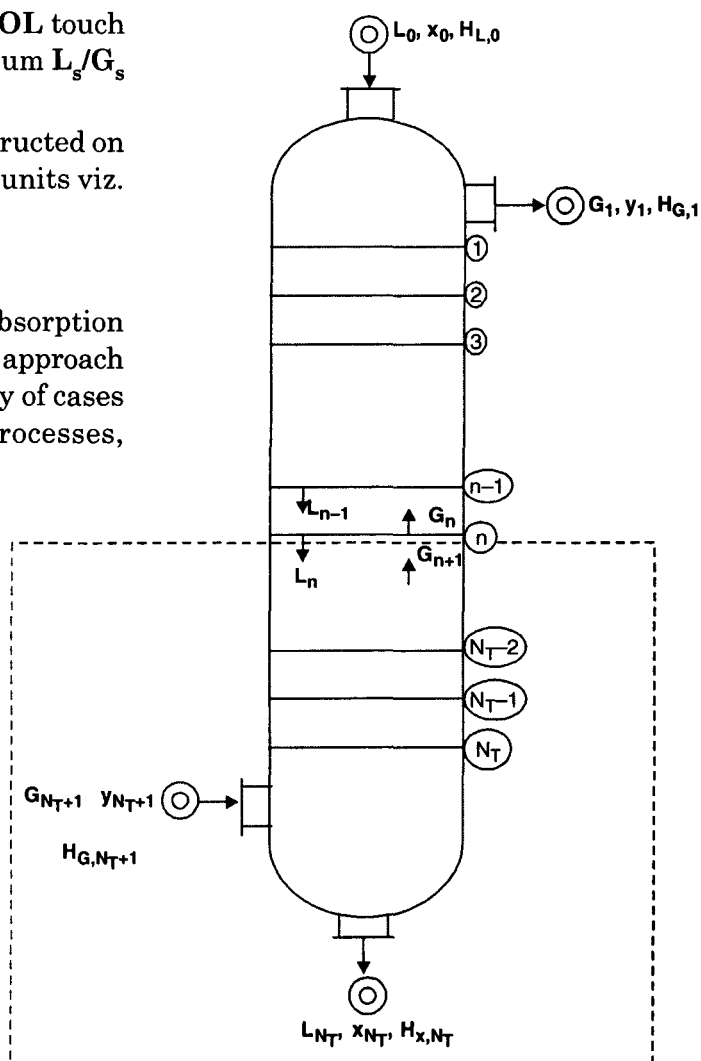
Fig. 1.10. 2.1. *Mass & Energy Balances for A Non-Isothermal Absorption Operation.*

Total heat entering the sytem = Total heat going out of the system

Or,
$$L_O \cdot H_{L,O} + G_{N_T+1} \cdot H_{G,N_T+1}$$
$$= L_{N_T} \cdot H_{L,N_T} + G_1 \cdot H_{G,1} + Q_T \qquad \qquad ...(1.54)$$

where, L = total molar liq rate, kmol/h

G = total molar gas rate, kmol/h

H_G = molar enthalpy of a gas referred to pure substance at some base temperature θ_O, kJ/kmol

H_L = molar enthalpy of a liq solution referred to pure substance at temp. θ_O, kJ/kmol

Q_T = rate of total heat removal from the entire tower, kW

The molar enthalpy of a liq soln., H_L at temperature θ_L and containing x mole fraction of solute is given by

$$H_L = C_L \cdot \Delta\theta + \Delta H_S \qquad \qquad ...(1.55)$$

where, C_L = heat capacity of liq. kJ/(kmol. K)

$\Delta\theta = \theta_L - \theta_O$

ΔH_s = molar enthalpy of mixing, kJ/kmol.

It is negative in case of heat evolution on mixing.

Adiabatic Operation

In case the column is operated adiabatically, the column will receive no heat from any external source nor it will give up any heat to any external agency (*e.g.*, cooling coil) *i.e.*,

$$Q_T = O$$

whereupon the overall enthalpy balance of the column becomes :

$$L_O \cdot H_{L,O} + G_{N_T+1} \cdot H_{G,N_T+1} = L_{N_T} \cdot H_{L,N_T} + G_1 \cdot H_{G,1} \qquad \qquad ...(1.56)$$

However, due to adiabatic operation, the exit streams will leave the absorber at higher temperature than the corresponding inlet streams because of heat generation during absorption and the absence of external cooling system. This rise in temperature reduces the solute solubility for the obvious reason and as a consequence, the value of $[L/G]_{min}$ becomes larger and a far greater number of trays than for isothermal operation is required for the same absorption duty.

Following the principle of an ideal tray*, the tray calculation from the bottom to the top of the column may be performed in the numerical design of such absorbers.

Considering the control volume (the broken-line enclosure)

Total Mass Balance :

$$L_n + G_{N_T+1} = L_{N_T+1} + G_{n+1} \qquad \qquad ...(1.57)$$

Total Solute Balance

$$L_n \cdot x_n + G_{N_T+1} \cdot y_{N_T+1} = L_{N_T} \cdot x_{N_T} + G_{n+1} \cdot y_{n+1} \qquad \qquad ...(1.58)$$

Enthalpy Balance

$$L_n \cdot H_{L,n} + G_{N_T+1} \cdot H_{G,N_T+1} = L_{N_T} \cdot H_{L,N_T} + G_{n+1} \cdot H_{G,n+1} \qquad \qquad ...(1.59)$$

---

*the gas and liq streams leaving the tray are in equilibrium both with respect to composition and temperature.

Design Procedure

Usually the temperature of feed streams L_O & G_{N_T+1} are known.

Exit gas stream G_1 temperature is the same as the top tray temperature θ_t. Assume a suitable value of θ_t.

Exit liq stream L_{N_T} temperature is the same as the bottom tray temperature θ_b.

Solve Eqns. 1.57 and 1.58 to compute L_n and x_n.

Use Eqn. 1.59 to determine the temperature θ_n of liq stream L_n

Stream G_n and stream L_n are at same temperature θ_n and have their composition in equilibrium, since **tray-n** is ideal. Therefore, gas composition y_n gets known.

Harness Eqns. 1.57 to 1.59 this way to perform tray by tray calculation up the column till **tray-1** is reached & θ_1 is calculated.

Check whether $\theta_1 = \theta_t$ (assumed). If not, repeat the calculations till θ_1 converges on θ_t.

Use Eqn. 1.54 to compute θ_b, the temperature of the liq leaving at the bottom of the column.

1.10.3. Absorption Factor

The absorption factor is the fraction of the kmol of solute or mass of solute absorbed :

$$e_a = \frac{\overline{Y}_b - \overline{Y}_t}{\overline{Y}_b} = \frac{Y_b - Y_t}{Y_b} \qquad \qquad ...(1.60)$$

where e_a = **absorption factor** also called **extraction factor**
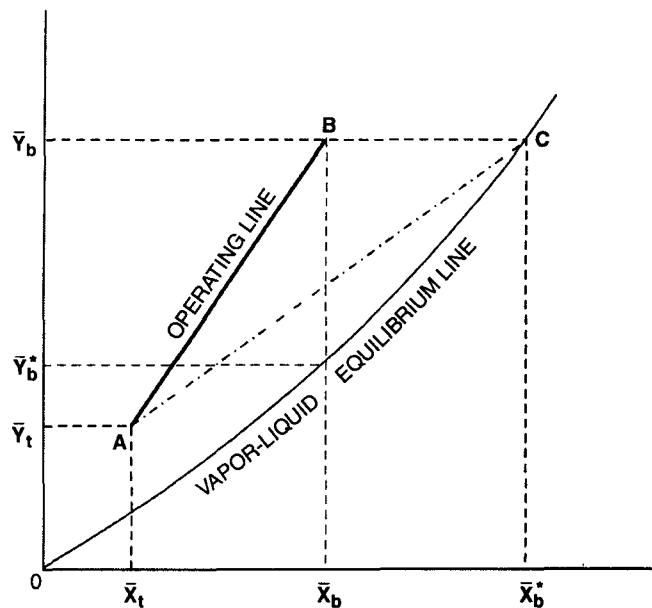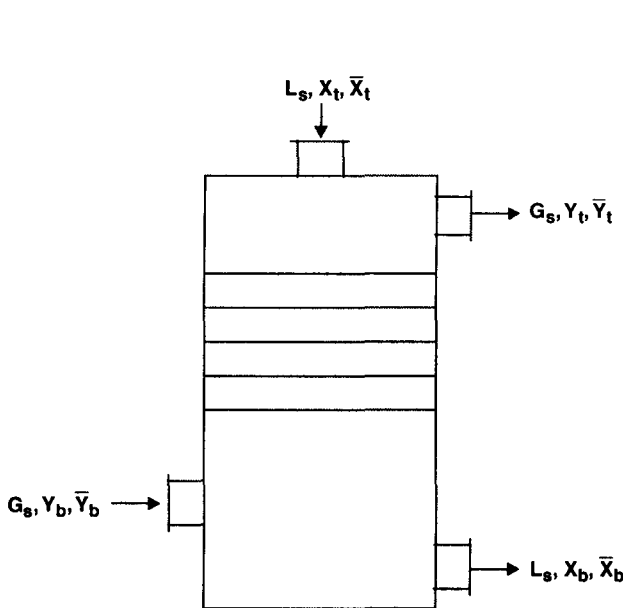
Fig. 1.10.3.1. *Schematic Diagram of An Absorber.*

Fig. 1.10.3.2. *OL and VLE-Line of An Absorber.*

$\overline{Y}_b$ = mass fraction of solute in the inlet stream

$\overline{Y}_t$ = mass fraction of solute in the exit stream

Y_b = mol fraction of solute in the inlet stream

Y_t = mol fraction of solute in the exit stream

The absorption factor is also defined by the ratio of the slope of the operating line **(OL)** to that of the vapor-liq equilibrium **(VLE)** line :

$$e_a = \frac{L_s / G_s}{m} = \frac{L_s}{m.G_s} \qquad \qquad ...(1.61)$$

For $e_a < 1$ The **OL** and **VLE** curve converge for the bottom of the absorber, *i.e.*, *AB* falls upon *AC* **[Figure 1.10.3.2]**. L becomes L_{min} and infinite number of theoretical trays are required even for fractional solute absorption.

For $e_a > 1$ No absorption limitation.

         Any degree of absorption is possible if sufficient trays are provided.

1.10.4. Number of Trays by Use of Absorption Factor

The number of theoretical trays (plates) required for a given degree of absorption can be conveniently determined as follows.

Overall gas and liquid rates vary thruout the column as the solute is transferred from gas to liq stream. However, the solute-free gas rate (*i.e.*, the flowrate of inert gas which is negligibly soluble in the solvent) remains constant thruout the column, *i.e.*,

$$G_{s,1} = G_{s,2} = G_{s,3} = ... = G_s$$

Likewise, on solute-free basis the flowrate of solvent (which is very little evaporated) remains practically constant all thru, *i.e.*,

$$L_{s,1} = L_{s,2} = L_{s,3} = ... = L_s$$

The material balance around the **n-th tray** of the absorption column **Figure 1.10.4.1** gives :

$$L_s . x_{n-1} + G_s . y_{n+1} = L_s . x_n + G_s . y_n$$

Or, $\dfrac{L_s}{G_s} = \dfrac{y_{n+1} - y_n}{x_n - x_{n-1}}$ ...(1.62)

Taking all the plates to be ideal :

$$y_n = m . x_n$$

$$y_{n-1} = m . x_{n-1}$$

where, **m** = slope of the **VLE** curve whose eqn. is **y* = m.x**

Combining these eqns. with the Eqn. 1.62 we get :

$$\frac{L_s}{m.G_s} = \frac{y_{n+1} - y_n}{y_n - y_{n-1}}$$

Or, $e_a = \dfrac{y_{n+1} - y_n}{y_n - y_{n-1}}$

$\therefore$ $y_n = \dfrac{y_{n+1} + e_a . y_{n-1}}{1 + e_a}$ ...(1.63)
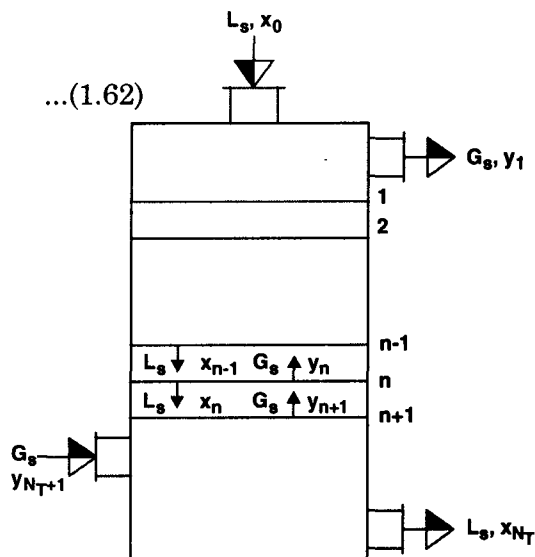
Fig. 1.10.4.1.

Substituting **n = 1, 2, 3, ...etc.** in Eqn. 1.63 we get for

Top Tray
$$y_1 = \frac{y_2 + e_a \cdot y_o}{1 + e_a}$$

2nd Tray From Top
$$y_2 = \frac{y_3 + e_a \cdot y_1}{1 + e_a}$$

$$= \frac{(1 + e_a) \cdot y_3 + e_a \cdot y_2 + e_a^2 \cdot y_o}{(1 + e_a)^2}$$

Or, $(1 + e_a)^2 \cdot y_2 - e_a \cdot y_2 = (1 + e_a) \cdot y_3 + e_a^2 \cdot y_o$

$\therefore$
$$y_2 = \frac{(1 + e_a) \cdot y_3 + e_a^2 \cdot y_o}{e_a^2 + e_a + 1}$$

3rd Tray From Top
$$y_3 = \frac{(1 + e_a + e_a^2) \cdot y_4 + e_a^3 \cdot y_o}{e_a^3 + e_a^2 + e_a + 1}$$

Now, $1 + e_a + e_a^2$ is in Geometric Progression

$\therefore$
$$\sum = 1 \cdot \frac{[e_a^3 - 1]}{[e_a - 1]}$$

Also, $1 + e_a + e_a^2 + e_a^3$ is in G.P.

$\therefore$
$$\sum = 1 \cdot \frac{[e_a^4 - 1]}{[e_a - 1]}$$

$\therefore$
$$y_3 = \frac{(e_a^3 - 1) \cdot y_4 + e_a^3 (e_a - 1) \cdot y_o}{e_a^4 - 1}$$

Therefore, for n-th tray

$$y_n = \frac{(e_a^n - 1) \cdot y_{n+1} + e_a^n (e_a - 1) \cdot y_o}{e_a^{n+1} - 1}$$

Since $y_n = m.x_n$,

$$x_n = \frac{(e_a^n - 1) \cdot y_{n+1} + e_a^n \cdot (e_a - 1) \cdot y_o}{m \cdot (e_a^{n+1} - 1)}$$

The material balance from the top to the n-th tray of the column **(Figure 1.10.4.2)** yields :

$$L_s \cdot x_n - L_s \cdot x_o = G_s \cdot y_{n+1} - G_s \cdot y_1$$

or,
$$\frac{L_s}{G_s} \cdot (x_n - x_o) = y_{n+1} - y_1$$

$$\boxed{\begin{array}{l} \text{cf. } a + ar + ar^2 + \ldots\ldots + ar^n \text{ is in G.P.} \\[2mm] S = a \cdot \frac{(r^n - 1)}{r - 1} \end{array}}$$
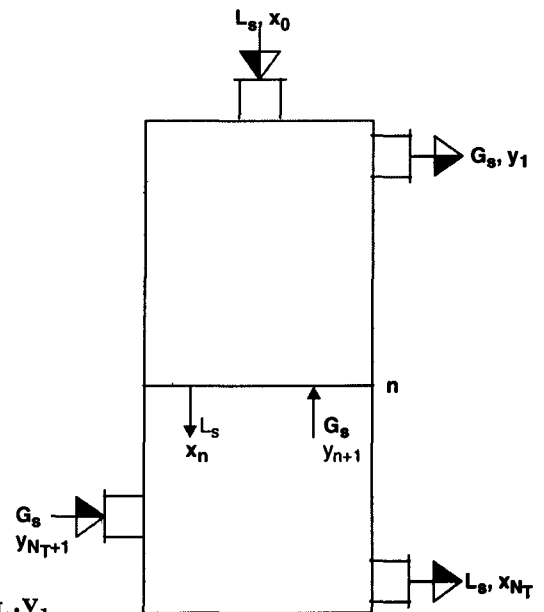
Fig. 1.10.4.2

or, $$\frac{L_s}{m.G_s} \cdot (m.x_n - m.x_0) = y_{n+1} - y_1$$

or, $$e_a (y_n - y_0) = y_{n+1} - y_1$$

$\therefore$ $$\frac{y_{n+1} - y_1 + e_a \cdot y_0}{e_a} = y_n = \frac{(e_a^n - 1) \cdot y_{n+1} + e_a^n \cdot (e_a - 1) \cdot y_0}{e_a^{n+1} - 1}$$

$\therefore$ $$y_1 = y_{n+1} \cdot \left[\frac{e_a - 1}{e_a^{n+1} - 1} \right] + y_0 \cdot \left[\frac{e_a^{n+1} - e_a}{e_a^{n+1} - 1} \right]$$

Now, $$\frac{e_a - 1}{e_a^{n+1} - 1} = 1 - \left[\frac{e_a^{n+1} - e_a}{e_a^{n+1} - 1} \right]$$

$\therefore$ $$y_1 = y_{n+1} + (y_0 - y_{n+1}) \left[\frac{e_a^{n+1} - e_a}{e_a^{n+1} - 1} \right]$$

$\therefore$ $$\frac{y_{n+1} - y_1}{y_{n+1} - y_0} = \frac{e_a^{n+1} - e_a}{e_a^{n+1} - 1} \qquad \qquad ...(1.64)$$

where, $y_{n+1} - y_1$ = actual change in gas composition.

$y_{n+1} - y_0$ = maximum possible change in gas composition, *i.e.*, if the gas leaving the absorber is in equilibrium with entering liquid.

Putting $n = N_T$, the total number of trays, the Eqn. 1.64 yields :

$$\frac{y_{N_T+1} - y_1}{y_{N_T+1} - y_0} = \frac{e_a^{N_T+1} - e_a}{e_a^{N_T+1} - 1}$$

Solving for N_T we get :

$$N_T = \frac{\log\left(\frac{y_{N_T+1} - m.x_0}{y_1 - m.x_0} \left(1 - \frac{1}{e_a} \right) + \frac{1}{e_a} \right)}{\log e_a} \qquad \qquad ...(1.65)$$

Expressed in mole ratio terms, Eqn. 1.65 transforms to : $\boxed{\text{cf. } y_0 = m.x_0}$

$$N_T = \frac{\log\left(\frac{Y_{N_T+1} - m.X_0}{Y_1 - m.X_0} \left(1 - \frac{1}{e_a} \right) + \frac{1}{e_a} \right)}{\log e_a} \qquad \qquad ...(1.65\ A)$$

1.10.5. Real Trays & Tray Efficiency

The number of real trays, *i.e.*, the number of actual plates to be insalled in an absorption column for a specific absorption duty can be determined by the efficiency.

Three kinds of efficiencies have been distinguished :

- **Local or Point Efficiency,** η_o
- **Plate Efficiency,** η_p
- **Overall Efficiency,** η

Point Efficiency (η_o) is the ratio of the change in vapor or liq composition effected at a given point on a real, (*i.e.*, actual) plate to that effected by an ideal, (*i.e.*, theoretical) plate at the same point :

$$\eta_{o,\,y} = \frac{y_n - y_{n+1}}{y_n^* - y_{n+1}} \qquad ...(1.66)$$

and   (Refer **Fig. 1.10.5.1**)

$$\eta_{o,\,x} = \frac{x_{n-1} - x_n}{x_{n-1} - x_n^*} \qquad ...(1.67)$$
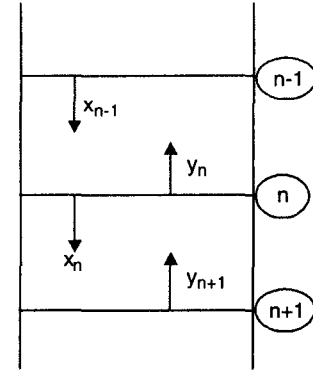
Fig. 1.10.5.1. *Determining Plate Efficiency & Point Efficiency*

where, y_{n+1} = composition of the vap stream reaching the **n**-th plate at the given point.

y_n = composition of the two vapor stream leaving the **n**-th plate.

y_n^* = vapor composition in equilibrium with the liq at the given point on plate **n**.

x_n = composition of the liquid stream leaving at the given point from the plate **n**.

x_{n-1} = composition of the liquid stream reaching the given point on the **n**-th plate

x_n^* = liquid composition in equilibrium with the vapor at the given point on plate **n**.

Therefore,

$y_n - y_{n+1}$ = change in vap composition effected at the given point by the **n**-th actual plate.

$y_n^* - y_{n+1}$ = change in vap composition effected at the given point by the **n**-th theoretical plate.

Similarly,

$x_{n-1} - x_n$ = change in liq composition effected at the given point by the **n**-th actual plate.

$x_{n-1} - x_n^*$ = change in liq composition effected at the given point by the **n**-th theoretical plate.

Plate Efficiency $\left(\eta_p\right)$, also known as **Murphee Efficiency** (η_M) is the ratio of the change in mean composition of vapor or liquid on the actual plate to the change in composition at equilibrium on the same plate :

$$\eta_{p,\,y} = \frac{\dot{y}_n - \dot{y}_{n+1}}{y_n^* - \dot{y}_{n+1}} \qquad ...(1.68)$$

$$h_{p,\,x} = \frac{x_{n-1} - x_n}{x_{n-1} - x_n^*} \qquad ...(1.69)$$

where, $\dot{y}_n$ = mean composition of the vapor stream rising from the **n**-th plate

$\dot{y}_{n+1}$ = mean composition of the vapor stream reaching the **n**-th plate from the tray below.

y_n^* = composition of the vapor in equilibrium with the liquid leaving the **n**-th plate.

The point & plate efficiencies are used to evaluate the effectiveness of a plate. They represent the ratio of driving force and the real plate to that on the ideal plate :

$$\eta_o = \frac{\text{Driving force at a given point on the n-th real plate}}{\text{Driving force at the same point on the n-th ideal plate}}$$

$$\eta_p \quad \text{or,} \quad \eta_M = \frac{\text{Driving force on the n-th real plate}}{\text{Driving force on the n-th ideal plate}}$$

Overall Tray Efficiency (η) : is the efficiency of the entire column (η). It is defined as **the ratio of the number of theoretical trays (No. of ideal trays) to the number of actual trays (No. of real trays) required to perform the same absorption duty under the same operating conditions :**

$$\eta = \frac{n}{n_a} \qquad \qquad ...(1.70)$$

where, n = number of ideal trays required.

         n_a = number of actual trays required.

The overall tray efficiency presupposes :

- Plate efficiency (Murphree efficiency) is constant for all trays.

- OL is a straight line and so is the **VLE**-line.

- Henry's Law is obeyed.

- Operating conditions being isothermal.

- System involves dilute solutions.

The overall tray efficiency can be computed analytically :

$$\eta = \frac{\log\left(1 + \eta_{M,E}\left(\dfrac{1}{e_a} - 1\right)\right)}{\log\left(\dfrac{1}{e_a}\right)} \qquad ...(1.71)$$

where, $\eta_{M,\psi}$ = Murphree efficiency corrected for entrainment. Its value for the bottom tray is given by [see **figure 1.10.5.2**]

$$\left[\eta_{M,\psi}\right]_G = \frac{AB}{AC}$$

$$\left[\eta_{M,\psi}\right]_L = \frac{DB}{DE}$$

Fig. 1.10.5.2. *Use of Murphree Efficiencies in the Computation of the Number of Real Trays in an Absorber.*

The dotted line represents the real effluent (vap & liq) conditions from the trays, for instance while *AC* represents the change in vapor compositions effected by the theoretical bottom plate, *AB* represents the actual change in vapor composition as effected by the real bottom plate. Similarly, *BD* refers to the change in liq composition effected by the actual bottom plate.

Thus the actual VLE-curve (dotted line) is used, instead of the theoretical VLE-curve, to compute the stepwise stage construction, which now provides the number of real trays.

1.11. PACKED BED ABSORBER

Packed columns are most widely used for gas absorption applications. And most frequently the flow arrangements are countercurrent, *i.e.*, the gas and liq streams traffic countercurrent thru packed bed.

Countercurrent packed towers bring about continuous contact of gas and liq streams sharing the same flowpath in the packing. And as a consequence, the gas and liq compositions change continuously with the height of packing.

The gas pressure drop across the packed bed should be properly controlled and it should not be so high that the tower reaches flooding conditions during operation. That is the column must operate over a definite range of gas and liq rates so that the column does not flood with load variations.

Over and above, the column is operated at a sufficiently high liq rate in order to attain satisfactory wetting of the packing. Low liq rates entail the risk of partial wetting of packing surface, which means reduction in gas-liq contact resulting in loss in both tower capacity and packing efficiency. However, in some cases the difficulty of wetting can be overcome thru considerable recirculation of the liq over the tower. Also it can be drastically improved by using high performance dumped packing (viz, Norton's IMTP packing, KOCH's Flexirings, GLITSCH's Cascade Mini Rings) and modern structured packing (viz, Sulzer's Mellapak, Norton's Intalox structured packing, KOCH's flexipac) in combination with efficient liquid distributor.

In selecting the packing, efforts should be directed to choose the form that will give rise to as near complete wetting of the packing as possible.

Packed towers offer certain distinct advantages :

1. Eminently suitable for vacuum service.

Packed towers can frequently be designed to register a much lower ΔP thru the packed bed than for a plate column & still ensuring adequate gas-liq contact.

2. Foaming service.

Packed towers can handle foaming liquids more satisfactorily.

3. Low liquid holdup.

Geometries of modern packings beget good drainage capacity and that means much less liq holdup, so that heat-sensitive materials, together with those absorption processes that may have undesirable side reactions may be better handled.

4. Simpler and cheaper construction.

Packed bed absorbers lend to more constructional simplicity and economy than tray towers when the absorption system is corrosive to normal materials of construction.

5. Economy.

For small columns with dia 600mm, packed towers have been found to be more economic than tray towers.

1.11.1. Absorption in Packed Bed

The rate of mass transfer in a packed bed absorber is given by :

$$N = A \cdot Z \cdot k_{G,P} \cdot a \cdot (p - p_i) \qquad \qquad ...(1.72)$$

where, N = rate of soluble transfer, kmol/h.

A = column cross-sectional area, m^2.

Z = packed bed depth, m.

a = interfacial area, m^2/m^3.

p = partial pressure of the solute in the bulk gas phase, Pa.

p_i = partial pressure of the solute in the gas film at the interface, Pa.

The interfacial area is the actual mass transfer area between liq and gas phases. This area is not necessarily the same as the geometrical surface area of the tower packing. The product : **a × AZ** represents the total interfacial area within the entire packed bed.

If the driving force of absorption process is expressed with respect to the liquid phase ($\Delta x = x_i$ − **x**), the mass transfer expression becomes :

$$N = A \bullet Z \bullet k_{L,x} \bullet a \bullet (x_i - x) \qquad \qquad ...(1.73)$$

where, $x_i - x$ = driving force across the liq film for absorption

In the steady-state process, the rate of solute diffusing thru the gas film equals its rate of diffusion across the liq film, so

$$N = A \bullet Z \bullet k_{G,p} \bullet a \bullet (p - p_i) = A \bullet Z \bullet k_{L,x} \bullet a \bullet (x_i - x) \qquad ...(1.74)$$

$$\therefore \qquad \frac{k_{L,x}}{k_{G,p}} = \frac{p - p_i}{x_i - x} = \text{ratio of driving forces in gas phase to liq phase.}$$

The values of x_i and p_i are difficult to determine in practical cases, so is the value of **a** which may vary with the flowrates of the two phases. Hence it is convenient to adopt the overall terms :

$$N = A \bullet Z \bullet K_{G,p} \bullet a \bullet (p - p^*) \qquad \qquad ...(1.75)$$

<div align="right">for mass transfer in gas phase</div>

and

$$N = A \bullet Z \bullet K_{L,x} \bullet a \bullet (x^* - x) \qquad \qquad ...(1.76)$$

<div align="right">for mass transfer in liq phase</div>

where, $K_{G,p} \bullet a$ = overall volumetric coefficient [also called overall gas phase mass transfer coefficient in terms of partial pressure], kmol/(h.m^3. Pa)

$K_{L,x} \bullet a$ = overall volumetric coefficient [also called overall liq phase mass transfer coefficient in terms of mol fraction], kmol/(h.m^3. kmol/kmol)

Hence for steady-state physical transfer of solute from gas phase to liq phase :

$$N = A \bullet Z \bullet K_{G,p} \bullet a \bullet (p - p^*) \qquad N = A \bullet Z \bullet K_{L,x} \bullet a \bullet (x^* - x) \qquad ...(1.77)$$

$$\text{or,} \qquad \frac{K_{L,x}}{K_{G,p}} = \frac{p - p^*}{x^* - x} \qquad \qquad ...(1.78)$$

The interfacial area **a** should not be confused with the geometric surface area of the absorber packing. Interfacial area is not directly related to the wetted area of packing [H.L. Shulman *et. al.* — *American Institute of Chemical Engineers Journal, Vol. 6 (1) 1960].* For instance, metal Pall rings exhibit a substantially high mass transfer coefficient compared to metal Raschig rings yet both packings sport same surface area for the same size packing.

For absorption operation, it is customary to use $K_G \bullet a$ values since absorber design calculations are usually made from the compositions of the gas phase. The overall mass transfer coefficients for absorption are considered to be a function of gas & liq flowrates :

$$K_G \cdot a = \psi \cdot [L']^b \cdot [G']^c \qquad \qquad ...(1.79)$$

where ψ = proportionality constant

L' = liq mass flux, kg/(h.m^2)

G' = gas mass flux, kg/(h.m^2)

b & c are exponents whose values are given the below **(Table 1.11.1.1)**

Table 1.11.1.1. Values of Exponents b & c for Random Packings

Controlling Phase	b	c
Liq-film controlled	0.22 — 0.38 (0.3 in absence of data)	0.06 — 0.08
Gas-film controlled	0.22 — 0.38	0.67 — 0.80

For liq-film-controlled absorption processes, the value of $K_G \cdot a$ is chiefly determined by the liq flowrate. However, in gas-film-controlled systems, the value of $K_G \cdot a$ is a function of both the liq and gas flowrates. It should be noted that the value of $K_G \cdot a$ in gas-film-controlled systems is much greater than that in liq-film-controlled systems. This is because, the liq-film resistance in liq-film-controlled processes reduces the value of overall mass transfer coefficient while it has only a small effect on overall coefficient in gas-film controlled processes.

1.11.2. Advantages of High Performance Structured Packing in Absorption Columns

The structured packings with well-established performance, viz. Sulzer's **Mellapak**, Norton's **IMTP-T** series, Koch's **Flexipac**. etc. give rise to :

1. **Low Pressure Losses :** Small fans and compressors with efficient intake stages will be sufficient to ensure appropriate gas loading. That means lower utility (electricity & cooling water) costs.

2. **Lower Liquid Loads :** Very high wettability of packing's surface requires only a small liq loads to gas-liq contacting. Therefore smaller liq flows save pumping and processing costs.

3. **Compact Columns :** These high efficiency packings permit high gas and liq thruputs, resulting in smaller column diameters (important for pressurized columns or upgrading existing columns). Because of the high separation capacities of structured packings, only a small height of packing is just sufficient to ensure desired separation duty and that reduces the column height.

4. **Low Weight :** These structured packings are generally lighter than comparable tray columns. This is particularly important for offshore applications.

5. **Flexibility :** Performance remains unaffected despite extreme input fluctuations.

6. **Insensitive to Dirt & Fouling :** Structured packings are less sensitive to dirt or foaming than random packings or trays. This allows absorption process applicable to those systems that involve solids suspension.

7. **Up-Grading of Existing Columns :** The structured packings can considerably improve separation, increase thruput & reduce pressure losses in existing columns. These plus points make column revamping with structured packing a very rewarding and more cost-effective solution than installing a second column.

8. **Scale Up :** Pilot test results on structured packings can be scaled up to full-size plants reliably & without difficulty.

1.11.3. Height of Transfer Units & Number of Transfer Units

The driving force behind mass transfer in absorption process can be expressed by a term known as Height of Transfer Units (HTU). The entire packed bed may be visulized as the sum of a number of identical transfer units thru which the mass is transported. The height of each such transfer units is called the height of transfer unit.

> This term has been coined by Chilton & Colburn *[Industrial & Engineering Chemistry, Vol. 27/1935]* to define a nearly constant quantity obtained by dividing the flowrate of solute in liq or gas phase by the volumetric mass transfer coefficient in that phase. The mass transfer coefficients vary with the flowrates, but HTU remains nearly constant.

Consider a packed be absorber (**Figure 1.11.3.1**) of area of cross-section A. Liq and gas traffic countercurrent thru the column with constant flowrates : L_s & G_s.

where L_s & G_s are liq and gas molar velocity on solute-free basis, kmol/(h·m²).

Mass balance over a packed bed height dZ yields :

$$A.L.\left[(x+dx)-x\right] = A.G.\left[(y-dy)-y\right]$$

or, $$A.L.\ dx = -\ A.G.\ dy = N$$ ...(1.80)

where, L = liq rate across the elementary bed depth **dZ**, kmol/(h.m²)

G = gas rate across the elementary bed depth **dZ**, kmol/(h.m²)

N = rate of solute transfer, kmol/h.

Because of continuous mass transfer in packed bed absorber, the gas & liq rates vary thruout the column; however L_s and G_s remain essentially constant foramuch as the carrier gas (inert gas) is practically insoluble in the solvent and a very little of solvent vaporizes into the gas stream.

Again, the rate of mass transfer in a packed bed absorber is given by :

$$N = A.K_{G,y}.a.(y-y^*).dZ = A.K_{L,x}.a.(x^*-x).dZ \qquad ...(1.81)$$

where, $y - y^*$ = driving force in the gas phase

$x^* - x$ = driving force in the liq phase

a = interfacial area, m²/m³

$K_{G,y}$ = overall gas phase mass transfer coefficient, kmol/ (h.m². driving force)

$K_{L,x}$ = overall liq phase mass transfer coefficient, kmol/ (h.m². driving force)

Combining Eqns. 1.80 we get :
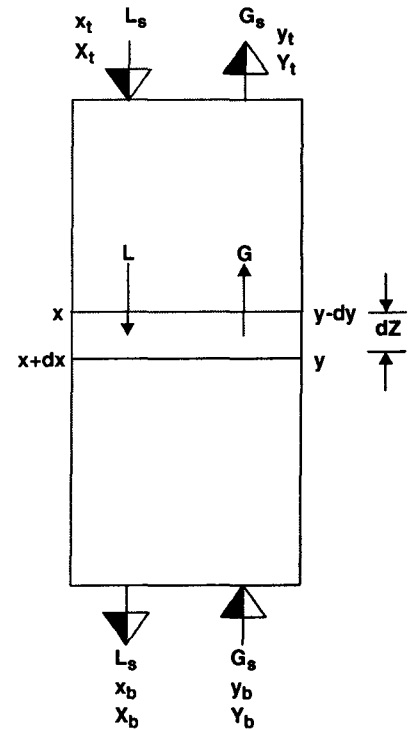
Fig. 1.11.3.1. *Countercurrent Absorber.*

$$dZ = -\ \frac{G}{K_{G,y}.a}.\frac{dy}{y-y^*} \qquad\qquad ...(1.82)$$

$$dZ = \frac{L}{K_{L,x} \cdot a} \cdot \frac{dx}{x^* - x} \qquad ...(1.83)$$

Assuming $G/[K_{G,y} \cdot a]$ and $L/[K_{L,x} \cdot a]$ constant*, upon integration, we get the height of contact zone, *i.e.*, height of the packed bed

$$Z = \frac{G}{K_{G,y} \cdot a} \cdot \int_{y_b}^{y_t} - \frac{dy}{y - y^*} = \frac{G}{K_{G,y} \cdot a} \cdot \int_{y_t}^{y_b} \frac{dy}{y - y^*} \qquad ...(1.84)$$

$$Z = \frac{L}{K_{L,x} \cdot a} \cdot \int_{x_t}^{x_b} \frac{dx}{x^* - x} \qquad ...(1.85)$$

The terms $\dfrac{G}{K_{G,y} \cdot a}$ & $\dfrac{L}{K_{L,x} \cdot a}$ have the dimension of height. They are called **Height of Transfer Unit.**

$$[HTU]_G = \frac{G}{K_{G,y} \cdot a} \qquad ...(1.86)$$

$$[HTU]_L = \frac{L}{K_{L,x} \cdot a} \qquad ...(1.87)$$

The height of one transfer unit expresses the height of packed bed required to carry out a separation of standard difficulty [Perry & Chilton (Eds.) — **Chemical Engineer's Handbook, McGraw-Hill Co., 5th edition**].

The limits of integration of the Eqns. 1.84 & 1.85 are the initial & final concentrations of the gas & liq streams.

The integrals $\int \dfrac{dy}{y - y^*}$ and $\int \dfrac{dx}{x^* - x}$ are dimensionless quantities. They are called the **Number of Transfer Units (NTU)** :

$$[NTU]_G = \int_{y_t}^{y_b} \frac{dy}{y - y^*} \qquad ...(1.88)$$

$$[NTU]_G = \int_{x_t}^{x_b} \frac{dx}{x^* - x} \qquad ...(1.89)$$

The number of transfer units required for a given separation is closely related to the number of theoretical plates or stages required to accomplish the same separation in plate towers.

The ratio $G/[K_{G,y} \cdot a]$ or, $L/[K_{L,x} \cdot a]$ is very much more constant than G, L, $K_{G,y}$ or $K_{L,x}$ which vary thruout the packed height. Hence, advantage is taken out of the fact that these ratios may be considered constant in many cases within the accuracy of the available data.

Height of transfer units (HTU) *multiplied by the number of transfer units* (NTU) *yields the height of the packed bed :*

$$Z = [HTU]_G \cdot [NTU]_G = [HTU]_L \cdot [NTU]_L \qquad ...(1.90)$$

1.11.3.1. HTU & NTU Based on Gas Film

Consider mass transfer over an elemental height **dZ** of a packed bed in a countercurrent absorber [Figure 11.3.1-1].

the mols of solute		the mols of solute
leaving gas phase	=	diffusing into the liq phase

$$i.e., \text{A.G}_s \cdot dY \qquad = \qquad A.\, L_s \cdot dX \qquad ...(1.91)$$

where, **A** = area of cross-section of packed bed, m^2

G_S = molar flux of solute-free gas, $\dfrac{\text{kmols of solute - free gas}}{h.\,m^2}$

L_S = molar flux of solute-free solvent,

$$\dfrac{\text{kmols of solute - free solvent}}{h.\,m^2}$$

Y = mole ratio of solute in gas phase

$$= \left(\dfrac{\text{Mols of solute}}{\text{Mols of solute - free gas}} \right) \text{in gas phase}$$

X = mole ratio of solute in liq phase

$$= \left(\dfrac{\text{Mols of solute}}{\text{Mols of solute - free solvent}} \right) \text{in liq phase}$$

Fig. 1.11.3.1-1. *Countercurrent Absorber.*

Again due to diffusional mass transfer across the gas-film in the gas-liq interface,

$$A.G_s \cdot dY = N = A.k_{G,p} \cdot a.(p - p_i).dZ \qquad ...(1.92)$$

where, $k_{G,p}$ = gas-film mass transfer coefficient on the basis of partial pressure, $kmol/(h.m^2 . Pa)$.

But,
$$p = \dfrac{Y}{1+Y}.P$$

$\therefore$
$$A.\, G_s \cdot dY = A.\, k_{G,p} \cdot a.P \left(\dfrac{Y}{1+Y} - \dfrac{Y_i}{1+Y_i} \right) \cdot dZ$$

or,
$$G_s.dY = k_{G,p} \cdot a.P. \left(\dfrac{Y - Y_i}{(1+Y)(1+Y_i)} \right) \cdot dZ$$

Therefore, the packed bed height **Z** required to achieve a change in **Y** from Y_b at the bottom to Y_t at the top of the bed is given by :

$$\int_0^Z dZ = \dfrac{G_s}{k_{G,p} \cdot a.P} \cdot \int_{Y_t}^{Y_b} \dfrac{(1+Y)(1+Y_i)}{Y - Y_i} \bullet dY \qquad ...(1.93)$$

or,
$$Z = [HTU]_{i,\,G} \cdot [NTU]_{i,\,G} \qquad ...(1.94)$$

where, $[HTU]_{i,G} = \dfrac{G_s}{k_{G,p} \cdot a \cdot P}$ = height of a transfer unit based on gas film, m

$$[NTU]_{i,G} = \int_{Y_t}^{Y_b} \frac{(1+Y)(1+Y_i)}{Y - Y_i} \cdot dY = \text{number of transfer units based on gas film} \qquad ...(1.96)$$

For weak gas mixtures, Eqn. 1.93 simplifies down to :

$$\int_0^Z dZ = \frac{G_s}{k_{G,p} \cdot a \cdot P} \cdot \int_{Y_t}^{Y_b} \frac{dY}{Y - Y_i} \qquad ...(1.97)$$

1.11.3.2. HTU & NTU Based on Liq Film

A similar analysis can be made on the basis of liq film :

$$A. \, G_s \cdot dY = A. \, L_s \cdot dX = A. \, k_{L,c} \cdot a \cdot (c_i - c) \cdot dZ \qquad ...(1.98)$$

Refer to Figure 1.11.3.1-1.

where, $k_{L,c}$ = liq-film mass transfer coefficient on the basis of concentration driving force, kmol/ $(h \cdot m^2 \cdot kmol/m^3)$

Again, X = mole ratio of solute in liq phase

$$= \frac{c}{c_T - c}$$

where, c = mols of solute per unit vol. of liq kmol/m^3

c_T = total mols of solute + solvent per unit vol. of liq, kmol/m^3

$\therefore \qquad c = \dfrac{X}{1 + X} \cdot c_T \qquad ...(1.99)$

$\therefore \qquad L_s \cdot dX = k_{L,c} \cdot a \cdot c_T \cdot \left(\dfrac{X_i}{1 + X_i} - \dfrac{X}{1 + X} \right) \cdot dZ$

$$= k_{L,c} \cdot a \cdot c_T \cdot \left(\frac{X_i - X}{(1 + X_i)(1 + X)} \right) \cdot dZ$$

$\therefore \qquad \displaystyle\int_0^Z dZ = \dfrac{L_s}{k_{L,c} \cdot a \cdot c_T} \cdot \int_{X_t}^{X_b} \dfrac{(1 + X_i)(1 + X)}{X_i - X} \cdot dX \qquad ...(1.100)$

or, $\qquad\qquad Z = [HTU]_{i,L} \cdot [NTU]_{i,L} \qquad\qquad ...(1.101)$

where, $[HTU]_{i,L}$ = height of transfer unit on the basis of liq film, m

$$= \frac{L_s}{k_{L,c} \cdot a \cdot c_T} \qquad ...(1.102)$$

$[NTU]_{i, L}$ = number of transfer units based on liq film

$$= \int_{X_t}^{X_b} \frac{(1+X_i)(1+X)}{X_i - X} \cdot dX \qquad \qquad ...(1.103)$$

For dilute solutions, the Eqn. 1.100 simplifies to

$$\int_0^Z dZ = \frac{L_s}{k_{L,c} \cdot a \cdot c_T} \cdot \int_{X_t}^{X_b} \frac{dX}{X_i - X} \qquad \qquad ...(1.104)$$

1.11.3.3. Overall Transfer Units

The use of overall mass transfer coefficients becomes convenient when the **VLE**-curve is straight and **OL** is a straight, *i.e.*, $(-k_{L,x}/k_{G,y})$ is constant. Under these circumstances we can transform Eqn. 1.93 to :

$$\int_0^Z dZ = \frac{G_s}{K_{G,p} \cdot a \cdot P} \cdot \int_{Y_t}^{Y_b} \frac{(1+Y)(1+Y^*)}{Y - Y^*} \cdot dY \qquad \qquad ...(1.106)$$

Eqn. 1.94 to :

$$Z = [HTU]_{O,G} \cdot [NTU]_{O,G} \qquad \qquad ...(1.107)$$

Eqn. 1.97 becomes :

$$\int_0^Z dZ = \frac{G_s}{K_{G,p} \cdot a \cdot P} \cdot \int_{Y_t}^{Y_b} \frac{dY}{Y - Y^*} \qquad \qquad ...(1.108)$$

Likewise Eqns. 1.100, 1.101 & 1.104 transform to :

$$\int_0^Z dZ = \frac{L_s}{K_{L,c} \cdot a \cdot c_T} \cdot \int_{X_t}^{X_b} \frac{(1+X^*)(1+X)}{X^* - X} \cdot dX \qquad \qquad ...(1.109)$$

$$Z = [HTU]_{O,L} \cdot [NTU]_{O,L} \qquad \qquad ...(1.110)$$

$$\int_0^Z dZ = \frac{L_s}{K_{L,c} \cdot a \cdot c_T} \cdot \int_{X_t}^{X_b} \frac{dX}{X^* - X} \qquad \qquad ...(1.111)$$

The height of an overall gas transfer unit is :

$$[HTU]_{O,G} = \frac{G_s}{K_{G,p} \cdot a \cdot P} \qquad \qquad ...(1.112)$$

The height of an overall liq transfer unit is :

$$[HTU]_{O,L} = \frac{L_s}{k_{L,c} \cdot a \cdot c_T} \qquad \qquad ...(1.113)$$

The number of overall gas transfer units is :

$$[NTU]_{O,G} = \int_{Y_t}^{Y_b} \frac{(1+Y)(1+Y^*)}{Y-Y^*} \cdot dY \qquad ...(1.114)$$

and the number of overall liq transfer of units is :

$$[NTU]_{O,L} = \int_{X_t}^{X_b} \frac{(1+X^*)(1+X)}{X^*-X} \cdot dX \qquad ...(1.115)$$

For Dilute Concentrations The molar ratios equal mol fraction terms whereupon

$$[NTU]_{O,G} = \int_{Y_t}^{Y_b} \frac{dY}{Y-Y^*} = \int_{y_t}^{y_b} \frac{dy}{y-y^*} \qquad ...(1.116)$$

$$[NTU]_{O,L} = \int_{X_t}^{X_b} \frac{dX}{X^*-X} = \int_{x_t}^{x_b} \frac{dx}{x^*-x} \qquad ...(1.117)$$

These integrals can be determined analytically & graphically as well.

1.11.3.4. Analytical Determination of NTU

If the **VLE**-line is straight, then it can be represented by

$$y^* = mx + b \qquad ...(1.118)$$

If (x_1, y_1^*) & (x_2, y_2^*) be the two points on it, then

$$y_2^* = mx_2 + b$$

$$y_1^* = mx_1 + b$$

$$\therefore \qquad m = \frac{y_2^* - y_1^*}{x_2 - x_1} \qquad ...(1.119)$$

Material balance over the control volume
(Figure 1.11.3.4.1) of the column gives :

$$L_s(x - x_b) = G_s \cdot (y - y_b)$$

$$\therefore \qquad x = x_b + \frac{G_s}{L_s} \cdot (y - y_b) \qquad ...(1.120)$$

Material balance over the entire column
(Figure 1.11.3.4.1 yields :)

$$x_t = x_b + \frac{G_s}{L_s} \cdot (y_t - y_b) \qquad ...(1.121)$$

where, L_s & G_s are liq and gas rates on solute-free basis, kmol/(h.m^2)
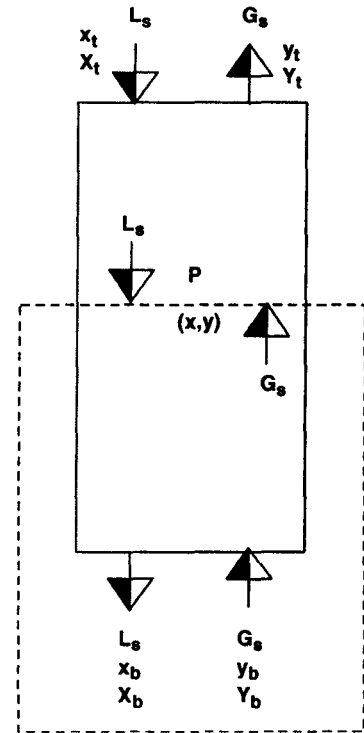
Fig. 1.11.3.4.1. Material Balance of a Countercurrent Packed Bed Absorber

Dilute Solutions

$$[NTU]_{O,G} = \int_{Y_t}^{Y_b} \frac{dy}{y - y^*}$$

$$= \int_{y_t}^{y_b} \frac{dy}{y - m\left(x_b + \dfrac{G_s}{L_s} \cdot (y - y_b)\right) - b} \qquad \text{From Eqn. 1.120}$$

$$= \frac{1}{1 - m \cdot \left(\dfrac{G_s}{L_s}\right)} \cdot \ln \frac{y_b - mx_1 - b}{y_t - m\left(x_b + \dfrac{G_s}{L_s} \cdot (y_t - y_b)\right) - b}$$

$$= \frac{1}{1 - \dfrac{y_b^* - y_t^*}{x_b - x_t} \cdot \dfrac{x_b - x_t}{y_b - y_t}} \cdot \ln \frac{y_b - y_b^*}{y_t - mx_t - b}$$

$$= \frac{1}{1 - \dfrac{y_b^* - y_t^*}{y_b - y_t}} \cdot \ln \frac{y_b - y_b^*}{y_t - y_t^*}$$

$$= \frac{y_b - y_t}{(y_b - y_t) - \left(y_b^* - y_t^*\right)} \cdot \ln \frac{[y - y^*]_b}{[y - y^*]_t}$$

$$= \frac{y_b - y_t}{[y - y^*]_{lm}} \qquad \qquad \dots(1.122)$$

where, $[y - y^*]_b = y_b - y_b^* = \Delta y_b = $ driving force at bottom end

$[y - y^*]_t = y_t - y_t^* = \Delta y_t = $ driving force at top end

$[y - y^*]_{lm} = $ log-mean of driving force

$$= \frac{\left[y_b - y_b^*\right] - \left[y_t - y_t^*\right]}{\ln\left(\dfrac{y_b - y_b^*}{y_t - y_t^*}\right)}$$

$$= \frac{[y - y^*]_b - [y - y^*]_t}{\ln \dfrac{[y - y^*]_b}{[y - y^*]_t}}$$

$$= \frac{\Delta y_b - \Delta y_t}{\ln\left(\dfrac{\Delta y_b}{\Delta y_t}\right)} \qquad \qquad \text{...(1.123)}$$

If Henry's Law applies, the **VLE**-curve's equation becomes :

$$y^* = m.x$$

Therefore,

$$[NTU]_{O,G} = \int_{Y_t}^{Y_b} \frac{dy}{y - y^*}$$

> $y^* = m.x$
>
> $$= m.\left(x_t + \frac{G_s}{L_s}.(y - y_t)\right)$$
>
> Assuming the feed solvent solute-free, *i.e.*, $x_t = 0$,
>
> $$y_t = m.\frac{G_s}{L_s}.(y - y_t)$$

$$= \int_{y_t}^{y_b} \frac{dy}{y - m.\dfrac{G_s}{L_s}.(y - y_t)}$$

$$= \int_{y_t}^{y_b} \frac{dy}{y\left(1 - m.\dfrac{G_s}{L_s}\right) + m.\dfrac{G_s}{L_s}.y_t}$$

$$\therefore \quad [NTU]_{O,G} = \frac{1}{1 - m.\dfrac{G_s}{L_s}}.\ln\left[\left(1 - m.\frac{G_s}{L_s}\right).\frac{y_b}{y_t} + m.\frac{G_s}{L_s}\right]$$

$$= \frac{1}{1 - \dfrac{1}{e_a}}.\ln\left[\left(1 - \frac{1}{e_a}\right).\frac{y_b}{y_t} + \frac{1}{e_a}\right] \qquad \text{...(1.124)}$$

where, e_a = absorption factor = $\dfrac{L_s}{m.G_s}$

Figure 1.11.3.4.2. illustrates the graphical relationship between $[NTU]_{O,G}$ and $\left(\dfrac{y_b}{y_t}\right)$.

These curves show that the greater the $m.\dfrac{L_s}{G_s}$ is, (*i.e.*, lower the absorption factor is), the

greater becomes the value of $[NTU]_{O,G}$ for a given ratio of $\left(\dfrac{y_b}{y_t}\right)$.

C
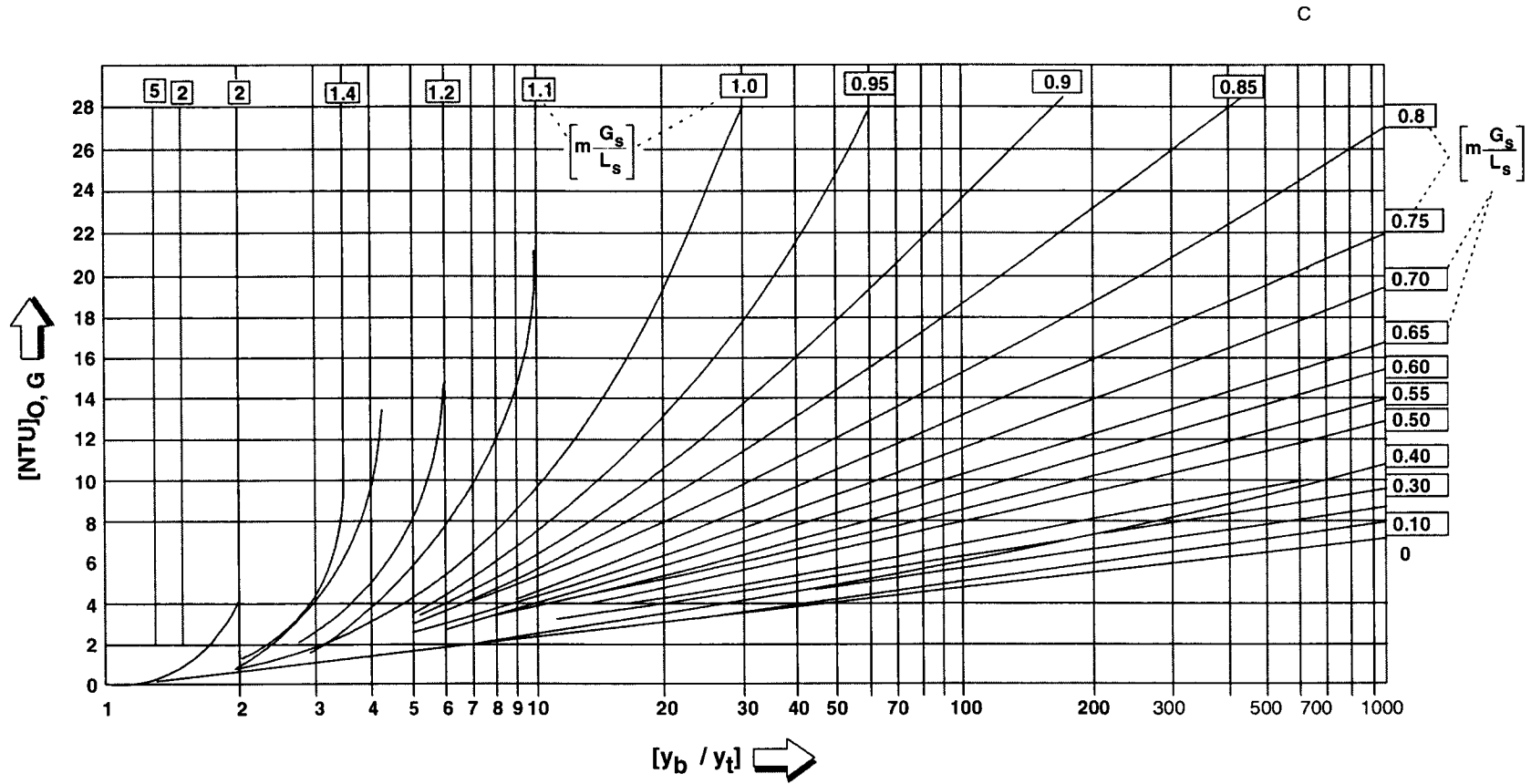
Fig. 1.11.3.4.2. *[NTU]$_{o,o}$ as a Function of $\left[\dfrac{y_b}{y_t}\right]$ with m.$\left[\dfrac{G_s}{L_s}\right]$ appearing as the Curve Parameter.*

The value of $m.\dfrac{L_s}{G_s}$ can be obtained as follows :

Solute balance over the entire column yields :

$$Gs.(y_b - y_t) = L_s.(x_b - x_t) \qquad \text{Refer Figure 1.11.3.4.3.}$$

If the entering solvent is solute free, then $x_t = 0$

$$\therefore \qquad x_b = \frac{G_s}{L_s} . (y_b - y_t)$$

$$\therefore \qquad m.\frac{G_s}{L_s} = \frac{m.x_b}{y_b - y_t} = \frac{y_b^*}{y_b - y_t} \qquad\qquad ...(1.125)$$

In case the entering liquid is not solute-free, the expression for $[NTU]_{O,G}$ would become :

$$\frac{y_i - K\,x_i}{y_0 - K\,x_i}$$
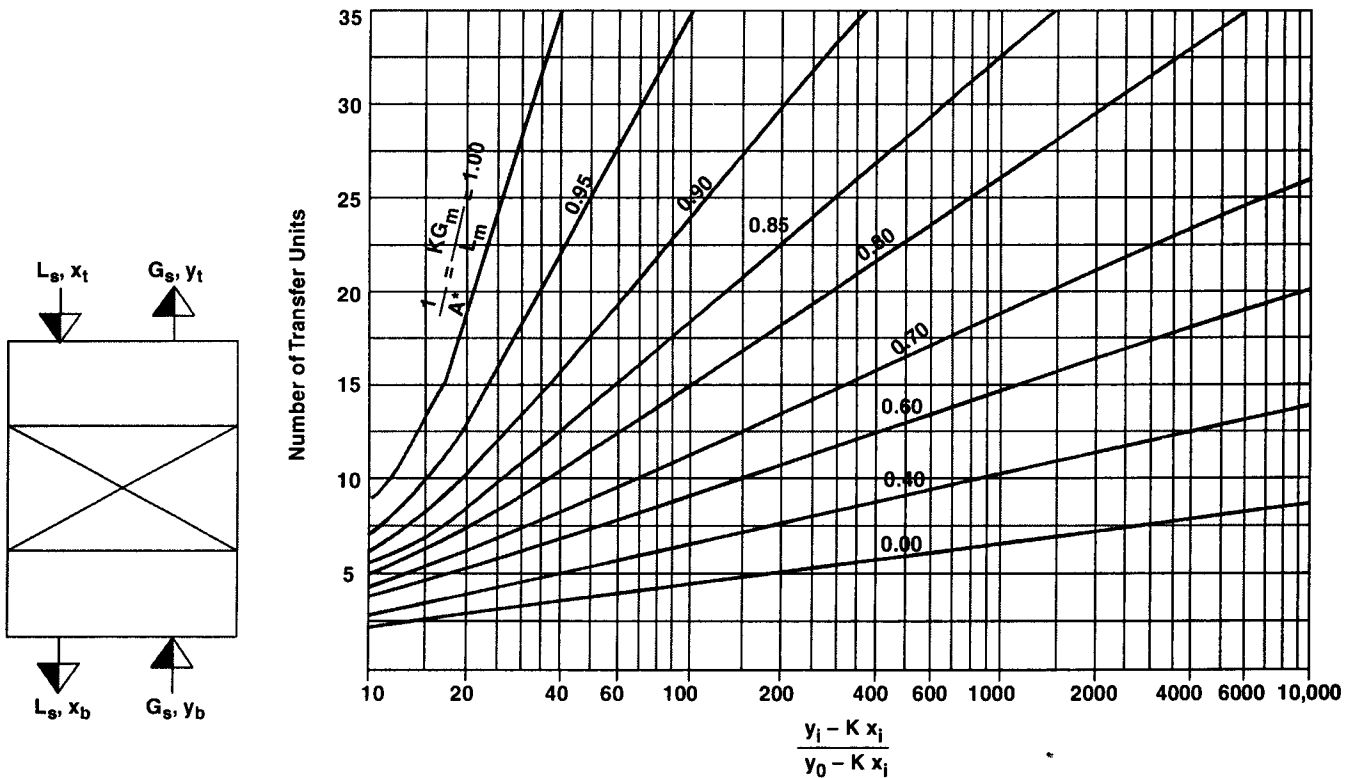
Fig. 1.11.3.4.3.
Material Balance in a Countercurrent Packed Bed Absorber

Fig. 1.11.3.4.4. *Colburn's Correlation for Absorber Design. The Number of Transfer Units is Ploted Against the Ratio of Inlet to Outlet Gas Compositions [A.P. Colburn — Industrial & Engineering Chemistry, vol.33 (1941)].*

$$[NTU]_{O,G} = \int_{y_t}^{y_b} \frac{dy}{y - m.\left(x_t + \dfrac{G_s}{L_s}.(y - y_t)\right)}$$

$$= \int_{y_t}^{y_b} \frac{d_y}{y \left(1 - m \cdot \frac{G_s}{L_s}\right) - m \cdot x_t + m \cdot \frac{G_s}{L_s} \cdot y_t}$$

$$= \frac{1}{1 - m\frac{G_s}{L_s}} \cdot \ln\left[\left(1 - m \cdot \frac{G_s}{L_s}\right) \frac{y_b - mx_t}{y_t - mx_t} + m \cdot \frac{G_s}{L_s}\right]$$

$$= \frac{1}{1 - \frac{1}{e_a}} \cdot \ln\left[\left(1 - \frac{1}{e_a}\right) \cdot \frac{y_b - mx_t}{y_t - mx_t} + \frac{1}{e_a}\right] \qquad \ldots(1.124\ A)$$

The number of transfer units can be obtained straightway from $[NTU]_{O,G}$ vs. the ratio of inlet to outlet gas compositions $\dfrac{y_b - mx_t}{y_t - mx_t}$ plot where absorption factor appears as curve parameter [**Figure 1.11.3.4.4**].

CONCENTRATED SOLUTIONS

During absorption, the mass transfer is predominantly a unidirectional diffusion process and Colburn has shown that the number of transfer units for concentrated solution is given by :

$$[NTU]_{O,G} = \int_{y_t}^{y_b} \frac{(1 - y)_{lm}}{1 - y} \cdot \frac{dy}{y - y^*} \qquad \ldots(1.126)$$

For gas controlled absorption

where, $(1 - y)_{lm} = \dfrac{(1 - y^*) - (1 - y)}{\ln\left(\dfrac{1 - y^*}{1 - y}\right)}$ $\qquad \ldots(1.127)$

However, Eqn. 1.127 can be further be simplified by substituting the arithmatic average for the logarithmic average, *i.e.*,

$$(1 - y)_{lm} \approx \frac{1}{2} \left[(1 - y^*) + (1 - y)\right]$$

$$\therefore \qquad \frac{(1 - y)_{lm}}{1 - y} \approx \frac{(1 - y^*) + (1 - y)}{2(1 - y)} = \frac{y - y^*}{2(1 - y)} + 1$$

which involves little error and as a result $[NTU]_{O,G}$ becomes

$$[NTU]_{O,G} = \frac{1}{2} \ln\left(\frac{1 - y_t}{1 - y_b}\right) + \int_{y_t}^{y_b} \frac{dy}{y - y^*} \qquad \ldots(1.128)$$

Expressed in mole ratios :

$$y_b = \frac{Y_b}{1 + Y_b}$$

$$y_t = \frac{Y_t}{1 + Y_t}$$

the Equation 1.128 transforms to :

$$[NTU]_{O,G} = \frac{1}{2} \ln\left(\frac{1 + Y_t}{1 + Y_b}\right) + \int_{Y_t}^{Y_b} \frac{dY}{Y - Y^*} \qquad \text{...(1.129)}$$

For liq controlled absorption processes, *i.e.*, for systems where the principal mass transfer resistance lies within the liquid, it is more convenient to express number of transfer units in terms of solute concentrations in liquid :

$$[NTU]_{O,L} = \frac{1}{2} \ln\left(\frac{1 - x_b}{1 - x_t}\right) + \int_{x_t}^{x_b} \frac{dx}{x^* - x} \qquad \text{...(1.130)}$$

In terms of mole ratios :

$$[NTU]_{O,L} = \frac{1}{2} \ln\left(\frac{1 + X_b}{1 + X_t}\right) + \int_{X_t}^{X_b} \frac{dX}{X^* - X} \qquad \text{...(1.131)}$$

$$\boxed{\text{cf. } x_b = \frac{X_b}{1 + X_b} \quad ; \quad x_t = \frac{X_t}{1 + X_t}}$$

For dilute solutions, the 1st term of RHS of Eqns. 1.128, 1.129, 1.130 & 1.131 becomes negligible whereupon these eqns. reduce to :

$$[NTU]_{O,G} = \int_{y_t}^{y_b} \frac{dy}{y - y^*} = \int_{Y_t}^{Y_b} \frac{dY}{Y - Y^*} \qquad \text{...(1.116)}$$

$$[NTU]_{O,L} = \int_{x_t}^{x_b} \frac{dx}{x^* - x} = \int_{X_t}^{X_b} \frac{dX}{X^* - X} \qquad \text{...(1.117)}$$

1.11.3.5. Graphical Estimation of NTU

Taking material balance on the solute from the bottom of the column to any horizontal plane passing thru the point *P* (X,Y) of the packed bed :

$$A \cdot L_s \cdot (X_b - X) = A \cdot G_s \cdot (Y_b - Y) \qquad \text{Refer Fig. 1.11.3.5.1.}$$

or, $$Y_b - Y = \frac{L_s}{G_s} \cdot (X_b - X) \qquad \text{...(1.132)}$$

where, A = area of cross-section of packed bed, m^2

L_s & G_s are liq and gas molar flowrates on solute-free basis, kmol/(h.m^2)
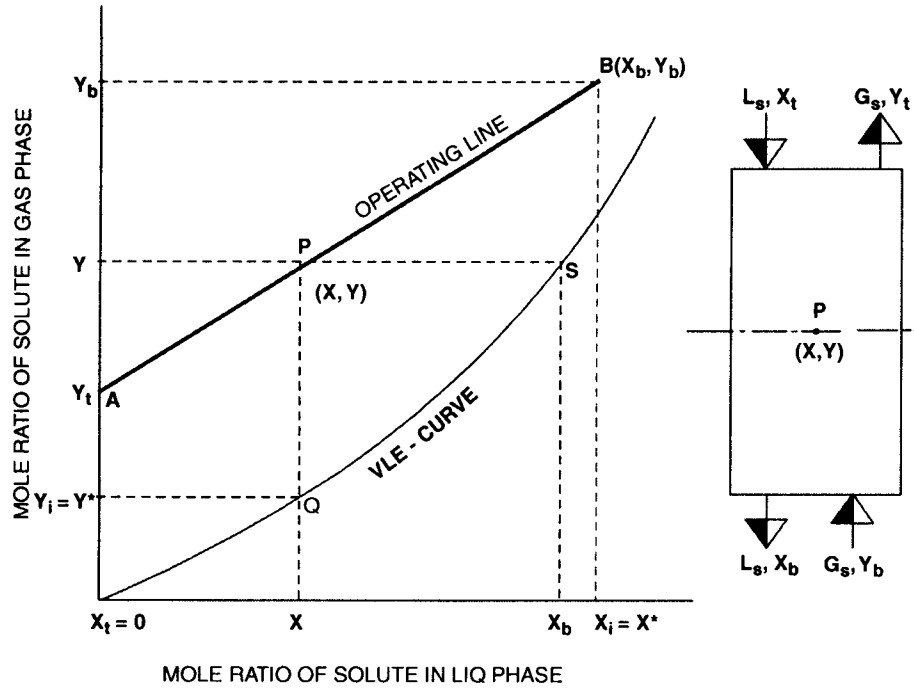
Fig. 1.11.3.5.1. *Driving Force in Gas-Film & Liq-Film Controlled Absorption Process.*

This is the eqn. of a straight of slope $\dfrac{L_s}{G_s}$ and it passes thru the point (X_1, Y_1).

A solute balance over the whole column yields :

$$A \cdot L_s \cdot (X_b - X_t) = A \cdot G_s \cdot (Y_b - Y_t)$$

Or, $Y_b - Y_t = \dfrac{L_s}{G_s} \cdot (X_b - X_t)$ ...(1.133)

This eqn. is identical to Eqn. 1.132 with (X,Y) replaced by (X_t, Y_t).

Eqn. 1.132 & 1.133 represent the operating line **(OL)** of the packed bed absorber.

The point **P** (X,Y) represents the condition of the bulk of the liq and gas at any point in the column.

Now if the absorption is a gas-film controlled process.

$$Y_i = Y^*$$

and is given by a point **Q** (X, Y_i) on the **VLE**-curve. The driving force causing solute transfer is then given by the distance **PQ**

$$PQ = Y - Y^*$$

DILUTE SOLUTIONS

NTU is evaluated from the graphical integration of the expression :

$$[NTU]_{O,G} = \int_{Y_t}^{Y_b} \frac{dY}{Y - Y^*} \qquad \qquad ...(1.116)$$

by selecting values of Y (arbitrarily), reading off from the diagram **(Figure 1.11.3.5-1)** the corresponding values of Y^* and thereafter calculating the values of $\dfrac{1}{Y - Y^*}$.

Next a graph *(AOC)* is drawn by plotting $\dfrac{1}{Y - Y^*}$ against Y
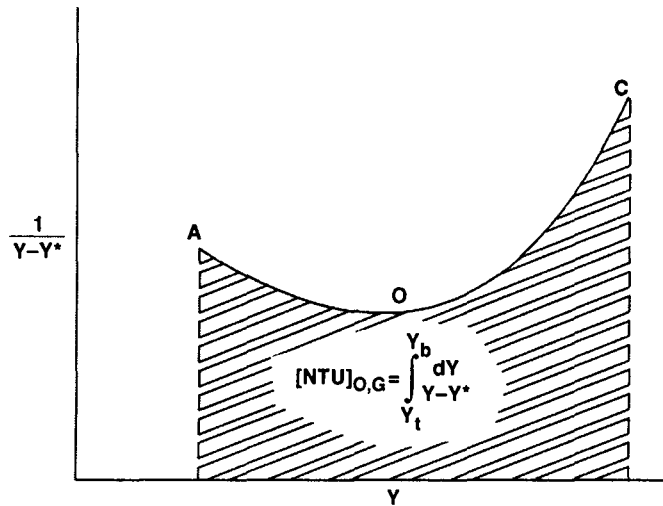
Fig. 1.11.3.5.2. *Graphical Determination of [NTU]$_{O,G}$*

The hatched area under the curve *AOC* gives the value of the integral $\int_{Y_t}^{Y_b} \dfrac{dY}{Y - Y^*}$, *i.e.*, $[NTU]_{O,G}$.

The method of trapeziums is usually followed to determine the numerical value of this hatched area.
In case the liq-film controls the process, X_i equals X^* whereupon $X^* - X$ represents the driving

$$PS = X_i - X = X^* - X$$

force and the number of transfer units is evaluated from the graphical integration of the expression :

$$[NTU]_{O,L} = \int_{X_t}^{X_b} \frac{dX}{X^* - X} \qquad \qquad ...(1.117)$$

exactly in the same way as we have for the gas-film controlled absorption process.

CONCENTRATED SOLUTIONS

For gas-controlled absorption processes, the number of transfer units as given by Eqn. 1.128

$$[NTU]_{O,G} = \frac{1}{2} \ln \left(\frac{1 - y_t}{1 - y_b} \right) + \int_{Y_t}^{Y_b} \frac{dy}{y - y^*} \qquad ...(1.128)$$

can be computed thru simple graphical integration.

The value of the integral $\int_{Y_t}^{Y_b} \frac{dy}{y - y^*}$ can be obtained by plotting $\frac{1}{y - y^*}$ as ordinate and **y** as

abscissa. However, such a plot for the graphical integration of Eqn. 1.128 often covers awkwardly large ranges of the ordinate. This can be overcome by replacing **dy** by **y•d(ln y)** term* whereupon total number of transfer units becomes :

$$[NTU]_{O,G} = 1.152 \log \left(\frac{1 - y_t}{1 - y_b} \right) + 2.303 \int_{\log y_t}^{\log y_b} \frac{dy}{y - y^*} \cdot d \log y \qquad ...(1.134)$$

Now the value of the integral of Eqn. 1.134 can be obtained by plotting $\frac{y}{y - y^*}$ as ordinate

versus **log y** as abscissa.

A similar treatment can be made to calculate **NTU** from Eqn. 1.129 which can be represented as :

$$[NTU]_{O,G} = 1.152 \log \left(\frac{1 + Y_t}{1 + Y_b} \right) + 2.303 \int_{\log Y_t}^{\log Y_b} \frac{Y}{Y - Y^*} \cdot d \log Y \qquad ...(1.135)$$

In this case the integral is obtained graphically by $\frac{Y}{Y - Y^*}$ against **log Y.**

Likewise, for liq-controlled absorption processes, the graphical evaluation of number of transfer units can be carried in analogous manner from Eqn. 1.30 and 1.131 :

$$[NTU]_{O,L} = \frac{1}{2} \ln \left(\frac{1 - x_b}{1 - x_t} \right) + \int_{x_t}^{x_b} \frac{dx}{x^* - x} \qquad ...(Eqn. 1.130)$$

$$= 1.152 \log \left(\frac{1 - x_b}{1 - x_t} \right) + 2.303 \int_{\log x_t}^{\log x_b} \frac{x}{x^* - x} \cdot d \log x \qquad ...(1.136)$$

$$[NTU]_{O,L} = \frac{1}{2} \ln \left(\frac{1 + X_b}{1 + X_t} \right) + \int_{X_t}^{X_b} \frac{dX}{X^* - X} \qquad ...(Eqn. 1.131)$$

$$\boxed{y. \, d \, (\ln y) = y \cdot \frac{1}{y} \cdot dy = dy}$$

$$= 1.152 \ \log\left(\frac{1+X_b}{1+X_t}\right) + 2.303 \int\limits_{\log X_t}^{\log X_b} \frac{X}{X^*-X} \cdot d \log X \quad \ldots(1.137)$$

1.11.3.6. Graphical Construction of Transfer Units

The number of overall gas transfer units as given by Eqn. 1.122

$$[NTU]_{O,G} = \frac{y_b - y_t}{[y - y^*]_{lm}} \qquad \ldots(1.122)$$

demonstrates that one overall gas transfer unit results when the change in gas composition over the entire packed bed equals the average overall driving force causing the change, *i.e.*,

$$[NTU]_{O,G} = 1$$

when

$$y_b - y_t = [y - y^*]_{lm}$$

$$\begin{bmatrix} \text{change in gas} \\ \text{composition} \end{bmatrix} \quad \begin{bmatrix} \text{average overall} \\ \text{driving force} \end{bmatrix}$$

For graphical construction of transfer units, draw **OL** and **VLE-** curve on **x-y** plot [**Figure 1.11.3.6.1**].

Draw another curve *HJK* passing thru the midpoints of all the vertical distances between the **OL** and **VLE**-line.
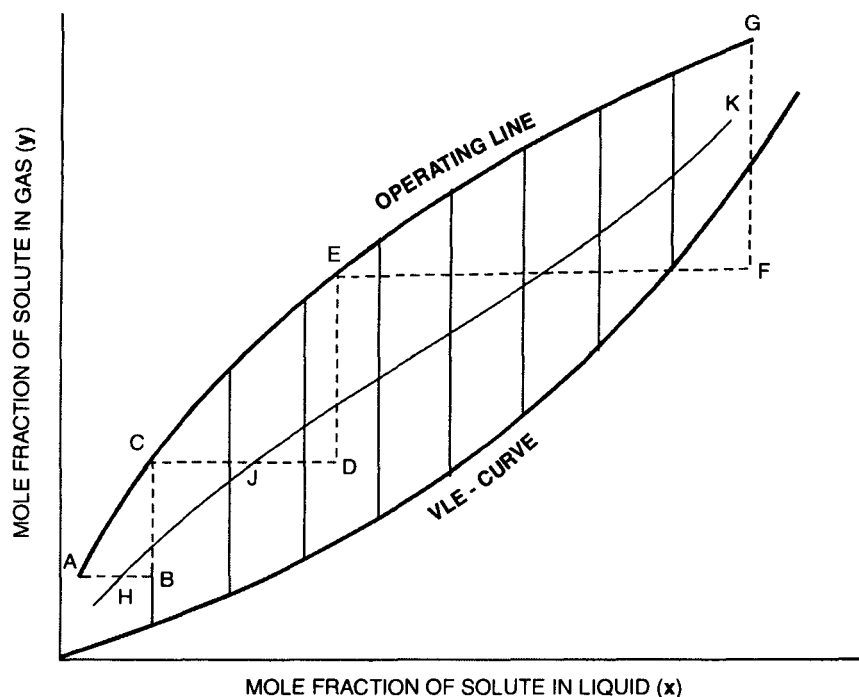
Fig. 1.11.3.6.1. *Graphical Construction of Transfer Units.* *[NTU]*$_{O,G}$.

From the point *A* draw a horizontal *AB* such that *AH* = *HB*. A vertical from *B* meets the **OL** at *C* and thus completing one transfer unit.

Similarly construct other steps — *CDE* and *EFG* etc. each corresponding to one transfer unit. Stepping off in this manner we'll get $[NTU]_{O,G}$.

Now, consider the transfer unit *CDE*. It brings about a change in gas composition $y_E - y_D$. The average driving force responsible for this change is $LM = y_L - y_M$. But $LJ = JM$. So if the OL is a straight line, then by geometry of the figure.

$$DE = 2LJ = LM$$

Likewise, $[NTU]_{O,L}$ can be computed by drawing the *HJK*-line Horizontally halfway between the OL & VLE-curve [**Figure 1.11.3.6.2**] and constructing the steps *ABC, CDE,* etc. whose vertical portions (*AB, CD,* ...etc.) get bisected by *HJK*.

MOLE FRACTION OF SOLUTE IN LIQUID (x)
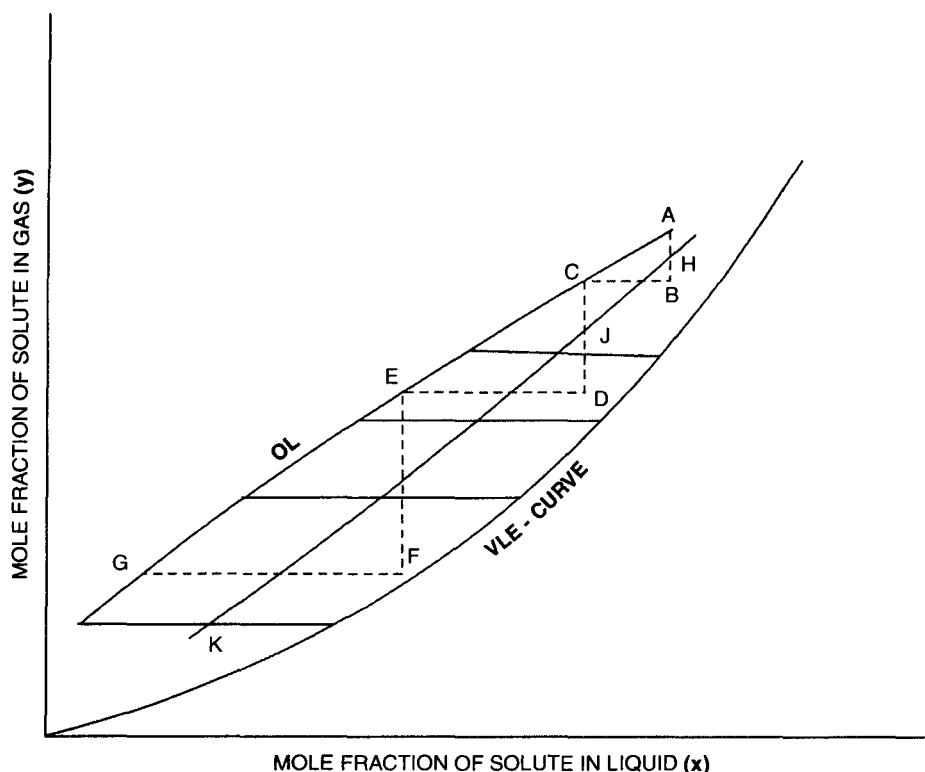
Fig. 1.11.3.6.2. *Graphical Construction of Transfer Units. [NTU]$_{O,L}$.*

1.11.3.7. Interrelationships of Gas & Liquid Transfer Units

The resistance to mass transfer as expressed thru **HTUs** is the sum of the individual gas-phase and liq-phase resistance [A.P. Colburn — *Transactions of American Institute of Chemical Engineers, Vol. 35 (1939)*] :

$$[HTU]_{O,G} = [HTU]_{i,G} \cdot \frac{(1-y)_{i,lm}}{(1-y)_{*,lm}} + \frac{m.G}{L} \cdot [HTU]_{i,L} \cdot \frac{(1-x)_{i,lm}}{(1-y)_{*,lm}} \qquad ...(1.138)$$

This equation reduces to :

$$[HTU]_{O,G} = [HTU]_{i,G} + \frac{m.G}{L} [HTU]_{i,L} \cdot \frac{(1-x)_{i,lm}}{(1-y)_{*,lm}} \qquad ...(1.139)$$

in case the resistance to mass transfer lies essentially all in the gas (whence $y_i \approx y^*$).

Likewise,

$$[HTU]_{O,L} = [HTU]_{i,L} \cdot \frac{(1-x)_{i,lm}}{(1-x)_{*,lm}} + \frac{m.G}{L} \cdot [HTU]_{i,G} \cdot \frac{(1-y)_{i,lm}}{(1-x)_{*,lm}} \qquad ...(1.140)$$

If the mass transfer resistance is essentially all in the liquid, this eqn. reduces to :

$$[HTU]_{O,L} = [HTU]_{i,L} + \frac{L}{m.G} [HTU]_{i,G} \cdot \frac{(1-y)_{i,lm}}{(1-x)_{*,lm}}$$

where, $[HTU]_{O,G}$, $[HTU]_{O,L}$, $[HTU]_{i,G}$ and $[HTU]_{i,G}$ = heights of transfer units, m, based on overall gas-phase resistance, overall liq-phase resistance, gas-phase resistance and liq-phase resistance respectively.

$(1-y)_{i,lm}$ = logarithmic mean of $(1-y)$ and $(1-y_i)$

$(1-x)_{i,lm}$ = logarithmic mean of $(1-x)$ and $(1-x_i)$

$(1-y)_{*,lm}$ = logarithmic mean of $(1-y)$ and $(1-y^*)$

$(1-x)_{*,lm}$ = logarithmic mean of $(1-x)$ and $(1-x^*)$

For dilute solutions Eqns. 1.139 & 1.141 further simplifies to :

$$[HTU]_{O,G} = [HTU]_{i,G} + \frac{m.G}{L} \cdot [HTU]_{i,L} \qquad ...(1.142)$$

$$[HTU]_{O,L} = [HTU]_{i,L} + \frac{m.G}{L} \cdot [HTU]_{i,G} \qquad ...(1.143)$$

1.11.4. Height Equivalent to A Theoretical Plate (HETP)

HETP affords to a simple method for designing packed towers :

the number of theoretical trays required to effect a specified change in solute concentration multiplied by the packed height equivalent to one theoretical plate gives the required height of the packing to accomplish the same task, *i.e.*,

$$Z = N_T \times HETP$$

HETP expresses the efficiency of a packing material for carrying out a separation. However, this concept ignores the difference between stagewise and continuous contact. Over and above, **HETP** varies with the type and size of packing, flowrates of gas & liq as well as for every system with concentration. Hence it requires enormous experimental data to permit utilization of this method.

However, it is more convenient to report experimental data in terms of **HTUs** rather than **HETPs**. This is because, **HTU** is theoretically more appropriate for packed columns in which mass is transferred by a differential rather than a stagewise manner.

If the **OL** & **VLE**-line are parallel, *i.e.*, if $m.\dfrac{G_s}{L_s} = 1$, then HETP = HTU

If the **OL** & **VLE**-line are straight but not parallel,

$$\frac{[HTU]_{O,G}}{HETP} = \frac{m.\dfrac{G_s}{L_s} - 1}{\ln\left[m.\dfrac{G_s}{L_s}\right]} \qquad ...(1.144)$$

1.11.5. Design Theory

The design of a packed bed absorber requires three basic parameters :

1. The rate of solute transfer

2. The knowledge of overall mass transfer coefficient

3. The driving force, usually measured in terms of pressure.

The pressure driving force difference must be determined at the bottom of the packed bed (Δp_b) as well as the top of the packed bed (Δp_t). For a gas stream containing a low concentration of solute, L_s/G_s is almost constant and the operating line **(OL)** of the absorber

$$Y - Y_1 = \frac{L_s}{G_s} \cdot (X - X_1)$$

is nearly straight. Also for dilute solutions there is negligible heat of solution as the solute transfers itself from gas to liquid phase. Therefore, the value of Henry's Law constant **H** or **m** (slope of the **VLE**-line) :

$$y^* = m.x$$

may be constant. Under these circumstances the pressure driving force is the logarithmic average of the driving forces at the bottom and top of the packed bed :

$$\Delta p_{lm} = \frac{\Delta p_b - \Delta p_t}{\ln\left(\dfrac{\Delta p_b}{\Delta p_t}\right)} \qquad \qquad ...(1.145)$$

Therefore, the volume of the tower packing required for the absorber can be calculated from :

$$A.Z = \frac{N}{K_{G,P} \cdot a \cdot \Delta p_{lm}} \qquad \qquad ...(1.146)$$

where, Δp_{lm} = log-mean of pressure difference driving force, Pa

A = area of cross-section of packed bed, m^2

Z = height of packed bed, m

a = interfacial area, m^2/m^3

$K_{G,P}$ = overall gas-phase mass transfer coefficient, $kmol/(h.m^2.Pa)$

X_1, Y_1 = liq and gas composition at any point in the packed bed in terms of mol ratios.

L_s, G_s = liq and gas molar flowrates on solute-free basis, $kmol/(h.m^2)$

This straightforward approach to design as described in Eqn. 1.146 endows a quick method for specifying industrial absorption columns. However, in practice this is not so, because of the following reasons :

- The rate of mass transfer is never constant. It decreases significantly as the concentration of solute approaches the solubility limit.

- Some systems change from gas-film control to liq-film control during operation as a result of change in liq-phase properties, solute concentration in the liquid or pH of the liquid phase.

- Complete analogy between heat transfer and mass transfer is lacking. During heat transfer the driving force is the terminal temperature differences which lend themselves to a logarithmic average since sensible heat transfer usually means a straight operating line and a straight equilibrium curve. In a heat transfer equipment the terminal temperature differences usually have values which differ by less than 10-fold. Whereas in the case of mass transfer the terminal partial pressure differences driving forces vary by 100 or 1000 times. Obviously it is quite unlikely that the operating line and the vapor-liq equilibrium curve, in particular, will remain linear over such a wide concentration ranges. And therefore, a logarithmic average is not a true representive of the driving force in typical absorption operations.

1.11.5.1. Simplified Design Procedures

Procedure - I

Credit goes to Kremser [A. Kremser — **National Petroleum News, Vol. 22/ No. 21 (1930]** who first developed a systematic procedure for design calculation of absorbers. He introduced the term absorption factor and based his calculation on the assumption of straight OL-line of constant slope **(m).**

- Calculate the absorption factor (e_a) :

$$e_a = \frac{L_s}{m.G_s} \qquad \ldots(1.61)$$

where, m = slope of VLE-line

$$\frac{L_s}{G_s} = \text{slope of the OL}$$

- Calculate each theoretical stage by using the following eqn. :

$$y_n = \frac{y_{n+1} + e_a . m . x_{n-1}}{1 + e_a} \qquad \ldots(\text{cf. Eqn. 1.63})$$

- Determine the total number of theoretical stages this way to satisfy the desired absorption specification.

- Estimate stage efficiency to calculate the packed depth required.

However, this method has its limitations :

1. It does not estimate the vap & liq compositions or temperature profiles in the column [R.N. Maddox — *Process Engineers Absorption Pocket Handbook, Gulf Publishing, 1985].*

2. It assumes straight operating line, and an equilibrium line of constant slope. But these are seldom linear over wide concentration ranges encountered in industrial absorbers.

Procedure - II

Enters the transfer unit concept in order to obtain more consistency with mass transfer theory.

- Calculate the absorption factor (e_a)

- Determine the number of gas-phase transfer units $[NTU]_{O,G}$ from the eqn. :

$$[\text{NTU}]_{\text{O,G}} = \frac{\ln\left[\left(1 - \frac{1}{e_a}\right) \cdot \frac{y_b - mx_t}{y_t - mx_t} + \frac{1}{e_a}\right]}{1 + e_a}$$

...(Refer Eqn. 1.124 A)

This eqn. assumes linear (although not parallel), operating line and equilibrium curve (VLE-line).

For preliminary absorber design, use may be made of the **Colburn Correlation [Figure 1.11.3.4.4]** to determine the number of gas-phase transfer units. For this one requires

– the ratio of inlet to outlet gas compositions :

$$\frac{y_b - mx_t}{y_t - mx_t}$$

– the absorption factor (e_a).

If the feed solvent is solute free, then

$$[\text{NTU}]_{\text{O,G}} = \frac{\ln\left[\left(1 - \frac{1}{e_a}\right) \cdot \frac{y_b}{y_t} + \frac{1}{e_a}\right]}{1 - \frac{1}{e_a}}$$

● Calculate the height of a transfer unit — the depth of packing producing a change in composition equal to the mass transfer driving force causing that change :

$$[\text{NTU}]_{\text{O,G}} = \frac{G}{K_{G,p} \cdot a \cdot P}$$

...(1.147)

where, G = gas molar velocity, kmol/(h.m^2).

$K_{G,p}$ = overall gas-phase mass transfer coefficient on the basis of pressure difference driving force, kmol/(h.m^2.Pa).

a = interfacial area of packing, m^2/m^3.

P = total system pressure, Pa.

$$[\text{HTU}]_{\text{O,L}} = \frac{G}{K_{L,y} \cdot a}$$

where, L = liq molar velocity, kmol/(h.m^2).

$K_{L,y}$ = overall liq-phase mass transfer coefficient based on mole fraction driving force, kmol/(h.m^2.kmol/kmol).

$K_{G,P}.a$ & $k_{L,y}.a$ are respectively known as overall gas-phase & liq phase volumetric coefficients.

● Calculate packed bed height :

$$Z = [NTU]_{O,G} \times [HTU]_{O,G}$$

The height of packing layer can also be calculated by eqn. :

$$Z = HETP \times N_T$$

where, **HETP** = height equivalent to a theoretical plate, m.

N_T = number of theoretical plates (stages of changes in concentration). It is usually determined graphically **[Figure 1.11.5.1.1]**.

MOLE RATIO OF SOLUTE IN LIQ PHASE
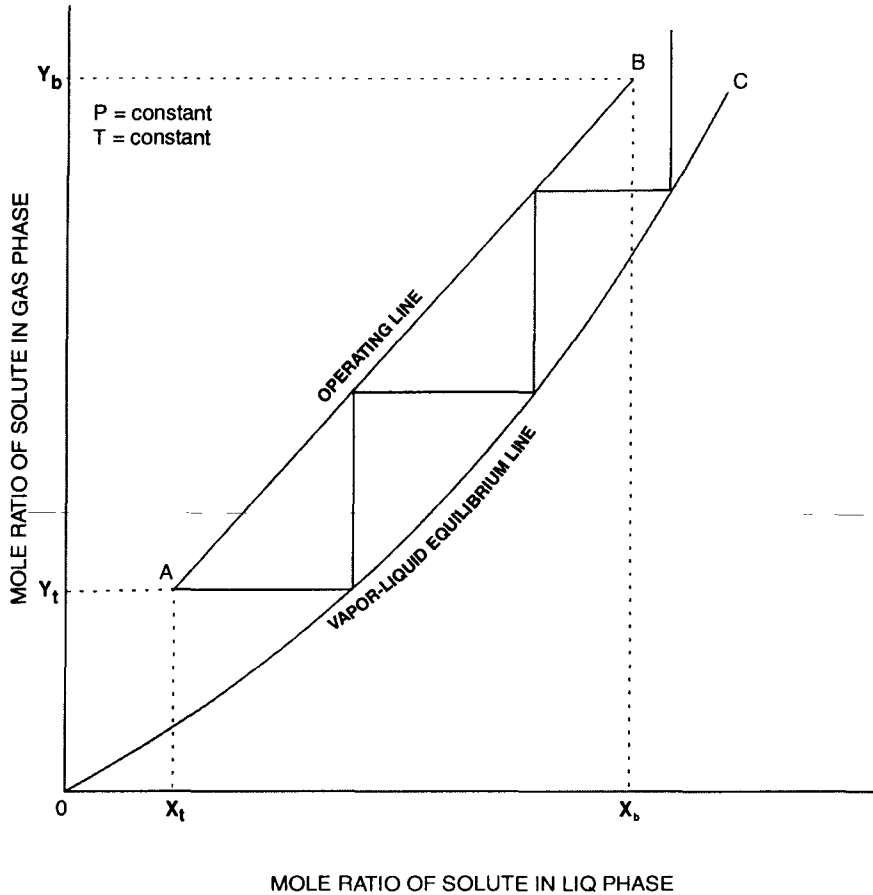
Fig. 1.11.5.1.1. *Graphical Determination of the Number of Stages (Theoretical Plates) in An Absorber.*
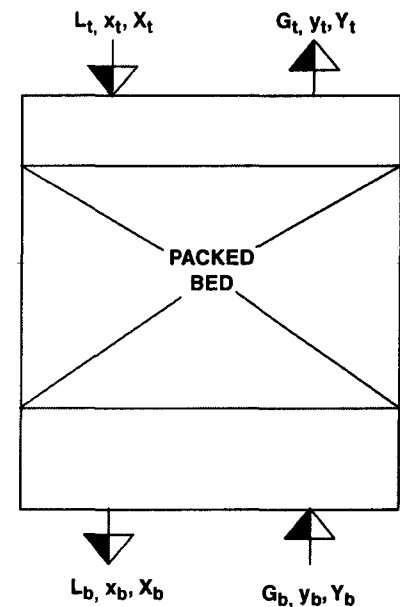
Fig. 1.11.6.1. *Gas-Liq Traffic in A Counter-Current Packed Bed Absorber.*

1.11.6. General Design Concept

Seldom any absorption process of commercial importance obeys Henry's Law for equilibrium values. Nor do they operate at constant gas rates or liquid rates.

Frequently the solute concentration in the inlet gas stream represents a significantly large percentage of feedgas. Therefore, after absorption of solute, the exit gas flowrate gets reduced. Likewise, the liquid rate down the tower progressively increases with the absorption of solute.

A mass balance across such absorption tower **(Fig. 1.11.6.1)**

$$y \cdot G_b + x_t \cdot L_t = y_t \cdot G_t + x_b \cdot L_b$$

where x and y represent liq and gas composition in terms of mole fraction of solute; G & L represent gas & liq flowrates, kmol. $h^{-1}.m^{-2}$. Subscripts 'b' & 't' stand for bottom and top of the column.

1.11.6.1. Diameter of A Packed Bed Absorber

The diameter of an absorption column can be obtained from :

$$Q_v = \frac{\pi}{4} \cdot D^2 \cdot v$$

∴
$$D = \left(\frac{Q_v}{0.785 \, v} \right)^{\frac{1}{2}} \qquad \qquad ...(1.148)$$

where, **D** = packed bed dia, m

Q_v = volumetric gas flowrate, m³/s

v = velocity of the gas stream related to the total cross-sectional area of the column, m/s

The gas velocity (v) can be computed from the flooding velocity (v_{fl}) by the eqn. :

$$\log\left(\frac{v_{fl}^2}{\epsilon^3} \cdot \frac{a}{g} \cdot \frac{\rho_G}{\rho_L} \cdot \mu_L^{0.16} \right) = C - 1.75 \left(\frac{\dot{L}_m}{\dot{G}_m} \right)^{\frac{1}{4}} \cdot \left(\frac{\rho_G}{\rho_L} \right)^{\frac{1}{8}} \qquad ...(1.149)$$

where, v_{fl} = gas velocity at the point of flooding (inversion), m/s

ϵ = void fraction, also called fractional void of packing. It is the free volume of packing, m³/ m³.

a = interfacial area of packing, *i.e.*, unit surface area of packing, m²/m³

ρ_G = density of the gas stream, kg/m³

ρ_L = density of the liq stream, kg/m³

μ_G = dynamic viscosity of the liq, mPa.s

C = constant

= 0.22 for a packing of rings or spirals.

$\dot{L}_m$ = mass flowrate of liq, kg/s

$\dot{G}_m$ = mass flowrate of gas, kg/s

Flooding velocity being computed, the operating velocity of the gas is taken as 75 – 90% of flooding velocity :

$$v = (0.75 - 0.90).v_{fl} \qquad \qquad ...(1.150)$$

Now, the actual velocity of the gas in the free section of the packing is given by :

$$v_{ac} = \frac{v}{\epsilon}, m/s \qquad \qquad ...(1.151)$$

It can be obtained from the relationship :

$$Re_G = 0.045 \, Ar^{0.57} \cdot [\dot{G} / \dot{L}]^{0.43} \qquad \qquad ...(1.152)$$

where, Re_G = gas Reynolds number in the so-called optimal hydrodynamic conditions

$$= \frac{D_{eq} \cdot v_{ac} \cdot \rho_G}{\mu_G}$$

$$= \frac{4\,\epsilon}{a} \cdot \frac{v}{\epsilon} \cdot \frac{\rho_G}{\mu_G}$$

$$= \frac{4v}{a} \cdot \frac{\rho_G}{\mu_G} \qquad\qquad ...(1.153)$$

D_{eq} = equivalent diameter of packing

$$= \frac{4\,\epsilon}{a}$$

Ar = Archimedes number

$$= \frac{D_{eq}^3 \cdot \rho_G \cdot \rho_L \cdot g}{\mu_G^2} \qquad\qquad ...(1.154)$$

μ_G = dynamic viscosity of the gas, Pa.s

1.11.7. Principal Dimensionless Numbers in Mass Transfer Operations

Nusselt Number, Nu

The Nusselt number for mass transfer is :

$$Nu = \frac{k.l}{D_{ff}} \qquad\qquad ...(1.155)$$

where, k = gas-film or liq-film mass transfer coefficient, kmol/(m^2.s.kmol/m^3) or, kg/(m^2.s.kg/m^3)

l = characteristic linear dimensions, m

D_{ff} = coefficient of molecular diffusion, m^2/s

$$[Nu]_G = \frac{k_G \cdot l}{D_{ff}} \qquad\qquad ...(1.155\ A)$$

$$[Nu]_L = \frac{k_L \cdot l}{D_{ff}} \qquad\qquad ...(1.155\ B)$$

cf. Nusselt No. for heat transfer is

$$Nu = \frac{h.d}{k}$$

where, h = heat transfer coefficient, W/m^2.K

d = linear dimension, m

k = thermal conductivity, W/m.K

Peclet Number, Pe

The Peclet number for mass transfer is :

$$Pe = \frac{v.l}{D_{ff}}$$

...(1.156)

where, v = gas or liq velocity, m/s

$$Pe = Re.\ Pr$$

Reynolds Number, Re

The Reynolds number for mass transfer is :

$$Re = \frac{l.v.\rho}{\mu} = \frac{l.v}{\nu}$$

...(1.157)

where, l = characteristic linear dimension, m

v = gas or liq velocity, m/s

ρ = gas or liq density, kg/m^3

μ = dynamic viscosity of gas or liq, Pa.s

ν = kinematic viscosity of gas or liq, m^2/s = $\dfrac{\mu}{\rho}$

$$Re_G = \frac{l.v_G.\rho_G}{\mu_G} = \frac{l.\ v_G}{\nu_G}$$

...(1.157 A)

$$Re_L = \frac{l.v_L.\rho_L}{\mu_L} = \frac{l.\ v_L}{\nu_L}$$

...(1.157 B)

Prandtl Number, Pr

The Prandtl number for mass transfer is :

$$Pr = \frac{\mu}{\rho.D_{ff}} = \frac{\nu}{D_{ff}}$$

...(1.158)

Now,

$$\frac{Pe}{Re} = \frac{\dfrac{v.l}{D_{ff}}}{\dfrac{v.l}{\nu}} = \frac{\nu}{D_{ff}} = Pr$$

...(1.159)

In heat transfer, the value of Prandtl No. is :

$$Pr = \frac{\mu.C_p}{k} = \frac{v.\rho.C_p}{k} = \frac{\nu}{\alpha}$$

where, C_p = heat capacity of gas at constant pressure, kJ/kg.K

α = thermal diffusivity, m^2/s = $\dfrac{k}{\rho.C_p}$

1.11.8. Dimensionless Formulae For Calculating Mass Transfer Coefficients

The following empirical relationships are used for the estimation of gas-film or liq-film mass transfer coefficient in the course of design calculations of packed-bed absorbers :

I. Gas-Film Mass Transfer Coefficient

$$Nu_G = 0.407 \, [Re_G]^{0.655} \cdot [Pr_G]^{0.33} \qquad \text{...(1.160)}$$

$$\text{where, } Nu_G = \frac{k_G \cdot D_{eq}}{D_{ff,G}} \qquad \text{...(1.161)}$$

$$Re_G = \frac{4v}{a} \cdot \frac{\rho_G}{\mu_G} \qquad \text{...(1.153)}$$

$$Pr_G = \frac{\mu_G}{\rho_G \cdot D_{ff,G}} = \frac{\nu_G}{D_{ff,G}} \qquad \text{...(1.158 A)}$$

k_G = gas-film mass transfer coefficient, $kmol/(s.m^2.kmol/m^3)$

$D_{ff,G}$ = diffusion coefficient of solute in the gas, m^2/s

Eqn. 1.160 holds for

$$Re_G = 10 - 10^4$$

II. Liq-Film Mass Transfer Coefficient

$$Nu_L = 0.0021 \, [Re_L]^{0.75} \cdot [Pr_L]^{0.5} \qquad \text{...(1.162)}$$

$$\text{where, } Nu_L = \frac{k_L \cdot \delta_{red}}{D_{ff,L}} \qquad \text{...(1.163)}$$

k_L = liq-film mass transfer coefficient, $kmol/(s.m^2.kmol/m^3)$

δ_{red} = reduced liq-film thickness, m

$$= \left[\frac{\nu_L^2}{g} \right]^{\frac{1}{3}}$$

$D_{ff,L}$ = diffusion coefficient of solute in the liq phase, m^2/s

$$Re_L = \frac{4\dot{L}}{A.a.\mu_L} \qquad \text{...(1.164)}$$

$\dot{L}$ = mass rate of liq, kg/s
A = packed bed cross-section, m^2
a = interfacial area of packing, m^2/m^3
μ_L = dynamic viscosity of liq, Pa.s

The wetted perimeter of the packing is :

$$Pm = \frac{A_C}{Z} = A \cdot a \qquad \qquad ...(1.165)$$

where, A_C = surface area of contact of the phases in the absorber under film conditions, m^2
A = packed-bed cross-section, m^2

The liq-film velocity thru packing is :

$$v_{L,fl} = \frac{\dot{L}}{\rho_L \cdot Pm \cdot \delta} = \frac{\dot{L}}{\rho_L \cdot A \cdot a \cdot \delta} \qquad \qquad ...(1.166)$$

where, $v_{L,fl}$ = velocity of the liq-film in the packing, m/s
δ = mean thickness of liq film, m

The equivalent diameter of the liq-film (d_{fl}) is :

$$d_{fl} = \frac{4 Pm \cdot \delta}{Pm} = 4\delta \qquad \qquad ...(1.167)$$

Hence the Reynolds number in terms of liq-film velocity and equivalent dia is :

$$Re_L = \frac{v_{L,fl} \cdot d_{fl} \cdot \rho_L}{\mu_L} \qquad \qquad ...(1.164\,A)$$

$$= \frac{4\dot{L}}{A \cdot a \cdot \mu_L} \qquad \qquad ...(1.164)$$

1.12. DIAMETER OF A PLATE COLUMN

The diameter of a plate column — bubblecap, sieve plate or valve plate column — can be obtained from :

$$D = \left(\frac{Q_v}{0.785 v} \right)^{\frac{1}{2}} \qquad \qquad ...(1.168)$$

where, D = plate column dia, m
Q_v = volumetric flowrate of vapor thru the column, m^3/s
v = vapor velocity related to the total cross-sectional area of the column, m/s

Tower dia is usually calculated on the basis of permissible optimum vapor velocity in the column:

$$v = C \left(\frac{\rho_L - \rho_G}{\rho_G} \right)^{\frac{1}{2}} \qquad \qquad ...(1.169)$$

where, C = coefficient that depends on.
    − the operating pressure of the column.

– the column load (with respect to liq stream).
– the plate spacing.
– the plate types.
   Its value can be obtained from the **Figure 1.12.1.**

$$\rho_L = \text{liq density, kg/m}^3$$
$$\rho_G = \text{gas density, kg/m}^3$$

when $\rho_L > \rho_G$, Eqn. 1.169 simplifies to :

$$v = C \left(\frac{\rho_L}{\rho_G} \right)^{\frac{1}{2}}$$ ...(1.169 A)
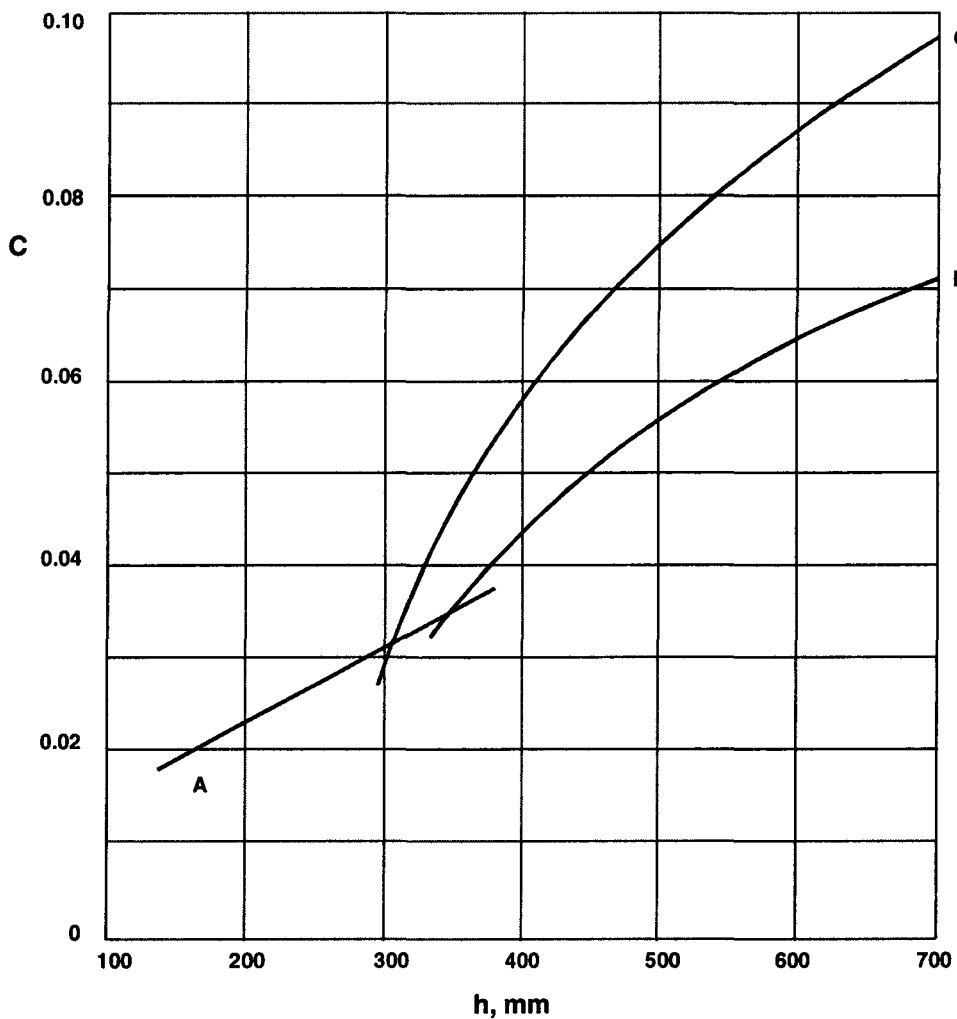
Fig. 1.12.1. *Dependence of Coefficient C on the Plate Spacing When the Tower Operates Under Atmospheric Pressure and With Medium Loads with Respect to the Liquid.*
   A & B — bubble-cap plates with round caps
   C — sieve plates

1.13. HEIGHT OF A PLATE COLUMN

The height of a plate column is the vertical distance between the top and bottom plates (Z_{Pl}). It is determined by :

$$Z_{Pl} = (N_T - 1).l \qquad \qquad ...(1.170)$$

where, N_T = total number of trays or plates

l = plate spacing, m

Use Eqn. 1.170 or 1.171 to get the value of N_T

The actual number of plates is :

$$N_{T,ac} = \frac{N_{T,th}}{\eta} \qquad \qquad ...(1.171)$$

where, $N_{T,ac}$ = total number of plates (actual).

$N_{T,th}$ = total number of plates (theoretical).

η = overall column efficiency.

1.14. CHOICE OF SOLVENT

Normally in all absorption operations three basic parameters are known :

1. the feed gas rate

2. solute content in the feed

3. operating pressure

while the solute concentration in the outlet gas stream is specified. It is the solvent whose chief function is to produce a specific solution in order to effect desired solute content in the outlet gas stream. The solvent is specified by the nature of the product. Forasmuch as the principal purpose is to remove some constituent from the gas, some choice is frequently possible. For instance, the solvent liq may be a low cost one – viz, water which is the cheapest and most plentiful solvent. Therefore, one can prescribe water as a solvent to be used on a once-thru basis when gas purification (scrubbing) rather than solute recovery is required. On the other hand, the solvent may be expensive and thus making it imperative to recycle the solvent thru a regenerator. Additionally, the following should be considered before selecting the solvent :

- *GAS SOLUBILITY* – The gas solubility should be high. The greater the solubility of solute in the solvent, the higher will be the rate of absorption and hence lower will be the necessary liq rate. This reduces the pumping cost as well as the cost of the solvent.

    Generally the solvents similar in chemical nature to the solute ensure good degree of solubility. For example, hydrocarbon oils are good solvents for absorbing benzene vapor from coke-oven gas. Hence, the coke-oven gas is scrubbed with hydrocarbon oils and not with water to remove benzene. Mind that water is a polar solvent while the HC-oils and benzene are non-polar liquids.

    Also a chemical reaction of the solvent with the solute frequently results in a very high gas solubility. But in case the solvent is to be recovered for reuse, the reaction, must be reversible.

- *VOLATILITY* – The solvent should preferably have a very low degree volatility, *i.e.*, should

have a low vapor pressure to avoid solvent loss with the exit gas stream. Usually the gas stream leaving the absorber at the top is saturated with the solvent and if the solvent is volatile it will mean much loss of the solvent.

To avoid this solvent loss, use may be made of a second, less volatile liq to recover the evaporated portion of the original solvent **(Figure 1.14.1)**

SCRUBBED GAS

NONVOLATILE ABSORBENT

RECOVERED SOLVENT + ABSORBENT

SOLVENT

Solvent Recovery Section

Absorption Section

RICH SOLUTION
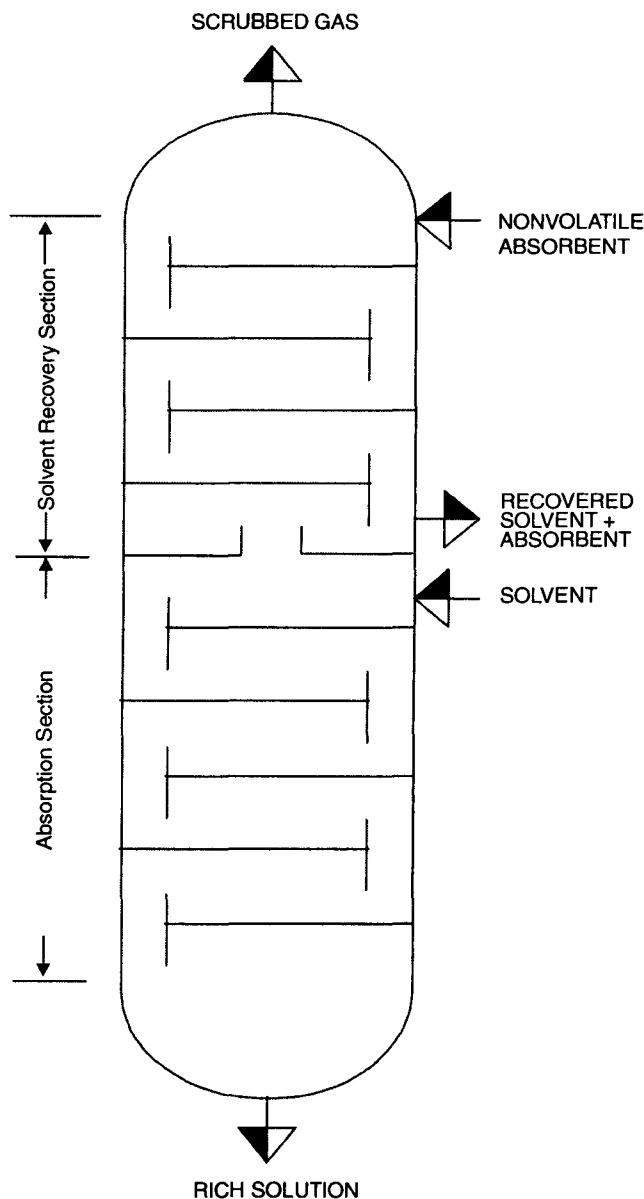
Fig. 1.14.1. *Tray Tower with the Provision of Volatile Solvent Recovery Section. A Relatively Volatile Solvent is Used in the Main Section of the Absorber Because of its Superior Solubility Characteristics and the Volatilized Solvent is Recovered by Using A Non-Volatile Absorbent Absorbing The Prime Solvent.*

• *CORROSIVENESS* – The solvent chosen must be chemically inert to the materials of construction of column internals.

- *COST* – The solvent should be inexpensive and readily available.

- *VISCOSITY* – Low viscosity solvent is always preferable. It begets certain distinct advantages.
  - rapid absorption rates
  - reduced flooding tendency
  - low pressure drops on pumping
  - good heat-transfer characteristics.

Over and above, the solvent selected should be chemically stable, noncorrosive, nontoxic, nonpolluting and of low flammability and should have a low freezing point.

Table 1.14.1. Different Concentration Terms For A Binary System of Ⓐ and Ⓑ

Concentration Term	Concentration of Ⓐ	Symbol For Concentration of Ⓐ in	
		Liq Phase	*Gas (Vap) Phase*
1. Mole Fraction	$\dfrac{\text{kmol of A}}{\text{kmol of}[A+B]}$	x_A	y_A
2. Mass Fraction	$\dfrac{\text{kg of A}}{\text{kg of}[A+B]}$	$\bar{x}_A$	$\bar{y}_A$
3. Mole Ratio	$\dfrac{\text{kmol of A}}{\text{kmol of B}}$	X_A	Y_A
4. Mass Ratio	$\dfrac{\text{kg of A}}{\text{kg of B}}$	$\bar{X}_A$	$\bar{Y}_A$
5. Molar Volume Concentration	$\dfrac{\text{kmol of A}}{\text{m}^3\text{ of }[A+B]}$	$c_{x,A}$	$c_{y,A}$
6. Mass Volume Concentration	$\dfrac{\text{kg of A}}{\text{m}^3\text{ of }[A+B]}$	$\bar{c}_{x,A}$	$\bar{c}_{y,A}$

Molar Percent To Mass Ratio and Mass-Volume Concentration

Example 1.1. A liq stream contains 60 mol% of Toluene and rest Carbon Tetrachloride. Determine :

1. Mass ratio of toluene

2. Mass-volume concentration of toluene in the liquid.

Given :

Component	*Density*
Toluene	*870 kg/m³*
Carbon tetrachloride	*1630 kg/m³*

Table 1.14.2. Concentration Conversion Table

Concentration of (A)	x_A	$\bar{x}_A$	X_A	$\bar{X}_A$	$c_{x,A}$	$\bar{c}_{x,A}$
x_A	—	$\dfrac{\dfrac{\bar{x}_A}{M_A}}{\dfrac{\bar{x}_A}{M_A}+\dfrac{1-\bar{x}_A}{M_B}}$ $= \bar{x}_A\cdot\dfrac{M_{mix}}{M_A}$	$\dfrac{X_A}{1+X_A}$	$\dfrac{\bar{X}_A}{\bar{X}_A+\dfrac{M_A}{M_B}}$	$\dfrac{c_{x,A}\cdot M_B}{\rho_{mix}+c_{x,A}(M_B-M_A)}$ $= \dfrac{c_{x,A}}{\rho_{mix}}\cdot M_{mix}$	$\dfrac{\bar{c}_{x,A}\cdot M_B}{\rho_{mix}\cdot M_A+\bar{c}_{x,A}(M_B-M_A)}$ $= \dfrac{\bar{c}_{x,A}}{\rho_{mix}}\cdot\dfrac{M_{mix}}{M_A}$
$\bar{x}_A$	$x_A\cdot\dfrac{M_A}{M_{mix}}$	—	$\dfrac{M_A\cdot X_A}{M_A\cdot X_A+M_B}$	$\dfrac{\bar{X}_A}{1+\bar{X}_A}$	$M_A\cdot\dfrac{c_{x,A}}{\rho_{mix}}$	$\dfrac{\bar{c}_{x,A}}{\rho_{mix}}$
X_A	$\dfrac{x_A}{1-x_A}$	$\dfrac{\bar{x}_A\cdot M_B}{(1-\bar{x}_A)\cdot M_A}$	—	$\bar{X}_A\cdot\dfrac{M_B}{M_A}$	$\dfrac{M_B\cdot c_{x,A}}{\rho_{mix}-M_A\cdot c_{x,A}}$	$\dfrac{\bar{c}_{x,A}}{\rho_{mix}-\bar{c}_{x,A}}\cdot\dfrac{M_B}{M_A}$
$\bar{X}_A$	$\dfrac{x_A}{1-x_A}\cdot\dfrac{M_A}{M_B}$	$\dfrac{\bar{x}_A}{1-\bar{x}_A}$	$X_A\cdot\dfrac{M_A}{M_B}$	—	$\dfrac{M_A\cdot c_{x,A}}{\rho_{mix}-M_A\cdot c_{x,A}}$	$\dfrac{\bar{c}_{x,A}}{\rho_{mix}-\bar{c}_{x,A}}$
$c_{x,A}$	$\dfrac{\rho_{mix}\cdot x_A}{M_{mix}}$	$\dfrac{\rho_{mix}\cdot\bar{x}_A}{M_A}$	$\dfrac{\rho_{mix}\cdot X_A}{M_A X_A+M_B}$	$\dfrac{\rho_{mix}\cdot\bar{X}_A}{M_A(1+\bar{X}_A)}$	—	$\dfrac{\bar{c}_{x,A}}{M_A}$
$\bar{c}_{x,A}$	$\rho_{mix}\cdot x_A\cdot\dfrac{M_A}{M_{mix}}$	$\rho_{mix}\cdot\bar{x}_A$	$(\rho_{mix}\cdot\bar{x}_A)\times$ $\dfrac{M_A}{M_A X_A+M_B}$	$\rho_{mix}\cdot\dfrac{\bar{X}_A}{1+\bar{X}_A}$	$c_{x,A}\cdot M_A$	—

M_A, M_B, M_{mix} = molar mass of A, B and the mixture, kg/kmol
M_{mix} = $M_A\cdot x_A + M_B\cdot x_B$
ρ_{mix} = density of mixture, kg/m³

Solution :

Step - (I) Mass Ratio of Toluene

Working Formula :
$$\overline{X}_T = \frac{x_T}{1-x_T} \cdot \frac{M_T}{M_C}$$

where the subscripts T and C refer to toluene and carbon tetrachloride respectively.

Now, M_T = molar mass of toluene

   = 92 kg/kmol

   M_C = molar mass of carbon tetrachloride

   = 154 kg/kmol

   x_T = mol fraction of toluene

   = 0.6

∴ $\overline{X}_T = \dfrac{0.6}{1-0.6} \cdot \dfrac{92}{154}$

   = 0.8961 kg of toluene/kg of carbon tetrachloride.   **Ans.**

Step - (II) Mass-Volume Concentration of Toluene

Working Formula : $\overline{c}_{x,T} = \rho_{mix} \cdot \overline{x}_T$

Mass ratio of toluene, $\overline{X}_T = 0.8961$

Mass fraction of toluene, $\overline{x}_T = \dfrac{\overline{X}_T}{1+\overline{X}_T} = \dfrac{0.8961}{1.8961} = 0.4726$

Now, the volume of the mixture

   = the vol. of toluene + the vol. of carbon tetrachloride

> Provided no change in volume occurs during mixing

Therefore, on the basis of 1 kg mass of the mixture,

$$\frac{0.4726}{870} + \frac{1-0.4726}{1630} = \text{vol. of 1kg mixture}$$

or. Vol. of 1 kg mixture = 8.6677 × 10⁻⁴ m³

∴ $\rho_{mix} = \dfrac{1}{8.6677 \times 10^{-4}}$

   = 1153.699 kg/m³

Therefore, the mass-volume concentration of the toluene is :

$$\overline{c}_{x,T} = \rho_{mix} \cdot \overline{x}_T = 1153.699 \times 0.4726 = 545.238 \text{ kg/m}^3.$$ **Ans.**

Volume Percent To Mass Ratio and Mass-Vol. Concentration

Example 1.2. The composition of a liq mixture is :

$$Toluene : CTC : : 58.8 : 41.2 \text{ (vol. percent)}$$

Calculate the mass ratio of toluene in the mixture, as well as its mass-vol. concentration is the same.

$$\rho_{Toluene} = 870 \text{ kg/m}^3$$

$$\rho_{CTC} = 1630 \text{ kg/m}^3$$

Solution : $\overline{X}_T = 0.8526$ kg TOL/kg CTC

$$\overline{c}_{X,T} = 535.034 \text{ kg/m}^3$$

Hints : $\overline{x}_T = \dfrac{\overline{X}_T}{1 + \overline{X}_T} = 0.4602$

$$\rho_{mix} = 1 \bigg/ \left[\frac{0.4602}{970} + \frac{1 - 0.4602}{1630} \right] = 1162.613 \text{ kg/m}^3$$

$$\overline{c}_{x,T} = \rho_{mix} \cdot \overline{x}_T = 535.034$$

Mole Fraction To Molar Volume Concentration and Mass-Volume Concentration

Example 1.3. The Composition of a liq mixture is :

Benzene : 0.4 mol fraction

Toluene : 0.6 mol fraction

Compute the

1. molar volume concentration of benzene.

2. mass-volume concentration of toluene.

Given :	*Component*	*Density*
	Benzene	*890 kg/m³*
	Toluene	*870 kg/m³*

Solution : We shall use the conversion formulae as presented in **Table 14.2.**

Step - (I) Molar Volume Concentration of Benzene

Working Formulae : $\qquad c_{x,B} = \dfrac{\rho_{mix} \cdot x_B}{M_{mix}}$

where, subscript 'B' stands for Benzene.

Now, $\quad x_B \quad = $ mol fraction of benzene $= 0.4$

$\qquad M_{mix} \quad = $ mol. wt. of the mixture

$\qquad\qquad\quad = M_B \cdot x_B + M_T \cdot x_T$

$\qquad\qquad\quad = 78 \times 0.4 + 92 \times 0.6$

$\qquad\qquad\quad = 86.4$ kg/kmol

$\qquad \rho_{mix} \quad = $ density of the mixture

$$\overline{X}_B = \frac{M_B}{M_T} \cdot \frac{x_B}{x_T}$$

$$= \frac{78}{92} \cdot \frac{0.4}{0.6}$$

$$= 0.5652 \text{ kg of benzene/kg of toluene}$$

$\therefore \quad \overline{x}_B = \text{mass fraction of benzene}$

$$= \frac{\overline{X}_B}{1 + \overline{X}_B}$$

$$= \frac{0.5652}{1 + 0.5652}$$

$$= 0.3611$$

Assuming no change in volume occurs upon mixing.

$$\frac{1}{\rho_{mix}} = \frac{\overline{x}_B}{\rho_B} + \frac{\overline{x}_T}{\rho_T}$$

$$= \frac{0.3611}{890} + \frac{1 - 0.3611}{870}$$

$$= 1.14009 \times 10^{-3}$$

$\therefore \quad\quad\quad\quad \rho_{mix} = 877.1174 \text{ kg/m}^3.$

Therefore, the molar volume concentration of benzene

$$c_{x,B} = \frac{877.1174 \times 0.4}{86.4}$$

$$= 4.0607 \text{ kmol of benzene/m}^3 \text{ of liq} \quad\quad\quad \textbf{Ans.}$$

Step - (II) Mass-Volume Concentration of Toluene

$$\overline{c}_{x,T} = \rho_{mix} \cdot x_T \cdot \frac{M_T}{M_{mix}}$$

$$= 877.1174 \, (0.6) \, \frac{92}{86.4}$$

$$= 560.3805 \text{ kg/m}^3. \quad\quad\quad \textbf{Ans.}$$

Aliter : $\quad\quad \overline{c}_{x,T} = \rho_{mix} \cdot \overline{x}_T$

$$= 877.1174 \, (1 - 0.3611)$$

$$= 560.3903 \text{ kg/m}^3$$

Density, Mass Ratio and Molar Volume Concentration

Example 1.4. Equal volumes of benzene and nitrobenzene are mixed to produce a liq mixture. Assuming no change in volume occurs upon mixing, determine :

1. the density of the mixture

2. the mass ratio of nitrobenzene in the mixture

3. the molar volume concentration of nitrobenzene in the mixture.

Given : Component   Density

*   Benzene   890 kg/m³*

*   Nitrobenzene 1200 kg/m³*

Solution :

Step - (I) Density of the Mixture

For as much as no volume change occurs upon mixing of equal volumes of benzene and nitrobenzene, so

Vol. of mix = vol. of benzene **(B)** + vol. of nitrobenzene **(NB)**

∴   2 m³ mix = 1m³ of **B** + 1m³ of **NB**

$$= 890 \frac{kg}{m^3} \times 1m^3 + 1200 \frac{kg}{m^3} \times 1m^3$$

$$= 2090 \text{ kg}$$

$$\rho_{mix} = \frac{1}{2}(2090) \text{ kg}/m^3$$

$$= 1045 \text{ kg/m}^3.$$

Step - (II) Mass Ratio of Nitrobenzene

Basis : 2m³ of mixture

Parameter	*Benzene*	*Nitrobenzene*
Volume	1m³	1m³
Mass	890 kg	1200 kg
Moles	$\frac{890}{78}$	$\frac{1200}{139}$
	= 11.41 kmol	= 8.633 kmol
Mole fraction	$\frac{11.41}{11.41 + 8.633}$	$1 - 0.5692$
		= 0.4308
	= 0.5692	

Therefore, the mass ratio of nitrobenzene in the mixture,

$$\overline{X}_{NB} = \frac{M_{NB}}{M_B} \cdot \frac{x_{NB}}{1 - x_{NB}}$$

$$= \frac{139}{78} \cdot \frac{0.4308}{0.5692}$$

$$= 1.3487 \text{ kg \textbf{NB}/kg \textbf{B}}$$ **Ans.**

Step - (III) Molar Volume Concentration of NB in the Mixture

Working Formulae : $\overline{c}_{x,NB} = \rho_{mix} \cdot \overline{x}_{NB}.$

$$c_{x,NB} = \bar{c}_{x,NB} / M_{NB}$$

Now,
$$\bar{x}_{NB} = \frac{\bar{X}_{NB}}{1 + \bar{X}_{NB}} = \frac{1.3487}{1 + 1.3487} = 0.57423$$

∴
$$\bar{c}_{x,NB} = (1045)(0.57423) = 600.073 \text{ kg/m}^3 \approx 600 \text{ kg/m}^3$$

∴
$$c_{x,NB} = \frac{600}{139} \text{ kmol/m}^3 = 4.3165 \text{ kmol/m}^3 \qquad \underline{\text{Ans.}}$$

DENSITY OF MIXTURE

Example 1.5. A liquid mixture consists of the following components :

Acetone : Carbon Disulfide : Chloroform :: 40 : 20 : 20 (mol %)

Calculate the density of the mixture considering that no change in volume did occur upon mixing.

Solution : We shall use the formula :

$$V_{mix} = \Sigma V_j \qquad \text{(where subscript j stands for individual component)}$$

Component	Molar Mass (kg/kmol)	Density (kg/m³)	Mol (%)
Acetone, $CH_3 COCH_3$	58	802	40
Carbon disulfide, CS_2	76	1290	40
Chloroform, $CHCl_3$	119.5	1530	20

Now **Mol % = Vol %**

∴ 100m³ of liquid mixture

= 40 m³ of acetone + 40 m³ of carbon disulfide + 20 m³ of chloroform

∴ $100 \times \rho_{mix} = 40 \times 802 + 40 \times 1290 + 20 \times 1530$

∴ $\rho_{mix} = 1142.8 \text{ kg/m}^3$ **Ans.**

Partial Pressure, Mole and Mass Fractions and Density

Example 1.6. Air at atmospheric pressure and a temperature of 307 K is saturated with water vapor. Determine the :

1. partial pressure of the air

2. mole fractions of the air

3. mass fractions of the air

4. density of air-vap mixture

Compare this density with the density of dry air.

Given : The atmospheric pressure = 99.33 kPa

Solution :

Step - (I) Partial Pressure of Air

$$p_{air} = P - p_{w/vap}$$
$$= 99.33 - 5.319 \text{ kPa}$$
$$= 94.011 \text{ kPa}$$

where, P = total pressure
$p_{w/vap}$ = partial pressure of water vapor

cf. Press. of satd. water vapor
$= 5.319$ kPa at 307 K

Step - (II) Mole Fraction of Water Vapor

Partial Press. = Mol fraction × Total Press.

$$y = \frac{p_{w/vap}}{P}$$

$$= \frac{5.319}{99.33}$$

$$= 0.0535$$

Step - (III) Mass Fraction of Water Vapor

$$\bar{y} = \frac{M_{H_2O} \cdot y}{M_{H_2O} \cdot y + M_{air}(1-y)}$$

$$= \frac{18(0.5356)}{18(0.0535) + 29(1 - 0.0535)}$$

$$= 0.03389$$

Step - (IV) Mass Ratio of Water Vapor

$$\bar{Y} = \frac{\bar{y}}{1 - \bar{y}}$$

$$= \frac{0.03389}{1 - 0.03389}$$

$$= 0.03507 \text{ kg water vap/kg of dry air}$$

Step - (V) Density of Air-Water Vapor Mixture

$$\rho_{mix} = \rho_{air} + \rho_{w/vap}$$

$$= \frac{M_{air}}{22.4} \cdot \frac{p_{air}}{P_o} \cdot \frac{T_o}{T} + \frac{M_{H_2O}}{22.4} \cdot \frac{p_{w/vap}}{P_o} \cdot \frac{T_o}{T}$$

$$= \frac{1}{22.4} \cdot \frac{T_o}{T} \cdot \frac{1}{P_o} \cdot \left[M_{air} \cdot p_{air} + M_{H_2O} \cdot p_{w/vap} \right]$$

$$= \frac{1}{22.4} \cdot \frac{273}{307} \cdot \frac{1}{101.325} [29 \times 94.011 + 18 \times 5.319]$$

$$= 1.1056 \text{ kg/m}^3$$

Aliter :
$$M_{mix} = M_{H_2O} \cdot y_{w/vap} + M_{air} \cdot (1 - y_{w/vap})$$

$$= 18 \times 0.0535 + 29\,(1 - 0.0535)$$
$$= 28.4115 \text{ kg/kmol}$$

$$\rho_{mix} = \frac{M_{mix}}{22.4} \cdot \frac{P}{P_o} \cdot \frac{T_o}{T}$$

$$= \frac{28.4115}{22.4} \cdot \frac{99.33}{101.325} \cdot \frac{273}{307}$$

$$= 1.1056 \text{ kg/m}^3$$

Now, density of dry air :

$$\rho_{air,dry} = \frac{M_{air}}{22.4} \cdot \frac{P}{P_o} \cdot \frac{T_o}{T}$$

$$= \frac{29}{22.4} \cdot \frac{99.33}{101.325} \cdot \frac{273}{307}$$

$$= 1.1285 \text{ kg/m}^3$$

Comparison : The moist-air (satd.) at 307 K and 99.33 kPa is lighter than dry air at the same temperature and pressure by

$$\frac{\rho_{air-vap}}{\rho_{air,dry}} = \frac{1.1056}{1.1285} = 0.979 \text{ times}$$

MASS RATIO AND DENSITY

Example 1.7. Air is saturated with ethyl alcohol vapor. The total system pressure of the air-alcohol vapor mixture is 80 kPa. The temperature is 333 K.

Determine :

1. the mass ratio of ethyl alcohol in the mixture

2. the density of the mixture.

Assume ideal behavior of both components of air-ethyl alcohol vapor mixture.

Solution : Saturated vap. press. of ethyl alcohol at 333 K

$$= 40 \text{ kPa.}$$

$$\therefore \qquad p_{air} = P - p_{air}$$
$$= 80 - 40$$
$$= 40 \text{ kPa}$$

Step - (I) Mole Fraction of Alcohol Vapor

Partial press. = Mole fraction × Total press.

$$\therefore \qquad y_{alc} = \frac{p_{alc}}{P}$$

$$= \frac{40}{80}$$

$$= 0.5$$

Step - (II) Mass Fraction of Water Vapor

$$\bar{y}_{alc} = \frac{M_{alc} \cdot y_{alc}}{M_{alc} \cdot y_{alc} + M_{air}(1 - y_{alc})}$$

where,

M_{alc} = mol. wt. of ethyl alcohol = 46 kg/kmol

M_{air} = mol. wt. of air = 29 kg/kmol

$$= \frac{46(0.5)}{46(0.5) + 29(1 - 0.5)}$$

$$= 0.61333$$

Step - (II) Mass Ratio of Ethyl Alcohol in the Vapor Mixture

$$\bar{Y}_{alc} = \frac{\bar{y}_{alc}}{1 - \bar{y}_{alc}}$$

$$= \frac{0.61333}{1 - 0.61333}$$

$$= 1.5861 \text{ kg EtOH/ kg of dry air} \qquad [\text{EtOH} = C_2H_5OH]$$

Step - (IV) Density of Air-Alcohol Vap. Mix.

$$\rho_{mix} = \rho_{air} + \rho_{alc}$$

$$= \frac{M_{air}}{22.4} \cdot \frac{p_{air}}{P_o} \cdot \frac{T_o}{T} + \frac{M_{alc}}{22.4} \cdot \frac{p_{alc}}{P_o} \cdot \frac{T_o}{T}$$

$$= \frac{1}{22.4} \cdot \frac{T_o}{T} \cdot \frac{1}{P_o} \left[M_{air} \cdot p_{air} + M_{alc} \cdot p_{alc} \right]$$

$$= \frac{1}{22.4} \cdot \frac{273}{333} \cdot \frac{1}{101.325} \left[29 \times 40 + 46 \times 40 \right]$$

$$= 1.0836 \text{ kg/m}^3 \qquad \qquad \underline{\text{Ans.}}$$

Mass-Volume Concentrations

Example 1.8. A gas mixture consists of :

Methane — 60 mol %

Hydrogen — 26 mol %

Ethylene — 14 mol %

Assuming the components of the mixture behaving ideally, compute the individual mass-volume concentrations.

The gas mixture is at a pressure of 3.0397 MPa and at a temperature of 293K.

Solution : The individual mass-volume concentration can be computed from the relationship :

$$\bar{c}_{x,A} = \rho_{mix} \cdot \frac{M_A}{M_{mix}} \cdot x_A$$

Component	Mol. Wt. (kg/kmol)	Mol (%)	Mol Fraction
Methane, CH_4	16	60	0.6
Hydrogen, H_2	2	26	0.26
Ethylene, C_2H_4	28	14	0.14

Now $\rho_{mix} = \rho_{Me} + \rho_H + \rho_{Et}$

$$= \frac{M_{Me}}{22.4} \cdot \frac{p_{Me}}{P_o} \cdot \frac{T_o}{T} + \frac{M_H}{22.4} \cdot \frac{p_H}{P_o} \cdot \frac{T_o}{T} + \frac{M_{Et}}{22.4} \cdot \frac{p_{Et}}{P_o} \cdot \frac{T_o}{T}$$

where, the subscripts :
Me = Methane
H   = Hydrogen
Et = Ethylene

$$= \frac{1}{22.4} \cdot \frac{T_o}{T} \cdot \frac{1}{P_o} \left[M_{Me} \cdot p_{Me} + M_H \cdot p_H + M_{Et} \cdot p_{Et} \right]$$

Now,

$p_{Me} = x_{Me} \cdot P = 0.6 \times 3.0397 = 1.8238$ MPa

$p_H = x_H \cdot P = 0.26 \times 3.0397 = 0.7903$ MPa

$p_{Et} = x_{Et} \cdot P = 0.14 \times 3.0397 = 0.4255$ MPa

$\therefore$ $\rho_{mix} = \frac{1}{22.4} \cdot \frac{273}{293} \cdot \frac{1}{0.101325} \left[16 \times 1.8238 + 2 \times 0.7903 + 28 \times 0.4255 \right]$

$= 17.5189$ kg/m^3

Now, $M_{mix} = M_{Me} \cdot x_{Me} + M_H \cdot x_H + M_{Et} \cdot x_{Et}$

$= 16 \times 0.6 + 2 \times 0.26 + 28 \times 0.14$

$= 14.04$ kg/kmol

$\therefore$ $\bar{c}_{x,Me} = \rho_{mix} \cdot \frac{M_{Me}}{M_{mix}} \cdot x_{Me}$

$= 17.5189 \frac{16}{14.04} (0.6)$

$= 11.9787$ kg/m^3 of gas mixture   **Ans.**

$\bar{c}_{x,H} = \rho_{mix} \cdot \frac{M_H}{M_{mix}} \cdot x_H$

$= 17.5189 \frac{2}{14.04} (0.26)$

$= 0.6488$ kg/m^3 of gas mixture   **Ans.**

$\bar{c}_{x,Et} = \rho_{mix} \cdot \frac{M_{Et}}{M_{mix}} \cdot x_{Et}$

$= 17.5189 \frac{28}{14.04} (0.14)$

$= 4.8913$ kg/m^3 of gas mixture   **Ans.**

Mole Fraction can Never be Negative

***Example 1.9.** For a binary gas mixture composed of components A and B, the following expression*

$$y_A = \frac{M_B \cdot c_{y,A}}{\rho_{mix} + (M_B - M_A) \cdot c_{y,A}}$$

represents the mole fraction of A. The mole fraction B also can be expressed thru similar relationship.

Show that for any values of M_B and M_A, the term y_A can never be negative.

Solution : The molecular weight of the gas mixture :

$$M_{mix} = M_A \cdot y_A + M_B \cdot y_B$$
$$= M_A \cdot y_A + M_B (1 - y_A)$$
$$= (M_A - M_B) \cdot y_A + M_B$$

Given :

$$y_A = \frac{M_B \cdot c_{y,A}}{\rho_{mix} + (M_B - M_A) \cdot c_{y,A}}$$

or, $y_A \cdot \rho_{mix} + y_A \cdot (M_A - M_B) \cdot c_{y,A} = M_B \cdot c_{y,A}$

or, $y_A \cdot \rho_{mix} = c_{y,A} \cdot [M_A - M_B] \cdot y_A + M_B \cdot c_{y,A} = c_{y,A} \cdot M_{mix}$

∴

$$y_A = \frac{c_{y,A}}{\rho_{mix}} \cdot M_{mix}$$

Now, $c_{y,A}$ and ρ_{mix} both are positive quantities.

M_{mix} being the sum of two positive quantities

$$M_{mix} = M_A \cdot x_A + M_B \cdot x_B$$

is also positive.

Therefore, y_A can never be negative irrespective of the values of M_B and M_A.

Likewise, y_B can never be negative irrespective of the values of M_B and M_A.

Overall Mass Transfer Coefficient and The Diffusion Resistance

***Example 1.10.** An absorption column is operated at a pressure of 314 kPa. The equilibrium compositions of the gaseous and liquid phases are characterized by the Henry's Law equation :*

$$p^* = 10.666 \times 10^6 \cdot x, \text{ Pascal.}$$

If the individual mass transfer coefficients are :

$$k_{G,y} = 1.075 \frac{kmol}{h.m^2.(\Delta y = 1)}$$

$$k_{L,x} = 22 \frac{kmol}{h.m^2.(\Delta x = 1)}$$

determine :

1. the overall mass transfer coefficients

2. the ratio of the different resistances of the liq and gas phases.

Check and Comment.

Solution : We can compute the values of overall gas-phase and liq-phase mass transfer coefficients by using Eqns. 1.27 and 1.30

$$\frac{1}{K_{G,y}} = \frac{1}{k_{G,y}} + \frac{m}{k_{L,x}}$$ [Eqn. 1.27]

$$\frac{1}{K_{L,x}} = \frac{1}{k_{G,y} \cdot m} + \frac{1}{k_{L,x}}$$ [Eqn. 1.27]

In order to find the value of m (the slope of the operating line), we are to transform the equilibrium relationship to the form :

$$y^* = m.x$$

Since for system obeys Henry's Law at equilibrium,

$$y^* = \frac{H.x}{P}$$ [Eqn. 1.3]

$$= \frac{10.666 \times 10^6}{314000}. x$$

$$= 33.968 \, x$$

∴ $$m = 33.968$$

Step - (I) Overall Gas Phase Mass Transfer Coefficient

$$\frac{1}{K_{G,y}} = \frac{1}{1.075} + \frac{33.968}{22}$$

$$= 2.47423$$

∴ $$K_{G,y} = 0.40416 \, kmol / \left[h.m^2. (\Delta y = 1) \right]$$ **Ans.**

Step - (II) Overall Liquid Phase Mass Transfer Coefficient

$$\frac{1}{K_{L,x}} = \frac{1}{(1.075)(33.968)} + \frac{1}{22}$$

$$= 0.07284$$

∴ $$K_{L,x} = 13.7287 \, kmol / \left[h.m^2. (\Delta x = 1) \right]$$

Step - (III) Check

When the main diffusion resistance is concentrated in the gaseous phase

$$K_{G,y} \approx k_{G,y}$$ [Eqn. 1.35)

In case the main diffusion resistance is concentrated in the liquid phase

$$K_{L,x} \approx k_{L,x} \qquad \text{[Eqn. 1.36)}$$

$$\therefore \qquad m = \frac{k_{L,x}}{k_{G,y}} \approx \frac{K_{L,x}}{K_{G,y}} = \frac{13.7287}{0.40416} = 33.9684$$

Step - (IV) Ratio of Diffusion Resistances

| *Overall mass transfer resistance* | = | *Gas-film resistance* | + | *Liquid-film resistance* |

Therefore, for driving force of Δy, the gas-film resistance

$$= \frac{1}{K_{G,y}} = \frac{1}{1.075} = 0.93023 \frac{h.m^2}{kmol}$$

liq-film resistance $\qquad = \dfrac{m}{k_{L,x}} = \dfrac{33.968}{22} = 1.544 \dfrac{h.m^2}{kmol}$

The ratio of liq-film to gas-film diffusion resistances :

$$\frac{m}{k_{L,x}} : \frac{1}{k_{G,y}} = 1.544 / 0.93023 = 1.6598$$

Similarly for a driving force Δx the ratio of liq-film to gas-film resistances is :

$$\frac{1}{k_{L,x}} : \frac{1}{k_{G,y}.m} = \frac{1}{22} : \frac{1}{1.075 \times 33.968} = 1.6598$$

Comment : The ratio of diffusion resistances to mass transfer remains the same irrespective of the driving force, with respect to gas-phase or liq-phase, taken into consideration.

The diffusion resistance of the liquid phase is 1.6598 times that of the gaseous phase.

DRIVING FORCE

Example. 1.11. Air (at 102 kPa) containing 15 mol% of acetylene (C_2H_2) is brought into contact with water (298 K) containing 0.30×10^{-3} kg C_2H_2 per kg of water.

Calculate the driving force to mass transfer and the direction of mass transfer.

Henry's Law constant for acetylene for its aqueous solution at 298 K

$$H = 1.3466 \times 10^8, Pa.$$

Solution : The driving force behind solute transfer across the gas-liq interface can be expressed in terms of

1. partial pressure difference
2. mole fraction difference
3. mole ratio difference

Step - (I) Partial Pressure of Acetylene

The partial pressure of acetylene in air

$$p = y.P$$

$$= 0.15 \times 102 \text{ kPa}$$
$$= 15.3 \text{ kPa}$$

Step - (II) Mole Fraction of Acetylene in Water

The given aq. phase contains 0.30×10^{-3} kg C_2H_2 per kg of water, *i.e.*,

$$\overline{X}_A = 0.30 \times 10^{-3}$$

Mole fraction of acetylene in water :

$$x_A = \dfrac{\overline{X}_A}{\overline{X}_A + \dfrac{M_A}{M_W}} = \dfrac{0.30 \times 10^{-3}}{0.30 \times 10^{-3} + \dfrac{26}{18}} = 2.076 \times 10^{-4}$$

Step - (III) Equilibrium Partial Pressure of Acetylene

Now the partial pressure of acetylene in the gaseous phase in equilibrium with the aq. phase containing 2.076×10^{-4} mol fraction of $C_2 H_2$ should according to Henry's Law, be :

$$\textbf{p* = H.x} \qquad\qquad\qquad\qquad\qquad\qquad\qquad \text{[Eqn. 1.1]}$$
$$= (1.3466 \times 10^8)\,(2.076 \times 10^{-4})$$
$$= 27955.416 \text{ Pa}$$
$$= 27.955 \text{ kPa}$$

However, the actual partial pressure of acetylene over this is lower :

$$\textbf{p = 15.3 kPa}$$

Therefore, the given gas-liq system will seek to attain the state of equilibrium thru transfer of solute (acetylene) from the liquid to the gas phase, *i.e.*, more and more dissolved acetylene will pass from water to air till the partial pressure of acetylene in the air equalizes the equilibrium partial pressure of acetylene **(p*)**.

Therefore, the direction of mass (acetylene) transfer is :
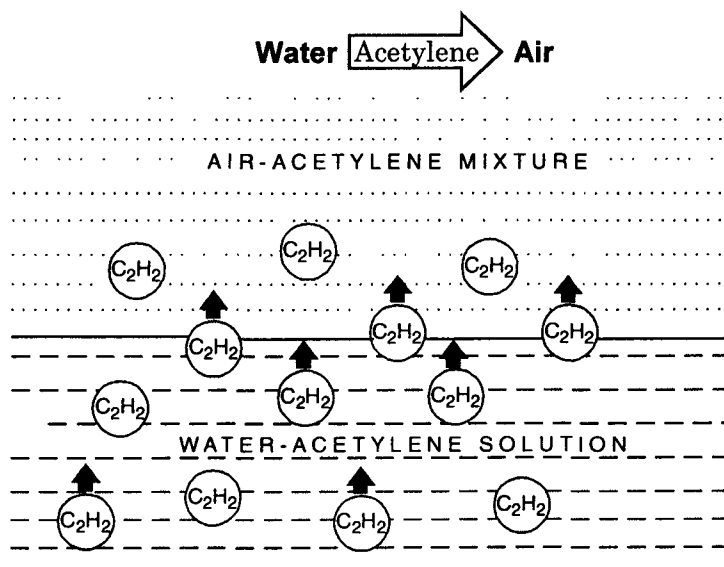
Fig. 1/Example 1.11. *Diffusion of Acetylene from Its Aqueous Solution to the Gas Phase because of its higher Equilibrium Partial Pressure than its Actual Partial Pressure Over the Liquid Phase.*

Step - (IV) Driving Force With Respect to Gas Phase

The driving force to this solute transfer at the beginning is :

1. Partial Pressure Difference

$$\Delta p = p^* - p_{actual}$$
$$= 27.955 - 15.3$$
$$= 12.655 \text{ kPa} \qquad \text{Ans.}$$

2. Mole Fraction Difference

$$\Delta y = y^* - y$$
$$= \frac{27.955}{102} - 0.15$$
$$= 0.1240 \qquad \text{Ans.}$$

3. Mole Ratio Difference

$$\Delta Y = Y^* - Y$$

$$= \frac{y^*}{1-y^*} - \frac{y}{1-y}$$

$$= \frac{\frac{27.955}{102}}{1-\frac{27.955}{102}} - \frac{0.15}{1-0.15}$$

$$= 0.37754 - 0.17647$$

$$= 0.20107 \text{ kmol of } C_2H_2 / \text{kmol of air} \qquad \text{Ans.}$$

Step - (V) Driving Force With Respect to Liquid Phase

The driving force for the transport of solute can also be expressed in terms of mole fraction difference or mole ratio difference of solute in liq phase.

The actual partial pressure of acetylene = 15.3 kPa

In order to exist in equilibrium with the air-acetylene gas phase containing this much amount of acetylene, the water, as per Henry's Law should have an acetylene concentration of

$$x^* = \frac{p_{actual}}{H} \qquad \qquad \text{...[Eqn. 1.1]}$$

$$= \frac{15.3 \times 1000}{1.3466 \times 10^8}$$

$$= 1.1361 \times 10^{-4}$$

However, the actual strength of acetylene in water is much greater

$$x = 2.076 \times 10^{-4}$$

Therefore, for this system to approach the state of equilibrium, the mole fraction of acetylene in the water should diminish, *i.e.*, the acetylene will pass from the water to the air.

Hence, the driving force to effect this mass transfer at the beginning is :

1. Mole Fraction Difference

$$\Delta x = x - x^*$$
$$= 2.076 \times 10^{-4} - 1.1361 \times 10^{-4}$$
$$= 0.9399 \times 10^{-4} \qquad\qquad \textbf{Ans.}$$

2. Mole Ratio Difference

$$\Delta X = X - X^*$$

$$= \frac{x}{1-x} - \frac{x^*}{1-x^*}$$

$$= \frac{2.076 \times 10^{-4}}{1 - 2.076 \times 10^{-4}} - \frac{1.1361 \times 10^{-4}}{1 - 1.1361 \times 10^{-4}}$$

$$= 2.0764 \times 10^{-4} - 1.1361 \times 10^{-4}$$

$$= 0.9402 \times 10^{-4} \text{ kmol of } C_2H_2 / \text{ kmol of water} \qquad \textbf{Ans.}$$

DRIVING FORCE

Problem 1.12. Solve above Example 1.11. when the water at 298K contains 0.164×10^{-3} kg C_2H_2 per kg of water.

Ans. No mass transfer will take place

Hints :

$$x = \frac{\dfrac{0.164 \times 10^{-3}}{26}}{\dfrac{1}{18}} \, 1.1353 \times 10^{-4}$$

$$p^* = H.x = 15.289 \text{ kPa}$$

$$p_{actual} = 15.3 \text{ kPa}$$

$$\Delta p \approx 0$$

$$\Delta y = y^* - y = \frac{15.289}{102} - 0.15 = 0.1498 - 0.15 \approx 0$$

$$\Delta Y = Y^* - Y = \frac{y^*}{1-y^*} - \frac{y}{1-y} = 0.1763 - 0.1764 \approx 0$$

Driving Force in Terms of Molar Volume and Mass-Volume Concentrations

Example 1.13. Calculate the driving forces in Example 1.11 in terms of :

1. molar volume concentration

2. mass-volume concentration

Solution : We shall use the relationship

$$c_{x,A} = \rho_{mix} \cdot \frac{x_A}{M_{mix}}$$

to determine the molar volume concentration of acetylene.

Now, $\quad x_A = 2.076 \times 10^{-4}.$ [Example 1.11]

$$x_w = 1 - 2.076 \times 10^{-4} = 0.9997 \approx 1$$

The solution is very dilute with respect to acetylene. Since the aq. soln. of acetylene is very dilute

$$\rho_{mix} \approx \rho_w$$

$$M_{mix} \approx M_w$$

$$\begin{aligned} M_{mix} &= M_A \cdot x_A + M_w \cdot (1 - x_A) \\ &= 2.076 \times 10^{-4} \times 26 + 18 \,(\, 1 - 2.076 \times 10^{-4}) \\ &= 18.0016 \text{ kg/kmol} \end{aligned}$$

$$\begin{aligned} M_{mix}^* &= M_A \cdot x_A^* + M_w \cdot (1 - x_A^*) \\ &= (26 - 18) \times 1.136 \times 10^{-4} + 18 \\ &= 18.0009 \end{aligned}$$

$$M_{mix} \approx M_{mix}^* \approx M_w$$

$$\therefore \qquad c_{x,A}^* = \frac{\rho_w}{M_w} \cdot x_A^*$$

and

$$c_{x,A} = \frac{\rho_w}{M_w} \cdot x_A$$

$\therefore$ Molar volume concentration driving force

$$\Delta c_{x,A} = c_{x,A} - c_{x,A}^*$$

$$= \frac{\rho_w}{M_w} \cdot [x_A - x_A^*]$$

$$= \frac{1000}{18} \cdot \left(0.9399 \times 10^{-4}\right) \frac{\text{kmol}}{\text{m}^3} \qquad \text{[Example 1.11]}$$

$$= 5.2216 \times 10^{-3} \text{ kmol } C_2H_2 \text{ /m}^3 \text{ of solution.}$$

Now, mass-volume concentration

$$\bar{c}_{x,A} = \rho_{mix} \cdot \frac{M_A}{M_{mix}} \cdot x_A \approx \rho_w \cdot \frac{M_A}{M_w} \cdot x_A$$

$\therefore$ Mass-volume concentration driving force

$$\Delta \bar{c}_{x,A} = \bar{c}_{x,A} - \bar{c}_{x,A}^*$$

$$\approx \rho_w \cdot \frac{M_A}{M_w} \cdot [x_A - x_A^*]$$

$$= 1000 \cdot \frac{26}{18} \cdot [0.9399 \times 10^{-4}]$$

$$= 0.1357 \text{ kg } C_2H_2 \text{ / kg of aq. soln.} \qquad \textbf{Ans.}$$

DRIVING FORCE OF MASS TRANSFER

Example 1.14. A binary vapor system containing equimolar quantities of Benzene and Chloroform is introduced to a column where it comes into contact with a liquid stream containing 56 mol% Benzene and rest Chloroform.

Determine the

1. direction of mass transfer

2. driving force of mass transfer process with respect to the vapor and the liquid phases at the point of vapor inlet.

The column operates at 98 kPa pressure.

Equilibrium Compositions of Liq and Vap for Benzene-Chloroform System At 98 kPa System Pressure

Chloroform in vapor (mol %)	*0*	*10*	*20*	*30*	*40*	*50*	*60*
Chloroform in liquid (mol %)	*0*	*8*	*15*	*22*	*29*	*36*	*44*

Solution : The vapor contains :

50 mol % **Benzene**

50 mol % **Chloroform**

The contacting liq contains :

56 mol % **Benzene**

44 mol % **Chloroform**

However as the given **Vap-Liq Eqil. Data** of benzene-chloroform system : 50 mol% of benzene in vap should remain in equilibrium with (100 − 36), *i.e.*, 64 mol% benzene in the liq.

Forasmuch as the given liquid contains 56 mol% of benzene, so there will occur benzene transfer from the vap to the liq phase.

Again as per the same **VLE-Data** of benzene-chloroform system :

50 mol% of chloroform in the vap should remain in equilibrium with 36 mol% of chloroform in the liquid.

However, the given liq contains 44 mol% of chloroform. So chloroform will diffuse into the vapor phase from the liquid to attend the equilibrium composition.

Therefore, there will occur *counterdiffusion* :

Benzene diffusing from the vap phase to the liq phase.

Chloroform diffusing from the liq phase to the vap phase.   **Ans.**

2. Now, $y_B = y_C = 0.5$ where subscripts

$x_B = 0.56$; $x_C = 0.44$ B = Benzene

C = Chloroform

From the given **VLE-Data** :

$$x_C^* = 0.36 \text{ for } y_C = 0.5$$

But $\qquad x_C = 0.44$

∴ Driving force the chloroform transfer in the liq phase is

$$\Delta x_C = x_C - x_C^*$$
$$= 0.44 - 0.36$$
$$= 0.10 \text{ kmol Chloroform / kmol of vap.} \qquad \textbf{Ans.}$$

Again, $\qquad y_C^* = 0.60 \text{ for } x_C = 0.44$

But $\qquad y_C = 0.5$

Similarly, the driving force for transfer of benzene in liq phase :

$$\Delta x_B = x_B^* - x_B$$
$$= 0.64 - 0.50$$
$$= 0.14 \text{ kmol Benzene / kmol of liq} \qquad \textbf{Ans.}$$

in vap phase

$$\Delta y_B = y_B - y_B^*$$
$$= 0.5 - 0.4$$
$$= 0.1 \text{ kmol Benzene / kmol of vap} \qquad \textbf{Ans.}$$

Overall Mass Transfer Coefficients in Different Units

Example 1.15. A solute gas carried by the inert gas (which does not pass into the liq) nitrogen is being absorbed in an absorber at a system pressure P_{abs} = 101.325 kPa and temperature of 293K such that the overall coefficient of mass transfer is :

$K_{G,c}$ = 12 kmol / (h.m².kmol/m³)

Determine the values of overall coefficient of mass transfer in the following units :

1. $K_{G,y}$, kmol / (h.m².kmol/kmol)

2. $K_{G,p}$, kmol / (h.m². Pa)

3. $K_{G,\bar{y}}$, kmol / (h.m². kg/kg of inert gas)

Solution : The **rate of solute transfer during any absorption process** is given by :

$$N = K_{G,c} . A . \Delta c_y = K_{G,y} . A . \Delta y = K_{G,p} . A . \Delta p$$

where, N = molar rate of mass transfer, kmol/h

1. From the foregoing relationship :

$$K_{G,y} . \Delta y = K_{G,c} . \Delta c$$

∴
$$K_{G,y} = K_{G,c} \frac{\Delta c}{\Delta y}$$

Now, from Table 14.2. we have :

$$c = \rho_{mix} \cdot \frac{y}{M_{mix}}$$

$$= \frac{1}{22.4} \cdot \frac{P}{P_O} \cdot \frac{T_O}{T}$$

> For a mixture of ideal gases we have :
>
> $$\frac{\rho_{mix}}{M_{mix}} = \frac{P}{R.T} = \frac{1}{22.4} \cdot \frac{P}{P_O} \cdot \frac{T_O}{T}$$

In the given example, $P = P_O$

$$\therefore \qquad \frac{\Delta c}{\Delta y} = \frac{1}{22.4} \cdot \frac{T_O}{T} = \frac{1}{22.4} \cdot \frac{273}{293} = 0.0415955$$

$$\therefore \qquad K_{G,y} = 12(0.0415955) = 0.499146 \text{ kmol/(h.m}^2\text{.kmol/kmol)} \qquad \textbf{Ans.}$$

2. Again $\qquad K_{G,y} \cdot \Delta y = K_{G,p} \cdot \Delta p$

Now, $\qquad\qquad y = \dfrac{p}{P}$

$$\therefore \qquad\qquad \frac{y}{p} = \frac{1}{P}$$

$$\therefore \qquad\qquad \frac{\Delta y}{\Delta p} = \frac{1}{P}$$

$$K_{G,p} = K_{G,y} \cdot \frac{\Delta y}{\Delta p}$$

$$= 0.499146 \left(\frac{1}{P} \right)$$

$$= 0.499146 / 101.325$$

$$= 4.9261 \times 10^{-3} \text{ kmol/(h.m}^2\text{.kPa)} \qquad \textbf{Ans.}$$

3. Now the mass rate of solute transfer

$$\dot{M} = M_S \cdot K_{G,y} \cdot A \cdot \Delta y = K_{G,\overline{y}} \cdot A \cdot \Delta \overline{Y}$$

where, $\dot{M}$ = mass rate of solute transfer, kg/h
          M_s = molar mass of solute, kg/kmol

$$\therefore \qquad K_{G,\overline{y}} = K_{G,y} \cdot \frac{\Delta y}{\Delta \overline{Y}} \cdot M_s$$

From Table 14.2

$$\overline{Y} = \frac{M_s}{M_{IG}} \cdot \frac{y}{(1-y)} \qquad \text{(where, } M_{IG} = \text{molar mass of inert gas, kg/kmol)}$$

For low values of y,

$$\frac{y}{1-y} \approx y$$

$$\therefore \qquad \frac{y}{\overline{Y}} = \frac{M_{IG}}{M_s}$$

$$\therefore \qquad \frac{\Delta y}{\Delta \overline{Y}} = \frac{M_{IG}}{M_s}$$

$$\therefore \qquad K_{G,\overline{Y}} = K_{G,y} \cdot M_{IG}$$
$$= 0.499146 \ (28)$$
$$= 13.9760 \ \text{kg/(h.m}^2. \ \text{kg solute/kg of inert gas)} \qquad \textbf{Ans.}$$

Overall Gas-Phase Mass Transfer Coefficient

Example 1.16. Carbon dioxide gas is absorbed in a packed tower 600mm dia and filled with 38mm Raschig rings up to a height of 3m. Air is used as carrier-gas while 2.5 (N) caustic soda solution as scrubbing liquid (solvent).

The gas rate is 1224 kg/(h.m²)

The liq rate is 14184 kg/(h.m²)

The carbon dioxide concentration in the inlet and outlet gas streams is 325 ppm and 35 ppm respectively.

Determine the value of overall volumetric gas-phase mass transfer coefficient, if the tower is operated at 101.325 kPa.

Solution : The solvent stream is solute-free.

The value of overall volumetric mass transfer coefficient w.r.t gas phase, $K_{G,y}$.a can be computed from the mass balance over the tower (**Figure 1/Example. 1.16**) :

$$G_s.A. \ (y_b - y_t) = N = A. \ Z. \ K_{G,y}.a. \ P. \ \Delta y_{1m}$$

From the given data :

$$y_b = 325 \ \text{ppm} = 325 \times 10^{-6}$$
$$G' = 1224 \ \text{kg/(h.m}^2)$$

$$\therefore \qquad G_s = \frac{1224}{29} = 42.2068 \ \text{kmol/(h.m}^2)$$

where, $M_{air} = 29$ kg/kmol

$y_t = 35$ ppm $= 35 \times 10^{-6}$

$x_t = 0$ as the solvent is solute-free

$L' = 14184$ kg/(h.m²)

Now, 2.5 (N) NaOH soln.

$$= 2.5 \times 40 \ \text{gm NaOH/litre of soln.}$$
$$= 100 \ \text{kg NaOH/m}^3 \ \text{soln.}$$

$\therefore$ 1m³ given NaOH soln. contains :
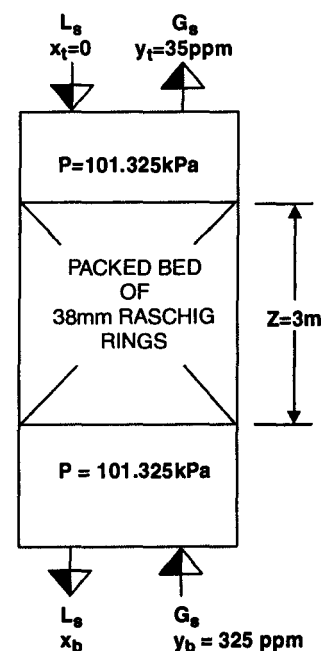
100 kg NaOH + 900 kg H₂O

Fig. 1/Example 1.16. *CO₂ Absorption By Caustic Soda 2.5 (N) Soln. In a 3m Packed Bed of 38mm Raschig Rings.*

i.e., $\dfrac{100}{40}$ kmol NaOH + $\dfrac{900}{18}$ kmol H$_2$O | Assuming density of solution = 1000 kg/m^3 |

i.e., 2.5 kmol NaOH + 50 kmol H$_2$O

∴ 52.5 kmol NaOH soln. weighs about 1000 kg.

∴ Mol. wt of the 2.5 (N) NaOH soln. = $\dfrac{1000}{52.5}$ = 19.0476 kg/kmol

Aliter :

1. $M_{mix} = \dfrac{x_A}{\bar{x}_A} \cdot M_A$

| $x_A = \dfrac{2.5}{50 + 2.5} = 0.0476$ |
| $\bar{x}_A = \dfrac{100}{100 + 900} = 0.1$ |

          $= \dfrac{0.0476}{0.1} \cdot (40)$

          $= 19.0476$

2. $M_{mix} = M_A \cdot x_A + M_B \cdot x_B$
          $= 40 \times 0.476 + 18 \times (1 - 0.476) = 19.0476$ kg/kmol

∴   Liq rate = 14185/19.0476 = 744.6607 $\dfrac{kmol}{h.m^2}$

Step - (I) Driving Force

The NaOH soln. used is fairly concentrated one. Therefore, the vap. press. of CO$_2$ over the soln. may be assumed to be negligible, *i.e.,*

$$p^* \approx 0$$

That means, the equilibrium mole fraction of solute in gas phase is practically zero, *i.e.,*

$$y^* \approx 0 \qquad \boxed{\text{cf. } p^* = y^* \cdot P}$$

Hence the entire resistance to CO$_2$ absorption lies in the gas phase. The driving force at the packed-bed-top

$$= y_t - y_t^*$$
$$= 35 \times 10^{-6} - 0$$
$$= 35 \times 10^{-6}$$

The driving force at the packed-bed bottom

$$= y_b - y_b^*$$
$$= 325 \times 10^{-6} - 0$$
$$= 325 \times 10^{-6}$$

∴ Log-mean driving force

$$\Delta y_{lm} = \frac{325 \times 10^{-6} - 35 \times 10^{-6}}{\ln\left(\dfrac{325 \times 10^{-6}}{35 \times 10^{-6}}\right)} = 1.30133 \times 10^{-4}$$

Substituting the known values in the foregoing mass balance :

$$42.2068 \times (325 - 35) \times 10^{-6} = 3 \times K_{G,y} \cdot a \times 101.325 \times 1.30133 \times 10^{-4}.$$

$$\left(\frac{kmol}{h.m^2}\right) \qquad\qquad (m) \qquad\qquad (kPa)$$

$$\therefore \qquad\qquad K_{G,y}.a = 0.30942 \; \frac{kmol}{h.m^3.kPa} \qquad\qquad \textbf{Ans.}$$

Variation of Overall Volumetric Gas-Phase Mass Transfer Coefficient With the Inlet Solute Concentration

Problem 1.17. Show how the overall volumetric transfer coefficient, $K_{G,y}.a$ in the above Example 1.16 will vary with the CO_2 content in the inlet gas stream changing to following values.

280 ; 300 ; 320 ; 330 ; 340 (ppm)

in order that same CO_2 concentration in the exit gas is to be maintained over the same packed bed and under same gas and liq rates.

The operating pressure and temperature and solvent strength remaining the same.

Show the variation graphically.

Solution :

y_b, [ppm]	280	300	320	330	340
$K_{G,Y}.a \left(\dfrac{kmol}{h.m^3.kPa}\right)$	0.28872	0.29830	0.30727	0.31154	0.31568
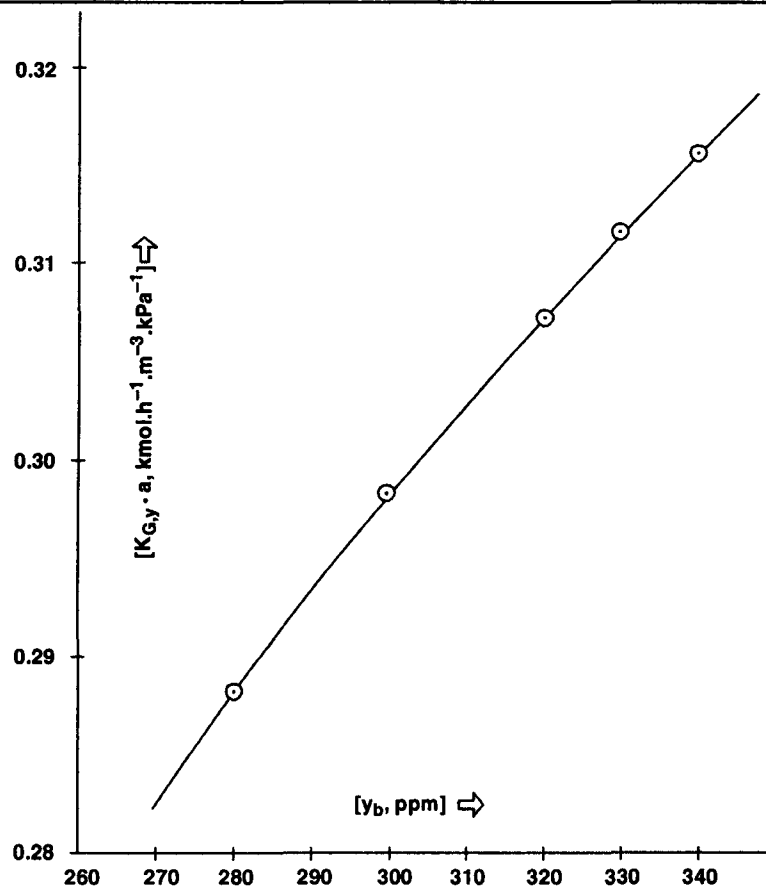
Hints : G_s = $42.2068 \, kmol/(h.m^2)$

   Z =   3m

   P =   101.325 kPa

   y_t = 35×10^{-6}

Mass balance relationship :

$$42.2068 \times (y_b - y_t) = 3 \times K_{G,y} \cdot a \times 101.325 \times \Delta y_{lm}$$

or, $$0.138849 \times (y_b - y_t) = K_{G,y} \cdot a \cdot \dfrac{y_b - y_t}{\ln\left(\dfrac{y_b}{y_t}\right)}$$

$\therefore$ $$K_{G,y} \cdot a = 0.138849 \times \ln\left(\dfrac{y_b}{y_t}\right)$$

$$\text{c.f. } \Delta y_{lm} = \dfrac{\Delta y_b - \Delta y_t}{\ln\left(\dfrac{\Delta y_b}{\Delta y_t}\right)}$$

$$= \dfrac{(y_b - 0) - (y_t - 0)}{\ln\left(\dfrac{y_b - 0}{y_t - 0}\right)}$$

Mass Fraction and Factor of Extraction

Example 1.18 . A binary mixture of air and carbon tetrachloride (CTC) vapor compressed to a pressure of 980 kPa is cooled in a tubular water-cooled condenser. Condensation of CTC sets in at 313 K.

Determine :

1. the mass fraction (in percent) of CTC in the air in the initial mixture.

2. the factor of extraction from the gas mixture after cooling it to 300K.

Solution : First of all we are to calculate the mole fraction of CTC at these two temperature : 313 K and 300 K.

Thereafter we'll determine the mass fraction, mole ratio and extraction factor in subsequence.

Step - (I) Mole Fraction of CTC at 313 K

Saturated vapor pressure of CTC at 313 K = 29.33 kPa

$$p = y.P$$

or, $$29.33 = y \, (980)$$

$\therefore$ $$y = 0.02993$$

Step - (II) Mass Fraction of CTC at 313 K

Working Formula : $$\bar{y}_{CTC} = \dfrac{M_{CTC}}{M_{mix}} \cdot y_{CTC}$$

M_{CTC} = molar mass of CTC = 154 kg/kmol

M_{mix} = molar mass of CTC-AIR mixture

$$= M_{CTC} \, y_{CTC} + M_{AIR} \, y_{AIR}$$
$$= 154 \times 0.02993 + 29 \times (1 - 0.02993)$$
$$= 32.7412 \, kg/kmol$$

$\therefore$ $$\bar{y}_{CTC} = \dfrac{154}{32.7412} (0.02993) = 0.1407 \; i.e., \, 14.07\%$$ **Ans.**

Step - (III) Mole Fraction of CTC at 300 K

Saturated vap. pressure of CTC at 300K = 17.066 kPa

$\therefore$ 17.066 = y (980)

or,   y = 0.017414

Step - (IV) Mass Fraction of CTC at 300 K

$$M_{mix} = 154 \, (0.017414) + 29 \, (1 - 0.017414)$$
$$= 31.176 \text{ kg/kmol}$$

$\therefore$ $\bar{y}_{CTC} = \dfrac{154}{31.176} \, (0.017414) = 0.08601$ *i.e.*, 8.60%

Step - (V) Extraction Factor : $e_a = \dfrac{\bar{Y}_{CTC, \, in} - \bar{Y}_{CTC, \, fin}}{\bar{Y}_{CTC, \, in}}$

where, $\bar{Y}_{CTC} = \dfrac{\bar{y}_{CTC}}{1 - \bar{y}_{CTC}}$

$\therefore$ $\bar{Y}_{CTC/313} = \dfrac{0.1407}{1 - 0.1407} = 0.1637$

$\bar{Y}_{CTC/300} = \dfrac{0.08601}{1 - 0.08601} = 0.0941$

$\therefore$ $e_a = \dfrac{0.1637 - 0.0941}{0.1637} = 0.4251 = 42.51\%$ **Ans.**

Solvent Flowrate

Example 1.19. In a packed-bed air drying tower, moist-air is scrubbed with concentrated sulfuric acid. The capacity of the scruber is 2000m³/h (based on dry air in standard conditions). The column is operated at atmospheric pressure with the following moisture content in the air and acid :

Stream	Initial Moisture Content	Final Moisture Content
Air	0.025 kg/kg of dry air	0.006 kg/kg of dry air
Acid	0.5 kg/kg of monohydrate	1.5 kg/kg of monohydrate

Solution : Drawing mass-balance on the overall column :

$$\overset{\bullet}{L}_s \left(\bar{X}_b - \bar{X}_t \right) = \overset{\bullet}{G}_s \cdot \left(\bar{Y}_b - \bar{Y}_t \right)$$

where, $\overset{\bullet}{L}_s$ = solvent rate on solute-free basis, *i.e.*, flowrates of monohydrates, kg/h

$\overset{\bullet}{G}_s$ = gas rate on solute-free basis, *i.e.*, flowrates of air on dry basis, kg/h

Now, $Q_{V,G}$ = volumetric flowrate of gas

                    = 2000 m³/h of dry air

Since the density of dry air under standard conditions is 1.293 kg/m^3,

$$\overset{\bullet}{G}_S = 2000 \times 1.293 = 2586 \text{ kg of dry air/h}$$

Given : $\overline{Y}_b = 0.025$ kg/kg of dry air

$\overline{Y}_t = 0.006$ kg/kg of dry air

$\overline{X}_b = 1.5$ kg/kg of monohydrate

$\overline{X}_t = 0.5$ kg/kg of monohydrate

$$\therefore \overset{\bullet}{L}_S (1.5 - 0.5) = 2586 (0.025 - 0.006)$$

or, $\overset{\bullet}{L}_S = 49.134$ kg/h   **Ans.**

Overall Mass Transfer Coefficient

Example 1.20 An absorber irrigated with water operates at a pressure of P = 104.857 kPa.

The film mass transfer coefficients are :

$$k_{G,p} = 2.76 \times 10^{-3} \text{ kmol/(m}^2.h.kPa)$$
$$k_{L,x} = 1.17 \times 10^{-4} \text{ m/s}$$

when the solute content in the liquid phase is 1 mol%

The equation of the equilibrium line is :

$$y^* = 1.02\ x$$

where, y = mol fraction of solute in the vap phase in equilibrium with the liq*

x = mol fraction of solute in the liq

Determine the overall mass transfer coefficient.

Solutions : Use is to be made of the eqn.

$$\frac{1}{K_{G,p}} = \frac{1}{k_{G,p}} + \frac{H}{k_{L,x}}$$

Now, $y^* = \dfrac{H}{P}.x$ ...[Eqn. 1.3]

$y^* = m.x$ Given

$\therefore$ $m = \dfrac{H}{P}$ where, H = Henry's Law Constant

m = slope of equilibrium line

$\therefore$ $H = m.p = 1.02 \times 104.857$ kpa $= 106.954$ kPa

$k_{G,p} = 2.76 \times 10^{-3}$ kmol/(h.m^2.kPa)

$k_{L,x} = 1.17 \times 10^{-4} \times 3600$ m/h

$= 0.4212 \text{ kmol}\Big/\Big(\text{h.m}^2.\dfrac{\text{kmol}}{\text{m}^3}\Big)$

$$= 0.4212 \, c_x \, \frac{kmol}{h.m^2}$$

where, c_x = concentration of solute in the liq phase

$$= \frac{\rho_{mix}}{M_{mix}} \cdot x_A$$

Since, the soln, is very dilute,

$$\rho_{mix} \approx \rho_w = 1000 \ kg/m^3$$

$$M_{mix} \approx M_w = 18 \ kg/kmol$$

$$x_A = \text{mol fraction of solute in liq}$$

$$= 0.01$$

$$\therefore \quad k_{L,x} = 0.4212 \left(\frac{1000}{18} \times 0.01 \right)$$

$$= 0.234 \, \frac{kmol}{h.m^2}$$

Substituting the known values in Eqn. 1.31 we get :

$$\frac{1}{K_{G,p}} = \frac{1}{2.76 \times 10^{-3}} + \frac{106.954}{0.234}$$

$$\therefore \quad K_{G,p} = 0.001220 \, \frac{kmol}{h.m^2.kPa} \qquad \qquad \textbf{Ans.}$$

Number of Overall Transfer Units

Example 1.21. An Acetone-Air mixture containing 1.5 mol% acetone is treated in a packed-bed absorption column where it is washed by a countercurrent stream of water to bring the acetone content of the exit gas stream down to 1% of the initial value.

Assume Henry's Law holds good here, estimate the number of transfer units required.

Given :

Gas Flowrate = 3600 kg/(h.m²)

Liq Flowrate = 5760 kg/(h.m²)

The VLE -relationship of air-acetone system is :

$$y^* = 1.75x$$

where, y* = mol fraction of acetone in the vap in equilibrium with a mol fraction x in the liq

Solution : The system is dilute, so

mol fraction = mol ratios

i.e., $\quad$ y = Y

and $\quad$ x = X

TOWER BOTTOM

$$y_b = 1.5\% = 0.015 = Y_b$$

$$G' = 3600 \text{ kg/(h.m}^2) \approx G_s'$$

$$x_b = \text{unknown}$$

TOWER TOP

$$y_t = 0.015 \times \frac{1}{100} = 0.00015 = Y_t$$

$$L' = 5760 \text{ kg/(h.m}^2) \approx L_s'$$

$$x_t = 0$$

Step - (I) Molar Flowrates on Solute-Free Basis

$$G_s = \frac{G_s'}{M_{air}} = \frac{3600}{29} = 124.1379 \text{ kmol}/(\text{h.m}^2)$$

$$L_s = \frac{L_s'}{M_w} = \frac{5760}{18} = 320 \text{ kmol}/(\text{h.m}^2)$$

Step - (II) Liq Composition at Tower Bottom

Use is to be made of overall mass balance :

$$G_s (y_b - y_t) = L_s (x_b - x_t)$$

or, $124.1379 (0.015 - 0.00015) = 320 (x_b - 0)$

$\therefore$ $x_b = 5.76 \times 10^{-3}$

Step - (III) Number of Overall Transfer Units

Working Formula : $[NTU]_{O,G} = \displaystyle\int_{y_t}^{y_b} \frac{dy}{y - y^*} = \frac{y_b - y_t}{[y - y^*]_{lm}}$ ...[Eqn. 1.22]

where, $[y-y^*]_{lm}$ = log-mean-driving-force = $\dfrac{\Delta y_b - \Delta y_t}{\ln\left(\dfrac{\Delta y_b}{\Delta y_t}\right)}$

Now,
$$\begin{aligned}
\Delta y_b &= [y - y^*]_b \\
&= y_b - y_b^* \\
&= y_b - m.x_b \\
&= 0.015 - 1.75 (5.76 \times 10^{-3}) \\
&= 0.00492 \\
\Delta y_t &= [y - y^*]_t \\
&= y_t - y_t^*
\end{aligned}$$

$$= y_t - m.x_t$$
$$= 0.00015 - 0$$
$$= 0.00015$$

$$\therefore \quad [y - y^*]_{lm} = \frac{0.00492 - 0.00015}{\ln\left(\dfrac{0.00492}{0.00015}\right)} = 1.366 \times 10^{-3}$$

$$\therefore \quad [NTU]_{O,G} = \frac{0.015 - 0.00015}{1.366 \times 10^{-3}} = 10.871 \qquad \textbf{Ans.}$$

Aliter : Absorption factor

$$e_a = \frac{L_s/G_s}{m} \qquad\qquad \text{...[Eqn. 1.60]}$$

$$= \frac{320/124.1379}{1.75}$$

$$= 1.473$$

$$[NTU]_{O,G} = \frac{\left[\ln\left(1 - \dfrac{1}{e_a}\right) \cdot \dfrac{y_b}{y_t} + \dfrac{1}{e_a}\right]}{1 - \dfrac{1}{e_a}} \qquad\qquad \text{...[Eqn. 1.24]}$$

$$[NTU]_{O,G} = \frac{\ln\left[\left(1 - \dfrac{1}{1.473}\right) \cdot \dfrac{0.015}{0.0015} + \dfrac{1}{1.473}\right]}{1 - \dfrac{1}{1.473}}$$

$$= 10.868 \qquad\qquad \textbf{Ans.}$$

$$\text{Similarly,} \quad [NTU]_{O,L} = [NTU]_{O,G} \cdot \left(\frac{m.G_s}{L_s}\right)$$

$$= (10.871)\left(\frac{1.75 \times 124.1379}{320}\right)$$

$$= 7.38 \qquad\qquad \textbf{Ans.}$$

Number of Overall Transfer Units

Problem 1.22. If in the above Example 1.21, the concentration of acetone in the exit gas is to be reduced to the following values :

2% ; 3% ; 4% ; 5% ; 10% ; 15% of inlet concentration

determine how many overall transfer units would be required in each case. The gas and liquid rates remain the same and the same VLE-eqn. remains valid.

Plot the variation graphically.

Solution :

$[NTU]_{O,G} =$	8.802	7.578	6.760	6.115	4.231	3.227
$[NTU]_{O,L} =$	5.975	5.144	4.589	4.151	2.872	2.190
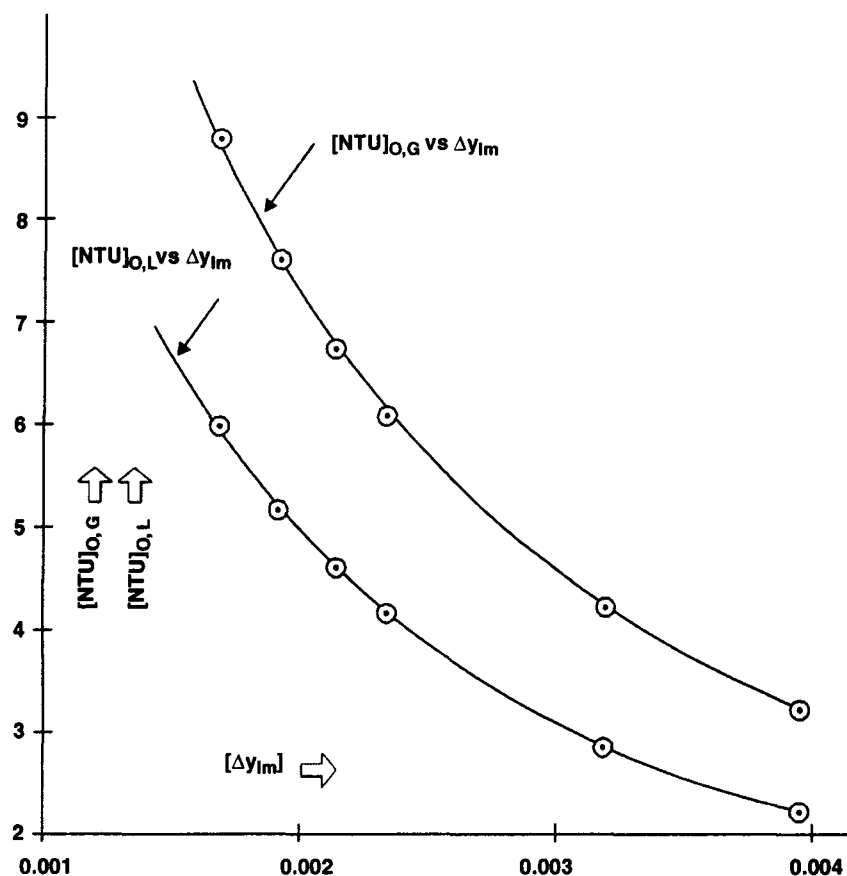
Figure 1/Example 1.22. *Dependence of Number of Transfer Units On Mean Driving Force*

Hints : $x_b = \dfrac{G_s}{L_s} \cdot (y_b - y_t) = \dfrac{124.1379}{320} (0.015 - y_t) = 0.3879 (0.015 - y_t)$

y_t	0.0003	0.00045	0.0006	0.00075	0.0015	0.00225
x_b	0.0057	0.00564	0.00558	0.00552	0.00523	0.00494
Δy_b	0.00502	0.00513	0.00523	0.00534	0.00584	0.00635
Δy_t	0.0003	0.00045	0.0006	0.00075	0.0015	0.00225
Δy_{lm}	0.00167	0.00192	0.00213	0.00233	0.00319	0.00395
$[NTU]_{O,G}$	8.802	7.578	6.760	6.115	4.231	3.227
$[NTU]_{O,L}$	5.975	5.144	4.589	4.151	2.872	2.190

Height of Transfer Unit. Number of Transfer Units and Packed Bed Height

Example 1.23. Hydrogen sulfide is absorbed in a packed bed absorption tower using triethanolamine-water solvent in a countercurrent arrangement.

The column operates at 300K and at atmospheric pressure.

The feed gas contains 0.03 kmol H_2S/kmol of inert hydrocarbon gas (which is insoluble in the scrubbing liquor). And it is desired to reduce the H_2S content of exit gas to 1% of its inlet concentration.

H_2S gets physically absorbed in the aq. TEA forming a solution such that the following VLE-relationship :

$$Y^* = 2X$$

holds good, where

Y^* = *mole ratio of solute in the vapor in equilibrium with the soln. kmol H_2S/kmol of inert gas*

X = *mole ratio of solute in the soln., kmol H_2S/kmol of solvent*

The solvent enters the tower H_2S-free and leaves with a load of 0.0135 kmol H_2S/kmol of solvent.

The feed gas stream enters the column at the rate of 60 kmol of inert HC/h per m^2 of tower cross-section.

If the absorption process is a gas controlled one, calculate

1. the height of the packed bed necessary

2. the height of a transfer unit

3. the number of such transfer units.

The overall volumetric coefficient for absorption is :

$$K_{G,Y}.a = 145 \frac{kmol}{h.m^3.(\Delta Y = 1)}$$

Solution : The rate of mass transfer, during absorption, in a packed bed of depth Z and area of cross-section A is

N = Mass transfer coefficient × Packed bed × Driving force
    (Volumetric)   *Volume*

$$= (K_{G,Y}.a)\,(A.Z)\,(\Delta Y_{lm}), \frac{kmol}{h}$$

where, N = rate of mass transfer, kmol/h

$$\Delta Y_{lm} = \text{log-mean driving force} = \frac{\Delta Y_b - \Delta Y_t}{\ln\left(\dfrac{\Delta Y_b}{\Delta Y_t}\right)}$$

Since the driving force varies thruout the packed bed, it is more appropriate to express the overall driving force in terms of logarithmic mean.

Again, $N = G_s \times [Y_b - Y_t] \times A$

$$\left(\frac{kmol\ inert}{h.m^2}\right)\left(\frac{kmol\ H_2S}{kmol\ inert}\right)[m^2]$$

$\therefore$ $G_s . [Y_b - Y_t]. A = K_{G,Y} . a. A. Z. \Delta Y_{lm}$ ....(1)

now, $G_s = 60\left(\dfrac{kmol\ inert\ HC}{h.m^2}\right)$

$$Y_b = 0.03\left(\frac{kmol\ H_2S}{kmol\ inert\ HC}\right)$$

$$Y_t = 1\%\ of\ 0.03 = 0.0003\ \frac{kmol\ H_2S}{kmol\ inert\ HC}$$

$$K_{G,Y}.\ a = 145\ \frac{kmol}{h.m^3.(\Delta Y = 1)}$$

$$\Delta Y_b = \Delta Y_b - Y_b^* = 0.03 - 2\ (0.0135) = 0.003\ \frac{kmol\ H_2S}{kmol\ inert\ HC}$$

$$\Delta Y_t = \Delta Y_t - Y_t^* = 0.0003 - 2\ (0) = 0.0003\ \frac{kmol\ H_2S}{kmol\ inert\ HC}$$

$\therefore$ $\Delta Y_{lm} = \dfrac{0.003 - 0.0003}{\ln\left(\dfrac{0.003}{0.0003}\right)} = 1.17259 \times 10^{-3}$

Substituting the known values in Eqn. (1) we get :

$60(0.03 - 0.0003) = 145 \times Z \times 5.8629 \times 10^{-4}$

$Z = 10.4807$ **Ans.**

Height of transfer unit :

$$[HTU]_{O,G} = \frac{G_s}{K_{G,Y}.a}$$

$$= \frac{60}{145},\ \frac{kmol\ inert\ HC / h.m^2}{kmol\ inert\ HC / h.m^3}$$

$= 0.41379$ **Ans.**

Number of transfer units

$$[NTU]_{O,G} = \frac{10.4807}{0.41379} = 25.32 \approx 25\ (say)$$ **Ans.**

Gas-Film Mass Transfer Coefficient

Example 1.24 In a packed-bed absorber, the overall liq film mass transfer coefficient $K_{L,c}$ .a for absorption of sulfur dioxide in water is 0.0025 kmol/(s.m³ .kmol/m³).

If the same column is used for the absorption of NH_3 in water at the same liquor rate but varying gas rates, derive an expression for the determination of overall liquid film coefficient $K_{L,c}.a$ for absorption of ammonia.

$$D_{ff,SO_2\text{-}air} = 10.3 \times 10 \ m^2/s \qquad at \ 273K$$

$$D_{ff,NH_3\text{-}air} = 17 \times 10^{-6} \ m^2/s \qquad at \ 273K$$

Henry's Law constant for aq. soln. of SO_2

$$= 50 \ kPa/(kmol/m^3)$$

All data are expressed at the same temperature.

Solution : We shall use Eqn. 1.32

$$\frac{1}{K_{L,c}} = \frac{1}{k_{G,p}.H} + \frac{1}{k_{L,c}} \qquad \qquad ...\text{Eqn. 1.32}$$

or,

$$\frac{1}{K_{L,c}.a} = \frac{1}{k_{G,p}.a.H} + \frac{1}{k_{L,c}.a}$$

or,

$$\frac{1}{0.0025} = \frac{1}{k_{G,p}.a.H} + \frac{1}{k_{L,c}.a} \qquad \qquad ....(1)$$

SO_2 is moderately soluble in water. Therefore, it is reasonable to assume that liq and gas phase resistances are equal :

i.e.,

$$\frac{1}{k_{G,p}.a.H} \approx \frac{1}{k_{L,c}.a}$$

Therefore, from Eqn. (1) :

$$\frac{1}{k_{G,p}.a.H} = \frac{1}{k_{L,c}.a} = \frac{1}{2 \times 0.0025}$$

$\therefore$

$$k_{G,p}.a.\ H = k_{L,c}.a = 0.005 \ \frac{kmol}{s.m^3.\left(kmol/m^3\right)}$$

For, SO_2,

$$H = 50 \ kPa/(kmol/m^3)$$

$$k_{G,p}.a = \frac{0.005}{50} \ \frac{\dfrac{kmol}{s.m^3.\left(kmol/m^3\right)}}{\dfrac{kPa}{kmol/m^3}} = 0.0001 \ \frac{kmol}{s.\ m^3.kPa}$$

Now,

$$Nu_G = 0.407 \ [Re_G]^{0.655} \cdot [Pr_G]^{0.33} \qquad \boxed{\text{Eqn. 1.60}}$$

or,

$$\frac{k_G.D_{eq}}{D_{ff,G}} = 0.407\left[Re_G\right]^{0.655} \cdot \left[\frac{G}{D_{ff,G}}\right]^{0.33}$$

$$\therefore \qquad k_G \propto [D_{ff,G}]^{0.67}$$

Therefore, for NH_3 absorption

$$k_{G,p}.a = 0.0001 \left(\frac{17 \times 10^{-6}}{10.3 \times 10^{-6}} \right)^{0.67} = 1.3989 \times 10^{-4} \ \frac{kmol}{s.m^3.kPa}$$

However, unlike sulfur dioxide NH_3 is highly soluble in water. Therefore, the liq-film resistance to the diffusion of ammonia is negligibly small, *i.e.*,

$$\frac{1}{k_{L,c}} \approx \frac{1}{k_{G,p}}$$

and as such

$$k_{G,p} \ .a = K_{G,p} \ .a = 1.389 \times 10^{-4} \ \frac{kmol}{s.m^3.kPa} \qquad\qquad \textbf{Ans.}$$

Mean Driving Force, Number of Transfer Units

Example 1.25. Benzene vapor carried by an inert gas mixture is scrubbed with hydrocarbon oil in a packed bed whereupon the benzene is absorbed in the countercurrent stream of scrubbing liquor which enters the column solute-free at the top of the column.

The feed gas contains 4% benzene vapor by volume and 80% of the benzene is extracted in the packed bed.

The concentration of benzene in the oil leaving the absorber is 0.02 kmol of C_6H_6/ kmol of pure oil.

The equilibrium reaction may be taken as

$$Y^* = 0.126X$$

where X and Y represent mole ratios of benzene in the soln. and in the feed gas.

Solution :   Vol % = Mol %

$\therefore$ $y_b = 0.04$

Extraction factor, $e_a = 80\% = 0.8$

$$\therefore \qquad \frac{Y_b - Y_t}{Y_b} = 0.8 \qquad\qquad\qquad\qquad ....(1)$$

$$X_t = 0$$

$$X_b = 0.02 \ kmol \ of \ C_6H_6/kmol \ of \ \textbf{pure oil}$$

$$Y^* = 0.126 \, X \qquad\qquad\qquad\qquad\qquad \text{Given}$$

$$\therefore \qquad m = 0.126$$

Now,

$$Y_b = \frac{y_b}{1 - y_b} = \frac{0.04}{1 - 0.04} = 0.041666$$

From Eqn. (1)

$$\frac{0.041666 - Y_t}{0.041666} = 0.8$$

$$\therefore \qquad \qquad \qquad Y_t = 0.008333 \text{ kmol of } C_6H_6/\text{kmol of inert gas}$$

Driving force at the column bottom :

$$\Delta Y_b = Y_b - Y_b^* = 0.04166 - 0.126 \times 0.02 = 0.03914 \; \frac{\text{kmol of } C_6H_6}{\text{kmol of inert gas}}$$

Driving force at the column top :

$$\Delta Y_t = Y_t - Y_t^* = 0.00833 - 0 = 0.00833 \; \frac{\text{kmol of } C_6H_6}{\text{kmol of inert gas}}$$

$\therefore$ MDF (*i.e.*, log-mean driving force)

$$\Delta Y_{lm} = \frac{Y_b - Y_t}{\ln\left(\dfrac{\Delta Y_b}{\Delta Y_t}\right)} = \frac{0.03914 - 0.00833}{\ln\left(\dfrac{0.03914}{0.00833}\right)} = 0.01991 \; \frac{\text{kmol of } C_6H_6}{\text{kmol of inert gas}} \qquad \textbf{Ans.}$$

The number of transfer units :

$$[NTU]_{O,G} = \frac{Y_b - Y_t}{\Delta Y_{lm}} = \frac{0.041666 - 0.00833}{0.01991} = 1.674$$

Solvent Rate; Mean Driving Force; Total Number of Transfer Units

Example 1.26. Sulfur dioxide carried by inert gas (nitrogen) is charged to an absorption tower operating at 101.325 kPa.

The gas is scrubbed in a countercurrent stream of water at 293K such that the amount of SO_2 in the feed system is 5% (vol.).

The solvent rate is 20% greater than the minimum theoretical value.

In order to achieve absorption at the rate of 1 ton SO_2 per hour, estimate :

1. the rate of waterflow needed

2. the MDF (mean driving force) of the process

3. the total number of transfer units.

The VLE-line may be assumed to be straight and the coordinates of two of its points are :

[p_{SO2} = 5.2 kPa . $\overline{X}$ = 0.007 kg SO_2/kg water]

[p_{SO2} = 3.78 kPa . $\overline{X}$ = 0.005 kg SO_2/kg water]

Solution : First of all, we're to establish the **VLE**-relationship; thereafter we will proceed to calculate the desired liq flowrate, **MDF** and **NTUs**.

Given : $\qquad\qquad\qquad y_b = 0.05$ $\qquad\qquad\qquad\qquad\qquad$ cf. Mol% = Vol%

$$\therefore \qquad\qquad Y_b = \frac{y_b}{1 - y_b} = \frac{0.05}{1 - 0.05} = 0.05263$$

and

$$\overline{Y}_b = \frac{64}{28} \cdot Y_b = \frac{64}{28} \cdot (0.05263) = 0.12029$$

Given : $\qquad\qquad \dot{L}_S = \dot{L}_{s,min} + 20\% \dot{L}_{s,min} = 1.2\,\dot{L}_{s,min}$

where, $\dot{L}_{s,min}$ = theoretical minimum rate of solvent on solute-free basis, kg/h

$$= \frac{\dot{M}}{\overline{X}_b^* - \overline{X}_t}$$
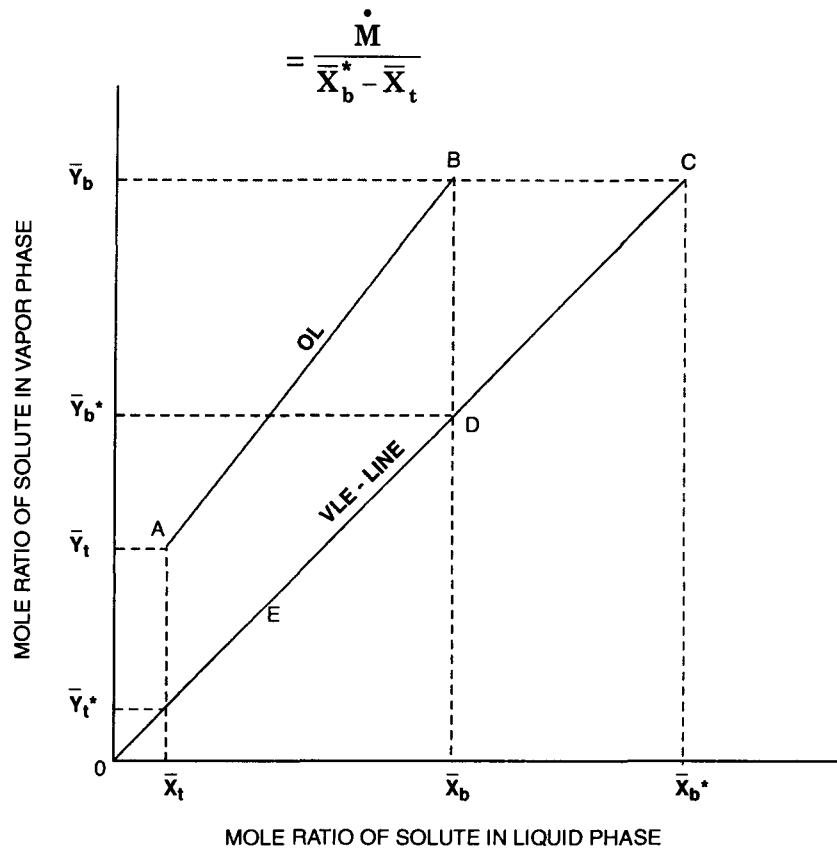
Fig. 1/Example 1.26. *OL and VLE-Line of An Absorber.*

$\overline{X}_b^*$ = mass ratio of solute at the bottom in equilibrium with the vap, kg solute/kg of solvent

$\overline{X}_t$ = mass ratio of solute at the col. top, kg solute/kg solvent

$\quad = 0$ **the feed solvent is solute-free**

Refer to **Figure 1/Example 1.26.** $\overline{X}_t$ has been deliberately not equated to zero for the case of understanding of theoretically minimum rate of solvent.

$\dot{M}$ = mass rate of solute absorption, kg/h

$\qquad$ = 1 t/h

$\qquad$ = 1000 kg/h

$\dot{L}_{s,min} = \dfrac{1000}{\overline{X}_b^* - 0}$

or, $\qquad \overset{\bullet}{L}_s = 1.2 \dfrac{1000}{\overline{X}_b^{\,*}} = \dfrac{1200}{\overline{X}_b^{\,*}}$ $\qquad$ ....(1)

Step - (I) Equilibrium Line

Now the eqn. of the equilibrium line is

$$\overline{Y}^* = m.\overline{X} \qquad ....(2)$$

where, m = slope of the equilibrium line.

The point ① with coordinates [p^* = 5.2 kPa, $\overline{X}$ = 0.007] lies on it.

$\therefore \qquad y_1^* = p_1^*/P$ $\qquad\qquad\qquad\qquad$ cf. $p^* = y^*.P$

$\qquad\qquad\quad = 5.2 / 101.325$

$\qquad\qquad\quad = 0.05132$

$\therefore \qquad \overline{Y}_1^* = \dfrac{64}{28} \cdot \dfrac{0.05132}{1 - 0.05132} = 0.12364$

$\therefore \qquad [\overline{X}_1 = 0.007,\ \overline{Y}_1^* = 0.12364]$ correspond to point ① lying on the **VLE-line**.

Likewise the point ② with coordinates [p^* = 3.78 kPa, $\overline{X}$ = 0.005]

$\therefore \qquad y_2^* = p_2^* / P = 3.78 / 101.325 = 0.03730$

$\therefore \qquad \overline{Y}_2^* = \dfrac{64}{28} \cdot \dfrac{0.0373}{1 - 0.0373} = 0.08856$

$[\overline{X}_2 = 0.005,\ \overline{Y}_2^* = 0.08856]$ correspond to point ② lying on the **VLE-line**.

$\therefore$ Slope of the VLE-line :

$$m = \dfrac{\overline{Y}_1^* - \overline{Y}_2^*}{\overline{X}_1 - \overline{X}_2}$$

$$= \dfrac{0.12364 - 0.08556}{0.007 - 0.005}$$

$$= 17.5397$$

Therefore, Eqn. (2) becomes :

$$\overline{Y}^* = 17.5397\,\overline{X} \qquad ....(2A)$$

Step - (II) Liquid Flowrate

Refer **Figure 1/Example 1.26**. The point ($\overline{X}_b^*$, $\overline{Y}_b$) lies on the VLE-line (Eqn. 2A), so

$$\overline{Y}_b = 17.5397\,\overline{X}_b^*$$

or, $\qquad 0.12029 = 17.5397\,\overline{X}_b^*$

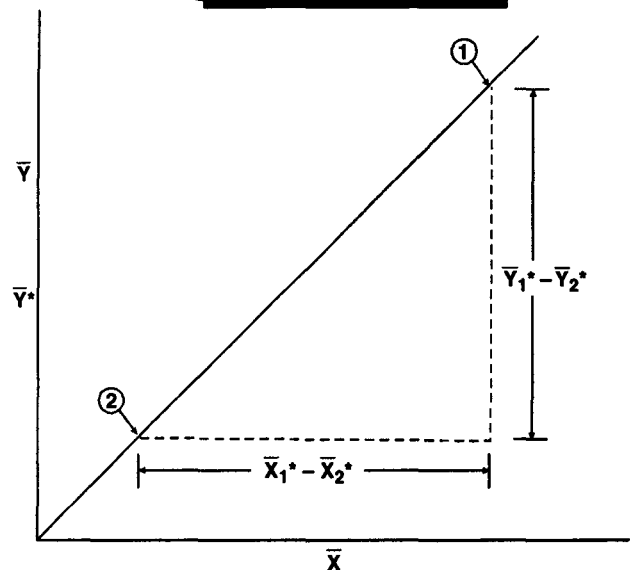$\therefore \qquad\qquad \overline{X}_b^* = 0.006858$

Fig. 2/Example 1.26

Fig. 2/Example 1.26. *VLE-Line of An Absorber.*

Therefore, from Eqn. 1,

$$\dot{L}_s = \frac{1200}{0.006858} = 174\,974 \text{ kg / h} \qquad \textbf{Ans.}$$

Step - (III) Driving Force
Mean Driving Force (MDF)

$$\Delta \overline{Y}_{lm} = \frac{\Delta \overline{Y}_b - \Delta \overline{Y}_t}{\ln\left(\dfrac{\Delta \overline{Y}_b}{\Delta \overline{Y}_t}\right)}$$

where, $\Delta \overline{Y}_b = \Delta \overline{Y}_b - \overline{Y}_b^*$

$$\Delta \overline{Y}_t = \Delta \overline{Y}_t - \overline{Y}_t^*$$

Given : $\qquad e_a = 90\%$

$\therefore \qquad \dfrac{\overline{Y}_b - \overline{Y}_t}{\overline{Y}_b} = 0.9$

or, $\qquad \dfrac{0.12029 - \overline{Y}_t}{\overline{Y}_t} = 0.9$

$\therefore \qquad \overline{Y}_t = 0.012029$

The point **D** $(\overline{X}_b, \overline{Y}_b)$ lies on the VLE-line [Refer **Figure 1/Example 1.26**]

$\therefore \qquad \overline{Y}_b^* = 17.5397 \dfrac{1000}{174\,974}$ $\boxed{b = \dfrac{1000 \text{ kg SO}_2}{174\,974 \text{ kg H}_2\text{O}}}$

$= 0.10024$

$\therefore \qquad \Delta \overline{Y}_b = 0.12029 - 0.10024 = 0.02005$

Similarly the point E $(\overline{X}_t, \overline{Y}_t^*)$ lies on the VLE-line **[Figure 1/Example 1.26].**

$\therefore \qquad \overline{Y}_t^* = 17.5397 \, \overline{X}_t$

$\therefore \qquad \overline{Y}_t = 0.012029$

$= 0 \qquad\qquad \boxed{\overline{X}_t = 0}$

$\therefore \qquad \Delta \overline{Y}_t = 0.012029$

$\therefore \qquad \Delta \overline{Y}_{lm} = \dfrac{0.02005 - 0.012029}{\ln\left(\dfrac{0.02005}{0.012029}\right)} = 0.01569 \dfrac{\text{kg SO}_2}{\text{kg of water}} \qquad \textbf{Ans.}$

Aliter : VLE-eqn. can also be presented as

$$p^* = \frac{5.2 - 3.78}{0.007 - 0.005} . \overline{X} = 710 \, \overline{X}$$

$$p_b^* = 710 \overline{X}_b = 710 \, \frac{1000}{174974} = 4.0577 \text{ kPa}$$

$$p_t^* = 710 \, \overline{X}_t = 0$$

$$\boxed{\begin{aligned} \overline{Y}_t &= 0.005263 \\ y_t &= \frac{Y_t}{1 + Y_t} = 0.005235 \\ p_t &= y_t . P \\ p_t^* &= 710 \times 0 = 0 \end{aligned}}$$

∴ $\Delta p_b = p_b - p_b^* = 0.05 \times 101.325 - 4.0577 = 1.0085 \text{ kPa}$

∴ $\Delta p_t = p_t - p_t^*$

$$= 0.005235 \times 101.325 - 0$$

$$= 0.53048$$

∴ **MDF :**

$$\Delta p_{lm} = \frac{\Delta p_b - \Delta p_t}{\ln\left(\dfrac{\Delta p_b}{\Delta p_t}\right)}$$

$$= \frac{1.0085 - 0.53048}{\ln\left(\dfrac{1.0085}{0.53048}\right)}$$

$$= 0.7440 \text{ kPa}$$ **Ans.**

$$= 5.580 \text{ mm Hg}$$

Packed Bed Height

Example 1.27. Acetone is to be recovered from air-acetone mixture using water as a solvent in a solvent in a packed tower with counterflow arrangement.

The feed stream contains acetone to the extent of 5% (vol.)

The liq rate = 3060 kg/(h.m²)

The gas rate = 1800 kg/(h.m²)

Assume the entire process is gas-film controlled.

The overall volumetric gas transfer coefficient

$$K_{G,p} . a = 0.54 \, \frac{kmol}{h.m^3.kPa}$$

Calculate the packed height to remove 98% of the acetone, if the tower is operated at 101.325 kPa.

Use may be made of the following equilibrium data for the system :

Acetone in gas (mol%) =	0.99	1.96	3.61	4
Acetone in liq (mol%) =	0.76	1.56	3.06	3.33

Solution : First we're to calculate the height of a single transfer unit. Next the number of such transfer units required. And finally the product of these two will give us the required packed depth.

Step - (I) VLE-Line

From the given equilibrium data we construct the VLE-line [**Figure 1/Exam. 1.27**]

y	=	0.0099	0.0196	0.0361	0.0400
x	=	0.0076	0.0156	0.0306	0.0333
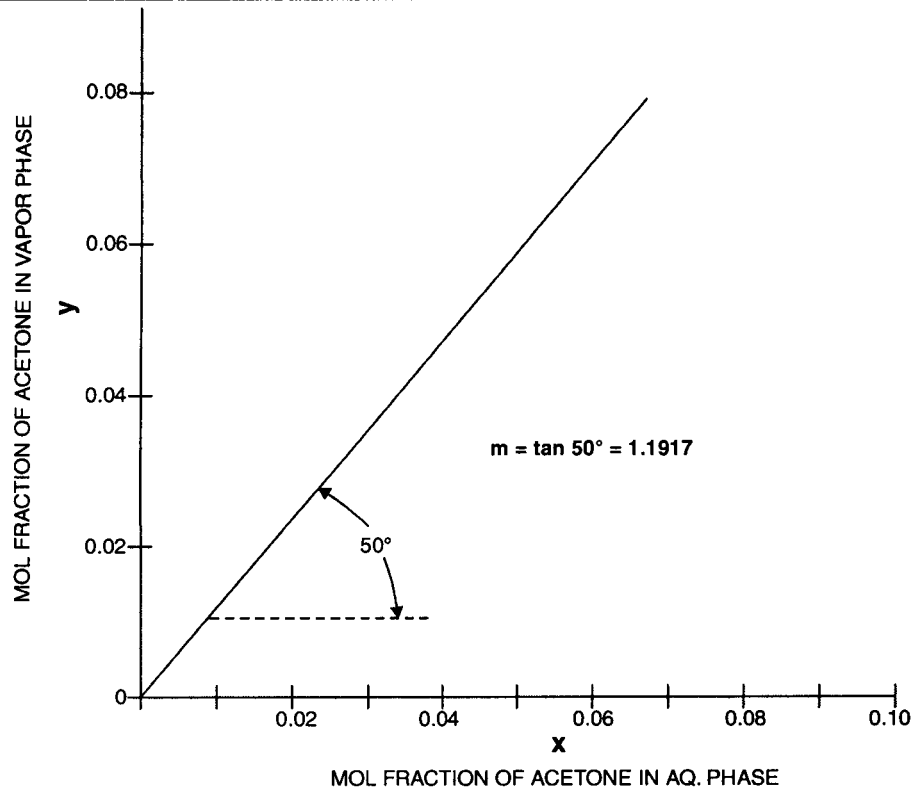
Figure. 1/Example 1.27. *VLE-line of Acetone. The Vapor Phase Consists of Air and Acetone-Vapor while the Liq-Phase Consists of Water and Acetone.*

From the graph, the slope of the eqil. line is

$$m = 1.1917$$

Step - (I) Height of Transfer Units

$$\text{Vol\%} = \text{Mol\%}$$

∴ $y_b = 0.05$ [TOWER BOTTOM]

$$G_s' = (1 - y_b) \cdot G'$$
$$= (1 - 0.05) \times 1800$$
$$= 1710 \text{ kg/(h.m}^2)$$

$$G_s = \frac{1710}{29} = 59.9655 \text{ kmol / (h.m}^2) \quad [\text{Molar mass of air = 29 kg/kmol}]$$

Since scrubbing removes 98% of acetone in the feed,

$$y_t = 0.02 \times 0.05 \qquad \text{[TOWER TOP]}$$
$$= 0.001$$
$$x_t = 0$$
$$L' = 3060 \text{ kg/(h.m}^2)$$

$$\therefore \qquad L'_s = (1-x). L' = 3060 \text{ kg/(h.m}^2)$$

$$\therefore \qquad L_s = \frac{3060}{18} = 170 \text{ kmol/(h.m}^2) \qquad \text{[Molar mass of water = 18 kg/kmol]}$$

Given : $\qquad K_{G,p} . a = 0.54 \dfrac{\text{kmol}}{[\text{h.m}^3.\text{kPa}]}$

$$\therefore \qquad [HTU]_{O,G} = \frac{G_s}{K_{G,p}.a.P}$$

$$= \frac{59.9655}{0.54 \times 101.325} \qquad \frac{\text{kmol}}{\text{h.m}^2} \frac{1}{\dfrac{\text{kmol}}{\text{h.m}^3.\text{kPa}}.\text{kPa}}$$

$$= 1.0959 \text{ m} \qquad\qquad \textbf{Ans.}$$

Step - (II) Number of Transfer Units

Working formula :

$$[NTU]_{O,G} = \frac{1}{\left(1 - m.\dfrac{G_s}{L_s}\right)} . \ln\left[\left(1 - m.\frac{G_s}{L_s}\right). \frac{y_b - m.x_t}{y_t - m.x_t} + m.\frac{G_s}{L_s}\right]$$

$$m = 1.1917 \text{ [Figure 1/Example 1.27]} \qquad ...\text{[Eqn. 1.124 A]}$$
$$G_s = 59.9655 \text{ kmol/(h.m}^2)$$
$$L_s = 170 \text{ kmol / (h.m}^2)$$

$$\therefore \qquad m.\frac{G_s}{L_s} = (1.1917)(59.965/170) = 0.42035$$

$$x_t = 0$$
$$y_b/y_t = 0.05/0.001 = 50$$

$$\therefore \qquad [NTU]_{O,G} = \frac{1}{1 - 0.42035} \cdot \ln\left[(1 - 0.42035) \times 50 + 0.42035\right]$$
$$= 5.8329 \qquad \textbf{Ans.}$$

Step – (III) Packed Height

$$Z = [HTU]_{O,G} \times [NTU]_{O,G}$$
$$= 1.0959 \times 5.8326$$
$$= 6.392 \text{ m} \qquad \textbf{Ans.}$$

Gas-Film Mass Transfere Coefficient

Example 1.28. Sulfur dioxide is removed from air stream by absorbing it in a 0.5(N) NaOH solution in a countercurrent packed-bed absorber.

The feed gas enters the column at a rate of 7200 kg/(h.m²)

The feed flowrate corresponds to a Reynolds number of 5200 and the friction factor is found to be 0.02.

If the tower is operated at 103 kPa, calculate the film transfer coefficient for SO_2 absorption which is predominantly gas-film controlled one.

Given :

Diffusion SO_2 in air   = 11.6 × 10⁻⁶m²/s
Gas viscosity   = 18 × 10⁻⁶ Pa.s   } *All at operating temperature 298K*
Density of gas stream = 1.155 kg/m³

Calculate the tower dia.

Solution : Use may be made of wetted wall column as the model for packed column. This may serve as the basis for the development of correlations for packed towers.

Work on wetted wall columns by Gilliland, *et. al.,* [E.R. Gilliland and T.K.Sherwood — *Industrial and Engineering Chemistry. Vol. 26/1934]* produced the following correlation :

$$\frac{h_d}{D_{ff,G}} \cdot D_t \cdot \frac{p_{IG,lm}}{P} = B. Re^{0.83}$$

To allow for the variation in the physical properties, Schmidt Number Sc is introduced, whereupon it takes the form :

$$\frac{h_d \cdot D_t}{D_{ff,G}} \cdot \frac{p_{IG,lm}}{P} = B'. Re^{0.83}. Sc^{0.44}$$

which can be rearranged to :

$$\frac{h_d \cdot D_t}{D_{ff,G}} \cdot \frac{p_{IG,lm}}{P} \cdot \frac{\mu}{D_t . v . r} \cdot \left(\frac{\mu}{\rho . D_{ff,G}}\right)^{0.56} = B'. Re^{-0.17} . \frac{\mu}{\rho . D_{ff,G}}$$

i.e., $$\frac{h_d}{v} \cdot \frac{p_{IG,lm}}{P} \cdot \left(\frac{\mu}{\rho . D_{ff,G}}\right)^{0.56} = \frac{B'}{Re^{0.17}} = j_D \qquad ....(1)$$

where, h_d = mass transfer coefficient = $\dfrac{D_{ff,G}}{Z_G}$, m.s⁻¹

$D_{ff,G}$ = diffusivity of solute in gas phase, m²/s

Z_G = thickness of gas-film, m

$p_{IG,lm}$ = log-mean partial pressure of inert gas, kPa

B' = constant

       = 0.021 — 0.027. However, a mean value of 0.023 can be taken.

j_D = j-factor (friction factor) introduced by Chilton and Colburn.

$$= \frac{R}{\rho . \mu^2}$$

μ = gas viscosity, Pa.s

v   = gas velocity, m/s

Given :

$$G' = 7200 \text{ kg/(h.m}^2)$$

$$\mathbf{Re} = 5200$$

$$j_D = 0.02$$

$$D_{ff, SO_2 \text{-Air}} = 11.6 \times 10^{-6} \text{ m}^2/\text{s}$$

$$\mu = 18 \times 10^{-6} \text{ Pa.s}$$

$$\rho = 1.155 \text{ kg/m}^3$$

$$\left[\frac{\mu}{\rho . D_{ff, SO_2 \text{-Air}}} \right]^{0.56} = \left[\frac{18 \times 10^{-6}}{1.155 \times 11.6 \times 10^{-6}} \right]^{0.56} = 1.1798$$

Now,

$$G' = \rho . v$$

or,

$$\frac{7200}{3600} = 1.155 \text{ v}$$

∴

$$v = 1.7316 \text{ m/s}$$

Substituting the known values in Eqn. (1) :

$$\frac{h_d}{1.7316} . \frac{P_{IG, lm}}{P} \times 1.1798 = 0.02$$

∴

$$h_d . \frac{P_{IG, lm}}{P} = 0.02935$$

Now,

$$k_{G, p} = \frac{h_d}{R.T} . \frac{P_{IG, lm}}{P}$$

$$= \frac{1}{8.314 \times 300} . (0.02935)$$

$$\boxed{R = 8.314 \ \frac{\text{kPa, m}^3}{\text{kmol. K}}}$$

$$= 1.17689 \times 10^{-5} \ \frac{\text{kmol SO}_2}{\text{s. m}^2. \text{kPa}}$$ **Ans.**

$$\boxed{7.532 \times 10^{-4} \ \frac{\text{kg SO}_2}{\text{s. m}^2. \text{kPa}}}$$

TOWER DIA This can be computed from the relationship :

$$\mathbf{Re} = \frac{D_t . \rho . v}{\mu}$$

or, $5200 = D_t . \dfrac{1.155 \times 1.7316}{18 \times 10^{-6}}$

∴ $D_t = 0.0468 \ m$ **Ans.**

Gas-Film Mass Transfer Coefficient

Problem 1.29. *Solve Example 1.28 using Morris-Jackson formula :*

$$\dfrac{h_d}{v} . \dfrac{p_{IG,lm}}{P} . \left[\dfrac{\mu}{\rho . D_{ff,G}} \right]^{0.5} = 0.04 / [\,Re\,]^{0.25}$$

Ans. $k_{G,p} = 2.8213 \times 10^{-6} \ kmol \ SO_2/(s.m^2.kPa)$

Hints :

∴ $\dfrac{h_d}{1.7316} . \dfrac{p_{IG,lm}}{P} . \left[\dfrac{18 \times 10^{-6}}{1.155 \times 11.6 \times 10^{-6}} \right]^{0.5} = \dfrac{0.04}{(5200)^{0.25}}$

∴ $h_d . \dfrac{p_{IG,lm}}{P} = 7.03704 \times 10^{-3}$

∴ $k_{G,p} = \dfrac{h_d}{R.T} . \dfrac{p_{IG,lm}}{P}$

$$= \dfrac{1}{8.314 \times 300} . (7.03704 \times 10^{-3})$$

$$= 2.8213 \times 10^{-6} \ kmol \ SO_2/(s.m^2.kPa)$$

Gas-Film Mass Transfer Coefficient

Example 1.30. *Ammonia is being absorbed from air at atmospheric pressure by acetic acid in a packed bed absorption column.*

The feed gas enters the column at a rate of 4000 kg/(h.m²) which corresponds to a Reynolds number of 5100 and a friction factor of 0.0198.

Absorption is carried out at 298K at which :

Viscosity of gas stream = 17.5 × 10⁻⁶ Pa.s

Density of gas stream = 1.154 kg/m³

Diffusion coefficient of ammonia in air = 19.6 × 10⁻⁶ m²/s

Determine the coefficient of mass transfer thru the gas-film.

Solution : We shall harness the Gilliland-Sherwood relationship for mass transfer in wetted-wall column :

$$\dfrac{h_d}{v} . \dfrac{p_{IG,lm}}{P} . \left[\dfrac{\mu}{\rho . D_{ff,G}} \right]^{0.56} = j_D \qquad\qquad ...(1)$$

Given :

$$G' = 4000 \text{ kg/(h.m}^2)$$

$$\mathbf{Re} = 5100$$

$$\mathbf{j_D} = 0.0198$$

$$\mu = 17.5 \times 10^{-6} \text{ Pa.s}$$

$$\rho = 1.154 \text{ kg/m}^3$$

$$D_{ff, NH_3-Air} = 19.6 \times 10^{-6} \text{ m}^2/\text{s}$$

Now,

$$v = \frac{G}{\rho} = \frac{4000/3600}{1.154} = 0.9628 \text{ m/s}$$

Substituting the known values in the Eqn. (1) :

$$\frac{h_d}{0.9628} \cdot \frac{p_{IG,lm}}{P} \cdot \left[\frac{17.5 \times 10^{-6}}{1.154 \times 19.6 \times 10^{-6}}\right]^{0.56} = 0.0198$$

$$\therefore \qquad h_d \cdot \frac{p_{IG,lm}}{P} = 0.022$$

$$\therefore \qquad k_{G,p} = \frac{h_d}{R.T} \cdot \frac{p_{IG,lm}}{P}$$

$$= \frac{0.022}{8.314 \times 298}$$

$$= 8.8796 \times 10^{-6} \cdot \frac{\text{kmol NH}_3}{\text{s.m}^2.\text{kPa}}$$

$$= 8.8796 \times 10^{-6} \times 17 \qquad \boxed{\text{Mol. wt of NH}_3 = 17 \frac{\text{kg}}{\text{kmol}}}$$

$$= 1.5095 \times 10^{-4} \frac{\text{kg.NH}_3}{\text{s.m}^2.\text{kPa}}$$

Gas-Film Transfer Coefficient

Problem 1.31. Solve Example 1.30 using Morris-Jackson relationship.

Ans. $k_{G,p} = 2.0911 \times 10^{-6}$ kmol $NH_3/(\text{s.m}^2.\text{kPa})$

Hints :

$$\frac{h_d}{0.9628} \cdot \frac{p_{IG,lm}}{P} \cdot \left[\frac{17.5 \times 10^{-6}}{1.154 \times 19.6 \times 10^{-6}}\right]^{0.5} = \frac{0.04}{(5100)^{0.25}}$$

$$\therefore \qquad h_d \cdot \frac{p_{IG,lm}}{P} = 5.1810 \times 10^{-3}$$

$$\therefore \qquad k_{G,p} = \frac{h_d}{R.T} \cdot \frac{p_{IG,lm}}{P}$$

$$= \frac{1}{8.314 \times 298} \cdot (5.181 \times 10^{-3})$$

$$= 2.0911 \times 10^{-6} \text{ kmol NH}_3/(\text{s.m}^2.\text{kPa})$$

Gas-Film Transfer Coefficient

Example 1.32. In a laboratory setup, a packed tower of dia 50mm is employed to carry out absorption of sulfur dioxide from an AIR-SO$_2$ mixture fed to the column at the rate of 6000 kg/(h.m^2).

The absorption is carried out at atmospheric pressure and temperature of 300K at which :

Gas stream viscosity = 18×10^{-6} Pa.s

Gas stream density = 1.155 kg/m^3

$D_{ff, SO_2\text{-}Air}$ = 11.6 × 10^{-6} m^2/s

If the resistance to mass transfer lies mostly in the gas phase, calculate the gas-film mass transfer coefficient.

Solution : We shall use Gilliland-Sherwood formula to work out the value of $k_{G,p}$

Gas density = 1.155 kg/m^3

$$\text{Gas rate } = 6000 \text{ kg/(h.m}^2) = \frac{6000}{3600} \text{ kg/(h.m}^2)$$

Now, $G' = \rho.v$

∴ $\dfrac{6000}{3600} = 1.155 \times v$

∴ $v = 1.443$ m/s

Given :   Tower dia, D_t = 50mm = 0.05m

$\mu = 18 \times 10^{-6}$ Pa.s

$\rho = 1.155 \times 10^{-6}$ m^2/s

$D_{ff, SO_2\text{-}Air} = 11.6 \times 10^{-6}$ m^2/s

Reynolds number :

$$\text{Re } = \frac{D_t.v.\rho}{\mu} = \frac{(0.05)(1.443)(1.155)}{18 \times 10^{-6}} = 4629$$

Gilliland-Sherwood relationship :

$$\frac{h_d}{v} \cdot \frac{p_{IG,lm}}{P} \cdot \left[\frac{\mu}{\rho.D_{ff,G}} \right]^{0.56} = \frac{B'}{Re^{0.17}}$$

Substituting **B' = 0.023** (Refer **Example 1.28**) and other known values :

$$\frac{h_d}{1.443} \cdot \frac{p_{IG,lm}}{P} \left[\frac{18 \times 10^{-6}}{1.155 \times 11.6 \times 10^{-6}} \right]^{0.56} = \frac{0.023}{(4629)^{0.17}}$$

$$\therefore \qquad h_d \cdot \frac{p_{IG,lm}}{P} = 6.6996 \times 10^{-3}$$

$$\therefore \qquad k_{G,p} = \frac{h_d}{R.T} \cdot \frac{p_{IG,lm}}{P}$$

$$= \frac{1}{8.314 \times 298} \cdot (6.6996 \times 10^{-3})$$

$$= 2.7041 \times 10^{-6} \; \frac{kmol \; SO_2}{s.m^2.kPa} \qquad \textbf{Ans.}$$

Packed Bed Height

Example 1.33. Ammonia is to be removed from an air-ammonia mixture by countercurrent scrubbing with water in a packed tower at 293K and a total pressure of 101.325 kPa.

The feed gas contains 10% ammonia of which 99% ammonia is to be removed.

The feed gas rate is 3425 kg/h per m² of tower cross-section and the liq rate is 2345 kg/ h per m² of tower cross-section.

Absorption coefficient $K_{G,p} \cdot a = 3.6 \; \dfrac{kmol}{h.m^2}$ per unit kPa partial pressure difference

The equilibrium data for the system :

$X_{NH_3} \cdot 1000 =$	21	31	42	53	80	105	160
$p_{NH_3} \cdot$ (kPa) $\;=$	1.599	2.426	3.319	4.226	6.733	9.266	15.332

where, $X_{NH_3} = \dfrac{kmol \; NH_3}{kmol \; water}$; p_{NH_3} = partial pressure of ammonia in air-ammonia mixture over the liq phase

Solution : Ammonia is a very soluble gas in water. Hence entire resistance to mass transfer in the process of absorption of ammonia is concentration in the gas phase. Therefore,

$$K_{G,p} \cdot a \approx k_{G,p} \cdot a$$

Therefore, from a mass balance over the column, the packed bed height Z can be computed from :

$$Z = \frac{G_s}{k_{G,p} \cdot a.P} \cdot \int_{Y_t}^{Y_b} \frac{(1+Y)(1+Y_i)}{(Y-Y_i)} .dY \qquad \text{...(Eqn. 1.93)}$$

Step - (I) Gas Composition at Tower Top and Bottom

From the given data :

$$y_b = 0.1 \qquad\qquad \text{[Vol\% = Mol\%]}$$

$\therefore \qquad\qquad Y_b = \dfrac{y_b}{1 - y_b} = 0.1111$

Since $\qquad\qquad e_a = 99\%$

$$0.99 = \dfrac{Y_b - Y_t}{Y_b}$$

$\therefore \qquad\qquad Y_t = Y_b\,[1 - 0.99] = 0.1111 \times 0.01 = 0.0011$

Step - (II) Gas and Liq Rates on Solute-Free Basis

The feed gas stream is composed of :

        10 mol% NH_3

        90 mol% Air   [Vol% = Mol%]

Therefore, the percent of air in the feed gas

$$= \dfrac{\dfrac{90}{100} \times 29}{\dfrac{90}{100} \times 29 + \dfrac{10}{100} \times 17} \times 100$$

Component	Molar Mass (kg/kmol)
AIR	29
NH_3	17

$$= 93.88\%$$

Mass flowrate of air

$$G_s' = \dfrac{93.88}{100} \times 3425 = 3215.55 \ \text{kg/(h.m}^2)$$

Molar flowrate of air

$$G_s = \dfrac{3215.55}{29} = 110.881 \ \text{kmol/(h.m}^2)$$

The scrubbing liquid at tower inlet contains zero solute. Therefore, molar flowrate of liq

$$L_s = \dfrac{2315}{18} = 130.277 \ \text{kmol/(h.m}^2)$$

Step - (III) Operating Line

Let us consider a horizontal plane in the packed bed where the compositions are X and Y. A mass balance between this plane and the top of the tower gives :

$$G_s \cdot (Y - Y_t) = L_s \cdot (X - X_t)$$

or,   110.881 $(Y - 0.0011) = 130.277\ (X - 0)$

$\therefore \qquad\qquad\qquad Y = 1.1749\,X + 0.0011$ $\boxed{X_t = 0}$ ....(1)

This is the eqn. of the **OL** in terms of mol ratios.

Step - (IV) Graphical Presentation of OL and VLE-Line

In order to present the OL and VLE-curve on the same X - Y plot, the given equilibrium data is converted to VLE-relationship on mol ratio basis :

$$p = y.P = \dfrac{Y}{1 + Y}.P$$

$\therefore \qquad\qquad\qquad y = \dfrac{p}{P - p}$

where, **p** = partial pressure of ammonia

P = total system pressure = 101.325 kPa

Y = mol ratio of NH_3 in vap phase

$$= \frac{kmol\ NH_3}{kmol\ air}$$

Operating Line : Y = 1.1749X + 0.0011

X	=	0	0.05	0.10	0.15
Y	=	0.0011	0.0598	0.11859	0.1773

VLE - Line.

X	=	0.021	0.031	0.042	0.053	0.080	0.105	0.160
p (kPa)	=	1.599	2.426	3.319	4.226	6.733	9.266	15.332
Y $\left[\dfrac{p}{P-p}\right]$	=	0.016	0.0245	0.0338	0.0435	0.0711	0.1006	0.1781

These data are plotted in **Figure 1/Example 1.33**

From the **Figure 1/Example 1.33** we complete the following table :

Y	Y_i	(1+Y) (1+Y_i)	$\dfrac{(1+Y)(1+Y_i)}{(Y-Y_i)}$
Y_t = 0.0011	0	1.0011	910
0.005	0.0024	1.0074	387.46
0.01	0.0055	1.0155	225.66
0.02	0.012	1.0322	129.15
0.04	0.026	1.0670	76.21
0.06	0.041	1.1034	58.07
0.08	0.058	1.1426	51.93
0.10	0.075	1.1836	49.31
Y_b = 0.1111	0.0865	1.2071	49.26

The values of $\dfrac{(1+Y)(1+Y_i)}{(Y-Y_i)}$ are plotted against the corresponding values of **Y** **(Figure 2/**

Example 1.33). The area under this curve equals the integral of Eqn. 1.93. This can be determined, though approximately, by using the formulae of trapeziums :

$$A_{curve} = \frac{Y_{in} - Y_{fin}}{n}\left(\frac{y_0 + y_n}{2} + \sum_{1}^{n-1} y\right)$$

where, Y_{in} = initial value of Y = Y_b

Y_{fin} = final value of $Y = Y_t$

n = ordinate number

y_o = ordinate value for n = 0

y_n = ordinate value for n = n

In our present case, we assume that **n = 11** and compile the following table, taking value of ordinates from the graph [**Figure 2/Example 1.33**]
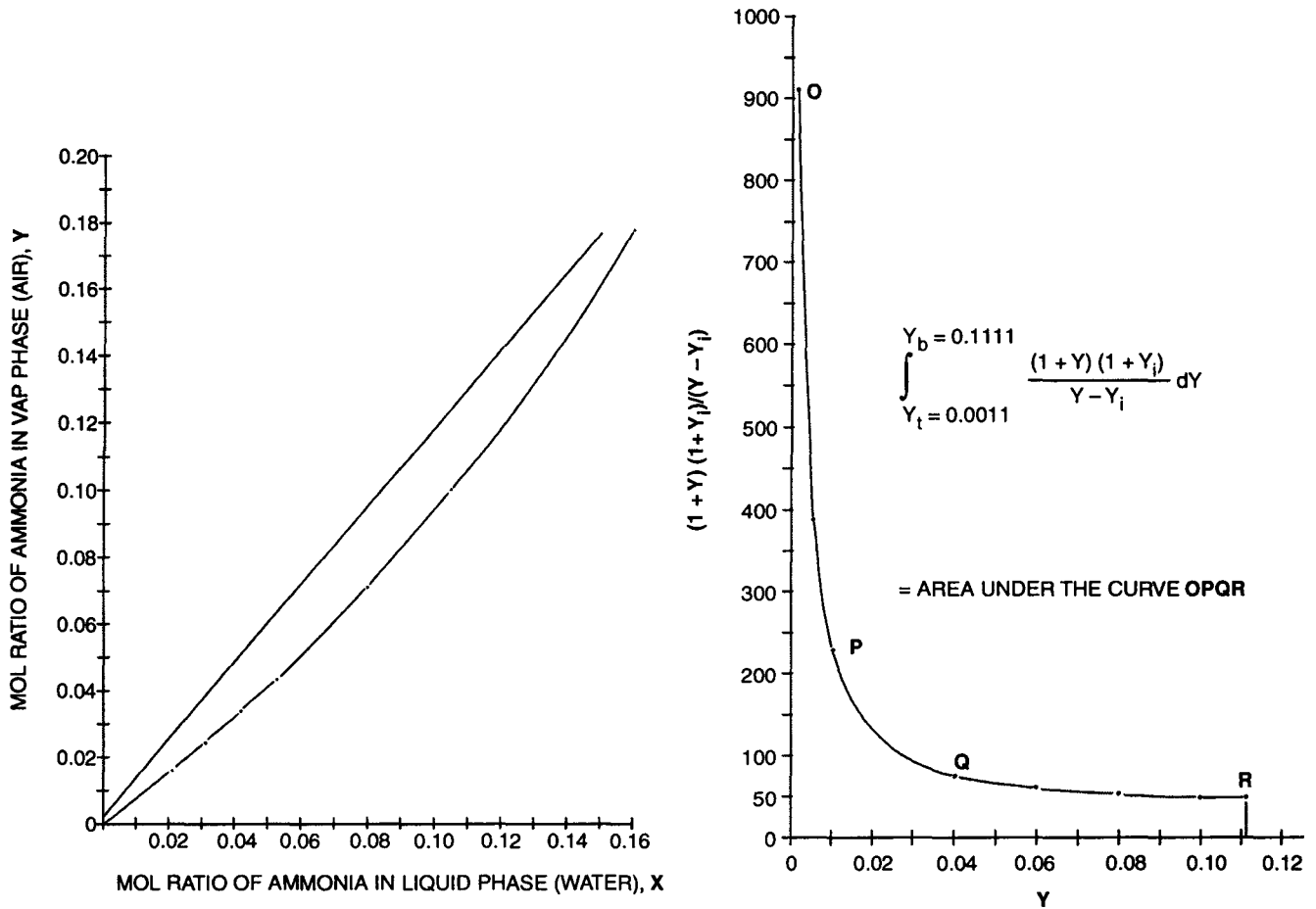

$$\int_{Y_t = 0.0011}^{Y_b = 0.1111} \frac{(1 + Y)(1 + Y_i)}{Y - Y_i} dY$$

= AREA UNDER THE CURVE **OPQR**

Fig 2/Example 1.33.

Fig 1/Example 1.33. *OL and VLE-Curve for Packed Absorption of Ammonia From Air-Ammonia Mixture Where Water is Used As a Solvent.*

Y	n	y	Y	n	y
0.001	0	910	0.061	6	60
0.011	1	210	0.071	7	55
0.021	2	124	0.081	8	51
0.031	3	90	0.091	9	50
0.041	4	75	0.101	10	50
0.051	5	67	0.111	11	49

$$\therefore \quad A_{curve} = \frac{0.111 - 0.0011}{11} \left[\frac{910 + 49}{2} + 210 + 124 + 90 + 75 + 67 + 60 + 55 + 51 + 50 + 50 \right]$$

$$= 13.1030$$

$$\therefore \quad Z = \frac{110.881}{3.6 \times 101.325} \times 13.1030 = 3.983 \text{ m} \qquad \textbf{Ans.}$$

Packed Bed Height

Problem 1.34. *Solve the Example 1.33, assuming the equilibrium line to be straight.*

Ans. Z = 4.421 m

Hints : In this case

$$G_s \cdot (Y_b - Y_t) = \frac{N}{A} = K_{G,p} \cdot a \cdot Z \cdot \Delta p_{lm}$$

TDF (top driving force) :

$$\Delta Y_t = Y_t - Y_t^*$$

$$= 0.0011 - 0 \qquad \text{(See Table/Example 1.33)}$$

$$= 0.0011$$

BDF (bottom driving force) :

$$\Delta Y_b = Y_b - Y_b^*$$

$$= 0.1111 - 0.0865 \qquad \text{(See Table/Example 1.33)}$$

$$= 0.0246$$

Scrubber Design

Example 1.35. A packed-bed scrubber is to be designed to absorb acetone vapor from air by irrigating the bed with water at the rate of 3t/h.

The packing to be used is ceramic rings of size 25mm × 25mm × 3mm.

The feed gas contains acetone by an extent of 6% by volume.

The scrubber is to operate at a mean temperature of 293K.

The feed gas will enter the column at atmospheric pressure at the rate of 1400 m³/h of pure air (referred to standard conditions).

The duty of the scrubber is to ensure an absorption factor of 98%.

Determine :

1. the diameter of the scrubber

2. the height of the packed bed.

Take the following equation

$$Y^* = 1.68X$$

valid for the VLE-relationship for the system where

   X = *kmol acetone/kmol of water*

   Y^* = *kmol of acetone vapor/kmol of air in equilibrium with the equilibrium phase.*

   Assume :

   1. Max. operating velocity = 75% of flooding velocity

   2. The resistance to mass transfer resides mainly in the vapor phase and the overall coefficient of mass transfer

$$K_{G,Y} = 0.4 \ \frac{kmol\ acetone}{h.m^2.(kmol\ acetone/kmol\ air)}$$

   3. Thorough and complete wetting of the packing.

Solution : Both the operating line and the equilibrium line, in this case, are straight. And therefore, the **MDF** (mean driving force) may be determined from these two straight lines drawn on the same x-y coordinates.

Step - (I) Acetone Absorption Rate

   Volumetric flowrate of feed gas

$$Q_{v,IG} = 1400 \ m^3/h \qquad \text{[at standard conditions]}$$

where **IG** = inert gas (here, air)

$$Q_{M,IG} = \frac{1400}{22.4} \ kmol/h$$

$$Q_{M,Ac} = \frac{1400}{22.4} \cdot Y$$

$$= \frac{1400}{22.4} \cdot \frac{y}{1-y}$$

$$= \frac{1400}{22.4} \cdot \frac{0.06}{1-0.06} \ kmol\ acetone\ /h$$

$\therefore$ Amount of acetone to be absorbed per hour

$$= \frac{1400}{22.4} \cdot \frac{0.06}{0.94} \times 0.98$$

$$= 3.9095 \ kmol/h$$

cf. e_a = 98% *i.e.*, 98% of acetone of feed stream is absorbed

Step - (II) Compositions at Tower Top and Bottom

   The scrubbing water at inlet is acetone-free, so

$$X_t = 0$$

At the scrubber outlet the solvent liquor carries out 3.9095 kmol acetone/h.

$$\therefore \qquad X_b = \frac{3.9095}{3000/18} \ \frac{kmol\ acetone/h}{\dfrac{kg\ water}{h}} \cdot \frac{1}{(kg/kmol)\ of\ water}$$

$$= 0.02345 \frac{\text{kmol acetone}}{\text{kmol water}}$$

The feed gas at tower inlet contains 6 vol% (*i.e.*, 6 mol%) of acetone.

$$\therefore \quad Y_b = \frac{y_b}{1 - y_b}$$

$$= \frac{0.06}{1 - 0.06}$$

$$= 0.06382 \frac{\text{kmol acetone vapor}}{\text{kmol of air}}$$

Forasmuch as 98% of the acetone is removed from the feedstream, so

$$Y_t = 2\% \, Y_b$$
$$= 0.02 \times 0.06382$$

$$= 0.001276 \frac{\text{kmol acetone vapor}}{\text{kmol of air}}$$

Step - (III) OL and VLE-Line

Hence the coordinates of **OL** are :
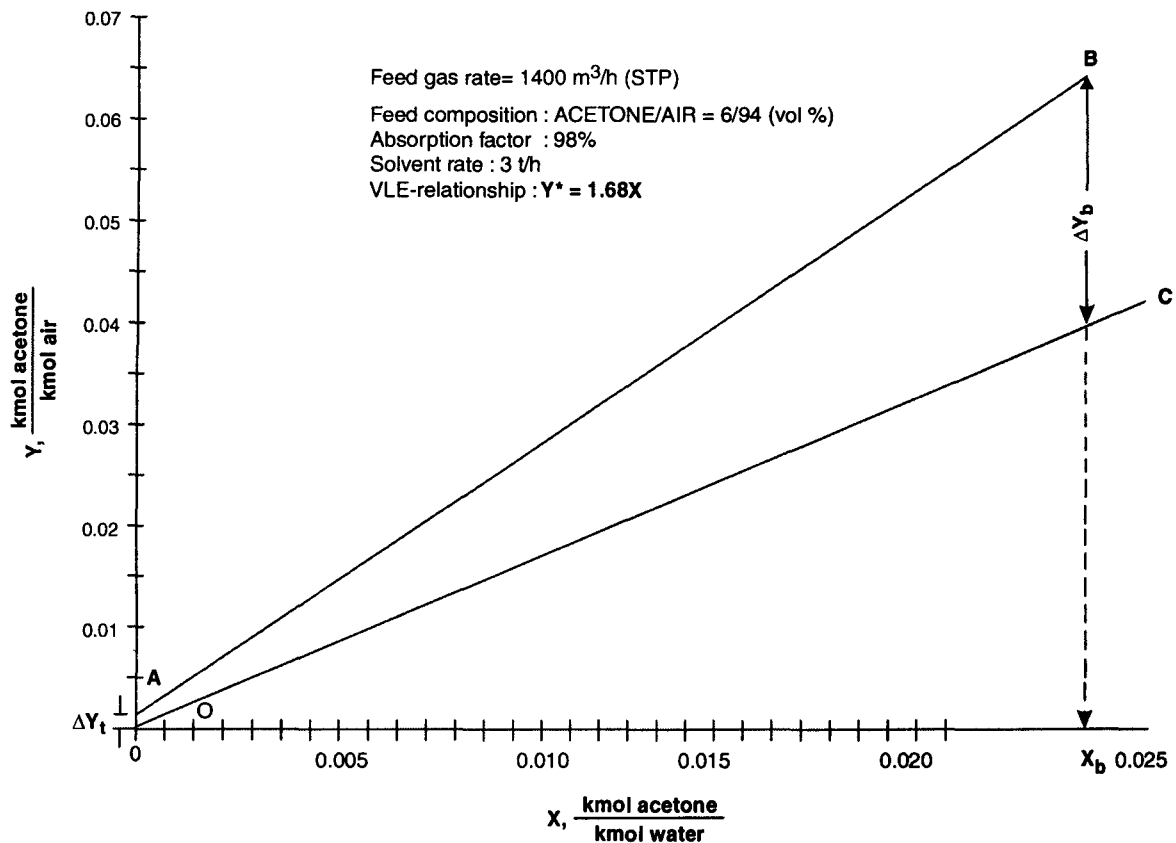
$$(X_t, Y_t) \quad \text{and} \quad (X_b, Y_b)$$

Fig. 1/Example 1.35. *VLE and Operating Lines of A Packed Bed Absorber in which Acetone Vapor is Absorbed from Air-Acetone Feed (6 Vol% Acetone) by Water at Atmospheric Pressure and at 293K.*

i.e., $(0, 0.001276)$ and $(0.02345, 0.06382)$

On **X-Y** coordinates the **OL** is drawn (straightline AB/**Figure 1/Example. 1.35**)

VLE-Line :   **Y* = 1.68X**

X	=	0	0.01	0.02	0.025
Y*	=	0	0.0168	0.0336	0.042

On the same plot the VLE-line is drawn (straightline OC/**Figure 1/Example 1.35**)

Step - (IV) Mean Driving Force (MDF)

$$\text{BDF} = Y_b - Y_b^*$$
$$= 0.06382 - 1.68X_b$$
$$= 0.06382 - 1.68\,(0.02345)$$
$$= 0.024424 \;\frac{\text{kmol acetone}}{\text{kmol water}}$$ **[Figure 1/Example 1.35]**

$$\text{TDF} = Y_t - Y_t^*$$
$$= 0.001276 - 1.68X_t$$
$$= 0.001276 \;\frac{\text{kmol acetone}}{\text{kmol air}}$$

$\therefore$ $$\text{MDF} = \frac{\Delta Y_b - \Delta Y_t}{\ln\left[\dfrac{\Delta Y_b}{\Delta Y_t}\right]}$$

$$= \frac{0.024424 - 0.001276}{\ln\left[\dfrac{0.024424}{0.001276}\right]}$$

$$= 0.007841 \;\frac{\text{kmol acetone}}{\text{kmol air}}$$

Step - (V) Mass Transfer Surface Area

The rate of solute transfer

$$N = K_{G,Y} \cdot A_c \cdot \Delta Y_{lm}$$
or, $$3.9095 = (0.4)\,(A_c)\,(0.007841)$$
$\therefore$ $$A_c = 1246.3499 \text{ m}^2$$

> A_c = surface area of contact of the phases in the absorber under film condition

Step - (VI) Packing Volume

$$V = \frac{A_c}{a}$$
$$= \frac{1246.3499}{204}$$
$$= 6.1095 \text{ m}^2$$

> a = 204 m^2/m^3 for ceramic packing of size 25mm × 25mm × 3mm

Step - (VI) Cross-Sectional Area of the Scrubber

For this we need to know the value of flooding velocity, v_{fl}. And we shall use Eqn. 1.149 to determine the flooding velocity. Next we'll calculate scrubber cross-section on the basis of operating velocity equal to 75% of flooding velocity.

$$\dot{L} = 3 \text{ t/h} = 3000 \text{ kg/h}$$

$$\dot{G} = 1400 \times 1.29 = 1806 \text{ kg/h} \qquad \boxed{\text{Density of air} = 1.29 \text{ kg/m}^3 \text{ at standard state}}$$

$$\mu_L = 10^{-3} \text{ Pa.s} = 1 \text{ mPa.s}$$

$$\rho_L = 1000 \text{ kg/m}^3 \; ; \rho_G = 1.29 \left[\frac{273}{293}\right] = 1.2019 \text{ kg/m}^3$$

$$\epsilon = 0.74 \text{m}^3/\text{m}^3 \; ; C = 0.022$$

Substituting the known values in Eqn. 1.149 :

$$\log\left[\frac{v_{fl}^2}{(0.74)^3} \cdot \frac{204}{9.81} \cdot \frac{1.2019}{1000} \cdot (1)^{0.16}\right]$$

$$= 0.022 - 1.75 \left[\frac{3000}{1806}\right]^{\frac{1}{4}} \cdot \left[\frac{1.2019}{1000}\right]^{\frac{1}{8}}$$

$$= -0.83527$$

$$\therefore \qquad v_{fl} = 1.5392 \text{ m/s}$$

∴ Design velocity

$$v = 75\% \, v_{fl}$$
$$= 0.75 \times 1.5392$$
$$= 1.1544 \text{ m/s}$$

Now, the gas input rate

$$\dot{G} = A.v.\rho_G$$

or,

$$\frac{1806}{3600} = A \cdot (1.1544) \cdot (1.2019)$$

∴

$$A = 0.36156 \text{ m}^2$$

Step - (VII) Scrubber Dia

$$\frac{\pi}{4} \cdot D_t^2 = A$$

or,

$$\frac{\pi}{4} \cdot D_t^2 = 0.36156$$

∴

$$D_t = 0.6785 \text{m}$$

Step - (VIII) Packed Bed Height

$$Z = \frac{V}{A}$$

$$= \frac{6.1095}{0.36156}$$

$$= 16.897 \text{ m} \qquad \qquad \textbf{Ans.}$$

Solvent Rate and Packed Bed Height

Example 1.36. A packed bed absorber is used to absorb methanol (MeOH) vapor with water from a carrier gas (inert gas) under atmospheric pressure and at a mean operating temperature of 300K. The packed bed is composed of randomly dumped ceramic packing having interfacial surface of 190 m²/m³ of packed volume.

If 98% recovery of methanol from the gas stream is required, calculate :

1. the solvent (water) flowrate to irrigate the packing

2. the height of the packed bed.

Given :

Feed gas rate = 1200 m³/h on the basis of inert gas at operating conditions

Alcohol content in the feed gas = 100 g per m³ of the inert gas referred to operating conditions

Methanol content in the liq effluent at absorber bottom

= 67% of the max. possible one, i.e., of the equilibrium one with the incoming gas.

The VLE-relationship for the system : Y = 1.15X*

where, Y* is the mol ratio of methanol vapor in gas stream in equilibrium with the mol ratio X of methanol in the aq. phase.

The overall mass transfer coefficient :

$$K_{L,X} = 0.5 \ \frac{kmol \ MeOH}{h.m^2.(kmol \ MeOH \ / \ kmol \ water)}$$

Coefficient of wetting of the packing :

$$\varphi = 0.87$$

Max. allowable gas velocity

$$v = 0.4 \ m/s$$

Solution : Methanol (MeOH) is soluble in water in all proportions. Forasmuch as the overall mass transfer coefficient is given in terms of $K_{L,X}$, so we've to determine the driving force with respect to liq phase ($\Delta X = X^* - X$) for the estimation of packed height.

Step - (I) Quantity of Methanol Absorbed

$$N = Q_{v,IG} \cdot \frac{y_b}{1 - y_b} \cdot e_a \cdot \frac{1}{22.4} \text{ , kmol/h}$$

Now, $\qquad$ c $\;=\;$ 100 g/m³ of IG

$$= 0.1 \text{ kg/m}^3 \text{ of IG}$$

$$= \frac{0.1}{32} \text{ kg/m}^3 \text{ of IG}$$

$$= 0.003125 \text{ kmol MeOH/m}^3 \text{ of IG}$$

$$\mathbf{y} = \mathbf{c} . \frac{\mathbf{M}_{mix}}{\rho}$$

$$= \frac{\mathbf{c}}{\rho / \mathbf{M}_{mix}}$$

$$= \frac{\mathbf{c}}{\dfrac{\mathbf{P} . \mathbf{T}_o}{\mathbf{P}_o . \mathbf{T}} . \dfrac{1}{22.4}}$$

$$= \frac{\mathbf{c} \times \mathbf{T} \times 22.4}{\mathbf{T}_o} \qquad [\text{cf. } \mathbf{P} = \mathbf{P}_o = 1 \text{ atm.}]$$

$$= \frac{0.003125 \times 300 \times 22.4}{273}$$

$$= 0.07692$$

$$\mathbf{e}_a = 98\% = 0.98$$

$$\mathbf{Q}_{v,IG} = 1200 \text{ m}^3/\text{h at operating conditions}$$

$$= 1200 \left(\frac{273}{300} \right) \text{m}^3/\text{h at standard conditions}$$

$$\mathbf{N} = 1200 \, \frac{273}{300} . \frac{0.07692}{1 - 0.07692} . (0.98) . \frac{1}{22.4}$$

$$\left[\frac{\mathbf{m}^3 \mathbf{IG}}{\mathbf{h}} \right] . \left[\frac{\mathbf{K}}{\mathbf{K}} \right] . \left[\frac{\mathbf{kmol MeOH}}{\mathbf{kmol water}} \right] . \left[\frac{1}{\mathbf{m}^3/\mathbf{kmol IG}} \right]$$

$$= 3.98108 \text{ kmol MeOH/h}$$

Step - (II) Liq and Gas Compositions at Tower Top and Bottom

Absorber Bottom

$$\mathbf{Y}_b = \frac{\mathbf{y}_b}{1 - \mathbf{y}_b} = \frac{0.07692}{1 - 0.07692} = 0.08332 \, \frac{\text{kmol MeOH}}{\text{kmol air}}$$

$$\mathbf{X}_b = 67\% \, \mathbf{X}_{max} \qquad \boxed{\text{Given}}$$

$$\mathbf{X}_{max} = \frac{0.08332}{1.15} = 0.07246 \, \frac{\text{kmol MeOH}}{\text{kmol water}}$$

$$\therefore \quad \mathbf{X}_b = (0.67)(0.07246) = 0.048548 \, \frac{\text{kmol MeOH}}{\text{kmol air}}$$

Absorber Top

The solvent enters the column solute-free.

$$\mathbf{X}_t = 0$$

$$Y_t = Y_b (1 - e_a) = 0.08332 (1 - 0.98) = 0.001666 \frac{\text{kmol MeOH}}{\text{kmol air}}$$

Step - (III) Mean Driving Force (MDF)

The equilibrium line $Y^* = 1.15X$ is drawn (**Figure 1/Example 1.36**)

For, $Y_b = 0.08332 \dfrac{\text{kmol MeOH}}{\text{kmol air}}$, $X_b = 0.07125 \dfrac{\text{kmol MeOH}}{\text{kmol air}}$ [**Figure 1/Example 1.36**]

For, $Y_t = 0.001666 \dfrac{\text{kmol MeOH}}{\text{kmol air}}$, $X_t = 0.00125 \dfrac{\text{kmol MeOH}}{\text{kmol air}}$ [**Figure 1/Example 1.36**]
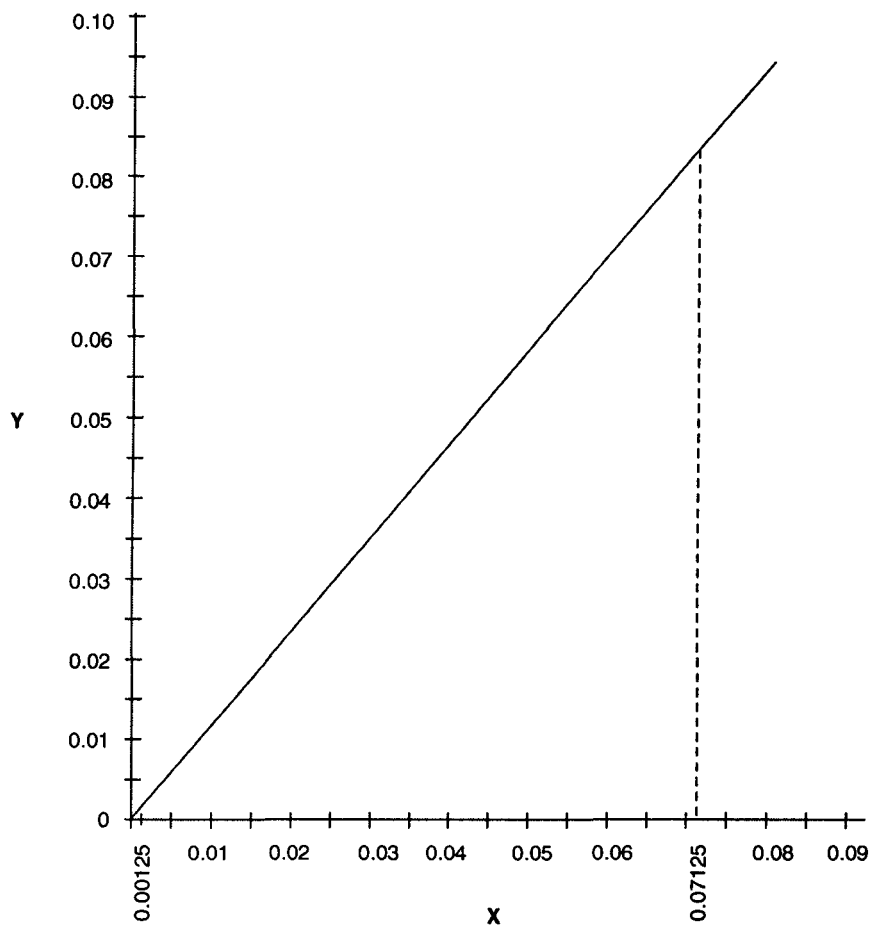
Fig.1/Example, 1.36.

$$\textbf{BDF}: \Delta X_b = X_b^* - X_b = 0.07125 - 0.048548 = 0.022702 \frac{\text{kmol MeOH}}{\text{kmol water}}$$

$$\textbf{TDF}: \Delta X_t = X_t^* - X_t = 0.00125 \frac{\text{kmol MeOH}}{\text{kmol water}}$$

$$\therefore \quad \text{MDF} \qquad \Delta X_{lm} = \frac{\Delta X_b - \Delta X_t}{\ln\left[\dfrac{\Delta X_b}{\Delta X_t}\right]}$$

$$= \frac{0.022702 - 0.00125}{\ln\left[\dfrac{0.022702}{0.00125}\right]}$$

$$= 0.007399 \frac{\text{kmol MeOH}}{\text{kmol water}}$$

Step - (IV) Liq Rate

If $\overset{\bullet}{L}$ be the solvent rate (kg/h) on solute-free basis, then

$$X_b = \frac{N}{\overset{\bullet}{L}/18} \cdot \frac{\text{kmol MeOH}/\text{h}}{\dfrac{\text{kg water}}{\text{h}} \cdot \dfrac{1}{\text{kg water}/\text{kmol water}}}$$

$$= 18\frac{N}{\overset{\bullet}{L}_s} \frac{\text{kmol MeOH}}{\text{kmol water}}$$

$$\therefore \qquad \overset{\bullet}{L}_s = 18\left[\frac{3.98108}{0.048548}\right] = 1476.0556 \text{ kg/h} \qquad \textbf{Ans.}$$

Step - (V) Surface Area of Contact between Vap and Liq Phases

$$A_c = \frac{N}{K_{L,X} \cdot \Delta X_{lm}}$$

$$= \frac{3.98108}{0.5 \times 0.007399} \cdot \frac{\text{kmol MeOH}/\text{h}}{\text{h.m}^2\left[\dfrac{\text{kmol MeOH}}{\text{kmol water}}\right]\left[\dfrac{\text{kmol MeOH}}{\text{kmol water}}\right]}$$

$$= 1076.1129 \text{ m}^2$$

Step - (VI) Effective Packing Volume

$$V_{eff} = \frac{A_c}{a} = \frac{1076.1129}{190} \cdot \frac{\text{m}^2}{\text{m}^2/\text{m}^3} = 5.66375 \text{ m}^2$$

Step - (VII) Actual Volume of Packing

$$V_{act} = \frac{V_{eff}}{\varphi} = \frac{5.66375}{0.87} = 6.5100 \text{ m}^3$$

Step - (VIII) Packed Bed Height

$$Q_{V,IG} = A.v = \frac{V_{act}}{Z} \cdot v$$

$$Z = \frac{V_{act}}{Q_{v,IG}} \cdot v = \left[\frac{6.51}{1200/3600}\right] \cdot (0.4) = 7.812 \text{ m} \qquad \textbf{Ans.}$$

Absorption Factor

Example 1.37. Acetone vapor is absorbed from air by water in a packed-bed absorber.

The absorber is provided with a bed of ceramic rings of 25mm × 25mm × 3mm in size irrigated with water.

The gas & liq phases move countercurrently in the column operated at a mean temperature of 293K and 1 atm. pressure.

Gas rate = 2000 kg/h

Gas composition at absorber inlet = 6 mol% of acetone vapor

Packed bed height = 10m

Column dia = 500 mm

Overall coefficient of mass transfer

$$K_{G,Y} = 0.42 \ \frac{kmol \ acetone}{h.m^2.(kmol \ acetone/kmol \ air)}$$

Determine the absorption factor of the absorber if the liq effluent contains 7.5 kg acetone per ton of pure water.

Assume the coefficient of wetting of the packing equals to 0.85

VLE-relationship for the system :

$$Y* = 1.68X$$

Solution : We shall resort to graphical technique to solve the problem.

Step - (I) Volume of Packing

$$V = Z.A$$

$$= 10 \left[\frac{\pi}{4} (0.5)^2 \right], m^3$$

$$= 1.96349 \ m^3$$

Step - (II) Effective Volume of Packing

$$V_{active} = V.\varphi = 1.96349 \times 0.85 = 1.66897 \ m^3$$

Step - (III) Surface Area of Phase Contact

$$A_c = V_{active}.a$$
$$= 1.66897 \times 204$$
$$= 340.470 \ m^2$$

Step - (IV) Gas Rate on Solute-Free Basis

Mass flowrate of gas, $\overset{\bullet}{G}$ = 2000 kg/h
Molar mass of the feed gas

$$= 0.06 \times 58 + 0.94 \times 29$$
$$= 30.74 \ kg/kmol$$

∴ Molar flowrate of gas

$$G = \frac{2000}{30.74} = 65.0618 \ kmol/h$$

Component (kg/kmol)	Molar Mass
Acetone	58
Air	29

Gas molar flowrate on solute-free basis

$$G_s = 65.0618 \times 0.94 = 61.1581 \text{ kmol air/h.}$$

Step - (V) Absorption Factor

The rate of acetone absorption :

$$
\begin{aligned}
N &= K_{G,Y} \cdot A_c \cdot \Delta Y_{lm} \\
&= (0.42)(340.470) \cdot \Delta Y_{lm} \\
&= 142.9974 \, \Delta Y_{lm}
\end{aligned}
\qquad \ldots(1)
$$

Overall material balance :

$$G_s (Y_b - Y_t) = L_s (X_b - X_t)$$

Now, $\qquad Y_b = 0.06$

$\therefore \qquad Y_b = \dfrac{y_b}{1 - y_b} = \dfrac{0.06}{1 - 0.06} = 0.06382$

$$\bar{x}_b = \frac{7.5}{1000} \frac{\text{kg acetone}}{\text{kg water}} = 0.0075 \frac{\text{kg acetone}}{\text{kg water}}$$

$$X_b = \frac{\bar{x}_b}{1 - \bar{x}_b} \cdot \frac{M_w}{M_{ac}} = \frac{0.0075}{1 - 0.0075} \cdot \frac{18}{58} = 0.002345 \frac{\text{kmol acetone}}{\text{kmol water}}$$

$$x_t = 0 \qquad \textbf{The solvent enters the column solute-free}$$

$\therefore \qquad X_t = 0$

Above mass balance reduces to :

$$61.1581 \, [0.06382 - Y_t] = L_s \left[\frac{N}{L_s} - 0 \right] = N \qquad \ldots(2)$$

Combining Eqns. (1) and (2) we get :

$$\boxed{ \text{cf. } X_b = \frac{N}{L_s} }$$

$$61.1581 \, (0.06382 - Y_t) = 142.9974 \, \Delta Y_{lm}$$

or, $\qquad 0.06382 - Y_t = 2.3381 \dfrac{\Delta Y_b - \Delta Y_t}{\ln\left[\dfrac{\Delta Y_b}{\Delta Y_t}\right]}$

or, $\qquad Y_b - Y_t = 2.3381 \dfrac{0.05988 - Y_t}{\ln\left[\dfrac{0.05988}{Y_t}\right]}$

or, $\qquad e_a \cdot Y_b \cdot \ln\left[\dfrac{0.05988}{Y_t}\right] = 2.3381 \, (0.05988 - Y_t)$

or, $\qquad e_a \cdot Y_b \cdot \ln\left[\dfrac{0.05988}{Y_t}\right] = 36.636 \, [0.05988 - Y_t]$

$$
\boxed{
\begin{aligned}
\Delta Y_b &= Y_b - Y_b^* \\
&= Y_b - 1.68 X_b \\
&= 0.06382 - 1.68(0.002345) \\
&= 0.05988 \\[4pt]
\Delta Y_t &= Y_t - Y_t^* \\
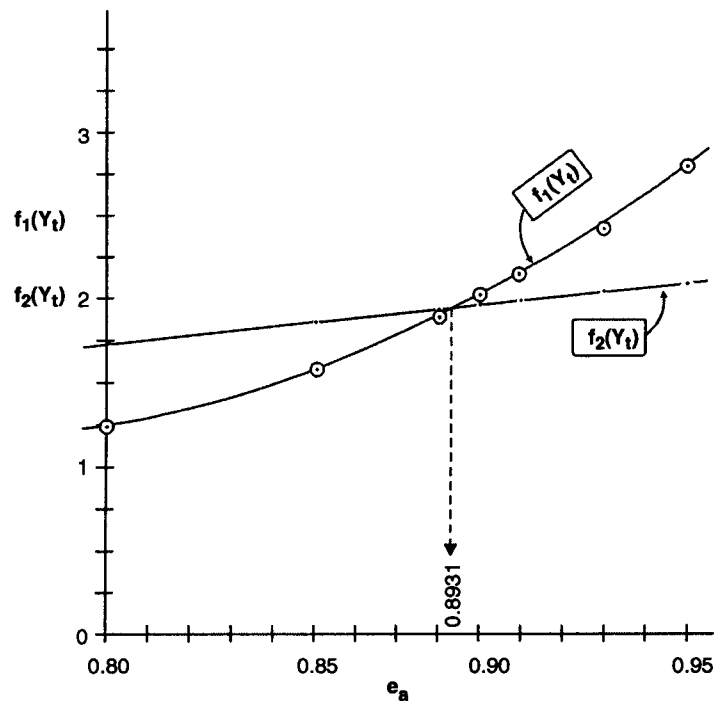&= Y_t - 1.68 X_t \\
&= Y_t
\end{aligned}
}
$$

Let   LHS = f_1 (Y_t) & RHS = $f_2(Y_t)$

$$e_a = \frac{Y_b - Y_t}{Y_b}$$

These two graphs are plotted against e_a

e_a	Y_t	$f_1(Y_t)$	$f_2(Y_t)$
0.80	0.01276	1.2365	1.7262
0.85	0.00957	1.5583	1.843
0.89	0.00702	1.9077	1.9365
0.90	0.006382	2.0149	1.9599
0.91	0.005743	2.1333	1.9833
0.93	0.004467	2.4139	2.0301
0.95	0.003191	2.7854	2.0768

These two lines intersect at e_a = 0.8931 [**Figure 1/Example 1.37**]

Fig 1/Exam. 1.37. $f_1(Y_t)$ *and* $f_2(Y_t)$ *as the Function of Absorption Factor.*

Hence the absorption factor of the given absorber under specified operating conditions is :

$$e_a = 89.31\%$$ **Ans.**

Solvent Rate

Problem 1.38. Calculate the solvent rate in Example 1.37

Ans. Solvent rate = 26.81 t/h

Hints : e_a = 0.8931

$$Y_t = Y_b (1 - e_a) = 0.06382 (1 - 0.8931) = 0.006822$$

BDF: $\Delta Y_b = Y_b - Y_b^*$

$$= Y_b - 1.68 X_b$$

$$= 0.06382 - 1.68 (0.002345)$$

$$= 0.05988$$

TDF: $\Delta Y_t = Y_t - Y_t^*$

$$= Y_t - 1.68 X_t$$

$$= 0.006822$$

MDF: $\Delta Y_{lm} = \dfrac{\Delta Y_b - \Delta Y_t}{\ln\left[\dfrac{\Delta Y_b}{\Delta Y_t}\right]} = \dfrac{0.05988 - 0.006822}{\ln\left[\dfrac{0.05988}{0.006822}\right]} = 0.024426$

$$N = K_{G,Y} \cdot A_c \cdot \Delta Y_{lm} = (0.42)(340.470)(0.024426)$$

$$= 3.49286 \text{ kmol acetone/h}$$

$$X_b = \frac{N}{L_s}$$

$\therefore$ $\quad L_s = \dfrac{N}{X_b} = \dfrac{3.49286}{0.002345} \dfrac{\text{kmol acetone/h}}{\text{kmol acetone/kmol water}}$

$$= 1489.4927 \text{ kmol water/h}$$

$$= 26810.868 \text{ kg water/h}$$

Flowrate of Solvent; NTU; Depth of Packing

Example 1.39. A scrubber with a diameter of 500mm is provided with a bed of ceramic packing of size 50m × 50mm × 5mm. Air at the rate of 550 m³/h (at 101.325 kPa/293°K) is charged at the bottom of the bed irrigated with water introduced to the column at the top.

The air contains ammonia of 2.8% by volume and it is to be absorbed by the countercurrent stream of water under atmospheric pressure.

Determine :

1. the solvent rate

2. the total number of transfer units $(NTU_{o,G})$

3. the packed bed depth.

Given :

Extraction factor = 0.95

Solvent rate is 40% greater than the theoretically minimum rate.

Overall gas phase mass transfer coefficient

$$K_{G,Y} = 0.001 \frac{kmol\ ammonia}{s.m^2.(kmol\ ammonia\,/\,kmol\ air)}$$

Coefficient of wetting of the packing, φ = 0.9

Concentration of ammonia in AIR-NH₃ Mixture in equilibrium with AQ. Soln. of ammonia at absorption temperature is :

X.1000	=	0	5	10	12.5	15	20	23
Y*.1000	=	0	4.5	10.2	13.8	18.3	27.3	32.7

Solution : Scrubber dia, D_t= 500mm = 0.5m

Q_V = 550 m³/h of air (101.325 kPa/293K)

$$y_b = \frac{2.8}{100} = 0.028$$ **Vol% = Mol%**

e_a = 0.95

$L_s = L_{s,min} + 45\% \, L_{s,min} = 1.45 L_{s,min}$

$$K_{G,Y} = 0.001 \, \frac{\text{kmol ammonia}}{\text{s.m}^2.(\text{kmol ammonia / kmol air})}$$

φ = 0.9

X.1000	=	0	5	10	12.5	15	20	23
Y*.1000	=	0	4.5	10.2	13.8	18.3	27.3	32.7

Step - (I) Feed Gas Rate at Standard Conditions

$$Q_v = 550 \times \frac{P}{P_o} \cdot \frac{T_o}{T}$$

$$= 550 \times \frac{273}{293}$$ cf. **P = P₀ = 101.325 kPa**

$$= 512.4573 \text{ m}^3/\text{h}$$

Step - (II) Rate of Ammonia Absorption

$$N = Q_v \cdot \frac{y_b}{1 - y_b} \cdot e_a \cdot \frac{1}{22.4}$$

$$= 512.4573 \, \frac{0.028}{1 - 0.028} \, (0.95) \cdot \frac{1}{22.4} \text{ kmol ammonia/h}$$

$$= 0.62607 \text{ kmol ammonia/h}$$

Step - (III) Liquid Rate

$$L_{s,min} = \frac{N}{X_b^* - X_t}, \text{ kmol/h}$$

Now, x_t= 0 as the solvent is introduced solute-free at the top of the column.

∴ $X_t = 0$

∴ $$Y_b = \frac{y_b}{1 - y_b} = \frac{0.028}{1 - 0.028} = 0.0288 \, \frac{\text{kmol ammonia}}{\text{kmol air}}$$

From the given equilibrium data, the VLE-curve **OA** is drawn **Figure 1/Exam. 1.39**
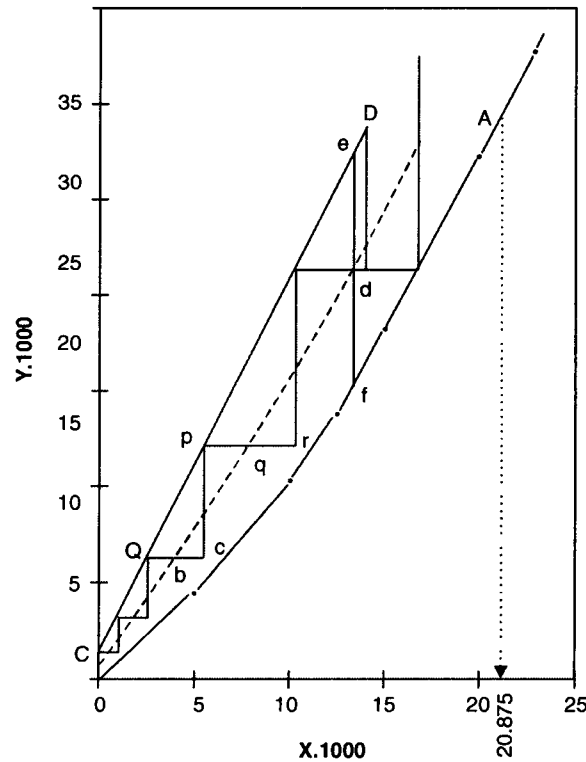

Fig. 1/Exam. 1.39.*VLE-curve For-Air-Ammonia Vapor in Equilibrium with AQ. Soln. of Ammonia at 293K & 101.325 kPa System Pressure.*

From the **Figure 1/Example 1.39**

$$X_b^* = 0.020875 \frac{\text{kmol ammonia}}{\text{kmol water}} \text{ for } Y_b = 0.0288 \frac{\text{kmol ammonia}}{\text{kmol air}}$$

$$\therefore \quad L_{s,\,min} = \frac{0.62607}{0.020875 - 0} = 29.9913 \text{ kmol/h}$$

$$\therefore \quad L_s = 1.45 \, L_{s,min}$$
$$= 1.45 \, (29.9913) \text{ kmol water/h}$$
$$= 43.48738 \text{ kmol water/h}$$
$$= 782.7729 \text{ kg water/h}$$

Step - (IV) Gas Rate & Liq Composition at Column Bottom

Overall material balance yields :

$$G_s \cdot (Y_b - Y_t) = L_s \cdot (X_b - X_t)$$

Now, $\qquad M_{mix} = 0.028 \times 17 + (1-0.028) \times 29 \text{ kg/kmol} = 28.664 \text{ kg/kmol}$

$$Q_v = 512.4573 \text{ m}^3/\text{h at STP}$$

$$\therefore \qquad G = \frac{512.4573}{22.4} \text{ kmol/h} = 22.8775 \text{ kmol/h}$$

$$\therefore \qquad G_s = G.\,(1 - y_b)$$
$$= 22.8775\,(1 - 0.028)\ \text{kmol air/h}$$
$$= 22.2369\ \text{kmol air/h}$$

Also, $\qquad Y_b - Y_t = Y_b.\,e_a = 0.0288 \times 0.95$

Substitution of the known value in the above material balance :

$$22.2369\,(0.0288 \times 0.95) = 43.48738\,(X_b - 0)$$

$\therefore \qquad X_b = 0.01399$ kmol ammonia/kmol water.

Step - (V) Number of Transfer Units

$$[\text{NTU}]_{o,G} = \int_{Y_t}^{Y_b} \frac{dY}{Y - Y^*}$$

The operating line *CD* is drawn by joining the points $C(X_t, Y_t)$ and $D(X_b, Y_b)$ on the same graph (**Figure 1/Example 1.39**)

$$X_t = 0$$
$$Y_t = Y_b(1 - e_a) = 0.0288\,(1 - 0.95) = 0.00144$$
$$X_b = 0.01399$$
$$Y_b = 0.0288$$

We draw an auxiliary dashline passing thru the midpoint of the oridinates between *CD* and *OA*.

Next starting from *C*, we step up such that ab = bc, pq = qr ...... etc. Each of these steps or stages correspond to one transfer unit **(NTU)**.

There are 4.608 stages in all.   **Ans.**

The last incomplete stage equals the ratio Dd/ef = 0.608

Comments : Upon inspection of the graph it becomes quickly apparent that a transfer unit is less than a step of the change in the concentration.

Aliter : Method of Graphical Integration

We compile the following table taking **VLE** data (given) and the data from **Figure 1/Example 1.39**)

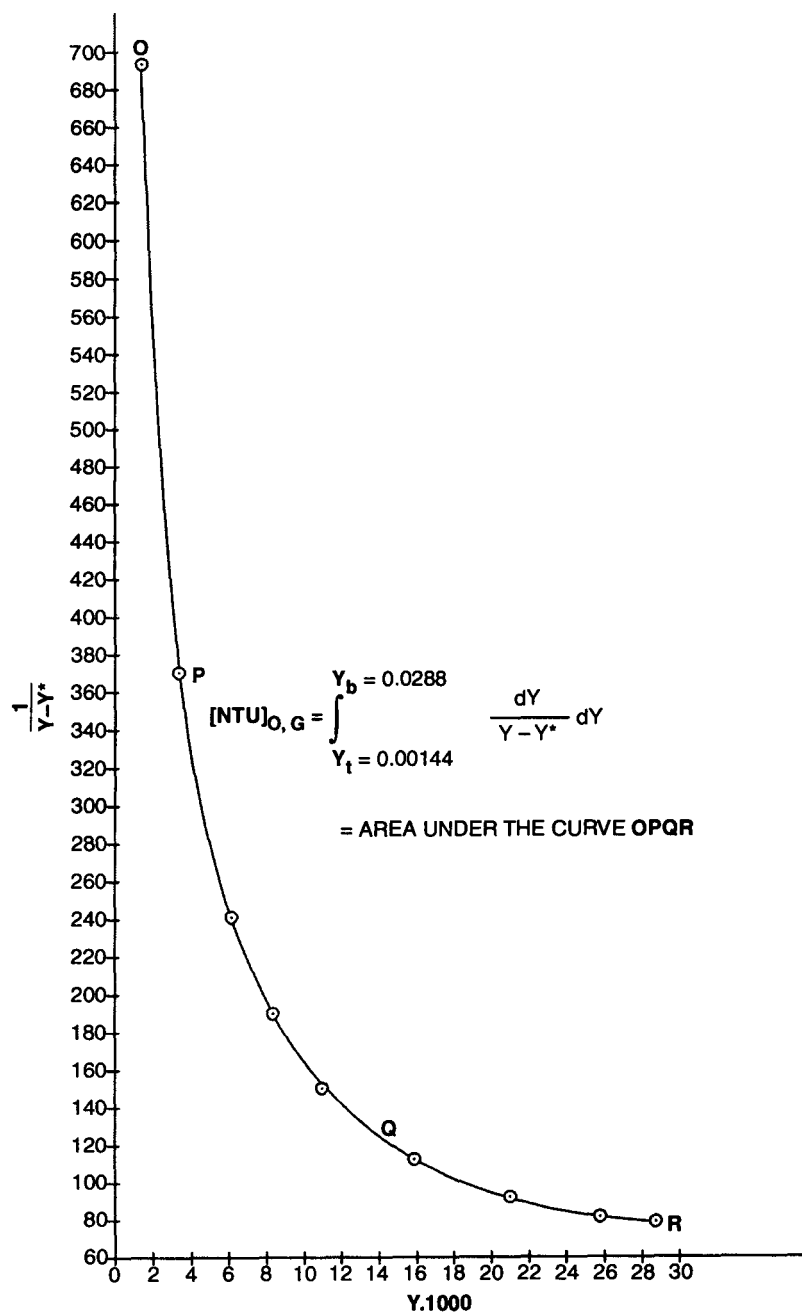| X	Y	Y*	Y – Y*	$\dfrac{1}{Y - Y^*}$
$X_t = 0$	0.00144	0	0.00144	694.444
0.00125	0.00375	0.00106	0.00269	371.747
0.0025	0.00625	0.002125	0.004125	242.424
0.00375	0.0085	0.00325	0.00525	190.476
0.005	0.0111	0.0045	0.00662	150.943
0.0075	0.016	0.00725	0.0875	114.285
0.010	0.021	0.0102	0.0108	92.592
0.0125	0.02587	0.0138	0.01207	82.815
$X_b = 0.01399$	0.0288	0.01625	0.01255	79.681

Fig. 2/Exam. 1.39. *Determination of the Number of Transfer Units By General Integration.*

We compile the following table for the graphical integration of $\dfrac{dY}{Y - Y^*}$

Y	n	$y = \dfrac{1}{Y-Y^*}$ *.(say)*	Y	n	$y = \dfrac{1}{Y-Y^*}$ *, (say)*
0.00144	0	694.444	0.0151	5	118
0.00417	1	330	0.0178	6	104
0.00691	2	224	0.02058	7	92
0.00964	3	170	0.0233	8	86
			0.02605	9	82
0.01237	4	139.9	0.02879	10	79.68

$$[NTU]_{o,G} = [A]_{curve\ OPQR}$$

$$= \frac{Y_{in} - Y_{fin}}{n}\left[\frac{y_o + y_n}{2} + \sum_1^{n-1} y\right] \quad \text{(Rule of Trapezium/Example 1.33)}$$

$$= \frac{0.02879 - 0.00144}{10}\left[\frac{694.444 + 79.68}{2} + 330 + 224 + 170 + 139.9 + 118 + 114 + 92 + 86 + 82 + 79.68\right]$$

$$= 4.9575$$

Step - (V) Height of A Transfer Unit

$$[HTU]_{o,G} = \frac{G_s}{K_{G,Y} \cdot a \cdot A_c}$$

Now, area of phase contact, $A_c = A.\varphi$

$$= \frac{\pi}{4} . D_t^2 . \varphi$$

$$= \frac{\pi}{4} .(0.5)^2. (0.9) , \text{m}^2.$$

Unit Surface Area of Packing

$$a = 87.5 \text{ m}^2/\text{m}^3 \text{ of packed bed of 50mm} \times 50\text{mm} \times 5\text{mm ceramic rings}$$

$$[HTU]_{o,G} = \frac{22.2369 / 3600}{(0.001)(87.5)\left(\dfrac{\pi}{4}\right)(0.5)^2(0.9)} , \frac{\dfrac{\text{kmol air / s}}{\dfrac{\text{kmol ammonia}}{\text{s.m}^2 . \left[\dfrac{\text{kmol ammonia}}{\text{kmol air}}\right]} . \dfrac{\text{m}^2}{\text{m}^3}}}{}. \text{m}^2$$

$$= 0.39947 \text{ m}$$

Step - (VI) Height of Packed Bed

$$Z = [HTU]_{o,G} . [NTU]_{o,G}$$

$$= (0.39947)(4.608) , \text{m} \qquad \textbf{[NTU determined graphically]}$$

$$= 1.80478 \text{ m} \qquad \qquad \textbf{Ans.}$$

$$Z = (0.39947)(4.9575) , \text{m} \qquad \textbf{[NTU] obtained thru graphical}$$
$$\textbf{integration}$$

$$= 1.9803 \text{ m} \qquad \textbf{Ans.}$$

Individual Film Transfer Coefficient

Example 1.40. Air-Ammonia mixture is passed thru a packed bed scrubber filled with dumped packings having interfacial surface area of 89.5 m^2/m^3. The bed is irrigated with water to absorb ammonia from the gas stream containing ammonia 5.8% by volume.

Determine the individual gas-film mass transfer coefficient.

The absorber is operated at :

Mean absorption temperature of 301K

Pressure of 101.325 kPa abs.

The feed gas rate = 3960 kg/h per m^2 of bed cross-section

Packing voidage = 0.79 m^3/m^3

Solution : We'll use the two following relationship :

$$k_G = \frac{Nu_G \cdot D_{ff}}{D_{eq}} \qquad \text{[Eqn. 1.16]}$$

and

$$Nu_G = 0.407 \, [Re_G]^{0.655} \cdot [Pr_G]^{0.33} \qquad \text{[Eqn. 1.160]}$$

Given :

$$a = 89.5 \text{ m}^3/\text{m}^3.$$
$$\epsilon = 0.79 \text{ m}^3/\text{m}^3.$$
$$T = 301K$$
$$P_{abs} = 101.325 \text{ kPa}$$
$$y_b = 0.058$$
$$G' = 3960 \text{ kg/(h.m}^2)$$

Step - (I) Average Molecular Weight of Feed Gas Stream

$$M_{mix} = 0.058 \, (17) + (1 - 0.058) \, (29)$$
$$= 28.304 \text{ kg/kmol}$$

Step - (II) Feed Gas Density

$$\rho_G = \frac{M_{mix}}{22.4} \cdot \frac{P}{P_o} \cdot \frac{T_o}{T} = \frac{28.304}{22.4} \cdot \frac{101.325}{101.325} \cdot \frac{273}{301} = 1.14603 \text{ kg/m}^3$$

Step - (III) Diffusivity of Ammonia in Air at Operating Temperature

$$D_{ff, T_2} = D_{ff, T_1} \cdot \frac{P_1}{P_2} \cdot \left[\frac{T_2}{T_1}\right]^{1.5}$$

$$= (17 \times 10^{-6}) \cdot \frac{101.325}{101.325} \cdot \left[\frac{301}{293}\right]^{1.5}$$

$$[D_{ff, NH_3\text{-}AIR/293K} = 17 \times 10^{-6} \text{ m}^2/\text{s}]$$

$$= 17.7 \times 10^{-6} \text{ m}^2/\text{s at } 301K/101.325 \text{ kPa}$$

Step - (IV) Equivalent Diameter

$$\mathbf{D_{eq}} = \frac{4 \in}{a} = \frac{4 \times 0.79}{89.5} = 0.0353 \, \text{m}$$

Step - (V) Gas Phase Reynolds Number

$$\mathbf{Re_G} = \frac{4v \cdot \rho_G}{a \cdot \mu_G} \hspace{3cm} \text{[Eqn. 1.153]}$$

$$= \frac{4 \cdot G'}{a \cdot \mu_G} \hspace{3cm} [\text{cf. } v \cdot \rho_G = G']$$

$$= \frac{4(3960 / 3600)}{89.5(18.75 \times 10^{-6})} \frac{\dfrac{\text{kg}}{\text{h.m}^2} \cdot \dfrac{1}{(\text{s/h})}}{\left[\dfrac{\text{m}^2}{\text{m}^3}\right] \cdot \left[\dfrac{\text{kg}}{\text{m.s}}\right]}$$

$$= 2621.97$$
$$= 2622$$

Step - (VI) Gas Phase Prandtl Number

$$\mathbf{Pr_G} = \frac{\mu_G}{\rho_G \cdot D_{ff}} = \frac{18.75 \times 10^{-6}}{(1.14603)(17.7 \times 10^{-6})} = 0.92434$$

Step - (VII) Gas Phase Nusselt Number

$$\mathbf{Nu_G} = 0.407 \, (2622)^{0.655} \cdot (0.92434)^{0.33} = 68.7896$$

Step (VIII) Gas-Film Mass Transfer Coefficient

$$\mathbf{k_G} = \mathbf{Nu_G} \cdot \mathbf{D}_{ff} / \mathbf{D}_{eq} = (68.7896) \, (17.7 \times 10^{-6}) / 0.0353 = 0.03449 \, \text{m/s} \hspace{2cm} \textbf{Ans.}$$

Packed Bed Volume and Height

Example 1.41. A smelter exit gas contains 3.5% by volume of SO₂ which is to be recovered by scrubbing the gas with water in a countercurrent absorption tower filled with random packing.

The feedgas is to be introduced to the column at the bottom and SO₂—free water to be fed at the top such that the exit gas from the top registers a SO₂—partial pressure SO₂ per 1000 kmol water.

The operating temperature of the scrubber = 293K

Operating pressure = 101.325 kPa

Vapor pressure of water at 293K = 2.3 kPa

Water rate = 27864 kg/h

If the area of cross-section of the tower is 1.357 m² determine the :

> *1. volume of packed bed*
>
> *2. height of packed bed*

to ensure the above separation.

Take the overall volumetric liquid phase mass transfer coefficient

$$K_{L,X} a = 684 \ \frac{kmol\,SO_2}{h.m^3.\left(kmol\,SO_2 / kmol\,H_2O\right)}$$

The equilibrium data for SO_2 and water at operating temperature are :

$X.10^4 =$	0.56	1.4	2.8	4.2	5.6	8.4	14.05
$Y.10^4 =$	7	16	43	79	116	194	363

where, X = kmol SO_2/ kmol water

Y = kmol SO_2/ kmol gas (air)

Solution : The packed volume is to be calculated from :

$$\underset{\left[\dfrac{kmol\,SO_2}{h}\right]}{N} = \underset{\left[\dfrac{kmol\,SO_2}{h.m^2.\dfrac{kmol\,SO_2}{kmol\,H_2O}}\right]}{K_{L,X}} \cdot \underset{[m^2]}{A} \cdot \underset{\left[\dfrac{kmol\,SO_2}{kmol\,H_2O}\right]}{\Delta X_{lm}}$$

which upon introducing the $K_L.a$ term takes the following form:

$$\underset{\left[\dfrac{kmol\,SO_2}{h}\right]}{N} = \underset{\left[\dfrac{kmol\,SO_2}{h.m^3.\dfrac{kmol\,SO_2}{kmol\,H_2O}}\right]}{[K_{L,X} \cdot a]} \cdot \underset{[m^3]}{V} \cdot \underset{\left[\dfrac{kmol\,SO_2}{kmol\,H_2O}\right]}{\Delta X_{lm}}$$

Given : $\quad$ P = 101.325 kPa

$\qquad\qquad\qquad$ T = 293 K

Column Top $\qquad$ L_s = 27864 kg/h

$\qquad\qquad\qquad$ L_s = 27864/18 = 1548 kmol/h

$\qquad\qquad\qquad$ p_{SO_2} = 1.145 kPa

$\qquad\qquad\qquad$ X_t = 0

Column Bottom $\qquad$ $X_b = \dfrac{1.145\,kmol\,SO_2}{1000\,kmol\,H_2O}$

Step - (I) Quantity of SO_2 Absorbed (N)

$$N = L_s\,(X_b - X_t)$$

$$= 1548\,(1.145 \times 10^{-3} - 0)$$

$$= 1.77246 \ kmol/h$$

Step - (II) Exit Gas Composition

Partial pressure of SO_2 content in the exit gas (tower top)

$$p_{SO_2} = 1.145 \text{ kPa}$$

$\therefore$
$$\begin{matrix} \text{Partial} & = & \text{Mol} & & \text{Total} \\ \text{Pressure} & & \text{fraction} & \times & \text{pressure} \end{matrix}$$

$$1.145 = y_t \times 101.325$$

$\therefore$
$$y_t = 0.0113$$

$\therefore$
$$Y_t = \frac{y_t}{1-y_t} = \frac{0.0113}{1-0.0113} = 0.011429 \frac{\text{kmol } SO_2}{\text{kmol inert}}$$

Step - (III) Inlet Gas Composition

Feed gas contains 3.5 vol% SO_2

$\therefore$
$$y_b = 0.035 \qquad\qquad\qquad \textbf{cf. Vol\% = Mol\%}$$

$\therefore$
$$Y_b = \frac{y_b}{1-y_b} = \frac{0.035}{1-0.035} = 0.03626 \frac{\text{kmol } SO_2}{\text{kmol inert}}$$

Step - (IV) Log-Mean-Driving-Force (ΔX_{lm})

$$\Delta X_{lm} = \frac{\Delta X_b - \Delta X_t}{\ln\left[\dfrac{\Delta X_b}{\Delta X_t}\right]}$$

where, $\Delta X_b = X_b^* - X_b$

$\Delta X_t = X_t^* - X_t$

For, $Y_b = 0.03626 , X_b^* = 14 \times 10^{-4}$ Fig. 1/Example 1.41

For, $Y_t = 0.011429 , X_t^* = 5.45 \times 10^{-4}$ Fig. 1/Example 1.41

$$\Delta X_b = (14 - 11.45) \times 10^{-4} = 2.55 \times 10^{-4} \frac{\text{kmol } SO_2}{\text{kmol } H_2O}$$

$$\Delta X_t = (5.45 - 0) \times 10^{-4} = 5.45 \times 10^{-4} \frac{\text{kmol } SO_2}{\text{kmol } H_2O}$$

$\therefore$
$$\Delta X_{lm} = \frac{2.55 \times 10^{-4} - 5.45 \times 10^{-4}}{\ln\left[\dfrac{2.55 \times 10^{-4}}{5.45 \times 10^{-4}}\right]} \times 10^{-4}$$

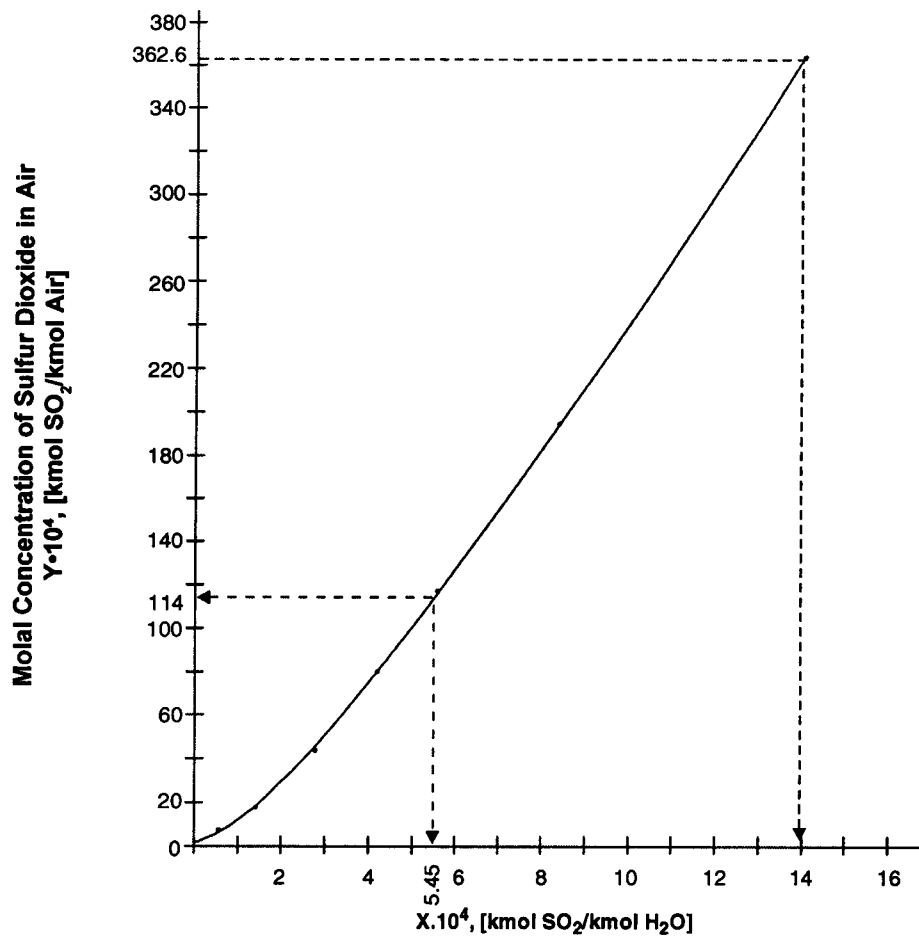$$= 3.81818 \times 10^{-4} \frac{\text{kmol } SO_2}{\text{kmol } H_2O}$$

Fig. 1/Exam. 1.41. *Extraplotation of Equilibrium Data for SO$_2$ And Water at 293K.*

Step - (V) Packed Bed Volume

Substituting the known value in the equation

$$N = K_{L,X} \cdot a \cdot V \cdot \Delta X_{lm}$$

We get

$$1.77246 = 694 \text{ (V) } (3.81818 \times 10^{-4})$$

∴
$$V = 6.78678 \text{ m}^3 \qquad \qquad \textbf{Ans.}$$

Step - (VI) Packed Bed Height

$$Z = \frac{V}{A}$$

$$= \frac{6.78678}{1.357}$$

$$= 5 \text{ m} \qquad \qquad \textbf{Ans.}$$

Liquid-Film Transfer Coefficient

Example 1.42 Carbon dioxide is absorbed by water in an absorber dumped with ceramic rings 35 mm × 35 mm × 4 mm in size.

If the density of irrigation is 60m³/(h.m²) and the coefficient of wetting of the packing is φ = 0.86, determine the liq-film mass transfer coefficient for the process taking place at the mean temperature of 293K.

Solution : The liq-film mass transfer coefficient can be computed from the relationship :

$$K_L = Nu_L \cdot D_{ff,L} / \delta_{red} \qquad ...(1.163)$$

where, $Nu_L = 0.0021 \, [Re_L]^{0.75} \cdot [Pr_L]^{0.5}$ $\qquad$ ...(1.162]

$$Re_L = \frac{4L'}{a \cdot \mu_L}$$

$$Pr_L = \frac{\mu_L}{\rho_L \cdot D_{ff,L}}$$

$$\delta_{red} = \text{reduced liq-film thickness} = \left[\frac{\upsilon_L^2}{g}\right]^{\frac{1}{3}}$$

Given :
$$Q_{v,L} = 60 \, \frac{m^3 \, liq}{h. \, (m^2 \, of \, bed \, cross - section)}$$

$$T = 293K$$

$$\varphi = 0.86$$

Step - (I) Liquid Rate

$$\rho_{L, 293K} = 1000 \, kg/m^3$$

$$L'_s = 60 \times 1000 \, \frac{kg}{h.m^2}$$

$$= \frac{60000}{3600} \, \frac{kg}{s.m^2}$$

Step - (II) Liquid Phase Reynolds Number

$$Re_L = \frac{4\overset{\bullet}{L}s}{A.a.\varphi.\mu_L} = \frac{4L'_s}{a.\varphi.\mu_L} \qquad\qquad \frac{\overset{\bullet}{L}}{A} = L'_s$$

$$= \frac{4(60000/3600)}{(140)(0.86)(1005\times10^{-6})}$$

a = 140 m²/m³; $\mu_{L, 293K}$ = 1005 × 10⁻⁶ Pa.s

$$= 550.955$$

Step - (III) Liquid Phase Prandtl Number

$$Pr_L = \frac{\mu_L}{\rho_L.D_{ff,L}} = \frac{1005\times10^{-6}}{(1000)(1.8\times10^{-9})} = 558.333$$

Step - (IV) Reduced Liq-Film Thickness

$$\delta_{red} = [\upsilon_L^2/g]^{1/3}$$

$$= \left[\frac{\mu_L^2}{\rho_L^2} \cdot \frac{1}{g}\right]^{\frac{1}{3}}$$

$$= \left[\left(\frac{1005\times10^{-6}}{1000}\right)^2 \frac{1}{9.81}\right]^{\frac{1}{3}}$$

$$= 4.6869 \times 10^{-5} \, m$$

Step - (V) Nusselt Number

$$Nu_L = 0.0021 \, [Re_L]^{0.75} \cdot [Pr_L]^{0.5}$$
$$= 0.0021 \, [550.955]^{0.75} \cdot [558.333]^{0.5}$$
$$= 5.6429$$

Step - (VI) Liquid-Film Transfer Coefficient

$$k = (5.6429)\,(1.8 \times 10^{-9})\,/\,(4.6869 \times 10^{-5})$$
$$= 2.167 \times 10^{-4} \, m/s \qquad\qquad \textbf{Ans.}$$

Gas-Film Transfer Coefficient

Example 1.43. Sulfur dioxide is absorbed from an inert gas (nitrogen) under atmospheric pressure in a packed tower operating under film conditions.

The temperature of absorption is 293K

Operating gas velocity = 0.35 m/s

The packed bed is composed of lumps of coke for which

the interfacial area of contact = 42 m²/m³ of packed bed

the fractional void = 0.58m³/m³ of packed bed.

Determine the gas-film transfer coefficient.

Solution : Use is to be made of the following equation :

$$k_G = \frac{Nu_G \cdot D_{ff,G}}{D_{eq}} \qquad \qquad \text{...(1.161)}$$

to evaluate the value of film transfer coefficient with respect to gas phase.

Gas phase Nusselt number is to be computed from :

$$Nu_G = 0.407 \, [Re_G]^{0.655} \cdot [Pr_G]^{0.33} \qquad\qquad \text{...(1.160)}$$

Equivalent dia of packing

$$D_{eq} = \frac{4 \in}{a}$$

Step (I) Gas Density

In absence of data let us assume the feed gas is dilute in SO_2 such that $\rho_G \approx \rho_{N_2}$

$$\therefore \qquad \rho_G = \frac{28}{22.4} \cdot \frac{273}{293} = 1.16467\ kg/m^3$$

Step - (II) Gas Phase Reynolds Number

$$\mathbf{Re} = \frac{4v \cdot \rho_G}{a \cdot \mu_G} \qquad\qquad ...(1.153)$$

where, v = operation velocity = 0.35 m/s

a = packing interfacial area = 42 m^2/m^3

μ_G = 17.5×10^{-6} Pa.s

$$\mathbf{Re}_G = \frac{4 \times 0.35 \times 1.16467}{42 \times \left(17.5 \times 10^{-6}\right)} = 2218.43$$

Step -(III) Diffusion Coefficient of SO_2 in N_2 at 293K

Assuming the diffusivity of SO_2 in N_2 is same as that in air,

$$\mathbf{D}_{ff,\ SO_2 - N_2 /293K} = \mathbf{D}_{ff,\ SO_2 - AIR/273K} \left[\frac{P_1}{P_2}\right] \cdot \left[\frac{T_2}{T_1}\right]^{1.5}$$

$$= 10.3 \times 10^{-6} \left[\frac{101.325}{101.325}\right] \cdot \left[\frac{293}{273}\right]^{1.5}$$

$$= 11.452 \times 10^{-6}\ m^2/s$$

Step - (IV) Gas Phase Prandtl No. (Pr$_G$)

$$\mathbf{Pr}_G = \frac{\mu_G}{\rho_G \cdot \mathbf{D}_{ff,G}} = \frac{17.5 \times 10^{-6}}{1.16467 \times \left(11.452 \times 10^{-6}\right)} = 1.312$$

Step - (V) Gas Phase Nusselt Number

$$\mathbf{Nu}_G = 0.407\ [2218.43]^{0.655} \cdot [1.312]^{0.33} = 69.21$$

Step - (VI) Equivalent Dia of Packing

$$\mathbf{D}_{eq} = \frac{4\ \epsilon}{a} = \frac{4 \times 0.58}{42} = 0.0552\ m$$

Step -(VI) Gas-Film Mass Transfer Coefficient

$$k = 69.21 \left[\frac{11.452 \times 10^{-6}}{0.0552}\right] = 0.01435\ m/s \qquad\qquad \textbf{Ans.}$$

Dependence of Gas-Film Transfer Coefficient on Gas Velocity

Problem 1.44. *Solve Example 1.43 if the gas velocity is changed to following values :*

0.20 ; 0.25 ; 0.30 ; 0.40 ; 0.45; 0.50 m/s

while all other parameters remain the same.

•

Show graphically how k_G *will vary with gas velocity.*

Ans.

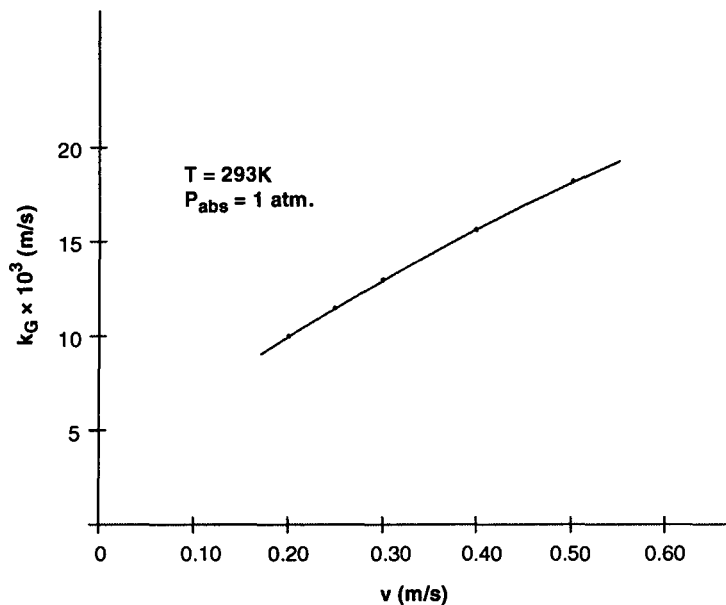| v (m/s) =	0.20	0.25	0.30	0.40	0.45	0.50
$k_G \times 10^3$ (m/s) =	9.952	11.5	12.9	15.67	16.92	18.13

Fig. 1/Example1.44. *Dependence of Gas-film Mass Transfer Coefficient on Gas Velocity For* SO_2 *Absorption in Water in An Absorber Filled with Coke Lumps* $[a = 42 \ m^2/m^3 \ ; \ \epsilon = 0.58m^3/m^3]$

Gas-Film Mass Transfer Coefficient

Example 1.45 *An absorber filled with grid packing with bars 12.5 mm × 100 mm in size having a spacing of b = 25 mm is used for the absorption of benzene vapor from the coke gas. If the coefficient of diffusion of benzene in the gas is 16 × 10⁻⁶ m²/s, determine the gas-film mass transfer coefficient.*

Given : For the packing, the equivalent dia is twice the grid bar width.

$$D_{eq} = 2b = 50 \ mm$$

Gas velocity = 0.95 m/s based on entire absorber cross-section

Gas density = 0.5 kg/m³

Dynamic viscosity of gas = 13 × 10⁻⁶ Pa.s

Film conditions prevail in the column.

Solution : The gas-film transfer coefficient can be computed from

$$k_G = \frac{Nu_G \cdot D_{ff, G}}{D_{eq}} \qquad ...(1.161)$$

where, Nu_G = Gas Phase Nusselt No.

$$= 0.407 \ [Re_G]^{0.655} \cdot [Pr_G]^{0.33}$$

$$D_{eq} = 2b = 2 \times 25mm = 50 \ mm = 0.05m$$

Step - (I) Gas Phase Reynolds Number (Re_G)

$$Re_G = \frac{4v \cdot \rho_G}{a \cdot \mu_G}$$

Now, $a = 50$ m^2/m^3 for the grid packing 12.5mm × 100mm in size with bar spacing 25 mm (b = 25 mm given)

$$\mu_G = 13 \times 10^{-6}\ \text{Pa.s}$$
$$\rho_G = 0.5\ \text{kg/m}^3$$
$$v = 0.95\ \text{m/s}$$

$$Re_G = \frac{4(0.95)(0.5)}{50(13 \times 10^{-6})} = 2923$$

Step - (II) Gas Phase Prandtl No. (Pr_G)

$$Pr_G = \frac{\mu_G}{\rho_G \cdot D_{ff,G}}$$

$$= \frac{13 \times 10^{-6}}{0.5(16 \times 10^{-6})}$$

$$= 1.625$$

Step - (III) Gas Phase Nusselt No. (Nu_G)

$$Nu_G = 0.407\,(2923)^{0.655} \cdot (1.625)^{0.33}.$$
$$= 88.9818$$

Step - (IV) Gas-Film Mass Transfer Coefficient

$$k_G = Nu_G \cdot \frac{D_{ff,G}}{D_{eq}}$$

$$= 88.9818\,\frac{16 \times 10^{-6}}{0.05}\ , \quad \frac{\text{m}^2/\text{s}}{\text{m}}$$

$$= 0.02847\ \text{m/s} \qquad\qquad\qquad\qquad \textbf{Ans.}$$

Packed Bed Height

Example 1.46. Ammonia is to be removed from a 9.688% (wt.) ammonia-air mixture by scrubbing with water in a packed tower, so that 98% of the ammonia is eliminated. What should be the height of the packed bed required for the purpose ?

Data :

Feed gas rate = 4458.855 kg/(h.m²)

Solvent (water) rate = 3384 kg/(h.m²)

$K_{G,p} \cdot a = 2.88$ kmol/h.m³.kPa

Operating pressure = 101.325 kPa

Operating temperature = 293K.

Solution : The packed bed height can be computed from

$$Z = \frac{G_s}{k_{G,p}.a.P} \cdot \int_{Y_t}^{Y_b} \frac{(1+Y)(1+Yi)}{Y-Y_i} \cdot dY \qquad \dots(1.93)$$

Since ammonia is a very soluble gas in water,

$$k_{G,p}.a \approx K_{G,P}.a$$

Therefore, the above expression transforms to

$$Z = \frac{G_s}{K_{G,p}.a.P} \cdot \int_{Y_t}^{Y_b} \frac{(1+Y)(1+Y^*)}{Y-Y^*} \cdot dY \qquad \dots(1.106)$$

Step - (I) Gas Composition at Tower Top and Bottom

The data in wt. % must be converted to mole fraction & then to mole ratio.

Gas composition at tower bottom : **9.688 wt% NH_3 + 90.312wt% Air**

Gas	Mol. Wt. (kg/kmol)
NH_3	17
Air	29

$$\frac{9.688}{100} = \frac{17y_b}{17y_b + 29(1-y_b)}$$

or, $\qquad 29 - 12y_b = 175.4748 y_b$

∴ $\qquad y_b = 0.15469$ mol fraction NH_3

∴ $\qquad Y_b = \frac{y_b}{1-y_b} = \frac{0.15469}{1-0.15469} = 0.1829 \dfrac{\text{kmol } NH_3}{\text{kmol Air}}$

Forasmuch as 98% ammonia in the feed gas is absorbed, so absorption factor is 98%, i.e.,

$$0.98 = \frac{Y_b - Y_t}{Y_b}$$

∴ $\qquad Y_t = Y_b - 0.98Y_b = 0.1829\,(1-0.98) = 0.003658 \dfrac{\text{kmol } NH_3}{\text{kmol Air}}$

Step - (II) Operating Line

The equation of the operating line is obtained from the mass balance between a horizontal section of the tower where the composition are X and Y and the top of the tower as :

$$G_s\,(Y - Y_t) = L_s\,(X - X_t)$$

Now, feed gas rate :

$$G' = 4458.855 \text{ kg/(h.m}^2)$$

$$y_{NH_3} = 0.15469 \text{ mol fraction}$$

$$y_{IG} = (1 - 0.15469) = 0.84531 \text{ mol fraction}$$

Average molecular weight of feed gas

$$M_{mix} = 0.15469\,(17) + 0.84531\,(29) = 27.1437 \text{ kg/kmol}$$

$$G = \frac{4458.855}{27.1437} \text{ kmol/(h.m}^2)$$

$$= 164.2684 \text{ kmol/(h.m}^2)$$

Feed gas rate on solute-free basis :

$$G_s = 164.2684 \times 0.84531 \text{ kmol IG/(h.m}^2)$$
$$= 138.8577 \text{ kmol IG/(h.m}^2)$$

Solvent rate :

$$L' = 3384 \text{ kg/(h.m}^2)$$

$$\therefore \quad L_s = \frac{3384}{18} \text{ kmol/(h.m}^2) \qquad \textbf{Assuming the solvent is solute free}$$

$$= 188 \text{ kmol/(h.m}^2)$$

$$X_t = 0 \qquad \textbf{The solvent enters the column solute-free}$$

$$\therefore \quad X_t = 0$$

Hence the foregoing mass balance becomes :

138.8577 (Y – 0.003658) = 188 (X – 0)

or, Y = 1.3539 X + 0.003658

Step – (III) Graphical Presentation of VLE and OL

VLE Data :

X.1000 =	21	31	42	53	79	106	159
Y.1000 =	16	24.5	33.9	43.5	70.4	101	176

where, X = kmol NH_3/kmol H_2O; Y = kmol NH_3/kmol AIR
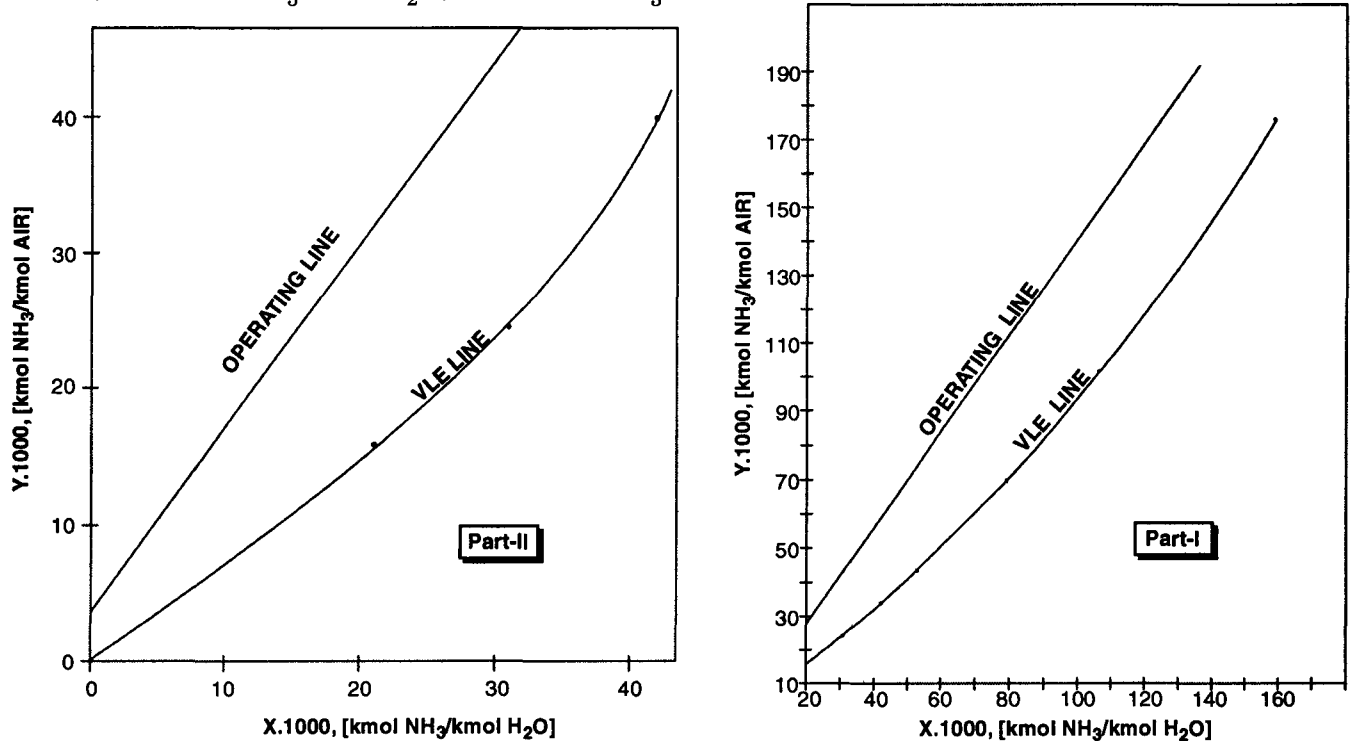
Fig. 1/Example.1.46 Graphical Representation of VLE & OL of Ammonia-Air System subjected to Scrubbing with Water in a Packed Tower wherein 98% of Ammonia of the Feed Gas is Absorbed under A Pressure of 101.325 kPa and at A Temperature of 293K while the Feed Gas Rate is 4458.855 kg/(h.m²) and Solvent Rate is 3384 kg/(h.m²).

Operating Line : Y = 1.3539 X + 0.003658

X =	0	0.05	01
Y =	0.003658	0.07135	0.13904

Taking these data we draw the OL & VLE curve **Figure 1/Example 1.46**

Step - (IV) Graphical Integration of NTU

$$[NTU]_{O,G} = \int_{Y_t}^{Y_b} \frac{(1+Y)(1+Y^*)}{Y-Y^*} \cdot dY$$

In order to determine **NTU** graphically, we construct the following table :

Y	Y* (Fig.1/Example 1.46)	Y - Y*	(1 + Y) (1 + Y*)	$\frac{(1+Y)(1+Y^*)}{Y-Y^*}$
Y_b = 0.1829	0.128	0.0549	1.3343	24.3043
0.17	0.120	0.05	1.3104	26.208
0.15	0.103	0.047	1.2684	26.988
0.10	0.062	0.038	1.1682	30.742
0.05	0.029	0.021	1.0804	51.45
0.04	0.023	0.017	1.0639	62.583
0.03	0.0155	0.0145	1.0459	72.135
0.02	0.009	0.011	1.02918	93.5618
0.01	0.0035	0.0065	1.0135	155.928
Y_t = 0.00365	0	0.00365	1.00365	274.972

— Values of $\frac{(1+Y)(1+Y^*)}{Y-Y^*}$ are plotted against the corresponding values of Y **[Figure 2/Example 1.46]**

The area under the curve OPQR corresponding to $[NTU]_{O,G}$ *i.e.*,

$$[NTU]_{O,G} = \int_{Y_t=0.00365}^{Y_b=0.1829} \frac{(1+Y)(1+Y^*)}{Y-Y^*}$$

We follow the rule of trapezium to obtain the value of this integral.

Y	n	$I = \frac{(1+Y)(1+Y^*)}{Y-Y^*}$ Figure 2/Example 1.46	Y	n	$I = \frac{(1+Y)(1+Y^*)}{Y-Y^*}$
0.1829	0	24.3043	0.0574	7	45.45
0.1649	1	26	0.0395	8	61
0.147	2	27	0.02157	9	90
0.129	3	28	0.00365	10	274.972
0.112	4	30.5			
0.0933	5	35			
0.0753	6	37			

$$[NTU]_{O,G} = \frac{Y_{fin} - Y_{in}}{n} \left[\frac{I_o + I_n}{2} + \sum_{1}^{n-1} I \right]$$

$$[NTU]_{O,G} = \int_{Y_t = 0.00365}^{Y_b = 0.189} \frac{(1 + Y)(1 + Y^*)}{Y - Y^*} \, dY$$
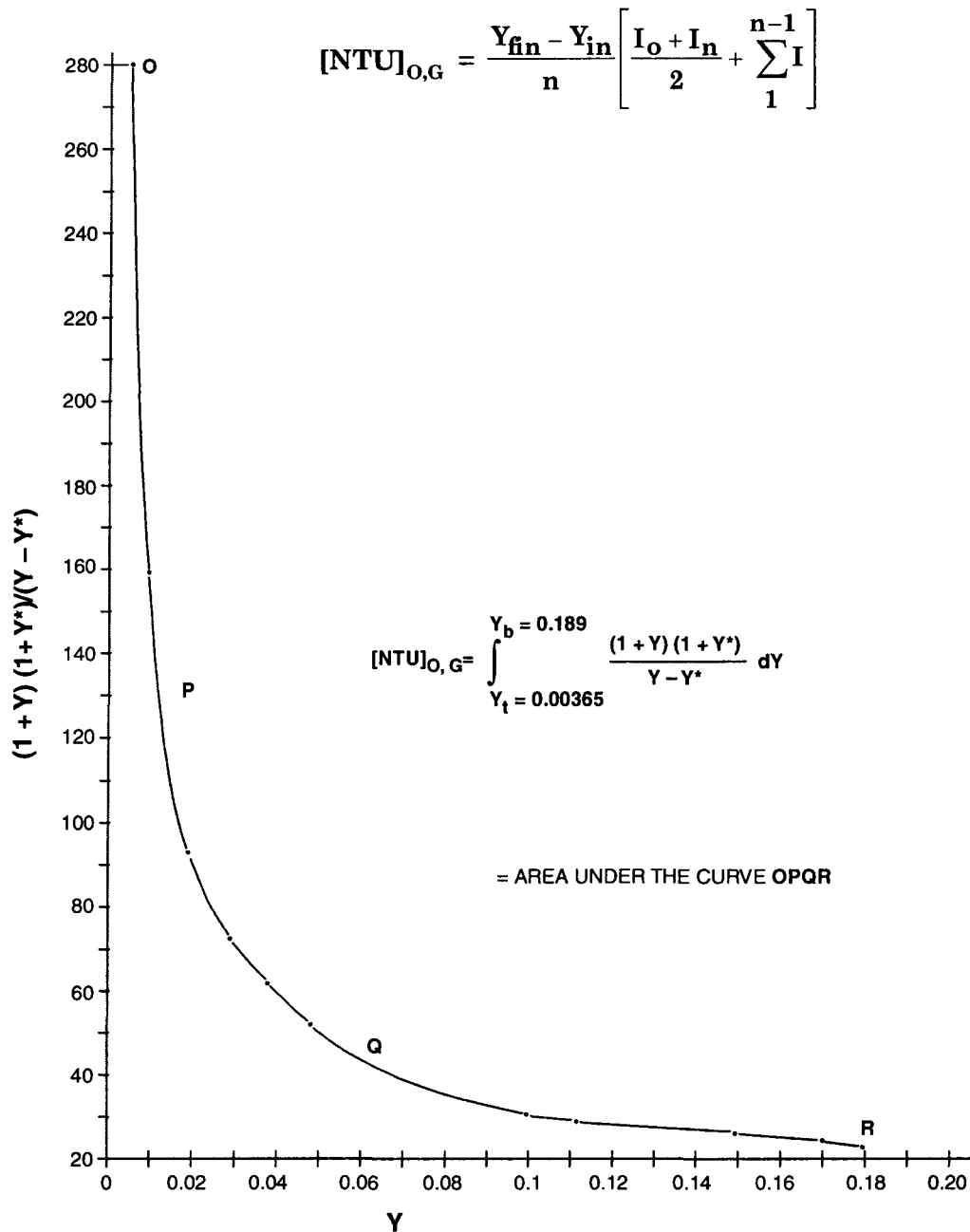
= AREA UNDER THE CURVE **OPQR**

Fig. 2/Exam 1.46 *Graphical Determine of [NTU]$_{O,G}$ for the Absorption of Ammonia with Water in A Packed Tower.*

$$= \frac{0.1829 - 0.00365}{10} \left[\frac{24.3043 + 274.972}{2} + 26 + 27 + 28 + 30.5 + 35 + 37 + 45.45 + 61 + 90 \right]$$

$$= 9.49286$$

$$\therefore \ Z = \frac{138.8577 \times 9.49286}{2.88 \times 101.325} = 4.517 \text{m} \qquad \textbf{Ans.}$$

PACKED BED HEIGHT

Problem. 1.47. Ammonia is to be removed from an Air-Ammonia mixture by scrubbing the gas with ammonia-free water in a packed tower, so that 99.9% of the ammonia is removed.

Feed gas composition : 10% ammonia by wt.

Feed gas rate : 4230 kg/h per m^2 of tower cross-section

Scrubbing liquor rate : 3384 kg/h per m^2 of tower cross-section

Overall volumetric gas phase mass transfer coefficient.

$$K_{G,P} \cdot a = 2.88 \; \frac{kmol\ NH_3}{h.m^3.kPa}$$

Operating pressure = 101.325 kPa

Operating temperature = 293 K

Equilibrium Data :

$\frac{kmol\ NH_3}{kmol\ H_2O} \times 1000$ =	21	31	42	53	79	106	159
$\frac{kmol\ NH_3}{kmol\ H_2O} \times 1000$ =	16	24.5	33.9	43.5	70.4	101	176

Calculate the packed height required for the purpose.

[Ans. Z = 29.482 m]

Hints :

Wt % $\Rightarrow$ Mol %

$$0.10 = \frac{17\,y_b}{17y_b + 29(1 - y_b)}$$

∴

y_b = 0.15934

Y_b = 0.18597 kmol NH$_3$/kmol Air

y_t = (1 – 0.999).y_b = 0.000159

Y_t = 0.000159 kmol NH$_3$/kmol Air

M_{mix} = 0.10(17) + 0.90(29) = 27.8 kg/kmol

G' = 4230 kg/(h.m^2)

G = 155.3956 kmol/(h.m^2)

G_s = $G(1 - y_{NH_3})$ = 130.6348 kmol IG/(h.m^2)

L_s = L'/M_{H_2O} = 188 kmol H$_2$O/(h.m^2)

x_t = 0

X_t = 0

Material Balance :

$$130.6348\ (Y - 0.000159) = 188\ (X - 0)$$

$$\therefore \qquad Y = 1.439\ X + 0.000159$$

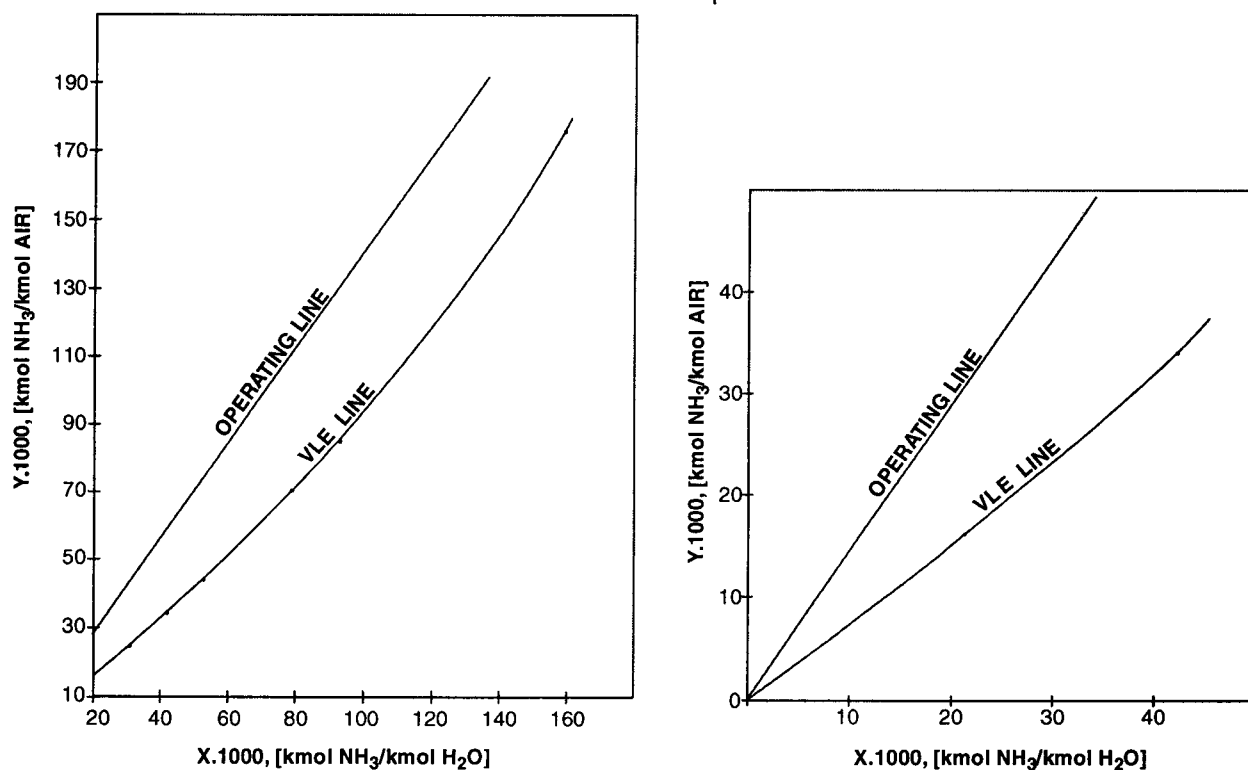$$Z = \frac{G_s}{K_{G,p} \cdot a \cdot P} \int_{Y_t}^{Y_b} \frac{(1+Y)(1+Y^*)}{Y - Y^*} \cdot dY$$

Fig. 1/Example 1.47.

Y	Y^*	$Y - Y^*$	$(1+Y)(1+Y^*)$	$\dfrac{(1+Y)(1+Y^*)}{Y-Y^*}$
	[Fig. 1/Example 1.47]			
$Y_b = 0.18597$	*0.134*	*0.05197*	*1.3448*	*25.8781*
0.18	0.126	0.054	1.32868	24.6051
0.17	0.117	0.053	1.30689	24.6583
0.15	0.100	0.05	1.265	25.3
0.13	0.083	0.047	1.22379	26.038
0.11	0.067	0.043	1.1843	27.543
0.090	0.053	0.037	1.1477	31.0208
0.07	0.0395	0.0305	1.1122	36.467
0.05	0.027	0.023	1.0783	46.884
0.04	0.021	0.019	1.06184	55.886
0.03	0.0155	0.0145	1.0459	72.135
0.02	0.0106	0.0094	1.0308	109.660
0.01	0.0051	0.0049	1.01515	207.173
$Y_t = 0.000159$	0.0000	0.000159	1.000159	6290.308

Determination of $[NTU]_{O,G}$ thru Graphical Method of Integration.
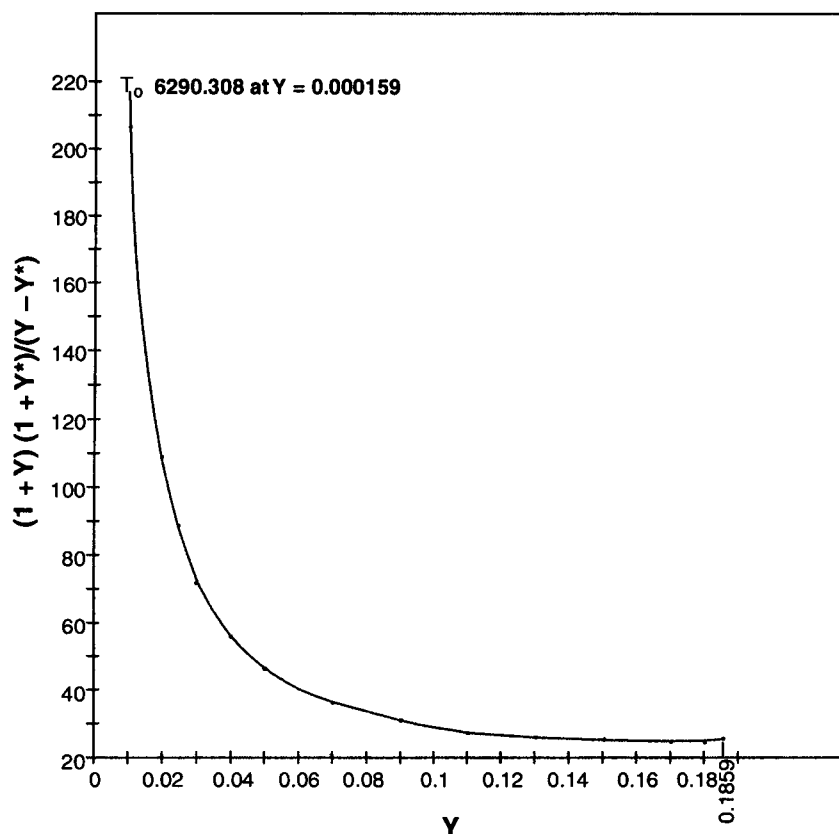
Fig. 2/Example 1.47.

Y	n [From Fig.2./Exam. 1.47]	$I = \dfrac{(1+Y)(1+Y^*)}{Y-Y^*}$	Y	n	$I = \dfrac{(1+Y)(1+Y^*)}{Y-Y^*}$ [From Fig.2/Exam. 1.47]
0.18597	0	25.8781	0.0744	6	35
0.1673	1	24.8	0.0559	7	42.5
0.1488	2	25	0.0373	8	60.5
0.1302	3	25.5	0.01874	9	116
0.1116	4	27	0.000159	10	6290.308
0.09306	5	30			

$$[NTU]_{O,G} = \int_{Y_t = 0.00159}^{Y_b = 0.18597} \frac{(1+Y)(1+Y^*)}{Y-Y^*}$$

$$= \left[\frac{0.18597 - 0.000159}{10}\right]\left[\frac{25.8781 + 6290.308}{2} + 24.8 + 25 + 25.5 + 27 + 30 + 35 + 42.5 + 60.5 + 116\right]$$

$$= 65.858$$

Packed bed height : $Z = \dfrac{130.6348 \times 65.858}{2.88 \times 101.325} = 29.482 \, m$

HEIGHT OF PACKING

Example 1.48. A soluble gas is absorbed from a dilute gas-air mixture by countercurrent scrubbing with a solvent in a packed tower. The solvent liquor introduced to the column at the top contains no solute and it is desired to recover 90% of the solute by using 50% more liquid than the minimum necessary.

What height of the packing will be required if the height of a transfer unit HTU of the proposed tower is 600mm.

Solution : The height of the packing

$$Z = [HTU]_{O,G} \times [NTU]_{O,G}$$

$$[HTU]_{O,G} = 600mm = 0.6 \, m \qquad\qquad\qquad \text{Given}$$
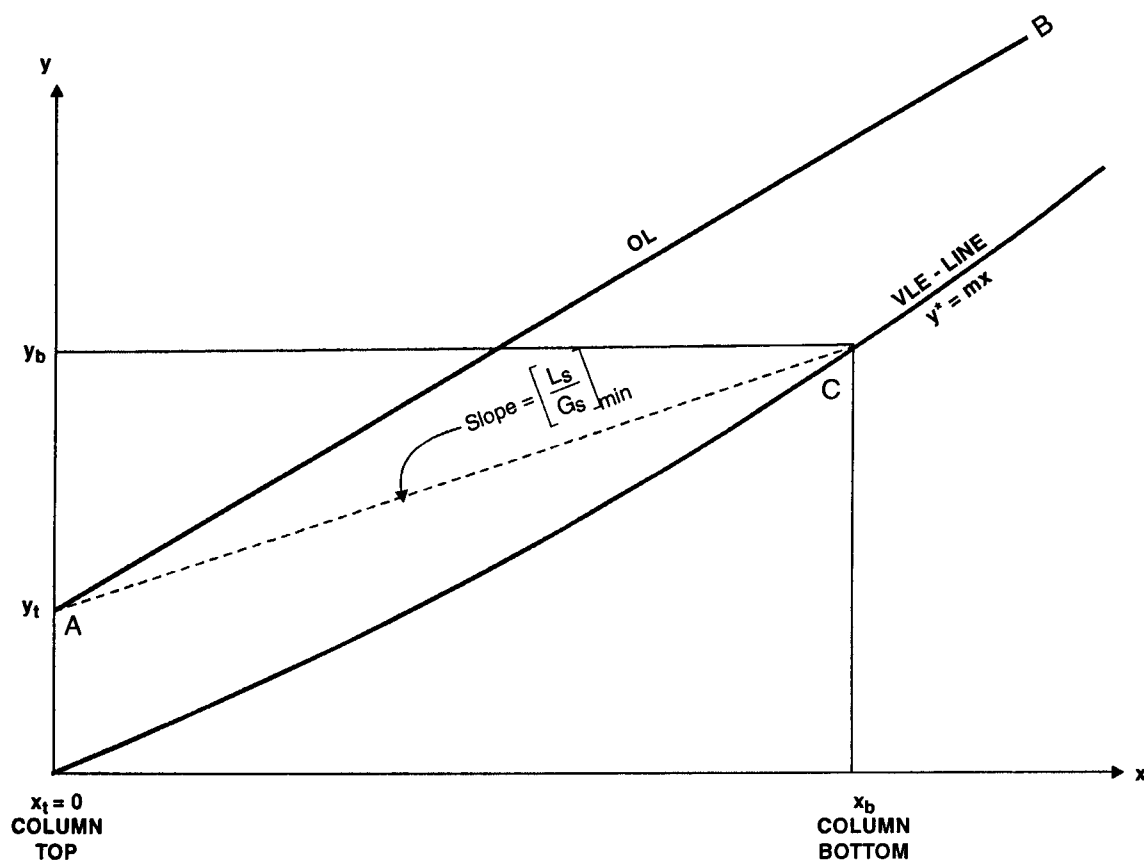
Fig. 1/Example/1.48. *Operating Line & Vap-Liq Equilibrium of An Absorber*
AB Represents OL when Liq Rate is L_s
AC Represents OL when Liq Rate is $L_{s, \, min}$

$$[NTU]_{O,G} = \frac{1}{\left[1 - \frac{1}{e_a}\right]} \cdot \ln\left[\left(1 - \frac{1}{e_a}\right) \cdot \frac{y_b}{y_t} + \frac{1}{e_a}\right] \qquad (1.124)$$

where e_a = extraction (*i.e.*, absorption) factor = $\frac{L_s}{m.G_s}$

m = slope of the equilibrium line

Now, AC represents the OL at limiting condition, *i.e.*, when $L_s = L_{s,\,min}$. The slope of AC is

$$\left[\frac{L_s}{G_s}\right]_{min} = \frac{y_b - y_t}{x_b}$$

(x_b, y_b) lies on the VLE curve.

$$\therefore \qquad y_b = m.x_b$$

$$\therefore \qquad \left[\frac{L_s}{G_s}\right]_{min} = \frac{y_b - y_t}{y_b / m} = m\left[1 - \frac{y_t}{y_b}\right] = m\left[1 - \frac{0.1y_b}{y_b}\right] = 0.9\,m$$

As per given condition

$$\frac{L_s}{G_s} = \left[\frac{L_s}{G_s}\right]_{min} + \left[\frac{L_s}{G_s}\right]_{min} \cdot (50\%) = 1.5\left[\frac{L_s}{G_s}\right]_{min}$$

$$\therefore \qquad \left[\frac{L_s}{G_s}\right] = 1.5 \times 0.9\,m = 1.35\,m$$

$$\therefore \qquad e_a = \frac{L_s}{m.G_s} = \frac{1.35\,m}{m} = 1.35$$

$$\therefore \qquad [NTU]_{O,G} = \frac{1}{\left[1 - \frac{1}{1.35}\right]} \ln\left[\left(1 - \frac{1}{1.35}\right) \cdot \frac{y_b}{0.1\,y_b} + \frac{1}{1.35}\right]$$

$$= 5.6438$$

$$\therefore \qquad Z = 0.6 \times 6.6438 = 2.786\,m \qquad \textbf{Ans.}$$

DEPENDENCE OF PACKING HEIGHT WITH LIQ RATE

Example 1.49. Show graphically how the height of packed bed will vary, in the Example 1.48, if the liq rate is changed to following values :

L_s = *40%, 45%, 55%, 60%, 65%, 70% more than* $L_{s,\,min}$.

The solute-free solvent is used as before to absorb 90% of solute in all cases. HTU remains the same.

Solution : The minimum value of the ratio of liq : gas ratio remains constant, *i.e.*,

$$\left[\frac{L_s}{G_s}\right]_{min} = 0.9 \ m[\text{where } m = \text{slope of VLE curve}]$$

L_s	$\dfrac{L_s}{G_s}$	$e_a = \dfrac{L_s}{m.G_s}$	$[NTU]_{O,G}$	$[HTU]_{o,G}$ (m)	Z (m)
40% more than $L_{s,\,min}$	1.4 × 0.9m = 1.26 m	1.26	5.0875	0.6	3.0525
45% more than $L_{s,\,min}$	1.45 × 0.9m = 1.305 m	1.305	4.8456	0.6	2.9074
55% more than $L_{s,\,min}$	1.55 × 0.9m = 1.395 m	1.395	4.4748	0.6	2.6836
60% more than $L_{s,\,min}$	1.60 × 0.9m = 1.44 m	1.44	4.3257	0.6	2.5954
65% more than $L_{s,\,min}$	1.65 × 0.9m = 1.485 m	1.485	4.1978	0.6	2.5187
70% more than $L_{s,\,min}$	1.70 × 0.9m = 1.53 m	1.53	4.0856	0.6	2.4513

Figure 1/Example 1.49 shows the variation of packed height with the liq rate to achieve the same solute removal efficiency.
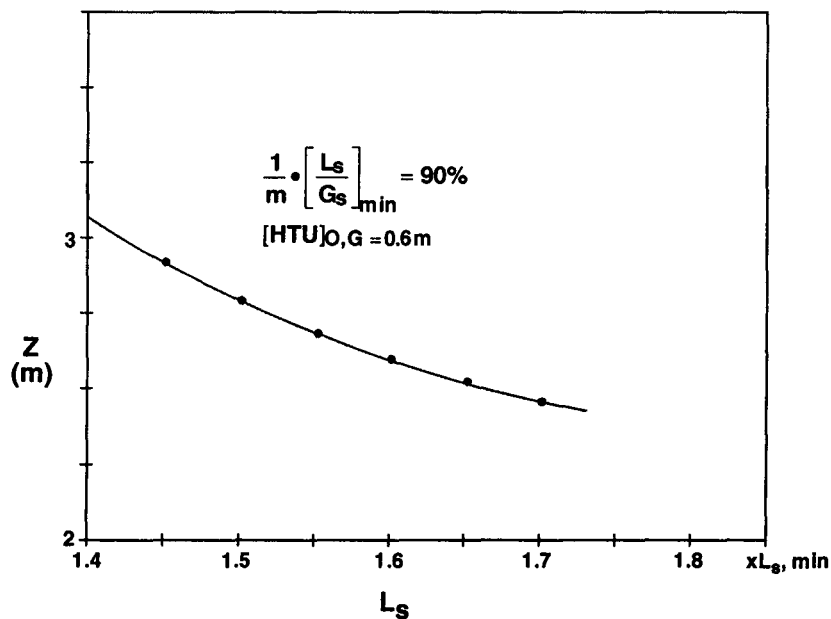
Fig. 1/Example 1.49. *Dependence of Packed Height with the Liq Rate to Achieve Constant Absorption Efficiency.*

OVERALL MASS TRANSFER COEFFICIENT

Example: 1.50 Carbon dioxide is absorbed from a gas mixture in a packed bed scrubber under the following conditions :

Feed gas rate = 5000m³/h

CO₂ Content	(% by volume)
Feed Gas	Exit Gas
28.4	0.2

Operating Pressure = 1671.45 kPa

Bed temperature = 288K

Pure water is used as solvent and fed to the column at the top at the rate of 650m³/h.

The scrubber consists of two packed beds :

BED	PACKING TYPE	WT. OF PACKING (tons)	BULK DENSITY OF PACKING (kg/m³)	PACKING INTERFACIAL AREA (m²/m³)
TOP	Ceramic rings of 35 mm × 35mm × 4mm in size	17	505	140
BOTTOM	Ceramic rings of 50mm × 50mm × 5mm in size	3	530	87.5

Assume coefficient of wetting of packing = 1

Determine the overall mass transfer coefficient

Solution : The overall mass transfer coefficient related to the pressure drop can be computed from :

$$K_{G,p} = \frac{\dot{G}}{A_c \cdot \Delta p_{lm}} \ , \quad \frac{kg}{m^2 . h . kPa}$$

where, $\dot{G}$ = rate of CO₂ absorption, kg/h

A_c = total surface area for gas-liq contact, m²

Δp = log-mean-partial-pressure-difference, kPa = MDF

Absorber Dia

Example 1.72. *Sulfur dioxide is to be removed, as an antipollution measure, from a gas stream with the characteristics of air by scrubbing with an aqueous ammonium salt solutions in a tower packed with 25-mm ceramic Rashig rings.*

Packing :
Packing factor, F_p = 155
Wall thickness = 3mm
Specific surface, a_p = 190 m^2/m^3
Fractional void of dry packing, = 0.73 m^3/m^3
Gas :
Feed rate = 3000 m^3/h at op. cond.
Pressure = 100 kPa
Temperature = 303K
Composition : 7% (vol.) SO_2 and rest IG
IG = Inert gas with the characteristics of air
Liquid :
Feed rate = 15000 kg/h
Density = 1235 kg/m^3
Viscosity = 0.0025 Pa.s
Surface tension, σ = 0.0745 N/m
Determine the absorber dia if 99% SO_2 removal is required.
Assume gas-pressure drop = 400 Pa per m of packed depth.
Solution :

The bulk of the gas quantity progressively diminishes from the absorber bottom to its top as SO_2 is increasingly absorbed from the upflowing gas stream. So there involves larger flow quantities at the tower bottom than at the top. As such the following calculations are directed to the estimation of bottom of the absorber.

Gas

$$\text{Volumetric rate} = 3000 \; \frac{100}{101.325} \; \frac{273}{303} \; \text{Nm}^3/\text{h}$$

$$\text{Molar rate} = \frac{3000}{22.41} \; \frac{100}{101.325} \; \frac{273}{303} \; , \text{kmol/h}$$

$$= 119.03722 \; \text{kmol/h}$$

$$= 0.033065 \; \text{kmol/s}$$

$$\text{Av. mol. wt.} = 0.07 M_{SO_2} + 0.93 \, M_{IG}$$

$$= 0.07 \, (64) + 0.93 \, (28.84) \qquad\qquad\qquad \text{[cf. IG} \approx \text{AIR]}$$

$$= 31.3012 \; \text{kg/kmol}$$

$$\text{Mass rate, } \dot{G} = 0.033065 \; \frac{\text{kmol}}{\text{s}} \times 31.3012 \; \frac{\text{kg}}{\text{kmol}} = 1.034974 \; \text{kg/s}$$

$$\text{Density, } \rho_G = \frac{1.034974}{3000/3600} \; \frac{\text{kg/s}}{\text{m}^3/\text{s}} = 1.24197 \; \text{kg/m}^3$$

Liquid

Rate, $\overset{\bullet}{L_s}$ = 15000 kg/h = 4.16666 kg/s at tower inlet

SO_2 removed : 99%

$$SO_2 \text{ removal rate} = 0.033065 \, \frac{\text{kmol FG}}{\text{s}} \, 0.99 \times \left[0.07 \frac{\text{kmol } SO_2}{\text{kmol FG}} \right] \left[64 \frac{\text{kg } SO_2}{\text{kmol } SO_2} \right]$$

$$= 0.14665 \, \frac{\text{kg } SO_2}{\text{s}}$$

Mass rate of liq effluents :

$$\overset{\bullet}{L_s} = 4.16666 + 0.14665 = 4.3133 \text{ kg/s}$$

Absorber Dia

$$\frac{L'}{G'} \cdot \left[\frac{\rho_G}{\rho_L - \rho_G} \right]^{0.5} = \frac{\overset{\bullet}{L}}{\overset{\bullet}{G}} \cdot \left[\frac{\rho_G}{\rho_L - \rho_G} \right]^{0.5} = \frac{4.3133}{1.034974} \left[\frac{1.24197}{1235 - 1.24197} \right]^{0.5}$$

From the pressure drop correlations **Figure 1/Example 1.72**, we get, for a ΔP = 400 Pa/m :
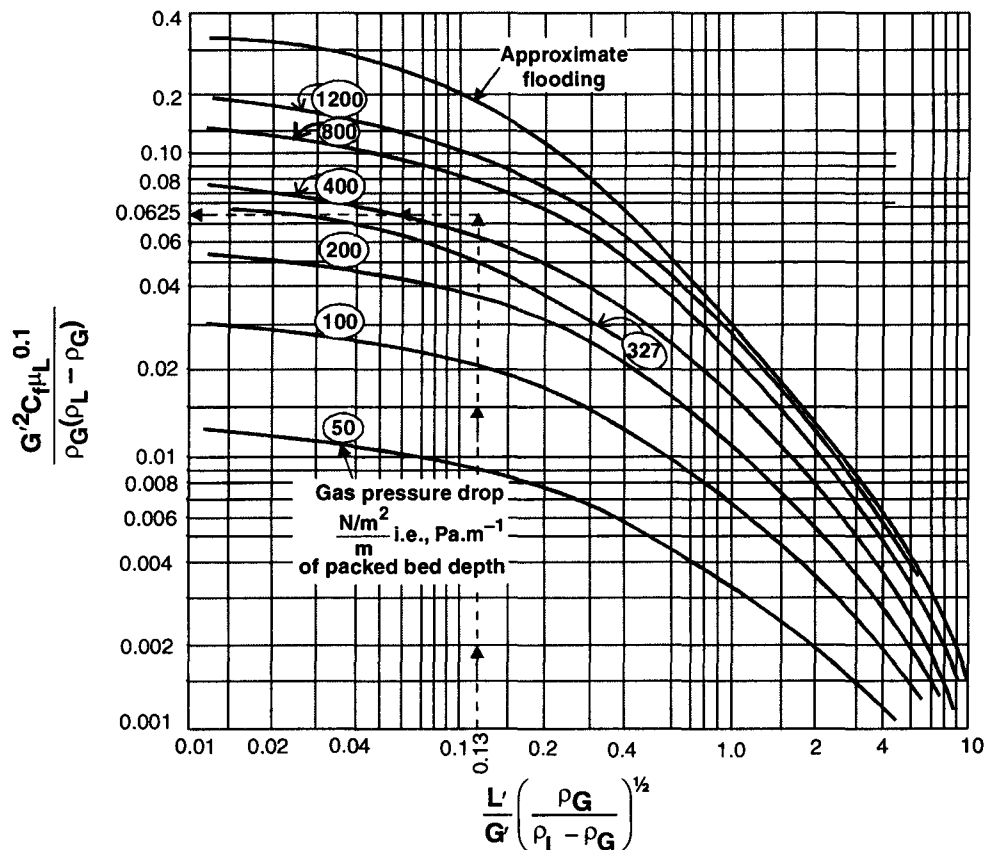
Fig. 1/Exampl. 1.72. *Pressure Drop Correlations in Towers Packed with Random Packings.*

$$\frac{G'^2 \cdot F_p \cdot \mu_L^{0.1}}{\rho_G(\rho_L - \rho_G)} \approx 0.0625$$

$$\text{or, } G' = \left[\frac{0.0625\,(1.24197)\,(1235 - 1.24197)}{155\,(0.0025)^{0.1}}\right]^{\frac{1}{2}} = 1.06059 \text{ kg/(s.m}^2)$$

Tower cross-sectional area :

$$A_t = \overset{\bullet}{G}/G' = 1.034974/1.06059 = 0.97584 \text{ m}^2$$

Tower dia :

$$D = \left[\frac{4}{\pi}(0.97584)\right]^{\frac{1}{2}} = 1.1146 \text{ m, say } 1.125 \text{ m} \qquad \textbf{Ans.}$$

Check Let us check for *Flooding.*

Flooding velocity v_{fl} is given by :

$$\log\left[\frac{v_{fl}^2 \cdot a_p \cdot \rho_G \cdot \mu_L^{0.16}}{g \cdot \varepsilon^3 \cdot \rho_L}\right] = C - 1.75 \left[\frac{\overset{\bullet}{L}}{\overset{\bullet}{G}}\right]^{0.25} \left[\frac{\rho_G}{\rho_L}\right]^{0.125}$$

where, C = 0.022 for a packing of rings or spirals

μ_L = liq viscosity, mPa.s

Examples and Problems to the Course of Unit Operations of Chemical Engineering
— P. G. Romankov (ed.)/ MIR Publ./Moscow (1979) / p-301

$$\text{or, } \log\left[\frac{v_{fl}^2\,(1.24197)\,(0.0025\times10^3)^{0.16}}{9.81\,(0.73)^3\,(1235)}\right] = 0.022 - 1.75\left[\frac{4.3133}{1.034974}\right]^{0.25}\left[\frac{1.24197}{1235}\right]^{0.125}$$

$$\text{or, } \qquad \log\left[v_{fl}^2\,(0.0579736)\right] = -1.0331485 \overset{\bullet}{G}$$

$$\therefore \qquad v_{fl} = 1.26419 \text{ m/s}$$

$$\therefore \qquad A_t = \frac{\pi}{4}\,(1.125)^2 = 0.994019 \text{ m}^2$$

$$\therefore \qquad G' = \frac{\overset{\bullet}{G}}{A_t} = \frac{1.034974}{0.994019}\,\frac{\text{kg/s}}{\text{m}^2} = 1.0412\,\frac{\text{kg}}{\text{s.m}^2}$$

Operating gas velocity :

$$v = \frac{G'}{\rho_G} = \frac{1.0412}{1.24197}\,\frac{\text{kg/(s.m}^2)}{\text{kg/m}^3} = 0.8383 \text{ m/s}$$

$$\therefore \qquad \frac{v}{v_{fl}} = \frac{0.8383}{1.26419} = 0.6631$$

Thus operating velocity, which is about 66% of flooding velocity, is in the safe range.

FAN-MOTOR POWER REQUIREMENT TO OVERCOME GAS-PRESSURE DROP

Example 1.73. If the irrigated packed height is 8m, and if an additional bed of 1100mm of 25-mm ceramic Intalox saddles is used above the liq distributor as an entrainment separator, estimate the power requirement of the fan motor to overcome the gas-pressure drop in Example 1.72

Overall efficiency of the fan and its motor = 60%

Solution :

The fan motor should develop the power to overcome : the pressure drop across the 8m bed of irrigated packings.   +

the pressure drop of the packing supports, liq distributors, inlet expansion and outlet contraction lossses for the gas.

Gas press. drop per m of irrigated packed bed = 400 Pa

Gas press. drop for the 8m of irrigated packing

$$= 400 \, (8)$$
$$= 3200 \, Pa$$

$$A_t \quad = 0.994019 \, m^2$$

$$\overset{\bullet}{G} \quad = 1.034974 \, kg/s$$

$$\overset{\bullet}{G}_s = 1.034974 - 0.14665 = 0.888324 \, kg/s$$

$$\therefore \quad G' = \frac{0.888324}{0.994019} \, \frac{kg/s}{m^2} = 0.893669 \, \frac{kg}{s.m^2}$$

This is the gas flowrate for the dry packing (entrainment arrestor) at a pressure of 100 000 − 3200 = 96800 Pa

The density of exit gas :

$$\rho_{G,s} = \frac{28.84}{22.41} \cdot \frac{273}{303} \cdot \frac{96\,800}{101325} = 1.1077 \, kg/m^3$$

where, $\rho_{G,s}$ = density of solute-free gas

Therefore, ***press. drop across*** the 1100mm bed for 25-mm Intalox saddles :

$$\frac{\Delta P}{Z} = C_D \cdot \frac{G_s'^2}{\rho_{G,s}}$$

where, C_D = empirical constant

= 241.5 for 25-mm Intalox saddles

$$\frac{\Delta P}{Z} = 241.5 \left[\frac{(0.893669)^2}{1.1077} \right] = 174.114 \, \text{Pa per m of packing}$$

Therefore, **the gas-phase drop across the top bed (1100-mm) of dry packing**

$$= 174.114 \, (1.1)$$
$$= 191.525 \, Pa$$

Total pressure drop across the irrigated and dry packed beds

$$= 3200 + 191.525$$

$$= 3391.525 \text{ Pa}$$

Let us take 1.5% of this bed press, drop as the press, drop to overcome the resistance of :

packing supports

liq distributors

gas inlet nozzle

gas outlet nozzle

Total gas-press. drop $= 3391.525 + \dfrac{1.5}{100} (3391.525) = 3442.39 \text{ Pa}$

Estimated **fan power output for the tower**

$$= \frac{3442.39 \, (0.888324)}{1.1077} \quad \frac{\text{Pa} \, (\text{kg/s})}{\text{kg/m}^3}$$

$$= 2760.637 \text{ N.m/s} = 2.7606 \text{ kW}$$

Overall efficiency of fan and motor is 60%

Fan motor power requirement

$$= \frac{2.7606}{0.60} = 4.601 \text{ kW}$$

Ans.

⬜⬜

2

Stripping

Stripping refers to the physical transfer of solute from the liquid phase to the gas phase. Generally, the stripping vapor of gas stream enters the column at the base, traffics up countercurrent to the liq-stream, enters into mass transfer operation as the gas-liquid contact is accomplished over a series of trays or packed bed. Some of the liq solvent also may get evaporated and pass into the gas phase; however, this is incidental to the stripping operation.

Many CPIs use a saturated vapor, such as steam, as the stripping agent that may get partially or totally condensed into the liquid phase.

Stripping is just the reverse of absorption & the solute (a gas) may be generated (desorbed) by reboiling the solvent (liq).

The essential condition for a successful stripping operation is that the solute must be more volatile than the solvent.

2.1. THE DRIVING FORCE

The liquid phase is a solution of the solute and if it follows Henry's Law, the vap press. of the solute above the liq phase is given by

$$P° = H.x \qquad ...(2.1)$$

where, $P° =$ vap. press. of solute, Pa

$H =$ Henry's Law constant, Pa/mol fraction **(Table. 2.1.1)**

$x =$ mole fraction of solute in liq phase

Again the partial pressure of solute in the vapor phase :

$$p = \text{mole fraction} \times \text{total press.}$$
$$= y.P \qquad ...(2.2)$$

Now, the stripping of the solute will continue as long as the vapor pressure of solute above the liq phase exceeds solute in the gas phase, *i.e.*,

$$P° > p$$

It is interesting to note that solute solubility in the liq is inversely proportional to the value of Henry's Law constant (cf. Eqn. 2.1)

2.1

Table 2.1.1. Henry's Law Constant For Organic Compounds in Water

Compound	H_{293K} *(MPa/mol fraction)*	H_{298K} *(MPa/mol fraction)*
Chloroform	17.225	
I, 4-Dichlorobenzene	19.251	
Benzene	24.318	
Toluene		34.450
1, 2, 4-Trimethylbenzene		35.767
Methyl Chloride	48.636	
Carbon tetrachloride	130.709	
Vinyl chloride	3970.375	

Therefore, anything that'll hike up the H-value will enhance the stripping operation. Inasmuch as Henry's Law constant increases with temperature, *higher temperature will accelerate stripping*. And that explains why a commonly utilized method involves preheating the liquid phase.

Since solute is transferred from the liq phase to the gas phase, it is convenient to base stripping calculations on the liq-phase concentrations. The driving force behind stripping operation is the difference between the solute concentration in the bulk-liq phase and that of the liq film at the interface between the gas and the liq phases **(Fig.2.1.1)**. That is, the driving force is :

$$\Delta x = x - x_{int} \qquad \qquad ...(2.3)$$
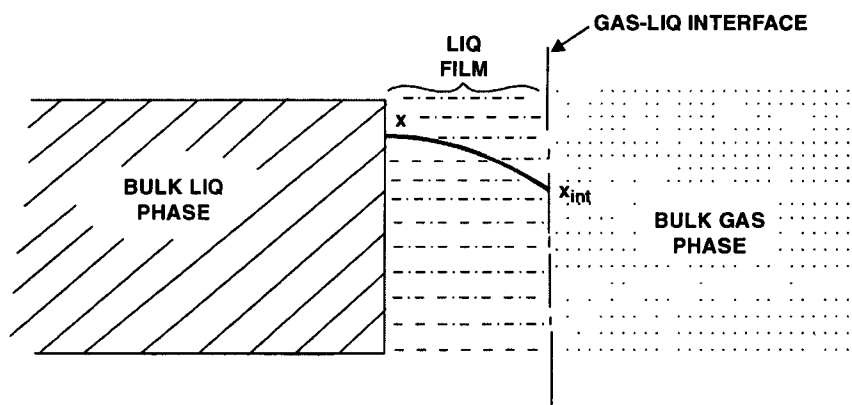
Fig. 2.1.1. Solute Diffuses from Bulk Liquid Phase to Bulk Gas Phase thru the Liquid Film at the Interface. The Driving Force being $\Delta x = x - x_{int}$

2.2. COUNTERCURRENT FLOW : MATERIAL BALANCE FOR SINGLE COMPONENT STRIPPING

Consider a countercurrent stripper column **(Fig. 2.2.1)** which may be either a packed tower or spray tower or bubble-cap column or filled with any internals that bring about gas-liq contact.

At any given section A – A of the tower, gas flowrate is G (total moles/unit tower cross-section × time) or G_s on solute free basis while liq flowrate is L (total moles/area × time) or L_s on solute-free basis.

The material balance of the solute over the envelop see **Fig. 2.2.1.** is

$$G_s \, [Y_b - Y] = L_s \, [X - X_b] \qquad \qquad ...(2.3)$$

This is the equation of the operating line **(OL)** on X,Y coordinates,of slope L_s/G_s , which passes thru (X_b , Y_b).

$$Y = \frac{y}{1-y}$$

$$X = \frac{x}{1-x}$$

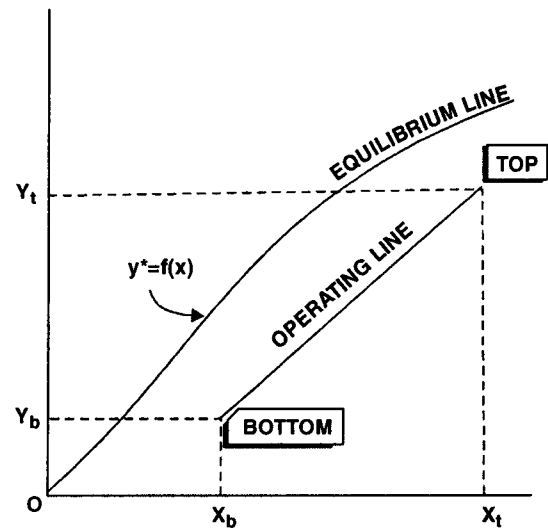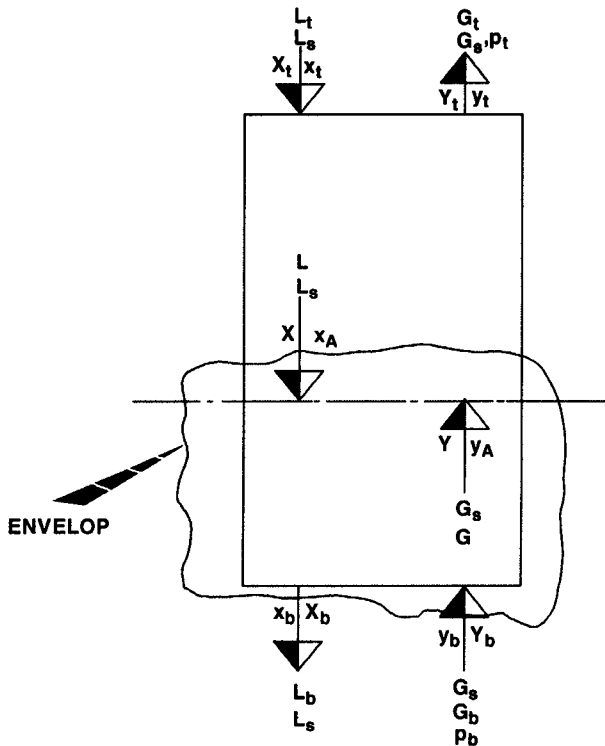The **OL** and **EL** for stripper are shown in **Fig. 2.2.2**

Fig. 2.2.1. *Countercurrent Strippr Column*   **Fig. 2.2.2.** *Equilibrium & Operating Lines for a Stripper.*

The above material balance **(Eqn. 2.3)** is applicable to both tray towers & packed columns. For tray towers it is more convenient to express Eqn. 2.3 with tray numbers presented in the subscript.

Thus Eqn. 2.3 becomes

$$G_s \left[Y_{N_p+1} - Y_1 \right] = L_s \left[X_0 - X_{N_p+1} \right] \qquad \qquad ...(2.4)$$

when applied to an entire tray tower **(Fig. 2.2.3)**

The number of theoretical plates required :

$$N_p = \frac{\log \left[\dfrac{X_0 - Y_{Np+1}/m}{X_{NP} - Y_{Np+1}/m} \left(1 - \dfrac{1}{S} \right) + \dfrac{1}{S} \right]}{\log S} \qquad \qquad ...(2.5)$$

where, m = slope of EL

$= Y_{n+1}/X_{n+1}$

S = stripping factor $= m\dfrac{G_s}{L_s}$

For S = 1

$$N_p = \dfrac{X_0 - X_{N_p}}{X_{N_p} - Y_{N_p+1}/m} \qquad \qquad ...(2.5A)$$

2.3. PACKED BED

If stripping is carried out in a packed bed, the mass transferred per unit time is expressed by

$$N = A.Z.k_L.a\ (x - x_{int}) \qquad \qquad ...(2.6)$$

where, A = col. cross-sectional area, m²

  Z = packed depth,

  k_L = liq-film mass transfer coefficient, kmol/(h.m².kmol/kmol)

  a = interfacial area, m²/m³ of packed bed

Please note that the interfacial area, **a** is not the geometric surface area of the packing but it is the mass transfer area between the gas and the liq phases. **AZ** is the bed volume. Thus **AZ.a** represents the total interfacial area within the entire packed bed.

As usual, the values of **a** and x_{int} are very difficult to evaluate. Hence in commercial operations, the overall terms have been utilized. The interfacial area is combined with the overall liquid phase **MTC** (mass transfer coefficient) to result an overall volumetric coefficient $(K_L.a)$.

Combining Eqns. 2.1. and 2.2 we get

$$x_{int} = \dfrac{y.P}{H} \qquad ...(2.7)$$

Hence the overall driving force is

$$\Delta x = x - \dfrac{y.P}{H} \qquad ...(2.8)$$

This expression is valid if the system obeys Henry's Law. When Henry's Law does not apply to the system, the equilibrium ratio **(K)** can be used to express the overall driving force :

$$K = \dfrac{y}{x} \qquad ...(2.9)$$

This equilibrium ratio is the function of temperature, pressure & composition. Thus Eqn. 2.3 modifies to

$$\Delta x = x - \dfrac{y}{K}$$
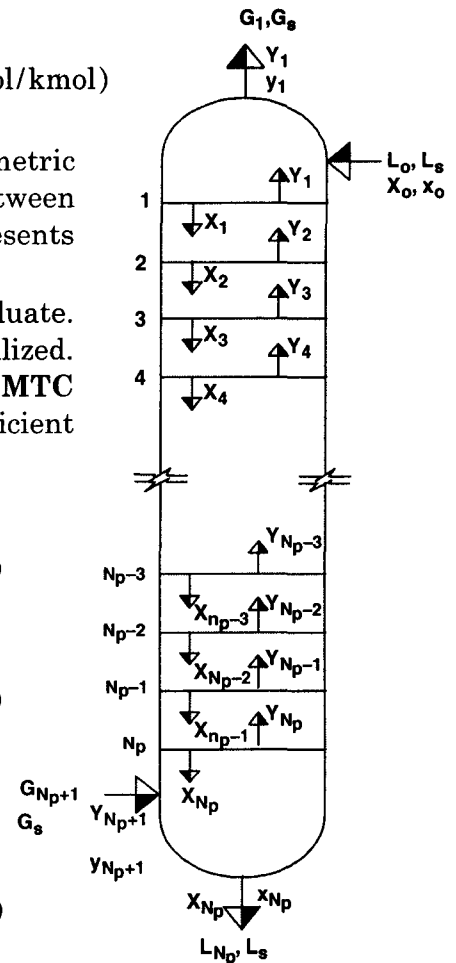
Fig. 2.2.3. *Multitray stripping column.*

$$...(2.10)$$

Therefore, overall mass transfer becomes

$$N = A.Z.K_L.a.\Delta x_{lm}. \qquad ...(2.11)$$

where, Δx_{lm} is the logarithmic mean average of the driving forces at the bottom & top of the packed bed

$$\Delta x_{lm} = \frac{\Delta x_t - \Delta x_b}{\ln\left|\frac{\Delta x_t}{\Delta x_b}\right|} \qquad ...(2.12)$$

where, Δx_t = mol fraction difference at tower top

Δx_b = mol fraction difference at tower bottom

This equation presupposes a straight **OL** & **EL**. And this is valid for systems where the solute mass transferred is small compared with the liquid & gas mass flowrate and the value of **H** or **K** is independent of solute concentration in the liq phase.

2.4. PACKED BED DESIGN

In stripping operations, the overall liq-phase MTC is related to individual film coefficients as :

$$\frac{1}{K_L.a} = \frac{1}{m.k_G.a.P} + \frac{1}{k_L.a} \qquad ...(2.13)$$

where, **m** = slope of the equil. curve

$= \dfrac{H}{P}$ for systems that obey Henry's Law

Henry's Law constant **(Table 2.4.1)** is applicable to slightly soluble gases, viz. aq. soln of acetylene, ethane, ethylene, hydrogen, nitrogen, oxygen, ozone etc.

Table 2.4.1. Henry's Law Constant

Gaseous Component	H_{283K} (MPa/mol fraction)	H_{298K} (MPa/mol fraction)
Acetylene	97.272	122.603
Ethylene	778.176	1033.515
Ethane	1915.042	2664.847
Carbonyl Sulfide	249.961	221.902
Hydrogen	6444.27	6920.497
Oxygen	3313.327	4063.132
Nitrogen	6768.51	8146.53
Ozone	251.286	380.982
Hydrogen Sulfide	3718.627	4893.997
Methane	3009.352	3809.82
Propylene	451.909	

Source : *International Critical Tables.*

The slope (**m**) of **OL** (operating line) varies. For solutes of greater solubility such as **C-3** and **C-4** hydrocarbons dissolved in light naphtha, **m** equals the equilibrium ratio. **K**. This ratio (**K**) is generally applicable to ideal liq-phase solutions at pressure up to 1 MPa.

The overall liq-phase **MTC, K_L** shows similar variations with gas and liq flowrates as in absorption. Likewise, temp. & press. are expected to exert same effect on the gas-film & liq-film MTC as in absorption operations. Forasmuch as liq-phase **MTC** as well as Henry's Law constant, increase with rising temperature, stripping is accentuated by heating the liquid phase.

The **Stripping Factor**, used to calculate the number of theoretical stages in a stripping operation, is the ratio of the equilibrium curve slope to the operating line slope :

$$S = \frac{EL\text{-slope}}{OL\text{-slope}} = \frac{K}{L_m/G_m} \qquad \qquad ...(2.14)$$

L_m = molar flowrate of liq, kmol/h

G_m = molar flowrate of gas, kmol/h

The product of stripping factor **(S)** and absorption factor **(A)** is unity.

$$A \times S = 1$$

$$\therefore \qquad \qquad S = A^{-1}$$

i.e., stripping factor is the reciprocal of absorption factor.

The number of liq-phase transfer units **($NTU_{o, L}$)** for a packed bed stripping column can be obtained from Colburn correlation **(Fig. 2.4.1)**
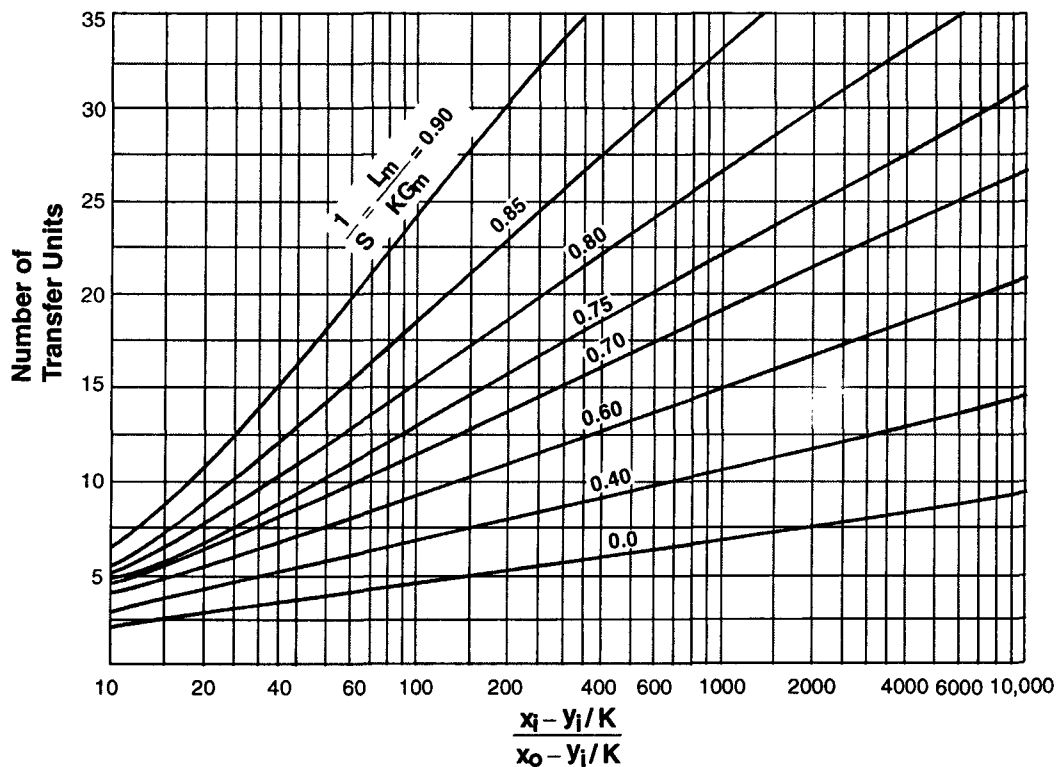
Fig. 2.4.1. *Colburn Correlation for Stripper Design.*

The abscissa of this correlation is

$$\frac{x_i - y_i/K}{x_o - y_i/K}$$

where, x_i = mole fraction of solute in the liq at inlet

x_o = mole fraction of solute in the liq at outlet

We need to have this abscissa value the stripping factor to determine the $NTU_{o, L}$ value. For these calculations the **EL** and **OL** should be linear and not necessarily parallel.

2.4.1 Packed Bed Dia

Stripping is carried out either on a once-thru process **(OTP)** or a recycle process. In case the solvent liq is a low-cost one, it is usually drained off as waste after being stripped **(OTP)**. On the other hand if the solvent is expensive it is recycled via an absorber. In the latter case, the designer must size the stripper first before he designs the absorber.

Stripper design requires following input data :

Input Data :

L_m	liq flowrate, kmol/h
x_i	inlet solute concentration, mol fraction
P	column operating pressure, Pa
x_o	solute concentration in the outlet stream, mol fraction

The first three parameters are known while the last one is to be specified.

Design Procedure

I. **Select the stripping gas**

II. **Determine the required flowrate of the stripping gas, G_m**

III. **Calculate the column dia**

IV. **Calculate the stripping factor, S, from**

$$\frac{1}{S} = \frac{L_m}{G_m \cdot K}$$

using the known K-value or from

$$S = \frac{H}{P} \cdot \frac{G_m}{L_m}$$

when Henry's Law is applicable.

V. **Using the known K-value determine the abscissa of the Fig. 2.4.1 :**

$$\frac{x_i - y_i / K}{x_o - y_i / K}$$

VI. **Read out $NTU_{o, L}$ from Fig. 2.4.1 taking S^{-1} as the curve parameter**

OR

Calculate $NTU_{o, L}$ from

$$NTU_{o, L} = \frac{\ln\left[\frac{x_i - y_i / K}{x_o - y_i / K}\left(1 - \frac{1}{S}\right) + \frac{1}{S}\right]}{1 - \frac{1}{S}}$$

$$= \frac{S-1}{S} \ln \left[\frac{\frac{x_i - y_i/K}{x_o - y_i/K}(S-1) + 1}{S} \right] \qquad \dots(2.16)$$

VII. The total packed depth required is

$$Z = [NTU]_{o,L} \times [HTU]_{o,L} \qquad \dots(2.17)$$

where, $[HTU]_{o,L}$ the overall height of a liq-film transfer unit, is the function of the liq flowrate and the operating temperature. The $[HTU]_{o,L}$ value for a particular packing at a specified liq rate & a given operating temperature is supplied by the packing vendor.

VIII. Calculate the pressure drop from the col. cross-sectional area.

Adjust the col. dia so as to maintain ΔP between 12.5 to 42 mm H_2O/m of packed depth at the point of maximum loading, *i.e.*, at the bed bottom.

For systems prone to foaming, the design press. dr. should not exceed **21mm H_2O/m** in operations using inert gas stripping. Where steam or reboiled solvent vapor is used as the stripping agent, the design press. dr. should be limited to a max. of **25mm. H_2O/m** for a moderately foaming system.

2.5. MULTI-TRAY STRIPPER

Refer to multitray stripper **(Fig 2.5.1)** for multicomponent system, the liquid may contain several volatile one for stripping. For such systems, there may be no component that passes thru at constant rate in the gas or liquid phase. Hence it becomes convenient to define all gas compositions in terms of the entering gas (not solute-free basis) and all liq compositions in terms of the entering liq (not solute-free basis). Thus, for any component in the liq (L_n) leaving any tray n is

$$X_n' = \frac{\text{moles of component in } L_n/\text{time}}{L_o} = \frac{x_n \cdot L_n}{L_o}$$

and for any component in the gas (G_n) leaving the same tray.

$$Y_n' = \frac{\text{moles of component in } G_n/\text{time}}{G_{N_p+1}} = \frac{y_n \cdot G_n}{G_{N_p+1}}$$

where, x_n = mole fraction of the component in the liq leaving tray-n
     y_n = mole fraction of the component in the gas leaving tray-n
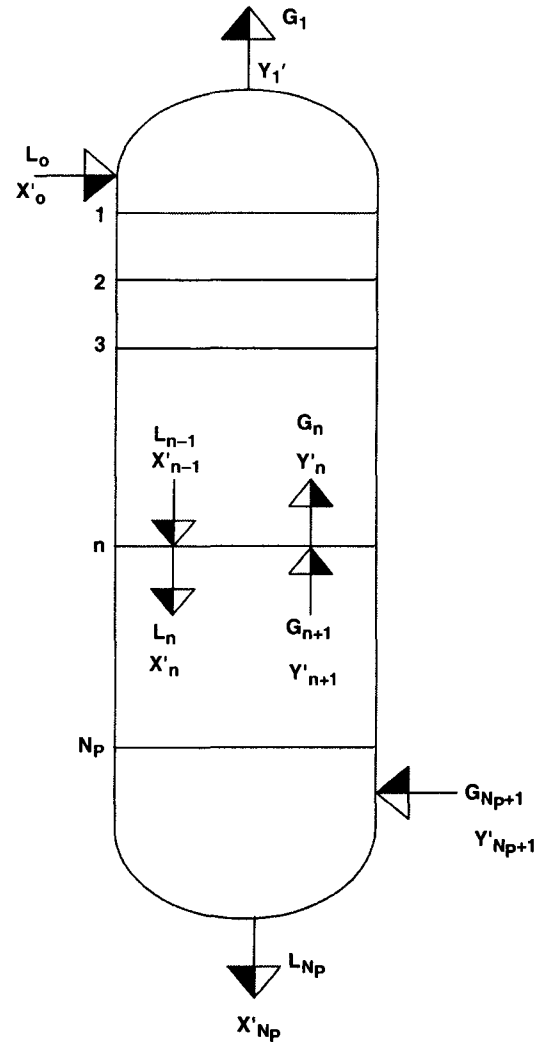 L_n = molar liq rate leaving tray-n, mol/time

Fig. 2.5.1 *Multitray Stripper.*

G_n = molar gas rate leaving tray-n, mol/time

L_0 = molar liq rate entering top tray, mol/time

G_{N_p+1} = molar gas rate entering bottom tray, mol/time.

Drawing material balance for any component about equilibrium tray-n yields :

$$L_0\left(X'_{n-1} - X'_n\right) = G_{N_p+1}\left(Y'_n - Y'_{n+1}\right) \qquad \text{...(2.18)}$$

Again the equilibrium relationship for this **n-th** tray is

$$y_n = K_n.x_n \qquad \text{...(2.19)}$$

where, K_n = equilibrium distribution ratio of any component on tray-n

or,

$$Y'_n \cdot \frac{G_{Np+1}}{G_N} = K_n.X'_n.\frac{L_0}{L_n}$$

or,

$$Y'_n = \frac{K_n.G_n}{L_n}.X'_n.\frac{L_0}{G_{N_p+1}} \qquad \text{...(2.20)}$$

$$= S_n.X'_n.\left|\frac{L_0}{G_{N_p+1}}\right| \qquad \text{...(2.20 A)}$$

where, S_n = stripping factor of any component on tray-n

A similar treatment on **(n+1)-th** equilibrium tray results.

$$Y'_{n+1} = S_{n+1}.X'_{n+1}.\left|\frac{L_0}{G_{N_p+1}}\right| \qquad \text{...(2.21)}$$

Substituting Y'_n and Y'_{n+1} values in Eqn. 2.18 :

$$\frac{L_0}{G_{N_p+1}}\left(X'_{n-1} - X'_n\right) = \left(S_n.X'_n - S'_{n+1}.X'_{n+1}\right)\frac{L_0}{G_{N_p+1}}$$

or,

$$X'_{n-1} + S_{n+1}.X'_{n+1} = X'_n\left(1 + S_n\right)$$

$$\therefore \qquad X'_n = \frac{X'_{n-1} + S_{n+1}.X'_{n+1}}{1 + S_n} \qquad \text{...(2.22)}$$

If the stripper contains only one tray (n = 1), Eqn. 2.20 becomes

$$X'_1 = \frac{X'_0 + S_2.X'_2}{1 + S_1} \qquad \text{...(2.22 A)}$$

From Eqn. 2.19 for n = 1

$$Y'_2 = S_2.X'_2.Z$$

$$S_2.X'_2 = Y'_2/Z \qquad\qquad \text{where, } Z = L_0/G_{Np+1}$$

Therefore, from Eqn. 2.20 A

$$X'_1 = \frac{X'_0 + Y'_2/Z}{1 + S_1} \qquad \text{...(2.23)}$$

If the stripper contains 2 trays (*i.e.*, n = 2), Eqn. 2.20 yields

$$X_2' = \frac{X_1' + S_3 . X_3'}{1 + S_2} \qquad ...(2.22\ B)$$

From Eqn. 2.21 for n = 2

$$Y_3' = S_3 . X_3' . Z$$

$$\therefore \qquad X_2' = \frac{\dfrac{X_0' + Y_2'/Z}{1 + S_1} + \dfrac{Y_3'}{Z}}{1 + S_2} \qquad ...(2.22\ A)$$

$$= \frac{X_0' . Z + Y_2' + Y_3'(1 + S_1)}{Z(1 + S_1)(1 + S_2)}$$

$$= \frac{X_0' + Y_2'/Z + Y_3'(1 + S_1)/Z}{(1 + S_1)(1 + S_2)} \qquad ...(2.23\ A)$$

The general expression for the fractional stripping of any component in the strippper having a total N_p number of trays is

$$\frac{X_0' - X_{N_p}'}{X_0'} = \frac{S_1 S_2 ... S_{N_P} + S_1 S_2 ... S_{N_P - 1} + ...S_1}{S_1 S_2 ... S_{N_P} + S_1 S_2 ... S_{N_P - 1} ..... + S_1 + 1} -$$

$$\frac{Y_{N_p + 1}'}{Z . X_0'} . \frac{S_1 S_2 ... S_{N_P - 1} + S_1 S_2 ... S_{N_P - 2} + ...S_1 + 1}{S_1 S_2 ... S_{N_P} + S_1 S_2 ... S_{N_P - 1} ..... + S_1 + 1} \qquad ...(2.24)$$

This is also called **Horton-Franklin Expression.**

In order to use the Eqn. 2.24, the L/G ratio for each tray & the tray temp. (that dictates the value of K) are required to compute the values of S terms.

Now if the liq is not ideal, K_j (for any component j) on any tray will additionally depend on the complete liq composition on the tray. Likewise fashion, if the gas solutions are not ideal, K_j will additionally depend on complete gas compositions. Thus, the Eqn. 2.24 becomes practically useful for ideal solutions only.

If it is assumed that the fractional stripping is the same for each tray, the liq rate L_n can be computed by drawing a material balance to the end of the tower :

$$L_n \approx L_0 \left[\frac{L_n}{L_o} \right]^{n/N_P} \qquad ...(2.25)$$

In case the molar latent heats and heat capacities happen to be all alike for all components, and if no heat of solution is absorbed, the temp. drop on stripping is roughly proportional to the amount of stripping whereupon.

$$\frac{L_0 - L_n}{L_0 - L_{N_p}} \approx \frac{\theta_0 - \theta_n}{\theta_0 - \theta_{N_p}} \qquad ...(2.26)$$

where, θ represents temperature.

Edmister introduced '**effective stripping**' term (S_E) to H-F expression replacing individual S factor for each tray whereupon Eqn. 2.24 simplifies to

$$\frac{X_o' - X_{N_P}'}{X_o'} = \left[1 - \frac{1}{S'} \cdot \frac{G_{N_P+1}}{L_o} \cdot \frac{Y_{N_P+1}'}{X_e'} \right] \frac{S_E^{N_P+1} - S_E}{S_E^{N_P+1} - 1} \qquad ...(2.27)$$

which becomes Kremser Eqn. if $Y_{N_P+1}' = 0$.

For a double-tray stripper $(N_P = 2)$, it develops to

$$S' = \frac{S_1(S_{N_P} + 1)}{S_1 + 1} \qquad ...(2.27\ A)$$

and

$$S_E = \left[S_1(S_{N_P} + 1) + 0.25 \right]^{0.5} - 0.5 \qquad ...(2.27\ B)$$

Eqn. 2.25 can be used to determine the number of equilibrium trays required to strip a component to a specified extent and provides the basis for using the exact equations of Horton & Franklin.

STRIPPER COLUMN OF A COAL GAS PLANT

Example 2.1. A Coal gas plant operates an absorber and a stripper in series to make free coal gas from its light oil content by scrubbing washoil and then regenerating the absorbent by stripping the resulting solution with heating steam.

Input Data :

Absorber :

Operating temperature = 299K

Operating pressure   = 0.107MPa

Gas rate (inlet)   = 900 m³/h

Benzene (Light Oil).   = 2 vol %

Wash Oil :

Mol. wt.   = 260

Light Oil content   = 0.005 mol fraction

Temperature   = 299K

Circulation rate   = 1.5 times minimum

Absorption factor   = 95%

Stripper :

Operating temperature = 395K

Rich solution temperature = 393K at entry

Stripping Steam :

Pressure   = 101.325 kPa

Temperature   = 395K

Flowrate   = 1.5 times the minimum

• Washoil-Benzene solutions are ideal

• *Lean solution (0.005 mol fraction benzene) cooled to 299K is fed to the top of the absorber.*

   Determine :

   I. washoil circulation rate

   II. Steam rate.

   Solution : Designate *B* for Benzene

                              WO for Washoil

                              IG   for Inert Gas*

ABSORBER CALCULATIONS

I. Feedgas Rate at Absorber Inlet

$$G_b = \frac{900}{3600}\left|\frac{m^3}{s}\right| \cdot \frac{273}{299}\left|\frac{K}{K}\right| \cdot \frac{0.107\times10^3}{101.325}\left|\frac{kPa}{kPa}\right|$$

$$= 0.241045 \, Nm^3/s$$

$$= \frac{0.241045}{22.41}\left|\frac{Nm^3/s}{Nm^3/kmol}\right|$$

$$= 0.010756 \, kmol/s$$

II. Feed Gas Composition

$$y_b = 0.02 \, mol \quad fraction \, benzene$$

$$Y_b = \frac{y_b}{1-y_b} = \frac{0.02}{1-0.02} = 0.020408 \left|\frac{kmol \, B}{kmol \, IG}\right|$$

III. Feedgas Rate on Solute-Free Basis

$$G_s = G_b(1-y_b)$$

$$= 0.010756 \left|\frac{kmol}{s}\right| \cdot (1-0.02) \, |mol \, fraction \, IG|$$

$$= 0.01054 \, kmol \, IG/s$$

IV. Equilibrium Line Equation

$$P^\circ_{Benzene/299K} = 13.33 \, kPa$$

Since Benzene-Washoil Solutions are ideal

$$y^* = \frac{P^\circ_B}{P} \cdot x = \frac{13.33 \, kPa}{107 \, kPa} \cdot x = 0.1245 \, x$$

or, $$\frac{Y^*}{1+Y^*} = 0.1245 \, \frac{X}{1+X}$$

$$Y^* = \frac{y^*}{1-y^*}$$

$$\therefore \, Y^*+1 = \frac{1}{1-y^*}$$

$$\therefore \, \frac{Y^*}{Y^*+1} = y^*$$

$$X = \frac{x}{1-x}$$

$$\therefore \, \frac{X}{1+X} = x$$

● Inert = solute-free gas

V. Equilibrium Curve on Graph

EL is a st. line passing thru (0, 0), *i.e.*, when

$X = 0, Y^* = 0$

X	0	0.06	0.08	0.1	0.14	0.16	0.2
Y	0	0.007	0.0093	0.0114	0.0155	0.0174	0.0211

Using these coordinates, **EL** curve is drawn **(Fig 1 to Soln. to Example. 2.1).**
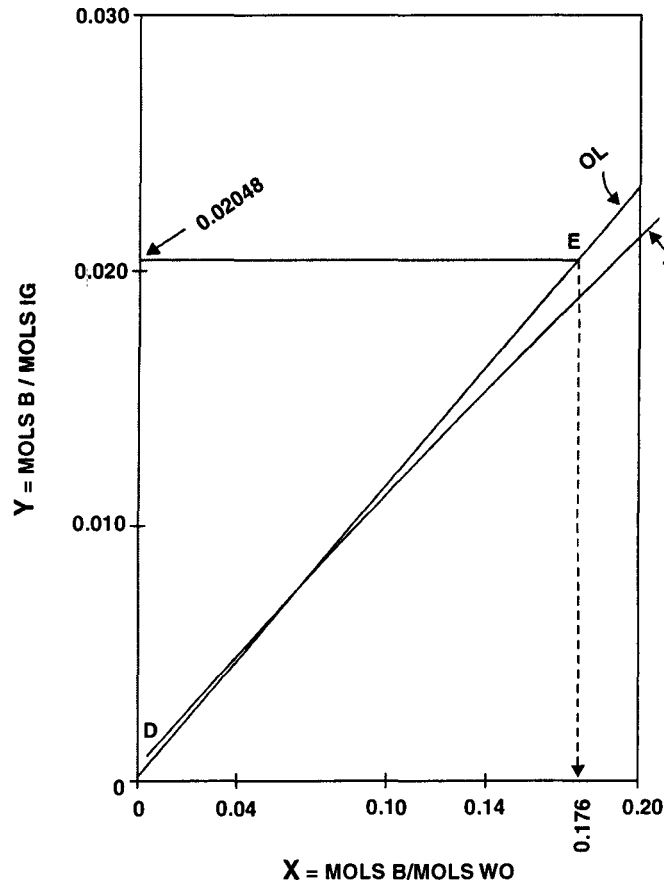
Fig. 1 to Soln. 2.1. *EL & OL of Absorber.*

VI. Operating Line

OL starts at point **D** (X_t, Y_t), see **Fig. 1 to Soln. 2.1.**

$$x_t = 0.005 \text{ mol fraction}$$

$\therefore$

$$X_t = \frac{x_t}{1-x_t} = \frac{0.005}{1-0.005} = 0.005025 \frac{\text{kmol } \mathbf{B}}{\text{kmol } \mathbf{WO}}$$

Since absorption factor is 95%,

$$Y_t = (1 - 95\%) Y_b$$
$$= 0.05 (0.02048) \text{ kmol } \mathbf{B}/\text{kmol } \mathbf{IG}$$
$$= 0.00102 \text{ kmol } \mathbf{B}/\text{kmol } \mathbf{IG}$$

For minimum oil circulation rate, **OL** becomes tangent to **EL**.

A horizontal corresponding to Y_b (=0.02048) is drawn, it intersects **OL** at **E**. The abscissa of **E** corresponds to

$$X_b = 0.176 \text{ kmol } \mathbf{B}/\text{kmol } \mathbf{WO}$$

DE is the **OL** with $L_{s, min}$ (see Fig. 1 to Soln. 2.1)

VII. Minimum Liquid Rate

$$L_{s, min} = G_s \left| \frac{Y_b - Y_t}{X_b - X_t} \right|$$

$$= 0.01054 \left| \frac{\text{kmol } \mathbf{IG}}{s} \right| \cdot \frac{0.02048 - 0.00102}{0.176 - 0.005025} \left| \frac{\text{kmol } \mathbf{B}/\text{kmol } \mathbf{IG}}{\text{kmol } \mathbf{B}/\text{kmol } \mathbf{WO}} \right|$$

$$= 0.001199 \text{ kmol } \mathbf{WO}/s$$

VIII. Operating Liquid Rate

$$L_{s, op} = 1.5 \ L_{s, min} = 1.5 \ (0.001199) = 1.798 \times 10^{-3} \text{ kmol } \mathbf{WO}/s$$

IX. Effluent Concentration at Absorber Bottom

Overall mass balance yields :

$$L_s \ (X_b - X_t) = G_s \ (Y_b - Y_t)$$

$$\therefore \qquad X_{b, op} = \left| \frac{G_s}{L_s} \right| (Y_b - Y_t) + X_t$$

$$= \frac{0.01054}{1.798 \times 10^{-3}} \left| \frac{\text{kmol } \mathbf{IG}/s}{\text{kmol } \mathbf{WO}/s} \right| (0.02048 - 0.00102) \left| \frac{\text{kmol } \mathbf{B}}{\text{kmol } \mathbf{IG}} \right| + 0.005025 \left| \frac{\text{kmol } \mathbf{B}}{\text{kmol } \mathbf{WO}} \right|$$

$$= 0.1191 \text{ kmol } \mathbf{B}/\text{kmol } \mathbf{WO}$$

STRIPPER

The absorber effluent becomes the feed liq to the stripper. It is fed to the top of the column while steam is introduced at the bottom as the stripping agent. Therefore, for the stripper

$$X_t = 0.1191 \text{ kmol } \mathbf{B}/\text{kmol } \mathbf{WO}.$$
$$X_b = 0.005025 \text{ kmol } \mathbf{B}/\text{kmol } \mathbf{WO}$$

Since the stripping steam is essentially solute **(Benzene)** free,

$$Y_b = 0 \text{ kmol } \mathbf{B}/\text{kmol Steam}$$

I. Equilibrium Line for The Absorber

$$P^\circ_{\mathbf{Benzene/395K}} = 320 \text{ kPa}$$

$$\therefore \qquad y^* = \frac{P^\circ_{\mathbf{B}}}{P} . x = \frac{320}{101.32} . \left| \frac{\text{kPa}}{\text{kPa}} \right| . x = 3.158 \, x$$

or, $$\qquad \frac{Y^*}{1 + Y^*} = 3.158 \, \frac{X}{1 + X} \text{ is the EL eqn.}$$

II. Equilibrium Curve

The coordinates of EL curve for stripper are tabulated below:

X	0	0.02	0.04	0.06	0.08	0.1	0.12	0.14
Y*	0	0.066	0.1382	0.2176	0.3053	0.4027	0.5113	0.6335

III. Operating Line for Minimum Steam Rate

OL starts at point **P** (0.005025, 0) corresponding to tower bottom composition. For the minimum steam rate, a tangent **PQ** is drawn from point **P** to EL.

PQ is the OL for minimum steam rate (**Fig. 2 to Soln. 2.1**)

IV. Minimum Steam Rate

From point $X_t = 0.1191$ a vertical is drawn intersecting the above **OL** at **Q**. The ordinate value of **Q**, as read out from figure, is 0.445.

$$Y_t = 0.445 \text{ kmol } \mathbf{B}/ \text{ kmol steam}$$

From overall material balance :

$$G_{s,\,min} = L_s \left| \frac{X_t - X_b}{Y_t - Y_b} \right|$$

$$= 1.798 \times 10^{-3} \left[\frac{\text{kmol } \mathbf{WO}}{s} \right] \cdot \frac{0.1191 - 0.005025}{0.445 - 0} \left[\frac{\text{kmol } \mathbf{B}/ \text{kmol } \mathbf{WO}}{\text{kmol } \mathbf{B}/ \text{kmol Steam}} \right]$$

$$= 4.6091 \times 10^{-4} \text{ kmol Steam/s}$$
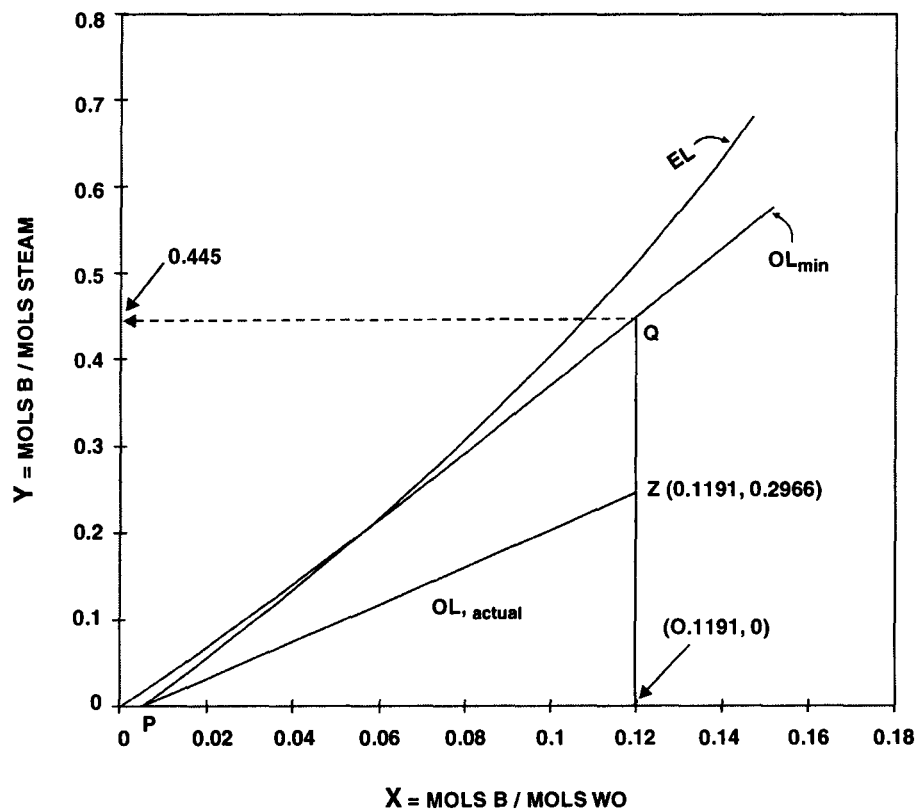
Fig. 2. To Solution 2.1

V. Operating Steam Rate & OL

The steam rate is 1.5 times the minimum.

$$G_{s,\,actual} = 1.5\,(4.6091 \times 10^{-4}) = 6.9136 \times 10^{-4}\ \text{kmol steam/s}$$

Actual operating line is **PZ** where the ordinate of **Z** is

$$Y_{t,\,z} = \frac{1.798 \times 10^{-3}}{6.9136 \times 10^{-4}}\left[\frac{\text{kmol } \mathbf{WO}}{\text{kmol Steam/s}}\right] \cdot (0.1191 - 0.005025)\left[\frac{\text{kmol } \mathbf{B}}{\text{kmol } \mathbf{WO}}\right]$$

$$= 0.29667\ \text{kmol } \mathbf{B}/\text{kmol Steam.}$$

2.6 ABSORPTION-STRIPPING SYSTEM

Many Chemical as well as Petrochemical units operate absorber & stripper hooked up in series. A suitable solvent is selected to abstract a number of components **(Absorption)** in the absorber and the resulting **'rich'** solution is regenerated **(Stripping)** in another column, called stripper, whereupon a 'lean' solution is resulting, which is pumped back to the absorber top as the solvent **(Fig. 2.6.1)**
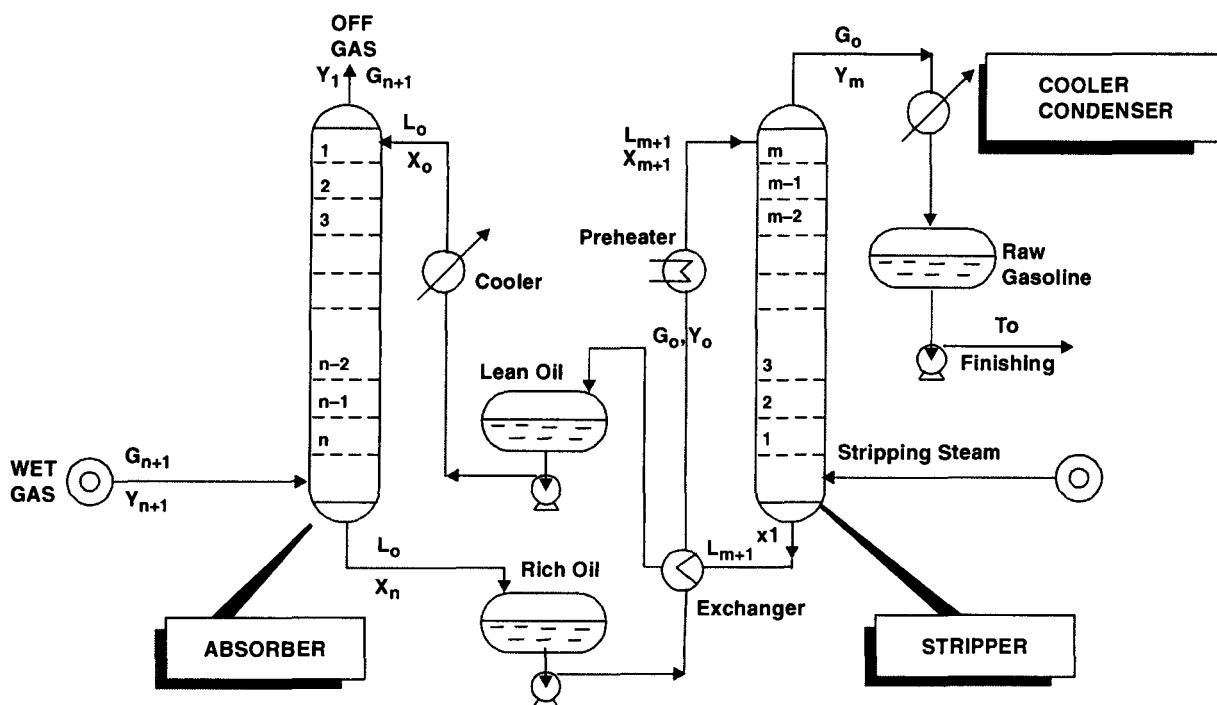
Fig. 2.6.1 *Absorber & Stripper Forming a Closed Loop in the Process of Hydrocarbon Recovery.*

Several methods for handling the simultaneous design of such systems are available. The approximate one is that offered by Kremser & Brown. While a more complete methods was forwarded by Edmister.

2.6.1. Kremser-Brown-Sherwood Method

This method gives reasonably good results for systems involving relatively small amount of solute transfer from gas to liq **(absorption)** or from liquid to gas **(stripping)** whereupon practically

zero heat of solution or dissolution takes place. Error becomes considerable with increasing solute concentration in the solvent (error may exceed 50% for some components). Nevertheless, this method works well on natural gas and related systems.

2.6.1A. Absorber—Determination of Component Absorption when Number of Trays Specified.

Input Data

• Feedgas rate	G_{n+1}	
• Feedgas composition	y_j	
• Feedgas temperature	θ_i	
• Feedgas pressure	P_{in}	
• Solvent feedrate	L_o	
• Solvent composition	x_o	Fig. 2.5.1
• Solvent temperature	$\theta_{S, o}$	
• Column operating pressure	P	
• Column operating temperature	θ	
• Total number of trays	N_P	

1. **Calculate individual component rates at inlet from feedgas rate & mole ratio of individual components in the feedgas.**

   For any component in the gas at inlet

   $$G_{N_P+1, j} = Y'_{N_P+1, j} \cdot G_{N_P+1}$$

   where, $Y'_{N_P+1, j}$ = moles of j in vap phase per mole of gas entering the absorber.

2. **Average the top & bottom temperatures of the tower. Read out equilibrium constant K_j values from the chart for each component in the gas at the tower operating pressure.**

3. **Lean solution (solvent) rate is usually given. If not, specify it to a suitable value.**

4. **Evaluate liq : gas flowratio**

   $$\frac{L_o}{G_{N_P+1}} = \frac{\text{Lean solution rate at inlet, mols/h}}{\text{Feed gas rate at inlet, mols/h}}$$

   Assume this value constant for tower design.

5. **Using this flowratio, calculate absorption factor A_j for each component**

   $$A_j = \frac{L_o}{G_{N_P+1}} \cdot K_j$$

6. **Calculate theoretical trays (N) :**

   $$N = \eta_o \cdot \times \text{No. of Actual Trays}$$

   where, η_o = overall tray efficiency (assume)

   N_P = No. of actual trays (specified)

7. Calculate fraction absorbed for each component ($E_{a,j}$)

$$E_{a,j} = \frac{Y_{N_p+1} - Y_1}{Y_{N_p+1} - Y_o^*} = \frac{[A_j]^{N_p+1} - A_j}{[A_j]^{N_p+1} - 1} \qquad \qquad ...(2.28)$$

Solve it using A_j values.

8. Determination the moles of each component absorbed :

$$G_j = G_o \cdot Y_{N_p+1,j} (E_{a,j}) \qquad \qquad ...(2.29)$$

9. Evaluate solute transfer rate to liq phase

$$X_{j,b} = \frac{\text{Component j absorbed, mols}}{\text{Lean solution rate, mol / h}}$$

10. Determine gas composition at tower top :

Moles/h of each component in the exit gas = Mols/h component in Inlet Gas

$$- \text{Mols/h component Absorbed}$$

$$= G_{N_p+1,j} - G_j$$

11. Compute Y_1 from :

$$\frac{Y_{N_p+1} - Y_1}{Y_{N_p+1} - Y_o^*} = E_{a,j} \text{ calculated in step-7}$$

Y_o^* is generally very small and hence equated to zero in most cases.

12. Determine $\Sigma X_{j,b}$ from Step-9. And correct the values from Step-1 thru Step-11 as follows.

13. Calculate A_j :

$$A_j = \frac{L_o}{G_{Np+1} \cdot K_j} \left(1 + \Sigma X_{j,b}\right) \qquad \qquad ...(2.30)$$

14. Recalculate absorption efficiency using new A_j value :

$$E_{a,j} = \frac{[A_j]^{N_p+1} - A_j}{[A_j]^{N_p+1} - 1}$$

or with the help of **Absorption Factor Curves (Fig. 2.6.1A-1)**

15. Calculate, using the value of corrected absorption coefficient, $E_{a,j}$, component absorbed/h:

$$G_j = G_o \cdot Y_{N_p+1,j} E_{a,j} \qquad \qquad ...(2.29)$$

16. Calculate mols of each component in the outlet gas ($Y_{1,j}$)

$$\frac{Y_{N_p+1} - Y_{1,j}}{Y_{N_p+1} - Y_o^*} = E_{a,j}$$

If X_1 in equilibrium with Y_1 is desired

$$X_1 = \frac{Y_1}{K \sum Y_1} (1 + \Sigma X_{j,b}) \qquad \qquad ...(2.30)$$
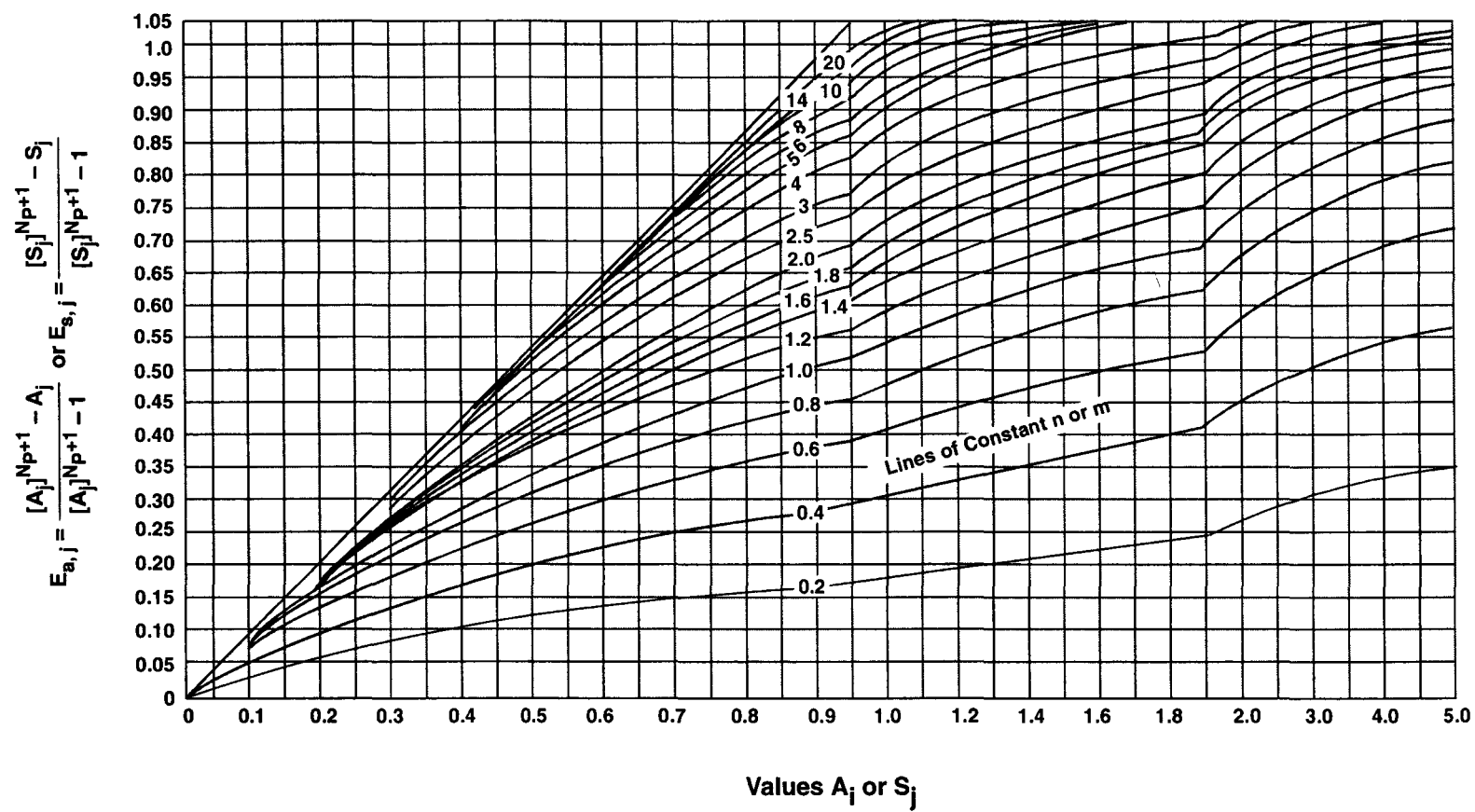
Fig. 2.6.1A-1. *Absorption and Strpping Factor Curves.*

17. Tabulate the result

First trial

Component	Inlet Composition $Y_{N_p+1,j}$ $= Y_{N_p+1,j} \cdot$ $\cdot G_{N_p+1}$	Component rate at Inlet G_{N_p+1}	Equil. Const. K_j	Absorption Factor A_j $= \dfrac{L_o}{G_{N_p+1}}$ $\cdot \dfrac{1}{K_j}$	Fraction Absorbed $E_{a,j}$	Abs. Rate $\left(\dfrac{mols}{h}\right)$	$X_{j,b}$	Exit Gas $\left(\dfrac{mol}{h}\right)$	$Y_{1,J}$
...	...	...	...	...	...	...	...	...	...
...	...	...	...	...	...	...	...	...	...
...	...	...	...	...	...	...	...	...	...
	$\sum Y_{N_p+1,j}$ $= 1.00$	$\sum G_{N_p+1,j}$ $=.....$				$\sum ...$	$\sum X = $ j, b	$\sum =$	

Go for 2nd trial following Steps 13 to 16.
    Check the difference between the Mols Absorbed from trial # 1 & trial # 2.
    If the difference is too much 3rd trial is needed.

2.6.1A.1. ABSORBER—Determination of Number of Trays for Specified Product Absorption

Input Data

• Operating temperature

• Operating pressure

• Feedgas rate

• Feedgas composition

• Operating liq : gas ratio either specified or taken equal to specified unit time's minimum value of liq : gas ratio.

Proceed as follows :

1. **Calculate feedgas component rates at absorber inlet**

$$G_{N_p+1,j} = Y_{N_p+1} \cdot G_{N_p+1}, \text{ mols/h}$$

2. **Calculate exitgas component rates at absorber top :**

$$Y_{t,j} = (1 - \% \text{ recovery}), Y_{b,j}$$

where, Y_j = mols of j in gas phase per unit mol of j-free gas

    Component rate in the exit gas

$$G_{t,j} = [Y_{b,j} - Y_{t,j}] \cdot G_s$$

3. **Evaluate component absorbed**

[mols/h]$_j$ absorbed = [mols/h]$_j$ IN − [mols/h]$_j$ OUT

The figure shows a chart with "Henry's Law Constant, H" on the vertical axis and "Tray Efficiency, % η_0" on the horizontal axis, with an "ABSORBERS" line.

Labels on the chart:
- O' Connell Correlation
- Use Average Tower Conditions
- Spread of Results ± 9%
- Includes CO_2 and NH_3 Data

Right side annotations:

[Henry's Law Constant, H, Mols/(cu.ft.) (Atm.)] [Pressure, P, Atm.]/[Viscosity of Absorbent, μ, Centipoises]

$$\left[\frac{H \times 10^{-3} \text{kmols}}{0.0283 \text{m}^3} \cdot \frac{1}{\text{kPa}}\right] \frac{[P, \text{kPa}]}{[\mu \times 10^{-3}\text{Pa.s}]} = K \left[\frac{\rho \times 16.018 \text{ kg.m}^{-3}}{453.6 \frac{\text{kg}}{\text{kmol}}}\right] / [\mu \times 10^{-3} \text{ Pa.s}]$$

$$\frac{H \times P}{\mu} = \frac{\rho \, (\text{kg.m}^{-3})}{K.M(\text{kg.kmol}^{-1}).\mu \, (\text{cP})} \times \frac{1}{16.018}$$

∴

Figure 2.6.1A.1.1.

4. Calculate $E_{a,j}$ for specified component (Input Data).

$$E_{a,j} = \frac{[\text{mols}/h]_j \text{ IN} - [\text{mols}/h]_j \text{ OUT}}{[\text{mols}/h]_j \text{ IN}}$$

= specified fraction recovery

5. Minimum liq : gas ratio for specified component

$$\left|\frac{L_o}{G_{N_p+1}}\right|_{min} = K.E_a \cdot \frac{\sum Y}{1 + \sum X} \simeq K_j.E_{a,j}$$

At tower bottom $\sum Y \simeq 1$ if equilibrium condition is assumed & $\sum X$ can be ignored since it gives slightly conservative value.

6. Determine operating liq : gas ratio

$$\left|\frac{L_o}{G_{N_p+1}}\right|_{op} = \left|\begin{array}{c}\text{specified}\\\text{unit}\end{array}\right| \cdot \left|\frac{L_o}{G_{N_p+1}}\right| \qquad \qquad ...(2.31)$$

7. Calculate operating absorption factor

$$A_{j,\,top} = \left|\frac{L_o}{G_{N_p+1}}\right|_{op} \cdot \frac{1}{K_j} \qquad \qquad ...(2.31)$$

8. Theoretical plates (n = N)

$$E_{a,\,j} = \frac{\left[A_{j,op}\right]^{N+1} - A_{j,op}}{\left[A_{j,op}\right]^{N+1} - 1} \qquad \qquad ...(2.32)$$

or, $(N + 1) \log_{10} |A_{j,\,op}| = \log \left|\dfrac{A_{j,op} - E_{a,j}}{1 - E_{a,j}}\right|$

Solve for N

9. Actual number of trays

$$N_P = N/\eta_o$$

where, η_o = overall tray-efficiency whose value can be determined from **Fig.2.6.1A.1.1** (see also **Table 2.6.1A.1.1**).

Table 2.6.1A.1.1. Absorption-Stripping Tray Efficiencies (Approximate Values).

Type	Pressure Range (MPa)	Temperature Range (K)	Efficiency Range (%)
ABSORPTION			
Hydrocarbon Oils & Vapors	0 – 5.5	272 – 327	35 – 50
Propane (Key)	0.7 – 14.5	—	30 – 38 (37)
Butane (Key)	0.7 – 14.5	—	28 – 33 (36)
STRIPPING			
Hydrocarbon Oils with steam	0 – 0.9	422 – 561	50 – 80
Unsaturates in Oil with closed reboiler	0 – 0.34		25 – 35

(Figure within parenthesis refers to average value)
Source : *Oil & Gas Journal (Nov.9/1953 - Mar.15/1954)* - R J Hull & K Raymond

10. Lean solution rate :

$$L_o = A_j \cdot K_j \cdot G_{N+1,\,op}, \text{ mols/h} \qquad \qquad ...(2.33)$$

11. For nonkey components, estimate $E_{a,\,j}$ by

$$E_{a,\,j} = E_{a,\,l} \cdot \left|\frac{K_1}{K_2}\right| \qquad \qquad ...(2.34)$$

with a limiting value of unity.

2.6.1B.STRIPPER–Determination of Number of Theoretical Trays & Stripping Steam (or Gas) Rate For a Specified Component Recovery

The rich solution (absorber effluent) from the absorption operation is usually stripped off

the desirable components and recycled back to the absorber **(Fig. 2.6.1)**. The stripping agent or medium may be process steam or inert gas (CH_4, N_2, CO_2, H_2, etc.)

Input Data :

- Rich solution rate, L_o
- Absorbed component composition in feed liq, X'_o
- Temp. level of coolant available at the battery limit
- Stripping stream's temp. & press
- Col. operating temp.
- Col. operating press.

Calculation procedure is as follows :

1. **Determine K_j values for each component at column temperature and pressure. Use K charts for this.**

2. **For specified component recovery, $E_{s,\,key}$ for key component is known. Calculate stripping rate of key**

$$G_{m,\,key} = L_{m+1} \cdot X_{m+1} \cdot E_{s,\,key}$$

3. **Estimate stripping efficiency of non-key components**

$$E_{s,\,j} = E_{s,\,key} \left| \frac{K_{key}}{K_j} \right|$$

4. **Calculate mols stripped per hour for each component as in Step - 2.**

5. **Estimate the minimum value of the ratio of flowrates of stripping stream & lean solution (V_o/L_o) by trial & error procedure based on key component & taking successive values of V_o.**

See Table in the next page

- **Assume several values of V_o**

- **L_o is known**

- **Compute a set of** $\dfrac{E_{s,\,key}\left(1 + \sum X_j\right)}{K_{key}\left(1 + \sum Y_j\right)}$ **values each corresponding to a particular V_o/L_o value.**

- **Plot V_o/L_o against $E_{s,\,key}\left(1 + \sum X_j\right)\big/K_{key}\left(1 + \sum Y_j\right)$.**

- **Get the minima, *i.e.*, the point where they are equal. Operation at this point required infinite number of trays. Therefore, values larger than the minimum should be used.**

- **Usually, 1.5 times $\left|V_o/L_o\right|_{min}$ is taken as the operating $\left|V_o/L_o\right|_{op}$.**

- **However, it is reasonable to try several values of $\left|V_o/L_o\right|_{op}$ and corresponding plates evaluated.**

V_o (assumed)	L_o (known)	$\dfrac{V_o}{L_o}$	$\sum X_j = \dfrac{\lvert L.X_j\rvert_{m+1}}{L_o}$	$(1 + \sum X_j)$	$E_{s,\,key} \times$ $(1 + \sum X_j)$	$\sum Y_j = \dfrac{\sum G_{m,j}}{G_{N_p+1}}$	$1 + \sum Y_j$	$K_{Key} \times$ $(1 + \Sigma Y_j)$	$\dfrac{E_{s,key}\left(1+\sum X_j\right)}{K_{key}\left(1+\sum Y_j\right)}$
...	...	...	...	...	...	...	...	...	...
...	...	...	...	...	...	...	...	...	...
...	...	...	...	...	...	...	...	...	...
...	...	...	...	...	...	...	...	...	...
...	...	...	...	...	...	...	...	...	...
...	...	...	...	...	...	...	...	...	...

V_o = mols/h of stripping medium (steam or gas) entering the stripper.

$$V_{o,\,op} = \text{assumed value} \left|\frac{V_o}{L_o\,_{op}}\right| \cdot L_{o,op},\ mols/h$$

6. Calculate $S_{j\,-\,key}$:

$$\left(1 + \sum Y_j\right) = 1 + \sum \frac{Y_{m,j}}{V_{o,op}}$$

$$\therefore \qquad S_{j,\,op} = K_j \left|\frac{V_o}{L_o}\right|_{op} \frac{1 + \sum Y_j}{1 + \sum X_j} \qquad \qquad ...(2.35)$$

7. Calculate the number of theoretical trays , M :

$$E_{s,\,j} = \frac{\left|S_{j,op}\right|^{M+1} - S_{j,op}}{\left|S_{j,op}\right|^{M+1} - 1} \qquad \qquad ...(2.36)$$

or, $\qquad (M + 1)\log_{10} S_{j,\,op} = \log_{10}\left|\frac{S_{j,op} - E_{s,\,j}}{1 - E_{s,\,j}}\right| \qquad \qquad ...(2.37)$

8. Calculate actual trays at operating reflux

$$M_{act} = \frac{M}{\eta_o}$$

9. Calculate for each component, the corrected amount stripped :

$$S_j = K_j \cdot \left|\frac{V_o}{L_o}\right|_{op} \cdot \frac{1 + \sum Y_j}{1 + \sum X_j}$$

$|V_o/L_o|_{op}$ is fixed in Step-5

$1 + \sum X_j$ and $1 + \sum Y_j$ come from Step-6

10. At each individual S_j values, read out, from Fig. 2.6.1A-1, the

$\dfrac{S^{M+1} - S}{S^{M+1} - 1} = E_{s,j}$ values taking theoretical number of trays (Step - 7) as the curve

parameter.

2.6.1B.1. STRIPPER—Determination of Rate of Stripping-Medium for Specified Recovery

Input Data :
- Rich solution rate, L_{m+1}
- Rich solution composition, X_{m+l}
- Column operating pressure
- Column operating temperature
- Precent recovery of a specified key component

Proceed as follows :

    1. Select a suitable value for theoretical trays (M)

    2. Refer to Fig. 2.6.1A.1

$E_{s,j}$ values for a key component specified

$$E_{s\,j-key} = \frac{|S|^{M+1}-S}{|S|^{M+1}-1}$$

Using **m = M** as curve parameter, read out S_e (effective stripping factor) corresponding to specified value of recovery for the key component.

    3. The value of $S_e = S_{key}$ for the key component

$$S_e = S_{key} = K_{key}\left|\frac{V_o}{L_o}\right| \cdot \frac{1+\sum Y_{key}}{1+\sum X_{key}}$$

or, $$\frac{V_o}{L_o} \cdot \frac{1+\sum Y_{key}}{1+\sum X_{key}} = \frac{S_{key}}{K_{key}}, \text{ known}$$

Construct the following table.

Component	*Component* *rate in rich* *soln. (mols/h)*	*K_j at Col.* *operating press* *and temp.*	*$S_j = Kj \times$* $\left\|\frac{V_o}{L_o}\right\| \cdot \frac{1+\sum Y_j}{1+\sum X_j}$	*$E_{S,j}$*	*Component* *stripped* *(mols/h)*
...	...	...	...	...	... ...
...	...	...	...	...	... ...
	$\sum$				$\sum$

Use K_j value for each component at col. op. press. & temp. to calculate column - 4 of the table.

From the values of S_j calculated (col. 4), read $E_{s,j}$ values from Fig. 2.6.1A.1 at the number of trays (M) assumed in Step-2.

    4. Calculate the mols of each component stripped per h

$$= |L_{m+1} \cdot X_{m+1}| \cdot E_{S,j}$$

    5. Calculate the stripping agent (steam or gas) rates, V_o, as follows

$$\frac{V_o}{L_o} \cdot \frac{1+\sum Y}{1+\sum X} = \frac{S_{key}}{K_{key}} \text{ (known)}$$

$$\therefore V_o = L_o \cdot \left|\frac{S_j}{K_j}\right|_{key} \left[\frac{1+\sum \dfrac{Mols/h \; in\,Rich\,Soln.}{L_o}}{1+\sum \dfrac{Mols/h \; Stripped*}{V_o}}\right]$$ *6th col. of Table (Step-3)

2.6.2. Absorption Edmister Method

This method utilizes the concept of average absorption and stripping factors and go into the details of a complicated problem.

Source : *Hydrocarbon Absorption & Fractionation Process Design Methods*— W C Edmister, Petroleum Engineer (May 1947 — March 1949)

2.6.2.A. Absorber Determination of Solvent Rate (Lean Soln.) for Specified Component Recovery in Fixed Tower

Input Data :

- Feedgas rate, G_{n+1}
- Feedgas composition, Y_{n+1}
- Specified recovery, E_a (for key component)
- Number of theoretical trays, $N = n$
- Operating pressure
- Operating temperature

Procedure

1. Read out A_e, from Fig. 2.6.1A.1 for the key component & its fixed recovery E_a, taking n = N as curve parameter

$$E_a = \frac{|A_e|^{N+1} - A_e}{|A_e|^{N+1} - 1} \qquad ...(2.38)$$

2. **Assume :**

(a) Lean soln. rate, L_o, mols/h

(b) Total mols absorbed

(c) Temp. rise of solvent (normally it goes up by 11 - 22K)

3. **Amount absorbed per tray**

$$= \left| \frac{G}{G_{N+1}} \right|^{1/N}$$

$$\therefore \qquad \left| \frac{G_1}{G_{N+1}} \right|^{1/N} = \frac{G_j}{G_{j+1}} \qquad ...(2.39)$$

Source : *Calculation of Absorber Performance & Design*—G Horton & W B Franklin (Industrial & Engineering Chemistry, vol. 32/P: 1384/1940)

Gas leaving top tray

$G_1 = G_{N+1}$ – Mols/h absorbed (assumed) , mols/h

Gas leaving bottom tray No. N

$$G_N = G_{N+1} \left| \frac{G_1}{G_{N+1}} \right|^{1/N}, \text{ mols/h}$$

Gas leaving tray No. 2 (from top)

$$G_2 = \frac{G_1}{\left|\dfrac{G_1}{G_{N+1}}\right|^{1/N}}, \quad \text{mols/h}$$

Liq leaving top tray No. 1

$L_1 = L_o + G_2 - G_1$, mols/h

where, Lo = lean soln. rate (solute free basis), mols/h

L_N = liq leaving bottom tray (solute free basis), mols/h

= L_0 + mols/h absorbed (assumed)

4. Calculate liq : gas flow ratios.

At top : L_1/G

At bottom : L_N/G_N

5. Use Horton-Franklin method to estimate tray temps. :

$$\frac{\theta_N - \theta_j}{\theta_N - \theta_o} = \frac{G_{N+1} - G_{j+1}}{G_{N+1} - G_1} \qquad\qquad ...(2.40)$$

i.e., temp. change is proportional to the vap. concentration (*i.e.*, amount absorbed) per tray.

where θ_o = lean oil temp., K

θ_N = bottom tray temp., K

θ_j = tray-j temp., K

θ_{N+1} = tower inlet gas temp., K

This relation is based on constant percent absorption per tray.

Temp. of bottom tray :

$$\theta_N = \theta_{N+1} + \Delta\theta \qquad\qquad \text{(assumed temp. rise)}$$

Temp. of top tray :

$$\theta_1 = \theta_N - \Delta\theta \left|\frac{G_{N+1} - G_2}{G_{N+1} - G_1}\right|$$

6. K values of components in the feed at

(*i*) top tray temp.

(*ii*) bottom tray temp.

from **Equilibrium Chart**

7. **Calculate absorption factor for each component at tower top and bottom conditions**

$$A_{t,j} = \frac{1}{K_j} \cdot \frac{L_1}{G_1}$$

$$A_{b,j} = \frac{1}{K_j} \cdot \frac{L_N}{G_N}$$

where, $A_{t,j}$ = absorption factor for component j at tower top conditions

$A_{b,j}$ = absorption factor for component j at tower bottom conditions

8. Use Fig. 2.6.2A.1 to read out A_e value corresponding to $A_{t,j}$ and $A_{b,j}$ values.
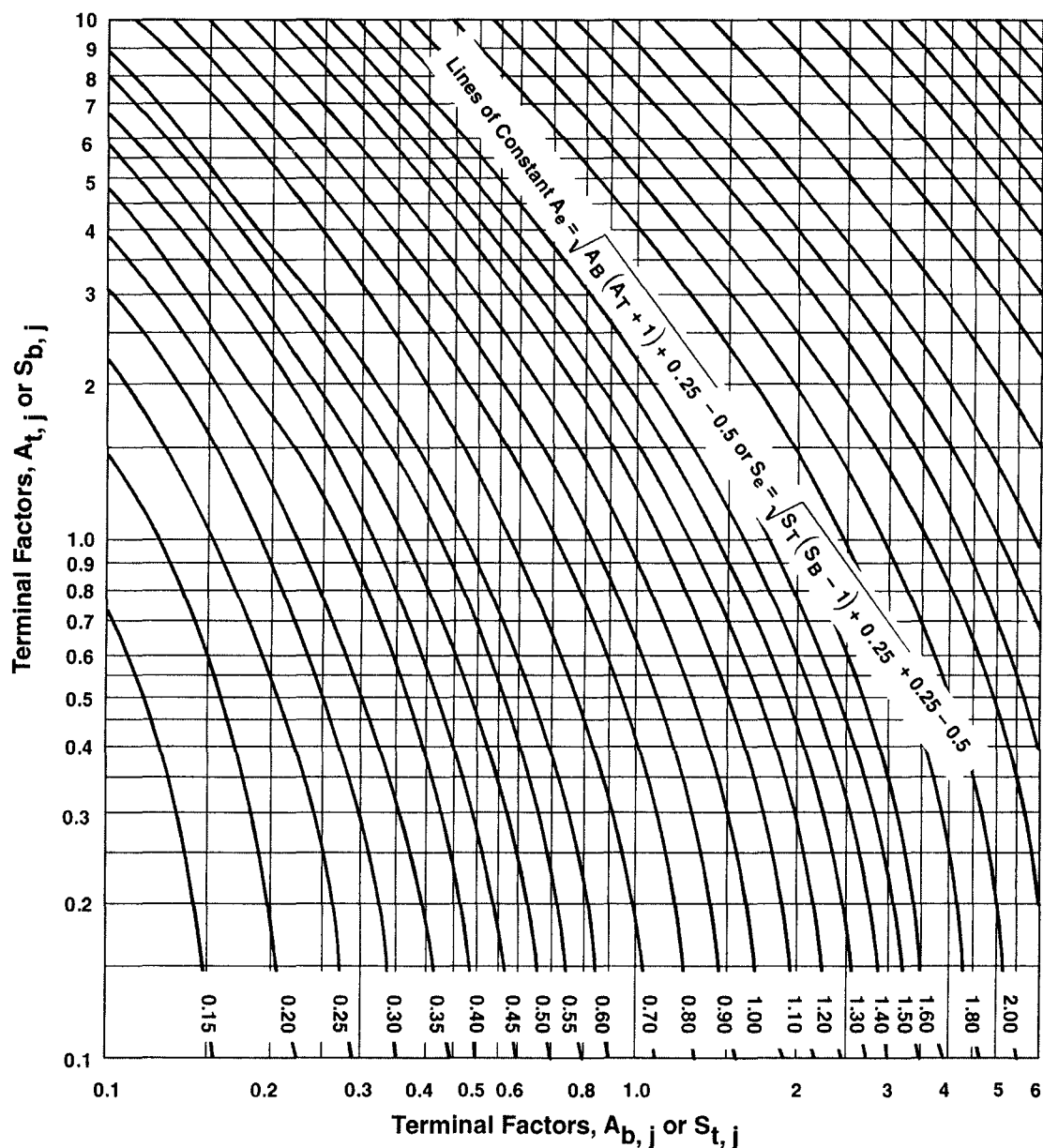
Fig. 2.6.2A.1. Absorption and Stripping Factors with Effective Absorption (and Stripping) Factor appearing as Curve Parameter.

9. Use Fig. 2.6.1A.1.

Determine $E_{a,j}$ corresponding to A_e obtained in Step-8 using $N = n$ (fixed or assumed) as curve parameter

10. Calculate the mols of each component absorbed

= [Mol component is Rich Gas at Inlet] $\times |E_{a,j}|$

Compile the following table.

Component	Mols in Rich Gas At Inlet	$K_{t,j}$	$K_{b,j}$	$A_{t,j}$	$A_{b,j}$	$A_{e,j}$	$E_{a,j}$	Mols Absorbed
...	...	...	...	...	...	...	...	...
...	...	...	...	...	...	...	...	...
...	...	...	...	...	...	...	...	...

11. Check whether the result yields the desired amount of key component absorbed. If the figure does not tally, go for 2nd trial assuming a new value of L_0. Adjustments may have to be made separately or simultaneously in the absorption quantity until an acceptable result is obtained.

2.6.2B. Absorber Determination of Number of Trays for Specified Recovery of Key Components

1. Assume n.

2. Draw material balance of key component over the tower

$$G_{1,j} = f_s \cdot L_{o,j} + (1 - f_a) \cdot G_{n+1,j} \qquad \qquad ...(2.41)$$

where, $G_{1,j}$ = molar gas rate of j leaving tray- 1, mols/h

f_s = fraction of $L_{o,j}$ stripped out, mols/h

$$= \frac{|S_e|^{n+1} - S_e}{|S_e|^{n+1} - 1} \qquad \qquad ...(2.42)$$

f_a = fraction of $G_{n+1,j}$ absorbed, mols/h

$$= \frac{|A_e|^{n+1} - A_e}{|A_e|^{n+1} - 1} \qquad \qquad ...(2.43)$$

$L_{o,j}$ = molar flowrate of a component j in liq phase entering the tower, mols/h

$G_{n+1,j}$ = molar flowrate of a component in gas phase entering the tower, mols/h

From Equ. 2.41

$$1 - f_a = \frac{A_e - 1}{|A_e|^{n+1} - 1} \qquad \qquad ...(2.43A)$$

Combining EQNs. 2.39, 2.41A and 2.40 results in

$$G_{1,j} = \frac{|S_e|^{n+1} - S_e}{|S_e|^{n+1} - 1} \bullet L_{o,j} + \frac{A_e - 1}{|A_e|^{n+1} - 1} \cdot G_{n+1,j} \qquad \qquad ...(2.44)$$

$$= \left[1 - \frac{S_e - 1}{|S_e|^{n+1} - 1} \right] . L_{o,j} + \left| \frac{A_e - 1}{A_e^{n+1} - 1} \right| . G_{n+1,j} \qquad \qquad ...(2.44)$$

For specified key-component recovery, $G_{1,j}$, $L_{o,j}$ and $G_{n+1,j}$ are fixed. Compute $G_{n,j}$

$$G_{n,j} = G_{n+1,j} \left| \frac{G_{1,j}}{G_{n+1,j}} \right|^{1/N}$$

$$\therefore \quad A_{t,\,key} = \frac{L_{1,key}}{G_{1,key}} . \frac{1}{K_{key}}$$

$$\& \quad A_{b,\,key} = \frac{L_{N,key}}{G_{N,key}} . \frac{1}{K_{key}}$$

3. Read out $A_{e,\,key}$ **corresponding to** $A_{t,\,key}$ **and** $A_{b,\,key}$ **values from Fig. 2.6.2A-1**

Calculate $S_{t,\,key}$ and $S_{b,\,key}$:

$S_{t,\,key} = 1 / A_{t,\,key}$

$S_{b,\,key} = 1 / A_{b,\,key}$

4. Estimate $S_{e,key}$ **from Fig. 2.6-2A-1 with the help of** $S_{t,\,key}$ **and** $S_{b,\,key}$ **values.**

5. A trial and error solution is necessary for the number of theoretical stages (n) by using EQN. 2.44A.

6. Calculate the values of $G_{1,\,key}$ **for non-key components using EQN. 2.44A with the calculated value of n**

7. If necessary, the entire procedure may be repeated using the better estimates of component flowrates in the exit streams that were estimated in the first iteration.

Absorber Design : Number of Theoretical Plates For Specified Product Absorption

Example 2*2. A gas stream, composed of C-1, C-2, C-3, C-4, and C-5 hydrocarbons is fed to an isothermal absorber operating at 305K and 0.51 MPa.

90% of nC-4 component is to be abstracted from the gas stream by lean solution containing no more than 0.002 mole fraction of nC-4 (see table below).

The individual component rates in the feedgas as well as the equilibrium constant values of each component at the operating temperature and pressure of the absorber are also presented in the table.

Component	$K_{j\ 305K/0.51MPa}$	FeedGas (kmols/h)	Lean Solution (mol fraction)
C-1	42.5	1639	—
C-2	7.29	166	—
C-3	2.25	95	—
iC-4	0.89	18	0.001
nC-4	0.65	33.6	0.002
iC-5	0.28	8	0.004
nC-5	0.225	16	0.006
Washoil	0	—	0.987
		$\Sigma = 1975.6$	$\Sigma = 1.000$

Lean solution rate = 1914.75 kmol/h

If the operating liq rate is 1.8 times the minimum rate, estimate the number of theoretical stages required.

Solution : The key component is nC-4

ABSORBER

Step - 1. Fraction Absorbed

Component	Fraction Absorbed (kmol)
nC-4	0.9

C-1 $0.9 \left|\dfrac{0.65}{42.5}\right|^* = 0.01376$

C-2 $0.9 \left|\dfrac{0.65}{7.29}\right| = 0.08024$

C-3 $0.9 \left|\dfrac{0.65}{2.25}\right| = 0.26$

iC-4 $0.9 \left|\dfrac{0.65}{0.89}\right| = 0.6573$

iC-5 $\simeq 1$ **as the case of Ist approximation**

nC-5 $\simeq 1$ **all the C-5s are assumed to be completely absorbed**

* As a rough approximation, assume the fraction absorbed of a given component is inversely proportional to its K-values :

$$E_{a,\,j} = E_{a,\,key} \cdot \left|\frac{K_{key}}{K_j}\right|$$

Step -2. Component Absorbed

1h Basis

Component	Absorbed(kmols)		OffGas(kmols)	
nC-4	0.9 × 33.6	= 30.24	33.6 – 30.24	= 3.36
C-1	0.01376 × 1639	= 22.552	1639 – 22.552	= 1616.44
C-2	0.08024 × 166	= 13.319	166 – 13.319	= 152.68
C-3	0.26 × 95	= 24.7	95 – 24.7	= 70.3
iC-4	0.6573 × 18	= 11.831	18 – 11.831	= 6.16
iC-5	1 × 8	= 8	8 – 8	= 0
nC-5	1 × 16	= 16	16 – 16	= 0
	Σ = 126.642		Σ = 1848.94 = G_1	

Step - 3. Operating Liq Rate

The EL EQN. is

$$y_j = K_j \cdot x_j$$

For the key component

$$\left|\frac{33.6}{1975.6}\right| = 0.65\, x_{key}$$

$\therefore$ $\qquad$ x_{key} = 0.02616 kmols/h in lean solution feed.

A material balance on key **(nC-4)** yields :

$$L_{n,\,key} = 0.002L_o + 0.9\,(33.6)$$
$$= 0.002L_o + 30.24$$

Overall material balance :

$$L_n = L_o + 126.642$$

Now, $\qquad$ $x_j = L_{n,\,j}\,/\,L_o$

Combining the above equations yields

$$0.02616 = \left| \frac{0.002L_{o,min} + 30.24}{L_{o,min} + 126.642} \right|$$

$\therefore$ $\qquad$ $L_{o,\,min}$ = 1114.53 kmols/h

$\qquad$ $L_{o,\,op}$ = $1.8L_{o,\,min}$ = 1.8 (1114.53) = 2006.154 kmols/h

Step - 4. Effective Absorption Factor For Key Component

Rich solution rate

$$L_n = L_{o,\,op} + \text{component absorbed}$$
$$= 2006.154 + (1975.6 - 1848.94) \text{ kmols/h}$$
$$= 2132.814 \text{ kmols/h}$$

The absorption factors for key component are computed :

$$A_{t,\,key} = \frac{L_{o,op}}{G_1} \cdot \frac{1}{K_{key}} = \frac{2006.154}{1848.94}\frac{\text{kmols}/\text{h}}{\text{kmols}/\text{h}} \cdot \frac{1}{0.65} = 1.6692$$

$$A_{b,\,key} = \frac{L_n}{G_{n+1}} \cdot \frac{1}{K_{key}} = \frac{2132.814}{1975.6} \cdot \frac{\text{kmols}/\text{h}}{\text{kmols}/\text{h}} \cdot \frac{1}{0.65} = 1.6608$$

$\therefore$ **Effective absorption factor for nC-4 (key) :**

$$A_e = [A_{b,\,key}\,(1 + A_{t,\,key}) + 0.25]^{\frac{1}{2}} - 0.5$$

$$= [1.6608(1 + 1.6692) + 0.25]^{\frac{1}{2}} - 0.5$$
$$= 1.6640$$

Step - 5. Calculation of Required No. of Theoretical Stages

$$G_{1,\,j} = \left[1 - \frac{S_e - 1}{|S_e|^{n+1} - 1} \right] L_{o,\,j} + \frac{A_e - 1}{|A_e|^{n+1} - 1} \cdot G_{n+1,\,j}$$

Now, for key component

$$G_{1,\,key} = 3.36 \text{ kmols/h}$$
$$A_e = 1.664$$
$\therefore$ $\qquad$ $$S_e = 1/1.664 = 0.6$$

$$G_{n+1, \text{key}} = 33.6 \text{ Kmols/h}$$

$$L_{o, \text{key}} = L_{o, op} \cdot x_{\text{key}} = 0.002(2006.154) \text{ kmols/h} = 4.012 \text{ kmols/h}$$

Substitution yields :

$$3.36 = \left| 1 - \frac{0.6 - 1}{0.6^{n+1} - 1} \right| 4.012 + \frac{1.664 - 1}{1.664^{n+1} - 1} (33.6) \quad (33.6)$$

or,

$$\frac{-1.6048}{0.6^{n+1} - 1} = 0.652 + \frac{22.31}{1.664^{n+1} - 1}$$

or,

$$\frac{-2.4613}{0.6^{n+1} - 1} = 1 + \frac{34.2177}{1.664^{n+1} - 1}$$

This EQN. is to solved by trial and error method.

n	L.H.S.	R.H.S.	Δ = R.H.S. – L.H.S.
5	+ 2.5817	2.6915	0.1098
5.1	+ 2.5754	2.6036	0.02823
5.12	+ 2.57426	2.58663	0.01237
5.13	+ 2.57366	2.67820	0.004545
5.14	+ 2.57306	2.56982	– 0.003228

Let us take **n = 5.14**

Comp.	K_j	$\dfrac{L_{o,op}}{G_1} \cdot \dfrac{1}{K_j} = A_{t,j}$	$\dfrac{L_n}{G_{n+1}} \cdot \dfrac{1}{K_j} = A_{b,j}$	$A_e = \left[A_{b,j}(1 + A_{t,j}) + 0.25 \right]^{\frac{1}{2}} - 0.5$
C-1	42.5	0.0255	0.0254	0.0254
C-2	7.29	0.1488	0.1480	0.1480
C-3	2.25	0.4822	0.4798	0.4818
iC-4	0.89	1.2191	1.2130	1.2151
nC-4(key)	0.65	1.6692	1.660	1.6635
iC-5	0.28	3.8751	3.8556	3.8642
nC-5	0.225	4.8223	4.7981	4.8090

Comp.	A_e	$S_e = 1/A_e$	$G_{n+1, j}$ (kmols/h)	x_j	$L_{o,j} = L_{o, op} \cdot x_j$ (kmols/h)	$G_{1, j}$ (kmols/h)
C-1	0.0254	39.37	1639	---	----------------	1597.369
C-2	0.1480	6.756	166	---	----------------	141.433
C-3	0.4818	2.075	95	---	----------------	49.791
iC-4	1.2151	0.8229	18	0.001	2.006	3.174
nC-4	1.6635	0.6011	33.6	0.002	4.0123	3.362
iC-5	3.8642	0.2587	8	0.004	8.0246	2.082
nC-5	4.8090	0.2079	16	0.006	12.0369	2.5057
						Σ =1779.176

Step - 6. 2nd Iteration

I. Operating Liq Rate

Components	FeedGas	OffGas (initial estimate) (kmols/h)	OffGas after Ist Iteration (kmols/h)
C-1	1639	1616.44	1579.369
C-2	166	152.68	141.433
C-3	95	70.3	49.791
iC-4	18	6.16	3.174
nC-4	33.6	3.36	3.362
iC-5	8	0	2.082
nC-5	16	0	2.5057
	$\sum$ = 1975.6	$\sum$ = 1848.94	$\sum$ = 1799.716 = G_1

After Ist iteration, the net amount absorbed

$$= 1975.6 - 1799.716$$

$$= 175.884 \text{ kmols/h}$$

$$x_j = \frac{0.002 L_{o,min} + 30.24}{L_{o min} + 175.884}$$

or, $$0.02616 = \frac{0.002 L_{o,min} + 30.24}{L_{o,min} + 175.884}$$

$\therefore$ $$L_{o,min} = 1061.2116 \text{ kmols/h}$$

$\therefore$ $$L_{o,op} = 1.8 L_{o,min} = 1910.18 \text{ kmols/h}$$

II. No. of Theoretical Plates

An overall material balance yields :

$$L_n = 1910.18 + 175.884 = 2086.064 \text{ kmols/h}$$

$$A_{t,key} = \frac{L_{o,op}}{G_1} \cdot \frac{1}{K_{key}} = \frac{1910.18}{1799.716} \cdot \frac{kmols/h}{kmols/h} \cdot \frac{1}{0.65} = 1.6328$$

$$A_{b,key} = \frac{L_n}{G_{n+1}} \cdot \frac{1}{K_{key}} = \frac{2086.064}{1975.6} \cdot \frac{kmols/h}{kmols/h} \cdot \frac{1}{0.65} = 1.6244$$

$\therefore$ Effective absorption factor for key

$$A_e = [A_{b,key}(1 + A_{t,key}) + 0.25]^{\frac{1}{2}} - 0.5$$

$$= [1.62.44(1 + 1.6328) + 0.25]^{\frac{1}{2}} - 0.5$$

$$= 1.6276$$

$\therefore$ $$S_e = 1/A_e = 0.6143$$

Substituting appropriate values in EQN. 2.44A

$$G_{1,j} = \left|1 - \frac{S_e - 1}{S_e^{n+1} - 1}\right| L_{o,j} + \left|\frac{A_e - 1}{A_e^{n+1} - 1}\right| \cdot G_{n+1,j}$$

$$= \left|1 - \frac{0.6143 - 1}{0.6143^{n+1}}\right| (1910.18 \times 0.002) + \frac{1.6276 - 1}{0.6143^{n+1} - 1} \quad (33.6)$$

Or,
$$\frac{-1.4735}{0.6143^{n+1} - 1} = 0.46 + \left|\frac{21.087 - 1}{1.6276^{n+1} - 1}\right|$$

Trial Solution :

n	L.H.S.	R.H.S.	Δ = R.H.S. − L.H.S.
5.2	1.5490	1.54179	−0.00720
5.21	1.5486	1.53627	0.01232
5.19	1.54939	1.54735	−0.002

Let us take **n = 5.19 theoretical stages.**

III. Absorption of Non-Key Components

Comp.	K_j	$\dfrac{L_{o,op}}{G_1} \cdot \dfrac{1}{K_j} = A_{t,j}$	$\dfrac{L_n}{G_{n+1}} \cdot \dfrac{1}{K_j} = A_{b,j}$	$A_e = [A_{b,j}\,(1 + A_{t,j}) + 0.25]^{\frac{1}{2}} - 0.5$
C-1	42.5	0.02497	0.02484	0.02484
C-2	7.29	0.14559	0.14484	0.1449
C-3	2.25	0.47172	0.4692	0.4698
iC-4	0.89	1.1925	1.1864	1.1885
nC-4	0.65	1.6328	1.6244	1.6276
iC-5	0.28	3.7906	3.7711	3.7796
nC-5	0.225	4.7172	4.6929	4.7038

Comp.	A_e	$S_e = 1/A_e$	$G_{n+1,j}$ (kmols/h)	x_j	$L_{o,j} = L_{o,op} \cdot x_j$ (kmols/h)	$G_{1,j}$ (kmols/h)
C-1	0.02484	40.2576	1639	---	---	1598.287
C-2	0.1449	6.9013	166	---	---	141.947
C-3	0.4698	2.1285	95	---	---	50.842
iC-4	1.1885	0.8413	18	0.001	1.9101	3.222
nC-4	1.6276	0.6144	33.6	0.002	3.8203	3.358
iC-5	3.7796	0.2645	8	0.004	7.6407	2.025
nC-5	4.7083	0.2126	16	0.006	11.4610	2.439

$$\Sigma = 1802.12$$

$$G_{1,j} = \left[1 - \frac{S_e - 1}{S_e^{n+1} - 1}\right] L_{o,j} + \left|\frac{A_e - 1}{A_e^{n+1} - 1}\right| G_{n+1,j}$$

Step - 7 3rd Iteration

1. Operating Liq Rate

Comp.	Feed Gas (kmols/h)	Off Gas Initial estimate (kmols/h)	Off Gas After Ist Iteration (kmols/h)	Off Gas After 2nd Iteration (kmols/h)
C-1	1639	1616.44	1579.369	1598.287
C-2	166	152.68	141.433	141.947
C-3	95	70.3	49.791	50.842
iC-4	18	6.16	3.174	3.222
nC-4	33.6	3.36	3.362	3.358
iC-5	8	0	2.082	2.025
nC-5	16	0	2.5057	2.439
	1975.6	1848.94	1799.716	1802.12 = G_1

After 2nd Iteration, the net amount absorbed = 1975.6 − 1802.12 kmols/h

$$= 173.48 \text{ kmols/h}$$

$$\therefore \qquad x_j = \frac{0.002 L_{o,min} + 30.24}{L_{o,min} + 173.48}$$

or,

$$0.02616 = \frac{0.002 L_{o,min} + 30.24}{L_{o,min} + 173.48}$$

$$\therefore \qquad L_{o,min} = 1063.814 \text{ kmols/h}$$

$$\therefore \qquad L_{o,op} = 1.8 L_{o,min} = 1914.865 \text{ kmols/h}$$

II. Number of Theoretical Plates :

$$L_n = L_{o,op} + 173.48 = 1914.865 + 173.48 = 2088.345 \text{ kmols/h}$$

$$A_{t,key} = \frac{L_{o,op}}{G_1} \bullet \frac{1}{K_{key}} = \frac{1914.865}{1802.12} \frac{\text{kmols}/\text{h}}{\text{kmols}/\text{h}} \cdot \frac{1}{0.65} = 1.6347$$

$$A_{b,key} = \frac{L_n}{G_{n+1}} \bullet \frac{1}{K_{key}} = \frac{2088.345}{1975.6} \frac{\text{kmols}/\text{h}}{\text{kmols}/\text{h}} \cdot \frac{1}{0.65} = 1.6262$$

$$A_e = \left[1.6262 (1 + 1.6347) + 0.25 \right]^{\frac{1}{2}} - 0.5 = 1.6294$$

$$S_e = 0.6137$$

Therefore, from EQN. 2.44A we get for nC-4 :

$$3.36 = \left| 1 - \frac{0.6137 - 1}{0.6137^{n+1} - 1} \right| (1914.865 \times 0.002) + \frac{1.6294 - 1}{1.6294^{n+1} - 1} (33.6)$$

or,

$$\frac{-1.4794}{0.6137^{n+1} - 1} = 0.4697 + \frac{21.1478}{1.6294^{n+1} - 1}$$

Trial Solution :

n	*L.H.S.*	*R.H.S.*	$\Delta = R.H.S. - L.H.S.$
5.19	1.5551	1.5523	-0.002727
5.20	1.5547	1.5468	-0.00786

Let us take **n = 5.19**

Comp.	K_j	$A_{t,j}$	$A_{b,j}$	A_e	S_e	x_j	L_o (kmols/h)	$L_{o,j} = L_o x_j$ (kmols/h)
C-1	42.5	0.02500	0.02487	0.02487	40.204	---	1914.865	---
C-2	7.29	0.1457	0.1450	0.1450	6.896	---	1914.865	---
C-3	2.25	0.4722	0.4698	0.47038	2.1259	---	1914.865	---
iC-4	0.89	1.1938	1.1877	1.1898	0.8404	0.001	1914.865	1.9148
nC-4	0.65	1.6347	1.6262	1.6294	0.6137	0.002	1914.865	3.8297
iC-5	0.28	3.7948	3.7752	3.7838	0.2642	0.004	1914.865	7.6594
nC-5	0.225	4.7224	4.6980	4.7090	0.2123	0.006	1914.865	11.4891

$$\frac{L_{o,op}}{G_1} \cdot \frac{1}{K_j} = A_{t,j}; \qquad \frac{L_n}{G_{n+1}} \cdot \frac{1}{K_j} = A_{b,j}$$

Comp.	$G_{n+1,j}$ (kmols/h)	A_e	S_e	$G_{1,j}$ (kmols/h)
C-1	1639.865	0.02487	40.204	1598.238
C-2	166	0.1450	6.896	141.931
C-3	95	0.47038	2.1259	50.790
iC-4	18	1.1898	0.8404	3.2193
nC-4	33.6	1.6294	0.6137	2.2992
iC-5	8	3.7838	0.2642	2.0042
nC-5	16	4.7090	0.2123	2.4425
				1800.924

Thus the 3rd iteration produced :

$L_{o,min}$ = 1063.814 kmols/h

$L_{o,op}$ = 1914.865 kmols/h

L_n = 2088.345 kmols/h

G_1 = 1800.924 kmols/h

which differ very little from the corresponding values obtained in 2nd iteration.

STRIPPER

I. Component Stripped Per Hour

Comp.	x_j	(Absorber in) lean Soln. $L_{o,j} = x_j \cdot L_{o,op}$	$G_{1,j}$ (Kmols/h)	(Absorber Out) Rich Soln. (kmols/h) (By Material balance)	
C-1	---	---	1598.238	1639 – 1598.238	= 40.762
C-2	---	---	141.931	166 – 141.931	= 24.069

Contd.

Comp.	x_j	(Absorber in) lean Soln. $L_{o,j} = x_j \cdot L_{o,op}$	$G_{l,j}$ (Kmols/h)	(Absorber Out) Rich Soln. (kmols/h) (By Material balance)
C-3	---	---	50.79	95 – 50.79 = 44.21
iC-4	0.001	1.1948	3.2193	18 + 1.1948 – 3.2193 = 16.695
nC-4	0.002	3.8297	2.992	33.6 + 3.8297 – 2.992 = 35.1305
iC-5	0.004	7.5694	2.0042	8 + 7.5694 – 2.0042 = 13.5652
nC-5	0.006	11.4891	2.4425	16 + 11.4891 – 2.4425 = 25.0466
Wash oil	0.987	1889.9717		[1889.9717]
		1914.865 = $L_{o,op}$		2089.45

$L_{o,op}$ = 1914.865 kmol.h^{-1}

$E_{s,key}$ (1 + ΣX_j)/[K_{key}(1 + ΣY_j)]
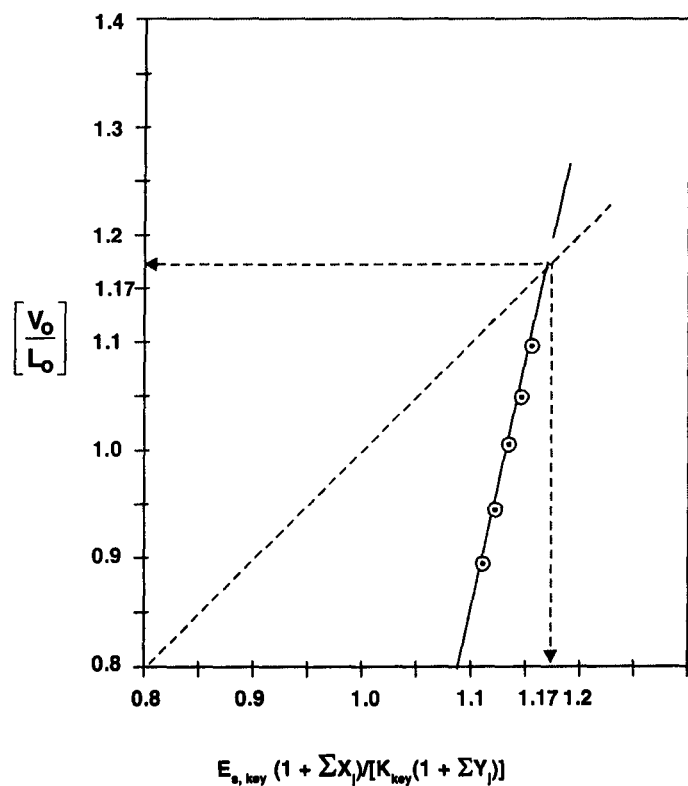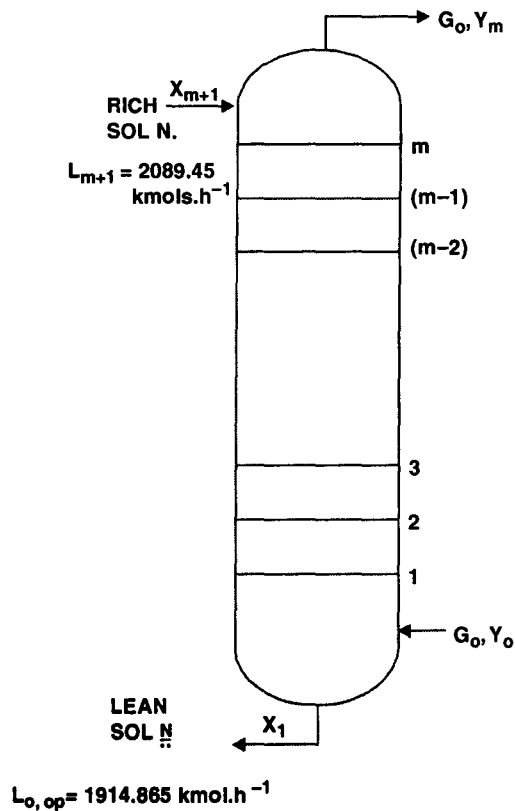
Fig. To Solution 2*2

Specified fraction stripping

$$E_{S,j} = \frac{\text{kmols key IN} - \text{kmols key OUT}}{\text{kmols key IN}}$$

Kmols of component · j stripped per hour

$$G_{m,j} = L_{m+1} \cdot X_{m+1} \cdot E_{S,j}$$

Comp.	Rich Soln. (IN) (kmols/h)	X_{m+1}	Lean Soln. (OUT) (kmols/h)	$E_{S,j}$	$G_{m,j}$ (kmols/h)
C-1	40.762	0.01950	--------	0.01420	0.5785
C-2	24.069	0.01151	-------	0.07943	1.91025
C-3	44.210	0.02115	-------	0.25737	11.373
iC-4	16.695	0.00799	1.9148	0.65065	10.8624
nC-4(key)	35.1305	0.01681	3.8297	0.8908	31.288
iC-5	13.5652	0.0065	7.5694	1.000	102.803
nC-5	25.0466	0.01198	11.4891	1.000	287.590
Wash oil	1889.9717				
	2089.4500 = L_{m+1}				446.4058

II. Minimum Stripping Medium Rate ($V_{o, min}$)

$$L_o = 1914.865 \text{ kmols/h}$$

$$\therefore \quad V_o/L_o = 0.5222$$

$$\Sigma\, X_j = (LX_j)_{m+1} / L_o = 35.1305/1914.865 = 0.01834$$

$$\therefore \quad E_{s,\,key}\,(1+\Sigma X_{key}) = 0.8908\,(1.01834) = 0.90713$$

V_o (kmols/h)	L_o (kmols/h)	V_o / L_o	$Y_j = G_{m,j}/V_o$	K_{key}	$K_{key}(1+\Sigma Y_j)$	$E_{s,\,key}(1+\Sigma X_j)/$ $K_{key}(1+\Sigma Y_j)$
1700	1914.865	0.8878	0.2626	0.65	0.82068	1.1053
1800	1914.865	0.9400	0.2480	0.65	0.8112	1.1182
1900	1914.865	0.9922	0.2349	0.65	0.8027	1.1300
2000	1914.865	1.044	0.2232	0.65	0.7950	1.1409
2100	1914.865	1.0966	0.2125	0.65	0.77881	1.1509
2200	1914.865	1.1489	0.2029	0.65	0.7818	1.1601
2500	1914.865	1.3055	0.1785	0.65	0.7660	1.1841

At point **P** (Fig. to. Soln. 2*2) the x – and y – coordinate become equal. This point marks the minimum V_o / L_o (= 1.17). Operation at this point requires infinite number of plates. Therefore, values larger than the minimum should be used.

III. Number of Theoretical Trays

V_o / L_o (assumed)	$V_{o,\,op} = \left\|\dfrac{V_o}{L_o}\right\|_{assum.} \cdot L_o$	$\Sigma Y_j = \Sigma G_{m,j} / V_o$	$S_{j,\,o} = K_j \left\|\dfrac{V_o}{L_o}\right\|_{op} \cdot \dfrac{\left\|1+\sum Y_j\right\|}{\left\|1+\sum X_j\right\|}$
1.2	2297.838	0.1942	$0.65\,(1.2)\,\dfrac{1.1942}{1.01834} = 0.9147$
1.25	2393.58	0.1865	$0.65\,(1.25)\,\dfrac{1.1865}{1.01834} = 0.9466$
1.30	2489.32	0.1793	$0.65\,(1.30)\,\dfrac{1.1793}{1.01834} = 0.9785$

Now, $(M_o + 1) \log S_{j,o} = \log \left[\dfrac{S_{j,o} - E_{S,j}}{1 - E_{S,j}} \right]$

For, $S_{j,o} = 0.9147$, $M_o = 18.0397$

$S_{j,o} = 0.9466$, $M_o = 13.234$

$S_{j,o} = 0.9785$, $M_o = 11.085$

IV. Number of Actual Trays

$S_{j,o}$	M_o	η_o	$M_{act} = M_o / \eta_o$
0.9147	18.0397	50%	36
0.9466	13.234	50%	26
0.9785	11.085	50%	22

Absorber Design : Number of Theoretical Trays and Solvent Flowrate For Specified Component Recovery

Example 2*3. *98% Ethylene recovery, thru absorption, from a gas stream of following composition has been envisaged :*

Component	Vol %
Hydrogen	*18.5*
Methane	*22.5*
Ethylene	*20.5*
Ethane	*0.5*
Propylene	*22.0*
Propane	*0.5*
n-Butane	*2.5*
n-Pentane	*13.0*
	100.0%

Feedgas rate = 9463 m³ / h

Feedgas pressure = 0.48 MPa

Feedgas temp. = 311K

The absorber operate at 0.48 MPa

The lean solvent (mol. wt. 160 kg/kmol ; density 825 kg/m³ ; dynamic viscosity 0.81 cP) is fed countercurrent to the gasflow to the tower at 300K.

Operating liq/gas ratio = 1.25 times the minimum liq/gas ratio.

Determine the solvent rate and the number of theoretical and actual trays.

Solution : We shall solve the problem thru stepwise sequence and at the same time checking unreasonable results.

Step - I. FeedGas Rate

$$G_{n+1/0.48Pa/311K} = 9463 \text{ M}^3/\text{h}$$

$$G_{n+1/NTP} = 9463(m^3/h) \frac{273K}{311K} \cdot \frac{0.48MPa}{0.101325MPa}$$

$$= 39350.994 \, Nm^3/h$$

$$= \frac{39350.994}{22.41} \, \frac{Nm^3/h}{Nm^3/kmol}$$

$$= 1755.956 \, kmols/h$$

$$\approx 1756 \, kmols/h$$

Step - II. Ethylene Absorbed

$$\text{Ethylene in (FeedGas)} = \left|\frac{20.5}{100}\right| \left|1756 \frac{kmols}{h}\right| = 359.98 kmols/h$$

$$\text{Ethylene out (Exit Gas)} = |1-0.98| \left|359.98 \frac{kmols}{h}\right| = 7.1996 kmols/h$$

$$\therefore \quad \text{Ethylene absorbed} = 359.98 - 7.1996 = 352.7804 \, kmols/h$$

Step - III. Specified Ethylene Separation

$$E_{a,j} = \frac{kmols \, IN - kmols \, OUT}{kmols \, IN} = 0.98$$

Step - IV. Minimum Liq : Gas Ratio

L/G ratio for ethylene :

$$\frac{L_o}{G_{n+1}} = K_j \cdot E_{a,j} \qquad\qquad\qquad \textbf{j = ethylene}$$

Average temperature conditions for **K** :

Tower temp. at top, $\theta_t = 300K$

Tower temp. at bottom, $\theta_t = 311K$

Average Tower temp., $\theta_{av} = \frac{1}{2}(300 + 311) = 305.5K$

Pressure :

Allowable $\Delta P \approx 0.14$ MPa in the column

$\therefore$ Absorber top pressure $= 0.48 - 0.14 = 0.34$ MPa

$\therefore$ Average col. press. $= \frac{1}{2}(0.48 + 0.34) = 0.41$ MPa

$\therefore \quad K_{C_2H_4/0.41 \, MPa/305.5K} = 11.5$ \hfill **Equilibrium Charts**

$$\therefore \qquad \left|\frac{L_o}{G_{n+1}}\right|_{minC_2H_4} = (11.5)(0.98) = 11.27$$

Step - V. Operating Liq : Gas Ratio

$$\left|\frac{L_o}{G_{n+1}}\right|_{op} = 1.25(11.27) = 14.087$$

Step - VI. Absorption Factor

$$A_{j,\,op} = \frac{L_o}{G_{n+1\,op}} \cdot \frac{1}{K_j} = \frac{14.087}{11.5} = 1.2249$$

Step - VII Theoretical Trays

At operating liq : gas ratio

$$E_{a,\,j} = \frac{A^{N+1} - A_j}{A^{N+1} - 1} = \frac{1.2249^{N+1} - 1.2249}{1.2249^{N+1} - 1}$$

or, $(N + 1)\, \log 1.2249 = \log \left| \dfrac{1.2249 - 0.98}{1 - 0.98} \right| = 1.08795$

$\therefore$ $N = 11.3489$

Step - VIII. Actual Plates

Now we're to calculate actual plates from the operating liq : gas ratio $\left[L_o / G_{n+1} \right]_{op}$

$$N_{act} = N \,/\, \eta_o$$

In absence of efficiency data, use is to be made of O'Connell's **Efficiency Correlation (Fig.2.6.1A1.1)**

$$\frac{HP}{\mu} = \frac{1}{16.018} \cdot \frac{\rho}{K.M.m}$$

where, H = Henry's Law Constant, $\dfrac{kmols}{m^3.kPa}$

   P = operating pressure, kPa

   μ = dynamic viscosity of solvent, cP

   ρ = density of solvent, kg/m^3

   M = molecular wt. of the solvent, kg/kmol

   K = distribution coefficient

For our solvent

$$\frac{H.P.}{\mu} = \frac{1}{16.018} \cdot \frac{825}{11.5(160)(0.81)} = 0.03455$$

Read off efficiency from **Fig. 2.6.1A.1.1.** It is 14%. This value is low. Since no better information is available, use $\eta_o = 15\%$

$\therefore$ Actual trays

$$N_{act} = 11.3489 \,/\, 0.15 = 75.659 \approx 76 \text{ trays}$$

Step - IX Lean Solution Rate

$$L_o = A_j \cdot K_j \, |\, G_{n+1} \,|_{op} = 1.2249\,(11.5)\,(1756 \text{ kmols/h}) = 24735.63 \text{ kmols/h}$$

This figure is too unrealistic to be acceptable. This high solution rate is the outcome of following reasons :

1. Op. press. being too low thus resulting in a high **K**-value.

2. Ethylene being light component and hence difficult to absorb.

3. Op. temp. too high

Let us increase operating pressure to 4.8 MPa whence K-value becomes 1.35

$$\therefore \qquad \left|\frac{L_o}{G_{n+1}}\right|_{min} = 1.35\,(0.98) = 1.323$$

Operating liq : gas ratio

$$\left|\frac{L_o}{G_{n+1}}\right|_{op} = 1.25\,(1.323) = 1.6537$$

Operating $A_{j,\,op} = 1.6537\,/\,1.35 = 1.2249$

Theoretical trays :

$$(N + 1)\log 1.2249 = \log\left|\frac{1.2249 - 0.98}{1 - 0.98}\right|$$

$$\therefore \qquad\qquad N = 11.349$$

Efficiency $\qquad\qquad = \dfrac{1}{16.018}\cdot\dfrac{825}{(1.35)(160)(0.81)} = 0.2943$

Refer to **Fig. 2.6.1A.1.1**

$$\eta_o \approx 29\%$$

$\therefore \qquad\qquad N_{act} = 11.349\,/\,0.29\ = 39.13\ \approx 39\text{ trays}$ $\qquad\qquad$ **Ans.**

Solvent feedrate = (1.2249) (1.35) (1756 kmols/h)

$$= 2903.74\text{ kmols/h}$$

$$\approx 2904\text{ kmols/h}$$ $\qquad\qquad\qquad\qquad$ **Ans.**

Comments : This final solvent rate is still a large qty to absorb ethylene. Therefore, it might be less expensive to separate ethylene by low-temp. fractionation (cryogenic distillation).

2.6.3. SEPARATION OF METHANE FROM CARBON MONOXIDE AND HYDROGEN

Methane is the major desired end-product in coal gasification processes such as flash hydrolysis or the Exxon Catalytic Process. Since it is always accompanied by carbon monoxide and/or hydrogen, it is necessary to develop economical methods of separation to obtain pipeline grade methane.

Several separation techniques are available :

1. absorption/stripping

2. cryogenic distillation

3. clathrate formation

The absorption/stripping method using liquid propane as solvent is a well-known chemical engineering operation that can be readily designed and constructed on a large scale.

Absorption/Stripping : Process Requirements

For the application of absorption/stripping, it is desirable to use a suitable solvent which has a high solubility for methane.

Enlisted in the following **Table 2.6.3.1** are a number of solvents with solubility data for methane.

Table 2.6.3.1. Solubility Data of Methane in Selected Solvents at various Pressures.

Solvents	m^3 of CH_4 (298K/101.325 kPa) dissolved in $1m^3$ of solvent at various pressures:					
	2 Mpa	*4 MPa*	*6 MPa*	*8.1 MPa*	*10.1 MPa*	*14.2 MPa*
Propane	41	83	125	174	200 at 9.1 MPa	
Butane	37	71	107	144		
Pentane	33	63	97	129	164	
Hexane	30	59	89	120		
Cyclohexane	15	33	56	83		
Benzene	11	24	41	59	80	
Methanol	9	19	29.5	41	55	
Ethanol	7.5	14.5	21.5	29.5	38	48 at 12 MPa
Water	0.9	1.2	1.8	2	2.6	3.3

It is seen that methane has highest solubility in propane than all other solvents at any pressure. Therefore, propane is the most suitable solvent (& economically available) for the absorption/stripping operation.

Operating conditions for the absorption and stripping tower are important design parameters for the process. Propane is always present, due to its low vap press. & entrainment, in the gas streams from both the absorber and the stripper. Usually this quantity of propane is not recovered & is lost. Obviously the amount of propane in the gas phase is determined by the operating temperature & pressure of the tower.

Shown in **Fig. 2.6.3.1** are the vapor pressure of selected compounds.

It is evident that the vap. press of propane is about 0.1 mm Hg and 1mm Hg at 127 K and 153K respectively. Typically, the absorber operates at 3.44 MPa abs. and the stripper at 3.35 MPa. abs. When the absorber and stripper operate at 127K & 153K respectively, the mole fractions of propane lost to outlet gas streams are 6.75×10^{-6} and 1×10^{-4} which tantamount to loss of about 0.085% & 3.28% respectively of the cost of methane (assuming the cost of methane and propane is the same). This low percentage of propane loss is commercially acceptable. The propane loss increases when the absorber operates at a higher temp. (see **Table 2.6.3.2**). Hence it is an acceptable proposition to operate absorber at 127K and stripper at 153K

Fig. 2.6.3.1 *Vapor pressure curves of selected compounds.*

Table 2.6.3.2 Propane Losses at Different Absorber Temperature
[Stripper Temp : 153K/Plant cap : 295000 sm³.h⁻¹]

T (K)	Ton Day⁻¹ Loss of Propane			% of Propane Cost Loss*
	Absorber	Stripper	Absorber + Stripper	
223	1265.5			
213	716.7			
193	218.2			
173	50.35	3.817	50.17	1.133
144	2.16	3.817	5.98	0.126
127	0.216	3.817	4.033	0.085

* assuming cost of methane equals cost of propane

Fig. 2.6.3.1 *Vapor pressure curves of selected compounds.*

Table 2.6.3.2 Propane Losses at Different Absorber Temperature
[Stripper Temp : 153K/Plant cap : 295000 $sm^3.h^{-1}$]

T (K)	Ton Day^{-1} Loss of Propane			% of Propane Cost Loss*
	Absorber	Stripper	Absorber + Stripper	
223	1265.5			
213	716.7			
193	218.2			
173	50.35	3.817	50.17	1.133
144	2.16	3.817	5.98	0.126
127	0.216	3.817	4.033	0.085

* assuming cost of methane equals cost of propane

Absorption/Stripping : Process Description

A schematic process flow diagram is shown in **Fig. 2.6.3.2.** Absorber feedgas **(stream 1)** a mixture of methane, hydrogen, and carbon monoxide at ~ 311K/3.446 MPa. abs. is successively cooled to 133K by the outlet gas stream from the absorber and some recycle gas. The absorber is a packed column filled with 25mm ring packing with ~50% void fraction. The rich liquid from the absorber bottom is heated in a HE by the liquid leaving the stripper at the bottom. The stripper is also a packed column filled with 25mm ring packings or saddles.
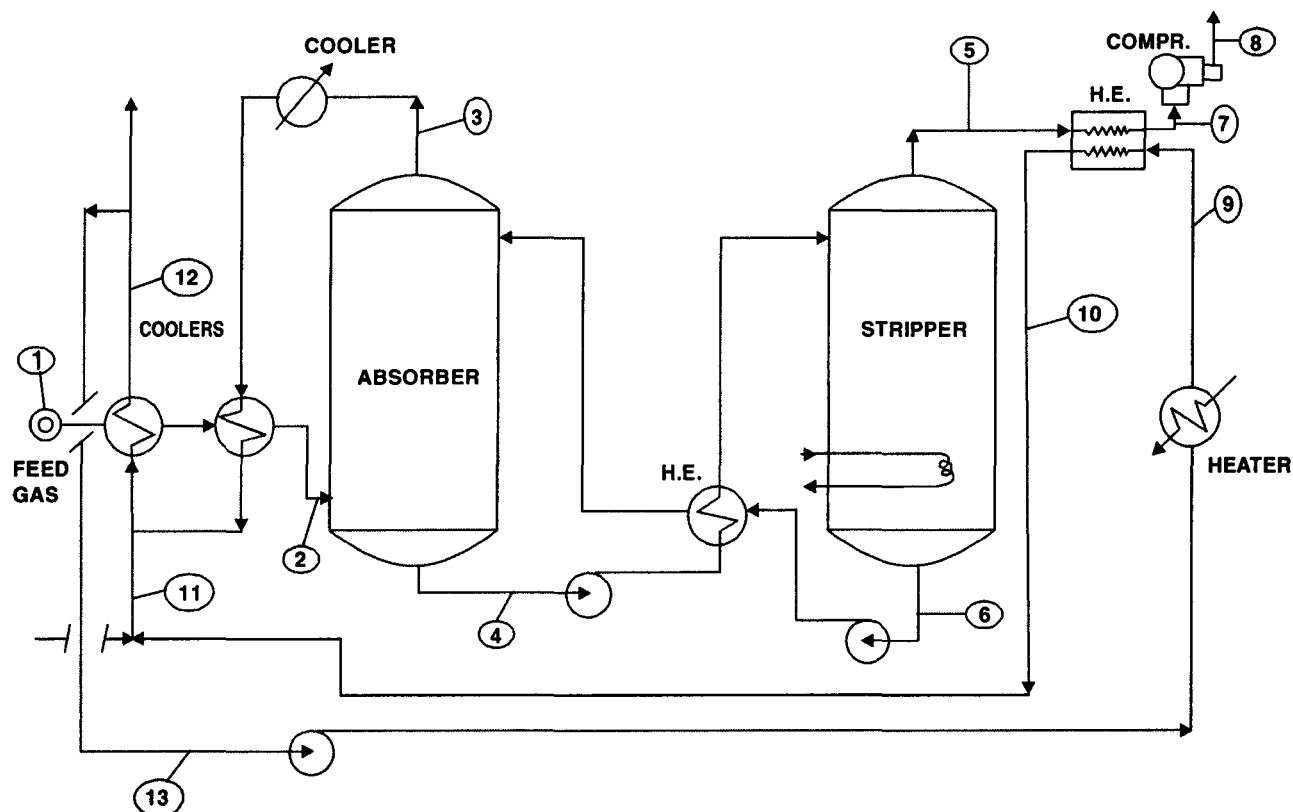
Fig. 2.6.3.2. *Flow Diagram for Methane Separation by Absorption/Stripping method.*

The heat supplied to the stripper at the bottom desorbs methane, hydrogen, and carbon monoxide from the rich liquid. The exit gas from the stripper top is heated in a HE by a recycle gas stream and is further compressed to produce the final methane product at 311 K/6.892 MPa. abs.

Design Example :

A typical feedgas composition is

> CH_4 : 40% (vol.)
>
> H_2 : 45% (vol.)
>
> CO : 15% (vol.)

Feedgas temperature : 311K

Feedgas pressure : 3.44 MPa. abs.

Plant capcacity : 295000 sm^3/h of methane output

[where sm³ is standard m³ referred to 288K/100 kPa]

Absorber :

Liquid Feedrate, L'	= 3838.59 th⁻¹
Gas Feedrate, G'	= 27372.95 m³.h⁻¹
Liquid Density, ρ_L	= 585 kg. m⁻³
Average operating temperature	= 127 K
Operating pressure	= 3.445 MPa. abs.
Liq rate in the absorber	= 1.5 kmol/kmol of feedgas
Absorbent : liq propane	**CH₄ absorption : 95%**

Stripper :

Liquid Feedrate, L'	= 1.5346 × 10⁷ kg. h⁻¹
Gas exit rate, G'	= 5.806 × 10⁵ kg. h⁻¹
Liquid Density, ρ_L	= 585 kg. m⁻³
Gas Density, ρ_G	= 50.67 kg. m⁻³

Design the absorber, stripper and evaluate the energy requirement for the separation of methane.

Solution :

Feed Gas Density at 127K

$\boxed{\textbf{CH}_4}$

$$T_r = \frac{127}{191} = 0.665$$

$$P_r = \frac{3.445 \times 10^6}{101325 \times 45.8} = 0.7412$$

$$Z_c = 0.56$$

$\boxed{\textbf{CO}}$

$$T_r = \frac{127}{133} = 0.955$$

$$P_r = \frac{3.445 \times 10^6}{101325 \times 34.5} = 0.984$$

$$Z_c = 0.32$$

$\boxed{\textbf{H}_2}$

$$T_r = \frac{127}{33.3} = 3.814$$

$$P_r = \frac{3.445 \times 10^6}{101325 \times 12.8} = 2.652$$

$$Z_c = 0.98$$

Vol % = Mol %

$$\therefore \quad Z_{av} = CH_4 \% \times Z_{CH_4} + CO\% \times Z_{co} + H_2 \% \times Z_{H_2}$$
$$= 0.40 \, (0.56) + 0.15 \, (28) + 0.45 \, (2)$$
$$= 0.713$$

Average molecular weight of the feedgas

$$M_{av} = 0.4 \, (16) + 0.15 \, (28) + 0.445 \, (2) = 11.15 \text{ kg. kmol}^{-1}$$

$$\therefore \quad \rho_G = \frac{P.M_{av}}{Z.RT}$$

$$= \frac{\left(3.445 \times 10^6 \, \text{Pa}\right)\left(11.15 \, \text{kg. kmol}^{-1}\right)}{0.713 \left[8313.846 \, \dfrac{\text{Pa. m}^3}{\text{K. kmol}}\right](127 \, \text{K})}$$

$$= 51.023 \, \text{kg. m}^{-3} \text{ at } 127 \, \text{K}$$

Absorber Design :

Basis : 100 kmol of feedgas

$$\begin{bmatrix} \text{CH}_4 : 40 \, \text{kmol} \\ \text{CO} \;: 15 \, \text{kmol} \\ \text{H}_2 \;\;: 45 \, \text{kmol} \end{bmatrix}$$

Methane absorption = 95%

∴ Methane absorbed = 38 kmol

As a preliminary estimate,

        CH_4 absorbed : 38 kmol

        CO absorbed : 13 kmol

        H_2 absorbed : 10 kmol

Liquid (propane) feedrate in the absorber

        = 1.5 kmol/kmol of feedgas

        = 150 kmol

Absorber top :

$$\left|\frac{L}{G}\right|_{Top} = \frac{150}{100 - (38 + 13 + 10)} = 3.846$$

L = liq mass velocity, kg. $\text{h}^{-1}.\text{m}^2$

G = Gas mass velocity, kg. h^{-1} . m^2

Absorber bottom :

$$\left|\frac{L}{G}\right|_{Bottom} = \frac{150 + 38 + 13 + 10}{100} = 2.11$$

∴ $$\left|\frac{L}{G}\right|_{av} = \frac{1}{2}(3.846 + 2.11) = 2.98$$

Therefore,

Liquid loading = **Flow Parameter** $= \left|\dfrac{L}{G}\right|_{av} \sqrt{\dfrac{\rho_G}{\rho_L}}$

$$= 2.98 \sqrt{\frac{51.023 \, \text{kg.m}^{-3}}{585 \, \text{kg.m}^{-3}}}$$

$$= 0.88$$

Corresponding to this liq loading, the gas loading at flood

$$\frac{G_{fl}^2 \left| a_P/\epsilon^3 \right| \cdot \mu_L^{0.2}}{\rho_G \cdot \rho_L} = 0.05$$

where, a_P = surface area of packing per unit bed vol, m^2/m^3

ϵ = void fraction of dry packing, m^3/m^3

μ_L = liq viscosity, cP

ρ_G = gas density, kg. m^{-3}

ρ_L = liq density, kg. m^{-3}

Considering max. allowable operating gas loading at 60% of floodpoint

$$\frac{G_{fl}^2 \left| a_P/\epsilon^3 \right| \cdot \mu_L^{0.2}}{\rho_G \cdot \rho_L} = 60\% \text{ of } 0.05$$

$\therefore$ G = 14257 kg. h^{-1}. m^{-2}, after computing a_P/ϵ^3 for 25mm Berl saddles.

Since methane recovery is 295000 sm³. h^{-1} (288 K/100 kPa), the feedgas rate at absorber inlet.

$$GA = G' = 1.066 \times 10^6 \text{ kg. } h^{-1} \qquad \text{where } A = \text{absorber cross-section}$$

$$\therefore \qquad A = \frac{G'}{G} = \frac{1.066 \times 10^6 \text{ kg.h}^{-1}}{14257 \text{ kg.h}^{-1}.\text{m}^{-2}}$$

$$= 74.767 \text{ m}^2$$

$$\therefore \qquad \frac{\pi}{4} D^2 = 74.767 \text{ m}^2$$

or,   D = 9.756 m   **Too large**

So let us go for 3#s of absorbers—each receiving $\frac{1}{3}$rd of total flow.

$$A = \frac{\frac{1}{3}\left[1.066 \times 10^6 \text{ kg.h}^{-1}\right]}{14257 \text{ kg.h}^{-1}.\text{m}^{-2}} = 24.9234 \text{ m}^2$$

$\therefore$ D = 5.633 m   where, D = absorber ID

The key component is methane for which average absorption factor = 6.478. For 95% removal

NTU = 2

HTU = 6.309 m

$\therefore$ Height of packed bed = HTU × NTU = 12.618 m

With the above conditions, **the gas composition at absorber outlet :**

CH_4 = 0.2 kmol

CO = 13 kmol   **Basis : 100 kmol of Feedgas**

H_2 = 44 kmol

Component	Mol Fraction
CH_4	3.48×10^{-3}
CO	0.2272

H_2	0.7692
C_3H_8	6.75×10^{-6}

Liquid (rich solution) composition at absorber outlet :

Component	*Mol Fraction*
CH_4	0.101
CO	0.005
H_2	0.003
C_3H_8	0.891

Pressure drop across the packed bed = 13.37 kPa. abs.

Tower wall-thickness = 76 mm

Stripper Design :

CH_4 ▶ key component

L' = 1.5346×10^7 kg. h^{-1}

G' = 5.806×10^5 kg. h^{-1}

ρ_L = 585 kg. m^{-3}

ρ_G = 50.67 kg. m^{-3}

∴ Liq loading = Flow Parameter

$$= \frac{L}{G} \sqrt{\frac{\rho_G}{\rho_L}} \qquad cf. \qquad \frac{L}{G} = \frac{L'/A}{G'/A} = \frac{L'}{G'}$$

$$= \frac{1.5346 \times 10^7 \text{ kg.} h^{-1}}{5.806 \times 10^{-5} \text{ kg.} h^{-1}} \sqrt{\frac{50.67 \text{ kg.} m^{-3}}{585 \text{ kg.} m^{-3}}}$$

$$\simeq 7.8$$

Corresponding to this liq loading, the floodpoint is at following gas loading

$$\frac{G_{fl}^2 \left(a_P/ \epsilon^3\right). \mu_L^{0.2}}{\rho_G . \rho_L} = 0.0018$$

Assuming maximum operating gas load = 60% of G_{fl}

∴ G = 6699 kg.h^{-1}. m^2

a_p/ϵ^3 has been computed for the same 25mm **Berl saddles.**

∴ Gas mass velocity, GA = 5.806×10^5 kg.h^{-1}

∴ Area of cross-section of stripper

$$= \frac{GA}{G}$$

$$= 86.6696 \text{ m}^2$$

∴ D = 10.505 m **Too large**

So, 3 Nos. of stripper are chosen

$$A = \frac{\frac{1}{3} \left| 5.806 \times 10^{-5} \text{ kg.} h^{-1} \right|}{6699 \text{ kg.} h^{-1}. m^{-2}} = 28.889 \text{ m}^2$$

$$\therefore \qquad D = \sqrt{\frac{4}{\pi} \left(28.859 \, m^2\right)} = 6.065 \text{ where } D= \text{stripper ID}$$

$$HTU = 3.474 \, m$$
$$NTU = 2$$

$\therefore$ Height of packed bed = (3.474 m) (2) = 6.948 m

ΔP across the packed bed = 2.82 kPa. abs.

Operating Parameters at Different Points on Flow Diagram

Point	Temp	Press	Flow Rate	Flow Rate	Composition (vol %)			
No.	(K)	(MPa. abs.)	(kg. h⁻¹)	(m³. h⁻¹)	CH_4	H_2	CO	C_3H_8
1.	311	3.445	1.066×10^6	27373	40	45	15	0
2.	127	3.445	1.066×10^6	11209	40	45	15	0
3.	127	3.356	4.214×10^5	10241	0.35	76.9	22.7	~Nil
4.	127	3.445	1.602×10^7		10.13	0.25	0.51	89.1
5.	153	3.343	5.783×10^5		96	2.1	1.9	0.01
6.	153	3.356	1.534×10^7		0.5	0.04	0.36	99.9
7.	311	3.343	5.783×10^5		96	2.1	1.9	0.01
8.	311	6.892	5.783×10^5	5474	96	2.1	1.9	~Nil
9.	316	3.356	1.342×10^5		0.35	76.9	22.7	~Nil
10	194	3.356	1.342×10^5		0.35	76.89	22.7	~Nil
11.	200	3.356	3.345×10^6		0.35	76.9	22.7	~Nil
12.	305	3.356	3.78×10^6		0.35	76.9	22.7	~Nil
13.	305	3.356	1.348×10^5		0.35	76.9	22.7	~Nil

[A] Pumping Energy Required To Pump Rich Solution From Absorber Bottom to Stripper Top (Fig. 2.6.3-3)
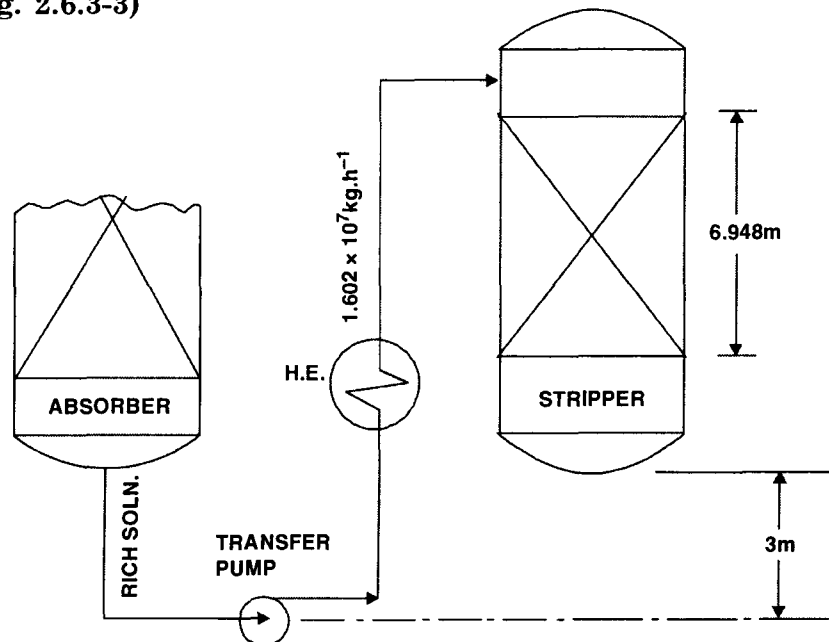
Fig. 2.6.3-3. *Rich Solution is Transferred From Absorber Bottom to Stripper Top By A Pump.*

Packed bed Height, **Z** = 6.948 m

Tower height, **H** = Z + 20% Z = 8.3376

Working formula :

$$H + 0.8\,W_s + h_{f\,r} = 0$$

where, W_s = head-loss per set of pipes (10 pipes) connecting each absorber & stripper

$h_{f,\,r}$ = fractional head-loss

$$= \frac{4\,flv^2}{2\,gd}$$

Since there are 3 sets of absorbers & 3 sets of strippers, the fluid (rich solution) is transported in 30 # s of pipes–each pair of absorber-stripper system is connected by 10 pipes.

Mass flow thru 30 pipes = 1.602 × 10⁷ kg. h⁻¹

Dia of each pipe, **d** = 76 mm

Therefore, velocity *v* in each pipe

$$v = \frac{1.602 \times 10^7 \left(\text{kg. h}^{-1}\right)}{30\left[\frac{\pi}{4}(0.076\text{ m})^2\right] \times 585\left(\text{kg}/\text{m}^3\right)}$$

$$= 201218.69 \text{ m.h}^{-1}$$

$$= 55.894 \text{ m.s}^{-1}$$

Liquid Reynolds No.

$$Re = \frac{v_L.d.\rho_L}{\mu_L} = \frac{\left(55.894\,m.s^{-1}\right)\left(0.076\,m\right)\left(585\,kg.m^{-3}\right)}{\left(7 \times 10^{-6}\,kg.m^{-1}.s^{-1}\right)} = 3.538 \times 10^8$$

Head loss due to friction

$$h_{fr} = \frac{4f\,L\,v_L^2}{2\,g\,d} \qquad \text{where, } \mathbf{4f} = \text{Fanning's friction factor}$$

L = 6.948 m + 20% (6.948 m) + 3 m height of stripper base from the eye of the pump impeller

= 11.3376 m

f = 0.004

$$h_{f,\,r} = \frac{4\left(0.004\right)\left(11.3376\text{ m}\right)\left(55.894\text{ m.s}^{-1}\right)^2}{2\left(9.81\text{ m.s}^{-2}\right)\left(0.076\text{ m}\right)}$$

$$= 380.065 \text{ m}$$

Therefore, head-loss per set of 10 pipes

$$= 380.065 \text{ m} \times 10$$

$$= 3800.65 \text{ m}$$

∴ 8.3376 **m** + 0.8**W**ₛ + 3800.65 = 0

∴   **W**ₛ = –4761.234 m

∴ Electrical power requirement for 30 pipes

$$P = \left| 4761.234 \text{ m} \right| \left| 1.602 \times 10^7 \frac{\text{kg}}{\text{h}} \right| \left| \frac{1}{3600} \frac{\text{h}}{\text{s}} \right| \left| 9.81 \frac{\text{m}}{\text{s}^2} \right|$$

$$= 207.849 \text{ MW}$$

[B] Energy Required to Pump Lean Solution From Stripper Bottom to Absorber Top (Fig. 2.6.3-4)

Packed bed height, $\mathbf{Z}$ = 12.618 m

Absorber height, $\mathbf{H}$ = $\mathbf{Z}$+20% $\mathbf{Z}$ = 15.1416 m

Applying energy balance equation

$$\mathbf{H} + 0.8 \, \mathbf{W_s} + \mathbf{h}_{fr} = 0$$

Liquid mass flowrate thru 30 pipes = 1.534×10^7 kg.h^{-1}

Dia of each pipe = 76 mm
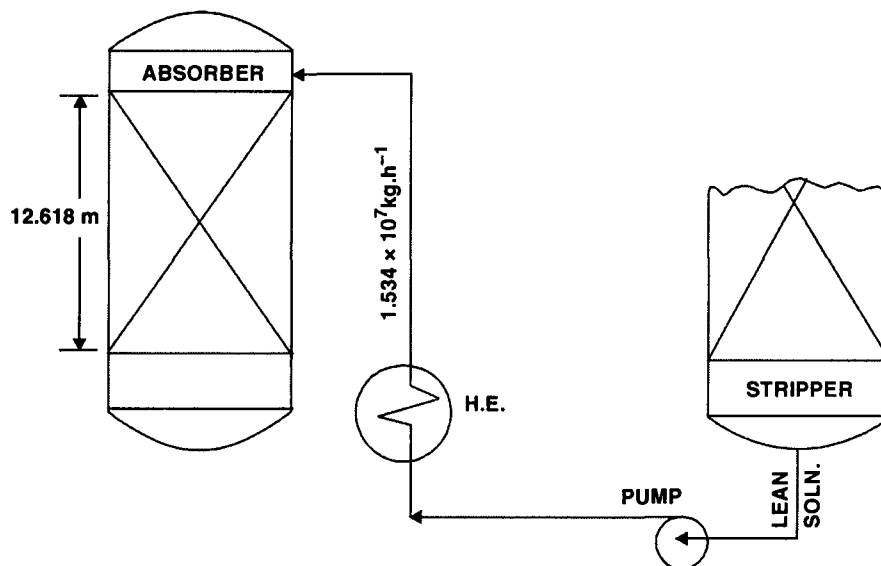
Fig. 2.6.3-4. *Lean solution is transferred from stripper bottom to absorber top by a pump.*

Liquid velocity in each pipe

$$v_L = \frac{1.534 \times 10^7 \text{ kg.h}^{-1}}{30 \left| \frac{\pi}{4} (0.076 \text{ m})^2 \right| \left| 585 \text{ kg.m}^{-3} \right|}$$

$$= 192677.57 \text{ m.h}^{-1} = 53.521 \text{ m.s}^{-1}$$

$$Re = \frac{d \cdot v_L \cdot \rho_L}{\mu_L} = \frac{(0.076 \text{ m})(53.521 \text{ m.s}^{-1})(585 \text{ kg.m}^{-3})}{7 \times 10^{-6} \text{ kg.m}^{-1}.\text{s}^{-1}}$$

$$= 3.399 \times 10^8$$

Using the relative roughness factor to be 0.0006,

$$\mathbf{f} = 0.004 \text{ for } Re = 10^8$$

∴ Frictional head loss in the pipe

$$h_{fr} = \frac{4f\,L\cdot v_L^2}{2\,g\,d} = \frac{4(0.004)\,(15.1416\text{ m})\,(53.521\text{ m.s}^{-1})^2}{2(9.81\text{ m.s}^{-2})(0.076\text{ m})}$$

$$= 465.40\text{ m}$$

This is the frictional head-loss in one pipe. So the total energy required per set (each set comprising 10 pipes) of pipes connecting stripper with the absorber

15.1416m + 0.8 W_s + 10 (465.40 m) = 0

∴ $\qquad\qquad W_s = -5836.427$m

∴ Total pumping power required

$$P = |\,5836.427\text{ m}\,|\ |\,1.534 \times 10^7\text{ kg.h}^{-1}\,|\ \left|\frac{1}{3600}\,\frac{h}{s}\right|\left|9.81\,\frac{m}{s^2}\right|$$

$$= 243.971\text{ MW}$$

[C] Energy Required by Blower at Absorber Inlet

$\qquad\qquad V_G = 27372.95\text{ m}^3\text{. h}^{-1}$

$\qquad\qquad G = 14257\text{ kg. h}^{-1}\text{. m}^{-2}$

$\qquad\qquad \rho_G = 51.023\text{ kg. m}^{-3}$

∴ $\qquad$ Gas velocity $= \dfrac{G}{\rho_G} = \dfrac{14257\text{ kg.h}^{-1}\text{.m}^{-2}}{51.023\text{ kg.m}^{-3}} = 279.423\text{ m.h}^{-1} = 0.0776\text{ m.s}^{-1}$

Let there are 30 pipes (76 mm ID) feeding the gas to the absorber.

∴ Gas velocity in each pipe

$$v_G = \frac{(27372.95\text{ m}^3\text{.h}^{-1})}{30\left|\dfrac{\pi}{4} \times (0.076\text{ m})^2\right|}$$

$$= 201133\text{ m.h}^{-1}$$

$$= 55.87\text{ m.s}^{-1}$$

Gas Reynolds No.

$$Re = \frac{d.\,v_G\cdot \rho_G}{\mu_G} = \frac{(0.076\text{ m})\,(55.87\text{ m.s}^{-1})\,(51.023\text{ kg.m}^{-3})}{7\times10^{-6}\text{kg.m}^{-1}\text{. s}^{-1}}$$

$$= 3.09 \times 10^7$$

Take, **f** = 0.004

∴ $\qquad h_{fr} = \dfrac{4f\,L\ v_G^2}{2g.d} = \dfrac{4(0.004)(3\text{ m})\,(55.87\text{ m.s}^{-1})^2}{2(9.81\text{ m.s}^{-2})(0.076\text{ m})} = 100.48\text{ m}$

Packed bed depth = 12.618 m (absorber)

Pressure drop in the absorber = 13.37 kPa.

Pressure drop per unit height of packed bed

$$= \frac{13.37}{12.618} \frac{\text{kPa}}{\text{m}} = 1.0595 \text{ kPa. m}^{-1} \text{ of packed depth} = 0.10637 \text{ m} \frac{\text{H}_2\text{O}}{\text{m}}$$

830 Pa. m^{-1} = 0.08333 m H$_2$O/meter of packed depth

∴ **Total pressure drop**

$$= (12.618 \text{ m}) (0.10637 \text{ m H}_2\text{O/m of packed height})$$
$$= 1.3422 \text{ m H}_2\text{O}$$

Now the energy balance equation for each pipe is

$$\mathbf{H} + \eta\mathbf{W_s} + \mathbf{h_{fr}} = 0$$

Applying this equation to one set of pipes (10 # s) for incoming gas into the absorber

$$(12.618 + 1.3422)\text{m} + 0.8 \, \mathbf{W_s} + 10 \, (100.48 \text{ m}) = 0$$

∴ $$\mathbf{W_s} = -1273.45 \text{ m}$$

∴ Blower energy required

$$= \left| 1.065 \times 10^6 \frac{\text{kg}}{\text{h}} \right| \left| \frac{1}{3600} \frac{\text{h}}{\text{s}} \right| \left| 1273.45 \text{ m} \right| \left| 9.81 \frac{\text{m}}{\text{s}^2} \right|$$

$$= 3695711 \text{ W}$$
$$= 3.695 \text{ MW}$$

[D] Compressor Power Required

Stripper exit gas (96% CH$_4$) is compressed by means of a compressor downstream of a H.E.

$$P = \frac{1}{\mathbf{k} - 1} \, \mathbf{P_7} . \, \mathbf{V_G} \left[\left(\frac{\mathbf{P_8}}{\mathbf{P_7}} \right)^{\frac{\mathbf{k-1}}{\mathbf{k}}} - 1 \right]$$

where,**k** = ratio of specific heats = C_P/C_V = 1.31 for methane

$\mathbf{P_7}$ = 3.343 MPa = 3.343 × 10^6 Pa.

$\mathbf{P_8}$ = 6.892 MPa = 6.892 × 10^6 Pa.

$\mathbf{V_G}$ = 5474 m^3.h^{-1} = $\dfrac{5474}{3600}$ m^3.s^{-1}

$$= 51.023 \text{ kg. m}^{-3} \text{ at } 127 \text{ K}$$

∴ $$P = \frac{1}{1.31 - 1} \left(3.343 \times 10^6 \frac{\text{N}}{\text{m}^2} \right) \left(\frac{5474}{3600} \text{m}^3. \text{ s}^{-1} \right) \left[\left(\frac{6.892}{3.343} \right)^{\frac{0.31}{1.31}} - 1 \right]$$

$$= 3062012 \text{ W}$$
$$= 3.062 \text{ MW}$$

Assuming the compressor to be 80% efficient, then the power required.

$$= \frac{1}{0.80} \, | \, 3.062 \text{ MW} \, | \, = 3.8275 \text{ MW}$$

[E] Heat Load of The Heater

This heater heats up 1.342 × 10^5 kg.h^{-1} gas stream from 305 K to 316 K.

∴ Heat load of the heater

$$Q = \left|1.342 \times 10^5 \frac{kg}{h}\right|\left|29307 \frac{J}{kmol.K}\right| \left|(316 - 305)\, K\right| \Big/ \left(7.89 \frac{kg}{kmol}\right)$$

$$= 5.48326 \times 10^8\, J.h^{-1}$$
$$= 1523130\, W$$
$$= 1.523\, MW$$

[F] Heat Load of The Cooler at Absorber Inlet

$$Q = \left|4.124 \times 10^5 \frac{kg}{h}\right|\left|29309 \frac{J}{kmol.K}\right|\left|117 - 127K\right| \Big/ \left(9.73 \frac{kg}{kmol}\right)$$

$$= -1.24224 \times 10^{11}\, J/h$$
$$= 3450677\, W$$
$$= 3.45\, MW$$

REFERENCE

1. V Dang – *Separation of Methane from Hydrogen & Carbon Monoxide by an Absorption/Stripping Process*, **Industrial Gas Separation** [ACS Symposium Series 223/Washington D.C./1983]

2.7. GENERAL EQUATIONS FOR CALCULATING ACUTAL PLATES IN ABSORBERS AND STRIPPERS

Here we'll develop a generalized, simplified method to calculate the number of actual plates of the absorbers/strippers using Murphree stage efficiency. These equations are more accurate and less tedious than conventional graphical technique* particularly if a large number of plates are involved.

Operating Line

Shown in **Fig. 2.7.1** is a countercurrent column (absorber/stripper). The material balance of the solute over the control volume is :

$$G_b \cdot y_b + L_i \cdot x_i = G_{i-1} \cdot y_{i-1} + L_b \cdot x_b \qquad ...(2.45)$$

where, G = flowrate of inert-gas, *i.e.*, solute-free gas, kmols/h

y = mole fraction of solute in vapor phase

L = flowrate of inert solvent, *i.e.*, solute-free solvent, kmols/h

x = mole fraction of solute in the liq phase.

Assuming equimolal overflow (*i.e.*, everytime a mole of vapor condenses a mole of liq evaporates whence

$$L_n = L_{n+1} = L_{n+2} = ... = L$$
$$G_n = G_{n+1} = G_{n+2} = ... = G$$
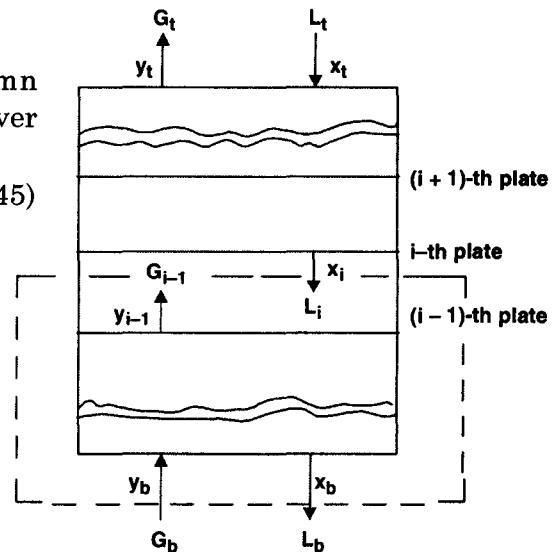
Fig. 2.7.1. *Countercurrent Gas-Liq traffic in an Absorber/Stripper*

the Eqn. 2.45, upon rearrangement yields :

$$y_{i-1} = \left| \frac{L}{G} \right| \cdot x_i + \left(y_b - \left[\frac{L}{G} \right] \cdot x_b \right)$$ ...(2.46)

• stepping off stages at the ends of the curves often leads to inaccuracies. This is the eqn. of operating line **(OL)** with a slope

$$m = \frac{L}{G} \qquad\qquad \& \qquad\qquad \text{y-intercept} = y_b - \frac{L}{G} \cdot x_b$$

DESIGN EQUATIONS

Assuming the gas and liq streams leaving each tray exist in equilibrium and that a linear relationship holds good between **x** and **y**, the equilibrium line **(EL)** equation becomes

$$y_i^* = mx_i + c$$ ...(2.47)

where, **m** = slope of **EL**

   c = y-intercept of **EL**

Elimination of x_i from Eqns. 2.46. & 2.47 yields :

$$y_{i-1} = \frac{L}{m.G} \cdot y_i^* - \frac{L}{m.G} \cdot c + y_b - x_b \left| \frac{L}{G} \right|$$ ...(2.48)

Again, the *Murphree vap-phase plate-efficiency* :

$$\eta_v = \frac{y_i - y_{i-1}}{y_i^* - y_{i-1}}$$ ...(2.49)

or,

$$y_i^* = \frac{y_i - y_{i-1}}{\eta_v} + y_{i-1}$$ ...(2.50)

Eliminating y_i^* from Eqns. (2.48) & (2.50) results :

$$y_i - \left(1 + \frac{m.G}{L} \cdot \eta_v - \eta_v \right) \cdot y_{i-1} = m.\eta_v \cdot x_b + c.\eta_v - \frac{m.G}{L} \eta_v \cdot y_b$$

or,

$$y_i - \left(1 + \frac{1}{A} \cdot \eta_v - \eta_v \right) \cdot y_{i-1} = m.\eta_v \cdot x_b + c.\eta_v - \frac{1}{A} \eta_v \cdot y_b$$

or, $$y_i - k_1 \cdot y_{i-1} = k_2$$ ...(2.51)

where, $A = \dfrac{1}{m.G}$ = **absorption factor**

$$k_1 = 1 + \frac{1}{A} \cdot \eta_v - \eta_v$$

$$k_2 = m.\eta_v \cdot x_b + c.\eta_v - \frac{1}{A} \cdot \eta_v \cdot y_b$$

Eqn. 2.51 is a linear difference equation which can be solved by Mickley method :

$$y_i = \lambda \cdot k_1^i + \frac{k_2}{1 - k_1} \qquad \ldots(2.52)$$

<div align="right">where, λ = constant</div>

$$= \lambda \cdot k_1^i + \frac{\eta_v \cdot \left(mx_b + c - \frac{1}{A} \cdot y_b\right)}{1 - \left(1 + \frac{1}{A} \cdot \eta_v - \eta_v\right)}$$

$$= \lambda \cdot k_1^i + \frac{\eta_v \cdot \left(mx_b + c - \frac{1}{A} \cdot y_b\right)}{\eta_v \cdot \left(1 - \frac{1}{A}\right)}$$

$$= \lambda \cdot k_1^i + \frac{mx_b + c - \frac{1}{A} \cdot y_b}{1 - \frac{1}{A}} \qquad \ldots(2.52)$$

When $i = 0$, $y_i = y_b$ whereupon Eqn. 2.52 becomes.

$$y_b = \lambda + \frac{mx_b + c - \frac{1}{A} \cdot y}{1 - \frac{1}{A}}$$

or,
$$\lambda = \frac{1}{1 - \frac{1}{A}}\left[y_b - \frac{1}{A} \cdot y_b - mx_b - c + \frac{1}{A} \cdot y_b\right]$$

$$= \frac{y_b - mx_b - c}{1 - \frac{1}{A}}$$

Therefore, the complete solution of n numbers of actual plates is (putting $i = n$)

$$y_n = \frac{y_b - mx_b - c}{1 - \frac{1}{A}}\left(1 + \frac{1}{A} \cdot \eta_v - \eta_v\right)^n + \frac{mx_b + c - \frac{1}{A} \cdot y_b}{1 - \frac{1}{A}}$$

or, $\left(1 - \frac{1}{A}\right) \cdot y_n - \left(mx_b + c - \frac{1}{A} \cdot y_b\right) = (y_b - mx_b - c)\left(1 + \frac{1}{A} \cdot \eta_v - \eta_v\right)^n$

or,
$$\left(1 + \frac{1}{A} \cdot \eta_v - \eta_v\right)^n = \frac{\left|1 - \frac{1}{A}\right| y_n - mx_b - c + \frac{1}{A} \cdot y_b}{y_b - mx_b - c} \qquad \ldots(2.53)$$

A material balance of the solute over the entire column yields :

$$x_b = \left|\frac{G}{L}\right| y_b - \left|\frac{G}{L}\right| y_t + x_t \qquad \qquad ...(2.54)$$

or,

$$mx_b = \frac{1}{A}\,[y_b - y_t] + mx_t$$

Eliminating mx_b from Eqns. 2.53 and 2.54 yields :

$$\left[1 + \eta_v\left(\frac{1}{A} - 1\right)\right]^n = \frac{(A-1)\,y_n - y_b + y_t - Amx_t - Ac + y_b}{(A-1)y_b + y_t - Amx_t}$$

$$= \frac{y_n + \left|\dfrac{y_t - A(mx_t + c)}{A-1}\right|}{y_b + \left|\dfrac{y_t - A(mx_t + c)}{A-1}\right|}$$

or,

$$\beta_v^n = \frac{y_b + \alpha}{y_n + \alpha} \qquad \qquad ...(2.55)$$

where, $\beta = \dfrac{1}{1 + \eta_v\left(\dfrac{1}{A} - 1\right)}$ $\qquad \qquad ...(2.56)$

$$\alpha = \frac{1}{(A-1)}\,|\,y_t - A\,(mx_t + c)\,| \qquad \qquad ...(2.57)$$

Eqn. 2.55 lends itself to compute actual compositions at each plate.

Note : When $\eta_v = 1$

$$\beta_v = 1 \qquad \qquad \text{From Eqn. 2.56}$$

Thus, β_v can be dubbed as modified absorption factor.

Upon rearranging & taking logarithm, Eqn. 2.55 gives the actual number of plates :

$$n = \frac{\ln\left|\dfrac{y_b + \alpha}{y_n + \alpha}\right|}{\ln \beta_v} \qquad \qquad ...(2.58)$$

and the number of theoretical (ideal) plates, n' is

$$n' = \frac{\ln\left|\dfrac{y_b + \alpha}{y_n + \alpha}\right|}{\ln A} \qquad \qquad ...(2.59)$$

where, $A = \dfrac{L}{m.\,G} = |\beta_v|_{\eta_v = 1}$

∴ *Overall efficiency*

$$\frac{n'}{n} = \frac{\ln\beta_V}{\ln A} = \frac{\ln\left[1 + \eta_V\left(\frac{1}{A} - 1\right)\right]}{\ln A} \qquad ...(2.60)$$

Liq-Phase Equations

The Murphree liq-phase plate efficiency

$$\eta_L = \frac{x_{i+1} - x_i}{x_{i+1}^* - x_i} \qquad ...(2.61)$$

Combining those eqn. with those of **EL** & **OL**, the following difference equation is resulted for boundary conditions

$$\begin{bmatrix} x_i = x_t \text{ at } i = 0 \\ \& \\ x_i = x_n = x_b \text{ at } i = n \end{bmatrix}$$

$$x_{i+1} - (1 - \eta_L + \eta_L \cdot A) \cdot x_i = \eta_L \cdot \frac{y_t}{m} - \eta_L \cdot A.x_t - \eta_L \cdot \frac{c}{m} \qquad ...(2.62)$$

Solving this linear difference equation as before, we get

$$\beta_L^n = \frac{x_n + \alpha'}{x_t + \alpha'} \qquad ...(2.63)$$

where, $\beta_L = 1 + \eta_L (A - 1)$ ...(2.64)

$$\alpha' = \frac{x_b - \frac{G}{L}|y_b - c|}{\frac{1}{A} - 1} \qquad ...(2.65)$$

Therefore,

$$n = \frac{\ln\left|\frac{x_n + \alpha'}{x_t + \alpha'}\right|}{\ln\beta_L} \qquad ...(2.66)$$

At $\eta_L = 1$, $\beta_L = A$, i.e., ideal conditions come to exist whereupon Eqn., 2.66 becomes

$$n' = \frac{\ln\left|\frac{x_n + \alpha'}{x_t + \alpha'}\right|}{\ln A} \qquad ...(2.67)$$

Therefore, the overall plate efficiency

$$\eta_o = \frac{n'}{n} = \frac{\ln\eta_L}{\ln A} = \frac{\ln\left[1 + \eta_L(A - 1)\right]}{\ln A} \qquad ...(2.68)$$

Eqns. 2.60 & 2.68 represent identical parameter, so equating these two gives relationship between η_V and η_L :

$$\frac{\ln\left[1+\eta_L\left(A-1\right)\right]}{\ln A} = \frac{\ln\left[1+\eta_V\left(\frac{1}{A}-1\right)\right]}{\ln\frac{1}{A}}$$

or,

$$-\ln\left[1+\eta_L\left(A-1\right)\right] = \ln\left[1+\eta_V\left(\frac{1}{A}-1\right)\right]$$

or,

$$\frac{1}{\left[1+\eta_L\left(A-1\right)\right]} = 1+\eta_V\left(\frac{1}{A}-1\right)$$

This is the fundamental relationship between η_L and η_V .Upon simplification it yields

$$\eta_V = \frac{A.\eta_L}{1+\eta_L\left(A-1\right)} \qquad \qquad ...(2.70)$$

$\therefore$

$$\eta_L = \frac{\eta_V}{\eta_V+A\left(1-\eta_V\right)} \qquad \qquad ...(2.71)$$

Stripper—Calculation of Actual and Theoretical No. of Plates for Specified Solute Removal

**Example 2.4.** A solute is to be desorbed from a solution by using a solute-free stripping gas in a plate column where gas and liq streams traffic in countercurrent direction.

The solution, containing 20 mol% of a solute Ⓐ, _enters the column at the top and exits the column at 2 mol% of_ Ⓐ _at the bottom._

The EL Eqn. : y = x + 0.025

OL Slope : m = 1.1

Determine :

1. the number of ideal plates

2. the number of actual plates

3. vapor composition at each plate

Given : Murphree vapor-phase efficiency

   η_V = 80%

Solution :

As the stripping gas is solute-free, so

$$y_b = 0$$

Inlet liq contains 20 mol% solute, so

$$x_t = 0.2$$

Exit liq contains 2 mol % solute, so

$$x_b = 0.02$$

OL slope = 1.1, *i.e,*

$$\frac{L}{G} = 1.1$$

EL is $y = x + 0.025$

$m = 1$

Drawing a material balance around the entire column begets y_t

$$y_t = \frac{L}{G}(x_t - x_b) + y_b$$

$$= 1.1 (0.2 - 0.02) + 0$$

$$= 0.198$$

$\therefore$ $$\beta_v = \frac{1}{1 + 0.8\left(\frac{1}{1.1} - 1\right)} \qquad \qquad ...(2.56)$$

$$= 1.0784$$

$$\alpha = \frac{1}{A - 1} \, |y_t - A(mx_t + c)| \qquad \qquad ...(2.57)$$

$$= \frac{1}{1.1 - 1} |0.198 - 1.1(1 \times 0.2 + 0.025)| \qquad \boxed{A = \frac{L}{m.G} = \frac{1.1}{1} = 1.1}$$

$$= -0.495$$

Therefore, **the number of theoretical plates**

$$n' = \frac{\ln\left|\dfrac{y_b + \alpha}{y_n + \alpha}\right|}{\ln A} \qquad \qquad ...(2.59)$$

$$= \frac{\ln\left|\dfrac{0 + (-0.495)}{0.198 + (-0.495)}\right|}{\ln 1.1}$$

$$= 5.359$$

The number of actual plates

$$n = \frac{\ln\left|\dfrac{0 - (0.495)}{0.198 + (-0.495)}\right|}{\ln 1.0784} \qquad \qquad ...Eqn. \, 2.58$$

$$= 6.767$$

$$\approx 7$$

The overall efficiency

$$\eta_0 = \frac{n'}{n} = \frac{5.359}{7} = 0.7655$$

Theoretical composition

$$A^{n'} = \frac{y_b + \alpha}{y_{n'} + \alpha} \qquad \text{...Eqn. 2.59}$$

$$\therefore \quad y_{n'} = \frac{y_b + \alpha}{A^{n'}} - \alpha = \frac{-0.495}{1.1^{n'}} + 0.495$$

$$x_{n'} = y_{n'} - 0.025 = \frac{-0.495}{1.1^{n'}} + 0.47$$

n	$y_{n'}$	$x_{n'}$
1	0.045	0.02
2	0.0859	0.0609
3	0.1230	0.0981
4	0.1569	0.1319
5	0.1876	0.1626
6	0.2155	0.1906

Eqns. 2.66 and 2.67 can be used to determine the actual and ideal number of stages :

$$= 1.0784$$

$$\alpha' = \frac{x_b - \dfrac{G}{L} \left| y_b - c \right|}{\dfrac{1}{A} - 1} \qquad \text{...(Eqn. 2.65)}$$

$$= \frac{0.02 - \dfrac{1}{1.1} \left| 0 - 0.025 \right|}{\dfrac{1}{1.1} - 1}$$

$$= -0.46999$$

$$\approx -0.47$$

$$\eta_L = \frac{\eta_v}{\eta_v + A\left(1 - \eta_v\right)} \qquad \text{...(Eqn. 2.71)}$$

$$= \frac{0.8}{0.8 + 1.1\left(1 - 0.8\right)}$$

$$= 0.7843$$

$$\beta_L = 1 + \eta_L\left(A - 1\right) \qquad \text{...(Eqn. 2.64)}$$

$$= 1 + 0.7843\left(1.1 - 1\right)$$

$$= 1.0784$$

$$\therefore \quad n = \frac{\ln\left|\dfrac{x_n + \alpha'}{x_t + \alpha'}\right|}{\ln \beta_L} \qquad \text{...(Eqn. 2.66)}$$

$$= \frac{\ln \left| \dfrac{0.02 + (-0.47)}{0.02 + (-0.47)} \right|}{\ln 1.0784}$$

$$= 6.767.$$

$$\approx 7$$

The number of ideal stages

$$\therefore \qquad n' = \frac{\ln \left| \dfrac{x_n + \alpha'}{x_t + \alpha'} \right|}{\ln A} \qquad \text{...(Eqn. 2.67)}$$

$$= \frac{\ln \left| \dfrac{0.02 - 0.47}{0.2 - 0.47} \right|}{\ln 1.1}$$

$$= 5.359$$

Absorber – Calculation of Actual Number of Plates for Specified Solute Removal

Example 2.5. An ammonia cracking plant cracks ammonia to generate hydrogen to be used in a downstream process. The unreacted ammonia is absorbed in water in a sieve-tray tower (750 mm ID) fitted with crossflow trays at 500mm tray spacing.

The cracker exit gas should contain $H_2 : N_2$ in 3:1 molar ratio with 3% ammonia by volume at 200 kPa/300K.

Determine the number of actual plates if :

liq rate (Inlet)	*= 0.322 kmol/s*
gas rate (Inlet)	*= 0.145 kmol/s*
exit gas composition	*= 0.0018 mol% NH_3*

Murphree vap-phase plate efficiency = 57.5 %

EL Equation $\qquad y = 0.707 x$

the scrubbing stream is free of ammonia.

Solution : Given :

$$L = 0.322$$
$$G = 0.145$$
$$m = 0.707$$
$$x_t = 0$$
$$y_t = 0.000018$$
$$y_b = 0.03$$
$$\eta_v = 0.575$$

$$\therefore \qquad A = \frac{L}{m.G} = \frac{0.322 \text{ kmol / s}}{0.707(0.145 \text{ kmol / s})} = 3.141$$

$$\therefore \qquad \beta_V = \frac{1}{1 + \eta_v \left(\dfrac{1}{A} - 1 \right)} \qquad \text{...(Eqn. 2.56)}$$

$$= \cfrac{1}{1 + 0.575 \left(\cfrac{1}{3.141} - 1 \right)}$$

$$= 1.64456$$

&

$$\alpha = \frac{1}{A-1} \left| y_t - A(mx_t + c) \right| \qquad \text{...(Eqn. 2.57)}$$

$$= \frac{0.000018}{3.141 - 1} \qquad \boxed{x_t = 0;\; c = 0}$$

$$= 8.407 \times 10^{-6}$$

$$\therefore \qquad n = \frac{\ln \left| \dfrac{y_b + \alpha}{y_n + \alpha} \right|}{\ln \beta_V} \qquad \text{...(Eqn. 2.58)}$$

$$= \frac{\ln \left| \dfrac{0.03 + 8.4 \times 10^{-6}}{0.000018 + 8.4 \times 10^{-6}} \right|}{\ln 1.64456}$$

$$= 14.143$$

$$\approx 14 \qquad \qquad \textbf{Ans.}$$

2.8 SOUR WATER STRIPPER

Water is frequently used to scrub ammonia, hydrogen sulfide and carbon dioxide from gas streams. The resulting foul water is called the **Sour Water** which must be stripped to contain less than 50 ppmw hydrogen sulfide before the water can be discharged to river basin or reused in the plant. The carbon dioxide, if present, is easily removed and its concentration in the stripped water is usually nil.

Sour-Water strippers widely used in oil refineries and petrochemical plants are also found in process industries. For example, the waste water effluent from ammonia-urea plants usually contains 5 to 10 wt% of ammonia and 2 to 3 wt% of carbon dioxide. The concentration of dissolved gases in the effulent can be brought down to permissible level by single-step stripping using steam as stripping medium. The process itself is profitable inasmuch as the stripped ammonia and carbon dioxide are recycled back to the synthesis section of the urea plant.

A typical stripping scheme commonly involved a stripper column hooked up with an optional heat recovery equipment and an overhead steam condenser. The refluxed stripper is recommended when a low water content in the top vapor is desired.

A stripper is merely a packed or trayed column down which the sour water is passed countercurrently to *'open'* steam. The excess steam and foul vapors then exiting the column at the top may then be burned. However, stricter environmental regulations do not permit such a crude design to operate now-a-days.

It is preferable to energize the stripper by inducting a reboiler instead of using *'open'* steam. This scheme begets certain advantages :

1. Conversion of steam condensate in pure form

2. Avoiding the adverse effect on combustion of foul gases in the furnace because of dilution effect by excess steam.

An overhead condenser is usually provided to condense out excess steam and a part of the condensate rich in NH_3 and H_2S is returned to the stripper as reflux, thereby increasing the load of the stripper.

Generally, it is preferable to return the reflux directly on to the feedtray which is the toptray designated as tray-1 **(Fig. 2.8.1)**
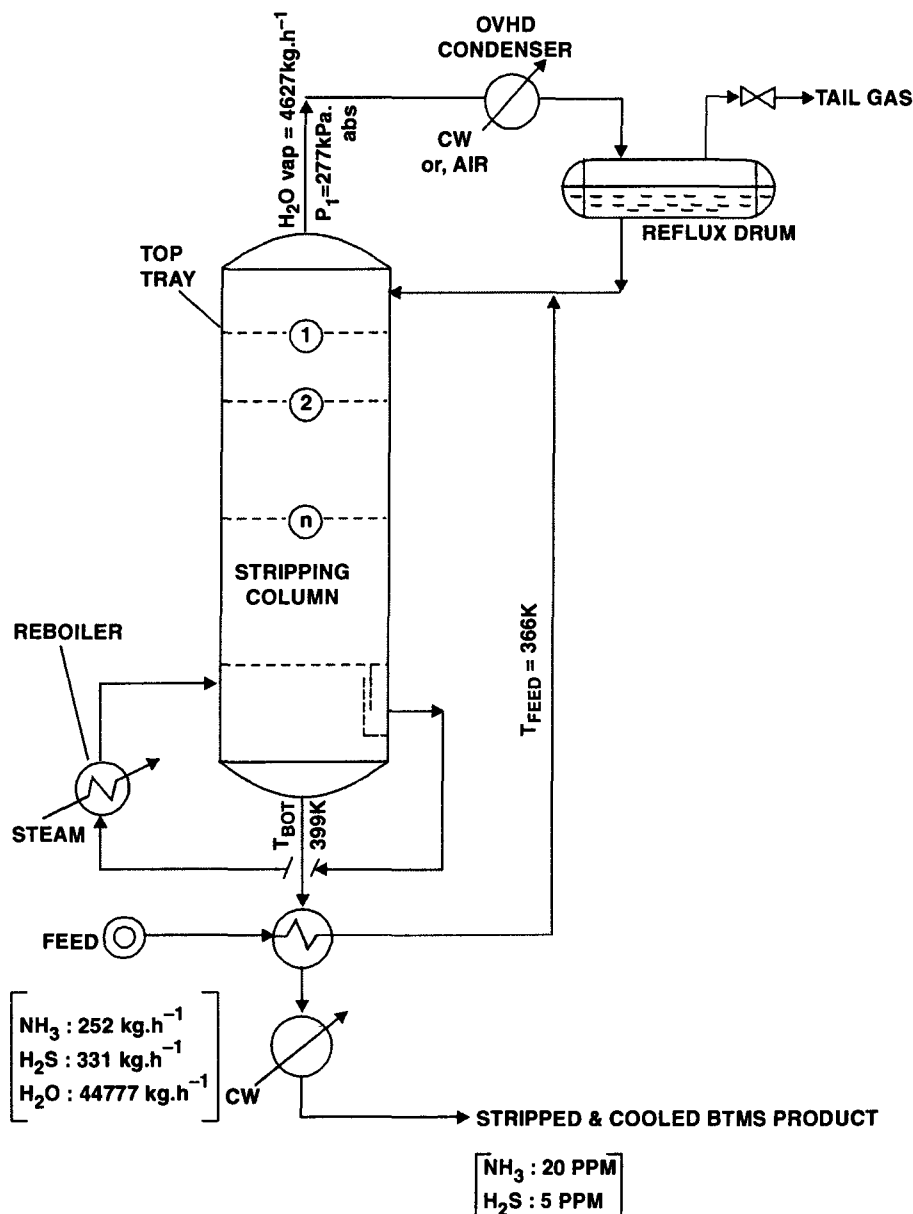
Fig. 2.8.1. *A Typical Sour Water Stripper.*

Since stripping is enhanced by heating, the feed is conveniently preheated by external heat exchange with the BTMS (bottoms) before entering the stripper.

Design Correlations

Credit goes to Van Krevelen whose pioneering effort led to the development of design correlations of sour-water stripper. Later, Krevelen's work was popularized by Beychok [**Aqueous Wastes From Petroleum and Petro-Chemical Plants** – M. R. BeyChok (John Wiley and Sons, London, 1967]. In subsequent time, other investigators independently developed modifications to the Van Krevelen's approach.

The method of tray-to-tray design calculation to determine the number of stripping trays is based on Beychok's procedure :

Step - 1. Feed flowrate and compositions are known. Determine the NH_3, H_2S rates in the feed.

Step - 2. NH_3 and H_2S contents in the BTMS liq are specified (usually in ppmw). Convert them into % concentrations :

$$\% \text{ in } NH_3 \text{ in } \mathbf{BTMS} = \frac{[ppmw]_{NH_3}}{10^6} \times 10^2$$

$$\% \text{ } H_2S \text{ in } \mathbf{BTMS} = \frac{[ppmw]_{H_2S}}{10^6} \times 10^2$$

And then calculate ammonia and hydrogen sulfide rates in the bottom :

$$NH_3 \text{ rate in the } \mathbf{BTMS}, \mathbf{B}_{NH_3} = [ppmw]_{NH_3} \times 10^{-4} \times \mathbf{L}$$

$$H_2S \text{ rate in the } \mathbf{BTMS}, \mathbf{B}_{H_2S} = [ppmw]_{H_2S} \times 10^{-4} \times \mathbf{L}$$

where,   L = water rate in the feed = F – [F_{NH_3} + F_{H_2S}]
        F = feedrate, kg/h
F_{NH_3} = ammonia rate in the feed, kg/h
F_{H_2S} = hydrogen sulfide rate in feed, kg/h

Step - 3. BTMS temperature is known.
Calculate partial pressure of water P_{H_2O} from modified Miles-Wilson Eqn. :
$$T = 7007 [14.465 - \ln p_{H_2S}] - 383$$
Mind that T is in °F and p in psia.

Step - 4 Reboiler operating pressure = BTMS pressure (a known qty)

$\therefore$ $y_{H_2O} = \dfrac{p_{H_2O}}{P}$

$\therefore$ Water rate in the BTMS, $B_{H_2O} = L \cdot y_{H_2O}$

Step - 5. Calculate components rate in Tail Gas
$$TG_{NH_3} = F_{NH_3} - B_{NH_3}$$
$$TG_{H_2S} = F_{H_2S} - B_{H_2S}$$
$$TG_{H_2O} = F_{H_2O} - B_{H_2O}$$

Step - 6. Calculate mole fraction of individual components in the tail gas :

$$y_{NH_3}\Big|_{TG} = \frac{T_{NH_3} / M_{NH_3}}{\sum y_{TG}}$$

$$y_{H_2S}\Big|_{TG} = \frac{T_{H_2S} / M_{H_2S}}{\sum y_{TG}}$$

$$y_{H_2O}\Big|_{TG} = 1 - \left(y_{NH_3}\Big|_{TG} + y_{H_2S}\Big|_{TG}\right)$$

where, $\sum y = y_{NH_3}\Big|_{TG} + y_{H_2S}\Big|_{TG} + y_{H_2O}\Big|_{TG}$

$\quad$ M = mol. wt., kg/kmol

Step - 7. Reflux drum is operated at a given pressure. So P_{RD} is known. Compute, the partial pressure of NH_3, H_2S and Water vapor in RD :

$$p_{NH_3}\Big|_{RD} = y_{NH_3}\Big|_{TG} \times P_{RD}$$

$$p_{H_2S}\Big|_{RD} = y_{H_2S}\Big|_{TG} \times P_{RD}$$

$$p_{H_2O}\Big|_{RD} = y_{H_2O}\Big|_{TG} \times P_{RD}$$

Step - 8. Determine K & C at

$$K = 121 \times 10^3 / 1.016298^T.$$

$$C = \left|\frac{2.84 \times 10^{-7}}{K}\right| . [1.27]^{(T-32)^{0.648}}$$

where, **K & C** are two temperature dependent variables used in Beychok-Van Krevelen Eqns.

$\quad$ Mind please, T is in °F.

Step - 9. K & C values at reflux drum temperature being evaluated, calculate H_2S content and NH_3 content in RD liquid from

$$S_{RD} = \left|\frac{p_{NH_3/RD} \cdot p_{H_2S/RD}}{C}\right|^{\frac{1}{2}}$$

$$A_{RD} = K \cdot p_{NH_3/RD} + \frac{1}{2}S_{RD}$$

where, $\quad$ S_{RD} = hydrogen sulfide content in RD liquid, ppm

$\quad$ A_{RD} = ammonia content in RD liquid, ppm

$p_{NH_3/RD}$ = partial pressure of ammonia in RD, psia

Step - 10. Calculate water flowrate (L_{RD}) in reflux.

Mass balance of water around RD :

$$L_{RD} = \text{Stripping Steam} - TG_{H_2O}$$

Step - 11. Flowrates of Reflux Components

$$L_{NH_3, RD} = A_{RD} \left| \frac{L_{RD}}{10^6 - A_{RD} - S_{RD}} \right|, \text{kg/h}$$

$$L_{H_2S, RD} = S_{RD} \left| \frac{L_{RD}}{10^6 - A_{RD} - S_{RD}} \right|, \text{kg/h}$$

Step - 12. Flowrates of OVHDs

$$V_{NH_3, 1} = NH_3 \text{ rate in vapor phase from Tray-1, kg/h}$$

$$V_{H_2S, 1} = H_2S \text{ rate in vapor phase from Tray-1, kg/h}$$

$$V_{H_2O, 1} = \text{stripping steam rate kg/h}$$

From mass balance

$$V_{NH_3, 1} = L_{NH_3, RD} + TG_{NH_3}$$

$$V_{H_2S, 1} = L_{H_2S, RD} + TG_{H_2S}$$

Molar rate of OVHDs :

$$NH_3 : V_{NH_3, 1}/17$$
$$H_2S : V_{H_2S, 1}/34$$
$$H_2O : V_{H_2O, 1}/18$$

Step - 13 Partial Pressures of OVHDs.

Calculate mole fractions of OVHDs, *i.e.*, components leaving Tray-1 in vapor phase

$$y_{NH_3, 1} = \frac{V_{NH_3, 1}/17}{\sum y_{j,1}}$$

$$y_{H_2S, 1} = \frac{V_{H_2S, 1}/34}{\sum y_{j,1}}$$

$$y_{H_2O, 1} = \frac{V_{H_2O, 1}/18}{\sum y_{j,1}}$$

$\therefore$ $p_{NH_3, 1}$ = partial pressure of NH_3 in vapor leaving Tray-1

$$= y_{NH_3, 1} \times P_1$$

$$P_1 = \text{total pressure on Tray-1}$$

Likewise,

$p_{H_2S, 1}$ = partial pressure of H_2S in vapor leaving Tray-1

$$= y_{H_2S, 1} \times P_1$$

$$p_{H_2O, 1} = y_{H_2O, 1} \times P_1$$

Step - 14. Tray-1 Temperature

Compute temperature of liquid leaving Tray-1 from

$$T_1 = 7007/[14.465 - \ln P_{H_2O,1}] - 383$$

where, T_1 is in °F & P_{H_2O} in psia (calculated in **Step - 13**)

Step - 15 Tray-2 Calculations

1. Calculate K_1 & C_1 using T_1

2. Calculate H_2S & NH_3 concentrations in liquid leaving Tray-1

$$S_1 = \left|\frac{P_{NH_3,1} \times P_{H_2S,1}}{C_1}\right|^{\frac{1}{2}}, \text{ppm}$$

$$A_1 = K_1 \cdot P_{NH_3,1} + \frac{1}{2}S_1 , \text{ppm}$$

3. Calculate NH_3 & H_2S contents in vapor leaving Tray-2 :

$$V_{NH_3,2} = A_1 \left|\frac{L_1}{10^6 - A_1 - S_1}\right| - B_{NH_3}, \text{ppm}$$

Determine L_1 from water mass balance around Tray-1.

$$V_{H_2S,2} = S_1 \left|\frac{L_1}{10^6 - A_1 - S_1}\right| - B_{H_2S}, \text{ppm}$$

SOUR WATER STRIPPER DESIGN

Problem 2.6. Design a plate-type sour-water stripper to remove NH_3 and H_2S down to level 20 ppmw and 5 ppmw respectively from a feed-stream of 45360 kg/h.

The stripper is to be hooked up with an OVHD (overhead) condenser and a partial reboiler heated by steam.

The liquid from the condenser is returned, as reflux, to the top tray via reflux drum (RD).

The RD operates at 357.44K/187.485 kPa, abs. Here tail gas is separated from the condensate and sent to the sulfur recovery plant.

The stripped liquor (BTMS) exchanges heat with the feed in the feed preheater preheating the feed stream to 365.77 K with no evaporation.

Calculate the number of trays & compute tray-to-tray composition.

Data :

Feed composition : NH_3 0.556 wt% ; H_2S 0.73 wt%

Operating Pressure

Tower top : 206.785 kPa

Reboiler : 241.249 kPa

ΔP per theoretical tray = 3.101 kPa

Stripping steam rate = 4626.72 kg/h

BTMS temperature   = 399.12K

Solution : In order that we can use Beychok-Krevelen's correlations, we must be careful to convert temperature from K to °F & pressure from kPa to psi.

Step - (1) Feed Composition
Ammonia rate in feedstream.

$$F_{NH_3} = 45360 \left| \frac{kg}{h} \right| \cdot (0.556\%) = 252.2016 \text{ kg/h}$$

Hydrogen sulfide rate in feedstream.

$$F_{H_2S} = 45360 \left| \frac{kg}{h} \right| \cdot (0.73\%) = 331.128 \text{ kg/h}$$

Water rate in feedstream.

$$F_{H_2O} = 45360 - (252.2016 + 331.128) = 44776.67 \text{ kg/h}$$

Step - (2) Bottoms Composition
Effluent liquid contains 20 ppmw NH_3 & 5 ppmw H_2S.

$$\therefore \qquad \% \ NH_3 \text{ in the bottoms} = \frac{20}{10^6} \times 10^2 = 0.002\%$$

$$\text{and } \% \ H_2S \text{ in the bottoms} = \frac{5}{10^6} \times 10^2 = 0.0005\%$$

$\therefore$ NH_3 rate in the **BTMS**

$$B_{NH_3} = 0.002\% \times 44776.67 \text{ (kg/h)} = 0.895533 \text{ kg/h}$$

$\therefore$ H_2S rate in the **BTMS**

$$B_{H_2S} = 0.0005\% \times 44776.67 \text{ (kg/h)} = 0.223883 \text{ kg/h}$$

Step - (3) Partial Pressure of Water in BTMS
Use is to be made of Miles-Wilson Eqn. :

$$T = 7007/[14.465 - \ln p_{H_2O}] - 383$$

with T in °F & p in psi.
For **BTMS** : T= 399.12K = 259.023 °F

$$\therefore \qquad\qquad 259.023 = 7007/[14.465 - \ln p_{H_2O}] - 383$$

$$p_{H_2O} = 34.8505 \text{ psia.}$$

Step - (4) Water Rate in the BTMS
Total pressure at the tower bottom = reboiler pressure
$$= 241.249 \text{ kPa. abs.}$$
$$= 35 \text{ psia}$$

$$\therefore \qquad y_{H_2O} = p_{H_2O}/P_{BTMS} = 34.8505/35 = 0.9957285$$

$$\therefore \qquad H_2O \text{ rate in the } \textbf{BTMS}, \ B_{H_2O} = (44776.67 \text{ kg/h}) (0.995728) = 44585.409 \ \frac{kg}{h}$$

Step - (5) Components Rate in Tail Gas

$$TG_{NH_3} = F_{NH_3} - B_{NH_3} = 252.2016 - 0.895523 = 251.30606 \text{ kg/h}$$

$$TG_{H_2S} = F_{H_2S} - B_{H_2S} = 331.128 - 0.223883 = 330.90411 \text{ kg/h}$$
$$TG_{H_2O} = F_{H_2O} - B_{H_2O} = 44776.67 - 44585.409 = 191.261 \text{ kg/h}$$

Step - (6) Reflux Drum–TG Composition

$$\text{Moles } NH_3 = \frac{251.30606}{17} = 14.7827 \; ; \; y_{NH_3}\big|_{TG} = 0.420677$$

$$\text{Moles } H_2S = \frac{330.90411}{34} = 9.7324 \; ; \; y_{H_2S}\big|_{TG} = 0.27695$$

$$\text{Moles } H_2O \text{ vap} = \frac{191.261}{18} = 10.6256 \; ; \; y_{H_2O}\big|_{TG} = 0.30237$$

$$\text{Total} = 35.1407$$

Step - (7) Reflux Drum–Partial Pressures of Components

$P_{RD} = 187.485 \text{ kPa.abs.}$

$$\therefore \; p_{NH_3}\big|_{RD} = y_{NH_3}\big|_{RD} . P_{RD} = 0.42067 \,(187.485 \text{ kPa.abs.}) = 78.8693 \text{ kPa.abs.}$$

$$p_{H_2S}\big|_{RD} = y_{H_2S}\big|_{RD} . P_{RD} = 0.27695 \,(187.485 \text{ kPa.abs.}) = 51.9239 \text{ kPa.abs.}$$

$$p_{NH_3}\big|_{RD} = p_{H_2O}\big|_{RD} . P_{RD} = 0.30237 \,(187.485 \text{ kPa.abs.}) = 56.6898 \text{ kPa.abs.}$$

Step - (8) K & C at RD

$$\text{Reflux drum temp.} = 357.44K = 183.992 \approx 184°F$$

$$\therefore \qquad K = 121000/(1.016298)^{184} = 6178.859$$

$$\& \qquad C = \left|\frac{2.84 \times 10^{-7}}{6178.859}\right| [1.27]^{(184-32)^{0.648}} = 2.26068 \times 10^{-8}$$

Step - (9) RD Liquid Composition

$$p_{NH_3}\big|_{RD} = 78.8693 \text{ kPa. abs} = 11.44 \text{ psia}$$

$$p_{H_2S}\big|_{RD} = 51.9239 \text{ kPa. abs} = 7.53 \text{ psia}$$

$$S_{RD} = \left[\frac{p_{NH_3}\big|_{RD} . p_{H_2S}\big|_{RD}}{C}\right]^{\frac{1}{2}} \text{ppmw} = \left[\frac{11.44 \times 7.53}{2.26068 \times 10^{-8}}\right]^{\frac{1}{2}} = 61729.243 \text{ ppmw}$$

$$A_{RD} = K . \, p_{NH_3}\big|_{RD} + \frac{1}{2} S_{RD}.$$

$$= 6178.859 \,(11.44) + \frac{1}{2} \,(61729.243)$$

$$= 101\,550.76 \text{ ppmw}$$

Step - (10) Water Flowrate in RD

$$L_{RD} = \text{Stripping Steam Rate} - TG_{H_2O}$$
$$= 4626.72 - 191.261$$
$$= 4435.459 \text{ kg/h}$$

Step - (11) Flowrates of Reflux Components

$$L_{NH_3}\big|_{RD} = A_{RD}\left|\frac{L_{RD}}{10^6 - A_{RD} - S_{RD}}\right|$$

$$= 101550.76 \left|\frac{4435.459 \text{ kg/h}}{10^6 - 101550.76 - 61729.243}\right| = 538.3213 \text{ kg/h}$$

$$L_{H_2S}\big|_{RD} = S_{RD}\left|\frac{L_{RD}}{10^6 - A_{RD} - S_{RD}}\right|$$

$$= 61729.243 \left|\frac{4435.459 \text{ kg/h}}{10^6 - 101550.76 - 61729.243}\right| = 327.2271 \text{ kg/h}$$

Mass balance of water around RD yields

$$4626.72 = L_{RD} + 191.261$$
$$\therefore \qquad\qquad L_{RD} = 4435.459 \text{ kg/h}$$

Step - (12) Flowrates OVHDs

NH_3 rate in vapor phase from Tray-1

$$V_{NH_3,1} = L_{NH_3}\big|_{RD} + TG_{NH_3}$$
$$= 538.3213 + 251.30606$$
$$= 789.6273 \text{ kg/h}$$

H_2S rate in vapor phase from Tray-1

$$V_{H_2S,1} = L_{H_2S}\big|_{RD} + TG_{H_2S}$$
$$= 327.2271 + 330.90411$$
$$= 658.1312 \text{ kg/h}$$

H_2O rate in vapor phase from Tray-1

$$V_{H_2O,1} = \text{Stripping steam rate}$$
$$= 4626.72 \text{ kg/h}$$

Molar Flowrates of OVHDs

Ammonia : $V_{NH_3,1}/17 = 789.6273/17 = 46.4486 \text{ kmol/h}$

Hydrogen sulfide : $V_{H_2S,1}/34 = 658.1312/34 = 19.3568 \text{ kmol/h}$

Water vapor : $V_{H_2O,1}/18 = 4626.72/18 = 257.04 \text{ kmol/h}$

Step - (13) Partial Pressures of OVHDs

Mole fraction of individual OVHD components :

$$y_{NH_3,1} = \frac{46.4486}{46.4486 + 19.3568 + 257.04} = 0.1438725$$

$$y_{H_2S,1} = \frac{19.3568}{46.4486 + 19.3568 + 257.04} = 0.0599568$$

$$y_{H_2O,1} = \frac{257.04}{46.4486 + 19.3568 + 257.04} = 0.7961705$$

$p_{NH_3,1} = y_{NH_3,1} \times P_1 = 0.1438725 \,(206.785 \text{ kPa. abs})= 29.7506 \text{ kPa. abs.}$
$p_{H_2S,1} = y_{H_2S,1} \times P_1 = 0.0599568 \,(206.785 \text{ kPa. abs})= 12.3981 \text{ kPa. abs.}$
$p_{H_2O,1} = y_{H_2O,1} \times P_1 = 0.7961705 \,(206.785 \text{ kPa. abs})= 164.6361 \text{ kPa. abs.}$

Step - (14) Tray-1 Temperature

$$P_{H_2O,1} = 164.6361 \text{ kPa. abs.} = 23.885 \text{ psia.}$$

$\therefore$ $\quad\quad\quad\quad T_1 = 7007/[14.465 - \ln 23.885] - 383 = 237.54°F \,(387.188K)$

Step - (15) K_1 & C_1 Values at Tray-1 Temperature

$$K_1 = 121 \times 10^3/(1.016298)^{237.54} = 2600.1606$$

$$C_1 = \left|\frac{2.84 \times 10^{-7}}{2600.1606}\right| [1.27]^{(237.54-32)^{0.648}} = 2.07043 \times 10^{-7}$$

Step - (16) H_2S and NH_3 Concentrations in Liquid Leaving Tray-1

$p_{NH_3,1} = 29.7506 \text{ kPa. abs.} = 4.31614 \text{ psia.}$
$p_{H_2S,1} = 12.3981 \text{ kPa. abs.} = 1.79868 \text{ psia.}$

$$S_1 = \left|\frac{p_{NH_3,1} \times p_{H_2S,1}}{C_1}\right|^{\frac{1}{2}}$$

$$= \left|\frac{4.31614 \times 1.79868}{2.07043 \times 10^{-7}}\right|^{\frac{1}{2}} = 6123.425 \text{ ppmw}$$

$$A_1 = K_1 \cdot p_{NH_3,1} + \frac{1}{2}S_1$$

$$= 2600.1606 \,(4.31614) + \frac{1}{2}(6123.425)$$

Step - (17) Ammonia and Hydrogen Sulfide Contents in Vapor Leaving Tray-2

$$V_{NH_3,2} = A_1 \left[\frac{L_1}{10^6 - A_1 - S_1}\right] - B_{NH_3}$$

where, L_1 = liquid flow from Tray-1

$$= F + L_{RD} + L_{NH_3,RD} + L_{H_2S,RD} + \text{Steam Condensed} - V_{NH_3,1} - V_{H_2S,1}$$

Now, the sensible heat absorbed by the Feed in heating from its entry temperature (365.77K) to the Tray-1 temperature (387.188K) :

$$\Delta H_{H_2O,1} = 44776.67 \left|\frac{kg}{h}\right| \times 4.187 \left|\frac{kJ}{kg.K}\right| \times (387.188 - 365.77) \text{ K} = 4015444.8 \frac{kJ}{h}$$

$$\Delta H_{NH_3(aq.),1} = 252.2016 \left|\frac{kg}{h}\right| \times \left(0.5 \times 4.187 \frac{kJ}{kg.K}\right) \times (387.188 - 365.77) \text{ K} = 11308.362 \frac{kJ}{h}$$

$$\Delta H_{H_2S(aq.),1} = 331.128 \left|\frac{kg}{h}\right| \times \left(0.2 \times 4.187 \frac{kJ}{kg.K}\right) \times (387.188 - 365.77) \text{ K} = 5938.9241\frac{kJ}{h}$$

$$\therefore \quad \Delta H_{feed, 1} = 4032692 \frac{kJ}{h}$$

Similarly, the sensible heat absorbed in heating the entering reflux from 357.44K to 387.188K:

$$\Delta H_{H_2O, RD} = 4435.459 \left|\frac{kg}{h}\right| \times 4.187 \left|\frac{kJ}{kg.K}\right| \times (387.188 - 357.44) \text{ K} = 552458.04 \left|\frac{kJ}{h}\right|$$

$$\Delta H_{NH_3(aq.),RD} = 538.3213 \left|\frac{kg}{h}\right| \times \left(0.5 \times 4.187 \frac{kJ}{kg.K}\right) \times (387.188 - 357.44) \text{ K} = 33525.271\frac{kJ}{h}$$

$$\Delta H_{H_2S(aq.),RD} = 327.2271 \left|\frac{kg}{h}\right| \times \left(0.2 \times 4.187 \frac{kJ}{kg.K}\right) \times (387.188 - 357.44) \text{ K} = 8151.5461\frac{kJ}{h}$$

$$\therefore \quad \Delta H_{RD, 1} = 594134.85 \frac{kJ}{h}$$

Now, heat required to vaporize all the H_2S from Tray-1

$$\Delta H_{H_2S} = (331.128 + 327.2271) \frac{kg}{h} \times \left(465.2 \frac{kJ}{kg}\right) = 306266.79 \frac{kJ}{h}$$

$\therefore$ Total heat absorbed on Tray-1

$$= 5383588.9 \frac{kJ}{h}$$

The mean latent heat for steam $= 2209.7 \frac{kJ}{kg}$

$$\therefore \textbf{Steam condensed on Tray-1} = \frac{5383588.9 \text{ kJ/h}}{2209.7 \text{ kJ/kg}} = 2436.3438 \frac{kJ}{h}$$

$\therefore$

$$L_1 = 45360 + 4435.459 + 538.3213 + 327.2271 + 2436.3438 -$$
$$789.6273 - 658.1312$$
$$= 51649.592 \text{ kg/h (113865.94 lb/h)}$$

$$V_{NH_3,2} = 14284.369 \left|\frac{113865.94}{10^6 - 14284.369 - 6123.425}\right| - \frac{0.895533}{0.4536}$$

$$= 1658.4136 \text{ lb/h (752.2564 kg/h)}$$

$$V_{H_2S,2} = S_1 \left|\frac{L_1}{10^6 - A_1 - S_1}\right| - B_{NH_3}$$

$$= 6123.425 \left|\frac{113865.94}{10^6 - 14284.369 - 6123.425}\right| - \frac{0.223883}{0.4536}$$

$$= 711.2817 \text{ lb/h (322.6373 kg/h)}$$

$V_{H_2O,2}$ = Stripping steam rate + Steam condensate from Tray-1

$$= 4626.72 + 2436.3438$$
$$= 7063.0638 \text{ kg/h}$$

Step - (18) Molar Flowrates of Vapors from Tray-2

Ammonia : $V_{NH_3,2}/17 = 752.2564/11{,}0115jjjjj7 \quad = 44.25037 \text{ kmol/h}$

Hydrogen sulfide : $V_{H_2S,2}/34 = 322.6373/34 \quad = 9.48933 \text{ kmol/h}$

Water vapor : $V_{H_2O,2}/18 = 7063.0638/18 \quad = 392.3924 \text{ kmol/h}$

$$\Sigma = 446.1321 \text{ kmol/h}$$

$$y_{NH_3,2} = (44.25037/446.1321) = 0.099186$$

$$y_{H_2S,2} = (9.48933/446.1321) = 0.021270$$

$$y_{H_2O,2} = (392.3924/446.1321) = 0.88178$$

$$P_2 = P_1 + \Delta P \text{ per tray} = 206.785 + 3.101 = 209.886 \text{ kPa. abs.}$$
$$p_{NH_3,2} = y_{NH_3,2} \times P_2 = 20.81775 \text{ kPa. abs.}$$
$$p_{H_2S,2} = y_{H_2S,2} \times P_2 = 4.46427 \text{ kPa. abs.}$$
$$p_{H_2O,2} = y_{H_2O,2} \times P_2 = 185.07327 \text{ kPa. abs.}$$

Step - (19) Temperature of Liquid on Tray-2

$$p_{H_2O,2} = 185.07327 \text{ kPa. abs.} = 26.85 \text{ psia.}$$
$$T_2 = 7007/[14.465 - \ln 26.85] - 383 = 244.039°F \ (390.7997K)$$

Step - (20) K_2 & C_2 Values at Tray-2 Temperature

$$K_2 = 121 \times 10^3/(1.016298)^{244.039} = 2340.8319$$

$$C_2 = \left|\frac{2.84 \times 10^{-7}}{2340.8319}\right| [1.27]^{(244.039 - 32)^{0.648}} = 2.65352 \times 10^{-7}$$

Step - (21) H_2S & NH_3 Concentrations

$$p_{NH_3,2} = 20.81775 \text{ kPa. abs.} = 3.02019 \text{ psia.}$$

$$p_{H_2S,2} = 4.46424 \text{ kPa. abs.} = 0.64766 \text{ psia.}$$

$$S_2 = \left|\frac{3.02019 \times 0.64766}{2.6535 \times 10^{-7}}\right|^{\frac{1}{2}} = 2715.0705 \text{ ppmw}$$

$$A_2 = K_2 \cdot p_{NH_3,2} + \frac{1}{2}S_2$$

$$= 2340.8319 + \frac{1}{2}(2715.0705)$$

$$= 8427.2933 \text{ ppmw}$$

Calculations thus proceeded from Tray-to-Tray.

Total number of Trays = 12

Compositions on last two trays are presented below :

Parameters		Tray-11	Tray-12
$L_{H_2O,(n-1)}$	Liq H_2O rate from Tray-(n-1)	52821.883 kg/h	52867.96 kg/h
$V_{NH_3,n}$	NH_3 vap leaving Tray-n	0.3810 kg/h	– 0.70308 kg/h
$V_{H_2S,n}$	H_2S vap leaving Tray-n	0.08618 kg/h	– 0.18144 kg/h
$V_{H_2O,n}$	H_2O vap leaving Tray-n	8236.437 kg/h	8282.513 kg/h
P_n.	Total press. on Tray-n	237.803 kPa. abs.	240.905 kPa. abs.
$P_{NH_3,n}$	Partial press. of NH_3 above Tray-n	0.011641 kPa. abs.	– 21.712 kPa. abs.
$P_{H_2S,n}$	Partial press. of H_2S above Tray-n	0.00131 kPa. abs.	– 27.640 kPa. abs.
$P_{H_2O,n}$	Partial press. of H_2O above Tray-n	237.7896 kPa. abs.	240.905 kPa. abs.
T_n	Temp. of liquid on Tray-n	398.79 K	399.22 K
A_n	Ammonia in liq leaving Tray-n	3.54 ppmw	– 4.95 ppmw
S_n	Hydrogen sulfide in liq leaving Tray-n	0.82 ppmw	1.62 ppmw

2.8.1. SOUR GAS SCRUBBER DESIGN BY CHARTS

Water is the cheapest & the most frequently used solvent to remove, by way of absorption., ammonia, hydrogen sulfide and carbon dioxide from gas streams.

To design a GAS SCRUBBER, use can be made of following charts **(Fig.2.8.1-1-2.8.1-8)** to identify the equilibria of ammonia and hydrogen sulfide between the gas stream and the washwater.

The require phase equilibria data must account for many simultaneous chemical reactions:

$$CO_2 + H_2O + \longleftrightarrow + HCO_3^{\ominus} + \overset{\oplus}{H}$$

$$HCO_3^- \longleftrightarrow + CO_3^{2-} + \overset{+}{H}$$

$$NH_3 + \overset{+}{H} \longleftrightarrow \overset{+}{N}H_4$$

$$NH_3 + HCO_3^- \longleftrightarrow NH_2CO_2^- + H_2O$$

$$H_3S \longleftrightarrow HS^- + \overset{+}{H}$$

$$HS^- \longleftrightarrow S^{2-} + \overset{+}{H}$$

$$H_2O \longleftrightarrow \overset{+}{H} + \overline{O}H$$
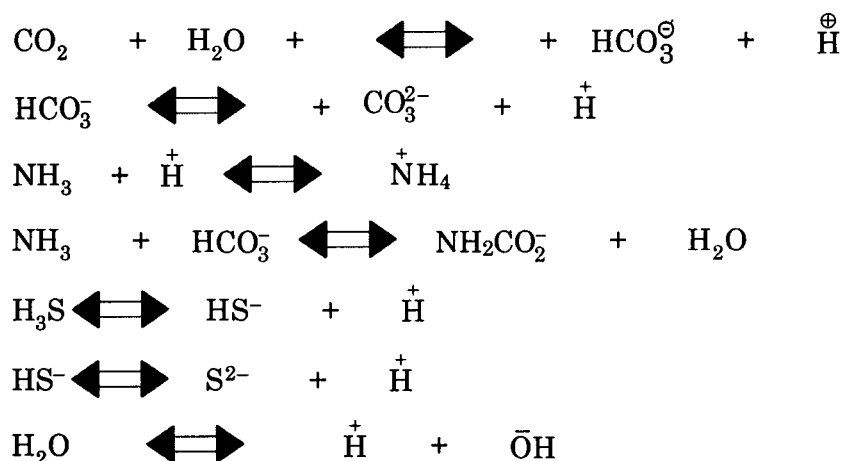
Design Limitation

1. The system is complicated. It is necessary to contend with both chemical and phase equilibria in establishing the design.

2. Each of the reactions and Henry's Law constants are not only temperature dependent, but are also functions of the type and concentration of components in solution and in some cases,

the ionic strength of the solution. Only those portions of ammonia, hydrogen sulfide and carbon dioxide that remain as discrete molecules than ionic form in solution can be stripped from the liquid phase.

NH₃ in solution, ppm wt.
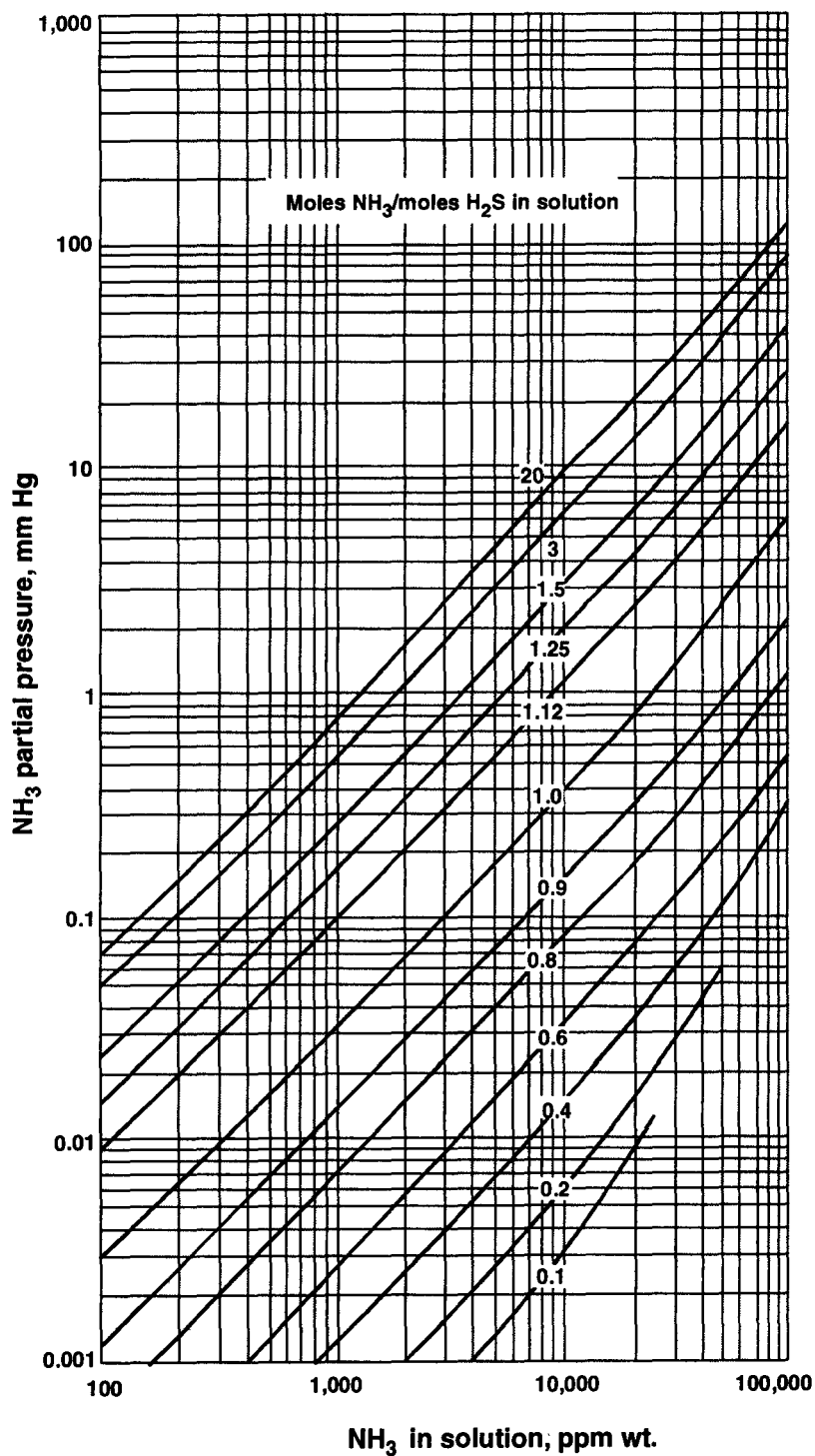
Fig. 2.8.1.1. *Ammonia equilibria at 80°F.*

Source: Hydrocarbon Processing, September 1991

© GULF PUBLISHING CO., HOUSTON, TX 77252-2608, USA.
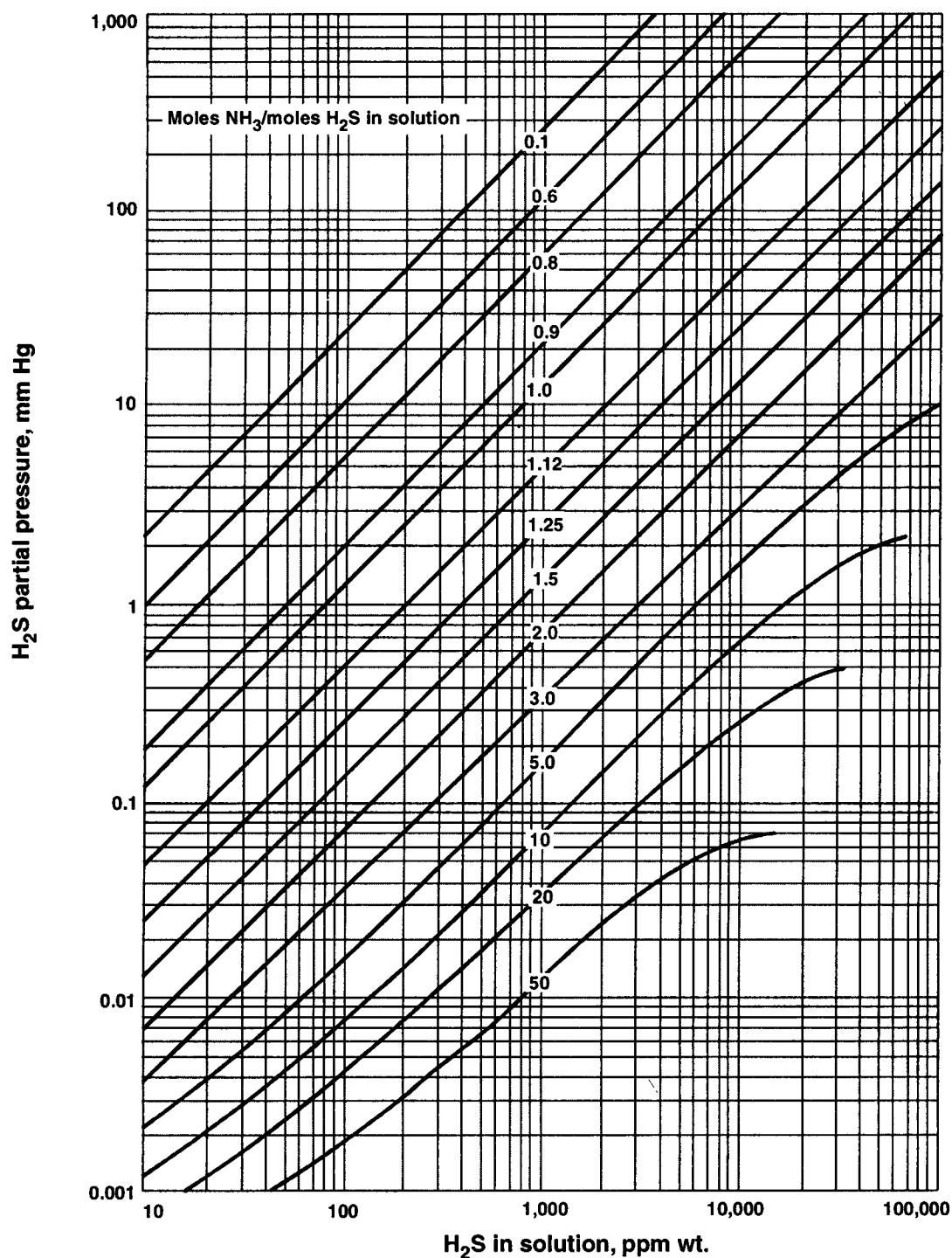
Fig.2.8.1.2. Hydrogen sulfide equilibria at 80°F.

Source : Hydrocarbon Processing, September 1991
© GULF PUBLISHING CO., HOUSTON, TX 77252-2608, USA.
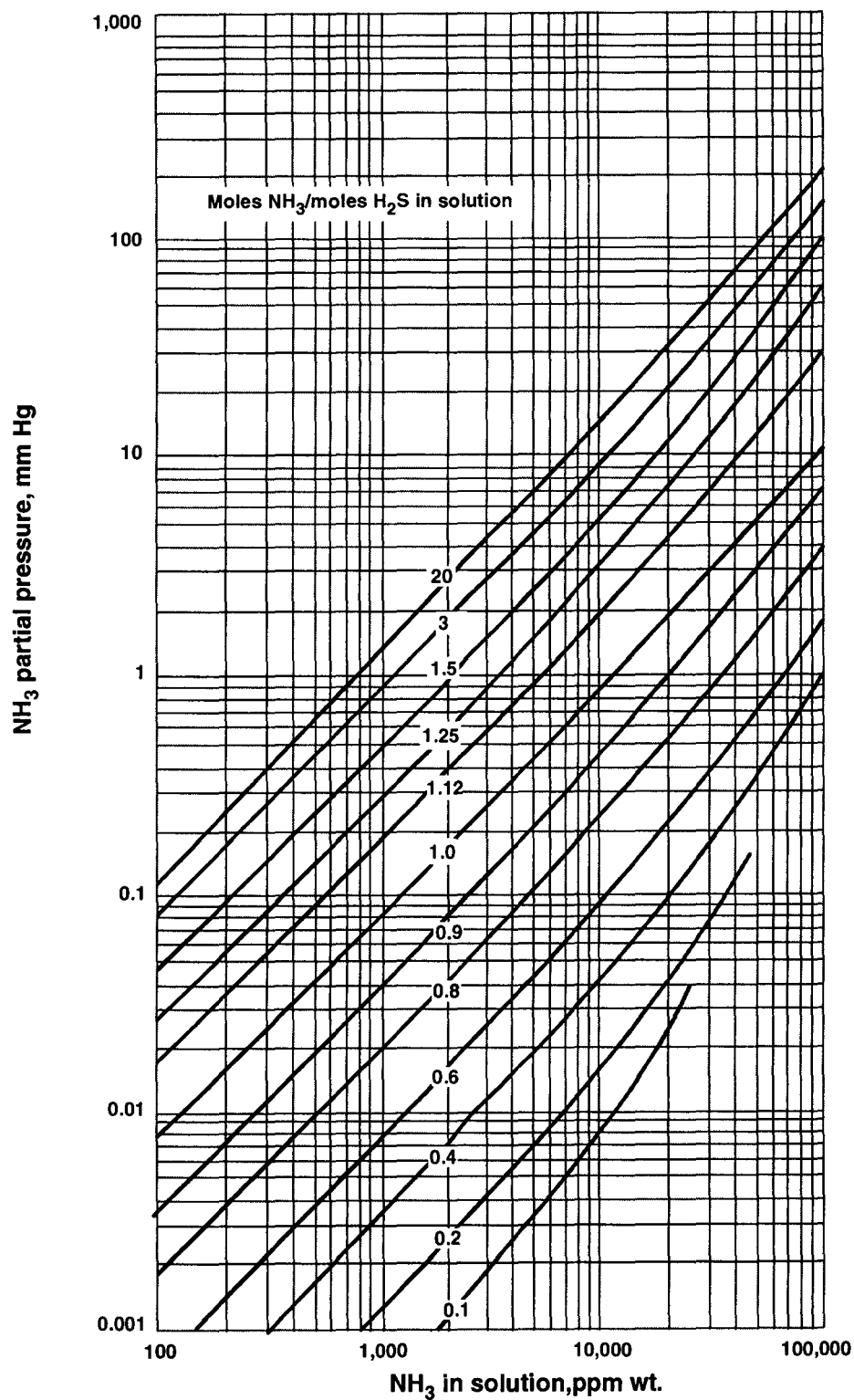
Fig. 2.8.1.3. *Ammonia equilibria at 100° F.*

Source: **Hydrocarbon Processing,** September 1991

© GULF PUBLISHING CO., HOUSTON, TX 77252-2608, USA
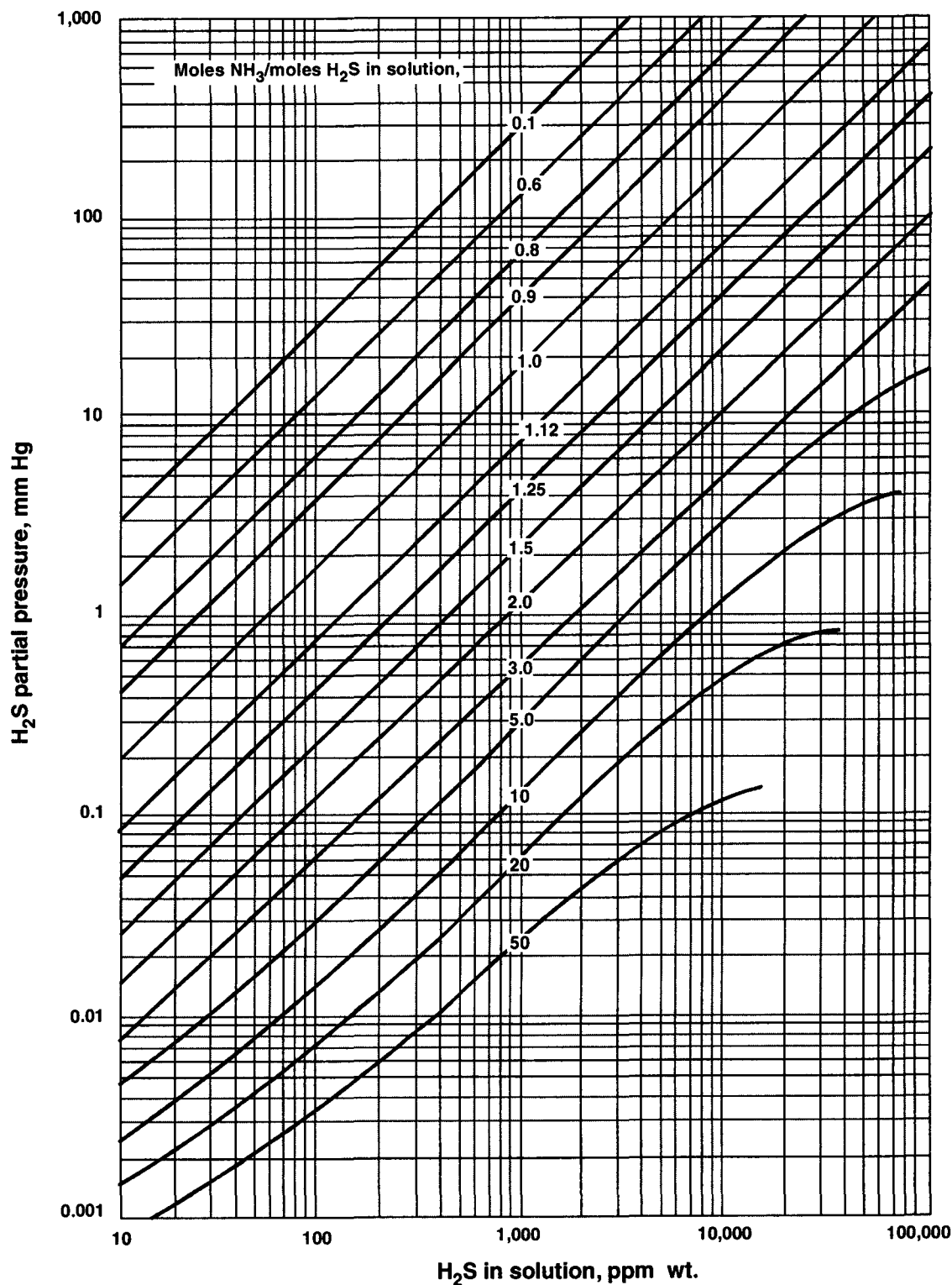
Fig.2.8.1.4. *Hydrogen sulfide equilibria at 100°F.*

Source : Hydrocarbon Processing, September 1991.

© GULF PUBLISHING CO., HOUSTON, TX 77252-2608, USA.
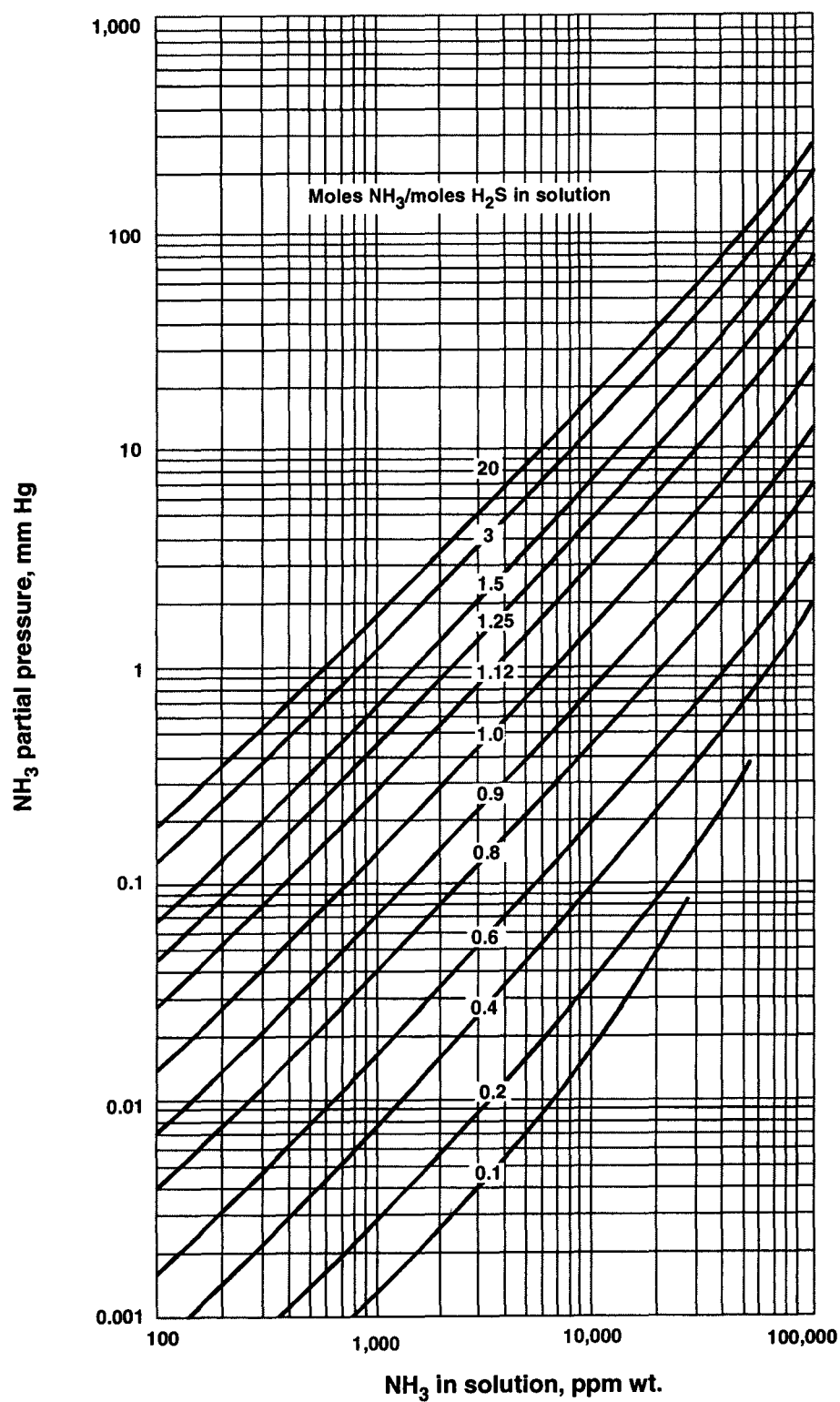
Fig. 2.8.1.5. *Ammonia equilibria at 120°F.*

Source : **Hydrocarbon Processing,** September 1991

© GULF PUBLISHING CO., HOUSTON, TX 77252-2608, USA
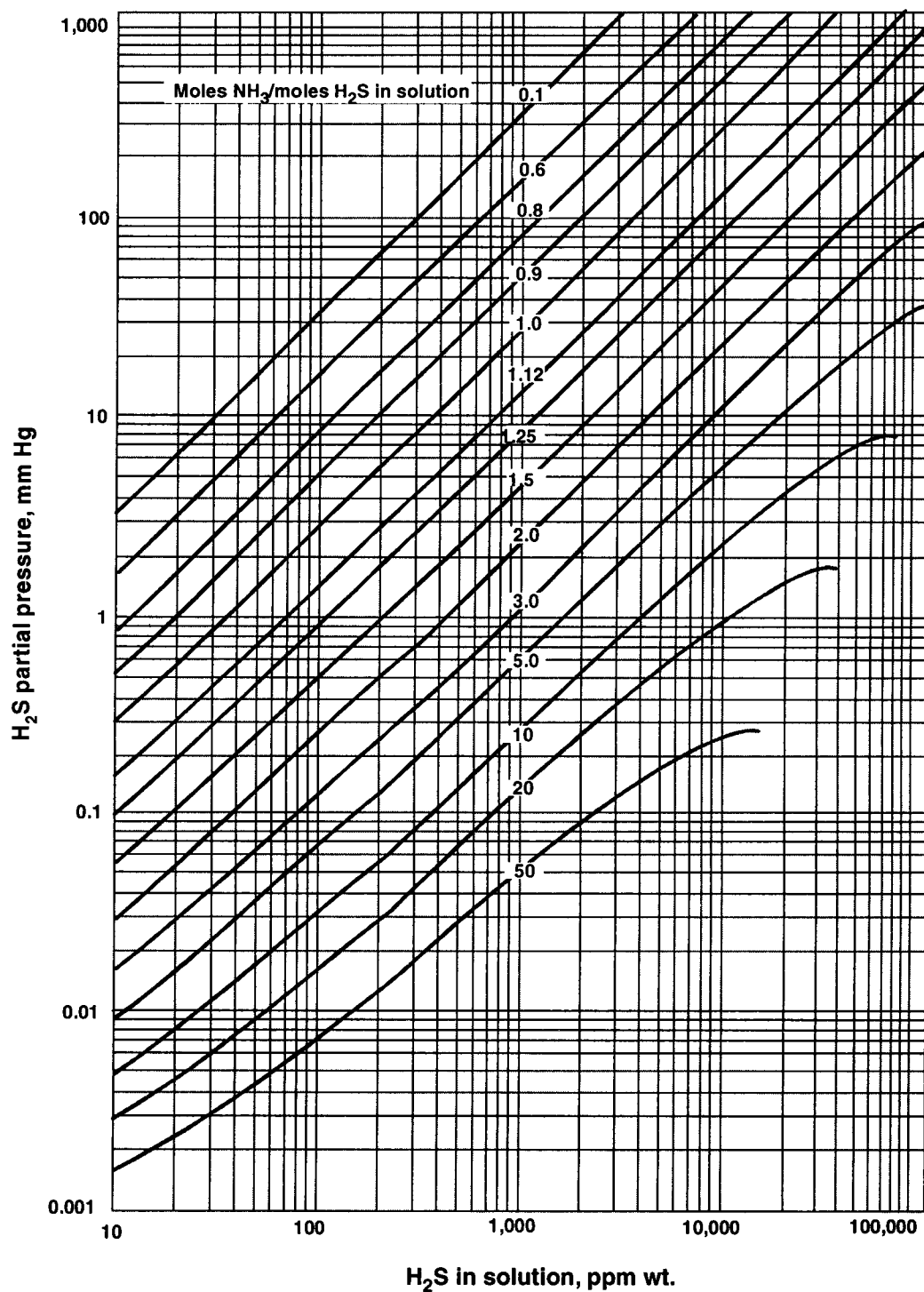
Fig, 2.8.1.6. *Hydrogen Sulfide Equilibria at 120°F.*

Source : **Hydrocarbon Processing,** September 1991

© GULF PUBLISHING CO., HOUSTON, TX 77252-2608, USA
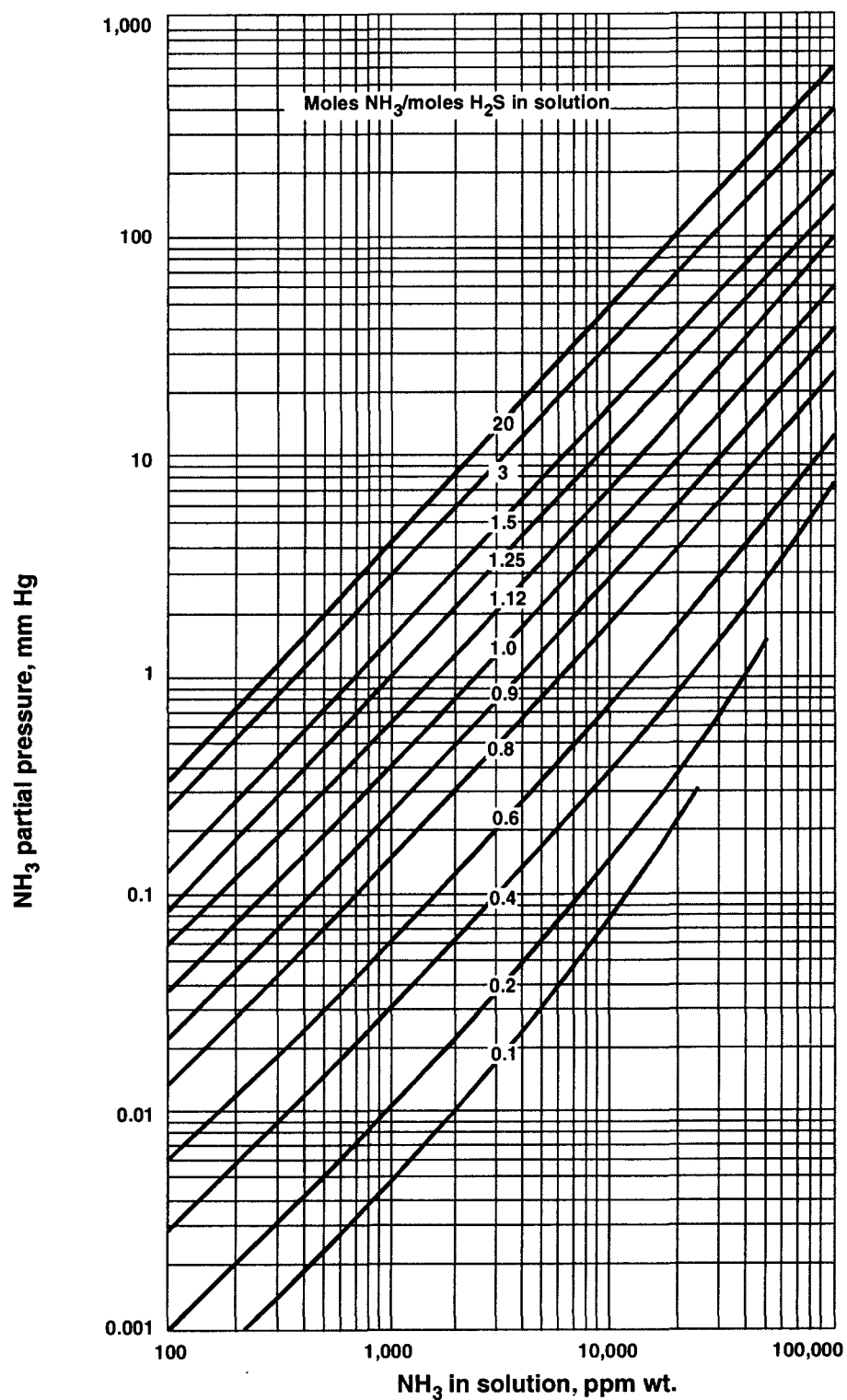
Fig. 2.8.1.7. *Ammonia equilibria at 150°F.*

Source : **Hydrocarbon Processing**, September 1991.
© GULF PUBLISHING CO., HOUSTON, TX 77252-2608, USA.
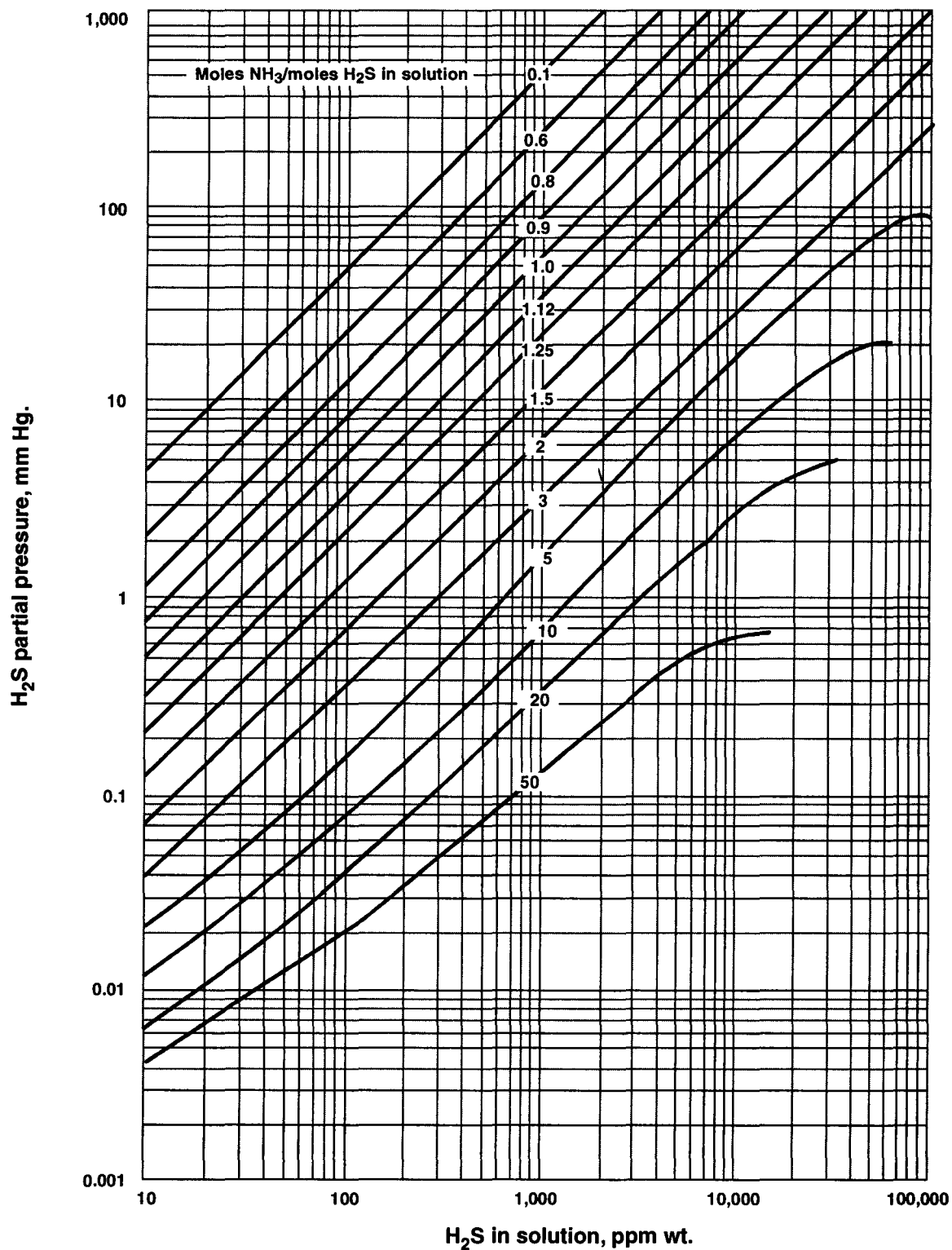
Fig. 2.8.1.8. *Hydrogen sulfide equilibria at 150°F*

Example Calculation : A sour gas scrubber is to be designed to absorb NH₃ and H₂S from a gas stream under following operating conditions.

Operating Conditions :

p_{NH_3} : *6 mm Hg*

p_{H_2S} : *6 mm Hg*

Temperature : 100°F

Solution: A trial-&-error method is adopted. The equilibrium concentrations of the NH_3 and H_2S in the aqueous phase are obtained by harnessing **Fig. 2.8.1.3** and **2.8.1.4** (Curves for 100°F).

Assumed NH₃/H₂S (molar)	NH₃ ppmw (Fig. 2.8.1-3)	H₂S ppmw (Fig. 2.8.1-4)	Calculated NH₃/H₂S	
			Wt.	Molar
1.5	13500	2800	4.71	9.4
2.0	9100	5500	1.65	3.3
2.3	8100	7000	1.16	2.3
3.0	6700	11000	0.61	1.2

Read out the ppmw of NH_3 and H_2S for several assumed molar ratios of NH_3/ H_2S in aqueous phase and for the given gaseous partial pressures, (expressed in mm Hg). Repeat until the calculated molar ratios of NH_3/ H_2S in aq. system tallies with the assumed value.

2.8.2. SOUR WATER STRIPPER DESIGN BY CHARTS

Having established the equilibria conditions associated with a gas scrubber to remove ammonia, hydrogen sulfide & carbon dioxide, the next step is to define the equilibria associated with stripping the ammonia and hydrogen sulfide from the sour water so it can be safely discarded without violating environmental regulations.

Sour water stripper operates at higher temperature and lower pressure than do sour gas scrubbers. Pressure than do sour gas scrubbers. Presented here is a set of charts (**Fig.2.8.2.1** thru **2.8.2.10**) for sour water stripper for the temperature range from 200°F to 280°F.

Example Calculation : Estimate the partial pressures of NH₃ & H₂S in outlet gas of a sour water stripper with following operating conditions.

Operating Conditions :

NH_3 in stripper effluent water :100 ppmw max

H_2S in stripper effluent water : 20 ppmw max

Stripper effluent water temperature : 220°F

NH_3/H_2S in stripper effluent water : 5 (wt. ratio)

NH_3/H_2S mole ratio in stripper effluent water :10

Solution : The maximum concentrations of the NH_3 and H_2S in the stripper gas are obtained from **Figs. 2.8.2.3** and **2.8.2.4** (curves for 220°F). Inasmuch as the outlet water (stripper effluent) concentrations are given, gas phase partial pressures can be read directly from the charts :

p_{NH_3} in stripper exit gas stream : 1.1 mm Hg (max) **(Fig. 2.8.2.3)**.

p_{H_2S} in stripper exit gas stream : 0.06 mm Hg (max) **(Fig..2.8.2.4)**.

Moles NH₃/moles H₂S

NH₃ partial pressure, mm Hg

NH₃ in solution, ppm wt.
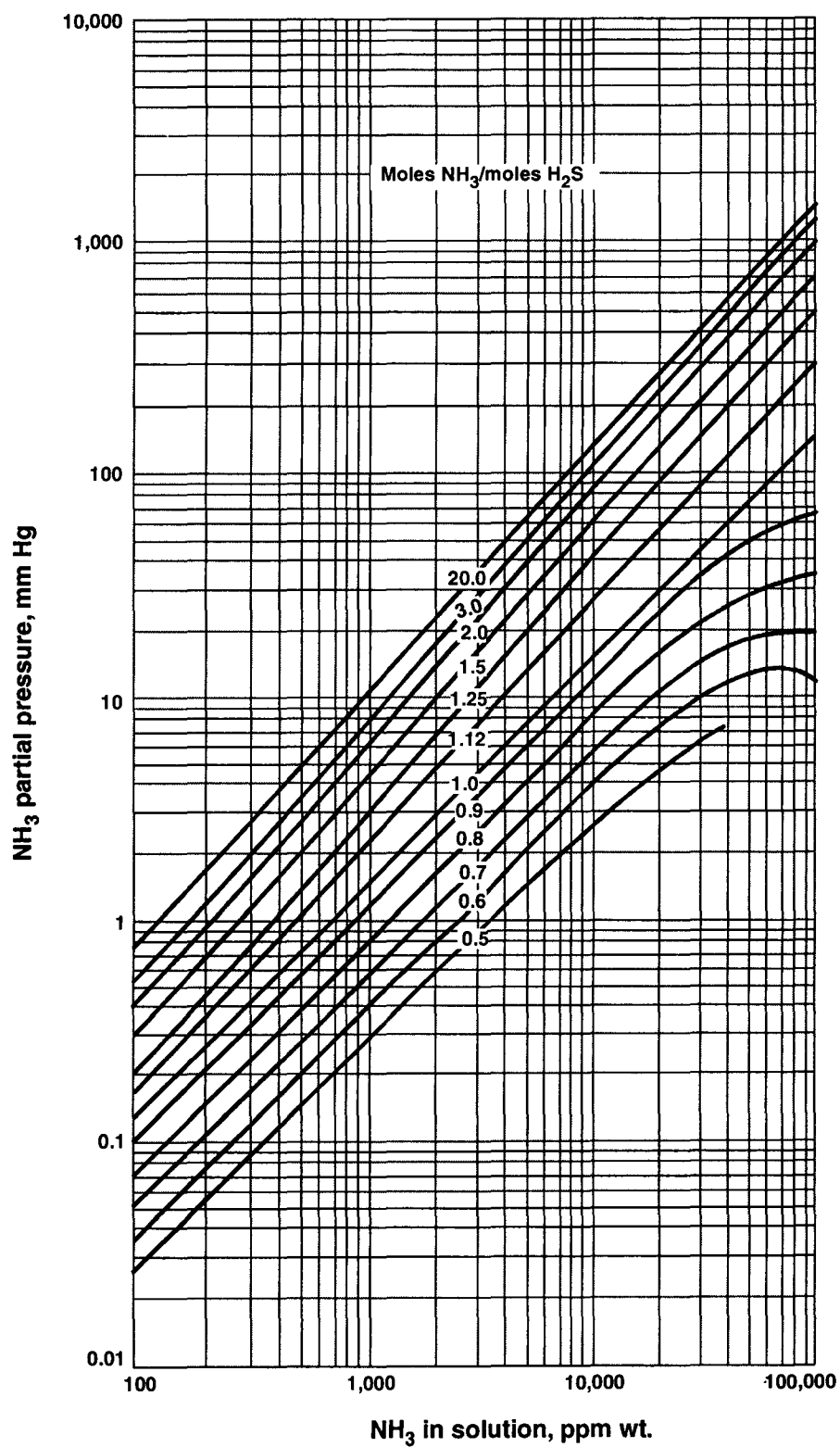
Fig. 2.8.2.1. *Ammonia equilibria at 200°F.*

Source : Hydrocarbon Processing, October 1991

© GULF PUBLISHING CO., HOUSTON, TX 77252-2608
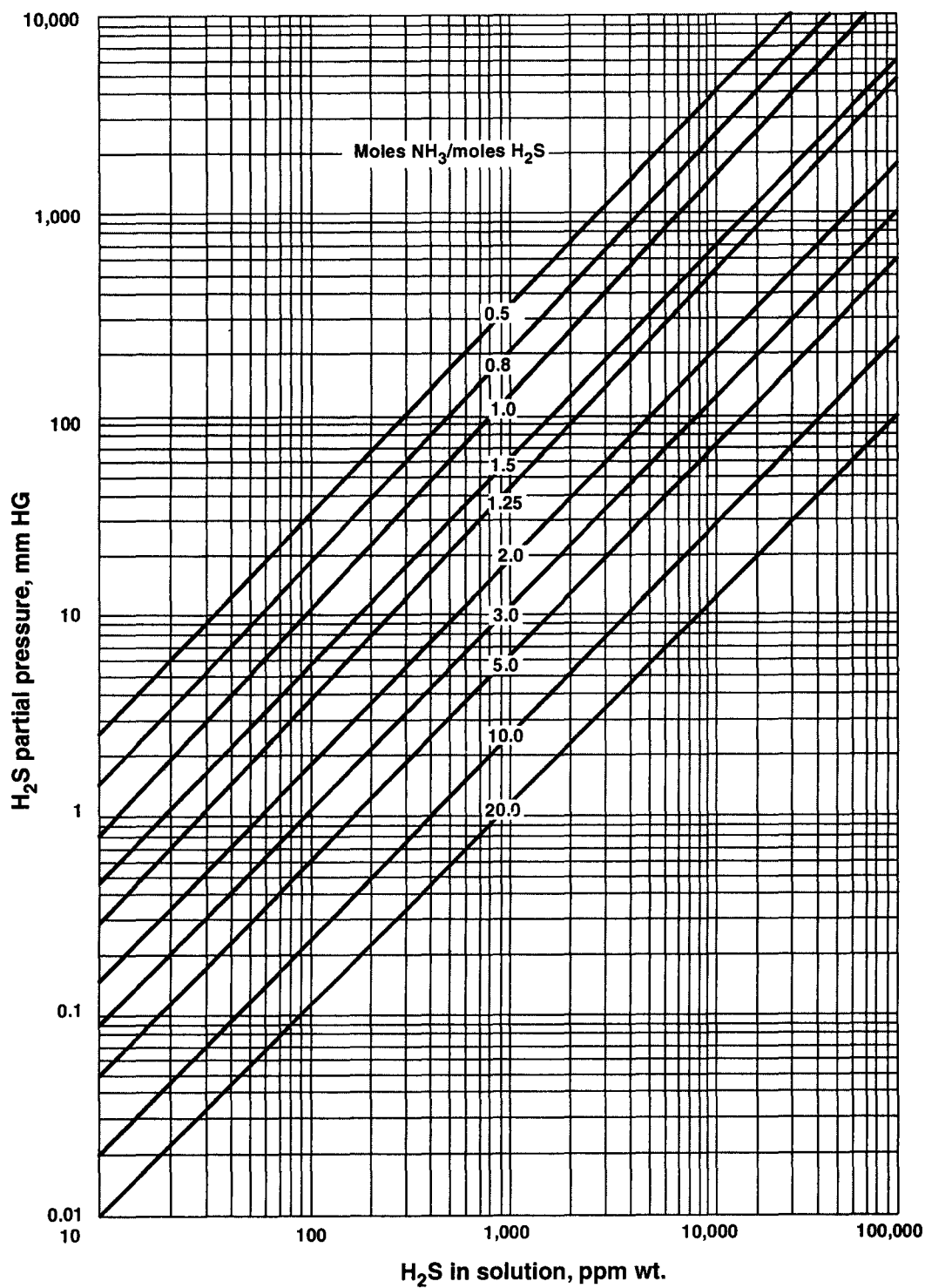
Fig. 2.8.2.2. *Hydrogen sulfide equilibria at 200°F.*
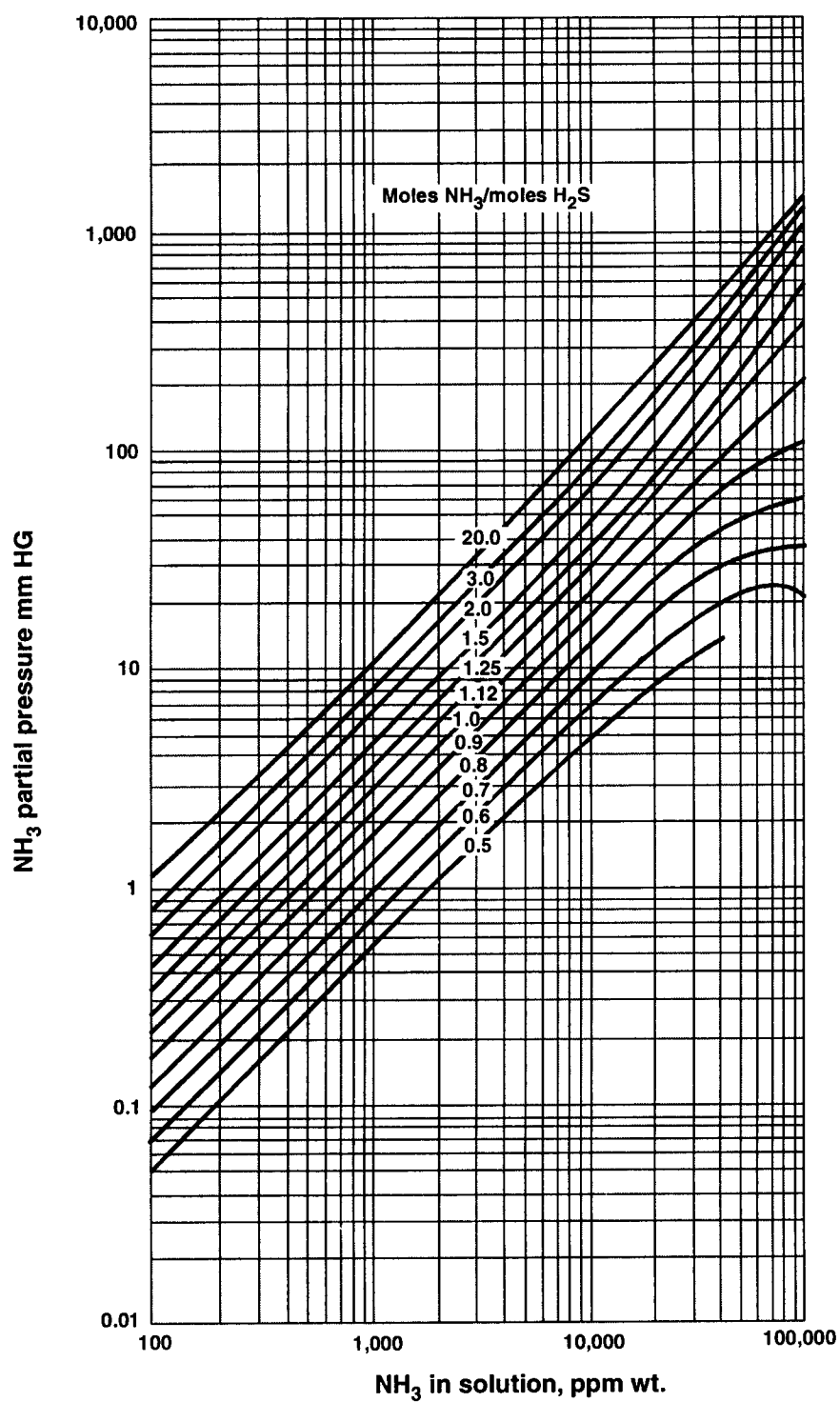
Fig. 2.8.2.3. *Ammonia equilibria at 220°F.*

Source : Hydrocarbon Processing, October 1991

© GULF PUBLISHING CO., HOUSTON, TX 77252-2608
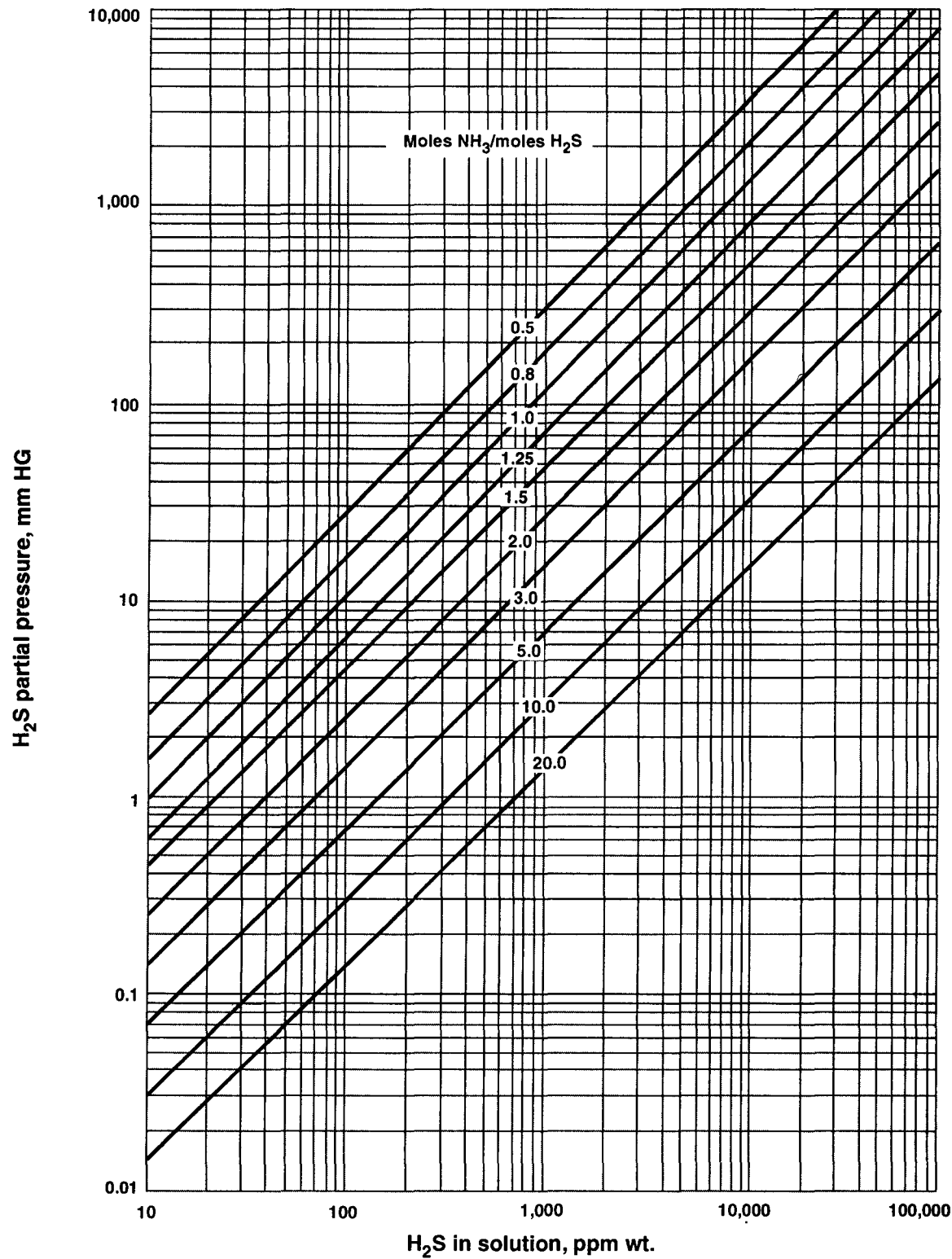
Fig. 2.8.2.4. *Hydrogen sulfide equilibria at 220°F.*

Source : **Hydrocarbon Processing**, October 1991

© GULF PUBLISHING CO., HOUSTON, TX 77252-2608
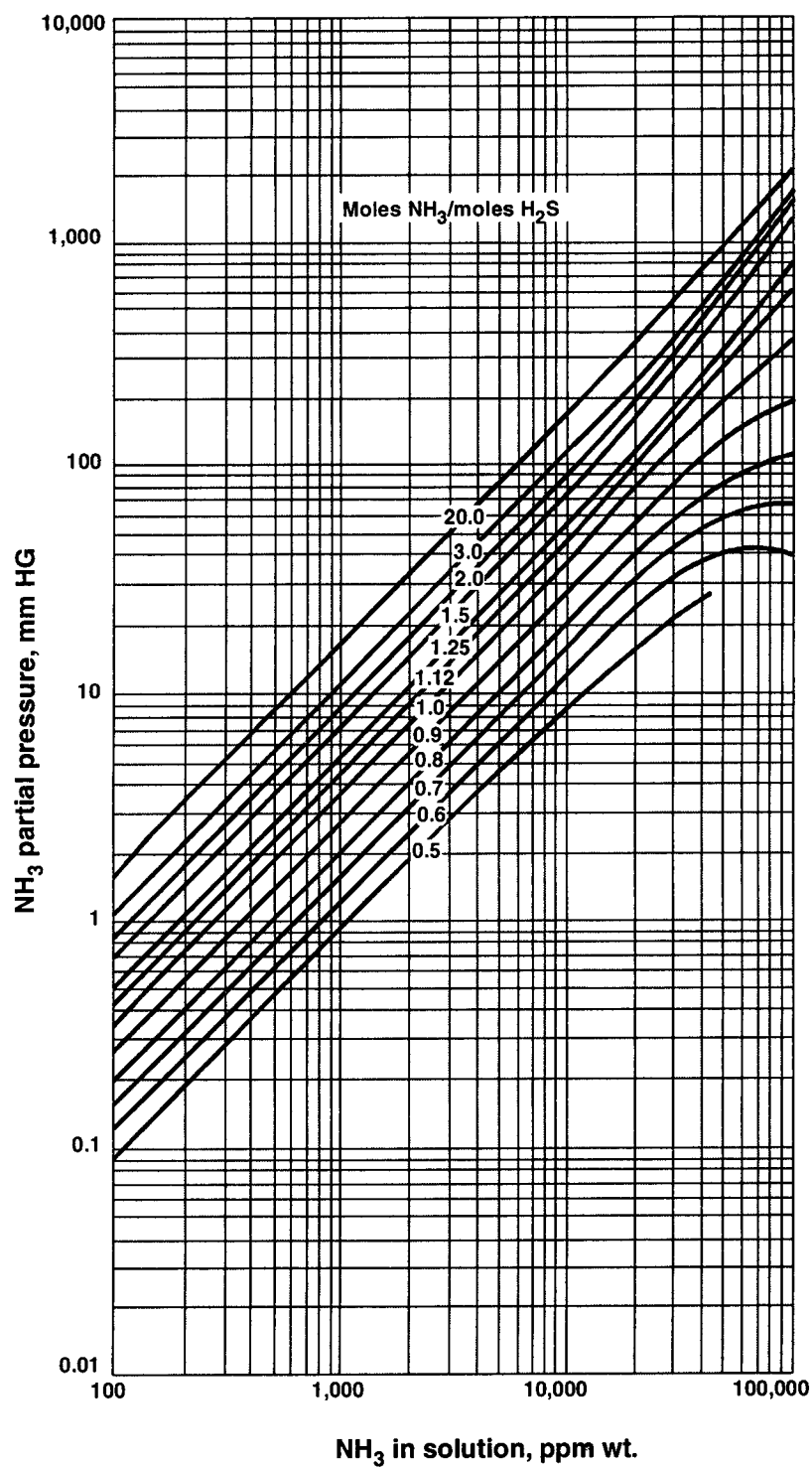
Fig. 2.8.2.5. *Ammonia equilibria at 240°F.*

Source : **Hydrocarbon Processing**, October 1991
© GULF PUBLISHING CO., HOUSTON, TX 77252-2608
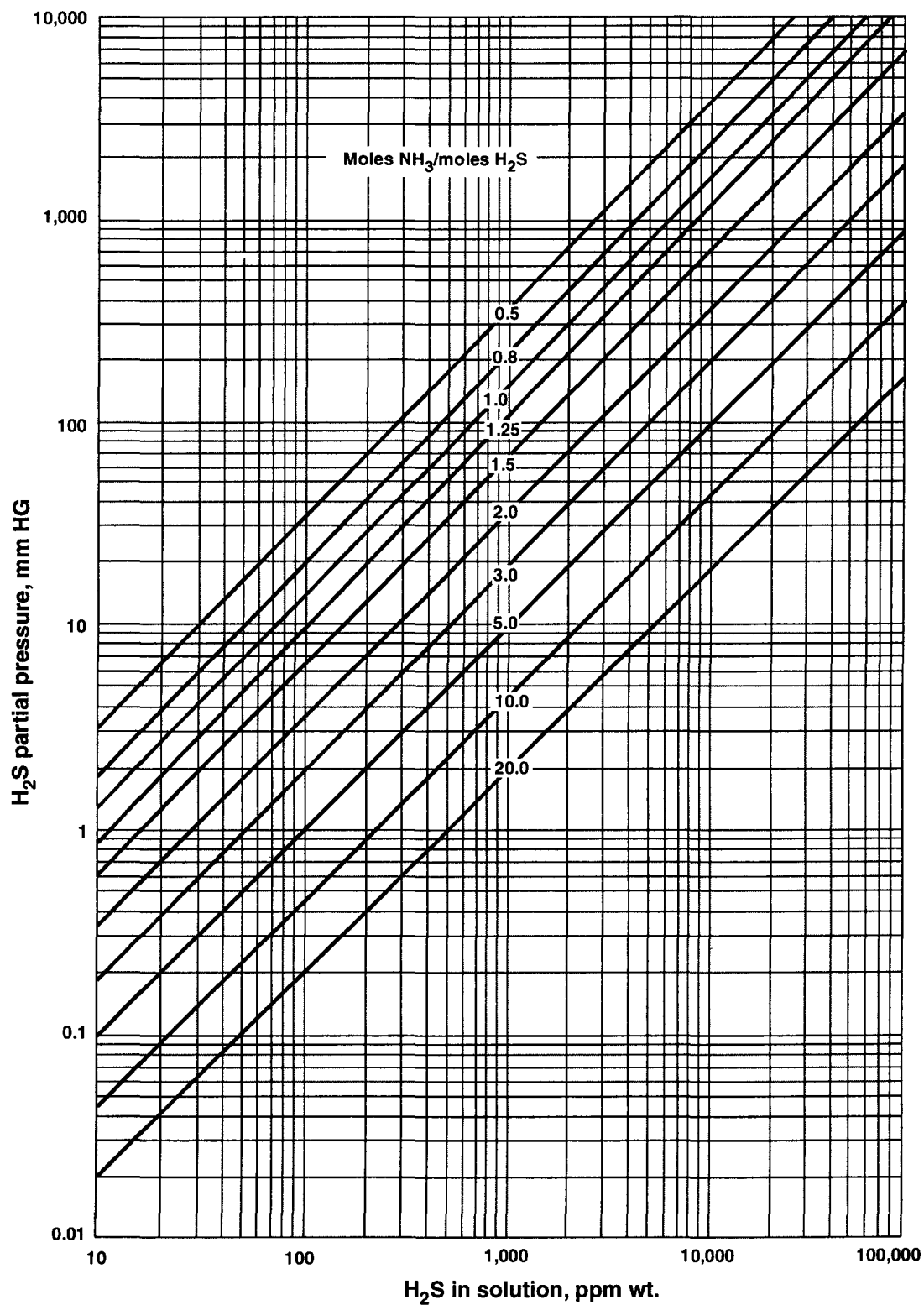
Fig. 2.8.2.6. *Hydrogen sulfide equilibria at 240°F.*

Source : **Hydrocarbon Processing,** October 1991

© GULF PUBLISHING CO., HOUSTON, TX 77252-2608
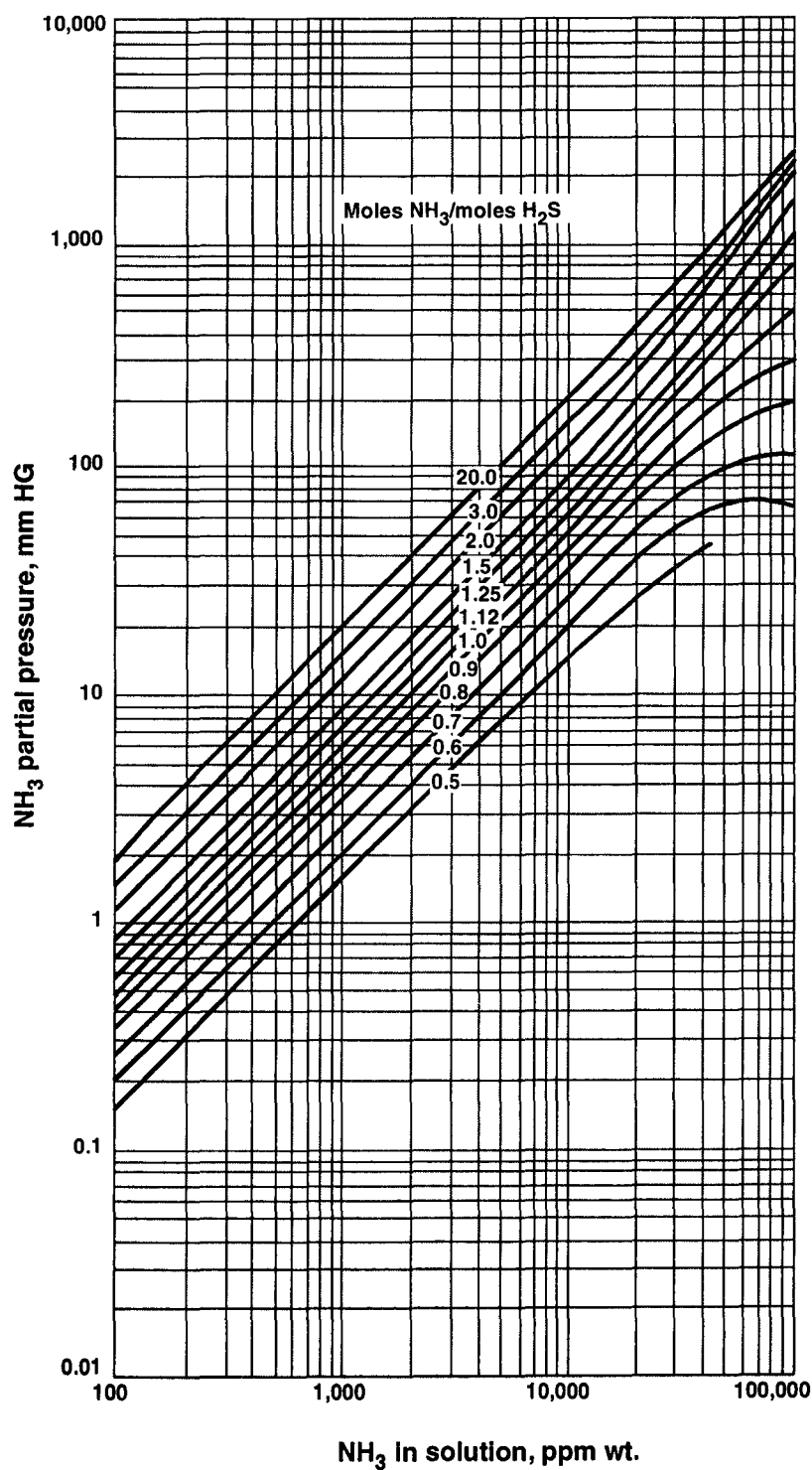
Fig. 2.8.2.7. *Ammonia equilibria at 260°F.*

Source : **Hydrocarbon Processing,** October 1991
© GULF PUBLISHING CO., HOUSTON, TX 77252-2608
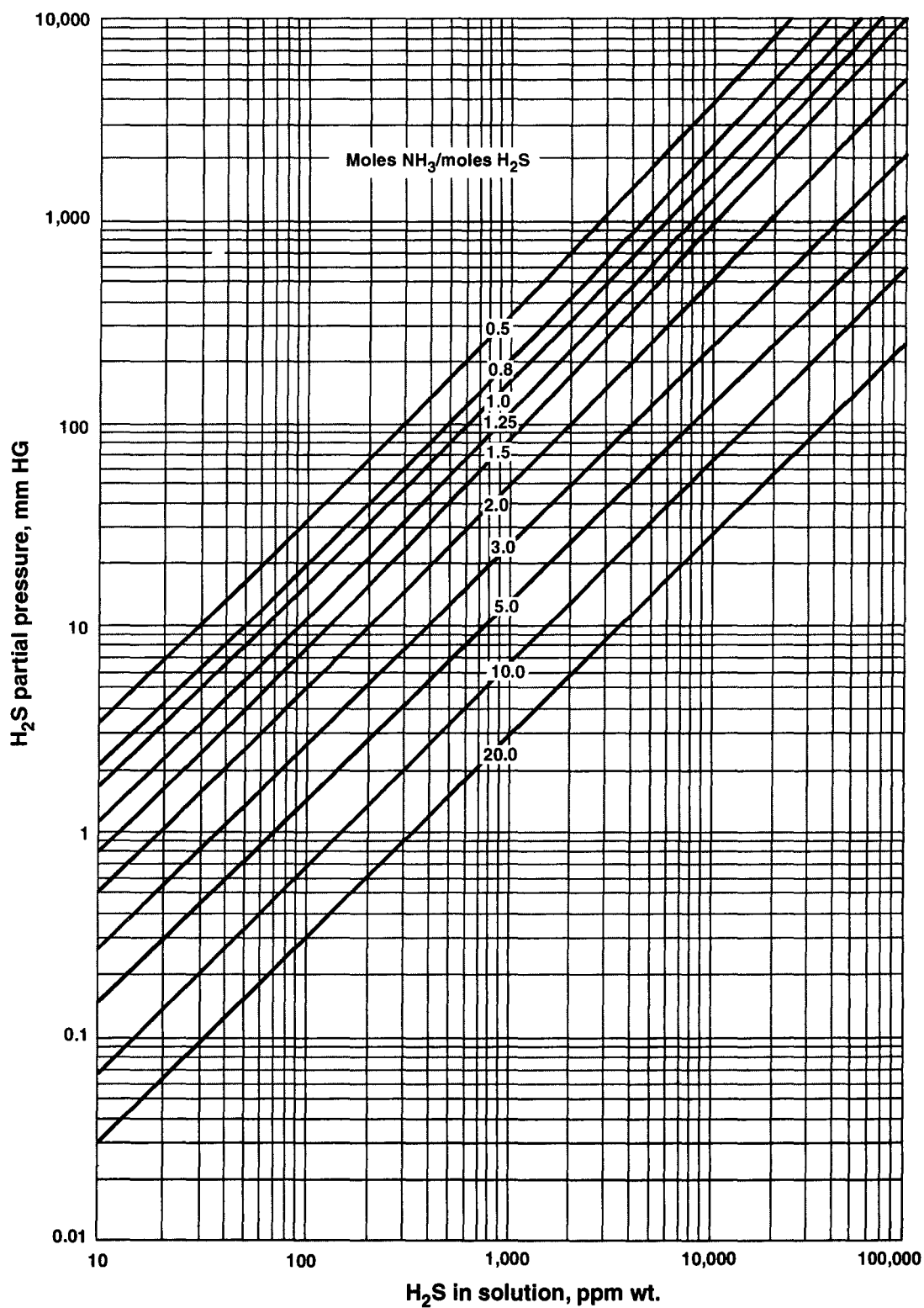
Fig. 2.8.2.8. *Hydrogen sulfide equilibria at 260°F.*

Source : Hydrocarbon Processing, October 1991

© GULF PUBLISHING CO., HOUSTON, TX 77252-2608
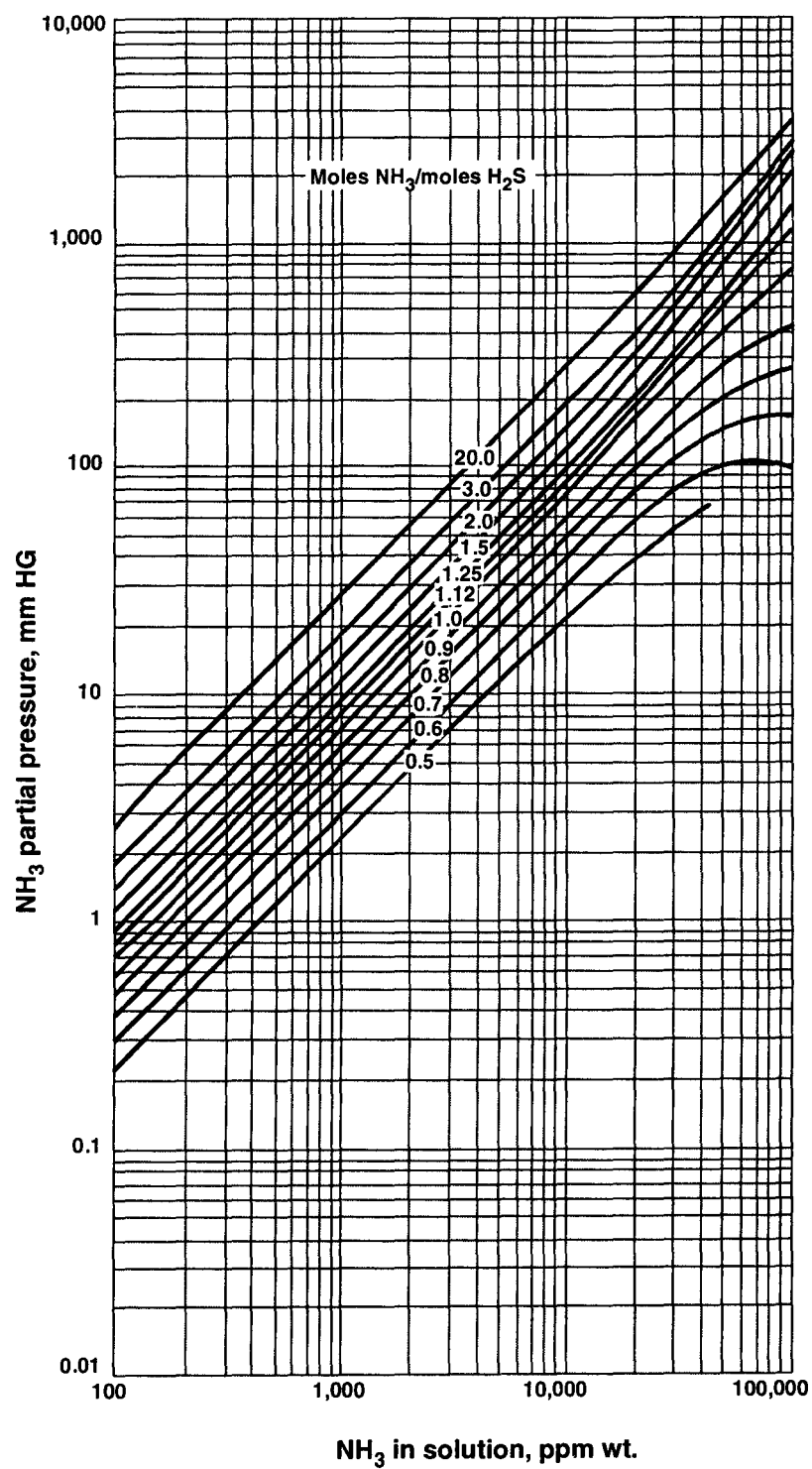
Fig. 2.8.2.9. *Ammonia equilibria at 280°F.*

Source : Hydrocarbon Processing, October 1991

© GULF PUBLISHING CO., HOUSTON, TX 77252-2608
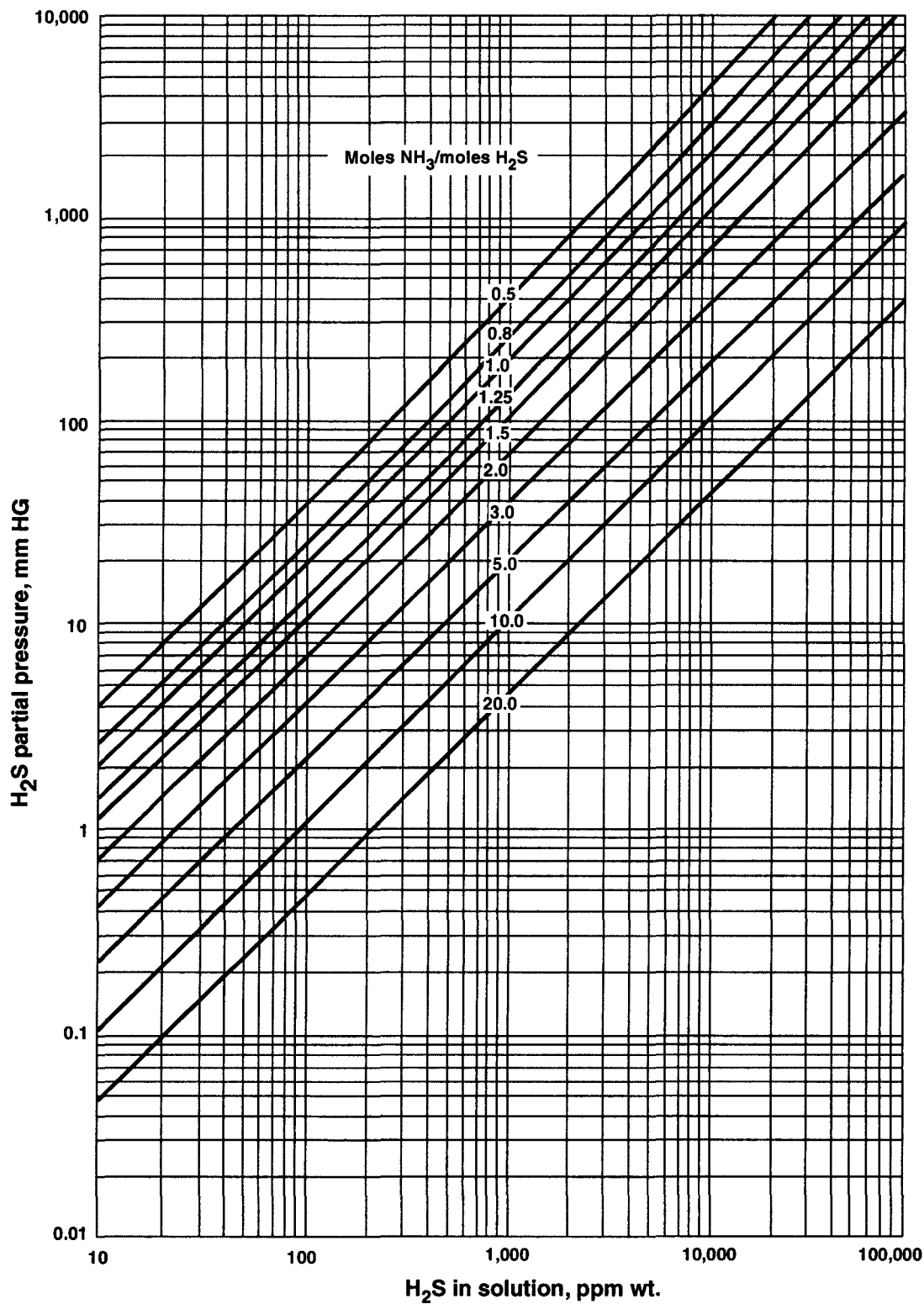
Fig. 2.8.2.10. *Hydrogen sulfide equilibria at 280°F.*

Source : Hydrocarbon Processing, October 1991

© GULF PUBLISHING CO., HOUSTON, TX 77252-2608

2.9. DIFFERENT METHODS FOR REMOVAL OF VOCS

Several methods are known for the removal of volatile organic compounds (VOCs) from water. Chemical oxidation is one them.

These oxidation techniques offer a degree of flexibility in tailoring treatment to a specific water or waste water at reasonable cost. However, chemical oxidation usually becomes most effective when it is used as a complementary process rather than a self-sufficient process. And particularly in wastewater applications it calls for careful consideration of the chemical & biological integrity of effluent streams.

Adsorption of VOCs on granular activated carbon is a potential VOC removal process. In the 1970s it was the most thoroughly proven technology for many organic pollution problems. But it still requires further design and system refinements to make it more attractive economically and more practical operationally.

Entered in the scenario in the 1980 is **air-stripping of VOC**. Experimental studies of bench, pilot, and industrial scale, have confirmed stripping to be an economically a better option than carbon adsorption to remove VOCs from groundwater.

Only in the 90's the steam-stripping began to compete with the air-stripping for the removal of VOCs.

Advantages of Steam-Stripping

Since stripping steam carries greater enthalpy than air, the organic contaminants easily transfer to the vapor phase, using smaller column dimensions and providing a rational use of many low-press - steams (*viz.* waste steam), thus improving energy consumption indices.

Another advantage of steam stripping is the possible recovery of the VOC when this forms a nonmiscible mixture with water. Hence upon condensing the stripper exit vapor, the VOC forms a distinct layer atop the condensate and can be easily separated out.

Air stripping merely transfers the VOC from water to air *i.e.* it doesn't reduce the actual amount of chemical discharge to the environment. Therefore, VOC stripped by air must be, due to environment reasons, chemically treated or burned out before being vented to the atmosphere. But steam stripping produces, in some cases, a recoverable phase, always as a minimum since it concentrates the VOC in the condensate. And as a result the VOC separated can be dealt with more effectively (by incineration, biological treatment, or recycling back to the process).

Overall, steam stripping is economically a better option than air stripping because of both capital and operational cost. For capital cost, the volume of a steam stripping column is in most cases lower than that for air stripping, and air blowers or compressors are expensive equipment. So far as operational cost is concerned, many CPIs and PCIs have low pressure steams that go into waste. This waste steam can be used as a stripping agent, improving the energy efficiency of the plant.

Source : *Design of steam − Stripping Column for Removal of VOCs.......JR Ortiz. Del Castillo et. al.* **(Industrial Engineering Chemistry and Research 2000/vol.39/P:731 - 739).**

2.10. AIR STRIPPING VOC IN TRAYED COLUMNS

Removal of volatile organic compounds (VOC) from water effluents by air stripping is a popular practice, particularly where low pressure heating steam (waste steam) is not available. The most commonly used vap-liq contactor in the stripping tower are packings because of their high separation

efficiency. However, a tray tower is sometimes used because of its easier operation and maintenance, especially if there are serious scaling problems inside the tower.

Design Procedure

The most important step in designing a trayed tower is to determine the number of trays for a required stripping separation. The procedure involves :

I. Calculation of the number of ideal trays by using the Kremser Equation.

II. Computing the number of nonideal trays as the number of ideal trays upon overall tray efficiency is the number of actual trays.

Two Bottlenecks

1. The above design calculation leaves the concentration distributions thru the tower uncertain.

2. Reliable values of the overall tray efficiency are difficult to obtain since tray efficiencies for various species and tray designs can differ.

Design Equations

The VOC stripper using tray is shown schematically in **Fig. 2.10.1**
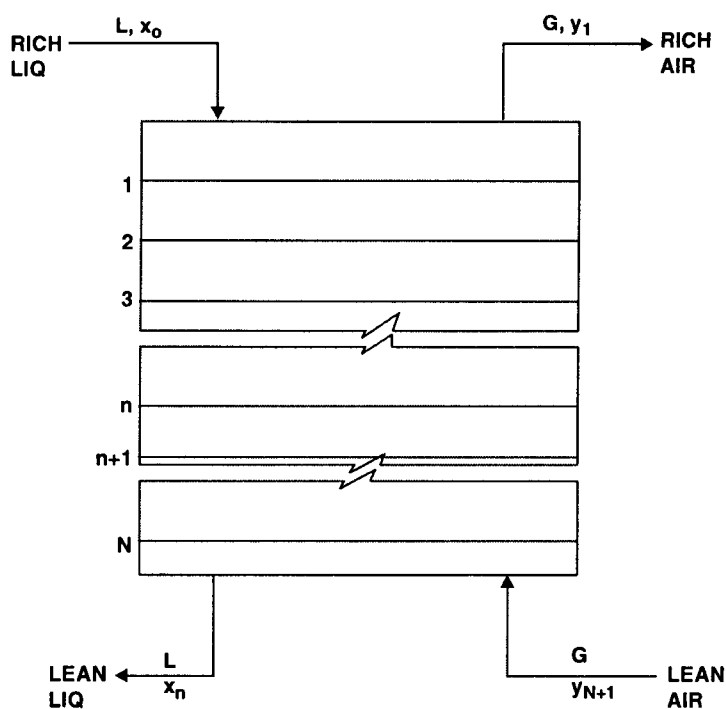
Fig. 2.10-1. *Air Stripper for VOC removal.*

A mass balance of **i**-component around the **n-th** tray of this countercurrent stripping operation gives

$$L.x_{n-1,\, i} + G.\, y_{n+1,\, i} = L.\, x_{n,\, i} + G.\, y_{n,i} \qquad \qquad ...(2.10.1)$$

where **L** and **G** are the molar flowrates (kmols. s^{-1}) of liq and air respectively.

$y_{n,i}$ = Composition of i-component in vapor leaving the **n-th** tray, mol fraction.

$x_{n,i}$ = Composition of i-component in liq phase the **n-th** tray, mol fraction.

Number of Ideal Trays : The configuration of a tray is depicted in **Fig. 2.10.2**
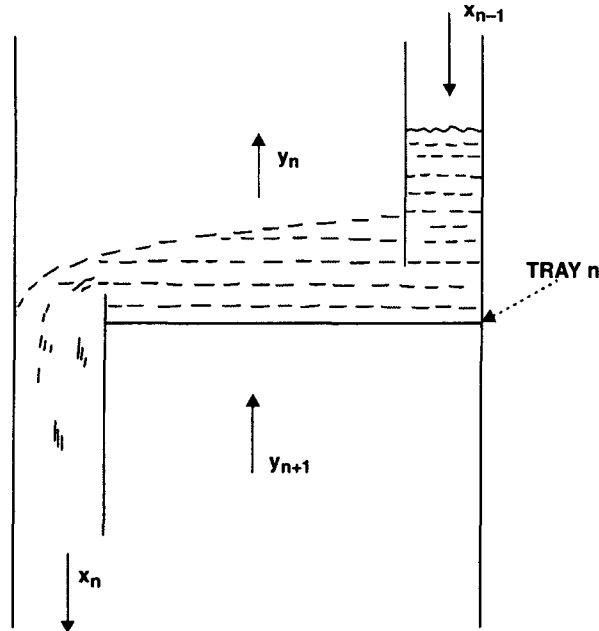
Fig. 2.10-2. *A single tray.*

For an ideal tray the gas concentration leaving the **n-th** tray, y, is in equilibrium with the liquid concentration, x_n . That is

$$y_{n,i} = K_i \cdot x_{n,i} \qquad \qquad \text{...(2.10.2)}$$

where K_i is the equilibrium constant of component **i**. Substitution of Eqn. 2.10.2 into Eqn. 2.10.1 yields

$$S_i \cdot x_{n+1,i} - (1 + S_i) \cdot x_{n,i} + x_{n-1,i} = 0 \qquad \qquad \text{...(2.10.3)}$$

where $S_i = K_i \dfrac{G}{L}$ is the **stripping factor,** which is an important parameter to determine the performance of a stripper.

In most cases the inlet air contains no organic components. Therefore

$$y_{N+1,i} = 0$$

whereupon the solution of Eqn. 2.10.3 results in

$$N = \frac{\ln\left[(S_i - 1)\left(x_{o,i}/x_{N,i}\right) + 1\right]}{\ln S_i} - 1 \qquad \qquad \text{...(2.10.4)}$$

$$\text{for } S_i \neq 1$$

or, $$N = \left[x_{o,i}/x_{N,i}\right] - 1 \qquad \qquad \text{...(2.10.5)}$$

$$\text{for } S_i = 1$$

Number of Non-Ideal Trays : For a non-ideal tray the gas concentration leaving the **n-th** tray, y_n, is not in equilibrium with the liquid on **n-th** tray, x_n as may be visualized from **Fig. 2.10-3**
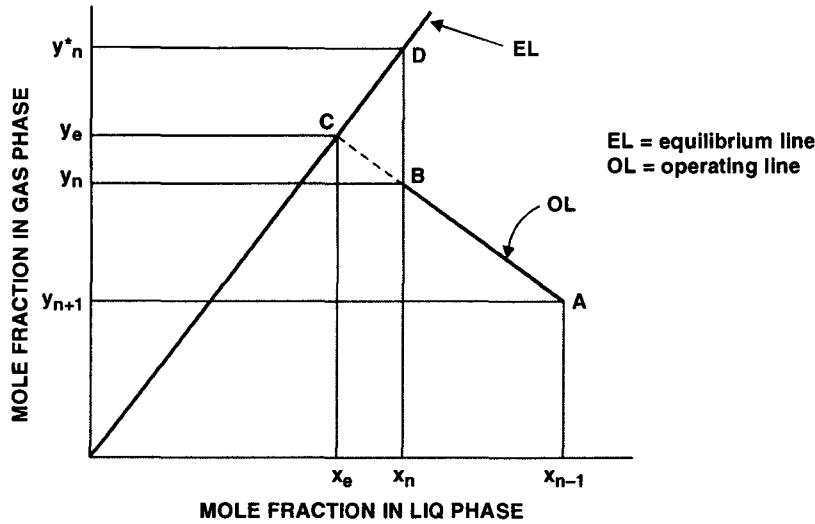
Fig. 2.10-3. *Tray input (A), output (B), and Equilibrium (C).*

The Murphree tray efficiency based on vapor phase is

$$\eta_{v,i} = (y_{n,i} - y_{n+1,i})/(y^*_{n,i} - y_{n+1,i}) \qquad \qquad ...(2.10.6)$$

where $y^*_{n,i}$ vap phase concentration of i-component in equilibrium with its concentration in the liquid phase, $x_{n,i}$ *i.e.*

$$y^*_{n,i} = K_i \cdot x_{n,i}$$

Plugging this in Equ. 2.10-6 results

$$y_{n+1,i} = [\eta_{v,i} \cdot K_i \cdot x_{n,i} - y_{n,i}]/(\eta_{v,i} - 1) \qquad \qquad ...(2.10.7)$$

A mass balance of component **i** around an envelop from the **n-th** tray to the bottom of the tower, the **N-th** tray begets

$$y_{n,i} = \left|\frac{L}{G}\right| \cdot x_{n,i} + y_{N+1,i} - \left|\frac{L}{G}\right| \cdot x_{N,i} \qquad \qquad ...(2.10.8)$$

For **(n+1)-th** tray

$$y_{n+1,i} = \left|\frac{L}{G}\right| \cdot x_{n,i} + y_{N+1,i} - \left|\frac{L}{G}\right| \cdot x_{N,i} \qquad \qquad ...(2.10.9)$$

Substitution of Eqns. 2.10-8 and 2.10-9 into Eqn. 2.10-7 produces

$$x_{n,i} - A_i \cdot x_{n-1,i} = A_i [(G/L) \cdot \eta_{v,i} \cdot y_{N+1,i} - \eta_{v,i} \cdot x_{N,i}] \qquad \qquad ...(2.10.10)$$

where $A_i = 1/[\eta_{v,i}(S_i - 1) + 1]$ $\qquad \qquad ...(2.10.11)$

Eqn. 2.10.10 is a linear first-order finite difference equation which may be solved with the aid of two boundary conditions

$$n = 0, \qquad x = x_0$$
$$n = N, \qquad x = x_N$$

As in most cases, the inlet air is fresh-air, free from VOC, so $y_{N+1} = 0$ whereupon the result is

$$N = \frac{\log(1/R_i) + (1-1/R_i)/S_i}{\log\left[\eta_{v,i}(S_i - 1) + 1\right]} \qquad \qquad ...(2.10.12)$$

$$\text{for } S_i \neq 1$$

or, $N = [(1/R_i) - 1]/\eta_{v, i}$ ...(2.10.13)

where, $R = x_{N,i}/x_{o, i}$ = fraction of VOC residue in water

When $S_i > 1$, the value of R_i decreases as N increases *i.e.* with the increase of number of tray more and more VOCs become depleted from feed of contaminated water and thereby reducing the fraction VOC residue in the exit water. However, when S_i approaches unity, N becomes very large since R_i is usually a very small number for the VOC stripping problem.

On the other hand, when $S_i < 1$, the fraction of VOC residue in stripper effluent, R_i, approaches a limiting value as N approaches infinity. This limiting value of R_i may be found from the following equation

$$R_i = x_{N, i} / x_{o, i} = 1 - S_i$$ ...(2.10-14)

Eqns. 2.10-12 and 2.10-13 can be used to generate design curves. Plots of N vs. S with η_v as the curve parameter for R = 0.01, 0.001, 0.0001 have been presented in **Figs. 2.10-4, 2.10-5 and 2.10.6** respectively.
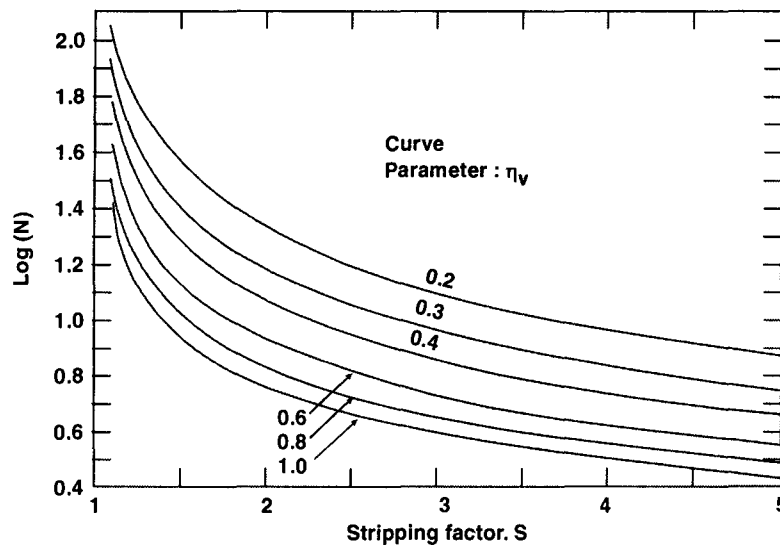
Fig. 2.10.4. *Number of real trays as a function of stripping factor R = 0.01.*
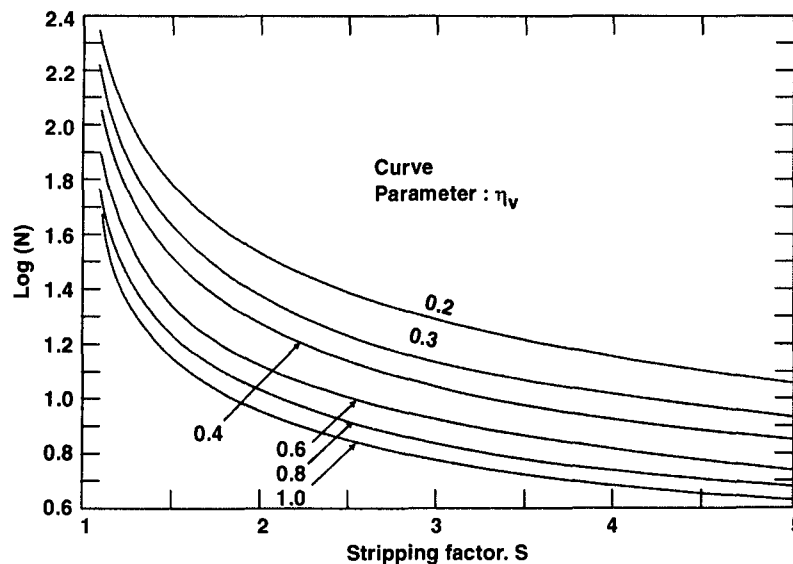
Fig. 2.10.5. *Number of real trays as a function at stripping factor for R = 0.001.*
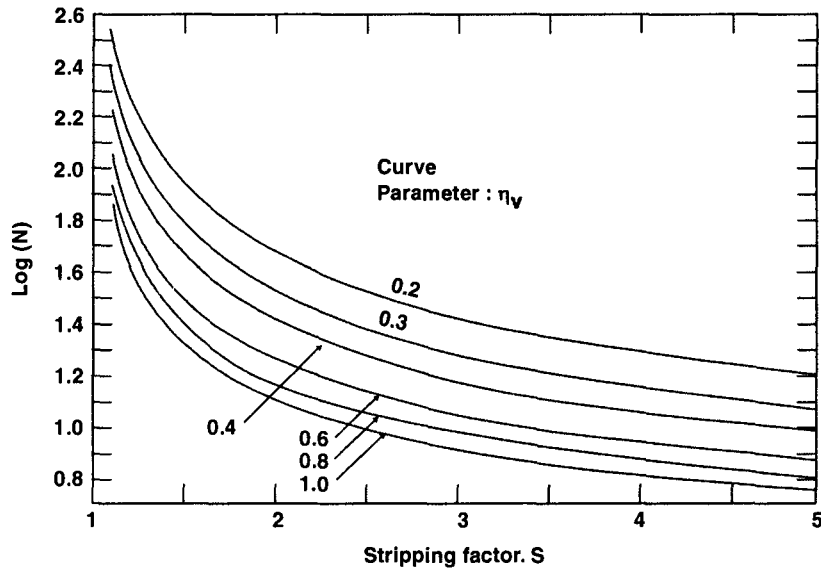
Fig. 2.10.6. *Number of real trays as a function at stripping factor for R = 0.0001.*

AIR STRIPPING OF TCE

Problem 2.7. *An air stripping column [operating pressure 1 atm.] is to be designed to reduce the concentration of trichloroethylene (TCE) from 100 ppm to ≤ 0.01 ppm in water.*

If the tower is operated with an airflow 1.75 times the minimum airflow, how many real trays are to be required for a Murphree vapor phase efficiency of 60% ?

If the treatable water flowrate is 315 $m^3.h^{-1}$, what is the air flowrate required ?

$K_{TCE, 298K/1.atm.} = 650$

Solution :

Given :

$$x_N = 0.01 \text{ ppm}$$
$$x_o = 100 \text{ ppm}$$
$$K = 650$$
$$G = 1.75\, G_{min}$$

Step - (I) Calculation of R

$$R = x_N/x_o = 0.01/100 = 0.0001$$

At this low ppm concentration it can be approximated that

$$K = \frac{L}{G_{min}}$$

Step - (II) Calculation of Stripping Factor

$$S = K.\frac{G}{L}$$

$$= \frac{L}{G_{min}}.\frac{G}{L}$$

$$= \frac{G}{G_{min}}$$

$$= 1.75$$

Step - (III) Determination of The Number of Real Trays

$S = 1.75 ;$ $\qquad$ $R = 0.0001 ;$ $\qquad$ $\eta_V = 60\% = 0.6$

$\therefore$ $\qquad$ From **Fig. 2.10.6, N** ≈ 24

Step - (IV) Operating Air Flow Rate

$$G \quad = 1.75 \, G_{min}$$

$$= 1.75 \, \frac{L}{K}$$

Now, $\qquad$ $L \quad = 315 \, \dfrac{m^3}{h}$

$$= 315 \, \frac{m^3}{h} \times 1000 \, \frac{kg}{m^3} \times \frac{1}{18} \, \frac{kmol}{kg}$$

$$= 17500 \, \frac{kmol}{h}$$

$$= 4.86111 \, kmol.s^{-1}$$

$\therefore$ $\qquad$ $G \quad = 1.75 \left| \dfrac{4.86111 \, kmol.s^{-1}}{650} \right|$

$$= 0.01308 \, kmol.s^{-1}$$

$$= \left| 0.01308 \, \frac{kmol}{s} \right| \times \left| 28.84 \, \frac{kg}{kmol. \, air} \right|$$

$$= 0.377227 \, kg.s^{-1}$$

$$= 1358.017 \, kg.h^{-1}$$

AIR STRIPPING OF TCE AND DCA

Problem 2.8. A tray tower is to be designed to strip both TCE and DCA (1, 1-dichloroethane) concentrations in a contaminated stream of factory effluent water from 100 ppm to ≤ 0.01 ppm by using air as the stripping agent.

The operating air-rate should be twice the minimum air rate.

How many real trays would be needed for such a system if the overall Murphree vap phase efficiency = 70%, i.e., 0.7.

If the effluent to be treated is 315 m^3 per hour, calculate the required air flowrate.

$K_{DCA, \, 298K/1 \, atm.} = 303$

$K_{TCE, \, 298K/1 \, atm.} = 650$

Solution :

Given :

$$x_N = 0.01 \text{ ppm}$$

$$x_o = 100 \text{ ppm}$$

$$\left.\begin{array}{l} K_{DCA} = 303 \\ \\ K_{TCA} = 650 \end{array}\right\} \; 298 \text{ K/1 atm.}$$

$$\eta_V = 70\%$$

Step - (I) Calculation of R

$$R = x_N/x_o = 0.01/100 = 0.0001$$

Step - (II) Determination of N

We can approximate

$$L/G_{min} \approx K$$

$$\therefore \qquad S = 2$$

From **Fig. 2.10.6** for S = 2 at η_V = 0.7, the total number of real trays

$$N = 16$$

Step - (III) Air Rate

Since $K_{DCA} < K_{TCE}$, we shall use, $K_{DCA} = 303$ in our calculation.

$$\text{Now,} \; \frac{L}{G_{min}} = K_{DCA} = 303$$

$$\therefore \qquad G_{min} = \frac{L}{303}$$

$L = 315 \text{ m}^3. \text{ h}^{-1} = 4.86111 \text{ kmol.s}^{-1}$ of [cf. **Problem 2.7**]

$$\therefore \qquad G_{min} = \frac{4.86111}{303} \text{ kmol.s}^{-1} = 0.01604 \text{ kmol.s}^{-1}$$

Now, $\qquad G_{op} = 2 \, G_{min}$

$$= 0.032086 \left|\frac{\text{kmol}}{\text{s}}\right| \times 28.84 \left|\frac{\text{kg}}{\text{kmol}}\right| \times 3600 \left|\frac{\text{s}}{\text{h}}\right|$$

$$= 3331.352 \text{ kg.h}^{-1}$$

AIR STRIPPING TCE AND DCA

Problem 2.9. If in Problem 2.8, the DCA concentration in the effluent is to be reduced to 0.01 ppm while the TCE concentration is to be reduced substantially to less than 0.01 ppm using the same air flowrate, i.e., 3331.352 kg.h⁻¹ what will be the TCE concentration in the effluent ?

Solution :

Given :

$$K_{DCA, \; 298K/1 \; atm.} = 303$$
$$K_{TCE, \; 298K/1 \; atm.} = 650$$

Step - (I) Determination of Equivalent Stripping Factor of TCE

$$S_{TCE} = K_{TCE} \cdot \frac{G}{L} = K_{TCE} \left| \frac{2\,G_{min}}{L} \right|$$

Since, $K_{DCA} < K_{TCE}$, it can be approximated that

$$L\,/G_{min} \approx K_{DCA}$$

$$\therefore \qquad S_{TCE} = 2 \left| \frac{K_{TCE}}{K_{DCA}} \right| = 2 \left| \frac{650}{303} \right| = 4.2904$$

Step - (II) TCE Concentration in The Stripper Effluent

Eqn. 2.10.12 upon rearrangement yields

$$x_{N,\,i} = \frac{S_i - 1}{S_i \left[(S_i - 1)\eta_{v,i} + 1 \right]^N - 1} \cdot x_{o,i}$$

$$= \frac{4.29 - 1}{4.29 \left[3.29 \times 0.70 + 1 \right]^{16} - 1}$$

$$= 3.8212 \times 10^7 \text{ ppm}$$

AIR STRIPPING TCE, DCA & HCB

Problem 2.10. If the column designed in Problem 2.8 were operated with the same operating gas & liq rates :

$G_{op} = 3331.352 \text{ kg.h}^{-1}$

$L\quad = 315 \text{ m}^3.h^{-1}$

but with the influent water containing 1 ppm of hexachlorobenzene (HCB) what will the effluent concentration of HCB be ?

$K_{HCB,\ 298\ K/1atm.} = 94.5$

Comment on the result.

Solution :

We shall proceed in the same way as we've done in solving the previous problem.

Step - (I) Determination of Equivalent Stripping Factor for HCB

$$S_{HCB} = K_{HCB} \cdot \frac{G}{L}$$

But $G = 2\,G_{min}$ $\boxed{\text{Problem 2.8}}$

$$\therefore \qquad S_{HCB} = 2\,K_{HCB} \cdot \left| \frac{G_{min}}{L} \right|$$

For such low ppm concentrations of contaminant, it is reasonable to assume that

$$L/G_{min} \approx K_{DCA}$$

$$\therefore \qquad S_{HCB} = 2 \left| \frac{K_{HCB}}{K_{DCA}} \right| = 2 \left| \frac{94.5}{303} \right| = 0.62376$$

Step - (II) HCB Concentration in Stripper Effluent

$$\eta_{V, i} = 70\%$$
$$N = 16$$
$$x_{0, HCB} = 1 \text{ ppm}$$

Rearranging Eqn. 2.10.12 it becomes

$$x_{N, i} = \frac{S_i - 1}{S_i \left[(S_i - 1) \eta_{v, i} + 1 \right]^N - 1} \cdot x_{o, i}$$

$$= \frac{0.62376 - 1}{0.62376 \left[(0.62376 - 1) 0.7 + 1 \right]^{16} - 1} (1 \text{ ppm})$$

$$= 0.378 \text{ ppm}$$

Comments : The stripping factor HCB being less than 1, the fraction of residue R_{HCB} approaches a limiting value as **N** approaches infinity. The limiting value of **R** is

$$R_{HCB} = x_{N,HCB} / x_{0,HCB} = 1 - S_{HCB} = 1 - 0.62376$$
$$= 0.3762$$

from which

$$x_{N,HCB} = 0.3762 \, (x_{0,HCB})$$
$$= 0.3762 \, (1 \text{ppm})$$
$$= 0.3762 \text{ ppm}$$

This confirms that the limiting value of x_N has been practically reached and no further increase of number of trays will help to bring down the **HCB** concentration.

AIR STRIPPING TCA, DCA, TCE, DCE, CTC

Problem 2.11 A company pumps 2 MGD(million gallons per day) of groundwater to supply drinking water to a community. However the groundwater contains five chlorohydrocarbons.

Organic Contaminant	Henry's Law Constant (K), atm	In-Flow Water Concentration (ppm)	Drinking Water Criteria (EPA Standard) (ppm)
TCA (1 : 1 : 1-Trichloroethane)	*273.6*	*100*	*0.200*
DCA (1 : 2-Dichloroethane)	*61.2*	*100*	*0.005*
TCE (Trichloroethylene)	*650*	*100*	*0.005*
DCE (1 : 1-Dichloroethylene)	*834*	*100*	*0.007*
CTC (Carbon tetrachloride)	*1679*	*100*	*0.005*

which must be removed so that the water meets the EPA drinking water criteria.

Design an air stripper for this purpose using operating air flowrate twice the minimum air flowrate.

Take, Murphree vapor phase efficiency equal to 60%.

Estimate the total number of trays & contaminant concentration in the effluent.

Solution : First to determine is the minimum air flowrate. For this DCA is taken as the key component since its equilibrium constant is lowest.

Step - (I) Stripping Factor for DCA

$$G = 2\,G_{min}$$

$$S_{DCA} = K_{DCA} \cdot \left|\frac{G}{L}\right| = K_{DCA} \cdot \left|\frac{2\,G_{min}}{L}\right| = \frac{2\,K_{DCA}}{L\,/\,G_{min}}$$

At the given low ppm concentration, it is reasonable to assume

$$L/G_{min} \approx K_{DCA}$$

$$\therefore \qquad S_{DCA} = 2$$

Step - (II) Total Number of Trays

$$R_{DCA} = x_{N,\,DCA}/\,x_{O,\,DCA} = 0.005 \text{ ppm}/100 \text{ ppm} = 0.00005$$

$$\eta_{V,\,DCA} = 0.60$$

$$N = \frac{\log\left[1/\,R_i + (1 - 1/\,R_i)/\,S_i\right]}{\log\left[(S_i - 1)\eta_{v,i} + 1\right]} \qquad \qquad ...(2.10.12)$$

$$= \frac{\log\left[1/\,0.00005 + (1 - 1/\,0.00005)/\,2\right]}{\log\left[(2 - 1)\,0.6 + 1\right]}$$

$$= 19.598$$

i.e., 20 trays

Step - (III) Relative Stripping Factors of Other Components

$$S_{TCE} = 2\,\frac{K_{TCE}}{K_{DCA}} = 2\left|\frac{650}{61.2}\right| = 21.241$$

$$S_{DCE} = 2\,\frac{K_{DCE}}{K_{DCA}} = 2\left|\frac{834}{61.2}\right| = 27.254$$

$$S_{TCA} = 2\,\frac{K_{TCA}}{K_{DCA}} = 2\left|\frac{273.6}{61.2}\right| = 8.941$$

$$S_{CTC} = 2\,\frac{K_{CTC}}{K_{DCA}} = 2\left|\frac{1679}{61.2}\right| = 54.869$$

Step - (III) Residual concentrations of VOCs in Stripper Effluent

$$x_{N,\,i} = \frac{S_i - 1}{S_i\left[\eta_{V,\,i}(S_i - 1) + 1\right]^N - 1}\,.x_{o,\,i}$$

$$x_{N, TCE} = \frac{21.241 - 1}{21.241[0.6 \times 20.241 + 1]^{20} - 1} \cdot (100 \text{ ppm})$$

$$= 4 \times 10^{-21} \text{ ppm}$$

$$x_{N, DCE} = \frac{27.254 - 1}{27.254[0.6 \times 26.254 + 1]^{20} - 1} \cdot (100 \text{ ppm})$$

$$= 3.17 \times 10^{-23} \text{ ppm}$$

$$x_{N, TCA} = \frac{8.941 - 1}{8.941[0.6 \times 7.941 + 1]^{20} - 1} \cdot (100 \text{ ppm})$$

$$= 5.40 \times 10^{-14} \text{ ppm}$$

$$x_{N, CTC} = \frac{54.869 - 1}{54.869[0.6 \times 53.869 + 1]^{20} - 1} (100 \text{ ppm})$$

$$= 3.44 \times 10^{-29} \text{ ppm}$$

2.11. DESIGNING AIR STRIPPERS [PACKED TOWERS]

VOC Air Stripper is always a countercurrent gas-liq contacting tower. Contaminated waste water introduced to column at the top is evenly distributed over a packed bed and flows downward [Fig. 2.11.1].
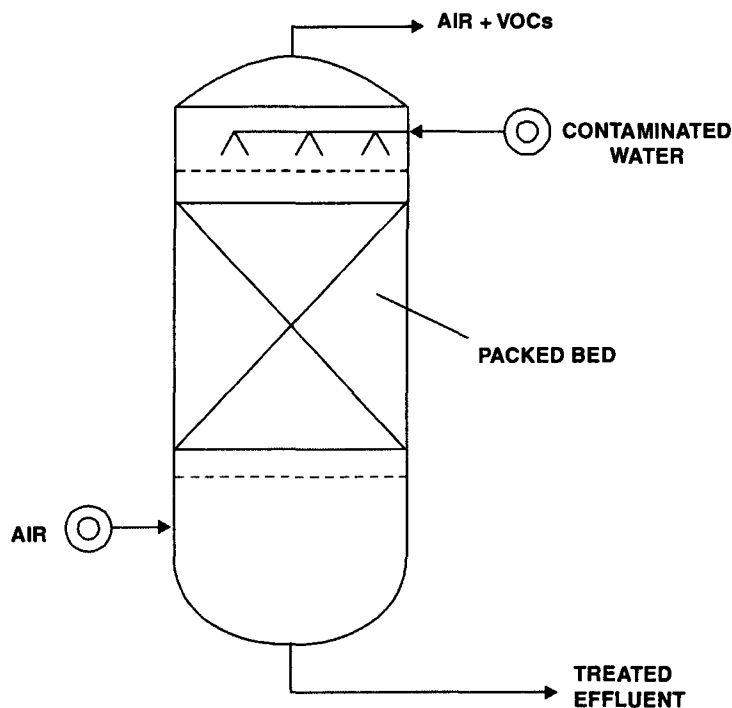
Fig. 2.11.1. *Packed bed air stripper*

Air blown up thru the packing from the bottom of the tower, comes into direct contact with the downflowing liquid stream forming a thin film over the packing surface. As a consequence of mass transfer across the gas-liq interface, VOCs pass into the gas stream. The VOC-laden gas is discharged thru the top of the tower while the VOC-free water exits the bottom as tower effluent.

The mass transfer rate of a VOC from the liquid phase to the gas phase depends on the Henry's Law Constant for that component, operating temperature, the concentration, and the gas-liq contact area.

From the Henry's Law, it follows that the partial pressure of a VOC in air equals the gas-liq equilibrium concentration of that substance in the liquid multiplied by a constant which is Henry's Law Constant :

$$p_A = H_A.X_A \qquad \qquad ...(2.11.1)$$

where, p_A = partial pressure of component A in gas phase, kPa

H_A = Henry's Law Constant for component A, kPa

X_A = Concentration of A in liquid phase, kmol A/kmol A-free liquid

Henry's constant (**H**) determines the equilibrium or, saturation concentration of the solute [VOC here] at a given temperature. The values of **H** may be available in handbooks or open literature.

Since, the mass transfer occurs at the air-water interface, it is beneficial to stretch the gas-liq intrafacial area as much as possible. This is accomplished by filling the tower with packing materials such as saddles, Raschig rings or Pall rings. The packings increase the interfacial (surface) area, thereby greatly enhancing the mass transfer of VOC from the liquid (water) to the gas (air) phase. That is, the packing increase the effectiveness of air stripping in the water.

The rate of mass transfer of a component depends on its concentration driving force in the liquid :

$$N_A = K_L.a.\Delta c \qquad \qquad ...(2.11.2)$$

where, N_A = mass transfer rate for component A, kmol.h^{-1}.m^{-3}

K_L = coefficient of liquid mass transfer, m.h^{-1}

a = interfacial area per unit volume of packing, m^2.m^{-3}

$\Delta c = c_A^* - c_A$.

c_A^* = Concentration of A in the liquid at equilibrium at the operating conditions, kmol. m^{-3}

For design purpose, the mass transfer rate in stripping tower can be expressed as :

$$N_A = \frac{Q_{V,L}}{A} . \frac{dc_A}{dZ} \qquad \qquad ...(2.11.3)$$

where, Q_{VL} = Volumetric flowrate of liquid, m^3, h^{-1}

A = Tower cross-sectional area, m^2

$\dfrac{dc_A}{dZ}$ = change in concentration of component A thru a bed depth of dZ.

Z = total packing depth

The values of tower cross-sectional area, A and the depth of packing, Z can be obtained from the known values of :

H, G, L and $K_L.a$ or $K_G.a$

The values of the coefficient of liquid or gas mass transfer ($K_L.a$ or $K_G.a$) depend on the size &

shape of the packing as well as the liquid and gas flowrates. These values are usually supplied by packing vendors, or can be obtained from published literature.

The liq-loading is set by the wastewater or groundwater flowrate. The air flowrate is so adjusted that air : water ratio exceeds 15 : 1

The height of the packing, **Z** , is *NTU* times *HTU*

where, *NTU* = number of mass transfer units

$\quad$ *HTU* = height of a mass transfer unit, m.

The *NTU* is defined as :

$$NTU = \frac{S}{S-1} \cdot \ln\left[\frac{c_{L,1} - c_{G,1}/H_A}{c_{L,2} - c_{G,1}/H_A} \cdot \frac{S-1}{S} + \frac{1}{S}\right] \quad ...(2.11.4)$$

where, S = stripping factor

$$= \frac{Q_{V,G}}{Q_{V,L}} \cdot H_A \qquad\qquad\qquad ...(2.11.5)$$

$Q_{V,G}$ = volumetric gas flowrate, m^3, h^{-1}.

$Q_{V,L}$ = volumetric liq flowrate, m^3, h^{-1}.

H_A = Henry's Law Constant for component A

$c_{L,1}$ = influent liquid concentration, kmol. m^{-3}

$c_{L,2}$ = effluent liquid concentration, kmol. m^{-3}

$c_{G,1}$ = inlet gas concentration, kmol. m^{-3}

$c_{G,2}$ = exit gas concentration, kmol. m^{-3}

The height of a transfer unit **HTU** is defined as

$$HTU = \frac{L}{K_L \cdot a \cdot \rho_{H_2O,molar}} \qquad\qquad ...(2.11.6)$$

where, $\quad$ L = liq loading, kmol. h^{-1}. m^{-2}

$\quad K_L \cdot a$ = liquid MTC, $(m.h^{-1})$ $(m^2.m^{-3})$

$\rho_{H_2O, molar}$ = molar density of water

$\quad\quad\quad\quad = 55.6$ kmol.m^{-3}

The Eqn. 2.11.6 defines **HTU** in terms of liquid phase **MTC**. Often, packing vendors provide $K_G \cdot a$ values, indicating that gas phase resistance rather than liquid phase resistance, holds sway in the mass transfer process. However, the **MTCs** can be related as follows :

$$K_L \cdot a = K_G \cdot a \, \frac{H_A}{\rho_{H_2O,molar}} \qquad\qquad ...(2.11.7)$$

Substitution of $K_L \cdot a$ value in Eqn. 2.11.6 results

$$HTU = \frac{1}{K_G \cdot a} \cdot \frac{L}{H_A} \qquad\qquad (2.11.8)$$

Inasmuch as the stripping air is essentially free of VOCs,

$$c_{G,1} = 0$$

and that simplifies Eqn. 2.11.4 down to

$$NTU = \frac{S}{S-1} \cdot \ln\left[\frac{c_{L,1}}{c_{L,2}} \cdot \frac{S-1}{S} + \frac{1}{S}\right] \qquad \ldots(2.11.4.1)$$

Sometimes it is convenient to express liq-phase concentration in mole fraction terms whereupon Eq. 2.11.4.1 becomes

$$NTU = \frac{S}{S-1} \cdot \ln\left[\frac{x_i}{x_o} \cdot \frac{S-1}{S} + \frac{1}{S}\right] \qquad \ldots(2.11.4.1A)$$

where, x_i = mole fraction of solute in influent liq

x_o = mole fraction of solute in effluent liq

Since the air stripping of VOC is countercurrent one

$$x_i = x_t$$

$$x_o = x_b$$

Therefore, Eqn. 2.11.4.1A can also be represented as

$$NTU = \frac{S}{S-1} \cdot \ln\left[\frac{x_t}{x_b} \cdot \frac{S-1}{S} + \frac{1}{S}\right] \qquad \ldots(2.11.4.1B)$$

For systems that obey Henry's Law, the slope of EL *(equilibrium line)*

$$m = \frac{H}{P}$$

Again the EL equation is given by

$$K = \frac{y}{x}$$

where, **K** (the equilibrium ratio) becomes the slope of EL, *i.e.*,

$$K = m = \frac{H}{P}$$

This modifies stripping factor

$$S = K\frac{G}{L} = \frac{H}{P} \cdot \frac{G}{L} \qquad \ldots(2.11.9)$$

Table 2.11.1 presents Henry's Law Constant for some volatile chlorinated hydrocarbons that are commonly found as well-water contaminants

Table 2.11.1 Henry's Law Constant at 298 K for some Typical Well-Water contaminants.

VOC	Typical Concentration (ppm)	H (MPa/mol fraction)
1, 1-Dichloroethane	0.05	25.3312
1, 1, 1-Trichloroethane	0.19	40.53
cis-1, 2-Dichloroethylene	0.27	36.447
Trichloroethylene	0.06	55.7287
Perchloroethylene	0.11	11.1457

TYPICAL ENERGY COST REDUCTION

Norton offers energy-efficient VOC removal with high performance Snowflake packing and

liquid distribution, at very low pressure drops. This saves both capital and especially operating cost compared with traditional packings. In an application involving the removal of 1, 1, 2, 2 - Tetrachloroethane from contaminated ground water, operating costs could be more than halved while maintaining the same number of transfer units. The following table compares a Snowflake design with the same number of transfer units as an actual customer design.

Liquid Rate	*664 m³/h (2925 gpm)*	*46.4 m³/m².h (19 gpm/ft²)*
Volumetric Vapor/Liquid Ratio	100:1	
Temperature	20°C	
1, 1, 2, 2 – Tetrachloroethane	IN – 3200 ppb	
	OUT–160 ppb (95% removal)	
	1 in. Saddles	**Snowflake packing**
Bed Depth, m	6.1	7.6
ft	20.0	25.0
Total Pressure Drop, mm H₂O	194.0	49.0
in H₂O	7.64	1.93
Power Required-Air Blower, HP	78.0	19.7
-Water Pump, HP	26.1	30.4
Annual Operating Cost, U.S.$	34, 000	16, 400

(Based on a Henry's Law constant of 21 atm/mf and a power cost of $0.05/kWh.)
Courtesy : NORTON Chemical Process Products Corporation, Ohio 44309, USA.

CONDITIONS OF TEST A

Southern California	Actual contaminated ground water
Tower–Internal Diameter	90.2 cm (35.5 in.)
Packing Height	5.13 m (16' 10")
Distributor	Norton Intalox High-performance Model 106 and V-notch trough type (non-Norton).
Support Plate	Flat Grid Type
Stripping Gas	Ambient Air
Contaminants	Trichloroethylene, TCE—11 ppb at inlet
	Perchloroethylene, PCE—95 ppb at inlet
	(Tetrachloroethylene)
Liquid Flow rate Measurement	102 mm (4in.) Hershey meter, on distributor inlet
Air Flow Rate Measurement	Fluid Control Inc., Model LT-81-41
Pressure Drop Measurement	U-Type manometer, just above support plate
Water Temperature	
– Norton Distributor	18°C (65°F)
– V-Notch Trough Distributor	20°C (68°F)
Air Temperature	21–27°C (70–80°F)

Sampling Points - Influent	Before water meter
- Effluent	As water left tower
Analysis	By certified laboratory using gas chromatography
Experimental Conditions	
– Liquid Rate	$35.7 - 103.1$ m^3/m^2.h ($14.6 - 42.2$ gpm/ft^2)
– Air Rate	$2661 - 5668$ m^3/m^2.h ($145.5 - 309.9$ cfm/ft^2)
Volumetric Vapor/Liquid Ratio	$40.0 - 93.2$:1.0
Equilibrium Constant, H$_{atm}$, PCE*	
– Norton Distributor	939
– V-Notch Trough Distributor	1035

* H equilibrium constant determined as Equation 6 in: Kavanaugh. M.C.,, and Trussel, R.R., *J Amer. Water Wks. Assoc., Vol. 72. No. 12, 1980, pp 684*. Conc.-mole fraction.

Courtesy : NORTON Chemical Process Products Corporation, Ohio 44309, USA.

Table 1 – Test Ⓐ VOC Removal Efficiencies with Snowflake Packing and Norton Distributor.

Water rate		Vapor/Liquid Volumetric Ratio	TCE			PCE			PCE Total Pressure			
			Inlet	*Outlet*	*%*	*Inlet*	*Outlet*	*%*	*HTU**		*Drop Water*	
m³/m².h	*gpm.ft²*	*Ratio*	*ppb*	*ppb*	*removal*	*ppb*	*ppb*	*removal*	*mm*	*ft*	*mm*	*in.*
35.7	14.6	93.2	11.3	0.10	99.1	98.3	0.55	99.4	975	3.2	22.2	0.875
35.7	14.6	82.0	10.8	0.20	98.1	83.6	0.5	99.4	975	3.2	15.9	0.625
35.7	14.6	74.5	12.6	0.04	99.7	94.1	0.2	99.8	823	2.7	12.7	0.500
53.3	21.8	62.4	10.4	0.15	98.6	83.4	0.75	99.2	1067	3.5	23.8	0.938
53.3	21.8	54.9	10.2	0.20	98.0	59.8	0.9	98.5	1189	3.9	15.9	0.625
53.5	21.8	49.9	11.3	0.10	99.1	95.9	0.8	99.3	1036	3.4	12.7	0.500
55.2	22.6	65.0	15.0	0.20	98.7	111.4	0.7	99.4	914	3.0	23.8	0.938
65.5	26.8	65.0	12.6	0.20	98.4	100.2	1.0	99.0	1097	3.6	33.4	1.313
66.4	27.2	50.0	11.0	0.20	98.2	89.5	0.9	99.0	1097	3.6	23.8	0.938
66.4	27.2	44.0	10.2	0.09	99.1	65.9	0.9	98.6	1158	3.8	17.5	0.688
66.4	27.2	40.0	10.9	0.10	99.1	89.7	0.9	99.0	1097	3.6	14.3	0.563
103.1	42.2	54.9	10.1	0.10	99.0	80.0	1.1	98.6	1158	3.8	71.4	2.813

Height of transfer unit

Courtesy : NORTON Chemical Process Products Corporation, Ohio 44309, USA.

Table 2 – Test Ⓐ Importance of Good Distribution (PCE)

Water Rate		Vapor/ Liquid Volumetric Ratio	V-Notch Trough Distributor			Norton Distributor			% Improvement with Norton Distributor
m³/(m².h)	*gpm/ft²*	*Ratio*	*HTU mm*	*HTU ft*	*% Removal*	*HTU mm*	*HTU ft*	*% Removal*	
35.7	14.6	93.2	1067	3.5	99.2	975	3.2	99.4	7.5
35.7	14.6	82.0	1006	3.3	99.4	975	3.2	99.4	1.8
35.7	14.6	74.5	1128	3.7	98.9	823	2.7	99.8	26.8
53.3	21.8	62.4	1158	3.8	98.7	1067	3.5	99.2	7.7
53.3	21.8	54.9	1189	3.9	98.5	1189	3.9	98.5	0.8
53.3	21.8	49.9	1250	4.1	98.2	1036	3.4	99.3	16.4
66.4	27.2	50.0	1158	3.8	98.7	1097	3.6	99.0	6.1
66.4	27.2	44.0	1280	4.2	97.9	1158	3.8	98.6	10.6
66.4	27.2	40.0	1128	3.7	98.8	1097	3.6	99.0	4.6

Note : The variability of the improvement obtained using a Norton distributor was due to the extremely non-linear fashion in which the V-notch trough distributor performed with varying air and water rates.

Courtesy : NORTON Chemical Process Products Corporation, Ohio 44309, USA.

DESIGN PARAMETERS

It requires a trial-&-error approach to determine the physical parameters designing an air-stripper to meet the specified level of stripping economically. Theoretical calculations form the basic guidelines for design, but these should be confirmed by pilotscale studies. This is chiefly because the calculations are often based on single solute system, *i.e.,* a lone VOC in solution. In constrast, most wastewaters and contaminated groundwaters contain more than one volatile organic compounds.

Nevertheless, the initial design calculations for the stripper column should be based on the compound with the highest concentration and hence lowest Henry's constant. That is, the calculations should be based on the VOC that is most difficult to remove by air stripping.

The physical parameters to be evaluated during design stage are

– **tower dia (ID)**

– **air-to-water ratio**

– **packing type & size**

– **height of the packed bed**

– **pressure drop of the gas thru the packing.**

These parameters are interrelated.

Liquid Rate The liquid irrigation rate is normally set between 50 $m^3.m^{-2}. h^{-1}$ and 100 $m^3.m^{-2}.h^{-1}$.

Tower dia is so selected as that liquid loading is maintained within this range. For example, if a 2500mm ID column is opted, a liquid rate of 340 $m^3.h^{-1}$ will be sufficient to keep the liquid loading within the above range.

However, the liquid flowrate thru a given tower is limited by the risk of flooding which greatly reduces removal efficiency. If the liquid rate is too high for a single column use of split-feed scheme may be used to treat the liquid in two or more tower in series or in parallel.

Tower Dia Tower diameters are usually 750 mm or greater. However, air-strippers of ID 2500 mm are not uncommon.

Packing Size The packing size is determined by the limit on pressure drop across the packed depth. As a rule of thumb, the ratio of packing size to tower dia should be 1:8 to 1:15.

Air-to -Water Ratio The air-to-water ratio is dependent on the stripping factor and Henry's constant (refer to Eqn. 2.11.9).

An air-to-water ratio of 15:1 is considered to be low. The ratios 22:1 to 30:1 are better while a ratio of 50:1 is high. The high ratio can remove more than 90% of VOCs at low concentrations and may be used within the limit of permissible pressure-drop.

The practical limit for the air-to-water is related to the permissible tower pressure drop which is again dictated by the available blower horse power. Usually 340 – 1020 $Nm^3.h^{-1}$ of stripping air is used per 23 $m^3.h^{-1}$ of water. At this gas loading the superficial gas velocity is about 0.3 – 1 $m.s^{-1}$.

Normal guideline for designing pressure drop is to keep ΔP within the range of 8 – 42 mm of water per m of packing.

Packed Bed Depth For VOCs, there is a limit for the packed height above which there are no gains in removal efficiency. The bed-depth is also influenced by the strength of packing. The packing may get deformed & crushed if the packing depth is too great. Hence bed height exceeding 9 – 12m are not generally recommended.

Bed height is affected by the type of packing & liq rate which dictate the height of a transfer unit **(HTU)**. For the same type of packing, the larger the packing size the greater is the HTU_L value for the same liquid rate & operating temperature. For example, when using 850 $Nm^3 h^{-1}$ of water, a 75 mm size **Super Intalox®** (of Norton CO.) packing will have HTU_L 25% greater than that for a 50 mm size of the same type of packing.

At lower gas loadings, *i.e.*, when using less than 500 $Nm^3.h^{-1}$ of air per 23 $m^3.h^{-1}$ of water, a 25mm size **Super Intalox®** packing will have its HTU_L about 20% less than that for a 50mm size for the same type of packing. That is larger packings require higher bed depth than their smaller and compact variants to achieve the same removal efficiency for the same operating conditions.

The number of transfer units **(NTU)**, air-to-water ratio and tower height affect removal efficiency and effluent quality. For instance if 98% removal efficiency is required.

$$x_o = 2\% \ x_i$$
$$x_i/x_o = 50$$

and that will require 4 to 5.3 transfer units for a stripper operating with an air rate of 340 – 1020 $m^3.h^{-1}$ and water rate of 23 $m^3.h^{-1}$ and at 100 kPa/293K.

If the water temperature is reduced to 286K, the Henry's Law constant for chlorinated hydrocarbons presented in **Table 2.11.1** will be 30% lower than at 293K. This will increase the number of transfer units required for the same percentage contaminant stripping.

If 99% contaminant removal is necessary, the number of transfer units required will be 18% greater than for 98% removal. On the other hand if 95% contaminant removal is satisfactory, the required **NTUs** will be 23% less than what required for 98% removal efficiency.

REFERENCES

1. E. D Heilshorn, *Chemical Engineering, March 1991/P :152-154*
2. J. P Bocard & B. J Mayland, *Hydrocarbon Processing April 1962, vol. 41/P-128*
3. A. L Kohl & F. C. R Riesenfeld, **Gas Purification (4th Edn.)**, Gulf Publishing Co., Houstan, TX, 1985.
4. R. N Maddox, **Process Engineer's Absorption Pocket HandBook** (Gulf Publishing, Houston, TX, 1985)
5. R. F Strigle (Jr.), **Random Packings & Packed Towers** (Gulf Publishing Co., Houston, TX, 1987)
6. M. C Kavanaugh & R. R Trussell, *Journal of American Water Works Association (No. 12/vol. 72/ 1980/P-684)*.

2.12 DESIGN OF STEAM STRIPPERS FOR VOC REMOVAL

Water pollution due to contamination by volatile organic compounds (VOCs) is a very prevalent problem. Either air or steam is used to strip off the contaminants.

VOCs commonly found in water include benzene, toluene, xylene, naphthalene, acetone, and a wide range of chlorinated hydrocarbons viz. TCA, DCA, TCE, DCE, CTC etc. They'are usually present in the water (surface waters, ground waters and wastewaters) in relatively small concentrations. Many of them are only partially miscible with water, but in general they all present a certain solubility.

Steam Stripping : Advantages and Disadvantages

Steam stripping takes place at higher temperatures than air stripping, usually very close to the boiling point of water. Since volatility of the organics is a very strong function of temperature, the high temperatures inherent in steam stripping ensures a very high stripping efficiency besides removal of heavier, most-soluble organics that are not strippable with air. Steam stripping can often achieve removal efficiency as high as > 99% and low effluent concentration (< 5 ppb.) No off-gas treatment is required.

The waste stream generated is a small qty of very concentrated organics that can be easily dealt with.

Steam stripping is a good and the most economical solution for wastewater streams containing more than 0.1% (wt.) organics and is the cost-effective at feed concentrations as low as 2 ppm.

It can be operated at vacuum or pressure with little penalty.

With heat integration, it can be made very energy efficient.

However, fouling is a nagging problem. And that is a major drawback of steam stripping.

Besides, steam stripping tends to be more capital-intensive than air-stripping. It does necessitate the presence off steam or process heat. MOC of the equipment should be more corrosion- and heat-resistant.

Set-Up :

Steam stripping for water cleanup is essentially a distillation process in which the volatile organics are distilled off as the light product **(OVHD)** while water goes down as residue and constitutes the heavy product **(BTMS)**.

The steam stripper is a packed or trayed tower. The wastewater feedstream is preheated in a recovery heater and charged to the tower at the top **(Fig. 2.12-1)**.

Steam is introduced to the stripper at the bottom to provide heat and vapor flow.

Packings or trays bring about intimate contact of feedwater with steam. Possessing high heat load, the saturated steam (frequently a wasteheat steam) transfers its heat to the feedwater causing organic materials to transfer from the liquid to the vapor phase.

These vapor-borne organics traffic up the column while the liquid move down the trays or thru the packings. And in that process the wastewater becomes leaner in organics whereas the vap-phase becomes progressively enriched with volatile organic materials.

While clean water leaves the tower at the bottom, steam, heavily laden with organics, leaves the tower at the top and is condensed, and processed further to separate the condensate from the VOCs.

Both the random and structured packings are used in steam stripping. And they are made of metal (stainless steel, aluminum) or plastic (viz. glass-reinforced polypropylene, polypropylene oxide, polyvinylidene fluoride, polytetrafluoroethylene). Structured packings are used to provide higher capacity and ensure higher separation efficiency.

Steam stripper are frequently associated with fouling. In such services, stainless steel sieve trays are a preferred choice.

Apart from packing, packed strippers are fitted with an assortment of gadgets viz. liq distributor, liq redistributor, packing support plates, mist eliminator etc.

Since heat load of the column is much higher at the bottom than at the top, it is necessary for the sake of energy conservation, to abstract as much heat from the bottoms before it is discharged off as environmentally safe effluent or recycled to the process. The extracted heat goes to preheat the feedwater to facilitate stripping. Such a heat recovery is not needed where strippers operate at reduced pressures because such systems operate at lower temperatures.

Feed	45.41 m³.h⁻¹

Feed 45.41 $m^3.h^{-1}$
397,000 ppb Chloroform
19,800 ppb Methylene Chloride
41,600 ppb Acetone
49,500 ppb Tetrahydrofuran

Bottoms 56.77 $m^3.h^{-1}$
5 ppb Chloroform
<5 ppb Methylene Chloride
41.6 ppb Acetone
49.5 ppb Tetrahydrofuran
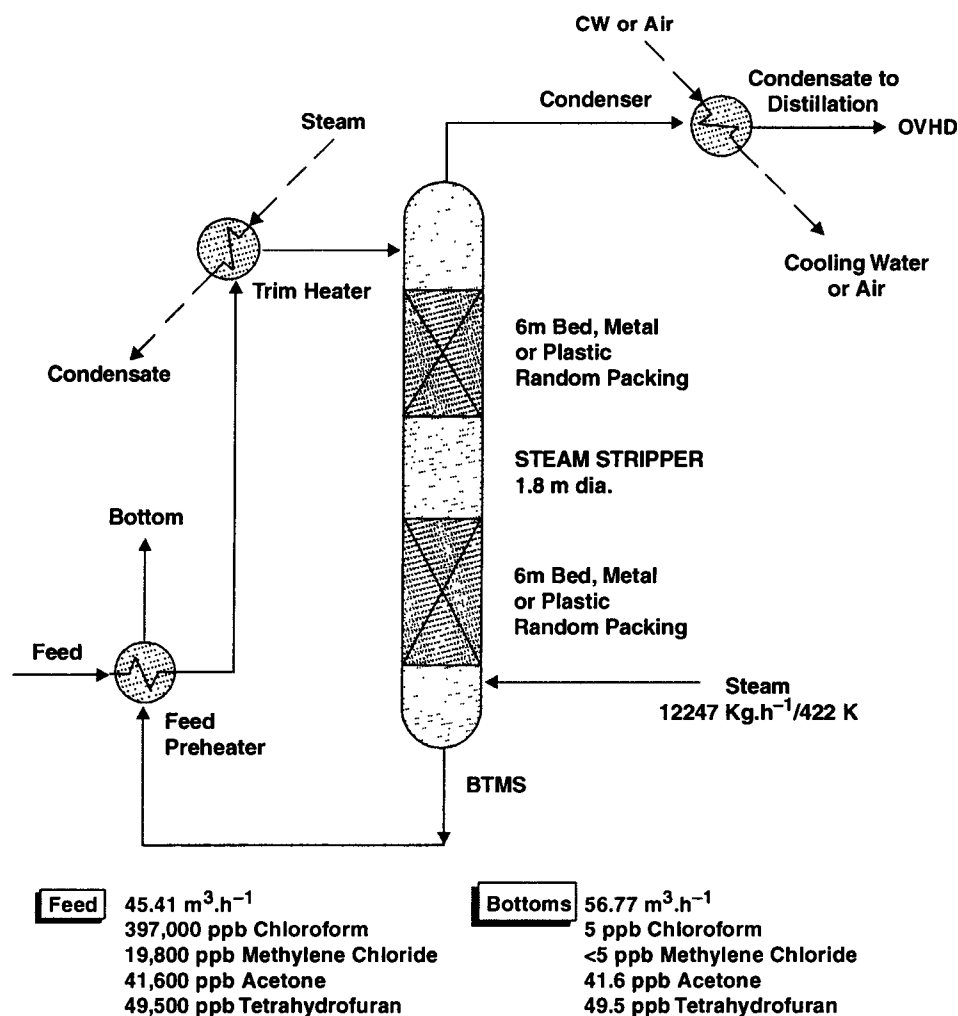
Fig. 2.12.1 : *A typical Steam Stripper with no solvent recovery.*

Steam requirements for stripping vary with

\# operating pressure of the stripper

\# operating pressure and temp. of the steam

\# the type of the VOCs

\# the degree of removal / recovery of VOCs

Important Design Considerations

I. The column must be capable of handling enough steam-flow to operate without the **BTMS-heat-recovery-exchanger**. This will be necessary during column startup and when the exchanger is on outage for cleaning / rectification.

II. Most of the aromatics and halogenated VOCs are only partially miscible in water. They separate into a distinct organic phase when the concentration exceeds a certain limit called the *solubility limit*. Steam stripping is very effective in such applications since **OVHD** vapor upon condensing separates out as a distinct layer from the aqueous layer and can be easily decanted **(Fig. 2.12-2)**

Design Conditions :

Vapor flow at bottom of column = 2548 $m^3.h^{-1}$ at 0.64 $kg.m^{-3}$
Vapor flow at top of column = 2141$m^3.h^{-1}$ at 1.44 $kg.m^{-3}$
Liquid flow below feed point = 31$m^3.h^{-1}$ at 800 $kg.m^{-3}$
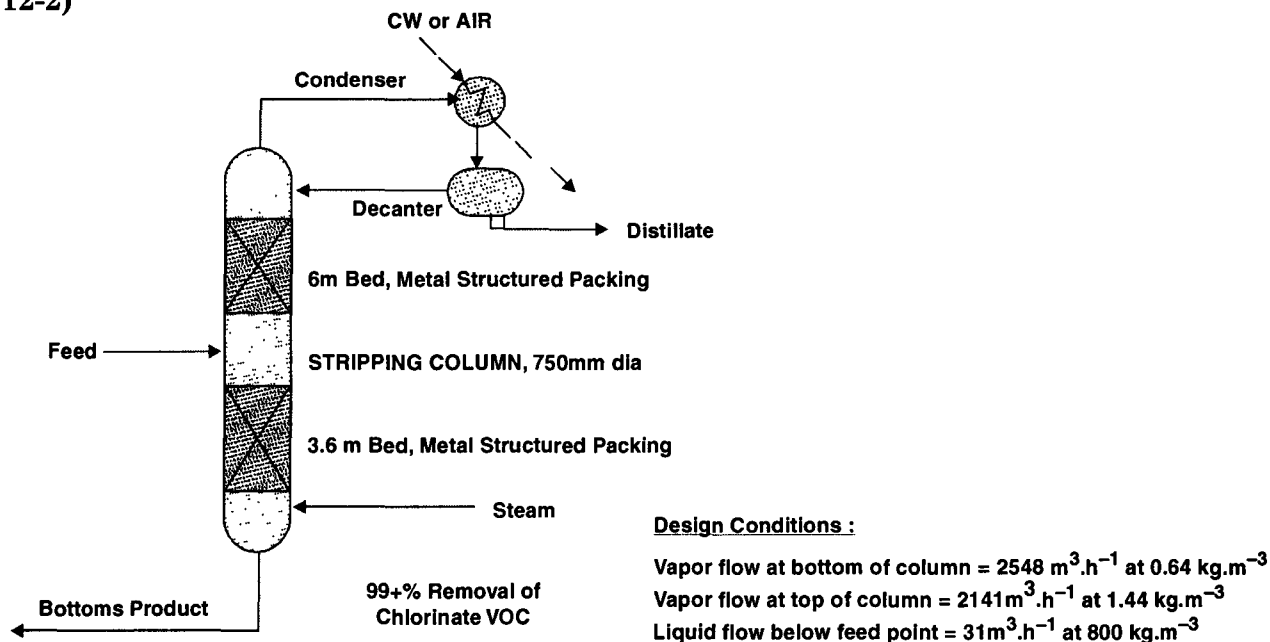
Fig. 2.12-2. *The steam stripper, condenser and decanter form a closed loop. While the water layer, in the decanter, is recycled to the stripping column for reprocessing, the VOC is collected as distillate.*

However, the design of decanter is beset with some problems :

- the condensate waterflow is much larger than the condensate organic flow
- in some cases the organics are lighter than water. Benzene, toluene are two good examples
- still in some cases the aq. phase is lighter than organic phase which includes halogenated organics

III. For better organic recoveries from more dilute streams, the stripper should be hooked up with a separate recovery column or, the stripper should be integrated with a distillation column at the top **(Fig. 2.12-3 A & 2.12-3B).**

The arrangement, as shown in **Fig. 2.12-3A,** is preferred where required steam flowrates are larger *i.e.* when contaminants are moderately volatile.

IV. Accurate and reliable equilibrium data are all but essential. Henry's law

$$yP = Hx$$

where y = mole fraction of VOC in the vapor phase
       x = mole fraction of VOC in the liquid phase
       P = total pressure
       H = Henry's Law Constant in pressure units

is to be used with due care because of broad concentration ranges, high temps., extensive interaction between components, and the existence of two liq phases.
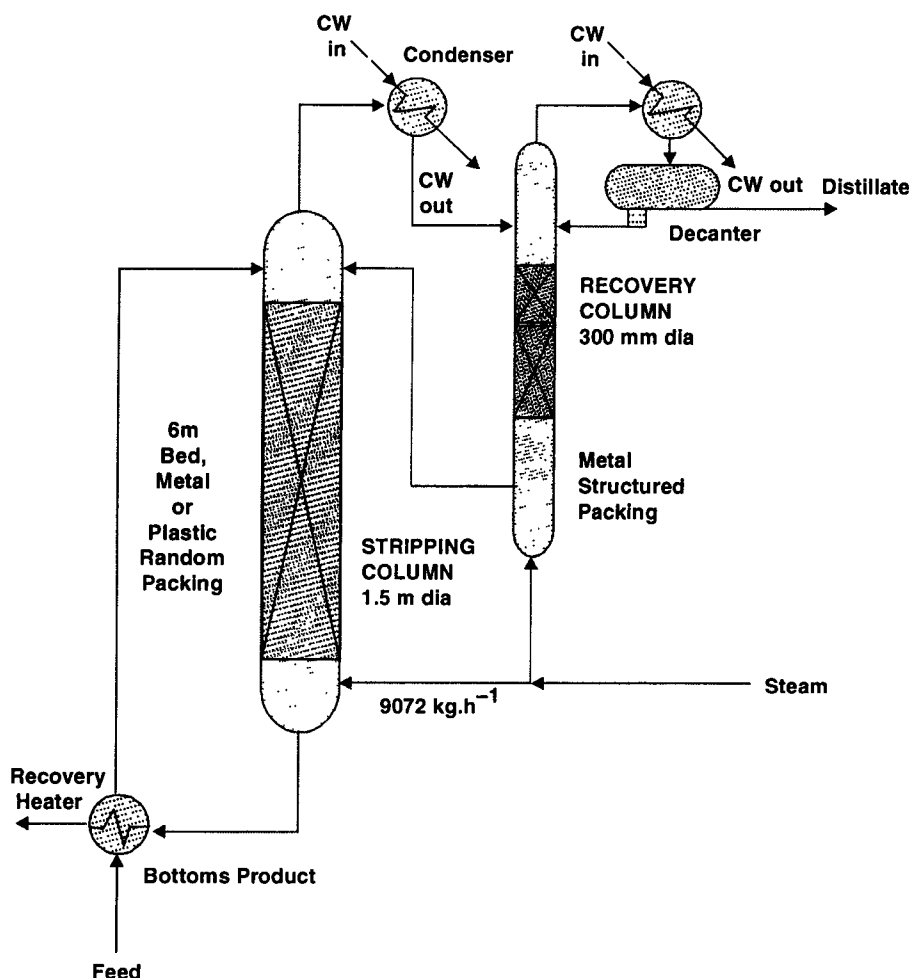
Fig. 2.12-3A. *Steam stripper coupled with a recovery column ensures better recovery of moderately and immiscible systems.*

V. Wastewaters can be very fouling, particulary when they are heated. As the temperature is raised, many inorganic salts precipitate.

Recovery exchanger is the most fouling-prone area. So it requires that the system design must take care to make provisions for frequent cleaning.

In the absence of recovery exchanger, the stripper bears the brunt of fouling. For fouling services trays are a better choice than packing.

Use of sequestering agents (antiscalants) recommended for good and reliable operation over a prolonged period.

VI. Plastics are good corrosion-resistant but they should be temperature-resistant as most of the plastic packings deform or tend to deform at temperature $\geq 410K$

Trays / packings made of stainless steel are costlier than plastic trays or packing. But capital savings achieved by using cheaper MOC generally translate into severe problems and added expenses later.

VII. Optimum design requires stripping factor between 1.5 and 6. Such a high value of λ mandates more stripping stages and that means taller tower and hence higher cost. Design under

these conditions becomes very sensitive to mass-trasfer models and **VLE** data. And, it is at this stage, high-performance trays and high-efficiency structured packings come in good stead. They keep **HETP**
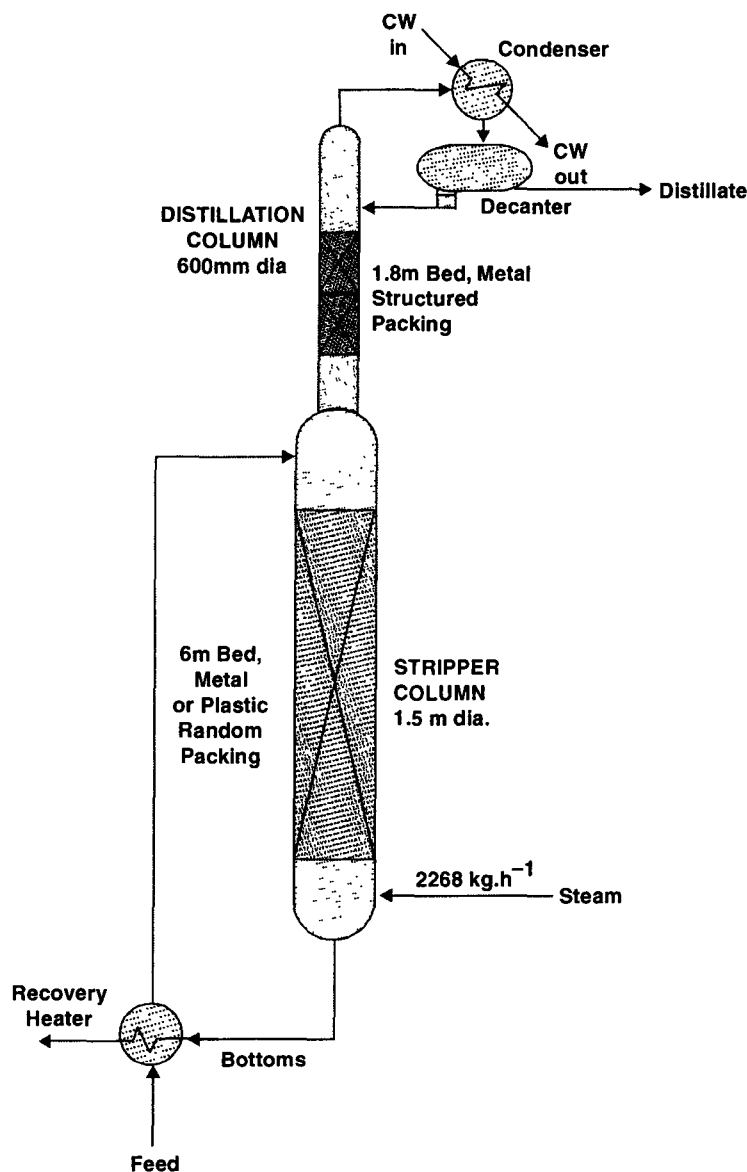
Fig. 2.12-3B. *Steam stripper integrated with a distillation column for better recovery of volatile and immiscible organic substances.*

or **HTU** down and ensure a more compact stripper design. Vendor's experience in the design of steam stripping is extremely valuable.

DESIGN PARAMETERS

1. Henry's Law Constant plays an important part in determining the required *steam : water* ratio in the stripper. Since *stripping factor is proportional to the vapor : liquid load in the column*, Henry's law constant determines the values of stripping factor and in that way it influences the number of transfer units **(NTUs)** and the height of a transfer unit **(HTU)**.

However, it is difficult to find reliable data on Henry's constant **H** because it

* varies dramatically with temperature

* changes abruptly due to the presence of other solutes

Generally, **H** increases with temp. and with the concentration of inorganic salts in water. The effect of inorganic salts is usually neglected but the effect of temperature should always be considered. Since a stripper is not operated with a uniform temperature thruout, a constant value of **H** is not applicable over the entire column. Therefore, Henry's law should be applied locally at each stage, allowing the variations of **H** from stage to stage depending on temperature and concentration.

Since a single **VOC** in wastewater is a rare occurence, the effect of additional organic solutes can be very important (see **Table 2.12-1** for benzene)

Table 2.12-1. Typical Values of Henry's Law Constant At 293K

VOC	H (atm)
Carbon tetrachloride (CTC)	1183
Perchloroethylene	800
Trichloroethylene (TCE)	500
Ethylbenzene (EB)	389
Benzene (B)	240
Benzene in presence of 2% wt. *iso*propanol	15
1:1:1- Trichloroethane (TCA)	200
Chloroform	180
Methylene chloride	125
Dichlorobenzene (DCB)	71
1:1:2:2- Tetrachloroethane	20
Methyl *iso*butyl ketone	7.1
Methyl ethyl ketone	1.7

From Henry's law

$$y.P = H . x$$

$$\therefore \qquad y = (H/P)x$$

$$= m.x$$

That's how equilibrium line **(EL)** is constructed (for the key VOC) with slope

$$= m$$

$$= H / P$$

At low pressure, $\qquad$ **H = f.P°**

where, $\quad$ **f** = activity coefficient of the organic component

$\qquad$ **P°** = vapor pressure of the pure organic component

2. Operating Pressure plays a decisive role in determining the separation efficiency, reliability and cost of steam stripping.

Operation at lower pressures (vacuum stripping) means lower volatility of VOC and hence enhanced stripping. Besides, operation at lower pressures means lower operating temperatures and hence reduced cost. So vacuum steam stripping is a low-cost option. Over and above, vacuum stripping

is associated with low degree of fouling by inorganic precipitation and imposes lower demand on heat recovery requirements.

As the vacuum stripper is operated at reduced temperature, vaccum stripping may be very energy efficient since feed need not be preheated to high temps. Since vacuum strippers operate at moderate temperature, use can be made of plastic packings, trays and tower internals to deal with corrosive systems effectively. However, vacuum strippers require vacuum pumps or ejectors that must be installed to pull vacuum into the system.

On the other hand pressurized strippers do not require a vacuum system. They operate hotter and the pressure of the stripper is determined by the pressure in the reflux accumulators.

Vacuum stripping normally operates at around 1.4kPa. abs. to prevent precipitation of inorganic salts whereas pressure stripping operates in the pressure range : 3.5 — 7kPa.

3. Stripping Factor (S) is the most important design variable in a stripper. It is defined by

$$S = m\,\frac{G}{L}$$

$$= \frac{H}{P} \cdot \frac{G}{L}$$

where   G = molar gas rate, kmols. h^{-1}

L = molar liq rate, kmols. h^{-1}

m is the slope of the equilibrium line and is equal to Henry's constant **(H)** upon operating pressure **(P)**.

Now greater the stripping factor, the more efficient is stripping. Obviously the stripping efficieny increases with higher steam-load, lower liq-load and lower operating pressure. Again, the most economical stripper designs are those that operate with minimum steam load but maximum possible liquid-load.

The stripping factor, for the sake of design should be always taken greater than unity. In cases where designer opts to reduce the rate of stripping medium to buy economy in stripper design, he should base his design with S value between 3 and **6.** S-value below 3 is not recommended because of the lack of reliability of **H** values in most cases of VOC combinations.

4. LIQ / VAP Ratio

Stripping towers are not commonly designed on the basis of floodpoint calculation. Since strippers are designed to operate with maximum possible liquid load and minimum steam load for the sake of economy, the diameter of the tower is dictated by the liquid rate.

Liq loading (L) in excess of 1.425 m^3.min^{-1}.m^{-2}(35 gpm / ft^2) and **vap loading** (F-factor = $v_G \cdot \sqrt{\rho_G}$) as low as 0.9 kg.s^{-1} (kg.m^{-3})$^{\frac{1}{2}}$ $\left(0.5\,\frac{ft}{s} \cdot \sqrt{\frac{lb}{ft^3}}\right)$ are commonly used. This tantamounts to a **L / G** ratio as high as 50 on a mass basis.

SELECTION OF HARDWARE

Trays but mostly packings find their way to steam strippers. Both have their advantages and limitations.

In fouling (biological and inorganic) services both trays and packings can be used but pretreatment of feed is required. Trays are more advantageous in this regard, especially if plugging is a serious problem. Steam strippers are prone to calcium fouling.

Since operating pressure for steam strippers should be kept as low as possible to minimize steam consumption and reduce fouling, high performance modern structured packings can be a good choice. They are particularly worthy for low pressure services.

The cardinal rule is :

use tray towers for fouling services

and

use packed towers for foaming services

The foaming tendencies should be checked under actual process. The plant should address water chemistry early in design and always consider pretreatment. For foaming services packings are always recommended to give mechanical deterrence to foamover. Trays must not be used in foaming systems, as foam from a tray below reaching the tray above will disturb the vap-liq equilibrium on the latter and degrades its efficiency.

For vacuum services packings perform much better than trays. Hence for system where pressure drop is crucial, trays are only marginally applicable but not recommended. Packings are far more suitable canditates.

Both high performance trays and packings fare at par to ensure high removal efficiency.

For heat recovery service, packings fare much better than trays which are applicable with limitations. However, ΔP is crucial.

If process characteristic is corrosive, plastic packings and internals are recommended. **SS** trays can be used but they are costly. Now-a-days plastic trays are available. They can be installed for steam stripping VOC.

Though turndown characteristics for trays and packings are equal, the initial cost for packed tower is higher than trayed tower.

DESIGNING A PACKED-BED VOC STRIPPER

For a given packing working under required operating condition, what the designer wants to know ultimately are :

● **the height (Z) of the packed bed required to achieve the specified separation**

● **press. dr. (ΔP) across the packed-bed**

The required height of packing **(Z)** is the product of the number of transfer units **(NTU)** and the height of a transfer unit **(HTU)** :

$$Z = NTU \times HTU$$

NTU is a variable that relates exclusively to the stripping factor **(S)** and the degree of removal. For a VOC stripper

$$NTU_{o,L} = \left| \frac{S}{S-1} \right| \cdot \ln\left[\left(1 - \frac{1}{S}\right) \frac{x_{IN}}{x_{OUT}} + \frac{1}{S} \right]$$

where x_{IN} and x_{OUT} are the inlet and outlet concentrations of a component VOC in the liquid phase.

At values of $S \geq 12$, this equation can be simplified to

$$NTU_{o,L} = \ln\left|\frac{x_{IN}}{x_{OUT}}\right|$$

HTU depends on the stripping factor, liquid load, and the packing efficiency.

The way to determine $HTU_{o,L}$ is to resort to a valid correlation or experimental data adapted to the conditions of the design and applicable to the packing being considered.

Experimental data are difficult to obtain and difficult to validate. Nevertheless, they represent the best basis for design. It is a good advice to compare always a design based on experimental data with a correlation method. The best correlation currently available is the **Onda model** developed by the **Separations Research Program** at the University of Texas, Austin, USA.

For packed-bed steam strippers for VOC removal, the resistance to mass-transfer lies mostly in the liquid phase and as such the packed bed depth required to achieve a separation will be

$$Z = HTU_{o,L} \times NTU_{o,L}$$

Typical design values of $HTU_{o,L}$ of a few selected random packings based on their performance are presented in **Table 2.12-2**.

Table 2.12-2. $HTU_{o,L}$ Values For Typical Random Packings In VOC Steam Stripping

Packing	MOC	S	Liq Load $(m^3.min^{-1}.m^{-2})$	$HTU_{o,L}(m)$
50mm Spherical Packing	Polypropylene	6		0.88
-do-	Polypropylene	9		0.96
89mm Spherical Packing	Polypropylene	6		1.02
-do-	Polypropylene	9		1.11
40mm Rings	Stainless Steel	6		0.96
-do-	Stainless Steel	9		1.08

The selection of the proper value of $HTU_{o,L}$ for the design should, better, be left on the shoulder of the packing vendor as a process guarantee is often associated with a design.

Important : The VOC stripper designer should avoid using **HETP** values of packings in the computation of $HTU_{o,L}$. These are supplied by packing vendors and also available in open literatures.

The height equivalent to a theoretical plate **(HETP)** is a popular concept adopted for design of distillation columns packed with random or structured packings. If used in the design of VOC stripper, **HETP** values become several times those found in conventional distillation using the same random or structured packings. This is because **HETP** values of packing as quoted by the packing vendors are defined, on the basis of distillation variable, in terms of height of a transfer unit in a gas phase. Therefore, **HETP** is a variable that is well-suited for systems where the resistance to mass transfer is in the gas phase. Stripping systems exhibit, in most cases, the majority of resistance to mass transfer in the liquid phase. Thus, when the values of $HTU_{o,L}$ are converted to HETP, the values of **HETP** become in the range 1.8—3.6m which is 2 to 4 times of $HTU_{o,L}$ for given packing at a specified

liq load and stripping factor. This is due to shift of mass-transfer resistance from liquid to gas phase and not due to inherent inefficiency in the packings.

Pressure drop is an important parameter in the design of strippers, particularly those for low pressure applications. Since packed towers operate at significantly lower ΔP than trays, they are more desirable for low-pressure applications. Press-drop correlations are presented in **Fig. 2.12-4.**

Estimation of pressure drop and maximum capacity of the packed strippers is critical. Since packed towers operate at much higher liquid loading than at top, the bottom pressure of stripper is much higher. Hence the bottoms pressure in the stripper has a pronounced effect on the **BTMS** temperature and on the volatility of VOC.

$$X = \frac{L'}{G'}\left[\frac{\rho_G}{\rho_L - \rho_G}\right]^{0.5}$$
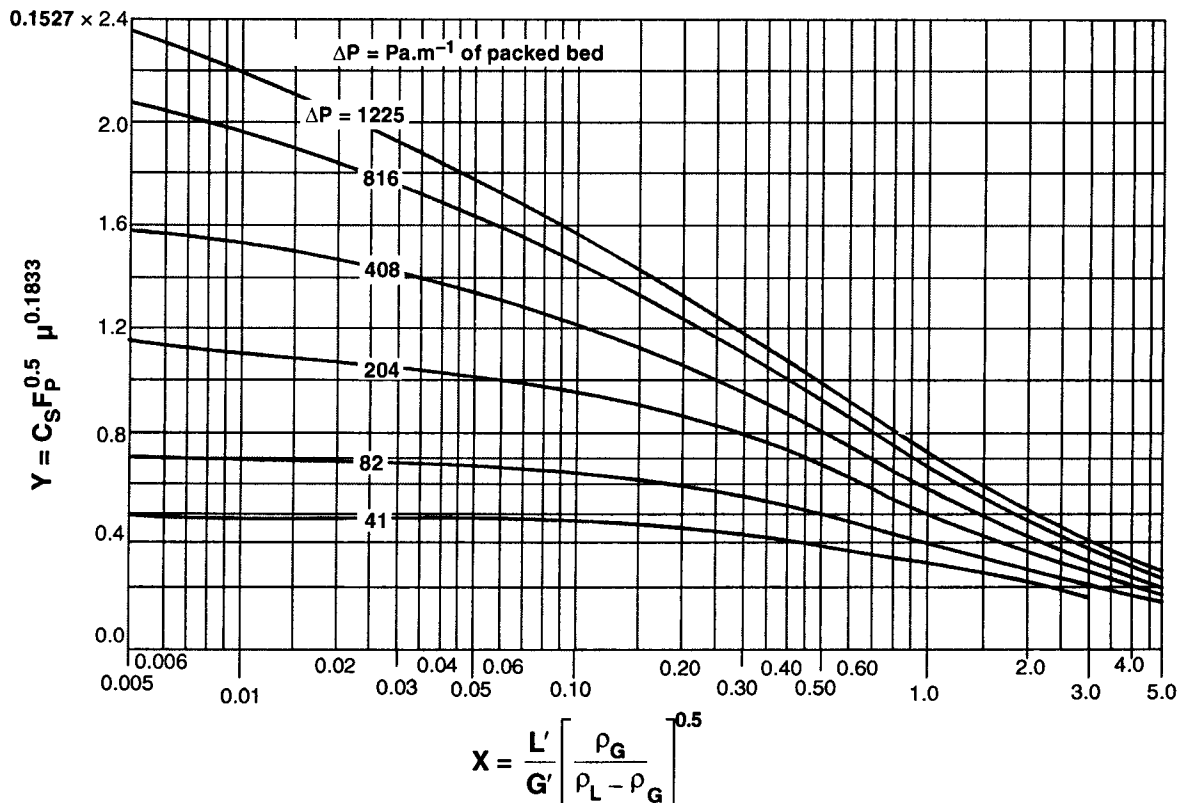
Fig. 2.12.4. *Generalized Pressure Drop Correlation*

SOME GUIDELINES

1. VLE Data : The design of a stripper is fundamentally based on Henry's constant for the target VOC. Experimental values of **H** are available in open literatures, but unfortunately they do not always agree with other published values or values obtained from field trials and installations.

The Henry's Law constant is a thermodynamic function that depends on temperature and composition. There have been many misguided efforts that've tried to link **H** to mass-transfer performance by regressing values of **H** from actual stripping data. This is an erroneous procedure that holds a fundamental thermodynamic variable dependent on totally unrelated parameters such as liquid distribution, packing shape and size, column levelness, gas distribution, instrument accuracy, and so on. Therefore, values of **H** determined in this way must not be used for design as they'll lead to dangerously unreliable scale-up and invite wrong answers.

What the designer ought to do is to determine the values of **H** from good experimental data on volatility and solubility [Gmehling *et. al.,* **Vapor-Liquid Equilibrium Data Collection, DECHEMA, Frankfurt, Germany**] and determine column efficiency separately using the proper value of **H**.

2. Gas and Liquid Distributions : Surprisingly some well designed strippers perform badly. And very often than not the blame is laid on packing. In most cases this allegation is unfounded as the packing performs only as well as the initial liquid and gas distribution to it. That is, if there is poor initial gas and liquid distributions, then packing will continue to perform badly.

Many a cases, badly designed liquid distributors and gas inlet nozzles have been found to be the main culprit in nonperforming strippers. Therefore, care should be taken to design and install proper distribution devices in the stripper.

Since strippers are designed to operate with minimum gas (air or steam) load and maximum liquid (contaminated water) load, many stripper applications involve very large liquid loads, sometimes exceeding $1.22 \text{ m}^3.\text{min}^{-1}.\text{m}^{-2}$, coupled with very low gas loading (**F-factor** $< 0.45 \text{ kg.s}^{-1} (\text{kg.m}^{-3})^{1/2}$. At such a high liq loading and low gas loading, the liq and gas distribution can act synergistically leading to disastrous consequences in terms of mass-transfer performance.

REFERENCES

1. H.Z. Kister, *Chemical Engineering Progress (Feb. 1994 / P:23–32)*
2. J.L. Bravo and J.R. Fair, *Industrial Engineering and Chemical Process Design and Development (Vol. 21, 1982 / P:162–170)*
3. H.Z. Kister and D. R. Gill, Distillation Design (McGraw–Hill, NY, 1992 / P:585–652)
4. J.L. Bravo, *Chemical Engineering Progress (APR 1993 / P:72–76)*
5. J.A. Bonilla, *Chemical Engineering Progress (Mar. 1993 / P:47–61)*
6. L.A. Robbins, *Chemical Engineering Progress (May 1991 / P:87–91)*
7. J.J. Carroll, *Chemical Engineering Progress (Sep. 1991 / P:48–52)*
8. J.J. Carroll, *Chemical Engineering Progress (Aug. 1992 / P:53–58)*
9. J.L. Bravo, *Chemical Engineering Progress (Dec. 1994 / P:56–63)*

2.13. STEAM STRIPPING TOLUENE FROM WATER : PERFORMANCE OF A SIEVE-TRAY TOWER

As more and more countries are imposing ever increasingly stringent environmental regulations and industrial criteria, air stripping for removal or reduction of volatile organic chemical discharge to the environment becomes increasingly incapable of yielding satisfactory results. The sole cause being : **air stripping simply transfers the organic pollutants from water to air and therefore, the actual amount of VOC discharge to the environment is not reduced.** In refineries & process plants where low level heat (waste steam) is available, steam stripping organic contaminants from the effluent water stands out to be the most desirable method of treatment. The contaminant in steam stripping is recovered as a concentrated, immiscible liq phase for recovery, recycle, or further treatment.

DESIGN HURDLES

Design of steam strippers on *industrial scale for removal of volatile* organic compounds from water is beset with a great deal of uncertainty. This is because :

1. Very often than not laboratory test data are scaled up to design industrial col. Determination of the required number of theoretical stages based on laboratory data is straightforward because the concentration levels involved place the VLE in the Henry's Law regime. However, converting the theoretical stage requirement into actual installed stages is another matter.

2. Such systems are liq-resistance controlled mass transfer systems. The predictive models that validate such systems in laboratory scale are seldom valid for industrial columns.

3. Industrial columns designed for VOC removal must meet design product specifications or the plant will be shut down. Hence, all uncertainty must be covered by safety factors. However, unnecessary, non-productive investment is a direct charge against plant profitability. Excessive oversizing may be counterproductive as it may tell upon otherwise obtainable mass transfer efficiency.

4. The concentration levels involved (10^{-9} mol fraction) may lie outside the range of validity of the mass transfer models.

5. Performance tests of operating commercial units are usually indeterminate. Those industrial units that operate successfully normally have their product which is at or below the detection limit of the analytical instrument. Thus the degree of overdesign is unknown.

In an effort to obtain design guidelines for columns which must remove hydrocarbons from water and to provide basic data to extend tray efficiency models to dilute, liq-resistance controlled sytems John G Kunesh *et.al.* conducted steam stripping toluene from water in a 1.22m dia column at **Fractionation Research, Inc.**, Stillwater, Oklahoma, U.S.A. They used sieve trays as gas-liq contacting device and measured the liq holdup. press. drop., and mass transfer efficiency of the tray stripping trace toluene from water at atmospheric pressure. Since a 1.22m dia col.. can be considered as an industrial-scale column, the measured efficiency provides immediate design guidelines for such services.

Why Toluene ?

Aromatic hydrocarbons, among all various types of organic compounds, possess highest solubility in water. And toluene is a good representative of this class. Besides, its solubility and volatility data are well-known. Its toxicity is moderate. Its b.p. is such that the reboiler and condenser temperatures are easily within the utility system capabilities.

Experimental Procedure

The column was operated in stripping mode for all runs. Liquid was pumped to the top of the column via a static mixture by means of toluene injection pump. The **OVHD** vapor was totally condensed and routed thru the reflux accumulator. Because of the low solubility of toluene in water at temperature below the column conditions, a water-rich phase and toluene-rich phase existed in the accumulator. The hydrocarbon-rich phase was decanted and recycled into the feedstream by the injection pump. The water-rich phase was cycled back to the feedtank.

Column Specification

The stripper was a vertical column of 1.22m ID giving a cross-sectional area of 1.17 m^2

6 Nos. of SS sieve trays (1.6 mm thick each) were set at a spacing of 686mm. Each tray was provided with an outlet weir of 50.8 mm high by 940 mm long. Each tray sported 508 holes (12.7 mm dia) punched in triangular layout with center-to-center hole distance of 38.1 mm (hole-pitch).

The trays having free-area of 1.01m² each provided a bubbling area of 0.86m² per tray. Hole area per tray was 0.0644m² **(Fig. 2.13.1).**

Vertically straight downcomers were installed on each tray and they occupied 13% tower cross-section. Downcomer area at top = Downcomer area at bottom = 0.14 m²
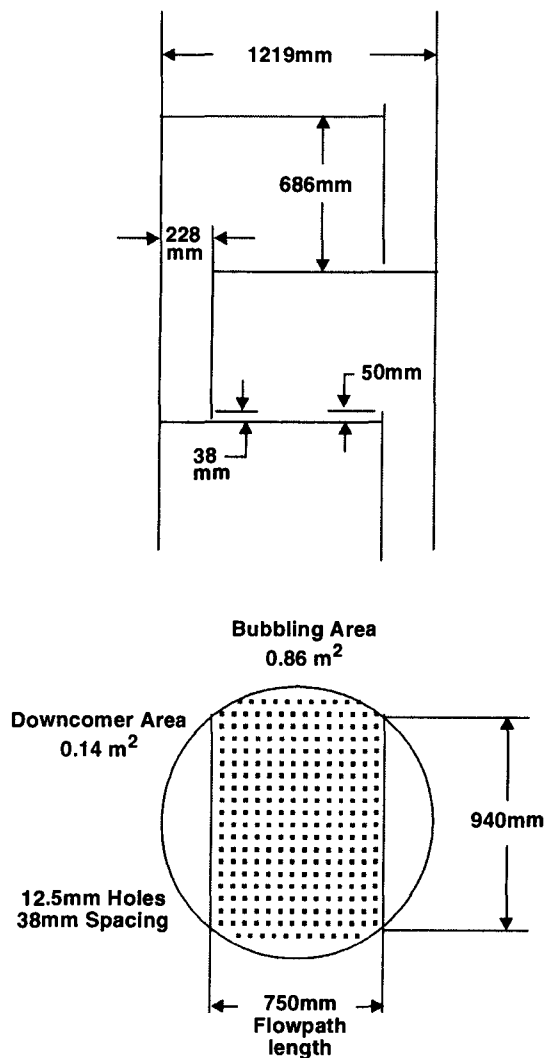
Fig. 2.13.1. *Sieve-tray dimensions.*

Theoretical Background

The feed composition was 1500mg/liter which corresponded to the solubility of toluene in water at 373K (~ 0.0003 mol fraction).

Stripping removes toluene from this maximum possible concentration level to succeedingly lower values depending upon the tray efficiency.

The equilibrium curve is essentially a st. line.

$$y^* = 2300x \text{ [at 1 atm]}$$

as the system obeys the Henry's Law relationship. After fewer than three theoretical stages [upon

McCabe-Thiele Diagram analysis] the liquid composition drops well below 1×10^{-9} mol fraction, or about 1 ppb. (part per billion).

Procedure

I. The internal liq rate was selected (arbitrary)

II. The feedrate to the column top was made equivalent to the liq rate.

III. Several reboiler steamrates were selected to obtain vap rates within a minimal entrainment & minimal weeping region.

Design Equations

A mass balance between the tray **n** and column bottom yields

$$G\,(y_n - y_o) = L\,(x_{n+1} - x_i) \qquad \qquad ...(2.13.1)$$

where, G = gas flowrate, $kmol.s^{-1}$

L = liq flowrate, $kmol.s^{-1}$

y_o = mole fraction of the light component of entering gas phase.

x_i = mole fraction of the light component of exiting liquid.

Rearranging Eqn. 2.13.1 results

$$y_n = \frac{L}{G} \cdot x_{n+1} - \frac{L}{G} \cdot x_1 + y_o \qquad \qquad ...(2.13.2)$$

Therefore, Murphree liq tray efficiency (η_L)

$$\eta_L = \frac{x_{n+1} - x_n}{x_{n+1} - x_n^*}$$

$$= \frac{x_{n+1} - x_n}{x_{n+1} - \dfrac{1}{m} \cdot y_n}$$

$$= \frac{x_{n+1} - x_n}{x_{n+1} - \dfrac{x_{n+1}}{\lambda} + \dfrac{x_1}{\lambda} - \dfrac{y_o}{m}}$$

where, m = slope of the vap-liq equilibrium line (VLE-line)

λ = stripping factor

$$= \frac{mG}{L}$$

$$= \frac{KG}{L}$$

K = equilibrium ratio for the light component. If $y_o = 0$ & $x_1 \ll x_{n+1}$, then Eqn. 2.13.3 simplifies to

$$\eta_L = \frac{x_{n+1} - x_n}{x_{n+1} - \dfrac{x_{n+1}}{\lambda}} = \frac{x_{n+1} - x_n}{x_{n+1}\left|1 - \dfrac{1}{\lambda}\right|} \qquad \qquad ...(2.13.4)$$

VOC being toluene, λ is large usually greater than 100. And this precises Eqn. 2.13.4 to

$$\eta_L = 1 - \frac{x_n}{x_{n+1}} \qquad \qquad ...(2.13.5)$$

which upon rearrangement yields

$$(1 - \eta_L)\, x_{n+1} = x_n \qquad \qquad ...(2.13.6)$$

When applied to each individual tray, Eqn. 2.13.6 becomes

$$(1 - \eta_L)\, x_2 = x_1$$
$$(1 - \eta_L)\, x_3 = x_2$$
$$\vdots \quad \vdots \quad \vdots$$
$$(1 - \eta_L)\, x_{n+1} = x_n$$

Multiplying the above equations both sides, gives

$$(1 - \eta_L)^n = \frac{x_n}{x_{n+1}}$$

or, $$\qquad n \ln(1 - \eta_L) = \ln x_1 - \ln x_{n+1}$$

$$n_{act} = \frac{\ln\left|\dfrac{x_n}{x_{n+1}}\right|}{\ln(1 - \eta_L)} = \frac{\ln\left|\dfrac{x_{OUT}}{x_{IN}}\right|}{\ln(1 - \eta_L)} \qquad \qquad ...(2.13.7)$$

where, n_{act} = actual number of trays.

Assuming that the liquid is completely mixed in the vertical direction and that the gas is completely mixed between trays, a steadystate mass balance over an elemental strip of froth [assuming the vapor is completely mixed in the vertical direction] gives.

$$- L.dx = k_{O,L}\,(x - x^*)\,.\, a.h_f dA \qquad \qquad ...(2.13.8)$$

where $k_{O,L}$ = overall liq phase *mtc*, kmol. s^{-1}. m^{-2}

x^* = mole fraction of light component in the liq in equilibrium with the bulk gas above the tray.

a = interfacial area of froth, m^2.m^{-3}

h_f = froth height, m

dA = area of cross-section of the elemental froth strip, m^2

Rearranging Eqn. 2.13.8 to get

$$\frac{dx}{x - x^*} = - \frac{k_{O,L}.a.h_f}{L}.dA \qquad \qquad (2.13.9)$$

which upon integration (assuming the liq is in plugflow from the inlet weir to the outlet weir without backmixing) results

$$\ln\left|\frac{x_n - x^*}{x_{n+1} - x^*}\right| = - \frac{k_{O,L}.a.h_f\, A_b}{L} \qquad \qquad ...(2.13.10)$$

where, A_b = tray bubbling area, m^2

Now, overall number of liq phase mass transfer unit $NTU_{O,L}$ is defined as

$$NTU_{O,L} \equiv \frac{k_{O,L} \cdot a \cdot h_f A_b}{L} = \frac{M_L}{r_L Q_L} \cdot k_{O,L} \cdot a \cdot h_f \cdot A_b \qquad (2.13.11)$$

Now, combining Eqns. 2.13.4, 2.13.10 & 2.13.11 begets

$$\eta_L = 1 - \exp(- NTU_{O,L}) \qquad \qquad ...(2.13.12)$$

For VOCs present in water, the vapor phase mass transfer resistance is practically absent and for such systems

$$k_{O,L} \approx k_L$$

Applying Higbie's penetration theory

$$k_L \propto \frac{\rho_L}{M_L} \cdot \mathcal{D}_L^{0.5} \qquad \qquad ...(2.13.13)$$

$$\therefore \qquad NTU_{O,L} \propto a \cdot h_f \cdot \frac{A_b}{Q_L} \cdot \mathcal{D}_L^{0.5}$$

$$= a \cdot \frac{h_{cl}}{\varnothing} \cdot \frac{A_b}{Q_L} \cdot \mathcal{D}_L^{0.5}$$

$$= a \cdot \tau_L \cdot \mathcal{D}_L^{0.5}/\varnothing \qquad \qquad ...(2.13.14)$$

where, $\mathcal{D}_L$ = liq molecular diffusion coefficient, $m^2 \cdot s^{-1}$

h_{cl} = height of clear liq on tray, m

$\varnothing$ = froth liq volume fraction

τ_L = liq resident time on tray, s = $\dfrac{h_{cl} \cdot A_b}{Q_L}$

Q_L = volumetric flowrate of clear liq , $m^3 \cdot s^{-1}$

a = interfacial area, $m^2 \cdot m^{-3}$ of froth = $\dfrac{6\epsilon}{\overline{d}}$

$\overline{d}$ = Sauter-mean bubble size

ϵ = froth-vapor volumetric fraction

Plugging the value of a in Eqn. 2.13.14 yields

$$NTU_{O,L} = \frac{1}{\overline{d}} \cdot \frac{\epsilon}{1- \epsilon} \tau_L \cdot \mathcal{D}_L^{0.5} \qquad \qquad ...(2.13.15)$$

The parameters of this equation were determined experimentally.

$NTU_{O,L}$ being known, the Murphree liq tray efficiency is computed from Eqn. 2.13.12.

The number of actual trays needed for designing the system is then obtained from Eqn. 2.13.7.

Liquid Holdup

Hofhuis and Zuiderweg's correlation

$$h_{cl} = 0.6 \, h_w^{\frac{1}{2}} \cdot p^{0.25} \cdot \left| \frac{FP}{I_w} \right|^{0.25} \qquad \qquad ...(2.13.16)$$

matched the experimental data quite well,

where, h_w = outlet weir height, m

p = hole pitch, m

FP = flow parameter, $X = \dfrac{L}{G}\sqrt{\dfrac{\rho_G}{\rho_L}}$

L_w = weir length per unit bubbling area, m.m^{-2}

H-Z correlation is applicable to both the froth & spray regimes.

At a constant liquid rate, the measured liq holdup decreases as the vapor velocity increases. The liq h/up measured near the outlet weir is higher than that measured at the center of the tray.

At low liquid rates, the tray tends to operate in the spray regime.

Pressure Drop

The total tray press. dr. can be approximately given by

$$\Delta P = h_{dry,\,T} + h_{cl} + h_r \qquad \qquad ...(2.13.17)$$

where, $h_{dry,\,T}$ = dry tray press. dr.

$$= \frac{\xi \cdot \rho_G \cdot \upsilon^2_{G,h}}{2g \cdot \rho_L} \qquad \qquad ...(2.13.18)$$

ξ = orifice coefficient

$$= 0.94 \left| \frac{1 - \theta^2}{\theta^{0.2}} \right| \cdot \left| \frac{d_h}{\tau} \right|^{0.2} \qquad \qquad ...(2.13.19)$$

> **Cervenka-Kolar Eqn.**

$\upsilon_{G,h}$ = vapor velocity thru holes, m.s^{-1}
θ = fractional open area
d_h = hole dia, m

Orifice coefficient, ξ can also be determined by applying Zuiderweg Equation

$$\xi = 0.7 \left| 1 - 0.14 \left(\frac{gh_{cl}}{\upsilon^2_{G,h}} \cdot \frac{\rho_L}{\rho_G} \right)^{\frac{2}{3}} \right| \qquad \qquad ...(2.13.20)$$

It was found that the ΔP increases as the liq rate increases at a fixed vapor rate. This is because the liq holdup increases as the liq rate increases. Both the press. dr. models–Cervenka-Kolar and Zuiderweg–predicted the measured press. drops reasonably well at low vapor rates and overpredicted them at high vapor rates especially at high liq rates **(Fig. 2.13.2).**
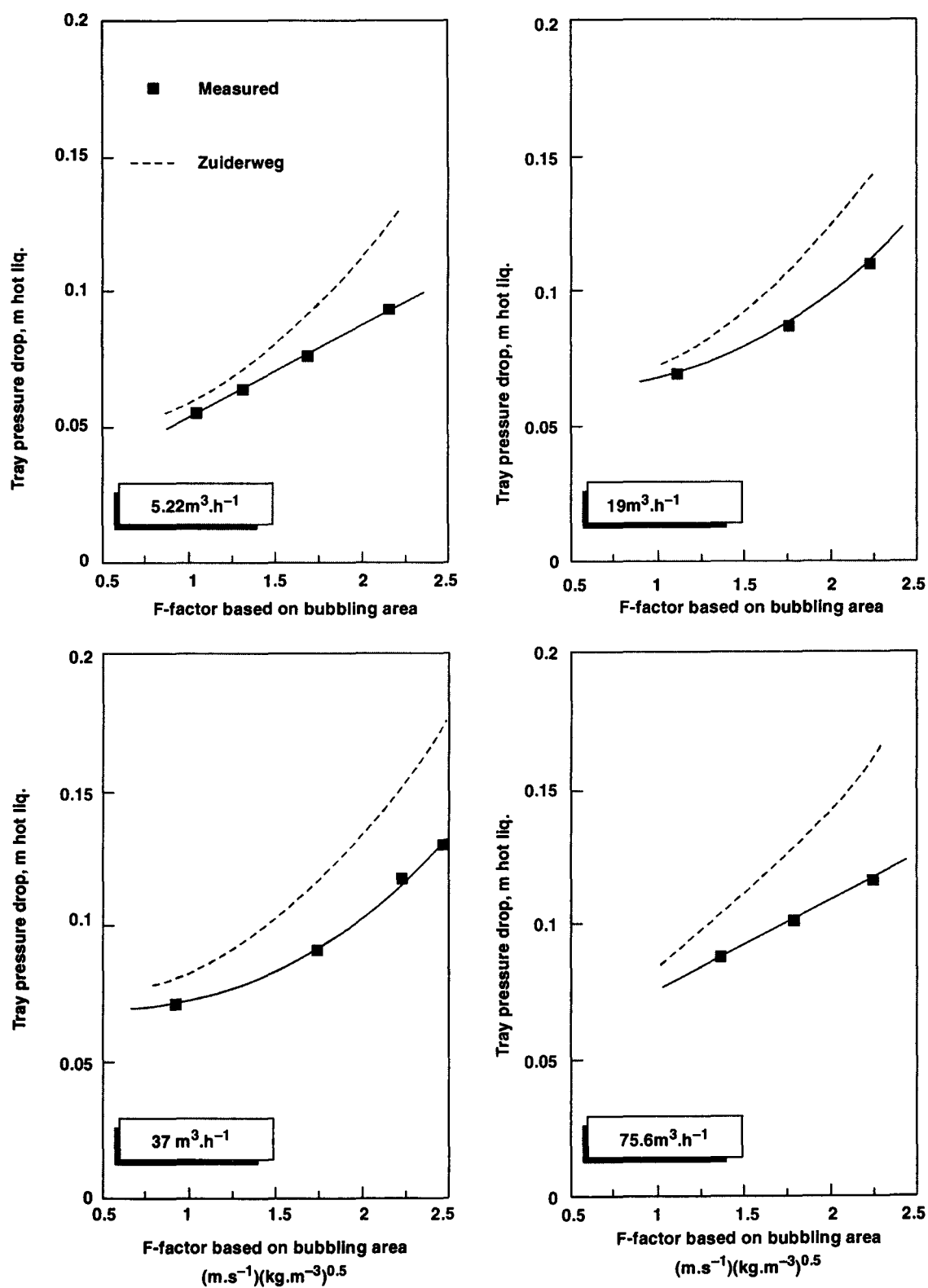
Fig. 2.13.2. *Comparison of measured and predicated pressure drops.*

Overall Tray Efficiency

The overall tray efficiency varied in the narrow range of 30—40%.

The AIChE model matches the measured efficiency at the low liq rate and underpredicts it at high liq rate.

Design Guidelines

1. On the basis of experimental data, a liquid tray efficiency of higher than 95% is not recommended in design.

2. Given the separation $x_{OUT}/x_{IN} = 10^{-20}$ in Eqn. 2.13.7, the total number of actual trays n_{act} needed for this separation can be calculated as a function of h_L from Eqn. 2.13.7.

3. The results show that an increase in tray efficiency from 0.8 to 0.9 reduces the total number of trays by 30% from 12.5 to 8.75. To compensate for this loss, an extra 2 to 3 trays should be inducted to the column.

REFERENCES

1. P. A. M Hofhuis & F. J Zuiderweg, **Institute of Chemical Engineering Symposium Series [No. 56/ 2.2-1/1979]**.
2. AIChE, **Bubble Tray Design Manual** [AIChE, NY, 1958].
3. F. J Zuiderweg, *Chemical Engineering Science [Vol. 37 (10)/P:1441/1982]*.
4. H. Z Kister, **Distillation Design** [McGraw-Hill, NY, 1992].
5. M. J Lockett, **Distillation Tray Fundamentals** [Cambridge University Press, Cambridge, UK, 1986].
6. H. Chan & J. R Fair, *Industrial Engineering Chemical Process Design Development [vol 23/P-814/ 1984]*.
7. G. X Chen & K. T Chuang, *Industrial & Engineering Chemistry Research [vol. 34/P/-3078-1995]*.
8. J. G Kunes et. at., *Industrial & Engineering Chemistry Research [Vol. 35/P-2660/1996]*.
9. M Sakata & T. Yanagi, *Institute of Chemical Engineering Symposium Series [No. 56/3.2-2.1/1999*.
10. T. Yanagi & M Sakata, *Industrial Engineering Chemical Process Design Development [vol. 21 (4)/ P : 712/1982]*.

VOC STRIPPER DESIGN

Problem 2.12. Water available from a ground-water source contains TCE as its chief contaminant to the extent 525 $\mu g.lt^{-1}$

Design an air-stripper to reduce TCE concentration in the effluent to a maximum level of 8 $\mu g.lt^{-1}$

Contaminated water (400 $m^3.s^{-1}$) is available at the battery limit at 289 K.

Blower available at the plant site has the capacity to deliver 12000 $Nm^3.h^{-1}$ of stripping air/289K.

Henry's Law Constant for TCE above water at 289K is 48.636 MPa/mol fraction.
Solution :

A trial-&-error approach, as usual, is to be followed taking an initial estimate of the column ID. This together with packing selected should give rise to a bed depth such that overall bed pressure drop can be overcome by blower specified.

As a case of **Ist Approximation**, let us select a **2500mm dia (ID) column & 50mm plastic Super Intalox® [Norton Co.] saddles for packing.**

Step - (I) Stripping Factor

$$S = \frac{H}{P} \cdot \frac{G_M}{L_M} \qquad \qquad ...(2.11.9)$$

$H_{TCE/289K}$ = 48.636 MPa/mol fraction

P = column operating pressure

= 1 atm. press. (let)

= 0.101325 MPa

A = column cross-section

$$= \frac{\pi}{4}(2.5)^2 \text{ m}^2$$

G_M = gas loading, $kmol.h^{-1}.m^{-2}$

$$= \frac{12000/22.41}{A} \cdot \frac{kmol}{h.m^2}$$

$\boxed{\begin{array}{l} M_{air} = 0.79(28) + 0.21\,(32) \\ = 28.84 \text{ kmol/kg} \end{array}}$

L_M = liq loading

$$= \frac{400 \left|\dfrac{m^3}{h}\right| \times 1000 \left|\dfrac{kg}{m^3}\right| \times \dfrac{1}{18.016} \left|\dfrac{kmol}{kg}\right|}{A, \left|m^2\right|}$$

$$= \frac{4 \times 10^5 / 18.016}{A} \; kmol.h^{-1}.m^{-2}$$

$$\therefore \qquad S = \frac{48.636 \text{ MPa/ mol fraction}}{0.101325 \text{MPa}} \cdot \frac{12000/22.41}{4 \times 10^5 / 18.016}$$

$$\frac{kmol /h.m^2}{kmol /h.m^2}$$

$$= 11.57654$$

Step - (II) Number of Transfer Units

$$NTU_{O,L} = \frac{S}{S-1}\ln\left|\frac{x_t}{x_b} \cdot \frac{S-1}{S} + \frac{1}{S}\right| \qquad \qquad ...(2.11.4.1B)$$

$$\frac{x_t}{x_b} = \frac{x_i}{x_o} = \frac{525 \; \mu g.lt^{-1}}{8 \; \mu g.lt^{-1}} = 65.625$$

$$\therefore \qquad NTU_{O,L} = \frac{11.57654}{10.57654} \ln\left[65.625\left(\frac{10.57654}{11.57654}\right) + \frac{1}{11.57654}\right]$$

$$= 4.4822$$

Step - (III) Packing Height

$$Z = NTU_{O,L} \times HTU_{O,L}$$

The liq loading is

$$L = \frac{400}{A} \frac{m^3.h^{-1}}{m^2} = \frac{400}{\frac{\pi}{4}(2.5)^2} = 814873 \ m^3.h^{-1}.m^{-2}$$

At this liquid loading the $HTU_{O,L}$ value for 50mm plastic **Super Intalox®** packing is 1.5m at 289K.

$$\therefore \qquad Z = 4.4822 \times 1.5m = 6.7233m$$

Step - (IV) Packed Bed Pressure Drop

Now let us check the hydraulic loading of the tower to see whether ΔP over the packed depth is within the permissible limit set by the blower. This is to be estimated from **Figure to problem 2.12.**

The **X** parameter of the figure is

$$X = \frac{L}{G} \cdot \left| \frac{\rho_G}{\Delta r} \right|^{\frac{1}{2}}$$

where, L = liq loading, $kg.h^{-1}.m^{-2}$

$$= 81.4873 \left| \frac{m^3}{m^2.h} \right| \times 998.2978 \left| \frac{kg}{m^3} \right|$$

$$= 81488.446 \ kg.m^{-2}.h^{-1}$$

G = gas loading, $kg.h^{-1}.m^{-2}$

$$= \frac{(12000/22.41)(28.84)\left(kg.h^{-1}\right)}{\frac{\pi}{4}(2.5)^2 \ m^2}$$

$$= 3146.0436 \ kg.h^{-1}.m^{-2}$$

$\rho_G = 1.22537 \ kg.m^{-3}$

$\rho_L = 999.5232 \ kg.m^{-3}$

$\Delta\rho = 998.2978 \ kg.m^{-3}$

$$\therefore \qquad X = \left| \frac{81448.446 \ kg.h^{-1}.m^{-2}}{3146.0436 \ kg.h^{-1}.m^{-2}} \right| \left| \frac{1.22537 \ kg.m^{-3}}{998.2978 \ kg.m^{-3}} \right|^{\frac{1}{2}}$$

$$= 0.9070$$

Likewise, the **Y**-parameter of the Figure is

$$Y = G^2 \cdot \frac{F_b}{\Delta\rho} \cdot \frac{\mu^{0.1}}{\rho_G}$$

where, G = gas loading, $kg.m^{-2}.s^{-1}$

$$= 0.8739 \ kg.m^{-2}.s^{-1}$$

F_p = packing factor

  = 28 for 50mm plastic **Super Intalox®** saddles

μ = dynamic viscosity of liq

  = 1.11×10^{-3} Pa.s

$$X = \frac{L'}{G'}\left[\frac{\rho_G}{\rho_L - \rho_G}\right]^{0.5}$$
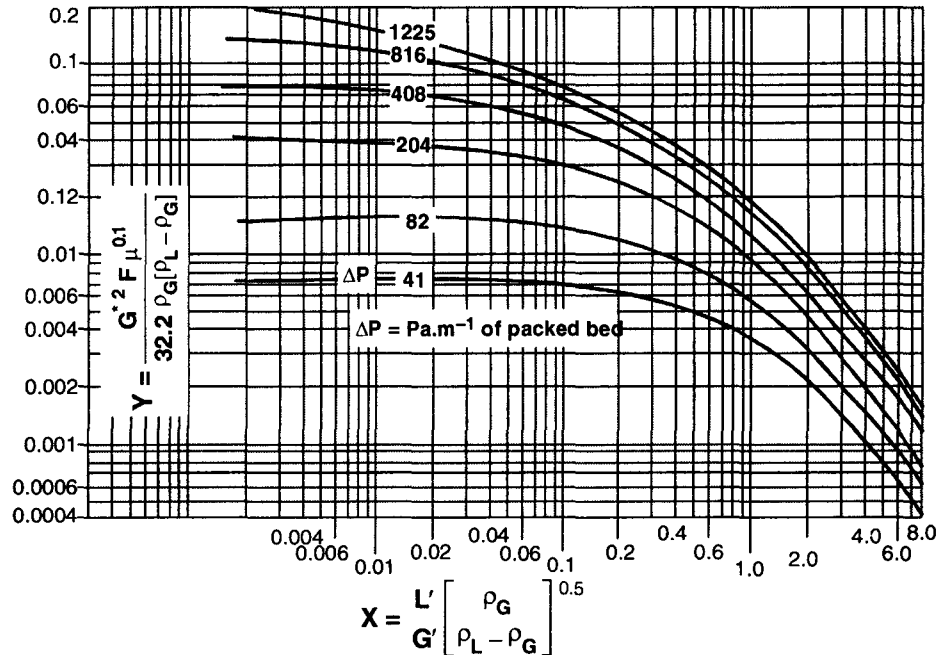
Fig. to Problem 2.12. *Generalized pressure-drop correlation in a packed tower.*
Note : *While evaluating G in FPS unit, take into account 32.2 in the denominator. Disregard this factor for G in SI units.

$\therefore$

$$Y = (0.8739)^2 \, \frac{28}{998.2978} \cdot \frac{\left(1.11 \times 10^{-3}\right)^{0.1}}{1.22537}$$

$$= 0.00885$$

$$\simeq 0.009$$

For

$$X = 0.9 \, \& \, Y \simeq 0.009$$

$$\Delta P \simeq 70 \, \text{Pa.m}^{-1} \text{ of packed depth [Fig. to Problem 2.12]}$$

$\therefore$ Overall bed press drop

$$= \left|170\frac{\text{Pa}}{\text{m}}\right| \times \left|6.7233 \, \text{m}\right|$$

$$= 1142.961 \, \text{Pa}$$

Therefore, the blower should be specified to deliver air at a positive pressure of 1.2 kPa at the inlet to the column.

ESTIMATION OF THE PERFORMANCE OF A PACKED–BED STEAM STRIPPER FOR VOC REMOVAL

Problem 2*13. In a certain stripping column, steam is used to strip trichloroethene (TCE) from water.

The tower (ID 2440mm) is filled with 25mm Pall Rings filled to a height of 7470mm.
Given :

Inlet concentration of TCE = 72 μg. l⁻¹

$\boxed{Liquid}$

rate = 456.277 t. h⁻¹

velocity = 0.028 m. s⁻¹

density = 958 kg. m⁻³

dynamic viscosity = 29 × 10⁻⁵ kg. m⁻¹. s⁻¹

equilibrium ratio = 8765

surface tension = 0.065 N. m⁻¹

diffusion coefficient = 4.16 × 10⁻⁹ m². s⁻¹

$\boxed{Steam}$

rate = 11 t.h⁻¹

velocity = 1.08 m. s⁻¹

denstiy = 0.605 kg. m⁻³

dynamic viscosity = 17 × 10⁻⁶ kg. m⁻¹. s⁻¹

diffusion coefficient = 1.24 × 10⁻⁵ m². s⁻¹

Calculate

- *liquid holdup*
- *pressure drop*
- *mass transfer coefficients*
- *the interfacial area for a steam stripping col.*
- *HTU*
- *NTU*
- *TCE concentration at stripper effluent (i.e. bottom liquid)*

Solution : For design of stripping columns, there are two parts :

– hydraulic calculations that provide the diameter of the column
– mass-transfer calculations that provide the effective bed height of the column

Hydraulic operation and the mass-transfer process should be simultaneously considered by using the Engel model for irrigated pressure drop and flooding. This method is an extension of the Stichlmair treatment for liquid holdup, irrigated, and flooding pressure drop predictions and is valid for both structured and dumped packings.

[A] Hydraulic Calculations

Step–(I) Equivalent DIA of Packing

The characteristic length of a ring type packing is its equivalent dia which is given by

$$d_p = \frac{6\,(1-\epsilon)}{a_p}$$

where, a_p = sp. surface area of packing, $m^2 \cdot m^{-3}$

= 215 for 25mm Pall rings

$\in$ = void fraction of packing

= 94% for 25mm Pall rings

$$\therefore \qquad d_p = \frac{6\,(1-0.94)}{215} = 1.674 \times 10^{-3} \text{ m}$$

Step – (II) Friction Factor

$$\psi = \frac{C_1}{Re_G} + \frac{C_2}{Re_G^{\frac{1}{2}}} + C_3$$

where C_1, C_2 and C_3 are Sticlmair constants

$$Re_G = \frac{d_p \cdot U_G \cdot \rho_G}{\mu_G}$$

$$= \frac{\left(1.674 \times 10^{-3}\text{m}\right)\left(1.08\,\text{m.s}^{-1}\right)\left(0.605\,\text{kg.m}^{-3}\right)}{\left(17 \times 10^{-6}\,\text{kg.m.s}^{-1}\right)}$$

$$= 64.34$$

$C_1 = 0.05$

$C_2 = 1.0$

$C_3 = 3.0$

$$\therefore \qquad \psi = \frac{0.05}{64.34} + \frac{1.0}{(64.34)^{\frac{1}{2}}} + 3 = 3.125$$

Step – (III) Dry Bed Pressure Drop

$$\Delta P_{dry} = \frac{1}{8} \cdot \psi \cdot a_p \cdot \frac{\rho_G \cdot U_G^2}{\in^{4.65}}$$

$$= \frac{1}{8} \cdot (3.125)\,(215)\,\frac{(0.605)\,(1.08)^2}{0.94^{4.65}}$$

$$= 79.022 \text{ Pa. m}^{-1} \text{ of packed height}$$

Step – (IV) Dynamic Holdup Below The Loading Point

$$h_{dyn,\,o} = 3.6 \left| \frac{U_L \cdot a_p^{0.5}}{g^{0.5}} \right|^{0.66} \cdot \left| \frac{\mu_L \cdot a_p^{1.5}}{\rho_L \cdot g^{0.5}} \right|^{0.25} \cdot \left| \frac{\sigma_L \cdot a_p^2}{\rho_L \cdot g} \right|^{0.1}$$

Now, $\qquad \left| \dfrac{U_L \cdot a_p^{0.5}}{g^{0.5}} \right|^{0.66} = \left| \dfrac{(0.028)\,(215)^{0.5}}{9.81^{0.5}} \right|^{0.66} = 0.26156$

$$\left|\frac{\mu_L \cdot a_p^{1.5}}{\rho_L \cdot g^{0.5}}\right|^{0.25} = \left|\frac{29 \times 10^{-5}(215)^{1.5}}{958(9.81)^{0.5}}\right|^{0.25} = 0.132118$$

$$\left|\frac{\sigma_L \cdot a_p^2}{\rho_L \cdot g}\right|^{0.1} = \left|\frac{0.065(215)^2}{958(9.81)}\right|^{0.1} = 0.89222$$

$$h_{dyn,o} = 3.6(0.26156)(0.1321128)(0.89222) \qquad = 0.11099$$

Step – (V) Dynamic Holdup Above the Loading Point

$$h_{dyn} = h_{dyn,o}\left[1+\left[6\,\frac{\Delta P_{tot}}{\rho_L \cdot g}\right]^2\right]$$

where, ΔP_{tot} = total specific press. dr., Pa. m^{-1}

$$\therefore \qquad h_{dyn} = 0.11099\left[1+\left[6\,\frac{\Delta P_{tot}}{958(9.81)}\right]^2\right]$$

$$= 0.11099 + 4.523 \times 10^{-8}\,\Delta P_{tot}^2$$

Step – (VI) DIA of Liquid Particles

$$d_L = C_L\sqrt{\frac{6\sigma_L}{\Delta\rho \cdot g}}$$

where, C_L = constant for evaluating liq particle dia

= 0.4 for random packing

= 0.8 for structured packing

$$\therefore \qquad d_L = 0.4\left|\frac{6(0.065)}{(958-0.605)9.81}\right|^{\frac{1}{2}} = 2.577 \times 10^{-3}\,m$$

Step – (VII) Specific Surface Area of Liquid Droplets

$$a_L = \frac{6h_{dyn}}{d_L} = \frac{6\left(0.11099 + 4.523 \times 10^{-8}\,\Delta P_{tot}^2\right)}{2.577 \times 10^{-3}}$$

$$= 258.4167 + 1.053 \times 10^{-4}\,\Delta P_{tot}^2$$

Step – (VIII) Total Pressure Drop (ΔP_{tot})

$$\frac{\Delta P_{tot}}{\Delta P_{dry}} = \frac{a_L + a_p}{a_p}\left|\frac{\epsilon}{\epsilon - h_{dyn}}\right|^{4.65}$$

$$\text{or,} \quad \frac{\Delta P_{tot}}{79.022} = \left[\frac{258.4167 + 1.053 \times 10^{-4} \Delta P_{tot} + 215}{215}\right] \left[\frac{0.94}{0.94 - 0.11099 - 4.523 \times 10^{-8} . \Delta P_{tot}^2}\right]^{4.65}$$

$$\therefore \quad \Delta P_{tot} = 332 \text{ Pa. m}^{-1}$$

Step – (IX) Holdup Above The Loading Point

$$h_{dyn} = 0.11099 + 4.523 \times 10^{-8} \Delta P_{tot}^2$$

$$= 0.11099 + 4.523 \times 10^{-8} (332)^2$$

$$= 0.11597$$

Step – (X) Pressure Drop At Flooding

$$\frac{\Delta P_{tot, fl}}{\rho_L . g} = \frac{\left[249 h_{dyn, o} \left(\sqrt{X} - 60 \in -558 h_{dyn, o} - 103 d_L . a_p\right)\right]^{\frac{1}{2}}}{2988 h_{dyn, o}}$$

where, $X = 3600 \in + 186480 \, h_{dyn, o} . \in + 32280 \, d_L . a_p . \in + 191844 \, h_{dyn, o}^2 + 95028 \, d_L . a_p . h_{dyn, o}$

$$+ 10609 \, d_L^2 . a_p^2$$

$$= 3600 (0.94)^2 + 186480 (0.11099) \, 0.94 + 32280 (2.577 \times 10^{-3}) (215) (0.94) + 191844 (0.11099)^2 + 95028$$

$$(2.577 \times 10^{-3}) (215) (0.11099) + 10609 (2.577 \times 10^{-3})^2 (215)^2$$

$$= 50912.039$$

$$\therefore \quad \frac{\Delta P_{tot, fl}}{\rho_L . g} = \frac{\left[249 (0.11099) \{\sqrt{50912.039} - 60 \times 0.94 - 558(0.11099) - 103 (2.577 \times 10^{-3}) (215)\}\right]^{\frac{1}{2}}}{2988 (0.11099)}$$

$$= 0.1123539$$

$$\therefore \quad \Delta P_{tot, fl} = 0.112353 (958) (9.81) \quad = 1055.8912 \text{ Pa. m}^{-1}$$

[B] Mass-Transfer Calculations

Step – (XI)   Effective Velocities

For random packing, the effective gas velocity

$$U_{G, e} = \frac{U_G}{\in (1 - h_{dyn})} \quad \text{where, } U_G = \text{superficial gas velocity, m.s}^{-1}$$

$$= \frac{1.08}{0.94 (1 - 0.11597)}$$

$$= 1.2996 \text{ m. s}^{-1}$$

The effective liquid velocity,

$$U_{L, e} = \frac{U_L}{\in h_{dyn}} = \frac{0.028}{0.94 (0.11597)} = 0.2568 \text{m.s}^{-1}$$

Step – (XII) Gas And Liq-Phase Mass-Transfer Coefficients

$$k_G = \frac{0.1\mathfrak{D}_G}{d_p}\left[\frac{d_p\,(U_{G,e}+U_{L,e})\rho_G}{\mu_G}\right]^{0.2405} \cdot \left[\frac{\mu_G}{\rho_G\cdot\mathfrak{D}_G}\right]^{\frac{1}{3}}$$

$$= \frac{0.1\,(1.24\times10^{-5})}{0.001674}\left[\frac{0.001674\,(1.2996+0.2568)\,0.605}{0.000017}\right]^{0.2405}\cdot\left[\frac{0.000017}{0.605\,(1.24\times10^{-5})}\right]^{\frac{1}{3}}$$

$$= (7.407\times10^{-4})\times2.97240\times1.31348$$

$$= 2.8919\times10^{-3}\ \text{m. s}^{-1}$$

$$k_L = \frac{0.3415\,\mathfrak{D}_L}{d_p}\cdot\left[\frac{d_p\,(U_{G,e}+U_{L,e})\,\rho_L}{\mu_L}\right]^{0.2337}\cdot\left|\frac{\mu_L}{\rho_L\cdot\mathfrak{D}_L}\right|^{\frac{1}{2}}$$

$$= \frac{0.3415\,(4.16\times10^{-9})}{0.001674}\left|\frac{0.001674\,(1.2996+0.2568)\,958}{0.00029}\right|^{0.2337}\left|\frac{0.00029}{958\,(4.16\times10^{-9})}\right|^{\frac{1}{2}}$$

$$= (8.4864\times10^{-7})\,(8.30946)\,(8.53040)$$

$$= 6.0154\times10^{-5}$$

Step – (XIII) Effective Interfacial Area

$$\frac{a_e}{a_p} = \frac{\left[\left(\dfrac{U_L^2\cdot\rho_L\cdot d_p}{\sigma}\right)\left(\dfrac{U_L^2}{g\cdot d_p}\right)\right]^{0.15}\ a_p\cdot d_p^{\,c}}{\left|\dfrac{U_L\cdot\rho_L\cdot d_p}{\mu_L}\right|^{0.2}\cdot\ \epsilon^{0.6}\,(1-\cos\gamma)}$$

where C is a constant whose value depends on packing.

Now,
$$\left[\left(\frac{U_L^2\cdot\rho_L\cdot d_p}{\sigma}\right)\left(\frac{U_L^2}{g\,d_p}\right)\right]^{0.5} = \left[\frac{(0.028)^2\,(958)\,(0.001647)}{0.065}\cdot\frac{(0.028)^2}{9.81(0.001674)}\right]^{0.5}$$

$$= 0.030388$$

$$a_p\cdot d_p^{\,c} = 215\,(0.001674)^{0.246} = 44.6151$$

$$C = 0.246 \text{ for } \textbf{25mm Pall Rings}$$

Value of C

Sulzer BX	0.9772
Mellapak 250Y	0.7312
25mm Fleximax	0.5005
25mm Flexirings	0.6298

$$\left|\frac{U_L\cdot\rho_L\cdot d_p}{\mu_L}\right|^{0.2} = \left|\frac{0.028\times958\times0.001674}{0.00029}\right|^{0.2} = 2.74142$$

$$\epsilon^{0.6} = (0.94)^{0.6} = 0.96355$$

$$1 - \cos\gamma = 1 - 0.41965 = 0.58034$$

where, γ = solid-liq contact angle in packing, degree.

$$\cos\gamma = 5.21 \times 10^{-16.83\sigma} \text{ for } \sigma > 0.045 \text{ N.m}^{-1}$$
$$= 5.21 \times 10^{-16.83 \times 0.065}$$
$$= 0.41965$$

$\therefore$
$$\frac{a_e}{a_p} = \frac{0.030388 \times 44.6151}{2.74142 \times 0.96355 \times 0.58034} = 0.8843$$

$\therefore$
$$a_e = a_p \times 0.8843 = 215 \text{ m}^2.\text{m}^{-3} \times 0.8843 = 190.1245 \text{ m}^2.\text{m}^{-3}$$

Step - (XIV) Overall Mass-Transfer Coefficient

$$\frac{1}{K_L.a} = \frac{1}{a_e}\left[\frac{1}{k_L} + \frac{1}{m.k_G}\right]$$

$$= \frac{1}{190.124}\left[\frac{1}{6.0154 \times 10^{-5}} + \frac{1}{8765(2.8919 \times 10^{-3})}\right]$$

$$= 87.437 \text{ s}$$

$\therefore$ $$K_L.a = 0.011436 \text{ s}^{-1}$$

Step - (XV) Height of A Transfer Unit (HTU)

$$\text{HTU} = \frac{U_L}{K_L.a} = 0.028 (87.437) = 2.448\text{m}$$

Step - (XVI) Number of Transfer Units (NTU)

$$\text{NTU} = \frac{Z}{\text{HTU}} \qquad \text{where, Z = packed bed depth}$$
$$= 7470 \text{ mm}$$
$$= \frac{7.47\text{ m}}{2.448\text{ m}} = 3.051 \qquad = 7.47 \text{ m}$$

Step - (XVII) TCE Concentration At Stripper Bottom

$$\lambda = m\frac{G}{L} = 8765\left|\frac{11}{456.277}\right| = 211.308$$

$$\frac{x_{IN}}{x_{OUT}} = \left[\exp\left|\frac{\lambda-1}{\lambda}\right|\text{NTU} - \frac{1}{\lambda}\right]\frac{\lambda}{\lambda-1}$$

$$= \left[\exp\left(\frac{210.308}{211.308} \times 3.051\right) - \frac{1}{211.308}\right]\frac{211.308}{210.308}$$

$$= 20.927$$

$\therefore$ $$x_{OUT} = \frac{72}{20.927} = 3.44049 \text{ µg.l}^{-1}$$

REFERENCES

1. J. Stichlmair, *et. al.*, **Gas Separation & Purification** *(vol. 3/1989/P-19)*.
2. J. A Rocha, *et. al.*, **Industrial & Engineering Chemistry Research** *(vol. 32/1993/P-641)*.

3. J. A Rocha, *et. al., Industrial & Engineering Chemistry Research (vol. 35/1996/P-1660).*

4. J. J Gualito, *et. al., Industrial & Engineering Chemistry Research (vol. 36/1997/P-1997).*

5. G. J Kunesh, *et. al., Industrial & Engineering Chemistry Research (vol. 35/1996/P-2660).*

6. Y. L. Hwang, *et. al., Industrial & Engineering Chemistry Research (vol. 31(7)/1992/P-1759).*

7. J. R. Ortizo–Del Castillo *et. al., Industrial & Engineering Chemistry Research (vol. 39/2000/P-731).*

2.14. IMPROVING SOUR WATER STRIPPERS

In conventional designs, stripper efficiency is related to steamflow which, in turn, is limited by stripper capacity. However, heat integration scheme can be implemented to hike up stripper capacity by as much as 50% cutting steamflow drastically down.

Stripping Conditions

Solutes (H_2S, CO_2, NH_3) dissolved in sour water are weak electrolytes which are partially dissolved into ions in the liquid phase :

$$\underset{(dis)}{CO_2} + \underset{(dis)}{NH_3} + H_2O \rightleftharpoons HCO_3^- + \overset{+}{N}H_4$$

$$HCO_3^- + \underset{(dis)}{NH_3} \rightleftharpoons CO_3^{2-} + \overset{+}{N}H_4$$

$$\underset{(dis)}{H_2O} + H_2O \rightleftharpoons \bar{S}H + H_3\overset{+}{O}$$
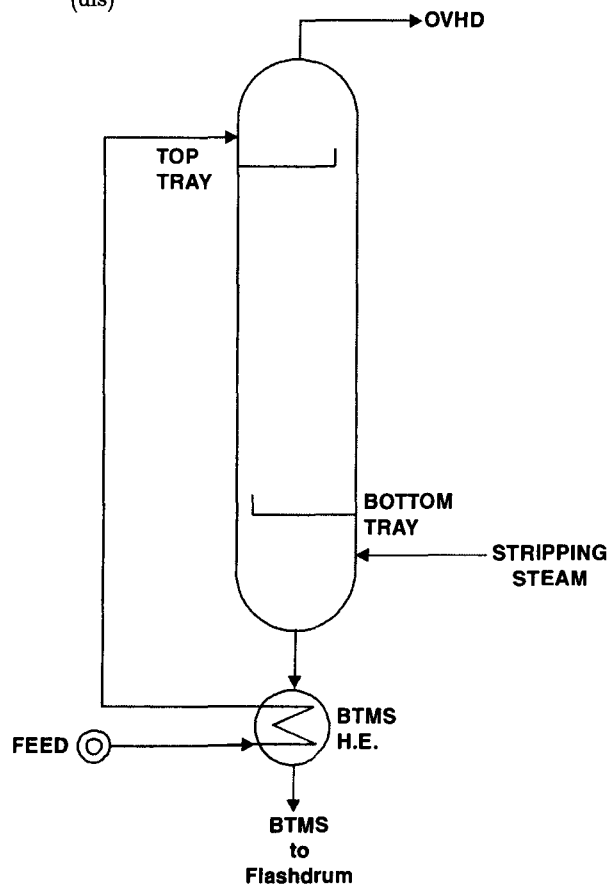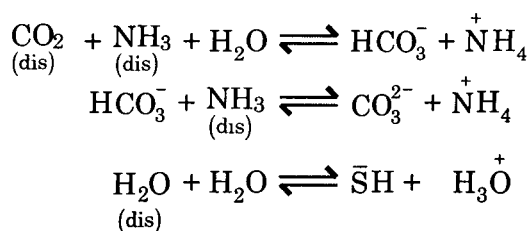
Fig. 2.14-1. *Conventional stripper design. The liquid feed introduced at the top of the column moves countercurrent to the stripping steam introduced at the bottom.*

Since the molecular form favors stripping, higher temperature accentuates desorption process of ammonia, carbon dioxide and hydrogen sulfide by way of shifting the above equilibrium to the left and increasing the relative volume of the components. And for sour water strippers, it has been observed that optimum temperature range in between 425K to 455K for strippers operating at 1.013MPa to 1.215MPa.

In this context the role played by the stripping steam is two :

- **supplying the necessary heat that goes to provide the heat of reactions taking place in the liq phase and the heat of desorption of NH₃, CO₂ and H₂S.**
- **increasing the feed temperature from its inlet value to BTMS value (Fig. 2.14-1).**

Major part of the steam gets condensed and adds to the flow of the bottom stream and the remaining supplied steam acts as a '**Carrier**' and leaves the tower at the top as overhead vapor with NH_3, H_2S and CO_2.
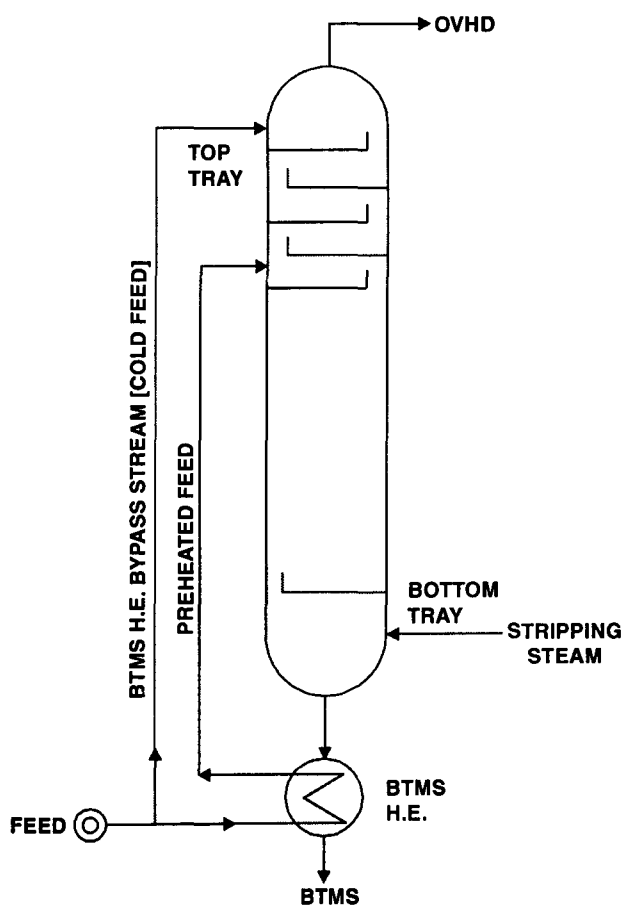
Fig. 2.14-2. *A heat integrated system. The feed is divided into two streams—one is preheated in the feed preheater by exchanging heat with BTMS and fed a few tray below the top tray while the remaining cold feed is directed to the top tray with the objective to 'quench' the upgoing vapor reducing the water load in OVHD vapor stream.*
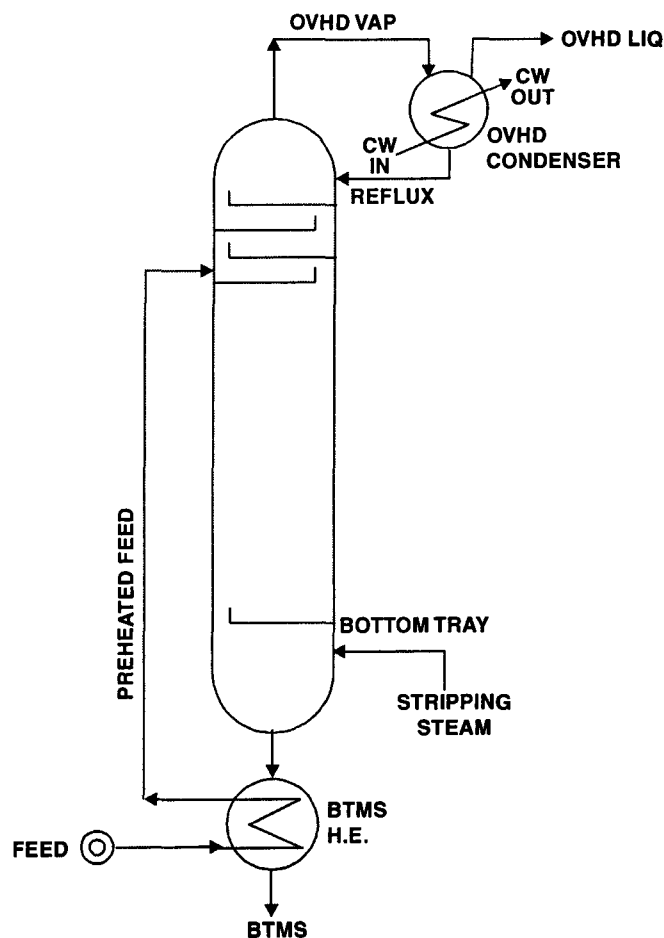
Fig. 2.14-3. *Another heat integrated stripper column. This one is with an OVHD condenser in line. The feed is preheated to extract much of input heat while the relatively cold reflux rich in H₂S, NH₃ is recirculated to the system to ensure better stripping, and keep Tray-1 temperature to a desired level. The OVHD condenser condenses out the water vapor in OVHD stream reducing H₂O load in exit gases.*

Since the steam load of the **OVHD** vapor is dictated by the column top temperature, the Tray–1 (top tray) temperature becomes the key variable to delimit the water vapor concentration in the **OVHD**, for it is the Tray–1 temperature that controls the partial pressure of water vapor leaving the Tray–1. This is very important for those systems where water-restricted overhead stream is an imperative.

To obviate this difficulty, scheme **B** and **C** are developed [**Fig. 2.14-2 and 2.14-3**]. In scheme –**B**, the stripper section above the inlet feed acts as a **'dryer'**, since water vapor going up gets quenched and condensed in contact with the colder downcoming liquid and thereby reducing the water content in the top vapor.

DESIGN OF A MULTITRAY-ABSORBER FOR THE SEPARATION OF ETHANE FROM NATURAL GAS

Problem 2.14. *Design an absorber (trayed column) for the separation of ethane from natural gas.*

Data

1. **Feed gas**

    [A] Composition (% by volume)

N_2	C-1	C-2	C-3	Moisture
2	78	16	4	250 K dewpoint

    [B] Rate : 5443 kmol. day^{-1}

    [C] Conditions : 302.5 K/2.825 MPa.

    $$[\text{C-1} \blacktriangleright CH_4; \text{C-2} \blacktriangleright C_2H_6; \text{C-3} \blacktriangleright C_3H_8]$$

2. **Absorbent**

    Absorption Oil : Commercial Hexane

    [D] Density : 730 kg.m^{-3}

    [E] Average Mol. Wt. :130 kg. kmol^{-1}

    Base your calculation on the following assumptions.

    1. *Ethane recovery 95%*
    2. *Propane recovery 95%*
    3. *Maximum methane content of the product 5%*
    4. *Recycle Gas Composition from Partial Stripper*

$C\text{-}1+N_2$	C-2	C-3
79% (vol)	20% (Vol)	1% (vol)

5. *Absorption factor at tower bottom, A_B = 1.1*
6. *Absorption temp. at tower bottom, T_{BOT} = 266 K*
7. *Use average pressure of 2.755 MPa. abs. for absorber design.*
8. *The recycle gas is cooled to 255K before entering the absorber.*
9. *N_2 + C-1 in recycle gas   : negligible*

    C-2 in recycle gas   : 0.7 mol%

Solution :

Heat and material balances dominate this type of calculation.

Step - (I)   Overall Material Balance

Component	Feed Gas		Product		Lean Gas	
	Mol%*	kmol.h^{-1}	Mol%	kmol.h^{-1}	Mol%	kmol.h^{-1}
N_2	2	4.536	0	0	2.5	4.536
C-1	78	176.904	5	2.268	96.25	174.636
C-2	16	36.288	76	34.473	1.0	1.815
C-3	4	9.072	19	8.618	0.25	0.454
Total	100	226.8	100	43.359	100	181.437

* Mol% = Volume % ; F = 5443 kmol. day^{-1} = 226.8 kmol.h^{-1}

Step - (II) Vaporization Constants at Tower Bottom

Bottom Temp   = 266 K

Bottom press. = 2.755 MPa. abs.

Feed Components Vaporization Constants

N_2	$k_o = 23$
C-1	$k_1 = 5.2$
C-2	$k_2 = 0.82$
C-3	$k_3 = 0.22$

Step - (III) Absorption Factors at Column Bottom By definition

$$A = \frac{L}{kG}$$

Component   **Absorption Factor**

C-2 $A_2 = \dfrac{L}{k_2 G} = \dfrac{1}{0.82} \cdot \dfrac{L}{G}$

> But $A_2 = 1.1$ (given)
>
> $\therefore \quad \dfrac{L}{G} = (1.1)(0.82) = 0.902$

N_2 $A_0 = \dfrac{L}{k_0 G} = \dfrac{0.902}{23} = 0.0392$

C-1 $A_1 = \dfrac{L}{k_1 G} = \dfrac{0.902}{5.2} = 0.1734$

C-3 $A_3 = \dfrac{L}{k_3 G} = \dfrac{0.902}{0.22} = 4.1$

Step - (IV) Column Efficiency For N_2 & C-1

For N_2 and C-1, the absorption factors are low. Hence the column efficiency is essentially the same as the absorption factor :

N_2 E_0 = A_o = 0.0392

C-1 E_1 = A_1 = 0.174

Step - (V). Nitrogen & C-1 Recycle

Parameter	N_2	C-1
Fraction absorbed, E	0.039	0.174
Fraction not absorbed, 1–E	0.961	0.826
Flowrate in lean gas, kmol.h^{-1}	4.536	174.636
Flowrate in total feed gas, kmol.h^{-1}	4.7174	211.377
Flowrate in NG feed, kmol.h^{-1}	4.536	176.904
Flowrate in Recycle stream, kmol.h^{-1}	0.1814	34.473

Step - (VI) C-2 & C-3 in Recycle

Recycle Stream

C-2 Content   : **20 kmol %**
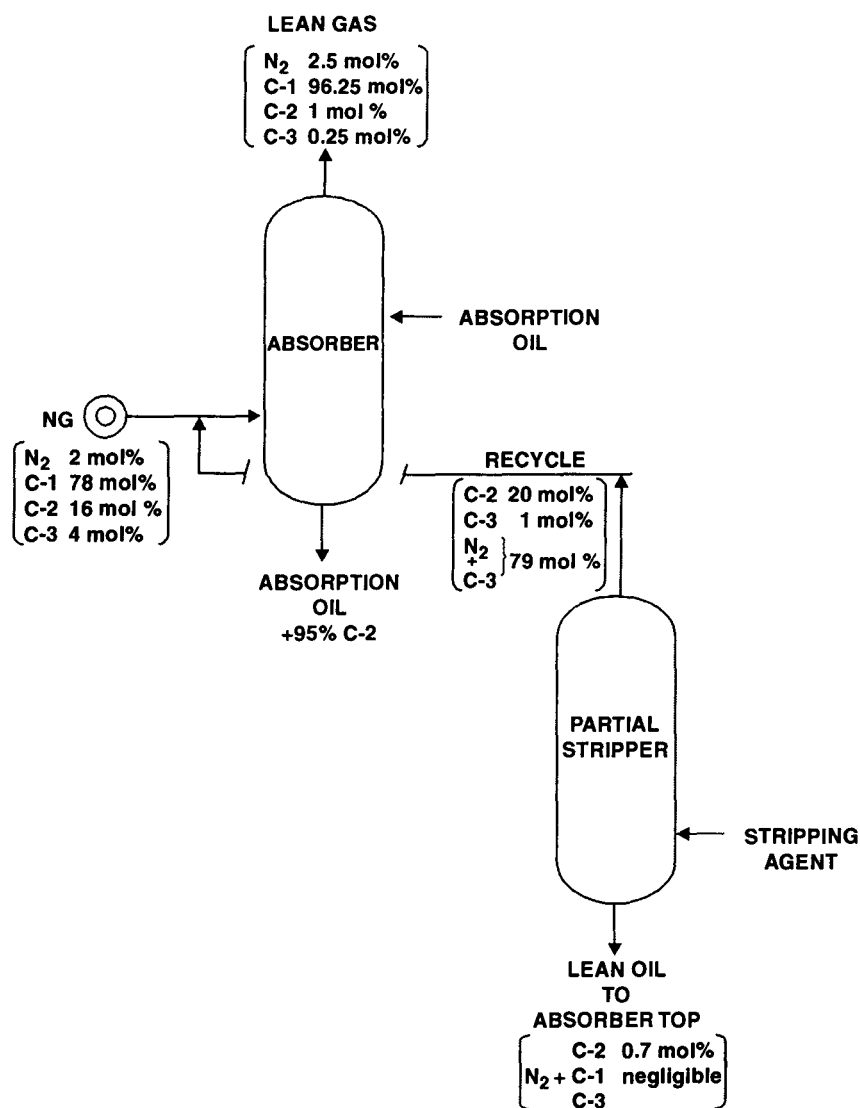
Fig./Prob. 2.14.1. *Material Balance Diagram of a typical C-2 Absorption Process.*

C-3 Content	:	1 kmol %
N_2 + C-1 rate	:	$0.1814 + 34.473 = 34.6544$ kmol.h^{-1}
∴ N_2 + C-1 content	:	$100 - (20 + 1) = 79$ kmol%
C-2 rate	:	$\dfrac{20}{79}$ (34.6544 kmol.h^{-1}) = 8.7732 kmol.h^{-1}
C-3 rate	:	$\dfrac{1}{79}$ (34.6544 kmol.h^{-1}) = 0.4386 kmol.h^{-1}

Step - (VII). Fractional Recoveries

Component	Absorber Feed, kmol.h^{-1}			LeanGas	Gas Absorbed	Fraction	
	NG	Recycle	Total	kmol.h^{-1}	kmol.h^{-1}	Not Absorbed	Absorbed
N_2	4.536	0.1814	4.7174	4.536	0.1814	0.9615	0.0384
C-1	176.904	34.473	211.377	174.632	36.745	0.8261	0.1738
C-2	36.298	8.7732	45.071	1.814	43.257	0.0402	0.9597
C-3	9.072	0.4386	9.5106	0.454	9.0566	0.0477	0.9522
Total	226.8	43.8662	270.676	181.436	89.24		

Step - (VIII) Solvent Circulation

$$\frac{L}{G} = 0.902 \qquad \textbf{Step - III}$$

$$G = 270.676 \text{ kmol.h}^{-1} \qquad \textbf{Step - VII}$$

$$L = 244.1497 \text{kmol.h}^{-1}$$

Gas absorbed in column   = 89.24 kmol.h^{-1} **Step - VII**

Oil feedrate to absorber top = $244.1497 - 89.24 = 154.9097$ kmol.h^{-1}

Oil feedrate to absorber top = | 154.9097 kmol.h^{-1} | | 130 kg. kmol^{-1} |

$$= 20138 \text{ kg.h}^{-1}$$

Step - (IX) Heat of Solution

Component	kmol.h^{-1}	Heat of Solution	
	Absorbed	kJ. kmol^{-1}	kJ.h^{-1}.
N_2	0.1814		
C-1	36.745	3489	128203
C-2	43.257	12993	562038
C-3	9.0566	15119	136927
Total	89.24		827168

Step - (X) Oil Temp at Absorber inlet

Heat absorbed by oil = | 20138 kg.h^{-1} | | Cp | | 266 - T_0 |

where **Cp** = specific heat of oil = 1.968 kJ.kg^{-1} K^{-1}

T_0 = oil temperature at absorber inlet, K

$\therefore$ | 20136 kg.h^{-1} | | 1.968 kJ. kg.K^{-1} | | 266 − T$_0$ | = 827168 kJ.h^{-1}

$\therefore$ 266 − T$_0$ = 20.87 $\simeq$ 21K

Allow ΔT = 22K to provide sensible heat of gas

$\therefore$ T$_0$ = 244 K

Step - (XI) Temperature of top plate
BASIS : Oil Inlet Temp. = 244K
1st Assumption : 250 K (top plate temp)

Component	Absorption Factor
N$_2$	k$_0$ = 19.5
C-1	k$_1$ = 4.2
C-2	k$_2$ = 0.60
C-3	k$_3$ = 0.15

Component	Liq composition on top plate x = y/k
N$_2$	x$_0$ = 0.025/19.5 = 0.00128
C-1	x$_1$ = 0.9625/4.2 = 0.2291
C-2	x$_2$ = 0.01/0.60 = 0.0166
C-3	x$_3$ = 0.0025/0.15 = 0.0166
	Σx$_j$ = 0.2636

STEP-I

$\therefore$ Gas-free oil, x$_8$ = 1 − 0.2636 = 0.7363

Actual feed oil composition

x$_2$ = 0.007 (see assumption # 9 given in the problem)

x$_3$ = 0.0166 (see above)

Component Flowrates in Feed Oil

Net Oil Rate top Absorber Top : 154.9097 kmol.h^{-1}

Component	Flowrate to The Top Plate
C-2	0.007 (154.9097 kmol.h^{-1}) = 1.08436 kmol.h^{-1}
C-3	0.0166 (154.9097 kmol.h^{-1}) = 2.57150 kmol.h^{-1}

Flow Rate Out of Top Plate

$$\text{Total flowrate} = \left| \frac{1 - 0.0236}{0.7363} \right| (154.9097 \text{ kmol.h}^{-1})$$

$$= 205.4241 \text{ kmol.h}^{-1}$$

Component	Exit Rate From Top Rate
N$_2$	0.00128 (205.4241) = 0.2629 kmol. h^{-1}
C-1	0.2291 (205.4241) = 47.0626 kmol. h^{-1}
C-2	0.0166 (205.4241) = 3.4100 kmol. h^{-1}
C-3	0.0166 (205.4241) = 3.4100 kmol. h^{-1}

Net Absorbed and Heat of Solution

Component	kmol.h⁻¹			k.J kmol⁻¹.	k.Jh⁻¹
	Σ	In Feed Oil	Net Absorbed		
N₂	0.2629	0	0.2629		
C-1	47.0626	0	47.0626	3489	164 201
C-2	3.4100	1.08436	2.32564	12793	29752
C-3	3.4100	2.57150	0.8385	15119	126 77
				Total	= 206630

Temp. rise on oil due to heat

$$= \frac{\left(206630 \text{ kJ.h}^{-1}\right)}{\left(20138 \text{ kg.h}^{-1}\right)\left(1.968 \text{ kJ. kg}^{-1}.\text{K}^{-1}\right)} = 5.21 \text{ K}$$

This is close enough to 5.5K rise assumed.

Step - (XII) Modified Heat Balance

Feed temp. 266K

Lean gas leaving at 250K

Δ Temp. = 16K of oil

Heat Balance

Component	kmol.h⁻¹	Molal Sp. Heat kJ. kmol⁻¹. K⁻¹	kJ.h⁻¹.K⁻¹
N₂	4.536	29.309	132.9456
C-1	174.632	35.170	6141.8074
C-2	1.814	47.313	85.8257
C-3	0.454	64.480	29.2739
	181.436		6389.8526

$$\text{Heat removed from gas} = \left(6389.8526\frac{\text{kJ}}{\text{h.K}}\right)(16 \text{ K}) = 102237.64 \frac{\text{kJ}}{\text{h}}$$

$$\text{Heat of solution, absorbed gas (Step - IX)} = 827168 \quad \frac{\text{kJ}}{\text{h}}$$

$$\Sigma = 929405 \quad \text{kJ.h}^{-1}.$$

Calculated temp. rise of oil:

$$266 - T_o = \frac{929405 \text{ kJ.h}^{-1}}{\left(20138 \text{ kg.h}^{-1}\right)\left(1.968 \text{kJ.kg}^{-1}.\text{K}^{-1}\right)}$$

$$\therefore \qquad T_o = 242.5\text{K}$$

This is somewhat cooler than the 266K assumed but acceptably close for preliminary design.

Step - (XIII) Absorption Factors at Absorber Top

L = total flow of liq out top plate = 205.4241 kmol.h^{-1} | Step - XIV |

G = lean gas rate = 181.437 kmol.h^{-1} | Step - I |

$$\therefore \frac{L}{G} = 1.1322$$

Component	Vaporization Constant	Absorption Factor	
	k	Top	Bottom
N$_2$	19.5	0.058	0.0392
C-1	4.2	0.269	0.1734
C-2	0.60	1.88	1.1
C-3	0.15	7.5	4.1

Step - (XIV) No. of Theoretical Plates

For equilibrium of ethane with inlet :

$$\text{Oil, } x_2 = 0.007$$

$$y_2 = 0.007 \, k_2 = 0.007 \, (0.6) = 0.0042$$

C-2 lost = (181.437 kmol.h^{-1}) (0.0042) = 0.7620 kmol.h^{-1}

$$\textbf{C-2 fractional loss} = \frac{0.7620}{45.071} = 0.0169$$

Actual recovery (C-2) desired is 95%

$\therefore$ $0.95 = (1 - 0.0169) \, E$ where E = column efficiency

$\therefore$ $E = 0.9663$

$$1 - E = 0.0337$$

$$F_1 = A_B = 1.1 \qquad\qquad \textbf{Step - III}$$

F_1 = enrichment factor at bottom of the absorber

$\therefore$ $$\text{Parameter } \theta = \frac{F_1 - E}{F_1} \, (1 - E)$$

$$= \frac{1.1 - 0.9663}{1.1} \, (1 - 0.9663)$$

$$= 0.004096$$

Now, F_2 = enrichment factor at the top of the stripper
$$= A_T$$
$$= 1.88 \qquad\qquad \textbf{Step - XIII}$$

For $\theta = 0.0041$ & $F_2 = 1.88$, the number of theoretical plates
n $\approx$ 7 [Fig. Prob. 2.6.2]

Step - XV Absorber Performance on Propane

| C-3 |

$$F_1 = 4.2$$

$$F_2 = 7.5$$

$$n = 7 \qquad\qquad \textbf{Step - XIII}$$

Colburn eqn. $(F_2 > F_1 > 1)$:

$$n = \frac{\log\left[\frac{F_1}{(1-E)(F_1-1)}\left(\frac{F_2-1}{F_2}\right)^2 - \frac{1}{F_2}\right]}{\log F_2}$$

or,

$$7 = \frac{\left[\frac{4.2}{(1-E)(3.2)}\left(\frac{6.5}{7.5}\right)^2 - \frac{1}{7.5}\right]}{\log 7.5}$$

or, $1 - E = 7.385 \times 10^{-7}$

∴ $E \approx 1$

That is, the absorption of propane (C-3 component) is virtually complete. Since 95% recovery is all that is required, the propane-content of the oil used may be allowed to rise to that in equilibrium with the desired lean gas. This justifies our assumption in **step-XI.**

Step - XVI Absorber Performance on N_2 & C-1

$$A_E = A_B \left|\frac{A_T + 2}{A_B + 2}\right|$$

For N_2, $A_E = 0.0392\left|\frac{0.058+2}{0.0392+2}\right| = 0.0395$

Fraction absorbed = $E = A_E = 0.0395$

For C-1, $A_E = 0.1734\left|\frac{0.269+2}{0.1734+2}\right| = 0.1810$

Fraction absorbed = $E = A_E = 0.181$

These values do not differ greatly from values used earlier. Hence revised assumption is not required.

2.14.1. Selecting and Optimizing A Sour Water Stripping Scheme

A sour water stream available at the battery limit at the rate of 130kg.min⁻¹ requires 14Nos. of ideal stages to reduce its ammonia and carbon dioxide content from **7** wt% and **3** wt% respectively to 25 ppmw and 0 ppm when a conventional stripping scheme [scheme–A] is adopted using saturated steam of **1.317** MPa.abs. Inasmuch as the stripper operates at 1.013 MPa.abs., the **BTMS** require a cooling down to 333K before it is flashed to the atmospheric one. As such the bottoms cooling load becomes as high as 1420KW.

The unit requires a steam consumption of 53.833 kg.min⁻¹ adding 6.5 kg.min⁻¹ of water vapor to the **OVHD** stream.

It requires the selection of an optimum scheme that'll minimize the input heat load while limiting water vapor load in the **OVHD** to a maximum of 850 kg.h⁻¹

The same stripping operation carried out in scheme-B with a feed-split of 80 kg.min⁻¹ of cold

feed going to the top tray and 50 kg.min^{-1} of preheated feed fed on to **Tray-4** requires 14 Nos. of trays to achieve same stripping efficiency. Steam consumption drops to 35.75 kg.min^{-1}; however, an additional constraint of an upper bound of 14.166 kg.min^{-1} of water vapor load in the **OVHD** stream is imposed.

74% of **BTMS** heat is recovered by way of feed preheating in the **BTMS HE** resulting in much colder BTMS stream reducing the **BTMS** cooling load down to about 312kW.

Yet another variant of heat integration improvising sour-water stripper operates on scheme – **C** which does not split the feed but tags an **OVHD** partial condenser while keeping **BTMS** exchanger in tact recovering 100% of **BTMS** heat. No further bottoms cooling, therefore, is required.

The system is more efficient than the previous split-feed system **(scheme–B)** in that it requires only 10 theoretical stages to achieve the same separation efficiency and requires no further BTMS cooling before it is flashed to atmospheric level.

However, this scheme consumes somewhat more steam (40.666 kg.min^{-1}) and yet fulfilling the upper limit of water rate 14.166 kg.min^{-1} in the **OVHD**.

It is obvious that water content in the overhead vapor can be controlled thru feed preheating adjustment. And that can be achieved in scheme–**D** that dispenses with **OVHD** condenser altogether (Fig. 2.14.1–1)
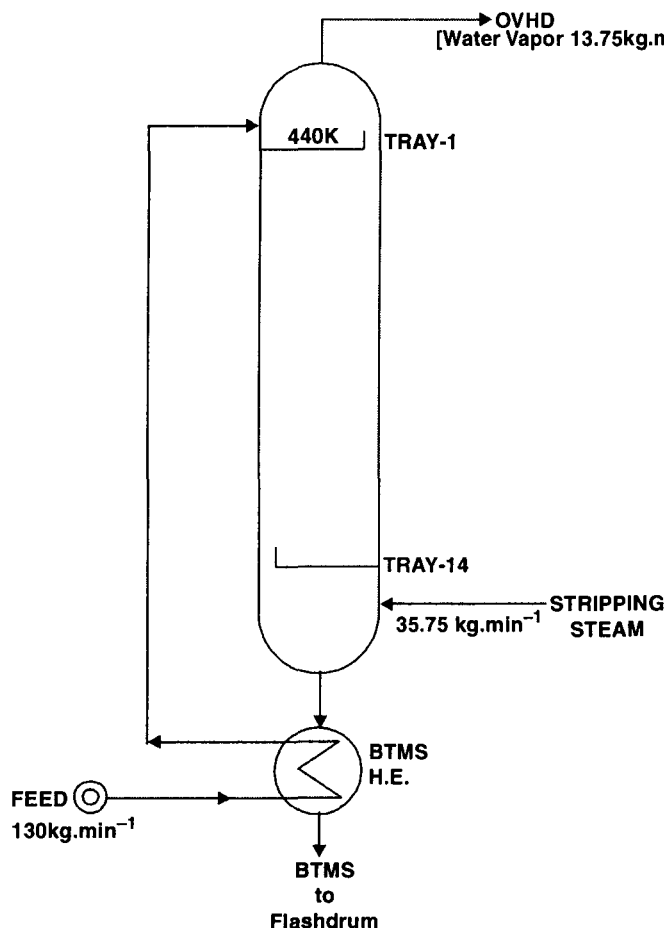
Fig. 2.14.1–1. *This simplified heat integration scheme abstracts the generated heat of stripping and returns it back to column thru feed preheating and thus optimizing the input heat. The water vapor load in the overhead stream is controlled by the degree of feed preheating.*

This scheme satisfies the design specifications (25 ppm NH_3 in the **BTMS**) while restricting **OVHD** water flowrate within the maximum allowable limit of 14.166 kg.min^{-1} (0.85t.h^{-1}).

Scheme–**D** and scheme–**B** are energetically equivalent but the latter scheme is the best one as it gives better control of top tray temperature, hence moisture load in the **OVHD** stream.

Nevertheless, scheme–**D** uses all plates to treat the whole input stream. As a result a continuous desorption process takes place. This begets a better temperature profile along the tower with a consequent increase in the overall plate efficiency. There is another favorable point that makes single feed scheme more interesting. For the same extent of heat recovery, the heat transfer area requirements are less in option scheme–**D** which also fulfils the upper bound to the top water flow without including the **OVHD** partial condenser (scheme–**C**).

The heat integrated scheme–**D** led to an important advantage. In the original design, the steamflow was limiting to the stripper capacity, as high steamrate would invite column flooding. Inasmuch as scheme–**D** operates with 30% less steam load, the stripper capacity can be boosted up by about 50% without the risk of column flooding.

2.15. REBOILED STRIPPER IMPROVES PERFORMANCE

Use of reboiled stripper rather than open steam strippers cuts waste and saves money. This is how the economy plays :

> a ton of steam fed to an open stripper ultimately becomes a ton of waste water that requires increasingly expensive water treatment. Now if the same amount of steam is used to heat a reboiled stripper, it ultimately becomes a ton of valuable condensate which can be recycled to boiler as BFW. Therefore, the chief economic incentive for reboiled stripping is the potential to upgrade waste water (which has a large negative value) and to recover boiler feed water with a large positive value. In many a case this savings repays the initial cost of the reboiler.

Design

The design is based on constant **stripping factor, S,** thruout the column

$$S = \frac{KG}{L}$$

where, **K** = volatility of the light key

     = y / x

y = mole fraction of light key in the vapor phase

x = mole fraction of light key in the liquid phase in equilibrium with the vapor above it

G = molar gas flowrate, kmol.h^{-1}

L = molar liq flowrate, kmol.h^{-1}

Note : Gas and vapor are synonymous.

Use is then made of Souder-Brown Equation

$$f_s = \frac{X_o - X_n}{X_o - X_{n+1}} = \frac{S^{n+1} - S}{S^{n+1} - S} \qquad \qquad ...(2.15.1)$$

relating fraction stripped f_s (in open stripper, refer to **Fig. 2.15.1**) with stripping factor, S, and the number of theoretical stages, **n.**

where X_0 = concentration of the light key entering in the feed, kmol light key / kmol solute-free solvent

X_n = concentration of the light key in the liq leaving the **n-th** stage (bottom) of the column, kmol light key / kmol solute-free solvent

X_{n+1} = concentration of the light key in a Hypothetical Liquid in equilibrium with the entering stripping medium (steam), kmol light-key / kmols solute-free hypothetical liquid
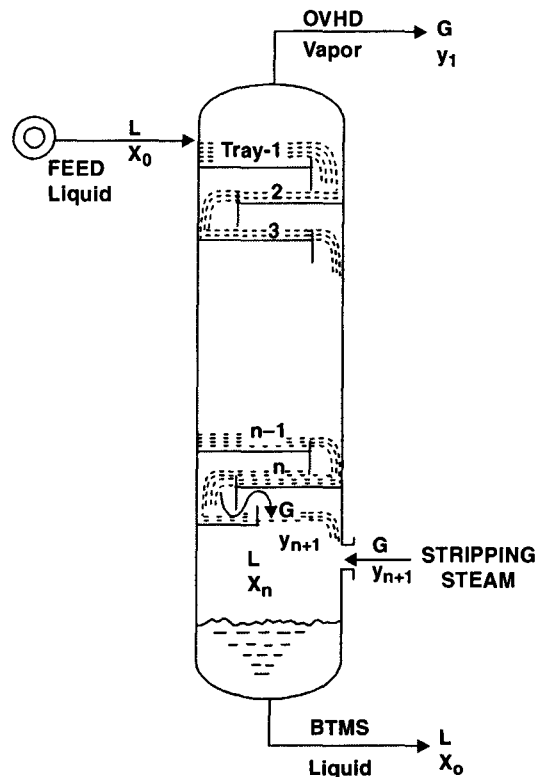
Fig. 2.15.1 Open stripper.

Eqn. 2.15.1 is most often in graphical form, familiarly known as Souder–Brown chart **(Fig. 2.15.2)**

The foregoing **S–B EQN.** presents f_s as the fractional approach of the feed liquid to equilibrium with the stripping medium. For open strippers, the stripping medium is free of light key *i.e.*

$$X_{n+1} = 0$$

whereupon fraction stripping f_s becomes

$$f_s = \frac{X_e - X_n}{X_e} = 1 - \frac{X_n}{X_e} \qquad \qquad ...(2.15.1A)$$

However, this fractional approach degenerates to an appropriate result if it is applied to reboiled stripper, for in this case the stripping vapor is in equilibrium with the bottoms and cannot, therefore, be free of light key **[Fig. 2.15.3]**

$$X_n = X_{n+1}$$

whereupon EQN. 2.15.1 yields
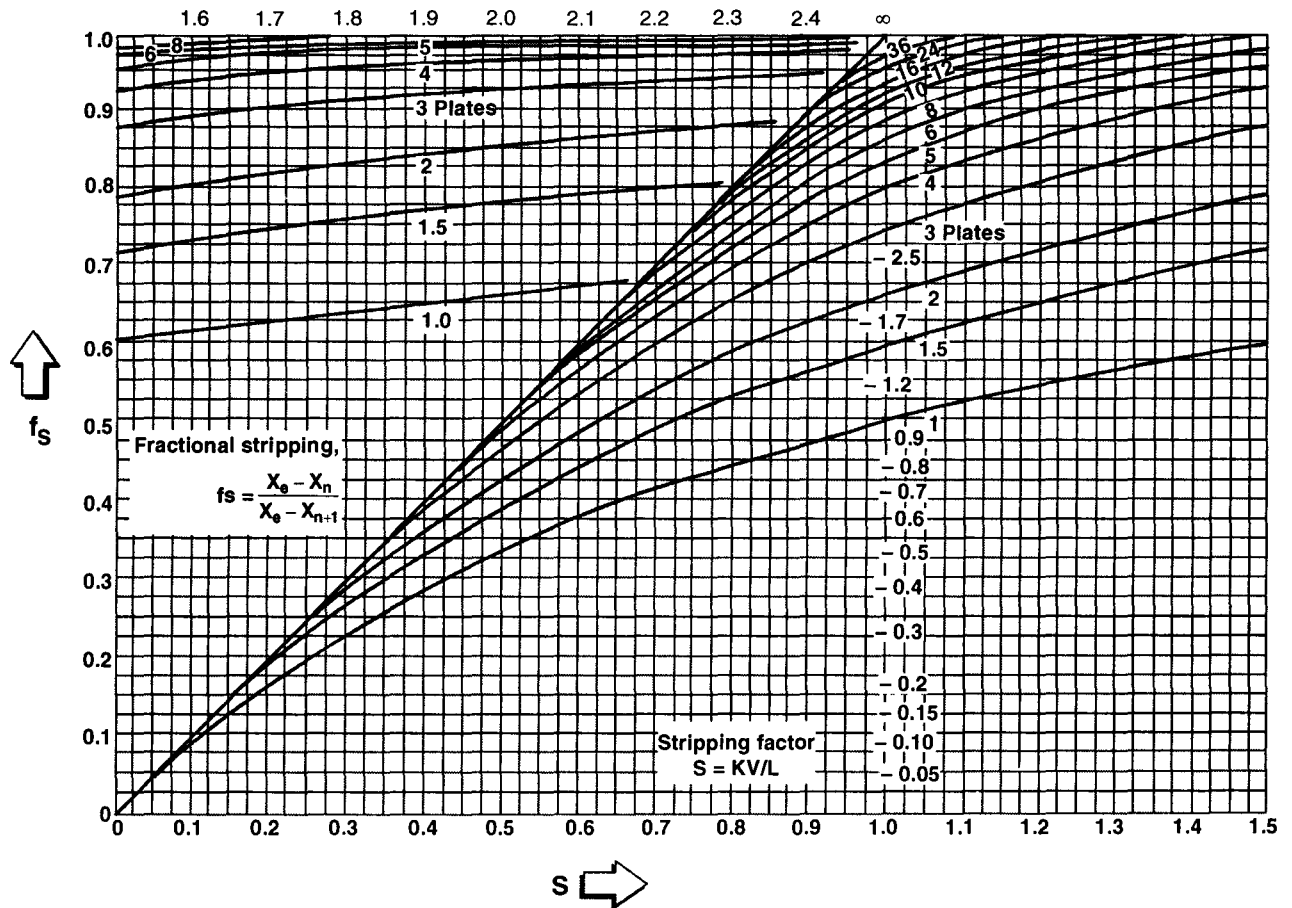
Fig. 2.15.2. *Souder–Brown Chart relating fraction stripped with stripping factor, number of stages and volatility of the light key.*

$$f_s = \frac{X_o - X_n}{X_o - X_n} = 1$$

and therefore infinite number of stages appear to be required for any value of S.

However, EQN. 2.15.1 is still valid for reboiled stripper, but it applies only to the trayed section of the column. And that requires modification of this equation in order to fit it to the design of reboild strippers, inasmuch as it is the bottoms liq composition $[X_{n+1}]$ and not the bottom tray liq composition $[X_n]$ that is of interest :

$$f'_s = \frac{X_e - X_{n+1}}{X_e} = 1 - \frac{X_{n+1}}{X_e} \qquad \ldots(2.15.2)$$

where f'_s is the newly defined fractional stripping parameter.

In order to develop a relationship between f_s and K, L, G, n so that it be represented in graphical form like EQN. 2.15.1, we rearrange EQN. 2.15.1 to give

$$X_o - X_{n+1} = \frac{1}{f_s}(X_e - X_n) = \left|\frac{S^{n+1} - 1}{S^{n+1} - S}\right|(X_e - X_n) \qquad \ldots(2.15.3)$$

Substituting into 2.15.2 and rearranging yields

$$f'_s = \left| \frac{S^{n+1} - 1}{S^{n+1} - S} \right| \cdot \frac{X_e - X_n}{X_e} = \left| \frac{S^{n+1} - 1}{S^{n+1} - S} \right| \cdot \left| 1 - \frac{X_n}{X_e} \right| \qquad \ldots(2.15.4)$$

Now refer to **Fig. 2.15.3.** A mass balance of the light key over the envelop gives

$$L \cdot X_n = G \cdot Y_{n+1} + B \cdot X_{n+1} \qquad \ldots(2.15.5)$$

where, L = liq rate on solute-free basis, kmol/h

G = gas rate on solute-free basis, kmol/h

B = bottoms liq rate on solute-free basis, kmol/h

Overall mass balance over the same envelop results
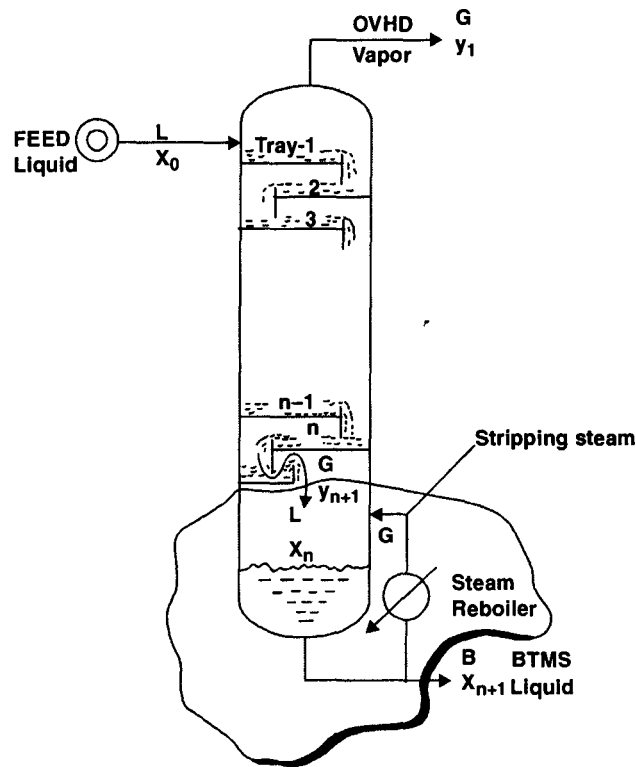
Fig. 2.15.3. *Reboiled stripper.*

$$L = B + G \qquad \ldots(2.15.6)$$

Assuming a high reboiler circulation rate, it is obvious from the definition of K that

$$y_{n+1} = K \cdot x_{n+1}$$

or,
$$\frac{Y_{n+1}}{1 + Y_{n+1}} = K \cdot \frac{X_{n+1}}{1 + X_{n+1}} \qquad \ldots(2.15.7)$$

Combining EQN. 2.15.5 and 2.15.6 and 2.15.7 and rearranging yields

$$X_n = \left|1 + \frac{K-1}{K} \cdot S\right| \cdot x_{n+1} \qquad \ldots(2.15.8)$$

Substituting EQN. 2.15.8 in EQN. 2.15.4 begets

$$f_s = \frac{S^{n+1}-1}{S^{n+1}-S}\left[1 - \left(1 + \frac{K-1}{K} \cdot S\right) \cdot \frac{X_{n+1}}{X_0}\right] \qquad \ldots(2.15.9)$$

EQN. 2.15.2 can be rearranged to

$$1 - f_s' = \frac{X_{n+1}}{X_0}$$

which upon substitution in EQN. 2.15.9 generates

$$f_s' = \frac{S^{n+1}-1}{S^{n+1}-S}\left[1 - \left(1 + \frac{K-1}{K} \cdot S\right)(1 - f_s')\right]$$

$$\ldots(2.15.10)$$

and this equation upon rearrangement and simplification yields

$$f_s' = \frac{\dfrac{S}{S-1}\left|S^{n+1}-1\right|}{\dfrac{S}{S-1}\left|S^{n+1}-1\right| + \dfrac{K}{K-1}} \qquad \ldots(2.15.11)$$

EQN. 2.15.11 presented in graphical form (**Fig. 2.15.4**) is the most useful one.

Note : Fractional stripping in open stripper is the function of **S** and **n** alone [**cf. EQN. 2.15.1**]. However, for reboiled stripper it depends on **S, n, K** (**slope of EL**) and $\dfrac{L}{G}$ (**slope of OL**). Additionally, the value of **K** for reboiled strippers must exceed unity for stripping to be possible.

REFERENCES

1. Thomas M. Snow, *Hydrocarbon Processing (Oct.1978)*.

2. M. Souder and G.S. Brown, *Industrial and Engineering Chemistry (vol. 24 / 1932 / P—519)*.

3. A. Kremser, *National Petroleum News (vol. 43 / May 21 / 1930)*.
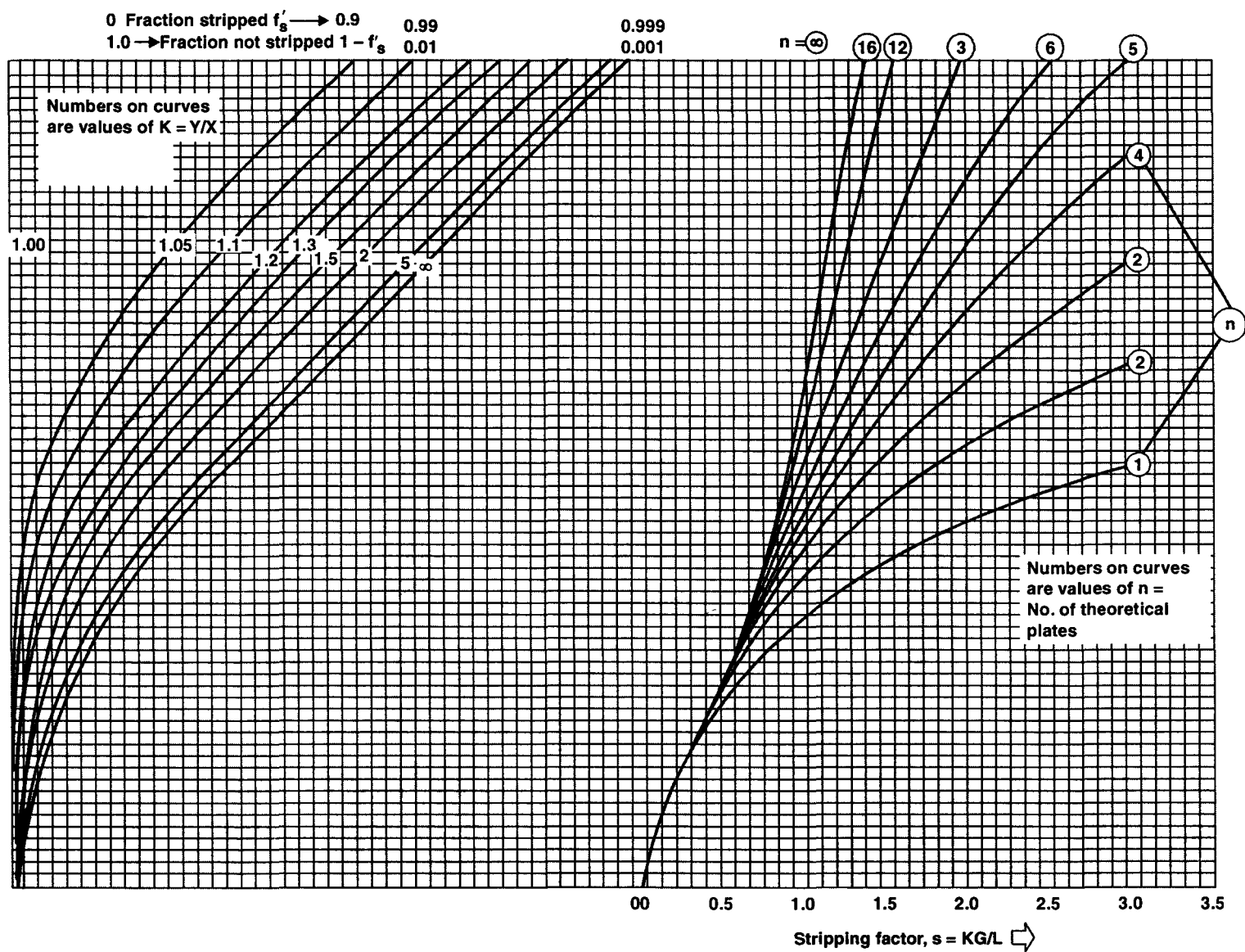
Fig. 2.15.4.

Problem 2.15. An Oil-Water stripper (Fig. 1/Problem 2.15) uses steam to strip waste water contaminated with oil (1 wt% of dissolved oil which is also the solubility limit at 311K).

Feedrate	$= 15000 \ kg. \ h^{-1}$
Stripping steam rate	$= 4500 \ kg.h^{-1}.$
Column operating pressure	$= 1 \ atm.$

Under these operating conditions the oil concentration in the BTMS is reduced to 50 ppmw.

Mol. wt. of oil = 100 kg. kmol^{-1}

Henry's Law Constant of oil in water at 375K = 5 atm for all concentrations up to its solubility limit.

It has been proposed to revamp the column to a reboiled stripper in order to reduce both the aq. effluent and the loss of steam condensate from the plant. Determine what the effect of this change on effluent quality will be.

Solution : The open steam stripper is depicted in **Fig. 2/Problem 2.15** a rather simplified way for the convenience of mass-balance.
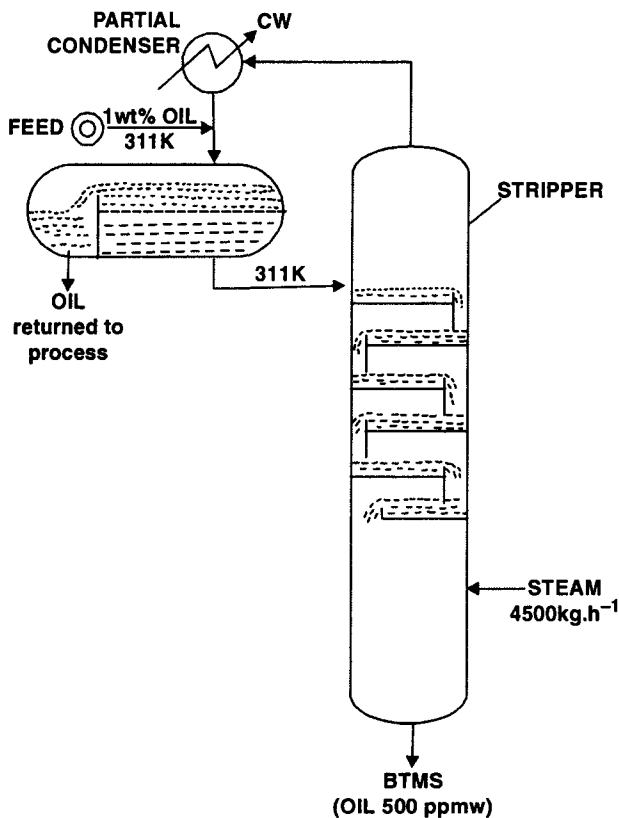
Fig. 1/Problem *2.15. Open Stripper.*	Fig. 2/Problem 2.15. *Mass-balance in Open Stripper.*
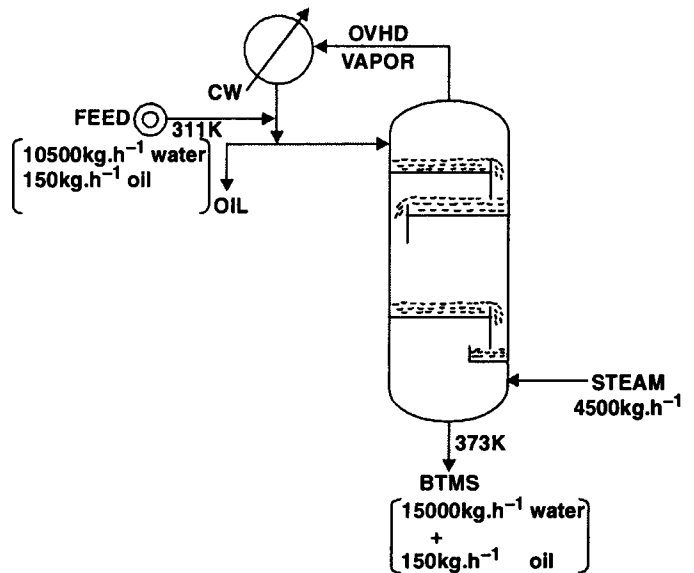
Vapor rate,
$$G = \frac{4500 \ \text{kg.h}^{-1}}{18 \ \text{kg.kmol}^{-1}} = 250 \ \text{kmol.h}^{-1}$$

Liquid Rate, $$L = \frac{(10500 + 4500) \text{ kg.h}^{-1}}{18} = 833.33 \text{ kmol.h}^{-1}$$

(on solute* - free basis)

(* Solute : Oil)

$$K = \frac{H}{P} = \frac{5 \text{ atm.}}{1 \text{ atm.}} = 5$$

$$S = K \frac{G}{L} = 5 \left| \frac{250 \text{ kmol.h}^{-1}}{833.33 \text{ kmol.h}^{-1}} \right| = 1.5$$

Oil (solute) content in the feed = 1% of 10500 kg.h^{-1} = 105 kg.h^{-1}.

$$\therefore \qquad X_o = \frac{\dfrac{105}{100} \dfrac{\text{kg oil. h}^{-1}}{\text{kg oil. kmol oil}^{-1}}}{\dfrac{10500}{18} \dfrac{\text{kg water. h}^{-1}}{\text{kg water. kmol water}^{-1}}}$$

$$= 0.0018 \frac{\text{kmol oil}}{\text{kmol oil - free water}}$$

Oil content in the bottoms = 500 ppmw

$$= \frac{500}{10^6} \times 15000 \text{ kg. oil. h}^{-1}$$

$$= 7.5 \text{ kg oil. h}^{-1}$$

$$X_n = \frac{\dfrac{7.5}{100} \dfrac{\text{kg oil. h}^{-1}}{\text{kg oil. kmol oil}^{-1}}}{\dfrac{15000}{18} \dfrac{\text{kg water. h}^{-1}}{\text{kg water. kmol water}^{-1}}}$$

$$= 0.00009 \frac{\text{kmol oil}}{\text{kmol oil - free water}^{-1}}$$

$X_{n+1} = 0$ for open stripper

$$\therefore \qquad f_s = \frac{X_e - X_n}{X_e - X_{n+1}} = \frac{0.0018 - 0.00009}{0.0018 - 0} = 0.95$$

For S = 1.5 & f_s = 0.95, the number of theoretical stages = 5 from **Fig. 2.15.2**

REBOILED STRIPPER

The reboiled stripper is presented schematically in **Fig. 3/Problem 2.15.** The vapor and liquid rates & compositions will remain very nearly the same as the open stripper.
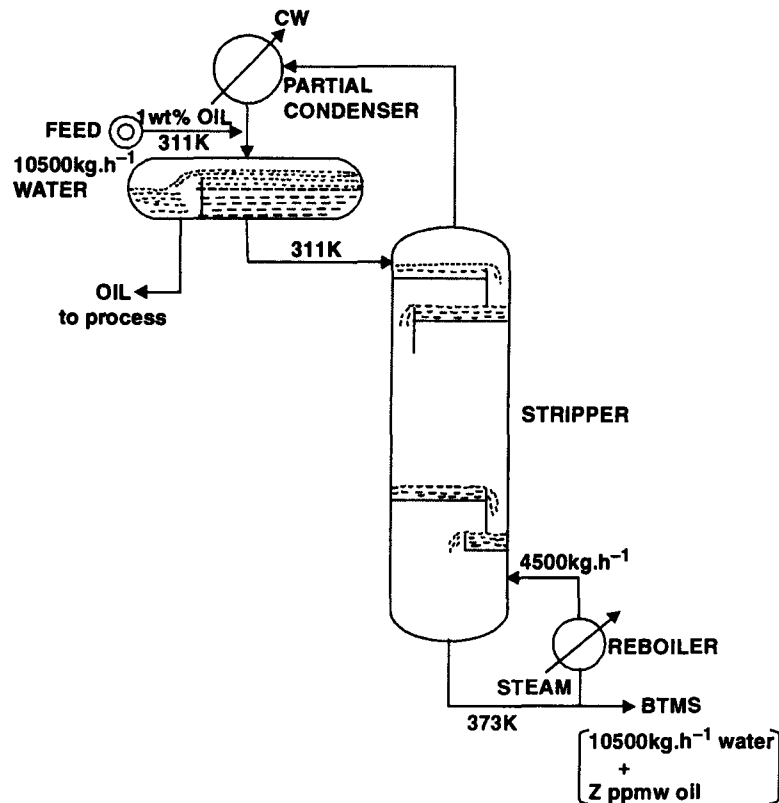
Fig. 3/Problem 2.15. *Reboiled Stripper*.

Therefore, it is reasonable to assume that the number of stages will also be unchanged. Thus for reboiled operation :

$$X_e = 0.0018$$
$$X_n = 0.00009$$
$$n = 5$$

$$G = 4500 \text{ kg.h}^{-1} = \frac{4500 \text{ kg.h}^{-1}}{18 \text{ kg.kmol}^{-1}} = 250 \text{ kmol.h}^{-1}$$

L = feedrate + vapor boilup rate
= 10500 + 4500 kg.h^{-1}
= 15000 kg.h^{-1}
= 833.333 kmol h^{-1}

$$S = K\frac{G}{L} = 5 \left| \frac{250 \text{ kmol.h}^{-1}}{833.333 \text{ kmol.h}^{-1}} \right| = 1.5$$

Refer to Fig. 2.15.4.

For **S** = 1.5, **n** = 5 & **K** = 5, the value of stripping factor is

$$f_s' = 0.962$$

Therefore from Eqn. 2.15.2

$$0.962 = 1 - \frac{X_{n+1}}{0.0018}$$

∴ $$X_{n+1} = 6.84 \times 10^{-5} \text{ kmol oil. kmol water}^{-1}$$

$$= 6.84 \times 10^{-5} \left| \frac{100}{18} \right| \frac{\text{kg oil}}{\text{kg water}}$$

$$= 3.8 \times 10^{-4} \text{ kg oil.kg water}^{-1}$$

$$= \frac{3.8 \times 10^{-4}}{10^6} \times 10^6 \text{ ppmw oil}$$

$$= 380 \text{ ppmw oil}$$

Comments : The provision of reboiler brings forth two benefits :

* the quantity of aq. effluent drops from 15000 kg.h⁻¹ to 10500 kg.h⁻¹
* the oil concentration reduces from 500 ppmw to 380 ppmw.
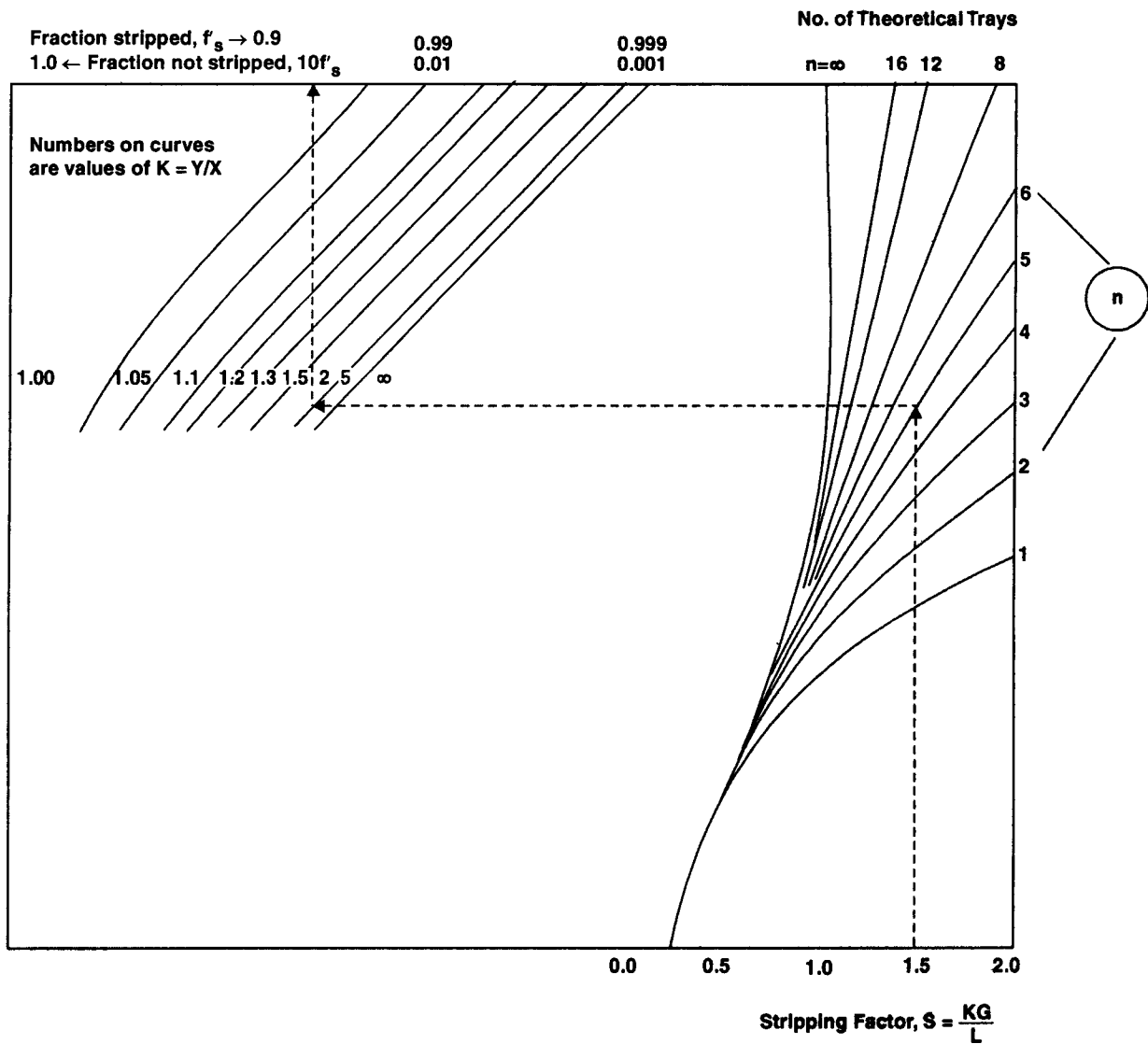
Fig. 2.15.4. *Stripping factor,* $S = \dfrac{kG}{L}$

2.16. WATER DEAERATION

A very widely practised stripping operation is deaeration of boiler feedwater (BFW) — a system that obeys Henry's Law. Dissolved air is removed from water by injecting stripping steam into it. The chief purpose of deaeration is to remove **DO** (dissolved oxygen causing waterside corrosion).

The pure steam stripping vapor contains no oxygen and therefore, the maximum possible driving force for mass transfer is available at the column bottom.

Frequently vacuum deaeration is utilized. When hot water is fed into a column under vacuum, it will flash to convert a part of the feed into vapor. The temperature of the resultant liquid then drops until its vapor pressure plus those of the dissolved gases equal the column pressure. Actually, the vapor pressure of water overwhelms the vapor pressure exerted by the dissolved gases and therefore, the latter can be neglected for practical purposes. Thus if a water at 294K is introduced to a column under pressure of 2000 Pa. abs., it will flash and be cooled to a temperature of 290.5K. At this lower temperature Henry's Law constant for **DO** is reduced by only 7% as compared to water at 294K. That is flashing will sustain considerable deaeration inspite of cooling.

Forasmuch as the water flashed to the lower temperature in one equilibrium stage, there is very little stripping vapor available in the lower part of the column. The amount of oxygen stripped is so small that there is practically no upward movement of vapor phase from column bottom. This together with high liquid flow used in these deaerators drags the small vapor phase out of the vacuum column where the oxygen is reabsorbed quickly.

Hence a double-stage vacuum deaeration is opted. This 2nd-stage column is operated in series with the first column, but at a lower absolute pressure. This generates additional flashed water vapor for stripping the **DO** to a lower concentration. Thus if the foregoing deaerator is hooked up with another deaerator operating at 1333 Pa. abs., the feedwater will flash further whereupon the generated vapor will scavenge the stripped oxygen out of the packed bed while the effluent will cool down to 284K.

A small amount of inert gas introduced to the bottom of the vacuum column causes a substantial reduction of oxygen concentration in the effluent water. For instance, 0.4 $Nm^3.h^{-1}$ of methane per 23 $m^3.h^{-1}$ of feedwater can reduce the effluent oxygen content by an additional 66%. Steam is even more effective in reducing oxygen content compared to straight vacuum deaeration. Higher enthalpy of steam accentuates its stripping potential.

DESIGN

The usual design procedure is a trial-and-error approach based on successive approximations on tower dia.

The vacuum deaerator dia is so selected as to give rise to a liquid irrigation rate of 100 $m^3.h^{-1}$ per m^2 of column cross-sectional area.

In erstwhile design, the vacuum deaerators used ceramic packing and operated at lower liquid rate. However, most modern column use plastic packing (50mm or larger) with a packed depth of 2—5m.

The operation is so overwhelmingly a liq-film controlled one that the gas-film resistance, for design purposes, can be dropped. Therefore, the number of transfer units

$$NTU_{O,L} = \ln \left| \frac{x_i}{x_o} \right| = \ln \left| \frac{x_t}{x_b} \right| \qquad \qquad ...(2.16.1)$$

The total packed depth required is

$$Z = NTU_{O,L} \times HTU_{O,L} \qquad \qquad ...(2.16.2)$$

Now, the overall height of a liquid-film transfer unit ($HTU_{O,L}$)of a particular packing at a specified liquid loading and temperature comes from packing vendor's data :

Packing Type	Liq Rate $(m^3.m^{-2}.h^{-1})$	Liq Temp. (K)	$HTU_{O,L}$ (m)
50mm Super Intalox®(plastic)	100	293	0.701
-do-	100	282	0.764
-do-	100	278	0.820
-do-	64	293	0.596
75mm Super Intalox®(plastic)	100	293	0.945

Oil Stripper : No. of Trays Required

Problem 2.16. *A trayed column is used to remove a contaminant hydrocarbon (2.55 mol%) from an oil by countercurrent steam stripping such that 4 kmol of steam is expended per 100 kmol of oil stripped.*

Determine the number of theoretical trays required to reduce the contaminant down to 0.05 mol %.

Given :

The VLE relationship of the hydrocarbon is
    y = 33x
The oil is non-volatile (assume).
No steam is condensed (due to internal heating)
Solution :

Since the steam does not condense, the **liq : gas flow ratio** in the column is

$$\frac{L}{G} = \frac{100}{4} = 25$$

Hydrocarbon concentration at inlet

$$x_t = 2.55 \ mol\% = 0.0255$$

∴
$$X_t = \frac{x_t}{1 - x_t} = \frac{0.0255}{1 - 0.0255} = 0.026167 \ \frac{mol \ HC}{mol \ of \ HC \text{-} free \ oil}$$

Hydrocarbon concentration at outlet

$$x_b = 0.05 \ mol\% = 0.0005$$

∴
$$X_b = \frac{0.0005}{1 - 0.0005} = 5 \times 10^{-4} \ \frac{mol \ HC}{mol \ of \ HC \text{-} free \ oil}$$

The **OL** equation is

$$Y - Y_b = \frac{L}{G} \ (X - X_b)$$

or, $$Y - 33 \ (5 \times 10^{-4}) = \frac{100}{4} \ (X - 5 \times 10^{-4})$$

or, $$Y = 25X - 0.012498 \qquad \qquad ...(1)$$

Again the **EL** equation is

$$y = 33x$$

$\therefore$ $$\frac{Y}{1 + Y} = 33 \ \frac{X}{1 + X}$$

or, $$Y = \frac{33X}{1 - 32X} \qquad \qquad ...(2)$$

Using Equations (1) and (2), the **OL** and **EL** are drawn on the graph paper **(Figure to Solution 2.16)** and the theoretical plates are stepped off.

$$Y = 25\,X - 0.012498$$

X	0	0.005	0.01	0.015	0.02	0.025
Y	– 0.012498	0.1125	0.2375	0.3625	0.4875	0.6125

$$Y = \frac{33\,X}{1 - 32\,X}$$

X	0	0.005	0.008	0.01	0.012	0.015
Y	0	0.1964	0.3548	0.4853	0.6428	0.9519
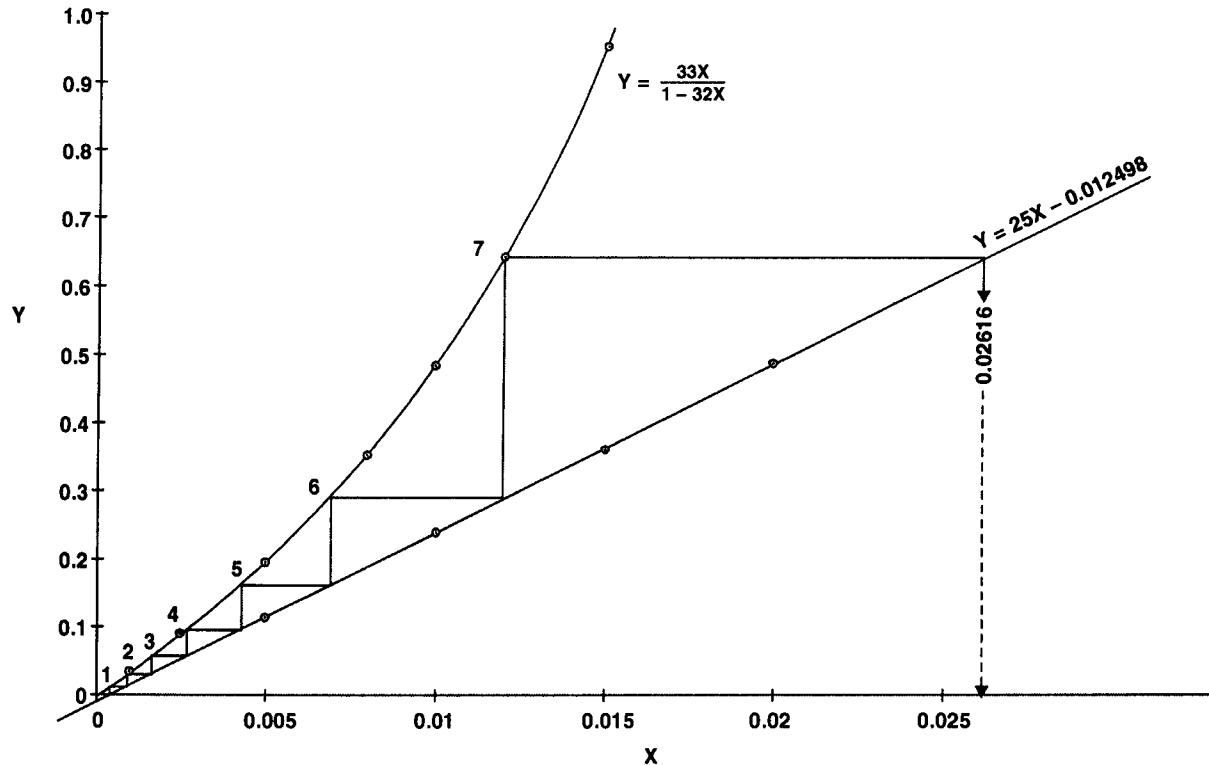
Fig. to Solution To Problem 2.16. *A total number of seven theoretical stages are required for steam stripping a hydrocarbon impurity from 2.55 mol% to 0.05 mol% in an oil.*

We step down in the usual way using **VLE** & **OL** simultaneously to get 7#s of theoretical plates.

Number of Theoretical Trays Required For Steam Stripping A Volatile Hydrocarbon

Problem 2.17. A contaminated organic liquor contains 8 wt% of paraffin hydrocarbon which is to be removed by using open steam in a stripper such that the effluent liquid contains 0.08 wt% paraffin.

The steam is saturated and at 373 K

The vap press of the paraffin = 53 kPa at 373 K

The vap press of the solvent may be neglected

The system obeys Raoult's Law.

Operating pressure = 1 atm.

Mol. wt. of paraffin = 114 kg. kmol⁻¹

Mol wt. of organic solvent = 135 kg. kmol⁻¹

If 3 times the minimum amount of steam is used, compute the number the theoretical stages required.

Solution :

We're to harness McCabe-Thiele method to work out the number of thoretical stages required for the given separation. For this we need two equations—one is **OL** and the other is **VLE** line.

Step - (I) VLE Equation

Raoult's Law is applicable to the system. Therefore,.

$$p = xP°$$

where **p** = partial pressure of the volatile paraffin

$P°$ = vap press of the pure component (paraffin contaminant)

Again for the vapor phase

$$y = p/P$$

where **y** = mole fraction of the paraffin **HC** in the vapor phase

P = total system pressure

∴ $\qquad\qquad\qquad y* = x\,|\,P°/P\,|$ during vap-liq equlibrium

$\qquad\qquad\qquad\quad = x\,|\,53/101.325\,|$

$\qquad\qquad\qquad\quad = 0.523x$ which is the **VLE** Equation.

In terms of mole ratios it becomes.

$$\frac{Y*}{1+Y*} = 0.523\,\frac{X}{1+X}$$

Step - (II) VLE Curve

The following table is completed to draw the VLE curve (see **Fig. to Soln. to Problem 2.17**).

X	$\dfrac{X}{1+X}$	$\dfrac{Y*}{1+Y*}$	$Y*$
0.005	0.004975	0.0026019	0.002602
0.01	0.00990	0.005177	0.005203

Contd..

X	$\dfrac{X}{1+X}$	$\dfrac{Y^*}{1+Y^*}$	Y^*
0.02	0.01960	0.01025	0.01035
0.04	0.03846	0.02011	0.02052
0.06	0.05660	0.02960	0.03050
0.08	0.07407	0.03874	0.04030
0.10	0.09090	0.04754	0.04991
0.12	0.107124	0.0560354	0.05936

Step - (III) Operating Line

$$X_t = \frac{\dfrac{0.08 \text{ kg HC}}{114 \text{ kg HC/kmol HC}}}{\dfrac{1-0.08}{135} \cdot \dfrac{\text{kg solvent}}{\text{kg solvent/kmol solvent}}}$$

$$= 0.10297 \, \frac{\text{kmol HC}}{\text{kmol solvent}}$$

$$X_b = \frac{\dfrac{0.0008 \text{ kg HC}}{114 \text{ kg HC/kmol HC}}}{\dfrac{1-0.0008}{135} \cdot \dfrac{\text{kg solvent}}{\text{kg solvent/kmol solvent}}}$$

$$= 0.0010297 \, \frac{\text{kmol HC}}{\text{kmol solvent}}$$

$Y_b = 0$ as the stripping steam is solute-free

Steam requirement is minimum when the exit streams are in equilibrium

When, $X_t = 0.10297$

$$\frac{Y_t^*}{1+Y^*} = 0.523 \, \frac{X_t}{1+X_t} = 0.048825$$

$\therefore$ $Y^* = 0.05133$

For an overall balance

$$L_{min} (0.10297 - 0.0010297) = G_{min} (0.05133 - 0)$$

$\therefore$ $\left.\dfrac{L}{G}\right|_{min} = 0.50353$

Since $G_{actual} = 3 \times G_{min}$

$$\left.\frac{L}{G}\right|_{actual} = \frac{1}{3} \cdot \left.\frac{L}{G}\right|_{min} = 0.16784 \text{ which is the slope of the OL Eqn.}$$

∴   OL Eqn. becomes

$$Y - Y_b = m (X - X_b)$$

or, $Y - 0 = 0.16784 (X - 0.0010297)$

or, $Y = 0.16784X - 0.0001728$ which is drawn on the **Fig.** **to Soln. to Problem 2.17**
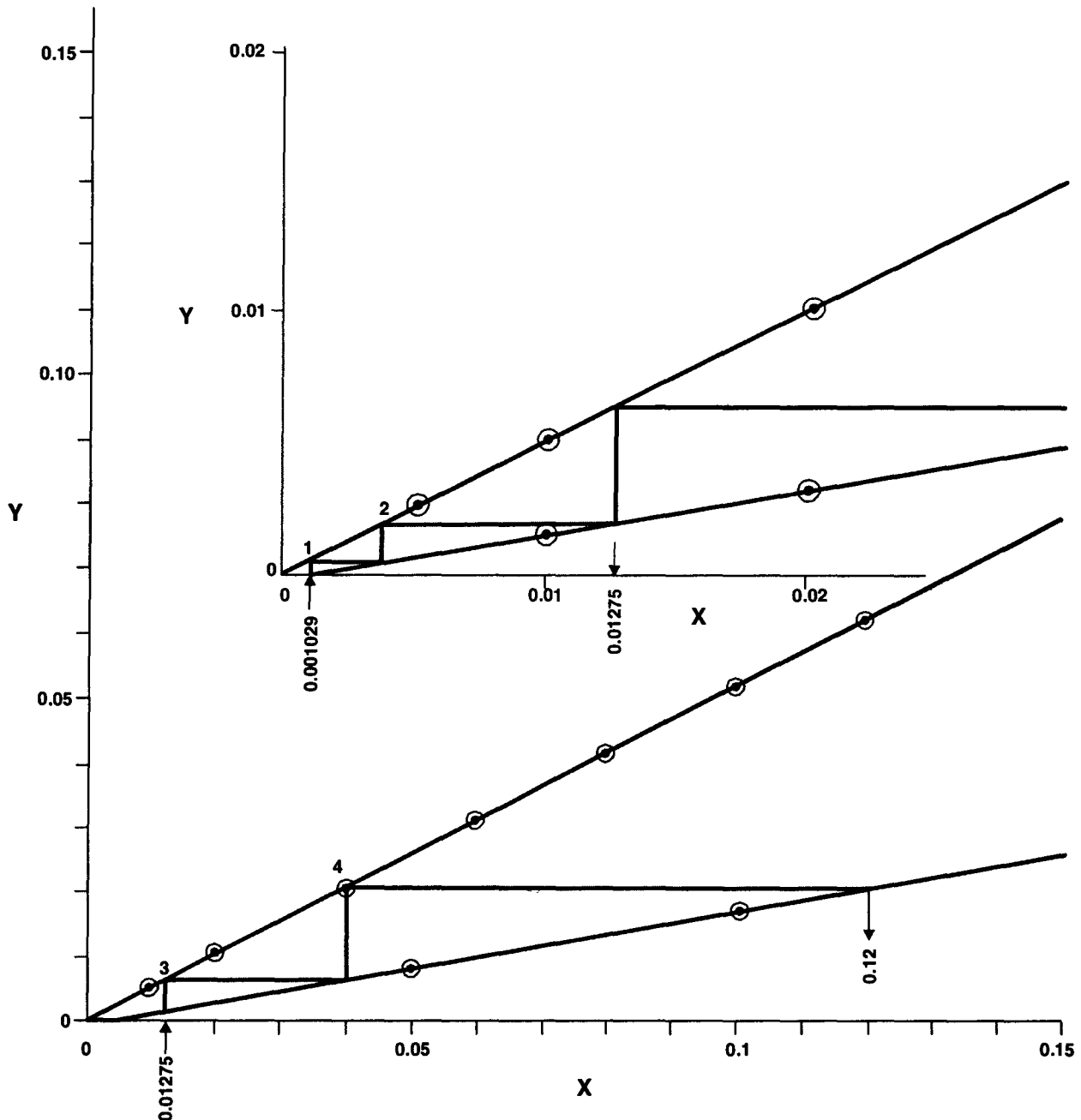
Fig. to Soln. To Problem 2.17.

From the figure, it is evident that nearly 4#s of theoretical stages are required to carry out the said stripping operation.

Pentane Stripper

Problem 2.18. *A 30-plate bubblecap column uses steam to strip n-pentane from solvent oil.*

Inlet oil concentration = 0.06 kmol n-pentane per kmol solvent
Effluent oil concentration = 0.001 kmol n-pentane per kmol solvent
The operation is close to isothermal one.
The Murphree overall plate efficiency is 30%.
Determine specific steam consumption, i.e., kmol of steam required per kmol of oil treated.
Also evaluate the ratio of specific and minimum steam consumptions. How many plates would be required if this ratio is raised to 2?
VLE Eqn. is Y* = 3X
where, Y* and X are expressed in mol ratios of n-pentane in the equilibrium gas and liquid phases respectively.

Solution :

$$\text{Number of actual plates} = 30$$

$$\text{Overall tray-efficiency} = 0.30$$

$$\text{Number of theoretical plates} = 30 \times 0.30 = 9$$

Tower Top

$$X_t = 0.06 \text{ kmol n-}C_5/\text{kmol solvent}$$

$$Y_t = \text{exit steam composition}$$

$$= 3X_t \text{ assuming exit vapor in equilibrium with feed liquid}$$

$$= 3 \ (0.06)$$

$$= 0.18$$

$$L = \text{Liq rate, kmol. h}^{-1}.\text{m}^{-2}$$

Tower Bottom

$$X_b = 0.001 \text{ kmol n-}C_5/\text{kmol solvent}$$

$$Y_b = 0, \text{ as stripping contains no n-pentane at inlet}$$

$$G = \text{Steam rate, kmol.h}^{-1}.\text{m}^{-2}$$

∴ **OL Eqn. at minimum steam rate**

$$Y_t - Y_b = \frac{L}{G}\bigg|_{\text{min}} . (X_t - X_b)$$

The minimum steam consumption occurs when the exit vapor is in equilibrium with the inlet feed.

∴

$$\frac{G}{L}\bigg|_{\text{min}} . = \frac{0.06 - 0.001}{0.18 - 0} = 0.3277$$

which represents minimum steam consumption per kmol of feed treated.

For operating steam consumption we must evaluate the operating stripping factor, **S.** We shall use Kremser Eqn. for this :

$$\frac{X_2 - X_1}{X_2 - Y_1/m} = \frac{S^{N+1} - S}{S^{N+1} - 1}$$

Substituing the appropriate data

$$\frac{S^{10} - S}{S^{10} - 1} = \frac{0.06 - 0.001}{0.06 - 0} = 0.98333$$

from which we get by trail & error

$$S = 1.37$$

$$\therefore \qquad K\left.\frac{G}{L}\right|_{actual} = 1.37$$

or, $$\qquad 3\left.\frac{G}{L}\right|_{actual} = 1.37$$

$$\therefore \qquad \left.\frac{G}{L}\right|_{actua} = 0.4566$$

$\therefore$ Specific steam consumption = 0.45666

$\therefore$ The ratio of actual to minimum steam consumption = 0.4566/0.3277

$$= 1.393$$

Now if this ratio is shot up to 2, the operating gas/liq ratio becomes

$$\frac{G}{L} = 2 \times \left.\frac{G}{L}\right|_{min} = 2 \times 0.3277 = 0.6554$$

$$\therefore \qquad S = K.\frac{G}{L} = 3\,(0.6554) = 1.9662$$

$$\therefore \qquad 0.9833 = \frac{(1.9662)^{N+1} - 1.9662}{(1.9662)^{N+1} - 1}$$

or, $\qquad (1.9662)^{N+1} = 58.856$

or, $\qquad (N+1)\ln 1.9662 = \ln 58.856$

$\therefore$ Actual number of plates
$$= \frac{5.027}{0.3}$$

$$= 16.757$$

$$\simeq 17 \qquad\qquad \textbf{Ans.}$$

$\square\square$

3

Hydraulics of Operation

Various hydraulic phenomena occur in tray towers, packed towers and wetted-wall columns*. They provide intimate contact of the gas and liquid streams in order to permit interphase diffusion of the constituents. Forasmuch as the basic characteristic of mass transfer in two - phase flows is the interaction of the phases that determines the size of the interfacial area, absorbers and strippers must, therefore, be so designed as to ensure a maximum area for phase contact.

Depending on their geometrical configurations and the hydrodynamic conditions setting up in them, the absorbers and strippers are classified into two groups :

Equipment with a fixed area for phase contact

Equipment with variable area for phase contact formed in the course of flow of the contacting phases.

Belonged to the Ist category are the wetted-wall columns while the plate columns (*i.e.* tray towers) and packed columns come under the IInd category.

3.1. PLATE COLUMNS

Plate columns or tray tower bring into effect countercurrent, multistage contact with gas phase dispersed as bubbles in the body of contacting liq phase. The bubbling layer, also called dispersion, usually appears as the gas passes thru the layer of liquid. This dispersion sports a very complex structure :

— it is a heterogeneous gas-liq system

— consistency in some of its physical parameters (viz. viscosity) is lacking

— there is no fixed interfacial area; its size and shape vary continuously.

There is no accurate quantitative description of the bubbling layer (dispersion) because of strong liq-recirculation induced by the rising bubbles and gas streams.

---

* Also there are spray chambers, agitated vessels and mixers for absorption and stripping operations to carry out.

The dispersion region is characterized by :

• detachment of bubbles from the distributor in an uniform manner and in equal intervals

• rising of bubbles up along a very short distance with an acceleration and thereafter with a uniform velocity thru the layer of liq.

Plate columns are classified according to the mode of gas-liq flow in their plates :

1. Crossflow plates

2. Counterflow plates

Crossflow Plates : Bring into effect crossflow between the gas and liq steams **(Fig. 3.1).**

Each plate is fitted with a baffle and downcomer. The liq overflows the baffle and descends thru the down-comer to the next tray below. Liq-flow patterns on crossflow plates can be altered by changing the location of downcomers on the plates **(Fig. 3.2)**
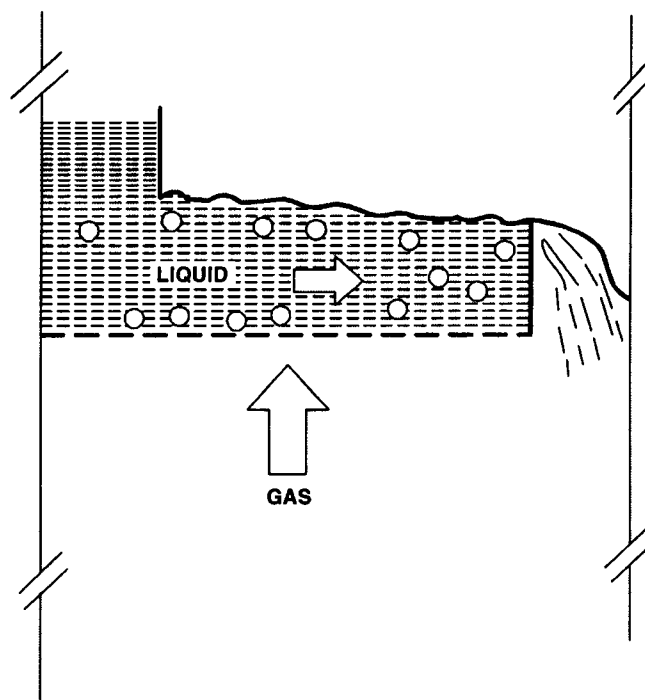
Fig. 3.1. *Crossflow Plate. The gas & the liq streams in any tray are in cross-flow to each other.*
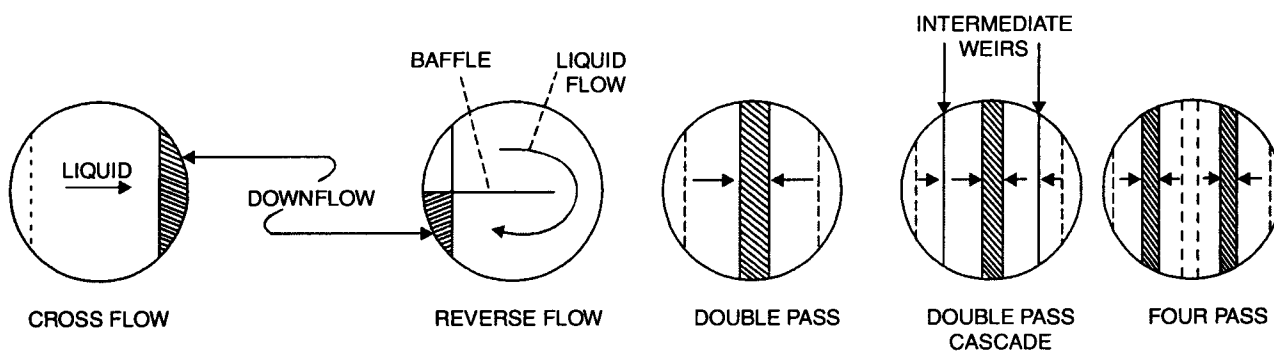
Fig. 3.2. *Common Liq-flow profiles on Crossflow Plates.*

Gas Dispersers : are perforations, bubblecaps etc. provided on the plate. Their sole function is to disperse gas into liq on the plate.

These perforations may be simple round orifices punched or drilled on the plate. These plates are called **Sieve Plates (Fig. 3.3)**
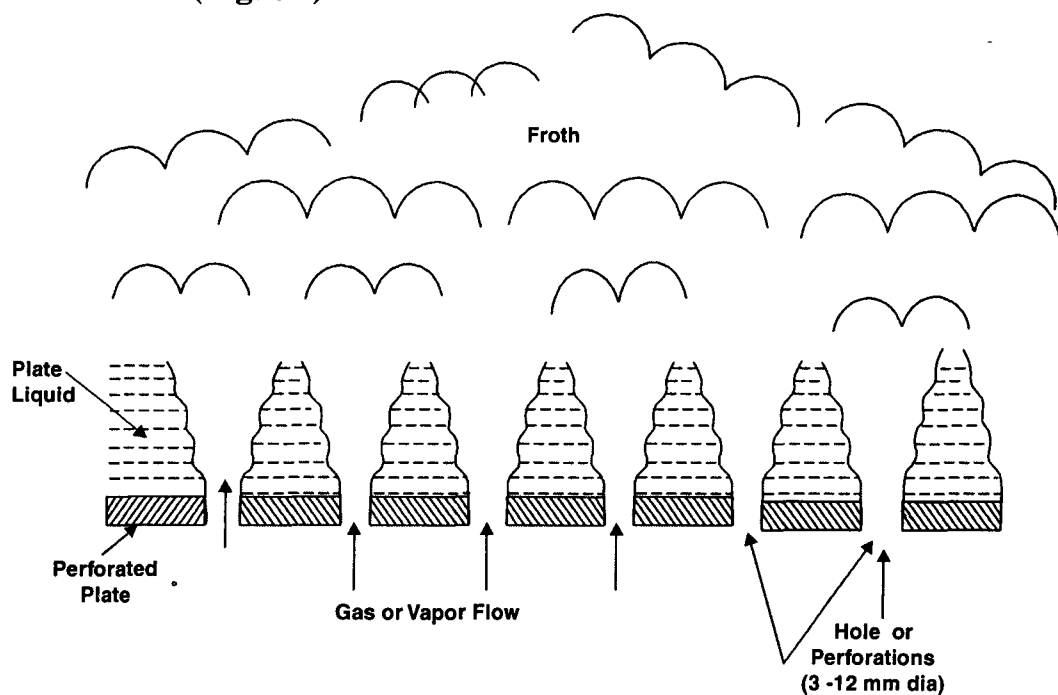
Fig. 3.3. *Sieve-plate Dispersers.*
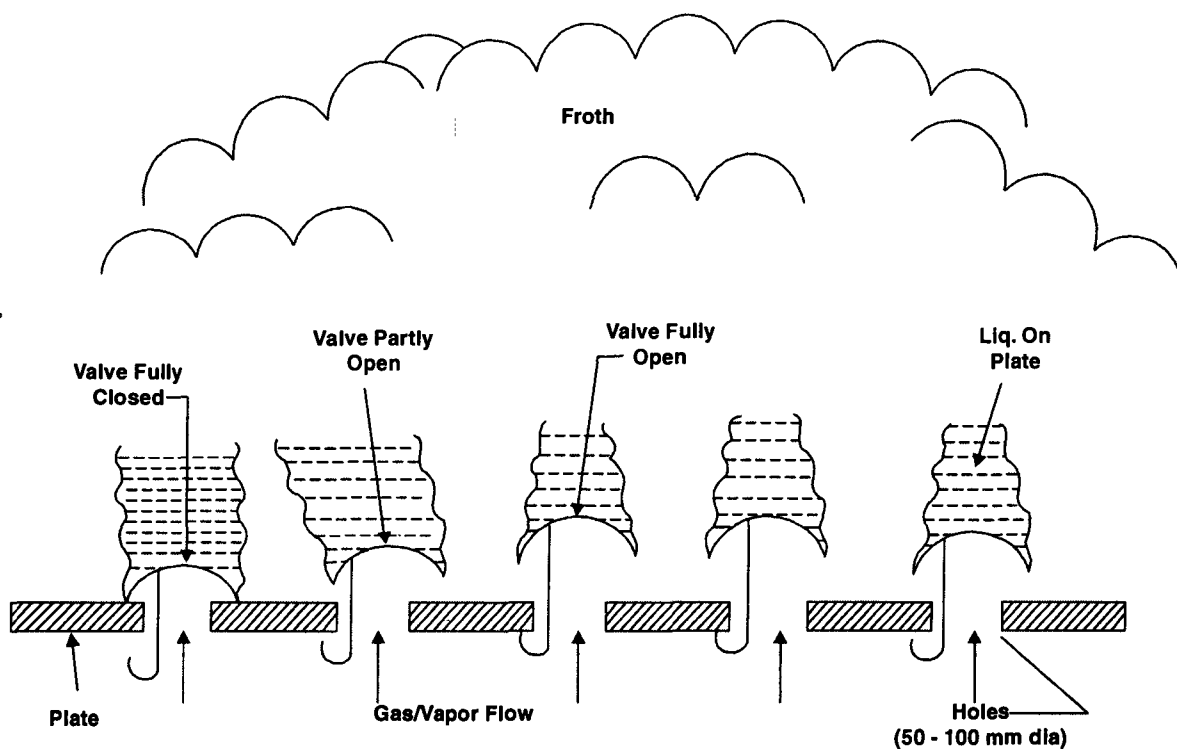
Fig. 3.4.1. *Valve-Plate Dispersers.*

If the holes are capped by liftable valves that provide variables orifices of nonuniform shape, the plates are called **Valve Plates (Fig. 3.4.1).** They're simply the extension of sieve plates.

Bubblecaps are the oldest gas dispersers. They've been used for over 150 years. Gas rises thru a central riser, reverses flow under the cap, flows downward thru the annulus between the riser and the cap and finally escaping, into the liq on tray, thru the slots or openings provided on the lower side of the cap **(Fig. 3.4.2)**
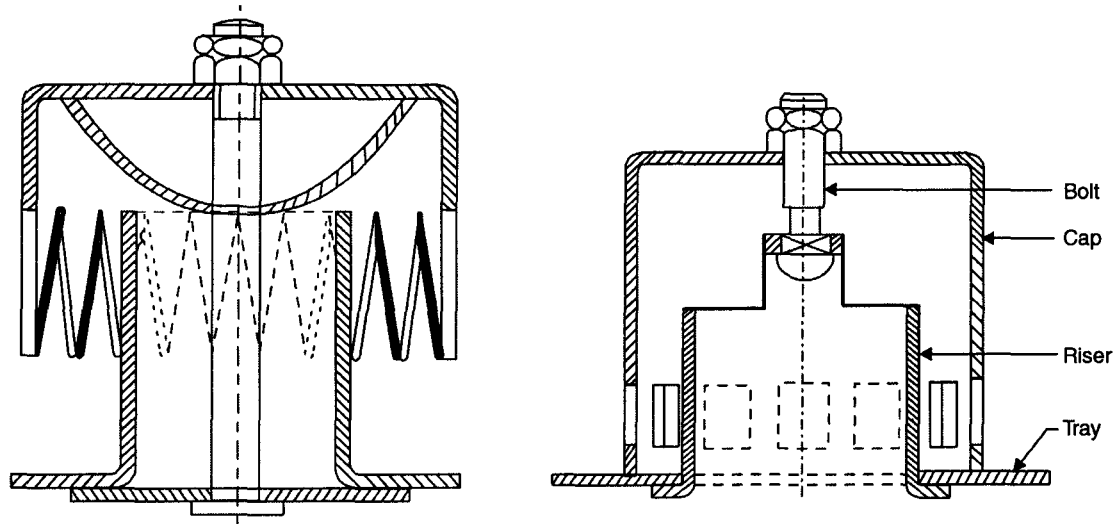
Fig. 3.4.2. *Bubblecaps.*

3.1.A. Hydraulics of Sieve-Plate Columns

Dry Pressure Drop : The dry plate drop thru a sieve plate is the sum of :

• **Entrance loss**

• **Friction loss**

• **Exit loss**

Entrance loss refers to gas pressure drop to overcome the resistance at the entrance to the perforations.

Friction loss arises out of gas pressure drop to overcome friction in the perforations.

Exit loss is the gas pressure drop due to expansion of gas stream as it emerges thru the perforations.

Hence, the **dry plate drop** in the sieve-plate :

$$h_d = C_o \left[0.4 \left(1.25 - \frac{A_o}{A_n} \right) + 4f \left(\frac{\delta_P}{d_o} \right) + \left(1 - \frac{A_o}{A_n} \right)^2 \right] \frac{v_{G,o}^2}{2g} \cdot \frac{\rho_G}{\rho_L} \qquad ...(3.1)$$

C.d 'A. Hunt *et.al.* — *AIChE Journal* **(Vol.1 / P – 441), 1955**

where, h_d = gas press drop thru a dry plate, m of clear liq

A_o = total area of orifices (perforations) , m^2

A_n = net tower cross-sectional area for gas flow , m^2

$= A_t - A_d$ for crossflow trays

δ_p = plate thickness, m

d_o = hole dia of perforations, m

$v_{G,o}$ = mean velocity thru orifices *i.e.* perforations, m/s

f = Fanning's friction factor which can be obtained from **Friction Factor vs. Reynolds No. Graph (Fig. 5.26 / Chemical Engineers' Handbook (5th ISE)**— Perry and Chilton)

C_o = orifice coefficient whose value depends on the ratio of δ_p / d_o. It can be obtained from the C_o vs. δ_P / d_O plot **[Figure 3.5]**
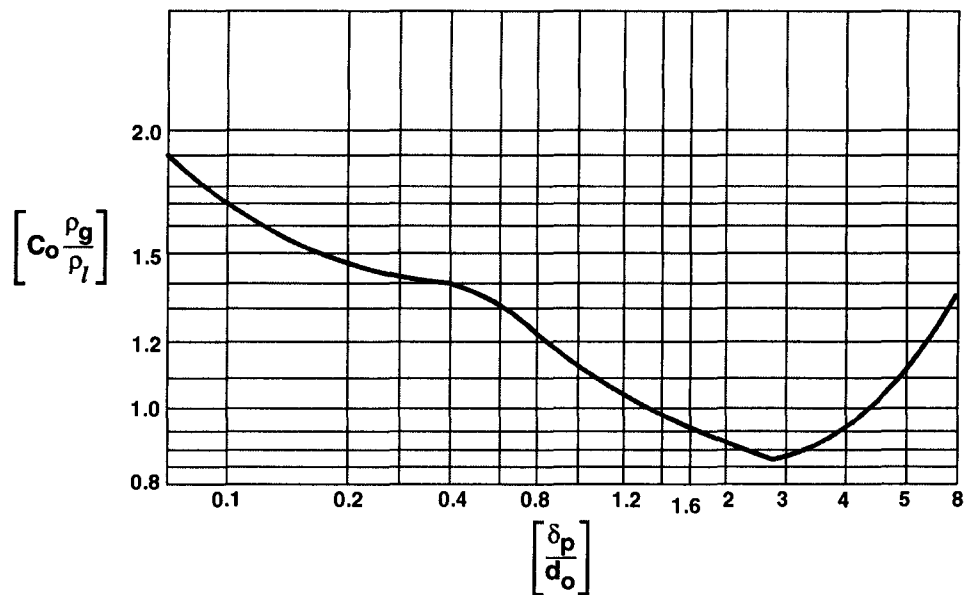
Fig. 3.5. *Orifice Coefficient (C_o) vs. Plate Thickness is to Hole Diameter (δ_p / d_o) Plot*

The value of orifice coefficient, C_o, can also be determined from :

$$C_o = 1.09 \left[\frac{d_o}{\delta p} \right]^{\frac{1}{4}} \qquad \qquad ...(3.2)$$

over the range of δ_p / d_o= 0.2 to 2.0

Hughmark and O'Connell

$$h_d = C_1^{-2} \cdot \frac{v_{G,o}^2}{2g} \left[1 - \left(\frac{A_h}{A_n} \right)^2 \right] \frac{\rho_G}{\rho_L} \qquad \qquad ...(3.1A)$$

where, $C_1 = 0.8806 - 0.0677 \left(\frac{d_o}{\delta p} \right) + 0.00732 \left(\frac{d_o}{\delta p} \right)^2 - 3.38 \times 10^{-4} \left(\frac{d_o}{\delta p} \right)^3 \qquad \qquad ...(3.2A)$

Note : Subscripts **h** stands for hole & **o** for orifice. Both are identical.

Leibson *et. al.*

$$h_d = C_2^{-2} \cdot \frac{v_{G,o}^2}{2g} \cdot \frac{\rho_G}{\rho_L} \qquad \qquad ...(3.1B)$$

$$\text{where, } C_2 = \left[0.836 + 0.273 \frac{\delta_P}{d_o}\right]\left[0.674 + 0.717 \frac{A_h}{A_n}\right] \qquad ...(3.2B)$$

while the comparable results are obtained from correlations of Hughmark-O'Connell and Hunt *et. al.*, the Leibson's orifice Eqn. 3.2A gives rise to somewhat higher dry-tray press. drop values.

If the plate thickness is ignored, the pressure drop thru a dry plate approximates to :

$$\Delta P_d = \xi \cdot \frac{v_{G,o}^2}{2} \cdot \rho_G \qquad \qquad ...(3.3)$$

where, ΔP_d = dry plate drop, Pa (*i.e.* N/m^2)

ξ = friction factor which is independent of the size and shape of the holes and their distribution on the plate

= 1.95—2.0 for A_o = (3—5)% A_n for ripple plates

= 1.4—1.5 for A_o = (15—20)% A_n for perforated and grid plates
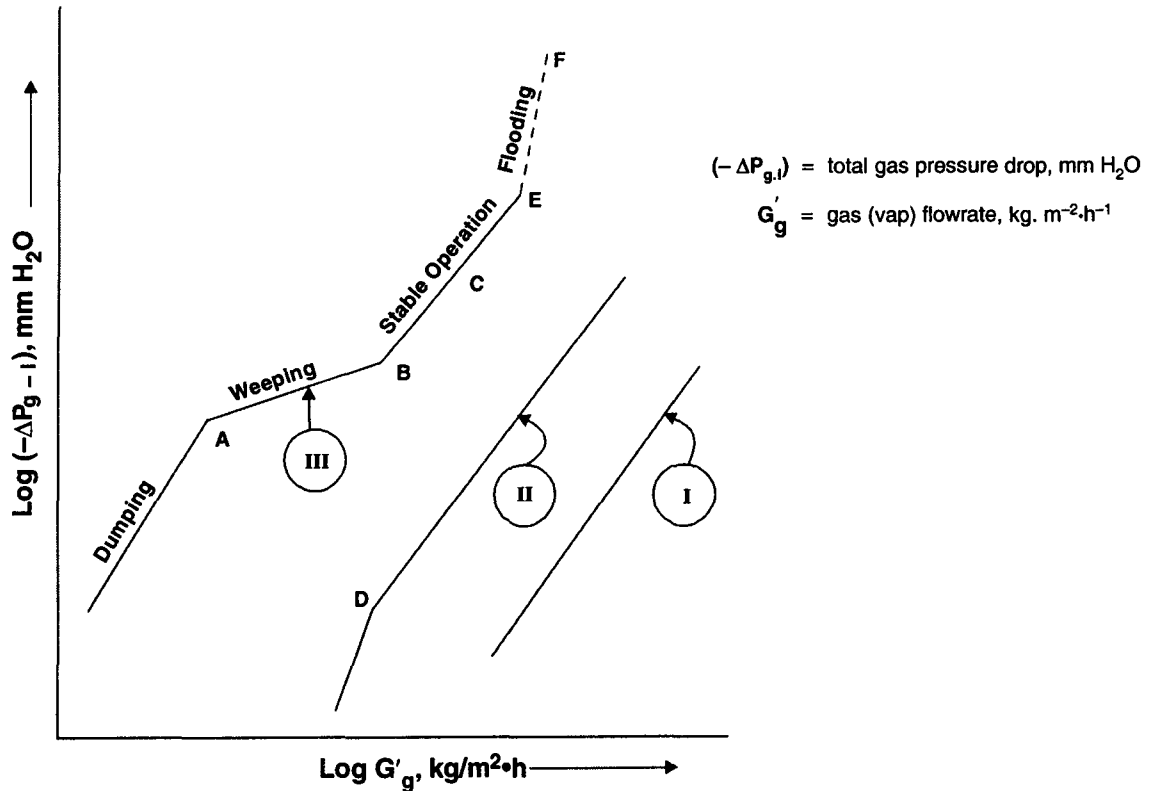
Fig. 3.6. *Gas Pressure Drop vs. Gas Rate Curves For Sieve Plates Under Three Different Conditions :*
   Curve-I : Dry Plate
   Curve-II : Irrigated Plate (Low Liq Rate)
   Curve-III : Irrigated Plate (Medium and High Liq Rates)

$v_{G,o}$ = gas velocity thru orifice (hole) , m/s

ρ_G = gas density , kg/m³

Irrigated Sieve Plates : The hydrodynamics of sieve plates is determined by

— *plate geometry i.e.* the number and size of the holes and the ratio of plate thickness to hole dia (δ_p/d_o)

— *liq rate*

— *gas rate*

— *physical properties of the gas-liq streams*

Fig. 3.6. represents the gas press drop variation under three typical operating conditions *viz.*

Curve (I) for dry plate

Curve (II) for irrigated plate at low liq rate

Curve (III) for medium and high liq rates

In absence of any liq flow in the column, the press. drop thru a dry plate changes linearly with the gas mass rate (G').Therefore,

$$\Delta P_d \propto v_{G,o}^2 \text{ approximately}$$

At constant moderate and high liq rates, the following regimes are observed :

Dumping (Showering) : At very low gas rates (less than pt. *A*), the liq flows freely over the plate but none of it reaches the downcomer. It entirely drains thru the perforations like showers **(Fig. 3.7).**
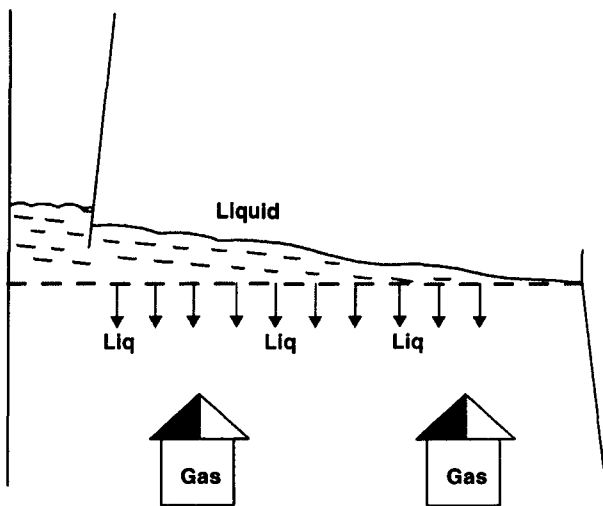
Fig. 3.7. *Dumping of tray liq thru perforations at low gas rates.*
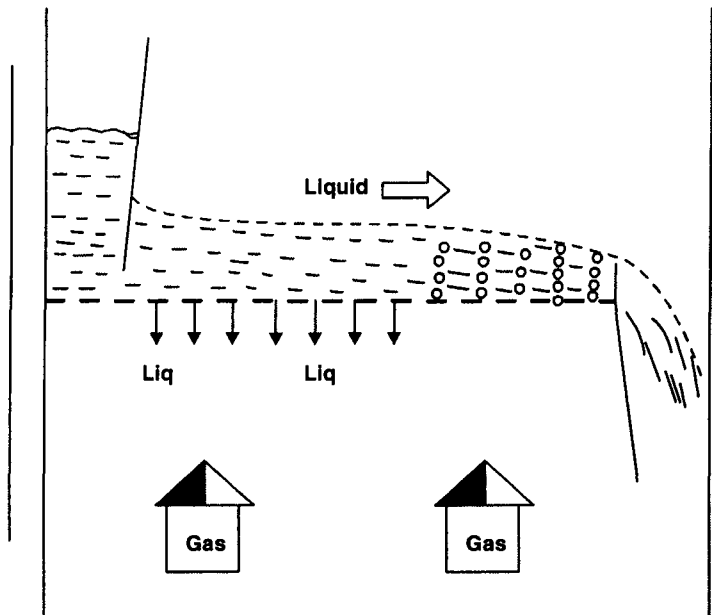
Fig. 3.8. *Weeping—A non-operating regime in which only a small number of holes constitute active zone.*

This is an unsteady-state operation.

Weeping : At gas velocities slightly higher than *A (Fig. 3.6),* a portion of the gas manages to pass thru only a limited number of holes and bubbles thru the liq-on-tray while much of the liq rains down thru the tray openings. This unsteady-state operation is called **weeping** *(Fig. 3.8).*

Operating Regime : At point **B** *(Fig. 3.6)* the gas or vap passes thru all the holes of the sieve-plate and the liq flows across the plate and overflows the weir into the downspout (downcomer). Thus normal operation sets in just at this point. **BC** marks the range of gas rate for stable operating regime—the entire gas stream bubbles thru the liq-on-tray gets dispersed very thoroughly into the liq producing gas-liq dispersion zone. This provides large interfacial surface areas and hence high tray efficiencies.

In this regime, high intensity of turbulence churns up a small fraction of the tray-liq into a froth and a mist of spray (the gas bubbles burst at the disengagement surface producing fine droplets of spray). The froth zone rests atop the dispersion zone while the spray zone caps the froth zone **(Fig. 3.9).**
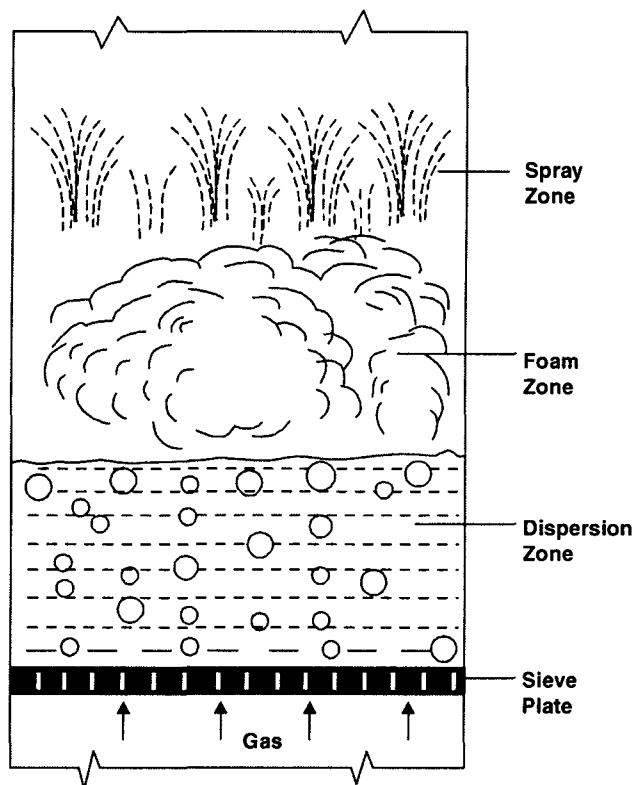
Fig. 3.9 : *Spray Zone Tops the Froth Zone that Caps the Dispersion Zone. A Stable Operating Regime.*

Priming : For gas-liq systems that tend to foam excessively, high gas velocities may lead to another inoperative regime called *priming* which is characterized by almost entire dispersion zone turned to a foamy mass leaving only a few mm thick bubbling layer (dispersion layer) on the tray deck and an insignificant zone of spray. The foam persists thruout the space between the trays and a great deal of liq gets gas-borne recirculates within the inter-tray spacing. This gives rise to excessive entrainment, (i.e., liq carryover) and high gas press drop that may lead to column flooding—called **Foamover or Foam Priming.**

Entrainment : When liq is carried up by the gas from the tray to the tray above, the phenomenon is called *entrainment* **(Fig. 3.10).** High gas rate and low liq rate are responsible for this. The entrained liquid is caught in the liq on the upper tray and counteracts the mass transfer operation. Entrainment is deleterious forasmuch as it

– exaggerates the liq loads on the upper trays.

- reduces the tray efficiency as liq from tray of lower volatility is carried to a tray of higher volatility with the effect that absorption effects get diluted.

- transports non-volatile impurities from the lower part of the column to the upper region and thereby contaminating the **OVHD**.

For the sake of convenience, liq entrainment is expressed in terms of fractional entrainment ψ

$$\psi = \frac{e}{L + e} \qquad\qquad ...(3.4)$$

where, e = absolute entrainment, $kmol/(h.m^2)$

L = liq rate, $kmol/(h.m^2)$

Flooding : For a constant liquid rate, increasing the gas rate results eventually in excessive entrainment of tray liq and flooding. **Point E (Fig. 3.6)** marks the onset of flooding. At the floodpoint there is very little or not at all liq flow down the col. Whatever liq fed to the col. is carried upward by the upflowing gas. As the col inventory of liq increases, ΔP across the col becomes quite large and control becomes difficult. Hence for a given liq rate, the max, allowable gas rate in a column must lie below this floodpoint by a safe margin.

Flooding may also be brought on by increasing the liq rate while keeping the gas rate constant. Excessive liq flow may become too much for the capacity of the downcomers whereupon the liq level in the downcomer rises up & reaches the liq level on the tray. This is called **DownComer Flooding** which is characterized by high gas press drop and other characteristics of flooded col. Line **CD** characterises flooding of a sieve-plate.

Fig. 3.10 shows the operating characteristic of sieve trays.
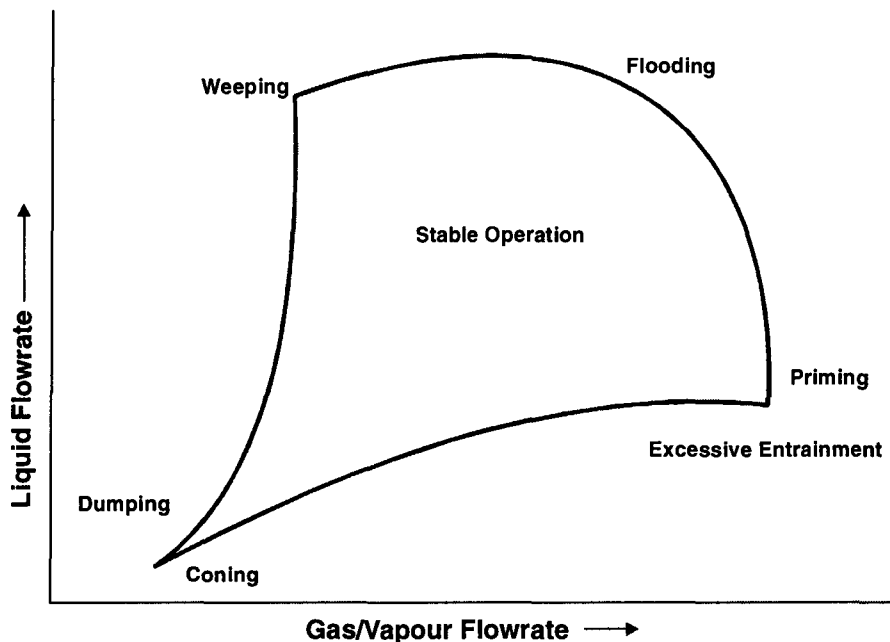
Fig. 3.10. *Operating Characteristics of Sieve Trays.*

Total Gas-Pressure Drop (h_{G-L}) thru an irrigated sieve-plate is the sum of :

■ *dry-plate drop* (h_d)

■ *hydraulic head* (h_L), *i.e., the press drop resulting from depth of liq on tray*

■ *residual pressure drop* (h_R)

– all the pressure drops being expressed in terms of head of clear liq of density ρ_L, *i.e.,*

$$h_{G-L} = h_d + h_L + h_R \qquad ...(3.5)$$

If expressed in terms of Pascals, (*i.e.,* N/m²), the above relationship would become

$$\Delta P_{G-L} = \Delta P_d + \Delta P_L + \Delta P_R \qquad ...(3.5)$$

Hydraulic Head (h_L) is the pressure drop required to overcome the weight of liquid pool on tray. It can be determined from Foss-Gerster relationship :

$$h_L = 0.0061 + 0.725h_w - 0.238\, h_w . v_{G,a} . \sqrt{\rho_G} + 1.225 \left(\frac{Q_{v,L}}{z} \right) \qquad ...(3.6)$$

A.S.Foss and J. A. Gerster — *Chemical Engineering Progress (Vol. 59/P-35), 1963*

where, h_L = hydraulic head, m of clear liq

h_w = weir height, m

$v_{G,a}$ = gas velocity based on active area A_a of the plate, m/s

$Q_{V,L}$ = volumetric flowrate of liq, m³/s

z = average flow width, m

$$= \frac{1}{2} [D_t + l_w]$$

D_t = tower dia, m

l_w = weir length, m

Fair correlated the effective liquid head to the operating liquid seal at outlet weir $(h_W + h_{OW})$ by means of an aeration factor β :

$$h_L = \beta (h_W + h_{OW}) \qquad ...(3.6A)$$

Source : J.F Fair in B. D. Smith's **Design of Equilibrium Stage Process** (McGraw-Hill, N.Y., 1963/Ch-15)

where β = aeration factor of liq in the active tray area, dimensionless

$$= 0.977 - 0.619\, F_{G,a} + 0.341\, (F_{G,a})^2 - 0.0636\, (F_{G,a})^3$$

$F_{G,a}$ = gas or vapor capacity based on active area, $kg^{\frac{1}{2}}.m^{-\frac{1}{2}}.s^{-1}$

$$= \frac{Q_{v,G}}{A_a} \sqrt{\rho_G}$$

$$= v_{G,a} . \sqrt{\rho_G}$$

The value of β can also be determined from the graph **Fig. 3.11**

The *pressure drop* resulting from the liquid pool on the tray (ΔP_L) can be calculated from
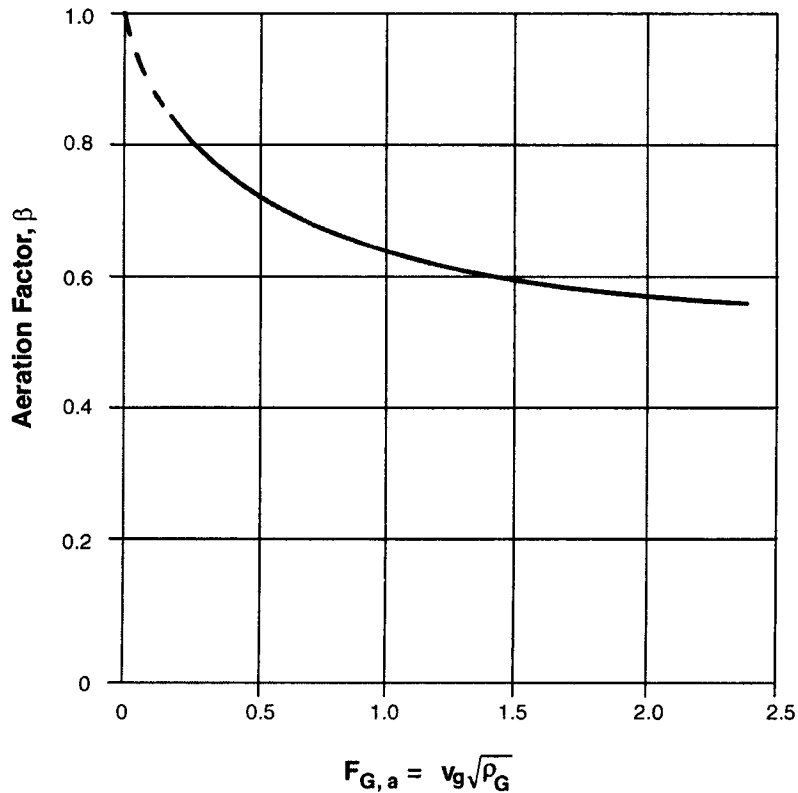
Fig. 3.11. *Aeration Factor for Bubble-Cap, Valve & Sieve Trays.*

$$\Delta P_L = 1.3 \left[\frac{\rho_f}{\rho_L} \cdot h_w + \left(\frac{\rho_f}{\rho_L} \cdot \Delta h \right)^{\frac{1}{3}} \right] \cdot \rho_L \cdot g \qquad \qquad ...(3.7)$$

> **Source** : Kafarov – **Fundamentals of Mass Transfer** (MIR Publ./Moscow), P : 354

where, ρ_f = density of foam on the tray, kg/m^3.

ρ_L = density of clear liq, kg/m^3

h_w = height of a weir, m

Δh = non-dispersed liq head at the weir, m of clear liq

$$= \left[\frac{Q_{m,l}}{\alpha . l_w} \right]^{\frac{2}{3}} \qquad \qquad ...(3.8)$$

$Q_{m,l}$ = liq. rate, kg.h^{-1}

α = coefficient of flow over the weir = 6400 – 10000

l_w = length of the weir, m

Residual Gas-Pressure Drop (h_R) : is the pressure drop required to overcome surface tension of the liq-on-tray as the gas issues from a perforation.

If ΔP_R is the excess pressure in the bubble due to surface tension (σ), then at the moment a bubble detaches from the perforation in the liq :

$$\pi . \frac{d_o^2}{4} . \Delta P_R = \pi . d_o . \sigma$$

$$\therefore \qquad \Delta P_R = \frac{4\sigma}{d_o} \text{ in N/m}^2 \qquad \qquad ...(3.9)$$

where, d_o = hole (perforation) dia, m

The relationship 3.9 is valid for bubbles less than 1mm in dia.

For holes of larger dia, the residual pressure drop must be computed from the formula :

$$\Delta P_R = \frac{4\sigma}{1.3\, d_o + 0.08\, d_o^2} \qquad \qquad ...(3.9A)$$

Source : Kafarov — *Fundamentals of Mass Transfer* (MIR Publ./Moscow/1975), p-35

But as per Eversole *et.al.* :

$$\Delta P_R = \frac{6\sigma}{d_b} \qquad \qquad ...(3.9B)$$

where, d_b = average bubble dia, m $\approx d_o$

Source : W.G. Eversole *et. al.*— *Industrial & Engineering Chemistry (Vo. 33/P-1459), 1941.*

$$\therefore \qquad h_R = \frac{6\sigma}{d_b} . \frac{1}{\rho_L . g} \qquad \qquad ...(3.10)$$

where, h_R = residual gas press drop expressed in m of clear liq

Head Loss Under Downcomer (h_{da}) : The head loss under downcomer apron as the liquid enters the tray may be estimated from :

$$h_{da} = 0.165 \left[\frac{Q_{v,L}}{A_{da}} \right]^2 \qquad \qquad ...(3.11)$$

where, A_{da} = area under downcomer apron, m^2

$Q_{v,L}$ = volumetric liq rate, m^3/s

The downspout is usually set at ($h_w - 0.025$) metre above the tray-deck, therefore,

$$A_{da} = l_w\, (h_w - 0.025) \text{ m}^2 \qquad \qquad ...(3.12)$$

where, l_w = length of weir, m

However, tray construction practice normally takes

$$A_{da} = 0.42\, A_d \qquad \qquad ...(3.12\text{ A})$$

J.R. Fair correlated head loss under downcomer to liq rate, $Q_{v,L}$ (m^3/s) thru :

$$h_{da} = 0.1526 \left[\frac{Q_{v,L}}{A_{da}} \right]^2 \qquad \qquad ...(3.11\ A)$$

Source : J. R. Fair in B. D. Smith's **Design of Equilibrium Stage Processes** (McGraw-Hill, NY, 1963/Ch-15).

3.1.B. Hydraulics of Valve-Plate Columns

Valve Plates are the extension of sieve-trays. The holes are provided with liftable caps that produce variable passages **[Fig. 3.12]** for the upflowing gas stream depending on the gas rate.

(A) Valve fully closed   (B) Valve partly open   (C) Valve fully open
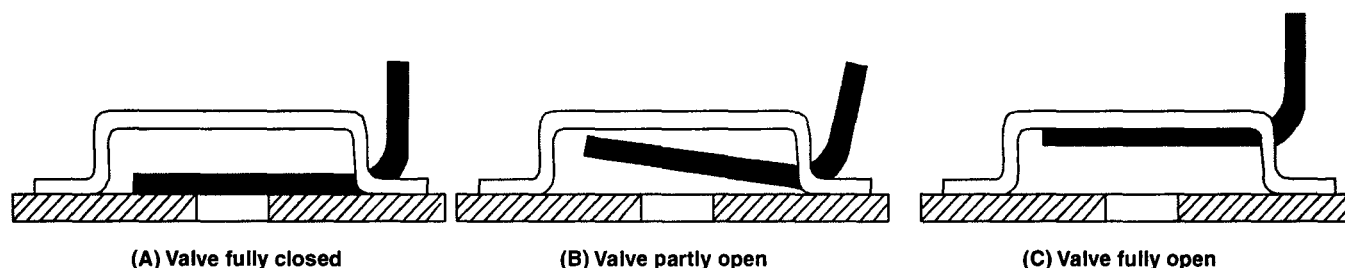
Fig. 3.12. *Three Different Positions of Valves on Valve Plate at Different Gas Load.*

TOTAL PRESSURE TOP

The total pressure drop thru an irrigated valve tray is the sum of gas pressure drop thru a dry plate and that thru pool of liquid-on-tray :

$$\Delta P_{G-L} = \Delta P_d + \Delta P_L \qquad \qquad ...(3.13)$$

Pressure Drop Curves

The pressure drop curves are obtained by plotting ΔP against gas velocity **[Fig. 3.13]**

For irrigated plates, ΔP_{G-L} is plotted against v_G while liquid rate appears as the curve parameter, *i.e.*, these curves are plotted against different constant liq rates.

It is quite clear from **Fig. 3.13** that the pressure drop thru a dry plate (ΔP_d) varies nonuniformly over the range of gas rate in the column. And therefore, it is not possible to frame a single ΔP_d − $v_{G,o}$ relationship that will express the dry plate drop from low to high gas rates.

The pressure drop curves can be divided into three zones depending on the gas velocity :

Zone - I : Low gas velocity 0.05 - 0.4 m/s

Zone - II : Moderate gas velocity 0.4 - 1.25 m/s

Zone - III : Higher gas velocity 1.25 - up m/s

The lower unit of gas velocity of **Zone - II** is determined from :

$$\left[v_G \right]_{II}^{low} = \left[\frac{f_2}{f_1} \cdot \frac{m_v \cdot g}{\rho_G \cdot a_o} \right]^{\frac{1}{2}} \qquad \qquad ...(3.14)$$
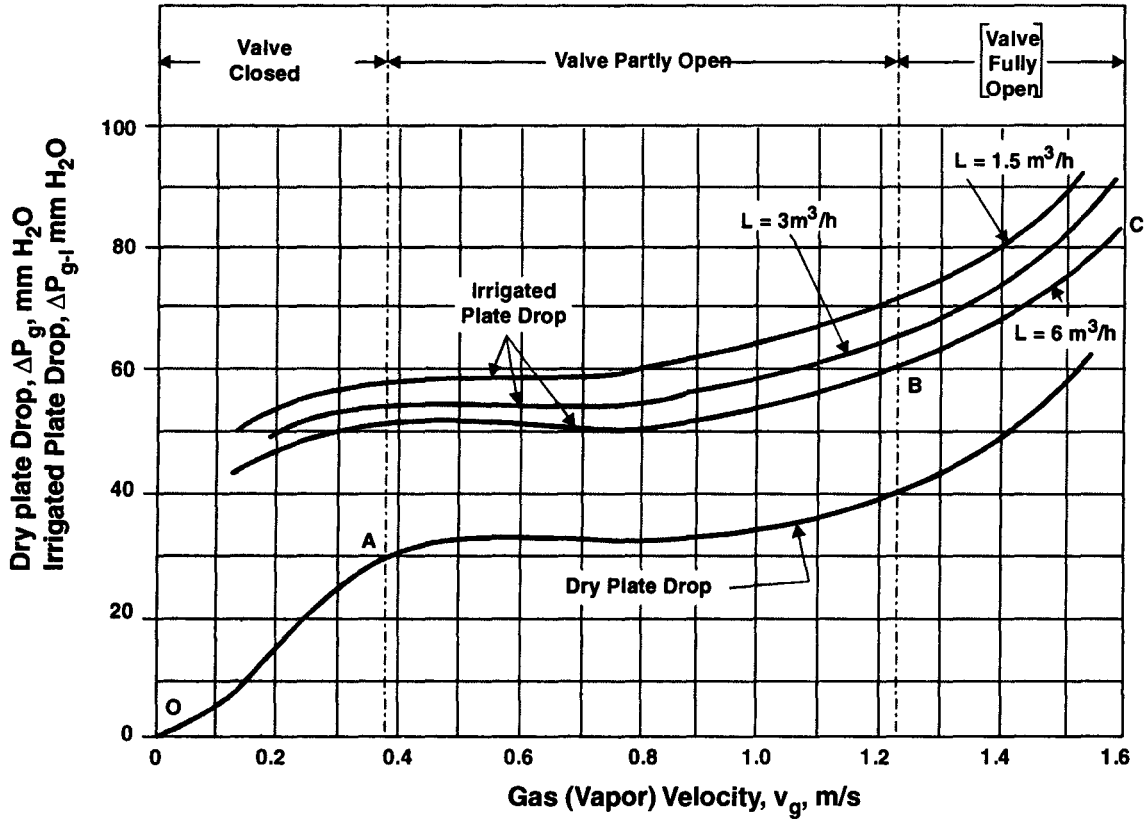
Fig. 3.13. *Pressure Drop Curves of A typical Valve Plate*

and the higher limit from :

$$[v_G]_{II}^{high} = 0.9\left[\frac{f_2}{f_4-f_3}\cdot\frac{m_v\cdot g}{\rho_G\cdot a_o}\right]^{\frac{1}{2}} \qquad ...(3.15)$$

where, $[v_G]_{II}$ = gas velocity in the region - II, m/s

   m_v = mass of a valve, kg

   ρ_G = gas density, kg/m^3

   a_o = area of a single hole, m^2

   f_1 , f_2 , f_3 , f_4 , are friction factors :

$$f_1 = 3500\left[\frac{A_o}{A_{v,i}}\right]^{1.2} \qquad ...(3.16)$$

$$f_2 = 6.71\left[\frac{A_o}{A_v}\right]^{-2.49}.exp\left[5.91\frac{A_o}{A_{v,}}\right] \qquad ...(3.17)$$

$$f_3 = 920\left[\frac{A_o}{A_{v,max}}\right]^{2.95} \qquad ...(3.18)$$

$$f_4 = 2160 \left[\frac{A_o}{A_{v,max}} \right]^{0.8} \qquad ...(3.19)$$

A_o = hole area of a plate, m^2

A_v = total open area of all valves on a plate, m^2

$A_{v,i}$ = total initial open area of all valves on a plate, m^2

The upper maximum, allowable hole velocity :

$$[v_{G,o}]_{max} = 1.3 \ [v_G]_{II}^{high} \qquad ...(3.20)$$

and the lower minimum allowable hole velocity :

$$[v_{G,o}]_{min} = 1.3 \ [v_G]_{II}^{low} \qquad ...(3.21)$$

Dry Pressure Drop

The dry plate drop across the plate with

valves fully closed :

Zone - I

$$[\Delta P_d]_I = \frac{f_1}{g} \left[\frac{Q_{v,G}}{A_o} \right]^2 \cdot \frac{\rho_G}{\rho_L}, \text{ m of liq} \qquad ...(3.22)$$

valves partly open :

Zone - II

$$[\Delta P_d]_{II} = f_2 \frac{m_v}{a_o \cdot L} + \frac{f_2}{g} \left[\frac{Q_{v,G}}{A_o} \right]^2 \cdot \frac{\rho_G}{\rho_L}, \text{ m of liq} \qquad ...(3.23)$$

valves fully open :

Zone - III

$$[\Delta P_d]_{III} = \frac{f_4}{g} \left[\frac{Q_{v,G}}{A_o} \right]^2 \cdot \frac{\rho_G}{\rho_L}, \text{ m of liq} \qquad ...(3.24)$$

Hydraulic Load

The gas pressure drop across the pool of liq-on-tray :

$$\Delta P_L = 0.27 \left[\frac{A_t}{A_o} \right]^{0.25} \cdot h_w^{0.85} \cdot \left[\frac{Q_{v,L}}{A_a} \right]^{0.35}, \text{ m of liq} \qquad ...(3.25)$$

where, A_t = tray area, m^2.

$Q_{v,L}$ = volumetric liq rate, m^3/h

h_w = weir height, m

A_a = active area (area of perforated sheet) of tray, m^2

3.1.C. Hydraulics of Bubblecap Tray Column

In bubblecap columns, the liquid and the gas or vapor are in crossflow. And the tray hydraulics depend on the gas and liq flowrates **(Fig. 3.14).**
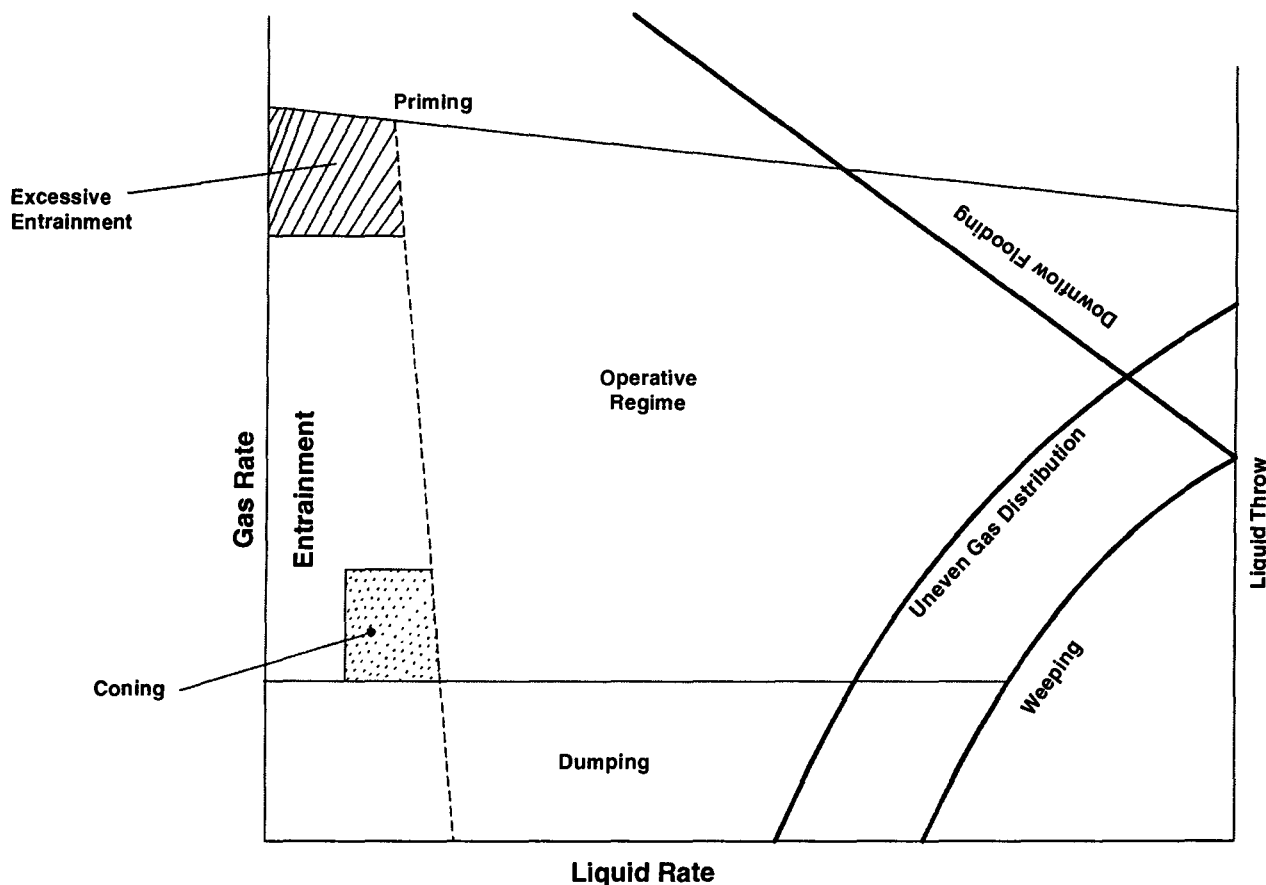
Fig. 3.14. *Different regimes of bubblecap tray hydraulics.*

At very low liquid rates.

I. low to moderate gas rate gives rise to **CONING** _____ an inoperative regime characterized by tray liquid being pushed away by the gas rising thru the bubblecap slots.

II. increasing gas rate gives rise to **ENTRAINMENT** _____ liquid carryout by gas stream.

III. and at still higher gas rates, excessive entrainment will occur.

At very low gas rates :

I. none of the liquid reaches the downspouts when the liquid rate is low. Entire tray liquid drains thru slots _____ a phenomenon called **DUMPING.**

II. with the increase of liquid rate, dumping yields to **WEEPING** _____ whence liq seeps thru all the tray openings plus some liq overflowing the weir.

III with the further increase of liq load, liq throw occurs, *i.e.*, at very high liquid rates, the liq. residence time on the tray is insufficient and the liquid flows in excess over the weir.

At very high gas rate and low liq rate, entrainment flooding **(PRIMING)** occurs and the liq fed to the column is carried out with the overhead gas. However, if under these circumstances liq rate is

gradually increased holding the gas constant, the col inventory of liq increases, press drop across the column becomes quite large and the excessive flow of liq overtaxes the capacity of downcomers and tray openings ultimately resulting in **DOWNFLOW FLOODING.**

Flow pattern

The placement of weirs make it possible to enforce the following liq-flow patterns on bubblecap trays :

— *crossflow*   — *reverse flow*

— *split flow, i.e., double-pass flow*   — *split flow cascade*

— *radial flow.*

The crossflow pattern is the most typical one for bubblecap plates.

The reverse flow pattern is limited to systems with small L/G ratios, because higher liquid loads increase hydraulic gradient on the tray.

For large dia columns or to accommodate large L/G ratios, the split flow arrangement is recommended. It can take up high liq rates and yet contributing to insignificant hydraulic gradient.

The double-pass cascading system is preferred where the column is to handle considerable L/G ratios or when the col dia is very large.

Superficial Gas velocity

It is the empty-column gas velocity attained by the gas while flowing thru the bubblecap trayed column when there is no liq flow in it.
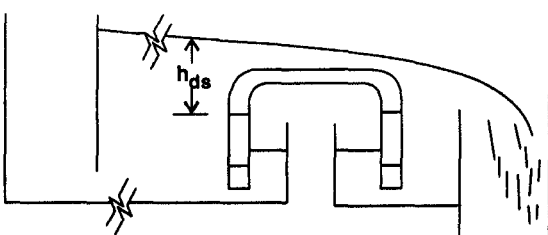
$$v_G = C_F \bullet \left[\frac{\rho_L - \rho_G}{\rho_G} \right]^{1/2}$$

where, ρ_L = liq phase density, kg/m^3

ρ_G = gas phase density, kg/m^3

C_F = **capacity factor** whose value depends on tray spacing and liq submergence (*i.e.*, the depth of liq pool on tray). See **Table 3.1.**

Table 3.1 Capacity Factor, C_F

Tray Spacing, l_t	Depth of liquid above the upper edge of slots, (h_{ds})			
(mm)	*12.5 mm*	*25 mm*	*50mm*	*75mm*
150	0.02 – 0.04	—	—	
300	0.09 – 0.11	0.07 – 0.09	0.05 – 0.07	
450	0.15	0.14	0.12	0.09
600	0.185	0.17	0.16	0.15
750	0.195	0.185	0.18	0.175
900	0.205	0.195	0.19	0.185

Maximum Allowable Gas Velocity

The maximum admissible gas velocity can be calculated from Souders-Brown equ.

$$v_{G,\,max} = 0.305\ C_F \left[\frac{\rho_L - \rho_G}{\rho_G}\right]^{1/2} \qquad\qquad ...(3.27)$$

> **Source :** M. Souders and G.G. Brown—*Industrial and Engineering Chemistry vol. 26 (1934)/P-98.*

Kirschbaum Equ. :

$$v_{G,\,max} = \frac{0.1578}{d_{cap}^{2/3}}\left[\frac{\rho_L}{\rho_G}\right]^{1/2} \cdot \Delta H \qquad\qquad ...(3.27A)$$

where, d_{cap} = cap dia, m

ΔH = height of upper edge of the cap from tray-deck, m

> **Source :** E.Kirschbaum —*Chem. Ing. Techn. vol. 28 (1956)/P-713.*
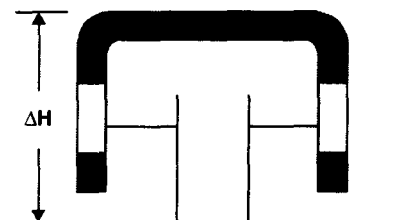
Bagaturov's Eqn. :

$$v_{G,\,max} = 0.38 \left[\frac{T}{M.P}\right]^{1/2} \qquad\qquad ...(3.27B)$$

where   T = gas temperature, K

M = mol. wt.of gas, kg/kmol

P = col. press., atm. abs.

This equation has been suggested for calculating maxm. admissible gas velocity in oil-refinery columns.

> **Source :** S.A. Bagaturov — *Petroleum and Gas [vol. 5(1959)/P-67].*

Pressure Drop

The gas pressure drop thru an irrigated bubblecap tray is the sum of dry plate drop and hydraulic head :

$$h_{G-L} = h_d + h_L \qquad\qquad ...(3.28)$$

where, h_{G-L} = total pressure drop thru an irrigated bubblecap tray, m of cl. liq.

h_d = pressure drop thru, *i.e.*, pressure drop thru gas-liq emulsion on the plate, m of cl. liq.

Dry-plate Drop : The dry-plate gas pressure drop is the sum of

— gas pressure drop thru risers (h_r)

— pressure drop thru the annulus of risers and bubblecap, including the circular clearance $(h_{C.C})$

— pressure drop thru slots (h_{sl})

$$h_d = h_r + h_{C.C} + h_{sl} \qquad\qquad ... (3.29)$$

Hydraulic head : The pressure drop thru the layer of the gas-liq emulsion on the tray is :

$$h_L = \beta \cdot h_{ds} = \beta \cdot (h_{ss} + h_{ow} + \frac{1}{2} h_{hg}) \qquad \qquad ...(3.30)$$

where, β = aeration factor, dimensionless

   h_{ds} = dynamic slot seal, m of clear liq

   h = static seal, m of cl. liq.

h_{ow} = height of crest over the weir, m of cl. liq

h_{hg} = hydraulic gradient on tray, m of cl. liq.

   The **dynamic slot seal, h_{ds}** varies depending on the operating conditions of the tray. The following values of h_{ds} are recommended :
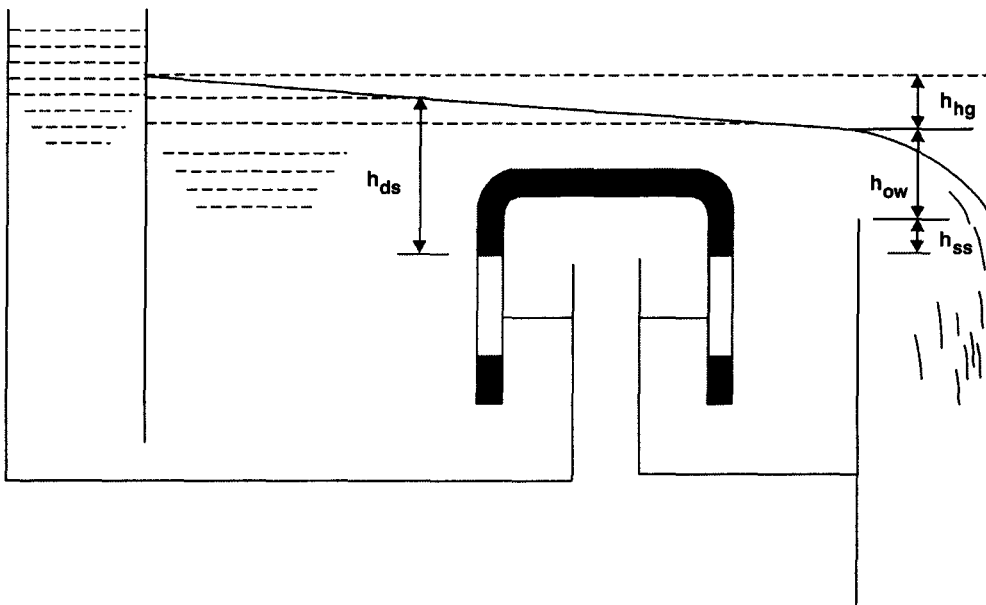
Table 3.2. Dynamic Seal

Col. Press. (kPa)	Dynamic Seal (h_{ds})
6 — 27	12.5 —38 mm
100	25 — 50 mm
> 100	50 — 100 mm

For segmental downcomer fitted with rectangular weir

$$h_{ow} = 0.666 \left[\frac{Q_{v,L}}{l_{w,eff}} \right]^{2/3} \qquad \qquad ...(3.31)$$

where, $Q_{v,L}$ = liq rate, m³/s

   $l_{w,eff}$ = effective weir length, m

   However, it is necessary to introduce a correction factor **k** into this equation to account for contraction of flow during its passage over the weir

$$h_{ow} = 0.666\ k\left[\frac{Q_{v,L}}{l_{w,eff}}\right]^{2/3}$$ ...(3.31A)

In practical calculations, k is taken equal to 1.12

3.2. HYDRAULICS OF PACKED TOWERS

A packed bed provides a mechanism for heat or mass transfer between gas and liquid phases usually flowing countercurrently in the column. However, the packing elements put up a resistance to these fluids. Of course, the resistance to the liquid flowing down thru the interspaces of packing is of not great importance because the liquid flows under the influence of gravity.

However, for the gas phase the picture is entirely different. As it flows upward, it must overcome the resistance offered by the packing element. In absence of any liquid flow, the bed may be treated as an extension of gas flow thru beds of granular solids.

The **dry bed-drop** (*i.e.*, gas-phase pressure drop thru dry bed) at low gas velocities is given by Carmen-Kozeny equation :

$$\Delta P_d = C\ \frac{v_G \cdot \mu_G}{\epsilon^3} \cdot \left[\frac{1-\epsilon}{d_p}\right]^2$$ ...(3.32)

assuming the flow is laminar and the gas pressure drop is mainly due to form drag loss.

ΔP_d = dry-gas pressure drop, Pa/m of Packed bed

v_G = superficial gas velocity, m/s

ϵ = void fraction, m^3 per m^3 of dry packing

d_p = packing diameter, m

μ_G = dynamic viscosity of gas, kg/(m.s)

C = proportionality constant.

Source : P.C. Carmen — *Journal of Society of Chemical Industry [vol. 57 (1938)/p-225].*

However, at higher gas velocities, as in most applications, the gas phase is in turbulent flow thru packed beds for which Burke and Plummer suggested :

$$\Delta P_d = C\ \frac{v_G^2 \cdot \rho_G}{d_p} \cdot \left[\frac{1-\epsilon}{\epsilon^3}\right]$$ ...(3.33)

assuming the pressure drop is mainly due to kinetic energy loss.

Source : S. P. Burke and W.B. Plummer—**Industrial and Engineering Chemistry [vol.20 (1928)/p-1196].**

Ergun combined the equation for form drag loss with the equation for kinetic energy loss :

$$\Delta P_d = C_1' \cdot \frac{v_G \cdot \mu_G}{\epsilon^3} \cdot \left[\frac{1-\epsilon}{d_p}\right]^2 + C_2' \cdot \frac{v_G^2 \cdot \rho_G}{d_p} \cdot \left[\frac{1-\epsilon}{\epsilon^3}\right]$$ ...(3.34)

Source : S. Ergun — **Chemical Engineering Progress [vol. 48, # 2, (1952)/p-89].**

This equation has been applied with some success to packed beds where dry-bed drop is small compared to the operating pressure of the column.

3.2.1. Influence of Packing Shape

Gas and liquid streams share the same flow channels in a packed bed. However, these flow channels have neither a fixed shape or diameter. The hydraulic radius [flow channel area divided by the wetted perimeter] varies quite significantly with the channel shape. The matter complicates as the flow channels are not straight nor are they of uniform length. Forasmuch as the gas pressure drop per m of bed-depth is constant, the actual gas velocity varies with the hydraulic radius as well as the effective length of the flow channel.

The effect of packing shape on ΔP is not well defined, even with the single-phase flow thru a packed bed. And therefore, the pressure drop produced in the actual packed bed must be experimentally determined.

Because of aerodynamic drag factor, the shape of packing element greatly influences resistance to flow. Because of this, the resistance to flow (*i.e.*, bed pressure drop), even for single-phase flow vary from one packing element to other though they have close characteristics :

Ceramic Intalox® saddles and **ceramic Raschig rings** have similar void fractions and bulk density, but greatly different pressure drop under same gas loading

Packing	*Void Fraction* (m^3/m^3)	*Bulk Density* (kg/m^3)	*Dry Bed Drop (Pa/m of bed depth)*	
			G' = 4394 kg/(h.m²)	*G' = 7811 kg/(h.m²)*
25 mm Intalox® Saddle	0.721	703	245	784
38 mm Raschig Rings	0.720	705	220	710

A similar situation exists between **Intalox® Metal Tower Packing (IMTP)** and **metal Pall** rings :

Packing	*Void Fraction* $kg/(h.m^2)$	*Bulk Density* $kg/(h.m^2)$	*Dry Bed Drop (Pa/m of bed depth)*	
			G' = 7324 kg.h⁻¹.m⁻²	*G' = 13182 kg.h⁻¹.m⁻²*
# 25 IMTP®	0.962	301	310	1012
50 mm Pall Rings	0.965	280	180	588

The test data show that the **IMTP®** and **ceramic Intalox® saddle** packing, by virtue of their shapes, produce less pressure drop than metal **Pall rings** and ceramic **Raschig ring**, respectively, for the same gas mass flow.

In single-phase gas flow, *i.e.*, for gas flow thru dry packing the pressure drop may be calculated from

$$\Delta P = C_1 . v_G^2 . \rho_G \qquad \qquad ...(3.35)$$

where, ΔP = gas pressure drop thru dry packed bed, Pa/m of bed depth

C_1 = dry-bed pressure-drop coefficient. It is constant for a given packing (**Table 3.3**)

Table 3.3. Dry-Bed Pressure-Drop Coefficient

Packing Type	*Material*	*Size (mm)*	*Wall Thickness (mm)*	C_1
Raschig ring	Ceramic	25	3.175	290.675
	Ceramic	38	4.76	175.556
	Ceramic	50	6.35	137.153
Raschig ring	Metal	25	1.58	296.251
	Metal	38	1.58	175.556
	Metal	50	1.58	137.153
Intalox saddle	Ceramic	25		235.904
	Ceramic	38		98.750
	Ceramic	50		76.806
	Ceramic	75		40.058
Pall ring	Metal	25	1.58	98.750
	Metal	38	1.58	60.347

The coefficient of dry-bed pressure-drop C_1 is actually the combined effect of packing shape factor, bed void fraction and hydraulic radius of the packing as indicated in Eqn. 3.33. It can be measured from the dry pressure drop line for any particular type and size of packing so long as the gas is in turbulent flow thru packed bed.

3.2.2. Irrigated Bed

Gas and liquid streams, during absorption, are either in *counterflow* (flowing mutually opposite direction) or in *cocurrent flow* (flowing in the same direction) within the packed bed. There is no theoretical model to predict the pressure-drop in irrigated packed beds. **Experimental** results are correlated in terms of **log ΔP vs. log G'** plot.

Countercurrent operation: As soon as a flowing liquid phase is introduced onto a packed bed, while a gas phase already been flowing upward thru the bed, the pressure drop will be greater than that developed only with gas flow.

Tower Dia = 750 mm
Packings used : 25mm Plastic Pall Rings
Packed Bed Height = 3m
ΔP = inch H_2O
Z = ft of packed bed
L' = liq loading, $lb.ft^{-2}.h^{-1}$ (water, here)
G' = gas loading, $lb.ft^{-2}.h^{-1}$
air
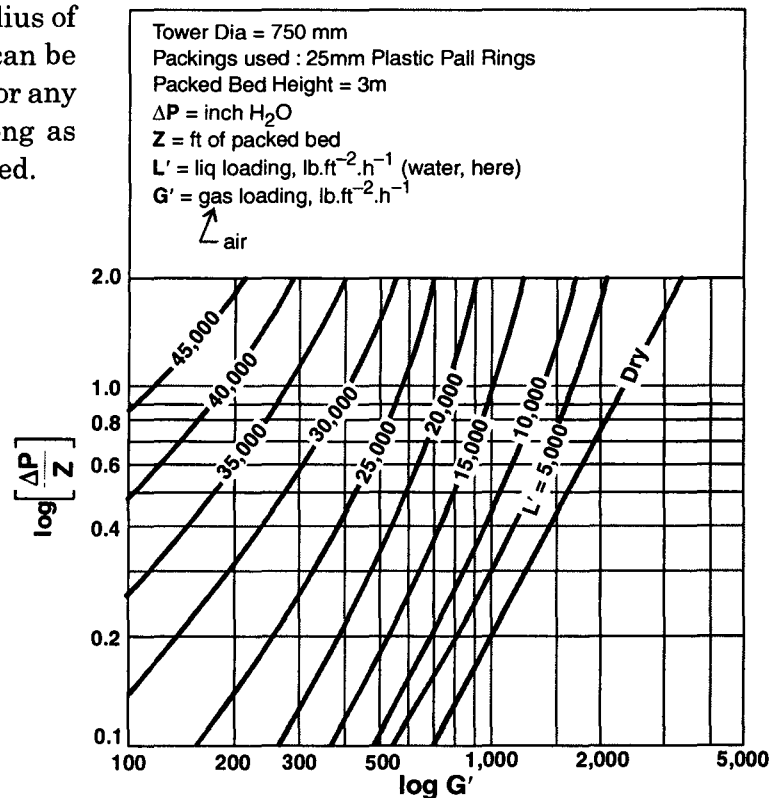
Fig. 3.15. *Pressure drop curves obtained by plotting Log [ΔP/Z] vs. Log G'*

At low gas rates, the pressure drop curves **log ΔP** *vs.* **log G'** run parallel to the dry line up to high liquid rates **(Fig. 3.15).**

But as the gas velocity is gradually increased the curves bend away from the dry line curve (*i.e.*, their slope increases). The highest gas rate at which pressure drop ΔP can be expressed by Eqn. 3.35 is called the LOWER LOADING POINT. **(Fig.3.16)**
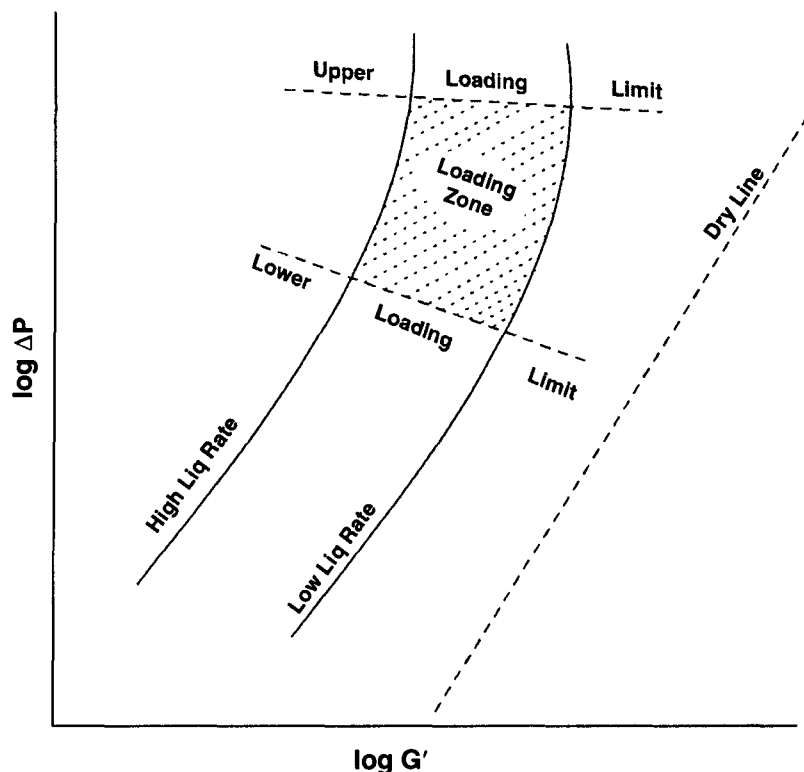
Fig. 3.16. *Pressure-drop characteristics of a packed bed.*

However, the dry-gas pressure drop represents a minimum value; when the packing is irrigated, the pressure drop increases. Leva modified C_1 to account for the effect of liquid rate

$$\Delta P = C_2 . 10^{C_3 v_L} . \rho_G . v_G^2 \qquad \qquad ...(3.36)$$

where, C_2 and C_3 are constants **(Table 3.4)**

v_L = superficial liq velocity, m/s

Source : M. Leva — *Chemical Engineering Symposium Series vol. 50 and 51 (1954).*

Table 3.4. Coefficients For Pressure Drop Correlation Of Leva

Type of Packing	*Nominal Size (mm)* (mm)	*Wall thickness* (mm)	C_2	C_3	*Range of L'* [kg/(h.m²)]
Raschig ring	13	2.4	1920	0.1893	1460—4200
	19	2.4	450	0.1184	8790—52750
	25	3	439	0.1141	1750—131800

Contd.,

Type of Packing	*Nominal Size (mm)* (mm)	*Wall thickness* (mm)	C_2	C_3	*Range of L'* [kg/(h.m²)]
Berl saddles	38	6	165	0.1049	3500—87900
	50	6	154	0.0774	3500—105450
	13	—	823	0.0892	1460—68840
	19		329	0.0774	1750—70300
	25		219	0.0774	3500—140600
	38		110	0.0594	3500—105450
Intalox saddles	25		170	0.0728	12300—70300
	38		77	0.0594	12300—70300

As the gas rate increases, the gas phase begins to interact with the liquid affecting the liquid flow regime. At higher gas rates, the rate of change of bed pressure drop increases more drastically than a constant value. This is because liquid holdup increases with increasing gas rate. This gas rate is called **Upper Loading Point (Fig. 3.16)**.

The upper loading limit defines the maximum capacity of the column. Gas rates higher than this limit will bring about either massive liquid entrainment in the gas phase **(entrainment)** or excessive liquid holdup in the packed bed **(Flooding)**.

At high liquid rates, depending on the size of the packing element, the bed voids largely tend to be filled with liquid as the gas flowrate approaches zero. As a result some of the input gas is aspirated down the column in the liquid phase. After the lapse of sufficient retention time of the liquid at the base of the column, these aspirated gas bubbles begin to disengage from the liquid phase and escape back into the gas phase. The packed bed, therefore, exhibits a pressure drop which is the outcome of the internal gas flow passing upward thru the bed. This internal gas flow is the sum of the externally introduced gas flowrate plus the recirculated gas stream released from the liquid at the bottom of the column.

Therefore, packed columns are not designed at very high liquid rates because pressure drop cannot be predicted by the usual correlations. And the designer should normally select a large enough packing element to avoid this area of operation. For instance :

50 mm packings do not exhibit this phenomenon below liq rate of 170 m³/h per m² of bed cross-section. Likewise 89 mm packings have been reported to operate at liq rates as high as up to 300 m³/(h.m²) without this gas-aspiration effect.

3.2.3. Flooding

At constant gas rate, an increase in liq thruput is accompanied by an increase in pressure drop. This is because the liquid inventory takes up more and more room in the packing with the increase of liquid rate, *i.e.*, greater restriction to gas flow is imposed. This ultimately leads to *flooding*— a point that represents the maximum capacity condition for a packed bed column. Any slight increase in liquid rates beyond this point builds up a deeper and deeper liquid pool atop the packing whereupon pressure drop hypothetically reaching an infinite value **(Fig. 3.17)**.

Likewise at constant liquid downflow rates L'_1, L'_2 ...... etc. increasing gas flow is again accompained by rising pressure drop until the floodpoint (marked by the dotted ΔP_{fl} line) is reached, whereupon the slightest increase in gas rate will cause a decline in permissible liquid thruput. This

Table 3.5. Liquid Holdup in packed towers

Packing type	Size (mm)	d_s	$\varphi_{L,\,s}$	$\varphi_{L,\,s/W}$	$\varphi_{L,\,t/W}$	H
Raschig Rings (ceramic)	13	17.74×10^{-3}	$0.0486 \dfrac{\mu_L^{0.02}}{\rho_L^{0.37}} \cdot \dfrac{\sigma^{0.99}}{d_s^{1.21}}$	$\dfrac{2.47 \times 10^{-4}}{d_s^{1.21}}$	$\dfrac{\left(2.09 \times 10^{-6}\right)\left(737.5L'\right)^{\beta}}{d_s^2}$	$\dfrac{975.7 L'^{0.57} \cdot \mu_L^{0.13}}{\rho_L^{0.84}\left(2.024 L'^{0.43} - 1\right)} \times$ $\cdot \left[\dfrac{\sigma}{0.073}\right]^{0.1737 - 0.262 \log L'}$ for $\mu_L < 0.012$ kg/(m.s)
	25	35.6×10^{-3}				
	38	53×10^{-3}				
	50	72.5×10^{-3}				
					$\beta = 1.508\, d_s^{0.376}$	$\dfrac{2168 L'^{0.57} \cdot \mu_L^{0.31}}{\rho_L^{0.84}\left(2.024 L'^{0.43} - 1\right)}$ $\cdot \left[\dfrac{\sigma}{0.073}\right]^{0.1737 - 0.262 \log L'}$ for $\mu_L > 0.012$ kg/(m.s)
Berl saddles (ceramic)	13	31.62×10^{-2}	$0.00423 \dfrac{\mu_L^{0.04}}{\rho_L^{0.37}} \cdot \dfrac{\sigma^{0.55}}{d_s^{1.56}}$	$\dfrac{5.014 \times 10^{-5}}{d_s^{1.56}}$	$\dfrac{\left(2.32 \times 10^{-6}\right)\left(737.5L'\right)^{\beta}}{d_s^2}$	$\dfrac{1404\ L'^{0.57} \cdot \mu_L^{0.13}}{\rho_L^{0.84}\left(3.24 L'^{0.413} - 1\right)}$ $\cdot \left[\dfrac{\sigma}{0.073}\right]^{0.2817 - 0.262 \log L'}$ for $\mu_L < 0.012$ kg/(m.s)
	25	3.2×10^{-2}				
	38	4.72×10^{-2}				
					$\beta = 1.508\, d_s^{0.376}$	$\dfrac{2830 L'^{0.57} \cdot \mu_L^{0.31}}{\rho_L^{0.84}\left(3.24 L'^{0.413} - 1\right)}$ $\cdot \left[\dfrac{\sigma}{0.073}\right]^{0.2817 - 0.262 \log L'}$ for $\mu_L > 0.012$ kg/(m.s)

μ_L in Pa.S, *i.e.*, kg/(m.s); ρ_L in kg/m³; L' in kg/(s.m²); σ = surface tension, N/m;
d_s dia of a sphere of same surface as the single packing element, m

causes the remaining liquid to again accumulate atop the packing with the effect that pressure drop again increases infinitely.

ΔP = press.drop per unit height of packing. $Pa.m^{-1}$
P = total pressure, Pa
ΔP_{fl} = press.drop per unit height of packing at incipient flooding
G'_{fl} = gas rate at incipient flooding, $kg.h^{-1}$
L' = liq rate.$kg.h^{-1}$
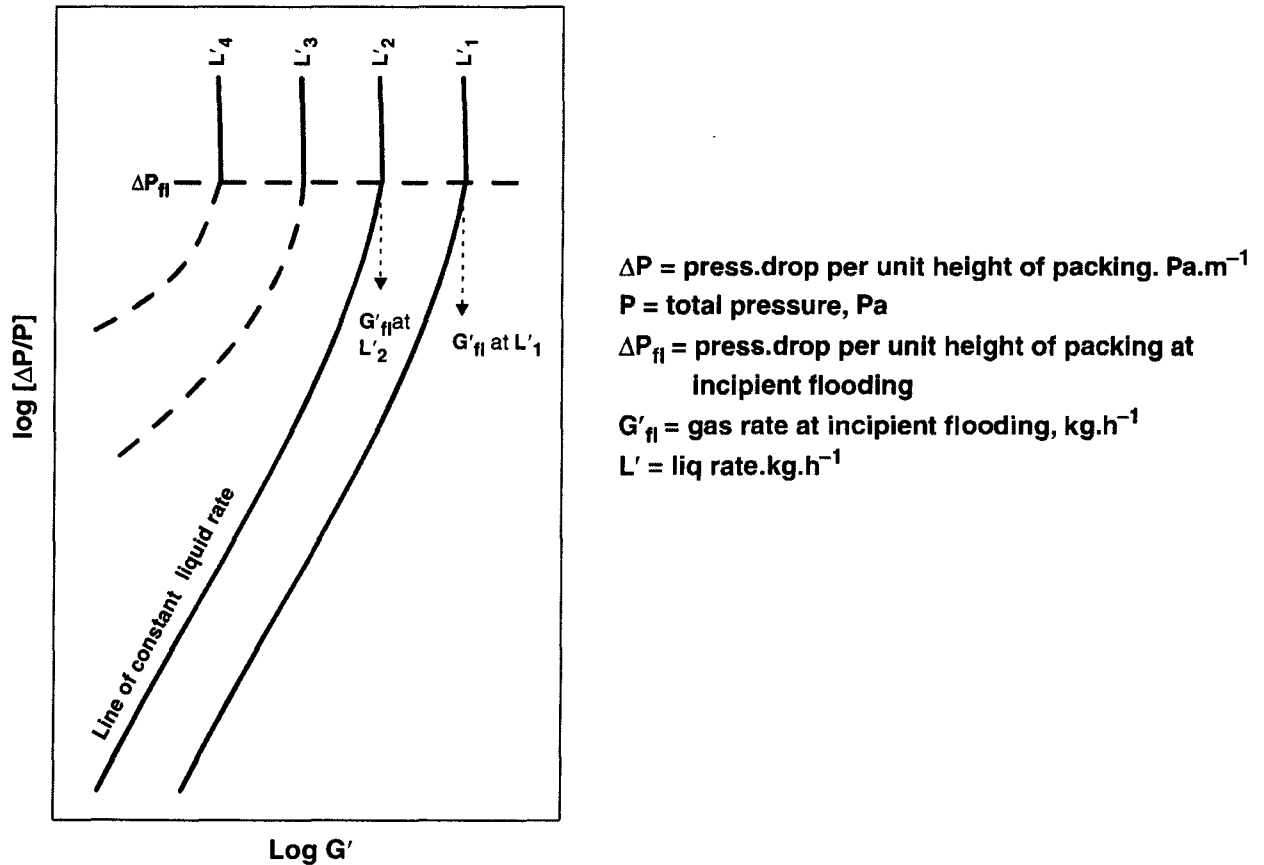
Fig. 3.17. *Pressure drop vs. Gas rate.*

3.2.4. Liquid Holdup

A packed bed demonstrates two different types of liquid holdup :

— *static holdup*, $\varphi_{L,S}$

— *operating holdup*, $\varphi_{L,o}$

Static holdup represents that volume of liquid per unit volume of packing which remains in the bed that has been fully wetted and then drained after the gas and liquid flows have been discontinued. Normally, the static holdup is not large and hence its effect on column hydraulics is insignificant.

The static holdup depends on :

packing surface area

the roughness of the packing surface

angle of contact between the packing surface and the liquid.

Besides, the capillary forces hold liquid at the junctions between the individual packing elements contribute to static holdup to some extent. Modern tower packings normally do not trap stagnant pools of liquid within the packing element itself.

Operating holdup is that volume of liquid per unit volume of packing that drains out of the bed after the gas and liquid flows to the column are discontinued.

Gas rate below the loading region exercises little effect on holdup.

Liquid surface tension has practically no effect on operating holdup for high surface tension liquid such as water.

However, liquid holdup increases with increasing liquid viscosity. For instance, if the v_L is increased from 10^{-6} m²/s to 2×10^{-6} m²/s, the liq holdup will increase by 10%. At about 16×10^{-6} m²/s liq viscosity, the holdup will be about 50% greater.

Viscous liquids tend to bridge the void space between the packing elements of a bed whereupon the bed undergoes a rapid loss of its gas handling capacity as liquid rates are increased. Smaller the packing size, greater is this effect. Therefore, it is recommended that only 38mm and larger size packing be used for handling liquids of 50×10^{-6} m²/s or higher viscosity.

The pressure drop thru a packed bed is not only due to the frictional loss and kinetic energy loss thru the packing but also due to the force exerted by the operating liquid holdup. Thus, for the same pressure drop a given packed bed has much less liquid holdup with high density liquid systems than with low density liquids.

The liquid holdup in packed towers can be estimated from Shulman's data **(Table 3.5)**

$$\varphi_{L,\,t} = \varphi_{L,s} + \varphi_{L,\,o} \qquad \qquad \text{...(3.37)}$$

$$\varphi_{L,\,o} = \varphi_{L,o/W} \cdot H \qquad \qquad \text{...(3.38)}$$

$$\varphi_{L,\,t/W} = \varphi_{L,s/W} + \varphi_{L,\,o/W} \qquad \qquad \text{...(3.39)}$$

where, $\varphi_{L,\,s/W}$, $\varphi_{L,o/W}$ and $\varphi_{L,\,t/W}$ refer to static, operating and total holdup when water or dil. aq. soln. is the liq stream.

$$H = \text{holdup correction factor.}$$

3.2.5. Interfacial Area

The interfacial area a_A, also called **specific interfacial surface**, for absorption and desorption with non-aqueous liquids is given by

$$a_A = a_{a|w} \frac{\varphi_{L,o}}{\varphi_{L,o/W}} \qquad \qquad \text{...(3.40)}$$

where, $a_{A|W}$ = interfacial area for absorption/desorption with water or very dil. aq. solns., m²/m³ of packed bed

$$a_{A/W} = m \left[\frac{808\,G'}{\rho_G^{0.5}} \right]^n \cdot L'^{\,p}$$

For conditions below loading, Shulman proposed :

where, **m, n, p** are all empirical constants whose values are given in **Table 3.6**

Table 3.6. Empirical Constants of Shulman's Relationship

Packing	Size (mm)	L' (kg/s.m²)	m	n	p
Raschig rings	13	0.678–2.0	28.01	0.2323 L' – 0.3	–1.04
		2.03–6.10	14.69	0.0111L' + 0.148	–0.111
	25	0.678–2.03	34.42	0	0.552
		2.03–6.10	68.2	0.0389L' – 0.0793	–0.47
	38	0.678–2.03	36.5	0.0498L' – 0.1013	0.274
		2.03–6.10	40.11	0.0109 L'– 0.022	0.140
	50	0.678–2.03	31.52	0	0.481
		2.03–6.10	34.03	0	0.362
Berl saddles	13	0.678–2.03	16.28	0.0529	0.761
		2.03–6.10	25.61	0.0529	0.170
	25	0.678–2.03	52.14	0.0506L' – 0.1029	0
		2.03–6.10	73.0	0.0310L' – 0.063	–0.359
	38	0.678–2.03	40.6	–0.0508	0.455
		2.03–6.10	62.4	0.024 L' – 0.0996	–0.1355

Source : H.L.Shulman *et. al.— American Institute of Chemical Engineers Journal*

Vol.1 (1955)/P–247, 253, 259; Vol.3 (1955)/P–157

Vol.5 (1959)/P–280; Vol.6 (1960)/P–469;

Vol.9 (1963)/P–479; Vol.13 (1967)/P–1137;

Vol.17 (1971)/P–631

3.2.6. Generalized Pressure-Drop Correlation

Since flooding normally represents the maximum capacity condition of a packed column, it is, therefore, a must to predict its value for new designs. For that it is highly desirable to have a generalized pressure-drop correlation to predict pressure drop in a packed bed.

Although the pressure-drop plots are available for most commercial random packings, these data are usually based on air-water system. While the air flowrate can be corrected for changes in gas densities, no reliable method exits to take into account the change of physiochemical properties of different liquids.

On the basis of laboratory measurements primarily on the air-water system, Sherwood *et.al.* developed the following generalized pressure-drop correlation of packed column for counterflow operations :

$$v_G^2 \cdot \frac{a_p}{\epsilon^3} \cdot \frac{\rho_G}{\rho_L} \cdot \frac{\mu_L^{0.2}}{g} = \text{function} \; \frac{L'}{G'} \left[\frac{\rho_G}{\rho_L} \right]^{0.5} \qquad \qquad \text{...(3.42)}$$

Source : T.K. Sherwood *et.al.—Industrial and Engineering Chemistry Vol. 30(1998)/P–765*

where v_g = superficial gas velocity , m/s

a_p = surface area of packing , m²/m³

ϵ = fractional voids in dry packing , m³/m³

ρ_L = liq density, kg/m³

ρ_G = liq density, kg/m³

μ_L = dynamic viscosity of liq, kg/(ms)

L' = liq mass rate , kg/(h.m²)

G' = gas mass rate , kg/(h.m²) = $v_G \cdot \rho_G$

The right handside of the Eqn. 3.42 is known as **Flow Parameter**

$$F_{L-G} = \frac{L'}{G'} \left[\frac{\rho_G}{\rho_L} \right]^{0.5} \qquad \qquad ...(3.43)$$

The flow parameter is the square root of the ratio of the liquid kinetic energy to gas kinetic energy :

Flow Parameter

$$= \frac{kg_L/(h.m^2)}{kg_G/(h.m^2)} \cdot \left[\frac{kg_G/m_G^3}{kg_L/m_L^3} \right]^{0.5}$$

$$= \sqrt{\frac{kg_L \cdot \left[\dfrac{m}{h}\right]_L^2}{kg_G \cdot \left[\dfrac{m}{h}\right]_G^2} \cdot \frac{m_L}{m_G}}$$

$$= \sqrt{\frac{(K.E.)_L}{(K.E.)_G}}$$

Lobo *et.al.*, modified Sherwood's equation by replacing the a_p/ϵ^3 term with F_p, called PACKING FACTOR :

$$v_G^{0.2} \cdot F_p \cdot \frac{\rho_G}{\rho_L} \cdot \frac{\mu_L^{0.2}}{g} = \text{function } F_{L-G} \qquad \qquad ... (3.44)$$

Source : W.E. Lobo *et.al*—*Transactions of American Institute of Chemical Engineers vol. 41 (1945)/p-693.*

The ratio a_p/ϵ^3 characterizes the size and shape of a particular packing, but it failed, the above researchers showed, to adequately predict packing hydraulic performance.

Eckert further modified this correlation. He introduced the term ψ, the ratio of density of water to the density of the liquid :

$$G'^2 \cdot F_p \cdot \frac{\psi}{\rho_G \cdot \rho_L} \cdot \frac{\mu_L^{0.2}}{g} = \text{function } \frac{L'}{G'} \left[\frac{\rho_G}{\rho_L} \right]^{0.5} \qquad \qquad ...(3.45)$$

where, $G' = v_G \cdot \rho_G$

and the generalized pressure-drop correlation is represented graphically in Fig. 3.18.

Eckert's further modification led to the development of the following correlation :

$$G'^2 \cdot \frac{F_p}{\rho_G \cdot (\rho_L - \rho_G)} \cdot \frac{\mu_L^{0.1}}{g} = \text{function } \frac{L'}{G'} \cdot \left[\frac{\rho_G}{\rho_L - \rho_G} \right]^{0.5} \qquad \qquad ...(3.45A)$$
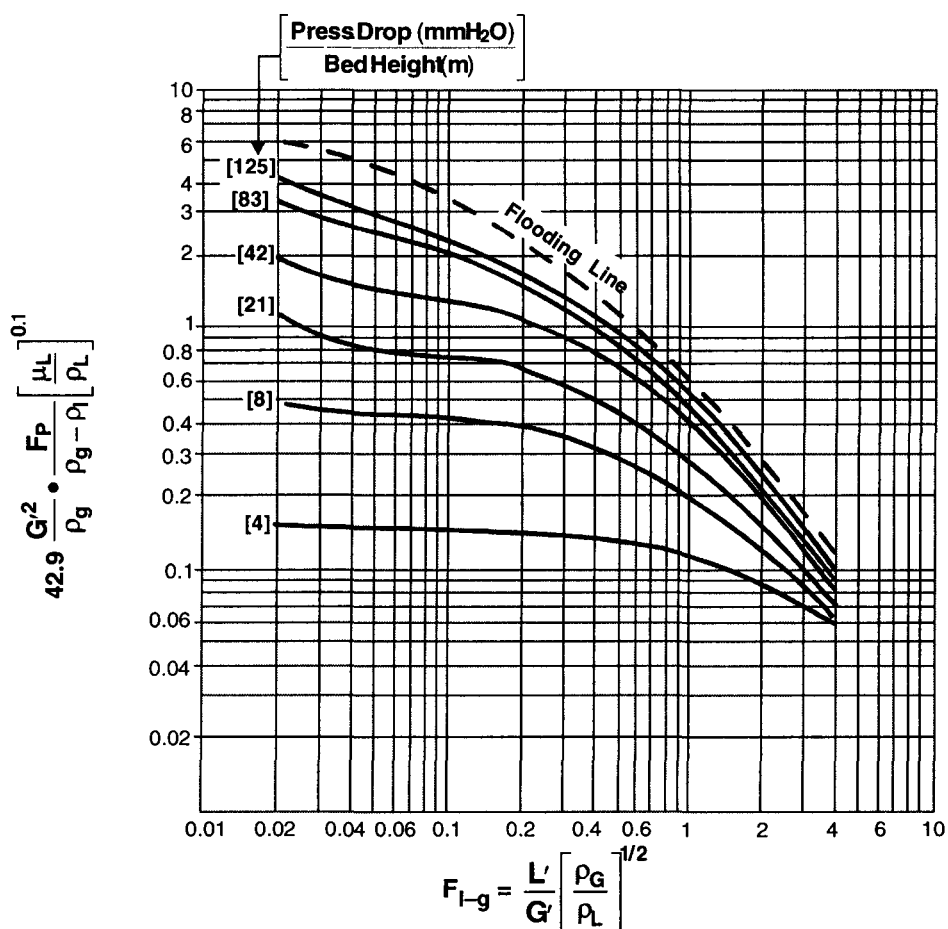
Fig. 3.18. *Generalized Pressure-drop Correlation for Packing.*

Source : J.S.Eckert — *Chemical Engineering Progress vol. 66, # 3 (1970)/P-39.*

and this generalized pressure-drop correlation is represented graphically in **Fig. 3.19.**

Norton Chemical Process Products Corporation, Akron, Ohio, USA carried out an extensive investigation to determine the optimum location of these pressure-drop parameters. Statistical survey of its 4500 press-dr. measurements data showed that over the following range of

$$\Delta P = 40\text{—}1630 \text{ Pa/m of packed bed}$$

$$F_{G\text{-}L} = 0.005\text{—}8$$

— about 55% of packing types and sizes would give rise to a constant packing factor at all pressure drops

— however packings smaller than 25mm size exhibited a small increment in F_p as the ΔP was reduced

— a few large-size packings with high-voidage showed a small decrease in the packing factor.

Based on these extensive data, the generalized press-drop correlation [**Fig. 3.20**] predicts pressure drop within ± 17% of measured values thruout its entire range. This accuracy shoots up to ± 11% in the most-widely-used-range of flow parameter and pressure-drop values :

The y-axis is labeled:

$$3.98 \frac{v_{G,gr}^2 \, a_p}{g \, \epsilon^3} \cdot \frac{\rho_g}{\rho_L} \cdot \mu_L^{0.2}$$

Curves labeled: **Stacked Rings** and **Dumped Rings**

Packing Size	Tower Dia
12.7 mm	76 mm
15 mm	305 mm
25 mm	152 mm
25 mm	305 mm
36 mm	305 mm

The x-axis is labeled:

$$\frac{L'}{G'} \left[\frac{\rho_g}{\rho_L} \right]^{\frac{1}{2}}$$
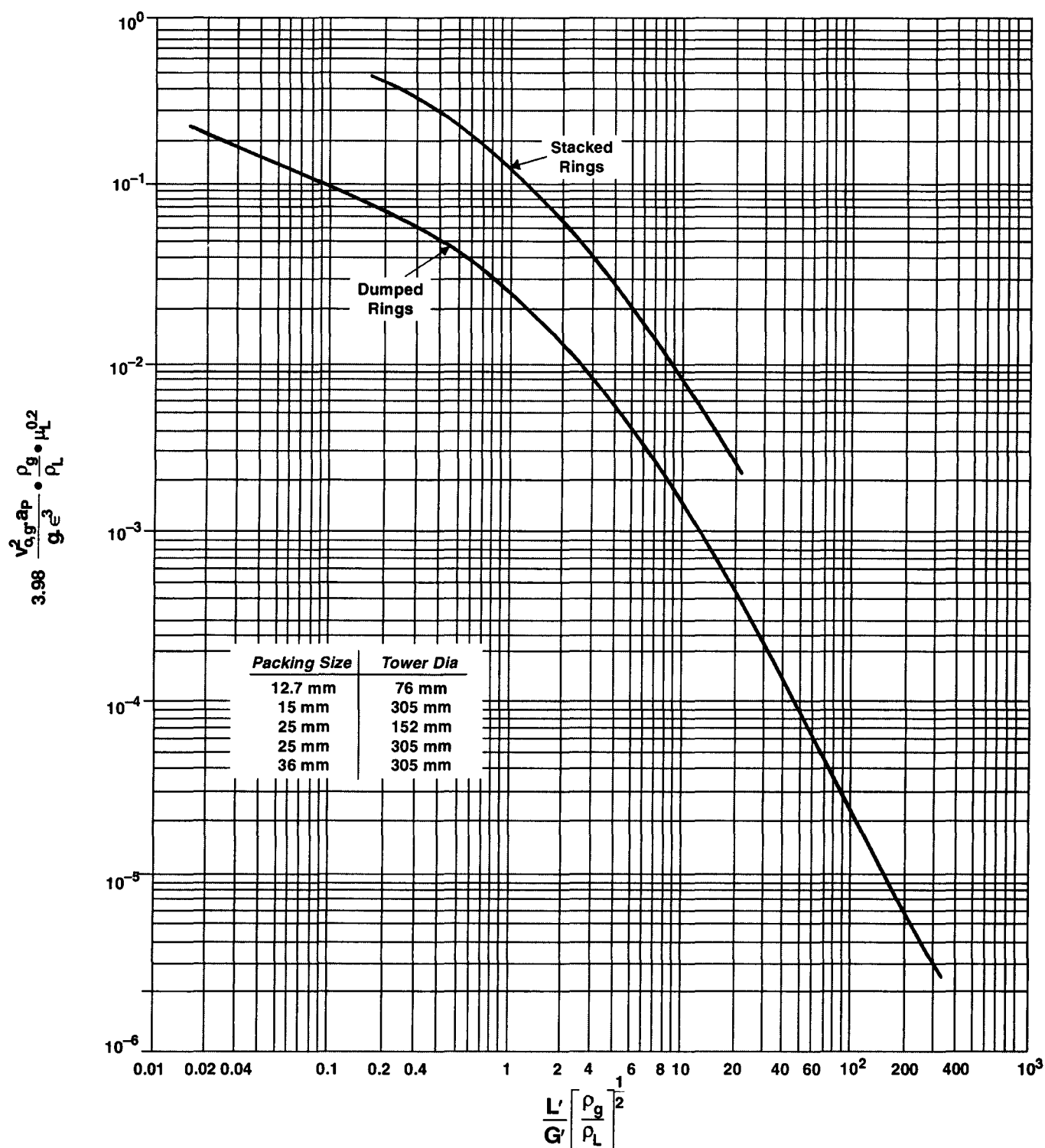
Fig. 3.19. *Generalized Pressure–Drop Correlation For Packing.*

Source : J.S.Eckert—*Chemical Engineering Progress vol. 82 (1975)/P-70.*

$F_{G-L} = 0.01—10$

$\Delta P = 204—816$ Pa/m of packed bed
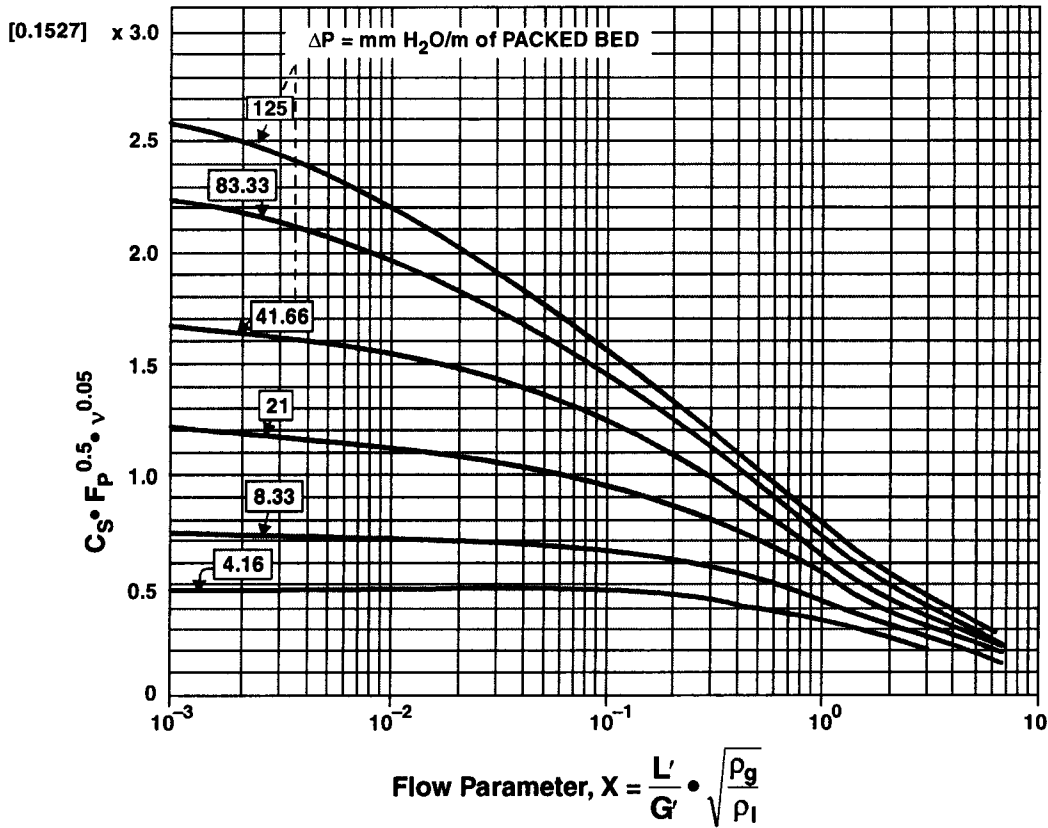
Figure 3.20. *Generalized Pressure-Drop Correlation.*

This correlation in its present form is probably the one that represents the max. accuracy possible, given the packing of varied sizes and shapes available. If greater accuracy is required for design purpose, one should go for separate-correlation available for each specific type and shape of packing.

The ordinate of this correlation is

$$Y = F_p \cdot C_s^2 . \upsilon^{0.1}$$

where, C_s = **capacity factor**, m/s

$$= v_G \left[\frac{\rho_G}{\rho_L - \rho_G} \right]^{0.5}$$

$\therefore$ $$Y = F_p . v_G^2 \frac{\rho_G}{\rho_L - \rho_G} . \upsilon^{0.1} = G'^2 . F_p . \frac{\upsilon^{0.1}}{\rho_G(\rho_L - \rho_G)}$$

The abscissa of this correlation is   cf. $G' = v_G . \rho_G$

$$X = F_{G-L} = v_G \left[\frac{\rho_G}{\rho_L - \rho_G} \right]^{0.5}$$

3.2.7.Packing Factor

It is purely a number (dimensionless) that relates the pressure drop to flowrates thru a bed of particular packing element. It characterizes a particular packing shape and size :

Table 3.7. Packing Factors (F_p) of Random Packings

	Packing Type				Nominal size (mm)					
	6.35	9.5	13	16	19	25	32	38	50	75
IMTP®				51	—	41	—	24	18	12
HY-PAK® (metal)						45	—	29	26	16
Super Intalox®Saddles (ceramic)					60	60	—	—	30	—
Super Intalox®Saddles (plastic)						40	—	—	28	18
Intalox Saddles (ceramic)	725	330	200	—	145	98	—	52	40	22
Intalox Saddles (plastic)						33	—	—	21	16
Pall Rings (plastic)				95	—	55	—	40	26	17
Pall Rings (metal)				70	—	48	—	28	20	18
Raschig Rings (ceramic)	1600* (1.6)	1000* (1.6)	580 (2.4)	380 (2.4)	255 (2.4)	155 (3)	125* (4.75)	95 (4.75)	65 (6.35)	37* (9.5)
Raschig Rings (metal) (W/thick = 0.8 mm)	700*	390*	300*	170	155	115*	—	—	—	—
Raschig Rings (metal) (W/thick = 1.6 mm)	—	—	410	300	220	144	110	83	57	32
Berl Saddles (ceramic)	900*	—	240*	—	170	110	—	65	45*	—

Figures within parenthesis indicate wall thickness in mm.

*Extrapolated value.

□□

Design : Basic Concepts

Be it an absorber or stripper, a good design aims at intimate contacting of a gas and a liquid stream under specified conditions. Maximizing the exposure of gas and liquid to each other is the only way to bring about such a contact. Conceptually this can be achieved in one of the three ways :

   # dispersing the liquid in the form of multiple, slow moving thin-films thru a volume of gas (as in packed towers)

   # dispersing the gas in the form of bubbles thru a volume of gas (as in trayed towers)

   # breaking up the liquid stream into fine sprays that are dispersed thru a volume of gas (as in spray towers).

However, none conforms entirely to its conceptual classification in reality. Each one is beset with certain advantages and disadvantages. And if process criteria is not the limiting factor on choice, the speed of installation or simply investment cost may be the decisive factor.

[A]   TRAYED TOWERS

An almost infinite variety of tray-type gas-liq contacting towers are there. And based on their *modus operandi*, they can be grouped into three general forms :
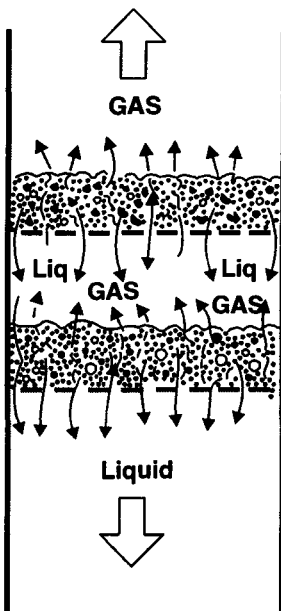
Fig. 4.1. *Turbogrid Trays.*
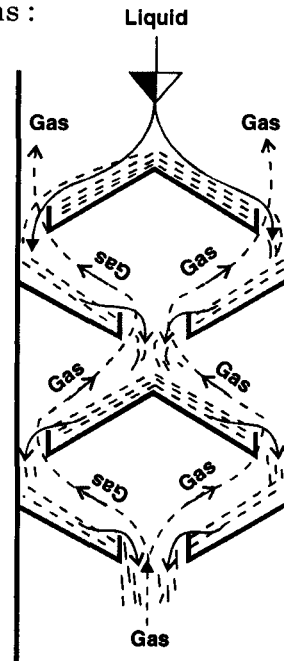
Fig. 4.2. *Schematic diagram of Disk-&-Donut Trays*

1. Random counterflow thru weeping grids, in which the gas and liquid share the same passageways

Example : *Shell Turbogrid Trays*

These are downcomerless trays.

2. Directed counterflow setup by means of some head differential or by single opening in which contact occurs principally by flow thru a series of liquid curtains.

Example : *Disk-and-Donut Trays* [Fig. 4.2]

3. Directed counterflow by channeling the liquid from tray to tray down the column thru the downcomers **(Fig. 4.3)**. Gas-liq contact takes place on the tray proper.

Example : *Bubblecap trays, sieve trays, valve trays*
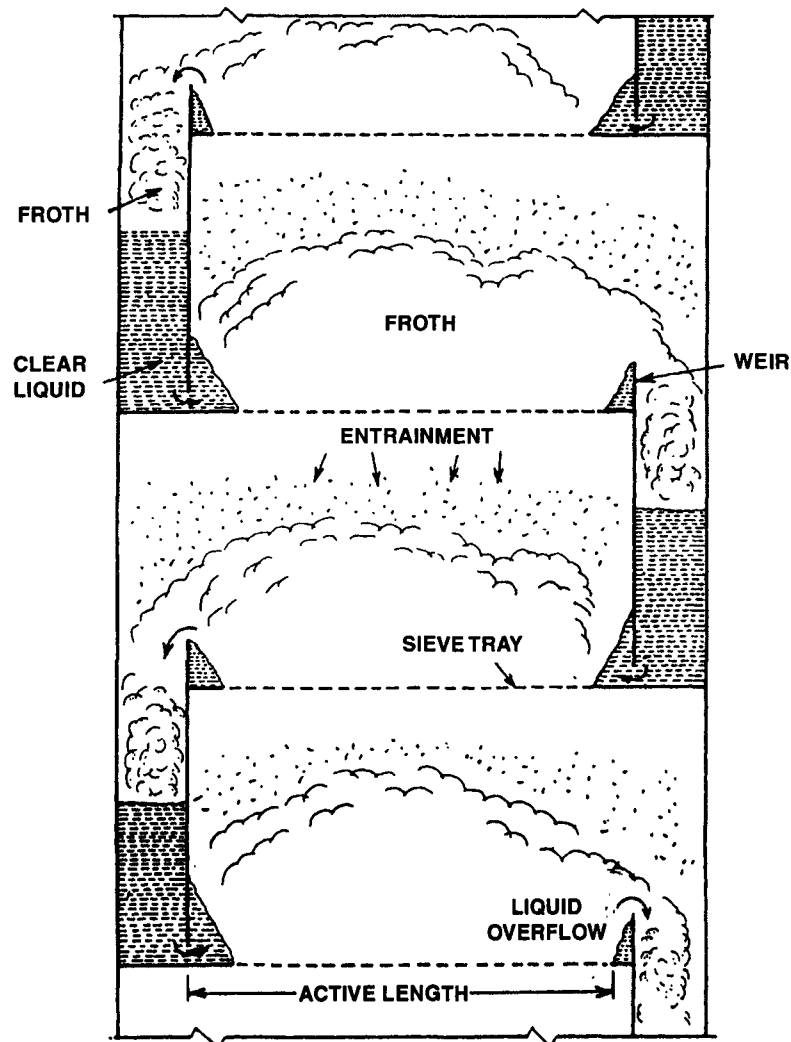
Fig. 4.3A. *Schematic diagram of a sieve tray tower.*
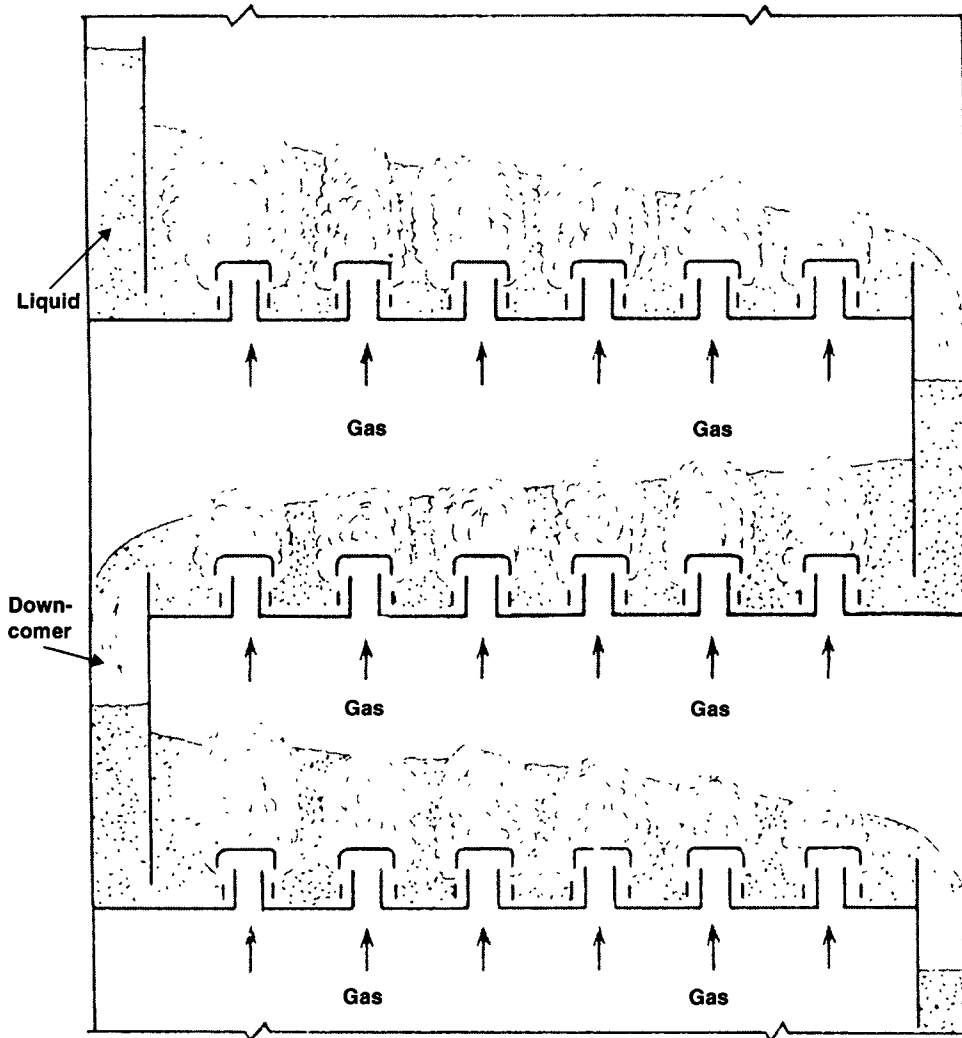
Fig. 4.3B. *Schematic diagram of a bubblecap tray tower. The rising gas flows thru the slots of each cap and bubbles thru the liquid that flows past the caps.*

4.A.1. Design Concepts : Basic

The basic requirements of a perforated gas-liq contacting tray are that it should :

• ensure intimate gas-liq contact

• provide sufficient liq holdup for good mass transfer

• sport sufficient area and spacing to keep entrainment at a bay and pressure drop within acceptable limits

• have sufficient downcomer area for the liquid overflowing freely from tray to tray without column flood.

Successful plate design results from happy wedding of theory with practical experience obtained from the operation of commercial columns. Proven layouts are used and the tray dimensions are kept within the range of values known to give satisfactory performance.

4.A.1.1. Operating Range

The column operates satisfactorily only over a limited range of gas and liquid rates. While the upper limit of gas rate is set by the condition of entrainment flooding, the lower limit of gas rate is set by the condition of weeping.

Likewise the higher limit of liquid rate is set by the downflow flooding and its lower limit by coning.

Flooding results in high gas pressure drop and a sharp drop in plate efficiency. Both weeping and coning is characterized by poor gas-liq contact.

4.A.1.2. Gas Pressure Drop

The general equation of total pressure drop across a crossflow plate—whether the plate is a bubblecap or sieve or valve type—is :

$$h_{G-L} = h_d + h_L + h_R \qquad ...(4.1)$$

where, h_{G-L} = total gas pressure drop across the irrigated plate, m of clear liq.

h_d = press drop across the dry plate, m of cl. liq.

= *dry cap + slot drop :* **Bubblecap Trays**

= *dry hole drop. :* **Sieve Plates**

= *dry valve drop :* **Valve Plates**

h_L = press drop to overcome the liq depth on the tray, m of cl. liq

h_R = residual gas pressure drop, m of cl. liq

Dry Plate Drop : It is calculated from the general orifice equation :

$$h_d = K_1 + K_2 \cdot v_{G,o}^2 \cdot \frac{\rho_G}{\rho_L} \qquad ...(4.2)$$

where, K_1 and K_2 are constants

$v_{G,o}$ = linear gas velocity thru risers for bubblecaps or holes for sieve plates, m/s
For Bubblecaps

$$K_1 = 0.9258 \, H_{sl}^{0.8} \cdot v_{G,sl}^{0.4} \cdot \left[\frac{\rho_G}{\rho_L - \rho_G} \right]^{0.2} \qquad ...(4.3)$$

$v_{G,o}$ = linear gas velocity thru risers for bubblecaps or holes for sieve plates, m/s
where, h_{sl} = cap slot height, m

$v_{G,sl}$ = gas velocity thru slot, m/s

K_2 is obtained from the **Fig. 4.4**

$$\therefore \qquad h_d = 0.9258 \, H_{sl}^{0.8} \cdot v_{G,sl}^{0.4} \cdot \left[\frac{\rho_G}{\Delta\rho} \right]^{0.2} + K_2 \cdot v_{G,o}^2 \frac{\rho_G}{\rho_L} \qquad ...(4.2A)$$

For Sieve Plates

$$K_1 = 0$$
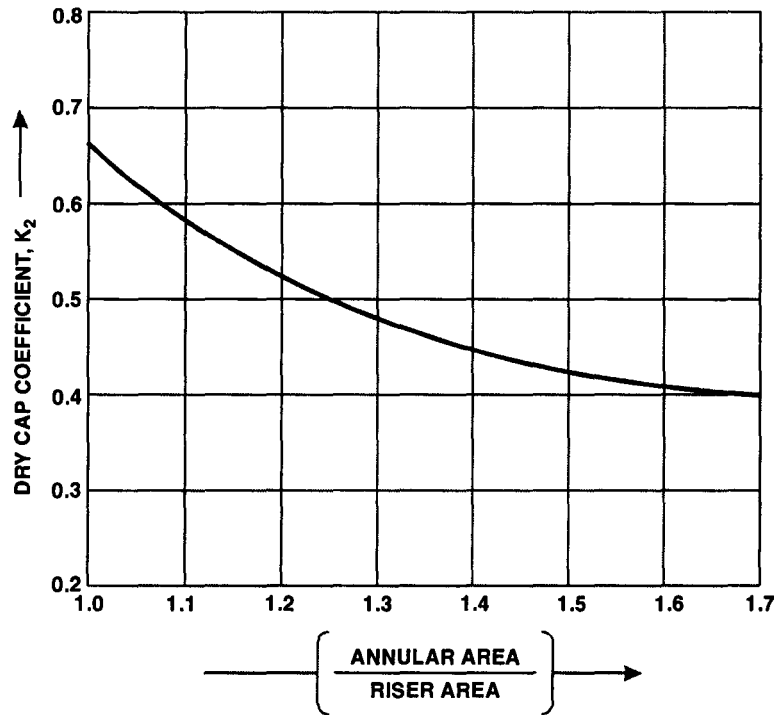
Fig. 4.4. *Dry-Cap Head Loss Coefficient.*

$$K_2 = 50.85 \times 10^{-3} \, C_v^{-2} \qquad \qquad \ldots (4.4)$$

where, C_v = discharge coeff. whose value can be obtained from **Fig. 4.5**

$$\therefore \qquad \qquad h_d = 50.85 \times 10^{-3} \left[\frac{v_{G,o}}{C_v} \right]^2 \cdot \frac{\rho_G}{\rho_L} \qquad \qquad \ldots (4.2B)$$

Hydraulic Head : It is the gas pressure drop to overcome the static liquid head on the plate:

$$h_L = \beta \cdot h_{ds} \qquad \qquad \ldots (4.5)$$

where, β = aeration factor [see **Fig. 3.11**]

h_{ds} = dynamic seal of tray *i.e.* it is the cl. liq height on the plate, m of cl. liq

$$= h_w + h_{ow} + \frac{1}{2} h_{hg} \text{ for } \textbf{Sieve} \text{ and } \textbf{Valve Plates} \qquad \qquad \ldots (4.6)$$

$$= h_s + h_{ow} + \frac{1}{2} h_{hg} \text{ for } \textbf{Bubblecap Plates} \qquad \qquad \ldots (4.6A)$$

h_w = weir height, m

h_{ow} = height of crest over the weir, m of cl.liq

h_{hg} = hydraulic gradient across the plate, m of cl. liq

Residual Head : It is the surface-tension head defined as the necessary pressure to form a vapor bubble thru the disperser :
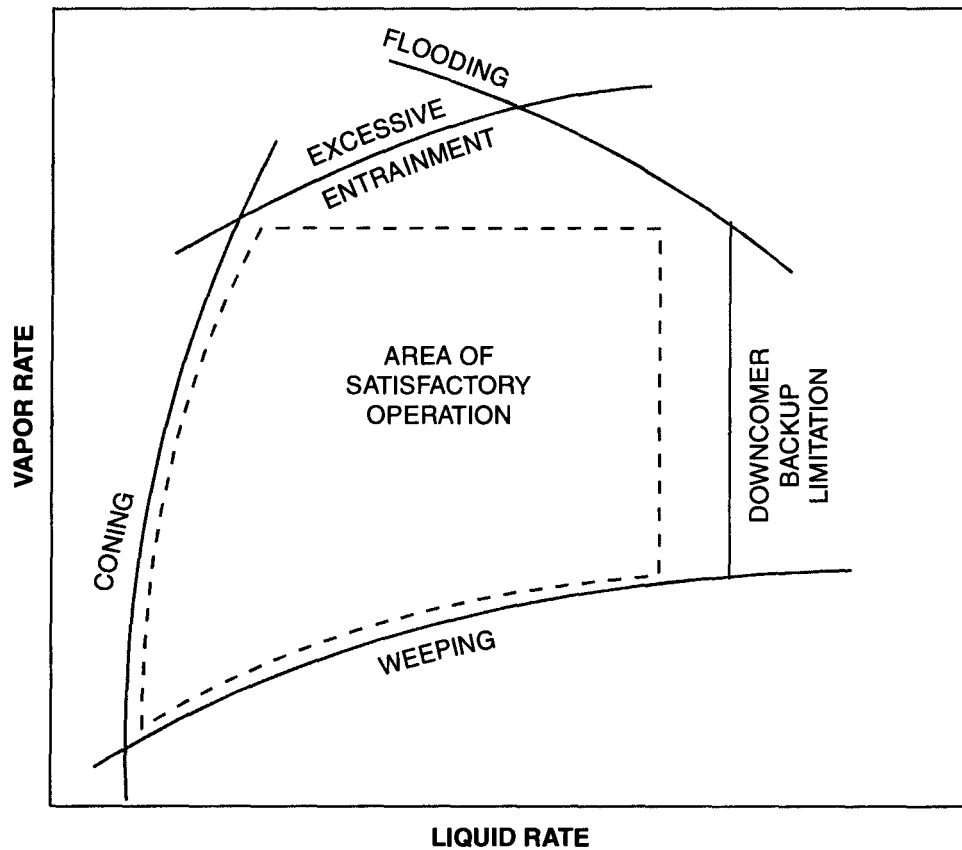
Fig. 4.5. *Discharge Coefficient For Gas Flow Thru Sieve Plates.*

$$h_R = \frac{6\sigma}{d_b} \cdot \frac{1}{\rho_{L,g}} \text{ , m of cl . liq} \qquad \qquad ...(4.7)$$

where, σ = surface tension of the liq, N/m

d_b = bubble dia, m

$\approx d_o$

The contribution of h_R to total gas pressure drop is so small that in some cases it may be dropped from the general pressure-drop equation :

$$h_{G-L} \approx h_d + h_L \qquad \qquad ...(4.1A)$$

4.A.1.3. Liquid Holdup

The liquid holdup on the tray is the effective liquid head in active and downcomer areas :

$$U = [h_L \cdot A_a + h_{dc} \cdot A_d]\rho_L \qquad \qquad ...(4.8)$$

where U = liq holdup *i.e.* mass of liq on the tray, kg

h_L = hydraulic head *i.e.* clear or effective liquid height on the tray, m of cl. liq

h_{dc} = downcomer backup *i.e.* height of clear or effective liq in the downcomer, m of cl. liq

A_a = active area or bubbling area, m²

A_d = downcomer cross-sectional area, m²

4.A.1.4. Submergence

It is the equivalent depth of unaerated liquid that would flow across the tray if all the perforations are plugged. It is calculated by

$$S = h_w + h_{ow} \qquad \ldots(4.8)$$

It is also called **liq depth**.

4.A.1.5. Hole Velocity

It is taken as the gas load (m³/s) divided by the total area of perforations :

$$v_{G,o} = \frac{Q_{v,G}}{A_o} \qquad \ldots(4.9)$$

4.A.1.6. Tray-To-Tray Liquid Flow and Liquid Distribution

During normal column operation, liquid overflows the tray to the next tray below. And a number of variations are possible in the manner of conducting liquid from tray to tray down the column. **Segmental downcomer** is one of them. In such an arrangement, the tower shell forms one wall of the downspout out and the liquid flows down thru an area that has the shape of a segment of a circle **(Fig. 4.6A)**.

[A]   [B]
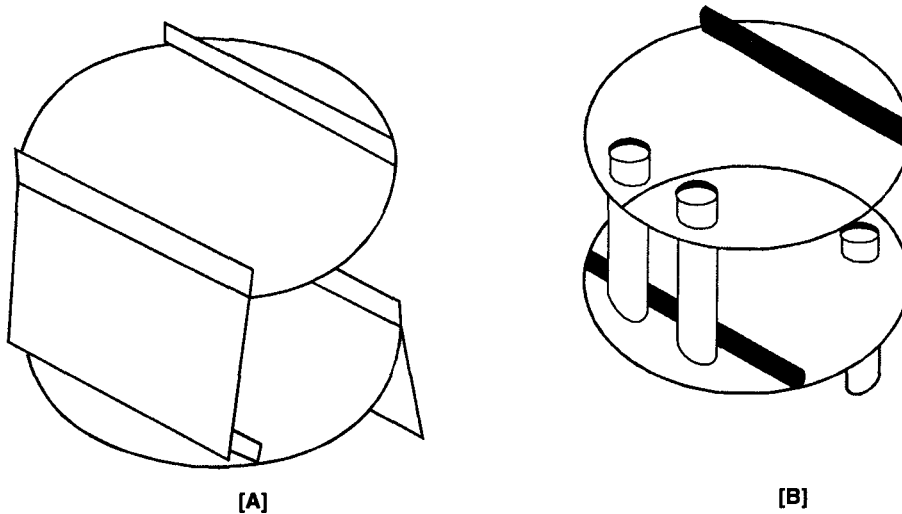
Fig. 4.6. *Two Most Popular Downcomer Types.*

In another variation, circular pipes are used to direct liquid from higher tray to lower tray down the column **(Fig. 4.6B)**.

For segmental downcomers, the straight overflow weir length sets the **crest height** :

$$h_{ow} = 0.666 \left[\frac{Q_{v,L}}{D\,l_{w,eff}} \right]^{\frac{2}{3}} \qquad \ldots(4.10)$$

where, $l_{w,\,eff}$ = effective length of rectangular weir, m

$Q_{v,\,L}$ = volumetric rate of liq, m³/s

For circular downpipes, the perimeter of the downpipes protruding above the tray determines the **crest height**

$$h_{ow} = 0.342 \left[\frac{Q_{v,L}}{D_w} \right]^{0.704}$$
　　　　　　　...(4.11)

where, D_w = diameter of the circular weir, m

Though the rectangular weir is the one most commonly used, it is common practice to serrate the edge of the overflow weir along one side of the tray when the liquid load is very low and it is desired to minimize the risk of uneven liquid flow across an unlevel tray. Under such circumstances the weir crest is calculated from :

$$h_{ow} = 0.851 \left[\frac{Q_{v,L}}{\tan\left(\frac{\theta}{2}\right)} \right]^{0.4}$$
　　　　　　　...(4.12)

where, θ = angle of the notch, degrees.

In addition to the single-pass crossflow segmental **(Fig. 4.7)** and pipe downcomer arrangements, radial flow and double-flow (split-flow) trays are relatively common **(Fig. 4.7)**. They are usually used for large-diameter towers, although every attempt is made to instal crossflow tray because of its lower cost.

The radial-flow arrangement **(Fig. 4.7A)** requires only every other tray to be sealed to the tower shell and provides equal flowpath-length for all the liquid. However, it is not suitable for handling high liquid loads because of the limitations in the weir.

The double-pass arrangement is the equivalent of two half-towers coaxed together with the wall between removed to let gas and liquid mix up between trays. This pattern of flow ensures a high liquid rate and gives rise to insignificant hydraulic gradient. Therefore, from design point of view it is preferable to use plates with splitflow (double-pass flow) at large L/G ratio or in large dia columns.
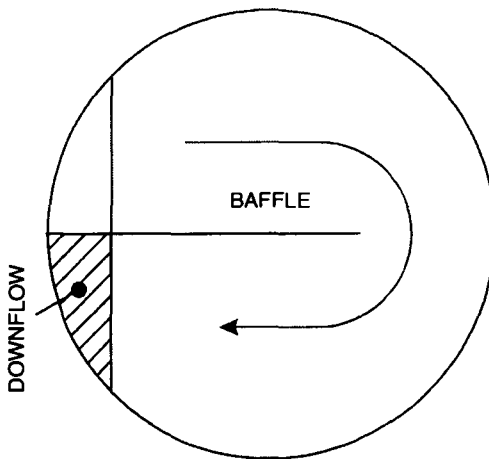
Fig. 4.7. *Reverse flow*   **Fig. 4.7A.** *Radial Flow Tray.*

DOUBLE PASS
SPLIT FLOW

FOUR PASS
SPLIT FLOW
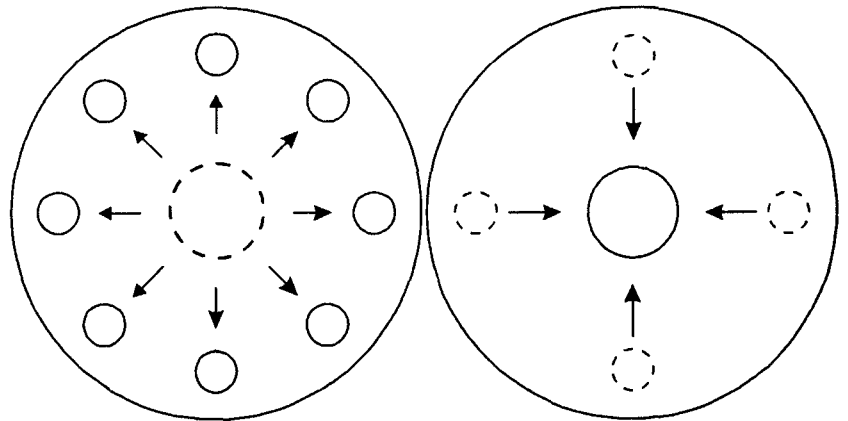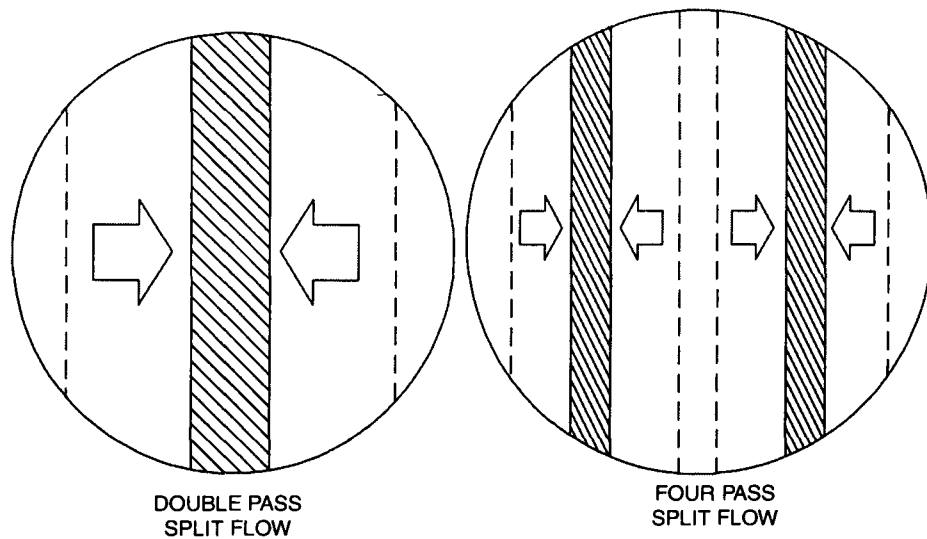
Fig. 4.7B. *Double-Flow Trays.*

For very large diameter towers fitted with bubblecap trays, cascade designs **(Fig. 4.8)** have been used, but their cost is considerable. The cascade system minimizes hydraulic gradient stagewise. This is particularly important for large dia columns where hydraulic gradient inherently becomes large.

[A] Cascade flow pattern of liquid on tray

[B] Split cascade flow (double pass)
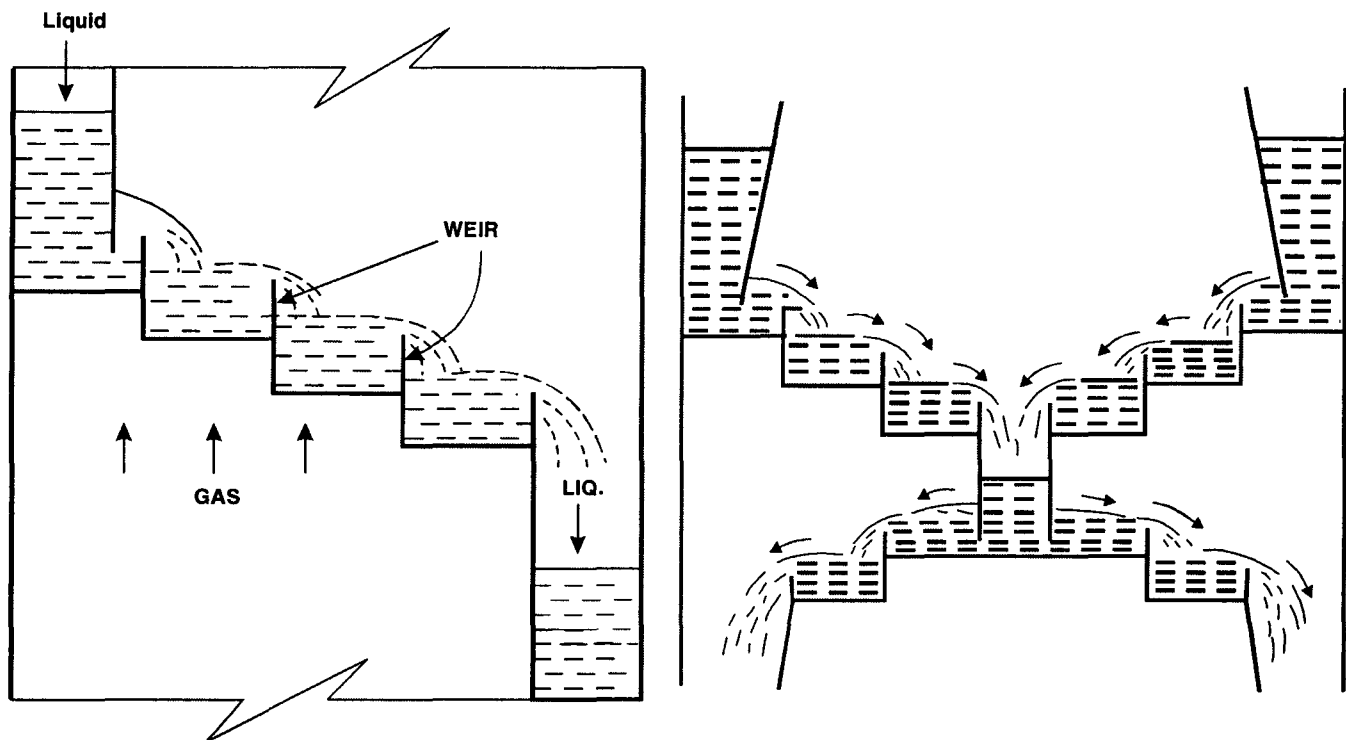
Fig. 4.8. *Cascade Trays are used in very large dia columns to Minimize Undesirable Hydraulic Gradient arising out of Long Liquid FlowPath on the Tray.*

It is important to note that the fraction of column cross-sectional area available for gas dispersers decreases when more than one downcomer is installed. Hence the optimum design requires a balance between accommodation of liquid flow and effective utilization of tray cross-section for gas flow.

4.A.1.7. Number of Flow Passes

The number of flow passes is dictated by liquid loading. For a given tray, the number of flow passes is increased, as necessary to bring the weir liq-loading within proper design limits so as to satisfy the condition :

$$\frac{Q_{v,L}}{l_w} \leq 0.01986$$

where, $Q_{v,L}$ = liq rate, m^3/s

l_w = weir length, m

The very size of the tray puts a limit on the number of flow passes :

$$[N_P]_{max} = 1.2368 \sqrt{A_t} \qquad ...(4.13)$$

where, $[N_P]_{max}$ = max. no. of flow passes which is rounded to the next higher integer but is never less than 1 for the obvious reason.

This limit as set by the tray cross-section is necessary to make room for constructing internal manways as well as to obtain satisfactory tray efficiency.

4.A.1.8. Weir Length, Flowpath Length, Flowpath Width

For rectangular weir dividing the tray into equal flowpath lengths, Economopoulos suggests:

$$l_w = l_{w,sd} + D_t (N_p - 1)^{0.946} \qquad ...(4.14)$$

$$Z.N_P = D_t - 2H_{sd} - 2\left[\frac{A_t}{D_t}\right].[N_P - 1]^{0.054}\left[1 - \frac{A_{d,sd}}{A_d}\right] \qquad ...(4.15)$$

$$\frac{A_{d,sd}}{A_d} = \frac{1}{\pi}\left[\cos^{-1}\left(1 - \frac{2H_{sd}}{D_t}\right) - 2\left(1 - \frac{2H_{sd}}{D_t}\right)\sqrt{\frac{H_{sd}}{D_t}\left(1 - \frac{H_{sd}}{D_t}\right)}\right] \qquad ...(4.16)$$

$$l_{w,sd} = 2\left[H_{sd}(D_t - H_{sd}\right]^{\frac{1}{2}} \qquad ...(4.17)$$

$$A_{d,sd} = A_d / N_P^{(0.916 + 0.0476N_P)} \qquad ...(4.18)$$

$$z = A_a / Z$$

where, l_w = length of weir, m

$l_{w,sd}$ = weir length of side downcomer, m

D_t = tower dia, m

H_{sd} = chord height of the side downcomer, m

A_t = tower area of cross-section, m^2

A_d = downcomer cross-sectional area, m^2

$A_{d,sd}$ = cross-sectional area of side-downcomer, m^2

z = flowpath width, m

Z = flowpath length, m

A_a = tray active area, m^2

Source : Alexander P. Economopoulos — *Chemical Engineering (Dec. 4/1978).*

4.A.1.9. The Feed Inlet and Distribution System

The feed liquor is introduced onto the top tray (the feedtray). Sound design requires the feed
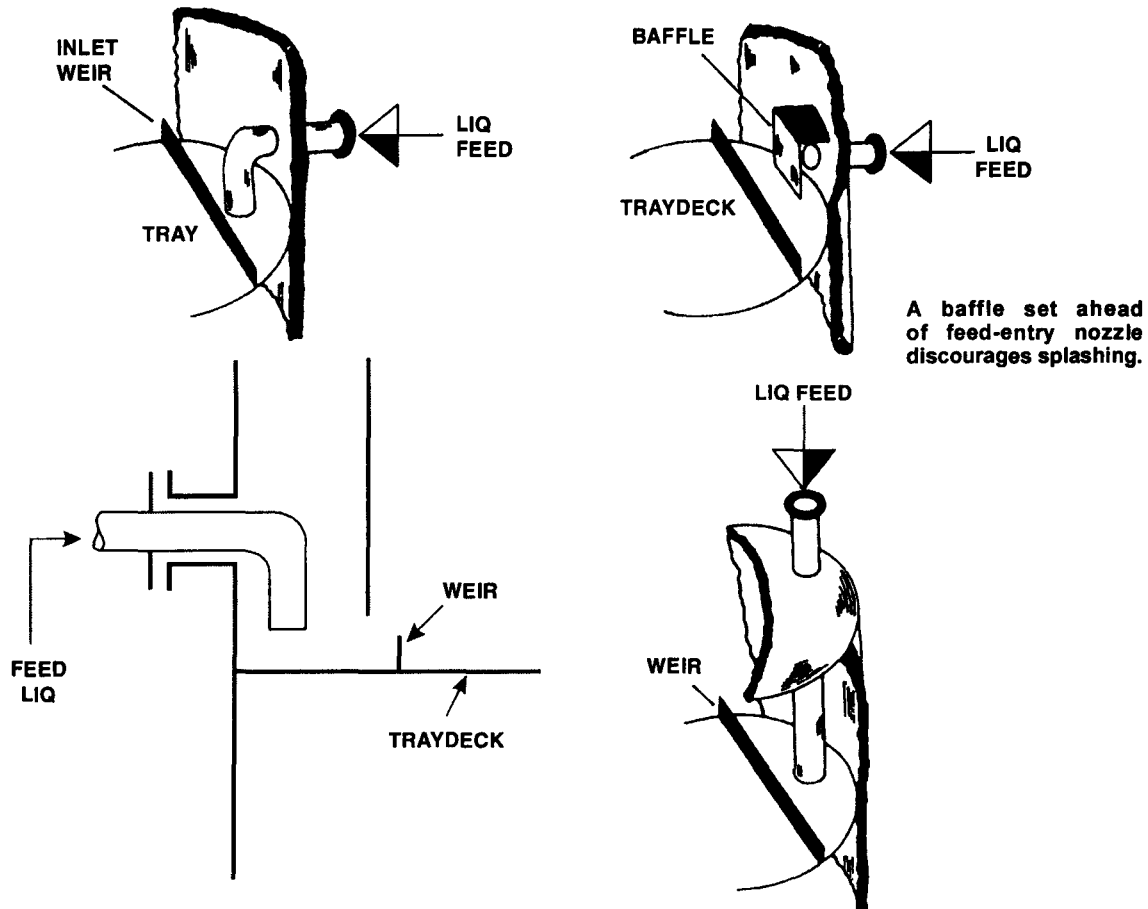
Fig. 4.9. *The Feed should be introduced to the Column with Minimum Splashing and be Distributed Evenly.*

be introduced thru such an arrangement as will distribute the feed more or less evenly on the feedtray with a minimum of splashing or jetting. Depending on designer's choice, expediency requirement and piping available, a wide variety feed inlet arrangements find their way to the absorbers and strippers. Sometimes a manufacturer's proprietrary high performance distributor system overrides a practical design which may be more economic.

Shown in **Fig. 4.9** are some forms of simplest arrangement for introducing feed on single-pass crossflow trays : an *internal baffle* **ahead of the feed nozzle, extended inlet nozzle with an elbow or a long straight pipe down thru the column headcover.**

The feedpipe, for large dia towers, is provided with a much wider splash baffle ahead of the nozzle-end above the feedtray or the elbow-end may be extended into a slotted or perforated distributor pipe **(Fig. 4.10).**
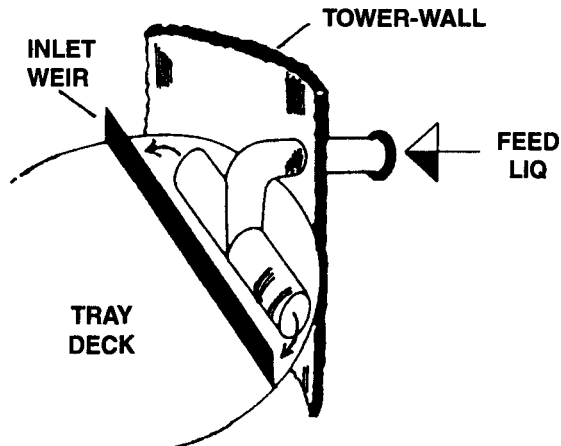
Fig. 4.10. *The Elbow-End of the FeedPipe inside the Column may be Further Extended into A Perforated/Slotted Horizontal Distributor Pipe to allow the Liquid To Flow Out More or Less Uniformly Over the Feedtray without Splashing.*
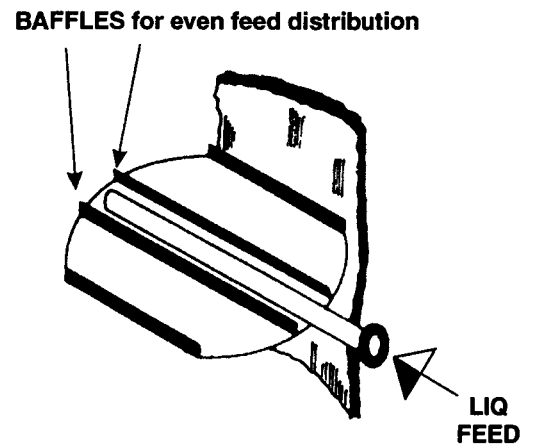
Fig. 4.11. *Extended Feed-Nozzle is either Slotted or Perforated Underside*

The most convenient way to introduce feed on a double-pass tray is to extend the feed-nozzle with a horizontal pipe having slotted or perforated underside and locating this 'extended nozzle' at the center of an outer downflow tray **(Fig. 4.11).**

4.A.1.10 Liquid Drawoff

Liquid is withdrawn from the absorber or stripper at the bottom usually via a **drawoff pot** (also called **sealpot**) which is essentially a closed-off downcomer **(Fig. 4.12)**

Frequently the column bottom itself acts as a sealpot, *i.e.,* is used to seal the bottom downcomer and the liquid is withdrawn straightaway from the bottom without breaking this seal **(Fig. 4.13)**

For sealpot system, the horizontal drawoff nozzle [see **Fig. 4.12**] can be sized by means of Eqn. 4.20 :

$$H = 0.1434 \ \frac{Q_{v,L}^2}{D_n^4} \qquad \qquad ...(4.20)$$

where, **H** = seal height, m **(Fig. 4.12)**

   D_n = dia of drawoff nozzle, m **(Fig. 4.12)**

   $Q_{v,L}$ = liq rate, m³/s

[A] Drawoff nozzle

[B] Chimney tray drawoff
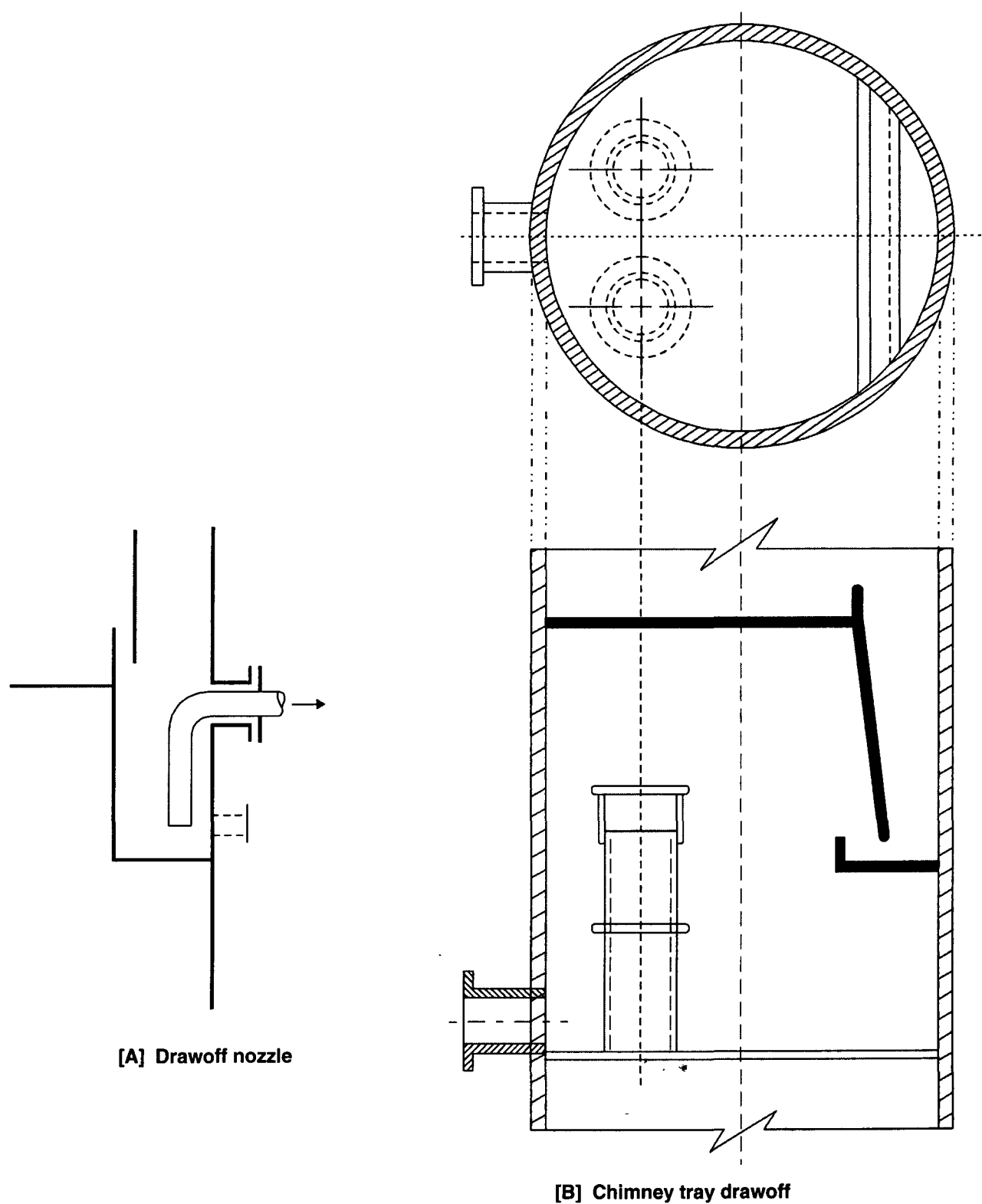
Fig. 4.12. *Liquid Drawoff is usually accomplished by a Sealpot.*
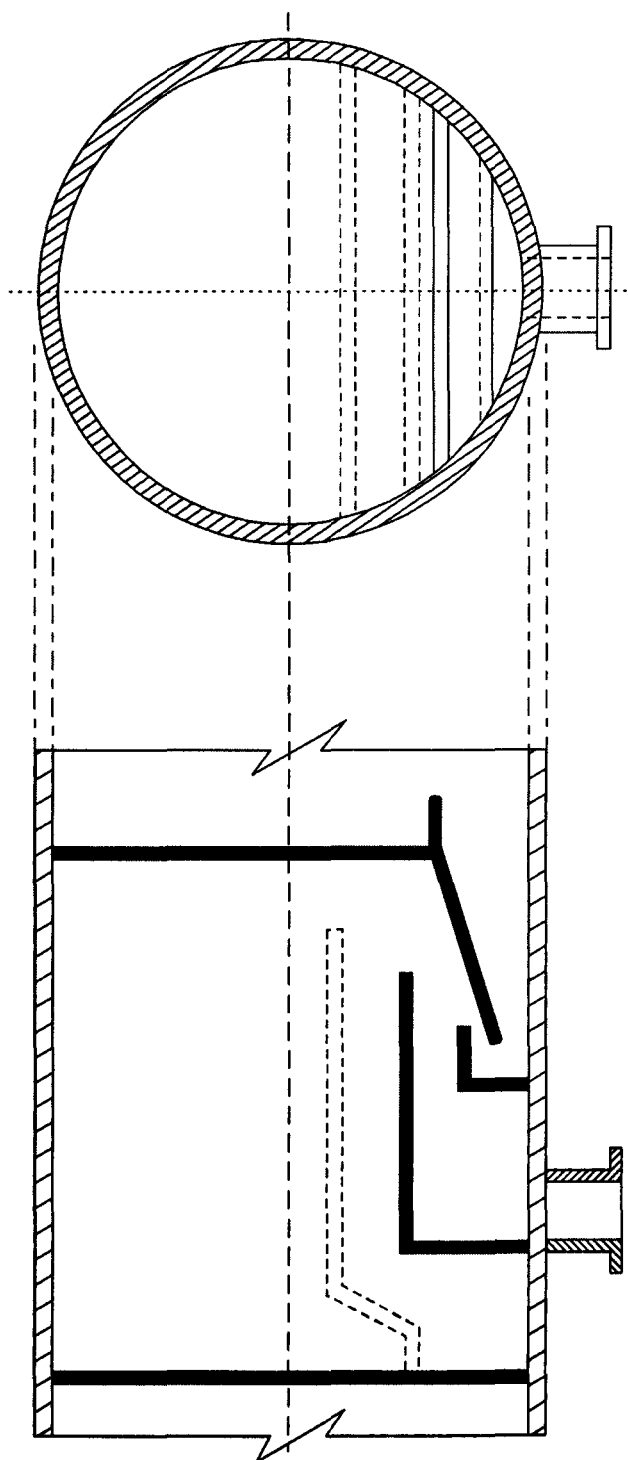
Fig. 4.12C. Draw-pan arrangement for drawoff
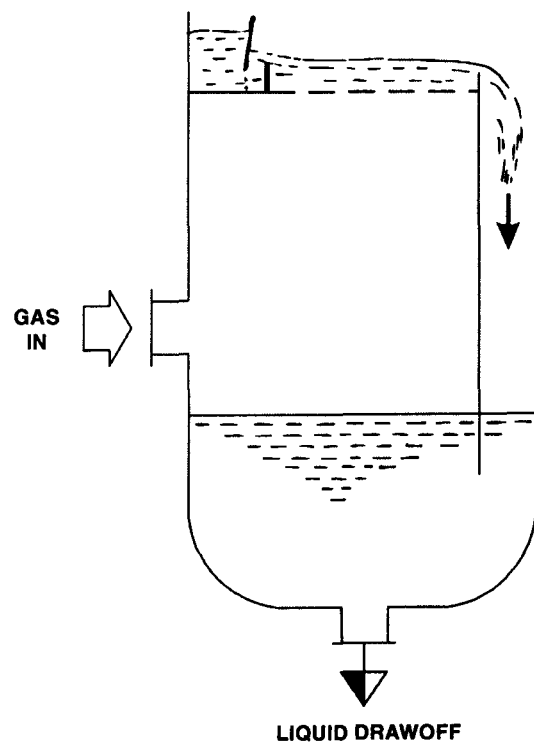
Fig. 4.13. *In absence of Sealpot, Liquid can be withdrawn from the Column Bottom by Maintaining a Liquid Seal at the Bottom Downcomer.*

For double-pass tray tower, the bottom tray is a center downflow one **(Fig. 4.14).** One sealpot and one drawoff nozzle are to be provided, if the tower bottom is not a sealpot.

The center downcomer of the bottom tray must be connected to a spout so that the feedgas can get around to its opposite side. If the downcomer is sealed to the towerwall it must be provided with two diametrically opposed feedgas nozzle **(Fig. 4.15).**
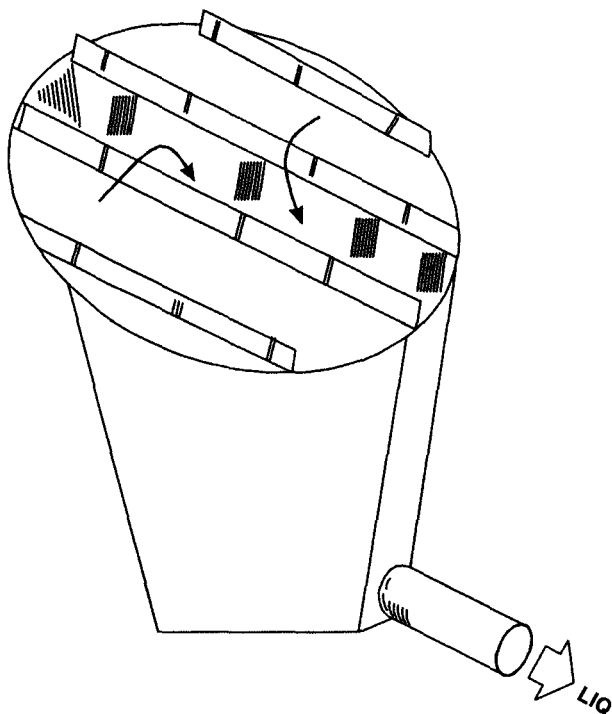
Fig. 4.14. *Double-Pass Crossflow Tray Tower is preferably provided with a Center Downflow Bottom Tray.*
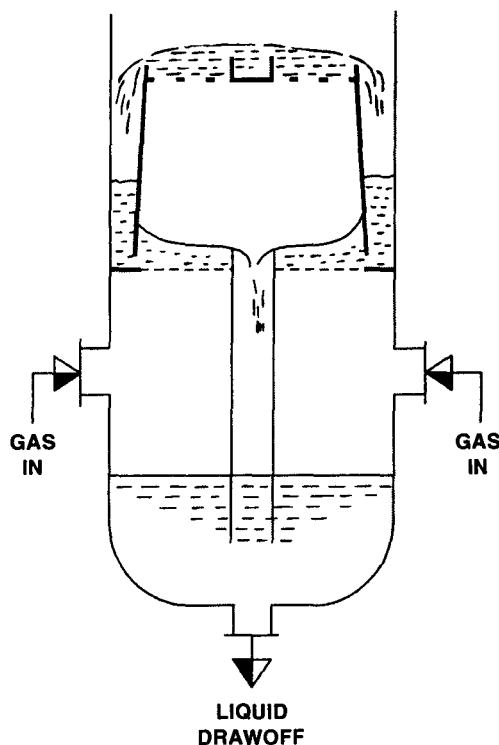
Fig. 4.15. *Two Gas Inlet Nozzles Set Diametrically Opposite on the Tower Shell if the Downcomer is Sealed to the Tower Wall.*

or the downcomer must be pierced with a sealed pipe to give feedgas access to both halves of the column from a single gas-inlet nozzle **(Fig. 4.16).**

If the double-pass tray tower is provided with an outflow bottom tray, the gas inlet and liquid drawoff nozzles are as shown in **Fig. 4.17.** Liquid seal is maintained at both side-downcomers by the liquid pool at the tower bottom.
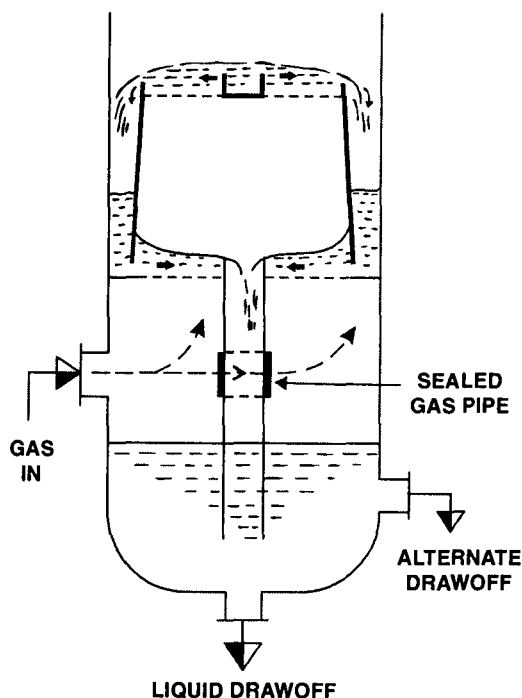
Fig. 4.16. *A Transverse Pipe thru the Downcomer and Sealed to each Side Equalizes Gasflow on both Sides of the Downcomer Sealed to the Tower Wall.*
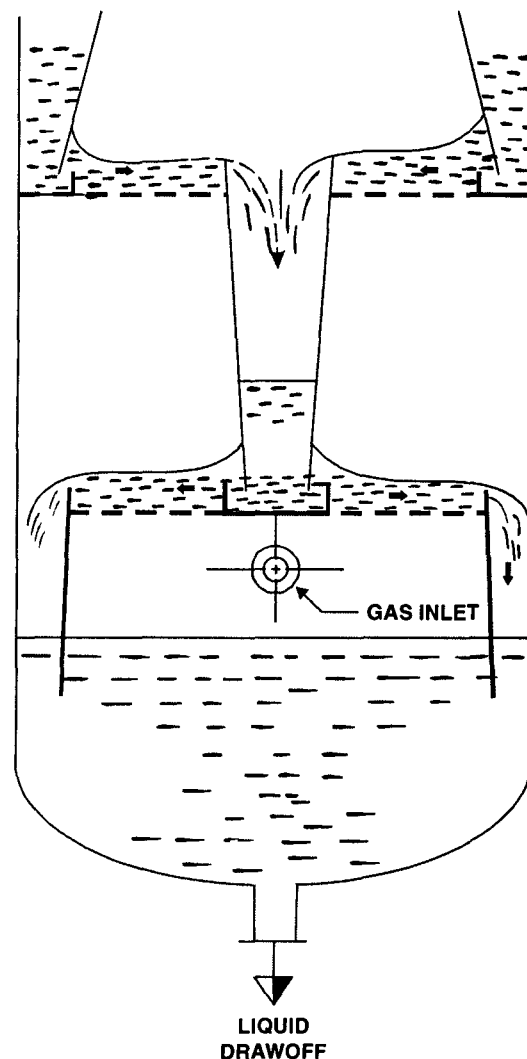
Fig. 4.17. *Liquid Seal maintained at both Side-Downcomers while the Drawoff is made right from the Bottom.*

4.A.1.11 Liquid Seal

Normal column operation requires the gas pass up the column by flowing thru the perforations on each tray, rather than up thru the downcomer. And for this, it is necessary to maintain a liquid seal at the bottom of every downcomer. This means, there must be a liquid pool submerging the downcomer leg. This is achieved by setting up an inlet weir **(Fig. 4.18A)** or putting up a depressed sealpan **(Fig.18B).**

Either system can alone give sufficient liquid depth on each tray at liquid inlet so as to submerge the bottom edge of the downcomer from the tray above and thereby sealing the downcomer from any gas flowing thru it.

The depressed sealpan arrangement is generally costlier than inlet weir system. However, it is sometimes preferred when a high liquid inventory would give rise to inordinate spashing or additional kinetic head on the tray if the liquid is allowed to flow over a conventional inlet weir.
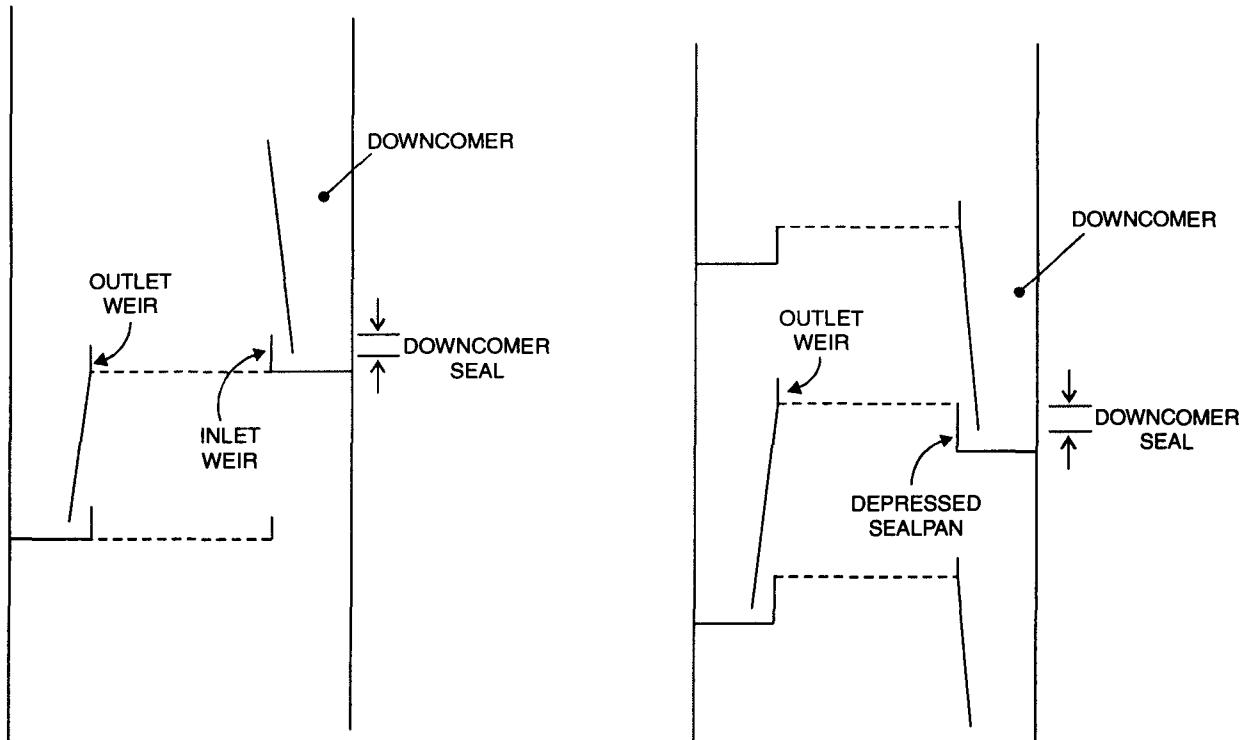
[A] Liquid Seal Established by An Inlet Weir   [B] Liquid Seal Created by A Depressed Sealpan

Fig. 4.18. *Liquid Seal Ensures Gas Flow thru Tray Perforations Instead of thru the Downcomer.*

4.A.1.12 Liquid Backup

There is a limit to the quantity of liquid and gas that can be passed simultaneously thru the column in countercurrent flow. This is referred as the ultimate capacity (**floodpoint**) of the column A perforated-plate tower with sealed downcomers can reach its floodpoint under three circumstances :

1. when the tray pressure drop is excessive **[Downflow Flooding]**

2. when the liq entrainment from tray to tray is excessive **[Entrainment Flooding]**

3. when the downcomers become vapor locked.

A sealed downcomer is basically a manometer leg **(Fig. 4.19.A)**. If there is no gas flow up thru the trays.

$$P_1 = P_2$$

assuming liquid surface tension holds up tray leakage.

If the clearance **R** between the bottom-edge of the downcomer and traydeck **(TR-1)** offers no resistance to the liquid flow, the downcomer liquid level coincides with the tray liquid level, marked by point **A (Fig.4.19A)**. The inlet weirs' height & length matches with those of outlet weirs.

If the downcomer skirt clearance **(R)** were so restrictive (as in **Fig. 4.19B**) that the liquid would have to acquire an additional head to overcome the resistance at the desired liquid thruput, the liquid level in the downcomer would climb to the level **B** such that the height **BA** represents the downcomer clearance loss (also called **head loss under downcomer apron, h_{da}**]. This loss can be computed from :

[A] Sealed downcomer
with clearance R. No gas
pass-up. No tray weepage

[B] Sealed downcomer
with restricted clearance. No gas
pass-up. No tray weepage.
Downcomer liq level is raised
to point B to overcome the
resistance due to restricted
clearance

[C] Sealed downcomer
with restricted clearance. Gas
passes up thru tray perforations.
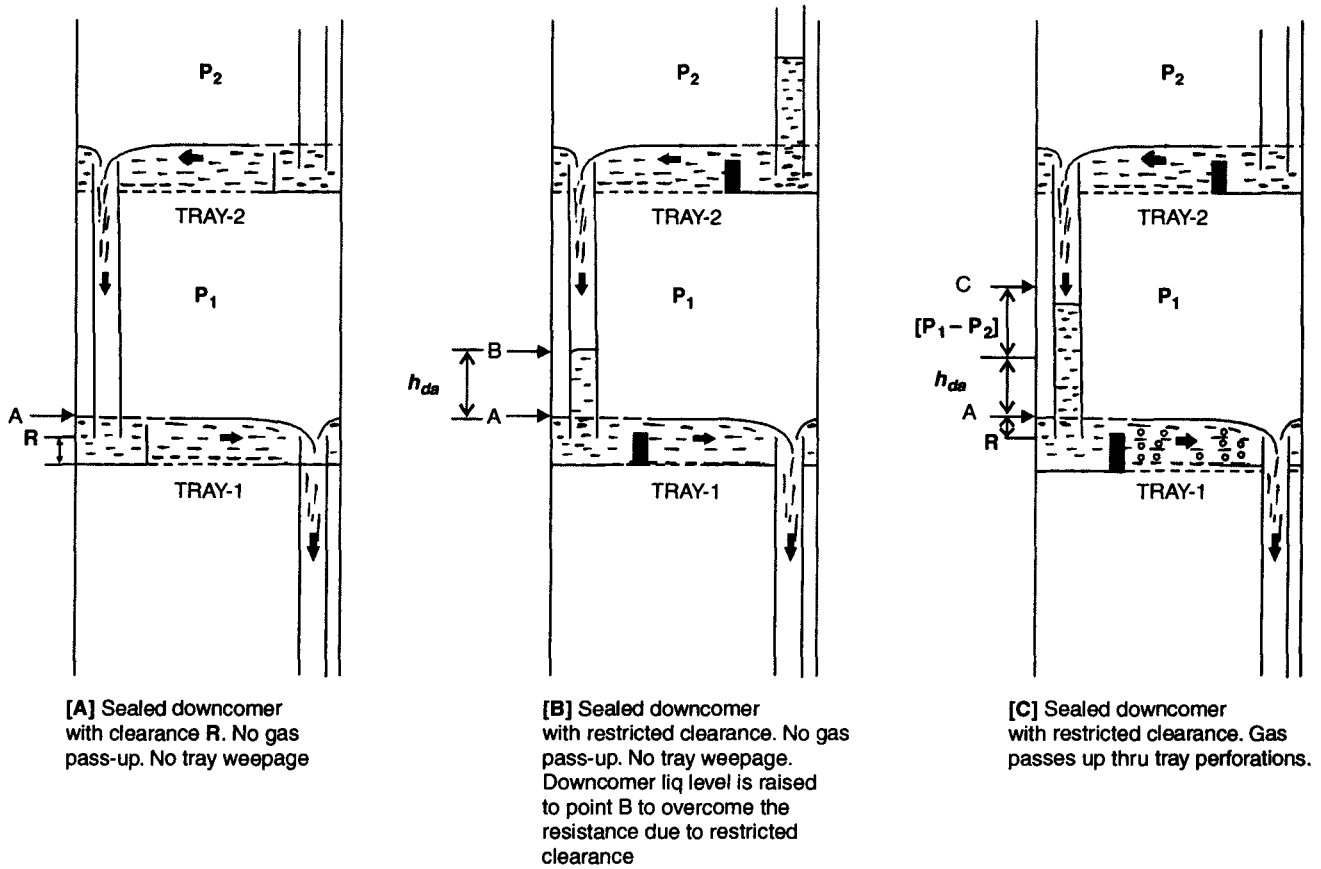
Fig. 4.19. *The Sealed Downcomer is, in effect, One Leg of a Manometer.*

$$\mathbf{h_{ad}} = 0.165 \left[\frac{\mathbf{Q_{v,L}}}{\mathbf{A_{da}}}\right]^2 \qquad \qquad ...(4.21)$$

$$= 0.165 \; v_{L,da}^2$$

where, $\mathbf{h_{da}}$ = head loss under downcomer apron, m of cl. liq

$\mathbf{Q_{v,L}}$ = liq rate, m³/s

$\mathbf{A_{da}}$ = area under downcomer apron, m²

$\qquad = \mathbf{l_w(h_w - 0.025)}$ \qquad \qquad \qquad \qquad ...(4.22)

$v_{L,da}$ = liq velocity thru the constricted area, *i.e.*, under downcomer apron, m/s

Therefore, the designer must give sufficient downcomer-skirt-clearance to minimize this loss without unduly sacrificing reasonable sealing.

We've so far discussed the tray hydraulics when

• there is no gas flow, *i.e.,* $P_1 = P_2$

• there is no tray seepage.

Now if the gas is allowed to pass up thru the tray perforations, P_1 becomes greater than P_2 because the upflowing gas suffers a head loss while passing thru **tray-2.** The pressure inside the downcomer is P_2 and that on the outside is P_1

Therefore, the manometric difference $P_1 - P_2$ is manifested in the rise of downcomer liquid level (Point **C**, in **Fig. 4.19.C**). The height of liquid level in the downcomer is called downcomer backup which, therefore, can be represented by :

$$h_{dc} = h_w + h_{ow} + h_{da} + (P_1 - P_2) \qquad ...(4.23)$$

But $(P_1 - P_2)$ represents total gas pressure drop thru an irrigated plate, *i.e.*,

$$\frac{(P_1 - P_2)}{\rho \cdot g} = h_{G-L} = h_d + h_L + h_R \qquad ...(4.1)$$

where, h_d = dry plate gas pressure drop, m of cl. liq

h_L = liq submergence = $h_w + h_{ow}$

h_R = residual pressure drop, m of cl. liq

$$\therefore \qquad h_{dc} = h_d + 2 (h_w + h_{ow}) + h_{da} + h_R \qquad ...(4.24)$$

ignoring the hydraulic gradient

Usually the residual gas pressure drop is too small & so it can be dropped from Eqn. 4.24 :

$$h_{dc} = h_d + h_{da} + 2 (h_w + h_{ow}) \qquad ...(4.24\ A)$$

From the design point of view, it is the normal practice not to allow the liquid backup to exceed half of the tray spacing. :

$$h_{dc} \ngtr \frac{1}{2} l_t.$$

otherwise at higher liquid loads the downcomer backup may lead to column flooding.

4.A.1.13 Percent Free Area

It refers to the unit 'cell' of the perforated portion of the tray (hatched area in **Fig. 4.20**).
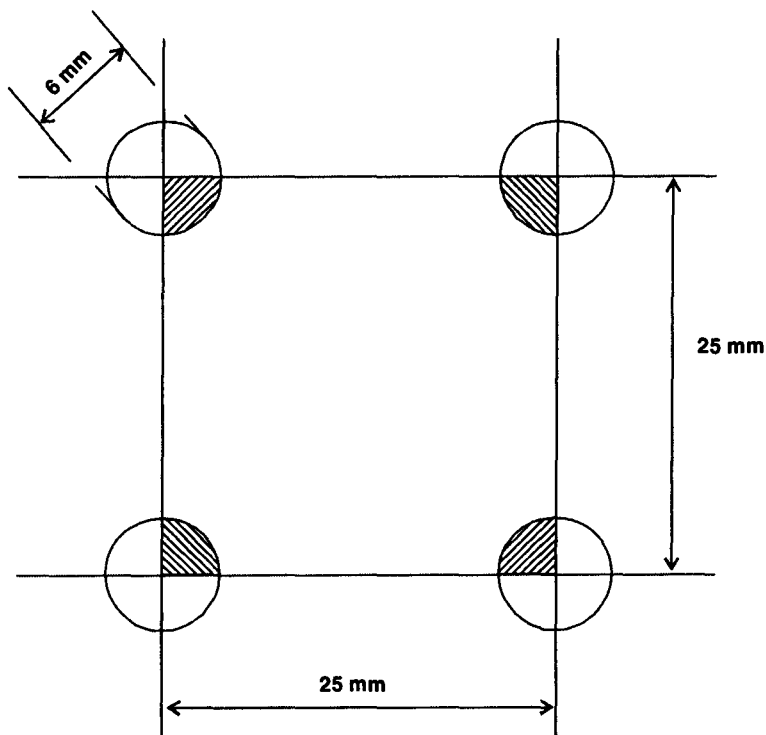
Fig. 4.20. *Percent Free Area.*

For instance the percent free area of a tray with perforations of 6mm dia arranged in 25mm square pitch

$$= \frac{4\left[\frac{1}{4} \cdot \frac{\pi}{4}(6)^2\right]}{25 \times 25} \times 100\% \quad \text{[see Fig. 4.20]}$$

$$= 5\%$$

That is, the percent free area does not mean the hole area divided by net tray area (A_o/A_n) or hole area divided by tower cross-sectional area.

4.A.1.14. Weepage Rate

If conditions so demand that the tray tower is to be operated below the weepage limit (which represents the combination of minimum vapor capacity and maximum static liquid submergence at which the tray will begin to weep), the amount of liquid weepage can be quantitatively estimated from :

$$7.3 \log_{10} [1473W + 1] = \left[v_{G,o} \cdot \sqrt{\rho_G}\right]_{v_{G,weep} \to 0} - \left[v_{G,o} \cdot \sqrt{\rho_G}\right] \quad \text{...(4.25)}$$

where, w = weepage, m^3/s per m^2 of tray hole area

$v_{G,o}$ = gas velocity thru holes, m/s

In practice, a trial and error method is followed to predict the weepage rate thru a tray :

1. At a particular liquid load on a tray assume a weepage rate.
2. The difference between the two is the weir overflow rate
3. Calculate h_{ow} by using Eqn. 4.10 or, 4.11 or, 4.12

$$h_w + h_{ow}$$

4. Determine liquid submergence on tray :

5. Determine the min. gas capacity, $\left[v_{G,o} \cdot \sqrt{\rho_G}\right]_{v_{G,weep} \to 0}$ at incipient weepage from the **Capacity Chart** (see later) for given tray with specified hole size & layout.

6. Calculate the operating gas capacity $\left[v_{G,o} \cdot \sqrt{\rho_G}\right]$

7. Compute weepage rate from Eqn. 4.25

8. Check whether the calculated value of weepage rate matches with its assumed value. If it fails to tally, go for 2nd approximation and repeat steps 2 to 8 all over again.

4.A.2. Tray Performance

The tray performance is measured in terms of tray efficiency which is the fractional approach to an equilibrium stage attained by a real tray. A rigorous estimation of tray efficiency is extremely complex. The best-established theoretical method for predicting column efficiency is the sequential prediction of :

$$\eta_{o,y} \to \eta_{p,y} \to \eta$$

where, $\eta_{o,y}$ = point gas-phase tray efficiency, also called **Murphree point efficiency**

$\eta_{p,y}$ = plate efficiency, also called **Murphree gas-phase plate efficiency**

η = overall tray efficiency, also called **Murphree overall tray efficiency.**

Based on two-film theory, the point efficiency can be expressed in terms of transfer units :

$$\eta_{o,y} = 1 - \exp. \ [- NTU]_{o,G} \qquad \qquad ...(4.26)$$

where, $[NTU]_{o,G}$ = number of overall gas-phase transfer units

$$\frac{1}{[NTU]_{o,G}} = \frac{1}{[NTU]_G} + \frac{m.G}{L} \cdot \frac{1}{[NTU]_L} \qquad \qquad ...(4.27)$$

$[NTU]_G$ = No. of gas-phase transfer units.

$[NTU]_L$ = No. of liq-phase transfer units.

G = molar gas rate, $kmol/(h.m^2)$ or, $kmol/(s.m^2)$

L = molar liq rate, $kmol/(h.m^2)$ or, $kmol/(s.m^2)$

The gas-phase transfer units can be obtained from :

$$[NTU]_G = k_G . a . \tau_G \qquad \qquad ...(4.28)$$

where, k_G = gas-phase mass transfer coefficient, $\dfrac{kmols}{\left(s.m^2\right)\left(kmols/m^3\right)}$

a = effective interfacial surface area for mass transfer, m^2/m^3 of froth on plate

τ_G = residence time of gas in froth zone, s

The AIChE data correlated $[NTU]_G$ directly :

$$[NTU]_G = \frac{1}{Sc_G^{\frac{1}{2}}} \left[0.776 + 4.57 \cdot h_w - 0.238 v_{G,a} \sqrt{\rho_G} + 104.6 \frac{Q_{v,L}}{Z} \right] \qquad \qquad ...(4.29)$$

Sc_G = gas-phase Schmidt No. = $\dfrac{\mu_G}{\rho_G . D_{ff,G}}$

$Q_{v,L}$ = volumetric liq rate, m^3/s

Z = length of liq travel on tray, m

$D_{ff,G}$ = gas phase diffusivity, m^2/s

The liquid phase transfer units can be obtained from :

$$[NTU]_L = k_L . a . \tau_L \qquad \qquad ...(4.30)$$

where, k_L = liq-phase mass transfer coefficient, $\dfrac{kmols}{\left(s.m^2\right)\left(kmols/m^3\right)}$

τ_L = residence time of liq in froth zone, s

As per AIChE data for **sieve trays** :

$$[NTU]_L = 40000 \; D_{ff,L}^{0.5} \left[0.213 \; v_{G,a} \sqrt{\rho_G} + 0.15 \right] \tau_L \qquad ...(4.31)$$

$$\tau_L = \frac{h_f \cdot A_a \cdot \varnothing_t}{Q_{v,L}} \qquad ...(4.32)$$

where, A_a = active area of tray, m^2

$\varnothing_t$ = average relative froth density on tray = $\dfrac{h_L}{h_f}$

$Q_{v,L}$ = liquid rate, m^3/s

h_f = froth height (see **Fig. 4.21**)

$$= 1.7 \; v_{G,a}^2 \; \rho_G + 74.41 \; h_w - 1.6 \qquad \text{[AIChE Eqn.]} \qquad ...(4.33)$$
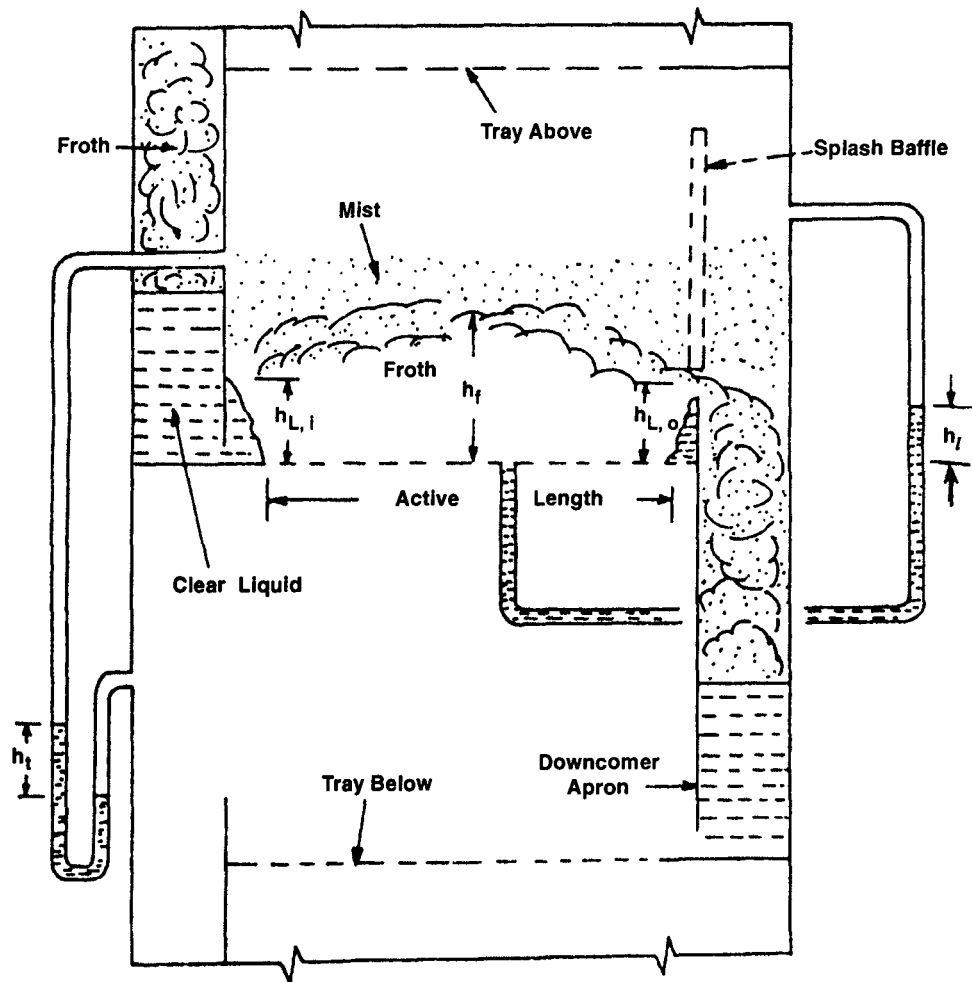
Fig. 4.21. *Schematic Diagram of A Cross-Flow Perforated Tray in Operation.*

Also,
$$\tau_L = \frac{h_L . A_a}{Q_{v,L}}$$
...(4.32 A)

But as per AIChE relationship for sieve trays
$$\tau_L = \frac{h_L . z . Z}{Q_{v,L}}$$
...(4.32 B)

In order to convert point efficiency, $\eta_{o,y}$ to Murphree plate efficiency, $\eta_{p,y}$, Lewis analyzed the effects of gas and liquid mixing on crossflow plates whereupon three distinct cases arise :

1. **Gas completely mixed between the trays**

2. **Gas unmixed and liquid flows in the same direction on successive trays**

3. **Gas unmixed and liquid flows in the reverse direction on successive trays.**

Most tray columns operate under conditions such that gas is completely mixed as it flows between the trays. Therefore, we shall limit the conversion $\eta_{o,y} \rightarrow \eta_{p,y}$ to **Case - 1** only.

As the consequence of complete gas mixing under the plate, gas enters the plate at uniform composition whereupon the Murphree plate efficiency is related to point efficiency thru the following relationship :

$$\eta_{p,y} = \frac{1}{e_s}\left[\exp\left(e_s . \eta_{o,y}\right) - 1\right]$$
...(4.33)

where, e_s = stripping factor, $m.\dfrac{G}{L}$

The Eqn. 4.33 holds good under the conditions of :

1. m = constant

2. $\dfrac{L}{G}$ = constant

3. $h_{o,y}$ = constant

According to eddy-diffusion model of AIChE :

$$\frac{\eta_{p,y}}{\eta_{o,y}} = \frac{1 - \exp.\{-(n'+Pe)\}}{[n'+Pe]\left[1 + \dfrac{n'+Pe}{n'}\right]} + \frac{\exp(n') - 1}{n'\left[1 + \dfrac{n'}{n'+Pe}\right]}$$
...(4.34)

where, $n' = \dfrac{1}{2}Pe\left[\left(1 + 4\dfrac{m.G}{L} . \dfrac{\eta_{o,y}}{Pe}\right)^{\frac{1}{2}} - 1\right]$

Pe = Peclet No.

$$= \frac{Z^2}{\tau_L . D_{ff,e}}$$

Z = length of travel on tray, m

$D_{ff,e}$ = eddy-diffusivity, m^2/s

For sieve tray, according to AIChE data,

$$D_{ff,\,e} = [3.93 \times 10^{-3} + 0.0171\, v_{G,\,a} + 3.67\, \frac{Q_{v,L}}{Z} + 1800 h_w]^2$$

...(4.35)

The calculated value of $\eta_{p,\,y}$ must be corrected for entrainment

$$\left[\eta_{p,\,y}\right]_\psi = \frac{\eta_{p,\,y}}{1 + \eta_{p,\,y}\left[\dfrac{\psi}{1 - \psi}\right]}$$

...(4.36)

where, $\left[\eta_{p,\,y}\right]_\psi$ = Murphree gas-phase plate efficiency corrected for entrainment

ψ = fractional entrainment

The resulting corrected efficiency is then converted to column efficiency

$$\eta = \frac{n}{n_t} = \frac{\log\left\{1 + \left[\eta_{p,\,y}\right]_\psi \left(e_s - 1\right)\right\}}{\log\left(e_s\right)}$$

...(4.37)

4.A.3. Tray Construction & Installation

Trays are supported on channels or I-beams particularly for large-dia towers. When tower dia is 6m or more, the web of such a beam may influence selection of tray spacing.

Large dia trays are made up in sections. Each such section is transported thru the tower manhole, set in appropriate position and bolted together inside the vessel with metal-to-metal sealing or with asbestos gasket. Such joints should preferably be leak proof or leakage, if there is any should not be excessive.

Also the tray sections at the peripheral waste zone are to be bolted to tray support-clips that are spot welded to the tower shell.

In large towers, each tray is provided with at least 600mm × 600mm manway to let in maintenance workers up and down the column since it is not practical to remove the entire trays during shutdown (**Fig. 4.22**).

The tray perforations are punched rather than gang-drilled. This is because punching costs far less than drilling. As a rule of thumb, punching is carried out on trays when tray thickness is to hole dia is less than unity, *i.e.*,

$$\frac{\delta_p}{d_o} < 1$$

However, this ratio may exceed unity in the case of very soft metals or when using some of the harder variety of stainless steels that may cause excessive drill-bit failure.

Weepage holes are provided so that towers can be fully drained for shutdowns. These holes
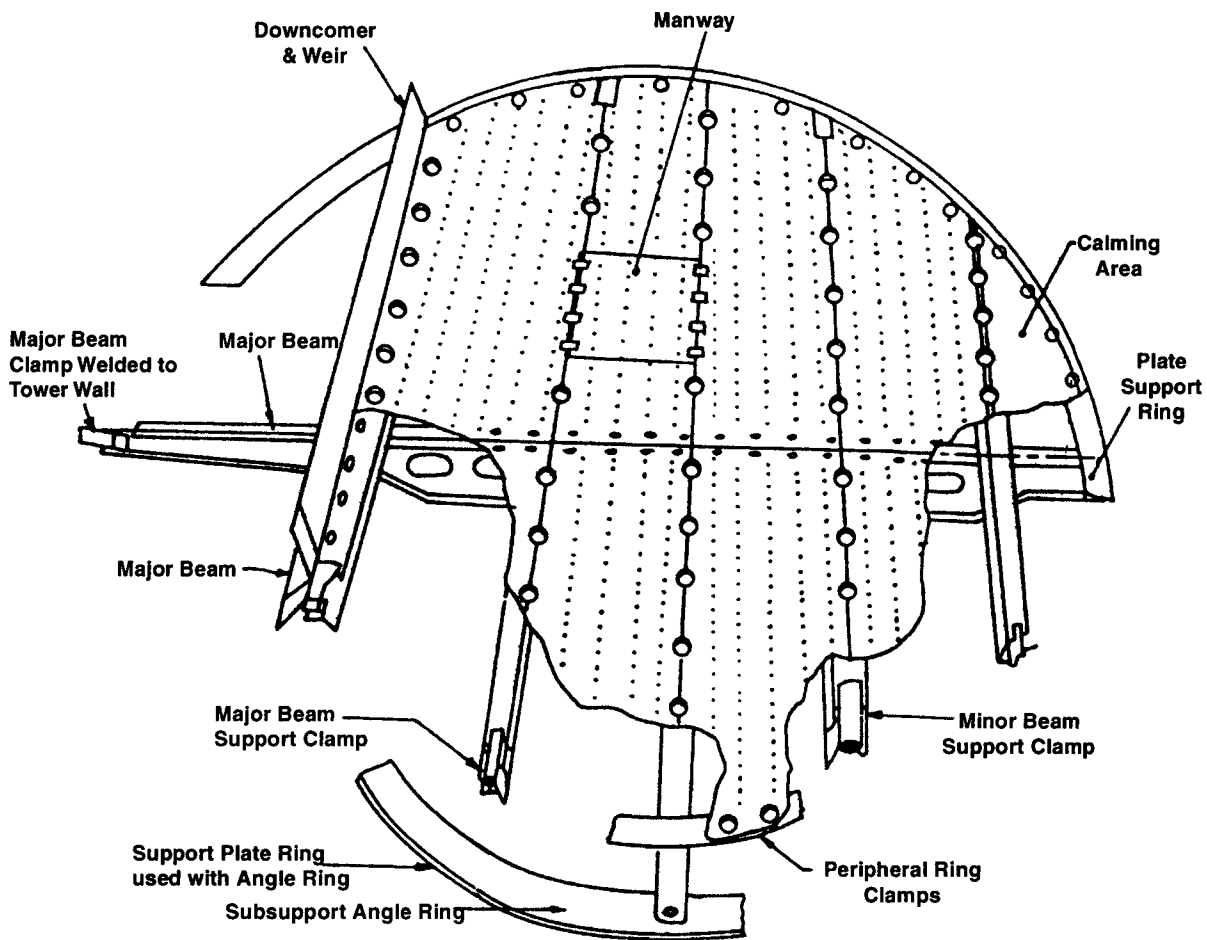
Fig. 4.22. *A Typical Tray Assembly (Sieve Tray) showing the Major Structural and Mechanical Components that Make up the Tray and its Supports.*

are customarily drilled in the tray inlet weirs. The number and size of these holes are based on a capacity of about 2% of the liquid thruput at full load.

When the tower is too small (< 1200 mm) to admit a technician to assemble the plates or when it is deemed desirable to provide for the rapid changing of internal tray details, the **stacked-type** (also called **cartridge-type**) of construction ought to be considered. Although adaptable to any tray form, this construction is particularly an attractive scheme for radial-flow designs.

Each tray is fabricated complete with the downcomer and joined to the plate above and below using screwed rods, called *spacers* [Fig. 4.23].

Ten or so plates are assembled into a stack which is inserted into the tower by overhead crane. Tall columns are usually divided into flanged sections so that the plate assemblies can be easily installed & removed.

The plates slide into the shell like a series of pistons. So there is no positive liquid seal at the edge of the plate and as a result a small amount of leakage always occurs.
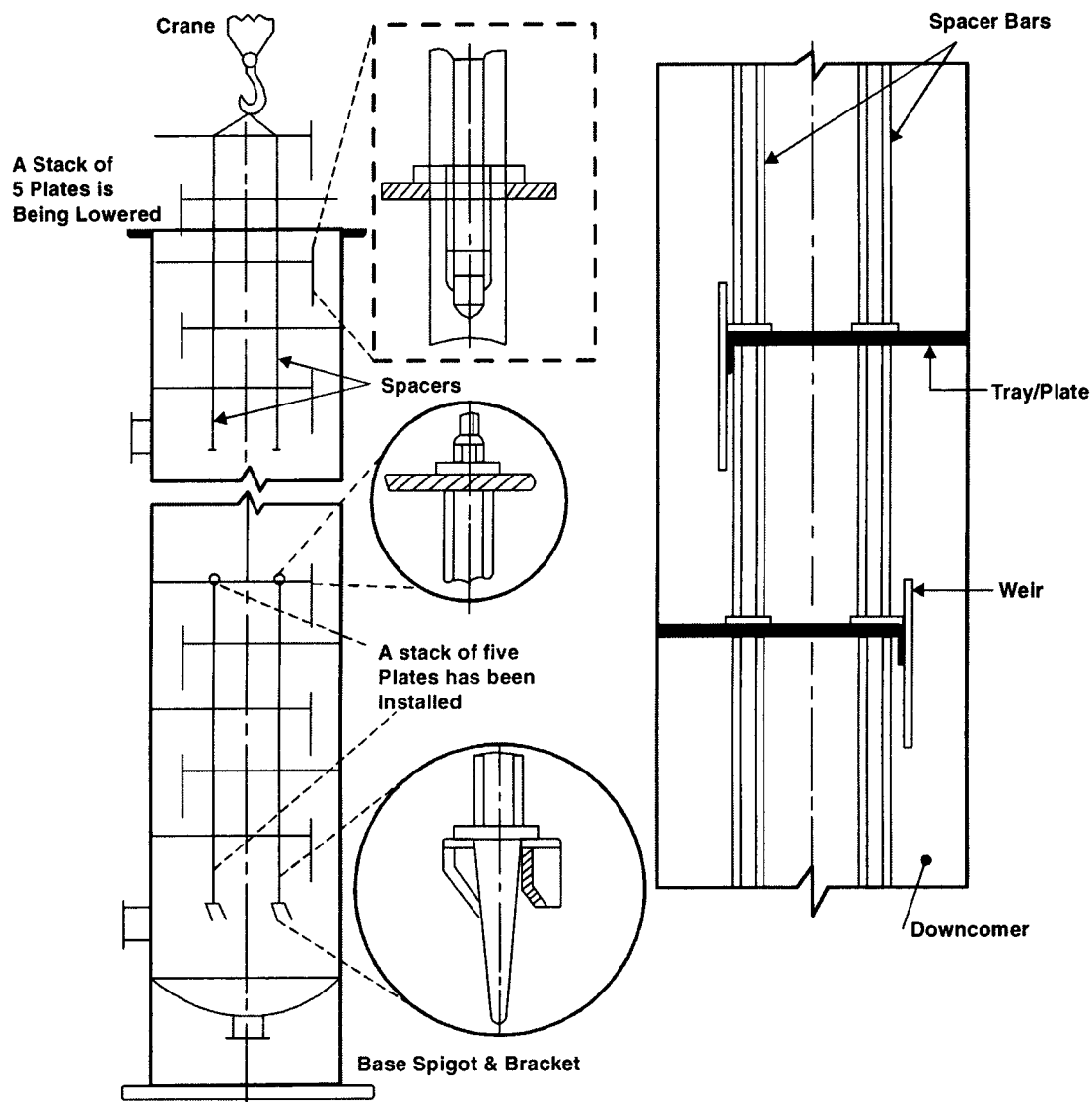
Figure. 4.23. *Typical Stacked Plate Construction.*

4.A.4. PERFORATED TRAY DESIGN USING CHARTS

An absorber or a stripper must operate within set limits of gas and liquid flows. Increasing the gas velocity thru the perforations eventually leads to excessive entrainment giving rise to backmixing that raises the internal tray-to-tray circulating liquid loads and destroys the staging, *i.e.*, temperature and concentration gradients from the bottom to the top of the tower.

The same effect is induced by an excessive liquid load. If the liquid thruput is increased (or more correctly, the depth of liquid pool on the tray is raised), there will occur greater droplet entrainment to the tray above.

Just as it is undesirable to operate with excessive liquid entrainment, it is equally undesirable to operate with insufficient gas velocity thru the perforations. This causes the liquid to weep excessively,

shortcutting its residence time on tray and bypassing gas contacts along its flowpath across the tray. The deeper the liquid pool-on-tray, the higher the hole velocity required to prevent this counterflowing weepage.

The **Capacity Charts** [Fig. 4.24] are quite handy and convenient to understand the relationship between gas and liquid thruputs, tray spacing (froth height) and weepage. These curves are drawn for a given gas-liq systems and for a fixed perforations size and pattern.
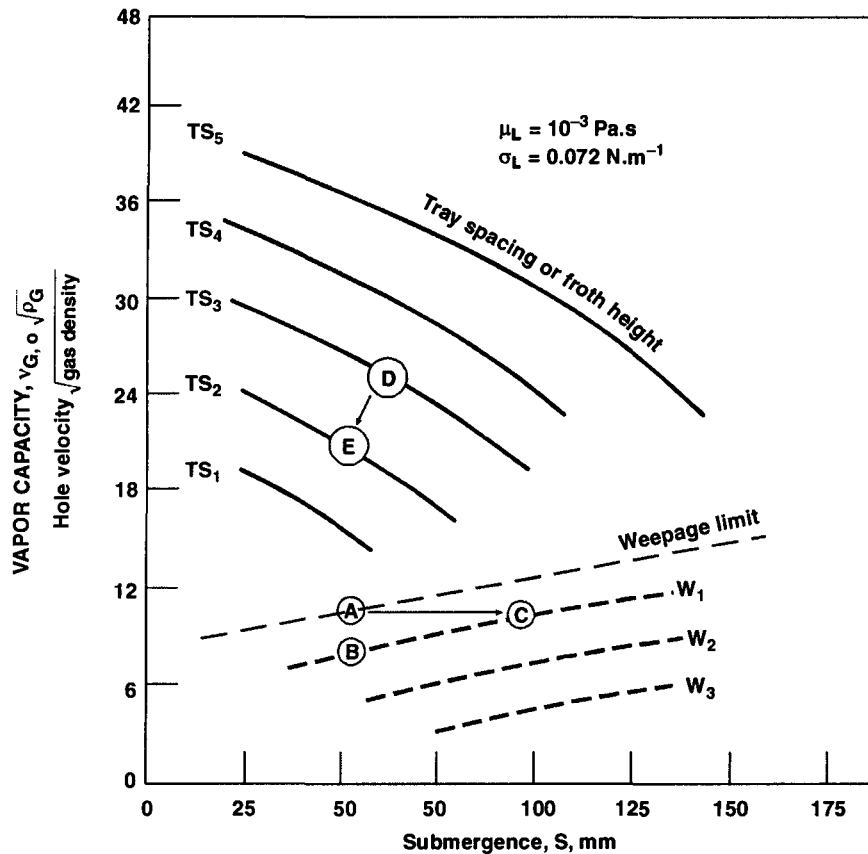
Fig. 4.24. *Capacity Chart for a Sieve-Tray [Hole Dia = 4.5 mm ; A_o = 8.35% A_t] for A Typical Gas-Liq System [μ_L = 10^{-3} Pa.s; σ_L = 0.072 N/m].*

The **weepage limit** (dashed line) is the locus of incipient weepage the particular plate *[d_o = 4.75 mm; A_o = 8.35% A_t]* will exhibit at different combination of maximum liquid submergence and minimum gas loads for the given gas-liq system.

Now, if the column operates at a liquid load corresponding to a crest-height of 25mm over a weir-height of 25mm (*i.e.*, a static submergence of 50mm), the tray will not weep even at a minimum gas load provided the gas (vapor) capacity product of hole velocity and the square root of gas density exceeds. 23.76 $kg^{1/2}$. s^{-1}. $m^{-1/2}$ [Point Ⓐ in *Fig. 4.24*], *i.e.*, if the operating point lies above Ⓐ no liquid will weep thru the perforations. Now, if the gas rate is reduced by 30% [to point Ⓑ in *Fig. 4.24*], the tray will weep. If, instead, the liquid load were increased to yield a static submergence of 100mm, liquid weep thru tray perforations at a rate of W_1 m^3/s per m^2 of hole area (A_o), *i.e.*, the same weep rate can be achieved by either decreasing the gas load down to Ⓑ or increasing the liquid load to yield a higher submergence at Ⓒ.

Therefore, the column must be designed at some point well above the incipient weepage locus so that operations at reduced load fall above it. Normally this is quite feasible forasmuch as a reduction in vapor load is usually accompanied by a reduction in liquid load. However, the reduced load condition may shift the operating point from a design condition corresponding to Point Ⓓ to a condition corresponding to Point Ⓔ. However, the pressure-drop factor may force the design point to be quite close to the incident weepage limit and in such cases, column operation at partial load may lead to weepage.

However, the above capacity chart [**Fig. 4.24**] is qualitative for a given perforated plate and for a particular gas-liq system. The position of the *Weepage Limit* and *Tray Spacing Curves* shifts with the change of the liquid properties (σ_L, μ_L etc.) and physical configuration of the trays. For instance :

- Lowering of surface tension of liq-on-tray shifts the weepage limit of **Fig. 4.24.** upwards, *i.e.*, it increases the weepage—limit gas rates. That is even at higher gas loads tray will weep.

- Reducing the tray perforation size lowers the weepage limit, *i.e.*, it shifts the weepage limit curve downcomers with the effect that if the holes are small enough, it is possible to hold liquid on tray without any weep, even when gas is not flowing up thru the holes (e.g., zero gas rate).

- At constant hole velocity and submergence, reduction of hole dia shifts the tray spacing curves diagonally up and to the right. That is smaller perforations permit closer tray spacing.

- Decreasing the plate thickness pushes up the weepage limit curve, *i.e.*, thin plates weep more easily than thick plates.

- Increasing the percentage free area (*i.e.*, increasing the number of holes or the hole dia or both) raises the weepage limit, *i.e.*, the dashed curve of *Fig. 4.24* is raised up and at the same time tray spacing curves shift diagonally up to the right.

4.A.4.1 DESIGN PROCEDURE

1. Choose arbitrarily a **hole size** and **percent free area**, *i.e.*, select a particular *Capacity Chart*

2. Select a **submergence** value in the range :
$$50 - 75\text{mm}$$

3. Select an appropriate design point, say about 20% above the weepage limit. This automatically fixes the ordinate value (tentative)

4. This oridinate value equals *Gas Capacity* $\left(v_{G,o} \sqrt{\rho_o} \right)$

5. **Compute hole area :**

$$A_o = \frac{Q_{v,G}}{v_{G,o}}$$

and the **active area** from the A_o/A_a ratio from the chart.

6. Multiply active area by 1.6 to account for downcomer and distributing zones peripheral hole-area losses.

$$A_t = 1.6 \, A_a$$

7. Calculate **tower dia**

$$D_t = \left[\frac{4}{\pi} \cdot A_t \right]^{\frac{1}{2}}$$

8. Make a trial layout sketch. Determine the weir length, l_w

9. Estimate **height of crest, h_{ow}** from

$$h_{ow} = 0.666 \left[\frac{Q_{v,L}}{l_w} \right]^{\frac{1}{2}} \qquad \qquad ...(4.10)$$

10. Set a weir height, h_w

Check the sum of h_w and h_{ow} does not exceed the submergence, *i.e.*,

$$h_w + h_{ow} \approx S \text{ for OK design} \qquad \qquad ...(4.8)$$

A_o , A_t are in m² ; h_w, h_{ow}, S, D_t are all in m

Note : Repeat the above procedure with a series of hole size of pattern until you get the most economical tower design to accommodate a desired range of loads.

Design : Sieve Tray

Example 4.1 : *Design a sieve tray tower to handle a liquid load :*
$Q_{v,L} = 1.5 \text{ m}^3/min$ *of water*
and a gas load :
$Q_{v,G} = 320 \text{ m}^3/min$ *of gas*
which is essentially nitrogen with a density of 1.20135 kg/m³
Solution : The design is carried out stepwise,

Step - (I) Arbitrarily choose a Capacity Chart (Fig. 4.25) that corresponds to the plate data of :

- 3 mm holes

- triangular pitch

- 3 holes per 25mm

i.e., pitch = 11mm

- Hole area

= 12.7% of active area

Step - (II) Take submergence value

$$S = 60mm$$

Select a tray spacing so that the design point at this submergence lies at least 20–25% above the weepage-limit. According, take $l_t = 360mm$

Set weir height h_w to 25mm
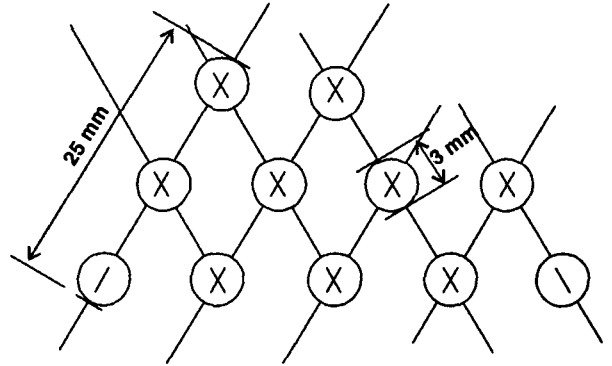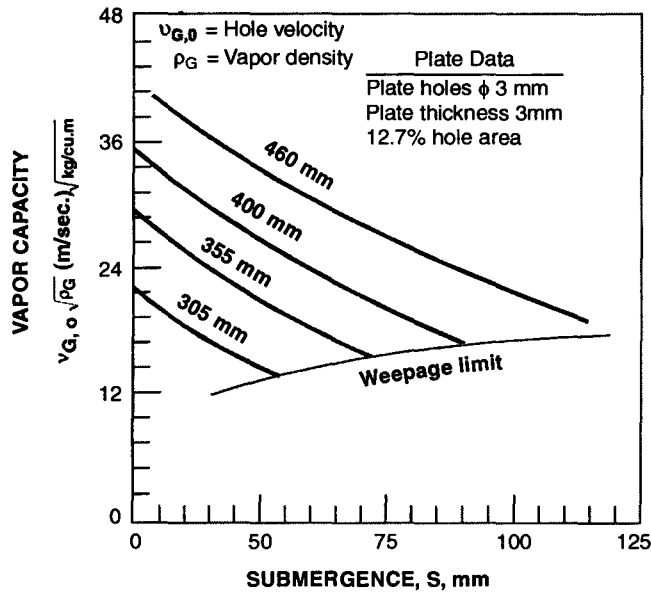
Fig. 4.25. *Capacity Chart for an Air-Water System.*

Step - (III) The Oridinate value that intersects the 360mm – tray spacing curve at submergence of 60mm is about 18.9, *i.e.*,

$$v_{G, o} \sqrt{\rho_G} = 18.9$$

or,

$$\frac{Q_{v,G}}{A_o} \sqrt{\rho_G} = 18.9$$

or,

$$A_o = \frac{320/60}{18.9} \sqrt{1.20135} = 0.30929 \text{ m}^2$$

Step - (IV) Active Area

$$A_a = \frac{A_o}{0.127} = \frac{0.30929}{0.127} = 2.43538 \text{ m}^2$$

Step - (V) Tower Cross-Section

$$A_t = 1.6A_a = 1.6 \, (2.43538) = 3.896619 \text{ m}^2$$

Step - (VI) Tower Dia

$$D_t = \left[\frac{4}{\pi} (3.896619) \right]^{\frac{1}{2}} = 2.2274 \text{ m}$$

Let us take

$$D_t = 2.25 \text{ m}$$
$$A_t = 3.9760 \text{ m}^2$$

$$A_a = \frac{1}{1.6} \, A_t = 2.4850 \text{ m}^2 \qquad\qquad\qquad \text{[corrected]}$$

$$A_o = 0.127 \, A_a = 0.3156 \text{ m}^2$$

Step - (VII) Tray Layout

The tray layout is drawn.
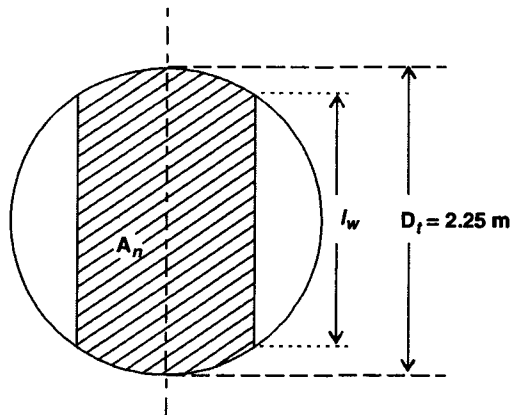
Take **Net Area = 20% more than Active area**

i.e., A_n $\quad = 1.2 \, A_a$

$\qquad = 1.2 \, (2.43538)$

$\qquad = 2.922456 \text{ m}^2$

Therefore, area of each segment :
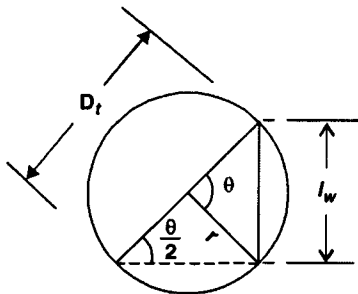
$$A_{seg} = \frac{1}{2} A_t - \frac{1}{2} A_n$$

$$= \frac{1}{2} \, (3.976 - 2.922456)$$

$$= 0.52677 \text{ m}^2$$

l_w	D_t	$r = \frac{1}{2} D_t$	$\theta = 2 \sin^{-1} \left[\dfrac{l_w}{D_t} \right]$	θ^{rad}	$\left[A_{seg} = \dfrac{1}{2} r^2 \left(\theta^{rad} - \sin \theta^\circ \right) \right]$
(m)	*(m)*	*(m)*	*(degrees)*	*(radian)*	*(m²)*
1.75	2.25	1.125	102.115	1.7822	0.50908
1.80	2.25	1.125	106.2602	1.8546	0.5661
1.76	2.25	1.125	102.928	1.7964	0.5200 which is very close to the value calculated above

with $\qquad\qquad l_w = 1.76 \text{ m}$

$$h_{ow} = 0.666 \left[\frac{1.5/60}{1.76} \right]^{\frac{2}{3}} = 0.0390 \text{ m}$$

Submergence $\qquad S = h_w + h_{ow}$

$\qquad\qquad\qquad = 0.025 + 0.039 \text{ m}$

$\qquad\qquad\qquad = 0.064 \text{ m}$ which is very close to our assumed value (60 mm of submergence)

Conclusion :

Tower dia	= 2250 mm
Tower cross-section	= 3.976 m²
Active area	= 2.485 m²
Hole area	= 0.3156 m²
Hole dia	= 3mm
Hole pitch	= 11mm
Hole layout	= equilateral-triangular
Weir length	= 1760mm
Weir height	= 25mm

4.A.5. Tower Design Using Rapid-Sizing Chart

We've designed trayed tower on the basis of fixed submergence and a selected tray spacing. However, by using **Rapid Tower Sizing Chart** (Fig. 4.26) we can estimate, for a given gas and liquid load, tray spacing at different tentative tower dia.

Perforated Plate
Tower Sizing Chart
Single-Flow Trays, High L/V
ϕ 3 mm holes on equilateral triangular pitch,
12 holes/100 mm, 12.7% hole area

Vapor load, $V\sqrt{\rho_G}$ = cu.m/sec $\sqrt{\text{vapor density}}$, kg / cu.m

Vapor capacity $v_{G,0}\sqrt{\rho_G}$ = m/sec $\sqrt{\text{vapor density}}$, kg / cu.m

Weir height, 25 mm
liquid backup based on 2 × solid liquid head
Hole velocity, v_{Go}, m.s^{-1}
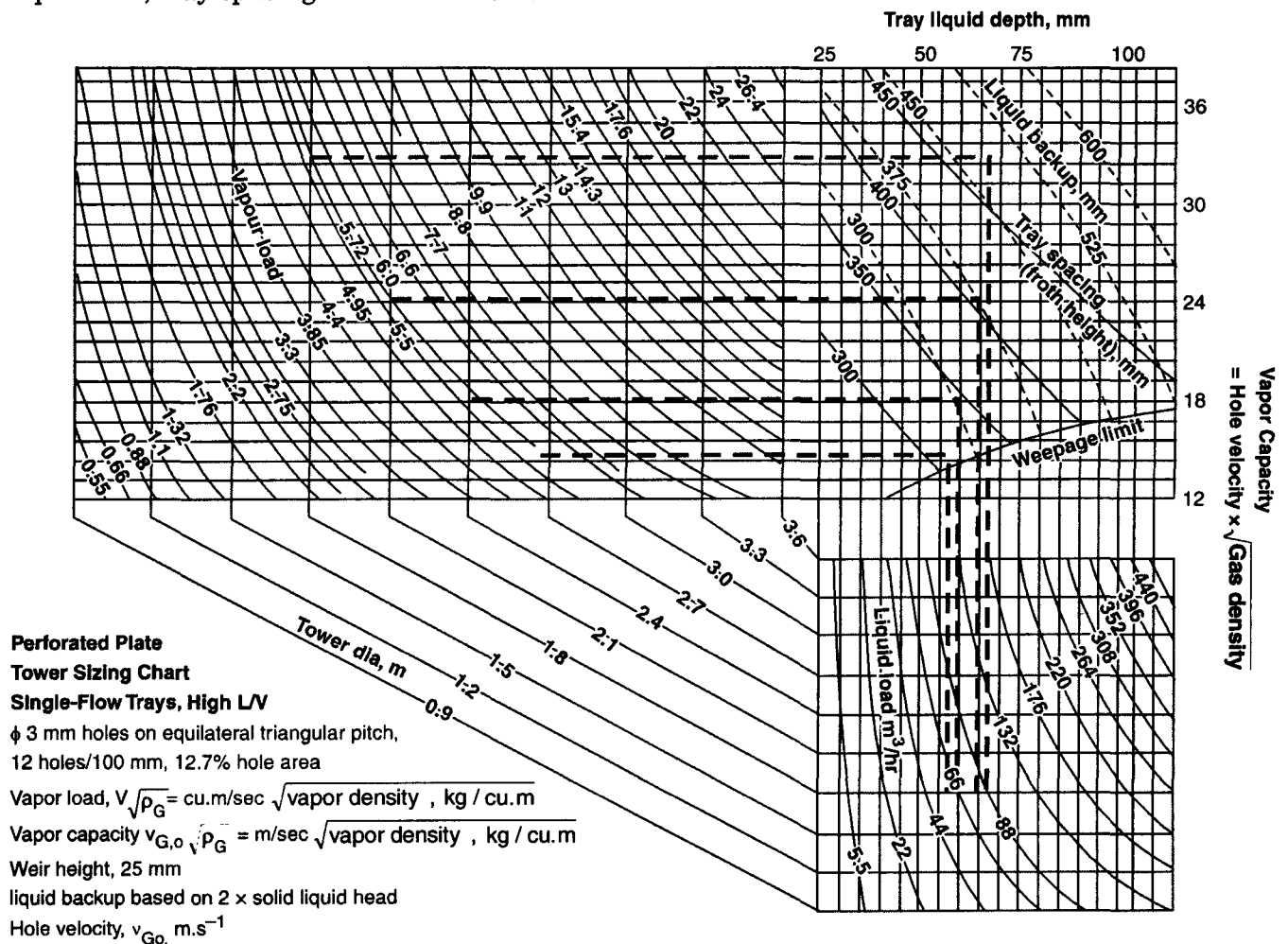
Fig. 4.26. *Rapid Tower Chart for a Single-Flow Perforated Trays with High Liq-To-Gas Ratio.*
Hole Dia = 3mm; Hole Pitch = 12 holes per 100mm
Hole Area = 12.7% of Active Area.

Procedure : 1. Locate gas-load line **(GL).**

2. Locate the liq-load line **(LL).**

3. Select those tower dia lines **(TD)** that intersect both the **GL** and **LL** lines.

4. Draw horizontals from the points of intersection of **LL** lines with the **TD** lines.

5. Draw verticals from the points of intersection of **LL** lines with the **TD** lines.

6. Locate the tray spacings on which the points of intersection of these verticals and horizontals lie. (Interpolation may be required).

Reconsider the previous design example.

Gas rate : 320 m³/min of nitrogen

Liq rate : 1.5 m³/min of water

Gas density : 1.20135 kg/m³

Gas load $$Q_{v,G}\sqrt{\rho_G} = \frac{320}{60}\sqrt{1.20135} = 5.8456 \text{ kg}^{0.5}.\text{s}^{-1}.\text{m}^{+1.5}$$

Liq Load $Q_{v,L} = 1.5 \text{ m}^3/\text{min}$

On the **Rapid-Sizing Chart,** locate the above GL and LL lines.

In **Fig. 4.26,** the GL line is intersected by the TD lines of

$$D_t = 1.8\text{m} ; 2.1\text{m} ; 2.44\text{m} ; 2.74\text{m}$$

Follow these **TD** lines to where they intersect the **LL** lines. Draw the verticals from the points of intersection of **TD** and **LL** lines.

Similarly draw horizontals from the points of intersection of **TD** and **GL** lines.

Read off the design tray spacings at the pt. of intersection of these vertical and horizontal lines.

Result :

Tower Dia (m)	$Q_{v,G}\sqrt{\rho_G}$ (kg$^{0.5}$.s^{-1}.m$^{-0.5}$)	Tray Spacing (mm)
1.8	34.16	500
2.1	24.39	400
2.44	18.29	350
2.74	14.64	312.5

Discussion : Therefore, for handling the given gas and liq loads without weeping and negligible entrainment, the 1.8m tower dia with 500mm tray spacing is as good as any of the following combinations

$$D_t = 2100 \text{ mm with} \quad l_t = 400\text{mm}$$
$$D_t = 2440 \text{ mm with} \quad l_t = 350\text{mm}$$
$$D_t = 2740 \text{ mm with} \quad l_t = 312.5\text{mm}$$

when tray of identical specification [d_o = 3mm ; Δ = 11mm ; A_o = 12.7% A_a] is used in each case.

However, the last combination [D_t/l_t :: 2740mm/312.5mm] puts the design point very close to the *Weepage Limit* entailing the risk of weepage at lower gas load or higher liq load. So let us abandon it.

Out of the remaining three, the choice of optimum design is the matter of capital cost or operating expenditure. The tower of 1.8m dia and with 500mm tray spacing will cost less in metal than any of the larger sizes. However, it gives rise to the maximum pressure drop which is proportional to $\left[Q_{v,G}\sqrt{\rho_G}\right]^2$. Though the tower of specification : $D_t/l_t :: 2740mm/312.5mm$ will give least gas press-drop but it'll be costliest among the three.

Therefore, let us select tower of **ID** = 2100mm with tray spacing of 400mm. It will be neither too costly nor it'll give rise to high gas pressure-drop.

4.A.6. Mechanical Design of Sieve Trays

The complete design of sieve trays involves two stages :

– *Basic Design Procedure*

– *Detailed Layout of the Tray Components*

We've already discussed at length, the basic design procedure that deals with the determination of the following basic parameters :

• **Tray diameter and area**

• **Bubbling area and hole area**

• **Hole dia**

And the details of tray layout belongs to the domain of mechanical design of sieve tray. But before we go for the layout of sieve trays, it is imperative to consider the following general factors that affect the details for tray layout.

Corrosion – is a mind-boggling problem. For trays subjected to corrosive environment, the likelihood of corrosion, the extent of damage and its possible impact on column internals must be evaluated. This involves objective analysis of the consequence of operating with corroded internals (viz, tray damage, tray collapse, upset of gas-liq flow, product quality deterioration and so on), and the cost of replacement of damaged tray/internals plus the cost of production must be taken into account. And therefore, the maximum limit of corrosion tolerance must be defined.

Fouling – may result either from ingression of foreign materials thru feed or from product polymerization inside the column.

Fouling is a naughty problem. For columns operating in fouling services, the type, degree and consequences of fouling must be eliminated at an early stage, and the method of cleaning its internals should be established.

Answer to fouling problems comes in the forms

– **dozing of additives that inhibit the polymerization process**

– **designing the column so that fouling has a marginal chance to occur.**

– **modifying operating conditions so that fouling does not significantly affect column performance.**

– **keeping feed free from foreign materials.**

In any case, the effect of fouling on column performance, frequency of shutdowns and method of cleansing have an important bearing on tray layout and design.

Tolerances : Tighter tolerances than necessary must be avoided as it means a significant waste of money. Tolerance of each specified tray component must be weighed in the context of its

contribution to the functional or mechanical integrity of the tray. The magnitude of the various tolerances should be realistic and as large as feasible for the particular application.

Sieve Tray Layout involves

- **– selecting hole dia**
- **– setting of tray spacing**
- **– establishing calming zones**
- **– designing outlet weirs-length and height**
- **– establishing levelness of the tray.**

Hole Dia : For industrial columns hole dia range from 3mm to 25mm. The following factors should be considered while selecting hole diameters.

I. Service Conditions: Small holes should be avoided for fouling or corrosive services.

If the service is a fouling one, small holes may get clogged partially or completely, leading to excessive tray drop (*i.e.*, pressure buildup) inviting premature flooding. Besides, hole blockage may arise from nonuniformly distributed flow pattern inflicting uneven vapor flows and lower tray efficiencies.

In case the service is corrosive, large holes beget two distinct advantages :

1. the rate of change of hole area and the rate of change of tray ΔP with time becomes much smaller.

2. the allowable tray thickness is greater with the consequent benefit of greater corrosion tolerance.

In any case, holes smaller than 12.5mm are not recommended whether the service is corrosive or fouling one.

II. Weeping : True it is that smaller the size of the holes, the lower is the tray weeping rate, That means, smaller holes augment capacity advantages. This is particularly true if tray spacing is small and/or the liquid surface tension is high, *i.e.*, tray operates in froth-regime. Plus small holes also reduce entrainment, most notably in low-pass services, *i.e.*, sieve-trays punched with small holes act as strainers.

III. Mass Transfer : Small holes ensure better vap-liq contact and hence higher efficiency if the operation is in froth-regime.

In case, the column operates in the spray-regime, the hole-size becomes an immaterial factor and under these circumstances, larger holes are preferred.

IV. Frothing : Recommendations are specially made for small holes (3mm) in clean vacuum services operating in the froth-regime in order to keep entrainment at bay and tray efficiency not to hamper.

V. Turn-Down : Small holes are always a favored choice in the context of higher turndown characteristics as they reduce tray weeping and entrainment and enhance tray capacity.

VI. Costs : Larger holes are punched while smaller holes ($d_o \approx 4.75$mm) are drilled. Drilling is more expensive than punching. However, punching has its limitation. A minimum plate thickness is required for a given dia of holes, to avoid tray warpage. As a rule-of-thumb, carbon-steels and copper-steels and copper-alloys can be punched when hole dia is equal to greater than tray thickness ; for SS materials, the hole dia must be 1.5 to 2 times the tray thickness.

VII. Errors in Dia : For trays with small holes, a small error in hole dia when drilling a punching has a greater impact on tray pressure drop, capacity & turndown than the same error in a large hole.

VIII. Installation : Tray pannels should be installed with the rough edge of the hole facing down (*i.e.*, facing the vapor low) **Fig. 4.27 A.**

D I R E C T I O N   O F   P U N C H I N G

TRAYDECK

D I R E C T I O N   O F   V A P O R   F L O W

[A] Normal

T R A Y   F A C E   G R O U N D   &   F R E E   O F   B U R R S

TRAYDECK

D I R E C T I O N   O F   V A P O R   F L O W

D I R E C T I O N   O F   P U N C H I N G

[B] Pressure Drop is Important
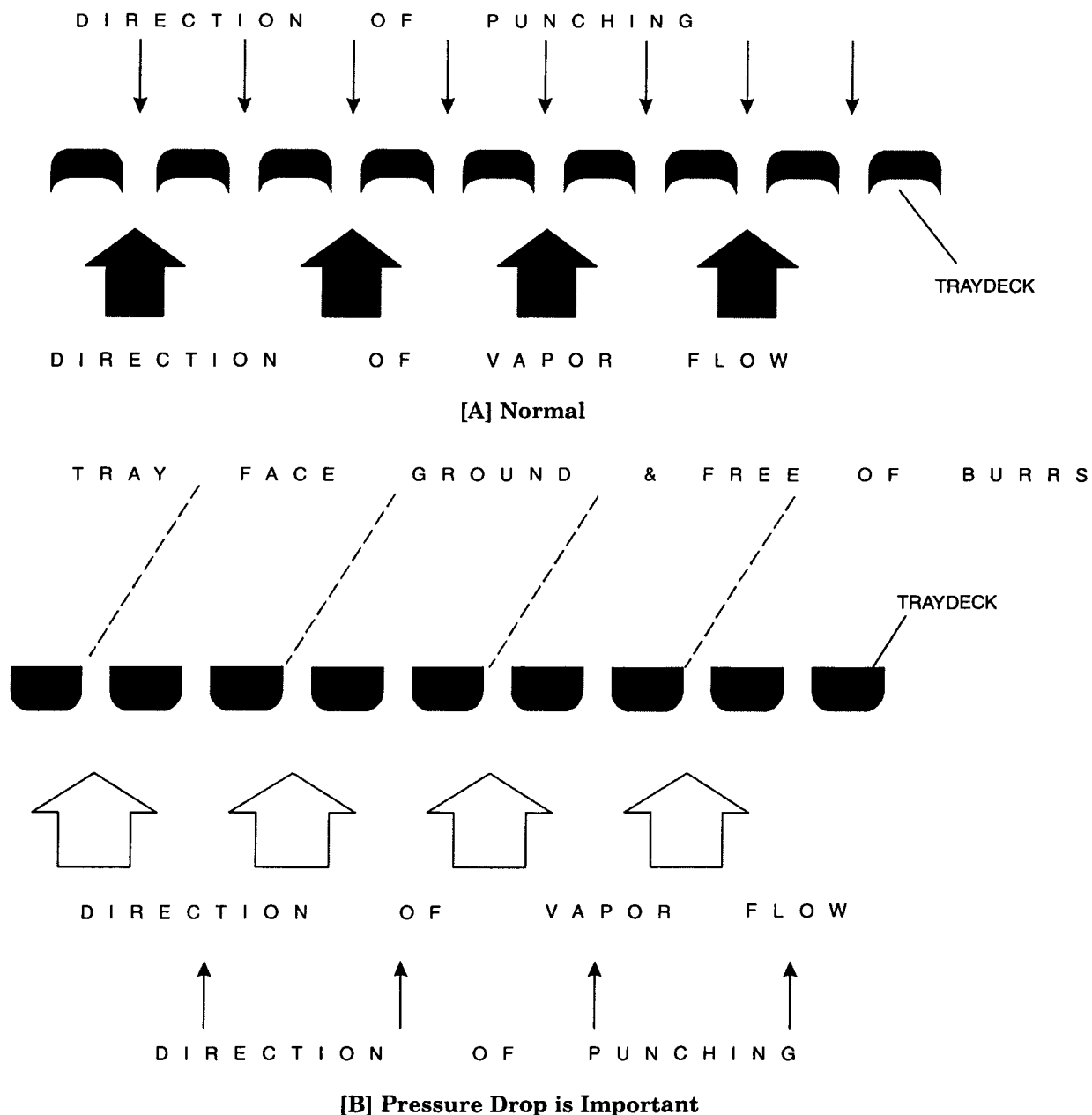
Figure 4.27. *Recommended Practice for Tray Installation.*

This is a normal practice for columns operating under higher ΔP, for it increases tray pressure drop slightly (due to venturi effect) of course, it reduces the risk if injury to workers working in the column or installing the trays, besides diminishing slightly the weeping tendency.

If, however, press-drop factor is of overwhelming importance, it is better to put rough side up and the burrs ground smooth **(Fig. 4.27B)**.

Normally, sieve trays with smaller holes (with dia 4.5mm being the general choice) are always preferred for nonfouling and non-corrosive services. Whereas large trayholes are recommended for fouling and corrosive operating conditions and for spray-regime operations, provided in latter case, the tray spacing is sufficiently large.

Hole Spacing

The sieve tray holes are spaced on staggered configuration with liq flowing perpendicularly to the rows **(Fig. 4.20)**
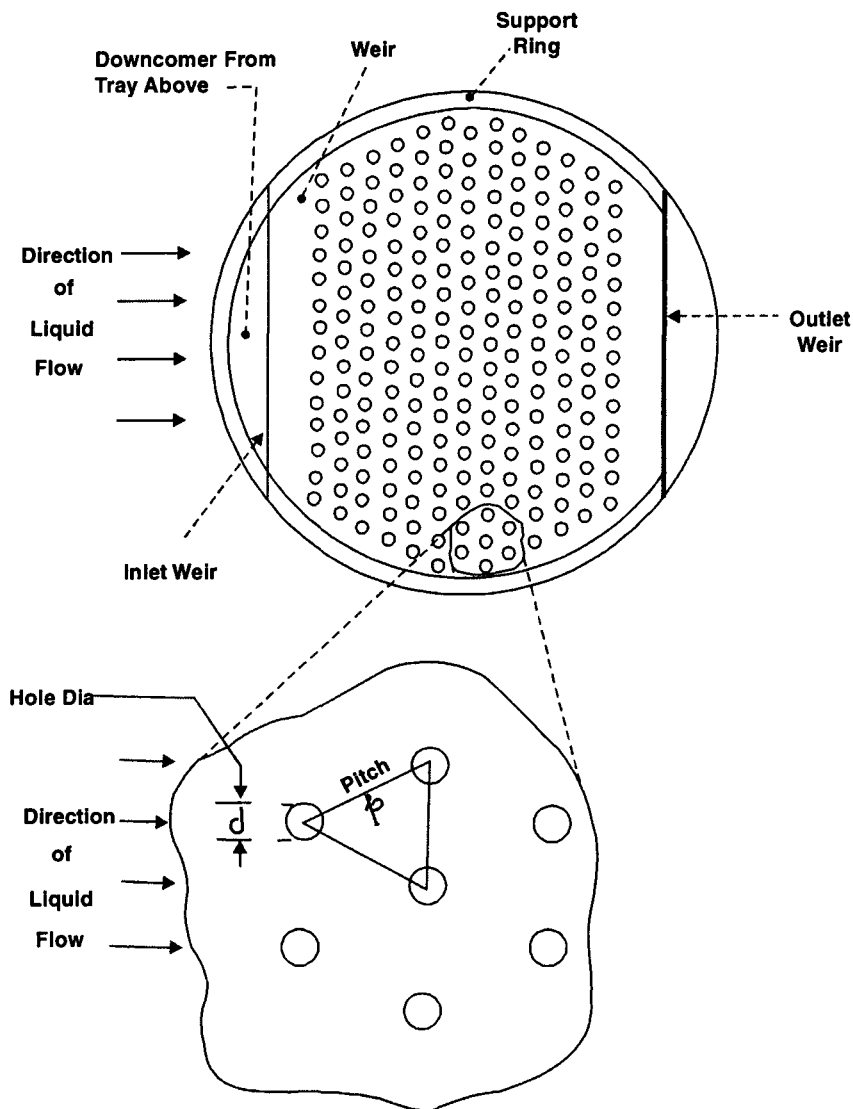
Figure 4.28. *Typical Layout of Components for Sieve Trays (Top View).*

This pattern of layout gives equilateral triangular hole-pitch.

Now, the pitch-to-diameter ratio (p/d_o) should lie between 2 and 5, preferably between 2.5 and 4 while 3.8 being recommended as optimum.

A p/d_o ratio smaller than 2 may give rise to interaction between vapor streams flowing thru adjacent holes and that reduces the contacting area betwen the counterflowing vapor and liquid streams. Also a p/d_o ratio smaller than 2 may lead to tray instability and invite excessive dumping. However, there should be an upper limit. For a p/d_o ratio exceeding 5 gives rise to higher percent of tray-waste area and curtails vap-liq contact area.

Once tray dia, hole area and hole dia are specified, the hole spacing becomes a dependent variable, *i.e.*, it cannot be directly specified. It must fall within the required range.

In case the hole spacing is lower than the minimum limit, the calming zone area should be
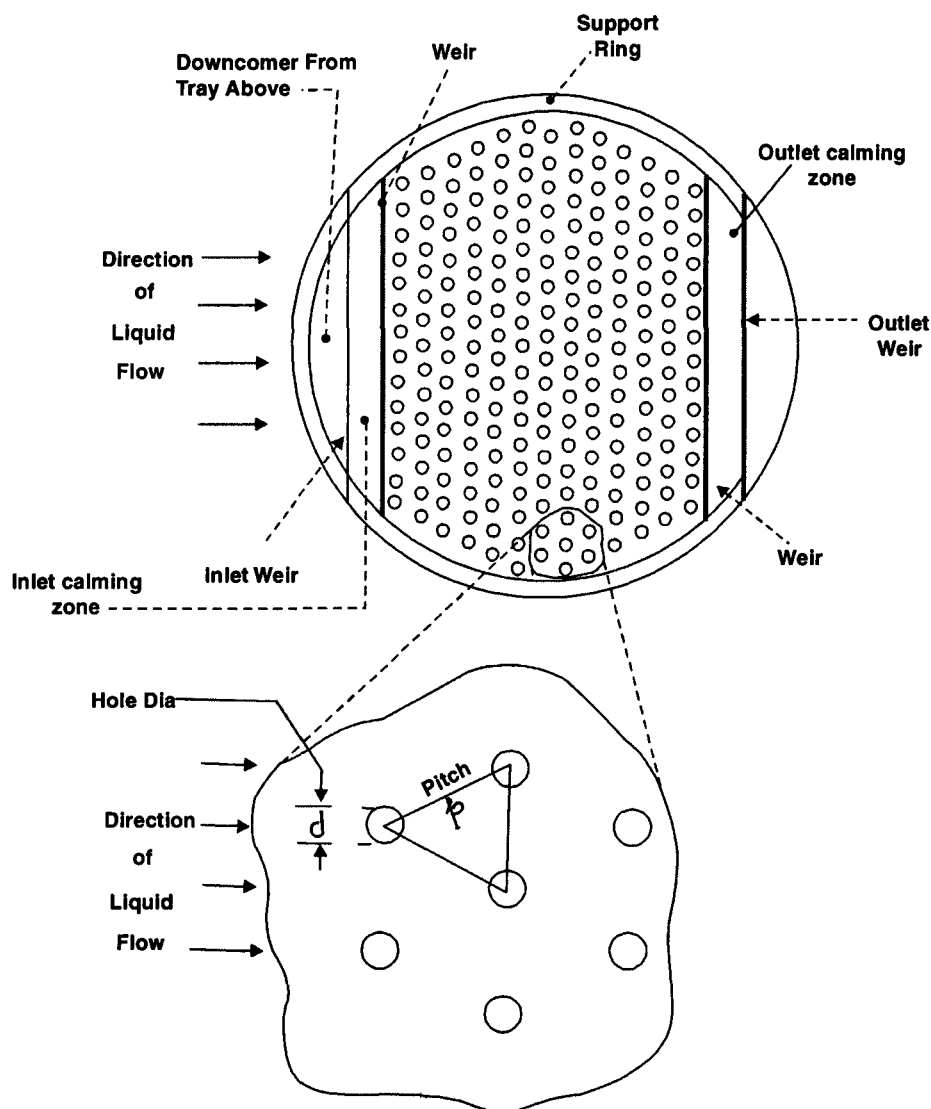
Fig. 4.29. *Typical Layout of Components of Sieve Tray.*

• Turn-Down = Maximum Load : Minimum Load

reduced or sloped downcomer should be used or column dia should be increased. If it is above the maximum limit, the number of holes should be increased to the optimum, and the excess holes should be blanked (using blanking strips)

However, the blanking strips should be installed obeying the following guidelines:

• The blanking strips should be installed from one wall to another.

• The width of each strip should not exceed 100mm to avoid formation of inactive regions.

• At least 4 nos. of blanking strips per tray and they should be scattered across the tray.

• The blanked area should not exceed a quarter of the tray area.

Calming Zones : are provided both at tray inlet and tray outlet. It is a blank area provided between the inlet downcomer or inlet weir and the hole field and the area between the hole field and the outlet weir **(Fig. 4.29)**

The liquid entering a tray via downcomer possesses a vertical velocity component in the downward direction. This velocity component results in excessive weeping and inhibits bubble formation at the first row of tray holes. To counterpoise this vertical component, a calming zone is to be provided at the inlet section. This calming zone should be at least 100mm wide. However, a calming zone of 50mm is satisfactory for trays fitted with recessed inlet weir, as in this case this downward vertical component is almost attenuated. Likewise outlet calming zone is to be provided to permit vapor disengagement from the froth on the tray prior to liquid entering the downcomer. For trays operating in the froth regime **[Fig. 4.30]** an outlet calming zone of at least 100mm is recommended. However, excessive width of the outlet calming zone is to be avoided as it represents a waste of space and promotes weeping and backmixing.

However, different considerations need apply if the trays operate in the spray regime. Under this condition, the liq does not enter the downcomer by flowing over the outlet weir. Instead, it enters as fine liq droplets suspended in vapor space and descends into the downcomer **(Fig. 4.31)**.
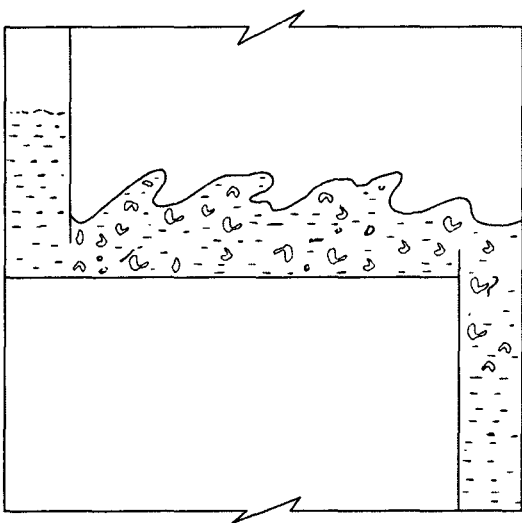
Fig. 4.30. *Froth Regime on Sieve Tray.*
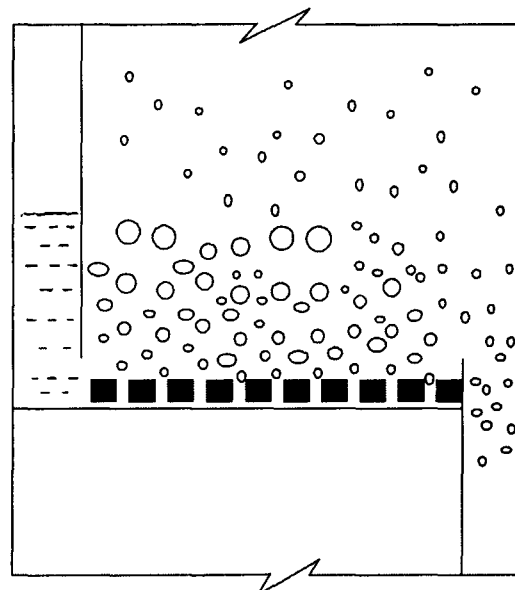
Fig. 4.31. *Spray Regime.*

For this reason, the closer the weir to the holes, the more easier it becomes for the suspended droplets to reach the downcomer. Therefore, it is recommended to place outlet weir as close to the holes as possible for spray-regime operation. For tray operation in this regime, the minimum width of the outlet calming zone is limited to about 50mm by plate-support ring.

Outlet Weirs :

Outlet weirs are required to maintain desired liq level on the tray. This is essential, particularly when the tray operates in the bubble or froth regime **(Fig. 4.30).** For it ensures liq holdup, even distribution of liq on the tray and insures adequate gas-liq contact time. That is, weir height will be high enough to provide sufficient liq-vap contact time and good bubble formation but not high enough to exceed the tray pressure drop above the permissible limit entailing the risk of more weeping and lower tray capacity. Again in the processing of hazardous liquids, higher liq-depth-on-tray risks higher column inventories.

For most applications, a liq level ranging between 50 mm, and 100mm provides the best value. Weir height can be determined from the following relation

$$100 - h_{ow} - \frac{1}{2} h_{hg} \geq h_w \geq 50 - h_{ow} - \frac{1}{2} h_{hg}$$

where, h_w = weir height, mm

h_{ow} = height of liq crest over the weir, mm

h_{hg} = hydraulic gradient, mm

However, an exception to this applies to those systems where a long liq-residence time is necessary, *e.g.*, where a chemical reaction takes place on a tray. Under such circumstances a weir height of up to 150mm can be used.

If weir height exceeds 15% of tray spacing, the designer should take care to allow for the reduction in effective tray spacing when capacity limits are estimated.

However, for trays operating in the spray regime*, the weir looses its significance and purpose and hence can be eliminated altogether. But it is a good advice to provide outlet weirs even with columns designed to operate normally in the spray regime. This is because, at low rates the columns may swing to operate in the froth regime.

Weir Dimensions :

Recommended weir height	= 12.7mm (minimum)
Preferred weir height	= 19mm
Weir height for most services	= 50mm (in general)
Weir height for vacuum services	= 25mm (in general)

Inasmuch as vacuum columns usually operate in the spray regime for most of their operating range, low weir height are suitable for them.

---

* **Spray Regime :** When trays operate in this regime **(Fig. 4.31)**, liq enters the downcomer as a shower of liq droplets, precipitating from the vapor space above the downcomer. This being the condition, liq holdup on the tray becomes independent of weir height.

Note : Adjustable weirs **(Fig. 4.32)** were common in early designs.
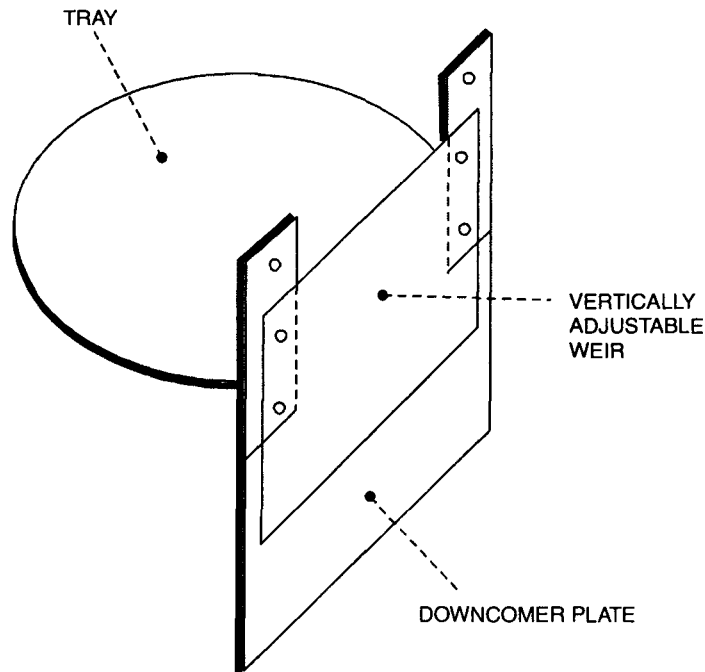
Fig. 4.32. *Adjustable Weir. They are fraught with Maladjustment possibilities and hence seldom Used Now-A-Days.*

But they're no longer recommended today as they're prone to maladjustments during plant operation outweighing their potential benefits.

Weir height tolerance = 1.6 – 3.2 mm

Weir length should be so adjusted as to **maintain at least 6 to 12mm liq crest above the weir,** *i.e.,*

$$h_{ow} = 6 — 12mm$$
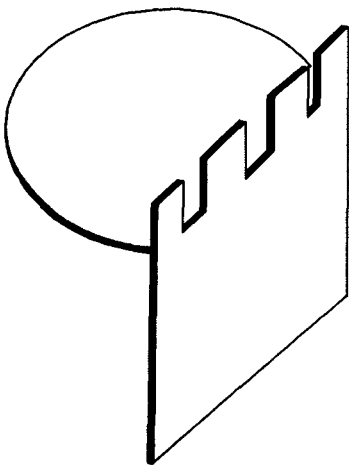
Fig. 4.33A. *A Rectangular -Notch Weir*
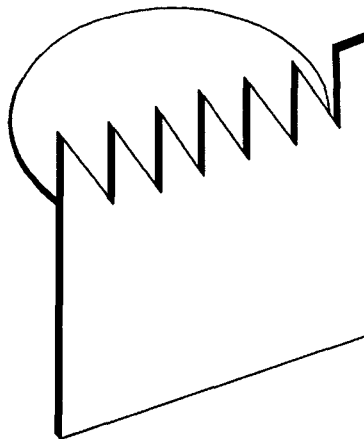
Fig. 4.33B. *Continuous Triangular-Notch Weir*
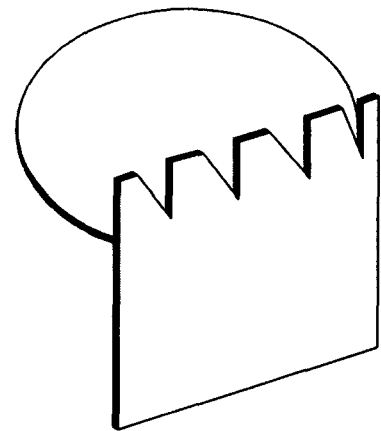
Fig. 4.33 C. *Intermittent Triangular-Notch Weir*

This is a measure to ensure good liq distribution on the tray. Select the higher value of h_{ow} (*i.e.*, 12mm) in case the tolerance is high, *i.e.*, 3.2mm.

Note : If the tolerance is too high relative to the liq crest, h_{ow} will vary all along the weir length inducing large flow variations from one end of the weir to the other with the effect that tray efficiency will go down.

Select notched weir (**Fig. 4.33.A, 4.33 B, 4.33 C**) for low weir loadings, whence a liq crest of 6 to 13mm may be difficult to obtain. Notches are made in rectangular or triangular profile. Such weirs are recommended for liq loading of less than 2.235 m³/h per meter of weir length.

TRAY LEVELNESS

During tray-design calculations, it is normally assumed that the tray is perfectly level. However, in practice it is not so. It is impossible to lay a tray perfectly horizontal in a column. And tilting tells upon tray performance in one or more ways :

I. **Weeping** – Tilting invites weeping which becomes considerable at low liq loading (less than 4.5m³/h per 100mm weir height) than at higher loading.

Apparently weeping thru sieve tray holes may be expected to increase with tilting, however, tests have proved otherwise.

II. **Vortexing** – Off-level tray can promote vortexing which is particularly evident in bubblecap trays that operate with a low slot, *e.g.*, atmospheric and vacuum columns.

III. **Vapor Load Excursions** – Out-of-levelness of tray may invite vapor load variations across the tray with a consequent loss of efficiency

IV. **Liq Maldistribution** – Tray unlevelness may lead to maldistribution of liquid flowing across the weir. This occurs particularly when liq crest is low.

V. **Loss Efficiency** – Unlevelness may significantly affect the performance of trays operating at low liq rates and trays that have a low liq crest whereupon some loss of efficiency is resulted.

The factors that throw tray out of level are :

Tray Levelness Tolerance :

The highest tolerance that will not affect tray performance is always recommended. Tower costs mount as this tolerance diminishes.

Many designers recommended a tolerance of ± 3.2mm for most services. This is probably unnecessarily fine.

Since, the effect of unlevelness depend more on the tray-slope than on tray flatness, it is logical to specify diameter-dependent tolerance. Follow Ernest E. Ludwig's guidelines :

ColumnDia	Tray-Levelness Tolerance
< 900 mm	± 3.2 mm
900 – 1500 mm	± 4.75 mm
1500 mm	± 6.35 mm

For columns larger than 3000 mm dia, **a** ± 9.5 mm tolerance may be permitted.

• Vertical Alignment

The column initially is fixed in its foundation so that its axis may be within 25–50 mm from the vertical at the top. Closer alignment is of little value forasmuch as the tolerance on the straightness of the col-shell axis is often greater than the vertical alignment. In a column 36m tall and 3.6 m dia this renders the top trays to be upto 3 mm out of level.

• Tower of Pisa Effect

Col. foundations often settle somewhat unevenly on their substrate. This causes tray tilting.

• Tray Deflection

Tray deflection throws tray off the level. This tray deflection occurs under load and may also result from uneven corrosion of the tray deck.

• Wind Loading

Tower may get deflected under a high wind load. However, this effect is usually small and temporary.

• Thermal Expansion

If the column is uninsulated and one side of the column becomes hotter under the sun, there'll occur relative expansion of the hotter side with respect to the *'colder'* side. This can inflict tray tilting. For example, in a 30m col. such a thermal expansion can add up to 6mm of tilt to the top tray.

• Tray Drainage :

Weepholes are provided to drain a tray. Tray drainage is required to drain out residual liq trapped on trays (particularly bubblecap and valve trays) and at low point (such as sealpans, inlet-weir areas).

Weephole size range : 6 – 16mm

Avoid small holes if the service conditions is fouling or corrosive ones.

Ludwig recommends a hole area :

$$280 \text{ mm}^2 \text{ per m of tray area}$$

REFERENCES :

1. Koch Engineering Co. Wichita, Kansas, USA, *Koch Flexitray Design Manual (Bulletin No. 960).*
2. Mathew Van Winkle, *Distillation (McGraw-Hill Co., NY, 1967).*
3. Glitsch, Inc., Dallas., Texas, USA, *Bulletin No. 4900 (3rd ed).*
4. O. Frank, *Chemical Engineering (Mar. 14, 1977 p: 110).*
5. D. B McLaren and J. C Upchurch, *Chemical Engineering (Jun 1, 1970/p: 139).*
6. F. A Zenz, *Chemical Engineering (Nov. 13, 1972/ p: 120).*
7. E. Interess, *Chemical Engineering (Nov. 15, 1971/p: 167).*
8. H.Z Kister, *Chemical Engineering (Sept. 8, 1980/p: 119–123).*
9. A. Sewell, *Chemical Engineering (London) (NO. 299/300, 442/1975).*
10. C. J. D. Fell and W. V. Pinczewski, *Chemical Engineering (London) (No. 316/P:45/77).*

11. L. Friend *et. at.*, *Chemical Engineering (Oct. 31, 1960/P:101)*.
12. J. D. Chase, *Chemical Engineering (Jul 31, 1967/P:105 and Aug. 28, 1967/P:139)*.
13. D. S Arnold, *et. al.*, *Chemical Engineering Progress (vol. 48, 1952/P:633)*.
14. E. J Lemieux and L. J Scotti, *Chemical Engineering Progress (Mar 1969/P:52)*.
15. C. M Bosworth, *Chemical Engineering Progress (Sep. 1965/P:82)*.
16. Ernest E. Ludwig, *Applied Process Design for Chemical and Petrochemical Plants – vol. 2* (GULF PUBL., Houston, Texas, USA, 1964).

4A.7. MECHANICAL DESIGN OF BUBBLECAP TRAYS

Bubblecap trays have been extensively studied and as a consequence a number of design recommendations have been forwarded. However, the most complete and generally accepted one is that of W L Bolles presented in *Petroleum Processing*. (FEB' 56/Mar' 56/APR' 56/May' 56).

The trays and the bubblecaps fitted on it operate as an integrated system, *i.e.*, as a unit. Hence both must be considered in the design.

It is pertinent to note at this point that custom design bubblecap trays are seldom recommended now as in most cases they have proved to be uneconomical and in some cases unnecessary. This explains why designers prefer to adhere to standard tray layout and cap size.

Standardization of layouts, downcomer areas, weir lengths, cap sizes buy time in mechanical engineering design.

Design Objectives

Five point design objectives control the overall design of bubblecap trays :

I. **Capacity :** should be high for vapor and/or liquid rates. This means the smallest column dia for given thruput. High column capacity is also desirable to accommodate fluctuations in vap and liq loadings.

II. **Pressure drop :** should preferably be low to reduce temperature gradients between top and bottom of the column. High pressure drop is usually, but not always, associated with uneconomical design.

III. **Efficiency :** high tray efficiency is the primary design objective. The better the intimate gas-liq contact over a wide range of capacities the higher will be the tray performance and hence efficiency over this range.

IV. **Fabrication and Installation Costs :** should be as low as possible. That means mechanical design should be simple.

V. **Operating and Maintenance Costs :** mechanical design details should account for peculiarities of system fluids (coking, polymerization, suspended particles, immiscible fluids, corrosiveness) and accordingly keep adequate provision for drainage/cleaning (mechanical or chemical) to keep the daily costs of operation and downtime to a minimum.

1. GAS VELOCITY

Use Souders-Brown equation

$$G' = C[\rho_G \cdot \Delta\rho]^{1/2}$$

to calculate the maximum permissible mass velocity,

where,

G' = maximum permissible mass velocity thru bubblecap-tray column, $kg.h^{-1} \cdot m^{-2}$

C = factor related to entrainment. Determine it from **Fig. 4a.7.1.**
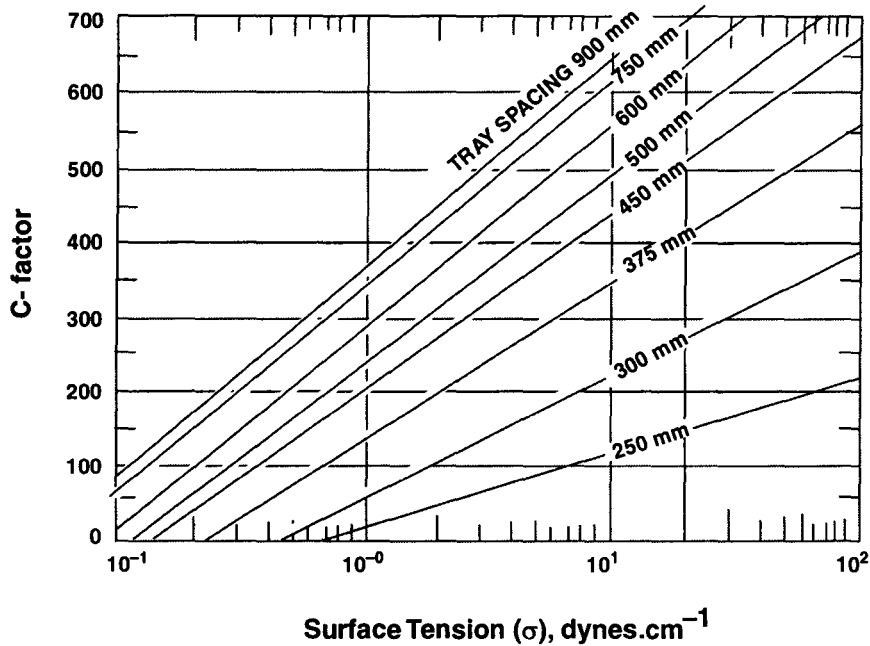
Fig. 4a.7-1. *C-factor for Bubblecap-Tray Column.*

ρ_G = gas (or vapor) density, $kg.m^{-3}$

$\Delta\rho = \rho_L - \rho_G$, density difference between liq and gas phases.

ρ_L = liq density, $kg.m^{-3}$

Determine **C-factor** at tower top and bottom. Get the average and then compute G'.

However, the gas mass rate obtained this way is the maximum allowable one and hence corresponds to minimum acceptable diameter for operation with essentially no entrainment carryover from plate to plate.

Hence, introduce a factor of safety of $1.10 - 1.25$, *i.e.*,

$$G' = \frac{1}{1.10 \text{ to } 1.25} G'_{max}$$

2. COLUMN DIA

The diameter is based on vapor flowrate, $\dot{G}$, in the region of greatest flow

$$D_T = \left| \frac{4}{\pi} \cdot \frac{\dot{G}}{G'_{DSGN}} \right|^{1/2} \qquad \text{DSGN : design}$$

Aliter :

Calculate gas velocity

$$v_G = C_F \left| \frac{\rho_L - \rho_G}{\rho_G} \right|^{1/2}, \text{m.s}^{-1}$$

where C_F = **capacity factor**. Its values are given in **Table 4A.7.1.**

Table 4A.7.1. Values of Capacity Factor, C_F

Tray spacing H, mm	Capacity Factor, $C_F \times 10^3$			
	$h_{ds} = 12\ mm$	$h_{ds} = 25\ mm$	$h_{ds} = 50\ mm$	$h_{ds} = 75\ mm$
150	6—12	—	—	—
300	27—34	21—27	15—21	—
450	46	43	37	27
600	56	52	49	46
750	60	56	55	53
900	63	60	58	56

Dynamic slot seal, $h_{ds} = h_{ss} + h_{ow} + \dfrac{1}{2} h_{hg}$

Dynamic slot seal, $h_{ds} = h_{ss} + h_{ow} + \dfrac{1}{2} h_{hg}$
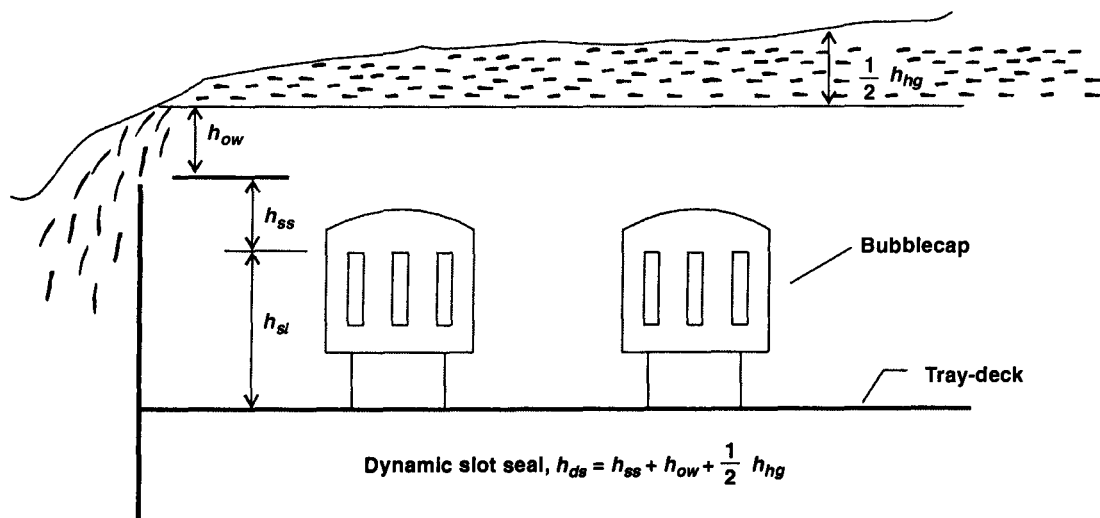
The velocity determined this way is the maximum permissible velocity, and should not be exceeded. Hence, somewhat lower gas velocity $0.80\ v_G$ — $0.65\ v_G$ is recommended leaving some safety margin.

Compute the column dia from

$$\frac{\pi}{4} D_T^2 = \frac{Q_{v,G}}{v_G|_{DSGN}}$$

3. TRAY TYPES

There are four basic tray types depending on the location of the overflow weirs, and hence the mode of liquid flow on the tray :

1. *Reverseflow*
2. *Crossflow*
3. *Double-pass*
4. *Cascade double-pass*

Fig. 4A.7.2.
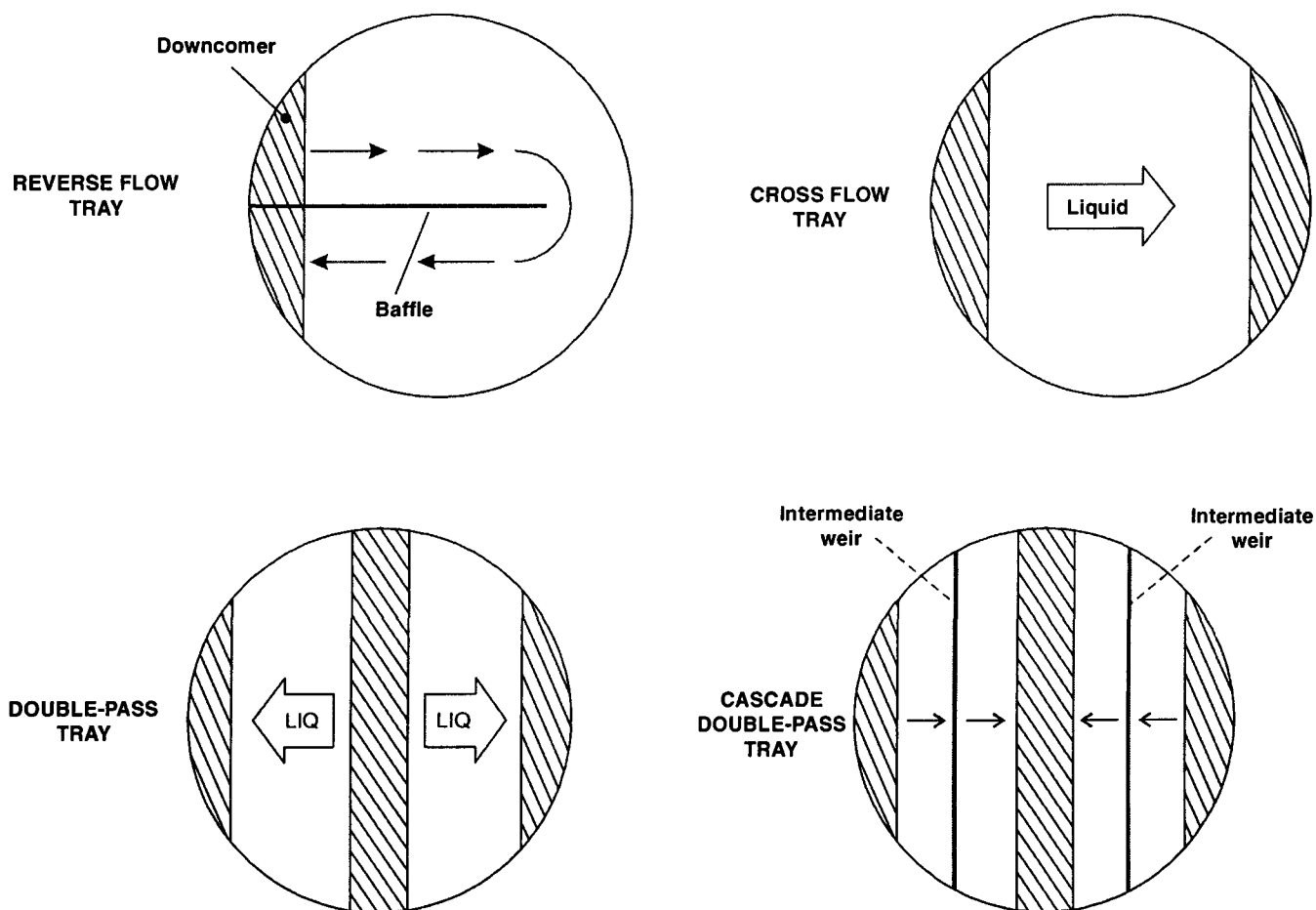
Fig. 4A.7.2. *Basic Tray Types.*

Reverseflow Tray : A center baffle divides this plate. The downcomers are all located on one side of the column.

The cross-section available for the liquid flow is small and the liquid path rather long. So this tray is recommended where liquid flows are small with respect to the vapor flows.

Crossflow Tray : The liquid traffics across the whole tray surface from inlet to the outlet

weir. It is the most common type of tray that operates at much higher liq load than the reverseflow tray.

Double-Pass Tray : When liquid load is high w.r.t. vapor, the double-pass tray is recommended. Such a tray has two inlets located on the edges of the tray, and one exit at the center. It provides short liquid path but large flow cross-section for liquid flow. Hence it provides more liquid capacity than the reverseflow or crossflow systems. Usually encountered in large dia towers.

Double-Pass Cascade Tray : The stepwise construction of the plate and the provision of intermediate weirs, the liquid gradient is diminished. For this reason the plate has exceptionally high liquid capacity.

A guide for tentative selection of the tray type for a given capacity is presented in **Table 4A.7.2.**

Table 4A.7.2. Guide for Tentative Selection of Tray Types.

Tower dia, D (mm)	Allowable flowrate of liquid, $m^3.h^{-1}$			
	Reverse-flow tray	Cross-flow tray	Double-pass tray	Cascade double-pass tray
900-1000	0–7	7–45	—	—
1200-1400	0–9	9–70	—	—
1800-2000	0–11	11–90	90–160	—
2400-2600	0–11	11–115	115–180	
3000-3400	0–11	11–115	115–205	205–320
3600-4000	0–11	11–115	115–230	230–360
4500-5000	0–11	11–115	115–250	250–410
6000-7000	0–11	11–115	115–250	250–455

BUBBLECAP LAYOUT

Make a 60° equilateral triangular layout of the caps on the plate with the liquid flowing into the apex of the triangle rather than parallel to the base, *i.e.*, liquid flowing normal to each row of caps.

CAP PITCH

Table 4A.7.3 Cap Pitch for Bubblecaps of Various Sizes.

Bubblecap Sizes	*Cap Lane*		
	Min.	*Max.*	*Recommended*
50 mm⎫ 75 mm⎬ 100 mm⎭	$\begin{bmatrix} 32\,mm \\ + \\ d_0 \end{bmatrix}$	$\begin{bmatrix} 44\,mm \\ + \\ d_0 \end{bmatrix}$	$\begin{bmatrix} 38\,mm \\ + \\ d_0 \end{bmatrix}$
150 mm⎫ 200 mm⎭	$\begin{bmatrix} 38\,mm \\ + \\ d_0 \end{bmatrix}$	$\begin{bmatrix} 64\,mm \\ + \\ d_0 \end{bmatrix}$	$\begin{bmatrix} 38\,mm \\ + \\ d_0 \end{bmatrix}$

where d_0 = cap OD

Inlet Weirs

These are installed to ensure uniform distribution of liquid as it enters the tray from the downcomer.

For dirty services, better avoid this gadget.

Set the 1st row of caps next to inlet weirs far enough to prevent gas stream bubbling into the downcomer. Also this can be prevented without inlet weirs provided a margin of 75 mm is kept between inlet downcomer and the nearest face of the 1st row of bubblecaps.

Height of inlet weir

$h_{w, in}$ = slot top height + 25 to 38 mm (see **Fig. 4A.7.3**)
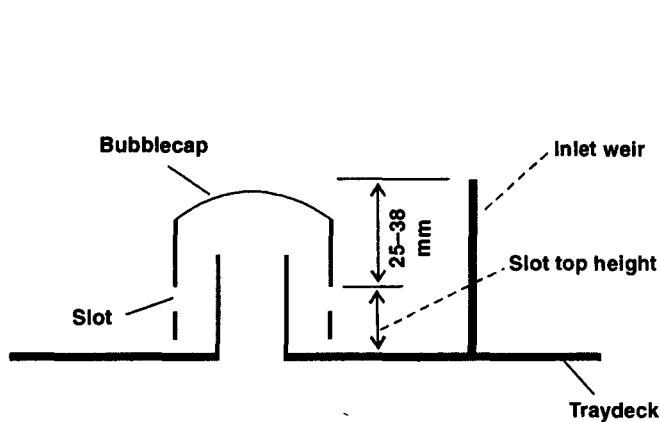
Fig. 4A.7.3. *Inlet weir height.*
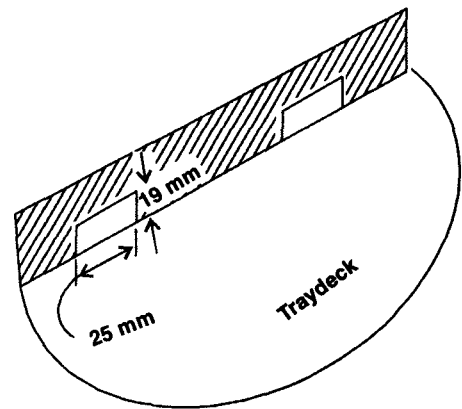
Fig. 4A.7-4. *A pair of small openings at inlet weir base is meant for tray flushing.*

Make provisions for tray flushing by providing two openings of 25 mm × 19mm (**Fig. 4A.7-4**) in the weir at its base.

Make a drainhole or weephole of 9.5 mm (minimum) size in the weir sealpot below the inlet downcomer. This is a measure to flush out any trapped sediment or other material.

Outlet Weir

These are necessary to maintain a liquid seal on the tray. It controls cap submergence, h_{ds} (*i.e.*, the vertical distance between slot top and the liquid level on the tray) insuring bubbling of gas/vap thru the liquid (**Fig. 4A.7-5**).

So the outlet weir height ($h_{w, out}$) should be so adjusted that a minimum submergence of 6 to 10 mm is maintained to avoid excessive bypassing of vapor thru void spots during surging.

The weir top must not be lower than top of the slots of the bubblecaps.
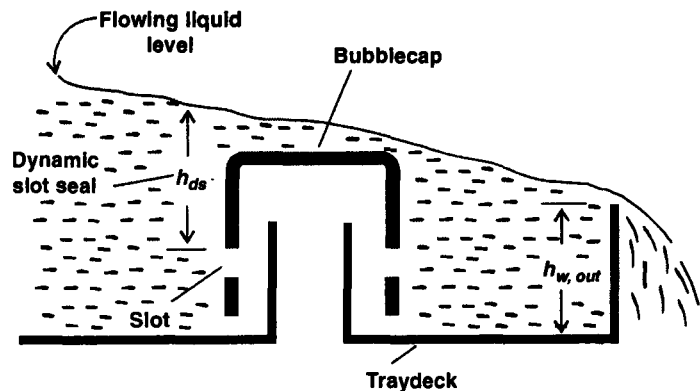
Fig. 4A.7.5. *Dynamic slot seal ensures a liquid gradient above the bubblecap and that insures gas/vapor bubbling thru the liquid.*

Downcomer

The downcomer must be sized to take care of the liquid loading plus the entrained foam and froth. This foamy material is disengagged in the downcomer whereupon only clear liq flows onto the tray below.

Erstwhile downflow pipes have been successfully replaced by segmental downcomers with the cross-section of a circular segment.

Prefer vertical and straight segmental downcomer. Segmental tapered design has also been used with some success; it gives better foam disengagement.

Refer to **Fig. 4A.7-6** to determine downcomer area and downcomer width.
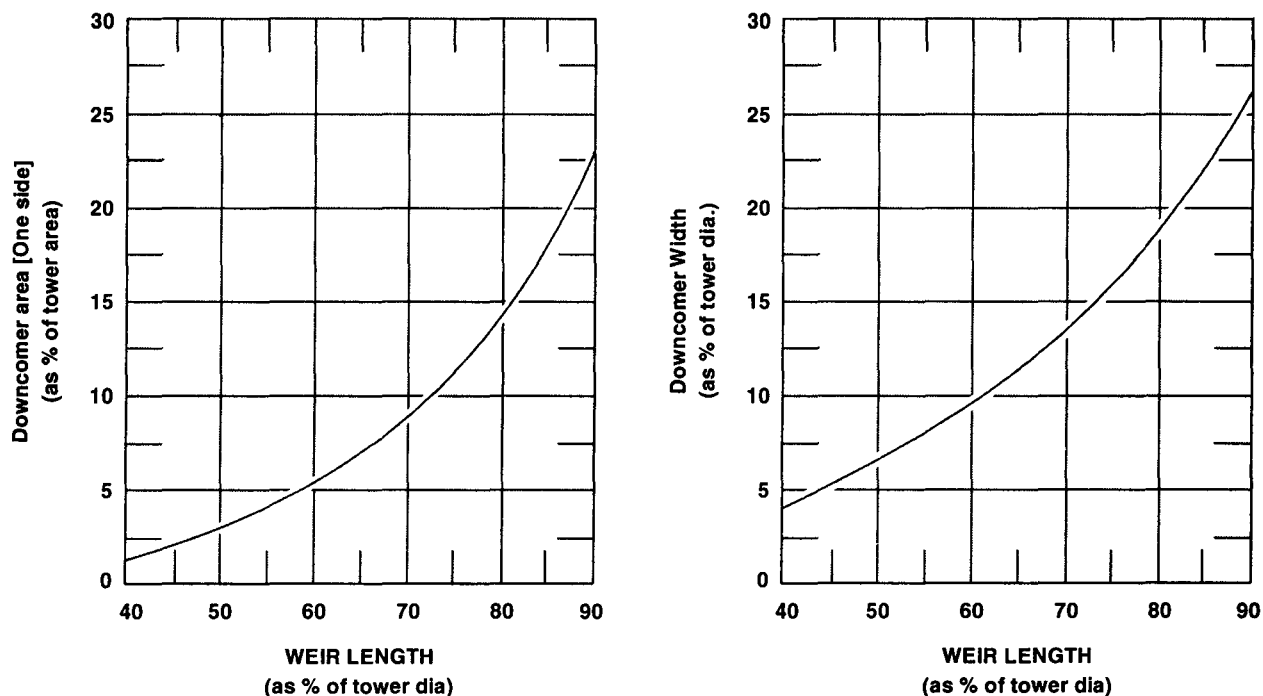
Fig. 4A.7.6. *Graphical Determination of Area & Width of Segmental Downcomer.*

Downcomer Seal

The downcomer seal is dictated by the liquid flowpath (see **Table 4A.7.4**)

Table 4A.7.4 Downcomer Seal

Liq Path*	DC Seal
< 1.5 m	13 mm
1.5 – 3 m	25 mm
> 3 m	38 mm

*Downcomer to outlet weir

Liquid bypass baffles

These are short stub baffles, also called redistribution baffles, that guide the liquid flowpath to prevent excessive liq bypassing of active area.

Location : All rows where endspace is 25 mm > cap spacing

Clearance to Caps : Same as cap spacing

Height : Twice the height of the clear liquid

Weepholes

These are provided for tray drainage, *i.e.*, to drain the liq holdup from the column when it is taken shutdown.

Each tray should be provided with enough drain holes (of 10 mm dia), so that a 2.5 cm^2 of area of the drainholes is apportioned for every square meter of tray. These holes are located in the deadspace of the tray.

W. L. Bolles recommended to provide *280 mm^2 of weepholes area per m^2 of net open liquid tray area in the tower*. This latter refers to the total of all trays in the tower.

Bottom Tray Sealpan

The bottom tray must have its downcomer sealed to prevent vapor traffic thru the downcomer. The downcomer of this tray is made equal to or 150 mm longer than other downcomers to insure against feed vapor surges.

4. BUBBLECAPS

Prefer round bell shaped bubblecaps. They are efficient units and hence often recommended. However, there are a great variants of bubblecaps which are in use in CPI and PCI.

Cap Dimensions

The most popular and perhaps the adaptable version is the round bell shaped bubblecap of 100 mm OD. The other two popular units are 75 mm caps (mostly used in smaller dia tower) and 150 mm caps (preferred in larger dia towers). Although it is not necessary to change the cap size with change in tower dia, the following table (**Table 4A.7.5**) may be used as a preliminary guide for the selection of bubblecaps.

Table 4A.7.5. Selection of Bubblecap on The Basis of Tower Dia.

Tower Dia (mm)	*Bubblecap Dia (mm)*
600–1200	75
1200–3000	100
3000–6000	150

SELECTION PROCESS

Consider the following factors in bubblecap selection :

1. For a given active area the cost of installation of 80 mm caps is 10–15% greater than the 100 mm caps while the cost of installing 150 mm units are 15% cheaper than 100 mm units.

2. There is less waste tray area with the 75 mm caps than with the 100 mm caps and it's more greater with 150 mm caps than 100 mm caps.

3. Evaluate tray performance first with 100 mm bubblecaps which are good general purpose units. If there are points of poor performance, re-evaluate the tray performance with the cap sizes to adjust in the direction of optimum performance.

4. Select pressed steel caps.

In the case of corrosive service conditions, select alloy pressed caps. They're light weight too.

Also cast iron caps may be used in services involving chlorinated hydrocarbons, conc. sulfuric acid etc.

Special caps of porcelain, glass and plastic may be selected for specific applications.

Note : With heavier caps of porcelain glass, please take care to make the trays more robust and that increases the overall weight of the column.

BUBBLECAP SLOTS

Slots are usually rectangular or trapezoidal in shape, either one giving good performance*.

There are triangular slots too but they exhibit narrower limits of capacity.

Slot Width ranges from 3 to 13 mm.

Recommended Size

3 mm × 6 mm—6 mm × 19 mm (Rectangular)

4.75 mm × 8 mm (Trapezoidal)

Slot Height : Recommended dimensions are

19 mm—47.5 mm   (Rectangular)

32 mm—38 mm   (Trapezoidal)

The essential dimensions of a bubblecap are presented in **Table 4A.7.6.**
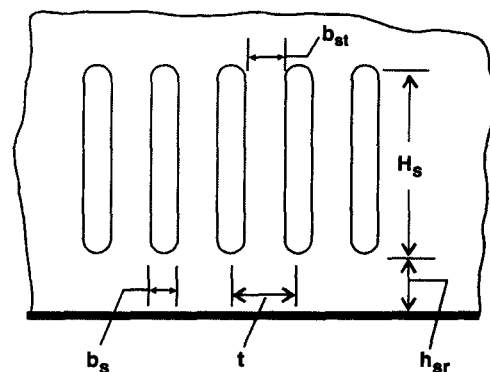
Table 4A.7.6. Dimensions of A Bubblecap

Outer dia of the cap (mm)	*Cap perimeter* πd *(mm)*	*No. of slots* n	*Slot width* b_s *(mm)*	*Slot spacing* b_{st} *(mm)*	*Height of the shroud* h_{sr} *(mm)*	*Pitch* t *(mm)*	*Thickness* s *(mm)*	*Slot height* H_s *(mm)*	*Slot area per cap* S_c *(mm)*
80	251	26	5	4.7	5	9.7	2	25	31
100	314	32	5	4.8	5	9.8	2	30	46.3
150	471	48	5	4.8	5	9.8	2	35	81.4

RISER DIA

The diameter of the riser should be selected so as to keep the ratio of **Annular Area : Riser Area** within 1.1 —1.4

---

* Bolles reported rectangular slots giving slightly greater capacity than the trapezoidal ones, while the trapezoidal slots give slightly better performance at low vapor loads.

RISER HEIGHT

The upper edge of the riser should be about 12.5 mm higher than the slot top **(Fig. 4A.7.7)**

REVERSAL AREA

It is the area between the top of the riser and the underface of the cap-roof. Keep it slightly greater than either the riser area or the annular area.

Fig. 4A.7.7. *Riser Height.*

SHROUD RING

This gives structural strength to the prongs or ends of the cap.

SKIRT CLEARANCE

13—25 mm for clean services

38 mm for dirty services

The face of the ring may rest directly on tray floor or it may have three short legs.
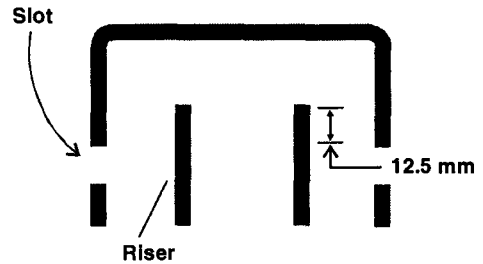
5. TRAY PERFORMANCE

A bubble cap tray must operate in dynamic balance closer to the optimum conditions to ensure better tray performance for a given capacity. And a mechanical interpretation of the relationship of tray components as they operate under a specified set of operating conditions is required to evaluate tray performance. This evaluation is based on the determination of :

1. Tray Pressure Drop

(*a*) slot opening, h_s

(*b*) static seal, h_{ss} and dynamic seal, h_{ds}

(*c*) liquid crest over the weir, h_{ow}

(*d*) liquid gradient across the tray, h_{hg}

2. Downcomer Conditions

(*a*) liq height in the downcomer, H_d

(*b*) liq residence time

(*c*) liq throw over weir into downcomer

3. Vapor Distribution
4. Entrainment
5. Tray Efficiency

TRAY PRESSURE DROP

(a) Slot Opening

The bubblecap is fully submerged in the liquid. With the increase of gas loading, the pressure under the cap increases, and the liquid is pressed down below the top of the slots whereupon the slots open for the gas flow. The vertical cap opening available for gas flow during operation of the cap under a given set of conditions is known as **Slot Opening, h_s**. It is independent of surface tension, viscosity and depth of liquid over the cap.

CAPS WITH RECTANGULAR SLOTS

For rectangular slots, the slot opening h_s may be estimated from the formula

$$h_s = 7.55 \left| \frac{\rho_G}{\Delta\rho} \right|^{\frac{1}{3}} \cdot H_s^{2/3} \cdot \left| \frac{Q_{v,G}}{A_s} \right|^{\frac{2}{3}} ,mm$$

where, h_s = slot opening, mm **(Fig. 4A.7.8)**

ρ_G = gas density, kg.m^{-3}

$\Delta\rho$ = $\rho_L - \rho_G$

ρ_L = liquid density, kg. m^{-3}

H_s = **Geometric slot height** (also called **full slot height**), mm

$Q_{v,G}$ = gas flowrate, m^3. s^{-1}

A_s = total slot area per tray, m^2

LEGEND

h_s = slot opening
H_s = full slot height
h_{ds} = dynamic slot seal
h_{ss} = static slot seal
h_l = height of clear liq on tray
h_{sc} = skirt clearance
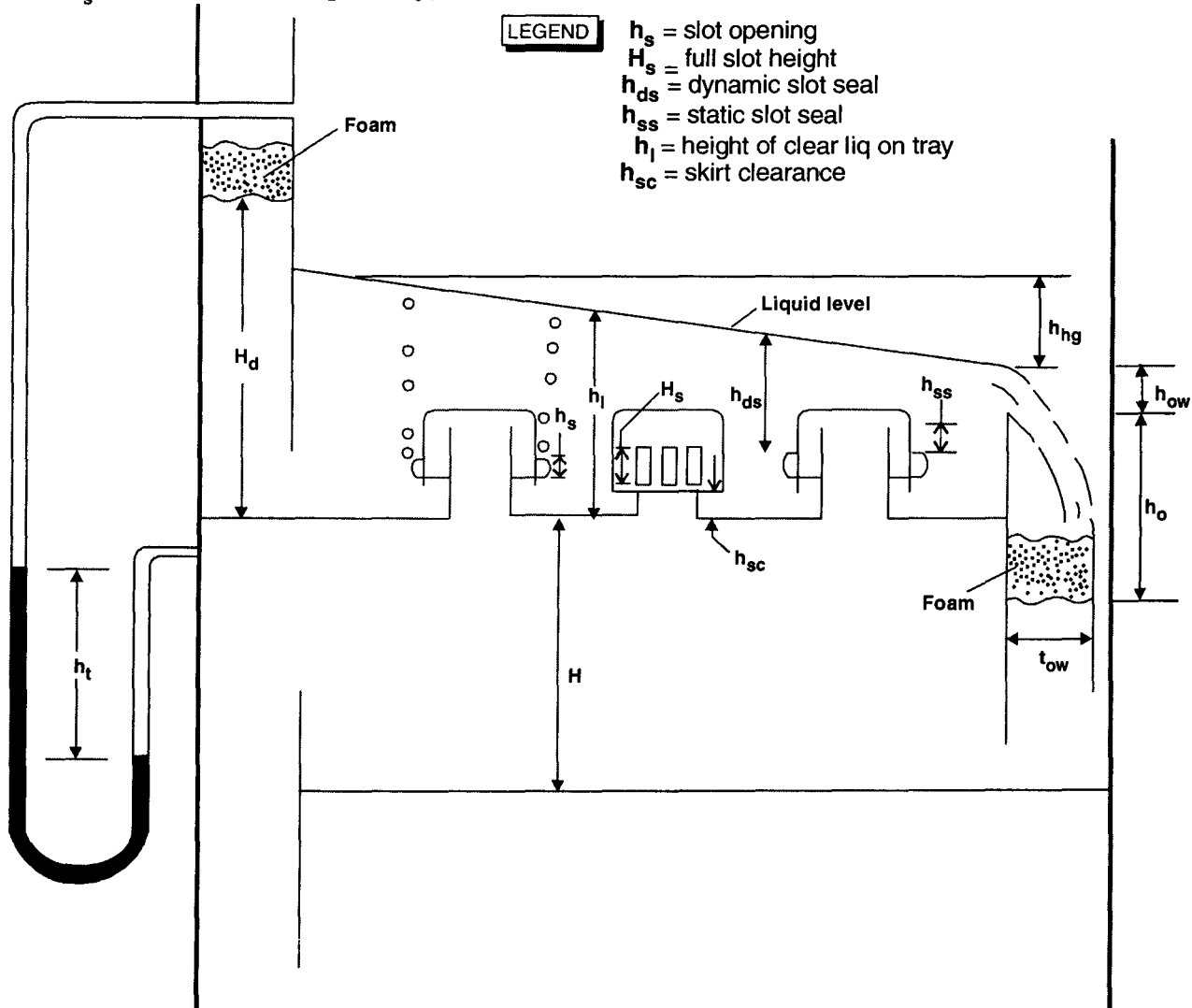
Fig. 4A.7.8. *Bubblecap tray hydraulics.*

Source : Mass Transfer and Absorbers—P.V.Danckwerts (ed.)

Also use can be made of Rogers-Thiele formula

$$h_s = 75597.53 \left|\frac{\rho_G}{\Delta p}\right|^{\frac{1}{3}} \cdot \left|\frac{Q_{v,G}}{N_c \cdot N_s \cdot W_s}\right|^{\frac{2}{3}}$$

where, N_c = number of caps per tray

N_s = number of slots per cap

W_s = slot width, mm

$Q_{v,G}$ = gas flowrate, $m^3 . s^{-1}$

Source : M.C.Rogers and E.W.Thiele, *Industrial and Engineering Chemistry (vol. 26, 1934/P:524).*

A quick estimation of the slot opening can be made from the **Chart (Fig. 4A.7.9).**
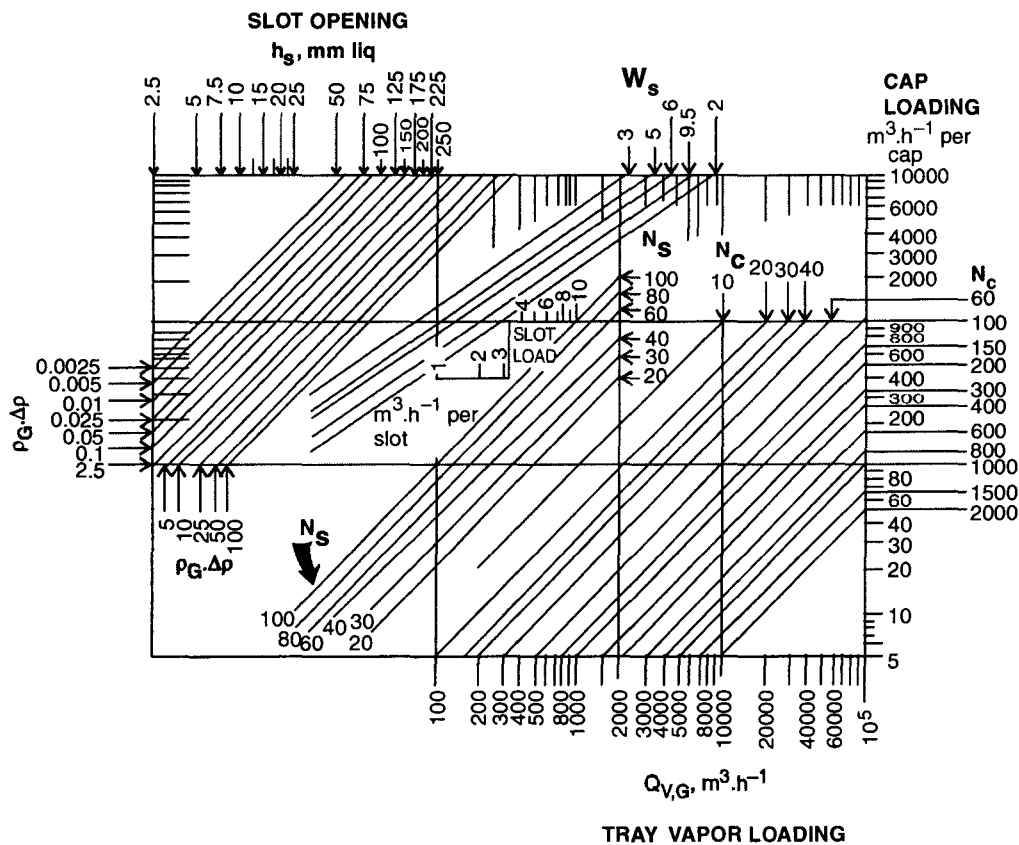
Fig. 4A.7.9. *Chart for estimating slot opening of rectangular slots for bell type bubblecap.*

Maximum slot capacity can be obtained from Bolles formula

$$Q_{v, G/max} = 4.777 \, A_s \left| H_s \cdot \frac{\Delta p}{\rho_G} \right|^{\frac{1}{2}}$$

where, $Q_{v, G/max}$ = maximum allowable gas load, $m^3.s^{-1}$

A_s = total slot area per tray, m^2

H_S = full slot-height, mm

Source : W.L.Bolles, *Petroleum Processing (Feb/Mar/Apr/May 1956).*

CAPS WITH TRAPEZOIDAL SLOTS

The maximum capacity at full slot opening is :

$$Q_{v, G/max} = 0.719\, A_s \left[\frac{2}{3}\left(\frac{R_s}{1+R_s}\right) + \frac{4}{15}\left(\frac{1-R_s}{1+R_s}\right)\right] \left| H_s \cdot \frac{\Delta\rho}{\rho_G}\right|^{\frac{1}{2}}$$

where, R_s = ratio of top to bottom widths of trapezoidal slots. It is also called **trapeziod shape factor.**

Fig. 4A.7.10. is a useful chart in solving slot height

R_s	SHAPE OF TRAPEZOID
0.00	Triangular
1.00	Rectangular
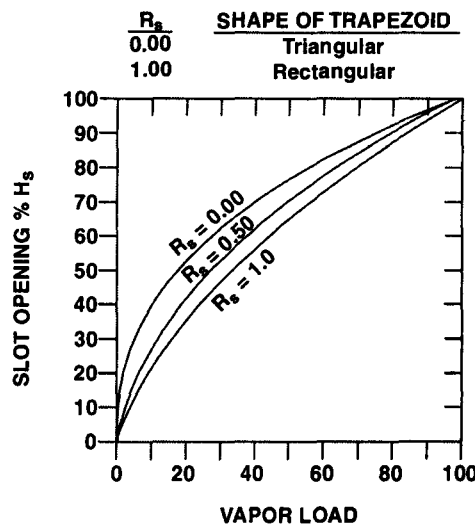
$$Q_{v, G/max} = 4.777\, A_s \left| H_s \cdot \frac{\Delta\rho}{\rho_G}\right|^{\frac{1}{2}}$$

R_s	C_s
0.00	0.63
0.50	0.74
1.00	0.79

Fig. 4A.7.10. *Generalized correlation for trapezoidal slot.*

Case – I When The Slot Is Opened Fully

This should be the case in a well-designed column whereupon the gas flows thru the whole slot.

Under this condition the equality

$$h_s = H_s$$

holds good.

Case – II Slight Overloading

With a slight overload the gas may escape under the edge of the cap.

Case – III. Low Gas Loading

With low load, h_s is too low with the effect that the bubblecaps are not being exploited well enough.

Note : It is recommended to design slots to remain 50 – 60% open during operation.

(b) Liquid Crest Over The Weir

Refer to **Fig. 4A.7.11**
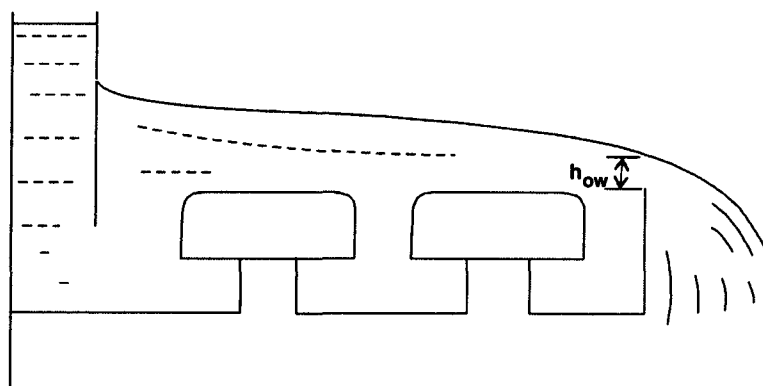
Fig. 4A.7.11.

As the liquid flows over the weir it develops some head, h_{ow}, called **liquid height over the weir.** The whole liquid surface on the tray rises due to it. This quantity can be expressed by the formula

$$h_{ow} = 2.84E \left| \frac{Q_{v,1}}{l_w} \right|^{\frac{2}{3}}, mm$$

where, $Q_{v,1}$ = liq rate, $m^3.h^{-1}$

l_w = length of weir, m

E = constriction coefficient.

Also,

$$E = f\left[\frac{Q_{v,1}}{l_w^{2.5}}, \frac{l_w}{D_T} \right] \text{ presented in } \textbf{Fig. 4A.7.12}$$

D_T = tower dia, m

(c) Liquid Gradient (h_{hg})

The difference in liquid height between the inlet and outlet sides of a tray is the **Liquid Gradient,** also called **Hydraulic Gradient,** h_{hg}. It occurs owing to the pressure drop of the liquid flow between the caps.

$$x = 0.226 \left[\frac{Q_{V,L}}{l_W} \right], \ m^3 h^{-1}.m^{-1} \ \Rightarrow$$

Liquid Loading on Tray
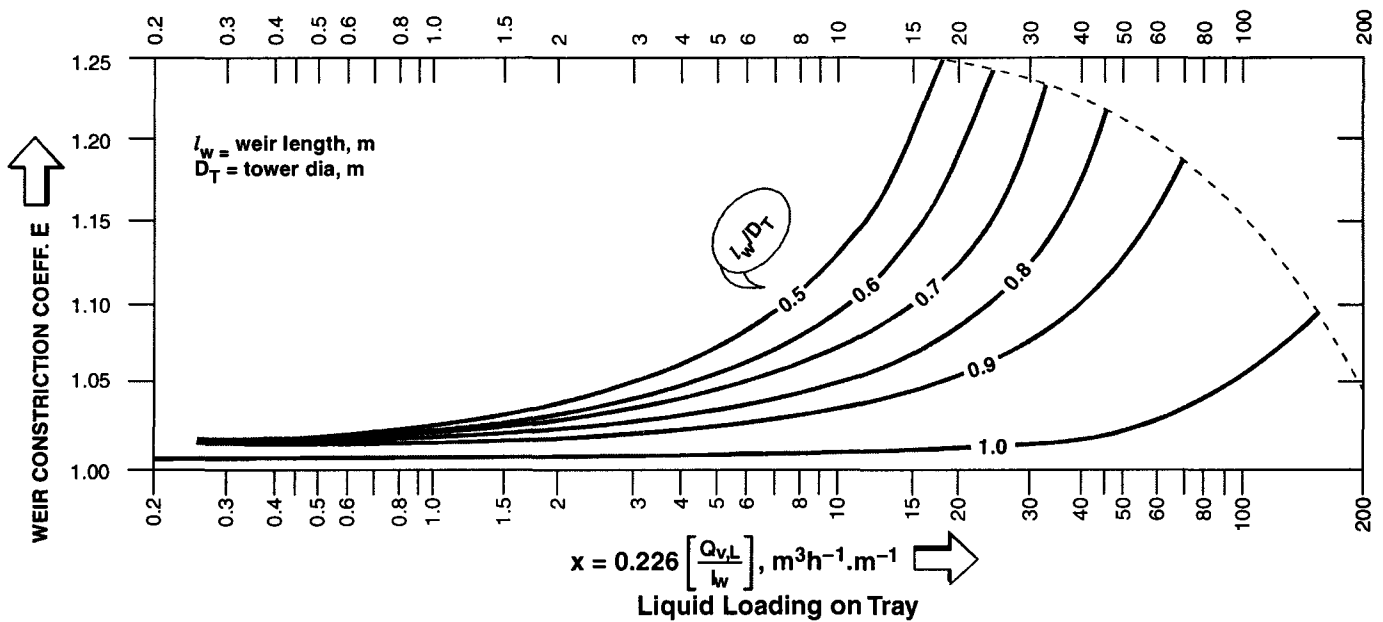
Fig. 4A.7.12. *Diagram for determining the constriction coefficient. The ratio of **weir length : tower dia** appears as curve parameter.*

Too high a liquid gradient is undesirable as it'll force all the gas stream pass thru the rows of caps nearer the tray outlet where the liquid head is lower *i.e.* the caps located close to the exit weir will get heavily loaded while those located at the entrance weir will not function at all. This means capacity reduction of the tray. That's how the liquid gradient is one of the criteria that must be checked to insure proper tray design and its efficient performance.

The hydraulic gradient is given by

$$h_l = h_w + h_{ow} + \frac{1}{2} h_{hg}$$

where h_l = height of clear liquid on tray, mm

h_w = weir height, mm

h_{ow} = height of crest over the weir, mm

h_{hg} = hydraulic gradient, mm

Some designers prefer to use $0.2h_{hg} - 0.33h_{hg}$ instead of $\frac{1}{2} h_{hg}$.

The data based on pratical experience suggest that for uniform gas distribution

$$h_{hg} \leq 0.5 \ (h_{fv} + h_s)$$

where, h_{fv} = press dr. due to friction and the changes of velocity as the gas traffics thru the cap, mm.

h_s = static pressure drop thru the slot

= slot opening, mm

Evaluate h_{hg} from

$$h_{hg} = C_G.h'_{hg}.n$$

where, n = number of rows of caps per tray encountered by the liquid

h'_{hg} = uncorrected hydraulic gradient per row of caps

C_G = gas load correction factor

Determine h'_{hg} from **Figures 4A.7.13, 4A.7.14, 4A.7.15 and 4A.7.16.**
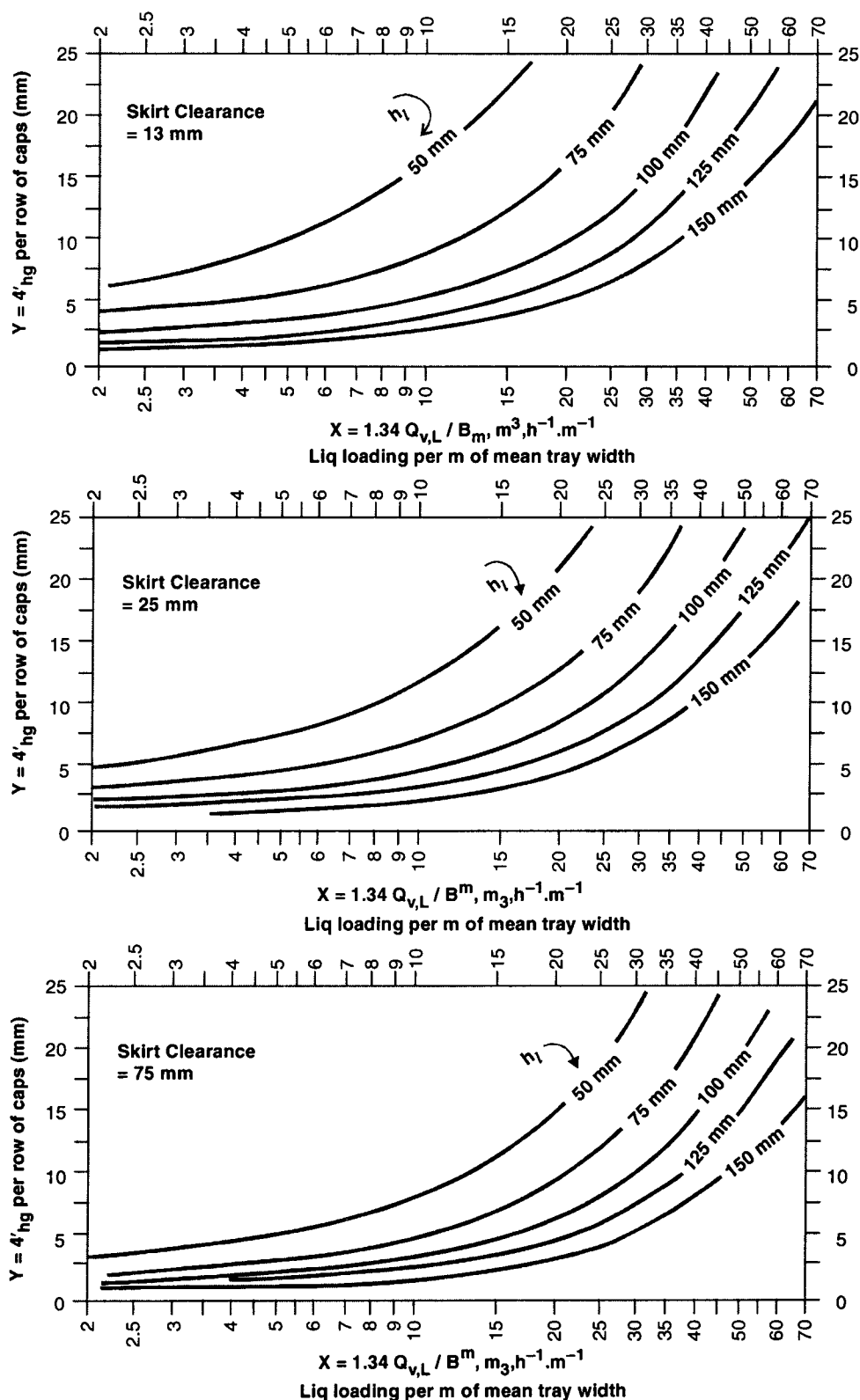
Fig. 4A.7.13. *Value of h'_{hg} for cap spacing = 25% cap dia.*
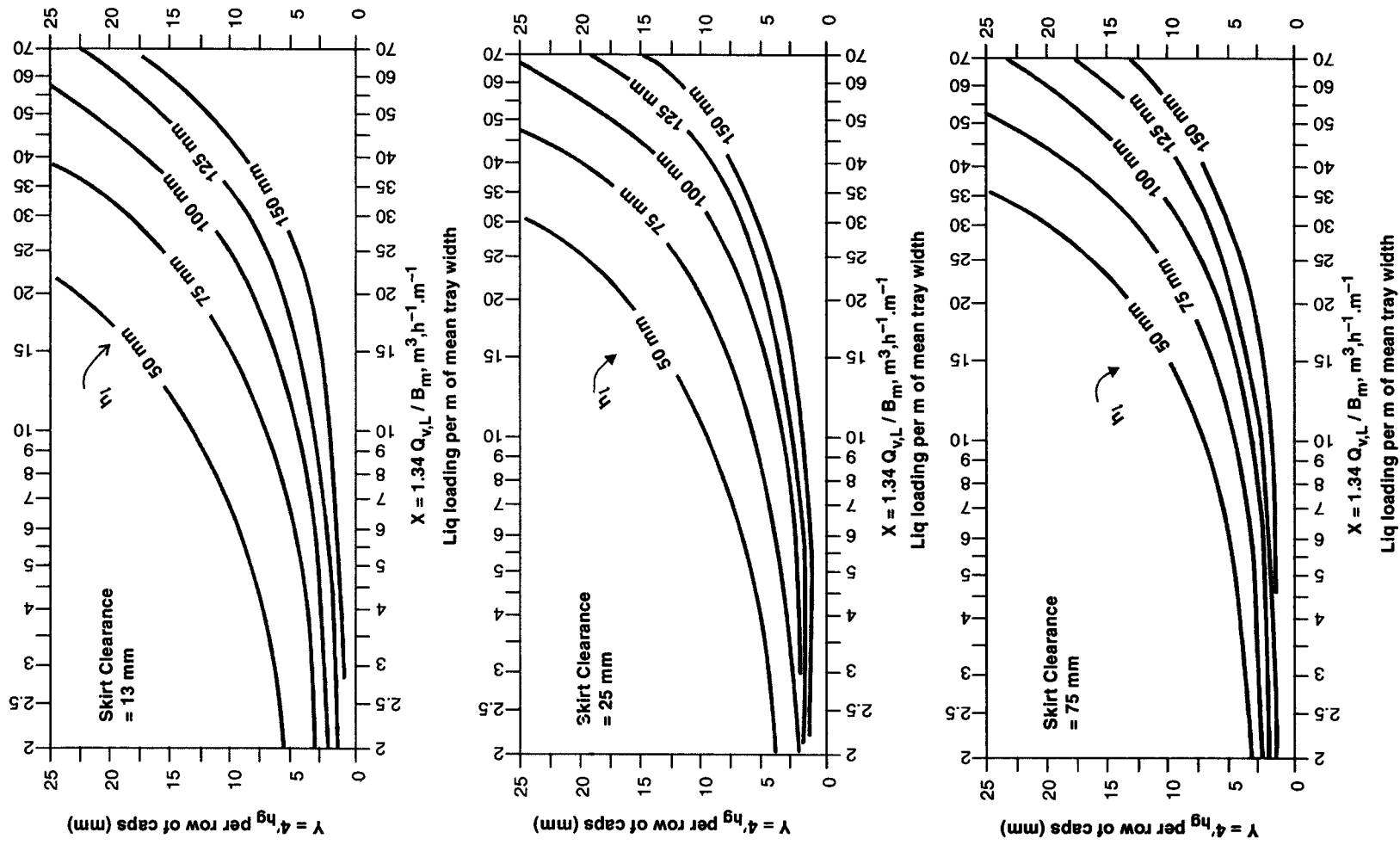
Fig. 4A.7.14. *Value of h'_{hg} for cap spacing = 31.25% cap dia.*
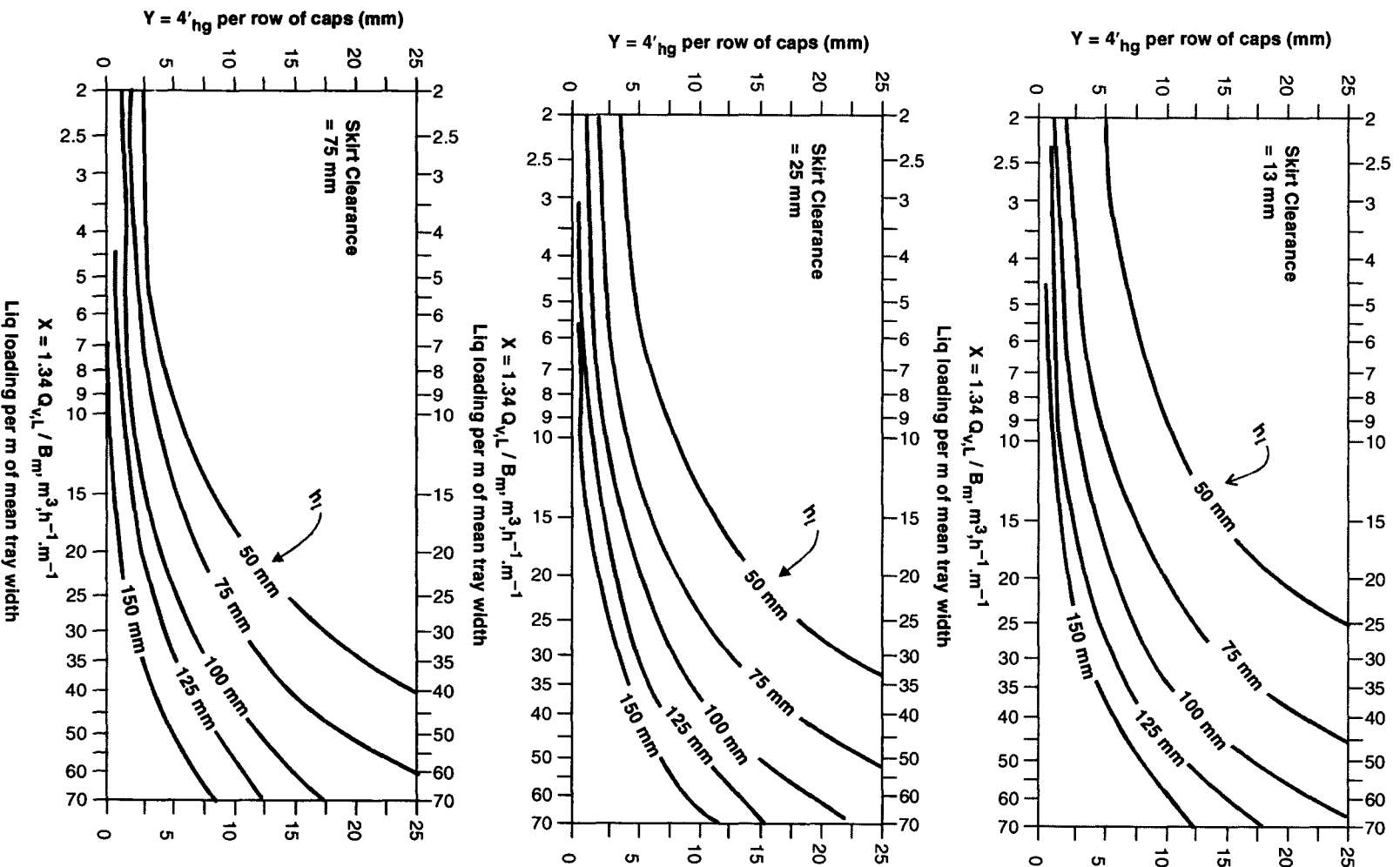
Fig. 4A.7.15. *Value of h_{hg}' for cap spacing = 37.25% cap dia.*
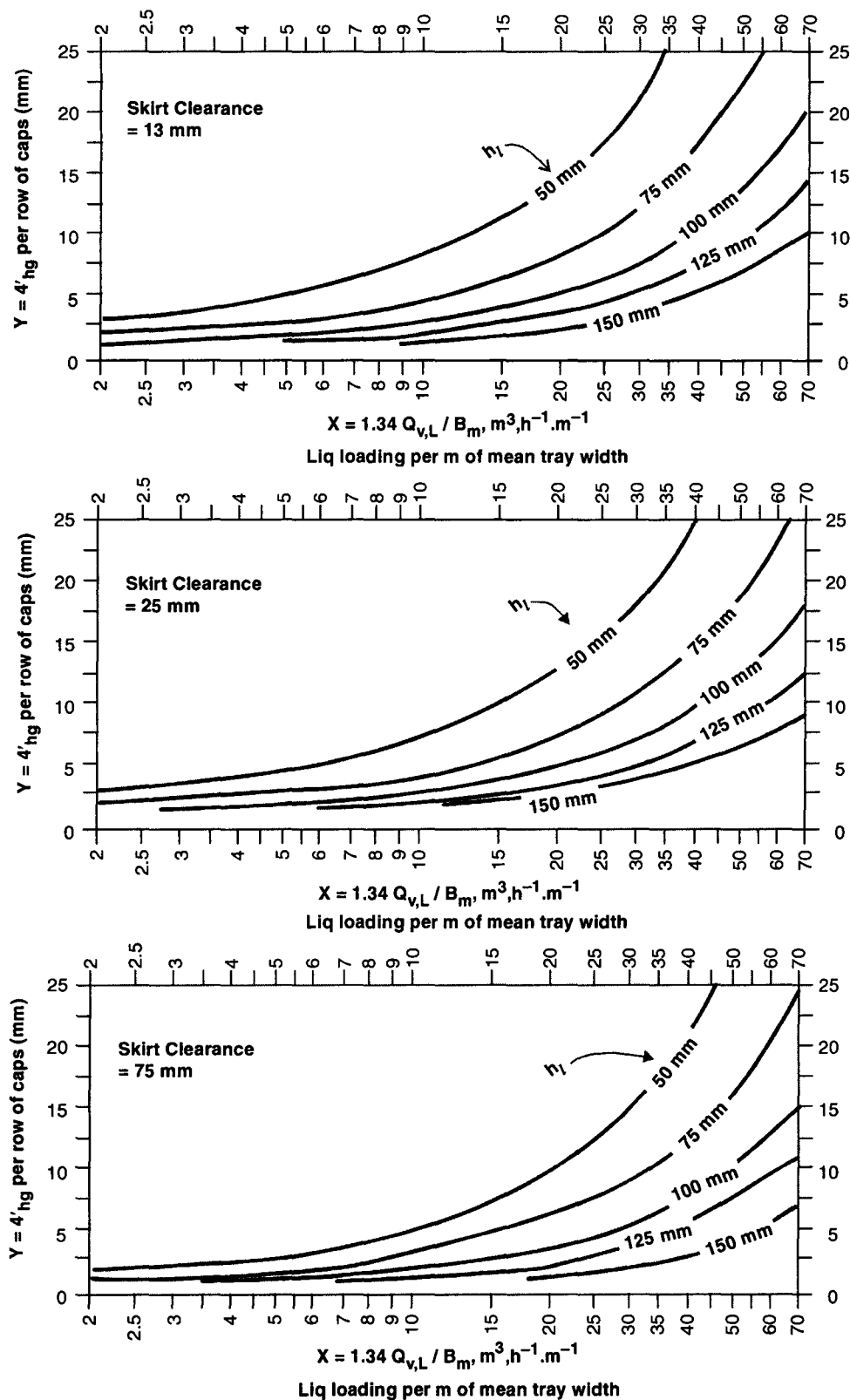
Fig. 4A.7.16. *Value of h'_{hg} for cap spacing = 50% cap dia.*

Determine the **Gas Load Correction** C_G from Fig. 4A.7.17.

$$C_G = \left[\frac{h_{hg}}{h'_{hg}}\right]$$
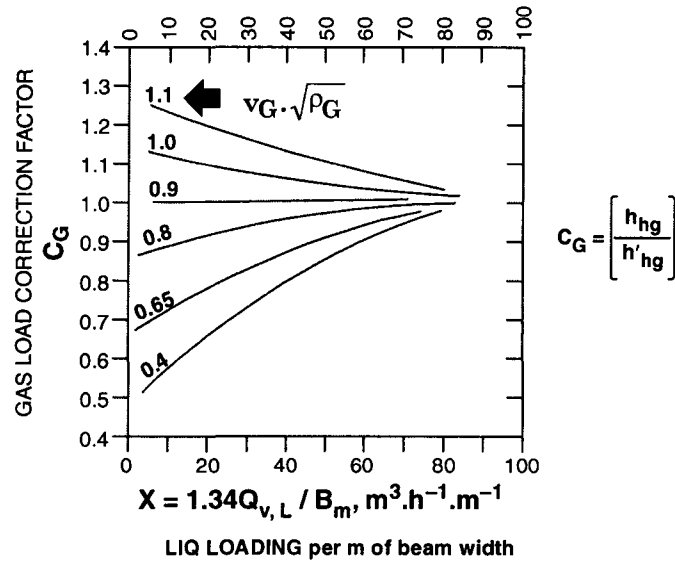
Fig. 4A.7.17. *Correction of liquid gradient for gas load.*

This method gives a conservative estimate of h_{hg} for average cases of bubblecap tray columns. Strictly speaking, it is not valid for towers with liquid overflowing the caps.

Calculated hydr. grad. in the range 12–25mm is usually considered acceptable for average cases. In case you find it exceeds 25mm, go for one of the following schemes to pull h_{hg} within above limits :

I. Raise cap. height, in inlet half of tower, by 25–50% of h_{hg} (calculated); but in no case it should exceed 25mm.

II. Slope the trays downward from liquid inlet to outlet so that

$$h_{hg} \not> \frac{1}{2} h_{hg} \text{ (calculated)}$$

(actual)

III. For large towers ($D_T > 2.5m$), check h_{hg} for sections of the tray normal to the liq flow. Adjust hydraulic gradient of each sections so that h_{hg} of individual sections does not exceed

$$\frac{1}{2}h_{hg} \text{ (calculated)}.$$

While you go for grad. adjustments, always keep in mind to ensure a fairly uniform head over the slots. Try to maintain average head over the cap slots for a section more or less equal to the average head over the adjacent section.

Total Gas Pressure Drop On One Tray

Compute the total pressure drop according to the formula

$$h_t = h_{fv} + h_s + h_{ss} + h_{ow} + \frac{1}{2} h_{hg} \text{ mm of liquid}$$

where, h_{fv} = riser press. dr. + reversal drop + annulus drop + slot press. drop

$$= 274 \; K_c \left| \frac{\rho_G}{\Delta \rho} \right| \left| \frac{Q_{v,G}}{A_r} \right|^{\frac{1}{2}}$$

A_r = total riser area per tray, mm^2

K_c = bubblecap press. dr. constant which is a **function of the ratio of annular area : riser area per cap.**

Determine its value from the **fig. 4A.7.18**
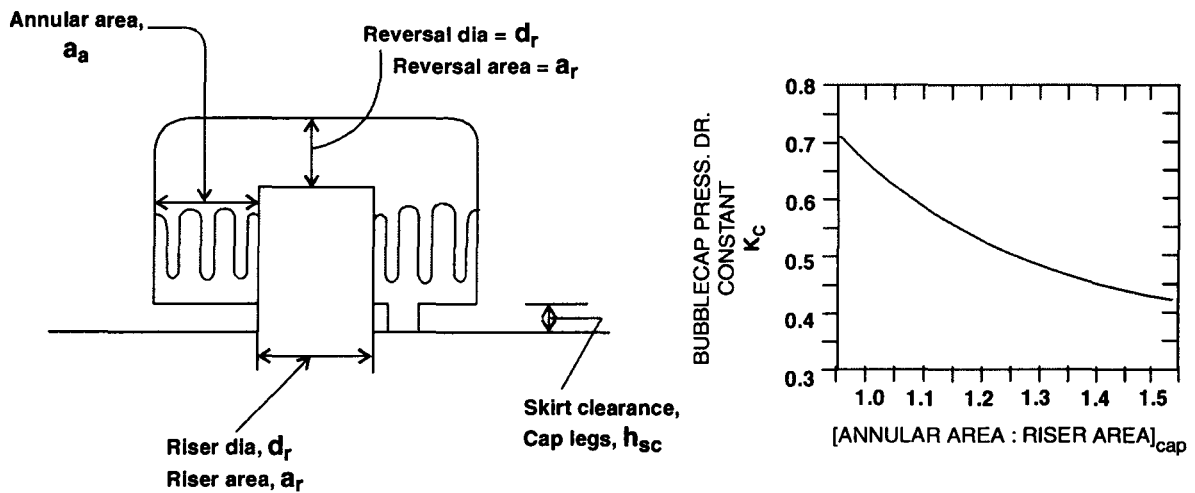
Fig. 4A.7.18. *Bubblecap Pressure Drop Constant.*

Downcomer Pressure Drop

(a) Height Of Clear Liq In the Downcomer

The **height of the clear liquid** (neglecting the presence of the foam) in the downcomer can be obtained from

$$H_d = h_w + h_{ow} + h_{hg} + h_d + h_t \; , \; mm \; of \; liq$$

where,

h_w = weir height, mm

h_{ow} = height of crest over the weir, mm

h_{hg} = hydraulic gradient, mm of liq

h_t = total tray press. dr., mm of liq

h_d = the liq head loss under the downcomer, mm liq

The quantity h_d can be obtained from the formula

$$h_d = 0.128 \left| \frac{Q_{v,L}}{100 \, A_d} \right|^2 \; , \; mm \; of \; liq$$

where, A_d = minimum area under the downcomer, m^2. It is usually the cross-section of the opening between the trayfloor and the edge of the vertical overflow baffle.

(b) Downcomer Seal

the bottom of the downcomer must be sealed below the operating liquid level on the tray. Refer to **Table 4A.7.7**

Table 4A.7.7. Downcomer Liquid Seal.

Tower Dia (mm)	*Downcomer Liquid Seal (mm)*
≤ 1.8	13
2 – 3.7	25
≥ 4	38

(c) Tray Spacing

Tray spacing is an important factor. It must be adequate for proper tray operation during normal as well as such abnormal conditions as surging, foaming and pulsing. And the **downcomer backup (H_d)** is needed to check whether the tray spacing is sufficient to ensure the flow.

Tray spacing is usually set at twice the liquid height in the downcomer :

$$l_t \geq 2H_d$$

for normal design

where, l_t = tray spacing, mm

The downcomer must provide adequate disengagement of foam / froth from clear liquid otherwise the foamy mass will back up the downcomer and reach the tray above. Hence tray spacing must be sufficient.

(d) Residence time In The Downcomer

The residence time in the downcomer is another criteria of adequate tray spacing. Because it gives reasonably adequate time for disengagement of foam and froth from the liquid in the downcomer. A minimum allowable residence time of **5s** is usually taken as an average.

Refer to **Table 4A.7.8** for suggested clear liq velocities in the downcomer.

Table 4A.7.8. Suggested Downcomer Velocities.

Tray Spacing (mm)	*Allowable Clear Liquid Velocities, $m.s^{-1}$*		
	High-Foaming System	*Medium-Foaming System*	*Low-Foaming System*
460	0.045–0.060	0.106–0.128	0.137–0.158
600	0.076–0.097	0.146–0.158	0.167–0.183
760	0.091–0.107	0.146–0.158	0.198–0.213

(e) Liquid Throw Over The Weir

It is useful to check whether the liquid overflowing the outlet weir on tray fails to cover the entire cross-section of the downcomer. Such a case might produce uneven liquid flow. Determine liq throw over the weir from

$$t_{ow} = 0.8 \sqrt{h_{ow} \cdot h_o}$$

and check t_{ow} should not exceed 60% of the width of the downcomer.

h_o = freefall distance

= $l_t + h_w - H_d$, mm

(f) Slot Seal

The **actual operating** or **dynamic slot seal** (h_{ds}) indicates the condition pertaining to the tray in operation

$$h_{ds} = h_{ss} + h_{ow} + \frac{1}{2}h_{hg}$$

This seal varies across the tray. But it is imperative to design the tray so as to render h_{ds} nearly the same for each row of caps.

The static slot seal (h_{ss}) is the fixed distance between the top of the outlet weir and top of the bubblecap slots.

GAS/VAPOR DISTRIBUTION

The bubblecap trays must be so designed as to insure uniformity of gas flow thru the caps thruout the entire range of operating conditions. It is indicated by the parameter **Vapor Distribution, R_v**,

$$R_v = h_{hg} / h_c$$

where h_c = head of liquid in the bubbling zone (i.e. wet-cap press. dr.), mm of clear liquid

Typical R_v values are :

R_v	
0. 4 and not exceeding 0. 6	(J.A. Davies)
0.5	(W.L. Bolles)

Only at values around **0.1** is essentially uniform vapor flow maintained thru all the caps.

As the **R_v** value increases, a smaller percentage of the gas / vapor flows thru the inlet tray caps and a larger percentage is shifted to the outlet caps. The crossflow of gas stream increases the effect of hydraulic gradient **(h_{hg})** on the tray and gives birth to dumping of liquid down the risers at the inlet row of caps. When **R_v** reaches the values equal to the cap drop at full slot opening.

Liquid Entrainment from Bubblecap Trays

Liq entrainment for design should be limited to **0.1 mol / mol dry gas (vap).**

Determine entrainment and its effect on tray spacing and efficiency as follows :

1. Assume acceptable level of entrainment to be 10%, *i.e.,* 0.1 mol of liquid entrained per mol of liq–free gas.

2. Using Colburn's correlation, determine the effect on efficiency.

3. Calculate total entrainment, **L_e**, kg. liq.h^{-1}.

4. Calculate tray area above caps. It is equal to

$$A_T - 2A_d$$

where **A_T** = tower cross-section

A_d = downcomer cross-section

5. Calculate liquid entrainment

$$W_e' = \frac{L_e}{A_T - 2A_d}, \frac{kg}{h.m^2}$$

6. Calculate gas velocity v_G' based on net tray area $(A_T - 2A_d)$.

7. Calculate density factor $\left|\frac{\rho_G}{\Delta\rho}\right|^{\frac{1}{2}}$

8. Calculate

$$v_G' \left|\frac{\rho_G}{\Delta\rho}\right|^{\frac{1}{2}}, m.s^{-1}$$
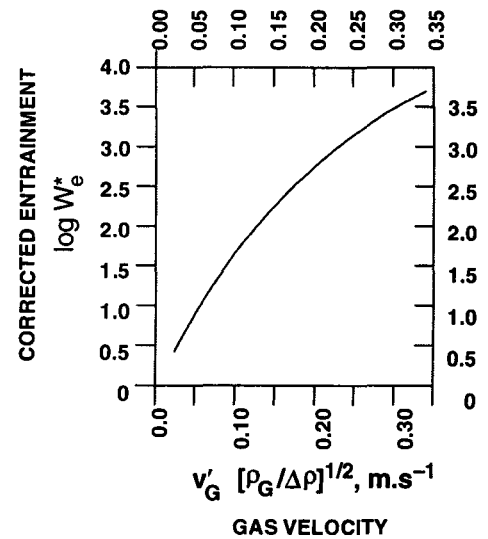
Fig. 4A.7.19. *Entrainment correlation.*

9. Determine W_e^* from **Fig. 4A.7.19**

10. Calculate corrected entrainment

$$\log_{10} W_e^* = \log_{10} W_e' + 2.59 \log_{10} S + \log_{10} \mu + 0.4 \log_{10} \sigma$$

where, W_e' = *corrected entrainment* (corrected for liq properties and plate spacing)

    S = clear height above the foam or froth, m

      = tray spacing minus foam height above the traydeck

    μ = viscosity of liq, Pa.s

    σ = surface tension of liq, $N.m^{-1}$

11. Adjust minimum tray spacing

$$l_t = h_f + S \times 1000, mm$$

where, h_f = **foam height** above traydeck, mm.

    $\simeq$ 2 × dynamic tray seal.

Bubblecap Column Design

Problem 4*2. Design a bubblecap tray column for following service :

- *Gas flowrate 12000 $m^3.h^{-1}$*
- *Liq rate 10$m^3.h^{-1}$*
- *Gas density 0.685 kg. m^{-3}*
- *Liq density 600 kg. m^{-3}*
- *Op. pressure 13.34 kPa*

Make a provision for 15% overload.

Cap Data

Total number of bubblecaps : 146

ID	*:100mm*
Spacing	*:140 mm*
Layout	*: equilateral triangular*
Slots	*: rectangular*
Total height	*: 100 mm*
Slot height, H_s	*: 30 mm*
Total slot area per tray, A_s	*: 0.5289 m^2*
Length of the weir, l_w	*: 935 mm*
Width of the segmental downcomer	*: 7% D_T*
Area of segmental downcomer	*: 4% A_T*
Skirt clearance, h_{sc}	*: 25 mm*
Height of the shroud ring, h_{sr}	*: 5 mm*
(distance between the slot and the lower edge of the cap)	
Mean liq depth on tray, h_l	*: 85 mm*
Number of rows of caps per tray	*: 11*
Riser cross-section per cap, a_r	*: 3840 mm^2*
Annular cross-section per cap, a_a	*: 3310 mm^2*

Solution : Tray hydraulics should take into account 15% overload.

Step – (I) Gas Rate

Normal gas flowrate = 12000 m³.h⁻¹

$$\text{Design gas flowrate} = \frac{12000}{3600}\left|\frac{m^3.h^{-1}}{s.h^{-1}}\right| \times 115\%$$

$$= 3.8333 \ m^{3\cdot}h^{-1}$$

Step – (II) Liq Rate

Normal liq rate   = 10 m³.h⁻¹

Design liq rate   = 10 $\left|m^3.h^{-1}\right|$ × 115%

= 11.5 m³.h⁻¹

Step – (III) Superficial Gas Velocity

Assume a tray spacing = 600 mm

Dynamic slot seal   = 25 mm (say)

$$v_G = C_F \left|\frac{\Delta\rho}{\rho}\right|^{\frac{1}{2}}$$

$C_F = 0.052$ [Table 4A.7.1]

$$\therefore \qquad\qquad v_G = 0.052 \left|\frac{600 - 0.685}{0.685}\right|^{\frac{1}{2}}$$

$$= 1.538 \text{ m. s}^{-1}$$

Step – (IV) Column Dia

$$v_{G, DSGN} = 0.8 \, v_G$$

$$= 0.8 \, (1.538 \text{ m. s}^{-1})$$

$$= 1.230 \text{ m.s}^{-1}$$

$$Q_{v, G} = 3.8333 \text{ m}^3. \text{ s}^{-1}$$

$$\therefore \qquad \frac{\pi}{4} D_T^2 = \frac{3.8333}{1.230} \left| \frac{\text{m}^3.\text{s}^{-1}}{\text{m.s}^{-1}} \right|$$

$$\therefore D_T = 1.9916 \text{ m and after rounding off, tower dia}$$

$$D_T = 2000 \text{ mm}$$

Note : According to **Table 4A.7.2** the operating liquid load of a bubblecap crossflow tray of 2m dia should lie in the range 11 – 90 m³. s⁻¹.

Per this Table, our liquid load is rather low.

Step – (V) Slot Opening (h_s)

$$h_s = 7.55 \left| \frac{\rho_G}{\Delta\rho} \right|^{\frac{1}{3}} . H_s^{\frac{2}{3}} . \left| \frac{Q_{v,G}}{A_s} \right|^{\frac{2}{3}}$$

$$\rho_G = 0.685 \text{ kg. m}^{-3}$$

$$\Delta\rho = 600 - 0.685$$

$$= 599.315 \text{ kg. m}^{-3}$$

$$H_s = 30 \text{ mm}$$

$$A_s = 0.5289 \text{ m}^2$$

$$h_s = 7.55 \left| \frac{0.685}{599.315} \right|^{\frac{1}{3}} . (30)^{\frac{2}{3}} . \left| \frac{3.8333}{0.5289} \right|^{\frac{2}{3}}$$

$$= 28.5433 \text{ mm}$$

Check : $h_s / H_s = 28.54 / 30 = 0.9514$ *i.e.* 95% of full slot height will be available and that is quite satisfactory.

Step – (VI) Liq Crest Over The Weir (h_{ow})

$$h_{ow} = 2.84 \, E \left| \frac{Q_{v,L}}{l_w^{2.5}} \right|^{\frac{2}{3}}$$

$$Q_{v, L} = 11.5 \text{ m}^3.\text{h}^{-1}$$

$$l_w = 0.935 \text{ m}$$

$$x = 0.226 \left| \frac{Q_{v,L}}{l_w^{2.5}} \right|$$

$$= 0.226 \left| \frac{11.5}{(0.935)^{2.5}} \right|$$

$$= 3.074$$

$$l_w / D_T = 0.935 / 2$$

$$= 0.465$$

for $x = 3.074$ and $l_w / D_T = 0.465$ we get from **Fig. 4A.7.12**

$$E \simeq 1.06$$

$$\therefore \qquad h_{ow} = 2.84 \, (1.07) \left| \frac{11.5}{0.935} \right|^{\frac{2}{3}}$$

$$= 16.19 \text{ mm} \simeq 16 \text{ mm}$$

Step – (VII) Mean Tray Width, B

Width of the segmental downcomer $= 7\% \, D_T$

Area of the segmental downcomer $\quad = 4\% \, D_T$

Distance between the segmental downcomers

$$l = D_T - 2 \times \textbf{Width of the segmental downcomer}$$

$$= D_T - 2 \times 7\% \, D_T$$

$$= 0.86 \, D_T$$

Tray area contained between the segments

$$A = A_T - 2 \, (4\% \, A_T)$$

$$= \frac{\pi}{4} D_T^2 - 8\% \left(\frac{\pi}{4} D_T^2 \right)$$

$$= 0.92 \left[\frac{\pi}{4} \cdot D_T^2 \right]$$

$$B = \frac{A}{l}$$

$$= \frac{0.92 \left| \frac{\pi}{4} D_T^2 \right|}{0.86 \, D_T}$$

$$= 0.84 \, D_T$$

$$= 0.84 \, (2000 \text{ mm})$$

$$= 1680 \text{ mm}$$

$$= 1.68 \text{ m}$$

Step – (VIII) Hydraulic Gradient On Tray (h_{hg})

$$h_{hg} = C_G \cdot h'_{hg} \cdot n$$

Gas load correction factor C_G is determined from **Fig. 4A.7.17.**
Liq load per **m** of mean tray width

$$\frac{Q_{v,L}}{B} = \frac{11.5 \, m^3 . h^{-1}}{1.68 \, m}$$

$$= 6.845 \, m^3 . \, h^{-1} \text{ per m of tray width}$$

Gas load

$$v_G \sqrt{\rho_G} = \frac{Q_{v,G}}{A_T} . \sqrt{\rho_G}$$

$$= \frac{3.8333 \left(m^3 . s^{-1} \right)}{\frac{\pi}{4} (2)^2 (m)^2} . \sqrt{0.685 \, kg . m^{-3}}$$

$$= 1.009 \, kg^{1/2} . \, m^{-1/2} . \, s^{-1}$$

Therefore, from the graph

$$C_G \simeq 0.86$$

h'_{hg} : Refer to **Fig. 4A.7.14**

For $\qquad \dfrac{Q_{v,L}}{B} = 6.84 \, m^3 . h^{-1}$ per **m** of tray width and

$$h_{sc} = 25 \, mm$$

and for the mean liq depth on tray, $h_l = 85 \, mm$

$$h'_{hg} \approx 0.94 \text{ mm per row of caps}$$

The number of rows, **n = 11**
Hence,

$$h_{hg} = 0.86 \, (0.94) \, (11)$$
$$= 8.89 \, mm \approx 9 \, mm$$

Check : Now let us check for the plate stability. For stable plate hydraulics

$$h_{hg} \leq \frac{1}{2} \left(h_{fv} + h_s \right)$$

Now, $\qquad\qquad h_{fv} = 274 \, K_c \left| \dfrac{\rho_G}{\Delta\rho} \right| . \left| \dfrac{Q_{v,G}}{A_r} \right|^2$, mm

$$h_s = \text{slot opening}$$
$$= 28.5 \, mm \qquad\qquad\qquad\qquad \textbf{(Step - V)}$$

$\boxed{\text{K}_\text{c}}$ Determine the ratio of

    annular area per cap to riser area per cap

i.e. $\text{a}_\text{a} : \text{a}_\text{r}$

From the given data

$$\text{a}_\text{a} : \text{a}_\text{r} \ :: 3310 \text{ mm}^2 : 3840 \text{ mm}^2$$
$$:: 0.8619$$

Refer to Fig. **4A.7.18.**

$$\text{K}_\text{c} \approx 0.67$$

Total number of caps   = 146

$$\text{Cap area per riser} = 3840 \times 10^{-6} \text{ m}^2$$

∴   Total riser area per tray $= 146 \, (3840 \times 10^{-6}) \text{ m}^2$

$$= 0.5606 \text{ m}^2$$

∴ $\text{h}_\text{fv} = 274 \, (0.67) \left| \dfrac{0.685}{600 - 0.685} \right| \left| \dfrac{3.8333}{0.5606} \right|^2$

$$= 9.809 \text{ mm}$$

∴ $\dfrac{1}{2} (\text{h}_\text{fv} + \text{h}_\text{s}) = \frac{1}{2} (9.8 + 28.5) \text{ mm}$

$$= 19.15 \text{ mm}$$

$$\text{h}_\text{hg} = 9 \text{ mm (calculated)}$$

∴ $\text{h}_\text{hg} < \dfrac{1}{2} (\text{h}_\text{fv} + \text{h}_\text{s})$

Hence the hydrodynamic stability of the plate is assured.

Step – (IX) Weir Height (h_w)

Since,

$$\text{h}_\text{l} = \text{h}_\text{w} + \text{h}_\text{ow} + \dfrac{1}{2} \text{h}_\text{hg}$$

$$\text{h}_\text{l} = 85 \text{ mm} \qquad\qquad\qquad \textbf{(given)}$$
$$\text{h}_\text{ow} = 16 \text{ mm} \qquad\qquad\qquad \textbf{(Step – VI)}$$
$$\text{h}_\text{hg} = 9 \text{ mm} \qquad\qquad\qquad \textbf{(Step – VIII)}$$

∴ $\text{h}_\text{w} = 85 - 16 - \frac{1}{2} \, (9)$

$$= 64.5 \text{ mm} \simeq 65 \text{ mm}$$

Step – (X) Total Gas Pressure Drop (h_t)

$$\text{h}_\text{t} = \text{h}_\text{fv} + \text{h}_\text{s} + \text{h}_\text{ss} + \text{h}_\text{ow} + \dfrac{1}{2} \text{h}_\text{hg} \text{ mm of liq}$$

$$\text{h}_\text{fv} = 9.8 \qquad\qquad\qquad \textbf{(Step – VIII)}$$

$$h_s = 28.5 \text{ mm} \qquad \text{(Step – V)}$$

$$h_{ss} = h_w - (h_{sc} + h_{sr} + H_s)$$

$$= 65 - (25 + 5 + 30) \ = 5 \text{ mm}$$

$$h_{ow} = 16 \text{ mm} \qquad \text{(Step – VI)}$$

$$h_{hg} = 9 \text{ mm} \qquad \text{(Step – VIII)}$$

$$\therefore \qquad h_t = 9.8 + 28.5 + 5 + 16 + \tfrac{1}{2}(9)$$

$$= 63.8 \text{ mm}$$

Step – (XI) Height of Clear Liquid in The Downcomer

$$H_d = h_w + h_{ow} + h_{hg} + h_d + h_t , \text{ mm of liq}$$

$$h_w = 65 \text{ mm} \qquad \text{(Step – IX)}$$

$$h_{ow} = 16 \text{ mm} \qquad \text{(Step – VI)}$$

$$h_{hg} = 9 \text{ mm}$$

$$h_d = \text{liq head loss under the downcomer}$$

$$= 0.128 \left| \frac{Q_{v,L}}{100 \, A_d} \right|^2 , \text{ mm}$$

The inlet downcomer liq seal= 25 mm for tower dia 2m **(see Table 4A.7.7)**

Thus the lower edge of the inlet downcomer will be 25 mm below the upper edge of the weir. Hence the distance between the lower edge of the inlet downcomer and the traydeck will be

$$= 65 - 25$$

$$= 40 \text{ mm}$$

Now, $\qquad l_w = 935 \text{ mm} \qquad \text{(Given)}$

$$\therefore \qquad A_d = 0.040 \times 0.935 \text{ m}^2$$

$$= 0.0374 \text{ m}^2$$

$$\therefore \qquad h_d = 0.128 \left| \frac{11.5}{100 \times 0.0374} \right|^2$$

$$= 1.21 \text{ mm}$$

$$H_d = 65 + 16 + 9 + 1.21 + 63.8$$

$$= 155.010 \text{ mm}$$

$$\simeq 155 \text{ mm}$$

Check

$$H_d = 155 \text{ mm} < \tfrac{1}{2} l_t \ (= 300 \text{ mm})$$

Hence our design is satisfactory.

Step – (XII) Liquid Throw Over The Weir (t_{ow})

$$t_{ow} = 0.8 \sqrt{h_{ow} \cdot h_o}$$

$$h_o = l_t + h_w - H_d, \text{ mm}$$

$$l_t = 600 \text{ mm}$$

$$h_w = 65 \text{ mm} \qquad \qquad \text{(Step - IX)}$$

$$H_d = 155 \text{ mm} \qquad \qquad \text{(Step - XI)}$$

$$\therefore \qquad h_o = 600 + 65 - 155$$

$$= 510 \text{ mm}$$

$$h_{ow} = 16 \text{ mm} \qquad \qquad \text{(Step - VI)}$$

$$\therefore \qquad t_{ow} = 0.8 \ \sqrt{(510)(16)}$$

$$= 72.26 \text{ mm} \approx 72 \text{ mm}$$

Check

Width of the segmental downcomer, $w_{dc} = 7\% \ D_T$

$$= \frac{7}{100} \times 2000 \text{mm}$$

$$= 140 \text{ mm}$$

$$\frac{t_{ow}}{w_{dc}} = \frac{72 \text{mm}}{140 \text{mm}}$$

$$= 0.514 \qquad \qquad \text{which is smaller than the highest}$$

recommended value (0.60)

Step – (XIII) Vertical Dimensions of The Downcomer

$$A_d = 0.0374 \text{ m}^2$$

$$\therefore \qquad D_{dc} = 0.2182 \text{ m}$$

$$= 218 \text{ mm}$$
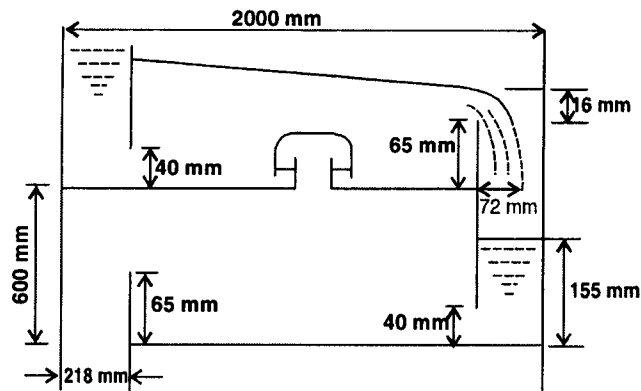
Design of A Bubblecap Stripping Column

Problem 4*3. A 1800 mm–ID stripping column fitted with 20 Nos. of crossflow bubblecap trays with following cap and tray data is to operate under following conditions :

	Tower Top	*Tower Bottom*
1. Operating pressure (kPa)	*10*	*13.34*
2. Operating temperature (K)	*300*	*350*
3. Vapor flow (kg. h⁻¹)	*2979*	*2979*
4. Vapor flow (m³. h⁻¹)	*13476*	*10704*
5. Vapor density (kg. m⁻³)	*0.2210*	*0.2779*
6. Liq rate (kg. h⁻¹)	*8620*	*8090*
7. Liq rate (m³. h⁻¹)	*10*	*10*
8. Liq density (kg. m⁻³)	*862*	*809*
9. Liq surface tension (dynes. cm⁻¹)	*9.5*	*12*

Cap data

Cap ID : 98 mm

Cap spacing : 140 mm

Cap layout : Δ 60° centers

Number of cap rows : 11

No. of caps per tray, N_c : 129

No. of slots per cap, N_s : 50

Cap height : 100 mm

Total slot height, H_s : 38 mm

Slot : rectangular

Slot width, w_s : 3 mm

Skirt clearance, h_{sc} : 25 mm

Height of the shroud ring, h_{sr} : 6 mm

Riser ID, d_r : 68 mm

Riser OD, $d_{r,o}$: 70 mm

Riser height above traydeck : 75 mm

Tray Data

Tray spacing, l_t : 600 mm

No. of downcomer per tray : 1

Downcomer location : end

Length of weir, l_w : 1200 mm

Weir height, h_w : 75 mm

Height of top of cap slots above traydeck : 50 mm

Static slot seal, h_{ss} : 13 mm

Height of the bottom of the downcomer above the traydeck : 70 mm

Area of segmental downcomer : 7.5% A_T

Downcomer Area between

- *downcomer and tower shell : 0.0823m²*
- *downcomer bottom and traydeck : 0.06596 m²*
- *downcomer and inlet weir : 0.06874 m²*

Riser slot seal : 25 mm

Evaluate the suitability of the trays for the operating conditions. Make modifications *if necessary.*

Solution : The suitability of the tray to accommodate the given operating conditions is to be determined on the basis of tray hydraulics.

Step – (I) Superficial Gas Velocity

$$v_G = Q_{v,\,G} / A_T$$

$$A_T = \frac{\pi}{4}(1.8)^2 = 2.54469 \text{ m}^2$$

	Top	Bottom
$Q_{v,\,G}$ (m³. h⁻¹)	13476	10704
A_T (m²)	2.54469	2.54469
v_G (m. s⁻¹)	1.471	1.1684

Step – (II) Superficial Gas Velocity Based on Active Tray Area

$$v_{G,\,active} = Q_{v,G}/A_{T,active}$$
$$A_{T,active} = A_T - 2\,(7.5\%A_T)$$
$$= 85\%\ A_T$$
$$= 0.85\,(2.54469)$$
$$= 2.1629 \text{ m}^2$$

		Top	Bottom
$Q_{v,\,G}$	(m³. h⁻¹)	13476	10704
$A_{T,\,active}$	(m²)	2.1629	2.1629
$v_{G,\,active}$	(m.s⁻¹)	1.730	1.3746

Step – (III) Superficial Gas Velocity Thru Slots

Slot height, $H_s = 38$ mm

Slot width, $w_s = 3$ mm

No. of slots per cap, $N_S = 50$

∴ Slot area per cap = 50 (3 mm) (38 mm)

$$= 5700 \text{ mm}^2$$

No. of caps per tray, $N_c = 129$

∴　　Total slot area per tray, $A_s = 129 \times 5700$ mm²

$$= 0.7353 \text{ m}^2$$

Superficial slot velocity, $v_o = Q_{v,G} / A_s$

	Top	**Bottom**
Q_v (m³. h⁻¹)	13476	10704
A_s (m²)	0.7353	0.7353
v_o (m.s⁻¹)	5.090	4.0437

Step – (IV) Height of Liquid Crest Over The Weir

$$h_{ow} = 2.84E \left| \frac{Q_{v,L}}{l_w} \right|^{\frac{2}{3}} , mm$$

$$l_w = 1200 \text{ mm}$$
$$= 1.2 \text{ m}$$
$$Q_{v,L} = \text{liq rate in m}^3. \text{ h}^{-1}$$
$$l_w : D_T = 1.2 : 1.8$$
$$= 0.666$$

$$x = 0.226 \left| \frac{Q_{v,L}}{l_w^{2.5}} \right|$$

	Top	**Bottom**
$Q_{v, L}$ (m³. h⁻¹)	10	10
x	1.432	1.432
E (Fig. 4A.7.11)	~ 1.02	~ 1.02
h_{ow}	11.9	12mm
	≈ 12 mm	

Step – (V) Hydraulic Gradient

$$\text{Mean tray width, } B = \frac{1}{2}(1.8 + 1.2) \text{ m}$$

$$= 1.5\text{m}$$

$$\frac{Q_{v,L}}{B} = \frac{10}{1.5} \frac{\text{m}^3.\text{h}^{-1}}{\text{m}}$$

$$= 6.666 \text{ m}^3.\text{h}^{-1} \text{ per m of tray width}$$

$$\text{Gas load} = v_G \sqrt{\rho_G}$$

$$h_{hg} = C_G \cdot h'_{hg} \cdot n$$

	Top	**Bottom**
v_G (m.s⁻¹)	1.471	1.1684
ρ_G (kg.m⁻³)	0.2210	0.2779
Gas load (kg¹ᐟ².m⁻¹ᐟ².s⁻¹)	0.6915	0.6159

Liq load (m³.h⁻¹ per m of tray width)	6.666	6.666
Mean liq depth on tray (mm)	85 (assumed)	85 (assumed)
h'_{hg} (Fig. 4A7.16), mm	0.625	0.625
n (No. of rows per tray)	11	11
C_G	~0.64	~0.56
h_{hg} (mm)	4.4	3.85
		≈ 4

Check

For hydrodynamic stability of tray, the following relationship

$$h_{hg} \leq 0.5 \, (h_{fv} + h_s)$$

must hold good.

h_s = static slot opening

$$= 7.55 \left|\frac{\rho_G}{\Delta\rho}\right|^{1/3} \cdot H_s^{2/3} \cdot \left|\frac{Q_{v,G}}{A_s}\right|^{2/3} \cdot mm$$

H_s = 38 mm

A_s = total slot area per tray = 0.7353 m²

	Top	Bottom
ρ_G (kg.m⁻³)	0.2210	0.2779
$\Delta\rho$ (kg.m⁻³)	861.779	808.722
H_s (mm)	38	38
$Q_{v,G}$ (m³.s⁻¹)	3.74333	2.97333
A_s (m²)	0.7353	0.7353
h_s (mm)	16	15

$$h_{fv} = 274 \, K_c \left|\frac{\rho_G}{\Delta\rho}\right| \cdot \left|\frac{Q_{v,G}}{A_r}\right|^2, mm$$

Riser area per cap, $a_r = \frac{\pi}{4}(d_r)^2$

$$= \frac{\pi}{4}(68)^2 \ mm^2$$

$$= 3631.68 \ mm^2$$

Total riser area per tray, $A_r = N_c \cdot a_r$

$$= 129 \, (3631.68) \ mm^2$$

$$= 0.46848 \text{ m}^2$$

Riser outside cross-sectional area, $a_{r,o} = \dfrac{\pi}{4}(d_{r,o})^2$

$$= \dfrac{\pi}{4}(70)^2 \text{ mm}^2$$

$$= 3848.451 \text{ mm}^2$$

Cap cross-sectional area, $a_r = \dfrac{\pi}{4} \cdot d_c^2$

$$= \dfrac{\pi}{4} \cdot (98)^2 \text{ mm}^2$$

$$= 7542.9639 \text{ mm}^2$$

Annular area per cap, $a_a = a_c - a_{r,o}$

$$= 7542.9639 - 3848.451 \text{ mm}^2$$

$$= 3694.5129 \text{ mm}^2$$

$\therefore$ $\qquad\qquad\qquad\qquad a_a : a_r :: 3694.5129 : 3631.68$

$$:: 1.017$$

$$K_c \simeq 0.66 \qquad\qquad\qquad \text{[Fig. 4A.7.18.]}$$

	Top	Bottom
$\rho_G/\Delta\rho$	0.0002564	0.0003436
$Q_{v,G}$ (m³.h⁻¹)	3.74333	2.97333
A_r (m²)	0.46848	0.46848
K_c	0.66	0.66
h_{fv} (mm)	2.96	2.50
$0.5\,(h_{fv} + h_s)$, mm	9.48	8.75
h_{hg}	$< 0.5\,(h_{fv} + h_s)$	$< 0.5\,(h_{fv} + h_s)$

This insures hydrodynamic stability of both top and bottom trays.

Step-(VI) Height of Clear Liquid on Tray (h_l)

$$h_l = h_w + h_{ow} + \frac{1}{2}\,h_{hg}$$

	Top	Bottom
h_w (mm)	75	75
h_{ow} (mm)	12	12
h_{hg} (mm)	4.4	4
h_l (mm)	89.2	89

Step - (VII) Total Gas Pressure Drop

$$h_t = h_{fv} + h_s + h_{ss} + h_{ow} + \frac{1}{2}h_{hg}$$

	Top	Bottom
h_{fv} (mm)	2.96	2.50
h_s (mm)	16	15
h_{ss} (mm)	13	13
h_{ow} (mm)	12	12
h_{hg} (mm)	4.4	4
h_t (mm)	46.16	44.50

Step - (VIII) Liq Head Loss Under the Downcomer

$$h_d = 0.128 \left| \frac{Q_{v,L}}{100 A_d} \right|^2 , \text{mm}$$

A_d = minimum area under the downcomer, m^2

$Q_{v,L}$ = 10 $m^3.h^{-1}$

$$A_d = \left(\frac{70}{1000} \, m \right) \left(\frac{1200}{1000} \, m \right) = 0.084 \, m^2.$$

$$h_d = 0.128 \left| \frac{10}{100 \times 0.084} \right|^2 = 0.181 \text{ mm} \simeq 0.2 \text{ mm}$$

Step - (IX) Height of Clear Liquid in the Downcomer

$$H_d = h_w + h_{ow} + h_{hg} + h_d + h_t , \text{mm}$$

	Top	Bottom
h_w (mm)	75	75
h_{ow} (mm)	12	12
h_{hg} (mm)	4.4	4
h_d (mm)	0.2	0.2
h_t (mm)	46.16	44.50
H_d (mm)	136.76	135.7

Check

$$\frac{1}{2} l_t = 300 \text{ mm}$$

$\therefore$
$$H_d < \frac{1}{2} l_t$$

Hence the tray spacing is satisfactory

Step - (X) Liq Throw Over the Weir (t_{ow})

$t_{ow} = 0.8 \sqrt{h_{ow} \cdot h_o}$

$h_o = l_t + h_w - H_d$, mm

l_t = 600 mm

h_w = 75 mm

	Top	*Bottom*
H_d (mm)	137.76	135.7
h_o (mm)	537.24	539.3
h_{ow} (mm)	12	12
t_{ow} (mm)	64.23	64.35
	$\simeq$ 64	$\simeq$ 64

Check

Width of the segmental downcomer

$$w_{dc} = 7\% \ D_T \ (\text{say})$$
$$= 0.07 \ (1800 \ \text{mm})$$
$$= 126 \ \text{mm}$$

Now,
$$\frac{t_{ow}}{w_{dc}} = \frac{64}{126} = 0.5079$$

which is smaller than the higher recommended value of t_{ow} = 60% of w_{dc}

4A.7.1. GENERAL GUIDELINE FOR BUBBLECAP TRAY DESIGN

Follow the following guidelines :

1. Tray

Select :

• cross flow tray for general use

• reverse flow tray for low **L/G ratio**

• double pass tray for high **L/G ratio** or larger towers

• double-pass, cascade tray for very high **L/G ratio** or very large towers.

• segmental downcomer

• vertical downflow baffle

2. Downcomer

Select :

• **segmental downcomer**

• **vertical downflow baffle**

• **Downcomer Length   Tray Type**

  $0.6D_T - 0.7D_T$ crossflow trays

  $0.5D_T - 0.6D_T$ double passtrays

• 200 – 300 mm of downcomer width for doublepass trays

3. WEIRS

Select :

- straight weirs for normal loads
- notched weirs for low loads

4. Bubble-Caps

Select :

- 80 mm OD bubblecaps for 600—1200mm dia towers
- 100 mm OD bubblecaps for 1200—3000mm dia towers
- 150 mm OD bubblecaps for 3000—6000mm dia towers

Bubble-Cap Size (OD) mm	No. of Slots (N_S)	Slot width (b_S) mm	Slot spacing (b_{St}) mm	Height of the Shroud Ring (h_{Sr}) mm	Slot Height (H_S) mm	Slot Pitch (t_S) mm	Slot Area per Cap (S_C) cm²
80	26	5	4.7	5	25	9.7	31.1
100	32	5	4.8	5	30	9.8	46.3
150	48	5	4.8	5	35	9.8	81.4

- equilateral triangular layout normal to flow
- cap spacing : 25 – 75 mm
- skirt height : 6 – 38 mm
- cap-to-towerwall clearance : 38 mm (minimum)
- cap-to-weir clearance : 75 mm (minimum)
- cap-to-downcomer clearance : 75 mm (minimum)
- removable fastening
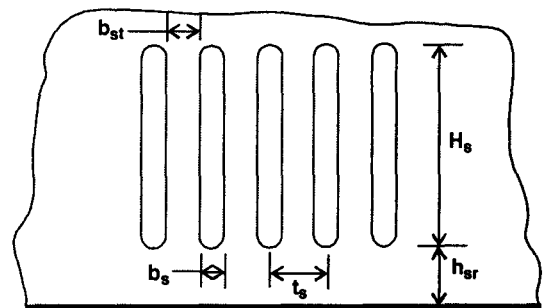
Fig. 4A. 7.1.1.

5. Tray Hydraulics

[A] Slot Opening

$$h_s = 100\% \ H_s \qquad \text{(maximum)}$$

$$h_s = 13mm \qquad \text{(minimum)}$$

[B] Dynamic Slot Seal

Select weir height so that dynamic slot seal (h_{ds}) becomes

12.5 – 37.5 for vacuum operation

25 – 50 for atmospheric press. operation

37.5 – 75 for 300 – 700 kPa operation

50 – 100 for 1300 – 3500 kPa operation

[C] Height of Clear Liquid in The Downcomer

$$H_d = 50\% \text{ of tray spacing } (l_t), \text{ maximum}$$

$$H_d < \frac{1}{2} \ l_t \text{ (Normally)}$$

[D] Downflow Residence Time

It should be a minimum of 5s.

[E] Liquid Throw Over the Weir

t_{ow} = 60% downcomer width (max.)

[F] Entrainment

Max 10% (mol % per mol dry vap)

[G] Pressure Drop

As dictated by the process

6. Tray Spacing

Select :

- 460 mm tray spacing for 750 – 3000 mm tower ID.
- 610 mm tray spacing for 1200 –6000 mm tower ID.

7. Baffles

Select :

- reverseflow baffle-height twice the height of the clear liquid (minimum)
- redistribution baffle-height twice the height of the clear liquid (minimum)
- **Locate**
- all redistribution baffle rows where endspace is 25mm > cap spacing

Keep

- cap-to-redistribution baffle clearance

= cap spacing

- downflow baffle seal should be

13 mm for mean tray width < 1525 mm

25 mm for mean tray width 1525 – 3050 mm

38 mm for mean tray width > 3050 mm

8. Tray Deflection

Design value : 3mm

9. Drain Holes

Hole dia : 9.5 – 16 mm

Hole area   : 280 mm^2/m^2 of tray area

10. Tray Levelness

3 mm (max.) for tower ID < 900 mm

4.75 mm (max.) for tower 900 – 1500 mm

6 mm (max.) for tower ID > 1500mm

11. Weir Levelness

± 1.6 mm

REFERENCES :

1. W. L Bolles, *Petroleum Processing (Feb./Mar./Apr./May 1956).*
2. J. A. Davies, *Industrial and Engineering Chemistry (vol. 39/1947/P:774).*
3. E. E. Ludwig, **Design for Chemical and Petrochemical Plants** (GULF PUBL. CO., Houston, Texas).
4. P. V. Danckwerts, **Mass Transfer and Absorbers.**
5. The American Institute of Chemical Engineering, **Bubble Tray Design Manual – Prediction of Fractionation Efficiency,** 1958.
6. H. E. Eduljee, *British Chemical Engineering (Sept. 1958/P :474).*
7. J. E. Broaddus, *et. al., Petroleum Refiner (Feb. 1955).*
8. M. C. Rogers and E. W. Thiele, *Industrial and Engineering Chemistry (vol. 26, 1934/ P: 524).*
9. D. J. Simkin, *et. al., Chemical Engineering Progress (vol 50, 1954/ P: 564)*

4 A. 8 VALVE-TRAY PRESSURE DROP CALCULATION : SIMPLIFIED MODEL

The total tray pressure drop is the sum of dry-tray drop and aerated-tray-liq pressure drop.

h_{tot} = h_d + h_{G-L}

h_d = dry-tray pressure drop

h_{G-L} = aerated-tray-liq pressure liq

= β (h_w + h_{ow})

h_w = weir height, m

h_{ow} = height of liq-crest over the weir, m of clear liquid

= 2.83 × 10^{-3} | $Q_{v,L}/l_w$ |$^{2/3}$ m of clear liquid

$Q_{v,L}$ = volumetric flowrate of liq, $m^3.h^{-1}$

l_w = weir length, m

β = aeration factor. Determine its value from **Fig. 4A.8.1**

F- FACTOR   1.22 F_a = $v_{G,a}$ $\sqrt{\rho_G}$, $kg^{1/2}.s^{-1}.m^{-1/2}$
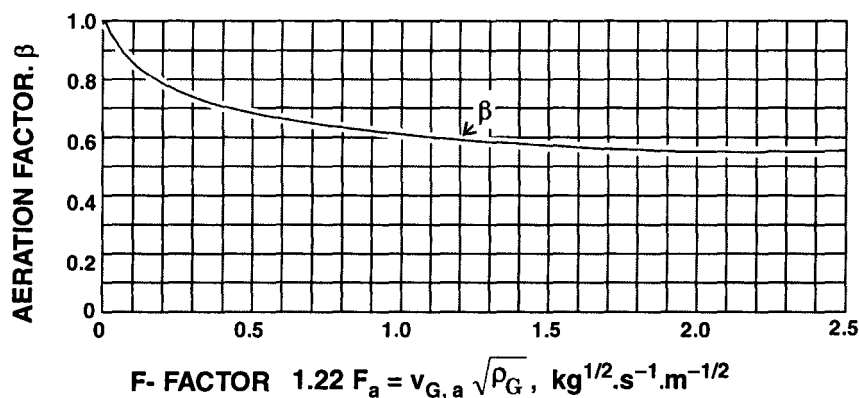
Fig. : 4 A. 8. 1. *Correlation for Aeration Factor.*

DRY-TRAY PRESSURE DROP

A typical valve-tray pressure drop profile is presented in **Figure 4A.8.2.**

$$1.22\ F_a = v_{G,a}\ \sqrt{\rho_G}\ ,\ kg^{1/2}.s^{-1}.m^{-1/2}$$
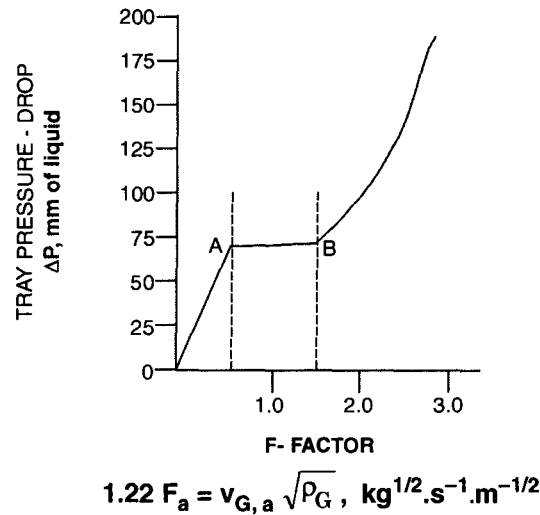
Fig. : 4 A.8.2. *Operating Valve-Tray Pressure-Drop Profile. Valve starts to open at A, remains open all along AB.*

At low hole-velocities, all valves remain closed (line **OA**). With the increase of gas-velocity, **DP** increases until the point **A** is reached when the valve-cap is about to lift off (**close balance point**). The hole velocity at **A**.

$$v_{o,\,cb} = \left| \Delta_v \cdot R. \left[\frac{C}{K_c} \right] \frac{\rho_m}{\rho_G} \right|^{\frac{1}{2}}$$

where, Δ_v = valve cap thickness, mm.

R = weight ratio of valve, *i.e.*, cap weight with legs : cap weight without legs. Its value depends on valve type and shape of the cap opening (see **Table 4A.8.1**).

Table 4A.8.1   R-Values for Different Shape of Cap Opening.

Valve Type	R-Value (Flat Orifice)	R-Value (Venturi Orifice)
3-leg valve	1.23	1.29
4-leg valve	1.34	1.45
No-leg valve	1.00	1.00

C = Eddy loss coefficient, dimensionless.

= 1.3 for flat and venturi valves.

K_C = loss coefficient for dry-tray press. drop, when the valve is just about to open, $s^2.mm.m^{-2}$ (see **Table 4A.8.2**).

Table 4A.8.2. *Loss Coefficient, K_c, when the Cap just Starts to Open.*

Orifice Type	K_C- Values ($s^2.mm.m^{-2}$) For Tray Deck Thickness		
	3.4mm	*2.65mm*	*1.88mm*
Flat	1682.524	1682.524	1682.524
Venturi	841.262	841.262	841.262

ρ_m = cap metal density, $kg.m^{-3}$ (see **Table 4A.8.3**)

Table 4A.8.3 Cap Metal Density

Cap Metal	Density ($kg.m^{-3}$)
Aluminium	2707
Titanium	4517
SS-400	7753
CS	7849
SS-316	8025
SS-304	8025
Monel-400	8826

Along **AB**, pressure drop remains constant provided liq load is not changed. At point **B** the valve is fully open [**opened balance point**]. The gas (vapor) velocity at this point is computed from

$$v_{0,\,ob} = \left| \Delta_v \cdot R. \left[\frac{C}{K_0} \right] \frac{\rho_m}{\rho_G} \right|^{\frac{1}{2}}$$

where,

K_0 = loss efficient for dry. press. dr. when the valve is full open but just about to close, $s^2.mm.m^{-2}$ (see **Table 4A.8.4**)

Table 4A.8.4 Loss Coefficient K_0 when the Valve is Full Open

Orifice Type	K_0- Values ($s^2.mm.m^{-2}$) For Tray Deck Thickness		
	3.4mm	**2.65mm**	**1.88mm**
Flat	224.464	254.538	301.837
Venturi	122.4846	122.4846	122.4846

The operating regime of the tray is **AB**, *i.e.*, the valve should operate between $v_{0,\,cb}$ and $v_{0,\,ob}$.

BOLLES METHOD

W. L. Bolles proposed the following correlations for hole-drop under closed and open conditions

Closed Valve : $\qquad\qquad h_0 = K_c \left| \frac{\rho_G}{\rho_L} \right| . v_0^2$

Open Valve :

$$h_o = K_o \left| \frac{\rho_G}{\rho_L} \right| \cdot v_o^2$$

where,

h_0 = press. dr. thru valve opening, m of tray. liq
v_0 = gas velocity thru valve openings, m/s

To determine a K_o not listed in the above table, use the following equation.

$$K_{o, 2} = K_{o, 1} \left| \frac{t_{D,1}}{t_{D,2}} \right|^{\frac{1}{2}}$$

where t_D refers to traydeck thickness

IRRIGATED-TRAY DROP

The aerated-liq ΔP correlation for virtually every type of valve tray—flat-orifice, venturi-orifice, round and rectangular is presented by the **Froth Density, $\varnothing$ vs. F-Factor** plot **(Fig. 4A. 8.3)**
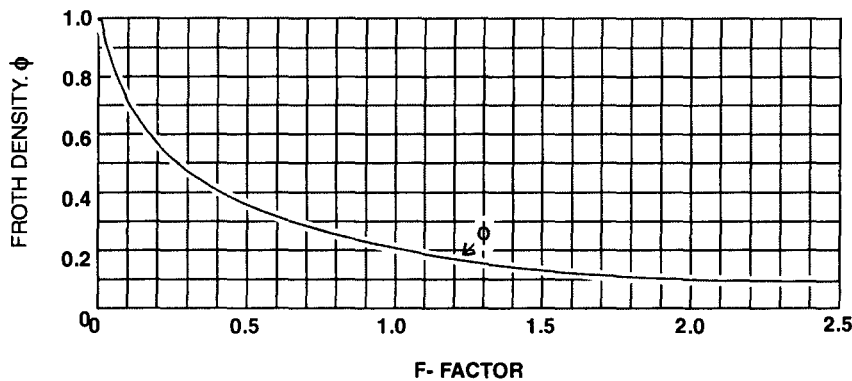
$$1.22 \; F_a = v_{G, a} \sqrt{\rho_G} \; , \; kg^{1/2}.s^{-1}.m^{-1/2}$$

Fig. 4A.8.3. *Correlation for Aerated Tray-Liq Pressure Drop.*

$v_{G, a}$ = gas velocity thru tray active area, $m.s^{-1}$

F_a = tray **F-factor** based on active (bubbling) tray area, $m.s^{-1} \, (kg.m^{-3})^{1/2}$.

A theoretical relation between β and $\varnothing$ was derived by Hutchinson, *et. al.*

$$\beta = \frac{\varnothing + 1}{2}$$

REFERENCES

1. B.D. Smith, **Design of Equilibrium Stage Processes** (McGRAW-HILL, N. Y, 1963)
2. D.C. Hausch, *Chemical Engineering Progress (vol. 60, 1964/P:55)*
3. W.L. Bolles, *Chemical Engineering Progress (vol.72, 1976 /P: 43)*
4. G.F. Klein, *Chemical Engineering (May 3, 1982 / P: 81-85)*
5. J.T. Thorngren, *Hydrocarbon Processing (Aug. 1978 / P: 111-113)*

TRAY HYDRAULICS

Problem 4.4.** **The operating parameters of a typical valve tray are as follows :

Vapor rate	$= 21500 \ kg.h^{-1}$
Liquid rate	$= 21483 \ kg.h^{-1}$
Vapor Density	$= 29 \ kg.m^{-3}$
Liquid Density	$= 490 \ kg.m^{-3}$
Weir Length	$= 1323 \ mm$
Height of weir	$= 75 \ mm$
Tray froth-height	$= 305 \ mm$
Percent of jet flood	$= 60 \ \%$
Tray F-factor	$= 0.8607$
Valve cap thickness	$= 1.5 \ mm$
Valve hole area	$= 0.1424 \ m^2$
Valve MOC*	$= 400 \ SS$
Valve type	$= 3\text{-}leg \ venturi \ orifice \ type$

*MOC : Materials of Construction

Compute :

1. tray press. drop

2. froth height

***Comment** if the measured value of total tray drop = 109mm and the measured value of froth height = 305 mm*

Solution : First, calculations should be made to check whether the valve tray operated between $v_{o,\,cb}$ and $v_{o,\,ob}$

Step - (I) Valve Orifice Velocity At Closed Balance Point

$$v_{o,\,cb} = \left| \Delta_v . R. \left[\frac{C}{K_c} \right] \frac{\rho_m}{\rho_G} \right|^{\frac{1}{2}}$$

$\Delta_v = 1.5 \ mm = 0.0015 \ m$

$R = 1.29$ for 3-legged valve with venturi orifice

$C = 1.3$ for flat and venturi orifice type valves

$K_C = 841.262 \ s^2.mm.m^{-2}$

$\rho_m = 8826 \ kg.m^{-3}$ for 400 SS

$\rho_G = 29 \ kg.m^{-3}$

Plugging these data into above eqn. yields

$$v_{o,\,cb} = \left| 1.5(1.29) \left[\frac{1.3}{841.262} \right] \frac{8826}{29} \right|^{\frac{1}{2}}$$

$$= 0.9539 \ m.s^{-1}$$

Step - (II) Valve Orifice Velocity At Open Balance Point

$$v_{o, cb} = \left| \Delta_v \cdot R \cdot \left[\frac{C}{K_o} \right] \frac{\rho_m}{\rho_G} \right|^{\frac{1}{2}}$$

$$K_o = 122.4846$$

$\therefore$

$$v_{o, ob} = \left| 1.5(1.29) \left[\frac{1.3}{122.4846} \right] \frac{8826}{29} \right|^{\frac{1}{2}}$$

$$= 2.5 \text{ m.s}^{-1}$$

Step - (III) Vapor Velocity Thru Valve Openings

Vapor rate = 21500 kg.h^{-1}

$$= 21500 \left| \frac{kg}{h} \right| \times \frac{1}{29} \left| \frac{m^3}{kg} \right| \times \frac{1}{3600} \left| \frac{h}{s} \right|$$

$$= 0.205938 \text{ m}^3\text{s}^{-1}$$

v_o = vap rate per tray/hole area of valves per tray

$$= 0.205938/0.1424 \left| \frac{m^3}{s} \right| \times \left| \frac{1}{m^2} \right|$$

$$= 1.44619 \text{ m.s}^{-1}$$

$\therefore$
$$v_{o, cb} < v_o < v_{o, ob}$$

Thus the valves on a tray operate between Closed Balance and Open Balance Points.

Step -(IV) Hole Drop

For a tray operating between closed and opened balance points, ΔP remains practically constant so one can use Bolles expressions but replacing v_o by $v_{o, cb}$ and $v_{o, ob}$ for calculating ΔP at closed balance and opened balance points. Thus,

$$h_{o, cb} = K_c \cdot \frac{\rho_G}{\rho_L} \cdot v^2_{o, cb}$$

$$= \left| 841.262 \frac{s^2 \cdot mm}{m^2} \right| \left| \frac{29 kg \cdot m^{-3}}{490 kg \cdot m^{-3}} \right| \left| 0.9539 m \cdot s^{-1} \right|$$

$$= 45.30 \text{ mm of liq on tray}$$

$$h_{o, ob} = K_o \cdot \frac{\rho_G}{\rho_L} \cdot v^2_{o, ob}$$

$$= \left| 122.4846 \frac{s^2 \cdot mm}{m^2} \right| \left| \frac{29 kg \cdot m^{-3}}{490 kg \cdot m^{-3}} \right| \left| 2.5 \text{ m.s}^{-1} \right|^2$$

$$= 45.306 \text{ mm of liq on tray}$$

The results are nearly identical

Step - (V) Total Tray Drop

The column is not near jet flooding. Therefore, no correction on h_o *is required.*

From **Fig. 4A.8.1**

for 1.22 $\mathbf{F_a}$ = 1.05, $\beta \simeq 0.64$

$$\therefore \qquad h_{ow} = 2.83 \times 10^{-3} \; |Q_{v,L}/l_w|^{2/3}$$

$$\therefore \qquad Q_{v,L} = \left|21483\frac{kg}{h}\right| \cdot \left|\frac{1}{490}\frac{m^3}{kg}\right| = 43.8428 \; m^3.h^{-1}.$$

$$l_w = 1323mm = 1.323m$$

$$h_{ow} = 2.83 \times 10^{-3} \left|\frac{43.8428}{1.323} \cdot \frac{m^3.h^{-1}}{m}\right|^{2/3}$$

$$= 0.02919 \; m \; of \; clear \; liq$$

$$= 29.19 \; mm \; of \; clear \; liquid$$

$$\therefore \qquad h_{G-L} = \beta(h_w + h_{ow})$$

$$= 0.604 \; (75 + 29.19) \; mm \; of \; clear \; liq$$

$$= 62.935 \; mm \; of \; clear \; liq$$

$$\therefore \qquad h_{tot} = h_d + h_{G-L}$$

$$= 45.30 + 62.935$$

$$= 108.235 \; mm \; of \; clear \; liquid$$

Comment :

The calculated value of total tray drop agrees well with the measured value (109 mm)

Step - (VI) Froth Height

$$h_{ow} = 29.19 \; mm \; of \; clear \; liq.$$

$$1.22 \; \mathbf{F_a} = 1.05 \; for \; which$$

$$\varnothing = 0.21 \qquad\qquad\qquad \textbf{Fig. 4A.8.3}$$

$$h_{G-L} = 62.935 \; mm \; of \; clear \; liquid$$

Froth height, $\qquad\qquad h_f = \dfrac{h_{G-L}}{\varnothing} = \dfrac{62.935}{0.21} = 299.69 \; mm$

Comment :

The calculated value of froth height approaches close to the measured value (305 mm).

[B] PACKED TOWER

Among the all types of gas-liq contacting devices, packings dominate the realm of absorption and stripping operation in CPIs (Chemical Process Industries). They characteristically operate with counterflow of the phases. Their popularity stems from the following salient features :

• Low press. drop. (unless operated at very high liq rates)

- Low capital investment (for columns of less than 600 mm dia, packings are cheaper than plates, unless alloy-metal packings)
- Wider range of operation (broader than a tray tower, unless the tray tower is conservatively designed with high-ΔP-trays)
- Versatility (the packing may be replaced with a type giving better efficiency, lower press. dr. or higher capacity)
- Corrosive fluid handling
- Minimum structure

4.B.1 DESIGN CONCEPTS : BASIC

Four basic steps are involved in the design of packed columns :

1. Selection of the type and size of packing
2. Determination of the column required for the specified separation
3. Determination of the col. dia to accommodate the liq and gas rates
4. Selection of column internals such as packing support, liq distributor system...etc.

4.B.1.2 TYPES OF PACKING

The chief requirements of a packing are that it should :

1. Expose a large surface area, *i.e.*, to provide a high gas-liq interfacial area

2. Sport an open structure so as to put up low resistance to gas flow.

3. Promote uniform wetting of packing, i.e., even distribution of liq on packing surface

4. Promote uniform gas flow across the bed cross-section, *i.e.*, no channelling.

In order to ensure these four goals, packings have undergone radical changes in their shapes and design pattern over the decades. Many diverse types and shapes of packing have been developed. However, they can be divided into two broad classes :

— *stacked*

— *random packings*

Stacked packings, which are regular arrangements of the packing elements, are mainly recommended for high gas rates and low pressure drop requirements.

Random packings are more commonly used. Raschig rings, Pall rings. Berl saddle; Intalox saddle are the principal types of random packings.

Raschig ring is the oldest random [dumped] tower packing which is still in substantial commercial use today.

Pall ring is the offshoot of Raschig ring – the improvement was made by BASF (Badische Aniline Soda Fabrik) Aktiengesellschaft in the early 1950s. Pall ring is a hollow cylindrical element of dia equal to its length while ten fingers punched from the cylinder wall extend into the interior of the packing element.

Although the Pall ring has the same geometric surface area as the Rashig ring, the interior surfaces of the pall ring are much more accessible to gas and liq flows due to the opening thru the wall.

The Pall ring underwent further modification by Mass Transfer Limited whereupon **Cascade®**
Mini Ring was born. It has features similar to Pall ring except its height is only one-third the outside
dia. This shape is said to orient itself preferentially when dumped.

Developed in the 1930s the **Berl saddle** has significantly increased surface area per unit of
packed volume compared to the Rashing ring. This design was further improved by Norton Chemical
Process Products. The outcome is : **Intalox® saddle** and **Super Intalox® saddle.**

Norton Co. combined the advantages of the shape of the Intalox® saddle with that of a modern
ring packing whereupon **IMTP® (Intalox Metal Tower Packing)** came into being in the late 1970
and is manufactured from metals only.

Ring and *saddle type packings* are available in a variety of materials :

• *ceramics*

• *metals and alloys*

• *plastics*

• *carbons*

Metal and plastic rings are more efficient than ceramics as they are lighter in weight. And
they make thinner-wall construction possible.

The choice of material is, however, dictated by the nature of the fluids and the operating
conditions. Ceramic packing normally becomes the first choice for corrosive liquids : *however they
are unsuitable for systems involving strong alkalies*. Plastic packings are cheap and light, but
they are attacked by some organic solvents and can only be used up to moderate temperatures.
Metal packings are efficient and sturdy — not susceptible to breakage (unlike ceramic packing) under
the load of the bed. But *they are, no doubt, costly.*

Raschig rings are cheaper per unit volume than **Pall rings** or saddles but are less efficient
and, therefore, the cost of the column usually becomes higher if **Raschig rings** are specified. For new
installation, the choice is normally between pall rings and **Berl/Intalox® saddles.**

For a given type of packing, the larger elements are more hollow (*i.e.,* having higher void
fraction) than their smaller counterparts. Hence the larger packing units give rise to less press. dr.
per unit bed height than the smaller size units under identical operating conditions (*i.e.,* same gas
massflow) :

Table 4.1. Characteristics of Metal Packings

Packing Type	Void Fraction	Bulk Density	Dry Bed Drop [Pa/m of bed depth]	
	$(m^3/m^3 \text{ of bed})$	(kg/m^3)	$G' = 7324 \left[\dfrac{kg}{h.m^2} \right]$	$G' = 13182 \ (kg/h.m^2)$
25 mm Pall Rings	0.942	464	375	1216
38 mm Pall Rings	0.956	352	261	841
50 mm Pall Rings	0.965	280	180	588
# 25 IMTP®	0.962	301	310	1012
# 40 IMTP®	0.971	232	196	645
# 50 IMTP®	0.977	181	122	408

4.2 Characteristics of Ceramic Packings

Packing Type	Void Fraction	Bulk Density	Dry Bed Drop [Pa/m of bed depth]	
	(m³/m³ of bed)	*(kg/m³)*	*G' = 4394(kg/h.m²)*	*G' = 7812 (kg/h.m²)*
25 mm Pall Rings	0.707	738	359	1127
38 mm Pall Rings	0.720	705	220	710
50 mm Pall Rings	0.737	663	180	596
# 25 Intalox®saddles	0.721	703	245	784
# 38 Intalox®saddles	0.734	669	131	424
# 50 Intalox®saddles	0.748	634	98	318

In general, the largest size of packing that is predominantly used is 50mm. Above 50mm the lower cost per m³ of packed bed does not normally compensate for the lower mass transfer efficiency. Though larger packing element bestows higher capacity, yet use of too large a size in a small column may contribute to poor liq distribution.

Smaller packing sizes beget higher mass transfer coefficient but are more expensive than the larger sizes. However, smaller packing elements give higher press. drop per unit bed depth than the larger elements of the same type for the same gasrate.

Recommended size ranges are :

Column Dia (mm)	Packing Size (mm)
< 300	< 25
300 – 900	25 – 38
> 900	50 – 75

The usual rule of the thumb is not to use packing size smaller than 25 mm when the gasrate is ≥ 850 m³/h. Likewise packing size smaller than 50mm is not recommended when the gasrate is ≥ 3400m³/h.

Source : F. A. Zenz – *Chemical Engineering, Nov. 13/1972.*

These rules depend on many other factors :

1. allowable press. dr.

2. possible height restriction

3. liq rate

Therefore, it is solely left to the discretion of the designer how he/she will apply these rules, barring the only general practical limitation :

the nominal size of the packing element should

not exceed $\left[\dfrac{1}{20}\right]$**th of the tower dia.**

This is imperative to reduce the greater voids at the vessel wall-packing element interface down to a negligibly small percentage of the total voids in the packed bed.

4.B.1.3 Column Dia

Normally the absorbers and stripper are designed for gas pressure drops of 200–400 Pa per m of packed depth.

Assume a suitable bed pressure-drop.

Calculate $\dfrac{L'}{G'} \cdot \left[\dfrac{\rho_G}{\rho_L - \rho_G} \right]^{0.5}$

Resort to the **Generalized Press.-Dr. Correlation (Fig. 3.19)**. Select the curve corresponding to ΔP (assumed) appearing as the curve parameter. Read out the ordinate Y for

$$X = \dfrac{L'}{G'} \cdot \left[\dfrac{\rho_G}{\rho_L - \rho_G} \right]^{0.5}$$

where $Y = G'^2 \cdot \dfrac{F_p}{\rho_G (\rho_L - \rho_G)} \cdot \dfrac{\mu_L^{0.1}}{g}$

The packing having been selected, the packing factor F_p is also known (from packing vendor's data or from **Table 3.7**)

Calculate G'

Therefore, tower cross-sectional area :

$$A_t = \dfrac{Q_{m,G}}{G'}, \qquad \dfrac{kg/s}{kg/(s.m^2)}$$

Calculate D_t :

$$D_t = | 4A_t/\pi |^{1/2}, \, m$$

Aliter Determine flooding velocity, v_{fl} by using Eqn. 1.149

Take **operating velocity,** $v = (75 - 90) \% \text{ of } v_{fl}$ ...(1.150)

Calculate packed bed dia

$$D = \left| \dfrac{Q_v}{0.785 \, v} \right|^{\frac{1}{2}}$$ ...(1.148)

Calculations at floodpoint yield the ultimate capacity limits or the minimum dia. However, how close the design diameter approach the minimum cannot be precisely defined.

The usual practice is to design on the basis of operating gas rate equal to 75% – 80% of the gas rate that would cause incipient floodpoint. Normally this is equivalent to a tower dia 15% greater than that calculated at floodpoint.

There are certain reasons as to why the design diameter should be somewhat larger than minimum tower dia :

- To allow for the uncertainties in the exact packing dimensions (*i.e.,* wall thickness of metal or ceramic rings)

- To take into account the improper distribution of packing arising out of vagaries of the crew that puts in the packing.
- To counter the probability of unexpected surges in either of the gas and liq flowrates
- To accommodate future changes in packing type and sizes if product specification tighten and limitation arise on pressure drop.

4.B.1.4 PACKED-BED DEPTH

The packed-bed depth height is the product of number of transfer units and the height of a transfer unit

$$Z = [NTU]_{o, G} \, [HTU]_{o, G} \qquad \qquad ...(1.107)$$

in terms of gas-phase transfer unit

or,

$$Z = [NTU]_{o, L} \, [HTU]_{o, L} \qquad \qquad ...(1.107)$$

in terms of liq-phase transfer unit

4.B.1.4.1 NUMBER OF GAS-PHASE TRANSFER UNITS

Calculate $[NTU]_{o, G}$ by either of :

$$[NTU]_{o, G} = \int_{y_t}^{y_b} \frac{(1 - y)_{lm} \cdot dy}{(1 - y)(y - y*)} \qquad \qquad ...(1.126)$$

$$[NTU]_{o, G} = \int_{y_t}^{y_b} \frac{dy}{y - y*} + \frac{1}{2} \ln \left| \frac{1 - y_t}{1 - y_b} \right| \qquad \qquad ...(1.128)$$

$$[NTU]_{o, G} = \int_{Y_t}^{Y_b} \frac{dY}{Y - Y*} + \frac{1}{2} \ln \left| \frac{1 + Y_t}{1 + Y_b} \right| \qquad \qquad ...(1.129)$$

For dilute solutions :

$$[NTU]_{o, G} = \frac{y_b - y_t}{(y - y*)_{lm}} = \frac{y_b - y_t}{\dfrac{\Delta y_b - \Delta y_t}{\ln \left| \dfrac{\Delta y_b}{\Delta y_t} \right|}} \qquad \qquad ...(1.122)$$

where, $\Delta y_b = y_b - y_b^*$

$\Delta y_t = y_t - y_t^*$

[See **Example 1.54**]

For dilute solutions obeying Henry's Law :

$$[NTU]_{o,G} = \frac{\ln\left[\dfrac{y_b - mx_t}{y_t - mx_t}\left(1 - \dfrac{1}{e_a}\right) + \dfrac{1}{e_a}\right]}{1 - \dfrac{1}{e_a}}$$ ...(1.124 A)

[See **Example 1.54**]

$[NTU]_{o,G}$ can also be determined graphically   [See **Example 1.54**]

4.B.1.4.2 NUMBER OF LIQUID-PHASE TRANSFER UNITS

Calculate $[NTU]_{o,L}$ by either of :

$$[NTU]_{o,L} = \int_{x_t}^{x_b} \frac{(1-x)_{lm}}{(1-x)(x^* - x)}$$

$$[NTU]_{o,L} = \int_{x_t}^{x_b} \frac{dx}{x^* - x} + \frac{1}{2}\ln\left|\frac{1-x_b}{1-x_t}\right|$$ ...(1.130)

$$[NTU]_{o,L} = \int_{X_t}^{X_b} \frac{dX}{X^* - X} + \frac{1}{2}\ln\left|\frac{1+X_b}{1+X_t}\right|$$ ...(1.131)

4.B.1.4.3 HEIGHT OF TRANSFER UNIT

For most standard packing, the data for volumetric overall mass transfer coefficient, $K_G \cdot a$, or the equivalent $[HTU]_{o,G}$ are avilable from the manufacturers, bulletins/literatures for specific systems. For some packings, data for $k_G.a$ (or, HTU_G) and $k_L.a$ (or, HTU_L) are also available.

For **Raschig Rings** and **Berl Saddles** calculates :

Gas-Phase Coefficient :

$$F_G.Sc_G^{2/3} = 1.195G\left|\frac{(1 - \varepsilon_{L,o}).\mu_G}{d_s.G'}\right|^{0.36}$$ ...(4.38)

where, F_G = gas phase mass transfer coefficient, kmol/(s.m^2)

Sc_G = Schmidt No. (gas phase), dimensionless = $\dfrac{\mu_G}{\rho_G.D_{ff,G}}$

$\varepsilon_{L,o}$ = operating void space = $\varepsilon - \varphi_{L,t}$ ...(4.39)

d_s = dia of the sphere of the same surface as a single packing element, m

G = superficial molar gas rate, kmol/(s.m^2)

G' = superficial gas mass rate, kg/(s.m^2)

Liquid Phase Coefficient :

$$k_L = 25.1 \frac{D_{ff,L}}{d_s} \left| \frac{d_s \cdot L'}{\mu_L} \right|^{0.45} \cdot \sqrt{Sc_L} \qquad \qquad ...(4.40)$$

where, k_L = liq phase MTC, kmol/(s.m^2.kmol/m^3)

   $D_{ff,L}$ = diffusivity of the solute in liq, m^2/s

   L' = superficial liq mass rate, kg/(s.m^2)

   Sc_L = Schmidt No. (Liq phase), dimensionless = $\dfrac{\mu_L}{\rho_L \cdot D_{ff,L}}$

Since liq data are normally obtained at very low solute concentrations, convert k_L to F_L thru

$$F_L = k_L \cdot C \qquad \qquad ...(4.41)$$

where, C = molar density of the solvent liq, kmol/m^3

   The overall height of a transfer unit is related to individual film transfer units $[HTU]_G$ and $[HTU]_L$ by :

$$[HTU]_{o,G} = [HTU]_G + m \cdot \frac{G}{L} [HTU]_L \qquad \qquad ...(4.42)$$

$$[HTU]_{o,G} = [HTU]_L + \frac{L}{m \cdot G} [HTU]_G \qquad \qquad ...(4.43)$$

where,   m = slope of the equilibrium line (EL)

   L/G = slope of the operating line (OL)

$[HTU]_G$ = height of a gas-phase transfer unit = $\dfrac{G}{F_G \cdot a}$

$[HTU]_L$ = height of a liq-phase transfer unit = $\dfrac{L}{F_L \cdot a}$

4.B.1.4.4 LIQUID HOLDUP

   Use Shulman's data to compute in sequence :

   1. Static liq holdup (water) $\varphi_{L,\,s/w}$

   2. Total liq holdup (water) $\varphi_{L,\,t/w}$

   3. Operating liq holdup (water) $\varphi_{L,\,o/w}$ [Eqn. 3.39]

   4. Operating liq holdup $\varphi_{L,\,o}$ [Eqn. 3.38]

   5. Static liq holdup $\varphi_{L,\,s}$

   6. Total liq holdup $\varphi_{L,\,t}$ [Eqn. 3.37]

4.B.1.4.5 INTERFACIAL AREA

   Calculate a_A from Eqn. 3.40

   For Packed Tower Design See **Example 1.57**

□□

Design : Absorbers & Strippers

5.1 DESIGN OF SIEVE TRAYS

The sieve-tray tower must be so designed as to accommodate large gas and liquid rates with the stable operating regime.

Tray layout details must be carefully selected on the basis of maximum allowable gas-pressure drop. Also the tower internals must be designed to guard against weeping, entrainment and flooding.

5.1.1 Tower Dia :

The tower dia and hence the column cross-sectional area is calculated on the basis of superficial gas velocity, v_G :

$$v_G = C_F \cdot \left[\frac{\rho_L - \rho_G}{\rho_G} \right]^{\frac{1}{2}} \qquad ...(5.1)$$

where, v_G = superficial (empty column) gas velocity, m/s.

ρ_L = liq density, kg/m^3.

ρ_G = gas density, kg/m^3.

G_F = *Capacity Factor* whose value at floodpoints can be determined from **Figure 5.1.**

From **Fig. 5.1**, the maximum allowable value of capacity factor, at specified tray spacing, can be estimated from a given tower loading (L'/G' ratio). And therefore gas velocity thru net area (A_n) at **flood** can be determined from :

$$v_{G, fl} = C_{F, fl} \cdot \left[\frac{\rho_L - \rho_G}{\rho_G} \right]^{\frac{1}{2}} \cdot \left[\frac{\sigma}{20} \right]^{0.2} \qquad ...(5.2)$$

[when σ is in dyne/cm]
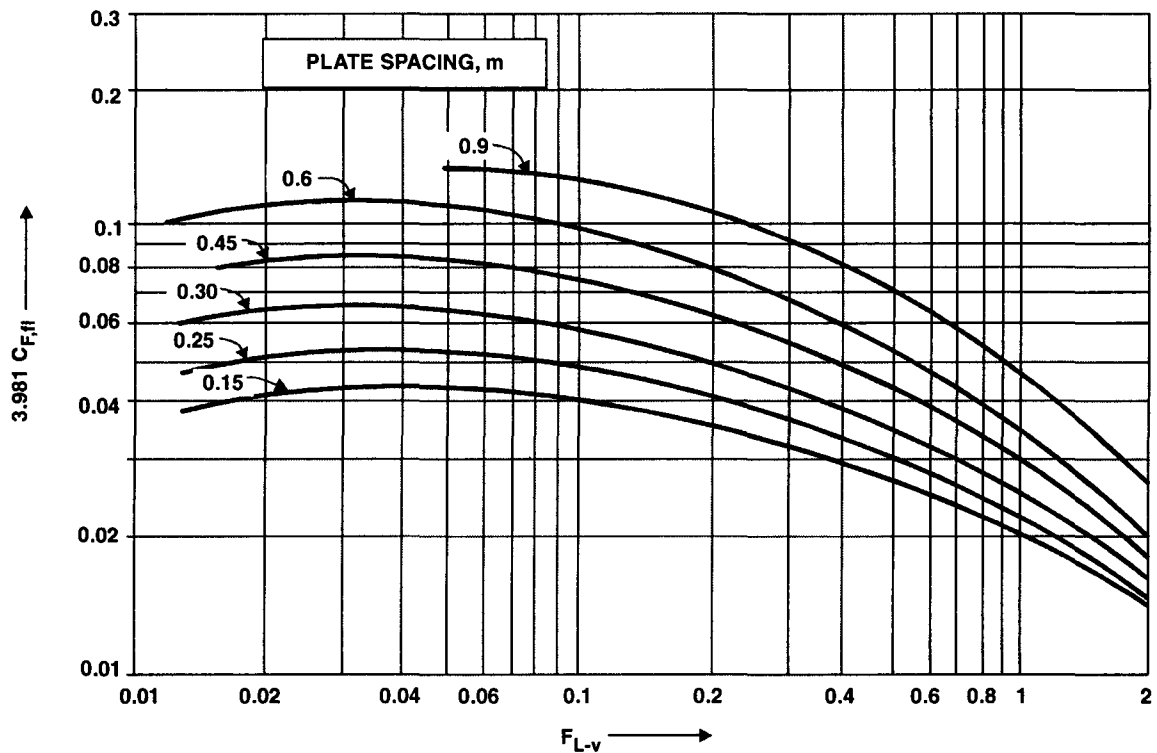
Fig. 5.1. *Capacity Factor (Max. Allowable) correlated against Flow Parameters for Sieve Trays, Valve Trays and Bubblecap Trays.*

$$= 3.981 C_{F, \, fl} \cdot \left[\frac{\rho_L - \rho_G}{\rho_G} \right]^{\frac{1}{2}} \cdot \left[\frac{\sigma}{20} \right]^{0.2} \qquad \ldots(5.2 \text{ A})$$

[when σ is in N/m]

where,

$v_{G, \, fl}$ = gas velocity thru net area at flood, m/s

$$= \left[\frac{Q_{v, \, G}}{A_n} \right]_{fl}$$

$Q_{v, \, G}$ = volumetric gas rate, m³/s.

A_n = tray net area, m².

= $A_t - A_d$ in case of cross-flow trays.

A_t = tower cross-section, m².

A_d = downcomer area, m².

$C_{F, \, fl}$ = capacity parameter at flood.

σ = liq surface tension, dyne/cm (**Eqn. 5.2**) or N/m(**Eqn. 5.2 A**).

For design, max. allowable gas velocity is taken 70 to 85% of flooding velocity.
Typically,

$v_G = (80 - 85)\% \; v_{G, fl}$ **for nonfoaming liquids**
$v_G = (70 - 75)\% \; v_{G, fl}$ **for foaming liquids** $\Big\}$ (subject to check for **Entrainment and ΔP**)

Therefore, **tower dia** is computed from :

$$D_t = \left[\frac{4}{\pi} \cdot \frac{Q_{v,G}}{v_G} \right]^{\frac{1}{2}} \qquad\qquad \text{...(5.3)}$$

The value of **capacity factor** C_F of Eqn. 5.1 can also be calculated from the empirical relationship

$$C_F = \alpha \; \log \left\langle \frac{1}{\left[\dfrac{L'}{G'}\right] \cdot \left[\dfrac{\rho_G}{\rho_L}\right]} \right\rangle + \beta \qquad \text{...(5.4)}$$

where, L' = liq mass rate, kg/(s.m²)

G' = gas mass rate, kg/(s.m²)

α , β are empirical constants :

$\alpha = 0.0744 \; l_t + 0.01173$ ...(5.5)

$\beta = 0.0304 \; l_t + 0.015$ ...(5.6)

l_t = tray spacing, m

Range
$[L'/G'] \; [\rho_G /\rho_L]^{0.5} = 0.1 - 1.0$
$A_o /A_a \geq 0.1$
$d_o \leq 6mm$

For $A_o /A_a < 0.1$, multiply α and β by $5 \left[\dfrac{A_o}{A_a} \right] + 0.5$

A_o = hole (perforation) area, m²
A_a = active area, m²

5.1.2. Hole : Size and Numbers

Hole dia of 3 to 12 mm are common, 4.5 mm size is the one most frequently used, although holes as large as 25mm have been successfully used.

Table 5.1 presents recommended hole dia and the number of such holes per m² of sieve trays depending on the ratio of hole area to tower cross-sectional area.

Table 5.1 Hole Dia and No. of Holes Per Unit Cross-Sectional Area :

Hole Dia d_o (mm)	No. of Holes Per Unit Column Cross-Sectional Area	$\left[\dfrac{A_o}{A_a}\right]$ %
3	1000	9.15
4.5	450	8
6	250	6.9

A_o = hole area, m² ; A_t = tower cross-sectional area, m².

5.1.3 Hole Dia and Sieve Thickness :

Sieve trays are made from carbon steels, alloy steels and other alloys. And the sheet thickness is less than $\frac{1}{2}$ d_0 for stainless steel and less than one hole dia for carbon steels and copper alloys.

Usually the plate thickness δ_p is assumed to be equal to $\left(\frac{1}{3} - \frac{1}{2}\right)d_0$. Some typical values are listed in Table 5.2.

Table 5.2 Hole Dia and Plate Thickness : Hole Dia Ratio

Hole Dia d_0 (mm)	*Plate Thickness (δ_p) (mm)*		*$\delta_p : d_0$*	
	SS	*CS*	*SS*	*CS*
3	1.95		0.65	
4.5	1.935		0.43	
6	1.92		0.32	
9	1.98	4.5	0.22	0.5
12	1.92	5.7	0.16	0.38
15	2.55	4.5	0.17	0.3
18	1.987	4.5	0.11	0.25

The ratio of plate thickness to hole dia ($\delta_p : d_0$), as the table shows, decreases steadily with the increase of hole dia.

5.1.4. Layout of Holes

The holes are arranged on an equilateral triangular layout – each hole occupying the apex of the triangle **Fig. 5.2**
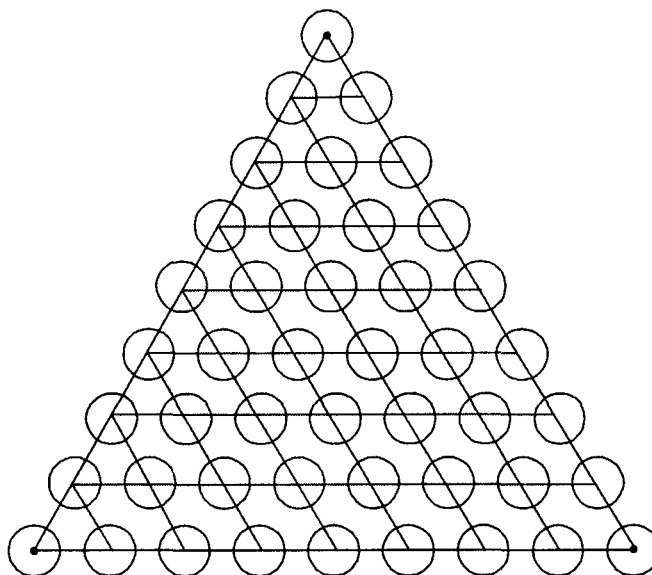
Fig. 5.2 *Sieve-Tray Holes are Distributed in Equilateral-Triangular Arrangement.*

Hole Pitch [Δ] varies from usually 2.5 to 5 hole dia – the commonest one is the **3d$_o$**. For such an arrangement

$$\frac{A_o}{A_a} = 0.907\left[\frac{d_o}{\Delta}\right]^2$$

...(5.7)

Depending on the ratio of hole area to active area, the hole pitch is selected (**Table 5.3**)

Table 5.3. Hole Pitch

$\frac{A_o}{A_a}$ (%)	$\left[\frac{\Delta}{d_o}\right]$
14.50	2.5
10.07	3.0
7.40	3.5
5.66	4.0
4.47	4.5

5.1.5 Plate Layout :

The crossflow sieve trays (**Figure 5.3**) consists of :

1. Active gas-distribution zone

2. Periphery waste and waste zone

3. Disengagement zone

4. Distribution zone

5. Downcomer zone

Periphery Waste and Support Zone : The periphery waste refers to the little dead area close to the walls.

The peripheral tray support zone is usually 25 – 50 mm wide and occupies 2 to 5 percent of tower cross-section—the fraction decreasing with the increase of tower dia.

The peripheral tray support (25—50 mm wide) and the beam supports generally occupy up to 15 percent of tower cross-sectional area.

Downcomer Zone : generally occupy 10 to 30 percent of the tower cross-section. A typical data, depending on the weir length for straight, rectangular weirs, is given below (**Table 5.4**)

Table 5.4 Downcomer Dia

Weir Length : Tower Dia $[l_w : D_t]$	*DownComer Area/Tower Area* $[A_d/A_t]$
(%)	(%)
55	3.877
60	5.257
65	6.899
70	8.808
75	11.255
80	14.145
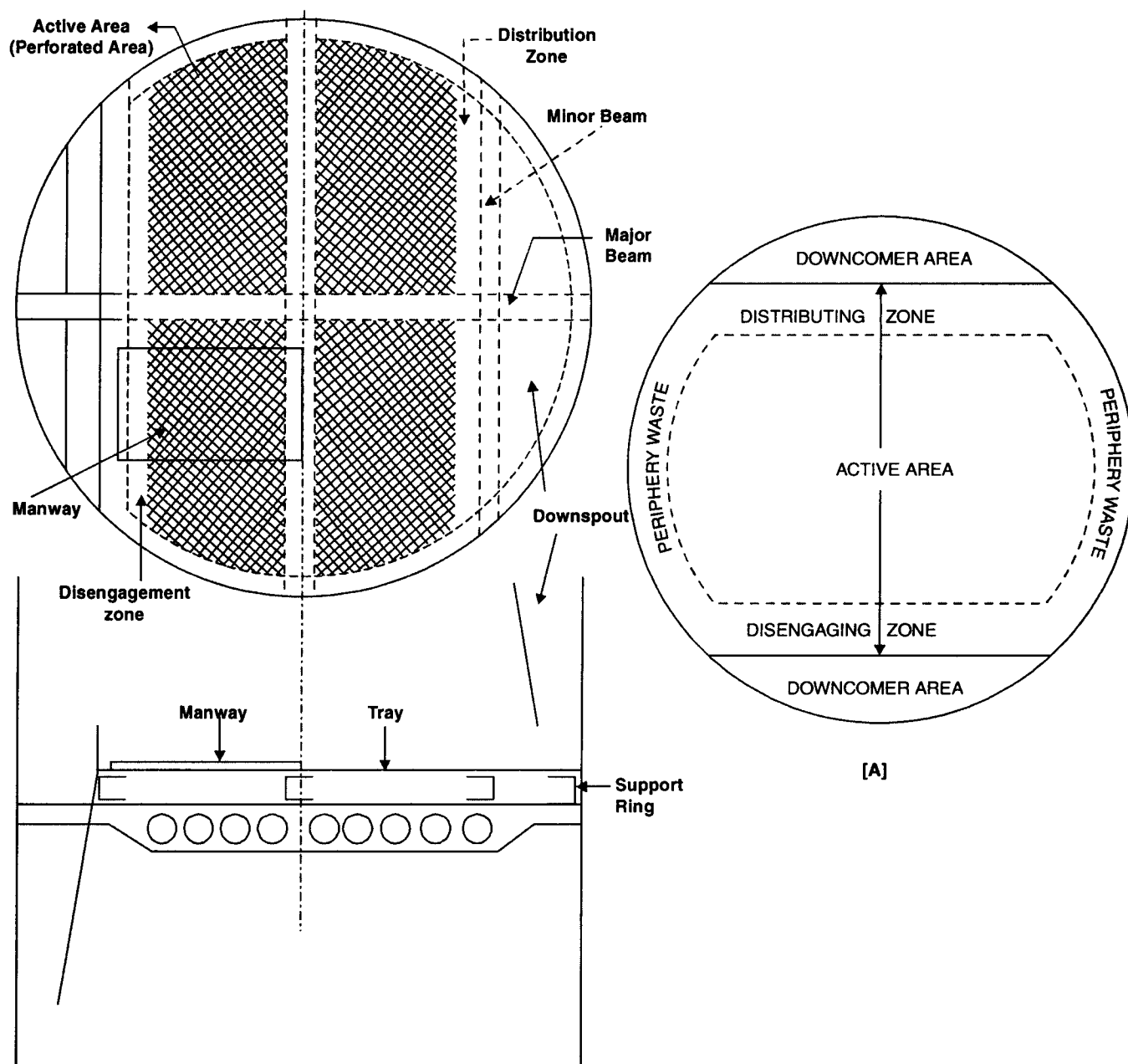
Fig. 5.3. *Zone Distribution of A Sieve Tray.*

Distribution Zone and Disengagement Zone : are respectively for liquid entering the tray and disengaging foam. Together they occupy 5% or more of the tower cross-section.

5.1.6 Active Area :

The tray cross-section minus the periphery waste and support zone, downcomer zone, distribution and disengagement zones combined is the area available for active perforations, also called **active area**. It counts for tray-area available for gas-liq contact :

$$A_a = A_t - \sum A_d - A_{dis} - A_{ws} \qquad ...(5.8)$$

where, A_a = active area, m^2

A_t = tower cross-sectional area, m^2

A_d = cross-sectional area for a single downcomer, m^2

A_{dis} = cross-sectional area of distribution and disengagement zones, m^2

A_{ws} = periphery waste zone, m^2

For ordinary cross-flow sieve-trays :

$$A_a = A_t - 2A_d - A_{dis} - A_{ws}$$

$$= 2\left[x\sqrt{r^2 - x^2} + 4\sin^{-1}\frac{x}{r}\right] \qquad ...(5.8\,A)$$

where, $x = \frac{1}{2}D_t - b_d + b_{dis}$ ...(5.9)

$r = \frac{1}{2}D_t - b_{ws}$ ...(5.10)

D_t = tower dia, m

b_d = downcomer width, m

b_{dis} = width of distribution and disengagement zones, m^2

b_{ws} = width of peripheral waste, m

Typical active areas for sieve tray are presented in **Table 5.5**

Table 5.5 Typical Active Area For Sieve Trays

Tower Dia (D_t) (m)	Active Area/Tower Cross-Section [A_a/A_t] (%)
1	65
1.25	70
2	74
2.5	76
3	78

5.1.7 Liquid Depth :

The depth of liq pool on tray liquid should not normally fall below 50mm to ensure good froth formation.

Liq depth = Weir height + Height of Crest over the weir

$$= h_w + h_{ow} \qquad \text{[See Fig 5.4]}$$

In most cases the sieves trays operate with a maxm. liq depth of 100 mm, though depths of 150mm have also been reported in certain cases.

[F.A.Zenz–*Chemical Engineering (vol. 79/P-120), Nov., 13, 1972*]
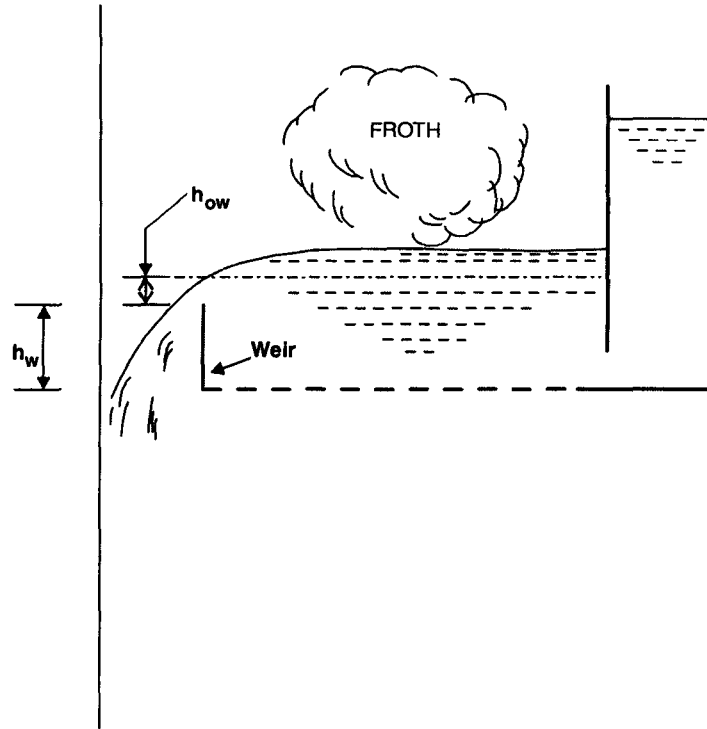
Fig. 5.4. *Weir Height and Height of Crest Over the Weir of a Sieve-Tray.*

5.1.8 Weir Height and Weir Crest :

The height of liq crest over the weir (h_{ow}) can be estimated from Francis formula :

Rectangular Weir :

$$h_{ow} = 0.666 \left[\frac{Q_{v,L}}{l_{w,eff}} \right]^{\frac{2}{3}}$$

...(5.11)

where, $Q_{v,L}$ = liq rate, m^3/s

$l_{w,eff}$ = effective length of weir, m

Serrated Weir :

$$h_{ow} = 0.851 \left[\frac{Q_{v,L}}{\tan\left(\frac{\theta}{2}\right)} \right]^{0.4}$$

...(5.11 A)

where, θ = angle of serration, degree

Circular Weir :

$$h_{ow} = 0.342 \left[\frac{Q_{v,L}}{D_w} \right]^{0.704}$$

...(5.11 B)

where, D_w = diameter of weir, m

The effective weir height is introduced to account for the fact that weir action is hampered by the curved surfaces of circular tower. From the geometry of the **Fig. 5.5** :
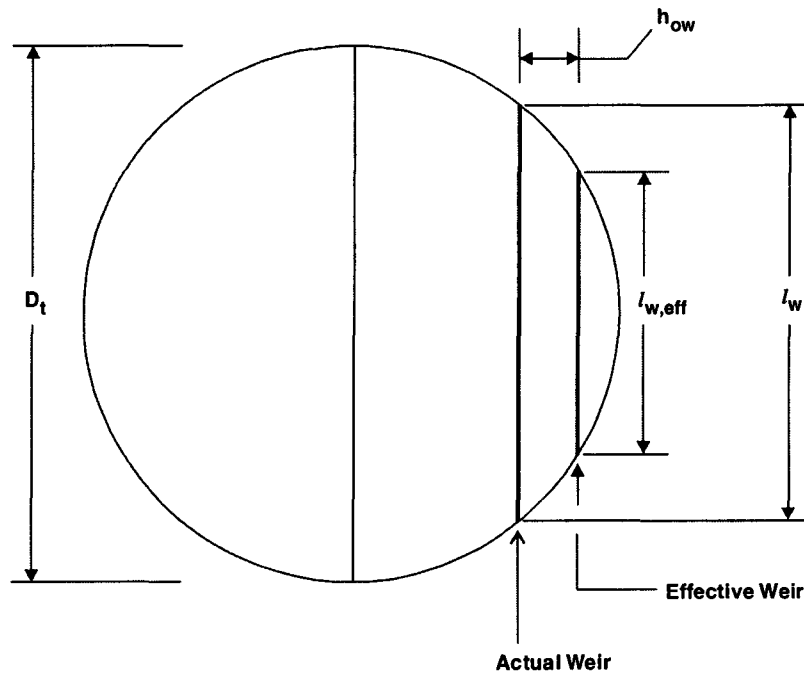
Fig. : 5.5. *Effective Weir Length is somewhat Shorter than Actual Weir Length because of Cylindrical Configuration of Tower.*

$$\left[\frac{l_{w,\,eff}}{l_w}\right]^2 = \left[\frac{D_t}{l_w}\right]^2 - \left\langle\left[\left(\frac{D_t}{l_w}\right)^2 - 1\right]^{0.5} + \frac{2h_{ow}}{D_t}\cdot\frac{D_t}{l_w}\right\rangle^2 \qquad ...(5.12)$$

5.1.9 Downcomer Backup :

The height of clear liq in the downcomer [Fig 5.6] *is called downcomer backup* and is calculated from the press-balance equation :

$$h_{dc} = h_{G-L} + h_w + h_{ow} + h_{da} + h_{hg} \qquad ...(5.13)$$

> **Source : R.H. Perry & C.H. Chilton — Chemical Engineers' HandBook (5th ISE) Page : 18-7.**

where, h_{dc} = height of liq in downcomer, m of clear liq

h_{G-L} = total press drop across the irrigated sieve-tray, m of clear liq.

h_w = height of weir at plate outlet, m

h_{ow} = height of liq crest over weir, m of cl. liq

h_{da} = head loss due to flow under downcomer apron, m of cl. liq

h_{hg} = hydraulic gradient, *i.e.,* head loss across the tray, m of clear liq, **(Figure 5.6)**
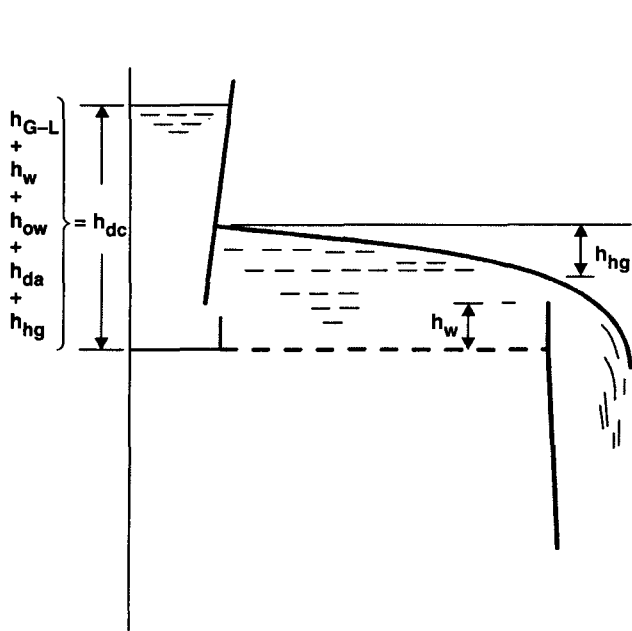
Fig. 5.6. *Downcomer Backup on A Sieve-Tray.*   **Fig. 5.7.** *Downcomer Backup.*
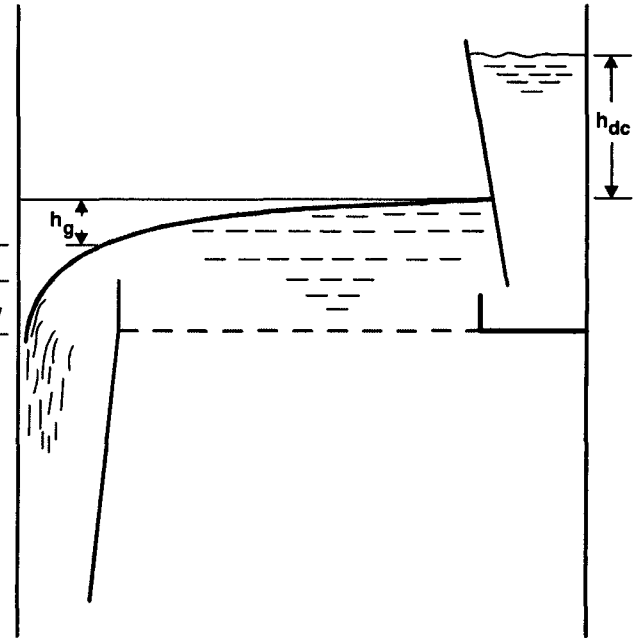
But in some text [R.E. Treybal–**Mass-Transfer Operations** (3rd ISE)/P-172] the difference in liq level inside and immediately outside the downspout (downcomer) is taken as downcomer backup

$$h_{dc} = h_{G-L} + h_{da}$$ **[Figure 5.7]**

$$= h_d + h_L + h_R + h_{da}$$ ...(5.13 A)

For stable operation, downflow flooding must be avoided. Therefore, the column must be so designed as to avoid excessive backup. Safe design requires that the maximum height of the clear liq in the downcomer be no more than half the tray spacing [R.E. Treybal—**Mass-Transfer Operations (3rd ISE)/P-172]**, *i.e.,*

Refer to Fig. : 5.7

$$h_{dc} + h_{hg} + h_{ow} + h_w < \frac{1}{2} l_t$$ ...(5.14)

Elsewhere* for safe design, the maxm. height of cl. liq. in downcomer is taken less than half the sum of the tray spacing and weir height :

Refer to **Fig. : 5.6**

$$h_{dc} \leq \frac{1}{2} [l_t + h_w]$$ ...(5.14 A)

The **downcomer backup** (h_{dc}) is calculated in terms of clear liq. However, the downcomer liq may be aerated and as such, the actual backup is

$$h'_{dc} = \frac{h_{dc}}{\phi_{dc}}$$ ...(5.15)

where, ϕ_{dc} = average froth density in downcomer

= 0.5 for gas-liq systems with rapid bubble formation

= 0.2 – 0.3 for gas-liq systems with slow bubble formation

To ensure vapor separation in the downcomer, it is necessary to have

$$b_{ow} \leq 0.6 \, b_d$$ ...(5.16)

where, b_d = downcomer width, m

b_{ow} = width of liq crest over the weir, m

$$= 0.8 \, \sqrt{h_{ow}[l_t + h_w - h_{dc}]}$$ ...(5.17)

*Kafarov— FUNDAMENTALS OF MASS TRANSFER (MIR Publ./1975)/ P-358.

R.K. Sinnott — CHEMICAL ENGINEERING : DESIGN (Vol.6)/Pergamon Press (U.K.), 1989.

l_t = tray spacing, m

5.1.10. Weeping

The column must be sized to guard against weeping which is deleterious in the sense that liq tends to short-circuit the perforations. Liquid will drain thru the holes when the gas velocity thru holes is too small, *i.e.*, the gas-press drop thru the holes is not sufficient to create bubble surface and support the static head of forth above the perforations. Of course, some mass transfer to and from the weeping liq occurs but it fails to reap the benefit of complete flow over the tray. Hence it is usual practice to design so that deleterious weeping does not occur.

Fig. 5.8. Shows the correlations for weeping on sieve-trays.
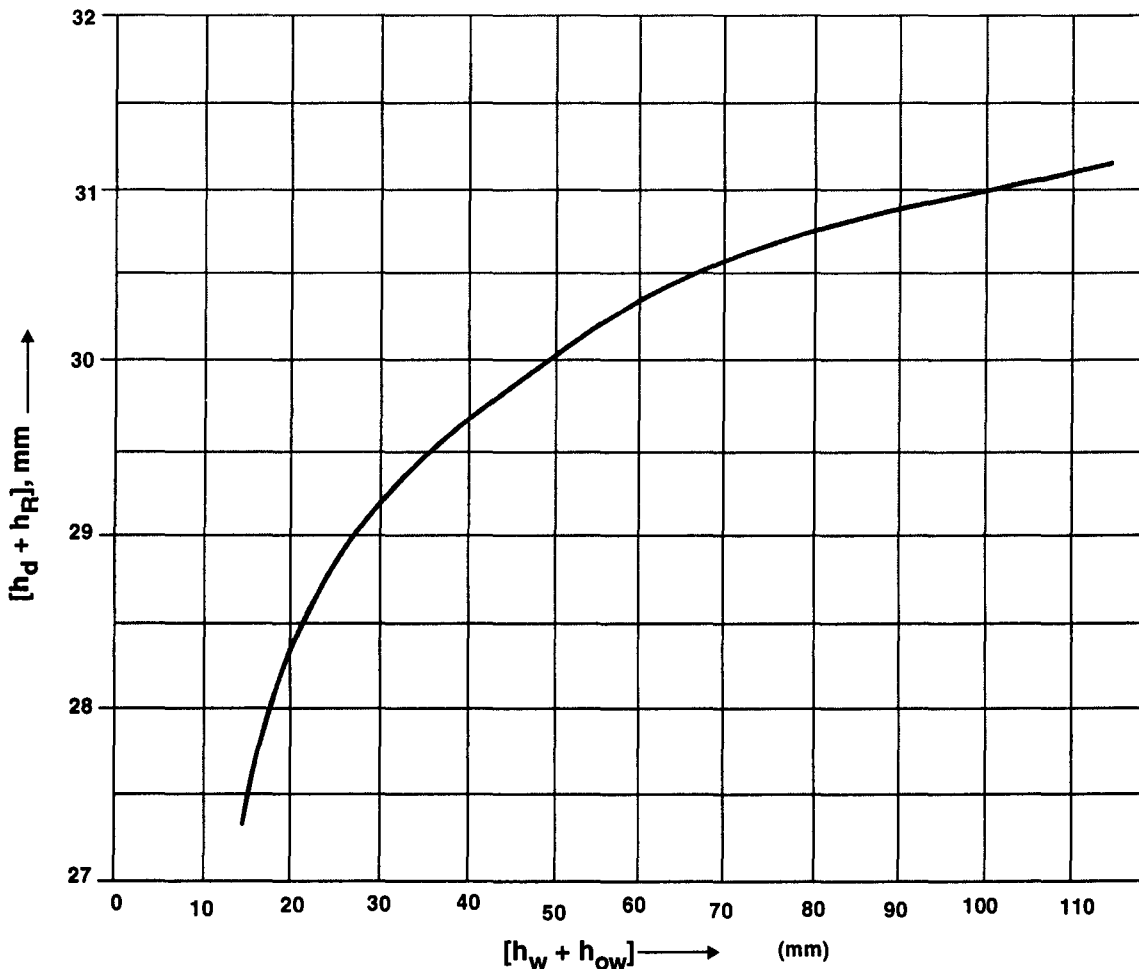
Fig. 5.8. *Weeping, sieve-trays.*

h_d = dry-plate press. drop, m of clear liq

h_R = residual gas-press. drop, m of cl. liq = $\dfrac{6\sigma}{\rho_L \cdot d_0 \cdot g}$

h_w = weir height, m

h_{ow} = height of liq crest on weir, m of cl. liq

The safe design must ensure that the col. operates at conditions above the appropriate curve of **Fig. 5.8** to avoid deleterious weeping.

Also the excessive weeping can be avoided if the col. operates above the min. gas velocity, $[v_{G,o}]_{weep}$

$$[v_{G,o}]_{weep} = 0.023\,\frac{\sigma}{\mu_G}\cdot\left[\frac{\mu_G^2 \cdot \rho_L}{\sigma \cdot \rho_G^2 \cdot d_o}\right]^{0.379}\cdot\left[\frac{\delta_p}{d_o}\right]^{0.293}\cdot\left[\frac{2}{\sqrt{3}}\cdot\frac{A_a \cdot d_o}{\Delta^3}\right]^{2.8/[Z/d_o]^{0.724}}$$

where $[v_{G,o}]_{weep}$ = minimum gas velocity thru orifices (holes) to avoid excessive weeping, m/s

σ = liq surface tension, N/m

μ_G = dynamic viscosity of gas, Pa.s

δ_p = plate thickness, m

d_o = hole dia, m

ρ_L = liq density, kg/m^3

Δ = hole pitch, m

Z = length of liq-travel on tray deck, m.

Its value can be obtained from the **Table 5.6.**

Table 5.6. Weir Distance from the Sieve-tray center $\left(\frac{1}{2}Z\right)$.

Weir length (l_w) : Tower dia (D_t) (%)	*Weir distance from the center of tray $\left(\frac{1}{2}Z\right)$: Tower Dia (D_t) (%)*
55	41.81
60	39.93
56	25.16
70	35.62
75	32.96
80	19.91

4.1.11. Entrainment

Liquid entrainment, in any proportion, is detrimental as it dilutes the effects of absorption (distillation) and increases liquid loads on the upper trays. Hence the column must be sized to guard against entrainment which is conveniently expressed in terms of fractional entrainment :

$$\Psi = \frac{e}{\overset{\bullet}{L} + e}$$ ...(5.4A)

where, Ψ = fractional entrainment, *i.e.*, the fractional of gross liq downflow that is entrained, kg/h or kmol/h

$\overset{\bullet}{L}$ = liq downflow rate without entrainment, kg/h or, kmol/h

e = absolute entrainment of liq, kg/h or, kmol/h

The fractional entrainment for sieve-trays can be obtained from ENTRAINMENT CORRELATION [**Fig. 5.9**] in which Ψ is plotted against $[L'/G']\ [\rho_G/\rho_L]^{1/2}$ while the ratio of superficial gas velocity to flooding velocity ($v_G : v_{G,\,fl}$) appearing as the curve parameter.
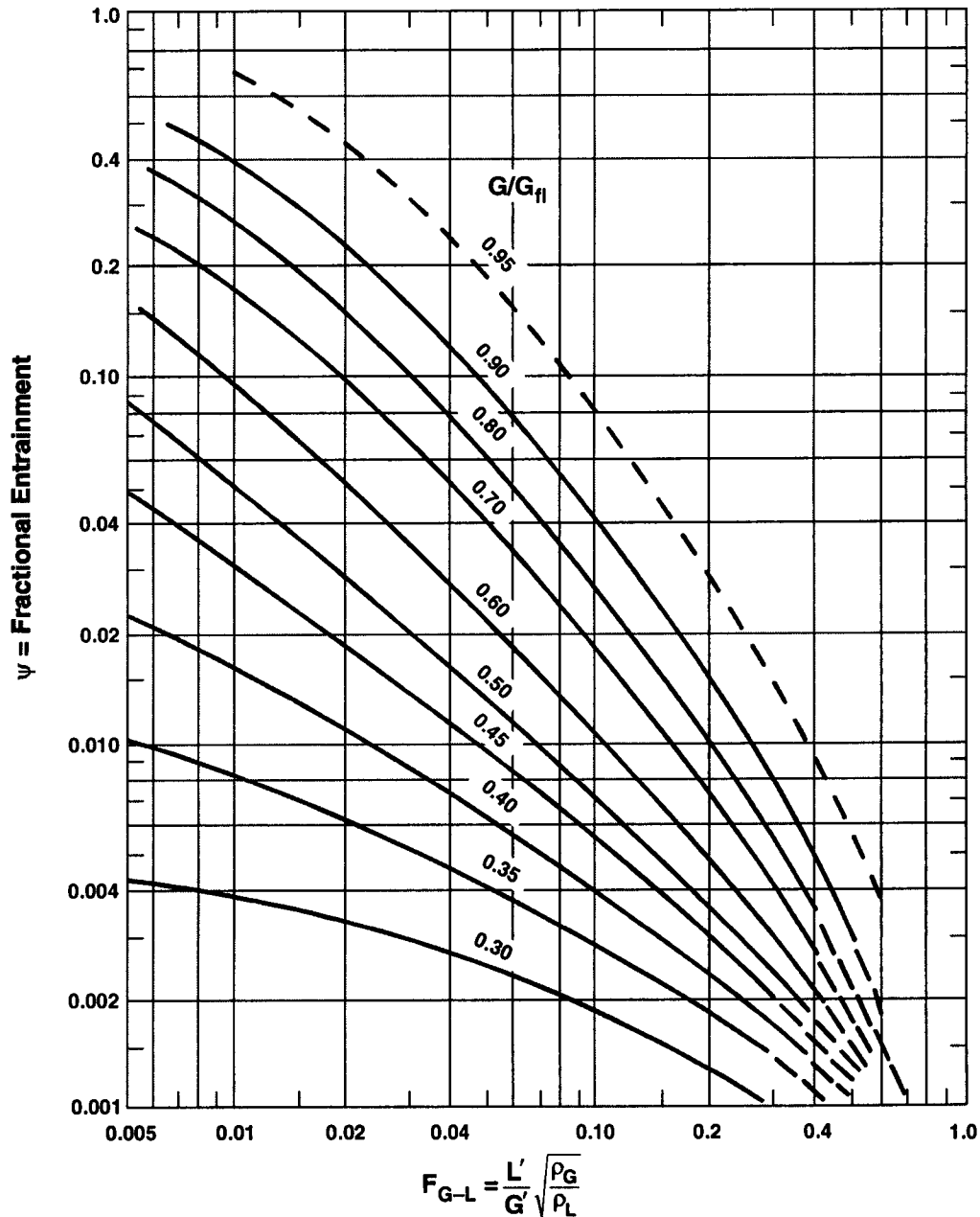
Fig. 5.9. *Entrainment correlation (Sieve-trays).*
L'/G' = *liq/gas mass ratio,* ρ_G/ρ_L = *liq/gas densities*

DESIGN OF A SIEVE-TRAY TOWER

Example 5.1. Design a crossflow sieve-tray tower for stripping aniline-water solution with steam from the following conditions specified for design :

Operating pressure	*= 101.325 kPa*
Operating temperature	*= 371.5K*
LIQUID	
Rate	*= 22.68 t/h*
Density	*= 961 kg/m³*
Dynamic viscosity	*= 3 × 10⁻⁴ Pa.s*
Surface tension	*= 0.058 N/m*
Composition	*= 7 mass% ANILINE*
GAS	
Rate	*= 11.34 t/h*
Dynamic viscosity	*= 12.5 × 10⁻⁶ Pa.s*

Report details of :

 # perforation size and layout

 # tower dia

 # tray spacing

 # weir length and weir height

 # total gas-pressure drop

Check for :

 # excessive weeping

 # entrainment

 # downflow flooding

Solution :

Liquid

Rate, $Q_{m, L}$ = 22.68 t/h = 6.3 kg/s

Density, ρ_L = 961 kg/m³

Viscosity, μ_L = 3 × 10⁻⁴ Pa.s

Surface tension, σ = 0.058 N/m

Composition : 7 mass% $C_6H_5NH_2$ + 93 mass% H_2O

Mol. wt. of aniline   = 93 kg/kmol

Av. mol. wt. of liq $= \dfrac{100}{\dfrac{7}{93} + \dfrac{93}{18}} = 19.0769$ kg/kmol

Vol. liq rate, $Q_{v, L} = \dfrac{6.3 \left[\dfrac{kg}{s}\right]}{961 \left[\dfrac{kg}{m^3}\right]} = 6.5556 \times 10^{-3}$ m³/s

GAS

Rate, $Q_{m, G}$ = 11.34 t/h = 3.15 kg/s

Composition : 3.6 mol% $C_6H_5NH_2$ + 96.4 mol% H_2O (vap)

Av. mol. wt. of gas $= \dfrac{3.6}{100}(93) + \dfrac{96.4}{100}(18) = 20.7$ kg/kmol

Gas density, $\rho_G = \dfrac{20.7}{22.41} \cdot \dfrac{101.325}{101.325} \cdot \dfrac{273}{371.5} = 0.67878$ kg/m³

Vol. gas rate, $Q_{v, G} = \left(\dfrac{3.15}{20.7}\right)\dfrac{kg/s}{kg/kmol} \cdot (22.41)\dfrac{m^3}{kmol} \cdot \left(\dfrac{371.5}{273}\right)\dfrac{K}{K}$

HOLES Hole dia from 3 mm to 12 mm are commonly used. Since 4.5 mm hole dia is the one frequently used, let us take

$$d_0 = 4.5 \text{ mm}$$

Layout : equilateral-triangular arrangement

Hole pitch : Δ = 12 mm (center to center distance)

Tower Dia

$$\dfrac{A_o}{A_a} = 0.907 \left[\dfrac{d_o}{\Delta}\right]^2 = 0.907 \left[\dfrac{4.5}{12}\right]^2 = 0.1275 > 0.1 \qquad \text{Eqn. 5.7}$$

$$\dfrac{L'}{G'} \cdot \left[\dfrac{\rho_G}{\rho_L}\right]^{1/2} = \dfrac{Q_{v,L} \cdot \rho_L / A_n}{Q_{v,G} \cdot \rho_G / A_n} \cdot \left[\dfrac{\rho_G}{\rho_L}\right]^{1/2} = \dfrac{Q_{v,L}}{Q_{v,G}} \cdot \left[\dfrac{\rho_L}{\rho_G}\right]^{1/2}$$

$$= \dfrac{6.5556 \times 10^{-3}}{4.6406} \cdot \left[\dfrac{961}{0.67878}\right]^{1/2} = 0.05315$$

Tray spacing, l_t = 600 mm = 0.6 m (tentative)

α = 0.0744 (0.6) + 0.01173 = 0.05637   Eqn. 5.5

β = 0.0304 (0.6) + 0.015 = 0.03324   Eqn. 5.6

Flooding Constant, C_F :

$[L'/G']\,[\rho_G/\rho_L]^{0.5} > 0.1$, so we'll take $\dfrac{L'}{G'} \cdot \left[\dfrac{\rho_G}{\rho_L}\right]^{1/2} = 0.1$

$$\sigma = 0.058 \text{ N/m}$$

$\therefore$ $C_F = 0.05637 \log\left[\dfrac{1}{0.1}\right] + 0.03324 = 0.08961$ Eqn. 5.4

Flooding velocity :

$$v_{G, fl} = 3.981(0.08961)\left[\dfrac{961 - 0.67878}{0.67878}\right]^{\frac{1}{2}}\left[\dfrac{0.058}{20}\right]^{0.2} \qquad \text{Eqn. 5.2A}$$

$$= 4.1703 \text{ m/s}$$

Fig. 5.1 : 3.981 $C_{F, fl} = 0.37;$ $\therefore$ $C_{F, fl} = 0.09294$

$$\therefore v_{G, fl} = 3.981(0.09294) \sqrt{\frac{961 - 0.67878}{0.67878}} \left[\frac{0.058}{20}\right]^{0.2} = 4.325 \text{ m/s}$$

Max. allowable gas velocity,

$$v_G = 80\% \ v_{G, fl}$$
$$= 0.8 \ (4.1703) \qquad\qquad\qquad \textbf{Assumed}$$
$$= 3.3362 \text{ m/s}$$

Net tower cross-sectional area for gas flow :

$$A_n = \frac{Q_{v, G}}{v_G} = \frac{4.6406}{3.3361} = 1.391 \text{ m}^2$$

Weir length, $l_w = 70\%$ of tower dia   **Tentative**

$\therefore$ Tray area occupied by one downspout = **8.8% of A_t**   **Table 5.4**

$\therefore$ **Tower area,** $\qquad A_t = \dfrac{A_n}{1 - 0.088} = \dfrac{1.391}{1 - 0.088} = 1.5252 \text{ m}^2$

Tower dia, $\qquad D_t = \left[\dfrac{4}{\pi}(1.5252)\right]^{1/2} = 1.3935 \text{ m} \approx 1.40 \text{ m (say)}$

$\therefore \qquad\qquad A_t \text{ (corrected)} = \dfrac{4}{\pi}(1.4)^2 = 1.53938 \text{ m}^2$

Weir Length

$$l_w = 0.70 \ (D_t) = 0.7(1.40) = 0.98 \text{ m}$$

Downcomer Area of cross-section

$$A_d = 8.8\% \text{ of } A_t = 0.088 \ (1.53938) = 0.13546 \text{ m}^2 \qquad \textbf{Table 5.4}$$

Active Area

$A_a = A_t - 2A_d$ – **Area taken by (tray support + distributing zone + disengagement zone)**

Area of periphery support + beam support = **15% A_t**   **say**

Distribution + Disengagement zones = **5% A_t**

$\therefore \qquad\qquad\qquad\qquad A_a = A_t - 2 A_d - 20\% A_t$
$$= 1.53935 - 2(0.13546) - 0.20 \ (1.53938)$$
$$= 0.96058 \text{ m}^2$$

Height of Crest over the Weir

$$h_{ow} = 25 \text{ mm} = 0.025 \text{ m} \qquad\qquad\qquad \textbf{1}^{\text{ST}} \textbf{ APPROXIMATION}$$

$$\left[\frac{l_{w,eff}}{0.98}\right]^2 = \left[\frac{1.4}{0.98}\right]^2 - \left\langle\left[\left(\frac{1.4}{0.98}\right)^2 - 1\right]^{0.5} + \frac{2\,(0.025)}{1.4} \cdot \frac{1.4}{0.98}\right\rangle^2 \qquad \text{Eqn. 5.12}$$

$$= 0.893288$$

$$\therefore \quad l_{w,eff} = 0.92623 \text{ m}$$

$$\therefore \quad h_{ow} = 0.666 \left(\frac{6.5556 \times 10^{-3}}{0.92623}\right)^{2/3} = 0.02455 \text{ m} \qquad \text{Eqn. 5.11}$$

The effective weir length resulting from h_{ow} (assumed) gives rise
to shorter weir crest $h_{ow} = 0.02455$ m   2$^{\text{ND}}$ APPROXIMATION

$$\left(\frac{l_{w,eff}}{0.98}\right)^2 = \left(\frac{1.4}{0.98}\right)^2 - \left\langle\left[\left(\frac{1.4}{0.98}\right)^2 - 1\right]^{0.5} + \frac{2\,(0.02455)}{1.4} \cdot \frac{1.4}{0.98}\right\rangle^2$$

$$= 0.89525$$

$$\therefore \quad l_{w,eff} = 0.927255 \text{ m}$$

$$\therefore \quad h_{ow} = 0.666 \left(\frac{6.5556 \times 10^{-3}}{0.927255}\right)^{2/3} = 0.02453 \text{ m}$$

$$\therefore \quad h_{ow} = 24.53 \text{ mm} \qquad\qquad\qquad \textbf{OK}$$

Weir height

$$h_w = 50 \text{ mm} = 0.05 \text{ m} \qquad \text{Let's take}$$

Dry Pressure Drop

$$d_o = 4.5 \text{ mm}$$

$$\delta_p = 2 \text{ mm} \qquad \text{Let's take}$$

$$C_o = 1.09 \left(\frac{4.5}{2}\right)^{1/4} = 1.33497 \qquad \text{Eqn. 3.2}$$

$$\Lambda = 12 \text{ m} \qquad \text{Let's take}$$

$$\frac{A_o}{A_a} = 0.907 \left(\frac{4.5}{12}\right)^2 = 0.127546 \qquad \text{Eqn. 5.7}$$

$$A_o = 0.127546\,(0.96058) = 0.122518 \text{ m}^2$$

$$v_{G,o} = \frac{Q_{v,G}}{A_o} = \frac{4.6406}{0.122518} = 37.8765 \text{ m/s}$$

$$\mu_G = 12.5 \times 10^{-6} \text{ Pa.s}$$

$$(Re_G)_{hole} = \frac{v_{G,o} \cdot d_o \cdot \rho_G}{\mu_G} = \frac{37.8765\,(0.0045)\,(0.67878)}{12.5 \times 10^{-6}} = 9255$$

At this value of Reynolds Number, the value of Fanning's friction factor :

$$f = 0.0078$$

Fig. 5.26 / Chemical Engineers' Handbook (5th ISE) — R.H. Perry & C.B. Chilton (McGraw-Hill)

$$h_d = 1.33497 \left[0.4 \left(1.25 - \frac{0.122518}{1.391} \right) + 4(0.0078) \left(\frac{2}{4.5} \right) + \left(1 - \frac{0.122518}{1.391} \right)^2 \right] \times \frac{(37.8765)}{2(9.81)} \cdot \frac{0.67878}{961}$$

$$= 0.09033$$

Hydraulic Head

$$h_w = 0.05 \text{ m} \qquad\qquad \text{see above}$$

$$v_{G,a} = \frac{Q_{v,G}}{A_a} = \frac{4.6406}{0.96058} = 4.8310 \text{ m/s}$$

$$z = \frac{1}{2}[D_t + l_w] = \frac{1}{2}[1.4 + 0.98] = 1.19 \text{ m}$$

$$h_L = 0.0061 + 0.725 (0.05) - 0.238(0.05)(4.831)\sqrt{0.67878} + 1.225 \left(\frac{6.5556 \times 10^{-3}}{1.19} \right) \qquad \text{Eqn. 3.6}$$

$$= 0.001734 \text{ m of clear liquid}$$

Residual Pressure Drop

$$d_b \approx d_o$$

$$h_R = \frac{6(0.058)}{0.0045} \cdot \frac{1}{961(9.81)} = 0.008203 \text{ m of cl. liq} \qquad \text{[Eqn. 3.10]}$$

Total Gas Pressure Drop

$$h_{G-L} = 0.09033 + 0.001734 + 0.008203 \qquad \text{[Eqn. 3.11]}$$
$$= 0.100267 \text{ m of cl. liq}$$

Head Loss Under Downcomer

$$l_w = 0.98 \text{ m}$$
$$h_w = 0.05 \text{ m}$$
$$\therefore \qquad A_{da} = 0.98 (0.05 - 0.025) = 0.0245 \text{ m}^2 \qquad \text{[Eqn. 3.12]}$$

Since $A_{da} < A_d$, the head loss under downcomer apron is

$$h_{da} = 0.165 \left[\frac{6.5556 \times 10^{-3}}{0.0245} \right]^2 \qquad \text{[Eqn. 3.13]}$$

$$= 0.011813 \text{ m of cl. liq}$$

Downcomer Backup

Ignoring hydraulic gradient factor (h_{hg}),

$$h_{dc} = 0.100267 + 0.05 + 0.02453 + 0.011813 \qquad \text{[Eqn. 5.13]}$$
$$= 0.18661 \text{ m of cl. liq}$$

$$h_{dc} = 0.100267 + 0.011813 \qquad \text{[Eqn. 5.13 A]}$$
$$= 0.11208 \text{ m of clear liq}$$

Check For Downflow Flooding

Use Eqn. 4.14 :

$$h_{dc} + h_w + h_{ow} + h_{hg} < \frac{1}{2} \, l_t \qquad \text{[Eqn. 5.14]}$$

$$h_{dc} = 0.11208 \text{ m of clear liq} \qquad \text{[Eqn. 5.13 A]}$$

$\therefore \qquad h_{dc} + h_w + h_{ow} + h_{hg} = 0.18661 \text{ m of cl. liq} \qquad \textbf{[Ignoring } h_{hg}\textbf{]}$

$$\frac{1}{2} \, l_t = \frac{1}{2} \, (0.6) = 0.3 \text{ m}$$

Therefore tray spacing is safely above the total liq level in the downcomer. Hence the design is safe.

Use Eqn. 4.14 A :

$$h_{dc} < \frac{1}{2} \, (l_t + h_w) \qquad \text{[Eqn. 5.14 A]}$$

$$h_{dc} = 0.18661 \text{ m of cl. liq}$$

$$\frac{1}{2} \, (l_t + h_w) = \frac{1}{2} \, (0.6 + 0.05) = 0.325 \text{ m}$$

$\therefore \qquad h_{dc} = 0.18661 \text{m} < \frac{1}{2} \, (l_t + h_w)$

Hence the column has been sized to avoid excessive liq backup, *i.e.*, the design is safe.

Check For Weeping

For $\qquad\qquad l_w = 70\% \, D_t$, the weir distance from the center of the tray

$$\frac{1}{2} Z = 35.62\% \, D_t \qquad \text{[Table 5.6]}$$

$$= 0.49868 \text{ m}$$

$\therefore \qquad Z = 2 \, (0.49868) = 0.99736 \text{ m}$

$$\left[\frac{\mu_G^2 \cdot \rho_L}{\sigma \cdot \rho_G^2 \cdot d_o} \right]^{0.379} = \left[\frac{\left(12.5 \times 10^{-6}\right)^2 961}{0.058(0.67878)^2 (0.0045)} \right]^{0.379} = 0.079351$$

$$\left[\frac{\delta_p}{d_o}\right]^{0.293} = \left[\frac{2}{4.5}\right]^{0.293} = 0.788516$$

$$\frac{2}{\sqrt{3}} \cdot \frac{A_a \cdot d_o}{\Delta^3} = \frac{2}{\sqrt{3}} \cdot \frac{0.96058(0.0045)}{(0.012)^3} = 2888.4954$$

$$\frac{2.8}{[Z/d_o]^{0.724}} = \frac{2.8}{[0.99736/0.0045]^{0.724}} = 0.05609$$

$$[v_{G,o}]_{weep} = 0.023 \frac{0.058}{12.5 \times 10^{-6}} [0.079351] [0.788516] [2888.4954]^{0.05609}$$

[Eqn. 5.16]

$$= 10.4404 \text{ m/s}$$

Now the gas velocity thru holes (37.8765 m/s) is well above the highest hole-velocity of the gas to cause deleterious weeping. So the design is safe from weepage.

Check For Entrainment

For stable operation of the column, we've taken maximum operating gas velocity

$$v_G = 80\% \ v_{G,fl}$$

$\therefore$
$$\frac{v_G}{v_{G,fl}} = 0.8$$

$$\frac{L'}{G'} \cdot \left[\frac{\rho_G}{\rho_L}\right]^{\frac{1}{2}} = 0.05315 \qquad \text{[See above]}$$

$$\psi = 0.068 \qquad \text{[From Fig. 5.9]}$$

Recycling of liq due to this small 'fractional entrainment' is too meagre to influence the tray hydraulics.

The above design is safe provided the col. operates in the range of stated operating conditions.

Result

Tower dia	= 1400 mm
Active area	= 0.96058 m²
Downcomer area	= 0.13546 m²
Weir length	= 980 mm
Weir crest	= 24.53mm
Weir height	= 50 mm
Weir spacing from the tray-center	= 498.7 mm
Tray spacing	= 600 mm

Tray sheet thickness	= 2 mm
Hole dia	= 4.5 mm
Hole layout	= equilateral-triangular
Hole pitch	= 12 mm
Hole area	= 0.122518 m^2

SIEVE-TRAY STRIPPER DESIGN

Problem 5.2 : A sieve-tray tower is to be designed for stripping a dilute aqueous solution of methanol with steam. The design conditions specified are :

Operating temperature	*= 368K*
Operating pressure	*= 101.325 kPa*
LIQUID	
Rate	*= 900 kmol/h*
Composition	*= 15% (mass) methanol (CH$_3$OH)*
Surface tension	*= 0.04 N/m*
Density	*= 961 kg/m^3*
GAS	
Rate	*= 360 kmol/h*
Composition	*: 18% (mol) methanol*
Dynamic viscosity	*= 12.5 × 10^{-6} Pa.s*

Design a suitable crossflow sieve-tray tower.

Ans.

Tower dia	=	1250 mm
Active area	=	0.82711 m^2
Hole area	=	0.10545 m^2
Weir height	=	50 mm
Weir length	=	875 mm
Weir spacing from the tray-center	=	445 mm
Tray spacing	=	500 mm
Tray thickness	=	2 mm
Downcomer area	=	0.10799 m^2
Hole dia	=	4.5 mm
Hole pitch	=	12 mm
Hole layout	=	equilateral-triangular

Hints :

Liquid

Av. mol wt. = 19.2642 kg/kmol

ρ_L = 961 kg/m^3

$$\dot{L}_M = 900 \text{ kmol/h}$$

$$Q_{v,L} = \frac{(900/3600)\dfrac{\text{kmol}}{\text{s}} \cdot (19.2642)\dfrac{\text{kg}}{\text{kmol}}}{961\dfrac{\text{kg}}{\text{m}^3}} = 5.0114 \times 10^{-4} \text{ m}^3/\text{s}$$

Gas

Av. mol. wt. $= 20.52 \text{ kg/kmol}$

$$\rho_G = 0.67928 \text{ kg/m}^3$$

$$\dot{G}_M = 360 \text{ kmol/h}$$

$$Q_{v,G} = \left(\frac{360}{3600}\right)\frac{\text{kmol}}{\text{s}} \cdot (22.41)\frac{\text{m}^3}{\text{kmol}} \cdot \left(\frac{368}{273}\right)\frac{\text{K}}{\text{K}} = 3.0208 \text{ m}^3/\text{s}$$

Perforations

Take $d_o = 4.5 \text{ mm}$; $\delta_p = 2 \text{ mm}$; $\Delta = 12 \text{ mm}$

$$\frac{A_o}{A_a} = 0.1275 > 0.1 \qquad\qquad\qquad\qquad\qquad\qquad \text{[Eqn. 5.7]}$$

Tower Dia

Take tray spacing, $l_t = 500 \text{ mm}$

$$\frac{L'}{G'} \cdot \left[\frac{\rho_G}{\rho_L}\right]^{\frac{1}{2}} = 0.06239$$

$$\alpha = 0.04893 \qquad\qquad\qquad\qquad\qquad\qquad\qquad \text{[Eqn. 5.5]}$$
$$\beta = 0.0302 \qquad\qquad\qquad\qquad\qquad\qquad\qquad\quad \text{[Eqn. 5.6]}$$
$$C_F = 0.07913 \qquad \text{[Eqn. 5.4]}$$

$$v_{G,fl} = 3.981\,(0.07913)\left[\frac{961 - 0.67928}{0.67928}\right]^{\frac{1}{2}}\left[\frac{0.04}{20}\right]^{0.2}$$

$$= 3.4176 \text{ m/s} \qquad\qquad\qquad\qquad\qquad \text{[Eqn. 5.2 A]}$$

Take, $v_G = 80\% \text{ of } v_{G,fl} = 2.73408 \text{ m/s}$

$$A_n = 1.10486 \text{ m}^2$$

$$l_w = 70\% \text{ of } D_t$$

$$A_t = \frac{1.10486}{1 - 0.088} = 1.211479 \text{ m}^2$$

$$D_t = 1.2419 \text{ m}$$

Take

$$D_t = 1.25 \text{ m}$$
$$A_t = 1.22718 \text{ m}^2$$
$$l_w = 0.875 \text{ m}$$
$$A_d = 0.088 \, (A_t) = 0.10799 \text{ m}^2$$
$$A_a = A_t - 2A_d - 15\% \, A_t = 0.82711 \text{ m}^2$$

Weir Height and Weir Crest

$$h_{ow} = 25 \text{ mm}$$ **[Tentative]**

$$\left[\frac{l_{w,eff}}{0.875}\right]^2 = 0.8801399$$ [Eqn. 5.12]

$\therefore$ $$l_{w, eff} = 0.82088$$

$$h_{ow} = 0.666 \left[\frac{5.0114 \times 10^{-3}}{0.82088}\right]^{2/3} = 0.02225 \text{ m}$$ [Eqn. 5.11]

Let $$h_{ow} = 0.02225 \text{ m}$$ [2ND APPROXIMATION]

$$\left[\frac{l_{w,eff}}{0.875}\right]^2 = 0.893644$$ [Eqn. 5.12]

$\therefore$ $$l_{w, eff} = 0.82716 \text{ m}$$
$$h_{ow} = 0.02213 \text{ m}$$ [Eqn. 5.11]
$$h_{ow} = 22 \text{ mm}$$ Ans.
$$h_w = 50 \text{ mm}$$ [TAKE]

Dry Pressure Drop

$$C_o = 1.33497$$
$$A_o = 0.10545 \text{ m}^2$$ [Eqn.3.2]
$$v_{G, o} = 28.6449 \text{ m/s}$$

$$Re_{G, o} = \frac{v_{G,o} \cdot d_o \cdot \rho_G}{\mu_G} = 7004.86$$

f = 0.0084 [*Fig. 5.26*/ Chemical Engineers Handbook (5th ISE) – R. H. Perry and C. B. Chilton]

$$0.4 \left(1.25 - \frac{A_o}{A_n}\right) = 0.461823$$

$$4f \left(\frac{\delta_p}{d_o}\right) = 0.014933$$

$$\left(1 - \frac{A_o}{A_n}\right)^2 = 0.81822$$

$$\frac{v_{G,o}^2}{2g} \cdot \frac{\rho_G}{\rho_L} = 0.02956$$

$\therefore$ $h_d = 1.33497 \,[0.4618232 + 0.014933 + 0.81822]\, 0.02956$

                                                                                    [Eqn. 3.1]

$$= 0.05110 \text{ m of cl. liq}$$

Hydraulic Head

$$v_{G,a} = Q_{v,G}/A_a = 3.6522 \text{ m/s}$$

$$z = \frac{1}{2}[D_t + l_w] = 1.0625 \text{ m}$$

$$h_L = 0.01230 \text{ m of cl. liq} \qquad\qquad [\text{Eqn. 3.6}]$$

Residual Pressure Drop

$$h_R = 5.657 \times 10^{-3} \text{ m of cl. liq} \qquad\qquad [\text{Eqn. 3.10}]$$

Total Gas-Pressure Drop

$$h_{G-L} = 0.06905 \text{ m of cl. liq} \qquad\qquad [\text{Eqn. 3.5}]$$

Head Loss Under Downcomer

$$A_{da} = 0.82711\,(0.05 - 0.025) = 0.020677 \text{ m}^2 < A_d \qquad\qquad \text{Eqn. 3.12}]$$

$\therefore$ $h_{da} = 0.00969 \text{ m of cl. liq} \qquad\qquad [\text{Eqn. 3.11}]$

Downcomer Backup

$$h_{dc} = 0.15074 \text{ m of clear liq} \qquad\qquad [\text{Eqn. 5.13}]$$

$$\frac{1}{2}(l_t + h_w) = 0.275 \text{ m}$$

$\therefore$ $h_{dc} < \frac{1}{2}(l_t + h_w) \qquad\qquad [\text{Eqn. 5.14 A}]$

Therefore, the design is safe from downflow-flooding point of view.

Check on Weeping

$$l_w = 70\% \ D_t$$

$$\frac{1}{2}\,Z = 0.445 \text{ m} \qquad\qquad [\text{Table 5.6}]$$

$$\left[\frac{\mu_G^2 \cdot \rho_L}{\sigma \cdot \rho_G^2 \cdot d_o}\right]^{0.379} = 0.091299$$

$$\left[\frac{\delta_p}{d_o}\right]^{0.293} = 0.788516$$

$$\frac{2}{\sqrt{3}} \cdot \frac{A_a \cdot d_o}{\Delta^3} = 2487.146$$

$$\frac{2.8}{\left[Z/d_o\right]^{0.724}} = 0.06089$$

$\therefore$ $[v_{G,o}]_{weep} = 8.5294$ m/s   **[Eqn. 5.18]**

$\therefore$ $v_{G,o} >> v_{G,o}]_{weep}$

Hence under prescribed operating conditions, the tower so designed is free from deleterious effect of weeping.

Check on Entrainment

$$\frac{v_G}{v_{G,fl}} = 0.8 \qquad\qquad\qquad \psi = 0.05 \qquad\qquad \textbf{[Fig. 5.9]}$$

$$\left[\frac{L'}{G'}\right]\left[\frac{\rho_G}{\rho_L}\right]^{\frac{1}{2}} = 0.06239 \quad \left.\right\} \text{ Hence entrainment is negligible}$$

Conclusion : Hence the tower design is safe from the standpoint of assigned operating conditions.

Sieve-Tray Absorber Design

Example 5.3 Design a suitable sieve-tray absorption tower to absorb principally the butane with a hydrocarbon oil from a gas mixture containing methane (CH₄), propane (C₃H₉) and butane (C₄H₁₀).

The operating conditions at the bottom of the tower are :

Pressure   *= 350 kPa*

Temperature   *= 311K*

Design the absorber at these conditions.

GAS

Rate   *= 900 kmol/h*

Composition : 85 vol% CH₄ + 10 vol% C₃H₈ + 5 vol% C₄H₁₀

μ_{CH_4} *= 11.3 × 10⁻⁶ Pa.s*

$\mu_{C_3H_8}$ *= 8.5 × 10⁻⁶ Pa.s* *at operating conditions*

$\mu_{C_4H_{10}}$ *= 8.7 × 10⁻⁶ Pa.s*

LIQUID

Rate	*= 540 kmol/h*
Average mol. wt.	*= 150 kg/kmol*
Density	*= 849 kg/m³*
Surface tension	*= 0.025 N/m*

Solution :

Liquid

Rate, $\dot{L}_M$ = 540 kmol/h = 0.15 kmol/s

Density, ρ_L = 849 kg/m³

Surface tension, σ_L = 0.025 N/m

Av. mol. wt., M_L = 150 kg/kmol

Vol. flowrate, $Q_{v,\,L} = \dfrac{0.15\left(\dfrac{kmol}{s}\right)150\left(\dfrac{kg}{kmol}\right)}{849\left(\dfrac{kg}{m^3}\right)} = 0.0265$ m³/s

Gas

μ_{CH_4} = 11.3 × 10⁻⁶ Pa.s

$\mu_{C_3H_8}$ = 8.5 × 10⁻⁶ Pa.s

$\mu_{C_4H_{10}}$ = 8.7 × 10⁻⁶ Pa.s

y_{CH_4} = 0.85

$y_{C_3H_8}$ = 0.10   **cf. vol% = mol%**

$y_{C_4H_{10}}$ = 0.05

$\mu_{mix} = \dfrac{\sum y_i . \mu_i . \sqrt{M_i}}{\sum y_i . \sqrt{M_i}}$

$= \dfrac{0.85\left(11.3 \times 10^{-6}\right)\sqrt{16} + 0.10\left(8.5 \times 10^{-6}\right)\sqrt{44} + 0.05\left(8.7 \times 10^{-6}\right)\sqrt{58}}{0.85\sqrt{16} + 0.10\sqrt{44} + 0.05\sqrt{58}}$

= 10.66 × 10⁻⁶ Pa.s.

M_{CH_4} = 16 kg/kmol ; $M_{C_3H_8}$ = 44 kg/kmol ; $M_{C_4H_{10}}$ = 58 kg/kmol

Av. mol. wt. M_G = 0.85 (16) + 0.10 (44) + 0.05 (58) = 20.9 kg/kmol

$\rho_G = \rho_o . \dfrac{P}{P_o} . \dfrac{T_o}{T} = \dfrac{20.9}{22.41} . \dfrac{350}{101.325} . \dfrac{273}{311} = 2.8278$ kg/m³

Rate, $\dot{G}_M$ = 900 kmol/h = 0.25 kmol/s

Vol. flowrate, $Q_{v,G} = 0.25 \left(\dfrac{kmol}{s} \right) 22.41 \left(\dfrac{m^3}{kmol} \right) \cdot \dfrac{311}{273} \left(\dfrac{K}{K} \right) = 6.3823 \text{ m}^3/\text{s}$

Perforations

Select : hole dia., $d_o = 5\text{mm}$

plates thickness, $\delta_p = 2.5\text{mm}$

hole layout $= \text{equilateral triangular}$

hole pitch $= 14 \text{ mm}$

Tower Dia

$$\frac{A_o}{A_a} = 0.907 \left[\frac{5}{14} \right]^2 = 0.11568 > 0.1 \qquad\qquad \text{[Eqn. 5.7]}$$

$$\frac{L'}{G'} \cdot \left[\frac{\rho_G}{\rho_L} \right]^{\frac{1}{2}} = \left[\frac{Q_{v,L} \cdot \rho_L / A_n}{Q_{v,G} \, \rho_G / A_n} \right] \cdot \left[\frac{\rho_G}{\rho_L} \right]^{\frac{1}{2}} = \left[\frac{Q_{v,L}}{Q_{v,G}} \right] \cdot \left[\frac{\rho_L}{\rho_G} \right]^{\frac{1}{2}}$$

$$= \frac{0.0265}{6.3823} \cdot \left[\frac{849}{2.8278} \right]^{\frac{1}{2}}$$

$$= 0.07194$$

Tray spacing, $l_t = 600 \text{ mm} = 0.6 \text{ m}$ [Tentative]

$\alpha = 0.0744 \, (0.6) + 0.01173 = 0.05637$ [Eqn. 5.5]

$\beta = 0.0304 \, (0.6) + 0.015 = 0.03324$ [Eqn. 5.6]

Capacity Factor, C_F :

$$[L'/G'] \, [\rho_G/\rho_L]^{0.5} > 0.1, \text{ so we'll take} \left[\frac{L'}{G'} \right]\left[\frac{\rho_G}{\rho_L} \right]^{\frac{1}{2}} = 0.1$$

$$\sigma = 0.025 \text{ N/m}$$

$\therefore$ $C_F = 0.05637 \log \left(\dfrac{1}{0.1} \right) + 0.03324 = 0.08961$ [Eqn.5.4]

Aliter : $3.981 \, C_{F,fl} = 0.34 \, (\text{Fig 5.1})$

$\therefore$ $C_{F,fl} = 0.0854$ which closely approaches the value of capacity factor at floodpoint obtained from Eqn. 5.4

Flooding velocity :

$$v_{G,fl} = 3.981 \, C_{F,fl} \left[\frac{\rho_L - \rho_G}{\rho_G} \right]^{\frac{1}{2}} \cdot \left[\frac{\sigma}{20} \right]^{0.2} \qquad\qquad \text{[Eqn. 5.2 A]}$$

$$= 3.981 \ (0.08961) \left[\frac{849 - 2.8278}{2.8278}\right]^{\frac{1}{2}} \cdot \left[\frac{0.025}{20}\right]^{0.2}$$

$$= 1.6208 \ \text{m/s}$$

Maximum allowable gas velocity :

$$v_G = 80\% \ v_{G,\,fl}$$
$$= 0.8 \ (1.6208)$$
$$= 1.29664 \ \text{m/s}$$

Net tower cross-sectional area for gas flow :

$$A_n = \frac{Q_{v,G}}{v_G} = \frac{6.3823}{1.29664} = 4.9221 \ \text{m}^2$$

Weir length, $l_w = 65\% \ D_t$ [Tentative]

Tray area occupied by one downcomer = 6.899% of A_t

Tower cross-sectional area :

$$A_t = A_n + A_d = A_n + 0.06899 \ A_t$$

or, $$A_t = \frac{A_n}{1 - 0.06899} = \frac{4.9221}{1 - 0.06899} = 5.28692 \ \text{m}^2$$

∴ **Tower dia :**

$$D_t = \left[\frac{4}{\pi}(5.28692)\right]^{\frac{1}{2}} = 2.5945 \ \text{m} \approx 2.60 \ \text{m}$$ [Say]

∴ $$A_t = \frac{\pi}{4}(2.6)^2 = 5.30929 \ \text{m}^2$$ [Corrected]

Weir Length

$$l_t = 0.65 \ D_t = 0.65 \ (2.60) = 1.69\text{m}$$

Downcomer Area of Cross-Section

$$A_d = 6.899\% \ A_t$$
$$= 0.06899 \ (5.30929)$$
$$= 0.36628 \ \text{m}^2$$

Active Area

$$A_a = A_t - 2A_d - \text{Area taken by [Tray Support + Disenga-}$$
$$\text{gement Zone + Distributing Zone)}$$
$$= A_t - 2A_d - 20\% \ A_t$$
$$= 0.8 \ A_t - 2A_d$$
$$= 0.8(5.30929) - 2(0.36628)$$
$$= 3.51485 \ \text{m}^2$$

Height of Crest Over The Weir

$$h_{ow} = 25mm \qquad \text{[Tentative]}$$

$$\left[\frac{l_{w,eff}}{1.69}\right]^2 = \left[\frac{2.6}{1.69}\right]^2 - \left\langle \left[\left(\frac{2.6}{1.69}\right)^2 - 1\right]^{0.5} + 2\frac{(0.025)}{2.6}\cdot\frac{2.6}{1.69}\right\rangle^2 \qquad \text{[Eqn. 5.12]}$$

$$= 0.929945$$

$$\therefore \qquad l_{w,\,eff} = 1.6297 \text{ m}$$

Calculated value of weir-crest :

$$h_{ow} = 0.666\left[\frac{0.0265}{1.6297}\right]^{\frac{2}{3}} = 0.04274 \text{ m} \qquad \text{[Eqn.5.11]}$$

$$h_{ow} = 0.043m$$

$$\left[\frac{l_{w,eff}}{1.69}\right]^2 = \left[\frac{2.6}{1.69}\right]^2 - \left\langle \left[\left(\frac{2.6}{1.69}\right)^2 - 1\right]^{0.5} + \frac{2(0.04274)}{2.6}\cdot\frac{2.6}{1.69}\right\rangle^2$$

$$\therefore \qquad l_{w,\,eff} = 1.5846 \text{ m}$$

$$\therefore \qquad h_{ow} = 0.666\left[\frac{0.0265}{1.5846}\right]^{\frac{2}{3}} = 0.04355m \approx 43.55 \text{ mm} \qquad \text{[OK]}$$

$$\therefore \qquad l_{w,\,eff} = 1.5846 \text{ m}$$

Weir Height

$$h_w = 60 \text{ mm} = 0.06 \text{ m} \qquad \text{[Let's take]}$$

Dry Pressure Drop

$$d_o = 5 \text{ mm} ; \delta_p = 2.5 \text{ mm} \And \Delta = 14 \text{ mm}$$

$$C_o = 1.09\left[\frac{5}{2.5}\right]^{\frac{1}{4}} = 1.37060 \qquad \text{[Eqn. 3.2]}$$

$$\frac{A_o}{A_a} = 0.907\left[\frac{5}{14}\right]^2 = 0.11568 \qquad \text{[Eqn.5.7]}$$

$$\therefore \qquad A_o = 0.11568 \, A_a = 0.11568 \, (3.51485) = 0.406628 \text{ m}^2$$

$$v_{G,\,o} = \frac{Q_{v,G}}{A_o} = \frac{6.3823}{0.406628} = 15.6956 \text{ m/s}$$

$$\mu_G = 10.66 \times 10^{-6}\ Pa.s$$

$$[Re_G]_{hole} = \frac{v_{G,o} \cdot d_o \cdot \rho_G}{\mu_G} = \frac{15.6956(0.005)(2.8278)}{10.66 \times 10^{-6}} = 20819$$

At this value of Reynolds number, the value of Fanning's friction factor :

$$f = 0.0065 \qquad\qquad [\textit{Fig.}: 5.26/\textbf{Chemical Engineer's Hand}$$
$$\textbf{Book (5th ISE)--Perry and Chilton]}$$

$$\therefore \qquad h_d = 1.3706\left[0.4\left(1.25 - \frac{0.406628}{4.9221}\right) + 4(0.0065)\left(\frac{2.5}{5}\right) + \left(1 - \frac{0.406628}{4.9221}\right)^2\right]$$

$$\times \frac{(15.6956)^2}{2(9.81)} \cdot \frac{2.8278}{849} \qquad\qquad [Eqn.3.1]$$

$$= 0.07575\ m\ of\ clear\ liq$$

Hydraulic Head

$$h_w = 0.06m \qquad\qquad [\textbf{See above}]$$

Gas velocity thru active area :

$$v_{G,a} = \frac{Q_{v,G}}{A_a} = \frac{6.3823}{3.51485} = 1.81581\ m/s$$

$$z = \frac{1}{2}[D_t + l_w] = \frac{1}{2}(2.6 + 1.69) = 2.145\ m$$

$$h_L = 0.0061 + 0.725\ (0.06) - 0.238\ (0.06)\ (1.8158)\ \sqrt{2.8278} + 1.225\left(\frac{0.0265}{2.145}\right)$$

$$\qquad\qquad\qquad\qquad\qquad\qquad\qquad\qquad\qquad\qquad\qquad [Eqn.\ 3.6]$$

$$= 0.021030\ m\ of\ cl.\ liq \qquad\qquad [Eqn.\ 3.6]$$

Residual Pressure Drop

$$h_R = \frac{6(0.025)}{0.005} \cdot \frac{1}{849(9.81)} = 0.003602\ m\ of\ cl.\ liq$$

$$\qquad\qquad\qquad\qquad\qquad\qquad\qquad\qquad [Eqn.3.10]$$

Taking $\qquad\qquad d_b \approx d_o$

Total Gas-Pressure Drop

$$h_{G-L} = 0.07575 + 0.02103 + 0.0036 = 0.10038\ m\ of\ cl.\ liq$$

Head Loss Under Downcomer

$$l_w = 1.69\ m$$

$$h_w = 0.06m$$

$$\therefore \qquad A_{da} = 1.69\ (0.06 - 0.025) = 0.05915 m^2 \qquad\qquad [Eqn.\ 3.12]$$

Since $$A_{da} < A_d$$
$$[0.05915 \text{ m}^2] \, [0.36628 \text{ m}^2]$$

$$h_{da} = 0.165 \left[\frac{0.0265}{0.05915} \right]^2 = 0.03311 \text{ m of cl. liq} \qquad \text{[Eqn. 3.11]}$$

Downcomer Backup

Ignoring the hydraulic gradient (h_{hg})

$$h_{dc} = 0.10038 + 0.06 + 0.04355 + 0.03311 \qquad \text{[Eqn.5.11]}$$
$$= 0.2370478 \text{ m of cl. liq}$$

Check For Downflow Flooding

$$\frac{1}{2} (l_t + h_w) = \frac{1}{2} (1.69 + 0.06) = 0.875 \text{ m}$$

$$\therefore \qquad h_{dc} < \frac{1}{2}(l_t + h_w)$$

Hence the height of the downcomer liq is safely below the tray spacing even at maximum permissible gas velocity, *i.e.*, the design is safe from downcomer flood.

Check For Weeping

Now let us estimate the maximum gas velocity that will set in deleterious weeping.

For $\qquad l_w = 65\% \, D_t$, the weir distance from the center of the tray :

$$\frac{1}{2} Z = 25.16\% \, D_t \qquad \qquad \text{[Table 5.16]}$$

$$= 0.2516 \, (2.6) \text{ m}$$
$$= 0.65416 \text{ m}$$

$$\therefore \qquad Z = 1.30832 \text{ m}$$

$$\left[\frac{\mu_G^2 \cdot \rho_L}{\sigma \cdot \rho_G^2 \cdot d_o} \right]^{0.379} = \left[\frac{\left(10.66 \times 10^{-6}\right)(849)}{0.025(2.8278)^2(0.005)} \right]^{0.379} = 0.030072$$

$$\left[\frac{\delta_p}{d_o} \right]^{0.293} = \left[\frac{2.5}{5} \right]^{0.293} = 0.81620$$

$$\frac{2}{\sqrt{3}} \cdot \frac{A_a \cdot d_o}{\Delta^3} = \frac{2}{\sqrt{3}} \cdot \frac{3.51485(0.005)}{(0.014)^3} = 7395.4066$$

$$\frac{2.8}{[Z/d_o]^{0.724}} = \frac{2.8}{[1.30832/0.005]^{0.724}} = 0.04974$$

$$\therefore \quad [v_{G,\,o}]_{weep} = 0.023 \, \frac{0.025}{10.66 \times 10^{-6}} \, [0.030072] \, [0.8162] \, [7395.4066]^{0.04974}$$

$$= 2.0621 \text{ m/s}$$

At the given liq load, the trays will begin to weep if the gas velocity thru holes falls to 2.062 m/s or below.

But as per our design, the hole velocity is :

$$v_{G,\,o} = 15.6956 \text{ m/s} \gg [v_{G,\,o}]_{weep}$$

Therefore, the trays will not weep and the tower design is OK.

Check For Entrainment

For design purpose, we've taken maximum operating gas velocity equal to 80% of flood velocity, *i.e.*,

$$\left[\frac{v_G}{v_{G,fl}}\right] = 0.8$$

Also,

$$\frac{L'}{G'} \cdot \left[\frac{\rho_G}{\rho_L}\right]^{\frac{1}{2}} = 0.07194 \qquad\qquad \text{[See above]}$$

$$\therefore \qquad\qquad \psi = 0.04 \qquad\qquad\qquad \textbf{[Fig. 5.9]}$$

The fractional entrainment is just too small to affect tray hydraulics.

5.2 DESIGN OF VALVE TRAYS

The inherent design characteristics of valve trays make high-intensity gas-liq mass transfer operation possible almost the entire range of permissible column-load variation, at an approximately constant pressure drop thru the plates.

The efficiency of valve plates is higher than that of ordinary bubblecap trays and it is rather stable **[Fig. 5.10].**

Also the output per unit volume of columns fitted with valve trays is considerably higher than those fitted with ordinary bubblecap trays.

The valve trays give rise to more or less constant pressure drop over the entire range of operating gas velocity **(Fig. 5.11)**

They have high turndown ratio, as high as to 8 :

$$\textbf{Turndown ratio} = \frac{\textbf{Max. gas load}}{\textbf{Min. gas load}}$$

F-factor is also called **Capacity Factor.**

(Reinhard Billet — **Gauze-Packed Columns for Vacuum Distillation**

(Chemical Engineering Feb. 21/1972).
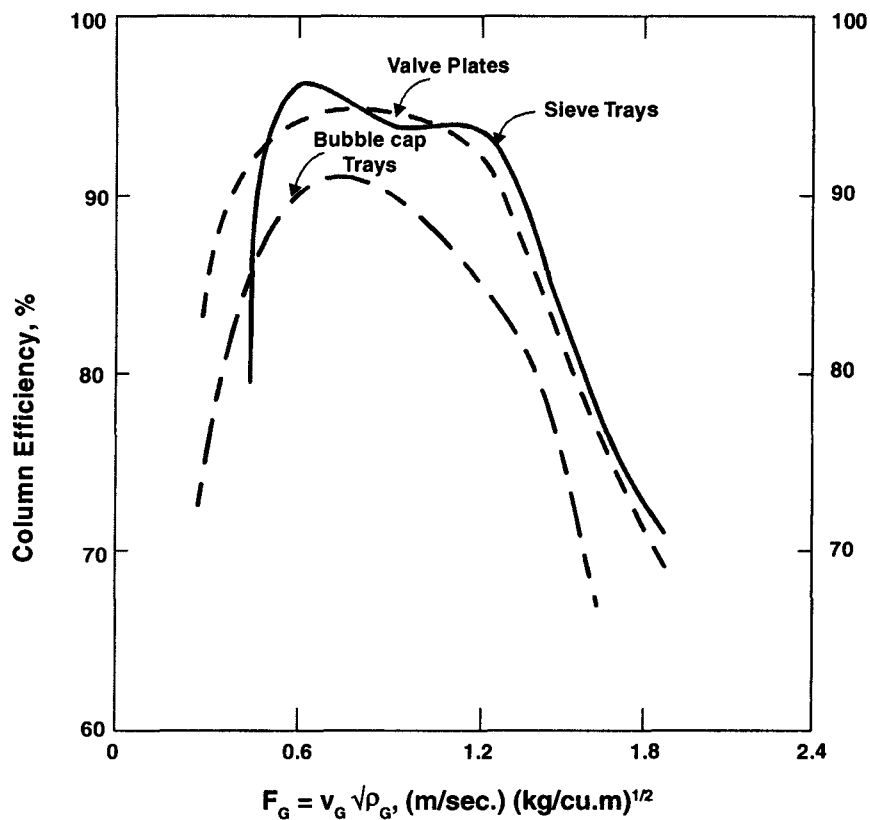
Fig. 5.10. *The Performance Profiles show that Valve TrayColumns Exhibit Higher and More Stable Column Efficiency than Bubblcap Trays.*
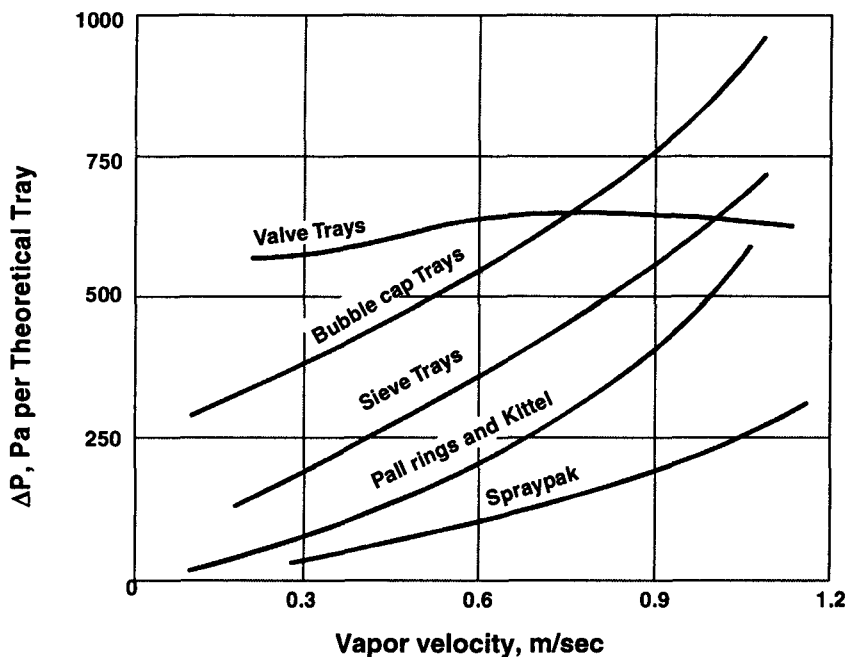
Fig. 5.11. *Pressure Drop-Efficiency Characteristics of Plates.*

Valve plates are available in single and multi-sector models which are selected on the basis of column dia :

Valve Tray Model	Column Dia
Single-sector valve tray	≤ 1.8 m
Double-sector valve tray	1.8 – 2.7
Triple-sector valve tray	2.7 – 3.6
Quadri-sector valve tray	> 3.6 m

The valves of different design are available. They cover the holes in the plate under gravity. In one such design, the valves are made in the shape of L-shaped plate covering the rectangular slots on the tray [**Fig. 5.12**].

(A) Valve fully closed   **(B) Valve partly open**

(C) Valve fully open

(A)   **(B)**
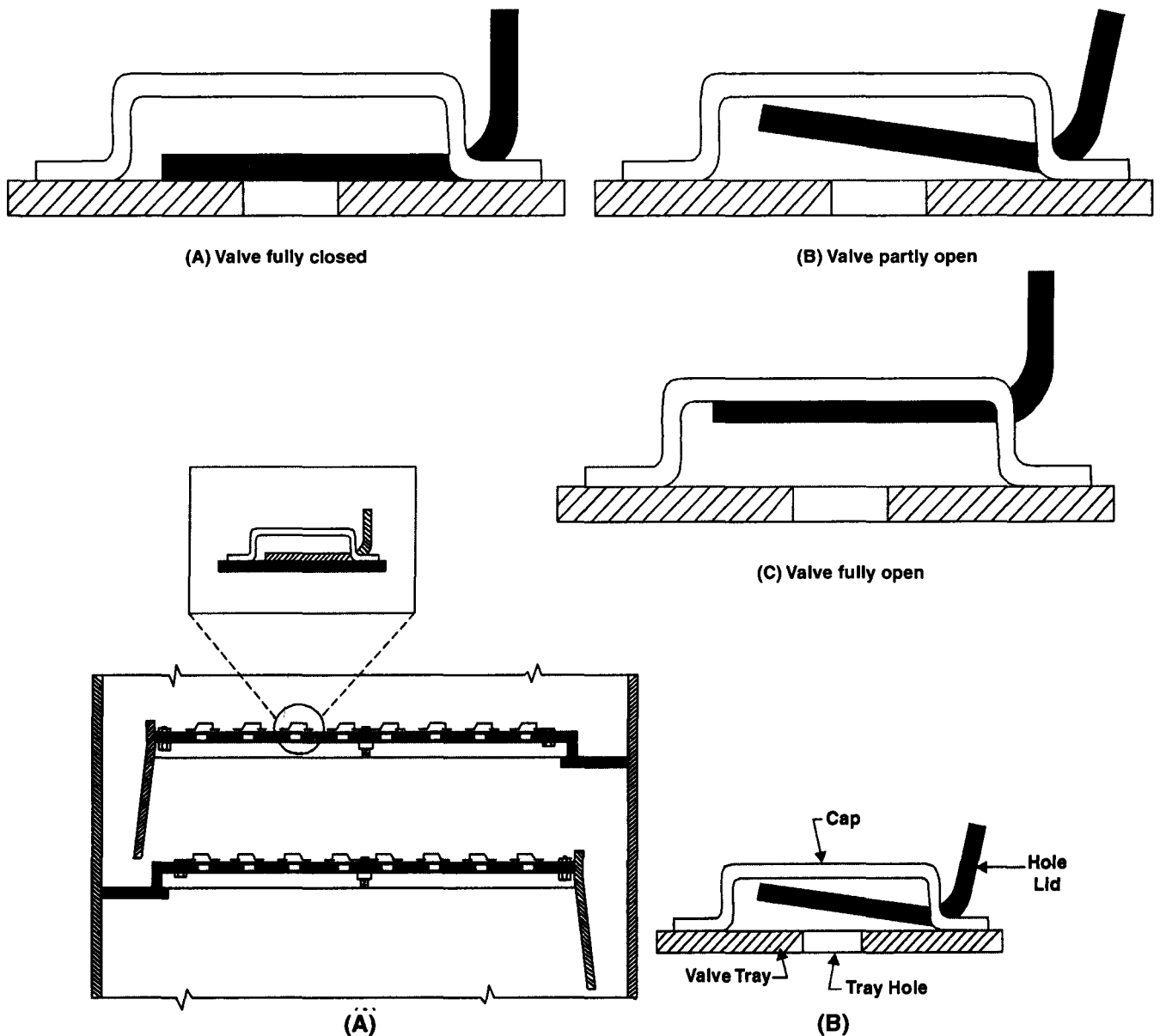
Fig. 5.12. *L-Shaped Valve.*

At very low gas rates the valve closes the slot due to gravity. With the increase of gas velocity, the gas lifts the lighter part of the valve creating an opening thru which the gas passes out and comes into contact with tray liquid. And ultimately at higher gas velocities the valves lift fully open.

There is another popular design : *disc valve fitted with a spider or guides*, e.g., **Flexi-tray plate** is valve tray (manufactured by *Koch Engineering Co.)* fitted with free-falling disc valves.

Active Area

For equilateral triangular layout, *i.e.*, valves occupying the corners of equilateral triangle, the **active area.**

$$A_a = 1.1 \left[\frac{\Delta}{d_v} \right]^2 A_o \qquad \qquad ...(5.7 \text{ A})$$

where, Δ = valve pitch, *i.e.*, center-.to-center distance between two consecutive valves, m

d_v = valve hole dia, m

A_o = area of perforations, m^2

Tray Area

The **tray area** is determined from the equation :

$$A_t = 1.2 \, [A_a + 2A_d] \qquad \qquad ...(5.19)$$

where, A_d = downcomer cross-sectional area^2

It is first determined tentatively on the basis of liq velocity of 0.1 m/s (**1st trial**) in the downcomer. Thereafter, A_d is defined more accurately settling the actual liq residence time in the downcomer (which should not be less than 5s)

Tray Spacing

The **tray spacing** is usually set equal to twice the downcomer backup :

$$l_t = 2h_{dc} \qquad \qquad ...(5.20)$$

This is to avoid downflow flooding and excessive entrainment.

l_t = tray spacing, m

h_{dc} = downcomer backup, m of clear liq

Downcomer Backup

The **height of gas-liq dispersion in the downcomer** is :

$$h_{dc} = \frac{1}{c} \, [\Delta P_{G-L} + h_w + h_{ow} + h_{hg}] \qquad \qquad ...(5.21)$$

where, c = coefficient of downcomer backup. Its value depends on the fraction of gas in the G-L dispersion and its foaming capacity.

= 0.5 —0.8

Weir Height

The **weir height** is usually set to 50mm. But under circumstances, where process demands longer liquid residence time on tray, weir height is extended up to 150mm.

Weir Length

The **length of the weir,** l_w is calculated from the weir equation:

$$h_{ow} = 3.7 \times 10^{-5} \left[\frac{Q_{m,L}}{l_w} \right]^{2/3}$$ ...(5.22)

where, $Q_{m,L}$ = liq rate, kg/h

l_w = weir length, m

h_{ow} = height of crest over the weir, m

Usually the weir-length should lie on the range

$$\frac{1}{2} D_t \leq l_w \leq 0.85 D_t$$

5.3. DESIGN OF BUBBLECAP TRAYS

Column Diameter

The bubblecap-tray column dia is calculated on the basis of superficial gas velocity :

$$D_t = \left[\frac{4Q_{v,G}}{\pi v_G} \right]^{\frac{1}{2}}$$ ...(5.23)

where, D_t = column dia, m

$Q_{v,G}$ = volumetric gas flowrate, m³/s

v_G = superficial gas velocity, m/s. It is also called empty column gas velocity forasmuch as it is the gas velocity when there is no liq flow in the column.

Downcomer Flooding

The column must be sized to guard against downflow flooding which occurs when the level of liquid in the downcomer reaches the top edge of the weir. It also corresponds to maximum loading of the downcomer.

The gas velocity at load ($v_{G,fl}$) can be calculated from Fair-Mathews Eqn. :

$$v_{G,fl} \left[\frac{\rho_G}{\rho_L - \rho_G} \right]^{\frac{1}{2}} = f \left[\frac{L'}{G'} \right] \left[\frac{\rho_G}{\rho_L} \right]^{\frac{1}{2}}$$ ...(5.24)

where, $v_{G,fl}$ = flooding velocity on the basis of net area of column cross-section

L' = mass rate of liq, kg/(h.m²)

G' = mass rate of gas, kg/(h.m²)

ρ_G = gas density, kg/m³

ρ_L = liq density, kg/m³

f = function

Source : I. Fair and R.L. Mathews — *Petroleum Refiner. vol. 37 (1958), No.4/P-153*

The Eqn. 5.24 can be solved with the aid of the chart [**Fig. 5.13**]
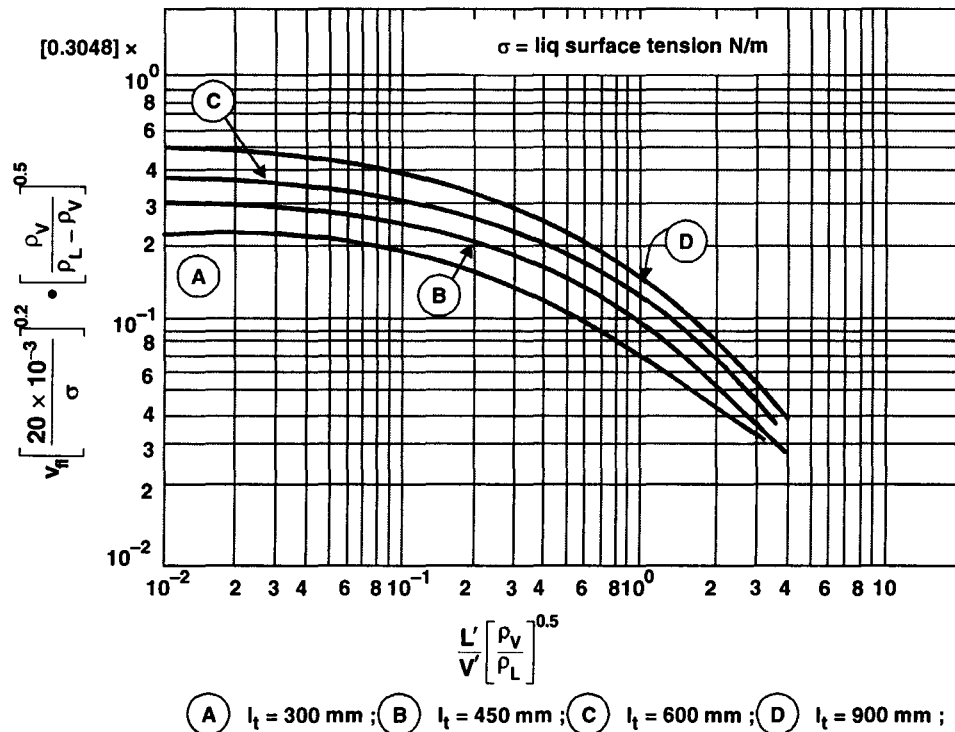
Fig. 5.13. *Calculating Flooding Velocity for Bubble cap Columns.*

The above chart is plotted on the basis of following assumptions :

1. Foaming is absent

2. $h_w < 15\%\ l_t$

3. Bubbling area prevails in the area between the weirs

Bubblecap Size

Bubblecaps come in two main types :

• *circular caps*

• *tunnel caps*

75 to 150mm dia caps are most common.

The circular caps sport rectangular or trapezoidal slots.

Because of design intricacy and fabrication difficulties, the cost of bubblecaps mounts with the reduction of cap size :

Bubblecap Dia (mm)	Relative Cost
150	1.00
100	1.20
75	1.35

Depending on the column dia, the caps of following sizes are recommended :

Column Dia (mm)	Bubblecap Size (Dia) Recommended
750 – 1200	75
1200 – 3000	100
3000 – 6000	150

Cap Layout

The caps are generally arranged on an equilateral triangular layout [**Fig. 5.14**].
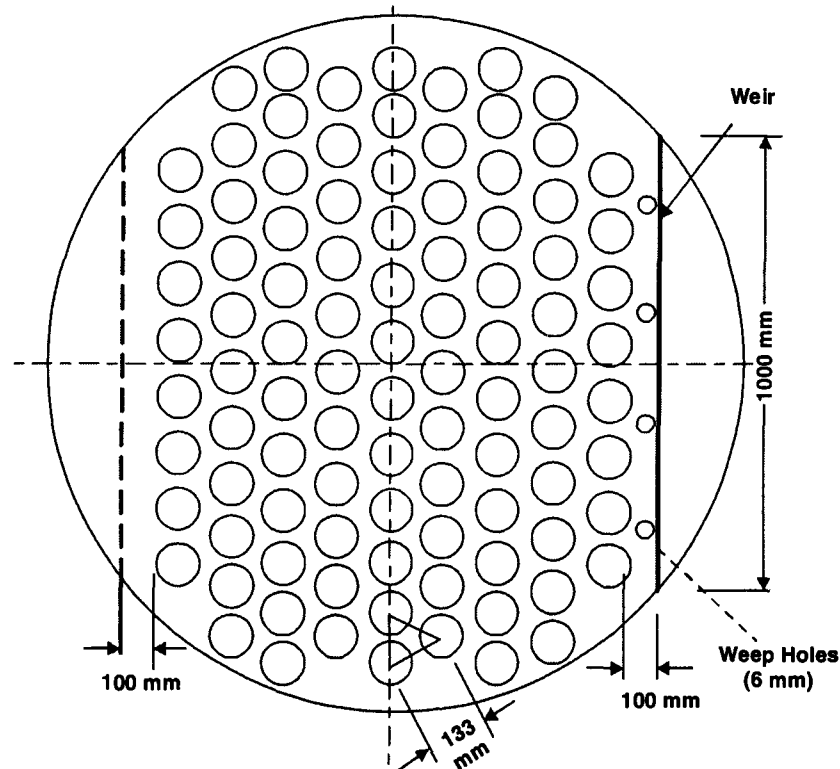
Fig. 5.14. *Bubblecap Layout.*

The caps are spaced 25 to 75mm apart. *Cap spacing should not be less than one cap dia plus 25mm*, in order to avoid impact of gas streams from the adjacent caps. In practice spacing varies from one cap dia + 25mm to one cap dia + 50mm.

Skirt Clearance : 12.5 – 38mm

Periphery Waste : It occurs due to inability to fit the cap layout to the circular form of the plate. The minimum distance from the cap to the column wall is 38mm and the distance from the cap to the weir is 75mm.

Cap Slots

Bubblecaps are provided with rectangular, trapezoidal or triangular slots thru which the gas disperses into the liquid.

Triangular slots ensure a greater opening and therefore sustain stable operation at very low loads. However, they are unfit for great loads. And as such their use is restricted.

Rectangular slots are the most suitable candidates for great loadings while trapezoidal slots approach closer to rectangular slots in service.

Slot Width (b_{sl}) : Recommended value = 3 – 12.5 mm

Fig. 5.15 Optimum value = 5.5 mm (approx)

Narrower the slots, higher the gas-liq interfacial area.
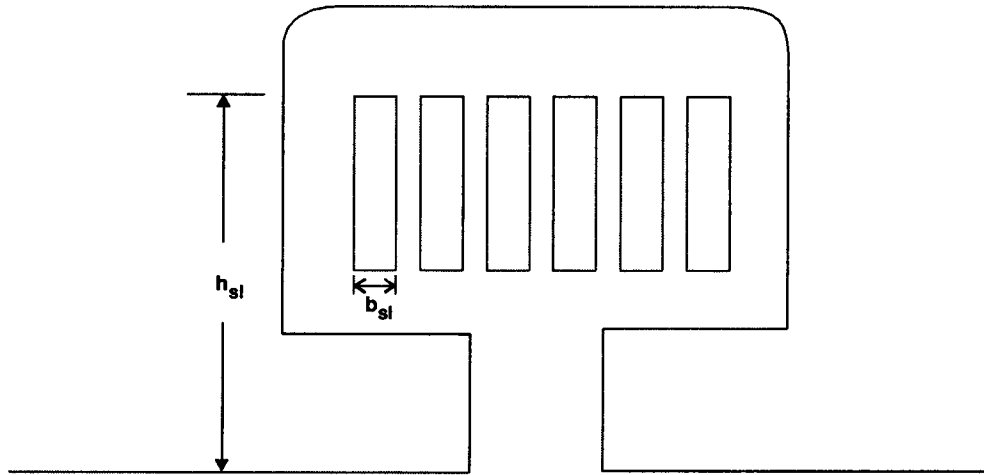
Fig. 5.15. *Slot Height and Width of A Bubblecap.*

Slot Height (h_{sl}) : **Recommended value = 12.5 – 50mm**

Slot height is determined by two factors

• **capacity of column**

• **plate performance**

While the lower limit is imposed by column capacity (small h_{sl} *values reduce the capacity of column*) the upper limit is restricted by the hydrodynamics of plate performance.

Bubblecap Dia (mm)	Slot Height (h_{sl}) (mm)
75	25
100	32
150	38

Risers

The size of the risers is determined after the size of the bubblecaps has been selected.

Smaller the riser dia, higher is the resistance to gas flow thru the riser but lower is the pressure drop thru the annular clearance between the riser and bubblecap. In likewise fashion, large dia risers yield opposite results. Therefore, the optimum value of riser dia is selected on the basis of

$$\frac{A_{an}}{A_r} = 1.1 - 1.4$$

where,A_{an} = area of cross-section of the annular space between the riser and the cap, m^2 (**Fig. 5.16**).

A_r = cross-sectional area of the riser, m^2 (**Fig. 5.16**).
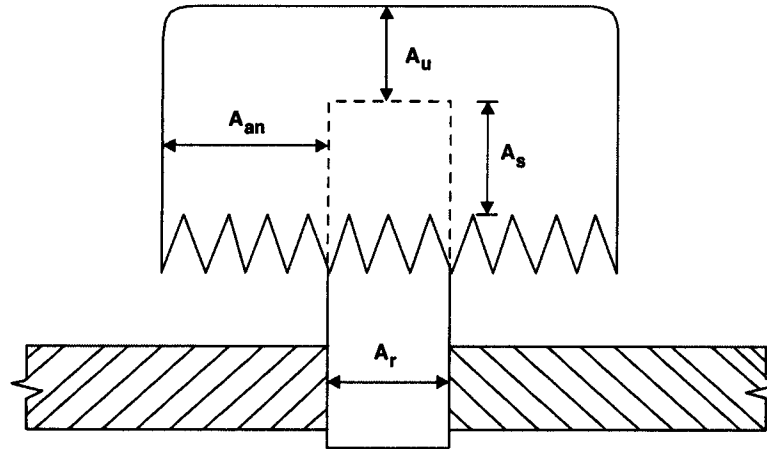
Fig. : 5.16. *Cross-Sectional Area of Riser and Annular Area Between Riser and Cap.*

For absorption columns, the tower area is taken equal to 6 – 12% of cross-sectional area of the tower (A_t).

Active Area

For cross-flow trays with a chord weir equal to 75% of the dia, some typical values of the fraction of the total cross-sectional area available for gas dispersion and contact with the liquid phase are given below :

Table 5.7 Active Area For Bubblecap Trays

Column Dia (mm)	*Cap Dia* (mm)	*Active Area, A_a* [% of Tower Cross-Section, $\frac{A_a}{A_t} \times 100$]
900	75	60
1200	100	57
1800	100	66
2400	100	70
3000	150	74

Weir Height

Weir Height is set within the range of
25 — 50mm

Liquid Seal

The bubblecap trays have an inbuilt liquid seal system preventing liq drainage at low gas rates.

With small liq rates, seals should be provided at the spot where the downspout is introduced into the plate below (a recess about 10mm deep).

ENTRAINMENT FLOODING

The column must be designed to avoid entrainment flooding at highest permissible gas rate.

Entrainment (fractional entrainment, ψ) is estimated from ψ vs. $v_G/v_{G,\,fl}$ plot in which $(L'/G')(\rho_G/\rho_L)^{1/2}$ appears as the curve parameter **(Fig. 5.17).**
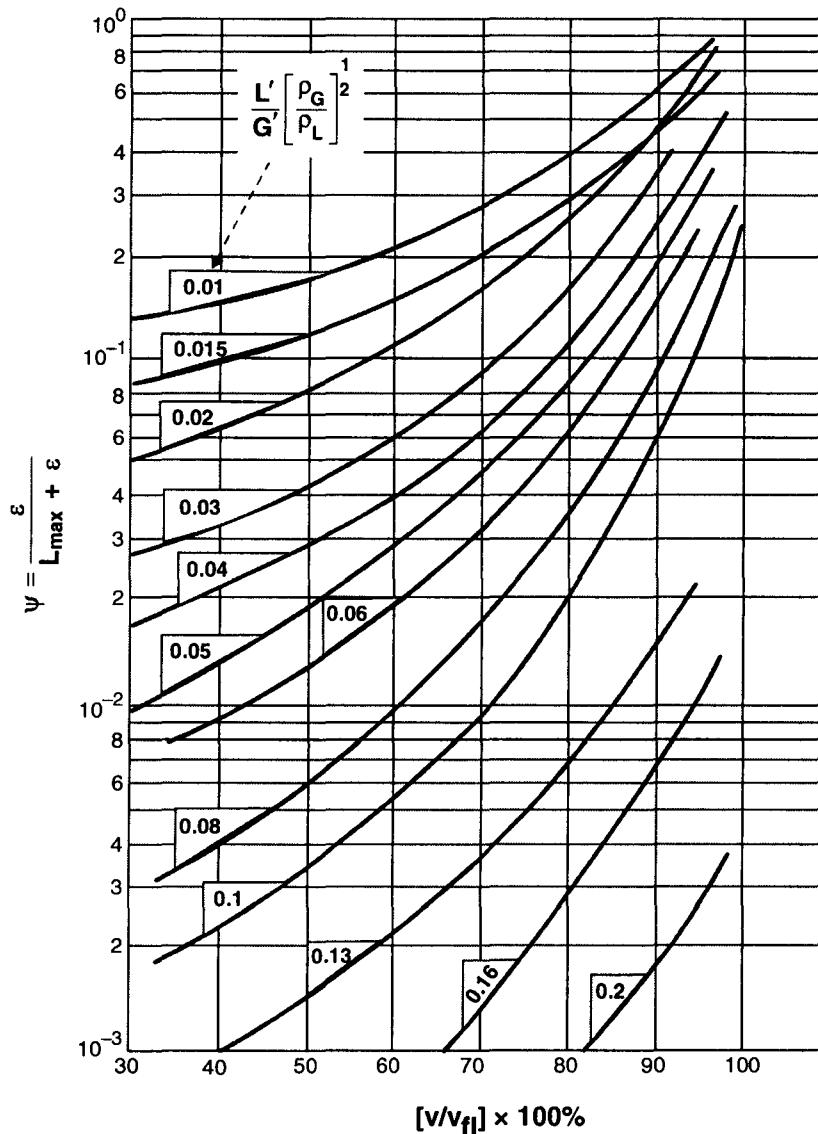
Fig. 5.17. *Entrainment For Bubblecap Plates.*

5.4 PACKED BED ABSORBER DESIGN

The usual procedure is :

\# Select a suitable packing

\# From the packing vendor's data **$K_G.a$ vs. Liq Rate Graph** read out the **$K_G.a$** value for a particular liq rate (assumed)

Calculate the log-mean-partial-press. difference of solute across the packed bed.

Calculate the volume of packing required from the relationship

$$N = K_G.a \; (V) \; (\Delta p_{lm})$$

where,   N = solute removal rate, kmol/h

$K_G.a$ = volumetric overall mass transfer coefficient, $\dfrac{kmol}{h.m^2.Pa} . \dfrac{m^2}{m^3}$

V = volume of packing required, m^3

Δp_{lm} = log-mean-partial-press. across the packed bed, Pa

Calculate the tower cross-sectional area from :

$$A_t = \dfrac{Q_{m,L}}{L'}$$

where, $Q_{m, L}$ = liq mass rate required to achieve the given absorption duty, kg/h

L' = mass velocity of liq across the bed, $kg/(h.m^2)$

Calculate tower dia and packed height :

$$D_t = \left[\dfrac{4}{\pi} . A_t \right]^{\frac{1}{2}}$$

$$H = V/A_t$$

#Calculate the **capacity factor***

$$\text{C-Factor} = v_G \sqrt{\dfrac{\rho_G}{\rho_L - \rho_G}}$$

Calculate the liq rate, $m^3 /(h.m^2)$

Check whether it matches with the assumed value. If the deviation is considerable, repeat the above steps all over again assuming a new liq rate.

C-factor = C_F

Determine the ΔP across the bed from the ΔP **vs. Capacity Factor Chart.**

CO₂ ABSORBER DESIGN

Example 5.4 : Design a packed bed absorber to reduce the CO_2 content of exhaust gas from 2% to 0.2% to (vol.) using 4% NaOH solution (Density = 65.08 lb/cu.ft.).

Assume 50% conversion of absorbed CO_2 to carbonate.

Gas density	*= 0.075 lb/cu.ft.*
Average mol. wt. of gas	*= 29.3 lb/lb mol*
Gas rate	*= 72110 lb/h*
Gas inlet temp.	*= 75°F*
Gas pressure	*= 15 inch water column*

Design the tower using 2" Pall rings and #2 metal Cascade Mini–Rings.
Make a comparative study.

Solution : The absorber is designed in stepwise details as follows :

Step – (I) Solute Absorption Rate

CO_2 removal required

$$= 72110 \left[\frac{lb}{hr} \right] \frac{1}{20.3} \left[\frac{lb\,mols}{lb} \right] \cdot \frac{2-0.2}{100}$$

$$= 44.2996 \text{ lb mols/hr}$$

$$\approx 44.3 \text{ lb mols/hr}$$

Step – (II) Alkali Requirement (4% NaOH Soln.)

$$2\,NaOH + CO_2 \rightarrow Na_2CO_3 + H_2O$$

<table>
<tr><td>2</td><td>1</td></tr>
<tr><td>lb mols</td><td>lb mol</td></tr>
</table>
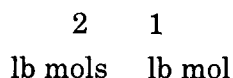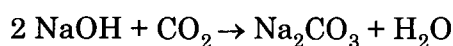
CO_2 Removal	*NaOH Requirement*
1 lb mol	2 lb mols
44.3 lb mols	2 (44.3) lb mols
	= 2 (44.3) (40) lb
	$= \dfrac{2(44.3)(40)}{0.04}$ lb 4% NaOH soln.
	$= \dfrac{2(44.3)(40)}{0.04 \,.(0.50)}$ lb of 4% NaOH soln.
	assuming 50% conversion
	= 177200 lb

NaOH soln. (4%) required = 177200 lb/hr

Step – (III) Volumetric Overall Mass Transfer Coefficient ($K_G.a$)

Assume liq rate = 7 GPM/sq. ft

Then from **Fig. 5.18** :

Packing	**$K_G.a$ (lb mols/(hr. cu.ft. atm.)**
2" Pall Rings (metal)	2.5
# 2 Cascade Mini-Rings (metal)	3.05
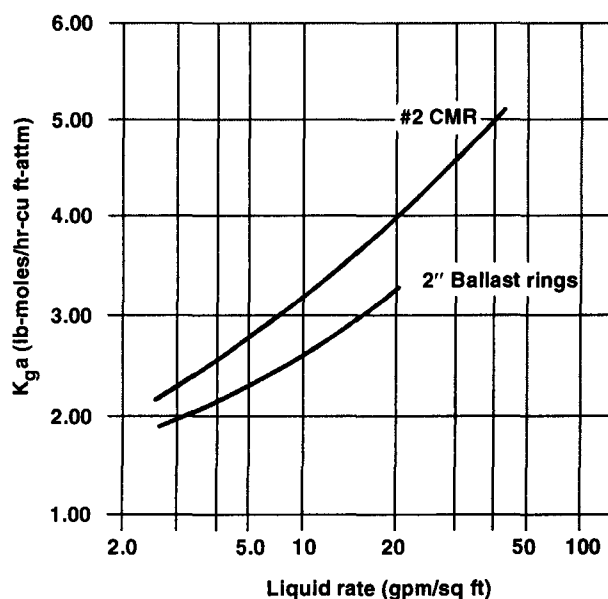
Fig. 5.18. *Efficiency vs. Liquid Rate For Metal Cascade Mini-Rings and Ballast Rings in a CO_2 Absorption Unit.*
Gas Rate = 900 lb/(hr.sq.ft)
CO_2 Content = 1% (vol)
NaOH Soln. = 4%
Conversion to Carbonate = 25%

Glitsch Test Data

Step – (IV) Packing Height

The chemisorption of CO_2 is the 2nd order irreversible reaction and there will be no CO_2 back pressure over the section.

$$\therefore \quad \Delta p_{lm} = \frac{0.02(1.0368) - 0.002(1)}{\ln\left|\dfrac{0.02(1.0368)}{0.002(1)}\right|}$$

$$= 406.8'' \text{ WC at } 39.1°F$$

1 atm = 33.90 WC at 39.1°F
= 406.8″ WC at 39.1°F
15″WC at 75°F ≈ 0.0368 atm gage
Absolute press of feed gas
= 1.0368 atm. abs.

Now, $\qquad N = K_G.a \ (V) \ (\Delta p_{lm})$

For 2″ metal Pall Rings $V = \dfrac{44.3}{2.5(0.008)} = 2215$ cu.ft of packing

For # 2 metal Cascade® Mini Rings

$$V = \frac{44.3}{3.05(0.008)} = 1815.5 \approx 1816 \text{ cu.ft of packing}$$

Liquid rate $= 4000 \ \dfrac{\text{lb}}{\text{hr(sq.ft)}}$ 1ST APPROXIMATION

Tower cross-sectional area

$$A_t = \frac{177200}{4000} = 44.3 \text{ sq. ft}$$

∴ **Tower ID**

$$D_t = \left[\frac{4}{\pi}\cdot A_t\right]^{\frac{1}{2}} = \left[\frac{4}{\pi}\cdot(44.3)\right]^{\frac{1}{2}} \quad = 7.5'$$

Packed bed heights for :

2″ PallRings	# 2 Cascade Mini - Rings
$\dfrac{2215}{44.3} = 50'$	$\dfrac{1816}{44.3} = 40.993' \approx 41'$

Step – (V) Pressure Drop
Superficial gas velocity

$$v_G = \frac{Q_{m,G}}{\rho_G \cdot A_p} = \frac{(72110/3600)}{(0.075)(44.18)} = 6.0451 \text{ ft/s}$$

A_p = packed bed area

$$\textbf{C-factor} = 6.0451 \left[\frac{0.075}{65.08 - 0.075}\right]^{\frac{1}{2}} = 0.2053 \text{ ft/s}$$

$$\text{Liq rate} = 177200 \left[\frac{\text{lb}}{\text{hr}}\right] \frac{1}{60} \left[\frac{\text{hr}}{\text{min}}\right] \cdot \frac{1}{65.08} \left[\frac{\text{cu.ft}}{\text{lb}}\right] 7.48 \left[\frac{\text{gallon}}{\text{cu.ft}}\right] \cdot \frac{1}{44.18} \left[\frac{1}{\text{sq.ft}}\right]$$

$$= 7.683 \text{ GPM/sq. ft}$$

Packing	ΔP	Figure
# 2 metal CMR	0.25" liq/ft of packed bed for a total press. drop of 10.2" of liq	5.19
2" metal Pall Rings	0.28" liq/ft of packed bed for a total press. drop of 14" of liq	*Reference : Glitsch Bulletin–217/P.26*

Final Comparison

Parameter	2"Pall Rings	#2 Cascade Mini-Rings
Column dia (ft)	7.5	7.5
Packed height (ft)	50	41
Packed volume (cu.ft)	2215	1816
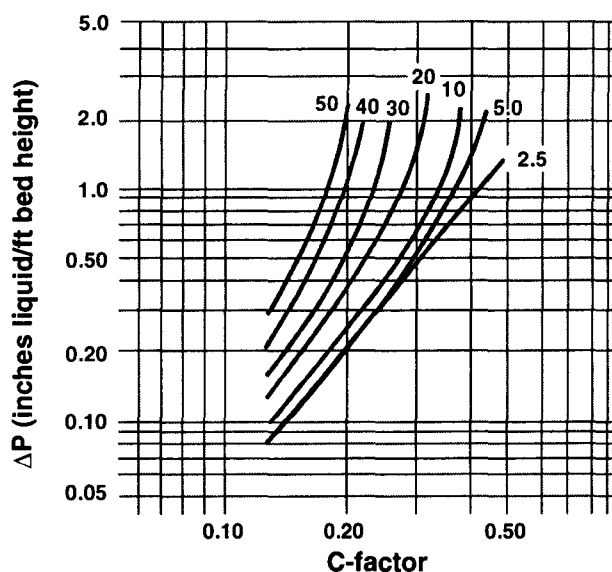
Fig. 5.19. *Pressure-Drop vs. C-Factor for # 2 metal Cascade Mini-Rings at Various Liquid Loadings (GPM/SQ. FT).*

5.4.1. Shortcut To Packed-Absorber Dia

Packed towers are widely used for absorption. While mass-transfer aspects or **VLE** dictate the tower dia, it is the hydrodynamic conditions of the contacting gas-liq streams that determine the tower dia.

Based on flooding velocity, the following empirical correlation :

$$\ln Y = -3.3861 - 1.0814 \ln X - 0.1273 \left[\ln X\right]^2 \qquad ...(5.25)$$

is used to determine the packed bed absorber dia for

$$0.015 < X < 10$$

where,

$$Y = G'^2 \cdot F \cdot \frac{\mu_L^{0.1}}{\rho_G \Delta\rho} \simeq G'^2 \cdot F \frac{\mu_L^{0.1}}{\rho_G \, \rho_L} \qquad ...(5.26)$$

$$X = \frac{\dot{L}}{\dot{G}} \cdot \left|\frac{\rho_G}{\Delta\rho}\right|^{0.5} \simeq \frac{\dot{L}}{\dot{G}} \left|\frac{\rho_G}{\rho_L}\right|^{0.5} \qquad ...(5.27)$$

G' = superficial mass velocity of gas, kg/(m^2.s). It is empty column gas velocity.

F = packing factor

$\quad = Z.d^{-n} \qquad\qquad\qquad\qquad\qquad\qquad ...(5.28)$

d = nominal packing dia, mm

Z and n are constants whose values depend on types of packings and materials of construction (see Table below)

$\dot{L}$ = liq mass flowrate, kg/s

$\dot{G}$ = gas mass flowrate, kg/s

$\quad = G'. A$

A = tower cross-section, m^2

$\therefore \qquad\qquad\qquad \dot{L}/\dot{G} = L'/G'$

Table 5.8 Constants For Typical Tower Packings

Packing Type	Z	n
Intalox Saddles		
— ceramic	7091	1.337
— plastic	268	0.651
Pall Rings		
— Hypak	139	1.021
— metal	843	0.913
— plastic	1641	1.043
— Flexiring	770	0.874
Berl Saddles		
— ceramic	9850	1.387
Rasching Rings		
— ceramic	27800	1.553
— metal (0.8mm wall thickness)	7364	1.305

Tower dia is designed on the basis of :

designed superficial gas velocity = 60% of flooding velocity

Once G'_{fl} at floodpoint is known, the tower dia is computed from

$$D = \left[\frac{4}{\pi} \cdot \frac{\dot{G}}{0.6 G'_{fl}} \right]^{0.5}$$

...(5.30)

Note :

$$G' = \frac{\dot{G}}{A}$$

$\therefore$

$$A = \frac{\dot{G}}{0.6 G'_{fl}}$$

or,

$$\frac{\pi}{4} \cdot D^2 = \dot{G}/0.6 G'_{fl}$$

$\therefore$

$$D = \left[\frac{4}{\pi} \cdot \dot{G}/0.6 G'_{fl} \right]^{\frac{1}{2}}$$

REFERENCE

1. *Mass Transfer Opertions* — R. E. Treybal (3rd Ed / McGraw-Hill Book Co. / NY 10020 / USA / 1980).

2. *How Tower Packings Behave* — J. S. Eckert (*Chem. Engg. / APR 14, 1975 and SEP. 15, 1975*).

PACKED BED ABSORBER DESIGN

Example 5*5. *A packed bed absorber is to be designed to remove sulfur dioxide from an effluent gas stream using aq. sodium hydroxide as the scrubbing liquor.*

The operating conditions and gas / liq properties at average column operating conditions are presented below :

G = *4 t/h*

L = *16 t/h*

ρ_G = *1.25 kg/m³*

ρ_L = *1200 kg/m³*

μ_L = *0.002 Pa.s*

Choose suitable packing to design the tower.

Solution : The absorption of SO_2 by aq. NaOH is a chemisorption which is proceeded by acid generation :

$$SO_2 + H_2O \rightarrow H_2SO_3$$
$$H_2SO_3 + NaOH \rightarrow NaHSO_3$$
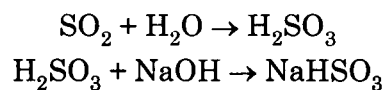
So let us select ceramic packing. **Ceramic Intalox saddle** is better off than **ceramic Raschig** rings.

Packing selected : 25mm-**ceramic INTALOX saddles**

∴   **d** = 25mm

                     Z = 7091

                     n = 1.337

∴   **F** = 7091 / (25)$^{1.337}$ = 95.865

$$X = \frac{L'}{G'} \left| \frac{\rho_G}{\rho_L} \right|^{0.5}$$

$$= \frac{16\,t/h}{4\,t/h} \left| \frac{1.25\ kg/m^3}{1200\ kg/m^3} \right|^{0.5}$$

$$= 0.12909$$

∴ ln **Y**= − 3.3861 − 1.0814 ln(0.12909) − 0.1273(ln 0.12909)^2 = − 1.70575

∴   **Y** = 0.18163

∴ $$G'^{\,2} = \frac{Y}{F} \cdot \frac{\rho_G\,\rho_L}{\mu_L^{0.1}}$$

$$= \frac{0.18163}{95.865} \cdot \frac{(1.25)(1200)}{(0.002)^{0.1}}$$

$$= 5.29073$$

∴   **G'** = 2.30015 kg/s.m^2

∴ $$D = \left[\frac{4}{\pi} \frac{(4000/3600)\ kg/s}{0.6 \times 2.30015\ kg/s.m^2} \right]^{0.5} = 1.0124\ m \qquad \textbf{Ans.}$$

5.4.2. Packed Tower Design (Modified Nguyen-Hess Method)

Based on the work of Sherwood *et. al,* ; Lobo *et. al.* and Zenz *et. al.* , H. X. Nguyen developed a mathematical model, later simplified by M. Hess, to determine the packed-tower dia :

$$G' = 0.2048(\beta)\ exp\left[-6.152362 + 3.165279\ \sqrt{21.0819 - 1.195736.\,ln\left(\alpha\beta^2\right)} \right]$$

where, α , β are two constants which are given by

$$\alpha = \frac{a \cdot \mu^{0.2}}{\epsilon^3 \cdot \rho_G \cdot \rho_L}$$

$$\beta = L' \left| \frac{\rho_G}{\rho_L} \right|^{\frac{1}{2}}$$

a = specific surface area of packing, m^2/m^3

L′ = liq loading, $kg/(h.m^2)$

G′ = gas loading, $kg/(h.m^2)$

$\dot{G}$ = mass flowrate of gas, kg/h

$\dot{L}$ = mass flowrate of liq, kg/h

ρ_G = gas density, kg/m^3

ρ_L = liq density. kg/m^3

μ = dynamic viscosity of liq, Pa.s

ϵ = void fraction of packing, m^3/m^3

The tower should be so designed as that it satisfies the following relationship

$$0.02 < \frac{L'}{G'} \left| \frac{\rho_G}{\rho_L} \right|^{\frac{1}{2}} < 7$$

holds good.

The term $\dfrac{L'}{G'} \left| \dfrac{\rho_G}{\rho_L} \right|^{\frac{1}{2}}$ is called **Control Parameter**

PACKED BED SCRUBBER DESIGN

Example 5*6. An organic vapor is to be retrieved from an air mixture by countercurrent scrubbing with a hydrocarbon oil in a tower randomly packed with 25mm Raschig rings.

Determine the tower dia if it operates at   :

gas flowrate	*= 820 kg/h*
liq loading	*= 7400 kg/h.m²*
gas density	*= 1.2013 kg/m³*
liq density	*= 891.56 kg/m³*
dynamic viscosity of liq	*= 34 × 10⁻³ Pa.s*
specific surface area of packing	*= 167 m²/m³*
packing voidage	*= 0.683 m³/m³*

The operating gas velocity is 50% of superficial gas velocity.

Solution : We shall use Nguyen's correlation to find the tower dia and check whether the control parameter lies within the permissible range.

Now,

$$\alpha = \frac{a.\mu^{0.2}}{\epsilon^3.\rho_G.\rho_L} = \frac{167\left(34\times10^{-3}\right)^{0.2}}{(0.683)^3(1.2013)(891.56)} = 0.248855$$

$$\beta = L'\left|\frac{\rho_G}{\rho_L}\right|^{\frac{1}{2}} = 7400\left|\frac{1.2013}{891.56}\right|^{\frac{1}{2}} = 271.6327 \text{ kg/h.m}^2$$

$$\ln(\alpha\beta^2) = 9.818017$$

$$\therefore G' = 0.2048(271.6327)\exp\left[-6.152362 + 3.165279\sqrt{21.0819 - 1.195736(9.818017)}\right]$$

$$= 1883.7454 \text{ kg/(h.m}^2)$$

$\therefore$ Area of tower cross-section,

$$A = \dot{G}/G'\ \frac{820(\text{kg}/\text{h})}{1883.7454\left(\text{kg}/\text{h.m}^2\right)} = 0.4353 \text{ m}^2$$

$$\therefore\ \ \frac{\pi}{4}.D_t^2 = 0.4353 \text{ m}^2$$

$$\therefore\ \ \dot{D}_t = 0.7444 \text{ m}$$

$$\simeq 750\text{mm}$$

Check :

Control parameter
$$= \frac{L'}{G'}.\left|\frac{\rho_G}{\rho_L}\right|^{\frac{1}{2}}$$

$$= \frac{7400\text{kg}/\text{h.m}^2}{1883.7454\text{ kg}/\text{h.m}^2}\left|\frac{1.2013\text{ kg}/\text{m}^3}{891.56\text{ kg}/\text{m}^3}\right|^{\frac{1}{2}}$$

$$= 0.144 \text{ which lies within the range } 0.02 \text{---}7$$

REFERENCES

1. T. K. Sherwood *et. el., Industrial Engineering Chemistry (vol. 30/1938).*

2. W. E. Lobo *et. al., Transaction of American Institute of Chemical Engineers (vol. 41 / P - 693 / 1945).*

3. F. A. Zenz *et. al., Chemical Engineering (Aug. 1953 / P: 176 - 184).*

4. N. H. Chen, *Industrial and Engineering Chemistry (June 1961).*

5. M. Hess, *Chemical Engineering (Apr. 09 / 1979 / P: 5).*

6. H. X. Nguyen, *Chemical Engineering (Nov. 20, 1978 / P: 181 - 184).*

7. V. I. Pancuska, *Chemical Engineering (May 5, 1980 / P: 113 - 114).*

5B.1.5. END EFFECTS IN PACKED TOWER DESIGN

Packed towers are designed on the basis of overall mass transfer coefficients, $K_G.a$ or $K_L.a$ in which the end effects are ignored. However, this factor should be taken into consideration for accurate experimental evaluation of mass transfer coefficient.

The end effect arises out of incomplete wetting of the packing immediately below the liquid distributor. This is the bedtop end effect that reduces the actual bed depth by Z_T **(Fig. 5.20)**

Likewise, the bottom end effect is the extension of actual bed depth **(Z)** by Z_B **(Fig. 5.20)**. It arises from an extended spray section below the packing support, where gas-liq mass exchange takes place.

Therefore, the **net end effect N** is

$$N = Z_B - Z_T$$

Z_T reduces absorption effect while Z_B stretches it,

whereupon the effective bed-depth comes out to be

Fig. 5.20. *Effective Packed Depth is the Actual Bed Depth Plus End Effect.*
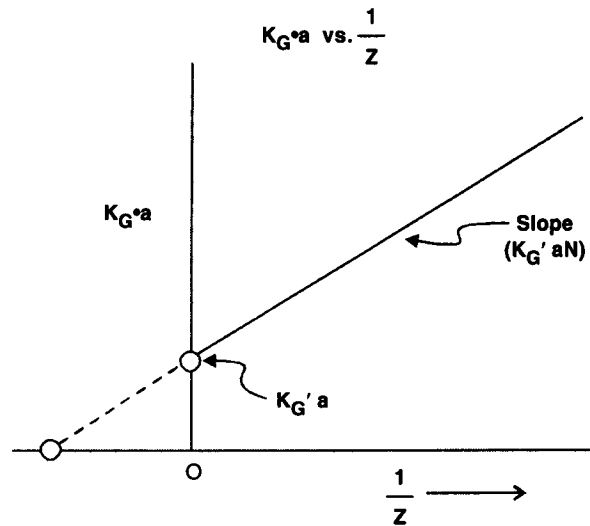
Fig. 5.21. *Apparent Overall Mass Transfer Coefficient vs. Reciprocal Packed Depth.*

$$Z_{eff} = Z + N = Z + Z_B - Z_T$$

where Z = actual bed depth **(Fig. 5.20)**.

Therefore, end effect is the difference between effective packed depth and actual packed depth.

For a given system obeying Henry's Law, the quantity of solute transfer over a packed depth Z may be represented by

$$G. Y = K_G.a.\Delta P_{LM}.Z \qquad \qquad ...(5.44)$$

where,   G = molar gas rate, kmol/(h.m^2)

$K_G.a$ = apparent overall mass transfer coefficient, $\dfrac{kmols}{h.m^3.kPa}$

ΔP_{LM} = log-mean-pressure-difference, kPa

Y = mole ratio of solute in gas phase *i.e.* mol solute/mol solute-free gas

Upon introducing the end effect, the EQN. 5.44 becomes

$$G.\Delta Y = K_G'.a.\Delta P_{LM} (Z + N) \qquad ...(5.45)$$

Combining EQN. 4.44 and 4.45 results

$$K_G.a = K_G'.a.N.\frac{1}{Z} + K_G'.a \qquad ...(5.46)$$

which is the equation of a st. line of the form **Y = mX + b** as shown in **Fig.5.21** *i.e.* the apparent overall mass transfer coefficient is a linear function of true overall mass transfer coefficient.

By the use of linear regression of the data the slope of the line = $K_G'.a.N$ \qquad **(Fig. 5.21)**

y-intercept of the line \qquad = $K_G'.a$ \qquad ...(Fig. 5.21)

End effect, \qquad $N = \dfrac{K_G'.a.N}{K_G'.a}$

The analysis of experimental data indicates that the apparent overall mass transfer coefficient can lead to errors exceeding 50%. Therefore, some caution should be exercised when using mass transfer coefficient, particularly with shallow beddepth column. It is advisable to repeat experiments under identical flow conditions with different packed depths and then evaluate the linear regression coefficients for $K_G.a$ to correct for end effects.

REFERENCES

1. O. E. Dwyer and B. F. Dodge, *Industrial and Engineering Chemistry (vol. 33(4) / P: 484 / 1941)*.

2. A. C. Mottola and L. L. Fellinger, *Chemical Engineering Progress (Oct. 1978 / P : 94 – 95)*.

□□

Packings

Tower packings come in various sizes and shapes. But they can be categorized into two broad groups.

    – random

    – regular

6.1. RANDOM PACKINGS

Random packings are simply dumped into the tower and they orient at random during installation.

They are made from ceramic, plastics, metals or carbon **(Fig. 6.1)**

The most frequently used random packing and some typical ones are described below.

6.1.1. Raschig Ring

It is the oldest random packing which is still in substantial commercial use today.

They are hollow cylinders with length equal to their outer dia. Their diameters range from 6 to 100 mm and even more.

Raschig rings are manufactured from ceramic, metals, plastics and carbon.

The ceramic Raschig rings are useful in contact with most liquids except alkalies and hydrofluoric acid.

© PARAS Towerpack Industries

Fig. 6.1. *Random packings are available in ceramic, plastics, metals or carbon.*

Table 6.1.1.1. Physical Data Ceramic Raschig Rings

Size O.D. and Length, mm	6	10	13	19	25	38	50	76
No., pcs/m³	3000000	872000	378000	109000	47700	13700	5800	1750
Wt. kg/m³	970	990	840	745	680	650	630	570
Void spaces %	60	59	65	69	72	73	74	77

©*Norton Co*. Reproduced with kind permission of Norton Chemical Process Products, Akron, Ohio (USA)
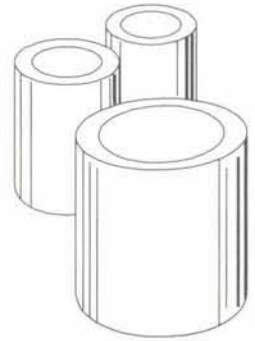
Table 6.1.1.2. Physical Data Metal Raschig Rings

Nominal Size, mm	10	12	16	19	25	32	38	50	75
No., pcs/m³	950000	395 000	205 000	115 000	49 500	25700	13 200	5800	1900
Void spaces %	82	84	86	88	85	87	90	92	95

©*Norton Co.* Reproduced with kind permission of Norton Chemical Process Products, Akron, Ohio (USA)

Table 6.1.1.3. Physical Data Carbon Raschig Rings

Size O.D. and Length, mm	6	13	19	25	38	50	76
No., pcs/m³	3000 000	374 000	111 000	47 000	13 800	5900	1750
Wt. kg/m³	745	440	550	440	550	440	370
Void spaces %	55	74	67	74	67	74	78

©*Norton Co.* Reproduced with kind permission of Norton Chemical Process Products, Akron, Ohio (USA)

6.1.2.1 Lessing Ring

It is a modified version of **Raschig ring** with one internal partition (**Fg. 6.1.2.1.1**)

It has been installed in both a dumped and a stacked (regular) manner

6.1.1.2 Cross Partition Ring (Fig. 6.1.1.2.1)

It is another modification of **Raschig ring** with two internal cross-partitions.
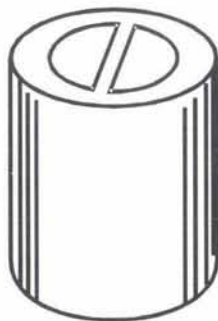
Fig. 6.1.2.1-1. *Lessing Ring.*   **Fig. 6.1.1.2.1.** *Cross Partition Ring.*

Like **Lessing ring** it has been installed in both a dumped and a stacked fashion

Table 6.1.1.2.1. Physical Data Ceramic Cross Partition Rings

Size O.D × and Length, mm	76 × 76	102 × 102	152 × 102	152 × 152
No., pcs/m³	1770	954	424	283
Wt. kg/m³	750	980	850	850
Void spaces %	69	59	64	64

© *Norton Co.* Reproduced with kind permission of Norton Chemical Process Products, Akron, Ohio (USA)

6.1.2. Saddles

The first of modern dumped packings was the **Berl saddle**. It was developed in the late 1930s. Its very shape bestowed on it a significant increase in surface area per unit volume compared to **Raschig ring.**

Table 6.1.2.1. Physical Data Ceramic Berl Saddles.

Size O.D × and Length, mm	12	25
Wt. kg/m³	865	721
Surface Area, m²/m³	466	249
Void spaces %	62	68
Packing factor	787	361
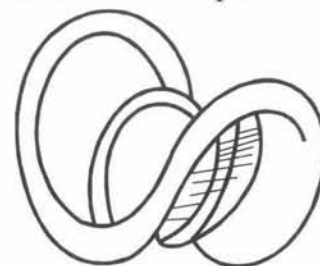
Berl Saddle

Saddles manufactured by different companies are given specific tradenames, *e.g.,* **Inatox®** (the trademark of Norton Chemical Process Products Corporation) **saddles** are manufactured by Norton Co. Likewise Koch Engineering Co., manufactures **Flexisaddle™** random packing in plastic and ceramic material.

6.1.2.1 Ceramic Intalox® Saddles

ensure two of the most important criteria of any tower packing :

- maximum usable area for gas-liq contact
- minimum resistance to the gas and liquid flows thru the column.

Regardless of how ceramic intalox packing falls when randomly dumped into a tower, the unique saddle shape minimizes pattern packing. Despite dumping, it is impossible for any two packing elements to cover one another to a degree which would significantly reduce the effective surface area for gas-liq contact.

Norton Co. manufactures **Super Intalox Saddle** also. They offer the advantages of random configuration and efficiency, but provide the additional benefit of 86% (or more) increased capacity when compared to **Raschig rings.**

Intalox Saddle

© *Norton Co.* Reproduced with kind permission of Norton Chemical Process Products Corporation, Akron, Ohio (USA).

K_Ga vs. Liquid Rate Liquid Rate lbs.(ft^2. hr) 10^3

Pressure Drop vs. Gas Rate Gas Mass Velocity lbs/(ft^2. hr) 10^2
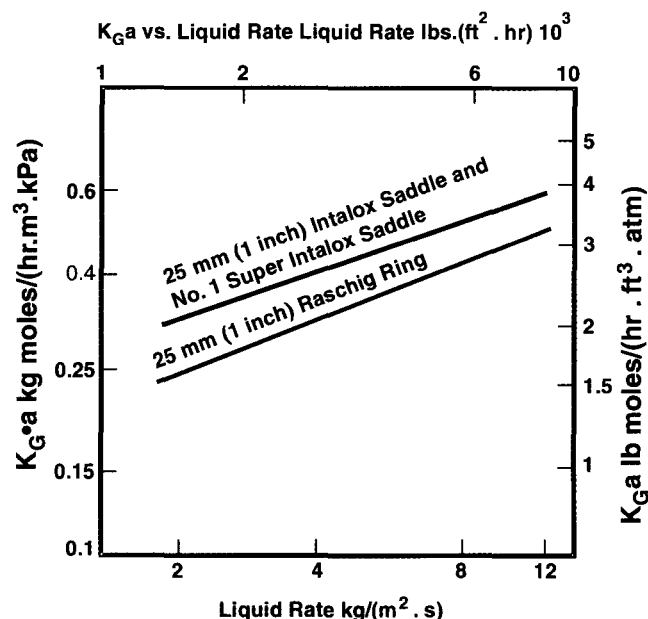
Fig. 6.1.2.1.1. *Performance Curve of Ceramic Intalox® and Super Intalox® saddles. They exhibit greater Efficiency (18% and even higher) than Raschig Rings.*
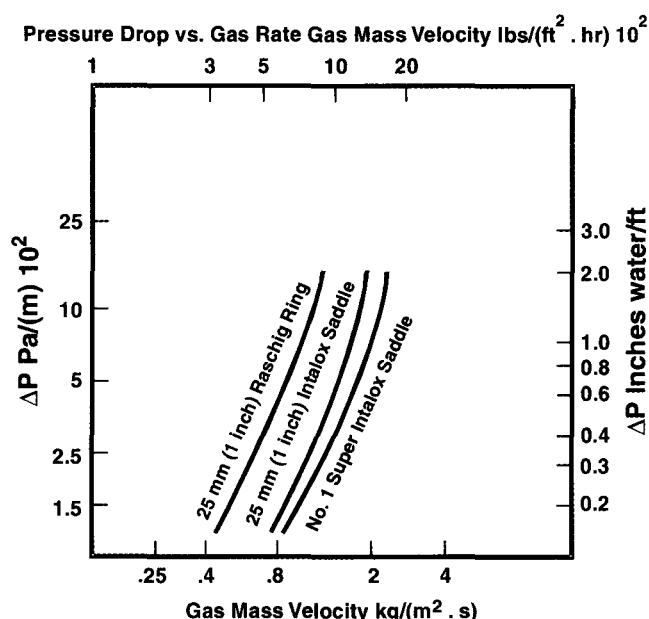
Fig. 6.1.2.1.2. *Pressure Drop Curves show Greater Capacity of Intalox and Super Intalox Saddles over Raschig Ring. Intalox Saddles provide 56% (or More) Greater Capacity than Raschig Ring. Super Intalox Saddles Ensure as much as 86% (or more) Greater Capacity than Raschig Rings.*

© **Norton Co. Reproduced with kind permission of Norton Chemical Process Corporation, Akron, Ohio (USA).**

Materials of Construction : Ceramic packings are available in chemical porcelain, chemical stoneware and Aceral® ceramic (a proprietary alumina formulation with superior acid resistance).

Of the three materials, chemical porcelain is specified for the majority of mass transfer applications because it is mechanically strong, completely non-porous, and more resistant to chemical attack than stoneware. In cases where even porcelain is subject to attack, Aceral ceramic is recommended for use.

Chemical Resistance : Chemical stoneware and chemical porcelain packings resist all acids, alkalies and solvents, other than hydrofluoric acid and hot caustics.

Porcelain is superior to stoneware in hot caustic service because it can withstand 10% sodium hydroxide service up to 325 K and 1% sodium hydroxide service up to 366 K.

In processes where ceramic packings are not viable, carbon is often a suitable material of construction.

· **Recommended Uses :** The chemical resistance and economical installed cost of ceramic packings have led to their extensive use in many mass transfer applications including the following absorption processes :

• Removal of CO_2 and H_2S by hot potassium carbonate solution

•.Cooling and drying of chlorine

•⁻Absorption of ClO_2, SO_2 and SO_3

- Removal of Mercaptan
- L.P.G sweetening

Table 6.1.2.1.1. Physical Data Ceramic Intalox Saddles.

Nominal Size, mm	6	10	13	19	25	38	50	76
No., pcs/m^3	4 150000	1800000	600000	219000	73000	23000	8600	1800
Wt. kg/m^3	875	810	745	710	680	630	600	600
Void spaces %	64	67	69	71	71	74	75	75

Fig. 6.1.2.1.3. *Ceramic Intalox® Saddle.*

© *Norton Co.* Reproduced with kind permission of Norton Chemical Process Products Corporation, Akron, Ohio (USA).

Table 6.1.2.1.2 Physical Data Ceramic Super Intalox Saddle

Nominal Size	No. 1	No. 2
No., pcs/m^3	52600	6350
Wt. kg/m^3	527	620
Void spaces %	77	75

Fig. 6.1.2.1.4. *Ceramic Super Intalox® Saddle.*

© *Norton Co.* Reproduced with kind permission of Norton Chemical Process Products Corporation, Akron, Ohio (USA).

6.1.2.2. Plastic Super Intalox® Saddles : are the improved version of Norton's **Intalox saddle.** They enhance internal gas and liquid distribution, allow higher capacities and maximum mass transfer efficiencies.

One of the keys to the saddles' high performance is the *scalloped edge.* This configuration provides many more interstitial transfer points per unit volume of packing than comparative packings. These transfer points continuously renew the liquid surface significantly increasing the rate of mass transfer. The scalloped edges also mobilize the packing within the bed, help resist settling effects, maintain packing free space and lower column pressure drop.

Applications : Plastic Super Intalox® saddles are eminently useful in a variety of processes:

- CO_2 absorption
- SO_2, HCl and HF absorption or stripping
- Cl_2 absorption in water or caustic
- ClO_2 absorption
- Cl_2 drying
- H_2S and mercaptan removal
- Deaerating
- Fume scrubbing

Unique shape minimizes channeling and wall streaming.

Scalloped edges provide numerous liquid transfer points.

High percentage of free space; excellent and uniform liquid distribution.

Courtesy : Norton Chemical Process Products Corpn.

Fig. : 6.1.2.2.1. *Plastic Super Intalox Saddle.*

Fig. 6.1.2.2.1-A *Courtesy :* Norton Chemical Process Products Corpn. Akron, Ohio, USA.

Norton took the advantages of the original **Intalox® saddles'** design and incorporated significant technological changes to come up with its plastic **Super Intalox® saddles. Super Intalox** saddles enhance internal gas and liquid distribution, allow higher capacity and maximize mass transfer efficiency

The unique scalloped edge is the key to the product's high performance. The configuration provides many more interstitial transfer points per unit of volume than standard saddle packings. By continuously renewing the liquid surface, the additional transfer points significantly increase the rate of mass transfer. The scalloped edges also immobilize the packing with the bed, which reduces settling, maintains packing free-space and lowers column pressure drop.

Fig. 6.1.2.2.2 *Performance curve of plastic Super Intalox Saddles.*

Greater Efficiency : Plastic Super Intalox saddles provide 30% (or more) greater efficiency than plastic **Pall rings** and maintain at least equal capacity.

Courtesy : *Norton Chemical Process Products Corpn.* Akron, Ohio, U.S.A

Table 6.1.2.2.1 Plastic Super Intalox Saddles

Physical Data

Nominal Size	No. 1	No. 2	No. 3
No. pcs/m^3	57500	6400	1400
No. pcs/ft^3	1630	190	42
Wt.* kg/m^3	95	60	48
Wt.* lbs/ft^3	5.85	3.75	3.00
Void Space %	90	93	94

•Refer to polypropylene.

Table 6.1.2.2.2 Plastic Super Intalox Saddles

Materials of Construction

Type of Plastic	Maximum Continuous operating temperature		Specific Gravity
	°C	°F	
General Grade Polypropylene	104	220	0.91
LTHA Polypropylene	119	247	0.91
LTHA Polypropylene (10% Glass reinforced)	127	260	0.97
High Density Polyethylene	100	212	0.95
Low Density Polyethylene	88	190	0.92
PVC	66	150	1.46
CPVC	85	185	1.55
Kynar[1] PVDF	143	290	1.77
Halar[2] E-CTFE	152	305	1.68
Tefzel[3] ETFE	149	300	1.70
Tefzel[3] ETFE (25% Glass reinforced)	200	392	1.86

1. Trademark of PennWalt Corp.
2. Trademark of Allied Corp.
3. Trademark of E.I Dupont de Nemours.

Data shown is from vendor's literature.

6.1.2.3 Flexisaddle™

Koch Engineering Co., Inc. manufactures **Flexisaddle™** random packing in plastic and ceramic materials **Plastic Flexisaddle™** packing is available in three sizes : *25mm, 50mm, and 76mm.* **Ceramic Flexisaddle™** packing is available in five sizes : *13mm, 25mm, 38mm, 50mm and 76mm.*
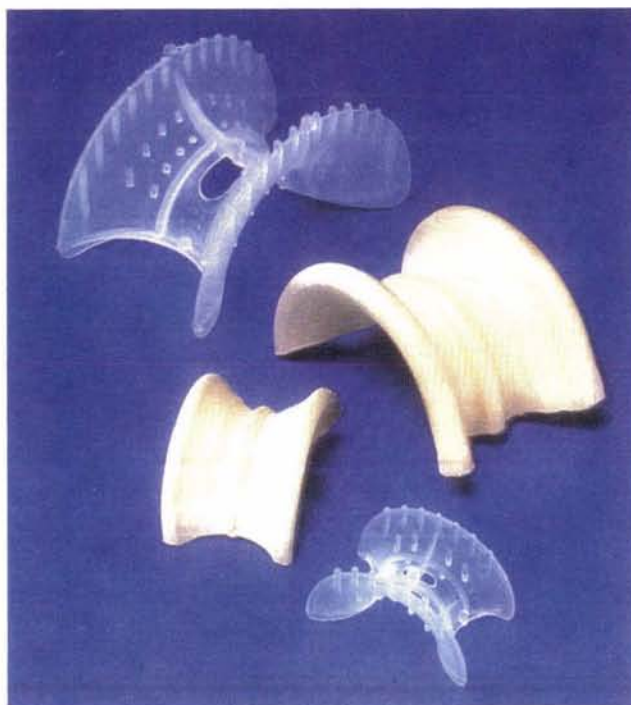
Fig. : 6.1.2.3.1. Flexisaddle™

Courtesy : Koch Engineering Co.
Source : Random Packing (KRP-2).
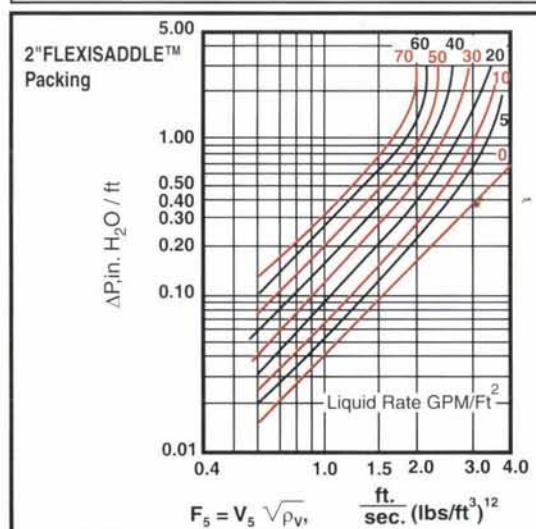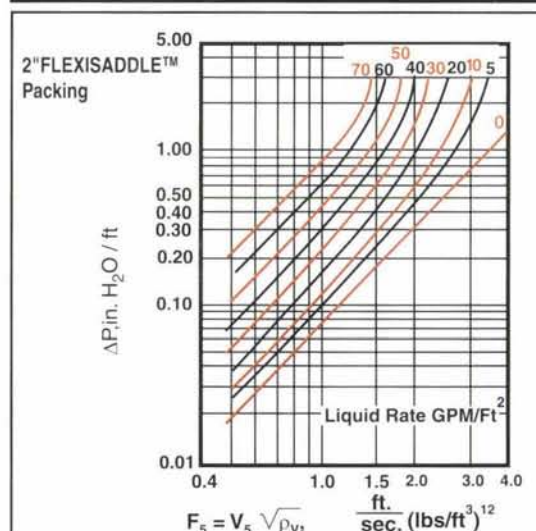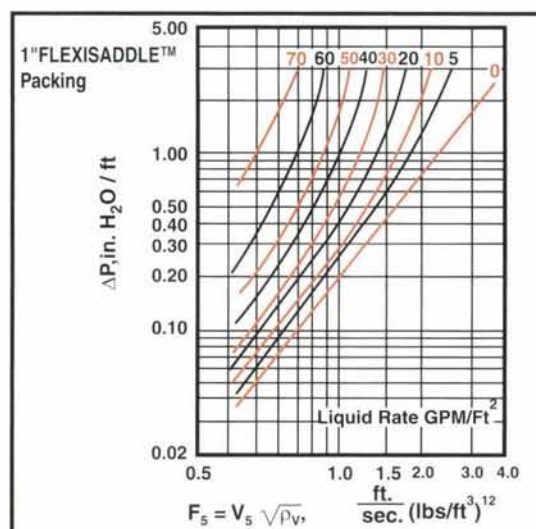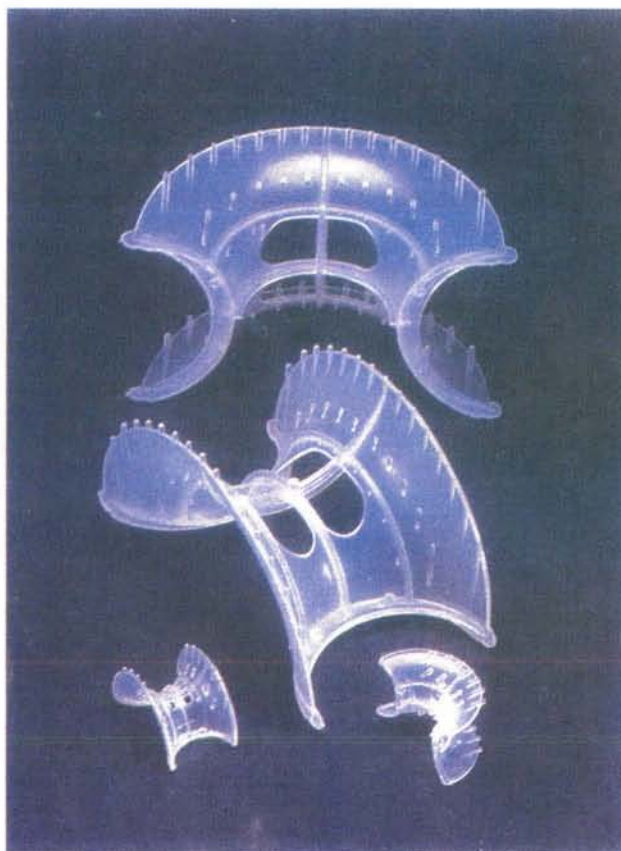
Fig. : 6.1.2.3.2. Plastic Flexisaddle packing is available in three sizes ranging from 1″ to 3″
Courtesy : Koch Engineering Co.

Ceramic FLEXISADDLE : packing is available in five sizes ranging from 1/2″ to 3″
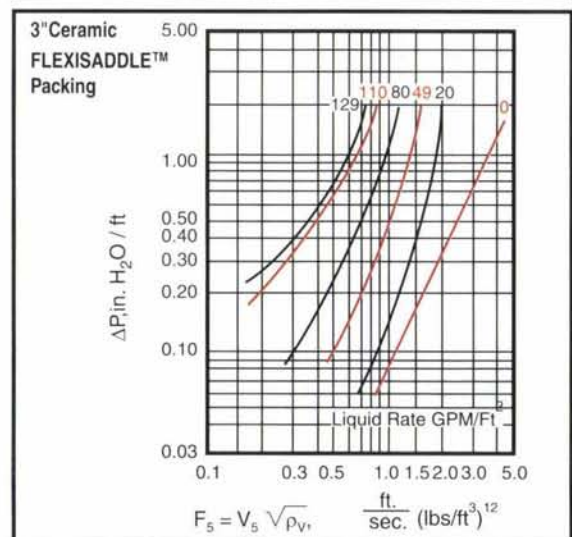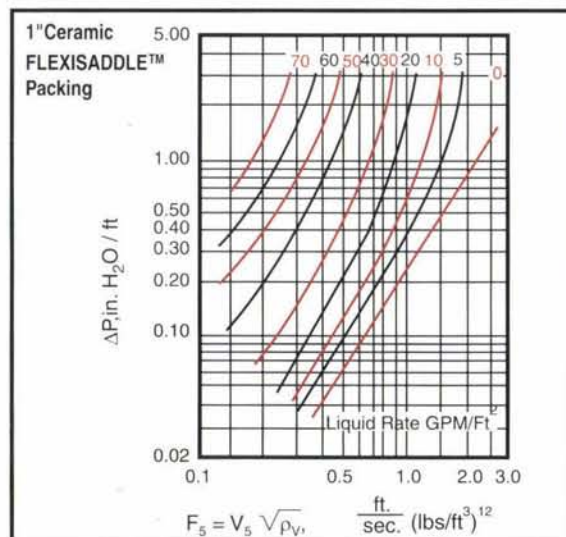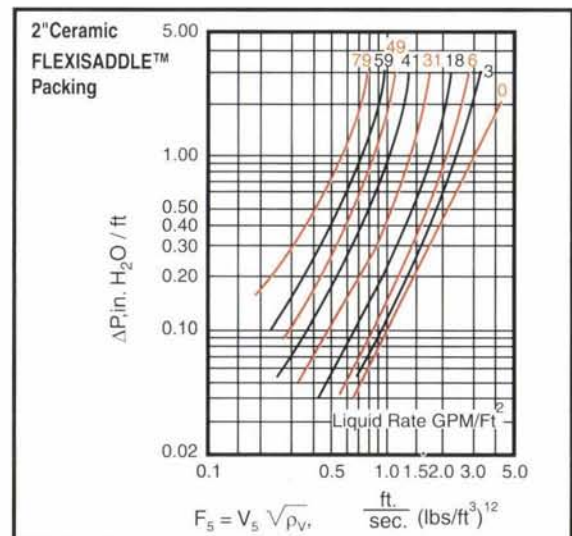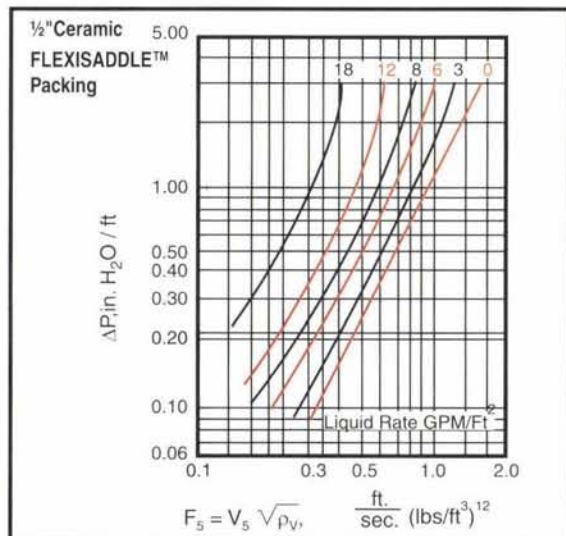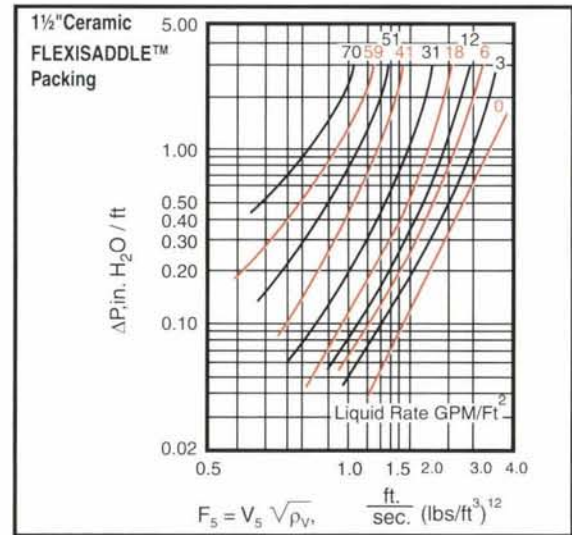
Fig. : 6.1.2.3.3. Ceramic Flexisaddle

6.1.3. Pall Rings

The **Pall ring** was born out of **Raschig ring** as a result of significant research work at BASF Aktiengesellschaft in the early 1950s.

Pall Ring [Fig. 6.1.3.1] is a cylindrical element of length equal to diameter with ten fingers punched from the cylinder wall extending into the packing element interior. Because of opening at the wall, the **Pall rings** make their interior more accessible to gas and liquid flows with the effect that Pall Ring having the same geometric surface area as the **Raschig ring** is much superior to the latter in mass transfer efficiency.

Pall rings are available in metals, plastic and ceramics.
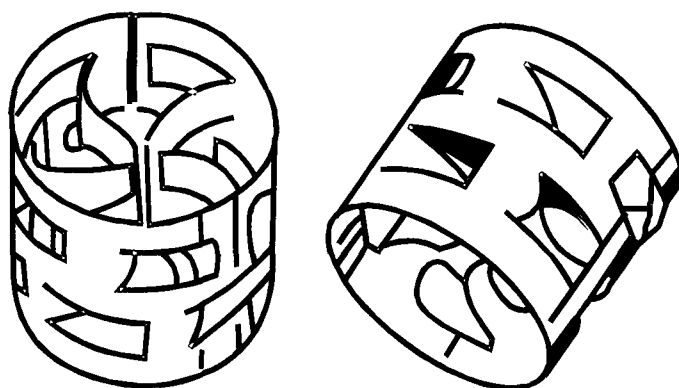
Pall Ring

Fig. 6.1.3.1. *Flexirings®. They are the Pall Rings manufactured by Koch Engineering Co.*

Metal FLEXIRING® tower packing is available in five sizes ranging from 5/6'' to 3½•'' india meter.

1½" Metal FLEXIRING® Packing

$F_5 = V_5 \sqrt{\rho_{V}}, \quad \dfrac{ft.}{sec.} \ (lbs/ft^3)^{1/2}$

5/8" Metal FLEXIRING® Packing

$F_5 = V_5 \sqrt{\rho_{V}}, \quad \dfrac{ft.}{sec.} \ (lbs/ft^3)^{1/2}$

2" Metal FLEXIRING® Packing

$F_5 = V_5 \sqrt{\rho_{V}}, \quad \dfrac{ft.}{sec.} \ (lbs/ft^3)^{1/2}$

3½" Metal FLEXIRING® Packing

$F_5 = V_5 \sqrt{\rho_{V}}, \quad \dfrac{ft.}{sec.} \ (lbs/ft^3)^{1/2}$

3½" Metal FLEXIRING® Packing

$F_5 = V_5 \sqrt{\rho_{V}}, \quad \dfrac{ft.}{sec.} \ (lbs/ft^3)^{1/2}$

Courtesy : Koch Engineering Co.

Plastic FLEXIRING® packing is available in five sizes ranging from 5/8'' to 3½•'' in diameter.

1½" Metal FLEXIRING® Packing

$\Delta P, \text{in. } H_2O \text{ / ft}$

Liquid Rate GPM/Ft^2

$F_5 = V_5 \sqrt{\rho_V}, \quad \dfrac{\text{ft.}}{\text{sec.}} (\text{lbs/ft}^3)^{1/2}$

5/8" Plastic FLEXIRING® Packing

$\Delta P, \text{in. } H_2O \text{ / ft}$

Liquid Rate GPM/Ft^2

$F_5 = V_5 \sqrt{\rho_V}, \quad \dfrac{\text{ft.}}{\text{sec.}} (\text{lbs/ft}^3)^{1/2}$

2" Plastic FLEXIRING® Packing

$\Delta P, \text{in. } H_2O \text{ / ft}$

Liquid Rate GPM/Ft^2

$F_5 = V_5 \sqrt{\rho_V}, \quad \dfrac{\text{ft.}}{\text{sec.}} (\text{lbs/ft}^3)^{1/2}$

3" Plastic FLEXIRING® Packing

$\Delta P, \text{in. } H_2O \text{ / ft}$

Liquid Rate GPM/Ft^2

$F_5 = V_5 \sqrt{\rho_V}, \quad \dfrac{\text{ft.}}{\text{sec.}} (\text{lbs/ft}^3)^{1/2}$

3½" Plastic FLEXIRING® Packing

$\Delta P, \text{in. } H_2O \text{ / ft}$

Liquid Rate GPM/Ft^2

$F_5 = V_5 \sqrt{\rho_V}, \quad \dfrac{\text{ft.}}{\text{sec.}} (\text{lbs/ft}^3)^{1/2}$

Courtesy : Koch Engineering Co.

Norton Co. manufactures metallic and plastic **Pall ring** in five different sizes each :

Table 6.1.3.1. Metal Pall Rings

Physical Data

Nominal Size, mm	16	25	38	50	90
No. of pcs/m³	205000	49500	13200	5800	1200
Void Space, %	93	94	95	96	97

© ***Norton Co.*** Reproduced with kind permission of Norton Chemical Process Products, Corporation, Akron, Ohio, USA.

Table 6.1.3.2. Plastic Pall Rings

Physical Data

Size O.D. and Length, mm	16	25	38	50	90
No. of pcs/m³	214000	50500	14700	6200	1200
Wt*, kg/m³	95	70	70	62	55
Void Space, %	87	90	91	92	92

© ***Norton Co.*** Reproduced with kind permission of Norton Chemical Process Products Corpn., Akron, Ohio (USA).

* Refers to polypropylene

Plastic Pall Rings

Norton's plastic **Pall rings** are used extensively in both new and retrofit installations. Unlike **Raschig rings,** the walls of Norton's pall rings are open. The high percentage of free space maintains superior, uniform liquid distribution. The ring's open space also provides gas and liquid full access to the ring's interior. The interior of each ring has diametrical ribs, which provide structural strength as well as additional surface area for gas-liquid contact.

Norton offers four sizes of **Pall rings** in standard polypropylene. Norton Pall rings are also available in high- and low-density polyethylene, glass-reinforced polypropylene and other thermoplastic materials.

Packing Material Data

Type of Plastic	*Maximum Continuous Operating Temperature*	
	°C	*°F*
General Grade Polypropylene	104	220
LTHA Polypropylene	119	247
LTHA Polypropylene (10% Glass reinforced)	127	260
High Density Polyethylene	100	212
Low Density Polyethylene	88	190
PVC	66	150
CPVC	85	185
Kynar[1] **PVDF**	143	290
Halar[2] **E-CTFE**	152	305
Tefzel[3] **ETFE**	149	300
Tefzel[3] **ETEF** (25% Glass reinforced)	200	392
Teflon[3] **PTEF**	250	482

1. Trademark of Pennwalt Corp.
2. Trademark of Ausimont Corp.
3. Trademark of E.I. DuPont de Nemours.
Data shown is from vendor's literature.

6.1.3.1. Hy-Pak® : Extensive research work at Norton. Co. modified **Pall ring** to **Hy-Pak®** (trademark Norton Chemical Process Products Corporation) system with enhanced interfacial area available for gas and liq contact.

Each packing is a cylinder with slotted walls (called *windows*) while tongues are projecting into the interior. The windows allow full access to the interior for both gas and liquid, while the tongues provide additional surface area for gas-liq contact.

Normally, as a packing's size enlarges, efficiency decreases and capacity increases. However, **Hy-Pak** packing, which is a sophisticated version of **Pall ring**, successfully overcomes this.

The size of **Hy-Pak** packing is slightly larger than the corresponding **Pall ring**, lowering its cost per unit volume. Yet there is no drop in efficiency. And there is more capacity.
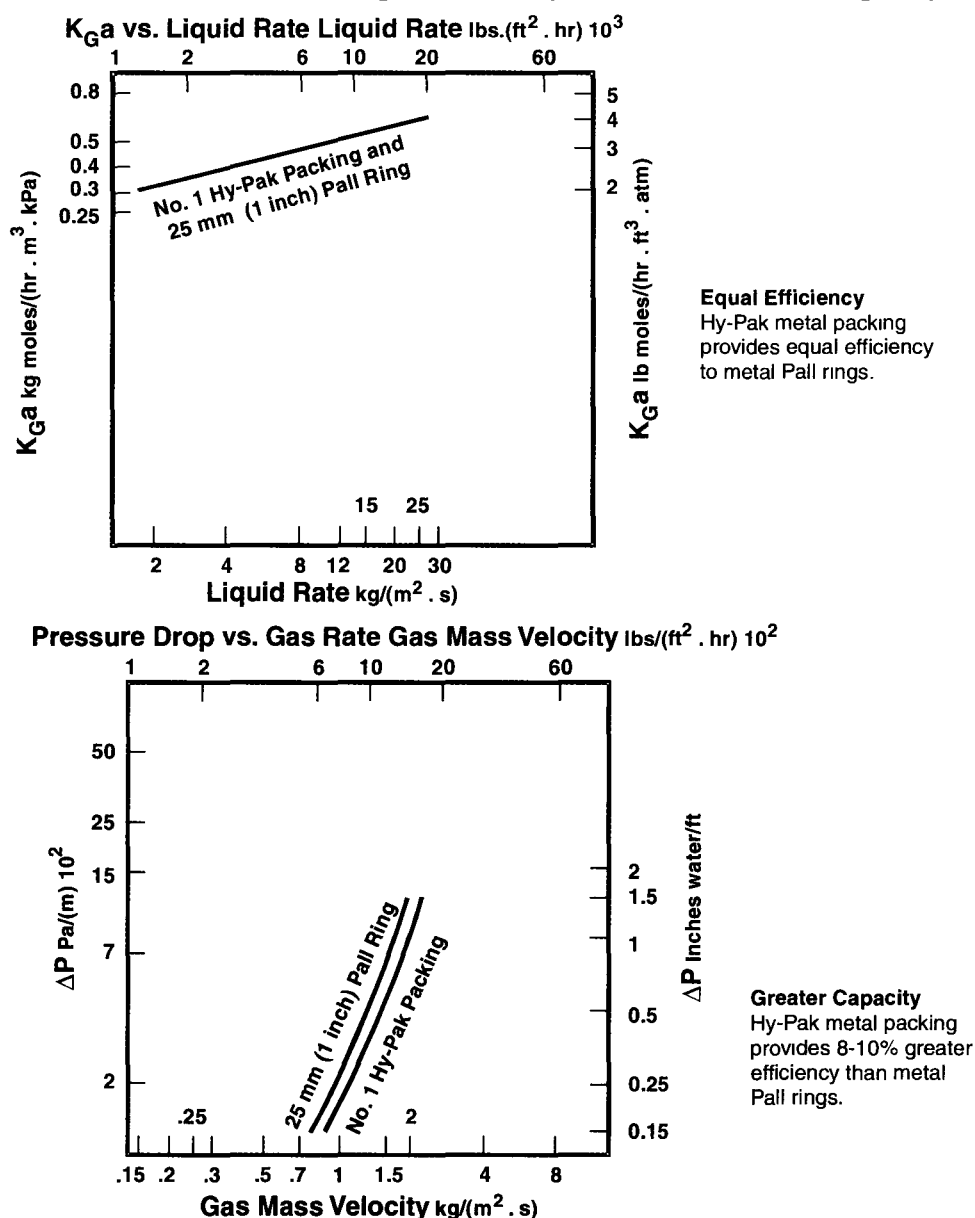
Fig. 6.1.3.1-1. *Performance Curves of Hy-Pak metal packing.*

© **Norton Co.** Reproduced with kind permission of Norton Chemical Process Products Corporation, Akron, Ohio (USA).

Materials of Construction : These packings are available in a choice of materials and sizes to meet a wide range of process requirements. Materials include carbon steel, stainless steels, and other exotic metals.

Applications : Hy-Pak metal packing is recommended for use in a variety of applications including :

CO_2 removal systems

H_2S absorbers

numerous other absorption systems.

Table 6.1.3.1.1. Hy- Pak Metal Packing.

Physical Data

Nominal Size, mm	25	38	50	90
No. of pcs/m³	30 000	9500	3700	1100
Void Space, %	97	97	98	98

© *Norton Co.* Reproduced with kind permission of Norton Chemical Process Products Corpn., Akron, Ohio (USA)
Courtesy : Norton Chemical Process Products Corpn., Akron, Ohio, USA.

6.1.3.2. HcKp™ : This random tower packing is an improved version of conventional **Pall-type** ring packing with an enhanced arrangement of internal drip tabs and a greater void **(Fig. 6.1.3.2.1)**.

© *KOCH Engineering Co.* Reproduced with kind permission from KOCH Engineering Co.

Fig. 6.1.3.2–1. KOCH HcKp™ Random Packings sport more Open Space than Pall Ring. That's Why They Exhibit Higher Capacity and Lower Pressure Drop than Pall-Type Rings Without Sacrificing Efficiency.

Together these improvements beget 15% higher capacity and 40% lower pressure drop than conventional **Pall rings** without sacrificing separation efficiency.

HcKp™ (trademark of Koch Engineering Co.) is ideal for use in high-liq-rate systems. It is available in several sizes.

Fig. 6.1.3.2-2 *HcKp*^{TM} *random packing comes in several sizes to meet varied requirements in capacity, efficiency, and pressure drop.*
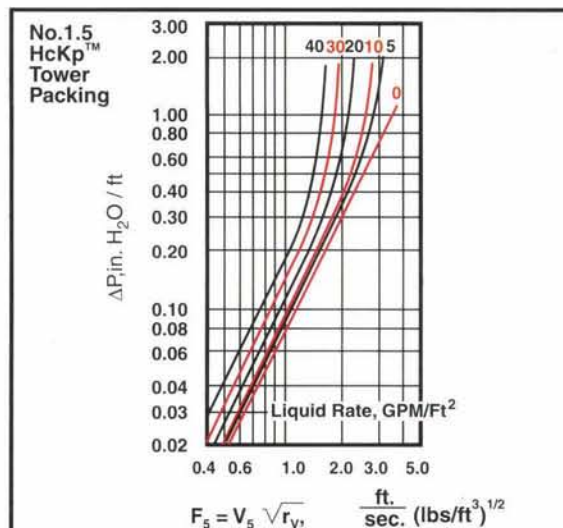
Fig. 6.1.3.2.2B
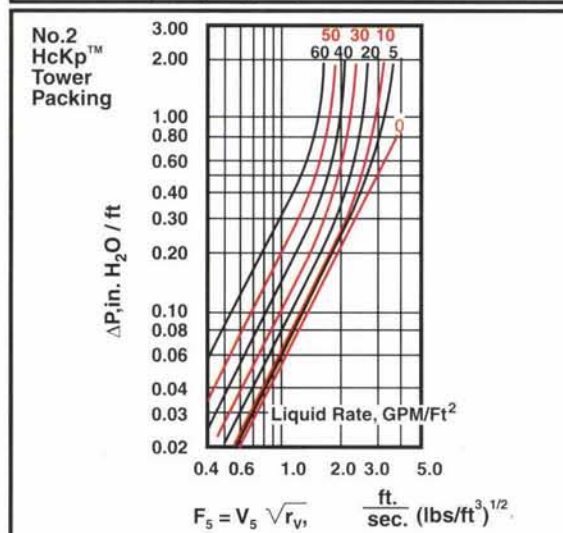
Fig. 6.1.3.2.2C
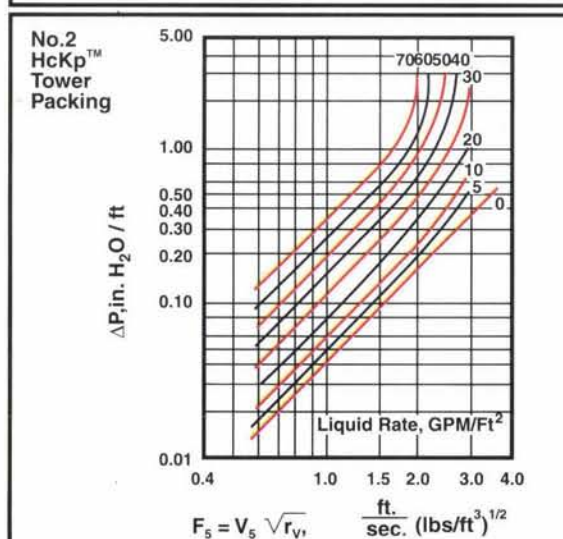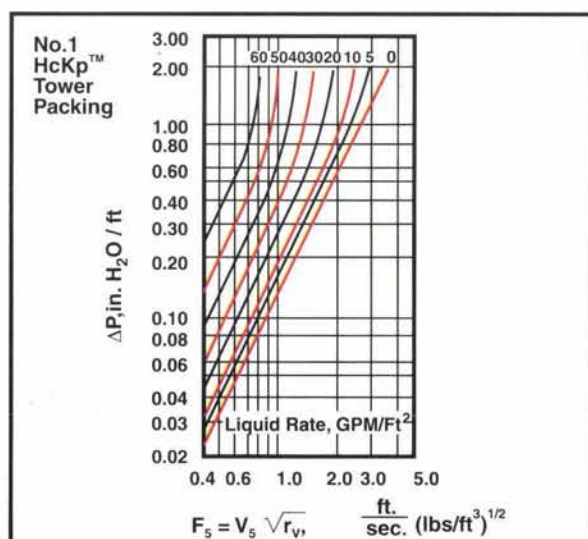
Courtesy : KOCH Engineering Co.

Fig.6.1.3.2.2A.

Fig. 6.1.3.2.2D

Norton's unique **High-Strength Pall ring Fig. 6.1.3.1.2** provides the performance of a 2-inch (50mm) **Pall ring** at a lower price and lower weight.

The shape of standard 2-inch **Pall rings** is structurally weaker than other packings. These rings attain adequate strength via extra-thick metal, which yields a heavy, costly packing.

The unique shape of Norton's high-strength **Pall ring** provides strength without the weight.

The high-strength **Pall ring** offers the same surface area as the standard 2-inch **Pall ring**.

Fig. 6.1.3.1.2.

*Courtesy : **Norton Chemical Process Products Corpn,** Akron, Ohio USA*

Fig. 6.1.3.1.3. *IMTP packing has a broad range of applicability as any mass transfer device. Many absorption and stripping towers, especially those aiming for high capacity or many stages have used IMTP packing.*

Courtesy : Norton Chemical Process Products Corporation, Akron Ohio, USA.

IMTP® High-performance Random Dumped packing (Fig. 6.1.3.1.3)

- Provides greater capacity and efficiency than fractionation trays and other random dumped packings.

- Pressure drop is approximately 40% lower than equivalent size **Pall rings.**

- Low liquid hold up minimizes liquid residence time.

- Quickly installed; requires minimal changes in existing vessels; structural strength allows packing depths to 15 m (50 ft) or more.

IMTP® PACKING PERFORMANCE

IMTP packing (Fig. 6.1.3.1.3) has a broad range of applicability as any mass transfer device. It has been heavily used in distillation — from deep vacuum towers, where its low pressure drop is crucial, to high pressure, where its capacity easily surpasses trays. Many absorption and stripping towers, especially those aiming for high capacity or many stages have used **IMTP** packing. The low pressure drop of **IMTP** packing also has been the key to its success in heat transfer towers such as refinery vacuum towers and olefin-plant hot sections.
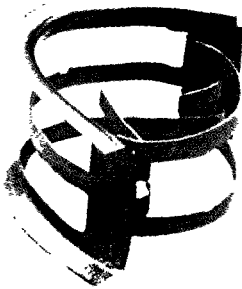
Fig. 6.1.3.1.4 . *IMTP Packing*
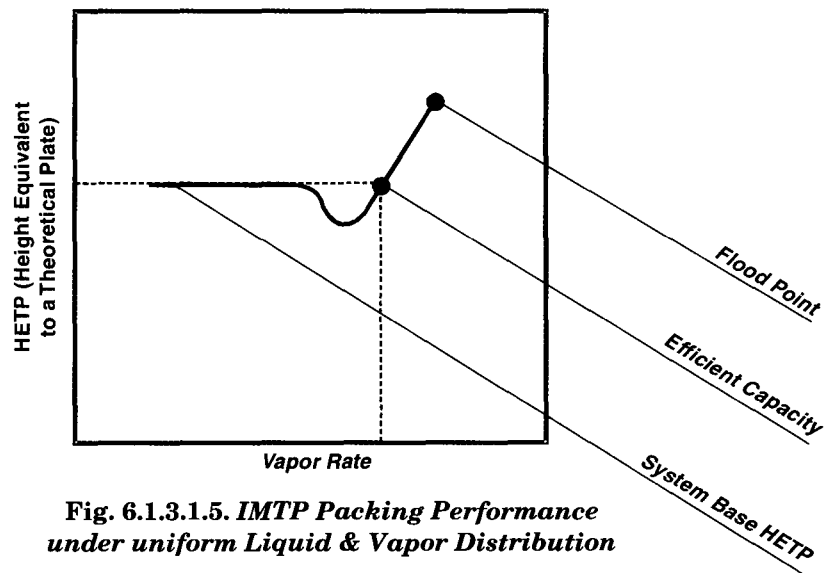
Fig. 6.1.3.1.5. *IMTP Packing Performance under uniform Liquid & Vapor Distribution*

To get an insight into the high-performance operating characteristics of Norton **IMTP packing**, consider the packing performance curve. **(Fig. 6.1.3.1.5)**

Norton defines two packing properties from a performance curve.

1. The System Base HETP of a packing, *which is the flat HETP value produced by uniform distribution.*

2. The **Efficient Capacity** of a packing, *which is the greatest vapor rate at which the packing still maintains the System Base HETP.*

NUTTER RING™—A SUPERIOR RANDOM PACKING

Nutter Ring enhances liquid spreading and film renewal on its surface and prevents droplet formation. Its performance tests in pilot plant facilities, as well as by Fractionation Research, Inc. **(F.R.I.).,** demonstrate that the **Nutter Ring** outperforms any other commercial random packing available today.

Successful performance in over 3000 installations worldwide, including columns over 8 m diameter, confirm that **Nutter Ring** test results can be scaled-up for commercial applications.

Fig. 6.1.3.3-6. *Nutter ring element*

Courtesy : Sulzer Chemtech

Fig. 6.1.3.3-7. *Nutter ring packed in a tower ensure very good piece-to-piece contact*

Nutter Ring Advantages

Fig. 6.1.3.3-8. *Nutter ring are available in a number of sizes.*

Courtesy : Sulzer Chemtech

- Efficiency enhanced by lateral liquid spreading and surface film removal.
- Superior surface utilization in mass and heat transfer, allowing shorter packed bed heights.
- Strength-to-weight ratio sufficient to withstand weight of a 15 m bed height.
- Maximum piece-to-piece contact with minimal nesting.
- Reproducible performance assured through uniform randomness.
- Free-flowing particle design promotes uniform randomizing and facilitates installation and removal.

Mechanical Specification	No. 0.7	No. 1.0	No. 1.5	No. 2.0	No.2.5	No.3.0
Pieces/m³	167,400	67,100	26,800	13,600	8,800	4,200
Surface area [m²/m³]	266	168	124	96	83	66
Weight [kg/m³]	176	178	181	173	145	133
Void [%]	97.8	97.8	97.8	97.9	98.2	98.4
Relative HETP Values	0.72	0.83	0.94	1.00	1.18	1.40

Fig. 6.1.3.3-9.

PLASTIC NUTTER RING

The inherent rigidity and energy efficient design characteristics of the patented **Nutter Ring** shape permits applications in plastics [**Fig. 6.1.3.1.9**] to produce pressure drops per theoretical stage and bed heights other packing types cannot achieve.

Performance Data

Capacity Diagram (Air/Water) (Fig. 6.1.3.1.10)

A — Nutter Ring No. 0.7

B — Nutter Ring No. 1.0

C — Nutter Ring No. 1.5

D — Nutter Ring No. 2.0

E — Nutter Ring No. 2.5

F — Nutter Ring No. 3.0

$C_G \text{ [m/s]} = F_V / \sqrt{\rho_L - \rho_G}$

$\text{Flow Parameter } [x] = \frac{L}{G} \sqrt{\frac{\rho_G}{\rho_L}}$
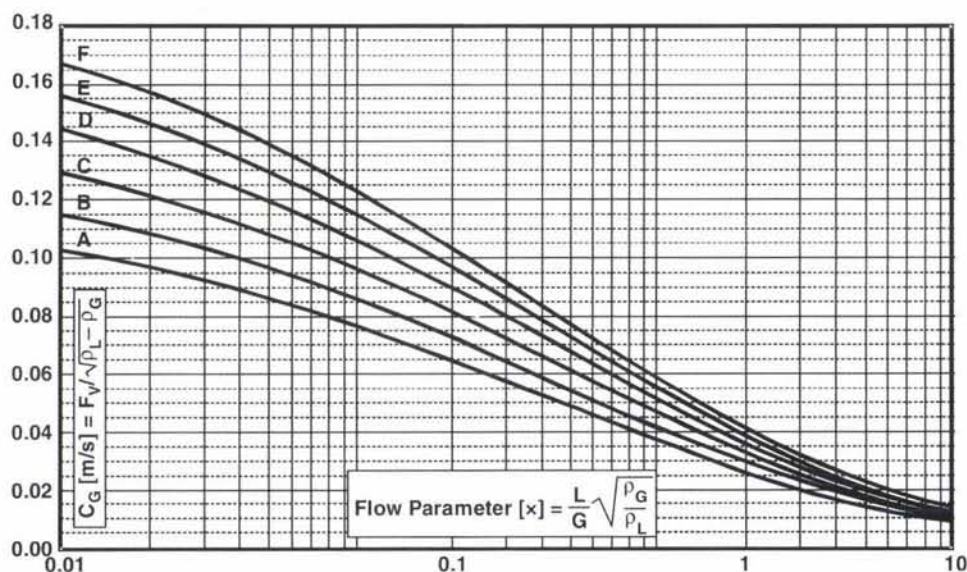
Fig. 6.1.3.1.10.

Courtesy : Sulzer Chemtech

Pressure Drop Nutter Ring No. 2.0

(I) — 0 m³/(m²h)

(II) — 10 m³/(m²h)

(III) — 25 m³/(m²h)

(IV) — 50 m³/(m²h)

(V) — 75 m³/(m²h)

(VI) — 100 m³/(m²h)

(VII) — 150 m³/(m²h)

(VIII) — 200 m³/(m²h)

Efficiency (F.R.I. Tests)

F.R.I. has never measured a better performance for any commercial random packing than the Nutter Ring. (Fig. 6.1.3.1.12 & 6.1.3.1.13)
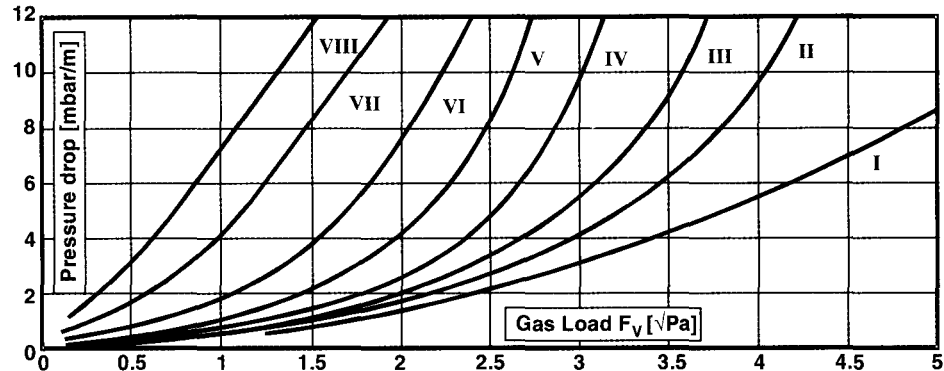
Fig. 6.1.3.1.11.
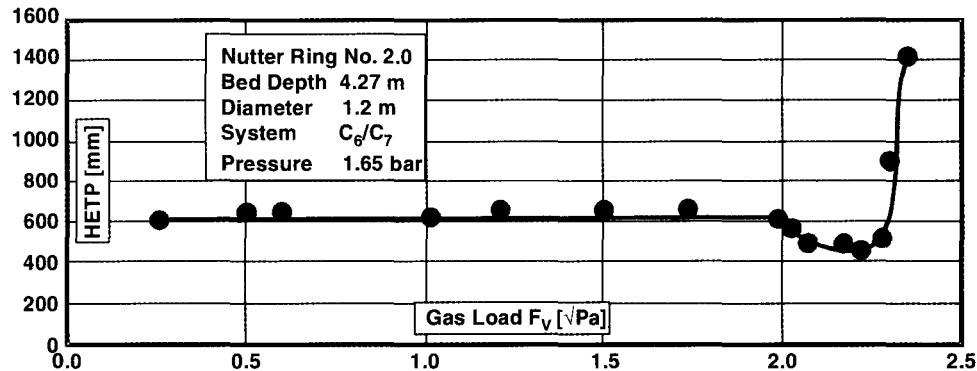
Fig. 6.1.3.1.12.
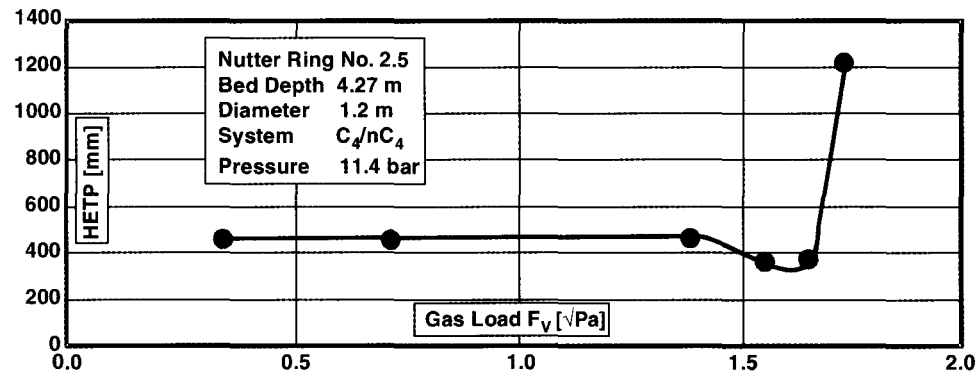
Fig. 6.1.3.1.13.

Effective Interfacial Area and $k_{OG}.a$ for CO_2-NaOH System

Compared to other random packings, Nutter Ring shows a better exploitation of the geometric surface for the mass and heat transfer. (Fig. 6.1.3.1.14)
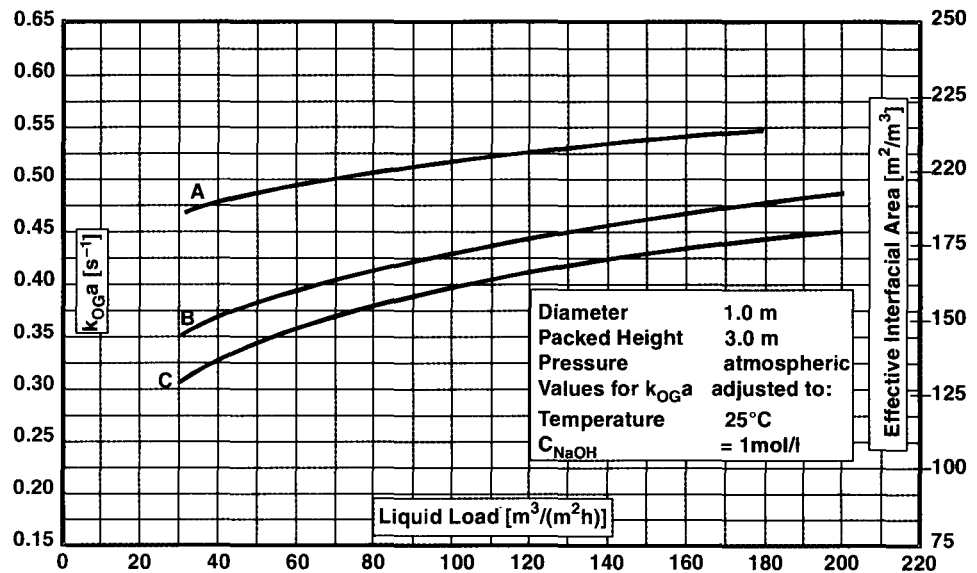
Fig. 6.1.3.1.14.

(A) — **Nutter Ring No. 1.0**

(B) — **Nutter Ring No. 2.0**

(C) — **Nutter Ring No. 2.5**

Gas and liquid distributors **Fig. 6.1.3.1.15** from *Sulzer Chemtech* ensure the peak performance of **Nutter Ring.**

Sulzer Chemtech uses the same types of liquid and gas distributors and the same quality standards for random as for its structured packing columns.

6.1.3.3. Cascade® Mini Rings

These are the random packings developed by *Glitsch, Inc.* Unlike other random column packings which generally have aspect ratio **(height : dia ratio)** approximately unity, the **Cascade**[R] **Mini Rings** have low aspect ratio which is the key to their superior performance. With an aspect ratio of only 0.3, the **Cascade Mini**

Fig. 6.1.3.1.15

Rings (CMR) undergo much greater degree of wetting of its internal surfaces than conventional dumped packings*.

Fig. 6.1.3.3-1. *Cascade Mini Rings are Cylindrical Elements With Height Only One–Third of the Outside Diameter. Fingers Punched From The Wall Project Into The Interior Increasing the Interfacial Area of the Packing Element.*

© Glitsch, Inc. Reproduced with kind permission of Topack Industries (India)— a licensee of Glitsch, Inc.

---

* Traditional dumped packings orient themselves at about 30° from the horizontal in a tower with the effect that much of their internal surfaces is shielded from liq by adjacent rings and is wetted very poorly.
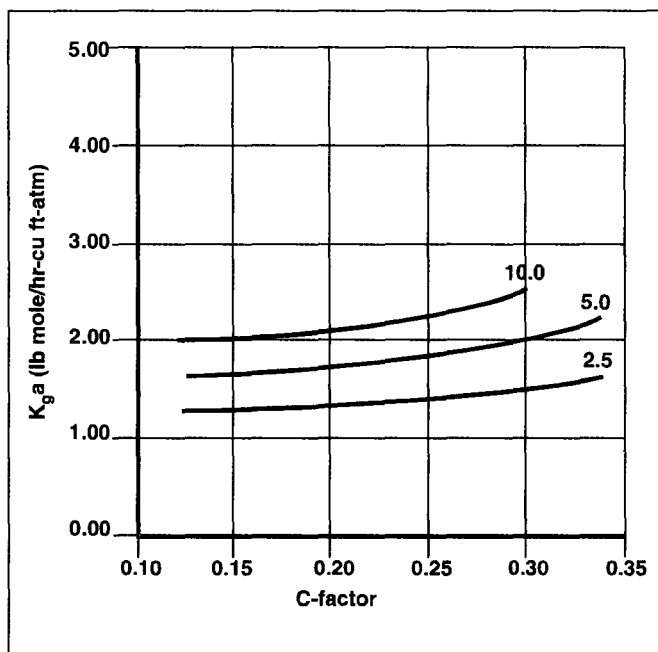
Fig. 6.1.3.3–1E. *Efficiency vs C-factor for # 3A polypropylene Cascade Mini-Rings at various liquid loadings (in gpm/sq ft).*
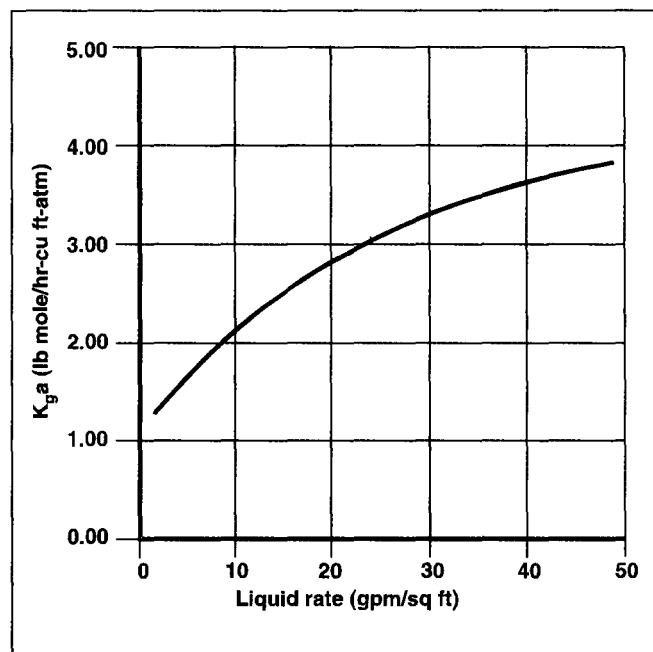
Fig. 6.1.3.3–1F. Efficiency vs liquid rate for # 3A polypropylene Cascade Mini-Rings. C-factor = 0.12.
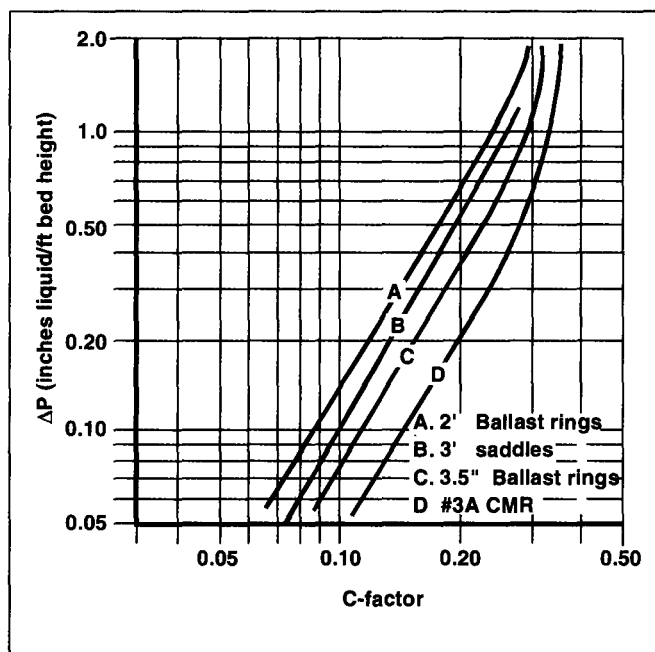
Fig. 6.1.3.3–1G. *Pressure drop vs C-factor for several polypropylene packings at 20 gpm/sq ft liquid loading.*
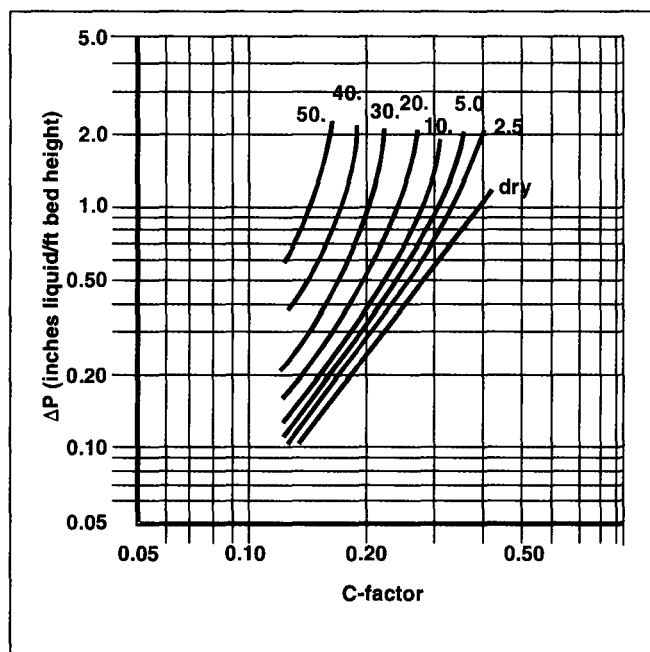
Fig. 6.1.3.3–1H. *Pressure drop vs C-factor for # 1A polypropylene Cascade Mini-Rings at various liquid loadings (in gpm/sq ft).*
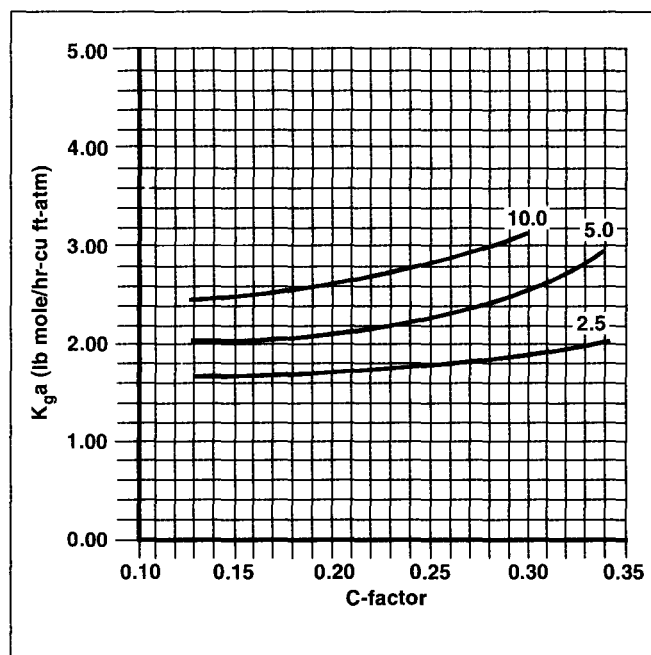
Fig. 6.1.3.3–1A. *Efficiency vs C-factor for # 1A polypropylene Cascade Mini-Rings at various liquid loadings (in gpm/sq ft).*
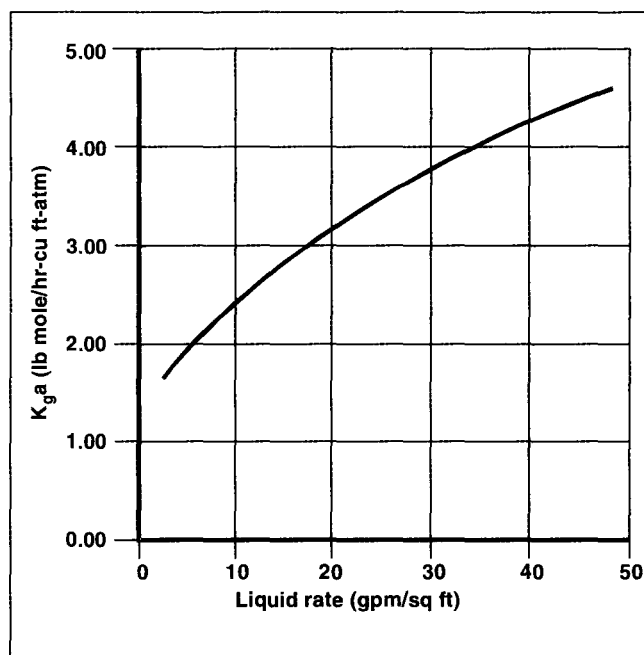
Fig. 6.1.3.3–1B. *Efficiency vs liquid rate of # 1A polypropylene Cascade Mini-Rings. C-factor = 0.12.*
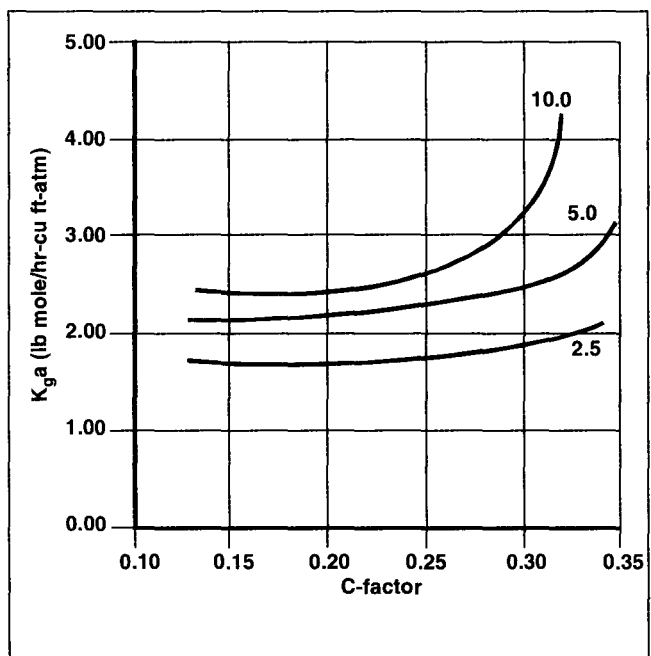
Fig. 6.1.3.3–1C. *Efficiency vs C-factor for # 2A polypropylene Cascade Mini-Rings at various liquid loadings (in gpm/sq ft).*
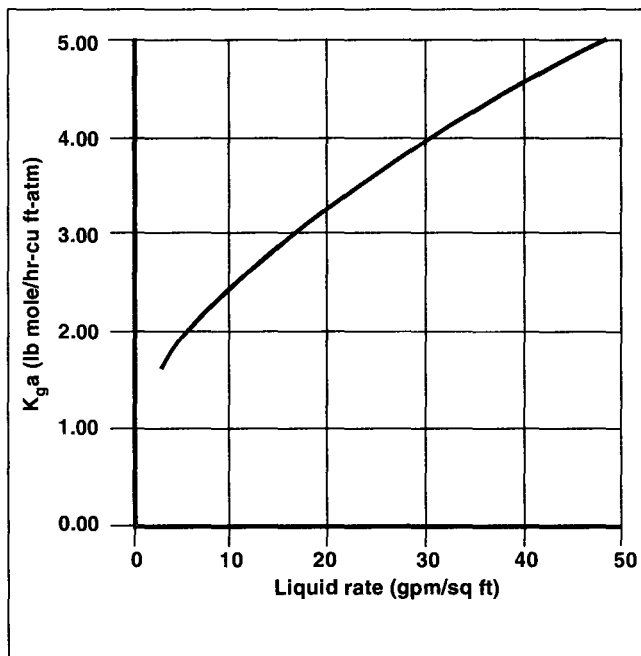
Fig. 6.1.3.3–1D. *Efficiency vs liquid rate for # 2A polypropylene Cascade Mini-Rings. C-factor = 0.12.*

Table 6.1.3.3-2. Reasonable Minimum Wetting Rates Of Cascade Mini-Rings.

Surface	m^3/h per m^2 of bed cross-section
Chemical stoneware (unglazed)	0.4888
Carbon steel or copper	0.733
Stainless steel (etched)	0.977
Ceramic (glazed)	1.955
Glass	2.444
Stainless steel, tantalus, other alloys	2.933
PVC/CPVC	3.666
Polypropylene	3.911
Fluoropolymers	4.888

Source TOPACK Bulletin : Cascade® Mini-Rings. Values are based on surface area of 141 m^2/m^3 of packed bed.

The added advantage of Cascade Mini-Rings is their high strength : **weight ratio** which permits use in deep beds with a minimum number of support plates. The **CMRs** also resist consolidation of bed during upsets and make removal easy during turnarounds.

MATERIALS OF CONSTRUCTION

Cascade Mini-Rings are fabricated from a variety of materials—from acid resistant ceramic to alloys to plastics.

Metals : Carbon steel; SS300 and SS400; aluminum; nickel; titanium; tantalum; zirconium; copper; brass; phosphor bronze; Alloy 20; Monel® 400; Inconel® 625; Incoloy® 600, 800 and 825; Hastelloy® A, B and C and other alloys also.

stics	*Recommended service Temp. (K)*
PVC	338
Polypropylene	358
CPVC	366
PVDF	413
Tefzel®	453
Halar®	473
PFA®	533
Xydar®	533

Source : **TOPACK Bulletin : Cascade® Mini-Rings**

More surface is available for formation of thin films and efficient mass transfer between liquid and gas phases.

Aerodynamic studies reveal that low aspect ratio holds form-drag to a minimum, the principal contribution to momentum, loss in the gas phase being due to **skin friction.** High gas velocities without liquid holdup are possible and that explains why the capacity of **CMR** is far greater than for **Pall rings** or **saddles.** Over and above, the unique geometry and orientation of **CMR** maximize turbulent mixing between gas and liquid phases while allowing free gas flow thru the packed bed. Pressure drop per unit of efficiency is thus low. Resulting incremental energy savings and yield increases can be so large that costs of revamping absorbers/strippers are often paid for in months rather than years.

Figure 6.1.3.3-1. Packing Factors For Cascade® Mini-Rings

Size	Plastic	Ceramic	Metal
0	---	---	55
0A	60	---	---
1	29	---	40
1A	30	---	---
1.5	---	---	29
2	15	38	22
2A	30	---	---
2B	18	---	---
2C	19	---	---
2.5	---	---	19
3	11	24	14
3A	12	---	---
4	---	---	10
5	---	18	8
7	---	15	---

Source : TOPACK Bulletin : Cascade® Mini-Rings

With **CMR** system, entrainment is very low. In any packing, entrainment is strongly influenced by stagnant liq pools and the length of surface over which waves can form in liquid films. Because of its unique design characteristics, **Cascade Mini-Ring** is less liable to nest than other random packings with the effect that liq pooling is diminished. Yet, unlike spherical packings, there is no high void space in the bed to impose a penalty on efficiency. The 0.3 aspect ratio of **CMR** means that liquid film wave formation is limited; wave height kept low and as a result entrainment goes low.

Reduced pooling and lower pressure drop also lead to less foaming (even with plastics) as well as a lower probability of solids being retained within the packing. More uniform liquid films mean fewer dry spots. This explains why **CMR packings** are less prone to fouling and corrosion than other packings.

Operating limits for a column are set at the lower end by wetting rates and at the upper by flooding. With **Cascade Mini-Rings,** towers have operated successfully in the 20–90% flooding range. Minimum wetting rates necessary are shown in **Table 6.1.3.3.2.** A turndown ratio of 4:1 is standard and some columns have been designed successfully to turndown ratio exceeding 8:1.
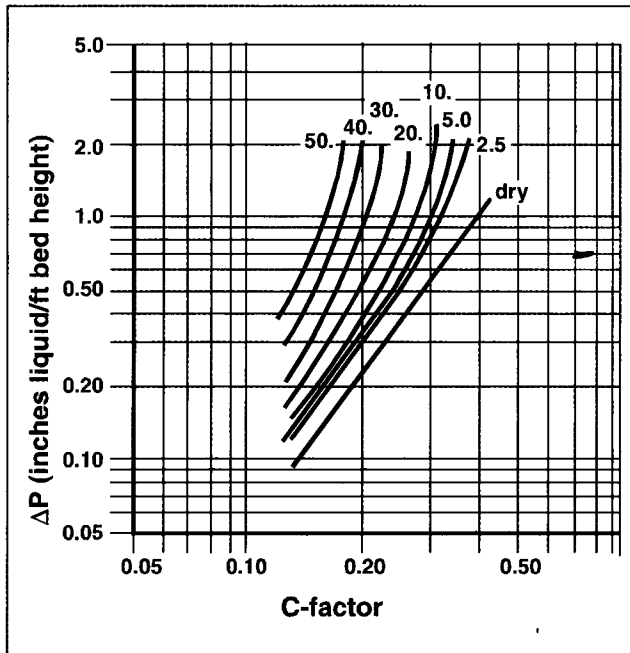
Fig. 6.1.3.3–1I. *Pressure drop vs C-factor for # 2A polypropylene Cascade Mini-Rings at various liquid loadings (in gpm/sq ft).*
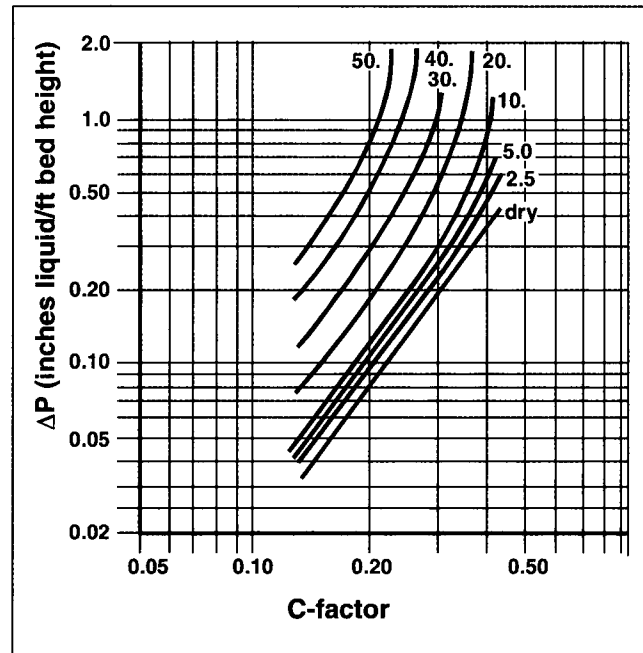
Fig. 6.1.3.3–1J. *Pressure drop vs C-factor for # 3A polypropylene Cascade Mini-Rings at various liquid loadings (in gpm/sq ft).*
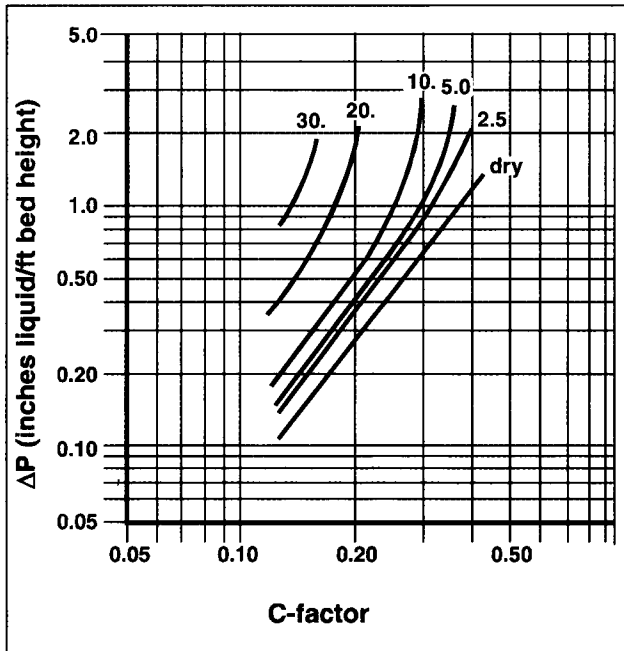
Fig. 6.1.3.3–1K. *Pressure drop vs C-factor for # 1 metal Cascade Mini-Rings at various liquid loadings (in gpm/sq ft).*
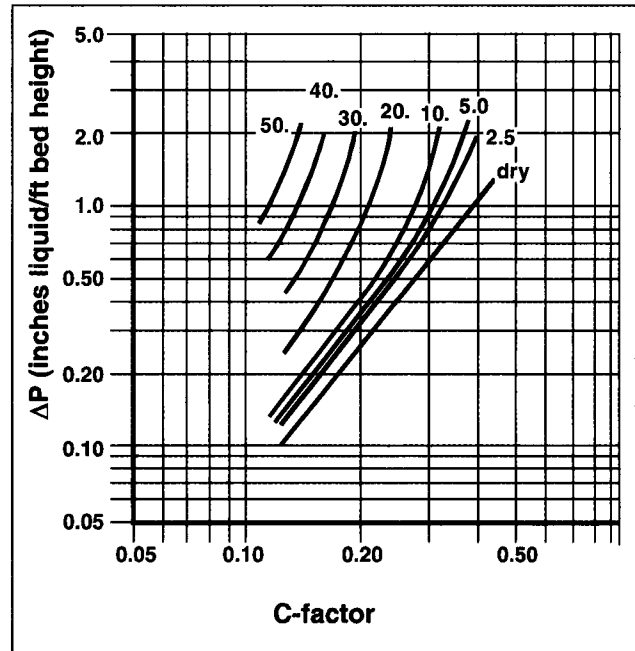
Fig. 6.1.3.3–1L. *Pressure drop vs C-factor for # 1.5 metal Cascade Mini-Rings at various liquid loadings (in gpm/sq ft).*
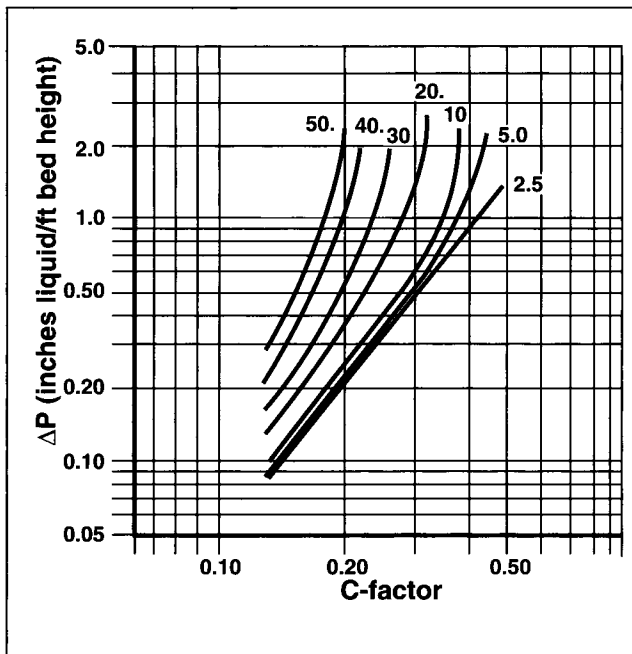
Fig. 6.1.3.3–1M. *Pressure drop vs C-factor for # 2A metal Cascade Mini-Rings at various liquid loadings (in gpm/sq ft).*
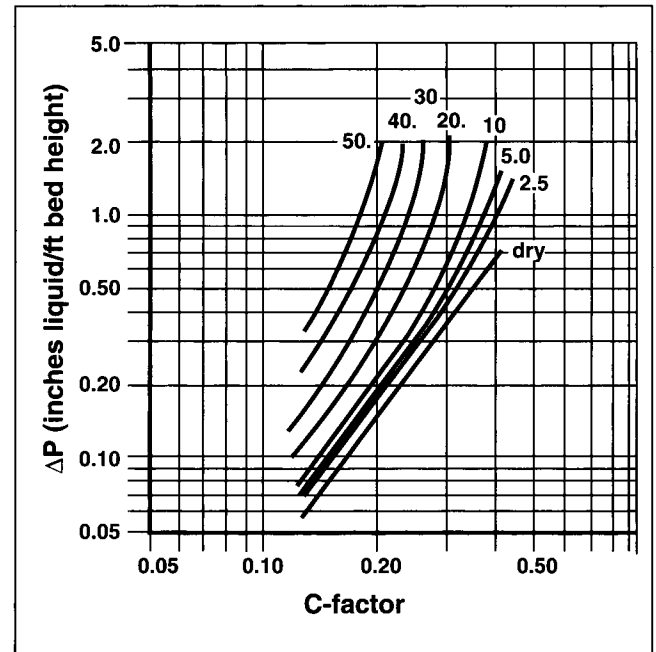
Fig. 6.1.3.3–1N. *Pressure drop vs C-factor for # 2.5 metal Cascade Mini-Rings at various liquid loadings (in gpm/sq ft).*
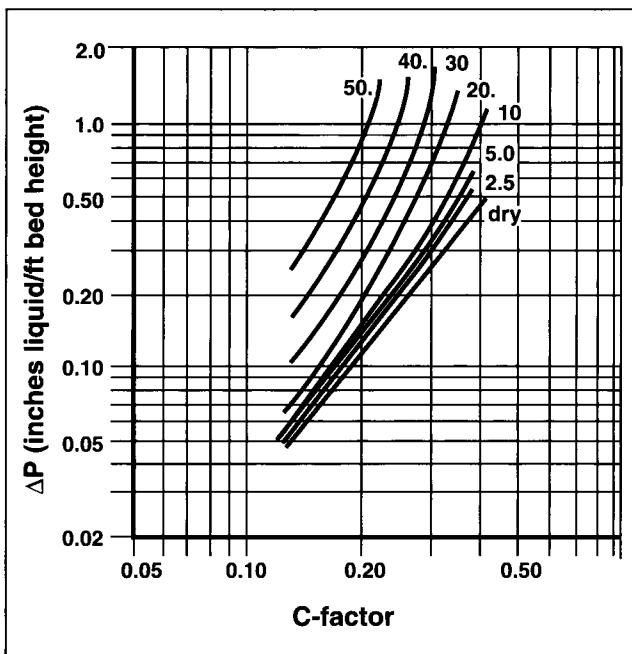
Fig. 6.1.3.3–1O. *Pressure drop vs C-factor for # 3 metal Cascade Mini-Rings at various liquid loadings (in gpm/sq ft).*
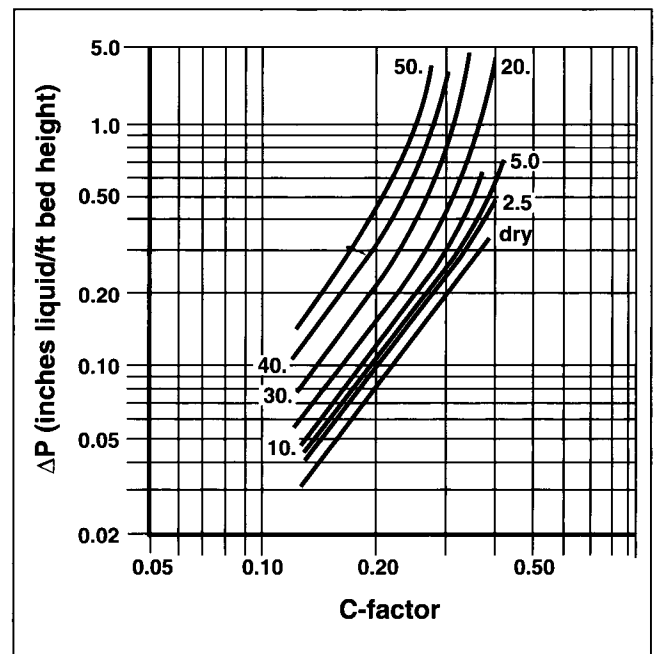
Fig. 6.1.3.3–1P. *Pressure drop vs C-factor for # 4 metal Cascade Mini-Rings at various liquid loadings (in gpm/sq ft).*

6.1.4. INTALOX® HIGH-PERFORMANCE SNOWFLAKE™ PACKING

It is the latest product of Norton. This plastic packing offers superior absorption and stripping efficiencies and, equally significant, lowers pressure drop to a point unmatched by standard plastic packing.

Fig. 6.1.4.1. *Intalox® Snowflake Tower Packing begets Superior Mass Transfer Efficiencies, lowers Pressure-Drop.*

Performance : As shown in fig. **6.1.4.1A. Intalox snowflake packing**
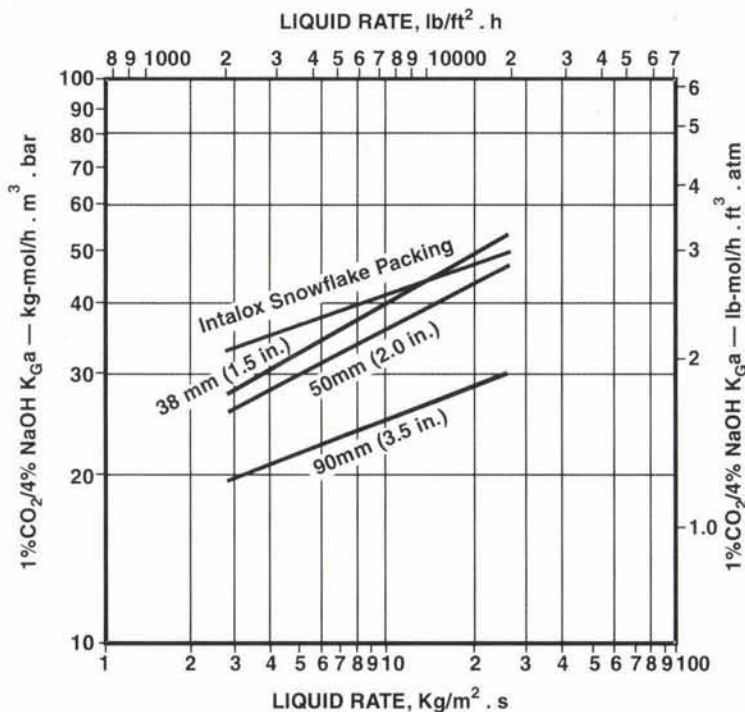
© *Norton Co.* Reproduced with kind permission of Norton Chemical Process Products Corpn, Akron, Ohio (USA).

Fig. 6.1.4-1A. *Intalox Snowflake Packing vs. Plastic Pall Rings.*

Packing Factor, F_p

Pall ring size, mm	38	50	90
Pall ring F_p	40	25	17
Intalox Snowflake packing, F_p	13	13	13

has:

— 68% greater efficiency than the 90 mm plastic **Pall ring**, with only 80% of the press-drop.

— 25% greater efficiency than the 50 mm plastic **Pall ring**, with only 50% of the press-drop.

— 10% greater efficiency than the 38 mm plastic **Pall ring**, with only 32% of the press-drop.

Operational Economics : In addition to increasing the efficiency of absorption and stripping operation, the proven performance characteristics of **Intalox Snowflake packing**, it has been reported, can substantially reduce the consumption of electrical energy.

Capital savings can also be realized for new installations because the size of towers and blowers can be significantly smaller than those required for standard packing.

The curves of the mass-transfer coefficients in **Fig. 6.1.4.1A.** show the tower height savings that are possible with **Intalox Snowflake packing**. The larger the $K_G.a$, the shorter the tower.

For the same amount of material transferred, the liquid holdup of **Intalox Snowflake packing** is normally less than standard packing. This not only reduces liquid inventory but also lowers the amount of absorbate degradation due to oxidation or thermal instability. This can be a significant benefit in situations where degradation products must be removed by a side-stream purification system.

Applications :   **# Fume scrubbing**

— formaldehyde

— ammonia

— acetic acid

 # Acid gas absorption

— HCl

— SO_2

— H_2S

 # Hot carbonate system

 # VOC stripper (volatile organic carbon stripping from ground water)

 # Deodorization (waste water treatment plant)

 # Direct contact cooling

 # Flue gas scrubbing

INTALOX® HIGH-PERFORMANCE SNOWFLAKE® PACKING DATA

For maximum tower performance, Norton's plastic Intalox® Snowflake® high-performance random packing offers superior separation efficiency and capacity in environmental applications, such as scrubbing and stripping. Independent tests have proven **Intalox Snowflake** packing to be the most

effective packing available for groundwater air stripping applications, yielding removal efficiencies of 99% and above.

Its unique shape lowers pressure drop, which substantially reduces electrical energy consumption. In typical system designs, **Intalox Snowflake packing** can save more than 50% in energy costs than traditional 1-in. plastic saddles. In new installations, the pressure drop advantage of **Intalox Snowflake** packing enables the designer to significantly reduce the size of towers and blowers.

Physical Data

Super Intalox Saddles				Intalox Snowflake Packing	Pall Rings			
Size	No. 1	No. 2	No. 3	50	25	38	50	90
pcs/m^3	57500	6400	1400	4925	50220	14870	6127	1171
pcs/ft^3	1620	190	42	144	1422	421	174	33
Wt.* kg/m^3	83	61	50	45	69	82	60	43
Wt.* lbs/ft^3	5.2	3.8	3.1	2.8	4.3	5.1	3.8	2.7
Void Space %	90	93	94	95	92	91	93	95

*Weights are nominal and are based upon polypropylene.

Physical Characteristics*

Packing Factor	13	13
Bulk Density	44.9 ± 3.2 kg/m^3	2.8 ± 0.2 lb/ft^3
Number of Pieces	4,925 pcs/m^3	140 pcs/ft^3
Surface Area	91.8 m^2/m^3	28 ft^2/ft^3
Void Fraction	95 ± 0.03%	95 ± 0.03%
Diameter	94 mm	3.7 in.
Height	30.5 mm	1.2 in.

*Typical values

PILOT PLANT TEST TOWER

Diameter	762 mm	30 in.
Bed Depth	3,048 mm	10ft.

GAS RATE, lb/ft².h
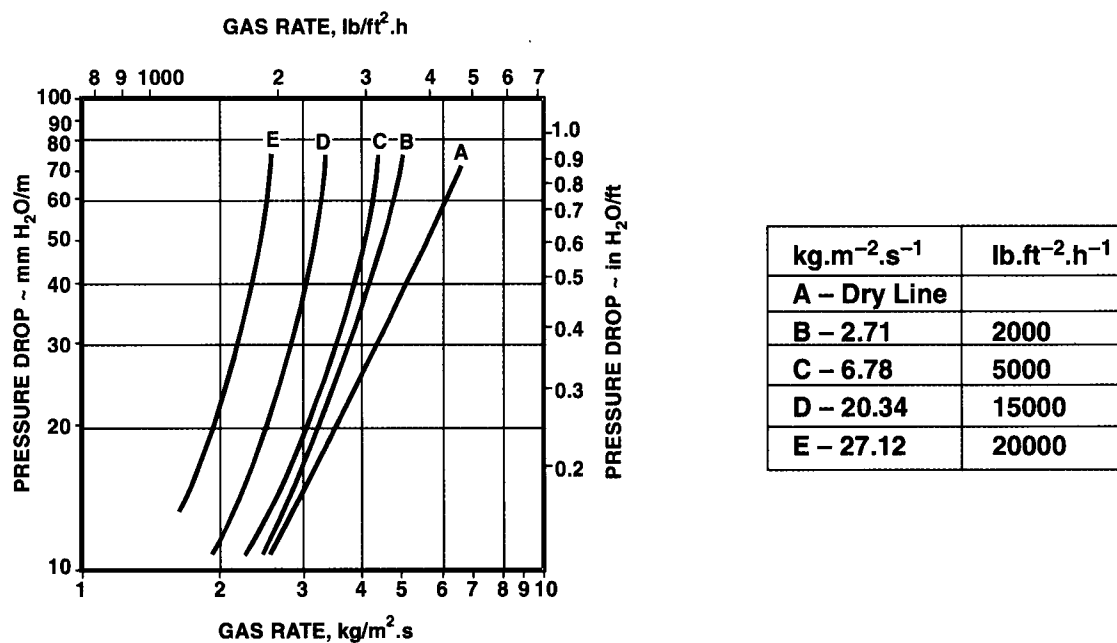
Fig. 6.1.4–1B. *Pressure Drop vs. Gas Rate.*

kg.m⁻².s⁻¹	lb.ft⁻².h⁻¹
A – Dry Line	
B – 2.71	2000
C – 6.78	5000
D – 20.34	15000
E – 27.12	20000

ΔP	
mm H₂O/m	inch H₂O/ft
A – 0	0.0
B – 42	0.5
C – 83	1.0
D – 125	1.5
E – 167	2.0

WATER LIQUID RATE, lb/ft².h

WATER LIQUID RATE, kg/m².s

Fig. 6.1.4–1D. K_Ga *vs. Liquid Rate.*

LIQUID RATE, lb/ft^2.h

CO$_2$/Air	1%
Caustic	4%
Carbonation	25%

LIQUID RATE, kg/m^2.s
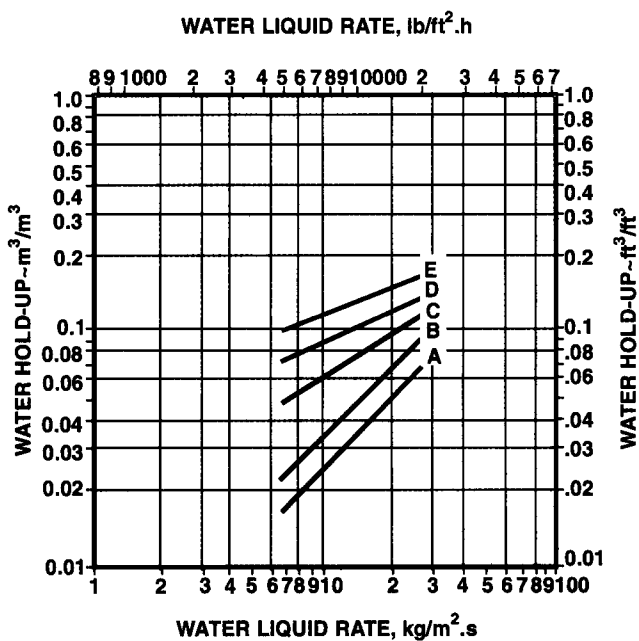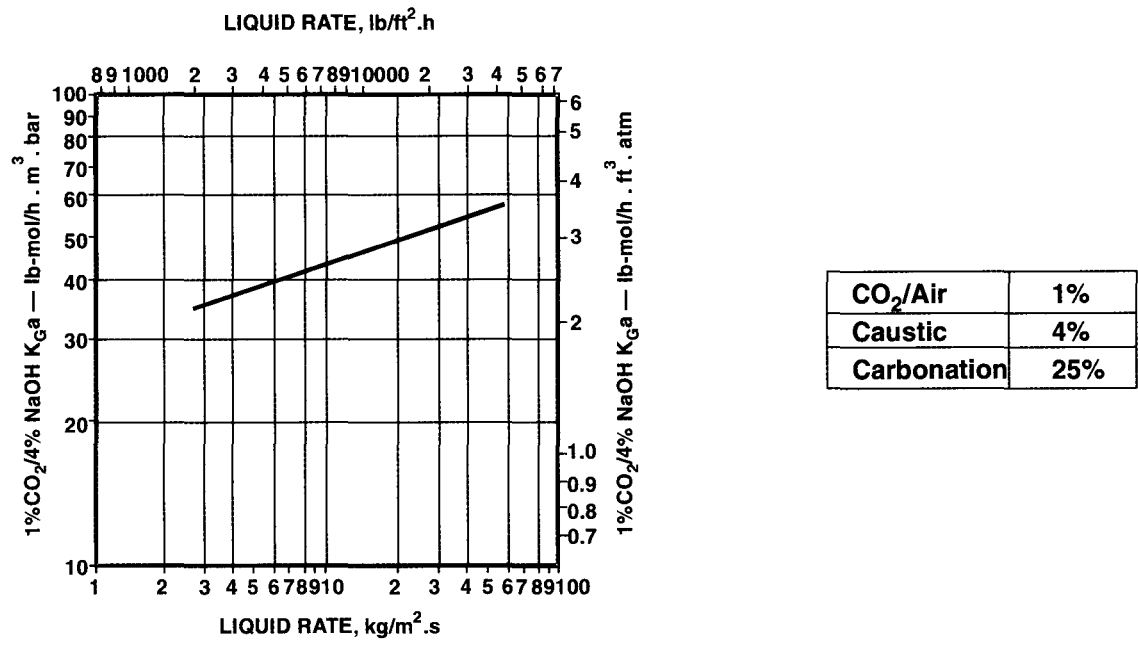
Fig. 6.1.4–1C. *Total Liquid Hold-Up vs. Liquid Rate.*

6.2. REGULAR PACKINGS

They are of a great variety. We shall limit out discussion to structured packings only.

Structured packings are of two general types : **knitted** and **nonknitted**. Both come in segmented as well as spiral forms.

The knitted structured packing is made of either knitted wire mesh or woven-wire gauze. **Series X/S** of ACS Industries, Inc. is a good example of knitted mesh structured packing **Fig. 6.2-1**
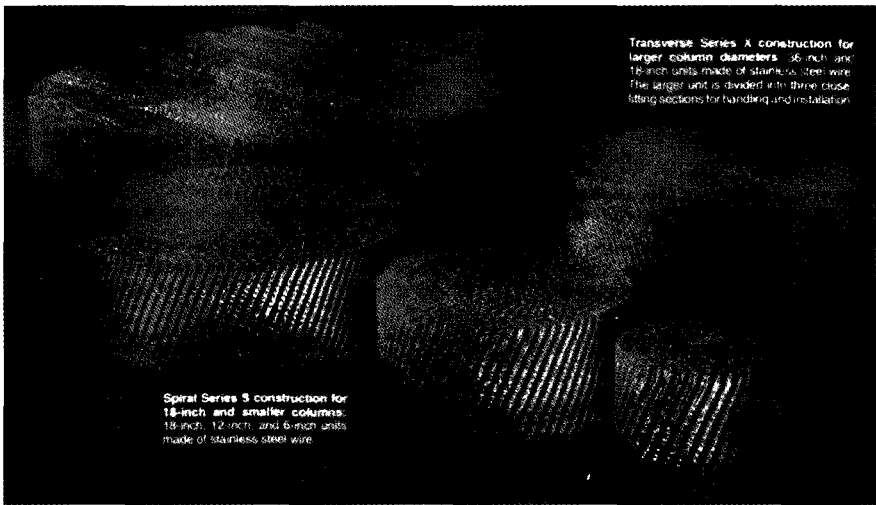
Fig. 6.2-2. *Spiral Series S and Transverse Series X are both Knit Mesh Packings.*
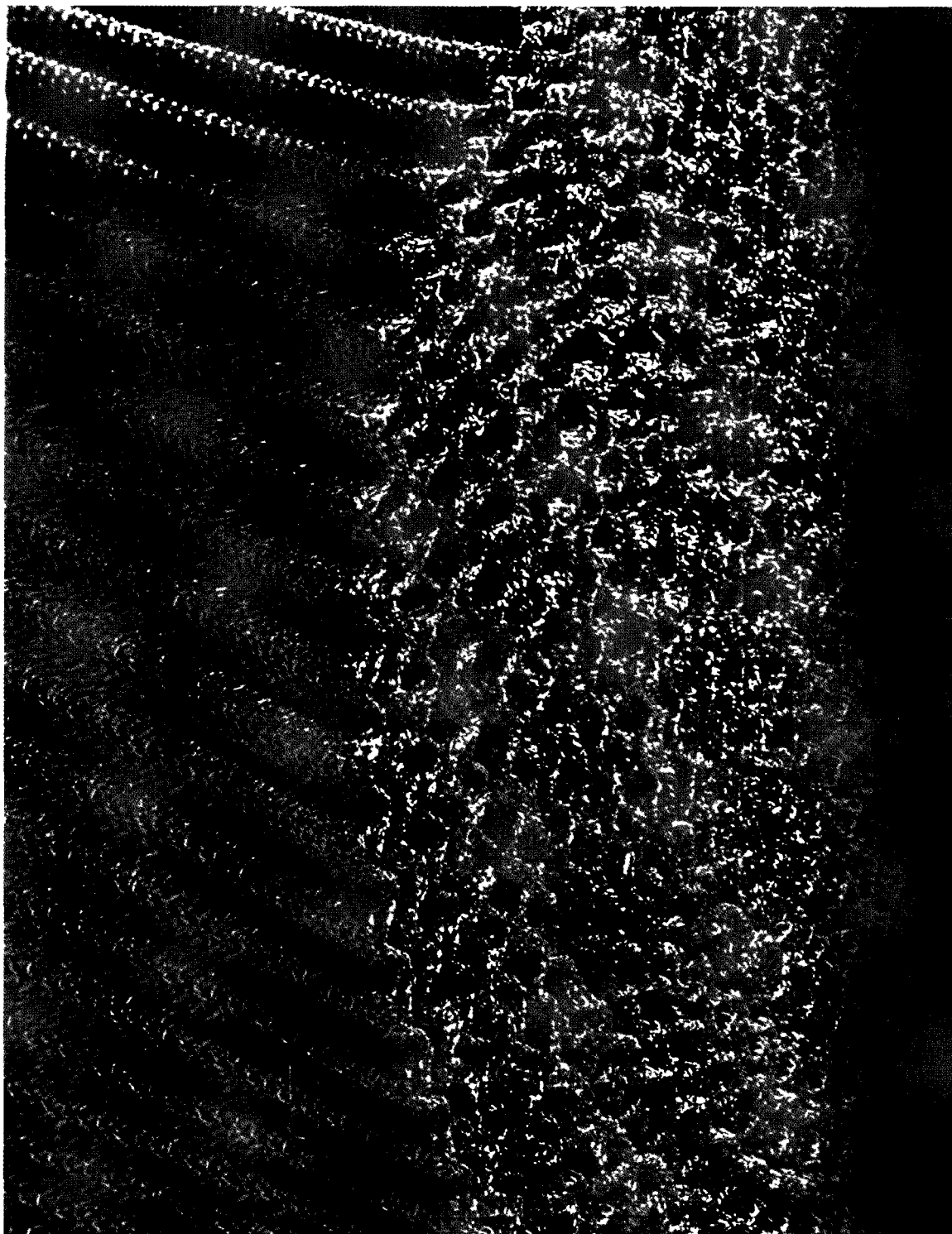
Bulletin : Series X/S Knitted Wire Mesh Structured Packing

ACS Industries, Inc.

Fig. 6.2-1. *Knit-Mesh structured packing. Spiral Series S.*

Spiral Series S construction is for columns of ID ≤ 450mm **Fig. 6.2-2** while **Transverse Series X** construction is for larger dia columns (ID ≥ 900mm) **Fig. 6.2-3**

The **S-Style** results when two ribbons with opposite corrugations are wrapped in spiral pattern (**Fig. 6.2-3**)
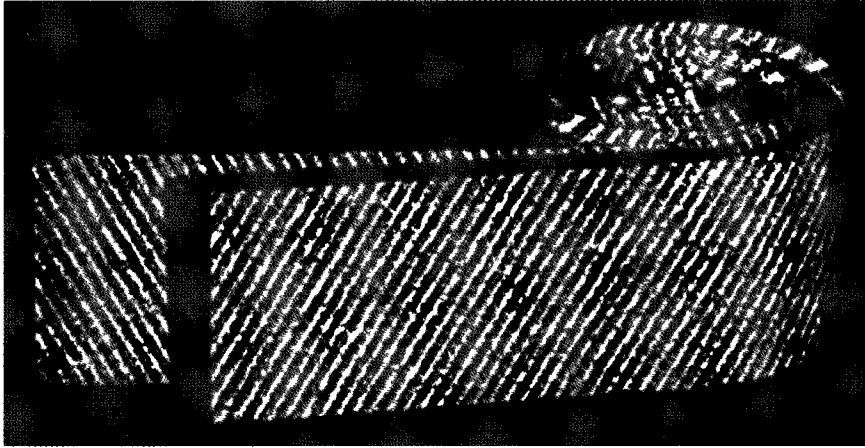
© **ACS Industries, Inc.**

Reproduced with kind permission of ACS Industries, Inc./Houston/Texas

Fig. 6.2-3. *Knit Mesh structured Packing—Spiral Type S-Style of ACS Industries, Inc. It Is Formed By Spiraling Two Ribbons With Opposite Corrugations Wrapped Together.*

The **X-Style** is built up of vertical sheets stacked with alternate corrugations (**Fig. 6.2-4**) that provide intersecting gas channels.
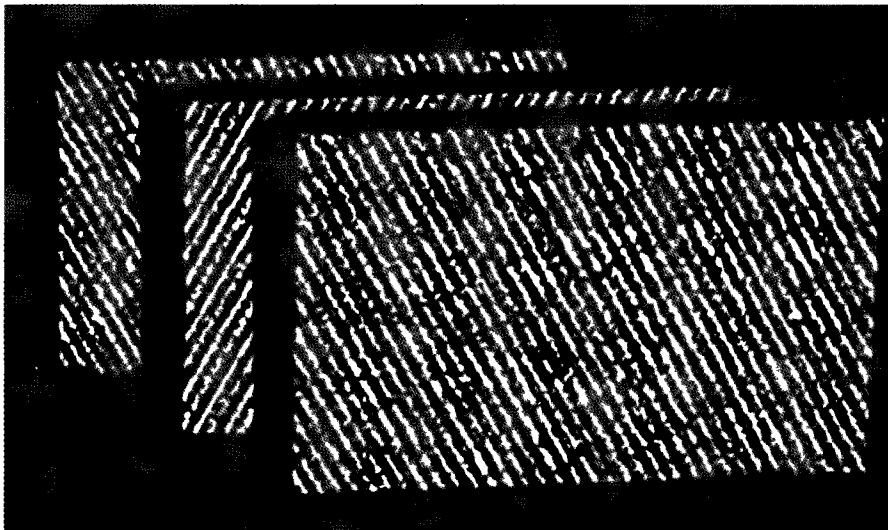
© ACS Industries, Inc. Reproduced with kind permission of ACS Industries, Inc./Houston/Texas.

Fig. 6.2-4. *X-Style is composed of Straight Sheets Stacked Together in a Rigid Structure.*

Fig. 6.2-5 and **6.2-6** are the two good examples of **gauze packing.**

Gauze Packings

Sulzer Metal Gauze Packing, Type BX
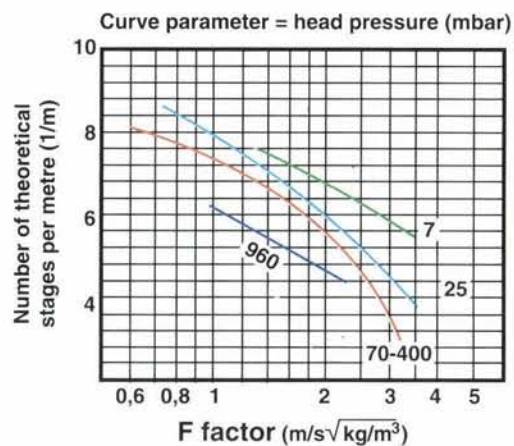
Fig.6.2.5A.

Bulletin : **Separation Columns For Distillation and Absorption**

Sulzer Chemtech

© **Sulzer Brothers Ltd. Switzerland**

Figure 6.2.5. *Gauze Packing.*

Shown here is the Sulzer Metal Gauze Packing,* Type BX. *It bestows :

• ***High Number of Theoretical Trays per Meter of Packed Bed Height.***

• ***Low Pressure Drop. As little as 0.1 – 0.5 mbar per Theoretical Stage***

• ***Small Holdup***

It Operates with A Minimum Liq Load of 0.2 m³/(h.m²)

This packing [**Fig. : 6.2.5**] has been in successful industrial use for more than 25 years. Greatest diameter supplied to date : 6m.

Special Features

■ High number of theoretical stages per meter

■ Pressure drop per theoretical stage 0.1 to 0.5 mbar

■ Most economical load range : **F-factor** 2—2.5 m/s $\sqrt{kg/m^3}$

■ Minimum liquid load approx. 0.2 m³/(m²h)

■ Small hold-up

Preferred Applications

- For a large number of theoretical stages
- In vacuum from 1 mbar to atmospheric pressure
- Where minimum pressure drop per theoretical stage is important
- For small overall height
- Batch and continuous columns
- Pilot columns (reliable scale-up)

Of only limited suitability for

- fouling substances that form deposits
- non-wetting liquids
  (*e.g.*, higher **HETP** with water)

Source : Separation Columns For Distillation and Absorption

Courtesy : Sulzer Chemtech

© Sulzer Brothers Ltd.

Reproduced with kind permission of Sulzer Brothers Limited/Winterthur/Switzerland

Curve parameters = liquid load (m³/m²h)
Ø = column diameter (mm)

Fig. : 6.2.5.B.

Gauze Packings

Sulzer Metal Gauze Packing, Type CY

Fig. : 6.2.6.

Curve parameter = head pressure (mbar)

Fig. : 6.2.6.A.

Bulletin : Separation Columns For Distillation and Absorption
Sulzer Chemtech
© Sulzer Rbrothers LTD.

Reproduced with kind permission of Sulzer Brothers LTD./Winter thur Switzerland

Fig. 6.2.6. Gauze Packing.

Shown here is the Sulzer Metal Gauze Packing, Type CY having the following Special Features.

- *Max. No. of Theoretical Stages Per Meter of Packed Height*
- *Small Holdup*

It comes into Operation with as Low Liq Load as 0.2 m³/(h.m³)
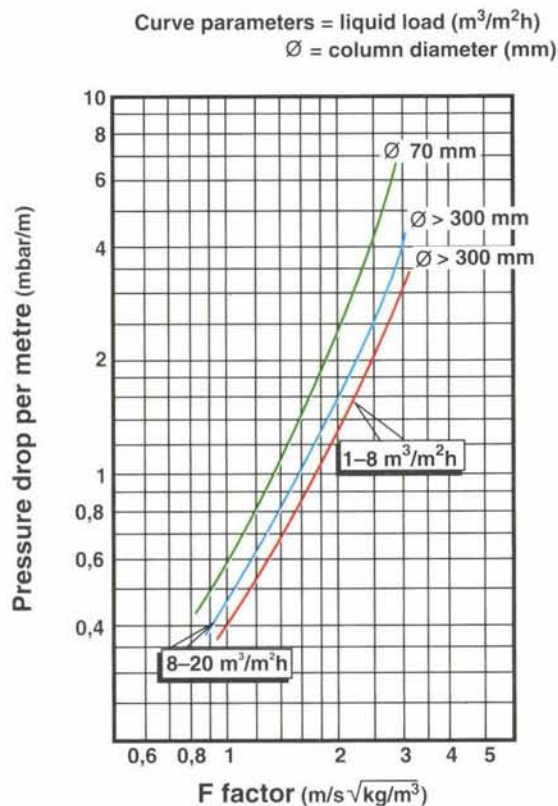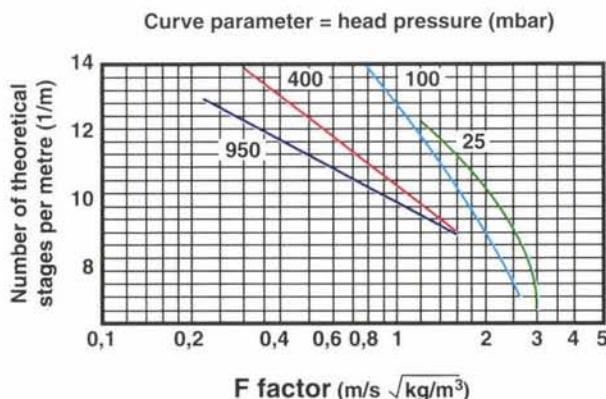
This packing [**Fig. : 6.2.6**] was developed for separation which require a large number of theoretical stages. Largest diameter supplied to date : 1.8 m.

Special Features

■ Maximum number of theoretical stages per meter

■ Most economical load range : **F-factor**

   1.5–2 m/s $\sqrt{kg/m^3}$

■ Minimum liquid load approx. 0.2 m³/(m² h)

■ Small hold-up

Preferred Applications

■ For a large number of theoretical stages

■ In vacuum from 1 mbar to atmospheric pressure

■ For small overall height

■ Batch and continuous columns

■ Pilot columns (reliable scale-up)

Of only limited suitability for

■ fouling substances that form deposits

■ non-wetting liquids (e.g., higher **HETP** with water)

Source : *Separation Columns For Distillation and Absorption.*

Courtesy : Sulzer Chemtech.

© **Sulzer Brothers Ltd.**

Curve parameter = head pressure (mbar)
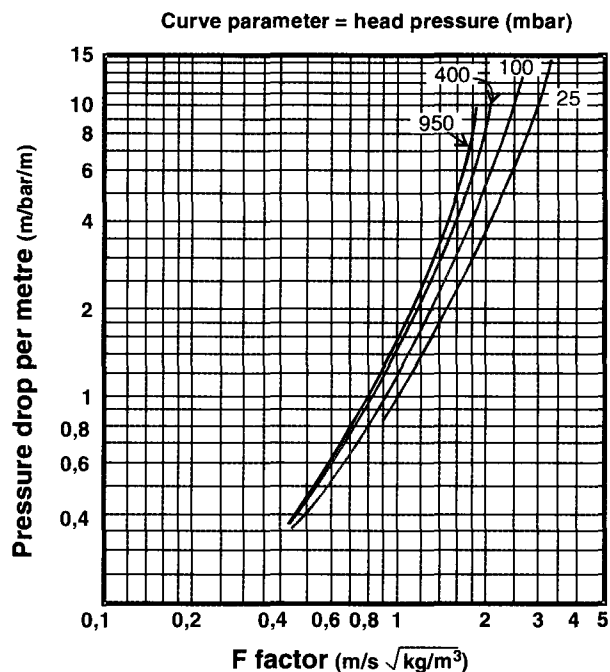
Fig. : 6.2.6.B.

Reproduced with kind permission of Sulzer Brothers Limited/Winterthur/Switzerland

These structured gauze packings are made from corrugated woven wire-gauze [**Fig. 6.2.7**]. The gauze is punctured with holes for liquid passage and then crimped to form diagonal gas channels. The crimped zigzags form angles of about 90°, with peaks about 12mm apart [**Fig. 6.2.8**]. Parallel ridges run at an angle of 30° from the vertical for liquid passage and then crimped to form
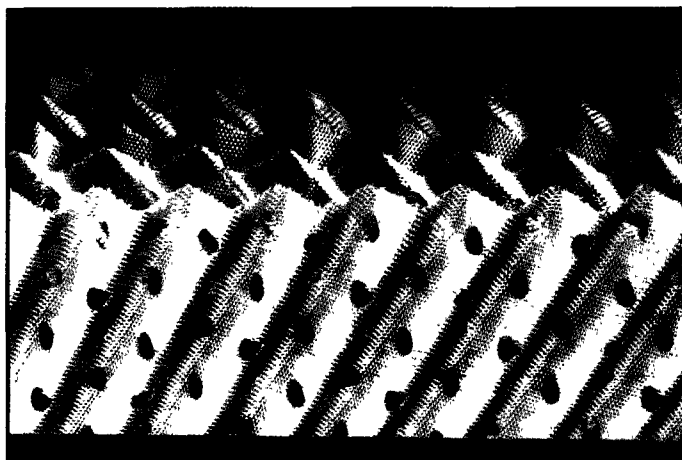
Fig. : 6.2.7. *Corrugated Woven Wire-Gauze Perforated With An Optimal Array of Small Widely Spaced Holes that Break up Liquid and Gas Flow. The Resulting Gas Turbulence Promotes Heat and Mass Transfer. The Holes Also Assist in Mixing and Spreading Liq Films.*

diagonal gas channels. The crimped zigzags form angles of about 90°, with about 12 mm [**Fig. 6.2.8**]. Parallel ridges run at an angle of 30° from the vertical.
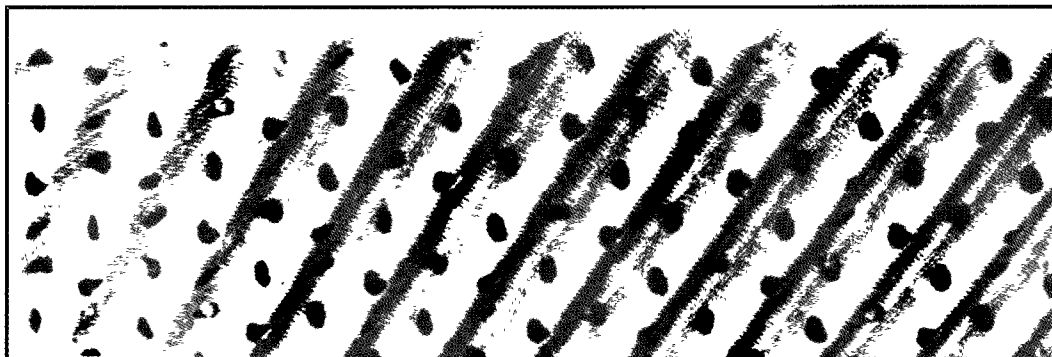
© **ACS Industries, INC.**

Reproduced with kind permission of ACS Industries, Inc./Houston/Texas

Fig. 6.2.8. *Angled Corrugations Provide Gas Channels.*

The crimped gauze sheets are packed tightly together, with corrugations running in alternate directions [**Fig. 6.2.9**]. This combination holds sheets apart from its two adjacent sheets in a rigid structure, while providing open gas passage with intersections forming a tortuous pattern. This design pattern enhances heat and mass transfer by gas turbulence and spreads the gas across the column.
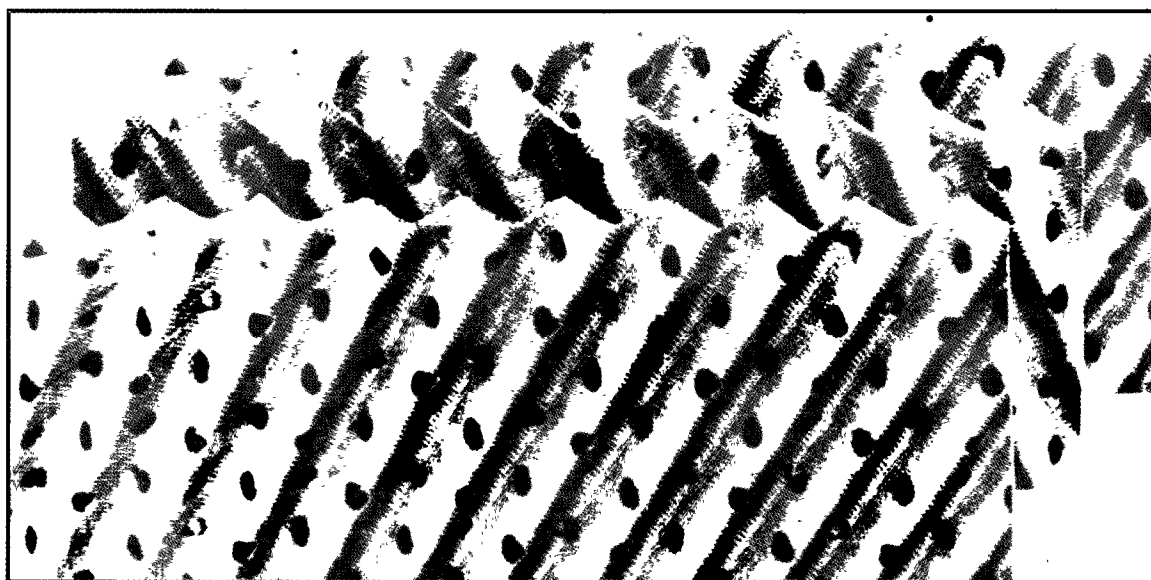
© **ACS Industries, INC.**

Reproduced with kind permission of ACS Industries, Inc./Houston/Texas.

Fig. 6.2.9. *Crossing the corrugations promotes gas turbulence.*

Nonknitted structured packing comes in sectionalized beds [**Fig. 6.2.10**] which are made up of corrugated plates in contact with each other and with the corrugations of adjacent plates inclined to each other [**Fig. 6.2.12**] and to the axis of the column.

© Sulzer Brothers Ltd. Reproduced with kind permission of Sulzer Brothers Ltd./Winterthur/Switzerland

Fig. 6.2.10. *Mellapak in Segmented Form. It is the Structured Plate Packing of SULZER CO.*

In its metal and plastics versions, **Mellapak** has a characteristic surface structure which results in a high separation performance of liquid loads ranging from small to high. The alternating arrangements of the individual corrugated sheets forms intersecting open channels. These effect an optimum intermixing of gas flows.

Depending on the chosen flow channel hydraulic diameter, different specific surface areas, for example 125, 250, 500 or $75m^2/m^3$, can be obtained. The angle of inclination of the channels is 30° for the **X series** and 45° for the **Y series.** By selecting appropriate combinations of the two parameters, MELLPAK provides the optimum configuration for any application.
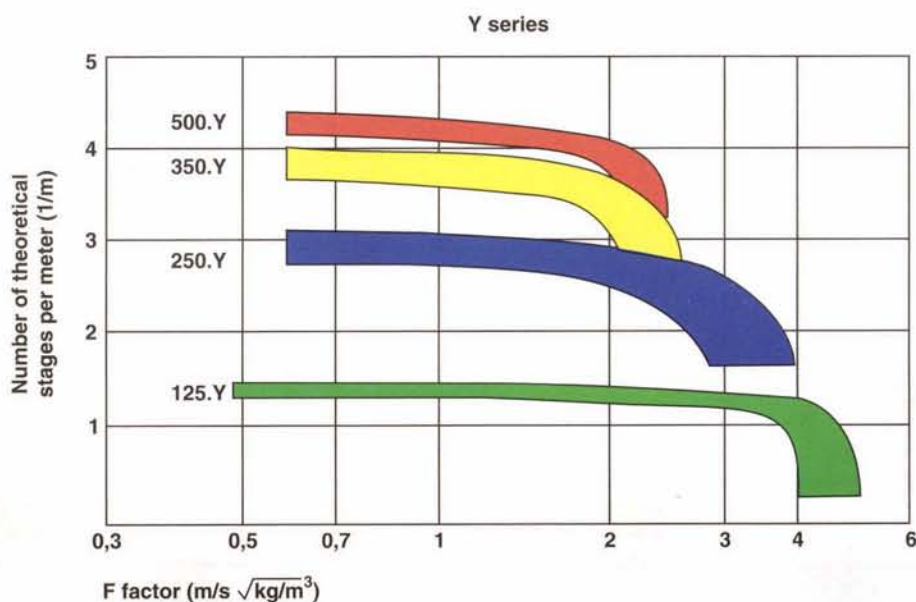
Fig. : 6.2.11.A. *NTUM vs. F-factor for Mellapak Y-series*

© **SULZER BROS. Ltd.**
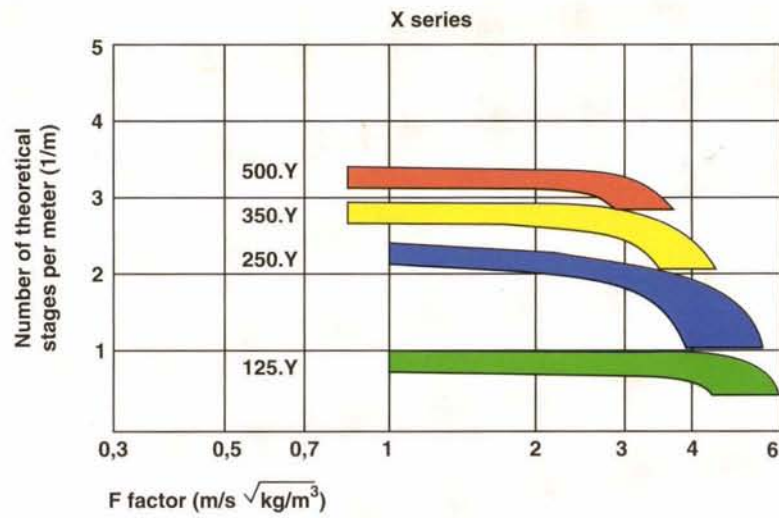
Fig. : 6.2.11.B. *NTUM vs. F-factor for Mellapak X-series*

© SULZER BROS. Ltd.

Fig. : 6.2.11.C. *Mellapak is also eminently suitable for services under positive pressure.*
© SULZER BROS. Ltd.

MELLAPAK functions also under positive pressures.
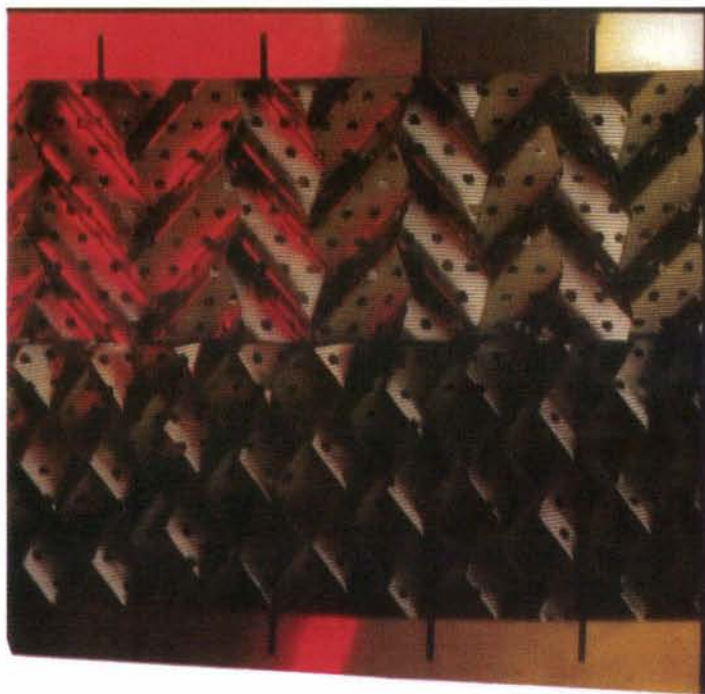
Fig. : 6.2.12. *The Corrugated Sheets are Combined in A Unique Geometric Pattern Forming Mixing Cells at Every Point Where the Corrugations Intersect.*

© **Koch Engineering Co.**

Reproduced with kind permission of Koch International, S.p.A., Bergamo, Italy.

The angled corrugations of adjacent layers are reversed with respect to the vertical column axis, forming mixing cells at every point where the corrugations intersect.

As shown in **Fig. 6.2.13,** the liquid and gas streams enter a cell, mix and form two new streams that flow into another mixing cell downstream in the element. After passing thru an element the gas and liq phases get thoroughly mixed across the surface of the corrugated sheets. Each subsequent element is oriented 90° from the previous one. Thus intimate mixing and radial distribution occur over the entire tower cross-section.

When operating, the liquid flows downward in zigzag patterns while the woven wire-gauze exercises a capillary effect that ensures complete wetting of its surface. This allows the uniform liquid flow in every unit cross-section of entire packed bed, even at very low liquid rates. Mass transfer takes place on both
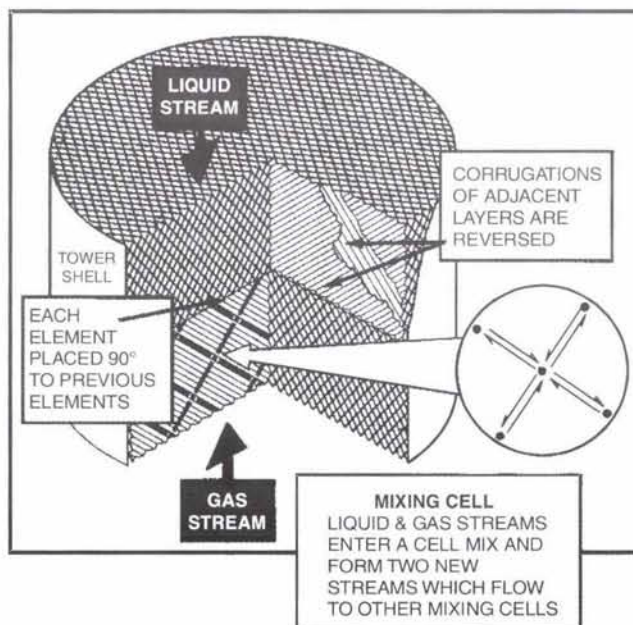
© *Koch Engineering Co.* Reproduced with kind permission of Koch International, S.p.A., Bergamo, Italy.

Fig. : 6.2.13. *Liquid and Gas Mixing in Koch/Sulzer Packing Elements.*

sides of the wire gauze. Inasmuch as only the kinetic energy of the gas is expended to move it thru the gas/liq interface, pressure drop remains extremely low.

The packing bodies are made of metal or synthetic material, preferably one that is self-wetting and textured or fibrous in nature.

While spiral-wound packing comes in modular, stackable cakes **[Fig. 6.2.14],** the segmented design is for installation thru manways in columns of large dia **[Fig. 6.2.15].**

© GLITSCH, Inc. Reproduced with kind permission of GLITSCH, Inc,/Dallas/ Texas (USA).

Fig. : 6.2.14. *Spiral Wound Design comes in Modular, Stackable Cakes. It consists of Corrugated Strips or Ribbons Coiling about A Central Axis to Form A Flat Cake of the Requisite Tower Dia. Such Modular Elements (Blocks) are Stacked One Upon the Other to give the Required Bed Depth.*
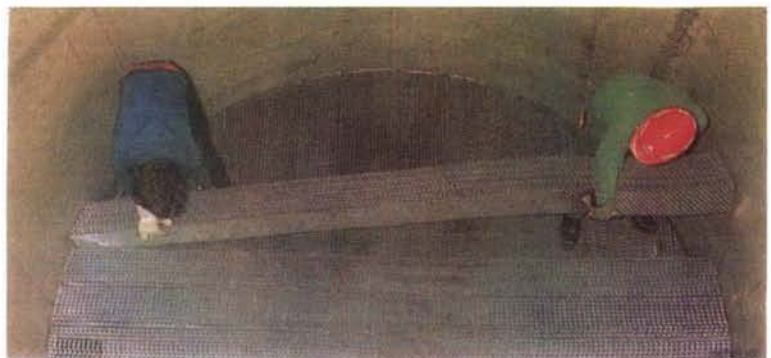
© *Sulzer Brothers LTD.* Reproduced with kind permission of Sulzer Brothers LTD./Winterthur/Switzerland.

Fig. : 6.2.15. *Packing is Inserted thru the Manhole. Packing, thereafter, is fitted inside the Column Sleeves at the Preassembly site.*

Structured Packings beget

- **greater capacity**
- **higher efficiency**
- **lower energy consumption**

than do random packing and trays. Plus, the scaleup of this type of packing is linear, i.e., laboratory model can be scaled up to fabricate a commercial column. However, these advantages come at the expense of a higher initial cost.

The use of high-performance structured packing should be considered :

- where tower revamping is required, by replacing trays or dumped packing with structured packing, to increase production capacity.

- where energy conservation is at a premium.

- when handling a high-value-added product, to minimize its inventory in the column.

- where process conditions demand operating at a low temperature to avoid thermal degradation or polymerization of the components.

- to hike up product purity or thruput in plants where headspace is a limitation.

- to cope with difficult separations requiring a large number of theoretical trays.

6.3. Selection and Design Guide to Random Packings

Obviously it is the tower operating conditions – temperature, pressure and corrosive nature of products and working fluids – that chiefly influence the choice of packing. O.Frank gives some general guideline :

■ **Metal packing should be avoided if the corrosion rate exceeds 10 mils/yr**

■ **Plastic packings must not be recommended for service beyond 340K of operating temperature.**

■ **Plastic packing may embrittle under prolonged exposure. So under conditions where they may be subjected to continuous heating, it is better, they should be glass-fibre-reinforced or an engineering plastic shall be used.**

■ **Ceramic packing is to be recommended for hot, corrosive service, although it is more fragile then metal or plastic packing.**

Source : O. Frank – *Shortcuts For Distillation Design* **Chemical Engineering, March 14 (1977).**

In general, the larger the packing elements of a given type, the smaller the available surface area for gas-liq contacting and hence lower the contacting efficiency, the lower the pressure drop, the higher the capacity, and the lower the cost.

There are four principal controlling factoring that dictate the economical choice of the random packing, These are :

● **Capacity**

● **Efficiency**

● **Pressure drop**

● **Material of Construction**

Table 6.3.A. outlines a general comparison of the four most commonly specified random packings.

Table 6.3.A Selection and Design Guide to The Most-Frequently-Specified Random Packing

Factor	*Packing*	*Type*		
	Raschig ring	*Berl saddle*	*Intalox saddle*	*Slotted ring*
Capacity	low	high (plastic) moderate (ceramic)	high (plastic) moderate (ceramic)	high (plastic and metal) moderate (ceramic)
In Bed Redistribution	poor	good	good	good
Turn-Down	poor	good	good	good
Efficiency	poor	good	good	good
Pressure Drop	high	low (plastic) moderate (ceramic)	low (plastic) moderate (ceramic)	low (plastic) moderate (ceramic)

Factor	Packing	Type		
	Raschig ring	*Berl saddle*	*Intalox saddle*	*Slotted ring*
Materials of Construction				
Plastic	no	yes	yes	yes
Metal	yes	no	no	yes
Ceramic	yes	yes	yes	yes
Carbon	yes	yes	no	no
Cost				
Plastic	–	low	high	low
Metal	moderate	–	–	moderate
Ceramic	low	moderate	high	high
Carbon	high	high	–	–

Source : G.K. Chen—*Packed Column Internals* **(Chemical Engineering, Reprint, March 5/1984)**. Reproduced with kind permission of GLITSHC, Inc./Dalls/Texas 75266-0053/USA

As the table shows, the slotted rings, especially the 50mm size, appear to be the best choice for cost of the mass-transfer application. This is due to their high capacity, good efficiency characteristics, low pressure drop, and low-to-moderate cost. They are available in metals, ceramics and plastic materials.

The separation efficiency in terms of **HETP** (height equivalent per theoretical plate), for 50mm slotted rings in various test systems viz. acetone-water, *iso*-octane-toulene, methanol-water, *iso*-propanol-water, ethylene-styrene, decreases as the bed-height increases. For instance, the **HETP** value increases from 600 mm to 750 mm to 800mm as the bed depth is increased from 1500 mm to 3000 mm to 6000 mm for *iso*-octane-toluene system. This phenomenon makes it imperative to use shorter beds laid up with liq collector/redistributor system in-between the beds. An alternative to this is to take higher-than-published values of **HETP** for a given size of packings in designing a commercial column.

6.4. LOADING OF RANDOM PACKING

Faulty loadings of random packing have been reported to be the root of a variety of malfunctions of packed bed columns. Hence adequate care must be taken during actual loading operation of random packings into the column.

Newer generation thin-walled metal/plastic packing themselves pose a problem. They may undergo crushing or deformation during loading. When loading is carried out thru successive instalments of small quantities of packing in tower of less than 1500mm dia, it is permissible to drop packing directly from the loading manhole, provided the manhole height is not exceeding 6 m from the support plate. During this process, the packing buckets/containers should be well shaked to disperse the elements more or less evenly across the tower dia. This must be supplemented by periodic visual checks by the supervisor as to ensure that the packing remains essentially level.

Another viable and effective technique is **chute-and-sock** arrangement [**Fig. 6.2.16**]. This method gently loads random packing and is recommended under three circumstances :

• For loading larger quantities of packing

- For filling large dia tower (≥1500 mm)
- When the loading-manhole is located more than 6m above the packing support plate.

Direct dumping of packings in small-dia towers is acceptable but is not preferable for large-dia towers due to the risk of natural (preferred) orientation of the packing near at the tower walls. So in the latter case, the **chute-and-sock** arrangement is the best choice.

In loading large-dia tower with random packings, it frequently becomes necessary for workers to ride the bed to physically distribute the packing element thruout the bed cross-section and level the packing. The workers should not stand directly on the packing for their entire body weight concentrated over the small area of their feet may subject the bed packing to crushing or deformation. They should, therefore, use plywood or wooden plank having **an area 1200mm x 1200mm** to stand on.*

The chances of breakage, crushing and deformation occur in the handling of plastic packings too. Therefore, the same general precautionary measures should be adopted as for metal packing. Nevertheless., these plastic packings require one extra care. When these plastic elements are loaded
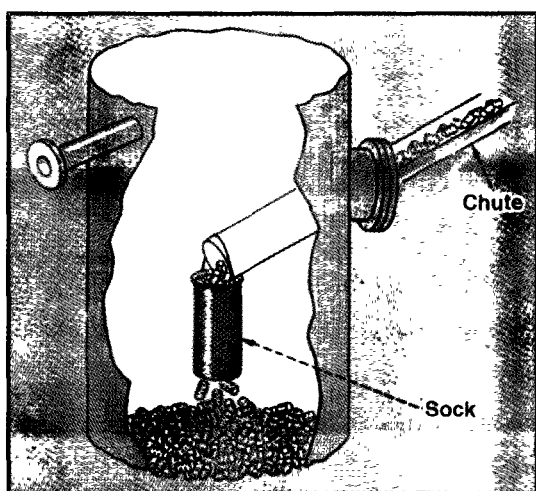
© GLITSCH, Inc. Reproduced with kind permission of GLITSCH, Inc,/Dallas/ Texas (USA)

Fig. : 6.2.16. *Chute-and-Sock Method of Loading is Very Helpful When Loading Random Packing Into A Tower From A Height More Than 6m.*

Fig. 6.2.17. *Packing 'Wet'. Water Height of at Least 1.2m is recommended.*

©Norton Co.

into a tower in subzero or near-freezing conditions extra care must be taken so that they're not dumped from a height more than 1200mm. Because at these low temperatures, the plastics become very brittle and less resilient to mechanical shock. Also it is almost a must to use gas-injection-type support plates instead of this metal grids to hold the plastic packings, as deep beds of plastic will extrude thru thin grids, which act like knife blades.

---

* These all foreign materials like plywood or plank must be removed before the workers leave the bedsite. Proper care must be taken so that any such external objects are not buried in the bed nor thrown into the column and left in the bed. Surely such carelessness will invite excess pressure buildup and poor performances.

Ceramic and porcelain packings are more susceptible to breakage and crushing than metal or plastic packings. So they must be handled with care. That is they must be given the status of glassware during shipment, loading and unloading.

Traditionally, *the best way to pack ceramic beds* is the **wet-packing procedure** :

• fill the tower with water

• slowly dump the packing **[Fig. 6.2.17]**

• drain the tower just before startup

The water cushions the mechanical shock of fall and promotes a true randomness of the packing elements.

Packing **'wet'** is fretted with certain inherent difficulties.

• the colume supports and the shell must be designed for full hydraulic load

• overhead liquid distributors become an impediment if they are installed prior to packing.

In case the wet-packing procedure is likely to entail the risk of damaging the support plate or the liquid distributors, a common alternative is to dump the ceramic packing from buckets lowered into the column **[Fig. 6.2.18]**.
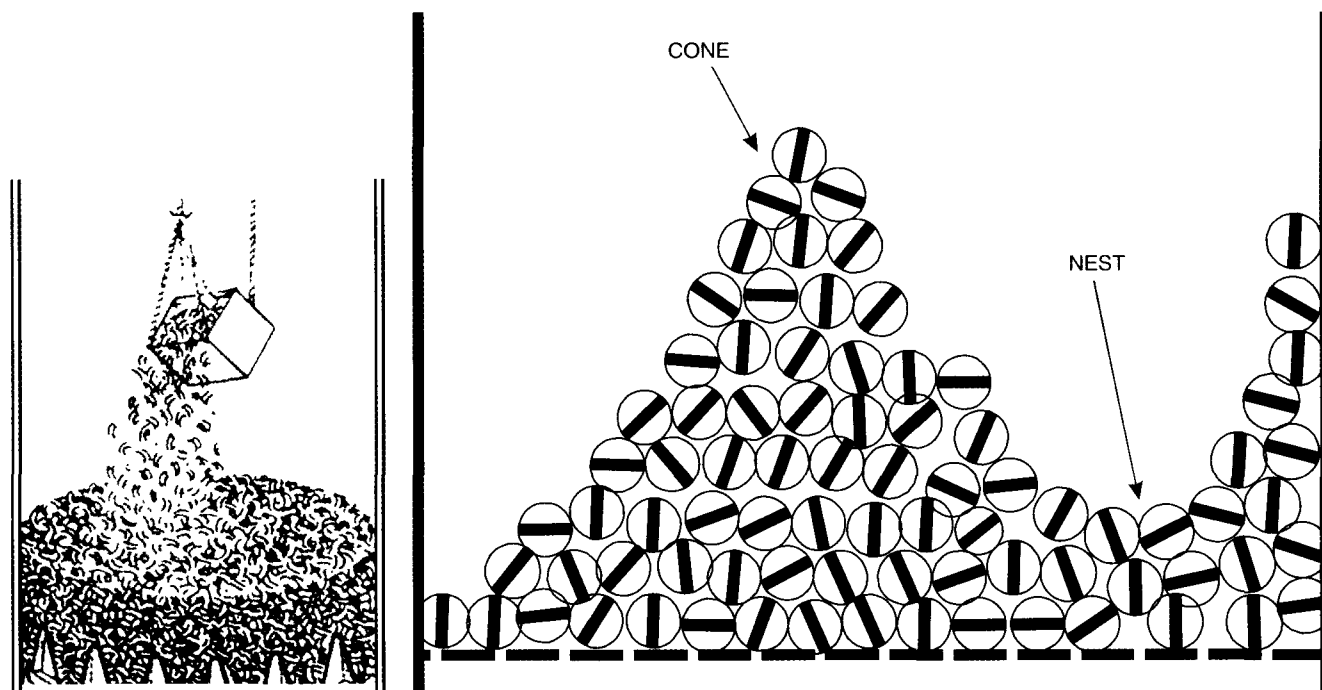
© **Norton Co.**

Fig. 6.2.18. *Packing 'Dry'*.	Fig. : 6.2.19. *Cones and Nests.*

The bucketful of packings are lowered into the column usually thru a manhole and emptied at several points. Thereafter the ceramic packings are hand spread evenly over the entire bed cross-section. Care must be taken so as not to dump, bump or throw any packing element piece. The supervisors must ensure that the packing is not being damaged before and during loading into the column. **'Nesting'** or **'coning'** must be avoided as they promote maldistribution.

Packings randomly dumped over the support plate at several points form conical heaps and *the valley between the adjacent 'cones' is called 'nest'* [Fig. 6.2.19]. While the cones give higher

bed drop. the nest gives lower—the net overall effect is gas-liq maldistribution. Hence these heaps must be leveled to a uniform packed depth thruout.

Packings undergo undesirable orientations when randomly dumped. This is particularly the case with ring type packing, viz. **Raschig rings, Pall rings** etc. If this type of tower packings is dumped only in the center of the tower, they build up a conical mound along the slopes of which the oncoming rings roll and tumble down and spread out to fill the tower periphery. As the rings do this, they tend to roll on their sides with the effect that horizontally oriented packing layers fill up the peripheral areas of the tower. This preferred orientation rather than completely random orientation of dumped packing renders the tower to perform far too poorly.

The procedure of loading packing in the column vary with the nature and type of packing and with each specific application for the obvious reason. For instance, wet-loading is not possible for all towers—particularly when the aqueous phase will adversely affect the process, and when completely drying of the bed and tower cannot be assured.

Plastic packings float on water and so they are usually dry-packed. However, some special additives may be dosed to the plastic melt before subjecting it to molding, if the density of the packing elements are to be raised higher than that of water for process reasons.

Carbon-steel packings undergo rusting when wetted. This factor must be taken into account though CS-packings normally come coated with oil prior to their shipment. It is very likely that the oil film may get erased out due to their prolonged weathering in the open storeyard. Also to be considered is the fact that this protective oily-film must be soap or solvent washed prior to loading the tower to prevent foaming or product contamination.

When wet-loading procedure is followed, one must be particularly wary of the fact that packing and internals can undergo serious damage, if live steam is injected into the column full of water.

□□

7

Packed Tower Internals

The most commonly employed tower internals are :

1. **Packing support plates**
2. **Gas distributors**
3. **Bed limiters and hold-down plates**
4. **Liquid distributors**
5. **Liquid redistributors**
6. **Wall wipers**
7. **Liquid collectors**

Not all of these internals are used in every absorber or stripper. In addition, some plate may serve more than one function.

7.1. PACKING SUPPORT PLATES

As the name implies, the primary function of the packing support plate is to lend physical support to the mass of tower packing plus the weight of the liquid holdup.

The packing support plate must give passage to the downward flow of liquid phase and upward flow of gas phase to the limit of the capacity of the tower packing itself.

The oldest packing support plate for random packings were flat ceramic plates sporting slots or perforations. They were chiefly used to support 25 to 50mm ceramic **Raschig rings**, common in those days, requiring small holes or narrow slots. And as such these plates had only 15—25% of plate cross-section as the open area. Despite these plates were heavy in construction, they lacked sufficient strength to support deep beds of ceramic tower packings.

Thereafter, large cast iron grids supporting stacked packings were used in the ammonia soda industry as well as in the manufacture of sulfuric acid. In addition, sections of subway gratings were used as packing support plates provided the metal could adequately stand against the corrosive action of the system liquid. However, the then commonly used **Raschig rings** tended to align themselves along these slots/openings in such support plates, thus leaving only marginal effective-free-area for gas and liquid passage. So *flooding was a common phenomenon that would initiate at the bed-bottom,* progressively move upward and flood the column eventually.

The first standardized line of column internals came into market at about 1960. Most of these were fabricated from ceramics and later from metals to meet the specific design requirements.

Leva proposed a **Gas Injection Weir-Type support plate** design to avoid excessive liquid buildup in the bed (M. Leva — **Tower Packing and Packed Tower Design**, U.S. Stoneware, 1953 /Ch–2). This design introduced the gas stream into the packed bed above the level where the liquid phase left the packed bed. The idea was to minimize the competition between the two countercurrent streams (gas and liq) vying for the same flowpath in the support plate.

This system proved to be adequate for ceramic random packings up to 50mm size. However, with 50mm metal **Pall ring,** it was observed that the ΔP thru the support plate and first 600mm of packing was much higher than the average pressure drop for the rest of the packed bed. Thus this packing support plate restricted the capacity of packing.

Further research work brought forth the improved **Multibeam Gas Injection support plate** to circumvent these difficulties. Multiple tests of this system using 50mm metal **Pall ring** have shown that the improved version gives rise to much less pressure drop as compared to the original design.

The multibeam support plate **(Fig. 7.1.1)** design meets the desired
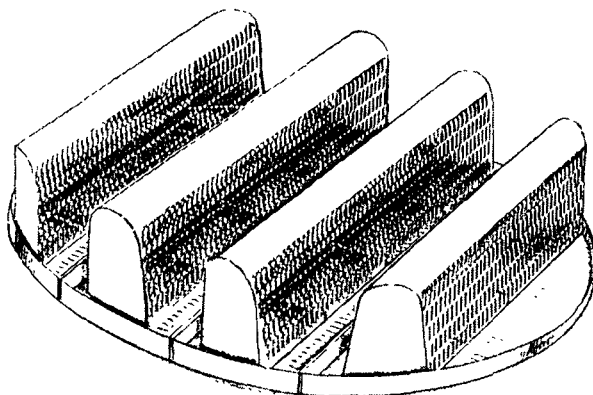
Models 101 and 101R

© KOCH Engineering Co. Reproduced with kind permission of KOCH International, S.p.A./ Bergamo (Italy)

Fig. 7.1.1. *Multibeam Gas-Injection Support Plate.*
While The Gas Gets Into The Bed Thru Slots–On–The–Side wall of each Beam, the Liq Flows Down the Near–Vertical Side wall and Drops onto the Horizontal Slotted Bottom Legs.

criteria for most applications :

low bed drop even at high liq rates. ΔP generally does not exceed 75 Pa in almost all applications.

high mechanical strength to hold a man's weight over and above the physical weight of packed bed.

installation is easy since it is available in parts. This is particularly useful for large dia (3.5m or more ID) large size columns — support plate parts (and later the packing also) enter the column thru manhole and assembled within the column itself.

The multibeam support plate is an assemblage of hollow individual beam with perforated (slotted) walls. That is, the support plates are fabricated in sections for installation thru tower manholes and are usually clamped to a support ring.

Gas passes up thru the slots in the archwalls while liquid passes thru the slots on the deck. Maximum thruput capacity and minimum pressure drop are maintained by keeping the gas passages clear of liquid.

At normal operating rates, the ΔP across the plate is low usually less than 60 Pa. Free area is normally 80% to 100% of the tower's cross-sectional area, depending on diameter, so the support plate does not bottleneck the tower operation.

The structural strength of these plates allows them to withstand the load of ≥ 9 m bed-depth of random packing. For towers of dia exceeding 2.7 m, a midspan beam is usually required. Also additional support is provided to guard against unusual loading or corrosion conditions.

KOCH's two models — **101** and **101R** — are very popular. **Model 101R** has a round unperforated top and is used in towers 750 mm ID and larger. **Model 101** has a flat, perforated top and is used in columns less than 750 mm ID.

Gas Injection Packing Support Plates

The **Models 101** and **101R** are the most common devices for supporting random packing. Model 101R has a round up perforated top and is used in towers 30"ID and larger. **Model 101** has a flat, perforated top and is used in columns less than 30"ID.

Vapor passes through slots in the arches while liquid passes through the slots on the deck. Maximum throughput capacity and minimum pressure drop are maintained by keeping the vapor passages clear of liquid.

Plan

At normal operating rates, the pressure drop across the plate is low, usually below $\frac{1}{4}$ inch water, free area is normally 80% to 100 + % of the tower's cross sectional area, depending on diameter, so the plate does not bottleneck the tower's operation. The support plates are fabricated in sections for installation through vessel manways, and are usually clamped to a support ring.

The structural strength of these plates allows bed depths of 30 feet and higher. A mid-span beam is usually required for diameters larger than 9 feet. Unusual loading or corrosion conditions may also require additional support.

© Copyright 1989, Koch Engineering Company, Inc

Models 101 and 101R Gas Injection Packing Support Plates

Tower I.D.	Support Ring Width	Load Capacity, Lbs./Sq.ft.	
		Carbon Steel	Stainless Steel
101			
12" – 17$\frac{3}{4}$"	$\frac{3}{4}$"	3980	2560
18" – 23$\frac{3}{4}$"	1"	2220	1430
24" – 39$\frac{3}{4}$"	1$\frac{1}{4}$"	1420	910

© KOCH Engineering Co. Reproduced with kind permission of KOCH Engineering Co., INC.
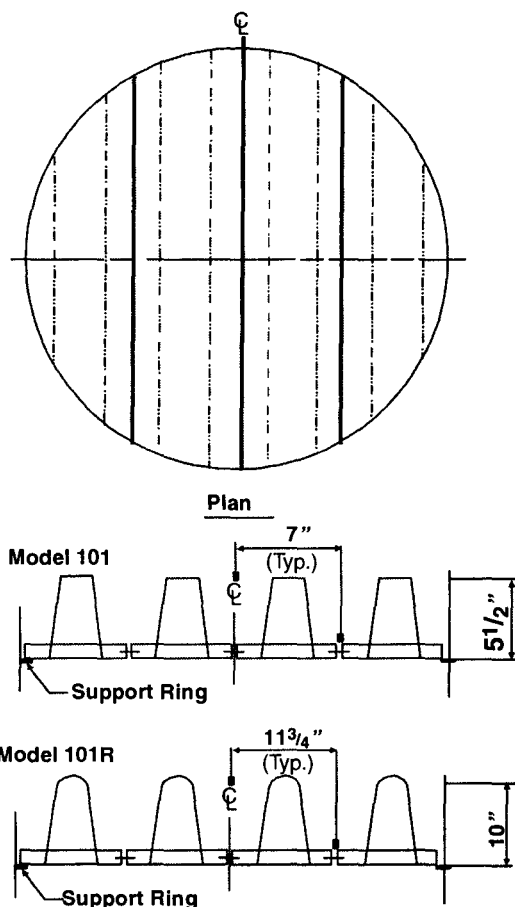
Fig. 7.1.2. Gas Injection Packing Support Plates Models 101 and 101R of KOCH Engg.

Tower I.D.	Support Ring Width	Load Capacity, Lbs./Sq.ft.	
		Carbon Steel	Stainless Steel
101R			
$30" - 59\frac{1}{2}"$	$1\frac{1}{2}"$	2000	1390
$60" - 89\frac{1}{2}"$	$2"$	1020	710
$90" - 119\frac{1}{2}"$	$2\frac{1}{2}"$	550	390
$120" - 137\frac{1}{2}"$	$2\frac{1}{2}"$	1650	1150
$138" - 179\frac{1}{2}"$	$3"$	1020	710

Notes :

• Approximate weight for standard construction: carbon steel: 8.4lbs./sq. ft. stainless steel: 5.0 lbs./sq. ft.

• These figures are typical values. Actual values will vary with temperature, diameter and material type and thickness.

• Larger sizes are available.

• All internals are segmented as required for installation.

• Center support beams may be required for diameters of 9 feet or larger.

Multibeam support plate is available in metal, thermoplastic and ceramic.

Shown in **Fig. 7.1.3.** is the metal multibeam support plate of Norton. Co.
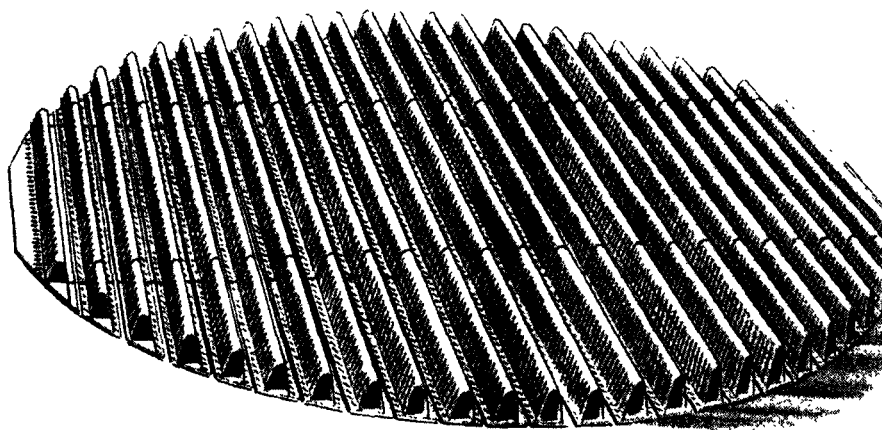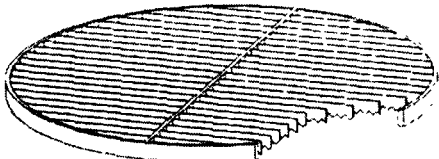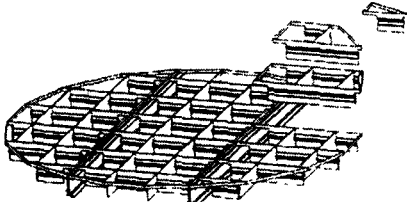
Model 804

© **Norton Chemical Process Products Corpn.** Reproduced with kind permission of Norton Chemical Process Products Corpn.

Fig. 7.1.3. *Metal Multibeam Support Plate (Model 804 of Norton Co.). Perforated Beams Provide Greater Gas and Liquid Handling Capacity than Units With Individual Risers. Most Units Provide Free Open Area in Excess of 100% of Column Cross-Sectional Area.*

Shown in **Fig. 7.1.4** are the support grids of Sulzer Brothers Ltd., Winterthur, Switzerland. They can be fitted to towers of dia from as small as 0.1m to as large as 4m.

Support grids

	TE	0.1 – 2 m	The **TE** support grid is supplied in one piece for flanged columns.
	TS	from 0.8 m	The **TS** segmented support grid is carried on support beams (type **TST**) or on lattice griders (type **TSL**). It is used for columns of larger diameter and high bed heights. Assembly takes place through the manhole.
	TSI	from 4 m	**TSI** support grid – similar to the **TS**, but with integrated support beams. It is self supporting and can be assembled and dismantled easily through the manhole. Suitable for large column diameters, it is made in stainless steel and in higher alloys.

Courtesy : *Sulzer Brothers Ltd.*, Winterthur, Switzerland.

Fig. 7.1.4. Support grids come in varied designs. Some are supplied as a single piece and lowered into the flanged column with top opened, while others come in sectional designs which are lowered thru column manhole and assembled at site.

7.2. GAS DISTRIBUTORS

The distribution of feed gas at the bottom of the packing is as important as that of the feed liquid at the top. This is because gas maldistribution can reduce column efficiency in the same way as liquid maldistribution; although the gas phase radial cross-mixing rate is at least three times that of the liq phase.

Inasmuch as a packing support plate usually is located immediately above the gas inlet in an absorber, this plate could be used to organize gas distribution. Since the gas phase has the inherent tendency to maintain a uniform distribution once it has been established, only the packing support plate immediately above the gas inlet needs only to act as gas distributor.

Normally, the gas flow control is accomplished by establishing a pressure drop across the support plate. This ∆P should be, at least, equal to the velocity head of gas at column inlet nozzle. However, the pressure drop thru the multibeam packing support plate is too low to control gas distribution.

Flat mesh packing support plate **(Fig. 7.2.1.)** is used with the idea that if liq is dripping uniformly from every piece of packing at the bottom of the tower, the gas could be admitted without specific direction. This is because the gas would, under these circumstances, naturally distribute itself equally between the raining liq streams.
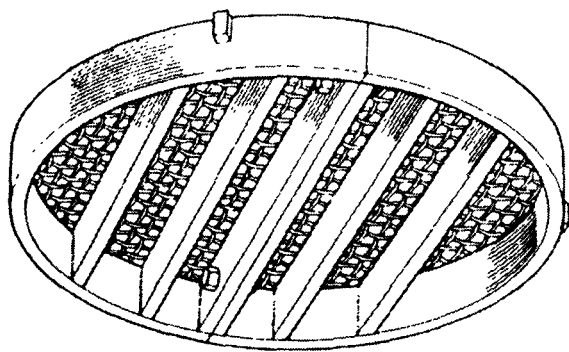
Fig. 7.2.1. *Flat Mesh Packing Support Plate.*

Courtesy : Norton Chemical Process Products
Corpn., Akron, Ohio, USA.
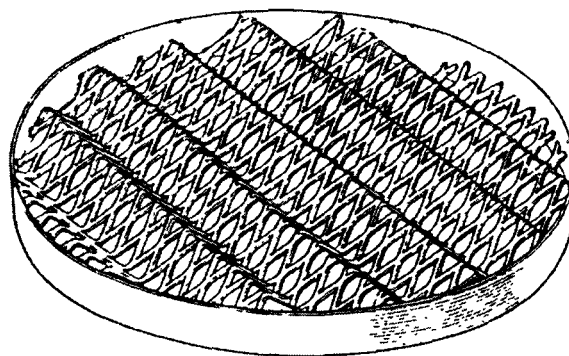
Fig. 7.2.1A. *Corrugated-mesh style packing support plate.*

Courtesy : Norton Chemical Process Products
Corpn., Akron, Ohio, USA.

Sometimes a very coarse mesh is used as packing support plate. In these cases, it is a common practice to put a few layers of larger packing atop the coarse mesh to support the main packing.

For high-pressure stripper columns, a vapor sparger is frequently used to bring into effect a uniform flow of stripping stream up the column.

When the inlet gas nozzle operates at a gas capacity factor exceeding 27 $kg^{\frac{1}{2}}/(m^{\frac{1}{2}}.s)$, a gas–distributing support plate **(Fig. 7.2.2.)** is used.

Reasonable assurance of gas distribution is afforded with support plate of the type illustrated in **Fig. 7.2.1A** and **Fig. 7.2.2.** They give rise to slightly shorter preferred paths of lower pressure drop for the gas distributed over their cross-section. The **"Cap"**. Style of **Fig. 7.2.2** is more positive and preferred but it is more costly than the corrugated mesh style of **Fig. 7.2.1A**
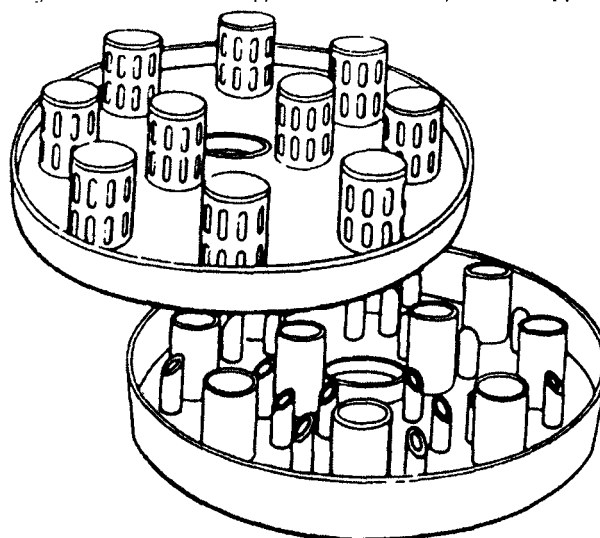
Fig. 7.2.2. *Gas Distributing Support Plate.*

Courtesy : Norton Chemical Products Corpn., Akron, Ohio, USA

Gas distributors come in a variety of designs :

Corrugated Mesh Style (Fig. 7.2.3.) : These are light-duty support plates designed usually for small-dia towers (less than 750mm ID) with lightweight beds.

© KOCH Engineering Co. Reproduced with kind permission of KOCH Engineering Co., INC.
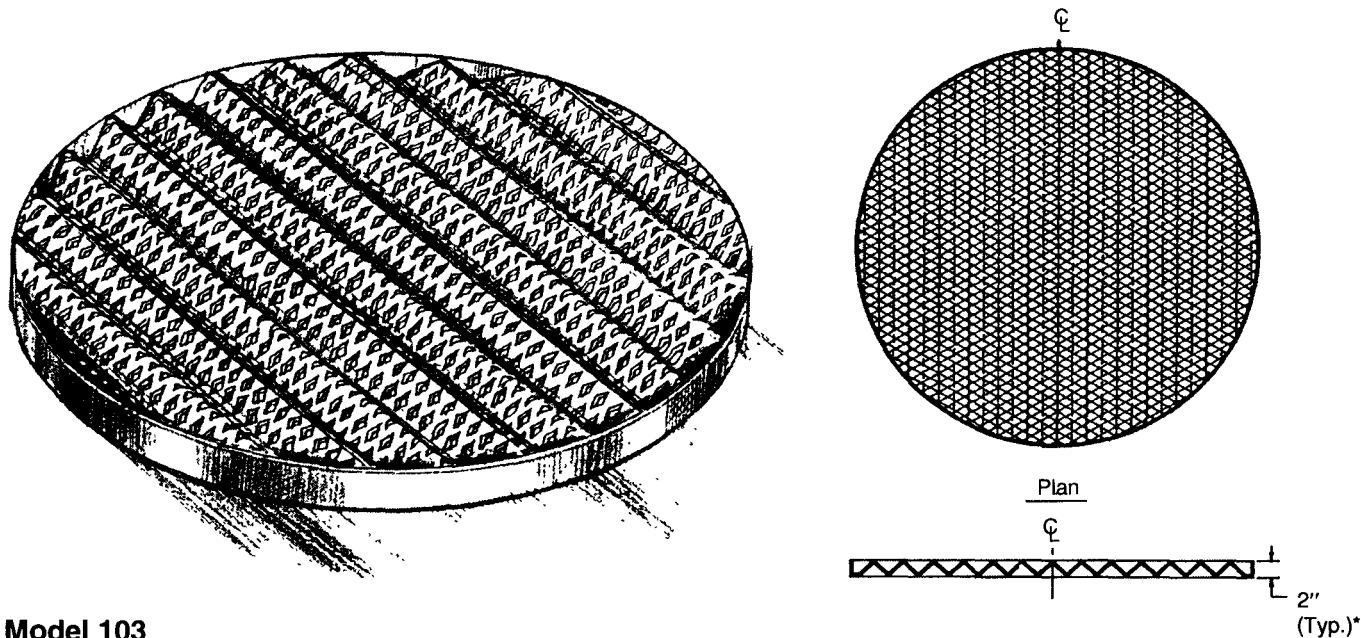
Model 103

Fig. 7.2.3. *Light-Duty Support Plate (Model 103 of KOCH Engineering Co.)*

© KOCH Engineering Co. Reproduced with kind permission of KOCH Engineering Co., INC.

Grid-Type Plate (Fig. 7.2.4) : These are used in columns with short bed depths and where efficient space utilization is essential.

Light-Duty Support Plates

These support plates are designed for small-diameter towers (less than 30"ID) with lightweight beds, where the fabrication of a **Model 101** is not practical. **Model 103** support plates are manufactured from expanded metal.

Model 103 Light-Duty Support Plates

For small-diameter Towers.

Tower I.D. (Inches)	Support Ring Width (Inches)	Min. Hand-Hole I.D. (Inches)	Load Capacity, Lbs./Sq.ft.	
			Carbon Steel	Stainless Steel
6–12	Clips	$6\frac{1}{2}$	2520	3140
$12\frac{1}{4}$–$17\frac{3}{4}$	$\frac{3}{4}$	9	1220	1520
$18-23\frac{3}{4}$	1	12	670	830
24 – 30	$1\frac{1}{4}$	15	400	500

Notes :

- Approximate weight for standard construction in carbon or stainless steel: 3.0 lbs.sq./ft.
- These figures are typical values. Actual values will vary with temperature, diameter, and material type and thickness.
- Larger sizes are available.
- All internals are segmented as required for installation.

Packing Support Plates

These grid-type plates are used in columns with short bed depths, and where efficient space utilization is essential, since they take up less tower height than a **Model 101R.**
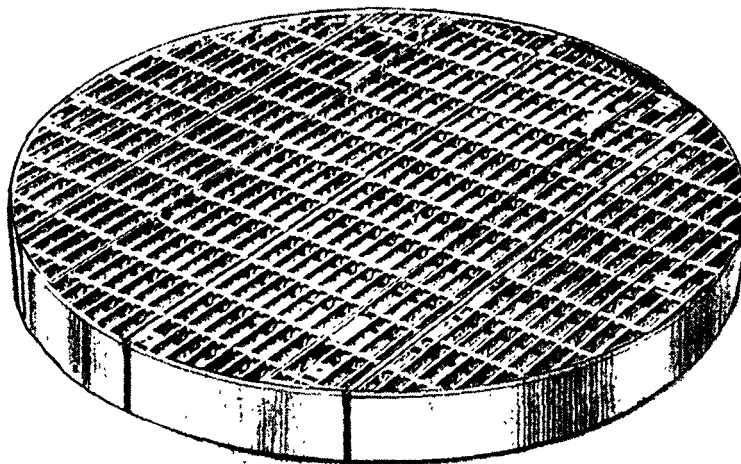
The **Model 104** is frequently used in the short packed beds of crude atmospheric and vacuum towers.

Fig. 7.2.4. *Grid-Type Packing Support Plate.*

Model 104 Packing Support Plates

Tower I.D.	Support Ring Width	Load Capacity, Lbs./Sq.ft.		Height (H)
		Carbon Steel	Stainless Steel	
$6''$–$11\frac{3}{4}''$	Clips	1170	1400	$1''$
$12\frac{1}{4}''$–$17\frac{3}{4}''$	$\frac{3}{4}''$	780	930	$1''$
$18''$ – $23\frac{3}{4}''$	$1''$	580	690	$1''$
$24''$ – $29\frac{3}{4}''$	$1\frac{1}{4}''$	580	690	$1\frac{1}{4}''$
$30''$–$59\frac{1}{2}''$	$1\frac{1}{2}''$	550	660	$2''$
$60''$–$89\frac{1}{2}''$	2	340	400	$2\frac{1}{2}''$
$90''$–$119\frac{1}{2}''$	$2\frac{1}{2}''$	550	660	$2''$
$120''$–$137\frac{1}{2}''$	$2\frac{1}{2}''$	510	610	$2\frac{1}{2}''$
$138''$–$179\frac{1}{2}''$	$3''$	330	400	$2\frac{1}{2}''$

Notes:

- Approximate weight for standard construction in carbon or stainless steel:12 lbs./sq.ft.

- These figures are typical values. Actual values will vary with temperature, diameter and material type and thickness.

- Larger sizes are available.

- All internals are segmented as required for installation.

- Centre support beams may be required for diameters of 9 feet or larger.

7.3. BED LIMITERS AND HOLD DOWN PLATES

During operation a gross maldistribution of system fluid can occur if the packing is physically lifted, or displaced near the top of the bed, or broken by abnormal flowrates or brief surges. This can be avoided by using some sort of bed limiters or hold down plates. Though functionally identical, bed limiters commonly are used with metal or plastics tower packings while hold down plates are used with ceramic or carbon tower packings.

Attached to support rings or bolting clips above the packed bed, a bed limiter prevents the loss of packings if high pressure drop or surge conditions cause sudden bed expansions.

Bed limiters are fabricated from a light weight metal or plastic structure. Usually a light weight mesh is attached to the bed limiter to prevent carry over of smaller-size packing **(Fig. 7.3.1)**

Shown in **Fig. 7.3.1A** is the thermoplastic bed limiter **(Model 1868** of Norton Co.). Beam-type plate is used primarily for plastic packing. Beam-type grids covered with mesh retain 19mm rings or 25mm saddles or larger. PVC is used to services up to 316K while polypropylene is used up to 339K.

Bed Limiters

Attached to support rings or belting clips above the packed bed, a **bed limiter** prevents the loss of packing if high pressure drop or surge conditions cause sudden bed expansions.

Lightweight mesh is attached to the bed limiter to prevent carry over of smaller-sized packing. Integral bed limiters may be used with most KOCH gravity distributors, thereby eliminating the need for a separate bed limiter. (See sketch above.) This reduces cost by
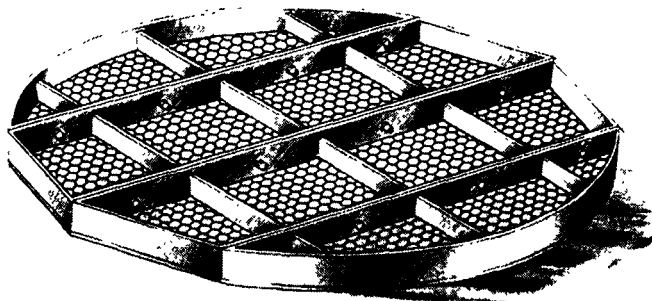
© **Norton Co.** Reproduced with kind permission of Norton Chemical Process Products Corporation., Akron, Ohio, USA.

Fig. 7.3.1A. *Thermoplastic Bed Limiter.*
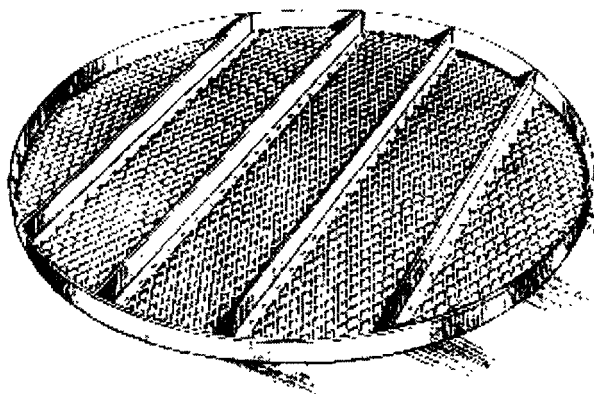
© *KOCH Engineering Co.* Reproduced with kind permission of KOCH Engineering Co., Inc.

Fig. 7.3.1. *Bed Limiter Sports a Lightweight Mesh Backing to prevent Bed Expansion and Dislocation of Top Layers of Packing Element.*

eliminating one device and its supporting, and minimizes the risk of maldistribution caused by liquid splashing on separate bed limiter.

The overall height of bed limiters is about 2 inches.

Plan

$L_{2''}$
(Typ.)*
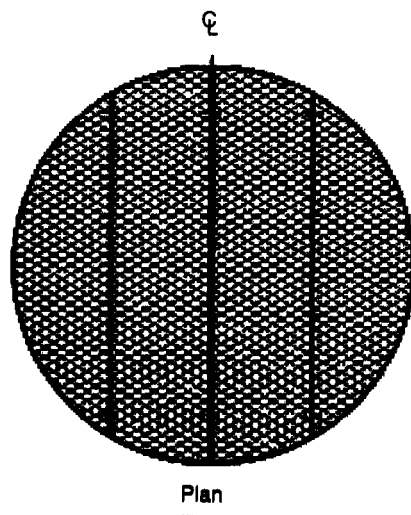
*Varies with process requirements

Model 401 Bed Limiter

| Tower I.D.	Support Ring Width	Approx. Wt., Lbs. Carbon or Stainless Steel
$6''-29\frac{3}{4}''$	$1\frac{1}{4}''$	30
$30''-59\frac{1}{2}''$	$1\frac{1}{2}''$	110
$60'' - 89\frac{1}{2}''$	$2''$	240
$90'' - 119\frac{1}{2}''$	$2\frac{1}{2}''$	430
$120''-137\frac{1}{2}''$	$2\frac{1}{2}''$	570

Notes :

• These figures are typical values. Actual values will vary with temperature, diameter and material type and thickness.

• Larger sizes are available.

• All internals are segmented as required for installation.

• Center support beams may be required for diameters of 9 feet or larger.

Since the bed limiter rests directly on the top of the packed bed, it must be structurally sound enough to resist any upward force acting on the bed. That's why it is fastened to clips on the column wall. Lugs protruding from the edges are fitted into mating slots welded to the inside of the tower shell. The lugs are clamped with a removable bolt or pin at the upper ends so that although the bed limiter plate can ride up and down on the packed bed its upward travel is restricted.

The overall height of bed limiters is about 50mm.

Hold down plates, like bed limiters, rest directly on top of the packed bed but are used exclusively to hold ceramic or carbon tower packing in place. They are not recommended for metal or plastic packing.

Hold down plates (Fig. 7.3.2) inhibit fluidization of the top layer of packing during tower operation. These brittle packing elements can get fractured during an operating upset whereupon the resulting fragments may channel deeper down the bed and clog the bed voidage telling upon the column capacity.

Plan

C̷

1″ (Typ.)*

3″ (Typ.)*

*Varies with process requirments
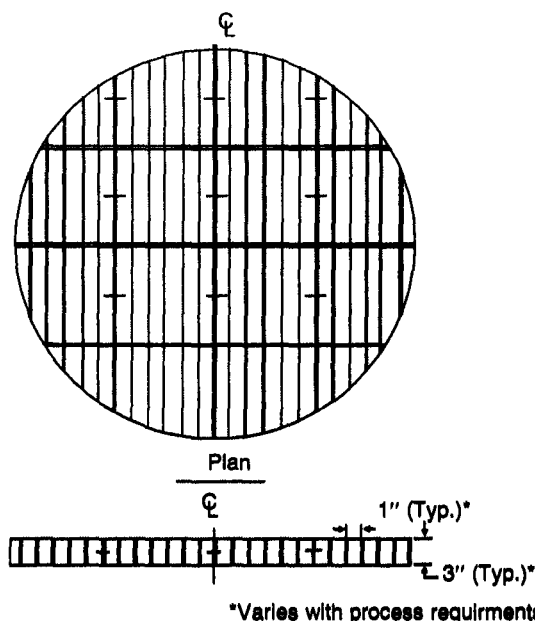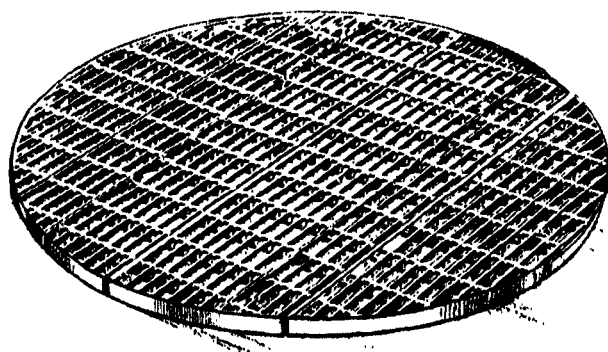
Fig. 7.3.2. *Hold down Plate rests Freely on The Top of the Packed Bed Because of Ceramic and Carbon Packing Tend to Settle During Operation.*

Bulletin : Packed Tower Internals (KOCH Engineering Co.)

© KOCH Engineering Co. Reproduced with kind permission of KOCH Engineering Co., Inc.

These plates, by virtue of their own weight, prevent expansion. Therefore, the plates weigh 100 — 150 kg/m². Like the bed limiters, they deliver at least as much thruput capacity as the packing at low pressure drops.

The overall height of hold down plates is usually 75mm but can be as high as 150mm.

Ideally hold down plates should be designed with slots or grids small enough to prevent the passage of individual pieces of packing. This is not always possible, since the plate must be designed

KOCH **Hold Down Plates** rest directly on top of the packed bed and are used exclusively to hold ceramic or tower packing in place. They are not recommended for metal or plastic packing.

The plates inhibit fluidization of the top layer of packing during tower operation. Like the bed limiters, they deliver at least as much throughput capacity as the packing at low pressure drops.

The overall height of hold down plates is usually 3 inches, but can be as high as 6 inches.

Model 501 Hold Down Plates

Tower I.D.	Support Ring Width	Approx. Wt., Lbs. Carbon or Stainless Stell
6″–29$\frac{3}{4}$″	Rests	110
30″–59$\frac{1}{2}$″		440
60″ – 89$\frac{1}{2}$″	on	1000
90″ – 119$\frac{1}{2}$″		1750
120″–137$\frac{1}{2}$″	Packing	2300

Notes :

- These figures are typical values. Actual values will vary with temperature, diameter and material type and thickness.
- Larger sizes are available.
- All internals are segmented as required for installation.
- Center support beams may be required for diameters of 9 feet or larger.

with a high percentage of free area as the packing. Where corrosion or fouling is not problem,

(a)   (b)

(c)
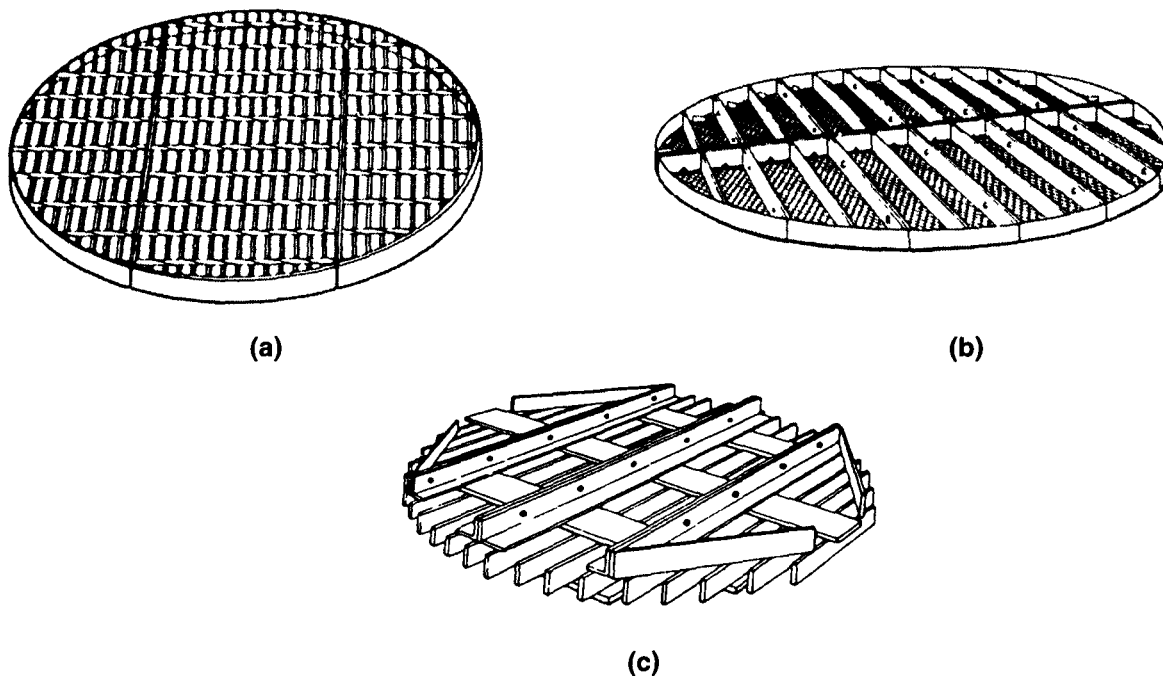
Fig. 7.3.2A. *Hold-Down Plates may float on three lugs.*

a lightweight mesh can be used to prevent the passage of packing without appreciably reducing free area. Such a **hold down plate** is shown in **Fig. 7.3.3.**
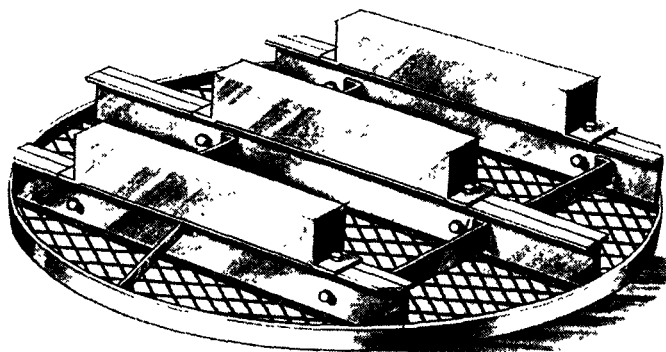
© **Norton Co.** Reproduced with kind permission of Norton Chemical Process Products Corporation.

Fig. 7.3.3. *Hold down Plate (Model 905 of Norton Co.). Backed by A Screen or Expanded Metal, it retains 50mm Saddles or 32mm Rings (Minimum). Designed for use with Ceramic or Carbon Packing. Not to be used with Metal or Plastic Packing.*

Bed limiters and hold down plates should be fabricated in sections so that these can be let into the tower thru manholes part by part and assembled on site. These plates must fit closely to the column wall to prevent escape of boudary packing elements. The free space for these plates must be high for the obvious reason of not to restrict the capacity of tower packing.

7.4 FEED LIQUID DISTRIBUTORS

The most important column internals are the liquid distributors. Forasmuch as maintaining good gas and liquid dispersion thruout the packing is of the greatest importance a liquid distributor, in addition to providing a uniform liquid distribution pattern to the top of the packed bed, must give sufficient room for gas passage to avoid pressure drop or liq entrainment. The distributor should sport high turndown ratio to accommodate load variation and must be resistant to fouling to avoid downtime loss.

The liquid distributor must ensure uniformity of liq flow from each point of irrigation.

The special disposition of every irrigation point must be symmetric with respect to bed cross-section. And this uniform geometric pattern must not be sacrificed to locate the gas risers into the distributor.

The number of irrigation points over every sq. meter of bed cross-section must be identical, provided flowrate per irrigation point is uniform, to ensure uniform bed-wettage. For this, the column cross-section is divided into quadrants plus concentric circles of equal area. Each such quadrant contains equal number of distribution points.

The liq distributors are designed with the number of distribution point per m² usually not to exceed 100. This is because a larger number than this does not improve packed bed efficiency though it is apparent that a larger number of distribution points can bring about a high degree of uniformity more easily. From the practical point of view, the geometric uniformity of liq distribution has more effect on packing efficiency than the number of distribution points per m² of tower cross-section.

The necessity for uniform irrigation increases with the increase of the number of theoretical stages per packed bed. For less than 5 theoretical stages per bed, column is not so sensitive to the uniformity of liq distribution. However, for more than 5 theoretical stages per bed, the liq distribution exercises influence on packing efficiency.

Packing itself does not adequately distribute the liquid that is simply poured on the surface from one point. The liq streams down by gravity over a relatively small cross-section—the path may, no doubt, be tortuous. That is, every packing has a natural liq flow distribution and a bed of random dumped packing develops a definite number of preferred paths of internal liq flow. Ideally, therefore, the liq should be distributed on the top of packed bed over an infinite number of points so that the number of liquid streams per unit bed cross-section exceeds the number of preferred liq paths (paths of least resistance). One such means is to spray the feed liq from one or more full-cone nozzles covering the entire tower cross-section. The method is not uncommon but it has certain inherent drawbacks. :

- more pumping elec. power is required
- less flexible in accommodating varying liq loads
- susceptible to nozzle clogging by dust or precipitated solid particles (particularly if the absorbing liq is recycled).
- installation of a mix-eliminator is almost a mandatory to control entrainment of fine droplets.

Liq distributors come in varied designs but basically they are of two general types :

■ **the gravity-fed distributor**

■ **the pressure-fed distributor**

The gravity-fed distributors are more common. They belong to two main classes :

• **Orifice plate distributors**

• **Trough distributor**

Orifice-Plate Distributor : is the most common liq distributor for general purpose, non-fouling applications. Gas passes thru the gas risers while liq flows thru holes on the deck **(Fig. 7.4.1).**

Pressure drop across the distributor ranges from typically **60-125 Pa** and the standard design has a turndown ratio of **2 : 1.** Higher turndown ratio is possible when taller vapor risers are used.

These distributor are fabricated in sections for installation thru manways and are usually clamped to a support ring. For tower dia less than 750mm where clamps are inaccessible, a rim is put around the periphery of the distributor to contain the liquid.

© *Norton Co.* Reproduced with kind permission of Norton Chemical Process Products Corporation/Akron/OHIO/ USA.

Fig. 7.4.1A. *Orifice Type Distributor. It Disperses the Liq Feed thru Small Perforations and permits the Upflowing Gas to Pass Out thru the Larger-Dia Chimneys.*

Shown in **Fig. 7.4.1A** is another very common type of liq distributor.

Orifice Plate Distributors

The **Model 301A Orifice Plate Distributor** [**Fig. 7.4.1**] is the most common liquid distributor for general purpose non-fouling applications. Vapor passes the plate through gas risers while liquid flows through holes on the deck.

Pressure drop across this distributor is typically **0.25"-0.5" w.c.,** and the standard design has a turndown ratio of **2:1.** Higher turndown ratios are possible when taller vapor risers are used.

Model 301A distributors are fabricated in sections for installation through manways, and

Model 301A

Fig. 7.4.1. *Orifice Plate Distributor*
© KOCH Engineering Co.

are usually clamped to a supporting. For tower diameters less than **30"** where clamps are inaccessible, a rim is put around the periphery of the distributor to contain the liquid.

Model 301A distributors are commonly used as redistributors by simply adding hats over the gas riser to prevent liquid from falling through. The **Model 301A** also can be used as a liquid collector by deleting the orifice holes and installing a downcomer or draw sump. The same style can be used as a vapor distributor of the bottom of a column, but the plate is designed with a higher pressure drop.

The **Model 301A** distributor can be specified as **Model 301AM,** with the **M** designating the antimigration feature. With this feature, bars or mesh are put under the gas riser to prevent lightweight packing from escaping, thus eliminating the need for a separate bed limiter.

Model 301A Orifice Plate Distributor

Tower I.D.	Support Ring Width	No. of Risers	Net Weight. Lbs. Carbon or Stainless Steel
6"— 17¾"	Clips	1—4	7—30
18"— 29¾"	1"	4	30—40
24"—29¾"	1¼"	4	40—60
30"—59½"	1½"	6-28	60—230
60"—89½"	2"	28-75	230—500
90"—119½"	2½"	75-128	500—800

Source : Packed Tower Internals (KOCH Engineering Co.)

© *Koch Engineering Co.* Reproduced with kind permission of Koch Engineering Co., Inc.

Fig. 7.4.1. *(continued) Orifice Plate Distributor. Shown here is the KOCH's Model 301A. This type of Distributors is very popular, General Purpose Liq Distributor Chiefly Employed for Non-Fouling Applications. They are Fabricated in Sections which are Inserted thru Man-Ways into the Column and Assembled within it.*

This Model 301A attains Anti-migration Feature when Bars or Mesh are put under the Gas Risers to Prevent Lightweight Packing from escaping, thus, eliminating the need for a separate Bed Limiter.

Notes :

● These figures are typical values. Actual values will vary with temperature, diameter, and materials type, and thickness

● Larger sizes are available

● All internals are segmented as required for installation.

● Center support beams may be required for diameters of 9 feet or larger

This type of distributor is restricted to relatively clean liquids and a narrow range of liq load. If the liq load is too low, some perforations may run dry and pass gas instead. If on the other hand, liq rate is too high, the liquid may overflow the gas chimneys and lead to flooding if the chimneys were not properly oversized. Also dirty liquid would plug the perforations.

Koch's **Model 301B** is capable of developing a high turndown ratio or accommodating a fouling service. With combination of holes and drip tubes, turndown ratios of 5 :1 are practical without increasing the riser height. When used for fouling service, solids settle out on the deck and clear liquid flows out thru the drip tubes.

When fitted with antimigration bars, it eliminates the need for a bed limiter. The antimigration feature is important because its cost is less than the cost of separate distributor and bed limiter. Also, when there is no bed limiter installed between the distributor and the packing, there arises less chance of maldistribution from liquid hitting the bed limiter.

Orifice Plate Distributors With Drip Tubes

Model 301B [Fig. 7.4.2] is similar to **Model 301A** except drip tubes are used in place of same or all of the plate orifices. The **301 B** is used to increase the turndown ratio or to accommodate a
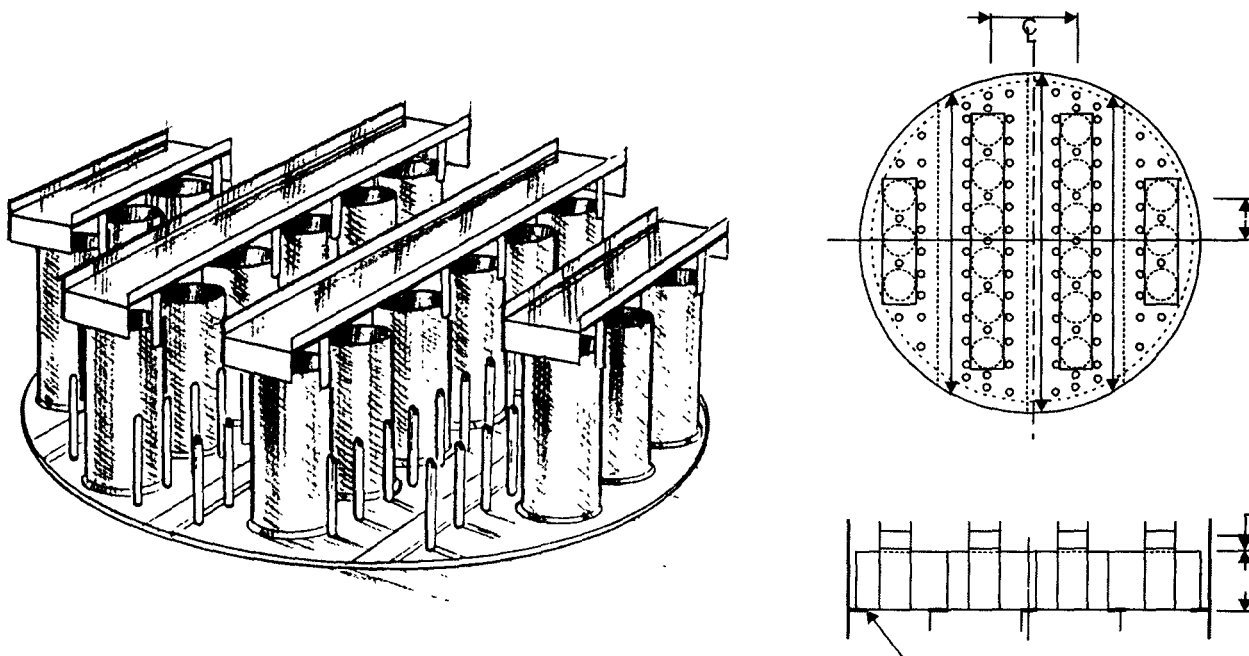
© *Koch Engineering Co.* Reproduced with kind permission of Koch Engineering Co., Inc.

Fig. 7.4.2. Orifice Plate Distributor with Drip Tubes. Shown Here is KOCH's Model 301B which is similar to model 301, except drip tubes are used in place of some or all of the plate orifices.

They can be used for fouling service or to accommodate high turndown ratios. Also they can be fitted with an Antimigration Bars eliminating the need for Bed Limiter.

fouling service. With a combination of holes and drip tubes, turndown ratios of **5:1** are practical without increasing riser height. When used for fouling service, solids settle out on the deck and clear liquid flows through the drip tubes.

Model 301BM has antimigration bars that eliminate the need for a bed limiter. The antimigration feature is important because its cost is less than the cost of a separate distributor and bed limiter. Also when there is no bed limiter installed between the distributor and the packing there is less chance of maldistribution from liquid hitting the bed limiter.

Model 301B Orifice Plate Distributor with Drip Tubes

Tower I.D.	Support Ring Width	No. of Risers	Net Weight. Lbs. Carbon or Stainless Steel
6"—17$\frac{3}{4}$"	Clips	1—4	7—30
18"—23$\frac{3}{4}$"	1"	4	30—40
24"—29$\frac{3}{4}$"	1$\frac{1}{4}$"	4	40—60
30"—59$\frac{1}{2}$"	1$\frac{1}{2}$"	6—28	60—230
60"—89$\frac{1}{2}$"	2"	28—75	230—500
90"—119$\frac{1}{2}$"	2$\frac{1}{2}$"	75—128	500—800

Notes :

■ These figures are typical values. Actual values will vary with temperature diameter and materials type and thickness

■ Larger sizes are available

■ All Internals are segmented as required for installation.

■ Center support beams may be required for diameters of 9 feet or larger

Trough Distributor : is generally used in tower with high liq rates or fouling service.

Trough distributors **(Fig. 7.4.3)** are fabricated in sections for installation thru manholes and are supported on a support ring (and beams if required)
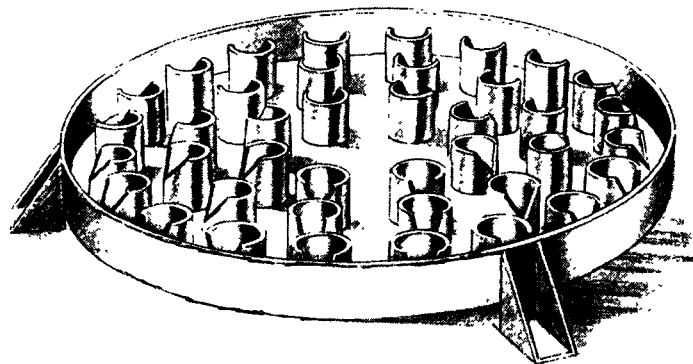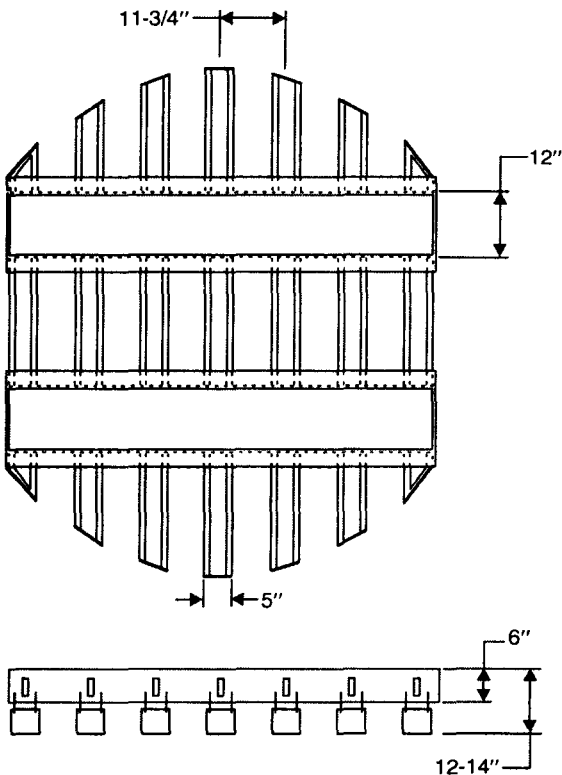
Source : Packed Tower Internals (KOCH Engineering Co.) © Koch Engineering Co. Reproduced with kind permission of Koch Engineering Co., Inc.

Fig. 7.4.3. *Trough Distributor (Model 302 of Koch Engineering Co.) Such Distributors can handle High Liq Rates or Fouling Service. They are fabricated in Sections for Installation Thru Manways.*

© *Norton Co.* Reproduced with kind permission of Norton Chemical Process Products Corporation/Akron/OHIO/ USA.

Fig. 7.4.3A. *Weir-Flow Distributor (Pan Type). Such Distributors provide for Countercurrent Passage of Gas and Liq thru Notched Chimneys.*

Turndown characteristics are very good (**4:1** and higher) because of the tapered notch designed.

Liq is introduced into the parting box, which properly distributes liq into the laterals. Generally, one parting box is required for tower up to **2.5m** in dia. Multiple parting boxes are used for larger diameter or high liquid rates.

Shown in **Fig. 7.4.3A** is the pan-style weir-flow distributor that is the same area for gas flow as does the pan orifice type. It is available in metal and ceramic.

TROUGH DISTRIBUTORS

The **model 302 Trough Distributor** [Fig. 7.4.3] is generally used in towers with high liquid rates or fouling service. Turndown characteristics are very good **(at least 4:1)** because of the tapered notch design.

Liquid is introduced into the parting box, which properly distributes the liquid into the laterals. Generally, one parting box is required for towers up to **8 feet** in diameter. Multiple parting boxes are used for larger diameters or high liquid rates.

Model 302 Trough Distributors are fabricated in sections for installation through manways and are supported on a support ring (and beams if required). This distributor also is available with an integral bed limiter as **Model 302M**.

Model 302 Trough Distributors

Tower I.D.	No. of Trough	Max. Flow Rate Nominal GPM	Net Weight, Lbs		No. of Parting Boxes
			Carbon Steel	Stainless Steel	
36"—42".	3	400	120	65	1
48"—54"	4	700	180	100	1
60"—66"	5	1000	275	150	1
72"—78"	6	1500	365	200	1
84"—90"	7	2000	475	260	1
96"—102"	8	2500	600	320	2
108"—114"	9	3100	730	400	2
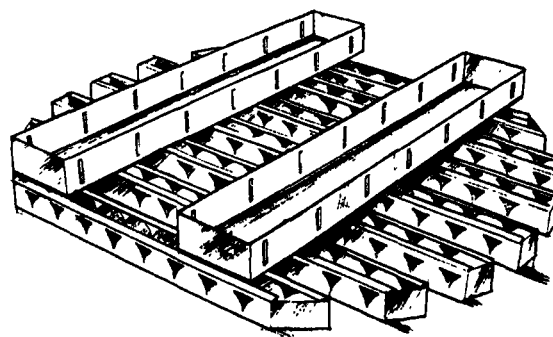
Model 302

Courtesy : KOCH Engineering Co.

Notes :

■ These figures are typical values. Actual values will vary with temperature, diameter and material type and thickness

■ Larger sizes are available

■ All Internals are segmented as required for installation.

■ Center support beams may be required for diameters of 9 feet or larger

■ Actual number of parting boxes will depend on liquid rates.

Norton's trough distributor–**Model 806 (Fig. 7.4.3B)** is similar to KOCH's **Model 302**. They call it weir-trough distributor recommended for large dia towers. Fit for non-fouling services they offer high turndown ratio.

The **model 806** is a metal weir-trough that operates thru gravity overflow thru weirs and hence resistant to fouling and can handle large volumes of suspended solids in the liquid. Functions efficiently during startup. Available in size range ≥ **1219 mm**.

Liquid Distributors
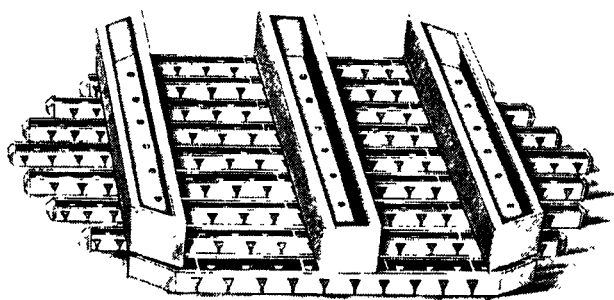
Courtesy : Norton Chemical Process Products Corpn., Akron. Ohio, USA

Fig. 7.4.3B. *Metal weir-trough distributor Model 806 offers high free area and a high turndown ratio.*

The weir-type notch directs the liquid down one edge of the chimneys, minimizing interference with the upflowing gas and, because the notch widens, accommodating everincreasing liquid flow in case the level in the pan rises with increased feedrate. Such distributors handle a wider range of flowrates more readily than orifice-type distributors with pan design.

For structured packing application in medium-to-large-dia columns, the liq distributor widely used is the trough distributor with multiple drip points. Shown in **Fig. 7.4.4** is the **Koch-Sulzer®** **Trough Distributor (MDP)** :
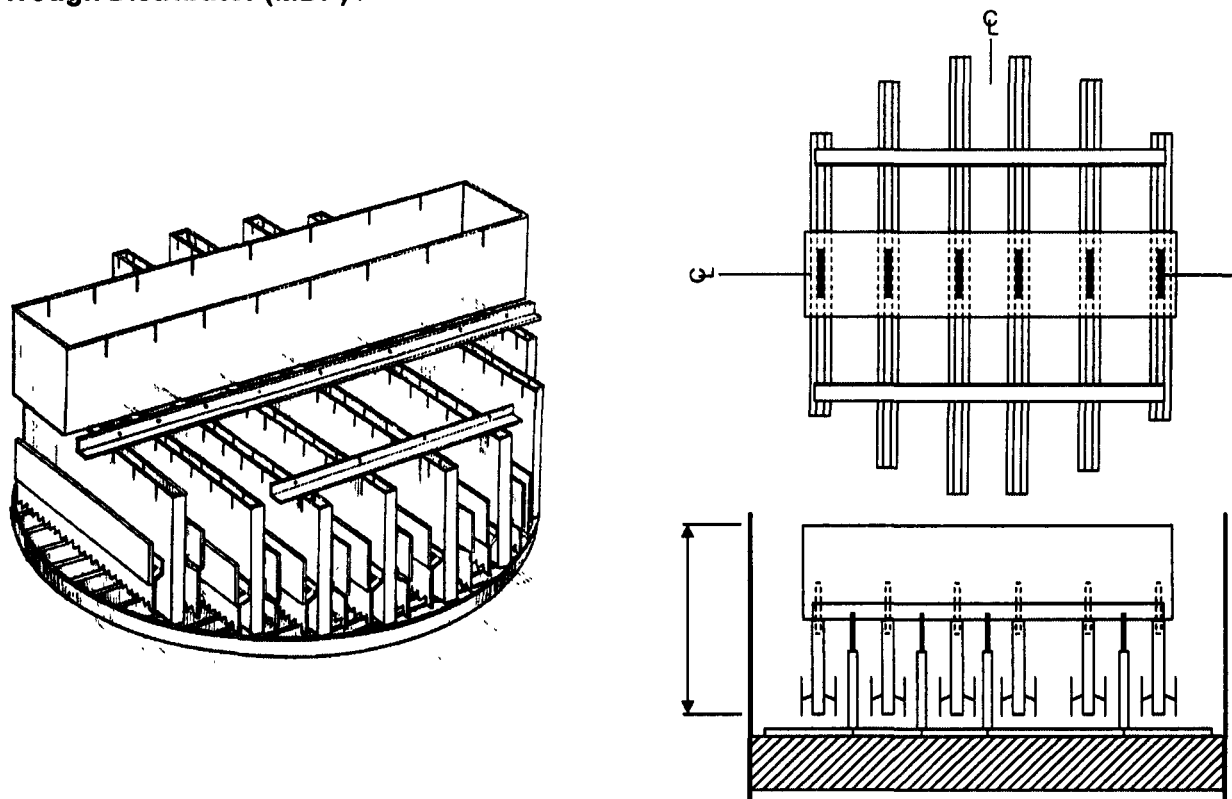
© *Koch Engineering Co.* Reproduced with permission of Koch Engineering Co., Inc.

Fig. 7.4.4. *Trough Distributor with Multiple Drip point Koch-Sulzer® Model Patented. This type of Distribution is widely used for Structured Packing Applications in Medium-to-Large Dia Columns. Highly Effective For Fouling Services Turndown Ratio is Typically 2.5:1 which can be improved by a Two-Stage Design. As a result of Multiple Drip Points (MDP) A Pall of Liq Rains Down Vertically on the Packed Bed below.*

The header above the lateral arrangement provides for sectionalized designs without the need for gaskets–a cost-effective design. Elevated holes in both the header and laterals ensure very high fouling resistance. Liquid streaming in a curtain from multiple drip points **(MDP)** falls perpendicularly to the top of the packing.

In a typical design, the header box may have holes in the floor or, for fouling services, holes in metering boxes that are welded inside the header. The header is leveled independently by lugs attached to the laterals. Laterals have holes punched in the sides above the floor of the lateral. The MDP baffle arrangement directs the liquid onto the packing with a typical lateral hole density of **100 points/m²**. Turndown capabilities :

typically 2.5:1 which can be boosted by installing two-stage design.

Another design which is widely used for structured packing applications is **trough distributor with drip tube system.** Shown in Fig. 7.4.5 is the **Koch-Sulzer® Trough Distributor (Drip Tube)** model meant for medium-to-large-dia column.
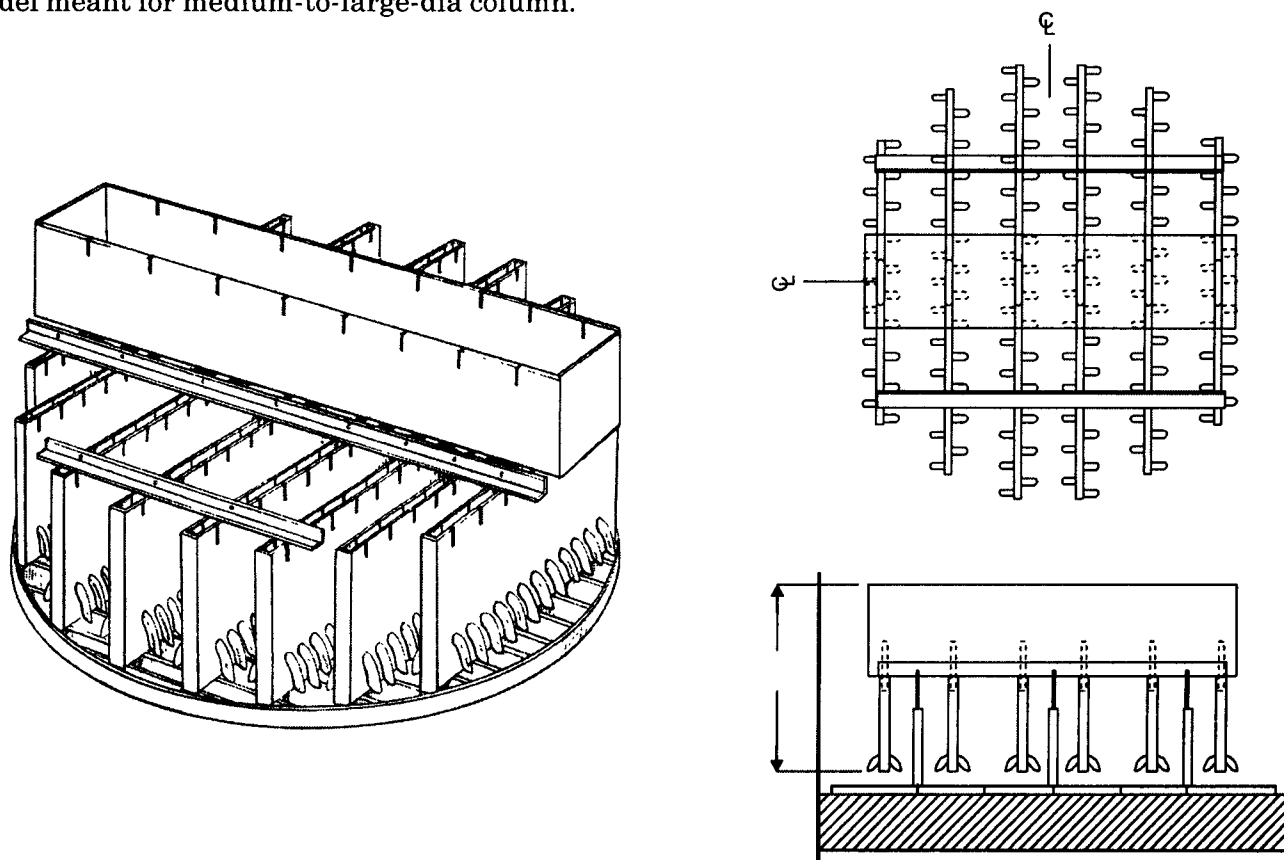
© *Koch Engineering Co.* Reproduced with kind permission of Koch Engineering Co., Inc.

Fig. 7.4.5. Trough Distributor with Drip Tube Koch-Sulzer® Model is widely used for Medium-To-Large-Dia Towers.

This Cost-Effective Sectionalized Design have Laterals with Holes Punched in the Sides above the Floor of the Lateral. The Drip Tube Arrangement Directs the Liquid onto the Packing. They are Superbly Suitable for Fouling Service and have Turndown Capability of 3:1 and more.

The header above the lateral arrangement allows cost-effective sectionalized designs without the need for gaskets. Elevated holes of both the header and laterals provide superb fouling protection. The liquid drip tubes provide a direct path for the liquid from each hole into the packing.

Koch/Sulzer® Trough Distributors [MDP]

This distributor is widely used for structured packing applications in medium-to-large-diameter columns. The header above the lateral arrangement provides for cost effective sectionalized designs without the need for gaskets. Elevated holes in both the header and laterals provide superb fouling protection. The liquid drip tubes provide a direct path for the liquid from each feed hole into the packing.

In a typical design, the header box may have holes in the floor or, for fouling services, holes in metering boxes that are welded inside the header. The header is leveled independently by lugs attached to the laterals. Laterals have holes punched in the sides above the floor of the lateral. The drip arrangement directs the liquid onto the packing with a typical lateral hole density of **110 points/m²**.

Turndown capabilities: typically 3 :1. A two-stage design can be provided for higher turndown requirements.

Overall distributor height is approximately **24"**, the distributor must be leveled from a grid, which normally rests on the top of the packed bed. The vessel manway however, is usually located at or above the header elevation.

*U.S. Patent : 4,557,877

TROUGH DISTRIBUTORS MDP

Tower ID	No. of Troughs	Max. Flow Rate GPM	Approx. Weight lbs
36"—42"	4	150	250
48"—54"	6	250	400
60"—66"	7	350	600
72"—78"	9	500	800
84"—90"	11	650	1100
108"—114"	13	1100	1700

Notes :

- These figures are typical values. Actual values will vary with temperature diameter and materials type and thickness
- Larger sizes are available
- All internals are segmented as required for installation.
- Center support beams may be required for diameters of **9 feet** or larger
- Actual number of parting boxes will depend on liquid rates.

Koch/Sulzer® Trough Distributors [Drip Tube]

This distributor is widely used for structured packing applications in medium-to-large-diameter columns. The header above the lateral arrangement provides for cost effective sectionalized designs without the need for gaskets. Elevated holes in both the header and laterals provide superb fouling protection. The liquid drip tubes provide a direct path for the liquid from each feed hole into the packing.

In a typical design, the header box may have holes in the floor or, for fouling services, holes in metering boxes that are welded inside the header. The header is leveled independently by lugs attached to the laterals. Laterals have holes punched in the sides above the floor of the lateral. The drip arrangement directs the liquid onto the packing with a typical lateral hole density of **10 points/ft²**.

Turndown capabilities: typically 3 :1. A two-stage design can be provided for higher turndown requirements.

Overall distributor height is approximately 24″. In addition the distributor must be leveled from a grid, which normally rests on the top of the packed bed. The vessel manway however, is usually located at or above the header elevation.

*U.S. Patent : 4,557,877

TROUGH DISTRIBUTORS [DRIP TUBE]

Tower ID	No. of Troughs	Max. Flow Rate GPM	Approx. Weight
36″—42″	4	150	200
48″—54″	6	250	350
60″—66″	7	350	450
72″—78″	9	500	650
84″—90″	11	650	850
108″—114″	13	1100	1300

Notes :

• These figures are typical values. Actual values will vary with temperature, diameter and materials type and thickness
• Larger sizes are available
• All Internals are segmented as required for installation.
• Center support beams may be required for diameters of 9 feet or larger
• Actual number of parting boxes will depend on liquid rates.

PLAN

18″ - 24″
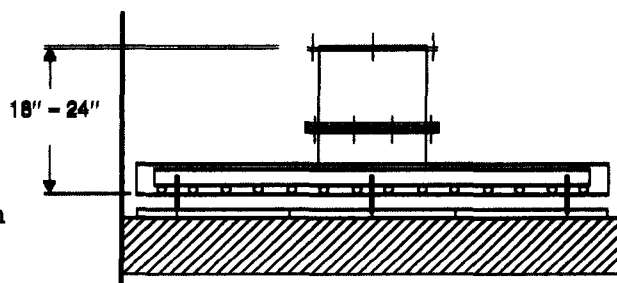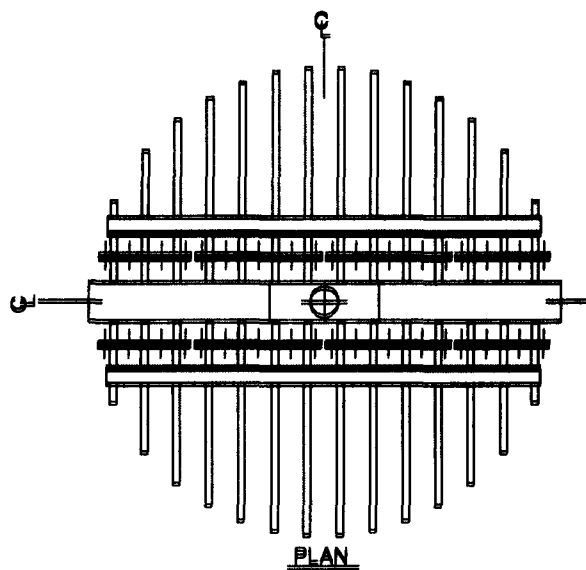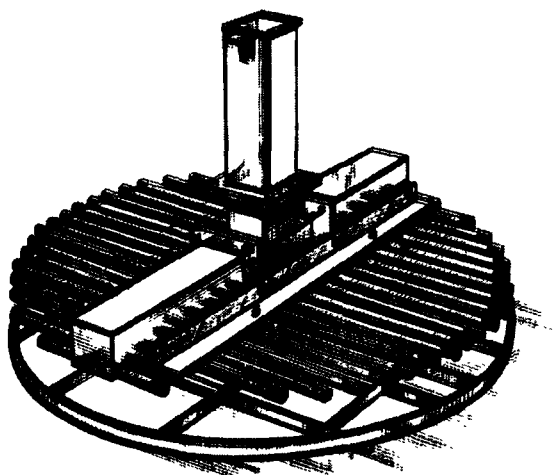
Source : Packed Tower Internals (KOCH Engineering Co.).
© Koch Engineering Co. Reproduced with permission of Koch Engineering Co., Inc.

Fig. 7.4.6. *KOCH-Sulzer tubular distributor is used in conjunction with Flexipac and Sulzer structured packing. They are used for clean service application with moderate liq load where packing efficiency is to be maximized. Minimum tower dia required is 150 mm.*

In a typical design, the header box may have holes in the floor or fouling services, holes in the metering boxes that are welded inside the header. Laterals have holes punched in the sides above the floor of the lateral and drip tube is fitted to each such hole. The drip tube arrangement directs the liquid onto the packing with typical lateral hole density of 100 points per sq.m.

Turndown capabilities are typically 3:1 which can be raised by installing a two-stages design.

Tubular distributor (Fig. 7.4.6.) used to irrigate structured packing, is chiefly used for non fouling applications where packing efficiency is to be maximized.

A typical design consists of laterals with holes not less than **1.15 mm** dia. Minimum lateral size is **12.5 mm** dia pipe. The header box is sized to ensure minimal pressure drop and a low velocity head. This prevents the gases from being entrained into the laterals and affecting liquid distribution.

Flashing feed distributor (Fig. 7.4.7) is used to disengage the vapor phase from a two-phase feed. Shown in **Fig. 7.4.7** is the **KOCH's flashing feed distributor (Model 300)** that consists of two plates — an upper gallery, which is 50% void for vapor disengagement, and a lower deck which is used for liquid distribution.

Koch/Sulzer® Tubular Distributors (Fig. 7.4.6)

The tubular distributor, used in conjunction with FLEXIPAC® and Sulzer® structured packing, is for non-fouling applications where packing efficiency is to be maximized.

A typical design consists of laterals with holes not less than **0.0465"**. Minimum lateral size is **1/2" Sch 40 pipe**, twice the area of the sum of the hole area. The header box is sized to provide minimal pressure drop and a low velocity head. This prevents gases from being entrained into the laterals and affecting liquid distribution. The receiver is designed with the same cross-sectional dimensions as the header box. The height of the receiver depends on turn-down requirements.

Tower height required : Allow typically 10—24", depending on turndown.

Turndown is typically **4 :1**. For high turndown requirements, a two-stage distributor (two alternating levels of laterals) may be used.

Tubular distributors are used for clean service application with moderate liquid load. Minimum tower diameter is **6"**.

TUBULAR DISTRIBUTORS

Tower ID	No. of Laterals	Max. Flow Rate [GPM]	Approx. Weight [Lbs]
16"—20"	5	20	100
22"—28"	7	40	150
32"—38"	11	80	200
42"—48"	15	125	300
52"—58"	18	185	400
62"—68"	21	250	500

Notes :

- Distributors are custom designed as required. These figures are typical values. Actual values will vary with specific application.
- Larger sizes are available
- All Internals are segmented as required for installation.

11-3/4"

6"
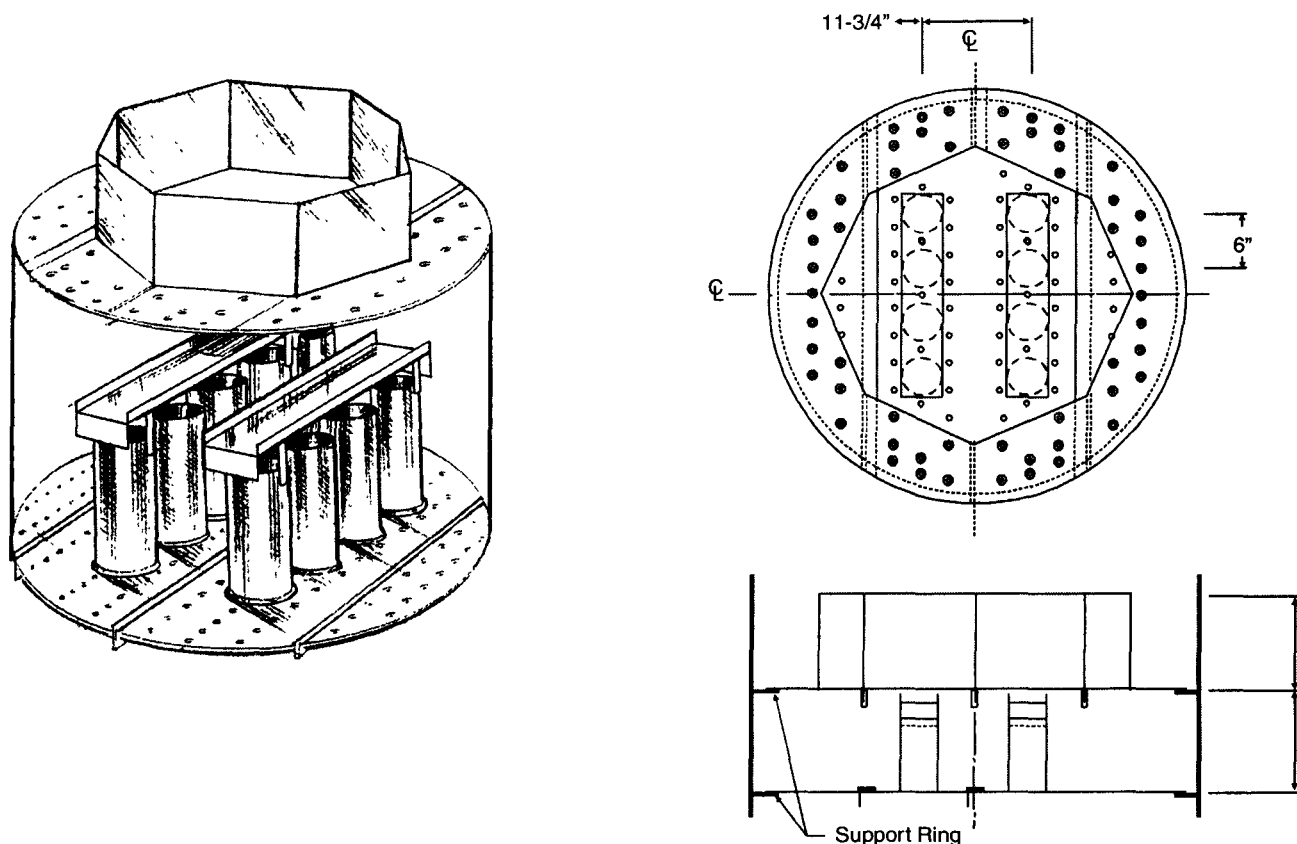
Source : Packed Tower Internals. (KOCH Engineering Co.)

© *Koch Engineering Co.* Reproduced with permission of Koch Engineering Co., Inc.

Fig. 7.4.7. *Flashing feed distributor. It is used to distribute feed that flashes as soon as it enters the distributor. It consists of two plates—an upper gallery which is 50% open for vapor distribution, and a lower plate for liquid distribution.*

The two-phase feed is introduced to the upper gallery where the vapor disengages from the liquid. A V-baffle is placed in front of the feed nozzle to deflect the feed around the tower wall. Holes in the bottom of the upper gallery transfer the liq to the lower plate where the liq is distributed over the packing.

The upper gallery height is typically 300 mm, and then spacing between the two plates is also 300 mm. This type of distributors is fabricated in sections for passage thru manways.

Pressure-fed distributors typically are of the ladder-type fitted with pipe arms sporting liq-metering orifices.

Flashing Feed Distributors

The **Flashing Feed Distributor** is used to disengage the vapor phase from a two-phase feed. The **Model 300** consists of two plates :an upper gallery, which is 50% open for vapor disengagement, and a lower plate for liquid distribution which is similar to a **Model 301A**. Each plate requires a separate supporting ring.

The two-phase feed is fed to the upper gallery where the vapor disengages from the liquid. A **Koch "V"** baffle is typically used in front of the feed nozzle to deflect the feed around the tower wall.

Holes in the bottom of the upper gallery transfer the liquid to the lower plate where the liquid is distributed over the packing.

The upper gallery height is typically **12 inches**, and the spacing between the two plates is also **12 inches**. The **Model 300 Flashing feed Distributor** is fabricated in sections for passage through column manways.

MODEL 300 FLASHING FEED DISTRIBUTORS

Tower ID	Support Ring Width	Typical Overall Height	Approx. Weight (Lbs)
48"—59½"	1½"	18"	140—230
60—89½"	2"	22"	345—750
90"—119½"	2½"	26"	750—1200
120"—137½"	2½"	29"	1200—1600
138"—179½"	3"	33"	1600—2700

Notes :

- These figures are typical values. Actual values will vary with temperature, diameter and material type and thickness.
- Larger sizes are available
- All Internals are segmented as required for installation.
- Center support beams may be required for diameters of 9 feet or larger.

Ladder pipe distributors : are used where the liq feed is under pressures, and is very effective when the tower height available for the distributor is limited. This distributor **(Fig. 7.4.8.)** is often specified over shallow bed depths where maximum efficiency is required, and in services with relatively low liq rates **[< 24 m³/(h.m²)]**. They are recommended for only non-fouling services, especially where low flow rates result in small holes being used.

A moderately high turndown **(4 :1)** is possible as higher hole pressure-drop is maintained than in a gravity distributor. It is also well suited for applications with high gas rates, since the free area for gas flow is relatively large and press.dr.across the distributor is generally negligible
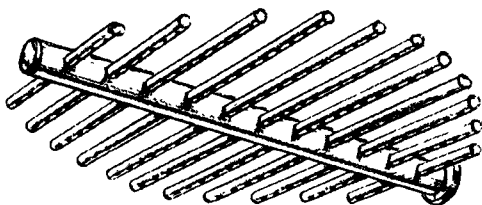
Model 304

Source : Packed Tower Internals (Koch Engineering Co.).

© *Koch Engineering Co.* Reproduced with kind permission of Koch Engineering Co., INC.

Fig. 7.4.8. *Ladder Type Distributor.*

Fig. 7.4.8-A

This pressure-fed liq Distribution System is very helpful when Tower Height Available for Placing the Distributor is limited.

They are recommended for only in Clean Services.. They are known to Operate with a High Turndown (4:1) because of Higher Hole Drop than Gravity Distributors.
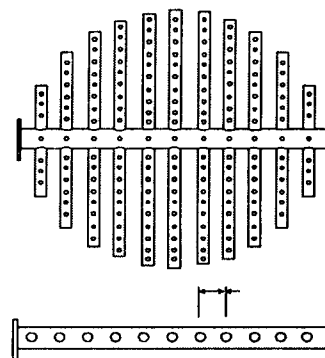
Ladder pipe distributors are fabricated in sections for passage thru column manholes. Standard design is for a horizontal feed from the side of the tower. However, vertical center-feed design is also available commercially.

Ladder Pipe Distributor

Model 304 Ladder Pipe Distributors [Fig. 7.4.8 & 7.4.8A] are used where the liquid feed is under pressure, and can be very helpful when the tower height available for the distributor is limited. This distributor is often specified over shallow bed depths where maximum efficiency is required, and in services with relatively low liquid rates (less than **10 gpm/sq. ft.**). They are recommended only in clean services, especially where low flow rates result in small holes being used. These distributors are commonly employed in liquid/liquid extraction columns.

A moderately high turndown is possible (about **4:1**) because the distributor can be designed for a higher hole pressure drop than a gravity distributor. The **Model 304** is well suited for applications with high vapor rates, since the free area for vapor flow is relatively large and pressure drop across the distributor is generally negligible.

Model 304 Ladder Pipe Distributors are fabricated for a passage through column manways. The distributor is supported by an internal nozzle flange on the main header and a support saddle on the opposite end of the header. Standard design is for a horizontal feed from the side of the tower. However, vertical center feed is also available.

Model 304 Ladder LPipe Distributor

Tower I.D.	Typical Flow, GPM	Header Diameter	No. of Laterals per side	Approx. wt., Lbs. Carbon or Stainless Steel
17¼"	18	1½"	2	10
23¼"	30	2"	3	17
29¼"	50	2"	4	25
36"	70	3"	5	50
42"	95	3"	6	65
48"	125	3"	7	85
54"	160	4"	8	115
60"	200	4"	9	140
66"	250	4"	10	160
72"	300	6"	11	300
84"	400	6"	12	340
96"	500	6"	13	450
108"	650	8"	14	625
120"	800	8"	15	700

NOTES :

- Distributors are custom designed as required. These figures are typical values. Actual values will vary with specific application
- Larger sizes are available
- All internals are segmented as required for installation
- Center support beams may be required for diameters of **9 feet** or larger.

Plan
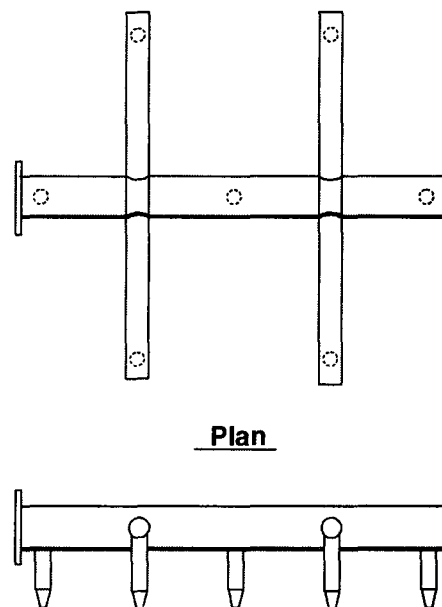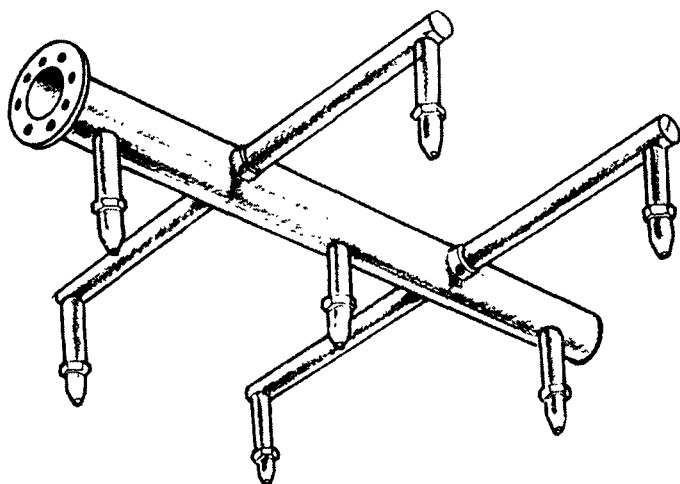
Model 305

Source : Packed Tower Internals. (Koch Engineering Co.)

© *Koch Engineering Co.* Reproduced with kind permission of Koch Engineering Co., Inc.

Fig. 7.4.9. *Spray Nozzle Distributor.*

Liq Under Pressure is Sprayed thru Multiple Nozzles onto a Packed Bed. They are imminently useful where a Uniform Distribution is Critical Due to Shallow Bed Depths.

Max. Turndown is 2:1 at a Typical ΔP Across Nozzles of 70 – 100 kPa.

Spray Nozzle Distributor

Spray Nozzle Distributors : are commonly used in scrubbers. They are particularly useful where a uniform distribution pattern is critical due to short bed heights.

Spray nozzle distributors **(Fig. 7.4.9)** are primarily used for heat transfer and refinery applications where a uniform distribution pattern is critical due to short bed heights. They are also commonly used in scrubbers and in wash zones, condensing zones and pumparound zones of crude oil vacuum towers.

They can be designed for liquid rates as low as **0.1 gpm/sq.ft.** of tower area, and have been used in columns with diameters in excess of **30 feet.**

The maximum turndown of a spray distributor is **2:1** at a typical pressure drop across the nozzles of **10-15 psi.**

Spray nozzle distributors are fabricated for passage through manways. They are supported by an internal flange on the main header, and by column wall attachment to support the opposite end of the header and the laterals, as required. The nozzle tips are typically **12"– 30"** above the packing, depending on spray nozzle layout, spray angle, flow-rate, and column diameter.

Model 305 Spray Nozzle Distributor (Fig. 7.4.9A)

Tower I.D.	Header Diameter	No. of Laterals per side	No. of Nozzles	Typical flow, GPM	Approx. wt., Lbs. Carbon or Stainless Steel
36″	2″	0	1	35	25
42″	2″	0	1	50	30
48″	3″	0	1	65	55
54″	3″	0	1	80	65
60″	3″	0	1	100	75
72″	4″	2	7	150	110
84″	4″	2	7	200	150
96²	4″	2	7	250	200
108″	6″	2	7	325	330
120″	6″	2	7	400	370

NOTES :
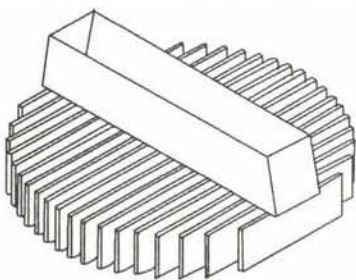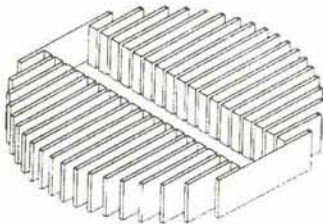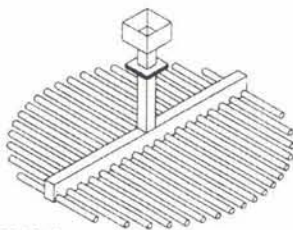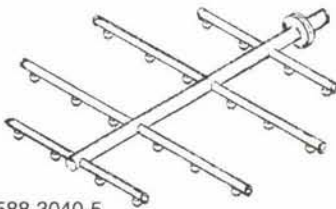
• Distributors are custom designed as required. These figures are typical values. Actual values will vary with specific application

• Larger sizes are available

• All internals are segmented as required for installation

They can be designed for liq rates as low as **25m³ per hour per sq. m.** of tower cross-section and have been installed in columns having dia exceeding 9m.

Spray nozzle distributor **(Fig. 7.4.9)** are fabricated for passage thru manways.

Sulzer Brothers are the fathers of structured packings. So it is little wonder that they will develop efficient liquid distributor and other column internals. Shown in Fig. **7.4.10** is an array of liquid distributors of SBL, Switzerland.

MELLATECH ® INTERNALS

Liquid distributors

Discharge Systems

Type L — patented — 4588 3039-1
Type P — patented — 4588 3039-2
Type G — 4588 3039-3
Type R — 4588 3039-4
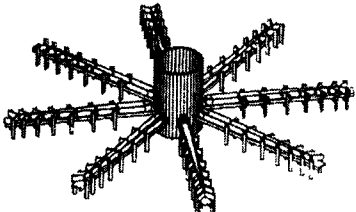
Distributor systems	*Type*	*Column diameter*	*Features*
 4588 3040-2	VE	from 0.8 m	The **VE** element distributor is supplied as standard with the types **P**, **L** and **G** discharge systems (distributor types **VEP**, **VEP** or **VEG**). It is made up from arm channels arranged in parallel, with a main channel or a main channel system located above them. Element distributors are assembled very easily through a manhole.
 4588 3040-3	VK	from 0.25 m	The **VK** channel distributor is preferably combined with the **G** and **R** discharge system (**VKG** and **VKR**). The flanged version can be assembled through the manhole. The main application is for smaller columns, wide operating ranges (type **VKR**) and markedly limited available space.
 4588 3040-1	VRG	0.25-1.6 m	**VRG** tube distributor for high drip point densities and small liquid loads, in particular for columns with gauze packings. In its flanged version (type **VRGF**), it can be assembled through the manhole. Only for clean liquids.
 4588 3040-5	VRD	from 0.8 m	The **VRD Spray nozzle** is used mainly in refinery columns and scrubber towers. It requires a head pressure. The operating range has a maximum of 1:2

Courtesy : Sulzer Brothers LTD., Winterthur., Switzerland

Fig. 7.4.10.

Sulzer has developed a very special type of liquid distributor **(Fig. 7.4.11)** for efficient distribution of liquids containing suspended solids.

The **VFS** special distributor is suitable for heavily contaminated liquids, suspensions or emulsions, such as milk of lime.

Distributor systems	Type	Column diameter	Features
	VRD	from 0.8 m	The **VFS** special distributor is suitable for heavily contaminated liquids, suspensions or emulsions, such as milk of lime.

Courtesy : Sulzer Brothers LTD., Winterthur., Switzerland

Fig. 7.4.11. *A special liq distributor (patented design) which is meant for handling liquids with solids suspensions. It is suitable for column dia ≥ 1m.*

7.5. LIQUID REDISTRIBUTOR

A liquid redistributor is installed between two packed beds to set liq maldistribution of the lower bed at right. Random packings are usually supported on gas injection multibeam support plate (**Fig. 7.1.1**) and the liquid flowing out from such a typical support plate is not sufficiently uniform to properly irrigate the next packed bed below. The multibeam support plate tends to segregate the liq downflow into a pair of parallel row of liq streams about **50 mm** apart with about **250mm** space between adjacent pairs. Likewise the gas-distributing support plate (**Fig. 7.2.2**) fails to ensure sufficiently uniform liquid irrigation pattern into the packed bed below because of the location of gas risers in such plates.

As a result of liq maldistribution, the compositions of the liq and gas phases will vary from those set by the column operating line. Redistributors collect the downcoming liq from the bed above and distribute it uniformly to the bed below. This renders the portion of liq filming down the column wall available for mass-transfer. The redistributor also corrects the coalescence of downflowing liq stream which occurs even with the most efficient type of packing. The purpose of the redistributor is to eliminate those factors that cause to the loss of efficiency in the tower and to reestablish a uniform pattern of liq irrigation.

Likewise, the redistributor must sustain uniform gas distribution that should have been established at the column bottom. Therefore, the redistributor must sport a large area available transverse to the gas risers since only very low gradient heads are available for cross-mixing of the liq. Over and above, the gasflow area must be sufficient to avoid a high press. dr. in the gas phase. And this area must be distributed uniformly across the column cross-section.

Redistributors are available only in metal construction.

The model shown in **Fig. 7.5.1** is Norton's liq redistributor available in the size range of **1219mm** and larger.
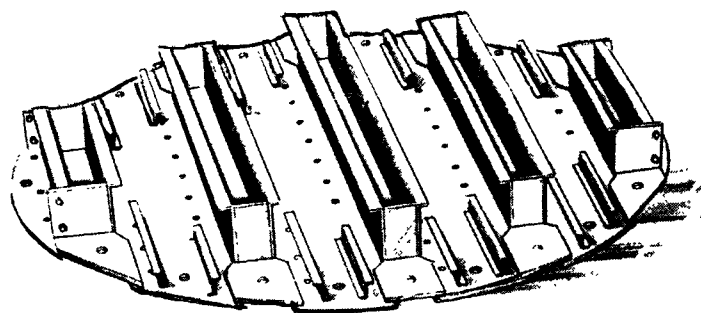
Source : Standard Tower Internals.

© **Norton Co.** Reproduced with kind permission of Norton Chemical Process Products Corporation/Akron/Ohio/USA

Fig. 7.5.1. *Redistributor achieves Total Collection of the Liq on the Plate and reestablishes a Uniform Pattern of Liq Irrigation. This Model 851 is Designed to be used with Norton Model 804 Multibeam Support Plate.*

Model 301A orifice distributors **(Fig. 7.4.1)** are commonly used as redistributors by simply adding hats over the gas risers to prevent liq from falling thru. This type of redistributors is meant for nonfouling applications.

For fouling services, **model 301B** type orifice plate distributors **(Fig. 7.4.2)** with drip tubes are used as redistributors. When used for fouling service, solids settle out on the deck and clear liq flows thru the drip tubes.

Redistributors may be used in combination with support plates. Shown in **fig. 7.5.2** is the KOCH's **Model 201A** which is simply a **Model 301A** distributor **(Fig. 7.4.1)** in combination with a **Model 101R** support plate **(Fig. 7.1.1)**
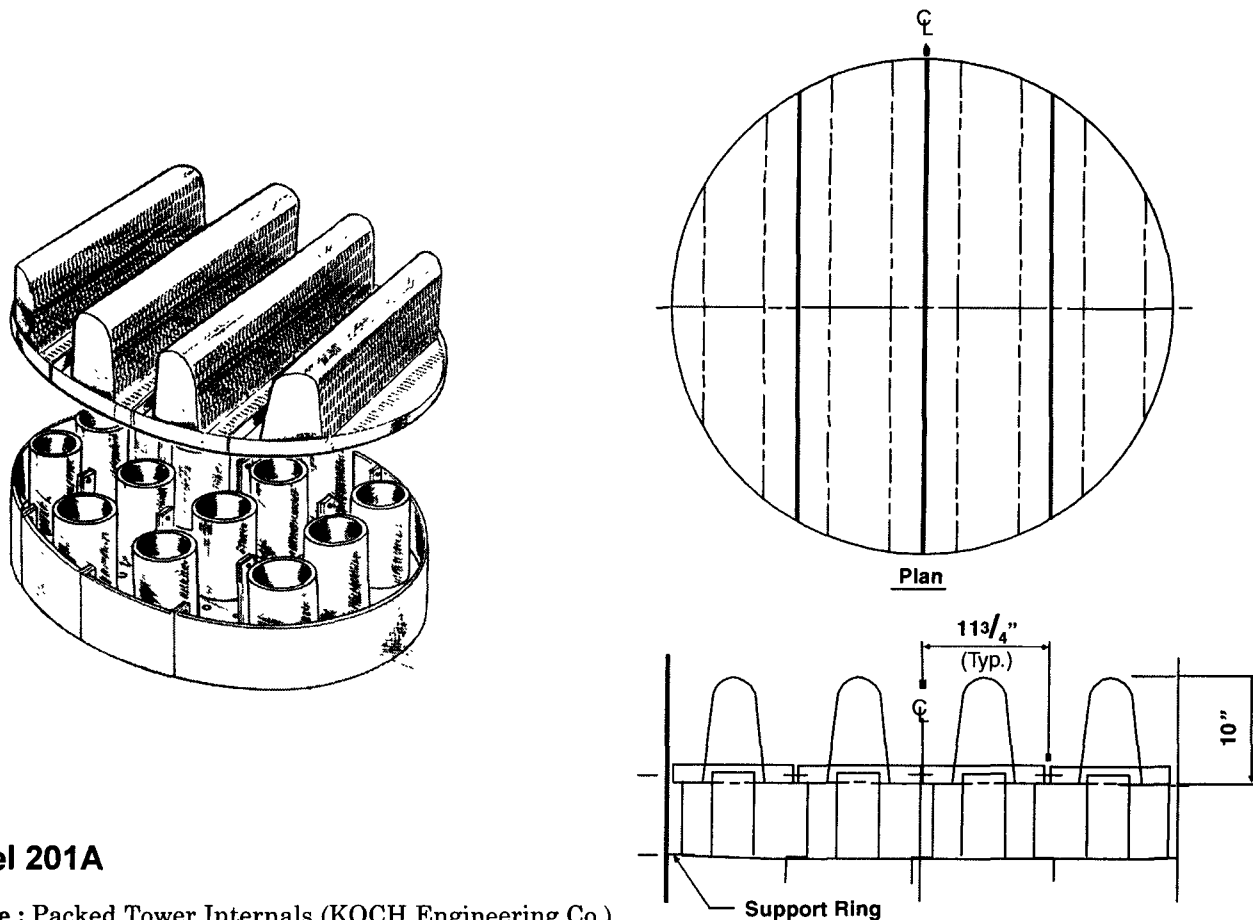
Model 201A

Source : Packed Tower Internals (KOCH Engineering Co.)

© *KOCH Engineering Co.* Reproduced with kind permission of KOCH Engineering Co., INC.

Fig. 7.5.2. *Redistributor–Support Plate Combination. The Packing Support Plate rests a top the Liq Distributor. The Liq Percolating Down the Support Plate Segregates to Preferential Flowpaths. The Distributor underneath Collects these Streams and Evenly Distribute the Liq onto the next Packed Bed Below.*

Combination Support Plates/Redistributors

Model 201A is simply a **Model 301A** distributor in combination with a **Model 101R** support plate. The support plate is supported by the rim of the redistributor. Therefore, only one support ring is required for the two internals. This reduces the tower height required for redistribution.

The combination plate is used where liquid redistribution is required between packed beds and no feed is introduced at that location.

The overall height is typically **14"–18"** and plates are fabricated in sections for installation through column manways.

For non-fouling serial the **Model 201A** is used. For fouling service or high turndown requirements, the **Model 201B** with drip tubes is used. These combination support plates/redistributors also are valuable with the same antimigration ratio feature as **Model 301AM** and **301BM** which eliminates the need for a separate be limiter.

Model 201A Combination Support Plates/ Redistributors

Tower I.D.	*Support Ring Width*	*No. of Sections*	*Load Capacity, Lbs./Sq.ft.*	
			Carbon Steel	*Stainless Steel*
$12" - 17\frac{3}{4}"$	**Clips**	1	4000	2600
$18" - 23\frac{3}{4}"$	1"	1	2200	1400
$24" - 29\frac{3}{4}"$	$1\frac{1}{4}"$	2	1400	900
$30" - 59\frac{1}{2}"$	$1\frac{1}{2}"$	2 – 5	2000	1400
$60" - 89\frac{1}{2}"$	2"	5 – 7	1000	700
$90" - 119\frac{1}{2}"$	2	7 – 10	550	400

Notes :

- Approximate weight for standard construction: carbon steel: 21.5 Lbs./ sq. ft. stainless steel: 13.0 Lbs./sq. ft.

- These figures are typical values. Actual values will vary with temperature, diameter and material type and thickness.

- Larger sizes are available.

- All internals are segmented as required for installation.

- Center support beams may be required for diameters of 9 feet or larger.

Norton's **Model 1006 (Fig. 7.5.3)** is essentially an orifice-type distributor (all metal) that can also be deployed as a collector-type redistributor. Available in size range ≥ **1219 mm**
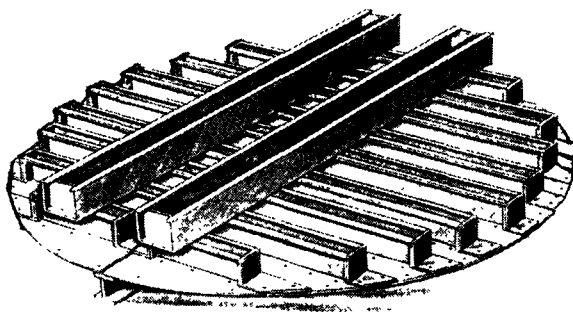
Model 1006

Courtesy : Norton Chemical Process Products Corpn., Akron, Ohio, USA

Fig. 7.5.3. *Model 1006 is Norton's orifice-type distributor (metal) that can function as redistributor also.*

7.6. WALL WIPERS

These area special class of tower internal often referred to as redistributors. They are generally installed in packed towers when tower efficiency is being reduced due to a large fraction of liq flowing down the column wall. This problem is more frequent in small-dia towers than in large dia columns. This is because, in small-dia cols., the tower wall surface is substantial when compared to the total packing surface area. As the column dia becomes larger, this wall surface area of the col diminishes progressively when compared to the packing area. For instance, in a **150mm-ID** col perhaps about 30% of the liq feed streams down the col wall whereas in a **1500mm-ID** col, liq flow down the col walls may thin out to as little as 3% of the liq feed.

Again the interface of the wall and packing represents a region of higher voidage, *i.e.*, greater open area relative to the internal regions of the packed bed. Therefore, it represents an area from which liq is less likely to leave. Means must, therefore be provided for redirecting liq from the walls back toward the center of the packed bed to ensure good distribution.

Fig. 7.6.1 Illustrates a design that collects wallflow liq and pipes it toward the center. It is most suitable for towers **600 mm (ID)** or less.
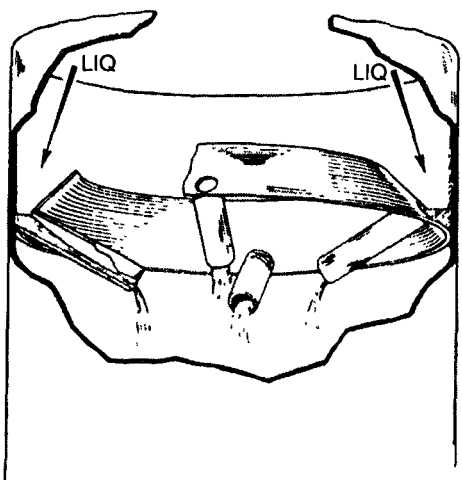
Fig. 7.6.1. *A Typical Wall Wiper. A Conical Shell Sealed to the tower wall, it Collects Liq Wallflow and Pipes it to the Central Position of the Packed Bed below. Ideal for Small Dia (≤ 600mm) Columns.*

Courtesy : Norton Chemical Process Products Corpn., Akron, Ohio, USA
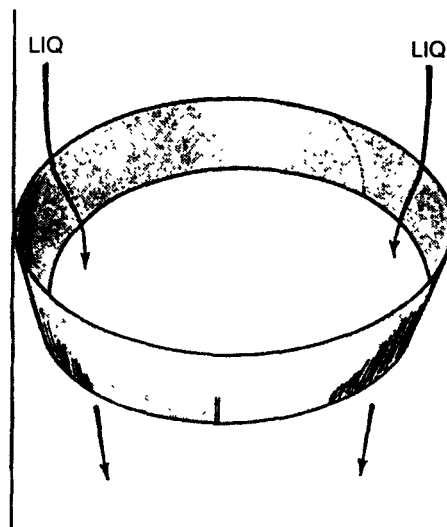
Fig. 7.6.2. *A Conical Shell Wall Wiper.*

Courtesy : Norton Chemical Process Products Corpn., Akron, Ohio, USA.

Fig. 7.6.2 shows another simple form of wiper. It is a conical shell that skims liquid off the walls and channels it towards to an inner dia.

This type of distributors has one limitation :

they restrict tower capacity of burried within the packing.

Therefore, their inner dia must be checked for approaching flooding.

However, this flooding hazard is avoided with the arrangement shown in **Fig. 7.6.3**
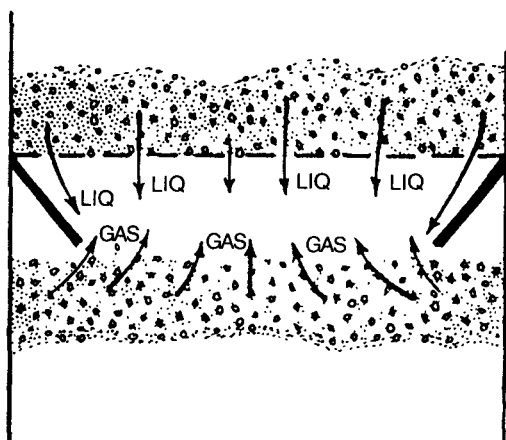
Fig. 7.6.3. *A Typical Wall Wiper Complete with a Packing Support Grid.*

Courtesy : Norton Chemical Process Products Corpn., Akron, Ohio, USA.
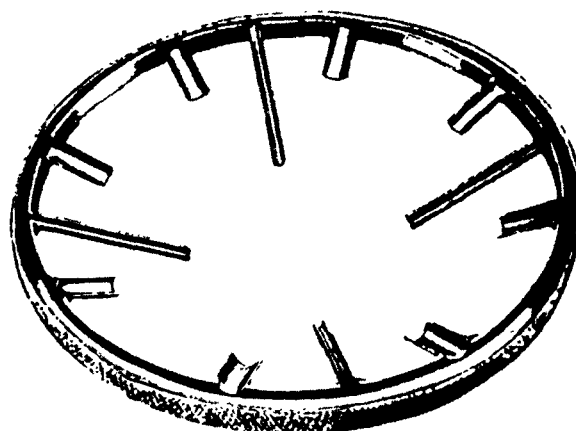
Fig. 7.6.4. *Wall Wiper With Channels for Directing Liquid Evenly Thruout the Packed Bed.*

Courtesy : Norton Chemical Process Products Corpn., Akron, Ohio, USA

Fig. 7.6.4 Illustrates a more effective version of **Fig. 7.6.2**

The cone sliced into a number of troughs directs the liq to various points along the tower radii.

Here again, care must be taken to avoid restrictions that will invite flooding at the redistribution level.

A wall wiper should also be considered in new installations when the bottom product must be completely stripped of volatile components.

Wall wipers may be fitted at virtually any point within a packed tower — within the bed, above the packing or above ordinary distributors. Their principal function is to remove liq from the column wall and transport it to the interior of the bed.

The wall wiper must sport a narrow ledge to avoid capacity limitation. However, the ledge itself cannot channel intercepted liq to a sufficient distance back into the packed bed to ensure its mixing with the mainstream of liquid. **Fig. 7.6.5** illustrates a patented design for a wiper plate that overcomes this problem.

Model 858

Fig. 7.6.5 : *Rosette Wall Wiper (Model 858 of Norton Co.) These Wall Wiper Redistributors Answer Redistribution Problems in Small Columns.*

Advantages Include :

• **Higher Liq Handling Capacity**

• **Eliminate Wall 'Streaming'**

• **Nonfouling**

• **Allow Greater Spacing Between Redistributors**

• **Provide Constant Percentage of Free-Space Regardless Of Tower Dia.**

This design, available in the size range : 102mm—610mm, maintains a very high percentage of column cross-sectional area open to gas and liq flows. This finger projections extended towards the center convey the intercepted liq to the interior of the packed bed and to the mainstream downflowing liquid.

7.7. LIQUID COLLECTORS

It is a specialty packed tower internal.

Very often it becomes imperative to intercept the entire liq downflow of the column. This condition arises due to an enlargement or contraction of the column dia.

If the lower part of the col is of a larger dia than the upper section and liq from the packed-bed located in the upper section is allowed to rain freely onto the larger-dia-packed-bed in the lower section, there will occur liq maldistribution on the lower bed for the obvious reason. The peripheral packings may not get irrigated at all.

Likewise, liq falling freely from a packed bed in the larger dia upper section will not distribute evenly over the packed bed located in the smaller-dia-lower-section. There will be excessive wallflow.
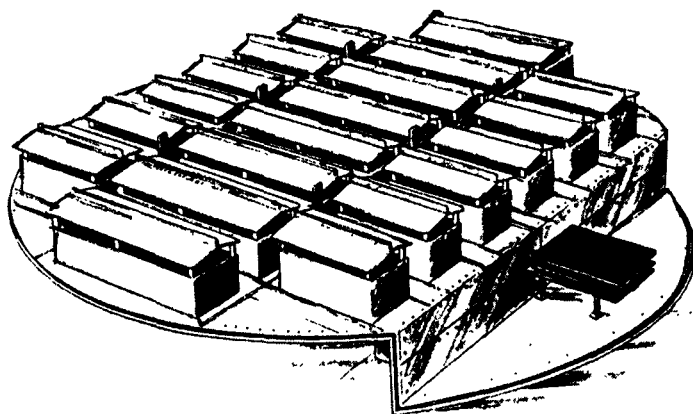
Model 933

© Norton Co. Reproduced with kind permission of Norton Chemical Process Products Corporation/Akron/Ohio/ USA.

Fig. 7.7.1. *Liquid Collector.*

Under these circumstances, a liquid collector plate **(Fig. 7.7.1)** must be installed where the column cross-section changes. The liq draining from packed bed above is collected and fed to a redistributor located just below the collector plate to irrigate uniformly in the lower bed.

A liq collector plate must be gasketed so that it can set liq-tight on the supporting ledge.

The collector plate is provided with a number of gas risers to maintain proper gas distribution. Each gas risers is fitted with a cover to deflect the falling liq onto this collector plate.

Vane Collectors (Fig.7.7.2) : are low-pressure-drop devices used to collect liquid for either redistribution or a side draw. They are available in various configurations for column dia ranging from 600mm to 6000mm.
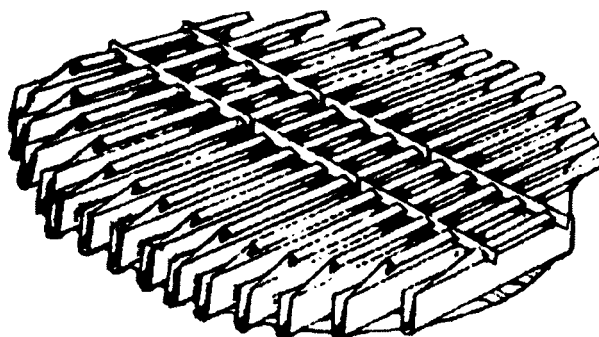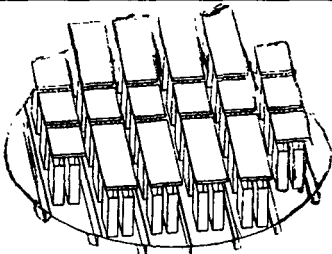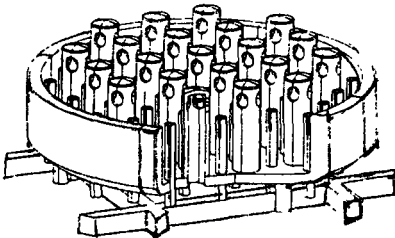
©KOCH Engineering Co. Reproduced with kind permission of KOCH Engineering Co.

Fig. 7.7.2. *A Typical Vane Collector* (KOCH Engineering Co.)

Shown in **Fig. 7.7.3** are two highly-efficient liquid collector-cum-distributor systems.

COLLECTOR–DISTRIBUTOR SYSTEM

	V/S	from 0.8 m	Chimney tray collector-distributor with discharge system, type **G**. Used for special applications (absorption, refineries) and operating conditions (high liquid loading, foams). It can be assembled through the manhole.
	V/ST	0.25–1.6 m	Socket-type collector-distribution pan made from graphite for use with highly corrosive media in conjunction with ceramic packings.

Courtesy : Sulzer Brothers Ltd., Winterthur, Switzerland

Fig. 7.7.3. *A pair of liquid collector-cum-distributor systems — proprietary designs.*

Typical Absorptions of Industrial Importance

8.1. GAS DEHYDRATION

Process Principle : Gas dehydration is a typical example of physical absorption that involves drying of an insoluble gas in contact with a dehydrating liquid.

The water vapor in the feedgas stream is the solute while the dehydrating liquid is the solvent. The driving force for mass transfer is the difference between the partial pressure of water vapor in the gas stream and the vapor pressure of water above the liquid phase.

The high heat of vaporization of water as well as its high heat of solution present high heat load to the liquid phase. As the dehydrating liquid is diluted by the condensed water and as the liquid temperature increases, the vapor pressure of the water above the liquid phase will increase and that will tell upon absorption efficiency. In order to outweigh this generic disadvantage, a high liquid circulation rate is usually maintained to minimize both the temperature rise and the dilution of the liquid dehydrating agent.

If absorption of a large amount of water vapor is required, a number of absorption towers, each recycling cooled liquid, are hooked up in series.

Typical Example # 1 Drying of Chlorine

The hot cell gas is cooled gas is cooled to about 288 – 291K before entering the first drying tower.

Operating Parameter

- **Inlet Gas Stream**

  Pressure : ~ 100 kPa

  % Water Vapor : 2 mol % (max)

- **Exit Gas Stream**

  % Water Vapor : 40 mol ppm

- **No. of tower :** 3 (usually) in series

- **Liq rate :** $10 - 12 \ m^3. \ m^{-2}.h^{-1}$

- **Dehydrating Agent :** H_2SO_4 (98 Wt %)

- **Acid consumption :** 9 kg per ton of Cl_2 dried

Important : Absorbent coolers normally become a necessity to cool the recirculated acid stream feed to the Ist and IIIrd towers in order to keep the outlet acid from each tower to 308 K max temp.

Design

1. *Pressure Drop :* the overall pressure drop desired for the entire drying system is only 0.98—1.2 kPa. Hence the three towers are sized to give a pressure drop of 82 to 121 $Pa.m^{-1}$ of packed depth.

2. *The process is, as expected, largely gas film controlled one.* Therefore, it is desirable to provide same packed depth in each of the three columns. To get to this configuration an iterative design procedure is followed.

3. Inasmuch as high liq rate is maintained in all the three columns, the acid concentration and temperature in each tower can be assumed, as first approximation, constant to determine the amount of water vapor removed in each column and thereby acid concentration

Important : If superdry chlorine [Cl_2 level:10 mol ppm max] is required, a fourth drying tower is tagged in. This column removes very little water vapor so that the recirculating acid's strength will be as high as 96 wt%. This highly concentrated acid gives rise to high liq-phase viscosity ($> 15000 \times 10^{-6}$ Pa.s), the absorption in this tower will be predominantly liq-film controlled.

Typical Example #2 : Natural Gas Dehydration

Natural gas usually contains water in liq and /or vapor form at source and/or as results of sweetening with an aqueous solution. And therefore it becomes necessary to remove the water to avoid the formation of hydrates during transport LNG thru pipelines, minimize corrosion and/or maximize the calorific values of gas.

The best way of drying the NG is generally the **absorption drying process** using glycol in which the gas stream, saturated with water vapors enters the absorption column at the bottom and comes into contact with triethylene glycol (TEG) either in countercurrent or cocurrent flow.

Historically TEG contactors were usually equipped with bubblecap trays. However, everincreasing stringent process requirements, such as everlower operating pressures arising from marginal recovery, and the constant search for weight reduction in off-shore operations, require selection of the optimal hardware for this process, and the minimization of uncertainties associated with its design.

In recent years structured packing has become the most frequently chosen such hardware. In about 1982 it was first used in Europe and then introduced in North America in about 1985.

Structured packing was first developed by Sulzer Brothers in the 1960s and registered dramatic success in such separation processes viz. distillation, absorption requiring a large number of separation stages. The key to the outstanding performance of structured packing is the way in which the gas and the liquid streams are handled by the packing.

Design

Many of the existing design rules for TEG natural gas dehydration units are purely empirical in nature or based on considerations such as flexibility of operation, plant safety etc. Complicacy mounts as there is still considerable controversy about some basic questions :

TEG – WATER equilibria
WATER CONTENT of sour NG etc.

1. Diameter : Using correlations of measured values, pressure drop and capacity for a given column dia are determined. Comprehensive sets of such measurements now exist over wide ranges of operating conditions for many structured packings and correlation of these data may be used with confidence for most applications particularly for TEG contactors as the design is usually far from the limits imposed by the hydrodynamics of the process.

For column dia **(D_t)** less than 1m, column cap. and press. dr. are strongly dependent on dia as a large portion of column cross sectional area lies within the column wall boundary layer. This requires correction for wall effects.

Hydrodynamic data over most of the pressure range at which TEG contactors operate are scarce and thus a correction is to be made to data obtained at pressures.

TEG contactors are so designed that capacity does not exceed 50% in order to accommodate fluctuations in gas feed and pressure. The limiting factor is more usually the mist eliminator operating range, however.

The column dia should be such that gas load **(F-factor)**

$$\text{F-factor} = v_G \cdot \sqrt{\rho_G}$$

does not exceed 3.0 Pa$^{1/2}$, where

v_G = gas velocity, m. s^{-1}

ρ_G = gas density, kg. m^{-3}

At higher gas flowrates liq entrainment becomes significant if liquid viscosity exceeds **(15 –20) × 10^{-3} Pa.s** (the $\mu_{TEG/303K}$).

For columns with an integral scrubbing system, the vaporload **(F-factor)** should not be increased beyond **2.8 Pa$^{1/2}$** as at higher flowrates the scrubbing section demister may become overloaded, leading to foaming problems due to entrained hydrocarbons in the packed section.

2. Packed Height : The packed height required for given absorption efficiency is determined in terms of **NTU (or NTS)**, and **NTUM (or NTSM)**,

where   **NTU** = No. of Transfer Units

NTS = No. of Theoretical Stages

NTUM = No. of Transfer Units per Meter

NTSM = No. of Theoretical Stages per Meter

The factor **NTUM (or NTSM)** defines the separation efficiency of the packing.

Though **NTS** method is more widely known and understood (not least because of a large number of tray columns still in service), the **NTU** approach is recommended for structured packing.

However, if **NTS** method is followed for structured packing, an **NTSM** value of 0.5 may be taken.

Accurate determination of packed height of **TEG** column is difficult because of:

• **NTUM / NTSM** data are approximate

• Paucity and inconsistency of available NG-Water and TEG-Water equilibrium data.

2.1. NTU CALCULATION

TEG contactor design is best based on the **NTU** instead of on the **NTS** due to several reasons :

■ The **NTU** approach is more accurate when the **EL** (equilibrium line) is comparatively **"flat",** resulting in a very low NTS value.

■ The heat of absorption of water vapor should be taken into account So long as operating pressure remains ≤ 10 bar, this is straight forward, to first-order accuracy.

In many cases the NG and TEG temperatures are not identical resulting in a net heat transfer between these two streams. This heat exchange factor should be taken into account whereupon the EL becomes curved at the top.

These two effects would be difficult to include in a standard stagewise calculation due to obvious reason.

■ Operating conditions in terms of **NTUM** but not in terms of **NTSM** give much better and satisfactory correlation of packing performance data.

The conventional method of determination of **NTU** is numerical integration

$$NTU = \int_{Y_t}^{Y_b} \frac{dY}{Y - Y^*}$$

If the **OL** and **EL** are assumed straight :

$$NTU = \frac{Y_b - Y_t}{\Delta Y_b - \Delta Y_t} \cdot \ln \left| \frac{\Delta Y_b}{\Delta Y_t} \right|$$

and

$$\frac{NTS}{NTU} = \frac{HTU}{HETP} = \frac{m\dfrac{G}{L} - 1}{\ln \left[m\dfrac{G}{L} \right]}$$

where **Y*** is the equilibrium value of mole fraction of water vapor.

Y_b and Y_t are the bottom and top-of-column operating values respectively.

G and **L** are molar gas and liq flowrates

m is the slope of the **EL**

The TEG contactor is an absorption column. The absorption of water in TEG involves a small number of **NTUs** (1 to 3 in any section).

The **NTUM** of a structured packing is a function of pressure, gas load, liquid load, and the packing density [**Figs. 8.1-1A, 8.1-1B, 8.1-1C, 8.1-1D**]

The **NTUM** value decreases with increasing pressure. This is due to lower diffusivity of the water vapor in the NG.

However, **NTUM** increases with increasing liquid load as higher liq rates stretch the gas-liq interfacial area.
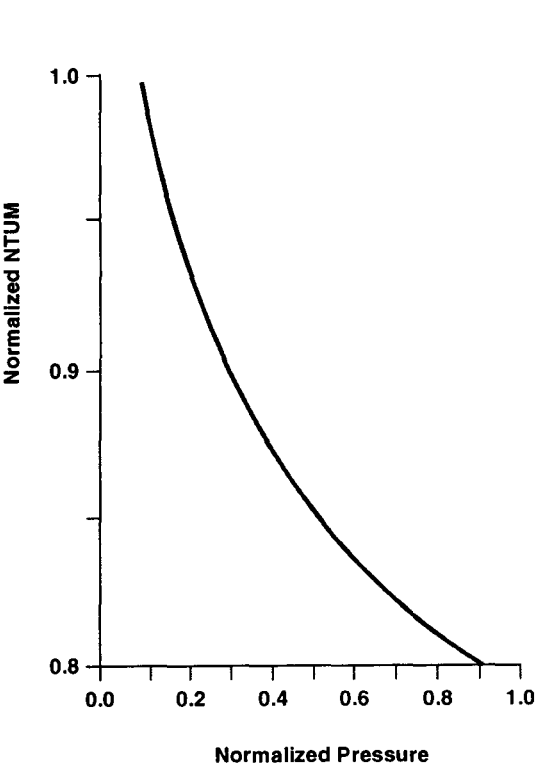
Fig. 8.1-1A.
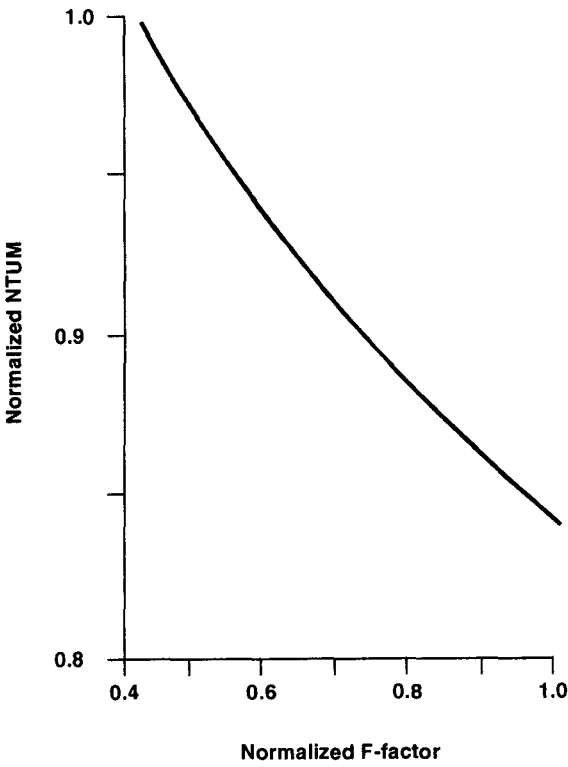
Fig. 8.1-1B.
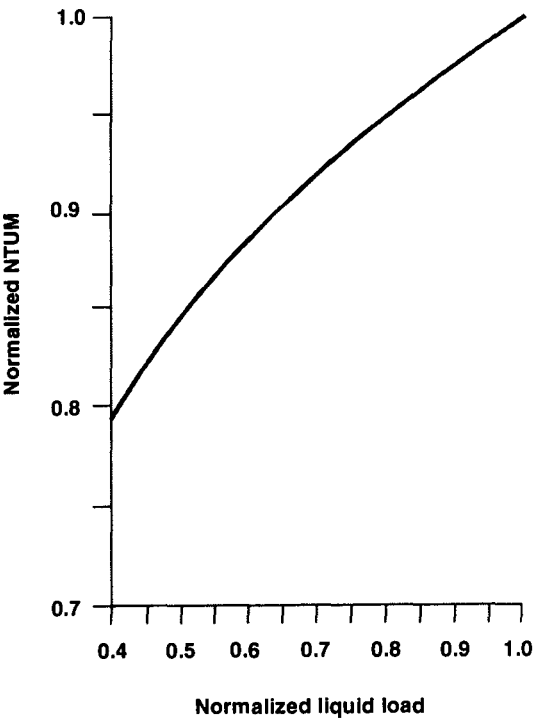
Fig. 8.1-1C.
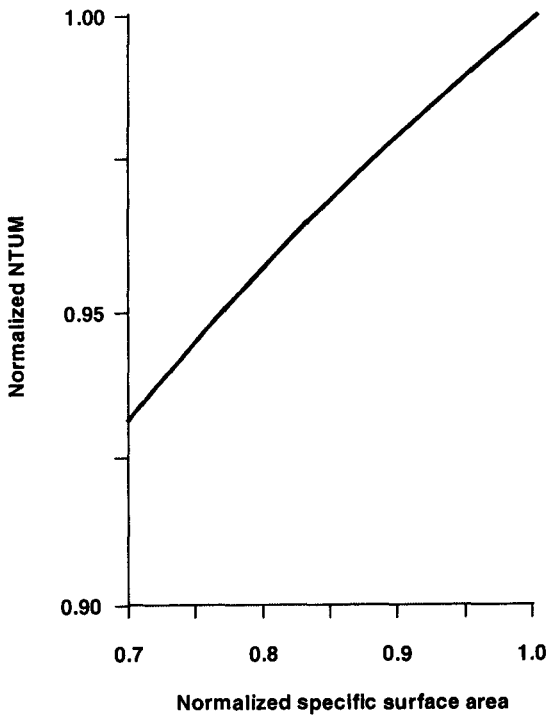
Fig. 8.1-1D.

NTUM decreases with increasing gas flowrate, as the contact time between gas and liq then decreases.

NTUM increases with increasing packing density due to obvious reason as greater gas-liq interfacial area becomes available with greater specific surface area.

3. TEG Flowrate

The flowrate of recirculated TEG recommended is 3 times the minimum flowrate required, i.e., at which the column is pinched. However, GPSA (Gas Processors Association, San Antonio, Texas) recommends for tray columns a TEG rate of 3US **gallons per pound of water in the feed.** This in most cases exceed the 3 × Minimum TEG Rate. However, GPSA recommendation what follows from ensuring the correct hydraulic performance of trays is in many cases unnecessarily conservative for structured packings.

For specific liquid loads (< **0.8 m³. m⁻². h⁻¹**) it is recommended that a higher factor of safety (30%) be taken for packed height. This is because, the liquid distributor may not perform optimally at such flowrates.

4. Hydrodynamics

For a given column dia structured packings offer greater capacity and smaller pressure drop than random packings, and substantially more so than trays.

$\Delta P \mid_{structured\ packing} \approx$ **0.2—0.3 kPa per m of bed depth for TEG**

The capacity difference, as is evident from **Fig. 8.1-2,** between tray columns and those equipped with structured packings is of the order of 80% for TEG contactors.

New design			Revamp	
	Trays	Structured packing	Trays	Structured packing
Capacity ref. %	100	100	100	185
Diameter mm	1500	1100	1500	1500
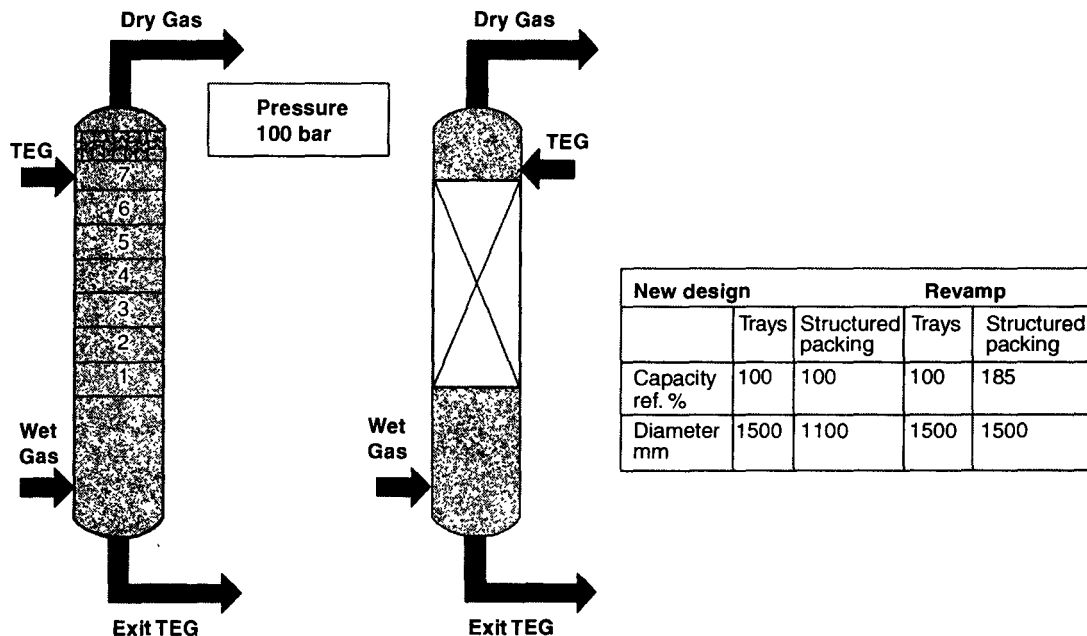
Fig. 8.1-2.

Revamping of trayed columns with structured packings will therefore enable the plant to process larger gas volumes where wellhead pressure has decreased, and thus continue to meet production targets.

If a new column is installed, the smaller column dia afforded by the use of structured packings will beget a substantial saving in column weight and cost, as the savings are more than linear with diameter—this is especially significant for TEG contactors, with their substantial shell thickness. The cost of structured packings is usually greater than that of other internals. However, the reduction in column dimensions means that the cost of the overall package — column plus internals — is less with structured packings.

This weight factor becomes an important consideration for offshore processing, where a reduction in platform superstructure mass of 1 ton permits a cut of 10—20 tons in substructure mass.

5. Liquid Holdup

Liquid holdup is a function of specific surface area, liquid flowrate, viscosity, and surface tension. NG dehydration columns fitted with structured packings encounter only 5% of the packed volume as liquid holdup.

6. TEG Losses

All glycols have a strong tendency to foam. Therefore, if NG is forced to flow thru it, it'll cause foaming. And no type of column internals can adequately handle severely foaming absorbents. And that means higher entrainment loss and loss of capacity. Usually control of this problem calls for dosing of an antifoaming agent.

But with TEG contactors packed with structured packing, NG is brought into tangential contact with the liquid phase (instead of being forced to flow thru it). This sort of gas-liq contacting ensures foaming does not occur, and the column is operated at around 80% capacity. Entrainment of liquid becomes negligible. And thus glycol carryover loss is virtually eliminated (**Fig. 8.1-3**).
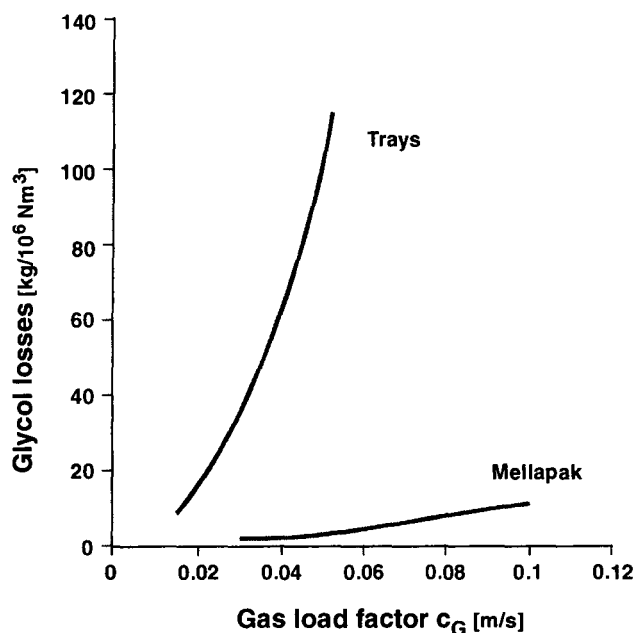
Fig. 8.1-3. *Comparison of glycol losses (due to entrainment) with trays and structured packings.*

Even if there is foaming, structured packing will continue to perform satisfactorily provided foaming level is moderate. However, care must be taken in design such that gas flowrates do not lead to demister overload or to liquid entrainment if the TEG viscosity is high, *i.e.*, if the TEG temperature is sufficiently low.

7. Plugging

Fouling is always a problem in NG dehydration column using TEG as absorbent. Glycols are very reactive to sulfur compounds. The resulting degradation products tend to polymerize and plug small openings. Although inlet separators are commonly installed just upstream of the TEG-Dehydrator Units, their efficiency is often low. Inadequate separator operation will allow a variety of extraneous particles to enter the absorber :

compressor oil, drilling mud,

corrosion inhibitors, pipeline dirt,

hydrates and/or salt water.

Plugging is particularly a critical problem for dumped packings, as they sport a wide spectrum of channel sizes. As the plugging material enters the column, it will accummulate in those channels of smallest diameter and slowly reduce capacity. Structured packing, on the other hand, has a single channel size, *i.e.*, it does not present small gaps where in plugging material will **preferentially** accummulate. That's why structured packings exhibit remarkable resistance to fouling even with highly polymerizing systems, clearly superior to dumped packings and comparable to that of trays.

Experience shows that the liquid distributor will always plug before the packing itself. So it is desirable to maximize distributor hole size, and there is thus a trade-off with distribution quality, achieved with high drip-nozzle density, and hence small hole size. Prefiltering of TEG will outdo this difficulty. However, to use too fine filter mesh is simply to exchange the risk of distributor plugging for that of filter plugging. Thus the designer must go for somewhat increased distributor hole size, and hence reduced drip-point density, reduced distribution quality. This should be counterpoised by somewhat greater packed height.

8. Turndown

For a TEG-column packed with structured packings, the gas turndown can be varied up to factor of 50, i.e. gas flowrate of only several percent of the design load without affecting the packings performance.

The extent of acceptable liquid turndown is governed chiefly by the liquid distributor. There is some decrease in packing performance with the decreasing flowrate. Also at very low liq flowrates, distribution quality may be difficult to maintain. Thus there is a trade-off between distribution quality and flexibility. **The distributor that provides for a liquid turndown ratio of 1:2 without loss of distribution quality is preferable.**

Construction

1. Liquid Distributor

For any packed column the quality of liquid distribution is crucial to its performance.

It is therefore recommended that packed column *TEG liq distributors should have a drip-point density of 80 per m² of column cross-section. The minimum recommended hole dia is 2 mm* to minimize the risk of plugging.

Overflow slots should be provided as an emergency precaution to avoid plugging. And for the same reason it is a good practice to filter the TEG at some point in the recirculation loop.

40% of column cross-sectional area must be provided for gas upflow (free area) to ensure that the $\Delta P < 50$ **Pa.**

A grid should be used to level the liquid distributor—this will rest on the top of the packing.

A gap of at least **50 mm** between the top of the packing and the bottom of the liquid distributor should be provided. The distributor tubes should not be more than 10mm from the top of the packing— this is a measure to avoid droplet entrainment.

Special care must be exercised in the choice of distributors for contactors in motion, e.g., offshore TEG contactors on platforms. Normally, a tube type **(Fig. 8.1-4.)** is an appropriate choice.
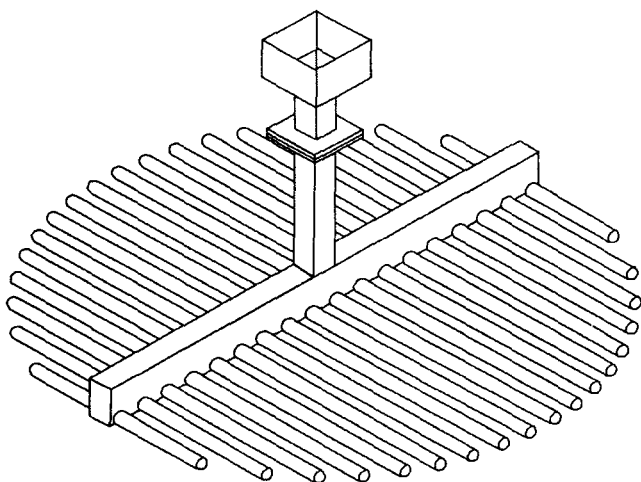
Source : Structured Packings for TEG Contactors — P. Collins and K. Breu

Courtesy : Sulzer Brothers LTD., Winterthur, Switzerland

Fig. 8.1.4. *Tube type liquid distributor for glycol contactor.*
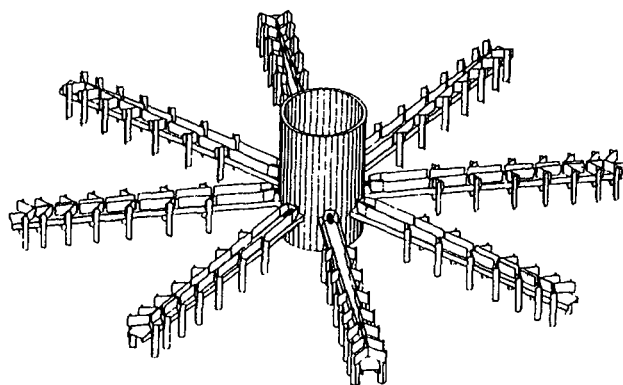
Source : Structured Packings for TEG Contactors — P. Collins and K. Breu

Courtesy : Sulzer Brothers LTD., Winterthur, Switzerland

Fig. 8.1.5. *Radial type liquid distributor for glycol contactor*

For systems with low gasrates, a radial type distributor **(Fig. 8.1.5)** is recommended

This is because at particularly low glycol flowrates the hole size will be so small that fouling is likely to be problem for tube type distributors.

2. Gas Inlet Nozzle

Gas nozzle size should be such that the **F-factor** does not exceed **60**. At higher gas flowrates with smaller gas inlet nozzles, the induced back-pressure may exceed the ΔP across the entire packed section with the effect that the suction effect immediately above the inlet will lead to severely non-uniform pressure and velocity profiles, and eventually to reverse flow, as shown in **Fig. 8.1.6.**

Once the maldistribution reaches this much proportion of severity, it'll propagate to much higher levels in the column telling upon packing performance badly.
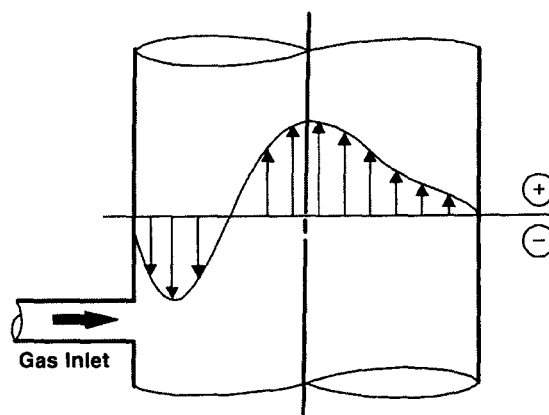
Fig. 8.1.6. *Form of column cross-section velocity profile above gas inlet resulting when inlet gas flowrate is excessive. This non-uniform velocity distribution is undesirable as it entails downflow above inlet.*

3. Scrubbing Section

Exit gas must be freed of droplets. Hence the use of a mist removal device is strongly recommended. Mesh demisters operated at the gas flowrate at which they're most efficient (usually in the **F-factor** range $2 - 2.8$ $Pa^{1/2}$) remove over 99.9% of droplets with diameters of the order of 20 μm and over 80% of droplets with diameters of the order of 8 μm.

Inasmuch as the new columns are installed with higher **F-factor** ($2.5 - 2.8$ $Pa^{1/2}$ in the absorbing section) such a demister can and should span the complete cross-sectional area.

Tray columns on the other hand operate at lower **F-factors** ($1.5 - 1.8$ $Pa^{1/2}$). Therefore if a column is revamped from trays to structured packing, its performance will be optimized if demister occupies the central portion of the column only. If sudden surges in water load, in the form of discrete droplet phase, are a possibility, it is better to over dimension the demister :

forasmuch as a demister with spare capacity will eliminate water droplets efficiently.

A chimney tray is usually recommended for glycol collection. If correctly designed, the tray will also improve gas distribution considerably. The distance between the top of the chimney hats and the bottom of the packing is recommended to be at least the width of the chimney hats and with an absolute minimum of 300 mm to ensure adequate gas distribution on entry to the packing.

Gas distribution may get unacceptably upset in the demister installed below the chimney tray if gas flowrates in the nozzle are sufficiently high. Also the gas distribution may be unacceptably poor when available height is insufficient to permit installation of a chimney tray. Under these circumstances, installation of a pressure relief device at the mouth of a nozzle is strongly recommended.

Where no scrubbing section is employed, the installation of a gas distributor is recommended if the column dia exceeds 2.5m.

4. Packing

Structured packing should be oriented to optimize gas-liq distribution. For this, ***the successive sections of a packing should be rotated by 90° to one another.*** This will also increase the capacity of the packed section to bear its own weight. Structured packings are so light weight that they can be packed to a height of over 10 m without any intermediate supporting structure. Of course, the use of a support beam is recommended for tower dia exceeding 2.5 m.

5. Revamping Tray Columns

In revamping NG-dehydration towers from trays to structured packing, the lowest tray-ring is left as it is to support the packing bed. Likewise, the uppermost ring is used to level the liquid distributor; all remaining tray rings and all trays are removed.

8.1A DESIGNING A TRAYED COLUMN FOR DEHYDRATING NATURAL GAS WITH TEG

Natural gas (NG) contains many impurities. The most undesirable among them is water vapor, which is present in varying degree in all NGs.

The NG must be dried before combustion or long-distance transmission thru pipelines because of following reasons :

- Gas hydrates plug equipment and pipelines
- Water vapor decreases the combustion temperature and hence lowers the combustion efficiency.
- NG containing water is corrosive, particularly if CO_2 and H_2S are present

$$H_2S + H_2O \rightleftharpoons \overset{\oplus}{H} + \overset{\ominus}{S}$$

$$CO_2 + H_2O \rightleftharpoons \overset{\oplus}{H} + \overset{\ominus}{HCO_3}$$
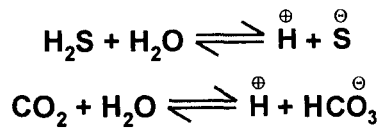
■ Water vapor upon condensing in NG pipelines induces slug-flow conditions damaging control valves.

■ Water vapor increases the volume and decreases the heating value of natural gas—this phenomenon reduces pipeline capacity.

■ A water dewpoint requirement of a sales-gas-contact specification ranges 32.8—117 kg per MMsm^3 (million standard cubic meter).

MMscm = million standard cubic meter [15°C/100 kPa. abs].

When triethlyene glycol (TEG)–a liquid desicant is used to dry natural gas in trayed column (**Fig. 8.1A.1**) the process engineers and design engineers need to estimate the circulation rate of lean TEG., and the diameter of the trayed column.
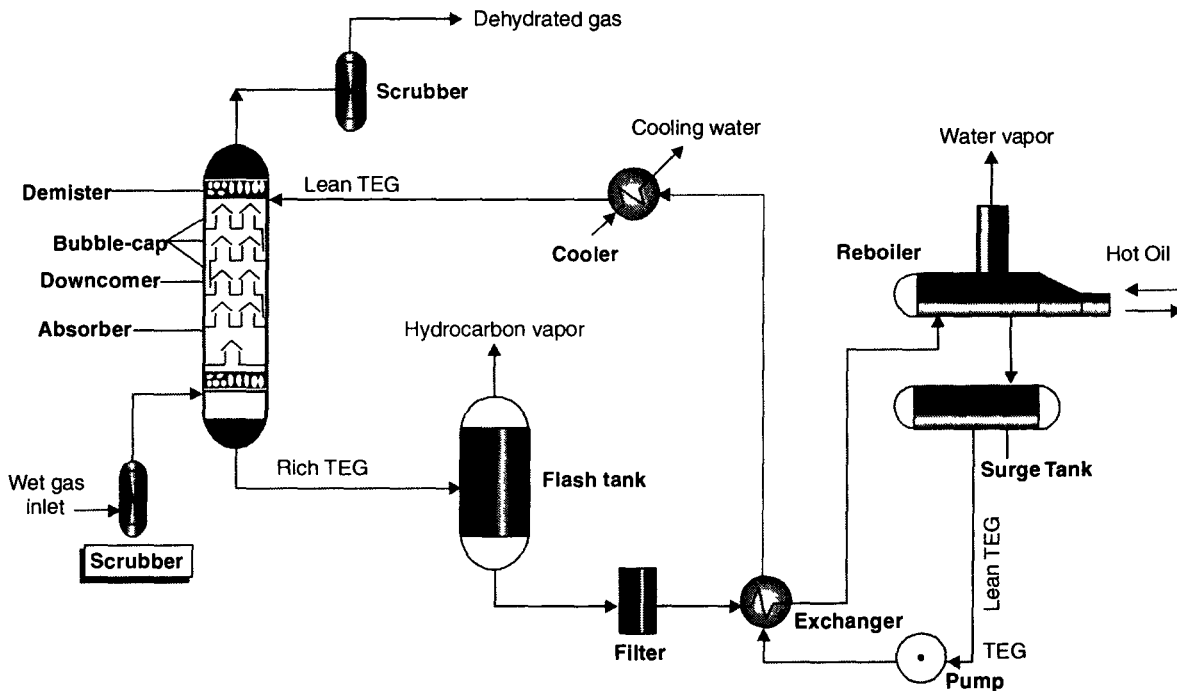
Fig. 8.1A.1. *TEG Dehydration Unit.*

DESIGNING A TRAYED COLUMN NG DEHYDRATOR

Example 8.1 A bubblecap trayed column is to be designed to dehydrate natural gas by using triethylene glycol (TEG). The input data are :

Volumetric flowrate of NG : 1 MMsm³/day
Gas temperature : 313 K
Gas pressure : 7 MPa
Concentration of lean TEG : 98.7 wt%
Water content in exit gas : 117 kg/MMm³

Assume tray efficiency :   *25%*

Solution :

We shall proceed on the basis of following assumptions :

1. The gas volume is constant at each point in the absorber

2. 1 mole of NG is entering the bottom tray per unit time. This will enable us to calculate the number of moles of lean TEG entering the top tray per unit time

3. ρ_{TEG} = 1.12 kg per liter

   ρ_G = 41.6 kg per m^3

4. The operating parameters of NG lie on the following range :

   Gas pressure :   2 — 10 MPa

   Gas temperature :   293 — 313 K

5. The gas volume is referred to standard temperature (T_s = 288K) and standard pressure (P_s = 100 kPa absolute).

6. The range of lean TEG varies from 97 to 99.85%

7. Mol wt. of TEG = 150 kg.kmol^{-1}

   Mol. wt of water = 18 kg.kmol^{-1}

8. The gas superficial velocity taken equal to 80% of flooding velocity to determine the column dia.

CALCULATION

Step - (I) Water Content of Saturated NG at Absorber Inlet

The water content of feed natural gas saturated at the operating conditions is

$$W_{IN} = 593.335 \ |\exp (0.0549 \ T)| .P^{-0.8146}$$

where, W_{IN} = water content of the entering gas, kg/MMsm^3

   T = temperature of NG feedstream, °C

   P = pressure of NG feedstream, MPa

Given :

$$T = 313 \ K = 40°C$$

$$P = 7 \ MPa$$

$\therefore$
$$W_{IN} = 593.335 \ |\exp (0.0549 \times 40| \ (7)^{-0.8146}$$

$$= 1092.9336 \ kg/MMsm^3$$

Step - (II) Mole fraction of Water in Lean TEG

Lean TEG is recycled to the absorber at the top. Its water content is evaluated from

$$x_{OUT} = \frac{|100 - x_{G,\,IN}|/M_W}{|100 - x_{G,\,IN}|/M_W + x_{G,\,IN}/M_{TEG}}$$

where, x_{OUT} = mole fraction of water in the lean TEG

$x_{G, IN}$ = concentration of lean TEG, wt%

M_W = molecular weight of water = 18 kg/kmol

M_{TEG} = molecular weight of TEG = 150 kg/kmol

Given :

$$x_{G, IN} = 98.7 \text{ wt\%}$$

$$x_{OUT} = \frac{|100 - 98.7|/18}{|100 - 98.7|/18 + 98.7/150} = 0.09890$$

Step - (III) Actual Amount of Water Absorbed

$$W_{act} = W_{IN} - W_e$$

where, W_e = water content in the exit gas (absorber outlet)

= 117 kg/MMsm^3

∴   Actual amount of water absorbed

$$W_{act} = 1092.9336 - 117 = 975.9336 \text{ kg/MMsm}^3$$

Step - (IV) Absorption Efficiency

$$\eta_a = 100 \left| \frac{W_{act}}{W_{max}} \right|, \%$$

where, W_{max} = maximum possible amount of water absorbed, kg/MMsm^3

$$= W_{IN} - W_{OUT}$$

W_{OUT} = water content in the exit gas (absorber outlet) if it is in equilibrium with the entering lean TEG, kg/MMsm^3

$$= W_{IN} \cdot x_{OUT} \cdot \gamma$$

γ = activity coefficient of water in TEG-water solutions

$$= -0.0585 \, x_{G, IN} + 6.2443$$

$$= -0.0585 \, (98.7) + 6.2443$$

$$= 0.47035$$

∴ $$W_{OUT} = (1092.9336) \, (0.0989) \, (0.47035)$$

$$= 50.8406 \text{ kg per MMsm}^3.$$

∴ $$W_{max} = 1092.9336 - 50.8406$$

$$= 1042.093 \text{ kg/MMsm}^3$$

∴ **Absorption efficiency**

$$\eta_a = 100 \left| \frac{975.9336}{1042.093} \right| = 93.65\%$$

Step - (V) Number of Actual Trays

The values of absorption factor **(A)** and the number of theoretical trays change with absorption factor

$$A = 4.158 + \exp(-19.17 + 23.02 \, \eta_a)$$
$$N = 1$$
$$\left. \right\} \quad \text{for } 86\% < \eta_a < 94\%$$

$$A = 5.79 + \exp(-54.88 + 58.02 \, \eta_a)$$
$$n = 1.5$$
$$\left. \right\} \quad \text{for } 94\% < \eta_a < 98\%$$

$$A = 7.21 + \exp(-267.83 + 271.113 \, \eta_a)$$
$$n = 2$$
$$\left. \right\} \quad \text{for } 98\% < \eta_a < 99.85\%$$

The number of actual trays is given by

$$N_{act} = 100 \left| \frac{N}{\eta_{tray}} \right|$$

For our system, $\eta_{tray} = 25\%$
η_a being 93.65%

$$A = 4.158 + \exp(-19.17 + 23.02 \times 0.9365)$$
$$= 15.052$$

and

$$N = 1$$

$\therefore$

$$N_{act} = 100 \left| \frac{1}{25} \right| = 4$$

Step - (VI) Mass Flowrate of Lean TEG Entering the top Tray of Absorber

$$m = A.K.G_v \, (1739) \, (M_{l, TEG}) \text{ in kg TEG/h}$$

where,   A = absorption factor

= 15.052 (see **Step - V**)

K = equilibrium constant for water in a TEG-H_2O system

$$= 1.33 \times 10^{-6} . W_{IN}, \gamma$$

$$= 1.33 \times 10^{-6} \, (1092.8299 \text{ kg/MMsm}^3) \, (0.47035)$$

$$= 683.6336 \times 10^{-6}$$

G_v = volumetric gas flowrate per day MMsm^3/day

= 1 MMsm^3/day

$M_{l, TEG}$ = molecular weight of lean TEG, kg/kmol

$$= x_{OUT} . M_W + (1 - x_{OUT}) \, M_{TEG}.$$

$$= 0.0989 \, (18) + (1 - 0.0989) \, (150)$$

$$= 136.945 \text{ kg/kmol}$$

$\therefore$ Mass rate of lean TEG entering the absorber top

$$m = (15.052) \, (683.6336 \times 10^{-6}) \, (1) \, (1739) \, (136.945)$$

$$= 2450.5596 \text{ kg TEG/h}$$

Step - (VII) Circulation Rate of TEG

$$C_{l, TEG} = \frac{m}{\rho_{TEG}}$$

$$= \frac{2450.5596}{1.12} \frac{kg \ TEG \ / \ h}{kg \ TEG \ / \ l}$$

$$= 2187.9996 \ l/h$$

Step - (VIII) Amount of Water Absorbed ($W_{act,h}$)

$$W_{act,h} = \frac{W_{act}}{24} \frac{kg / MMsm^3 \ of \ feedgas}{h}$$

$$= \frac{975.9336}{24} \frac{kg}{h}$$

$$= 40.6639 \ kg/h$$

Step - (IX) Circulation Rate of TEG

$$C_{TEG} = \frac{C_{l,TEG}}{W_{act,h}} \frac{lt}{kg \ water \ absorbed}$$

$$= \frac{2187.9996}{40.6639} \frac{lt / h}{kg / h}$$

$$= 53.8069 \ lt/kg \ of \ water \ absorbed$$

Step - (X) Flooding Velocity

$$v_{fl} = 0.055 \sqrt{\frac{\Delta\rho}{\rho_G}} \qquad where, \ \Delta\rho = \rho_L - \rho_G$$

$$= 0.055 \left| \frac{1.12 - 0.0416}{0.0416} \right|^{\frac{1}{2}}$$

$$= 0.2800 \ m/s$$

Step - (XI) Gas Superficial Velocity

$$v_s = design \ velocity$$
$$= 80\% \ of \ v_{fl}$$
$$= 0.8 \ (0.28 \ m/s)$$
$$= 0.2240 \ m/s$$

Step - (XII) Volumetric Flowrate of Gas

$$V = 10.8253 \left| \frac{T}{T_s} \right| \cdot \left| \frac{P_s}{P \times 10^{-3}} \right| \cdot G_v \ in \ m^3/s$$

where,

T = gas temperature, K

T_s = standard temperature, K

P_s = standard pressure, kPa

P = gas pressure, MPa

G_v = gas flowrate, MMsm³/day

$$V = 10.8253 \left| \frac{313}{288} \right| \cdot \left| \frac{100}{7 \times 10^3} \right| \quad (1)$$

$$= 0.16807 \text{ m}^3/\text{s}$$

Step - (XIII) Tower Cross-Section

$$A = \frac{V}{v_s}$$

$$= \frac{0.16807}{0.2240} \quad \frac{\text{m}^3/\text{s}}{\text{m/s}}$$

Step - (XIV) Dia of Tray Tower

$$D_{tower} = \sqrt{\frac{4 \, A_{tower}}{\pi}}$$

$$= \sqrt{\frac{4(0.7503)}{\pi}}$$

$$= 0.9774 \text{ m}$$

$$\simeq 98 \text{ cm}$$

8.2. SELECTIVE ABSORPTION

The term **"selective absorption"** refers to the preferential absorption of one component "A" from a mixture containing another gas "B" (usually with similar properties) whose co-absorption is for some reason not desired.

Selectivity can be achieved by two mechanisms : **Equilibrium** (or thermodynamic) **selectivity** and **kinetic selectivity**. They are based on completely different principles and should not be confused.

Several magnitudes have been defined as quantitative measures of the selectivity (either thermodynamic or kinetic) of a packing or of an absorption column. All of them are acceptable and useful, so long as consistency is kept. Two of the most usual simple definitions are the following :

$$\textbf{Selectivity of a process} = \frac{\% \text{ of A absorbed}}{\% \text{ of B absorbed}}$$

$$\textbf{Selectivity of a packing} = \frac{\text{NTUM for A}}{\text{NTUM for B}}$$

The first definition is mainly used for thermodynamic selectivity. For kinetically selective absorption the determination of the second value is the decisive step.

8.2.1. Thermodynamically selective absorption

Equilibrium (or thermodynamic) selectivity is based on the different solubilities of the two key components. Selectivity is achieved by choosing an **L/G** ratio that gives an absorption factor greater than 1 for the component to be absorbed (**A**) and less than 1 for the undesired component (**B**). In this way, "**A**" is absorbed while for "**B**" the column is "**pinched** " (**Fig. 8.2.1**) and only a small amount of "**B**" is absorbed.
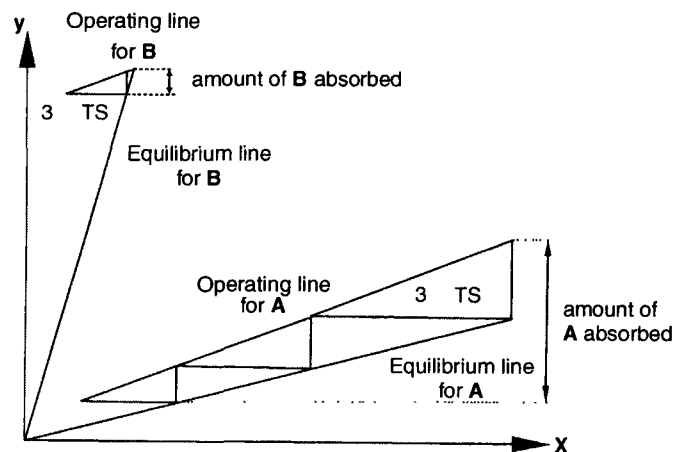
Fig. 8.2.1. *Equilibrium Selectivity.*

The greater the difference in solubilities between the two components, the more selective the absorption will be. Thus, equilibrium selectivity can be controlled by choosing the proper solvent and setting the correct **L/G** ratio. An increase in the number of theoretical stages improves equilibrium selectivity (**Fig. 8.2.2**). This feature makes high efficiency packings attractive for this application, but one has to consider that beyond a certain values, the increase in packing height results in only marginally better selectivity.
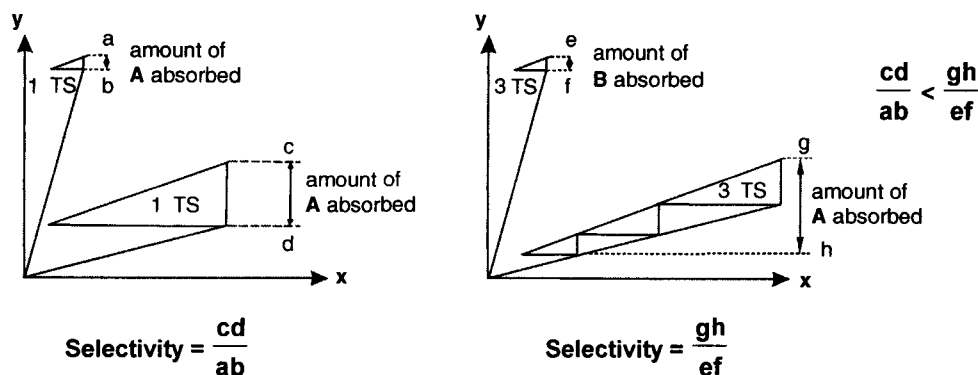
Fig. 8.2.2. *Improvement in equilibrium selectivity with increasing number of stages.*

In principle, the same equilibrium selectivity can be achieved with any type of packing, provided of course that enough packing height is available. On the other hand, no packing will be able to improve the selectivity of a process beyond the limits set by the gas-solvent equilibrium. The packing

selectivity has a value of about 1 in the whole operating range because the performance of the packing is roughly the same for "A" and "B"; the selectivity of the process varies in a very wide range (2—100) depending on the solvent (as an example, the process selectivity of the absorption of "A" with respect to the carrier gas is virtually infinite). An important factor is that there is no danger of overdesign: extra reserve height or unexpectedly high packing performance can only be beneficial.

Design of Thermodynamically Selective Absorption

The design of thermodynamic selectivity is straightforward and does not require any special knowhow. In most cases, only computational purposes, the two key components can be assumed to be absorbed independently. Only seldom is it necessary to consider the influence of simultaneous solubility on the equilibrium, that is, how the solubilities of the two key components influence each other. In such cases the corresponding simultaneous equilibrium data have to be available. The design can be performed by the usual hand calculation methods or with any tray-by-tray simulation programme if the equilibrium is highly nonlinear or if heat effects are important.

8.2.2 Kinetically Selective Absorption

Kinetically selective absorption is based on the difference in the velocity of absorption of the two key component. This difference is due to the presence of a chemically reactive component "C" in the solvent which reacts at different rates with the key components. Typically, "A" reacts instantaneously with "C", whereas "B" reacts only slowly with "C". The instantaneous reaction of "A" with "C" does not affect the absorption of "A", which remains being gas-side controlled, that is, HTU_{OG} for "A" is equal to HTU_G. The reaction of "B" with "C", however, shifts the resistance to the liquid side, so that HTU_{OG} is controlled by HTUL and has a much higher value. In this way, the same packing shows very different apparent efficiencies (HTU_{OG} or $NTUM_{OL}$) for "A" and "B", thus favouring the absorption of "A".

Unlike for thermodynamically selective absorption, it is not interesting to approach the equilibrium between the phases in the column; the closer the column is to equilibrium, the larger the amount of "B" that reacts, whereas the instantaneous absorption of "A" is not modified. This decreases the selectivity down to the thermodynamic or equilibrium value.

A typical case is the selective absorption of H_2S and CO_2 by means of tertiary amines, for example, MDEA. At equilibrium the solubilities of H_2S and CO_2 in MDEA would yield a process selectivity of around 5 to 10. But since CO_2 reacts slowly with the amine, the apparent **HTU** for CO_2 is much higher, thus resulting in a packing selectivity of 20 – 50 and process selectivities of 15 – 30.

Kinetic selectivity is radically different from equilibrium selectivity in several respects :

* For a given solvent and **L/G ratio**, the characteristics of the packing (more specifically, the ratio of the gas and liquid mass transfer coefficients) greatly influence kinetic selectivity. Due to their mass transfer characteristics, structured packings are intrinsically more selective than trays.

* Kinetic selectivity changes markedly at turndown because the gas and liquid mass transfer coefficients vary at different rates as a function of turndown. The best design at 100 % load may not be the optimal one at 50%.

* *There is danger of overdesign and underdesign:* too much packing would result in excessive absorption of "B" and lower selectivity. If the column is too short, the specification for "A" will not be reached.

* The applicability of stagewise models for the simulation of kinetically selective absorbers is limited, since the assumption of equilibrium stages is not justified.

Design of Kinetically Selective Absorption

The design of kinetically selective absorption is a complex task and, strictly speaking, each system should be treated individually. Due to its industrial importance, design procedures are currently available at Sulzer only for selective absorption of H_2S/CO_2 with MDEA.

The first design method is based on the special purpose program **AMSIM** (DB Robinson and Associates Ltd.). **AMSIM** contains reliable equilibrium data for the system $H_2O/CO_2/MDEA$, among others. Although it is based on a stagewise model, kinetic selectivity can be simulated roughly by defining different tray efficiencies (ε) for H_2S and CO_2. These tray efficiencies have to be related to or extrapolated from pilot or industrial plant data, and, as a first approximation, can be taken as inversely proportional to the experimental HTU values for H_2S and CO_2. A typical values range is :

$$\varepsilon_{H_2S} / \varepsilon_{CO_2} = 20 - 50$$

Specific values for the efficiency of the packing for CO_2/H_2S absorption and desorption with different amines can be found in open literature.

This design method is very straightforward and sufficiently accurate for many purposes, the whole effect of kinetic selectivity being lumped in a single parameter. The main disadvantage is the difficulty of estimating ε_{H_2S} and ε_{CO_2}, even if experimental data are available. Reliable extrapolation to different operating conditions is problematic.

If a more accurate and reliable design is required, a second method should be used. It is based on a continuous model of the absorber. The mass transfer, equilibrium and kinetic relationships between the different ionic and nonionic species are rigorously solved at each level in the column . It is important to note that it requires the mass transfer coefficients for the gas and liquid phase to be known (among other parameters). Therefore, its applicability and accuracy depend critically on the knowledge of the mass transfer coefficients. This model has not been implemented yet (June 1989), but should be made available in the near future if reliable and consistent designs for $CO_2/H_2S/MDEA$ are to be done routinely.

Source : Separation Columns TRK/0614.

Courtesy : Sulzer Chemtech.

8.2A. Selective Absorption Of H_2S [Removal of H_2S from Raw Gas by using Aqueous Carbonate Solution]

The raw gas (RG) coming from coal gasifier contains a considerable load of **H_2S** and **CO_2**. Since **H_2S** is highly toxic as well as corrosive and also can be used as a source of sulfur in a Claus plant, the removal of **H_2S** from the gasifier exit gas has been practised since the beginning of coal conversion industry.

Several processes are known to remove **H_2S** from a gasification gas which contains larger quantities of carbon dioxide. Most of them, however, involve simultaneous absorption of **H_2S** and **CO_2**.

There are, of course, a number of processes where **H_2S** is selectively absorbed. The most noteworthy among them is *selective absorption of H_2S from RG of coal gasifier in a solution of sodium carbonate :*

Aqueous carbonate solution has a tendency to react with acidic gases such as hydrogen sulfide and carbon dioxide

$$CO_2 + \overline{O}H \rightleftharpoons HC\overline{O}_3 \qquad \qquad ...(1)$$

$$H_2S + \overline{O}H \rightleftharpoons H\overset{\cdot}{S} + H_2O \qquad \qquad ...(2)$$

$$H_2S + CO_3^{2-} \rightleftharpoons HC\overline{O}_3 + H\overline{S} \qquad \qquad ...(3)$$

$$HC\overline{O}_3 + \overline{O}H \rightleftharpoons CO_3^{2-} + H_2O \qquad \qquad ...(4)$$

Reactions **(2)**, **(3)** and **(4)** are kinetically very fast, *i.e.*, they may be considered instantaneous, regardless of the reactant concentrations when compared to the rate of diffusion. Whereas, the reaction **(1)**, due to low concentration of $\overline{O}H$, can be considered as a very slow 1st order reaction w.r.t. CO_2.

It has been found that the selectivity of H_2S absorption increases at low temperatures, high carbonate concentrations and high gas to liquid flow ratios.

Removal Efficiency Of H₂S

The removal efficiency of H_2S decreases with increasing temperature while that of CO_2 increases **(Fig. 8.2A.1)**
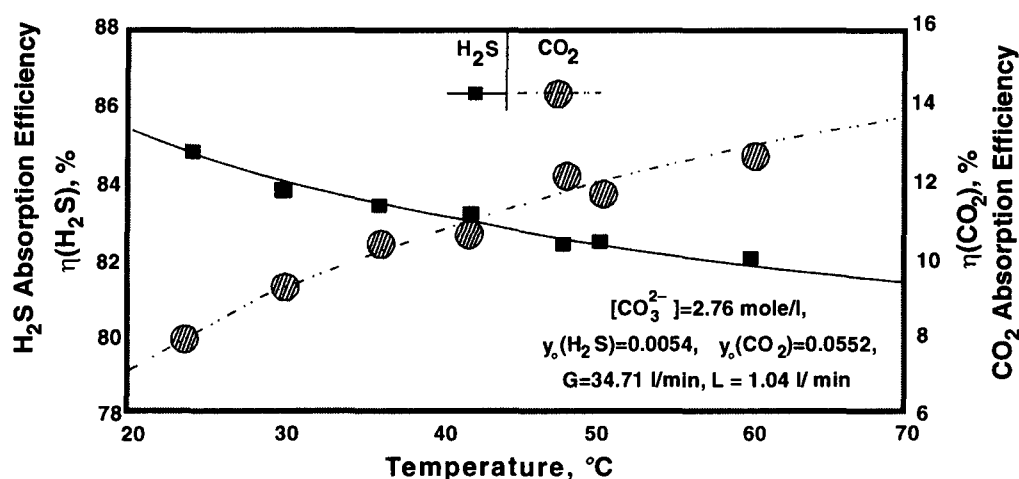
Fig. 8.2A.1. *Effect of Temperature on Removal Efficiency.*

The **removal efficiency,** *i.e.*, **absorption efficiency** is defined as the amount of the gas that has been absorbed divided by the total amount entering the column, *i.e.*,

$$\eta = \frac{p_{IN} - p_{OUT}}{p_{IN}} \times 100 \%$$

where, p_{IN} = inlet partial pressure of H_2S or, CO_2

p_{OUT} = outlet partial pressure of H_2S or, CO_2

Overall Mass Transfer

The overall mass transfer coefficient **(MTC)** is calculated on the basis of following relationship

$$K_G \cdot a = \frac{r}{A \cdot h \cdot \Delta p_{LM}}$$

where, **r = absorption rates of H_2S/CO_2,** mols.min^{-1}

$$= \frac{G \cdot P_T}{RT} \left(y_{IN} - y_{OUT} \right)$$

G = gas flowrate, lt. min^{-1}

P_T = total operating pressure, atm.

T = operating temperature, K

y_{IN} = mole fraction of **H_2S** or **CO_2** in inlet gas stream

y_{OUT} = mole fraction of **H_2S** or **CO_2** in outlet gas stream

a = specific area of packing material, m^2. m^{-3}

A = bed cross-section, m^2

h = packed bed depth, m

Δp_{LM} = logarithmic mean partial pressure difference, atm.

The overall **MTC** decreases only very slightly for **H_2S** while for **CO_2** it increases significantly with the increase of temperature **(Fig. 8.2A.2)**.
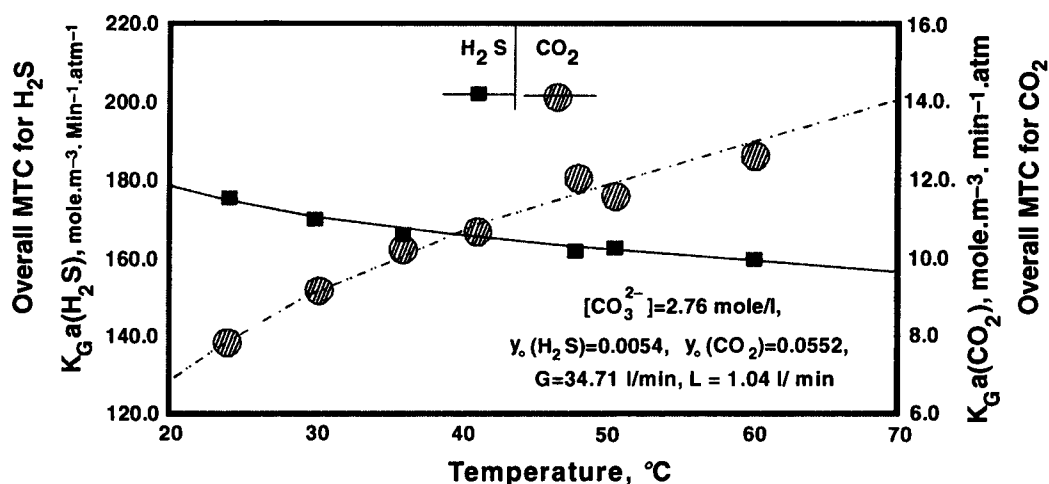
Fig. 8.2A.2. *Effect of Temperature on Overall MTC.*

Again the overall **MTC** for hydrogen sulfide absorption goes up with increasing concentration of **CO_3^{2-}** ions while that of **CO_2** decreases **(Fig. 8.2A.3)**.
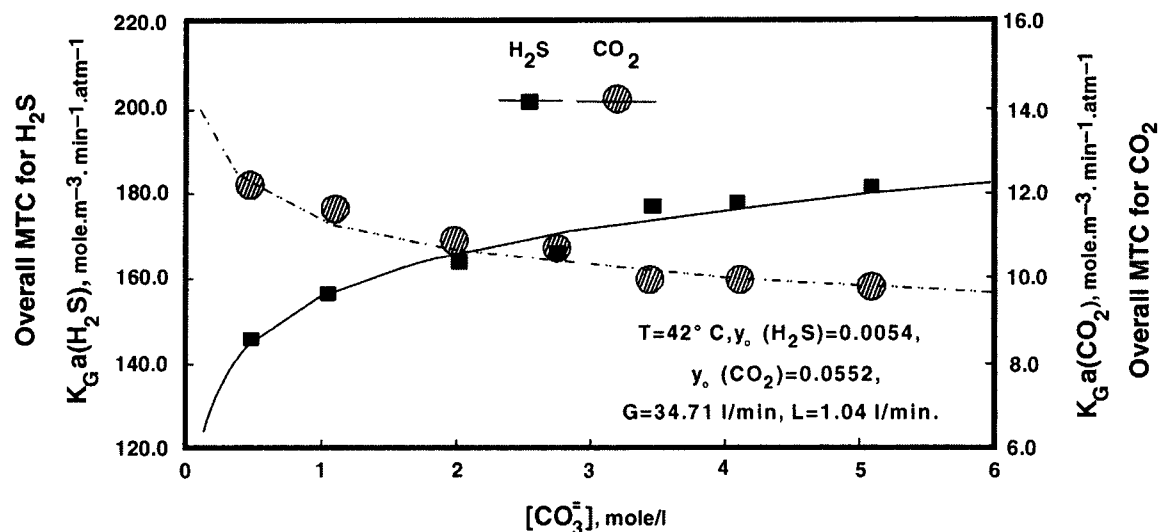
Fig. 8.2A.3. *Effect of Carbonate Concentration on the Overall MTC.*

The effect of feedgas **H₂S** and **CO₂** concentration at absorber inlet upon overall **MTCs** of H_2S and CO_2 are presented in **Fig. 8.2A.4** and **Fig. 8.2A.5.**
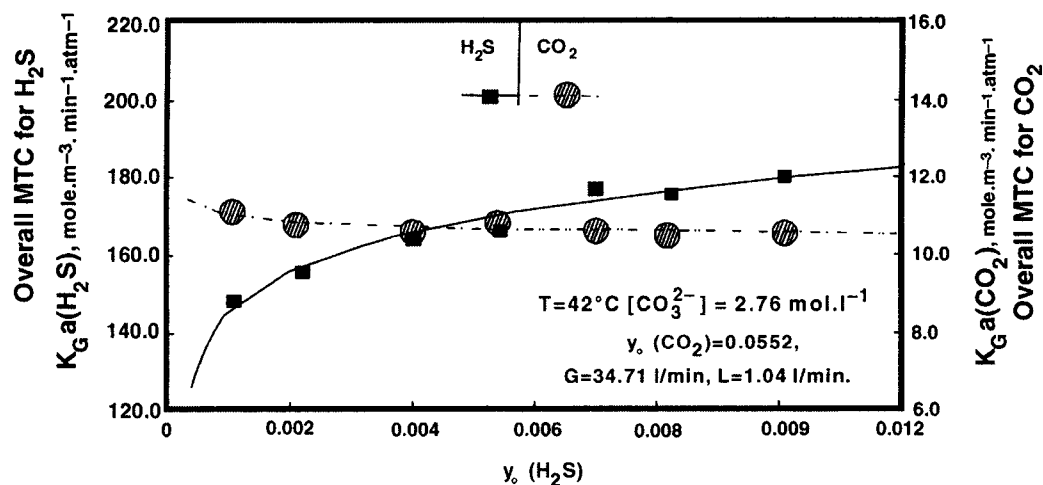
Fig. 8.2A.4. *Effect of H₂S inlet concentration on the Overall MTC.*
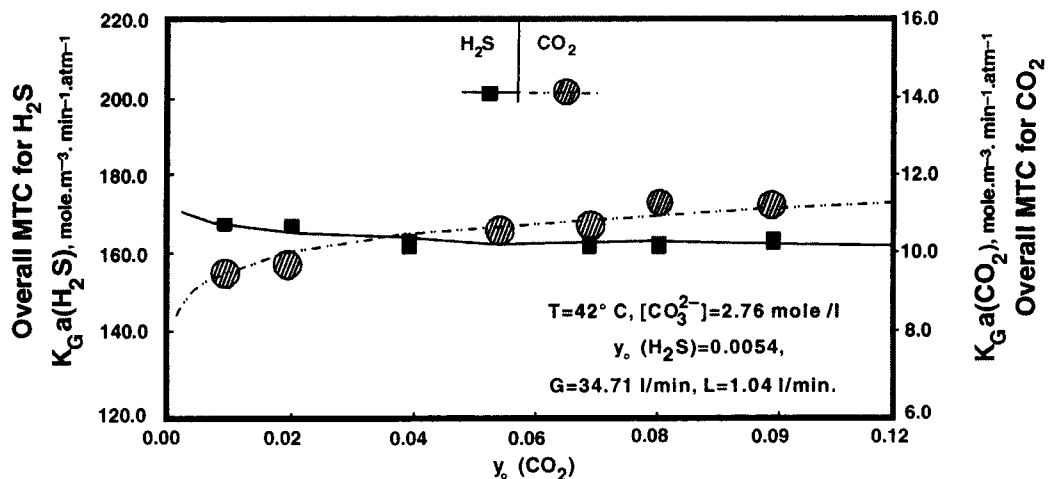
Fig. 8.2A.5. *Effect of CO₂ inlet concentration on the Overall MTC.*

From both figures it is evident that the overall MTCs of H_2S and CO_2 do not get much affected by the inlet concentration of respectively H_2S and CO_2. This is expected as long as the concentration of CO_3^{2-} and HCO_3^- do not change significantly as a result of the gas absorption.

However, the overall MTCs of both H_2S and CO_2 increase with increasing gas superficial velocity (Fig. 8.2A.6)
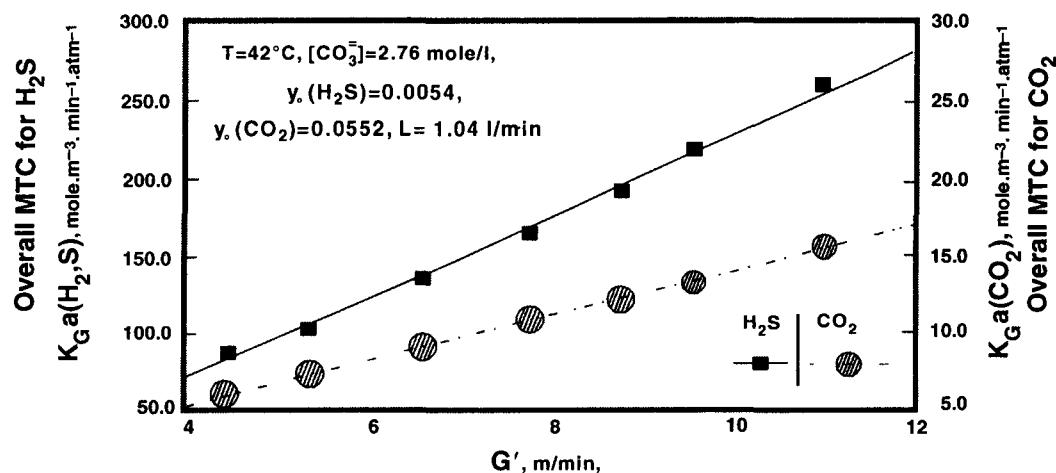
Fig. 8.2A.6. *Effect of Gas Velocity on the Overall MTC.*

Selectivity of H_2S Absorption

The selectivity of hydrogen sulfide absorption (S_0) by carbonate solutions is, as defined by Garner, *et. al.*, the ratio of overall MTC of H_2S to that of CO_2 :

$$S_0 = \frac{K_G \cdot a|_{H_2S}}{K_G \cdot a|_{CO_2}}$$

Fig. 8.2A.7 shows that the selectivity factor decreases with increasing the temperature. This is due to the fact that the rate of CO_2 absorption is increased while that of H_2S decreased with increasing temperature.
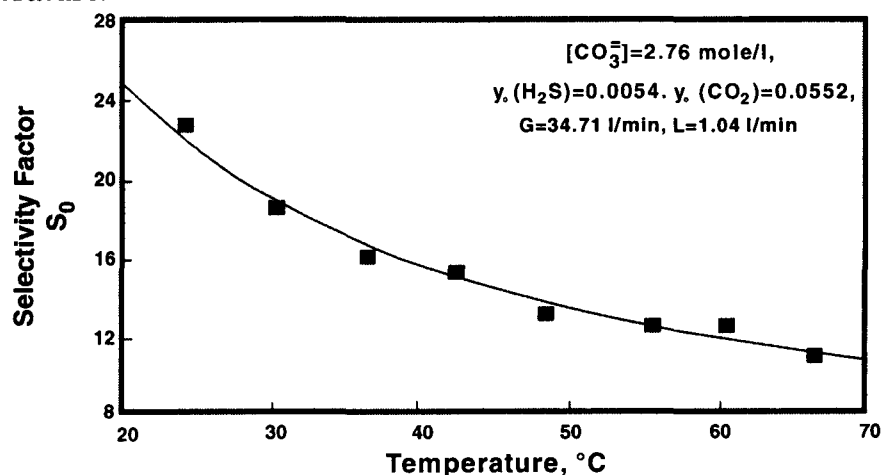
Fig. 8.2A.7. *Effect of Temperature on Selectivity Factor.*

Therefore, in order to improve the selectivity of hydrogen sulfide absorption lower operating temperatures are required.

The selectivity factor of H_2S increases somewhat with increasing concentration of CO_3^{2-} in the absorption solution **(Fig 8.2A.8)**.
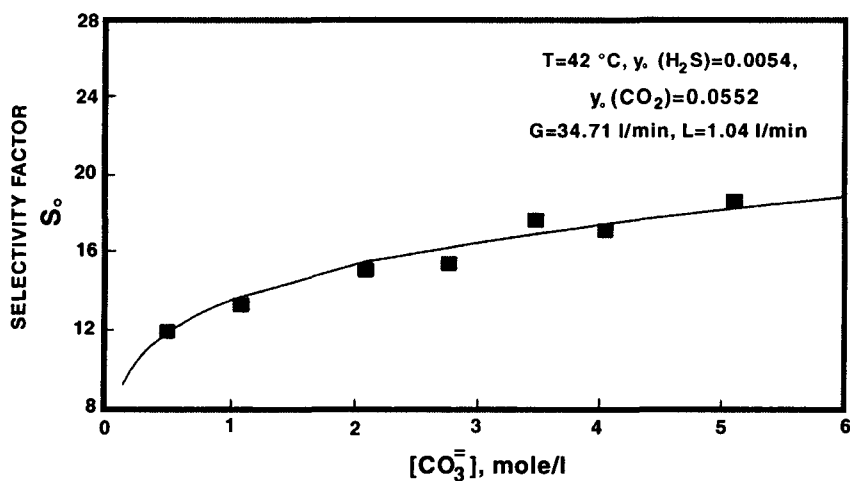
Fig. 8.2A.8. *Effect of Carbonate Concentration on the Selective Absorption of H_2S.*

And as expected, the selectivity factor changes very little with inlet hydrogen sulfide or carbon dioxide concentrations **(Fig. 8.2A.9** and **Fig. 8.2A.10)**
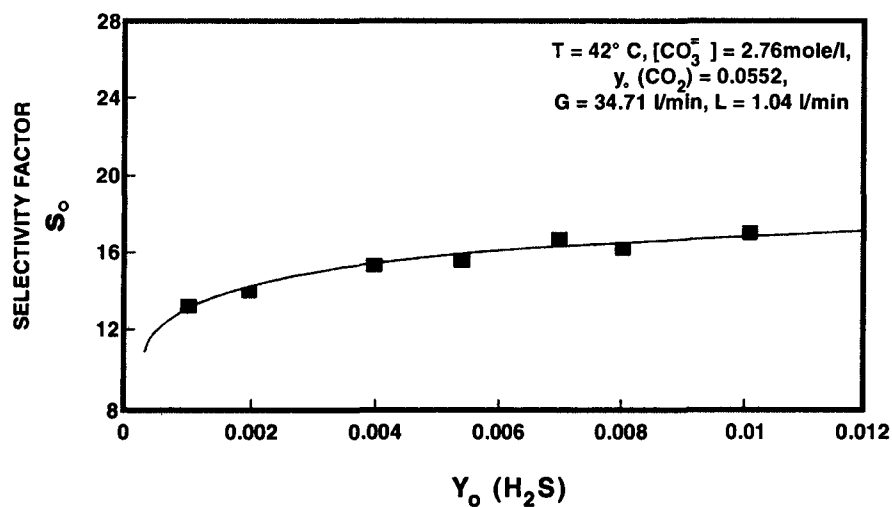
Fig. 8.2A.9. *Effect of H_2S concentration at absorber inlet on the Selectivity Factor.*
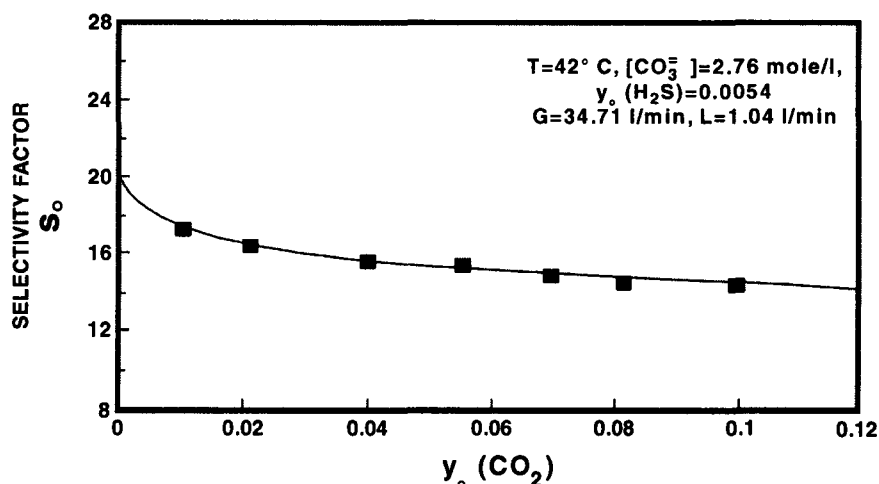
Fig. 8.2A.10. *Effect of* CO_2 *concentration at absorber inlet on the Selectivity Factor.*

Inasmuch as the overall MTCs for both H_2S and CO_2 increase with increasing gas superficial velocity, the selectivity factor S_o, increases only slightly with increasing gas velocity **(Fig. 8.2A.11).**
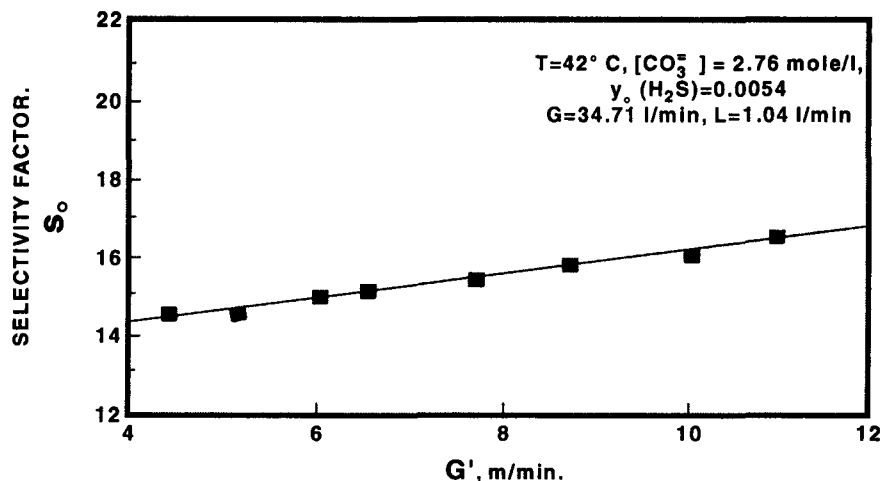
Fig. 8.2A.11. *Effect of Gas Velocity on the Selectivity Factor.*

However, the selectivity factor decreases with increasing liquid velocity **(Fig. 8.2A.12)**
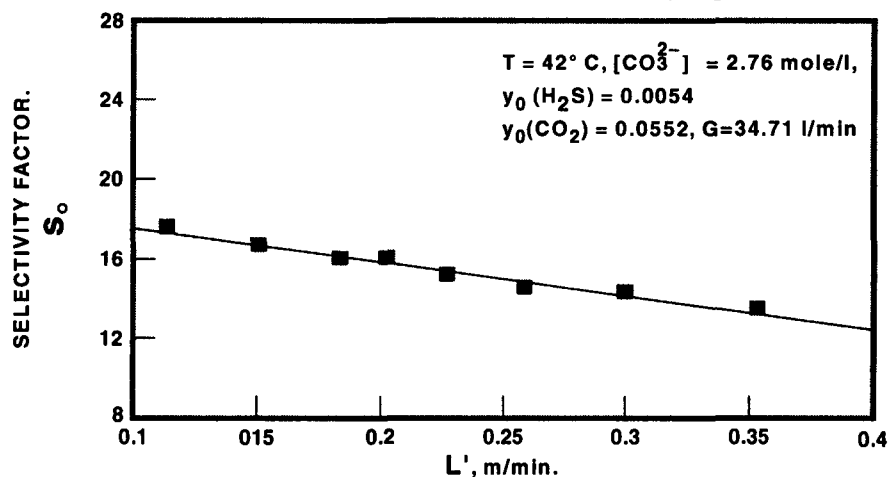
Fig. 8.2A.12. *Effect of Liquid Velocity on the Selectivity Factor.*

Conclusion

Therefore, the selective absorption of H_2S in aq. carbonate solution from a gas mixture containing a rich load of CO_2 can be enhanced under the following conditions :

- **low operating temperatures**

- **high carbonate (CO_3^{2-}) concentration**

- **high gas rate**

- **low liquid rate**

The removal efficiency of H_2S can be further improved by increasing the height of the packed bed and by increasing the gas/liq flowratio. The latter can be achieved by using a trickle bed mode and/or by increasing the size of the packing (hence higher voidage) to allow higher gas flowrates.

REFERENCES

1. K L Mai and A L Babb, *Industrial Engineering Chemistry (vol. 47/1955/P-1757).*

2. H Brenner, *Chemical Engineering Science (vol.17/1987/P-229).*

3. F Garner et.al., *Journal Of Applied Chemistry (May 1958/P-325).*

4. E Bendall, *AIChE Journal (vol. 29 (1)/1983/P-66).*

5. G Astarita and F Gioia, *Chemical Engineering Science (vol. 19/1964/P-963).*

6. MH Al-Wohoush et.al., *AIChE Symposium Series (No. 311/vol. 92/1996/P-106).*

8.3. SELECTIVE H_2S-ABSORPTION BY USING AQUEOUS AMMONIA SOLUTION

Selective absorption of H_2S from hydrocarbon gases containing CO_2 is important in many CPIs. Applications include gas processing, production of thioorganic compounds (viz. mercaptans), enriching Claus feedgas with H_2S to boost up S-recovery efficiency, prevention of SO_2 pollution, and heavy oil production.

Such selective extraction of H_2S leads to the processing of industrial gases having very wide range of compositions, pressures and temperatures. **Table 8.3.1** presents 5#s of typical gases treated on industrial scale thru selective H_2S absorption by using MDEA as the solvent.

Table 8.3.1. Typical Industrial Gases Subjected To Selective H_2S Extraction By MDEA Process.

	Raw Gas			Absorber Top	Treated Gas	Enriched Gas
No.	Total Press., P_{tot} (MPa)	P_{CO_2} (kPa)	P_{H_2S} (kPa)	Temp. (K)	Maximum H_2S Concentration (vpm)	Desired H_2S Concentration (%)
1.	0.115	43	72	310	3000	90
2.	0.12	22	0.3	348	250	indifferent
3.	0.12	103—88	17—32	313	500—1000	50—60
4.	0.8	160	240	313	100—1000	90
5.	8.0	16—160	0.08—0.25	287—293	2.5	indifferent

p refers to partial press of the component presented as its subscript.

Source : Hydrocarbon Processing, Aug. 1981/P-112

Selectivity for Hydrogen Sulfide

Selective removal of H_2S from CO_2 can be achieved by means of aqueous ammonia solution if short contact time is used (about 5s based on gas).

[Source : British Patent 520327 –by H. Bähr. 1940]

The difference in the rate of absorption of the two acid gases is based on the fact that hydrogen sulfide ionizes immediately to $\overline{S}H$ and $\overset{+}{H}$ ions, the latter react fast with the hydroxyl ions in the solution

$$H_2S \rightleftharpoons \overset{+}{H} + \overset{.}{S}H$$

$$\overset{+}{H} + \overset{.}{O}H \longrightarrow H_2O$$
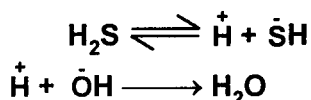
while carbon dioxide must first react with water, forming carbonic acid, before it can react ionically with ammonia

$$CO_2 + H_2O \rightleftharpoons H_2CO_3$$

$$H_2 + CO_3 \rightleftharpoons \overset{+}{H} + H\overset{.}{C}O_3$$

$$\overset{+}{N}H_4 + H\overset{.}{C}O_3 \rightleftharpoons NH_4HCO_3$$
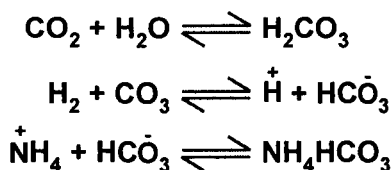
The rate of hydration of CO_2 is quite slow and that's why it is the controlling step of the overall reaction.

The selectivity is influenced by the method of contact between gas and liquid. When a mixture of H_2S and CO_2 is brought in contact with quiescent surface of dilute aq. ammonia soln (0.5–2%) 1 atm and room temperature, H_2S is found to dissolve twice as fast as CO_2. If the gases are absorbed by falling drop of ammonia solution of same dilution under identical conditions of pressure and temperature, the H_2S dissolves 85 times faster than the carbon dioxide. Experiments conducted on a typical coke-oven gas containing about 0.5% H_2S and 2% CO_2 showed that H_2S dissolved 17 times faster than CO_2 when the gas was contacted in a spray tower with an excess of dilute aq. ammonia at 294K.

[Source : *Gas-and-Wasserfach*—C.Eymann *vol. 89 (1/P-10/1948]*.
Brennstoff-Chem.—J.Bähr *[vol. 36 (9/10-129/1955]*.

The absorption of ammonia into water is quite rapid and it is essentially a gas-film controlled process. The rate of H_2S absorption in aq. ammonia solution is also rapid and depends on ammonia concentration. If an adequate ammonia is present at the inter-face, then of this absorption is governed by the gas-film resistance.

On the other hand, the absorption of CO_2 into water or weak alkaline solution is a typical liq-film CO_2, H_2S and ammonia is brought into contact with water, the ammonia and H_2S get absorbed much rapidly than CO_2. This differential absorption can be accentuated by operating under conditions which reduce gas-film resistance.

Absorption of CO_2 into water and dilute alkaline solutions largely depends on the physical solubility (which is not high), and more CO_2 cannot be absorbed until some molecules are removed from the interface by the hydration reaction. So the efficiency of CO_2 absorption is enhanced by the turbulence in the liquid film and by extended liq holdup (retention) time in the absorption zone. These conditions can be met in a tall, packed tower operating under relatively high liquid loading, or bubbling the gas thru a liquid-filled column.

H_2S and NH_3 absorption rates can be raised by inducing higher turbulence in the gas phase at the interface—a condition that requires a high relative velocity between gas and liquid streams. This can be accomplished by spraying water or dilute alkaline solution onto an upflowing gas stream than can be realized in gravity-flow devices. If maximum selectivity for H_2S is desired, use should be made of spray column in conjunction with relatively short contact-time.

Process Description

Under certain operating conditions, aqueous ammonia solutions absorb H_2S selectively from gas streams which also contain carbon dioxide.

However, selective H_2S-extraction processes do not result in complete elimination of H_2S. The degree of H_2S removal depends on several operating variables and it appears that H_2S elimination to the extent of 90% is the maximum limit that can be achieved economically.

[Note : Substantial quantity of HCN also gets removed in the selective absorber].

Selective H_2S removal processes operate without recycle of the wash liquor. The first two types of processes are usually integrated with the ammonia-removal system of a coke-oven gas. The ammonia content of the gas is almost entirely absorbed simultaneously with H_2S and thus serves as the active agent in the solution.

Selective H₂S-removal by Ammonia Solution without Recycle

The feedgas cooled in the gas cooler is contacted countercurrently in selective H_2S absorber
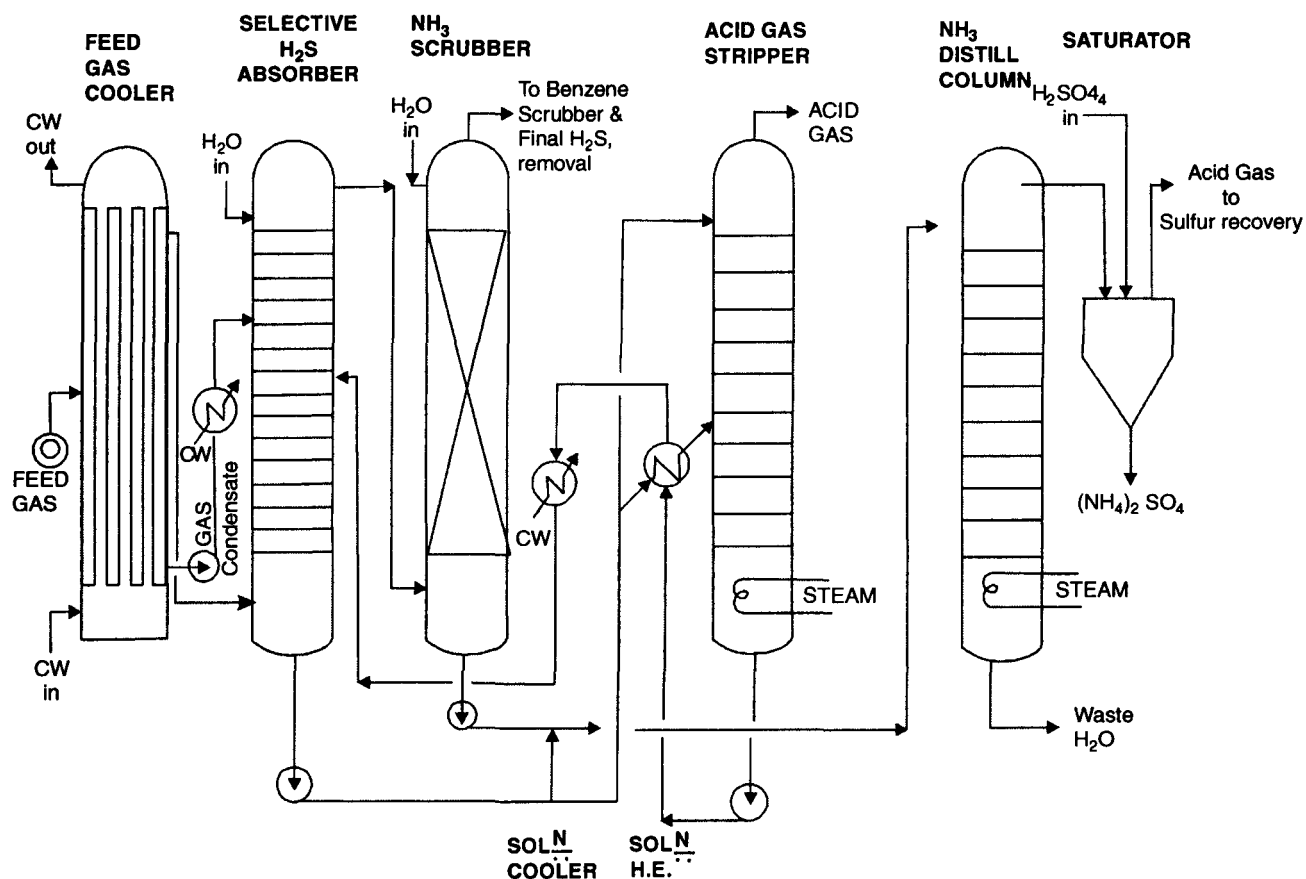
Fig. 8.3.1. *Typical Flow Diagram of a Selective Hydrogen Sulfide Removal Process without Solution Recycle.*

with water or a mixture of water and cooled gas condensate or recirculated, regenerated aq. ammonia solution **(Fig. 8.3.1)**

The absorber effluent together with **NH₃**-scrubber effluent is sent to ammonia distillation column to regenerate **NH₃**.

Insomuch as ammonia present in most coal gases is insufficient to remove more than 30—50% of the hydrogen sulfide, recycling of regenerated ammonia free from acid gas is necessary if more complete **H₂S** elimination is desired.

The overhead vapor from the ammonia distillation column is either converted to ammonium sulfate or condensed to strong ammonia liquor.

Selective H₂S-removal with Partial Solution Recycle

If partial liquid recycle is used, the rich ammonia solution that leaves the **H₂S**-absorber is fed to the acid gas stripper, after heat exchange with a portion of the stripped solutions **[Fig.8.3.2]**

The acid gases (**H₂S** and **CO₂**) are expelled from the solution by indirect heating with steam. A portion of the stripper effluent (acid-gas free solution) is recycled to the **H₂S**-absorber while the remainder is stripped of ammonia in **NH₃**-distillation column. The overhead vapors from this column, which is essentially ammonia, are recycled to the **H₂S**-absorber.
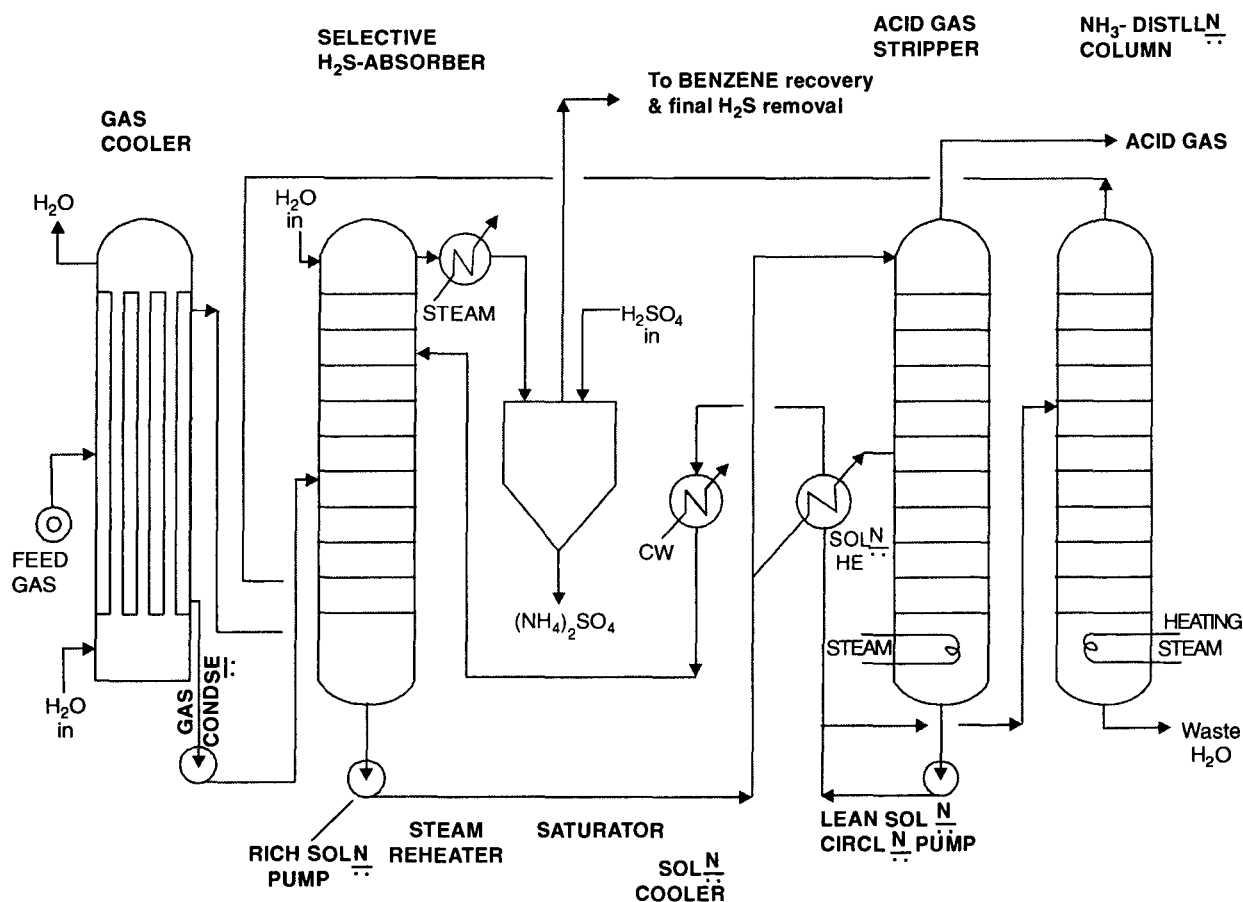
Fig. 8.3.2. *Typical Flow Diagram of Selective H₂S-removal process with Partial Solution Recycle.*

Selective H₂S-removal with Total Recycle

This process operates entirely independent of ammonia-recovery plant. The ammonia concentration in the wash liquor is maintained at such a level that the vapor pressure of ammonia over the solution is essentially the same as the partial pressure of ammonia in the gas with the effect that no ammonia is virtually removed from the gas in the **H₂S**-absorption. This mode of operation permits two completely separate **H₂S** and **NH₃**-removal systems.

A typical example of such a process is the Collin process which is presented schematically in **Fig. 8.3.3**
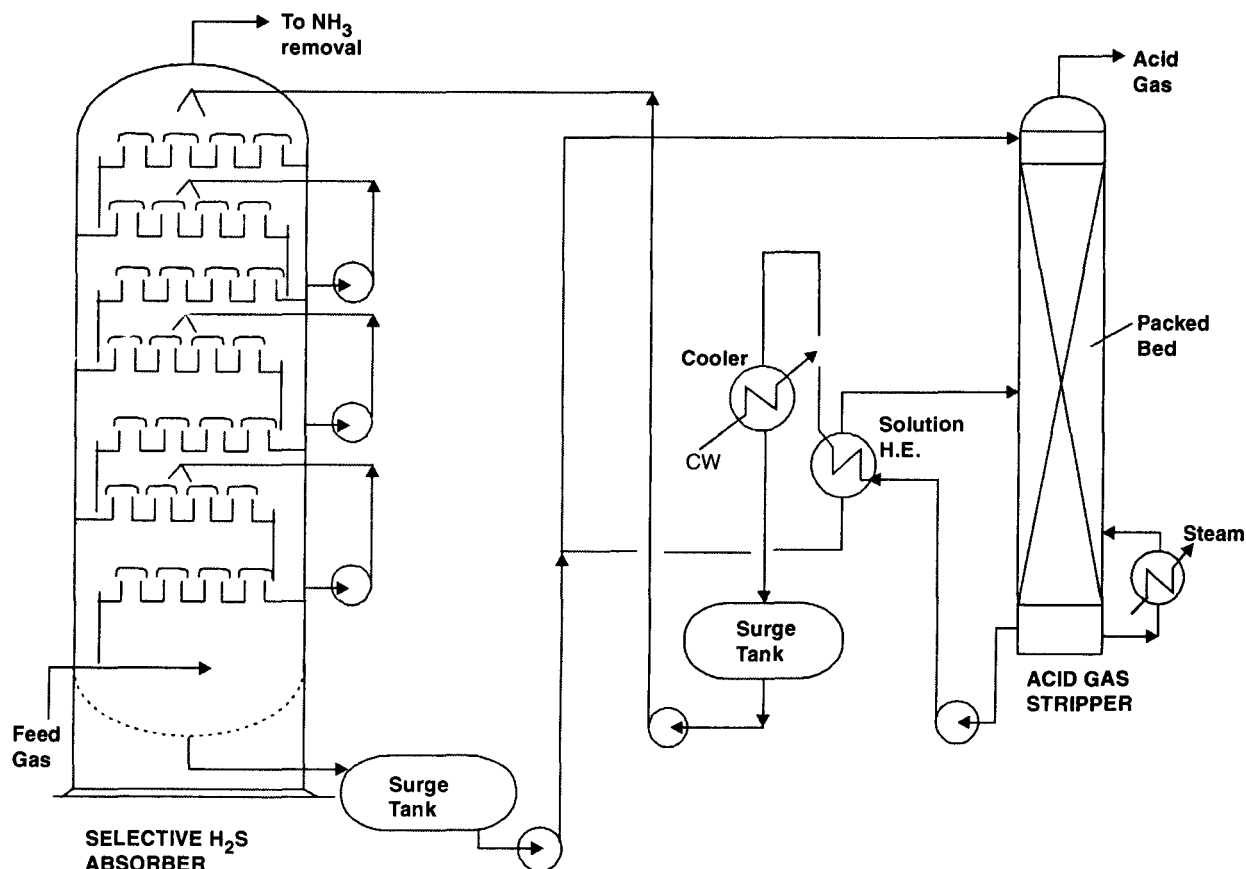
Fig. 8.3.3. *Selective Absorption of H₂S with Total Liquid Recycle (Collin Process).*

The feedgas is brought into countercurrent contact with wash liquor in **6-stage spraytower.** Solution is withdrawn from the bottom of each stage and pumped back to the top of the same stage where it is atomized thru small spray nozzles. The rich liquor from absorber bottom is fed to the acid gas stripper in two streams—one going to the top and the other to the middle via solution heat exchanger where it is preheated by heat exchange with the regenerated solution.

The upper section of the stripper column is fitted with bubblecap trays while ceramic packing is used in the lower section of the column. The solution is regenerated by indirect steam-heating in a reboiler and pumped back to the absorber via solution heat exchanger. The ammonia lost from the system is replaced by absorption of ammonia from the inlet gas.

Design

It is the mode of gas-liq contact that determines, by and large, the degree of selectivity for H_2S extraction from a mixture of gases. Hence the H_2S-absorber must be designed to ensure :

- **high relative gas and liq velocities so that contact time ≃ 5s based on the gas.**
- **intimate gas-liq contact**

Operating data with different types of columns are available in the open literature and may be used as guides to the design of selective H_2S absorbers. Operating data obtained with hurdle-packed, bubblecap and Kittel-tray columns in the treatment of typical coal gas are presented in **Table 8.3.2**

Table 8.3.2 Selective H_2S-Absorber Units Treating Coal-gas

Parameters	*Type of Column*		
	Dumped packed	*Bubblecap*	*Kittel-tray*
Feedgas Composition			
H_2S (mol%)	0.605	0.605	0.605
CO_2 (mol%)	2.73	2.73	2.73
NH_3 (mol%)	0.775	0.775	0.775
Absorber Effluent Composition			
H_2S (kg.m^{-3})	2.2	6.7	7.8
CO_2 (kg.m^{-3})	10.6	3.4	1.6
NH_3 (kg.m^{-3})	8.8	9.8	9.4
H_2S absorbed (% of Inlet)	16	42.5	52.5
CO_2 absorbed (% of Inlet)	13.1	3.7	1.8
Outlet Liquid (mol H_2S/mol CO_2)	0.27	2.5	6.25
Absorber Dia (mm) (mol H_2S/mol CO_2)	3200	3200	3200
Absorber Height (m)	30	6	5.5
Operating Press. (kPa)	112	112	112
Superficial Gas Velocity (m.s^{-1}) [Empty col. gas velocity]	0.64	0.64	1.61
Gas-Liq Contact Time (s) [based on gas]	47.5	6	3.5
Gas rate (MM^3.h^{-1})	18037	18037	18037

These data clearly show the superiority of Kittel-tray columns and bubblecap columns over the packed columns, so far as selective absorption of H_2S is concerned.

However, the H_2S removal is incomplete. This is due to low mol-ratio of NH_3 to H_2S in the feedgas. H_2S removal can be boosted up to as much as 70% to 80% if NH_3 :H_2S mole ratio is raised to

2. Somewhat better removal-up to 90%- is achievable with a large excess of available ammonia (**NH₃ : H₂S :: 4:1** mol ratio).

Bähr reported that as many as eight bubblecap trays and 15 Kittel-trays were just enough to extract maximum amount of **H₂S** removal. The selectivity does not change appreciably with the number of trays. This is mainly due to the fact that the bulk of the **NH₃** gets removed in the lower portion of the column and any additional tray at the top are not supplied with an active solution (**NH₃ + H₂O**) for absorption.

Bubblecap column is the second best, (Kittel-tray column being the best one) in achieving highest selective removal of **H₂S**. However, the degree of **H₂S** removal in bubblecap column is relatively unaffected by increasing gas velocity from **0.26 m.s⁻¹** to **0.60 m.s⁻¹**. It is primarily determined by the ammonia content of the feedgas.

One typical Kittel-tray absorber (**1930 mm dia** and **6 m high**) sporting 16 double trays produced as high as **10:1** mole ratio **H₂S : CO₂** in the absorber effluent while treating 21520 m³.h⁻¹ of coal gas (**H₂S – 0.63 mol%** ; **NH₃ – 0.71 mol%**) with fresh water without solution recycle. **H₂S** to the extent of 54% was removed indicating extremely high selectivity (CO₂ in feedgas was present in the range 2—3 mol%).

[Source : *Brennstoff-Chem.* – J. Bähr vol. 36 (9/10)/P:129/1955].

Bayerlein observed good result in selective absorption of **H₂S** in spray tower fitted with 6 stages, each 3 m high, and handling 11043 m³.h⁻¹ of coal gas (**NH₃ : 0.53 mol%** and **H₂S : 0.53 mol%**) using fresh water as wash liquid in once-thru process. The data obtained are presented in **Table 8.3.3** while the gradual enrichment of tower liquid with **H₂S, NH₃, CO₂** and **HCN** thru successive stages is shown graphically in **Fig. 8.3.4**.

Table 8.3.3 Operating Data of 6-Stage Spray Tower

Tower Characteristics	*Stages*	
	1 to 3	*4 to 6*
Feedgas Composition		
H₂S (mol%)	0.53	
CO₂ (mol%)	0.53	
NH₃ (mol%)	0.08	
Outlet Gas Composition		
H₂S (mol%)	0.32	
NH₃ (mol%)	0.003	
HCN (mol%)	0.04	
Column dia (mm)	1600	2362
Number of Stages	3	3
Height of each stage (m)	3	3
Feedgas rate (m³.h⁻¹)	11043	11043
Solution Composition	6.3	
(1st stage) (H₂S : CO₂ mol ratio)		
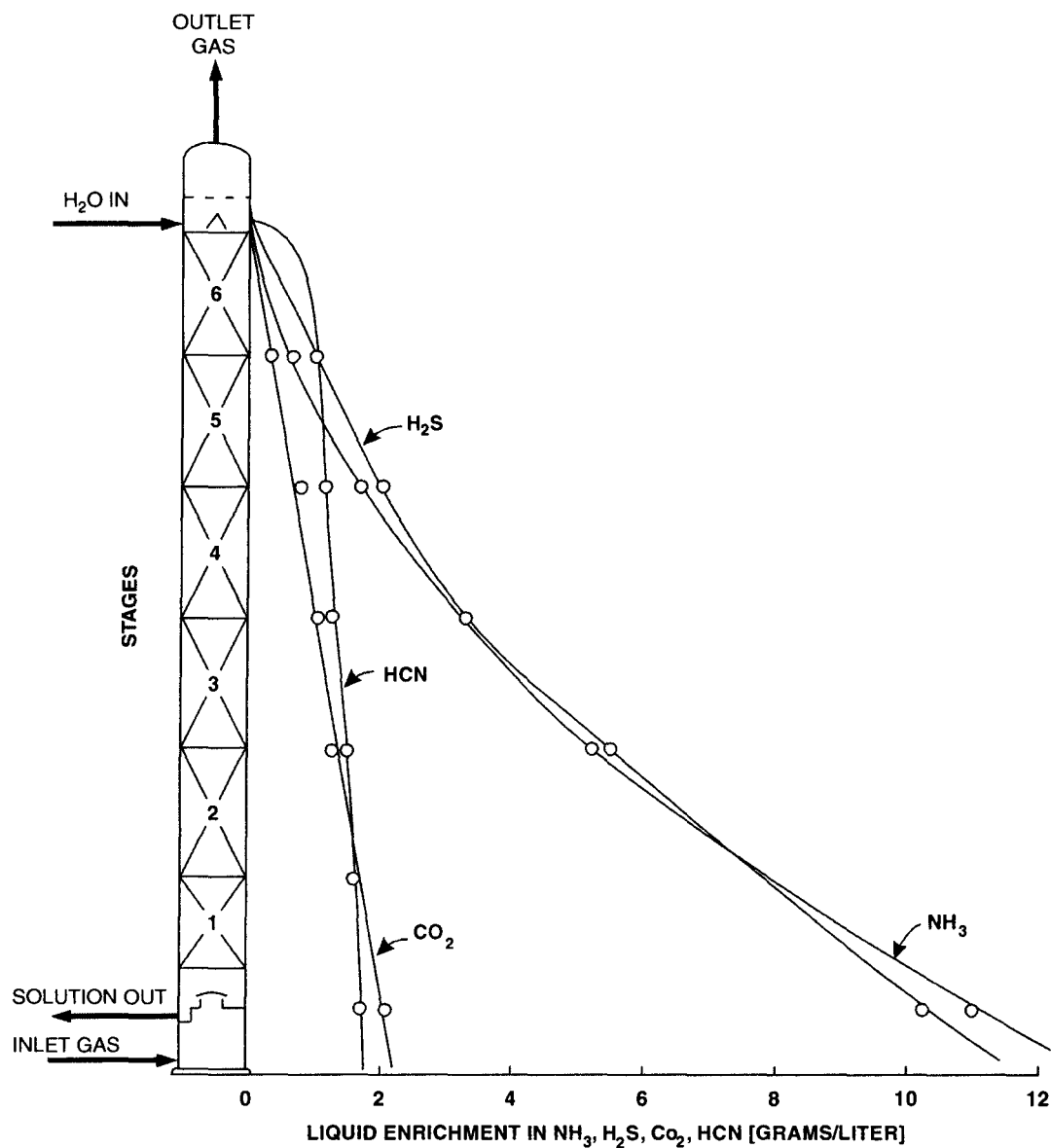
Fig. 8.3.4. *Change in liquid composition down the 6-stage absorption tower.*

Operating parameters of a typical selective H_2S-absorption process operating on total recycle is presented in the following **Table 8.3.4.**

Table 8.3.4 Typical Operating Data of Selective H_2S-Absorber Operating on Total Recycle.

Gas rate $(m^3.h^{-1})$	31856
Gas temperature (K)	294
Inlet Gas Composition	
$\quad H_2S$,	
$\quad NH_3$	

Exit Gas Composition
    H_2S

Acid Gas Composition (%)	
H_2S	74 – 77
CO_2	12 – 14
HCN	6 – 9
NH_3	0.4 – 0.5
H_2S Removal (%)	78
Liquid Rate	
Liquid Temperature (K)	**297**
Inlet Liquid Composition (kg.m⁻³)	
NH_3	11.7
H_2S	1.0
Outlet Liquid Composition (kg.m⁻³)	
H_2S	7.2

8.4. LOW-TEMPERATURE ACID GAS REMOVAL (AGR)

Acid Gas Removal (AGR) refers to the separation of hydrogen sulfide and carbon dioxide from gas mixtures. The major application of AGR are :

1. treating NG containing sulfurous compounds (H_2S, COS, CS_2, RSH) and carbon dioxide.

2. treating shift gases resulting from coal conversion.

3. treating synthesis gas made by partial oxidation of sulfur-contaminated feedstocks, *e.g.*, gasoline production from coal via Syn Gas (Fischers-Tropsch Process).

4. acid gas removal in hydrogen production from coal.

5. treating synthesis gas made from methane and steam (*e.g.*, production of ammonia, hydrogen, and oxo-compounds).

In fact, acid gas removal is a key step in the upgrading of natural gas and syn gas made from natural gas, coal or petroleum.

The Consolidated Natural Gas Research Company, Cleveland, Ohio, USA has developed a low-temp, energy-efficient AGR process, known as **CNG process** that removes sulfurous compounds, trace contaminants, and gas streams (MP and HP). The process features

I. absorption of sulfurous compounds and trace contaminants with pure liq CO_2.

II. regeneration of pure carbon dioxide by triple–point crystallization.

III. absorption of CO_2 with a slurry of organic liquid containing solid carbon dioxide.

The **CNG process** operates at a temperature of 193K and medium to high pressure (2 –15 MPa) gas mixtures containing substantial quantities of carbon dioxide.

Motivation for Alternative AGR Technology

There are two major types of acid gas removal processes :

I. Chemisorption

II. Physical Absorption

Typical chemisorption agents are amines, hot potassium arsenate, potassium carbonate. Typical physical absorbents are cold methanol (**Rectisol Process**), dimethyl ether of tetraethylene glycol (**Selexol Process**). While chemisorption is favored at low acid gas partial pressure (< 1400 kPa), physical absorption becomes the most favored option at acid gas partial press > 1400kPa. Existing **AGR** processes were developed in response to the needs of petroleum and natural-gas industries where crude gas mixtures are relatively well defined. But they fare badly to cleanse raw gas mixtures resulting from coal gasification. Because the raw gas obtained from coal gasifier contains a much higher load of carbon dioxide, a much higher ratio of CO_2 : H_2S plus many other trace contaminants result.

The **AGR** system to be compatible with coal gasification in the **syn fuels** manufacture must ensure:

1. separation of acid gases and trace contaminants from the crude gas.

2. separation of highly purified CO_2 from the hydrogen sulfide plus trace contaminants.

Capital and energy cost estimated for **AGR** in synfuels production are high because processing and environment requirements demand that these separations be sharp. In fact **AGR** plant is costlier than coal gasification plant or methanation unit.

Existing physical **AGR** processes are relatively energy inefficient for application in coal gasification. They consume substantial quantities of steam or stripping agent to regenerate the lean solvent into the **AGR** absorber. The raw gas from coal gasifier contains substantial qty of CO_2 and the potential amount of work, available by expansion of separated CO_2 from its partial pressure of 700–2100 kPa to atmospheric pressure, is not recovered in existing **AGR** processes.

The raw gas from gasifier contains high ratios of CO_2 : H_2S and this poses particular difficulties to conventional **AGR** processes to produce a sulfurous stream in sufficient concentration for conversion to elemental sulfur in a Claus plant. A Claus feed of 40% H_2S or greater is most desirable. Existing **AGR** processes treating coal gasifier gases typically produce an acid gas stream containing **25% H_2S** or less.

The raw gas resulting from coal gasification contains a much higher load of CO_2 than what is obtained from crude gas obtained from petroleum and natural gas. Separation of pure carbon dioxide for by-product use or for rejection to the atmosphere (environmental regulations restrict total **sulfur limit to 200 – 250 ppm** and **H_2S limit to 10 ppm**) is difficult to achieve with existing **AGR** processes.

Besides, there are many trace contaminant gases (**COS, RSH, CS_2, NH_3, HCN,** and **aliphatic and aromatic hydrocarbons**) in the raw gases coming from coal gasification plant. Existing **AGR** processes have difficulty removing all these trace downstream processing and carbon dioxide venting. They also face potential technical and economic problems in solvent recovery and regeneration, e.g., solvent (viz. method) loss with treated or vent gases, and increased nitrogen or steam stripping for effective removal of contaminants.

Goals for AGR Process Development

Any **AGR** process to be best fitted for gas cleaning in the production of synfuels from coal must target the following goals :

- **Low energy consumption**
- **Low capital cost**
- **Higher recovery (≥ 40%) of H_2S for sulfur recovery in Claus plant**
- **Pure CO_2 byproduct**
- **Environment friendly (pure CO_2 vent gas)**
- **Removal and rejection of trace contaminants**
- **Non-corrosive with ordinary MOC**

Process Description of CNG-AGR Process

The acid gas removal process developed by Consolidated Natural Gas Research Co. sports three unique features that differentiate with the existing **AGR** technologies :

I. use of pure liq carbon dioxide as absorbent for sulfurous compounds

II. use of triple-point crystallization to separate pure carbon dioxide from sulfurous compounds

III. use of a liq-acid slurry of saturated solution of CO_2 and an organic solvent containing suspended solid CO_2 particles to absorb carbon dioxide below the triple point temperature of carbon dioxide.

Pure liq CO_2 is a very effective absorbent for sulfurous compounds and trace contaminants.

Triple point crystallization of CO_2 (–56.6°C/5.1 atm at which solid, liq and vap phases of carbon dioxide can exist at equilibrium, **Fig. 8.4.1)** economically produces pure carbon dioxide and concentrated hydrogen sulfide.
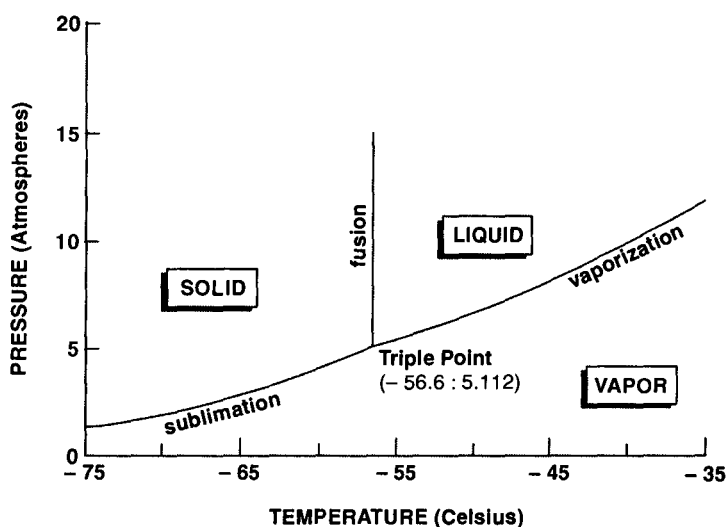
Fig. 8.4.1 *Carbon dioxide phase diagram.*

As far as bulk CO_2-absorption is concerned, the slurry absorbent (organic solvent) diminishes absorbent flow and restricts the rise of temperature of CO_2–absorber to an acceptable low value.

The sequence of gas treatment is shown in **Fig. 8.4.2.**
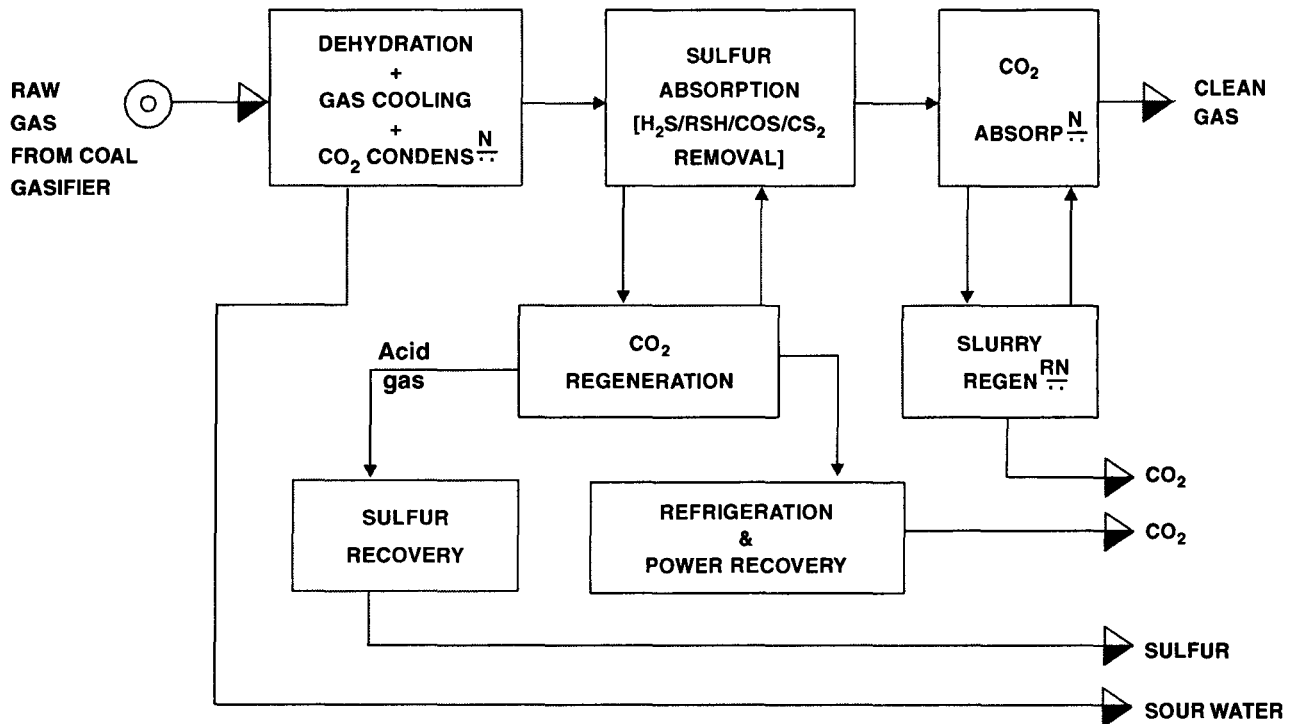
Fig. 8.4.2. *Schematic presentation of CNG process.*

Precooling

This is a water-removal step. The raw gas **(RG)** is cooled and the residual water vapor is removed to prevent subsequent icing.

If the **RG** is relatively free of C_2+ hydrocarbons, regenerable molecular sieve can be used to eliminate water. Otherwise, water is removed by solvent washing (e.g. dimethyl formamide) with dry solvent regenerated by distillation.

The water-free **RG** is further cooled to its CO_2 dewpoint by countercurrent heat exchange with return clean gas and separated carbon dioxide.

The dewpoint of the gas depends on the gas pressure and CO_2 partial pressure. At fixed CO_2 composition, the dewpoint is lowered as total pressure decreases while at fixed total pressure, the dewpoint is lowered as CO_2 composition decreases. **Fig. 8.4.3** shows variations of calculated dewpoints for synthesis gas (with 30 mol% carbon dioxide) for pressure up to 10.5 MPa.
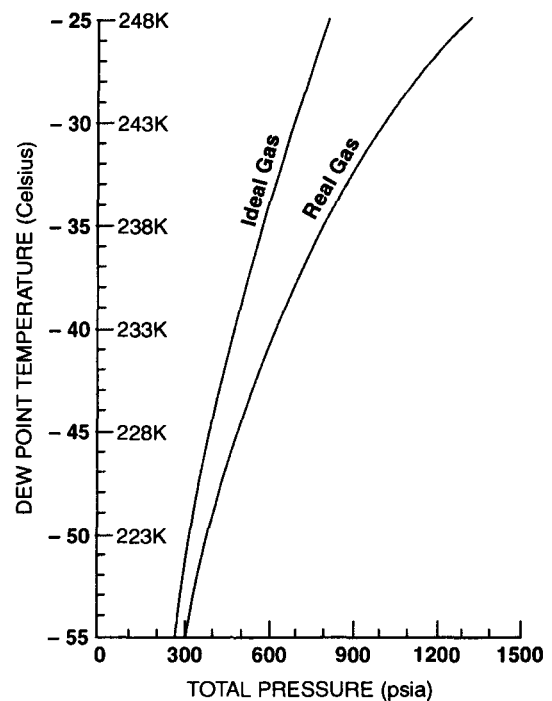
Fig. 8.4.3. *Dewpoint vs. Pressure, syn gas with 30 mol% CO_2.*

The dewpoint must be warmer than 216.4K (–56.6°C) to permit the use of liq CO_2 absorbent inasmuch as pure liq CO_2 cannot exist below the triple point. Shown in **Fig. 8.4.4** are variations of partial pressures of CO_2 with total pressure of syngas.
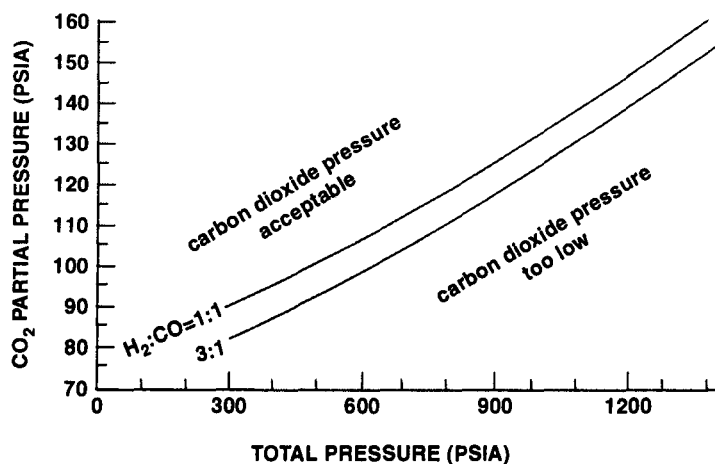
Fig. 8.4.4. *CO_2-Partial pressure vs. total pressure.*

Increasing the H_2 : CO ratio at any fixed total pressure decreases the CO_2-partial pressure required for 216.4K dewpoint. Liq carbon dioxide can be used to absorb sulfur molecules for any combination of gas pressure and CO_2-partial pressures which lies above the curves of **Fig. 8.4.4.**

Carbon Dioxide Condensation and Sulfurous Compound Absorption

From its dewpoint the **RG** is cooled to about 218K (–55°C) whereupon carbon dioxide is condensed out. The condensate is contaminated with sulfurous compounds. About 65% of CO_2 content of RG [With **30 mol% CO_2/7 MPa/243K (–30°C) dp**] condenses to a liq upon cooling to 243K.

Note : Removal of CO_2 by condensation is preferred over absorption because it is more reversible and hence more energy efficient and less capital intensive.

The gas at 218K (–55°C) is scrubbed with pure liq carbon dioxide to cleanse sulfurous compounds and remaining trace contaminants. Liq CO_2 has very good absorbing capacity for sulfurous compounds. It absorbs.**COS** more effectively than it absorbs H_2S. Thus, an absorber designed to remove H_2S using liq CO_2 absorbent will also remove **COS** and all other less volatile sulfurous compounds in the gas.

Note : The opposite is true concerning **COS** for both cold methanol (**Rectisol**) and dimethyl ether of polyethylene glycol (**Selexol**).

Besides, the physical properties of liq CO_2 is also favorable to promote high stage-efficiency :

• *its viscosity is low :* 0.35 cP at 218K (–55°C). [In comparison, methanol is 7 to 8 times more viscous over the temperature range of 273K (0°C) to 218K (–55°C). The **Selexol** solvent's viscosity is 5 to 10 cP around room temperature].

• *its density is high :* 1170 kg. m^{-3} at 218K (–55°C) which is higher than most absorbents.

$$\left\{ \begin{array}{l} \rho_{CH_3OH} : 850 \, kg.m^{-3} \text{ at } 233 \text{ K } (-40°C) \\ \rho_{selexol \; solvent} : 1030 \, kg.m^{-3} \text{ at room temp} \end{array} \right\}$$

This high density and low viscosity permit high liq and gas rates in the absorption tower.

Carbon dioxide has low mol. wt. of 44 compared to **Selexol** solvent's mol. wt. of over 200. Low molecular weight favours high gas solubility per unit volume of solvent.

Table 8.4.1 summarizes physical properties for methanol, **Selexol** solvent and liq CO_2 for comparison.

Table 8.4.1. Three Typical Absorbents and their physical Properties

Solvent	Mol. Wt.	Density/Temp. (kg. m⁻³/°C)	Viscosity, µ/Temp. (cP/ °C)	BP (°C)	FP (°C)
Liq CO_2	44	1170/−55	0.35/−55	− 78.5	− 56.6
Methanol	32	850/−40	1.8/−40	64.8	− 97.5
Selexol solvent	200	1030	6/+ 25	—	− 20 to − 30

The liq carbon dioxide used as absorbent of sulfurous compounds and other trace impurities is not purchased; it comes from the raw gas being processed.

The treated gas, containing less than 1 ppm H_2S, leaves the sulfur absorber at essentially 218K (− 55°C) with CO_2 as the only significant impurity yet to be removed.

Carbon Dioxide Regeneration by Triple Point Crystallization

Liquid carbon dioxide containing sulfurous and various other trace compounds is subjected to crystallization to yield pure solid carbon dioxide which does not form solid solutions with any of the trace contaminants likely to be absorbed by liq CO_2 in the absorber. Therefore, the CNG process sharply rejects trace contaminants with the H_2S-rich acid gas stream.

The crystallization process employed is direct-contact **triplepoint crystallization** with vapor compression. This is a continuous separation that operates at pressure and temperature near the triplepoint of carbon dioxide such that vapor liq and solid phases of CO_2 co-exist [See **Fig. 8.4.2**]. The liquid is flashed whereupon solid carbon dioxide is formed. Solid CO_2 melts by direct contact with condensing CO_2 vapor. No heat exchange surfaces are required to transfer the latent heat involved. CO_2 crystals form at pressure slightly below the triplepoint while crystal melting occurs at pressure slightly above the triplepoint. Carbon dioxide vapor is compressed from the crystal formation pressure to the crystal melting pressure (**Fig. 8.45**).
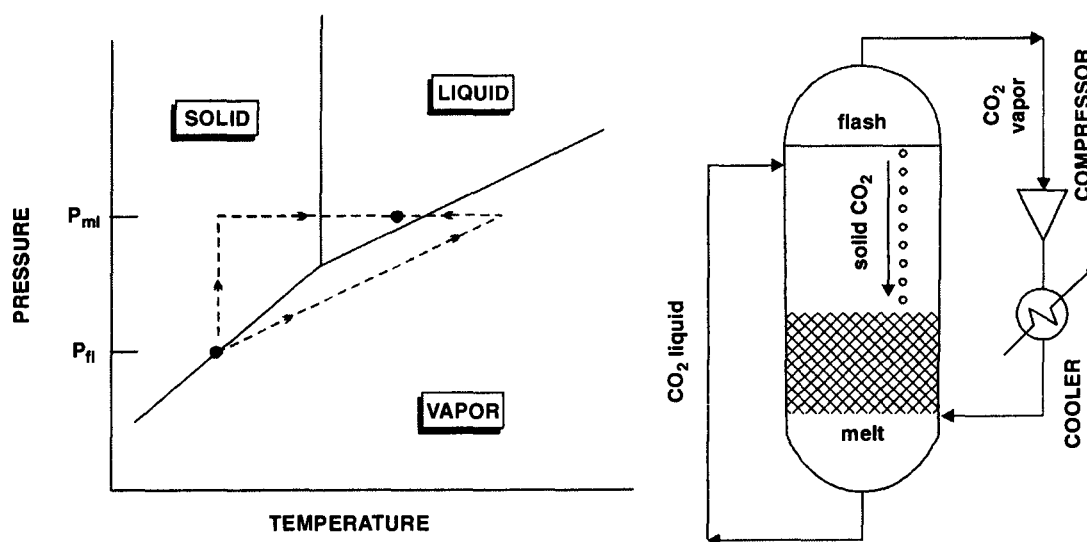
Fig. 8.4.5. *Triplepoint crystallization of carbon dioxide.*

Pure carbon dioxide solid precipitated by triplepoint crystallization is split into two streams:

— one is absorbent stream which is recycled to the absorber.

— other is used up as product or vented to the atmosphere after refrigeration and power recovery.

The amount of excess liq CO_2 generated by triplepoint crystallization can be substantial. For instance, a syn gas (7 MPa) with 30 mol% CO_2 yields, when subjected to triplepoint crystallization, nearly 40% of the total carbon dioxide as pure liq CO_2 for refrigeration and power recovery.

The other product of triplepoint crystallization is an acid gas stream rich in H_2S. This is sent to Claus plant for sulfur recovery after refrigeration recovery.

The triplepoint crystallizer operates in closed cycle. The **adiabatic flash pressure, P_{fp}** maintained slightly below the triplepoint pressure causes the liquid to spontaneously vaporize and solidify. The solid : liq ratio is determined by the heats of fusion and vaporization. For carbon dioxide it is 1.7, i.e., 1.7 moles of CO_2 solidify per mole of liq CO_2 evaporates. The solid being denser than the liq, drops thru the liquid and form a loosely packed crystal bed at the bottom. The liq head (3 –4 m) is enough to raise the hydrostatic pressure on the solid to the melter pressure, P_{ml}. The crystal bed depth is about 0.6 m.

In actual operation, a small backwash flow is maintained upward to wash out crystals off the bed and prevent mother liquor from penetrating into the bed.

The vapor is withdrawn from the flashzone, compressed to the melter pressure (P_{ml}), sensibly cooled to near saturation, and dispersed under the solid bed where it condenses and causes solid CO_2 to melt. The liq is withdrawn and pumped to the flashzone.

A dramatic concentration change of sulfurous compounds occurs between the mother liquor in the flashzone and the liq product in the meltzone. The

Fig. 8.4.6. *Concentration profile of sulfurous compounds and contaminants in liq CO_2 in triplepoint crystallizer.*

mother liquor concentration at bedtop and liquid product concentration at bedbottom are relatively uniform, but a sharp drop in concentration (of the order of 500 to 5000) of sulfurous compounds and trace contaminants occurs across the bed (**Fig. 8.4.6**).

Final Carbon Dioxide Removal

Carbon dioxide content of the purified gas (after removal of sulfurous compounds and trace components) at 218K (–55°C) is treated with slurry absorbent.

The slurry absorbent is a saturated sol^n of organic solvent and carbon dioxide containing suspended particles of solid CO_2. The difference in partial pressure of CO_2 in the feedgas and that in

the regenerated slurry absorbent, is considerable and this provides the driving force for carbon dioxide absorption.

CO_2 absorption is an exothermic process and the released heat supplies the latent heat for melting of the solid CO_2. The direct refrigeration provided by the melting of solid CO_2 moderates the appreciable solvent temperature rise normally associated with bulk CO_2 absorption.

The liq-solid slurry absorbent possesses large effective heat capacity and that enables relatively small slurry flows to absorb the carbon dioxide heat of condensation with only modest rise in temperature. Small slurry absorbent flows permit smaller absorption tower dia as operating vapor velocities generally increase with reduce liquid loading.

[**Note** : In contrast, the solvent flow in other AGR processes, is considerably larger and that requires larger dia tower].

The CO_2-rich solvent exits the absorber at about 218K (–55°C) and is stripped off. It is then cooled by external refrigeration and flashed in stages at successively lower pressures to generate a cold slurry of liq solvent and solid CO_2.

The carbon dioxide flashgas is recycled back thru the process for refrigeration and power recovery, and thereafter delivered as a product stream or vented to the atmosphere. The regenerated slurry absorbent is recirculated to the CO_2-absorber.

[**Note** : Compared to the other sub-ambient temperature CO_2 removal processes, the CNG process requires less refrigeration because absorption of CO_2 with slurry and the regeneration of the latter by flashing require small temperature and pressure driving forces.]

Note : The solubility of solid CO_2 in several solvents is shown in **Fig. 8.4.7.**

MOL % CARBON DIOXIDE, LIQUID PHASE
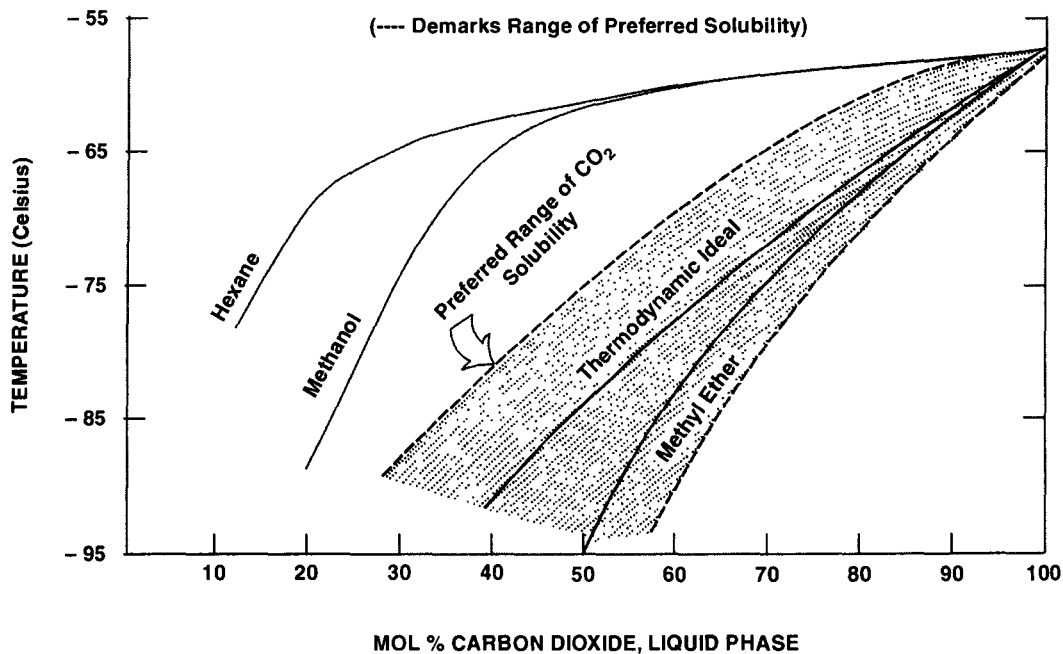
Fig. 8.4.7. *Solubility of solid carbon dioxide in selected solvents.*

The preferred range of CO_2 solubility is also shown. Belonged to this preferred solubility range are ethers and ketones *e.g.*

(1) Di-*n*-butyl ether

(2) Methyl ethyl ketone

These solvent

— exhibit relatively linear change in solubility with temperature

— have low viscosity when saturated with CO_2

— have low vapor pressures

— have low melting points

Note : CO_2 removal by slurry absorption is an attractive scheme down to 198K (−75°C) which can be easily achieved by slurry regeneration at slightly above 1 atm. CO_2 pressure. With a 198K (−75°C) exit gas temperature, slurry absorption reduces the CO_2 content of a 7 MPa syn gas stream from about 13 mol% to about 4 mol% — a 70% reduction.

REFERENCES

1. K G Christensen and W J Stupin, *Hydrocarbon Processing (Feb. 1978/P–125)*

2. D K Beavon *et.al.*, **Claus Processing of Novel Acid Gas Streams** (Symposium On Sulfur Recovery and Utilization, American Chemical Society, Atlanta Meeting March 29 — April 3, 1981)

3. R W Rosseau *et.al.*, **Evaluation of Methanol as a Solvent for Acid Gas Removal in Coal Gasification Processes** (Symposium On Gas Purification, AIChE Spring National Meeting, Houston, Texas, April 1981).

4. R E Hise *et.al.*, **A Low-Temperature Energy-Efficient Acid Gas Removal Process** (ACS Symposium Series 223 / Washington D.C., 1983).

8.5. SULFURIC ACID MANUFACTURE

Process Principle Sulfur trioxide upon absorption by the water content of 98% sulfuric acid produces oleum which is diluted by dosing polished water to produce 98% H_2SO_4 which is recirculated to the absorption tower.

In a sulfur-burning plant, the hot gas stream entering the SO_3-absorber contains 8 to 10 mol% of SO_3 which is to be absorbed almost completely so that exit gas contains 30 – 40 mol ppm SO_3. The absorbent is 98% H_2SO_4 which is sprayed from the top onto a packed bed of ceramic packed bed of ceramic packings while the feedgas moves up thru the bed coming in contact with acid-film spread over the packing surface. *The absorption of SO_3 is an exothermic process.* The liberated heat as well as the sensible heat of the feedgas are taken care of by the feed acid that enters the column at 350K to 355K and leaves the column 10 K to 15 K hotter.

Design SO_3 is highly soluble in 98% sulfuric acid and that renders the process almost a pure gas-film-controlled absorption. Thus an increase in gas flowrate at constant gas composition will hike up the mols of SO_3 to be absorbed in direct proportion. By increasing the flowrate but maintaining **L/G ratio** constant, the overall mass transfer coefficient will go up even at faster rate than the qty of SO_3 to be absorbed.

The first step of design of the absorber is to select the tower dia so that exit gas stream velocity

is not so high as to entrain liquid sulfuric acid out of the column. In the 1950s, sulfuric acid plant utilized some of the largest dia packed towers. Column dias up to **9m** were common for both drying tower and the SO_3 absorber. However, since mid 1960s, with the advent of new tower packing and advanced design procedures, column dias seldom approach this size in modern units.

The design ΔP at the bottom of the absorber commonly ranges from 21 to 25 mm H_2O per m of packed depth. This pressure drop may double up over at period of 9—10 yrs. of operation due to accumulation of sulfation products in the packed bed.

To avoid bed plugging from packing degradation products, larger size (50mm or 75mm) ceramic packing is normally specified.

The combined effect of modern tower packings, improved packing support systems and efficient liquid distributor designs has made it possible to raise the superficial gas velocity almost two-fold from designs common in the late 1950s.

The driving force for mass transfer, in the design of absorber, is the difference between the partial pressure of SO_3 over the sulfuric acid. The overall mass transfer coefficient are very high, in the order of **90 kmol.h^{-1}m^{-2}. atm^{-1}** for ceramic **Intalox saddles** at a liquid rate of **18 m^3.m^{-2}.h^{-1}**. This high K_G.a value indicates that there is very little liq-film resistance.

8.6. ABSORPTION WITH CHEMICAL REACTION

Many an absorption process of great industrial importance involves chemical reaction the solute and a component present in the liquid phase, of course, the solute must get dissolved into the liquid phase first, and then it enters into a chemical reaction. The driving force is the potential for the chemical reaction between the solute (*i.e.*, the component to be absorbed) and one or more component (s) of the liquid mixture. The absorbed component thus forms part of a new compound (s) in the liquid. In the majority cases, a fugacity gradient also plays a role, however.

Chemical absorption is either reversible or irreversible. The reversible reactions permit the resultant solution to be regenerated so that the regenerated solvent can be recycled and the solute is recovered in concentrated form. For instance H_2S or CO_2 can be absorbed into ethanolamines (**MEA** or **DEA**). Both of these solutions are alkaline and combine chemically with one-half mole of acid gas per mol of amine. And it is possible to regenerate the rich amine solution by stripping the heated solvent.

Again there are some absorption reactions which are irreversible. Absorption of NH_3 into dilute acids and the absorption of CO_2 into alkaline hydroxides are two good examples. The absorption process leads to the formation of a stable chemical compound to which the solute is so lightly bonded that there is no appreciable vapor pressure of the solute above the liq phase. Under these circumstances, regeneration of the solute is not possible and the active component* in the liquid gets consumed.

The overall mass transfer coefficient is

$$K_G.a = \frac{y_i G_i - y_o G_o}{A.Z.\Delta p_{lm}}$$

where, Δp_{lm} is the logarithmic mean partial pressure driving force.

---

* that enters into chemical reaction with the solute

$$\Delta p_{lm} = \frac{P(y_i - y_o)}{\ln(y_i/y_o)}$$

where, P = total system pressure, kPa

     Δp_{lm} = log-mean-partial pressure difference, kPa

     y_i = mol fraction of the solute in the inlet gas

     y_o = mol fraction of solute in the outlet gas

     A = column cross-sectional area, m^2

     Z = packed depth, m

     $K_G \cdot a$ = overall gas-phase mtc, $kmol.h^{-1}.m^{-3}.kPa^{-1}$

     G_i = inlet gas-flow, $kmol.h^{-1}$

     G_o = outlet gas-flow $kmol.h^{-1}$

8.6.1 H$_2$S-MDEA System

Selective extraction of H_2S from hydrocarbon gases containing CO_2 by using methydiethylamine (**MDEA**) has been successfully developed by Elf-Aquitaine, France. And the results have been proved to be satisfactory offering economic advantages over the approaches.

Techniques : There are only two ways available for separating H_2S from CO_2 :

1. **Harnessing thermodynamic properties of certain compounds that absorb preferentially more H$_2$S than CO$_2$**

2. **Using reactions with differential reaction rate between acid gases and a chemical reactant**

Physical solvent route presents too many disadvantages when natural gas is treated. Solvents can be used economically only if partial pressure of acidic components are relatively large. Moreover, due to simultaneous absorption of part of the hydrocarbons, a portion of hydrocarbon gases gets lost and their recovery leads to process complicacy. Moreover, physical solvent are expensive. Also they are not easily available always. Their vapor pressure being considerable, large solvent loss is incurred.

Reaction Mechanism A secondary amine reacts with H_2S to produce amine hydrosulfide

$$R_2NH + H_2S \rightleftharpoons \left(\begin{array}{c} R \\ | \\ R-N-H \\ | \\ H \end{array}\right)^{\oplus} (SH)^{\ominus} \qquad \ldots(1)$$
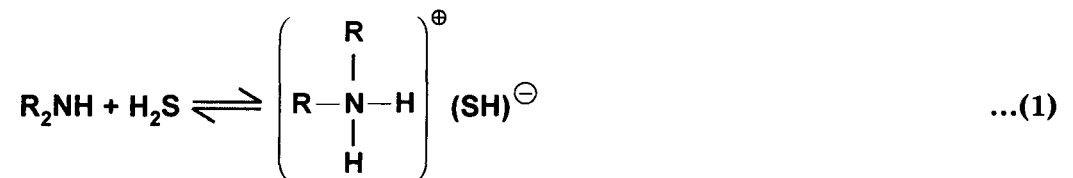
R represents alkyl group viz. **Me, Et,** *iso*-**Prop** ...etc.

On the other hand CO_2 also reacts with secondary amine, but only slowly, to form the amine carbonate

$$2R_2NH + CO_2 \rightleftharpoons \left(\begin{array}{c} R \\ | \\ R-N-C-\bar{O} \\ || \\ O \end{array}\right)\left(\begin{array}{c} R \\ | \\ R-N-H \\ | \\ H \end{array}\right)^{+} \qquad \ldots(2)$$
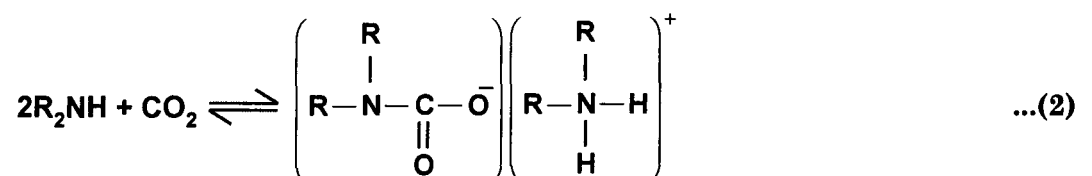
Carbon dioxide also reacts with water or hydroxyl ions,

$$CO_2 + H_2S \rightleftharpoons H_2CO_3 \qquad ...(3)$$

$$CO_2 + \dot{O}H \rightleftharpoons HC\dot{O}_3 \qquad ...(4)$$

which again react with the amine to yield amine bicarbonate and amine carbonate

$$R_2NH + H_2CO_3 \rightleftharpoons \left(R - \underset{\underset{H}{|}}{\overset{\overset{R}{|}}{N}} - H \right)^+ (HCO_3)^- \qquad ...(5)$$

$$R_2NH + HC\dot{O}_3 \rightleftharpoons \left(R - \underset{\underset{H}{|}}{\overset{\overset{R}{|}}{N}} - H \right)^+_2 (CO_3)^{2-} \qquad ...(6)$$
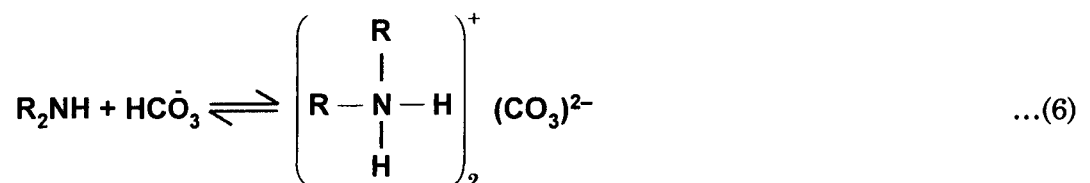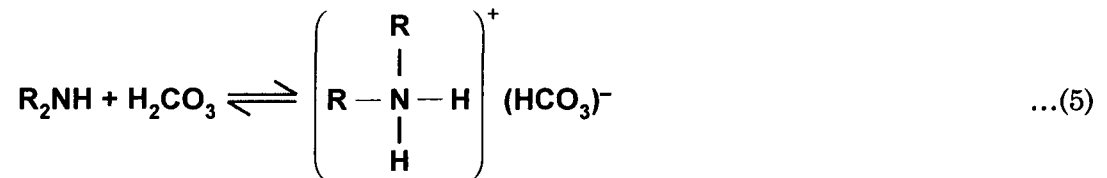
 # Reaction 1 : rate is very high

 # Reaction 2 : rate is moderate

 # Reactions 5 & 6 : rates are slow; largely controlled by reactions **3 & 4**

MDEA is a tertiary amine which reacts directly with H_2S but not with CO_2 as it lacks replaceable hydrogen :

$$R_3N + H_2S \rightleftharpoons \left(R - \underset{\underset{R}{|}}{\overset{\overset{R}{|}}{N}} - H \right)^{\oplus} (SH)^{\ominus} \qquad ...(7)$$

For CO_2 to react with tertiary amine (a base), it must go into the soln first to produce acid

$$H_2CO_3 + R_3N \rightleftharpoons \left(R - \underset{\underset{R}{|}}{\overset{\overset{R}{|}}{N}} - H \right)^{\oplus} (HCO_3)^{\ominus} \qquad ...(6)$$
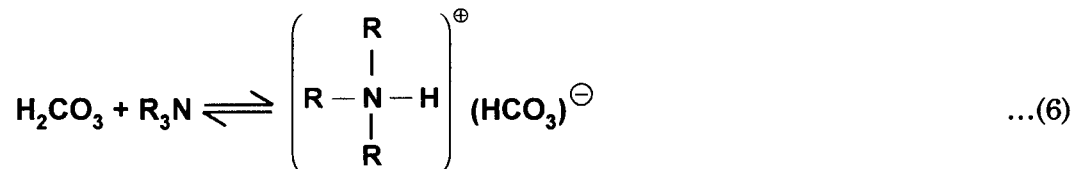
Since rates of reactions **3** and **4** are extremely low, the rate differential between reaction **7** and **8** becomes markedly pronounced and that forms the very basis of selective absorption of H_2S by **MDEA** from a gas stream containing CO_2.

The absorber should be so designed to permit gas-liq contact time large enough to remove H_2S but sufficiently short in order to retain CO_2 only partially.

MDEA advantages

Among all industrially available tertiary amines, the **MDEA** is the best choice considering :

- its pronounced selectivity between H_2S and CO_2
- its H_2S absorption capacity
- its ease of regeneration which depends on pK
- its low vapor pressure and other physical and chemical constants

Laboratory and pilot plant data attest to the fact that **TEA** (triethanolamine), **MDEA** and **DEEA** (diethylethanolamine) have the same selectivity for H_2S compared to CO_2. But because of bulk effect of diethyl group, the regeneration of **TEA** and **DEEA** presents difficulty. Over and above, **DEEA** and **TEA** exhibit larger vapor pressure that renders their industrial use for selective H_2S absorption impossible.

MDEA is a moderately strong base whose H_2S-selectivity was demonstrated by Frazier and Kohl.

[Source : *Industrial Engineering Chemistry (vol. 42/No. 11/P-2288/1950)* – H.D. Frazier and A.H. Kohl].

Design Equation Gas selective desulfurization is carried out by countercurrent scrubbing in a tray column using sieve trays, valve trays and bubblcap trays. Tower dia ranges between 760mm and 2750mm.

The number of absorber plates must be accurately determined to set the gas liq contact time to an optimum value that will render almost all H_2S and only a limited amount of CO_2 absorbed.

The total mass transferred per unit time from the main body of gas phase :

$$dN = k_g.\, a.dV.(p - p_i) = k_l.a\lambda.dV.(c_i - c)$$

where, $(p - p_i)$, the driving force at any point, is the difference between the partial pressure of solute of the main-body gas phase and that in the gas-film at the interface.

N = mass amount transferred from the gas phase to the liquid phase per unit time

a = interfacial are per unit volume of froth

V = froth volume

λ = enhancement factor due to liquid-phase chemical reaction

i.e.,
$$dN = \frac{1}{\dfrac{1}{k_g} + \dfrac{H}{\lambda k_l}} \cdot adV.\,(p - p^*)$$

where, p^* = partial pressure of the component in equilibrium with its concentration c in the liquid

$\quad\quad = H.c$

H = Henry's Law constant

Integrating above differential equation on a finite volume of froth leads to the expression of mass transfer local efficiency

$$E_o = 1 - \exp\left[-\frac{1}{\dfrac{1}{k_g} + \dfrac{H}{\lambda k_l}} \cdot a.\tau_g.zRT \right]$$

where, E_o = gas phase efficiency

$\quad\quad \tau_g$ = gas residence time in froth

$$\lambda = \left[1 + \frac{\mathcal{D}.k_2.B^o}{k_1^2} \right]^{\frac{1}{2}} \text{ for pseudo first order reaction.}$$

$\mathcal{D}$ = diffusivity of the component dissolved in the liquid phase

k_2 = 2nd-order reaction rate constant

B^o = reactant concentration

Industrial Experience In the Lacq Plant, France all gases from condensates and rich amine flashdrums, (averaging H_2S and CO_2 content **30%** and **20%** by volume) were treated with **DEA** under **800kPa** to produce treated gas used as fuel. The acid gas produced by **DEA** scrubbing contained H_2S 60% by volume being used as a raw material for thio-organic synthesis.

The capacity of the thio-organic units boosted up without modification following replacement of **DEA** by **MDEA** producing an H_2S enriched gas containing about **90% H_2S**.

Initially the absorber was equipped with bubblecap trays treating 0.4 $\text{MNm}^3.\text{day}^{-1}$ of fuel gas. Following laboratory simulations, the bubblecap trays were replaced by special sieve trays resulting in H_2S content of the enriched gas as high as **88%**.

Additional Advantages of MDEA

■ **Regeneration :** It takes less energy to regenerate **MDEA** than to regenerate other amines used for total deacidification of gases because :

■ low CO_2 loadings due to high selectivity for H_2S

■ heats of reactions for H_2S/MDEA and especially CO_2/MDEA are lower than with other amines (MEA, DIPA, DEA)

■ MDEA separations need relatively low reflux ratios

■ **Corrosion :** Detailed laboratory studies and field test data have demonstrated that corrosion rates of carbon steels are extremely low, about **0.04 mm per year** in the worse cases. This expressly excludes the need for any corrosion inhibitor.

■ **Degradation :** Most of the secondary amines, viz., **DEA**, upon degradation lead to the formation of heavier amines like diethanolpiperazine (**DEP**) and trihydroxyethylethylene diamine (**THEED**) because of secondary H-atom available for replacement. **MDEA**, a tertiary amine, cannot give this type of polymerization.

This explains why no reports has so far been made to show any **MDEA** degradation products in solutions, having been used for several years in industrial units.

■ **Foaming :** No foaming problem has been reported from any operating unit using **MDEA** process

■ **Economics :** Operating costs of **MDEA** process are compared to those of **SNPA-DEA** process in the following **Table 8.3.5**

Table 8.3.5 Comparative Costs of the MDEA and DEA Process for Fuel Gas Treatment

Raw Gas	*MDEA Process*	*DEA Process*
1. Flow rate ($\text{Nm}^3.\text{h}^{-1}$)	14000	14000
2. Pressure MPa	0.8	0.8

Contd.,

Raw Gas	MDEA Process	DEA Process
3. Composition (vol%)		
H_2S	30	30
CO_2	20	20
CH_4	50	50
Treated Gas		
Composition (vol%)		
H_2S	< 0.05	< 0.01
CO_2	20	0.5
Utilities		
LP Steam $(t.h^{-1})$	15	21
Electricity (kWh)	40	70
Chemicals consumption $(t.y^{-1})$	4	7

Source : *Hydrocarbon Processing, August 1980 /P-116.*

MDEA process requires far lesser number of absorber trays. The liquid flowrate is also smaller. Consequently, sizes of amine-amine H.E.s, regenerator and pump are reduced. Finally, the low CO_2 absorption brings about size reduction of reboilers and water condensers.

8.7. CO_2/H_2S-ABSORPTION BY AMINE

Many gases *viz.* Natural Gas, refinery gas, synthesis gas (*e.g*, **EO-Process,** Ammonia Production), coke oven gas and off-gas contain H_2S and/or CO_2. A number of solvents are used to remove these acid components. Alkanolamines are mostly the favored ones. Belonged to this groups are :

- monoethanolamine (**MEA**)
- diethanolamine (**DEA**)
- diglycolamine (**DGA**)
- diisopropanolamine (**DIPA**)
- triethanolamine (**TEA**)
- methyldiethanolamine (**MDEA**)

The solutions of alkanolamines are alkaline and chemically combine with $\frac{1}{2}$ mol of acid-gas per mol of amine.

Selectivity Inasmuch as H_2S reacts rapidly with all alkanolamines, its absorption rate is controlled largely by mass transfer consideration. CO_2-absorption on the other hand, is often liq-film controlled and governed by slower rates of reaction. Solvent selectivity for H_2S occurs as a result of these different absorption rates and is most pronounced for tertiary and sterically-hindered alkanolamines.

Primary & Secondary Amines

$$\begin{matrix} R_1 \\ \diagdown \\ R_2 \diagup \end{matrix} N{-}H + CO_2 \underset{k_{-2}}{\overset{k_2}{\rightleftharpoons}} \begin{matrix} R_1 \\ \diagdown \\ R_2 \diagup \end{matrix} \overset{+}{N} \begin{matrix} H \\ \diagup \\ \diagdown \\ COO^- \end{matrix} \qquad \text{[fast]}$$

$$\underset{R_2}{\overset{R_1}{>}}\!\!\overset{+}{N}\!\!\underset{COO^-}{\overset{H}{<}} \ + \ \underset{R_2}{\overset{R_1}{>}}\!\!NH \ \xrightarrow{k_b} \ \underset{R_2}{\overset{R_1}{>}}\!\!N\!\!-\!\!COO^- \ + \ \underset{R_2}{\overset{R_1}{>}}\!\!\overset{+}{N}\!\!\overset{H}{\underset{H}{<}}$$ [slow]

$$\underset{R_2}{\overset{R_1}{>}}\!\!N\!\!-\!\!COO^- \ + \ H_2O \ \xrightarrow{\ Hydrolysis\ } \ \underset{R_2}{\overset{R_1}{>}}\!\!N\!\!-\!\!H \ + \ HCO_3^-$$ [slow]

$$\underset{R_2}{\overset{R_1}{>}}\!\!N\!\!-\!\!H \ + \ S\overset{H}{\underset{H}{<}} \ \longrightarrow \ \underset{R_2}{\overset{R_1}{>}}\!\!\overset{+}{N}\!\!\overset{H}{\underset{H}{<}} \ + \ \overline{S}H$$ [very fast]

Tertiary Amines

$$\underset{R_2}{\overset{R_1}{>}}\!\!N\!\!-\!\!R_3 \ + \ CO_2 \ \longrightarrow \ \text{No reaction}$$

$$\underset{R_2}{\overset{R_1}{>}}\!\!N\!\!-\!\!R_3 \ + \ CO_2 \ + \ H_2O \ \xrightarrow{k_2} \ \underset{R_2}{\overset{R_1}{>}}\!\!\overset{\oplus}{N}\!\!\overset{R_3}{\underset{H}{<}} \ + \ HCO_3^-$$ [slow]

$$\underset{R_2}{\overset{R_1}{>}}\!\!N\!\!-\!\!R_3 \ + \ H_2S \ \longrightarrow \ \underset{R_2}{\overset{R_1}{>}}\!\!\overset{+}{N}\!\!\overset{R_3}{\underset{H}{<}} \ + \ \overline{S}H$$ [very fast]
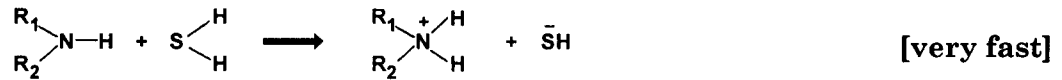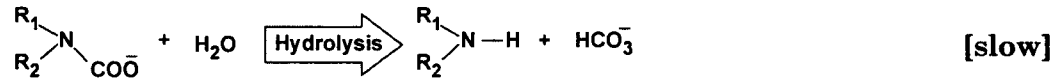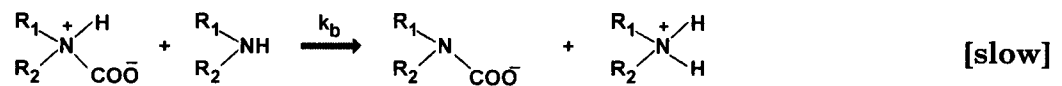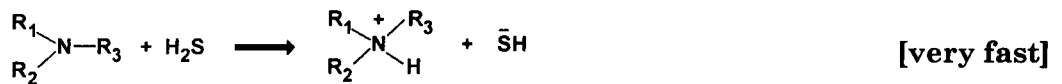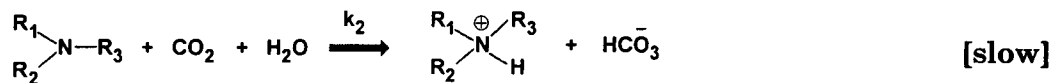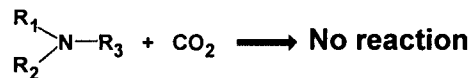
Mass Transfer Assuming the absorption process is accomplished thru three fundamental physical operations

- **the liquid is well mixed**
- **the vapor phase is mixed between the stages**
- **the vapor phase passes thru the liquid in plugflow**

a differential material balance can be drawn to relate the vap and liq flowrates to the efficiency

$$\frac{dY}{dZ} = \left[K_G \cdot a \cdot A \cdot P(KX - Y) - Y\frac{dV}{dZ} \right] \Big/ \left[V_{j+1} + Z\frac{dV}{dZ} \right]$$

The overall gas-phase *mtc* K_G is calculated by using the Whitman *two-resistance theory* :

$$\frac{1}{K_G} = \frac{1}{k_G} + \frac{H}{I \cdot k_L^\circ}$$

where $\ \ k_G$ = gas phase mtc

k_L° = liq phase mtc in absence of chemical reaction

H = Henry's Law constant for physical solubility

I = enhancement factor

This enhancement factor, I, accounts for the increase in the liq-phase mtc due to the chemical reactions taking place between the acid gas components and the alkanolamine in the liq phase. For **H₂S**, the enhancement factor is the function of molecular diffusion coefficient, $\mathcal{D}$ and the species concentration due to obvious reason — **H₂S** reacts instantaneously with the alkanolamine:

$$I_{H_2S} = 1 + \frac{\left(\mathcal{D}_{R_1R_2R_3N} / \mathcal{D}_{H_2S}\right)\left[R_1R_2R_3N\right]}{\left(\mathcal{D}_{H_2S} / \mathcal{D}_{R_1R_2R_3N}\right)\left[H_2S_i\right]}$$

where, [ ] refers to concentration of the component within it.

In the case of CO_2, the enhancement factor is a function of chemical reaction rates and the regime of mass transfer. The overall reaction rate constant, $k_{o,v}$

$$k_{o,v} = k_1 + k_{OH}\left[\overline{OH}\right]$$

may be harnessed to calculate the enhancement factor using

$$I_{CO_2} = k_L^o + \mathcal{D}_{CO_2} \cdot \frac{k_{o,v}}{k_L^o}$$

For primary and secondary amines, an apparent **1st-order** rate constant, k_1, for the reactions between amine and CO_2, may be defined as

$$k_1 = \frac{k_2\left[R_1R_2NH\right]}{1 + \dfrac{k_{-2}}{k_b\left[R_1R_2NH\right]}}$$

With tertiary amines, where no carbonate is formed, the reaction rate constant for the base-catalyzed CO_2 hydrolysis reaction is given by

$$k_1 = k_2\,[R_1R_2R_3N]$$

Equipment Arrangement Shown in **Fig. 8.7.1** is the schematic layout of a typical amine gas treatment system.
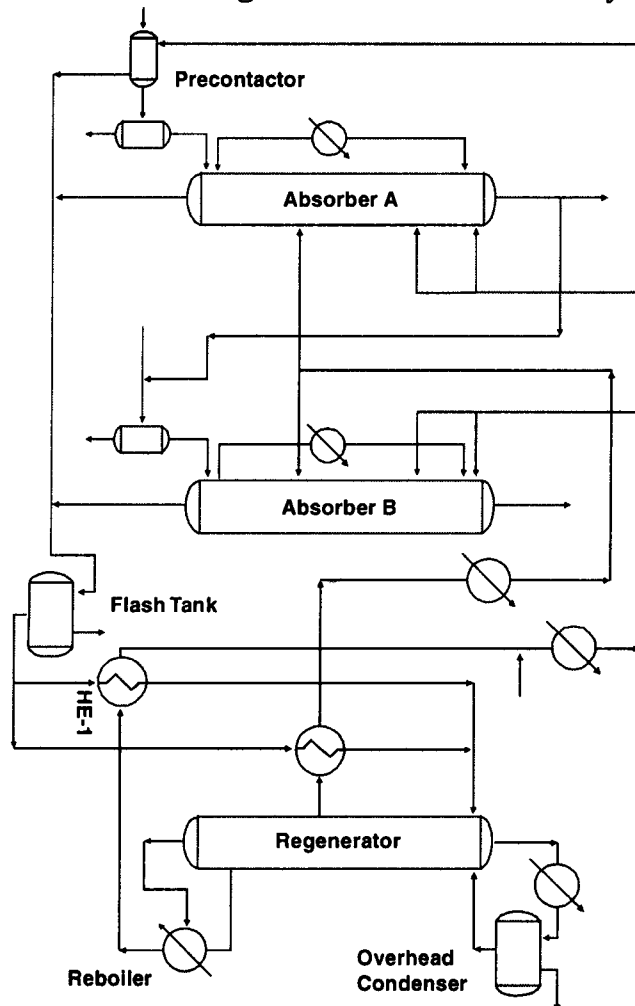
Courtesy : Sulzer Chemtech, Winterthur, Switzerland.

Fig. 8.7.1. *Basic equipment arrangement for Amine-Acid Gas Removal system.*

It consists of two parallel trains of absorber in which cooled lean solvent flows downward while the gas stream to be treated traffics up. The gas-liq contact and hence mass transfer takes place on the trays/packed bed.

The absorption of acid gas by amine is an exothermic reaction. The heat of the solution is taken care of by the tower effluent (the rich solvent) which is further heated in **HE-1 (Regenerator Feed Heater)** before being introduced to the stripper column **(Regenerator)** at the top. Inasmuch as the vapor pressure of the absorbed gas increase rapidly with the temperature increase, so preheating the rich amine solution will expedite its stripping in the regenerator **(stripper).**

The stripper bottom effluent is the lean solvent which is cooled in the **HE-1** before being fed to the absorber at the top. However, the lean solvent temperature should be kept above the dewpoint of the condensable hydrocarbons, in case in feed gas stream contains any such components in order to avert condensation of an immiscible hydrocarbon liquid which promotes foaming of the liquid phase in the absorber.

8.7.1. Design Consideration

■ **Solvent Strength** Usually 18 wt% **MEA** solution **(~3N)** is used as solvent for acid gases, Of course, it is desirable to operate with a high solution strength so as to reduce the liquid circulation requirement. However, certain physiochemical problems put a limit to the use of solvent with higher **MEA** concentration :

1. The vapor press of CO_2 above the rich solution at constant CO_2/MEA ratio increases with increasing **MEA** concentration.

2. Reboiler load increases to regenerate solvent of higher **MEA** concentration.

3. Higher the **MEA** concentrations, the higher becomes the rate of corrosion of common metals. *Strippers are operated at 70 kPa to minimize corrosion.*

4. **MEA** tends to degrade as the temperature increases. This mounts the operational cost in terms of solvent replacement and removal of the degradation product.

Use of higher strength amine through solution **(~5N MEA)** can be made provided suitable stabilizer is dozed. These are special chemical agents that inhibit corrosion of metals.

■ **Foaming** Amines are moderately foaming systems that restrict the bed pressure drop to a maximum of **21 mm $H_2O.m^{-1}$** of packed depth at the point of greatest loading to avoid the gas phase doing excessive work on the liquid phase as it would generate a greater degree of foaming. This pressure drop limitation specifies the absorber dia. Of course, the tower dia will vary with different size of tower packings as bed press dr varies with packing size. Normally, as the absorber operating pressure increases, the size of the packing used is increased.

■ **Vessel Size and Packed Depth** The thickness of the vessel shell of the absorber is the function of system pressure and the shell dia. Therefore, the absorber operating at higher pressure can be designed by increasing the dia and therefore, the larger shell thickness. Alternatively, the packed height can be increased by using larger size packing without going for larger dia tower with higher shell thickness. Usually, the last option is less expensive and hence preferred one.

■ **Solvent Flowrate** In general the lean solvent used to absorb CO_2 contains **0.12—0.15 mol CO_2** per mol **MEA**. This solution absorbs **0.3 to 0.35 mol CO_2** per mol of **MEA**. Since the gas

flowrate and inlet composition are known and the outlet gas composition is specified for the absorber, the solvent flowrate now can be computed from the material balance.

CO_2 Absorber

Example 8.2. A typical absorber (operating press. 22.10 atm abs.) receives feedgas (18 mol% CO_2) at the rate of 36000 kg.h^{-1} at 327.44 K.

The CO_2 content of inlet gas stream is to be reduced to 90mol ppm CO_2 in the outlet gas stream by absorbing the acid gas in 261000 kg.h^{-1} of lean solution containing 0.12 mol CO_2 per mol MEA. This liq feed is 30.2% (wt.) MEA solution at a temperature of 316K.

Density of feedgas at inlet temperature is 12.6878 kg.m^{-3}

Compute the rich liquid flowrate and CO_2 absorption rate.

Solution :

Refer to **Figure to Example 8.2**

$$\textbf{Volumetric flowrate of feedgas} = \frac{36000 \text{ kg.h}^{-1}}{12.6878 \text{ kg.m}^{-3}}$$

$$= 2837 \text{ m}^3.\text{h}^{-1}$$

Referred to NTP this volume comes out to be

$$\frac{V_o}{273} = \frac{2837.37 \times 23.10}{327.44}$$

or, $$V_o = 54667 \text{ Nm}^3.\text{h}^{-1}$$

$$= 2440.49 \text{ kmol.h}^{-1}$$

[cf. **1 kmol ≡ 22.4 Nm^3**]

∴ CO_2 flowrate = 18% of 2440.49 kmol.h^{-1}

$$= 439.28 \text{ kmol.h}^{-1}$$

MEA in the lean solution = 0.302 × 261000 kg.h^{-1}

$$= 78822 \text{ kg.h}^{-1}$$

$$= \frac{78822}{61} \frac{\text{kg.h}^{-1}}{\text{kg.kmol}^{-1}}$$

$$= 1292.1639 \text{ kmol.h}^{-1}$$

> MEA mol. wt
> = 14 + 2 + 12 + 2 + 12 + 2 + 16 + 1
> = 61 kg.kmol^{-1}

∴ **CO_2 content in the lean solution** = 1292.1639 × 0.12

$$= 155.059 \text{ kmol.h}^{-1}$$

Volumetric flowrate of

CO_2-free gas = 2440.49 − 439.28 = 2001.21 kmol.h^{-1}

∴ **CO_2 in the exit gas** = $\left[\dfrac{90}{10^6}\right]$ × 2001.21 kmol.h^{-1}

CO$_2$ (90 mol ppm)

261000 kg.h^{-1}
Lean MEA soln.

$\left(\dfrac{0.12 \text{ mol } CO_2}{\text{mol MEA}}\right)$

(30.2 wt % MEA Sol $\frac{n}{.}$)

36000 kg.h^{-1}
Feed gas
[18 mol %]
Density
= 12.6878 kg.m^{-3}

Rich MEA Soln.
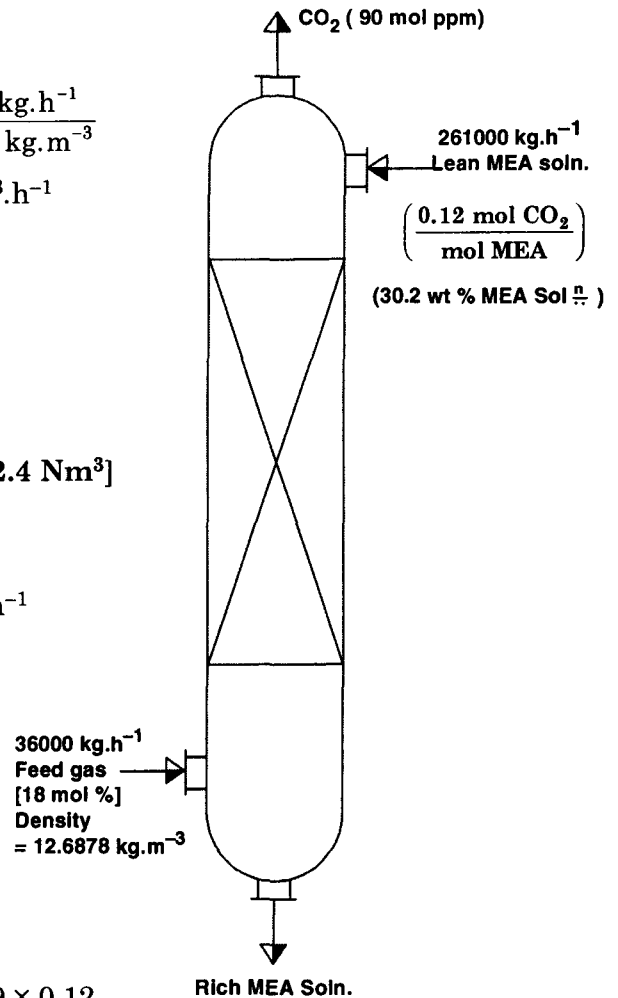
Fig. to Example 8.2

$$= 0.18010\ kmol.h^{-1}$$

∴   **CO₂ absorbed** $= 439.28 - 0.1801 \simeq 439.1\ kmol.h^{-1}$

∴   **Rich solution flowrate** $= 261000 + 439.1\ kmol.h^{-1} \times 44\ kg.kmol^{-1}$

$$= 280320.4\ kg.h^{-1}$$

■ Overall Mass Transfer Coefficient, $K_G.a$

CO_2 absorption is a liq-film-controlled process for which the overall **mtc** is influenced by the liquid and gas flowrates, solvent temperature and the mol CO_2 per mol of solvent in the lean solution.

For a packed-bed absorber using lean solvent containing 0.15 mol CO_2 per mol **MEA**, the $K_G.a$ values for different packings are presented in the following table compiled on the basis of

Liq flow rate, $L_v = 24.45\ m^3.m^{-2}.h^{-1}$

Gas capacity factor, $C_s = 1.1346\ kg^{\frac{1}{2}}.m^{-\frac{1}{2}}.s^{-1}$

Solvent temperature $= 297\ K$

Table 8.7.1.1 Overall Mass Transfer Coefficient [CO₂-MEA System)

Packing	MOC	$K_G.a$ (kmol h.$^{-1}$.m^{-3}.atm^{-1})
# 25 IMTP packing	metal	115.57
# 40 IMTP packing	metal	91.63
# 50 IMTP packing	metal	78.17
# 70 IMTP packing	metal	55.75
# 1 Hy-Pak packing	metal	92.59
# 1½ Hy-Pak packing	metal	77.53
# 2 Hy-Pak packing	metal	66.00
# 3 Hy-Pak packing	metal	46.46
# 1 Super Intalox packing	plastic	89.71
# 2 Super Intalox packing	plastic	61.51
# 3 Super Intalox packing	plastic	39.41
# 25 mm Intalox saddles	ceramic	90.35
# 38 mm Intalox saddles	ceramic	72.73
# 50 mm Intalox saddles	ceramic	60.23
# 75 mm Intalox saddles	ceramic	95.80
25 mm Pall rings	metal	99.32
38 mm Pall rings	metal	82.66
50 mm Pall rings	metal	69.84
89 mm Pall rings	metal	41.01
25 mm Pall rings	plastic	84.58
38 mm Pall rings	plastic	72.09
50 mm Pall rings	plastic	66.96
89 mm Pall rings	plastic	39.41
25 mm Pall rings	ceramic	74.01
38 mm Pall rings	ceramic	61.51
50 mm Pall rings	ceramic	52.22
89 mm Pall rings	ceramic	32.68

The $K_G.a$ values cited in the above table are for a solvent temperature of 297 K. They will get hiked up by 40% if the solvent temperature is raised to 311K and by 90% at solvent temperature 324.66 K.

Again these $K_G.a$ values get affected by CO_2 partial pressure. The $K_G.a$ values decline by 75% at a CO_2. partial pressure of 101.325 kPa (1 atm) and by 90% at 2026.5 kPa (20 atm) partial pressure.

Of course, the driving force for mass transfer increases at higher partial pressures of CO_2 and the solubility of CO_2 also increases at higher pressure, yet $K_G.a$ values do not increase contrary to the expectation. This is due to the fact that the **mtc** is restricted by the diffusion of the reactive amine.

The $K_G.a$ value decreases as the ratio of **mol CO_2/mol MEA** increases. If the CO_2 : **MEA** mol ratio value of 0.15 is doubled (0.31), the $K_G.a$ value will get reduced by 40%. If a solvent containing 0.43 mol CO_2 per mol **MEA** is used, the $K_G.a$ value will drop by 70%.

As expected, the $K_G.a$ value increases with the increase of **MEA** concentration in the solvent. However, increasing the **MEA** concentration also increases the viscosity of the liq phase that hinders the rate of CO_2 diffusion. The $K_G.a$ value has registered a decrease of 5% for 1N increase in the **MEA** concentration above 3N.

8.7.2. Design Guidelines

Dimensioning of absorption columns of CO_2 and/or H_2S absorption is complex because of a number of interacting parameters *viz.* physical absorption, chemisorption with resistance on gas side, resistance on the liquid side, different reactions and kinetics, pressures from *atmospheric pressure upto 100 bar, liq loads ranging from 1m³.m⁻².h⁻¹ to 150 m³.m⁻².h⁻¹* and *temperature from 223 K to 273 K.*

For the design of columns, some process knowledges are always necessary : *e.g.*, equilibrium, and kinetic data of the process. These data are not available for processes which are patented due to obvious reason. (For instance : **Sulfinol, Selexol, Ucarsol. Flexsorb, etc.**).

1. Trays vs. Packed Columns

Both packings and trays are used in the absorbers. Most of the older units contain either **bubblecap trays** or **Raschig** ring packing. However, in modern plants, alternate tray designs (*e.g.*, sieve trays and valve trays) and high performance packing (viz. **Hy-Pak, Super Intalox, IMTP, Goodloe** and **Gauze**) are used extensively.

The choice between the trays and packing is rather arbitrary because generally either can be designed to achieve targetted absorption efficiency and overall economics are seldom decisively in favor of one or the other. **Since CO_2/H_2S-absorption in alkanolamines present foaming problems, packing will generally fare better than tray.** More recently, foaming in bubblecap columns and other tray columns has been successfully tackled by dozing antifoam agents instead of going for costly revamp of tray by replacing them with packings.

The most forceful reason going in favor of packed bed CO_2-absorber is its high degree of CO_2 removal. The low tray efficiency normally obtained with plate columns may result in an unfavorably tall column. Packed column will alleviate this difficulty by its requirement of lower overall height.

For a rough design of packing height, one can use the formula for chemisorption (provided the column is working far away from equilibrium value).

$$NTU = \ln \left| \frac{y_{in}}{y_{out}} \right| \qquad ...(8.7.2.1)$$

The performance of a packing depends greatly on the absorption system, gas loads, liq loads and pressure level. **Table 8.7.2.1** gives NTUM values for CO_2 and H_2S absorption processes using different solvents in a packed bed of **Mellapack 250.Y**

Table 8.7.2.1 Design Guidelines for Absorption

Packing : Mellapak 250.Y

Liq load : $30m^3.m^{-2}.h^{-1}$

Solvent	Solute	NTUM
MEA	CO_2	0.8–1.2
MEA	H_2S	1–2
DEA	CO_2	0.5–0.8
DEA	H_2S	1–1.5
MDEA	CO_2	0.01–0.21
MDEA	H_2S	1–1.5
BASF-MDEA	CO_2	0.2–0.4
DIPA	CO_2	0.5–0.7
DIPA	H_2S	1–1.5
RECTISOL	CO_2	1–1.3
SELEXOL	CO_2	0.4
SELEXOL	H_2S	> 1
SULFINOL	H_2S	> 1
SULFINOL	CO_2	0.4–1.0
AMISOL	H_2S	0.8
GIAMMARCO VETROCOKE	CO_2	> 0.2

Source : SULZER CHEMTECH SEPARATION COLUMNS [TRK/0614].

2. Liquid Rate

Normally the gas flowrate and physical properties of the gas are known. So it is necessary, before detailed design of the absorption can be undertaken, to know the flowrates and physical properties of the liquid containing the solvent.

Vapor pressure data for H_2S and CO_2 over **MEA** and **DEA** solutions are presented in **Fig. 8.7.2.1 thru 8.7.2.17.**

Physical properties data of several ethanolamine solutions are presented in **Fig. 8.7.2.18— 8.7.2.29**
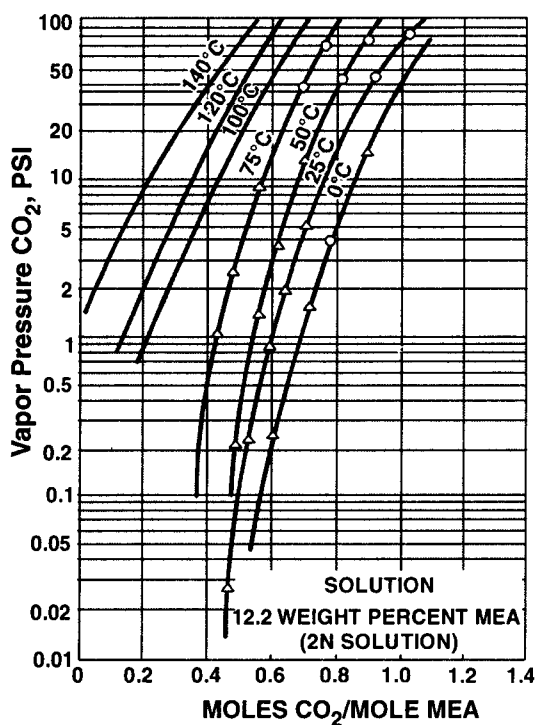
Fig. 8.7.2.1. *Vapor Pressure of CO₂ versus CO₂*
Concentration in 2N Monoethanolamine solutions.
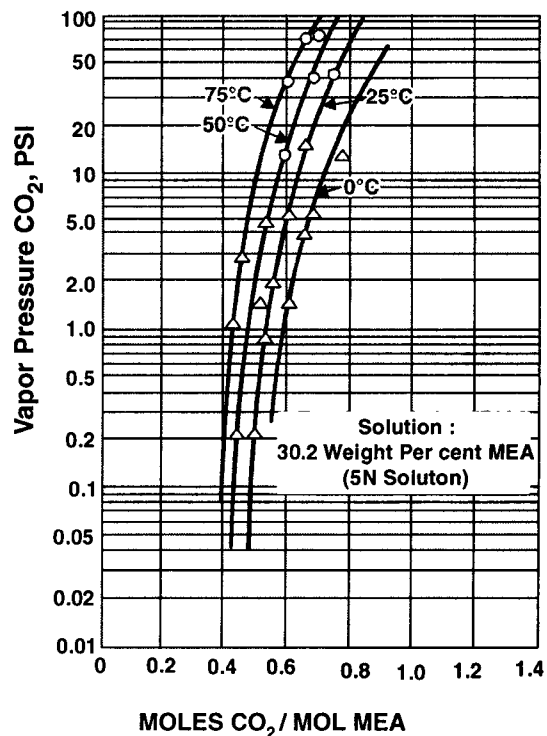
Fig. 8.7.2.2 . *Vapor Pressure of CO₂ versus CO₂*
Concentration in 5N Monoethanolamine solutions.
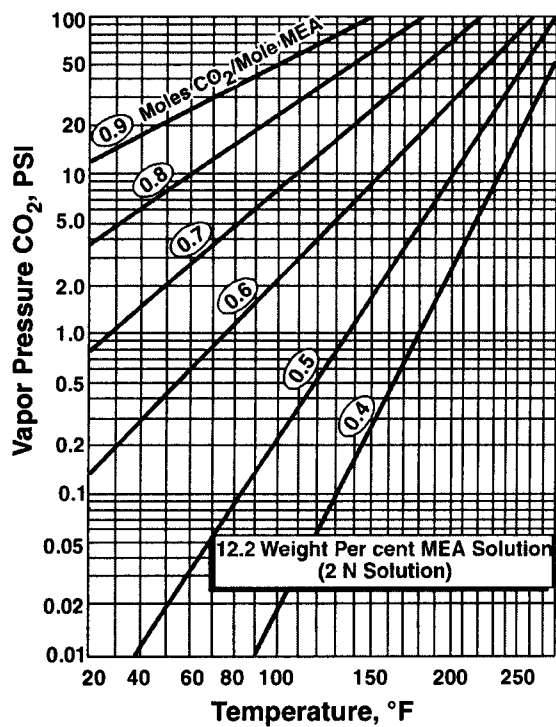
Fig. 8.7.2.3. *Effect of Temperature on CO₂ Vapor*
Pressure for various CO₂ Concentrations in 2N
Monoethanolamine solutions.
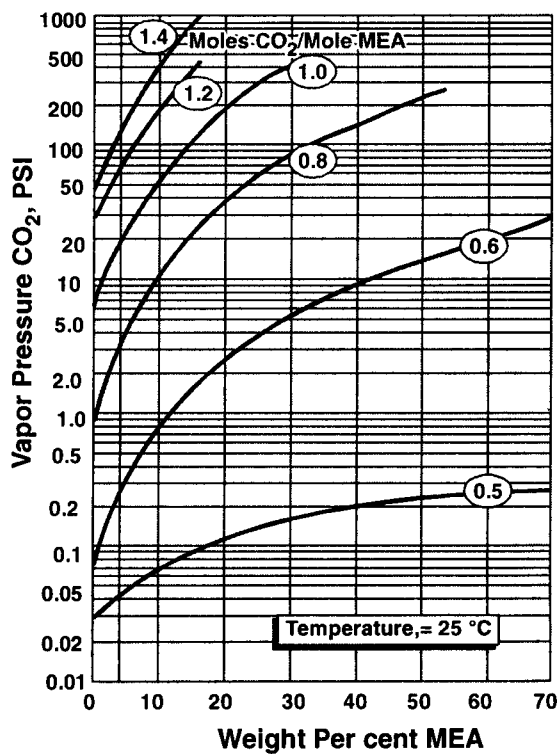
Fig. 8.7.2.4. *Effect of Amine Concentration*
on CO₂ Vapor Pressure.
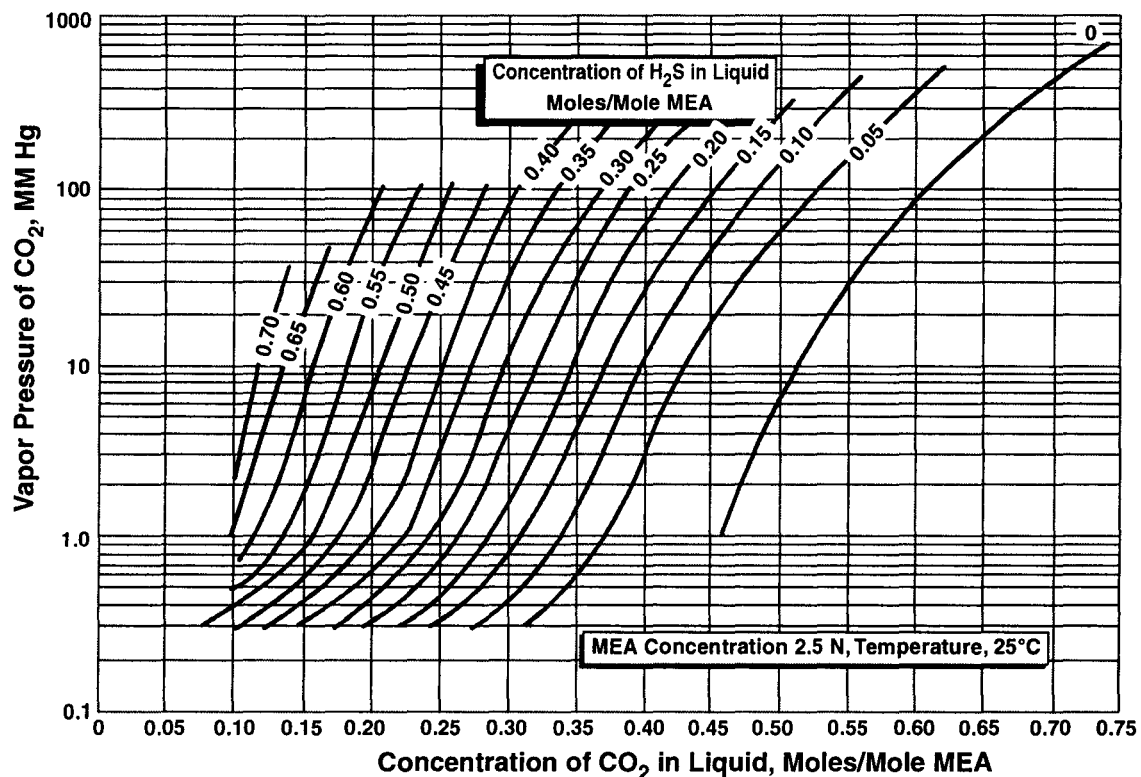
Fig. 8.7.2.5. *Effect of dissolved hydrogen sulfide on vapor pressure of CO_2 over 2.5N Monoethanolamine solution at 25°C.*
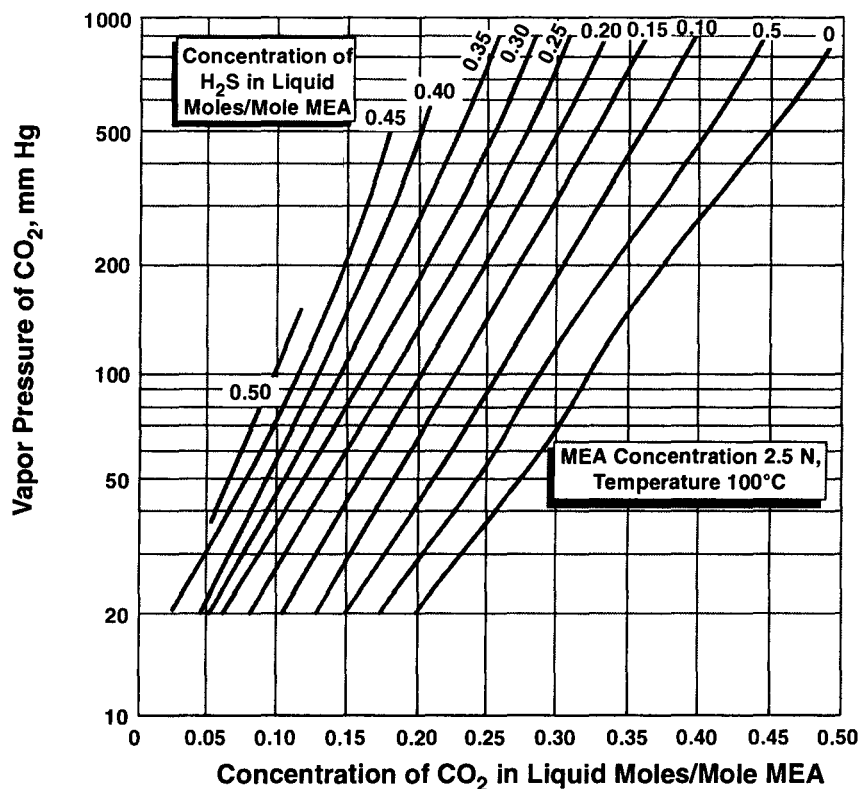
Fig. 8.7.2.6. *Effect of dissolved hydrogen sulfide on Vapor Pressure of CO_2 over 2.5N Monoethanolamine solution at 100°C.*
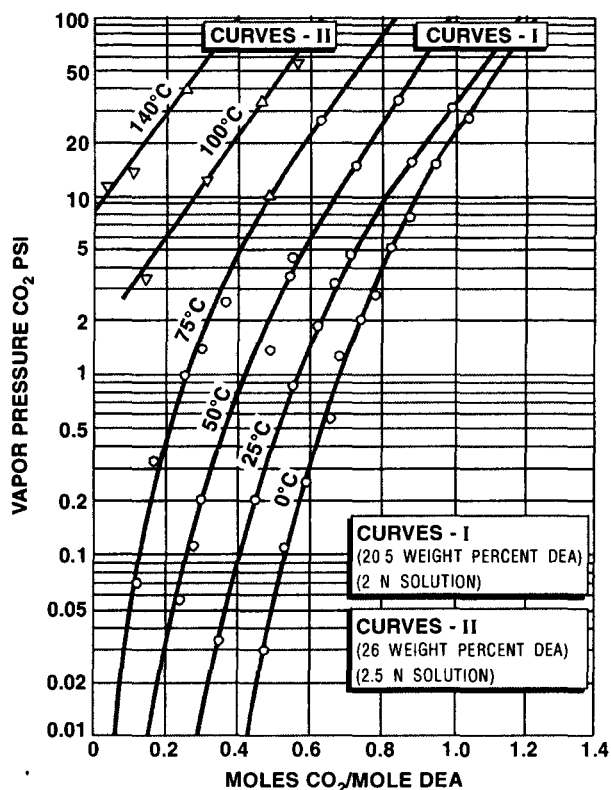
Fig. 8.7.2.7. *Vapor Pressure of CO_2 versus CO_2 Concentration in 2 and 2.5N Diethanolamine solutions.*
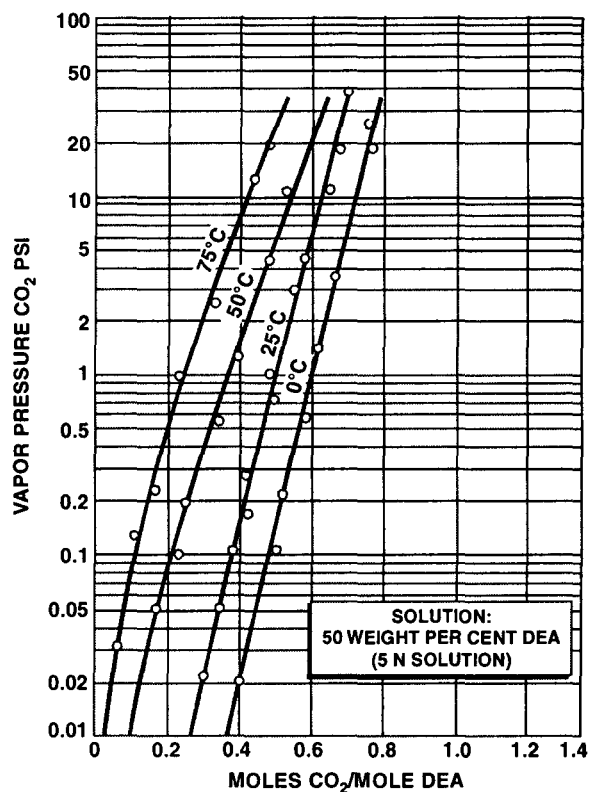
Fig. 8.7.2.8. *Vapor Pressure of CO_2 versus CO_2 Concentration in 5N Diethanolamine solution.*
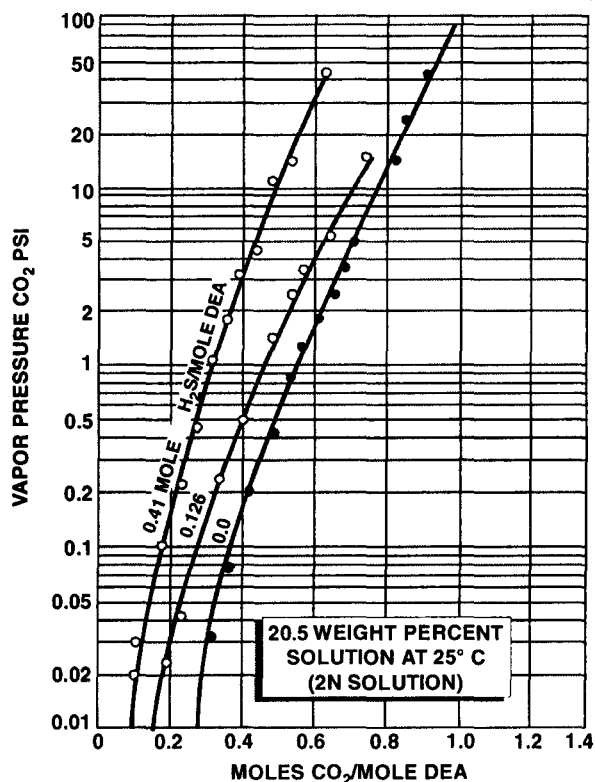
Fig. 8.7.2.9. *Effect of dissolved H_2S on CO_2 Vapor Pressure over 2N Diethanolamine solution containing both CO_2 and H_2S.*
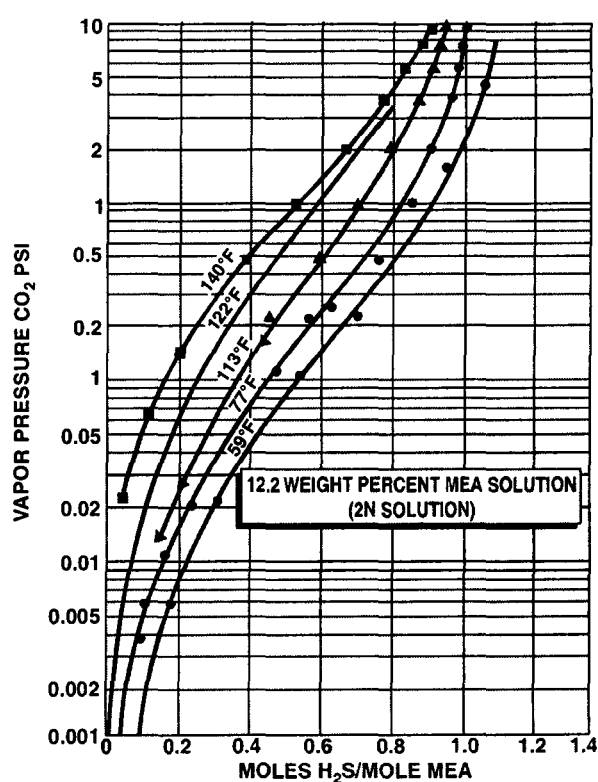
Fig. 8.7.2.10. *Vapor Pressure of H_2S versus H_2S Concentration in 2N Monoethanolamine solution.*
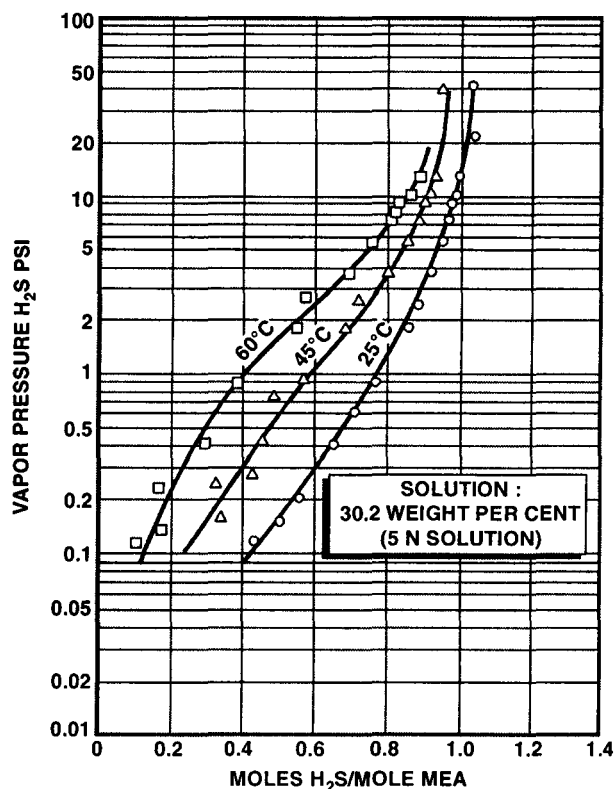
Fig. 8.7.2.11. *Vapor Pressure of H_2S versus H_2S Concentration in 5N Monoethanolamine solution.*
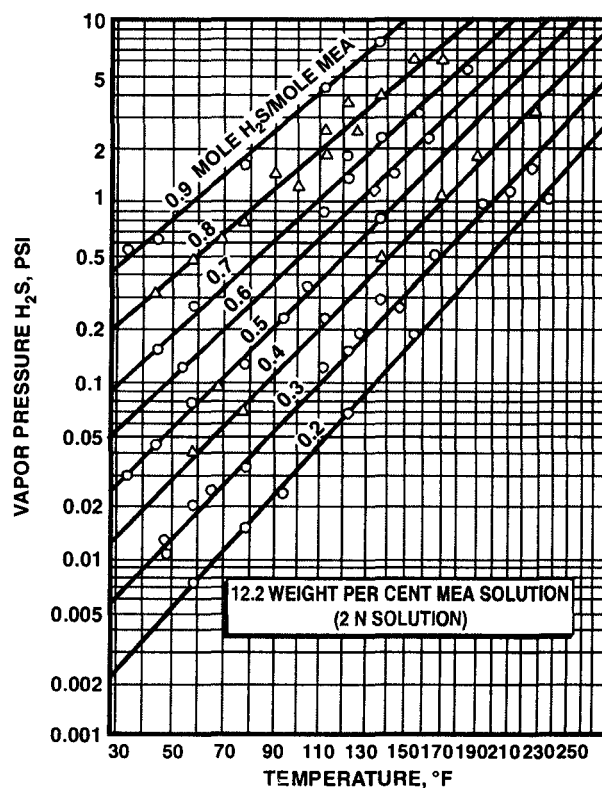
Fig. 8.7.2.12. *Effect of Temperature on Vapor Pressure of H_2S for various H_2S Concentrations in 2N Monoethanolamine solution.*
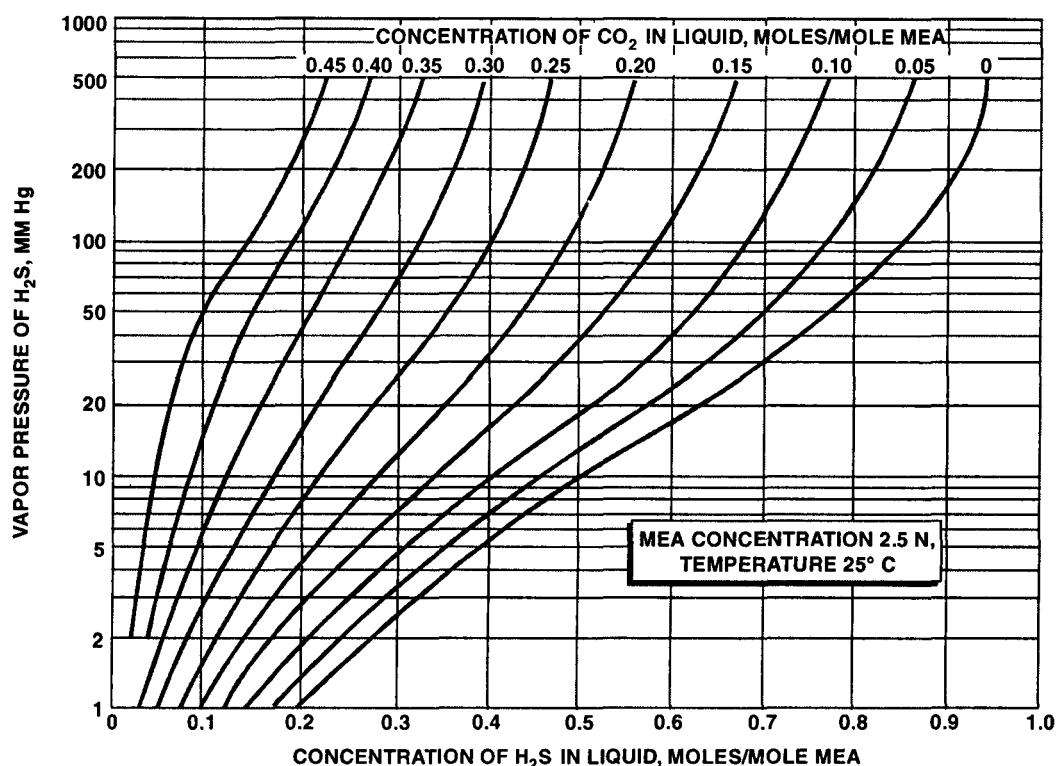
Fig. 8.7.2.13. *Vapor Pressure of H_2S vs. Concentration of H_2S in MEA*
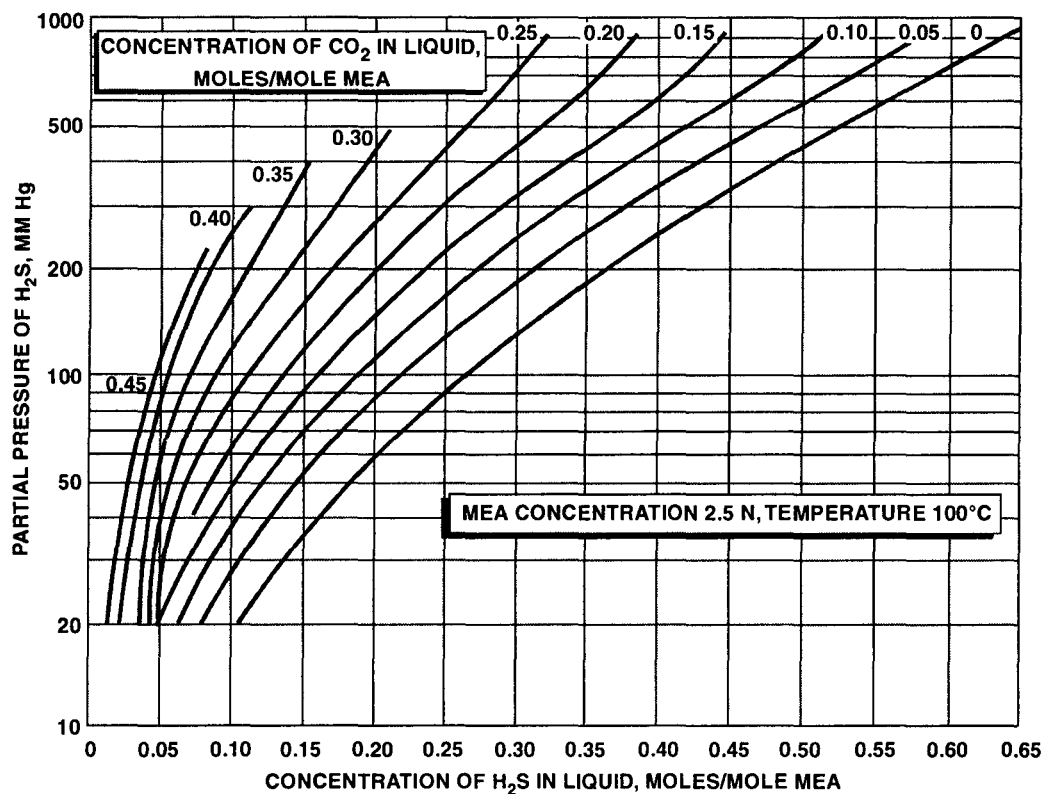
Fig. 8.7.2.14 *Effect of dissolved carbon dioxide on Vapor Pressure of H_2S over 2.5N Monoethanolamine solution at 100°C.*
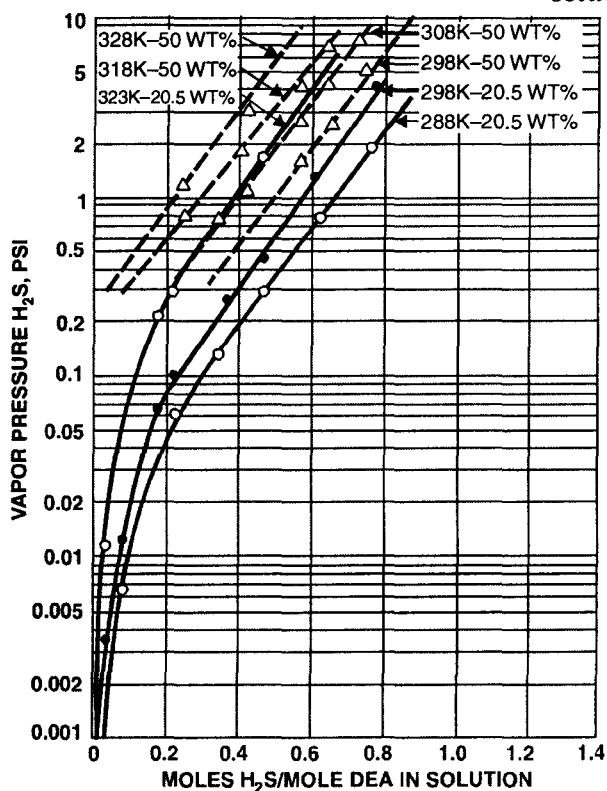
Fig. 8.7.2.15 *Vapor Pressure of H_2S versus H_2S Concentration in 2 and 5N Diethanolamine solutions.*
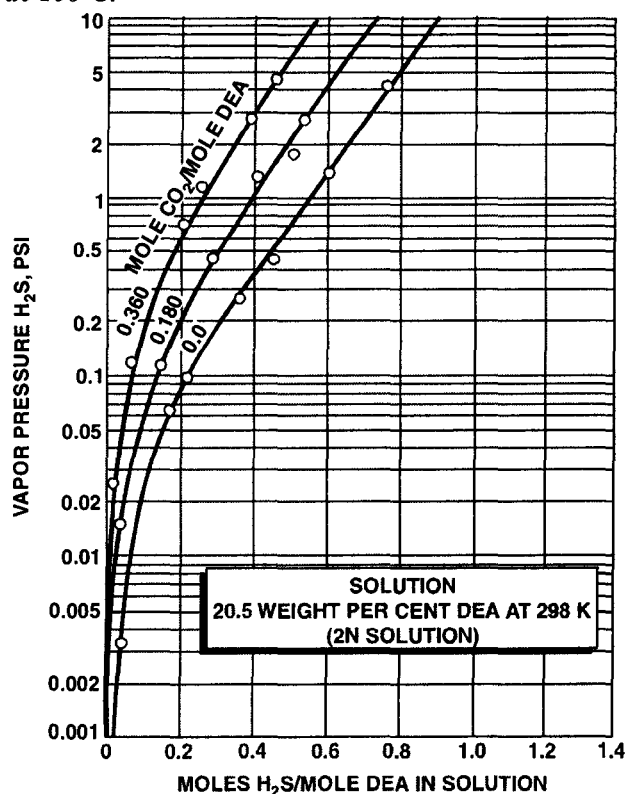
Fig. 8.7.2.16. *Effect of CO_2 on Vapor Pressure of H_2S over 2N Diethanolamine solution both CO_2 and H_2S.*
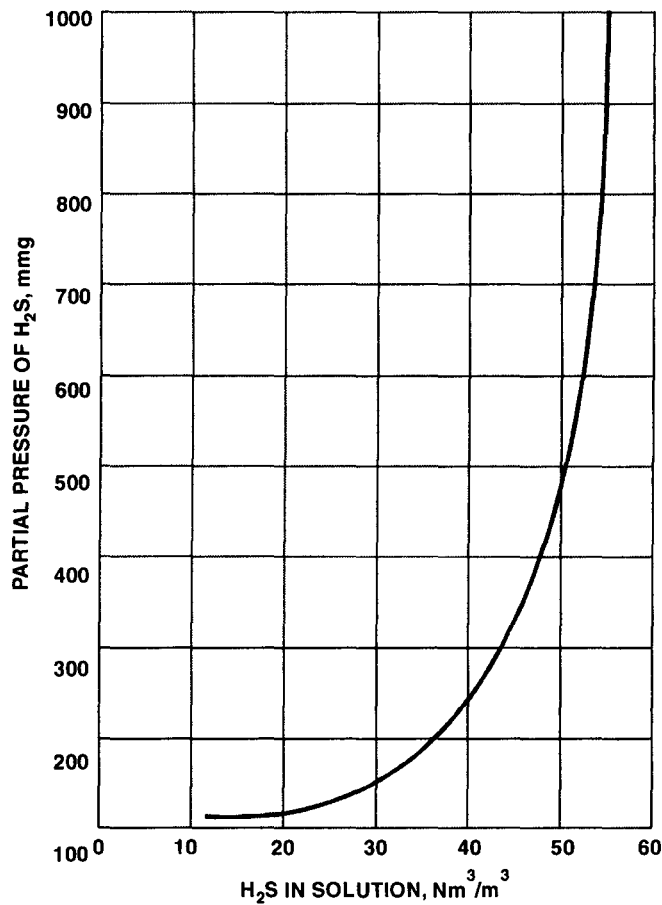
Fig. 8.7.2.17. *Equilibrium solubility of H_2S in ADIP solution.*
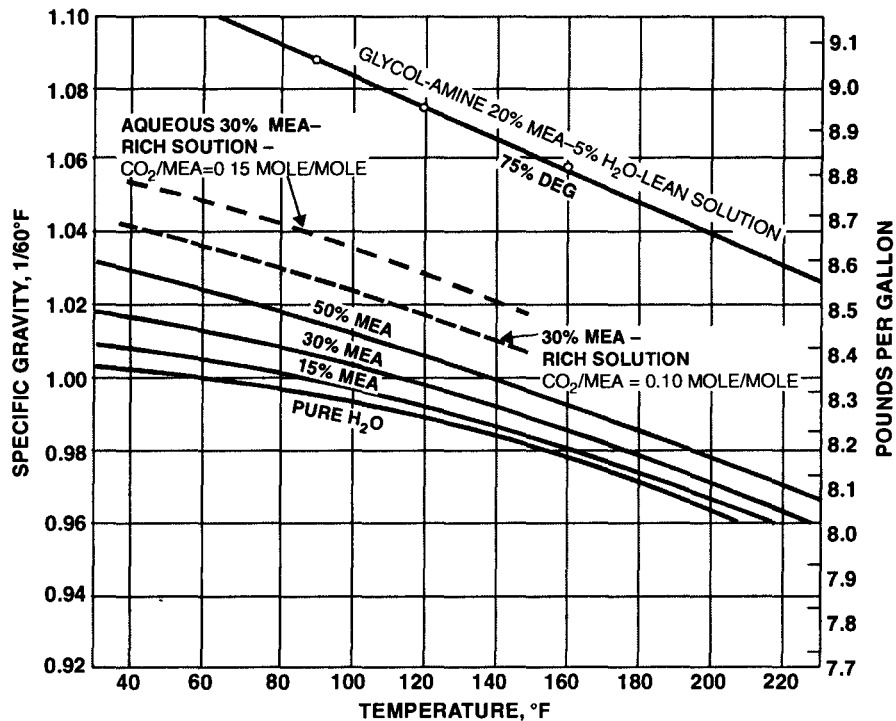
Fig. 8.7.2.18 *Specific gravity of Monoethanolamine solutions.*

TEMPERATURE, °C
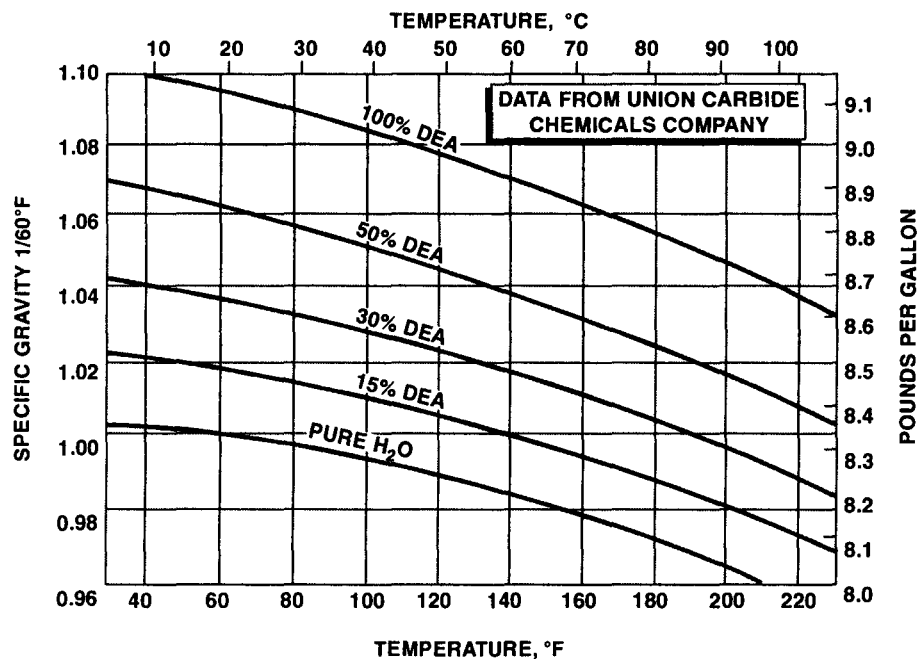
Fig. 8.7.2.19. *Specific gravity of diethanolamine solutions.*

TEMPERATURE, °C
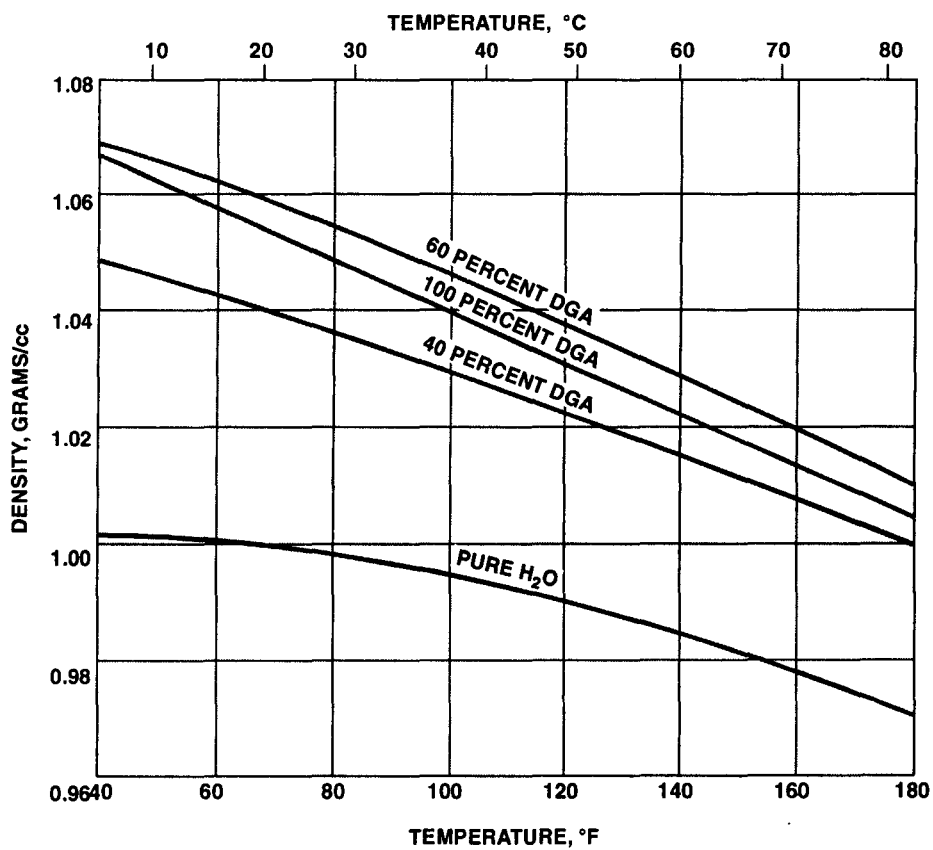
Fig. 8.7.2.20. *Density of Diglycolamine solutions.*
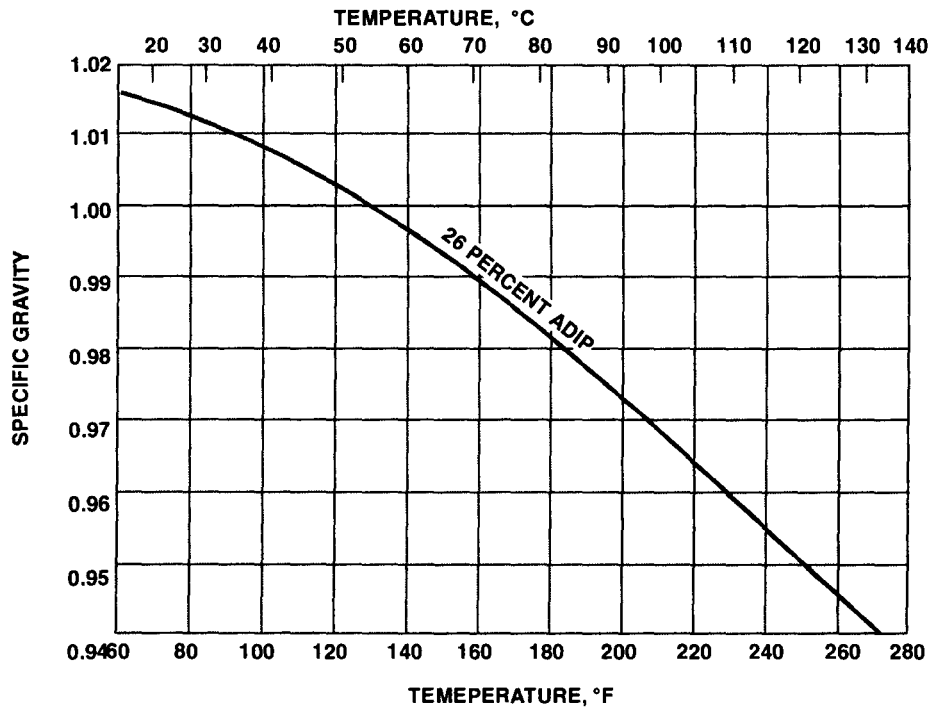
Fig. 8.7.2.21. *Specific gravity of ADIP solution.*
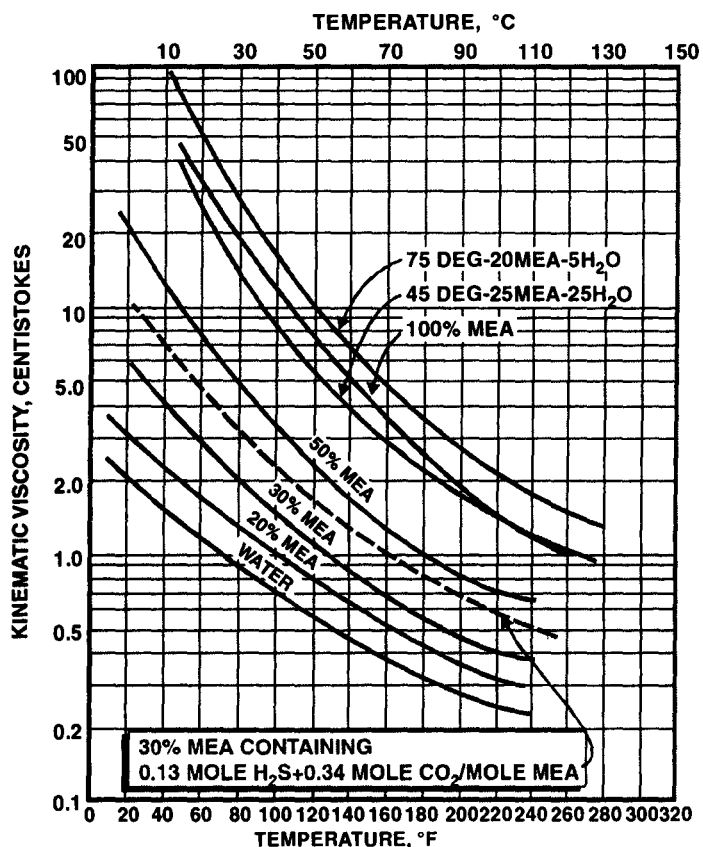
Fig. 8.7.2.22. *Viscosity of Monoethanolamine solutions.*
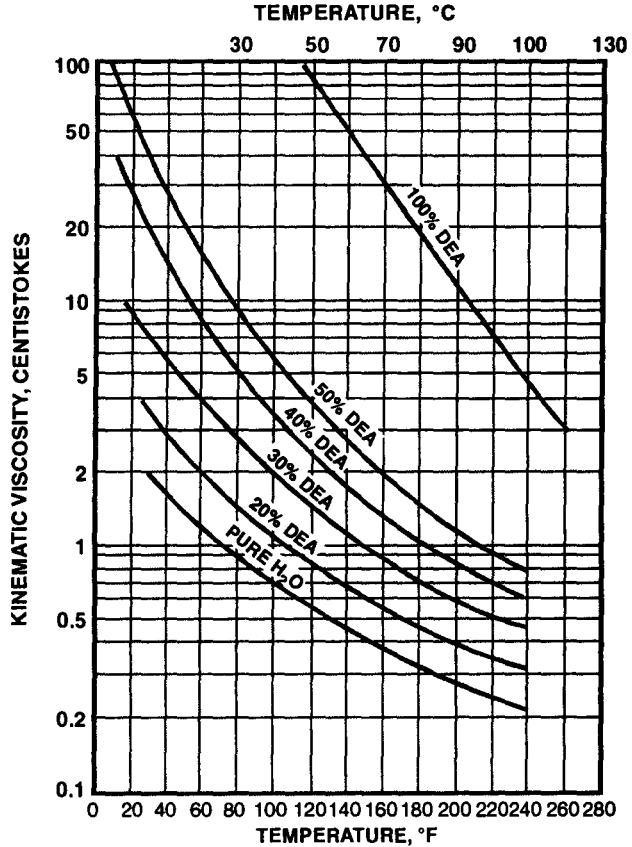
Fig. 8.7.2.23 *Viscosity of Diethanolamine solutions.*

TEMPERATURE, °C
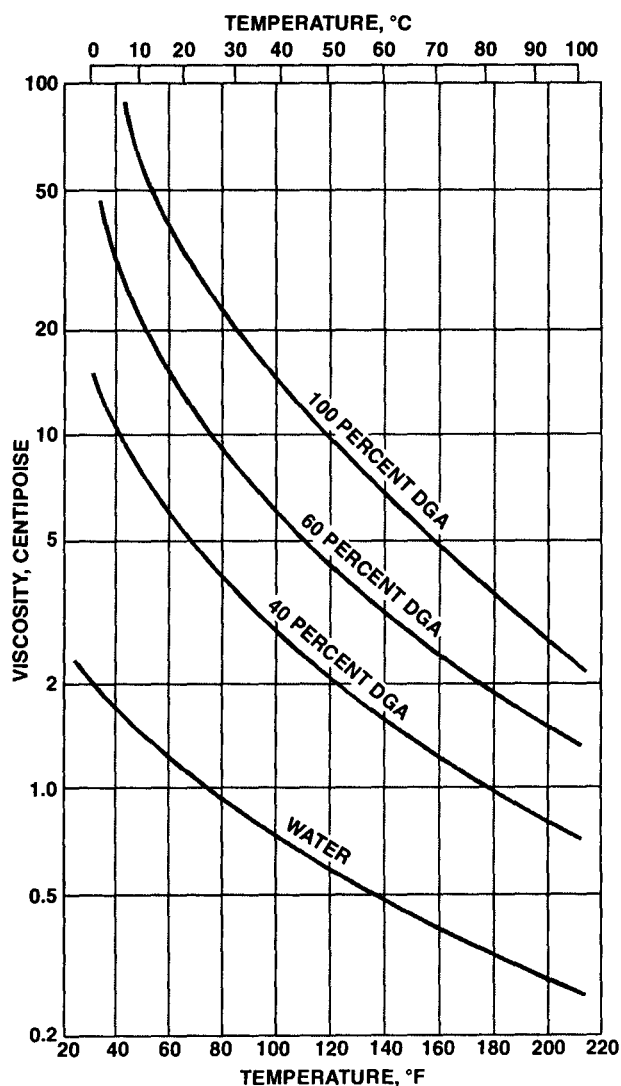
Fig. 8.7.2.24. *Viscosity of Diglycolamine solutions.*
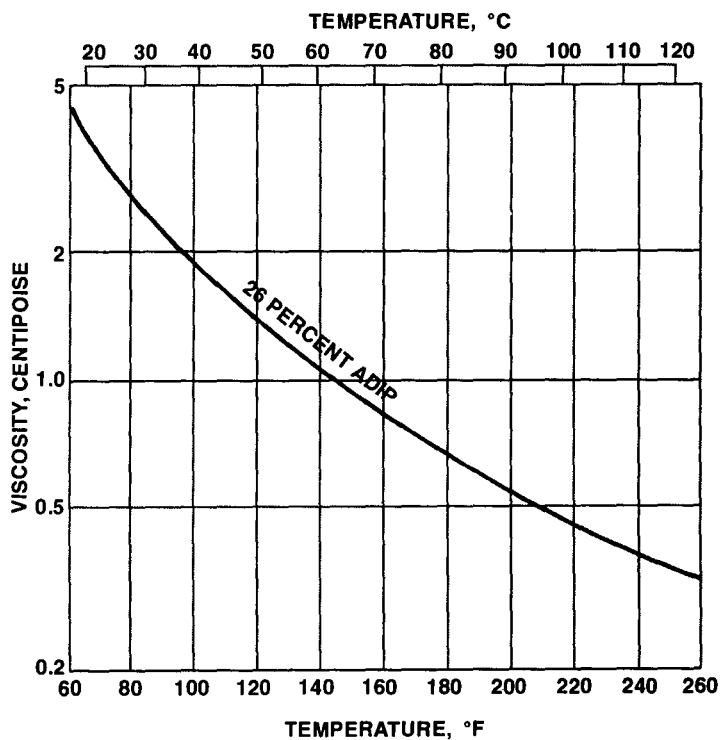
Fig. 8.7.2.25. *Viscosity of ADIP solution.*
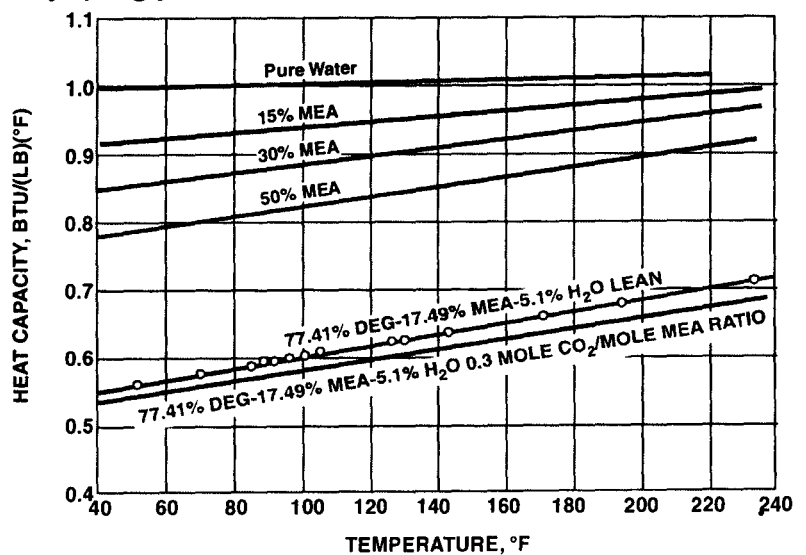
Fig. 8.7.2.26. *Heat Capacity of Monoethanolamine solutions.*
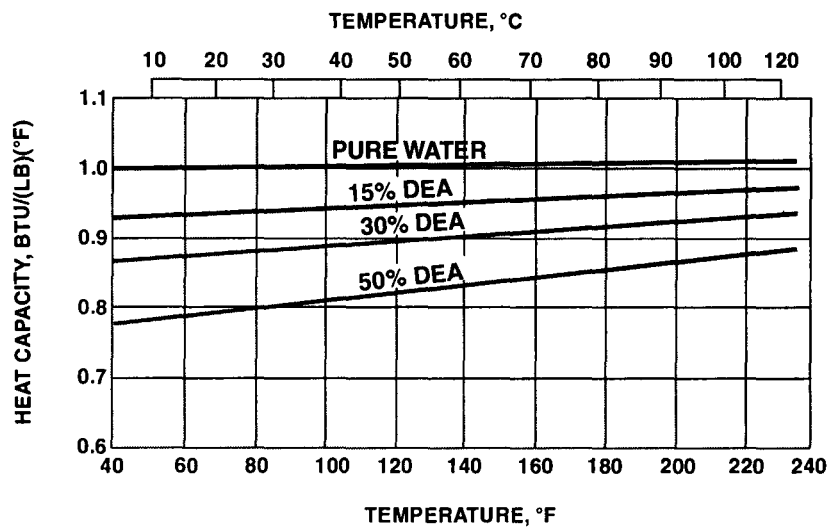
Fig. 8.7.2.27. *Heat Capacity of Diethanolamine solutions.*
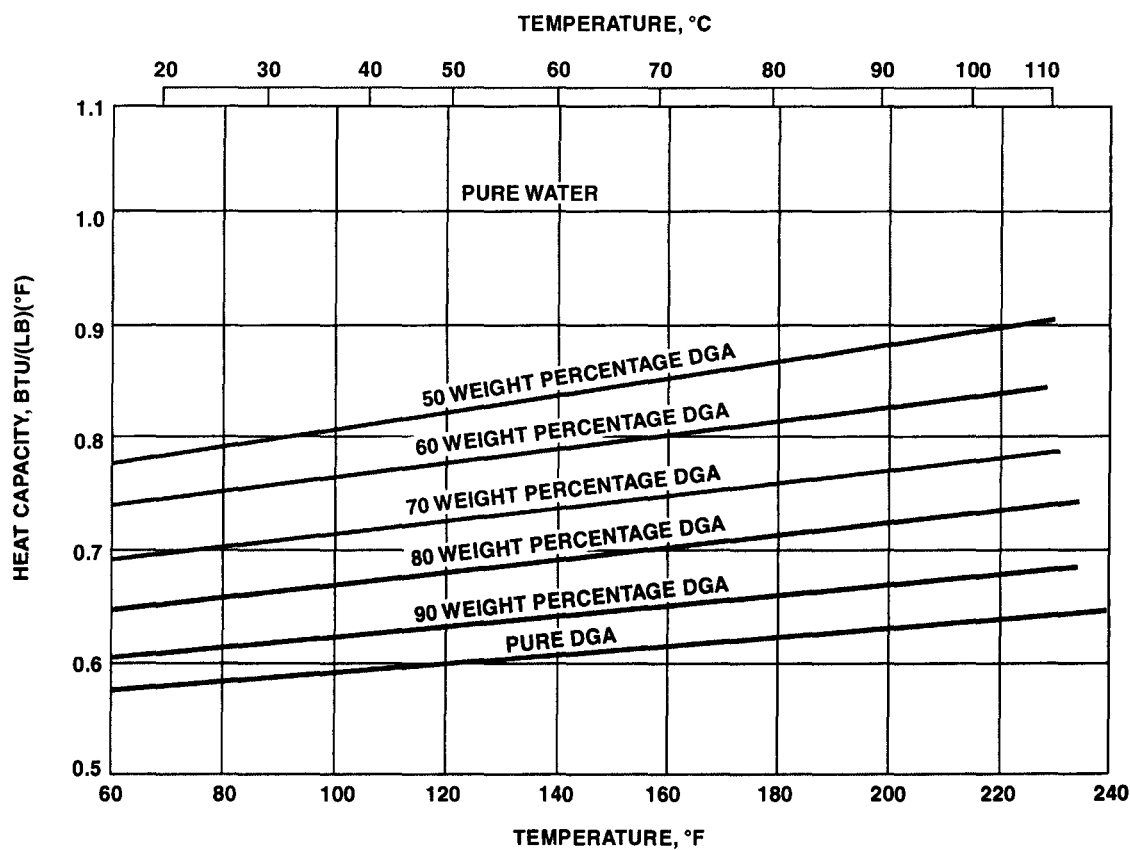
Fig. 8.7.2.28. *Heat Capacity of Diglycolamine solutions.*
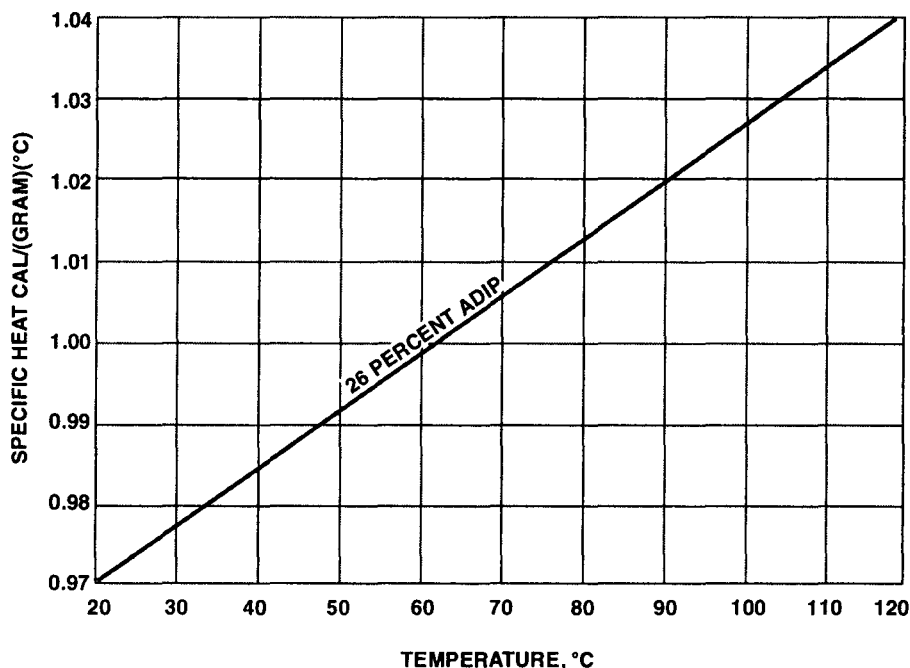
Fig. 8.7.2.29. *Heat Capacity of ADIP solution (26%)*

As a first approximation for calculating the required flowrate it is normally assumed that the acid-gas content of the rich solutions will approach to within 75—80% of the equilibrium value w.r.t. the feedgas at the temperature at the absorber bottom. In many commercial operations, the approach is not even this close, and appreciably closer approach is quite difficult to attain inasmuch as the rate of absorption drops rapidly with the acid-gas concentration in the solution.

Precise calculation of the liq loading requires the knowledge of the degree of stripping obtained in the stripping column, *i.e.,* the composition of the lean solution which is taken as absorber feed. However, an approximate rate can be estimated on the basis of absorber alone by assuming a lean solution composition and making a necessary correction after the stripping column is designed. For CO_2- **Amine systems** plant data indicate that the lean solution will contain between 0.05 and 0.2 mol CO_2 per mol of **MEA**, depending upon the stripping conditions. Normally, a value of 0.15 is considered to calculate absorber liq rate if a low-pressure stripper column is used. For material balance purposes, it is safe to assume that entire H_2S content of the stripper feed (rich solution from ABS. BTMS) gets stripped off in the stripper so that lean solution is virtually free of H_2S.

3. Column Temperature

To estimate the temperature of the solution leaving the absorber, it is essential to have the data on the heat of reaction [**Table 8.7.2.2**] and heat capacity of the solution [**Figure. 8.7.2.26–8.7.2.29**]

Table 8.7.2.2. Heat of the Reaction for Absorption of H_2S and CO_2 in Ethanolamine Solutions.

Acid-gas Component	Amine	Heat of Reaction $(kJ.kg^{-1}$ gas$)$
H_2S	MEA	1907.32
H_2S	DEA	1188.58
H_2S	TEA	930.40
H_2S	DIPA	1104.85
H_2S	DGA	1567.72
CO_2	MEA	1918.95
CO_2	DEA	1518.88
CO_2	TEA	1465.38
CO_2	DGA	1977.10

For gas streams containing large proportions of acid gases (>5%), the qty of lean solution required is so large that it virtually cools down the purified gas to within a few degrees of the lean solution temperature at the top of the column. That is, the lions's share of the heat of the reaction is abstracted by the solution which whereupon leaves the column at an elevated temperature [Fig. 8.7.2.30].
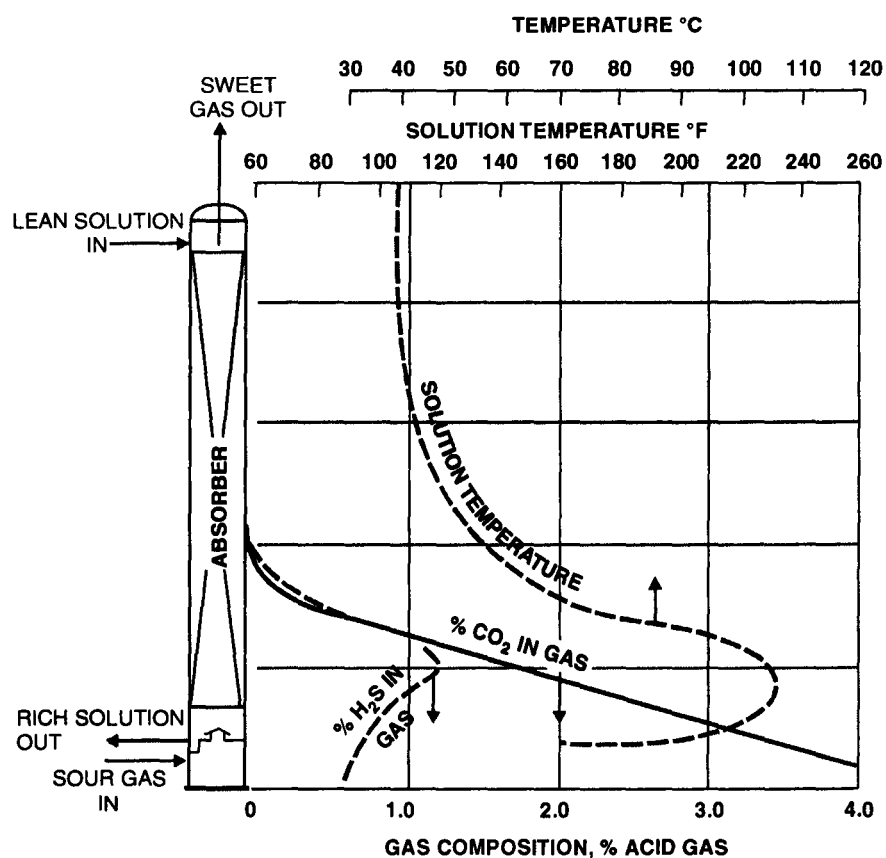
Fig. 8.7.2.30. *Temperature and concentration profiles in an absorber treating sour gas containing a high-concentration of acid gas. The temperature bulge results from cool feedgas absorbing heat from the rich solution.*

In the cases where more dilute gases are purified, the qty of gas handled may be so large in comparison to that of the solution that it is the gas, rather than the solutions, which takes care of the heat load of the absorption reaction. The solution is cooled to approximately the temperature of the incoming gas before it leaves the column, and essentially all the heat of the reaction is taken out of the column by the gas stream **(Fig. 8.7.2.31)**
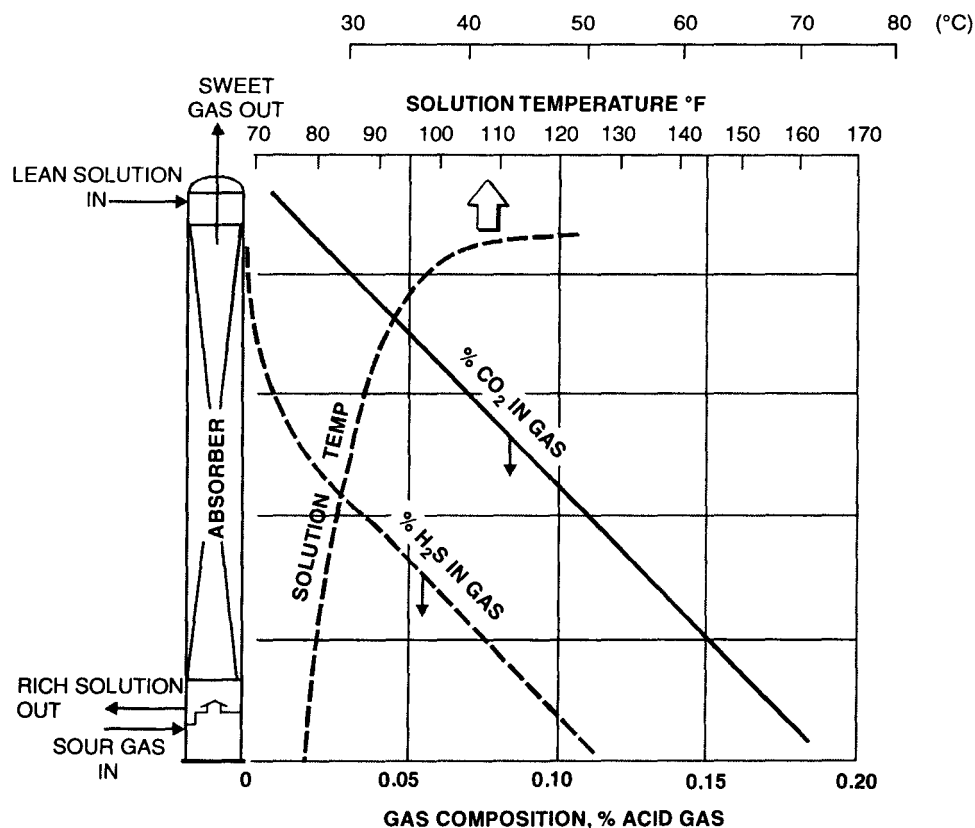
Fig. 8.7.2.31. *Temperature and Gas Composition Profiles in an absorber treating sour gas with a low concentration of acid-gas.*

4. Absorber Dia

When liquid and gas flowrates are known and their physical properties at hand, the required column dia of the CO_2-absorber can be estimated by conventional techniques.

PACKED BED ABSORBER

[A] Sherwood Method The generally accepted design procedure for sizing packed columns is the modified version of the Sherwood correlation **[Fig. 8.7.2.32]**

Packing Factor (F_p) : is a characteristic of packing. For any given tower packing it represents a number that relates the bed pressure-drop to flowrates through a packed bed of the said packing. It appears in the **generalized pressure-drop correlations** (cf. **Eqn. 8.7.2.32.1**) and **Fig. : 8.7.2.32 A** and **Fig. : 8.7.2.32B** of packed bed hydraulics.

$$42.9 \frac{G'^2 . F_p}{\rho_G(\rho_L - \rho_G)} . \left(\frac{\mu_L}{\rho_L}\right)^{0.1} = \text{function}\left(\frac{L'}{G'} . \sqrt{\frac{\rho_G}{\rho_L}}\right) \qquad ...(8.7.2.32.1)$$
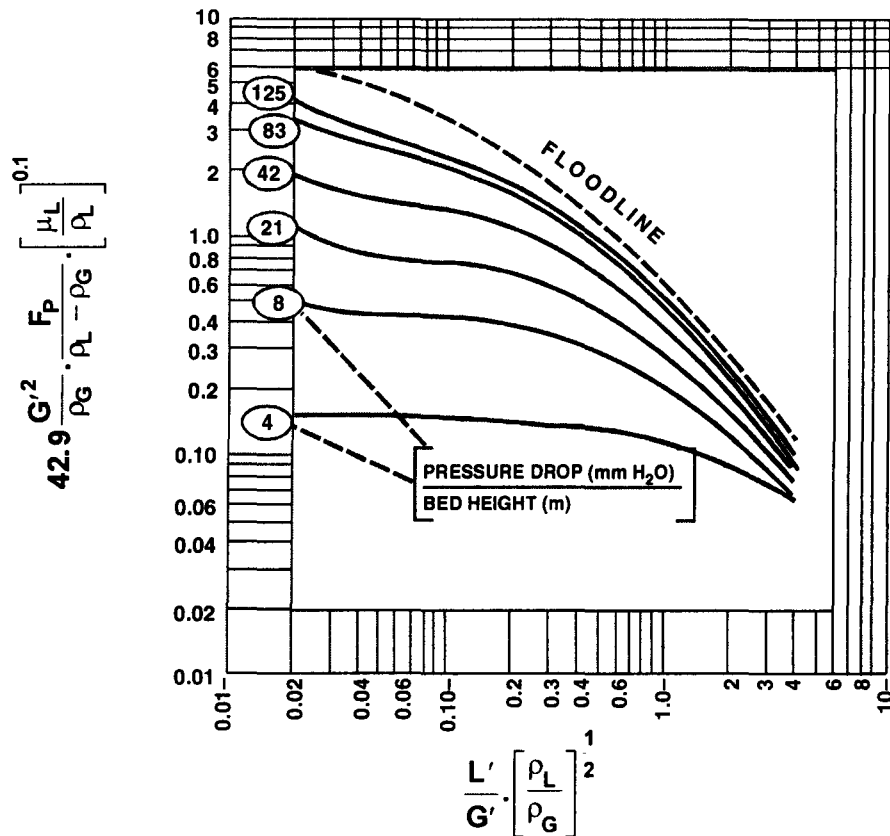
Fig. 8.7.2.32A. *Generalized Pressure Drop Correlation in randomly packed tower.*

or, $$42.9\frac{G'^2 \cdot F_p \cdot \upsilon_L^{0.1}}{\rho_G \cdot \Delta\rho} = \text{function (Flow Parameter)}$$

or, $$42.9\, C_s^2 \cdot F_p \cdot \upsilon_L^{0.1} = \text{function of (Flow Parameter)}$$

where, $G' =$ mass flowrate of gas, kg/(m^2.s)

$$C_s = \text{Capacity factor} = \frac{G'}{\left[\rho_G \cdot (\rho_L - \rho_G)\right]^{\frac{1}{2}}}$$

$F_p =$ packing factor

$\upsilon_L =$ kinematic liquid viscosity $= \dfrac{\mu_L}{\rho_L}$

$\Delta\rho = \rho_L - \rho_G$

$\dfrac{L'}{G'} \cdot \sqrt{\dfrac{\rho_G}{\rho_L}} = $ Flow parameter

The packing factors are determined from the experimental pressure drop data; hence they are empirical rather than theoretical in nature. The packing factor of some selected packing are listed in the **Table 8.7.2.32.1**

Table 8.7.2.32.1 Packing Factors for Selected Random Packing

Packing Factor (F$_p$)*

Nominal packing size (mm)	IMTP® Packing (Metal)	Hy-Pak® Packing (Metal)	Intalox Saddles (Cera-mic)	Super Intalox® Saddles (Cera-mic)	Super Intalox® Saddles (Plastic)	Berl Saddles (Cera-mic)	Pall Rings (Pla-stic)	Pall Rings (Metal)	Raschig Rings (Cera-mic)	Raschig Rings (Metal W/th : 0.8 mm)	Raschig Rings (Metal W/th : 1.6 mm)
12			200			240			580	300	410
16	51						95	81	380	170	300
19			145			170			255	155	220
25	41	45	92	60	40	110	55	56	179	115	144
31									125		110
37	24	29	52			65	40	40	93		83
50	18	26	40	30	28	45	26	27	65		57
75/87	12	16	22		18		17	18	37		32

* when C$_s$ in ft/s.

$$C_s = V_G \sqrt{\frac{\rho_G}{\rho_L - \rho_G}}$$

$$X = \frac{L'}{G'} \bullet \left| \frac{\rho_G}{\rho_L - \rho_G} \right|^{1/2}$$
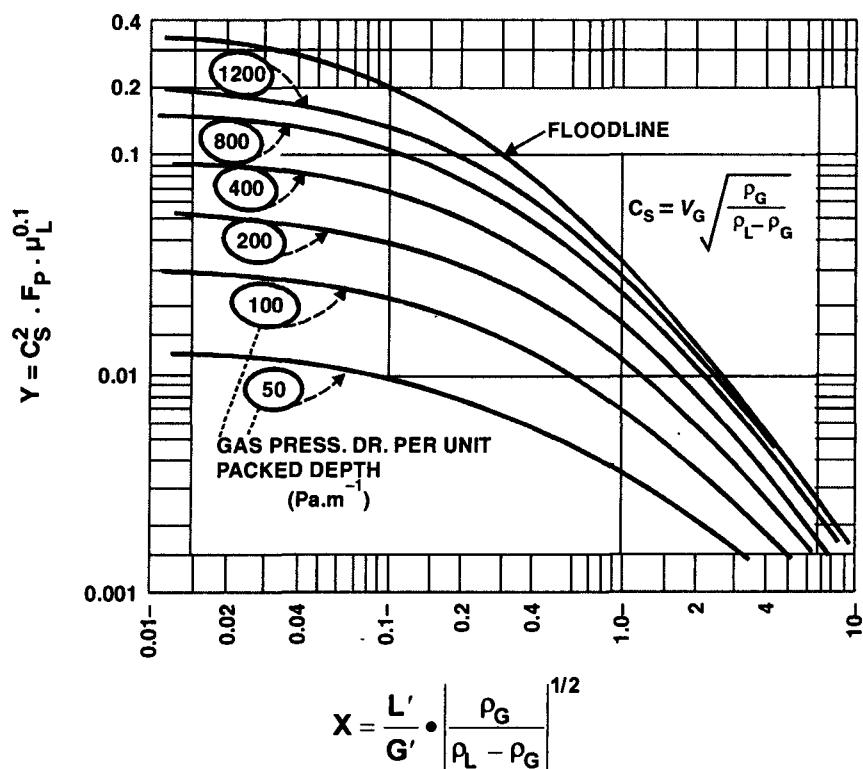
Fig. 8.7.2.32 B.

This correlation relates bed dia to fluid densities, flowrates and packing characterization factor **(Packing Factor, F)**

$$D = 1.13 \left[\frac{\dot{M}_G}{G'} \right]^{0.5}$$

...(8.7-2.2)

where, D = absorber dia. m

$\dot{M}_G$ = mass flowrate of gas, kg. s^{-1}

G' = gas mass velocity, kg. m^{-2}. s^{-1}

Designing commercial columns by using flooding correlations of this type should take care of two technical factors :

— flooding frequently occurs well below the values predicted by such correlations

— tendency for foaming of amine system

Due to these, Reed and Wood have recommended design rates not exceeding 60% of those flooding [R. M. Reed and W. R. Wood — **Transactions of American Institute of Chemical Engineers, vol. 37/1941/P-363—383]**

[B] Strigle Method The classical method of depicting generalized press-dr correlation (as illustrated in **Fig. 8.7-2.32 above**) uses a logarithmic scale for both the abscissa and the ordinate. And that makes interpolation between parameters of constant pressure-drop difficult. To overcome this difficulty, an alternate generalized press-drop correlation (**Fig. 8.7-2.33**) has been recommended [Ralph F. Strigle (Jr.) — **Random Packings and Packed Towers**, Gulf Publishing Co., Houseton, TX, 1987/P-19]. This correlation utilizes a linear scale for the ordinate into which has been introduced the **capacity factor** (C_s) term.

$$X = \frac{L'}{G'} \bullet \left| \frac{\rho_G}{\Delta \rho} \right|^{0.5}$$

where, $\Delta \rho = \rho_L - \rho_G$
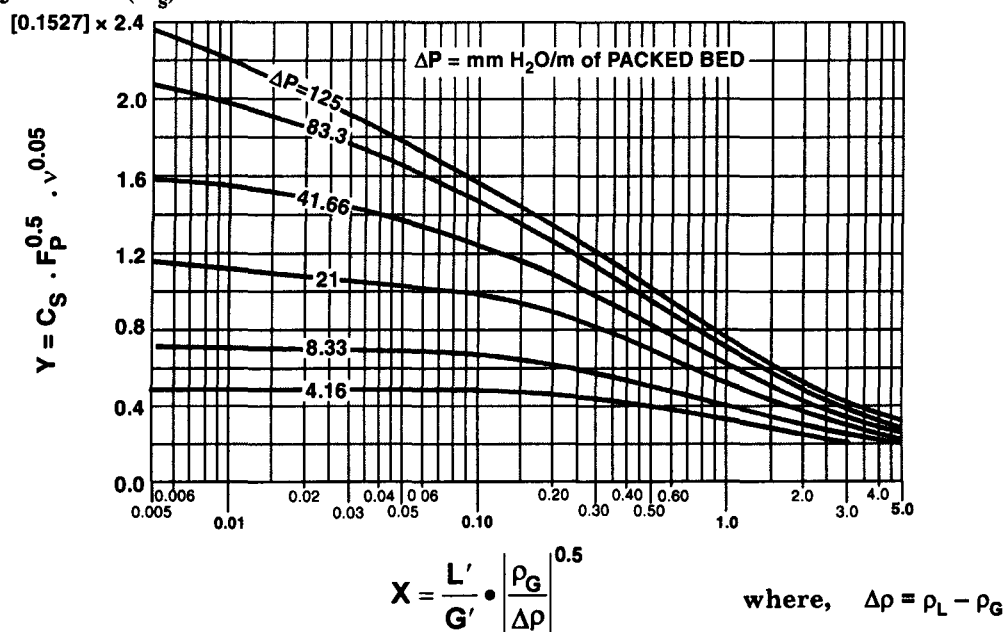
Fig. 8.7-2.33. *Alternate Generalized Pressure-Drop Correlation.*

CO_2-Absorber Design

Example 8.3. Design a CO_2-absorber to treat a dry, feedgas of composition

C-1 : 2.7 mol %

C-2 : 75 mol %

C-3 : 15 mol %

CO_2 : 7.3 mol %

The feed liq is a 30 wt% aqueous diethanolamine solution containing 0.10 mol CO_2 per mol of DEA.

The exit gas is to contain 0.5 mol % CO_2.

Design the absorber on the basis of :

Gas rate	*= 120000 kg. h^{-1}*
Operating pressure	*≈ 2.65 MPa*
Inlet gas temperature	*= 302 K*
Outlet gas temperature	*= 316 K*
Feedgas density	*= 44.53 kg. m^{-3} at operating conditions*
Absorbent liq density	*= 1006 kg. m^{-3}*
Absorbent liq viscosity	*= 2.5 cSt*

The system is foaming and hence bed press-dr is not to exceed 200 Pa. m^{-1} of packed depth.

Tower effluent composition : 0.35 mol CO_2/mol DEA.

Solution : We shall use flooding correlations to design the absorption column.

Step I Mol. Wt. of Feedgas

Basis : 100 kmol

Feedgas component	*Feedgas composition (kmol)*	*Mol. Wt. (kg. kmol^{-1})*	*Mass (kg)*
C-1 (CH_4)	2.7	16	43.2
C-2 (C_2H_6)	75	30	2250.0
C-3 (C_2H_8)	15	44	660.0
CO_2	7.3	44	321.2
		Total	3274.4

∴   Mol. wt. of the feedgas = 32.74 kg. kmol^{-1}

Step – II CO_2 Absorbed

Lean solution (absorbant) : 30 kg DEA/100 kg Sol^n

DEA :   H—N(CH$_2$CH$_2$OH)(CH$_2$CH$_2$OH)   ; Mol. wt. : 105 kg. kmol^{-1}
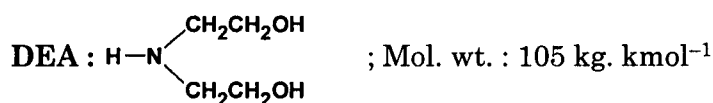
Lean solution concentration = $\dfrac{30}{105}$ kmol DEA/100 kg solution

= 0.2857 kmol DEA/100 kg solution

Mass Balance

Basis : 1000 kg lean solution feed

EXIT GAS $\begin{bmatrix} \text{100kmol INERT} \\ \text{0.5025 kmol } CO_2 \end{bmatrix}$

1000kg LEAN SOLUTION
$\begin{bmatrix} \text{2.857 kmol DEA} \\ \text{0.2857 kmol } CO_2 \end{bmatrix}$

FEED GAS
$\begin{bmatrix} \text{100 kmol INERT} \\ \text{7.874 kmol } CO_2 \end{bmatrix}$

1000 KG RICH SOLUTION
$\begin{bmatrix} \text{2.857 kmol DEA} \\ \text{0.9999 kmol } CO_2 \end{bmatrix}$
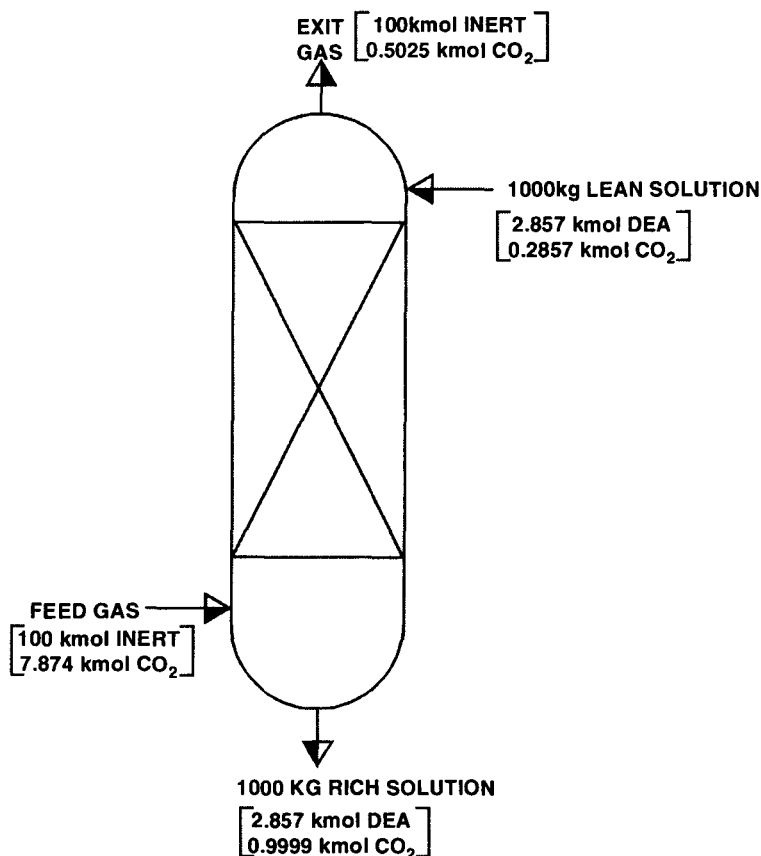
Fig. to Example 8.3

$$\text{Feedgas composition} = \frac{7.3 \text{ kmol } CO_2}{2.7 \text{ kmol C-1} + 75 \text{ kmol C-2} + 15 \text{ kmol C-3}}$$

$$= 0.07874 \text{ kmol } CO_2/\text{kmol Inert Gas}$$

$$= 7.874 \text{ kmol } CO_2 / 100 \text{ kmol Inert Gas}$$

$$\text{Exit gas composition} = \frac{0.5 \text{ kmol } CO_2}{(100 - 0.5) \text{ kmol Inert Gas}}$$

$$= 0.005025 \text{ kmol } CO_2/\text{kmol INERT}$$

$$= 0.5025 \text{ kmol } CO_2/100 \text{ kmol INERT}$$

∴ **CO_2 absorbed** $= 7.874 - 0.5025$

$$= 7.3715 \text{ kmol}/100 \text{ kmol Inert}$$

Now CO_2 absorbed $= 0.35 \text{ kmol per kmol of DEA feed}$

$$= 0.35 \times 2.857 \text{ kmol per 1000 kg absorbant}$$

$$= 0.9999 \text{ kmol } CO_2/1000 \text{ kg absorbant}$$

$$\therefore \quad \frac{7.3715 \text{ kmol CO}_2}{100 \text{ kmol Inert}} = \frac{0.9999 \text{ kmol CO}_2}{1000 \text{ kg absorbant}}$$

$\therefore$ **Inert gas flow** $= \dfrac{100}{7.3715} \times 0.9999$ per 1000 kg absorbant

$= 13.5644$ kmol per 1000 kg absorbant

$\therefore$ **Feedgas flow** $= 13.5644 + \dfrac{7.874}{100} \times 13.5644$

$= 14.6324$ kmol 1000 kg absorbant liq

Rich solution contains 0.9999 kmol CO_2/1000 kg liq

$= 44 \dfrac{\text{kg}}{\text{kmol}} \times 0.9999$ kmol CO_2/1000 kg liq

$= 43.9956$ kg CO_2/1000 kg liq

$\therefore$ **Tower effluent** $= 43.9956$ kg CO_2 + 1000 kg **Liq Feed**

$= 1043.9956$ kg for each 1000 kg **Liq Feed**

Inasmuch as the exit gas gets humidified to an equilibrium water content above the feed DEA solution, so the exit gas stream contains 0.30 mol% water vapor which comes from liq feed.

$\therefore$ **Water vaporized** $= \dfrac{0.30}{100} \times 18$ kg per 100 kg **Liq Feed**

$= 0.54$ kg per 1000 **Liq Feed**

$\therefore$ **Actual tower effluent flow** $= (1000 - 0.54) + 43.9956$ kg per 1000 kg **Liq Feed**

$= 1043.4556$ kg per 1000 kg **Liq Feed**

Step – III Flow Parameter at Tower Bottom

Maximum loading will occur at absorber bottom due to obvious reason

$$X = \frac{L'}{G'} \left[\frac{\rho_G}{\Delta\rho} \right]^{0.5} \qquad \qquad ...(8.7\text{-}2.3)$$

$L' = 1043.4556$ kg per 1000 kg **Liq Feed**

$G' = \left[14.6324 \text{ kmol} \times 32.74 \dfrac{\text{kg}}{\text{kmol}} + 0.54 \right]$ per 1000 kg **Liq Feed**

$= 479.6047$ kg per 1000 kg **Liq Feed**

$\rho_G = 44.53$ kg. m^{-3}

$\rho_L = 1006$ kg. m^{-3}

Substitution in above relationship begets

$$X = \frac{1043.4556}{479.6047} \left[\frac{44.53}{1006 - 44.53} \right]^{0.5} = 0.4682$$

Step – (IV) Capacity Factor (C_s)

The system is foaming and accordingly we're to design the tower so as to limit ΔP up to a maximum of *200Pa per m of packed depth.*

Hence from **Fig. 8.7-2.33**, for

$$X = 0.4682$$
$$\Delta P = 200 Pa.\ m^{-1}$$

we get an ordinate value $Y \approx 0.75$

Let us select 50 mm IMTP® packing.

For this packing, *packing factor is 18* when C_s in ft. s^{-1}.

$$\therefore \qquad Y = C_s.\ F_P^{0.5}.\ \upsilon^{0.05} \qquad\qquad ...(8.7\text{-}2.4)$$

where $F_P = $ *packing factor*, dimensionless

Step – (VII) Tower Cross-section and ID

$$\dot{M}_G = 120000\ kg.\ h^{-1}$$

$$\therefore \qquad A = \frac{\dot{M}_G}{G'/A} = \frac{120000/3600}{10.6413} \quad = 3.1324\ m^2$$

$$D = \sqrt{\frac{4A}{\pi}} = \sqrt{\frac{4\,(3.1324)}{\pi}} \quad = 1.997\ m \simeq 2m$$

Step – (VIII) Irrigation Rate

$$\text{Feedgas flow} = 14.6324\ kmol/1000\ kg\ \textbf{Liq Feed}$$
$$= 14.6324 \times 32.74\ kg/1000\ kg\ \textbf{Liq Feed}$$

$$\therefore \qquad \text{Liq feedrate} = \frac{120000}{14.6324 \times 32.74} \times 1000\ kg.\ h^{-1}$$

$$= 250488\ kg.\ h^{-1}$$

$$\therefore \quad \textbf{Bed irrigation rate} = \frac{250488\ kg.h^{-1}}{1000\ kg.m^{-3}} \times \frac{1}{3.1324\ m^2}$$

$$= 79.4898\ m^3.\ m^{-2}.\ h^{-1}$$

which is suitable for **# 50 IMTP® packing**

Step – (IX) Check

$$\text{Inlet gas rate} = 120000\ kg.\ h^{-1}$$

$$= \frac{120000}{32.74}\ kmol.\ h^{-1}$$

$$= 3665.2412\ kmol.\ h^{-1}$$

$$\upsilon = \text{kinematic viscosity, centiStokes}$$

$$C_s = \text{capacity factor}$$

$$= V\left[\frac{\rho_G}{\Delta\rho}\right]^{\frac{1}{2}} \qquad\qquad ...(8.7\text{-}2.5)$$

$$V = \text{superficial gas velocity, m. s}^{-1}$$

$$\therefore \quad 0.75 = C_s \, (194)^{0.5} \, (2.5)^{0.05}$$

$$\therefore \quad C_s = 0.05143 \text{ m. s}^{-1} \qquad\qquad F_p = 194 \text{ when } C_s \text{ in m. s}^{-1}$$

Step – (X) Feedgas Velocity

$$C_s = V \left[\frac{\rho_G}{\Delta\rho} \right]^{0.5}$$

$$\therefore \quad V = C_s \left[\frac{\Delta\rho}{\rho_G} \right]^{0.5}$$

$$= \left(0.05143 \text{ m.s}^{-1} \right) \left[\frac{1006 - 44.53}{44.53} \; \frac{\text{kg.m}^{-3}}{\text{kg.m}^{-3}} \right]^{0.5}$$

$$= 0.23897 \text{ m. s}^{-1}$$

Step – (XI) Gas Mass Velocity

$$\frac{G'}{A} = V.\rho_G, \text{ kg.m}^{-2}.\text{s}^{-1} \qquad\qquad\qquad ...(8.7\text{-}2.6)$$

$$= (0.23897 \text{ m. s}^{-1}) \, (44.53 \text{ kg. m}^{-3})$$

$$= 10.6413 \text{ kg. m}^{-2}.\text{s}^{-1}$$

$$\textbf{Inert} \text{ rate at inlet} = \left[\frac{2.7}{100} \times 16 + \frac{75}{100} \times 30 + \frac{15}{100} \times 44 \right] 3665.2412 \text{ kg. h}^{-1}$$

$$= 108241.9 \text{ kg. h}^{-1}$$

$$\therefore \textbf{Exit gas rate} = \left[108241.9 + \frac{0.5025}{100} \times 3397.6785 \times 44 \right] + \left[\frac{0.30}{100} \times 3397.6785 \times 18 \right] \text{ kg. h}^{-1}$$

<p align="center">Carbon Dioxide   Water Vapor</p>

$$= 109176.6 \text{ kg. h}^{-1}$$

$$\therefore \quad X_{top} = \frac{250488}{109176.6} \left[\frac{41.4866}{1006 - 41.4866} \right]^{0.5} = 0.4758$$

$$\therefore \text{Capacity factor at the top of the column}$$

$$C_{s,\,top} = 0.23897 \left[\frac{41.4866}{1006 - 41.4866} \right]^{0.5} = 0.04956 \text{ m. s}^{-1}$$

$$\therefore \quad Y = C_s.\, F_p^{0.5}.\, \upsilon^{0.05} = 0.04956 \, (194)^{0.5} \, (2.5)^{0.05} = 0.7226$$

For **X = 0.4758** and **Y = 0.7226**, we get bed press dr **ΔP = 180 Pa. m^{-1}** of packed depth **(Fig. 8.7-2.33)**.

The press dr at the top of the packed bed is **180 Pa. m⁻¹**, which is lower than at the bottom of the bed [ΔP = **200 Pa. m⁻¹**] as expected.

[C] Kohl's Method Carbon dioxide absorption by any of the commonly used amines is liq-film-controlled one. Nevertheless, correlation is generally made on the basis of $K_G.a$ values rather than $K_L.a$ values because $K_G.a$ values can be more readily calculated from experimental data and are more directly applicable to the design of commercial CO_2 absorbers.

Published data indicate that $K_G.a$ increases with increased liq loading and decreases with increased concentration of CO_2 in solution. Also $K_G.a$ decreases it has been reported, with increased partial pressure of CO_2 over the solution. Increasing temperature or amine concentration initially pushes up $K_G.a$ which, after a maxima, drops steadily with further rise in temperature or amine concentration.

Based on the observed effects of temperature, partial pressure, viscosity, CO_2 content of solution, and amine strength, the following correlation was proposed by Kohl for CO_2 absorption in **MEA** :

$$K_G.a = \frac{0.56}{\mu^{0.68}} \left[1 + 5.7\,(0.5 - C)\,M.\,\exp(0.0067\,T - 3.4p)\right] \qquad ...(8.7\text{-}2.7)$$

where,

$K_G.a$ = overall gas-film coefficient, lb mols. h⁻¹. ft⁻³. atm⁻¹

μ = dynamic viscosity of solution, cP

C = concentration of CO_2 in the solution, **mols CO_2 / mol MEA**

M = amine concentration is solution, g. mols. lt⁻¹

T = solution temperature, °F

p = partial pressure of CO_2 above solution, atm.

Source : A. L. Kohl — **AIChE Journal** Vol. **2** (June 1956)/P : 264

This equation can be developed on the basis of runs made at liq flowrate of 695 lb. h⁻¹. ft⁻² (3394 kg. h⁻¹. m⁻²) and gas velocities varying from 0.9 to 0.55 ft. s⁻¹ (0.0274 to 0.1676 m. s⁻¹). Gas velocity has been found not to have an appreciable effect; however liq flowrate is quite important. If the entire resistance to CO_2 absorption lies in the liquid phase, Kohl proposed that $K_G.a$ could be extrapolated to other liq flowrates by assuming it to vary approximately as $L^{2/3}$.

Sherwood and Holloway have found that packing size affected $K_L.a$ and the liq flowrate exponent was also affected by packing used.

Source : T K Sherwood and F A L Holloway — **Transaction of American Institute of Chemical Engineers**, vol. **36** (Dec. 25/1940) / P: 39.

To take into account the effect of liq flowrate and packing size, the following general equation has been suggested for CO_2 absorption by aq. **MEA** solutions in packed bed

$$K_G.a = F \left|\frac{L}{\mu}\right|^{2/3} \left[1 + 5.7\,(C_e - C).\,M.\,\exp(0.0067\,T - 3.4p)\right] \qquad ...(8.7\text{-}$$

$$2.8)$$

where, **L** = liq flowrate, lb. h⁻¹. ft⁻²

C_e = equilibrium concentration of CO_2 in soln, **mols CO_2 / mol MEA**

F = factor to correct for size and type of packing (see **Table 8.7-2.3**)

Table 8.7-2.3. Values of F for different packings

Packing	F × 10³
5 –6 mm Glass rings	7.1
9.5 mm Ceramic rings	3
19×50 mm Tellerettes (polyethylene)	3
25 mm Steel rings	2.1
25 mm Ceramic saddles	2.1
38×50 mm Ceramic rings	0.4 – 0.6

The performance of several commercial packing designs for CO_2 absorption by aq. **MEA** solutions at atmospheric pressure has been studied by several investigators using varied kinds of packings — **Berl saddles, Raschig rings, Tellerettes** etc. and their results are plotted in **Fig. 8.7-2.34.**
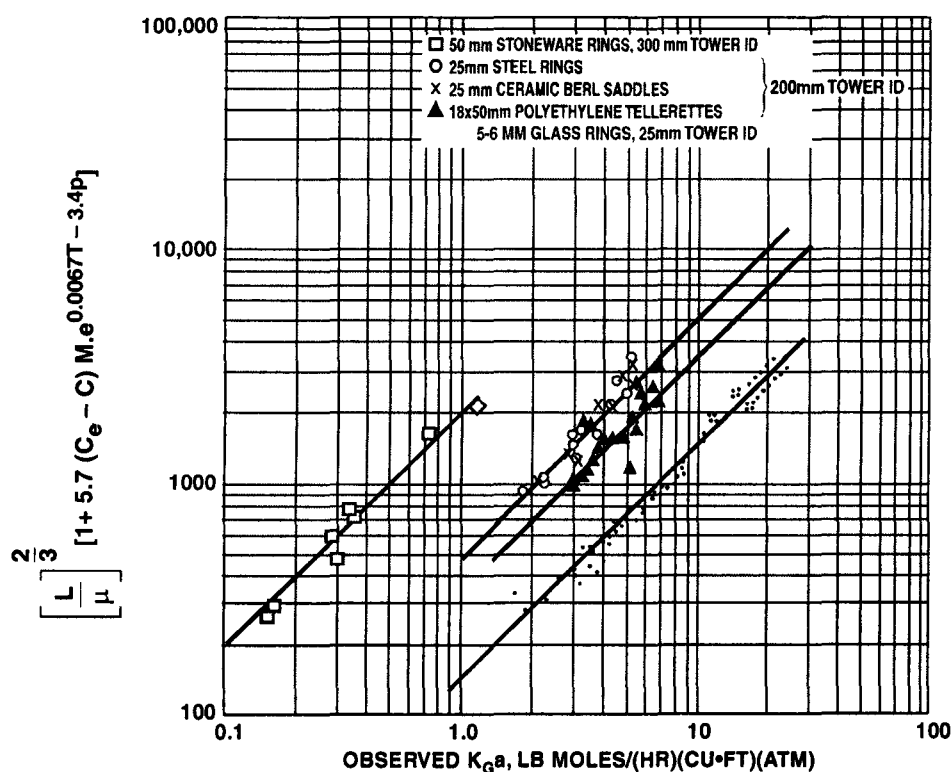
Fig. 8.7-2.34. *Correlation of $K_G \cdot a$ for CO_2 absorption by aqueous MEA solutions in packed towers.*

CO_2 Absorption in Packed Towers by DEA and TEA

Under certain circumstances, the absorption of CO_2 is carried out by using diethanolamine (DEA) and triethanolamine (TEA). However, their absorption coefficient is considerably much less than that with **MEA**. Under the same operating conditions, the $K_G \cdot a$ values for **MEA** solutions are 2 – 2.5 times greater than they are for **DEA** and 20 – 30 times greater than for **TEA**.

Source : A L Shneerson and A G Leibush — **Journal of Applied Chemistry**, vol. 19 (9) / 1946 / P : 869 – 880.

Cryder and Maloney, using 200 mm dia column packed with **18 mm Raschig rings**, found $K_G \cdot a$ values decrease with increased saturation of the solution, increase with increased liq flowrate, and decrease with increased CO_2 partial pressure. $K_G \cdot a$ values for 1N and 2N **DEA** solutions are plotted in **Fig. 8.7-2.35**
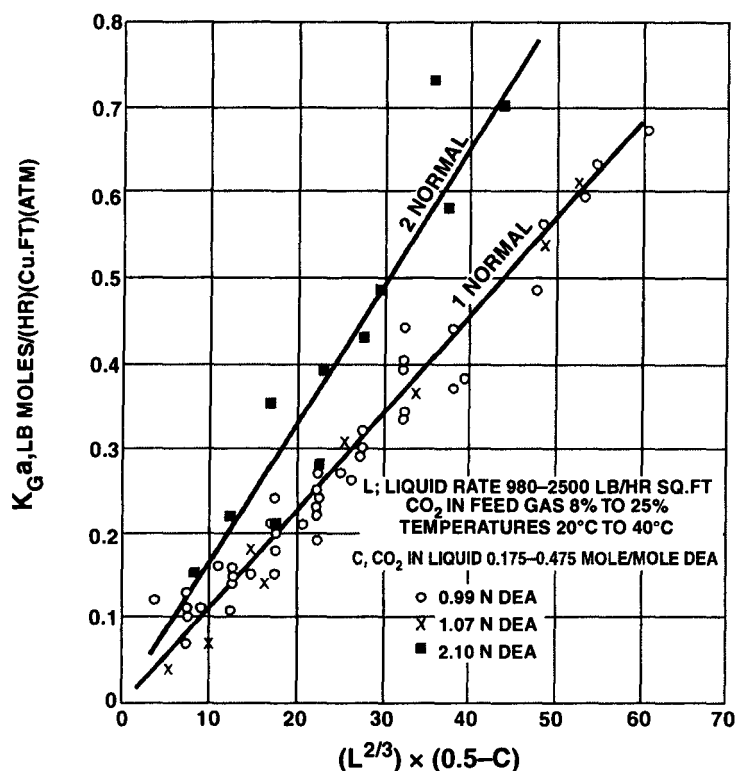
Source : D S Cryder and J O Maloney — Transactions of American Institute of Chemical Engineer, vol. 37 / Oct. 1941 / P : 827 – 852.

Fig. 8.7-2.35. *$K_G \cdot a$ values for CO_2 absorption in aq. DEA for 200 mm column packed with 18 mm Raschig rings.*

Runs made with 3N and 4N DEA solutions resulted in lower absorption coefficients, presumably due to increased viscosity.

Plate Column CO_2 Absorber

The problem of estimating plate efficiency for CO_2-MEA system in plate column was analyzed by Kohl. The following equation was used to relate the absorption coefficient to plate efficiency

$$E_{MV} = 1 - \exp\left[-K_G \cdot (A/V)\right] RT \qquad \ldots(8.7\text{-}2.9)$$

while the following expression was used to correlate the effects of viscosity, amine strength, CO_2-concentration, temperature and partial press of CO_2 on the absorption coefficient

$$K_G (A/V) = \frac{1.2 \times 10^{-4}}{\mu^{0.68}} \left[1 + 1.2 (0.5 - C) M. \exp(0.0067 T - 3.4p)\right] \qquad \ldots(8.7\text{-}2.10)$$

where E_{MV} = Murphree vap efficiency for a single plate

A = interfacial area of contact, $ft^2 \cdot ft^{-2}$ of tray

$\quad$ = **a.h**

a $\;=\;$ interfacial area, $ft^2 \cdot ft^{-3}$ of contact volume

h $\;=\;$ height of contact zone, ft

V $\;=\;$ actual gas velocity. $ft^3 \cdot h^{-1} \cdot ft^{-2}$ of tray

R $\;=\;$ gas constant

T $\;=\;$ temperature, $°R$

$\boldsymbol{\mu}$ $\;=\;$ dynamic viscosity of liq, cP

p $\;=\;$ partial press of CO_2, atm.

$\quad$ This equation was framed on the basis of data obtained on a commercial bubblecap column operating at atmospheric pressure with a gas rate which resulted in an approx. superficial gas velocity of 35 ft. s^{-1} thru cap slots. At reduced velocity an increased plate efficiency was observed presumably due to an increased in A/V. For lower gas velocities (<35 ft. s^{-1}), introduce a correction factor, taking the correction factor equal to unity at 35 ft. s^{-1} (**Fig. 8.7-2.36**)
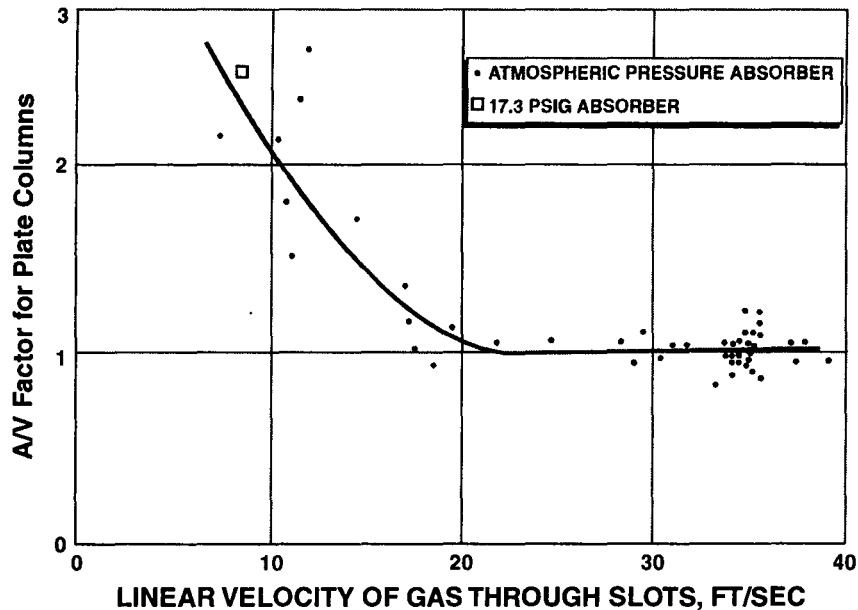
Fig. 8.7-2.36. *Correction factor to adjust K_G. (A/V) for lower gas rates.*

DESIGN PROCEDURE

- Calculate K_G. (A/V) by using equation 8.7-2.10
- Correct it upwards if necessary for a lower gas rate
- Estimate E_{MV} by using equation 8.7-2.9
- Compute the number of plates (n) required to reduce the CO_2 content of a gas stream from y_i to y_o by using the equation

$$n = -\frac{\ln(y_i/y_o)}{\ln(1 - E_{MV})} \qquad \dots(8.7\text{-}2.11)$$

Note : No correlation is available for estimating the plate efficiency of columns operating with **DEA**. Inasmuch as $K_G \cdot a$ for CO_2 absorption in **DEA** solutions is roughly one-half of that for **MEA** **(Table 8.7-2.4)**, it would be expected at approximate plate efficiencies would range from 5 to 15 %.

ACTIVATED MDEA

Application : Removal of CO_2, H_2S and COS from natural gas, synthesis gas and other gases.

Products

1. Treated gas with a CO_2 content of 5 vol % and < 1ppm H_2S.

2. Acid offgas with >99.5 vol% CO_2.

3. CO_2 recovery >99%.

Description The acid components in the feed gas (**Fig.8.7.1**) are removed by absorption in an aqueous solution of **MDEA** and activator with a total amine content of 40 to 50 wt%. The rich solution coming from the absorber column (**1**) is regenerated by flashing and stripping in a stripper column (**2**). Different process configurations can be combined with various solvent types in order to meet the requirement in each application.

Operating conditions

Absorber

Pressure up to 120 bar abs.

Temperature 308K—363K

Regenerator

Pressure 0.5bar abs. (vacuum flash) to 2.4 bar abs.

Economics

Energy consumption for CO_2 removal from ammonia synthesis gas

Power :1kWh/kmol CO_2

Thermal energy consumption for treatment of natural gas

15 to 20 MJ/kmol CO_2 and H_2S removed.

MOC

Mainly carbon steel equipment is deployed in as much as the MDEA solvent is non-corrosive.

AMINE GUARD FS

Application Removal of CO_2,H_2S,COS and RSH · from natural gas; CO_2 from ammonia syngas, etc., by using a solution containing one of the **Ucarsol** family of formulated solvents. When desired H_2S can be removed selectively to provide a superior Claus plant feed and reduce regeneration requirements.
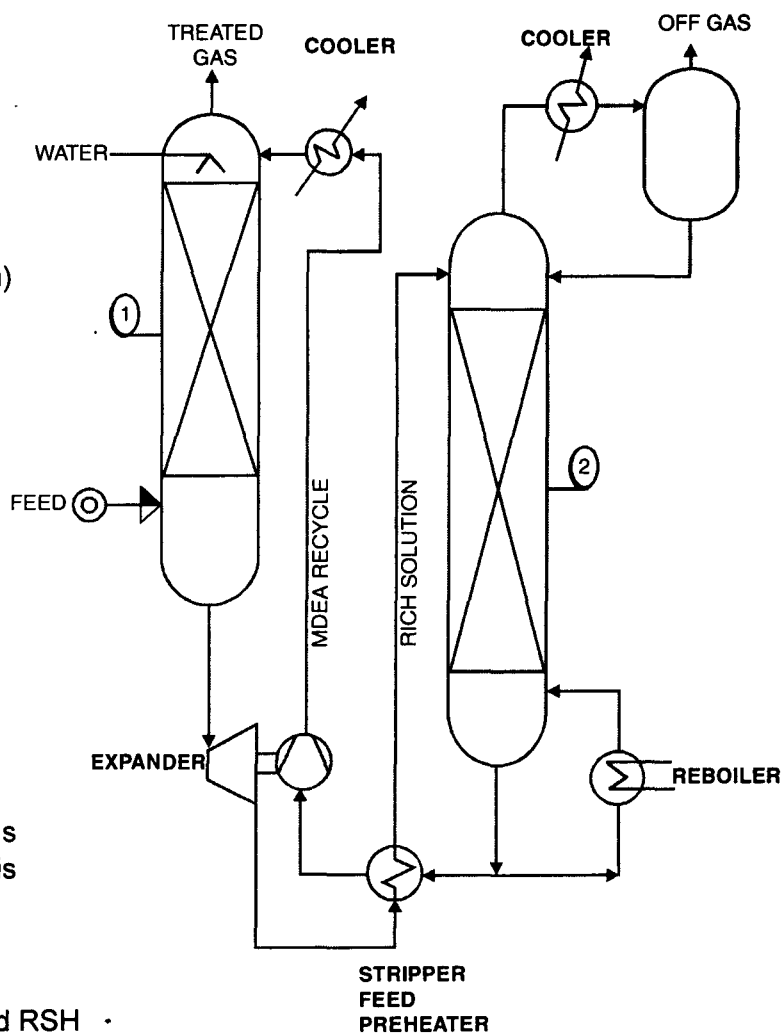
Fig. 8.7.1.

Product Purified gas meeting pipeline or LNG plant specifications or petrochemical specifications as appropriate.

Description The treating solution **(Ucarsol)** absorbs acid gases from the feed in an absorber column **(Fig. 8.7.2)(1)**. The rich solution, loaded with CO_2, H_2S, COS etc., is regenerated by reducing its pressure and then stripping with steam in the stripper tower**(2)**. Waste heat is recovered to generate the steam.

Regeneration energy is minimized by choosing the optimum **Ucarsol** solvent for the situation, using high solvent concentrations and proper selection of process parameters.

Operating conditions

Absorption pressure : 344kPa to 13.78MPa as available.

Feed temperature : ~339K.

(If the feed available at a higher temperature, that heat will be used to supply regeneration heat).

Acid gas content may be up to 50%.

Economics For a 14MMsm³.day⁻¹ natural gas unit having a feed gas containing 6% CO_2 and 1% H_2S, typical costs are as follows :

Fig. 8.7.2.

	Pipeline	LNG feed
Investment, $MM	14.0	17.0
Operating costs, $MM/y	6.0	7.0

1MMsm³ =1 million standard m³ (15° C/100kPa.abs)
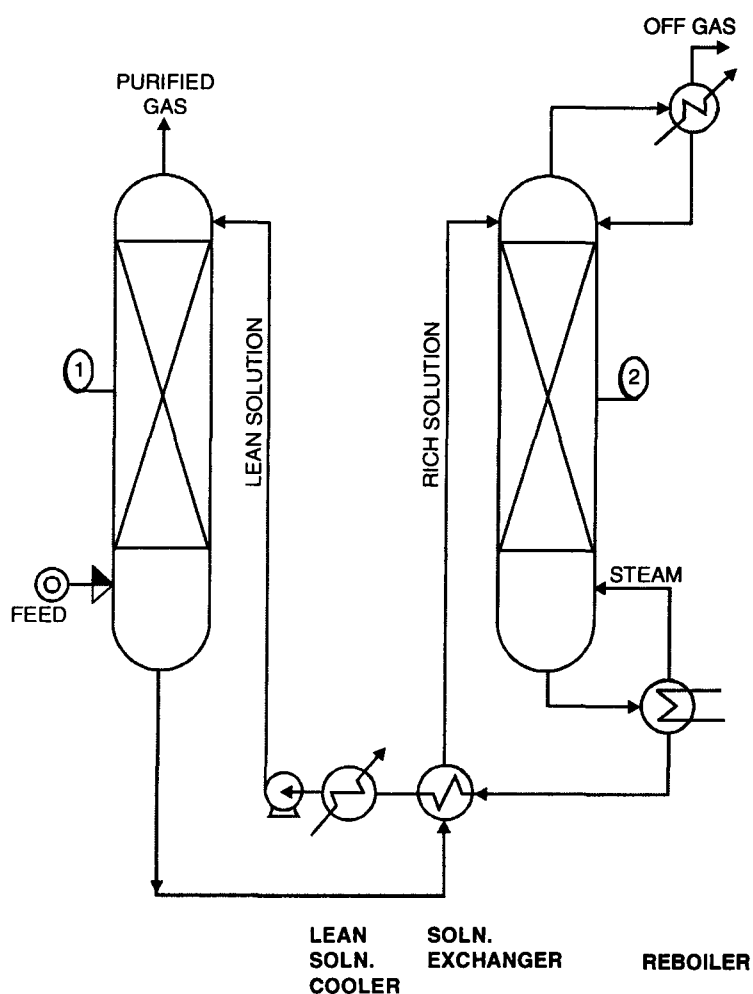
ARI LO-CAT II

Application Removal of H_2S and the production of high purity sulphur from both anaerobic and aerobic gas streams including well-head gas, fuel gas, acid gas, natural gas, carbon dioxide, Claus tail gas, synthesis gas and ventilating air streams.

Description Three types of processing configurations are available depending on the type of gas and the final deposition of the sweet gas. The conventional scheme, shown in **Fig. 8.7.3**, processes gas stream which are combustible or cannot be contaminated with air. In this scheme, the sour gas contacts a dilute, proprietary, iron chelate solution in an absorber **(1)** where the H_2S is absorbed and converted to solid sulphur while the valence state of the iron is reduced from +3 to +2. A variety of absorber configurations
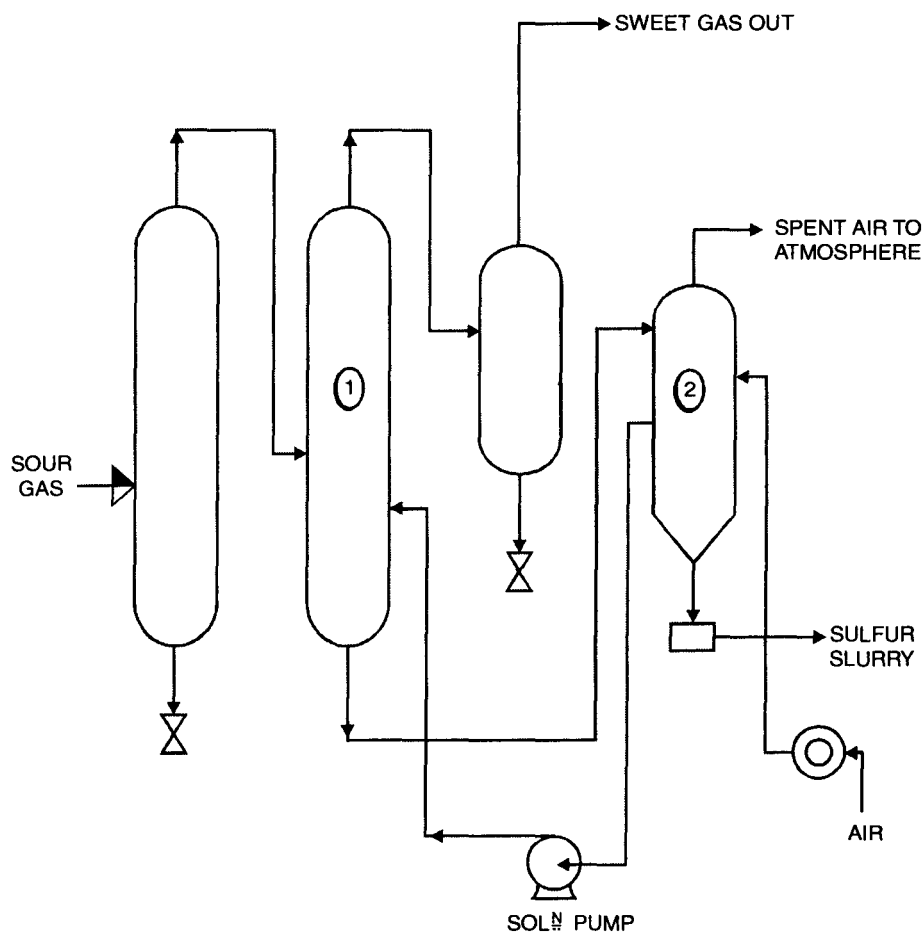
Fig. 8.7.3.

may be used depending on the application. The solution is regenerated in the oxidizer **(2)** and then recycled to the absorber.

In the proprietary auto-circulation processing scheme, the absorber **(1)** and the oxidizer **(2)** are combined into one vessel and separated internally by means of baffles. The design of the baffles enforces a series of "gas lift" pumps, which eliminates the need for circulation pumps. This configuration is ideally suited for treating amine acid gas streams.

The aerobic processing scheme is utilized when processing an air stream in which the absorption of H_2S, the oxidation of sulphide iron to sulphur, the reduction of ferric iron to ferrous iron and the subsequent re-oxidation of the iron all occur currently in the same vessel.

Operating conditions

Pressures From vacuum conditions to ~2MPa

Temperatures From 295K to 395K.

Hydrogen sulphide concentrations From a few ppm to 100%.

Sulphur loadings From about a Kg per day to 25+ ltpd.

NOTES : ☐ No restrictions on type of gas to be treated however, some contaminants such as SO_2 may increase operating costs.

□ Infinite turndown with respect to H_2S concentrations, sulphur loading and gas rate.

□ Recovery of the sulphur product as a slurry, a filter cake or as high purity, molten sulphur. In most cases, sulphur cake can be deposited in a non hazardous landfill.

□ Auto-circulation configuration when treating amine acid gas for remote or unattended operation typical for gas field operation.

BEAVON-OTHERS

Application Purification of **TG** (tail gas) from sulphur recovery units (such as Claus units) and gas stream containing low concentrations of SO_2.

The type of process to be combined with the Beavon treatment depends on the intended disposition of the treated product gas (*e.g.*, additional sulphur recovery; other component recovery; incineration or exhaust while meeting stringent air pollution standards).

> **Beavon processing** converts sulphur compounds to H_2S.
>
> **Beavon-MDEA processing** adds H_2S separation
>
> **Beavon-Selectox processing** converts H_2S to elemental sulphur
>
> **Beavon-Hi-Activity processing** converts H_2S to elemental sulphur.
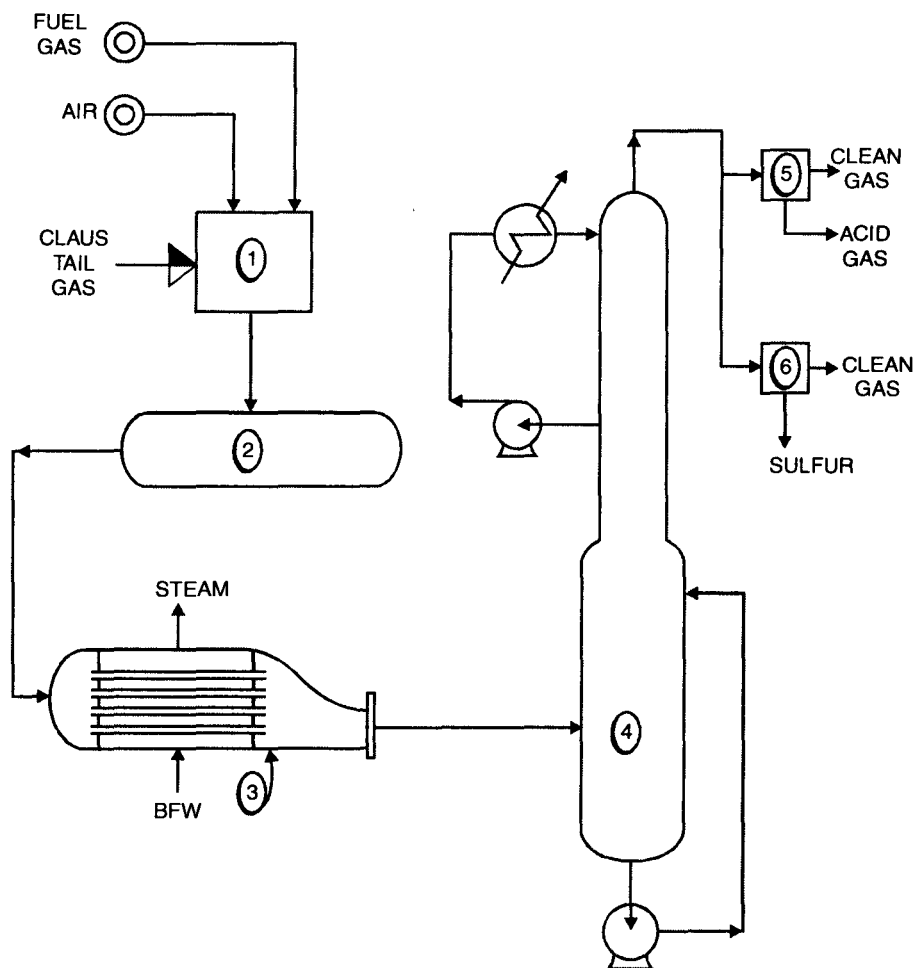
Fig. 8.7.4.

Description In the Beavon step, essentially all sulphur compounds in the feed gas (SO_2, S_x, COS, CS_2) are converted to H_2S.

The feed gas is heated (1) to reaction temperature by mixing with the hot combustion products of fuel gas and air (**Fig.8.7.4**). This combustion is carried out with a deficiency of air to provide sufficient H_2 and CO to convert all of the sulphur and sulphur compounds to H_2 S.

The heated gas mixture is then passed through a catalyst bed (2) where all sulphur compounds are converted to H_2S by hydrogenation and hydrolysis. The hydrogenated gas stream is cooled in a steam generator (3) and then by direct contact (4) with a buffer solution before entering the selected H_2S removal process.

Beavon-MDEA One of several processes used to remove H_2S is by absorption (5) in a solution of MDEA (methyl diethanolamine) or one of the recently developed highly selective amine type solvents. The clean tail gas contains less than 10ppm H_2S when using the newer solvents. When this combination is operating on a Claus tail gas, the separated H_2S can be recycled to the Claus unit.

Beavon-Selectox An alternative (6) for removing the H_2S is to convert it to elemental sulphur by the Selectox process.

Beavon-Hi-Activity Another alternate for removing the H_2S is to oxidize it directly to elemental sulphur by the Hi-Activity process.

OPERATING CONDITIONS

Operating pressures are near atmospheric (throughout the system)

Operating temperature 805K to 1005K (hydrogenation/hydrolysis reactor)

Efficiency Sulphur recovery of Claus plus Beavon-Selectox or Beavon MDEA is more than 99% or 99.9%, respectively.

MOC All equipment are essentially made of CS.

CLAUSPOL

Application This is a Claus tail gas treatment process. This is a simple, low capital/operating cost process that removes hydrogen sulphide and sulphur dioxide in Claus effluents without the use of hydrogen and little in the way of utilities.

Debottlenecking Claus systems is also attractive proposition as there are no recycle streams from *Clauspol* to Claus units to take up reactor space and there is no theoretical limit on the quantity of sulphur recoverable in the Clauspol process. Some of the Claus sulphur recovery duty can therefore be shifted to the Clauspol unit at the same time maintaining high sulphur recovery efficiencies.

Efficiency Overall sulphur recovery yields of 99.9% can be attained.

Description This is the 3rd generation of the *Clauspol* process first introduced in the 1970s.

Claus TG (1) enters the bottom of the Clauspol contacting column (packed bed) (2) where the circulating solvent absorbs the H_2S and SO_2 (**Fig.8.7.5**).

The solvent contains an inexpensive dissolved catalyst that promotes the Claus reaction in the liquid phase producing elemental sulphur.

The sulphur is recovered from the solution as liquid via a proprietary separation section (3) and is sent to the sulphur storage area.
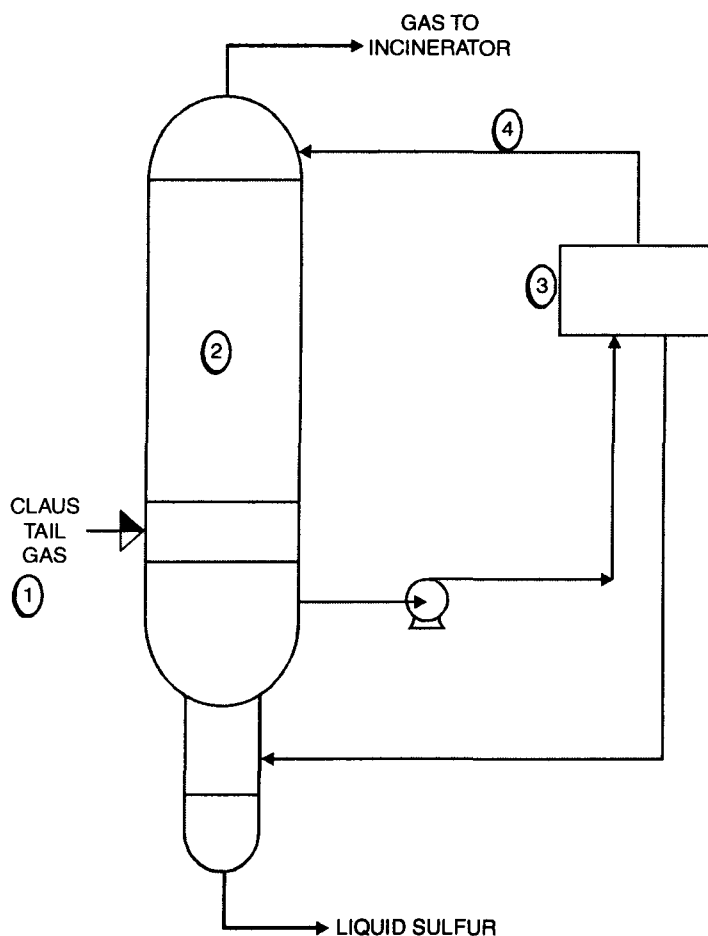
Fig. 8.7.5.

The lean solvent **(4)** is returned to the top of the contacting column.

Operating conditions The reaction proceeds at atmospheric pressure and at low temperatures (343K to 403K) for more favorable equilibrium. This and the continuous withdrawal of product sulphur from the reaction environment explain the high efficiency of the process. The pressure drop across the packing is very small so no blower is required.

Economics For a *Clauspol* unit treating a typical Claus unit tail gas, combined production of 100 metric tons of sulphur per day (ISBL 1996 Gulf Coast location).

Investment*, million US$	5
Catalyst consumption, million US$.y^{-1}	0.024
Initial solvent charge, million US$	0.13
Power ,kWh	170
Cooling water, m^3.h^{-1}	50
LP steam, metric tons.h^{-1}	1—3

*[excluding engineering & licence fees]

CO₂ RECOVERY

Application Recovery of high purity CO_2 from oxygen-containing gases such as boiler flue gases (FG), gas turbine exhausts and waste gases

Description This is Kerr-McGee/ABB Lummus Global absorption/stripping technology. CO_2-containing feed gases are first cooled and scrubbed **(1)**, if necessary, to reduce SO_2-levels **(Fig.8.7.6)**. The gases are boosted slightly in pressure before entering the recovery system.

This is an amine-based system that operates absorption/stripping using a 15% to 20% monoethanolamine **(MEA)** solution. Feed gases are sent to an amine absorber **(2)** where they are scrubbed with **MEA** to recover CO_2. The scrubbed gases are vented to the atmosphere after water washing in the absorber's top to minimize **MEA** losses.

Rich solution from the **MEA** absorber is preheated in an exchanger **(3)**, flashed **(4)** and sent to a stripper **(5)** where CO_2 is recovered overhead. Condensate from the stripper overhead is returned to the system

Lean **MEA** from the stripper **(5)** is cooled in the H.E.s **(3 & 7)**, filtered **(6)** and returned to the absorber. Periodically, a batch reclaiming operation **(8)** is conducted to purge MEA degradation products and to recover **MEA** by decomposing heat-stable salts. The bottoms from the reclaiming operation may be burned as boiler fuel.

CO_2 recovered from the stripper overhead is compressed and used as a vapor product, or in some cases, it is dried and liquefied using a standard ammonia refrigeration system to produce a liquid product.
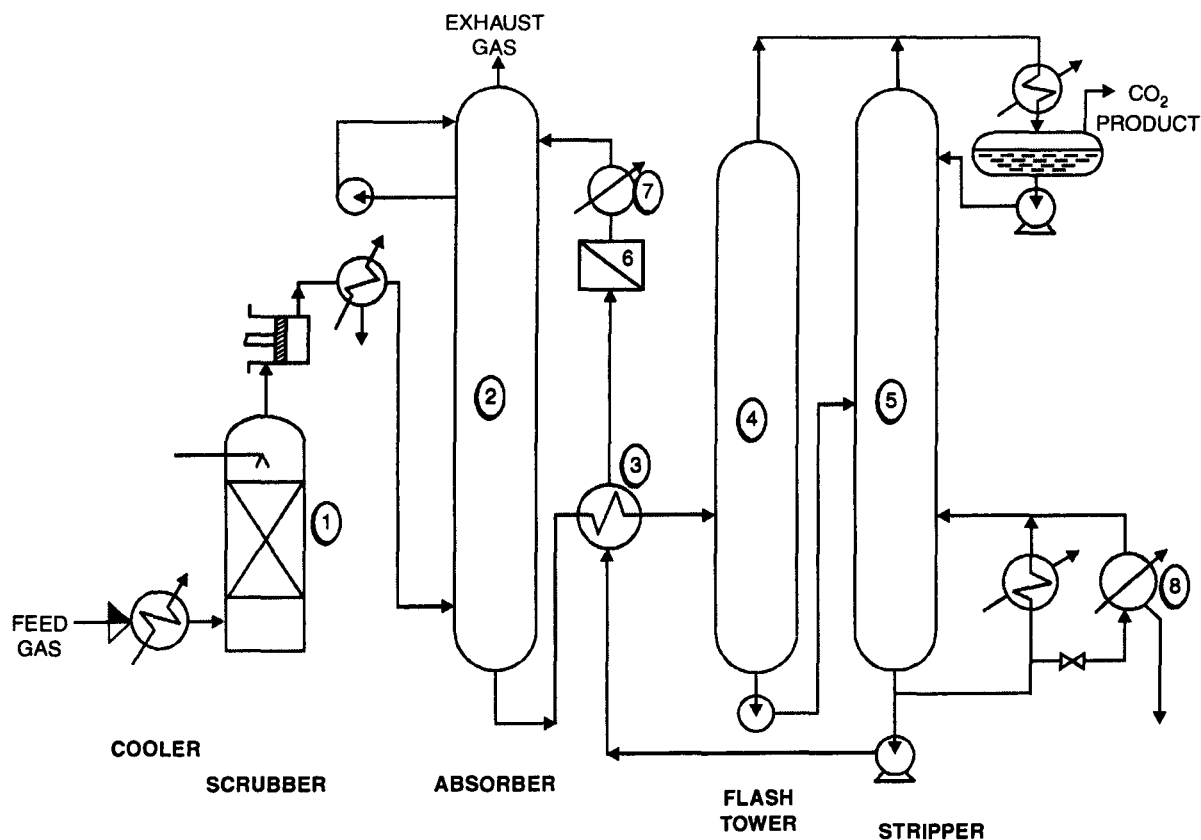
Fig. 8.7.6.

Operating conditions Absorption and stripping operations take place at slightly above atmospheric pressure. Feed gases can contain upto 15 vol% oxygen, though economics are favored by high CO_2 and low oxygen concentrations in the feed. The process can recover CO_2 from flue gases containing from 3 to 15 vol% (dry basis) CO_2. Moderate levels of SO_2 and NO_x in the feed are acceptable. SO_2 prescrubbing is required only with SO_2-levels higher than 100ppmv.

Plant Availability The plants have demonstrated high degree of availability. Operating units with availability factors in excess of 98% are common.

Economics Typical capital investment for a 200 tpd CO_2 plant is US$9 million. Liquefaction facilities would add roughly US$4 million to the capital investment. Typical utility and chemical requirements per ton of CO_2 recovered are as follows:

Product	Gaseous	Liquid
LP Steam, ton	2.3	2.3
Water, cooling, m^3	95	114
Power, kW. h	100	240
Chemicals, US $	2.25	3.00

CLINTOX

Application Reduction of SO_2 emissions from a Claus plant. As an add-on unit to an existing Claus plant, the **Clintox** process increases both the capacity and capability of the system.
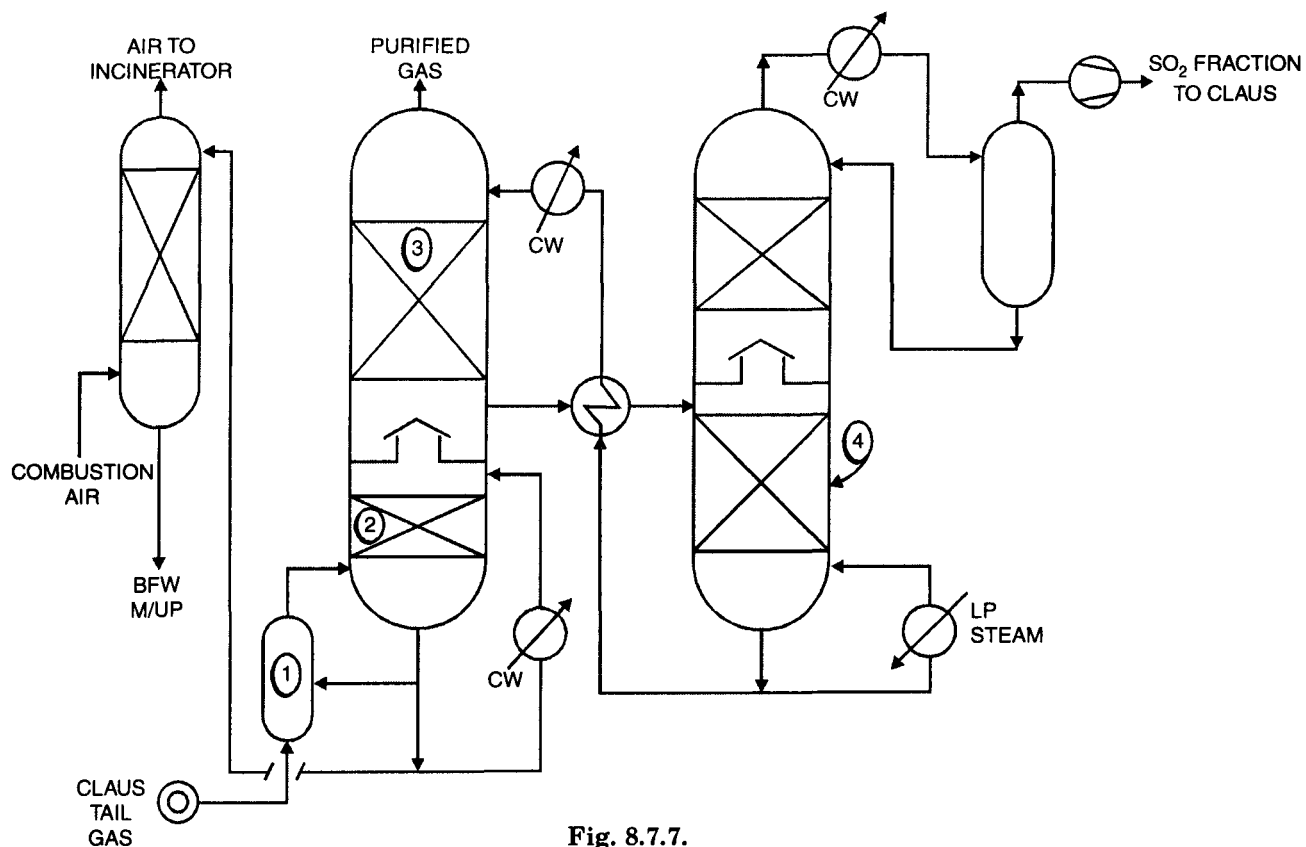
Fig. 8.7.7.

Description The process uses a highly efficient physical scrubbing mechanism to remove SO_2 from the incinerated TG (tail gas) of a Claus unit. The recovered SO_2 is recycled to the inlet of the Claus unit. Any reduced efficiency in the upstream Claus unit gets compensated for by an increase in the efficiency of the **Clintox** process to capture and recycle the uncovered SO_2.

The simplified flow diagram (**Fig.8.7.7**) shows how the Claus TG is quenched (**1**) by injection of water before entering the direct contact cooler (**2**). In the scrubbing section (**3**), SO_2 is washed from the gas. The purified TG is vented overhead.

The SO_2-rich scrubbing solvent is preheated and passed to the regenerator column (**4**). The reboiler for the column operates at about 373K to 413K and can be heated with waste heat, *e.g.*, low pressure steam from the last sulphur condenser of the upstream Claus unit. The concentrated SO_2 fraction leaving the regenerator is cooled (by heat exchange with cooling water), compressed (usually by a water seal pump) and recycled to the Claus plant front end. The lean solvent from the regenerator transfers heat to the rich solvent and to cooling water before returning to the scrubber (**3**).

Since the contact cooler (**2**) also captures most of the Claus reaction water, the surplus water is stripped (**5**) using combustion air intended for thru upstream incinerator. The stripped water can be used as boiler feed water makeup.

Operating conditions Since the efficiency of the **Clintox** physical scrubber increases when the tail gas SO_2 concentration increases, a less efficient Claus unit is tolerated. Thus a combination of **Claus** and **Clintox** units gives a sulphur recovery system that is emissions below 100 ppm total sulphur.

Economics Investment and operating costs run favorably with conventional processes.

Utilities Typical for unit, including incinerator, associated with a 100 long tpd **Claus** plant:

Electrical power (include. Cooling tower), kWh	240
Fuel (*e.g.*, sour water off gas), kmol.h^{-1}	8.5
Steam,> 25 bar press., tph (generated)	(2.9)
Steam, 1.5 bar press., tph	1.0
Solvent, U.S.\$.h^{-1}	5.80
Water, cooling makeup, m^3.h^{-1}	3.0

ECONAMINE

Application Removal of acidic impurities—H_2S and CO_2— with partial removal of COS from gas.

Product Treated gas (H_2S < 0.25 gr/100 scf; CO_2 as low as 50ppmv); concentrated acid gases.

[gr = grain; scf = standard cubic foot]

Description Absorption (**1**) using aqueous solution of diglycolamine (**DGA**), a primary alkanolamine (**Fig. 8.7.8**). Typical amine system flow.

Heated rich solution is regenerated (**2**). Regenerator heat furnished by any suitable media.

Condensed water is recycled for further processing.

Lean solution recycled through exchangers and coolers to contactor.

Operating conditions Solution is typically 65 wt% **DGA**. High concentration permits low circulation and regenerator heat.

Note: DGA degradation by COS and CO_2 is reversible by reclaiming at elevated temperatures.
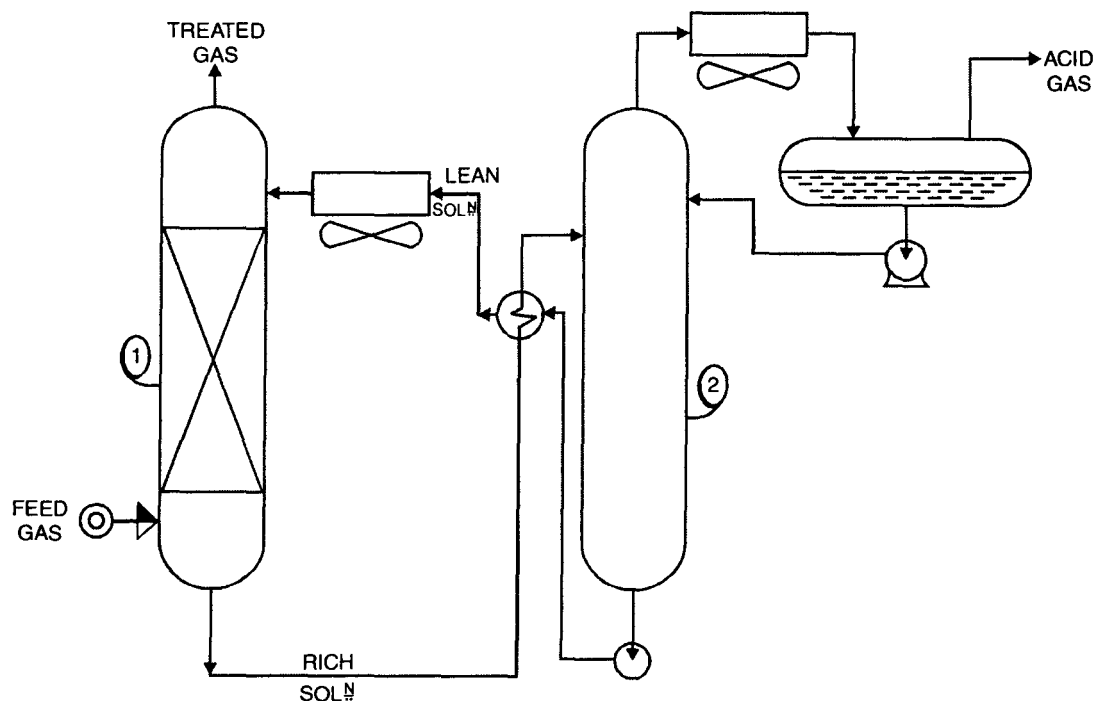
Fig. 8.7.8.

Economics Aqueous **DGA** freezes below 215K; thermally stable to 655K. Vapor phase losses are insignificant. HC (hydrocarbon) content of acid gases is also insignificant. **DGA** is suitable for air-cooling with high ambient temperatures.

FLEXSORB SOLVENTS

Application Removal of H_2S selectively or removal of a group of acidic impurities

(H_2S, CO_2,COS,CS_2 and mercaptans) from a variety of streams, depending on the solvent used.

Flexsorb SE or **SE Plus solvent** is used on : hydrogenated Claus plant **TG** (tail gas) to give H_2S ranging down to H_2S < 10 ppmv; pipeline natural gas to give H_2S < 0.25 gr/100 scf; or Flexicoking low kJ fuel gas. The resulting acid gas byproduct stream is rich in H_2S.

Flexsorb PS Solvent yields a treated gas with : H_2S < 0.25 gr/100scf, CO_2 £ 50 ppmv COS and CS_2 < 1 ppmv, mercaptans removal > 95%. This solvent is primarily aimed at natural gas cleanup. The byproduct stream is acid concentrated acid gases.

Flexsorb HP operates on hot potassium carbonate-based chemistry. The system is also compatible with H_2S. The gases can be purified to less than 30ppmv CO_2.

Description A typical amine system flow scheme is used **(Fig.8.7.9)**. The feed gas contacts the treating solvent in the absorber **(1)**. The resulting rich solvent [bottom stream] is heated and pumped to the regenerator **(2)**. Regenerator heat is supplied by any suitable heat source. The lean solvent from the regenerator is sent through rich/lean solvent exchangers and coolers before returning to the absorber.

Flexsorb SE solvent is an aqueous solution of a new hindered amine.

Flexsorb SE Plus solvent is an enhanced aqueous solution which has improved H_2S regenerability.

Flexsorb PS solvent is a hybrid solution consisting of a hindered amine, a physical solvent and water.
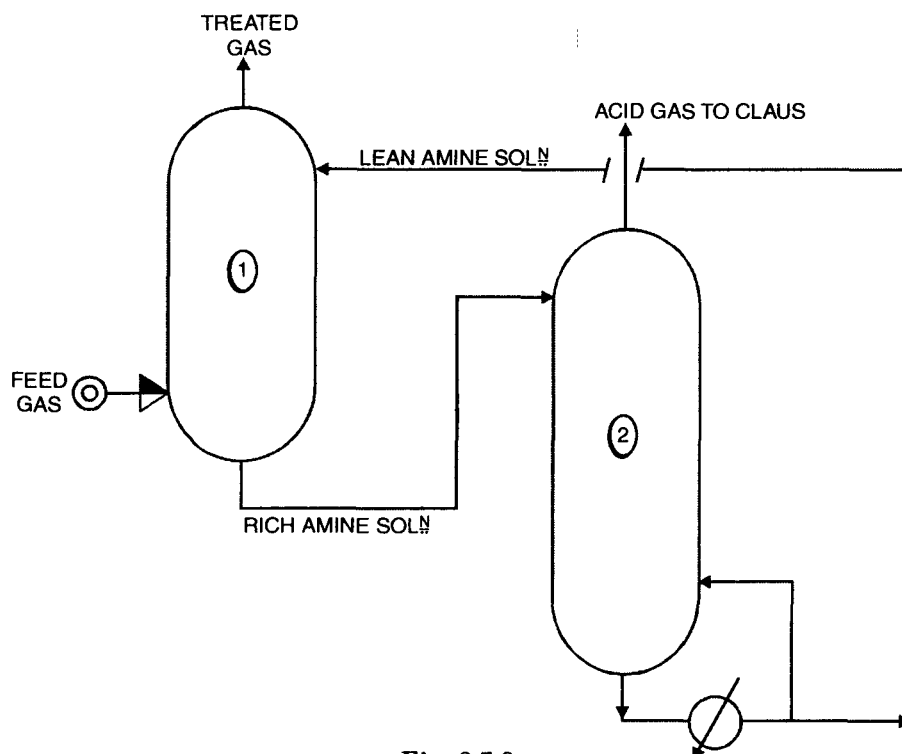
Fig. 8.7.9.

Flexsorb HP is a hot potassium carbonate-based system containing a hindered amine promoter.

Economics Lower investment and energy requirements based primarily on requiring 30% to 50% lower solution circulation rates.

PURISOL

Application Removal of acid gases from natural gas, fuel gas and syngas by physical absorption in NMP (N-methyl-pyrrolidone). Typical cases: 1. High CO_2 contents to low residual level, 2. Bulk acid gas removal to moderate purity by simple flash regeneration, 3. Selective H_2S removal. Ideally suited for (3) in an IGCC based on POX of coal or oil, as NMP is the most selective solvent on the market. It is a cheap, stable, non-corrosive and easily available solvent with a broad range of further industrial applications.

Description Raw gas from a POX of heavy residue is cooled **(Fig.8.7.10)**, HCN and organic sulphur compounds are removed in prewash **(1)**. Hot-regenerated, lean solvent, cooled slightly below ambient temperature removes the H_2S in the main absorber **(1)**. NMP traces are eliminated by back washing with H_2O on top of **(1)**. H_2S-laden solvent from **(1)** is flashed at medium pressure in a re-absorber **(2)** wherein H_2S traces in the flash gas are re-absorbed by a small quantity of lean NMP. The sulphur-free gas from **(2)** is compressed back to the produced fuel gas **(1)**. Flashed solvent from **(2)** is heated by heat exchange with hot lean solvent and flashed again **(3)**. It is finally hot regenerated in **(4)** .The resulting, cooled acid gas, very rich in H_2S is processed in an Oxy Claus unit, the tailgas is hydrogenated, water formed is removed by quenching, recompressed to re-absorber **(2)** for desulfurization and finally ending up in fuel gas.

The closed cycle is offgas free and allows for a high degree of desulfurization. It leads to a net gain of valuable gas plus the recycled CO_2 increasing power output of the gas turbine. Thus increasing overall efficiency of the IGCC plant.
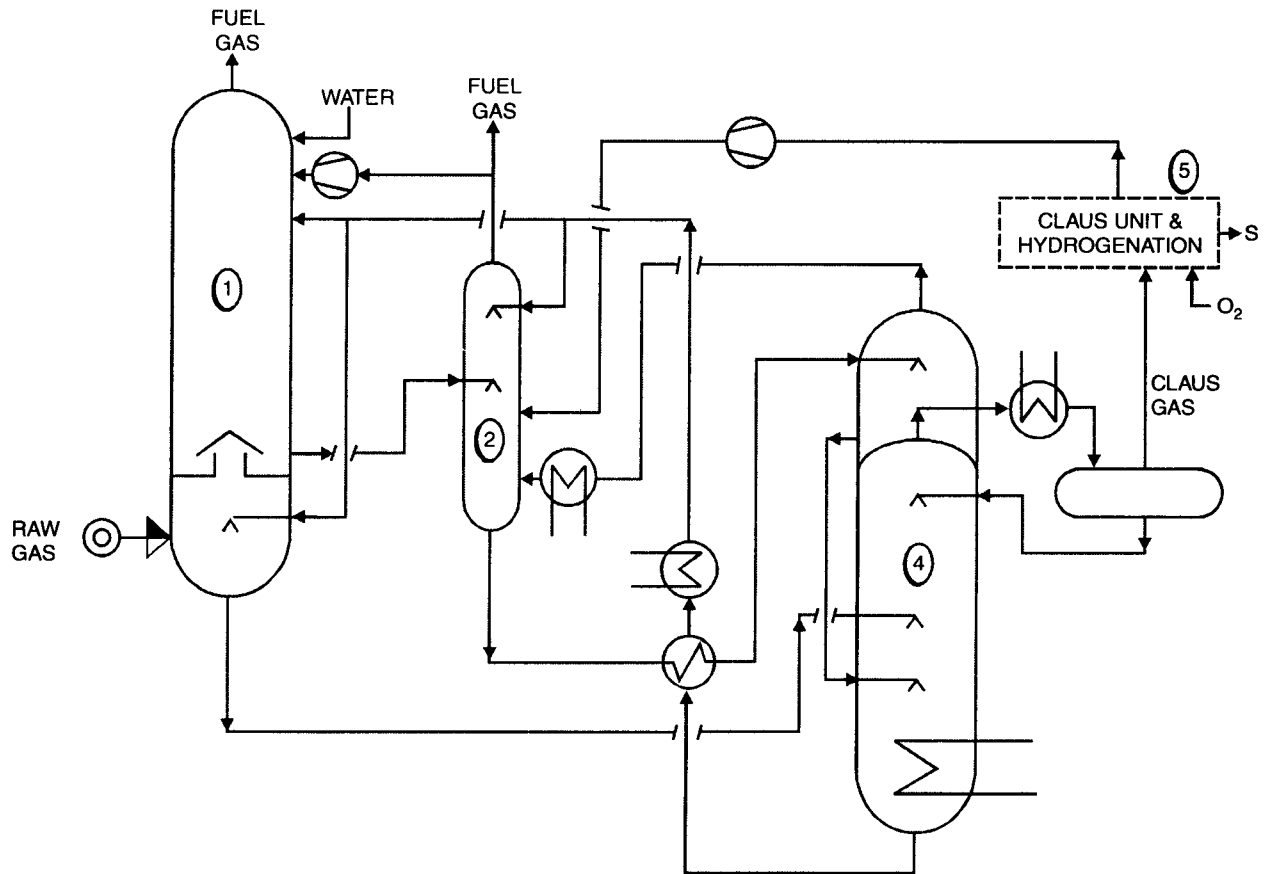
Fig. 8.7.10.

Material balance for a 500 MV IGCC power plant in mol%

Composition	Raw Gas	Fuel Gas
H_2	43.12	43.36
N_2 + Ar	1.49	2.39
CO + CH_4	45.9	45.96
CO_2	8.27	8.38
H_2S + COS	1.20	< 50 ppm
Flow, kmol.h^{-1}	18666.3	18610.0
Pressure, bar	52.0	49.5

Utilities

Power (shaft) (without power recovery)	4.3 MW
Medium pressure steam	20.6 tph
Cooling water (Δt=10°C)	1650 m^3.h^{-1}
NMP vapor loss	2 kg.h^{-1}
Demineralized water	2.2 tph

RESULF

Application Purification of TG from sulphur recovery unit (SRU) for incineration. **Resulf, Resulf-10** and **Resulf-MM** units are easily retrofitted to existing SRU complexes. They feature a low unit pressure drop and can make use of latest specialty solvents to lower energy consumption and maximize flexibility.

Products Treated vent gas from a **Resulf-MM** unit typically contains 1,000ppm H_2S and must be incinerated. Treated vent gas from a **Resulf** unit typically contains less than 150ppmv H_2S and is oxidized in an incinerator before venting to the atmosphere. Vent gas from a **Resulf-10** unit has a maximum of 10ppmv H_2S and may not require incineration.

Description Heated in the feed heater, SRU TG is mixed with a reducing gas containing H_2 **(Fig.8.7.11)**. The heated stream is then passed through the reactor **(1)**, where the SO_2, elemental sulphur and other sulphur containing compounds, such as COS and CO_2, are converted to H_2S. Hot gas leaving the reactor is cooled in a waste heat steam generator. The gas is further quenched in a direct contact water cooler **(2)** The overhead gas stream is fed to the absorber **(3)** where the downward flowing lean solvent contacts the up-flowing gas and absorbs nearly all the H_2S and only part of the CO_2. Rich solvent is then sent to the generator **(4)** where the H_2S and CO_2 are removed by steam stripping and lean solvent is produced. Acid gas from the regenerator is recycled to the SRU. Lean solvent from the regenerator is cooled and returned to the absorber.

Operating condition The **Resulf** units use **MDEA** or formulated **MDEA** as a solvent. **Resulf-10** units are
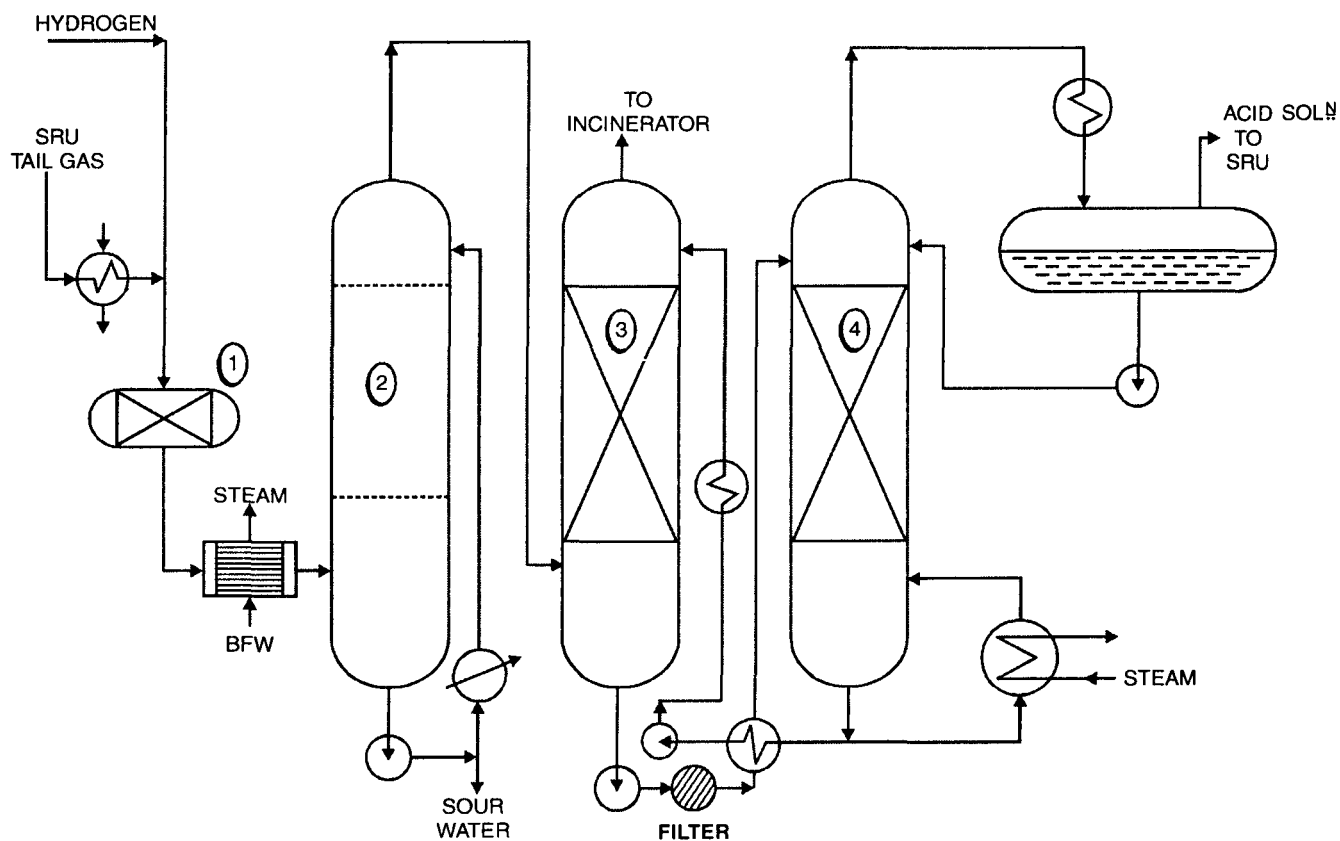
Fig. 8.7.11.

designed for using specialty amines such as formulated **MDEA**. **Resulf** units use generic **MDEA** solvents. **Resulf-MM** use amine from the primary amine unit (**MEA, DEA** or **MDEA**).

Economics Plate and frame heat exchangers have been used to reduce capital costs. Modular designs can also be used to reduce capital costs while maintaining critical project schedules. The cost for **Resulf-MM** is significantly lower than **Resulf** or **Resulf-MM** and **Resulf** technologies are that they can be inexpensively upgraded.

RECTISOL

Application Removal of acid gas using an organic solvent at low temperatures. In general, methanol is used as the preferred solvent for H_2S, COS and CO_2 removal whereby organic and inorganic impurities are also removed. It is possible to produce a clean gas with less than 0.1 ppm sulfur and a CO_2 content down to the ppm range. The main advantage over the other processes is the use of a cheap, stable and easily available solvent, a very flexible process and low utilities.

Description Rectisol unit is meant for the selective desulfurization and CO_2 removal from the raw gas for the production of DSG (desulfurized gas) and DCG (decarbonated gas) for the generation of methanol synthesis gas. Raw gas (from **SGP-POX**) is cooled and trace components are removed in the prewash **(1)** with cold methanol **(Fig. 8.7.12)**. Prewashed gas is desulfurized **(1)** by using CO_2-laden solvent down to
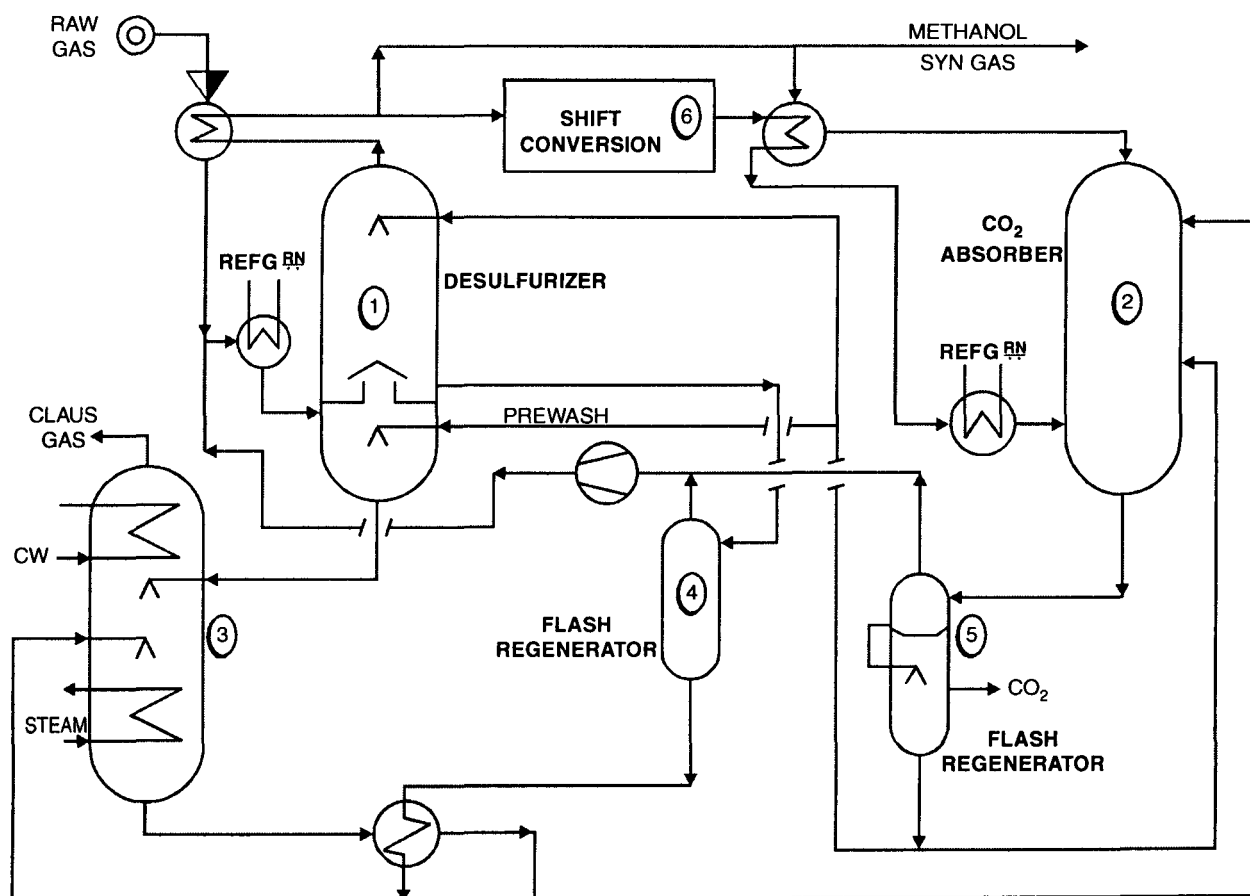
Fig. 8.7.12.

0.1 ppm. H_2S-laden solvent is then regenerated first by flashing to medium pressure **(4)** to recover H_2 and CO and second by heating to boiling temperature and stripping with methanol vapors **(3)**. The stripped H_2S enriched gases are sent to a Claus unit. The portion of the desulfurized gas which is shifted to the CO-Converter **(6)** has a typical CO_2 content 33%. Shifted gas reenters the **Rectisol unit**, is cooled and the CO_2 is removed in a two stage absorber **(2)**. In the lower section, the gas CO_2 content is reduced to about 5% using flash-regenerated methanol. Remaining CO_2 is removed using hot regenerated **(3)**, cold methanol in the upper section, thus about 3% CO_2 is contained in the synthesis gas. The flashed CO_2 is free of sulfur and can be discharged to atmosphere or used further. The refrigeration balance of the system is maintained by a conventional refrigeration unit. Methanol is injected in the raw gas cooling to prevent icing. The condensed methanol-water mixture is separated in a methanol-water column, (not shown).

Material balance for a 2,000-tpd methanol plant in mol%

Composition	Raw gas	Syngas	CO_2	Claus gas
H_2	43.80	67.69	0.59	1.38
N_2—Ar	0.25	0.25	<0.01	0.03
CO—CH_4	52.57	29.03	0.26	8.96
CO_2	2.30	3.03	99.15	42.28
H_2S + COS	1.08	<0.1 ppm	traces	47.35
Flow. $Kmol.h^{-1}$	8482.5	8,415.0	1,868.7	193.5
Pressure, bar	56	48.5	1.2/Ambient	2.5

Utilities

Power (shaft) (without power recovery)	1,640 kW
Low-pressure steam	5.5 tph
Refrigerant at 242K	4,200 kW
Cooling water ($\Delta t=10°C$)	133 $m^3.h^{-1}$
Methanol vapor loss	40 $kg.h^{-1}$

SCOT

Application Removal of sulfur compounds from TG of sulfur plants to comply with permissible air emission limits by using the **Shell Claus Offgas Treating (SCOT)** process.

Description The Claus tail gas feed to the **SCOT** process is heated to 523K to 673K with an in-line burner or heat exchanger **(1)** with optionally added H_2 or a mix of H_2/CO **(Fig. 8.7.13)**. If reducing gas H_2 or CO, is unavailable, an in-line burner **(1)** is operated substoichiometrically to produce reducing gas.

The heated gases are then allowed to flow through a catalyst bed **(2)** where sulfur compounds, including CS_2 and COS, get substantially reduced to H_2S.

The H_2S-laden gas is then cooled to about 313K in a heat recovery system **(3)** and in a quench tower **(4)**, followed by selective H_2S removal in an amine absorber **(5)**, to reduce H_2S load down to typically 10 to 400 ppm level.

The acid gas from the solvent regenerator is recycled to the sulfur plant for recovery of sales grade sulfur. The absorber offgas is thermally or catalytically incinerated, the liberated heat is recovered by generating steam or by exchange **(1)** with the Claus tail gas.
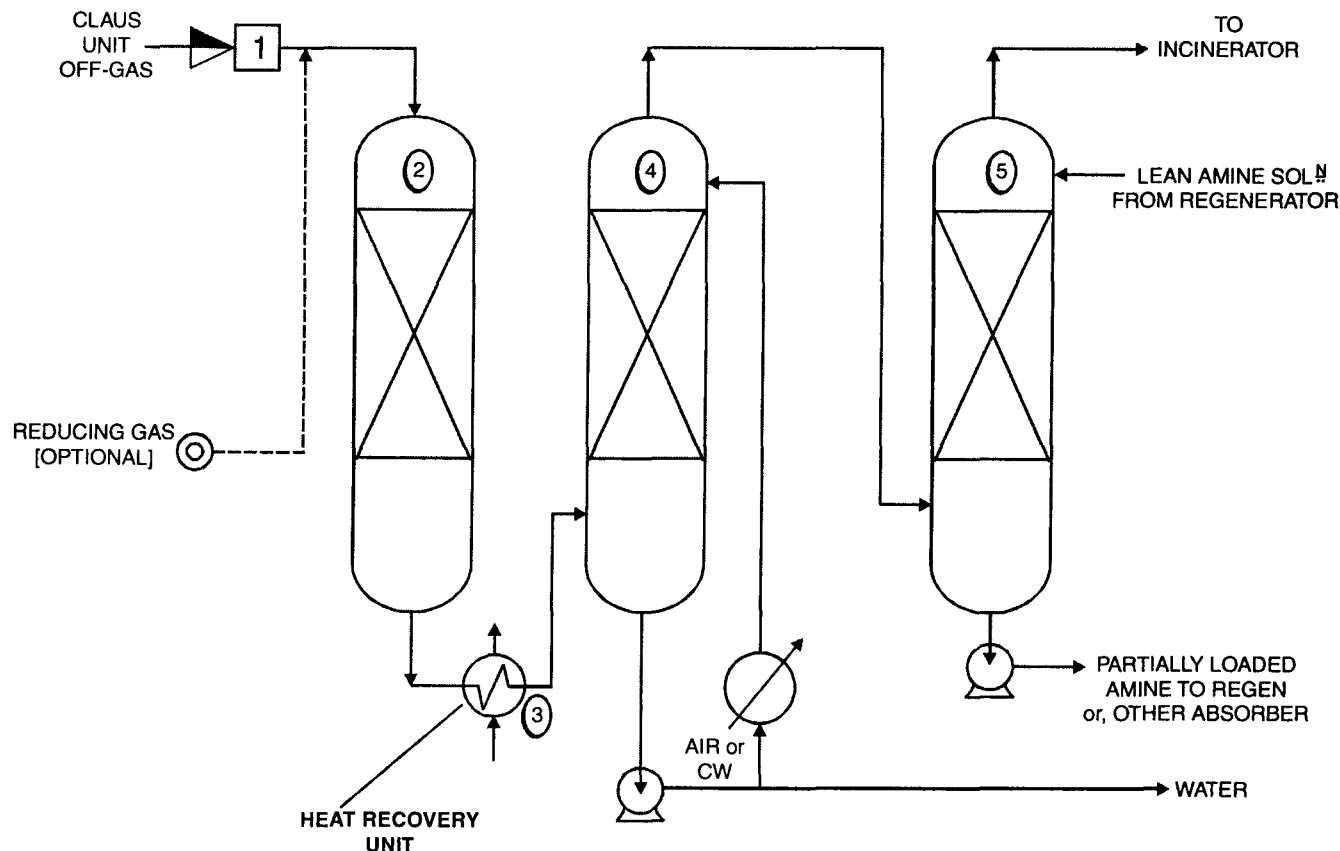
Fig. 8.7.13.

Efficiency The process is fully continuous, provides 99.7% sulfur recovery on Claus plant intake from design to zero turndown, and operates reliably with less than 1% unscheduled shutdown time. **SCOT** pressure drop is 27 kPa or lower.

Economics Scot produces an overall (**Claus + SCOT**) 99.7+% recovery of saleable sulfur. **SCOT** uses equipment common to plants and refineries with minimal operator attention over a wide range of sulfur intake and tail gas flows, which have a small effect on overall sulfur recovery.

SELEXOL

Application Selective or combined removal of H_2S, RSH, CS_2, COS, CO_2, BTX, water, hydrocarbon, VOC, and chlorinated and oxygenated hydrocarbons from gas or air by physical absorption. Used for treatment of natural gas, synthesis gas, partial oxidation, coal gasification, landfill gas, EOR and air cleanup projects.

Products

1. **Treated gas:** total sulfur less than 1 ppm; CO_2 can be retained or removed to ppm levels, water or less than 7 lb/MM scf; hydrocarbon and water dew point as desired.

2. **Offgases:** highly enriched H_2S stream for Claus processing

3. **High purity, high pressure CO_2** for urea, food or EOR projects

4. **Hydrocarbon-rich stream** for fuel or sales; and

5. Pollution-free vent gases or air.

Description **Selexol** solvent is a physical solvent and therefore absorbs various acid gas compounds in proportion to their partial pressure. Solvent regeneration is by pressure letdown of rich solvent. The solvent is essentially regenerated without heat. However, to reduce treated gas contaminants to low ppm, the solvent can be regenerated by stripping medium—such as gas, air or heat.

Feed gas enters absorber **(1)** where contaminants are absorbed by **Selexol solvent (Fig.8.7.14)**. Rich solvent from the absorber bottom flows to a recycle flash drum **(2)** to separate and recompress **(3)** any coabsorbed product gas back to the absorber. Further pressure reduction in the drum **(4)** releases offgases.
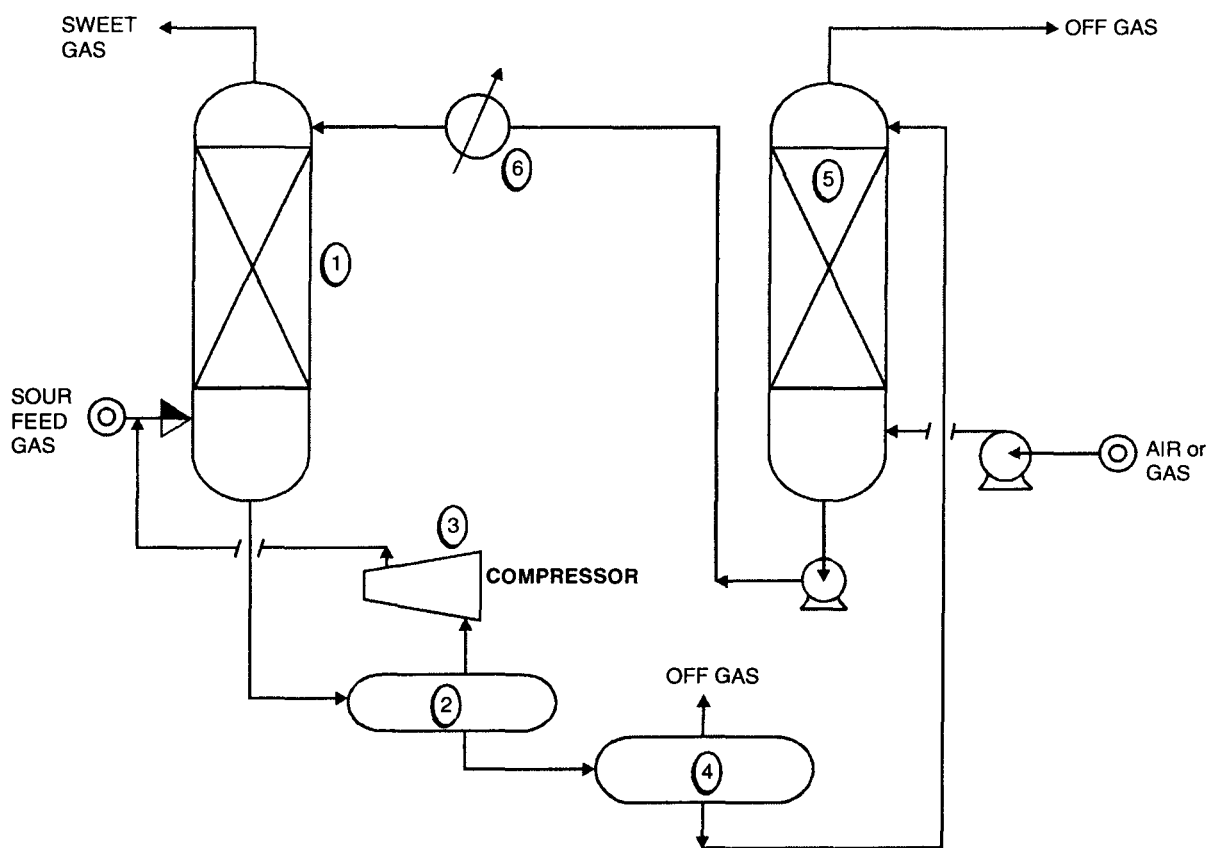
Fig. 8.7.14.

In some applications, the solvent is regenerated in a stripper column **(5)**. The regenerated solvent is then pumped through a cooler **(6)** and recycled back to the absorber **(1)**.

Operating conditions

Process: high on-stream efficiency under wide range of operating conditions and feed compositions, pressures to 2,000⁺ psig.

Temperatures from ambient to 255K.

Solvent : nonfoaming & has no degradation products; vapor pressure losses are negligible.

Economics Highly energy efficient process. A single unit simultaneously controls the treated gas water

and hydrocarbon dew points along with acid gas content, which further enhances its economic advantage. Also, due to high enrichment capability for H_2S stream, the process also results in substantial cost savings for sulfur recovery and tail gas cleanup units. The plant cost and utilities vary with the application and cannot be generalized.

STRETFORD

Application Selective removal of H_2S from gas streams with total sulfur recovery of 99.9+% and reduction of residual H_2S in the treated gas to a very low concentration, generally below 10ppmv. The feed can be Claus TG (tail gas) after conversion of SO_2 to H_2S, off gas from amine or physical solvent processes, coke oven gas, natural gas or geothermal power station offgases.

Description The process is a liquid redox process which includes the following steps:

- Absorption of H_2S **(1)** in the **Stretford solution (Fig.8.7.15).**

- Oxidation of H_2S in solution to elemental sulfur in the reaction tank **(2)**.

- Regeneration of the solution by oxidation **(3)** with air which also floats off the sulfur.

- Arresting the sulfur in a sulfur slurry tank **(4)** and then filtering or centrifuging **(5)** to produce a very clean cake, which can be melted in an autoclave.
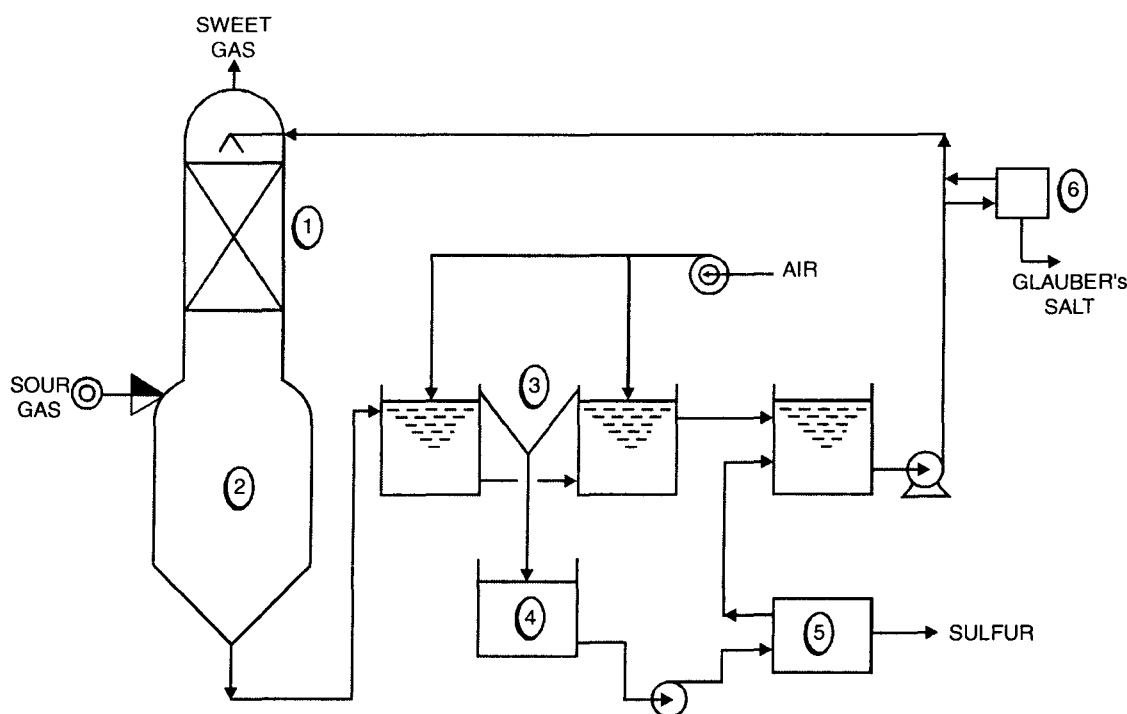
Fig. 8.7.15.

- An optional desalting unit **(6)** gives zero liquid effluent, minimal chemical costs and a Glauber's salt byproduct.

H_2S -contaminated streams with up to 99% CO_2 can be treated. Most gaseous organic compounds pass through the process as inerts. Plants incorporate either packed columns, venturis or a combination of both. The treated gas typically contains less than 10 ppmv H_2S.

Operating conditions The process is operated at solution temperatures between 325K and 365K. Design and operating experience ranges from atmospheric pressure up to 5MPa.

Economics The costs vary with scale and application. Typically for a **Claus TG unit** with a sulfur capacity 5 long tpd, the installed cost is about $4 to 5 million and costs of utilities and chemicals about $100 and $40, respectively, per long ton sulfur removed.

8.8. SO$_2$-SCRUBBER DESIGN

Packed towers are almost exclusively used for **FGD** operation in which SO$_2$ is scrubbed with water **(pH > 7)** in a countercurrent gas-liq operation.

Scrubbing is essentially an absorption process in which the mass-transfer aspects or vap-liq equilibria decide the tower height while the hydrodynamic conditions determine the tower dia. Here is a quick method for estimating scrubber diameter. This requires mass-flowrate, physical property and packing-property data.

Flooding Velocity The gas superficial mass velocity G at flooding conditions is given by

$$Y = \frac{G^2 . F . \mu_L^{0.1}}{\rho_G . \Delta\rho} \approx \frac{G^2 . F . \mu_L^{0.1}}{\rho_G . \rho_L} \qquad ...(8.8.1)$$

where,

$\quad$ **G** $=$ gas loading, kg.s^{-1}.m^{-2}

$\quad$ **F** $=$ packing factor

$\quad$ ρ_G $=$ gas density. kg.m^{-3}

$\quad$ $\Delta\rho$ $=$ $\rho_L - \rho_G$

$\quad$ ρ_L $=$ liq density. kg.m^{-3}

$\quad$ μ_L $=$ liq viscosity, kg.m^{-1}.s^{-1}

The parameter **Y** is given by

$$\ln Y = -3.3861 - 1.0814 \ (\ln X) - 0.1273 \ (\ln X)^2 \qquad ...(8.8.2)$$

where **X** $=$ flow parameter

$$= \frac{L'}{G'} \left(\frac{\rho_G}{\Delta\rho} \right)^{1/2} \qquad ...(8.8.3)$$

$\quad$ **L'** $=$ liq rate, kg.s^{-1}

$\quad$ **G'** $=$ gas rate, kg.s^{-1}

Note that no advance knowledge of superficial velocities is required, since **(L'/G')** in the flow parameter is numerically same as **(L/G)**.

L = liq loading. kg.s^{-1}.m^{-2}

When the values of **L'**, **G'** and the physical properties are available, one can calculate the **flow parameter, X** and then **Y-parameter** from Eqn. 8.8.2

Now to find the value of **G** from Eqn. 8.8.1, the value of packing factor, **F** is required. It is determined from the following empirical correlation

$$F = Z.d^{-n}$$

where Z and n are constants listed in the **Table 8.8.1** and **d** is nominal packing dia in mm.

TABLE 8.8.1 Constants for typical Tower Packings

Packing type	Z	n
Raschig rings		
Metal (W/thk 0.8mm)	7364	1.305
Ceramic	27800	1.553
Pall rings		
Metal	843	0.913
Plastic	1641	1.043
Hy-Pak	1139	1.021
Flexi-ring	770	0.874
INTALOX saddles		
Plastic	268	0.651
Ceramic	7091	1.337
Berl saddles (ceramic)	9850	1.387

It is a general design practice to take operating gas superficial mass velocity G_{OP} = 60 to 80% of G_{fl}. For the most conservative design

$$G_{OP} = 0.6\ G_{fl}$$

Once G_{fl} is known, it is easy to compute the tower diameter from

$$D = \left[\left(\frac{4}{\pi}\right) \frac{G'}{0.6 G_{fl}} \right]^{1/2} \qquad \text{... (8.8.5)}$$

Note : $G' = A_t \cdot G_{OP}$

PACKED-BED SO_2-SCRUBBER DIA

Example 8.4. Sulfur dioxide is to be removed from a fluegas stream by scrubbing the stream with an aq. solution of sodium hydroxide in a tower packed with 25mm ceramic INTALOX saddles. Estimate the required tower dia from the following data :

$G' = 3600\ kg.h^{-1}$

$L' = 14400\ kg.h^{-1}$

$\rho_G = 1.25\ kg.m^{-3}$

$\rho_L = 1200\ kg.m^{-3}$

$\mu_L = 0.002\ kg.m^{-1}.s^{-1}$

Solution

Step. (I) Flow Parameter, X

$$X = \frac{L'}{G'} \left| \frac{\rho_G}{\rho_L - \rho_G} \right|^{1/2}$$

$$= \frac{(14400 \text{ kg.h}^{-1})}{(3600 \text{ kg.h}^{-1})} \left| \frac{1.25}{1200 - 1.25} \right|^{1/2}$$

$$= 0.1290$$

Step.II   Y-Parameter

$$\ln Y = -3.3861 - 1.0814 \, (\ln 0.1290) - 0.1273 \, (\ln 0.1290)^2$$

$$= 1.7054$$

$$\therefore \quad Y = 0.1816$$

Step. (III) Packing Factor

$$F = Z.d^{-n}$$

For **ceramic INTALOX saddles (25mm)**

$$Z = 7091 \quad \& \quad n = 1.337$$

$$\therefore \quad F = 7091 \, (25)^{-1.337}$$

$$= 95.865$$

Step. (IV) Gas Superficial Velocity of Flood

$$G_{fl} = \left| \frac{Y.\rho_G.\rho_L}{F.\mu_L^{0.1}} \right|^{\frac{1}{2}}$$

$$G_{fl} = \left| \frac{0.1816(1.25)(1200)}{95.865(0.002)^{0.1}} \right|^{1/2}$$

$$= 2.2999 \text{ kg.s}^{-1}.\text{m}^{-2}$$

Step. (V) Operating Gas Loading

$$G_{OP} = 0.60 \, G_{fl}$$

$$= 0.60 \, (2.2999) \text{ kg.s}^{-1}.\text{m}^{-2}$$

$$= 1.37998 \text{ kg.s}^{-1}.\text{m}^{-2}$$

Step. (VI) Tower Dia

$$D = [(4/\pi) \, (G'/G_{op})]^{\frac{1}{2}}$$

$$= [(4/\pi) \, (1/1.37998)]^{\frac{1}{2}}$$

$$= 0.9605\text{m}$$

Therefore, a **tower of dia 1m** should be adequate for this duty.

8.9. NATURAL GAS TREATING : HELPFUL HINTS FOR PHYSICAL SOLVENT ABSORPTION

Sepasolv MPE and **Selexol** are two good physical solvents for removal of acid gases (H_2S, CO_2) and other impurities (COS, mercaptans) from natural gas (NG) and synthetic gases. They perform well and offer economical as well as problem-free purification of NG.

SEPASOLV MPE as a mixture of oligoethylene glycol methyl *iso*propyl ethers with an average molecular weight of ~316 kg.kmol^{-1}.

Developed by BASF [Badische Aniline Soda Fabrik], it has been found to be an excellent solvent for physical absorption of H_2S, CO_2 as well as impurities like COS, RSH etc. from NG & SYN gases.

SELEXOL is a mixture of dimethyl ethers of polyethylene glycol which may be tri- to nonaethylene glycol giving a mean molecular weight of 280.

Developed by Allied Chemical, **Selexol** was originally meant for CO_2 removal from synthesis gas. However, it was also used to remove small quantities of H_2S from NG. Of late, **Selexol** has been extensively applied for bulk and selective removal of H_2S from very sour NG.

Solvent Selection

Both **Sepasolv MPE** and **Selexol** are physical solvents whose properties differ basically from chemical solvents. Physical solvents offer substantial advantages over chemisorbents particularly when H_2S partial pressure $\left(P_{H_2S}\right)$ is greater than 1 bar. Concentration of dissolved gas increases almost linearly with pressure, and that means that lower amounts of circulating solvent and substantially lower energy consumption are required even when final washed gas stream contains as little as a few ppm H_2S. For selective removal of H_2S from sour gas with P_{H_2S} < **1 bar**, chemisorbents such as **Alkazid DIK** have an advantage over **Sepasolv MPE** (Fig. 8.9.1)
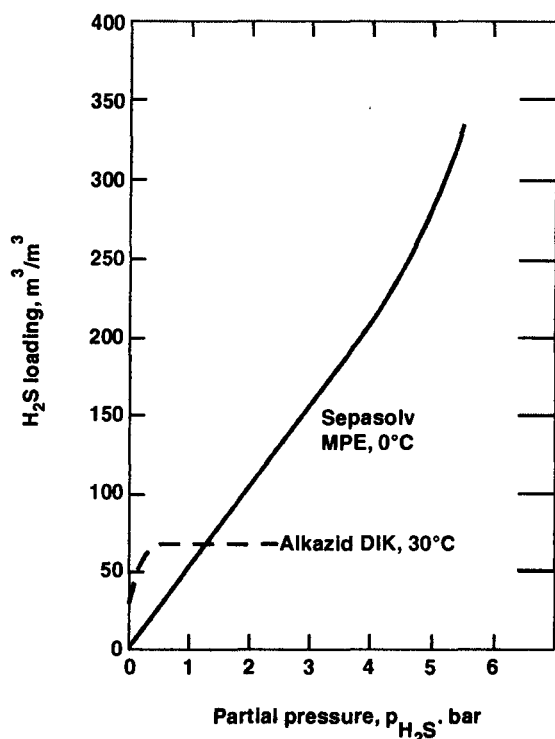
Fig. 8.9.1. *Relative H₂S loading capacity for physical & chemical solvents.*
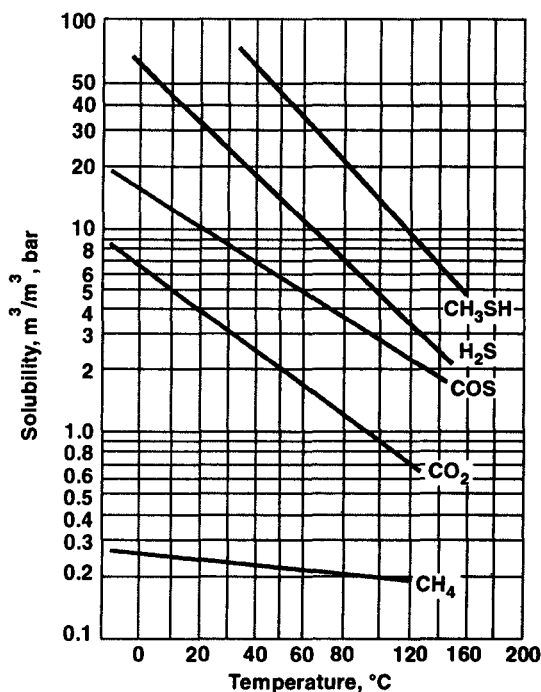
Fig. 8.9.2. *Acid gas solubility in Sepasolv MPE.*

The physical properties of **Sepasolv MPE** and **Selexol** are presented in **Table 8.9.1.**

TABLE 8.9.1. Physical Properties of Sepasolv MPE and Selexol

	SEPASOLV MPE	*SELEXOL*
Molecular weight, kg.kmol^{-1}	316	280
Density at 293K,kg.m^{-3}	1002	1035
$C_{P,273K}$, kJ.kg^{-1}.K^{-1}	1.94	2.05
$C_{P,373K}$, kJ.kg^{-1}.K^{-1}	2.18	2.14
μ_{293K}, Pa.s × 10^3	7.2	6.8
μ_{273K}, Pa.s × 10^3	15	13
Freezing point, K	248	251—244

• The selection of the physical solvent——whether **Sepasolv MPE** or **Selexol**—is determined by

• solvent availability

• price

• the difference in solubility of methane, COS & mercaptans **(Fig. 8.9.2)**

Absorber Taller absorber with 25—30% higher packed sections involves higher capital investment. But this extra cost burden is offset by energy savings. Within a year or so this extra cost can be recovered.

The packing volume, solvent circulation and energy consumption are interdependent. This interdependence is graphically demonstrated in **Fig. 8.9.3.**
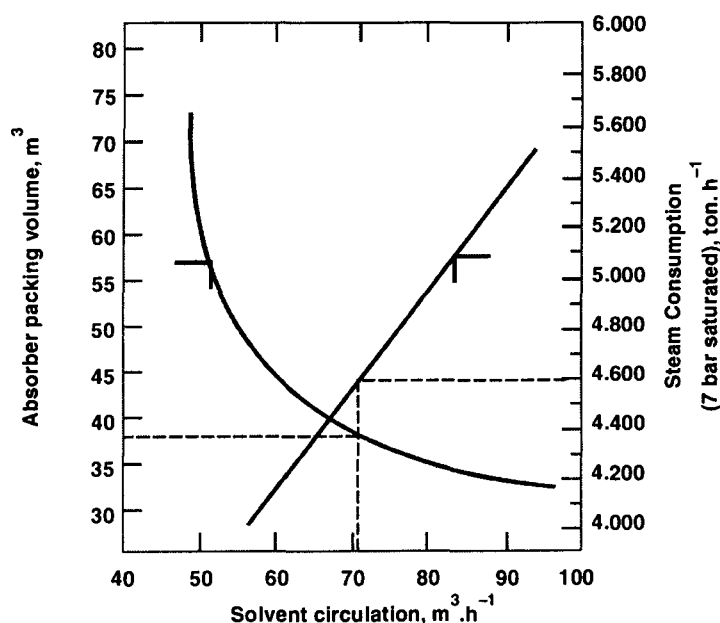
Fig. 8.9.3. *Effect of packing volume on required solvent circulation and steam consumption (A typical operating point shown by dashed line).*

Not only the energy consumption goes down when solvent circulation is lower, methane losses become less and methane slippage to Claus feed gas becomes lower.

Ring type packings are mostly used. However, difference in mass transfer efficiency is barely

visible if **Pall Rings** are replaced by **Cascade Mini Rings** of comparative size. Despite vendor's claim of better lateral distribution and reduced flow-channeling obtained using minirings, no improvement in absorber efficiency has been noted when **Pall Rings** were replaced by **CMR** of same size.

Packings used should be made of stainless material **1.4301 DIN** or **304SS** to maintain a rust-free & smooth surface texture compared to carbon steel rings, which rust when the column is opened for inspection and cleaning. When the column is returned to service, this iron oxide film gets reduced to iron sulfide in contact with H_2S. The iron sulfide spoils the solvent besides rendering the packing surface rough. Dirt particles settle more easily on the roughend surface pollute the packed bed, induce channeling reduce mass transfer.

Liquid Distributor *Equalized liq distribution throughout the packing is essential for optimal* mass transfer. One good choice is Sieve Tray Distributor with at least 225 feedpoints per m^2.

Liquid Residence Time in the sump should be at least two minutes to avoid entrainment of gas bubbles from the absorber. Though a control valve is there to maintain a minimum liq level as a safequard against the gas breakthru, a second valve should be installed and controlled by a level switch.

Flash Tank The loaded solvent leaving the absorber under level control is flashed in the flash vessel where the liquid residence time should also be at least 2 minutes irrespective of the horizontal or vertical configuration of the flash tank.

A vertical flash tank containing a layer of packing arranged above the liquid level **(Fig. 8.9.4)** has been found to be especially effective.

Recycle Compressor Since iron sulfide dust is always present in the system, it leads to severe wear at stuffing boxes and piston rings in non-lubricated machines.

Special care must be taken while selecting piston rod materials since they operate under strong stress. Rods must have a wear-resistant surface and be resistant to sulfide attack, *i.e.*, stress corrosion cracking induced by hydrogen sulfide. Rods manufactured from **1.4571 DIN** material and coated with a **0.6 m** layer of **CrNiBSi alloy** meet these requirements. The layer should be applied according to the Thermo Spray process with a surface hardness of R_c **62**.

Acid Attack Compressed gas must not be cooled below the dewpoint of water in the gas to avoid acid attack. The dewpoint depends on the solvent water content, flash temperature, flash pressure and compression pressure. **Figure 8.9.5** sketches the variation of partial pressure of water vapor with temperature when **Sepasolv MPE** is used as a solvent containing 3% water by weight.

Oil Separator Lube oil entering the solvent together with recycle gas should be removed by using a gravity oil separator.

Heat Exchangers Shell-&-tube heat exchangers are predominantly used as solvent/solvent exchangers. They're low-cost option & exhibit excellent heat transfer efficiency. However, their gasket material must be resistant to thermal & chemical stresses which can be a problem at temperature above 140°C. To address this problem, it is advised to install a small tubular H.E. between the plate heat exchanger and stripper so that the PHE can comfortably operate at lower temperature.

EPDM [Ethylen-Propylen-Dien-Caoutchouc] The EPDM gasket is very expensive and their replacement is time-consuming as well as costly. *It is better to instal stable partition plates to avert damage to the plates by pressure surges during operational troubles.*

Temperature Control Temperature in the stripper sump is dictated by the water load of the
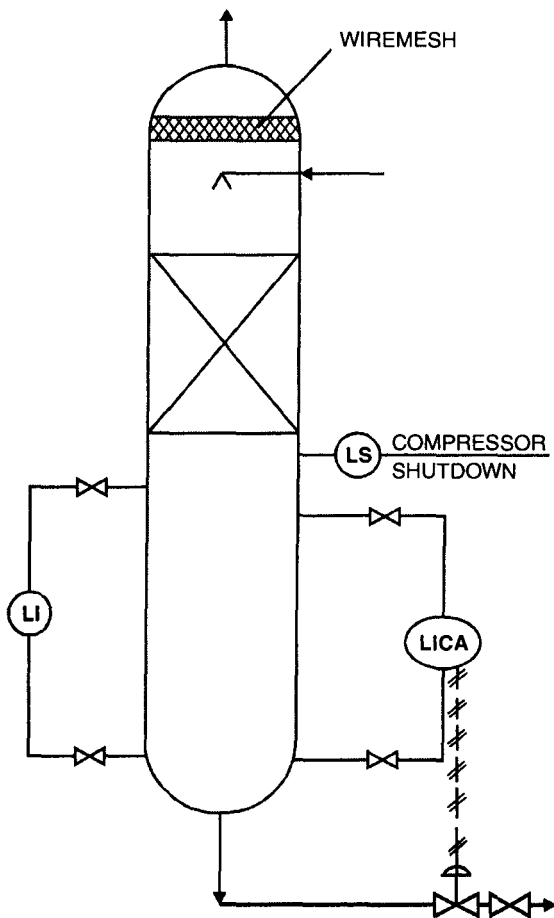
Fig. 8.9.4. *Vertical Flash Tank.*
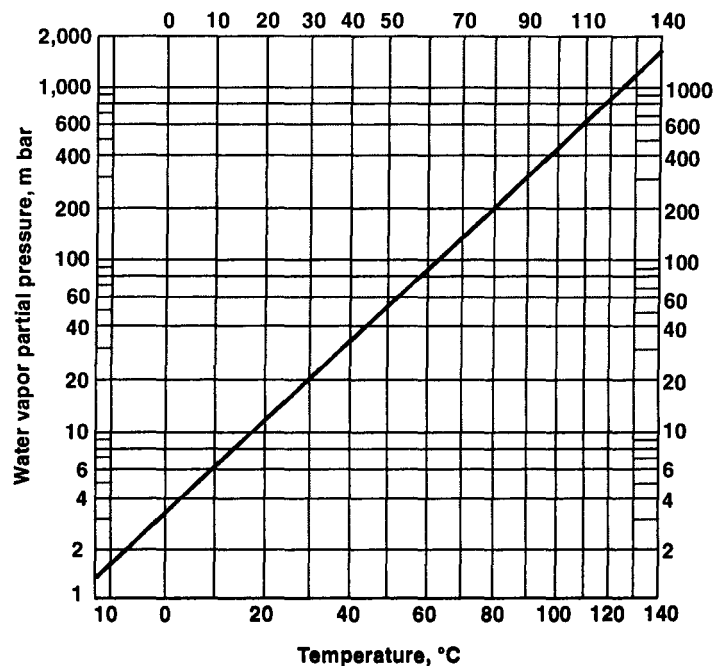
Fig. 8.9.5. *Water vapor partial pressure in Sepasolv MPE with 3 wt % water.*

solvent at a constant pressure. That means a constant reboiler (sump) temperature ensures a constant water content in the regenerated solvent.

With solvents like **MEA**, the system becomes more sensitive with a higher percentage of water; So it requires a careful adjustment of the control circuits.

Follow the following procedures to get a good result:

❑ Fix steam input by flow control

❑ Control M/up water flow as steam injected into the stripper

❑ Control condensation temperature in the condensers downstream. This will stabilize water content in Claus feedgas.

The variations in temperature as well as Claus gas qty call for a careful balance of steam or water M/up.

Filters Crude gas, solvent and reflux water must be filtered. *Good results have been reported in using cartridge filters for crude gas, cloth filters for solvent by-pass stream [10-20% of the main circulating flow], and bag filters for reflux water.*

The circulating solvent should be kept very clean to sustain smooth operations since iron sulfide sludge breeds troubles. Sludge is particularly troublesome in case it settles in the leveling bottles of the level transmitter. This blocks the level adjustment. Such a condition may invite gas break-thru from the absorber to the flash tank and possibly to the stripper as well. Use of piston valves for control functions should be avoided as they get easily fouled by solids which also shorten service easily fouled by solids which also shorten service life of mechanical seals on centrifugal pumps. The O or V-rings, the protective sleeve of the shaft are of a particular problem.

Foaming Solvent foaming is a problem that only occurs in the absorber. It is caused by the colloidal iron sulfide, oil, gas condensate, or chemical used as inhibitors for corrosion protection in gas wells and gas dehydration units.

Foaming is indicated by

❏ increase in ΔP across the absorber

❏ increase of recycle gas

❏ increase of Claus feedgas qty

❏ an increase in air requirement to the Claus plant

As foaming occurs, sump degasification in the flash tank becomes less and as a consequence oversaturated solvent is discharged. This additional gas contains substantial qty of methane which is stoichiometrically burned causing air requirements to the Claus plant to increase out of proportion.

Hence foaming must be minimized as far as possible by avoiding pollution of the solvent & then by injecting silicone defoaming agents [*A dose of 5 ppm to the ⊙n qty is sufficient*]

Note : An overdose may lead to increased foaming. ⊙n means circulation

Condensate : Higher hydrocarbons, being highly absorbed by solvent, cause problems with gases containing condensate.

Low-boiling HCs steamed out in the stripper can be removed in the reflux separator. Higher-boiling ones separate out like oil. However, long-chain paraffins beget particular difficulties if the feedgas is loaded with them. They precipitate in the coolers reducing heat transfer efficiency. This problem can be tackled by installing scrape chillers, better combined with preliminary washing.

Regeneration Stripping determines the composition of gas washed out and hence dictates the possibilities for further treatment.

Use of air, as stripping agent, is possible only with pure CO_2 washings. H_2S, if present, reacts with aireal oxygen to form water and sulfur. This goes into solution at the high stripper temperature but precipitates & plugs the chiller when cooled.

Uses of sweet gas as stripping agent begets least problems for desorption of H_2S from solvent. However, application range is narrow since the washed out gas cannot be processed further in a **Claus** or **sulfuric acid plant,** as these require higher H_2S contents.

Regeneration by using flue gas is another good option. Sweet gas is burned stoichiometrically in a special burner generating flue gas which is cooled (by direct water injection) and dried thru a glycol contact tower. Subsequently, the fluegas is blown into the stripper by using a blower.

The burner must be controlled carefully to reduce the flame temperature to minimize NO_x generation as NO_2 can form HNO_3 & HNO_2

$$2NO_2 + H_2O \rightarrow HNO_3 + HNO_2$$
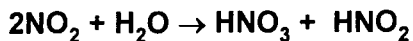
which may lead to corrosion, particularly in reboiler

Stripping by steam is most widely used and it adds 3—5% water to the solvent. Water partly evaporates in the reboiler, flows out into the stripper, stripping the gas-loaded solvent raining down. The gas-steam mixture off the top is condensed in the separator. This water, containing 3—5% solvent, is refluxed back to the column top. Inasmuch as some water is carried out with Claus gas, losses must be constantly made up by steam injection or addition of distilled water.

REFERENCES

1. Werner Wölfer *et.al.*, **Solvent shows Greater Efficiency in Sweetening of Gas** [OIL & GAS JOURNAL, vol. 78, 3.1980/p:66—70].

2. Werner Wölfer, **Helpful Hints for Physical Solvent Absorption** [HYDROCARBON PROCESSING, NOV. 1982 P:193—197].

8.10. PROCESS DESIGN FOR VOC REMOVAL

VOC removal involves two basic systems

(I) Absorption of VOC by a solvent in an **Absorber**

(II) Regeneration of solvent in a **Stripper**

Hence the process design for VOC removal involves chiefly the design of an absorber and a stripper.
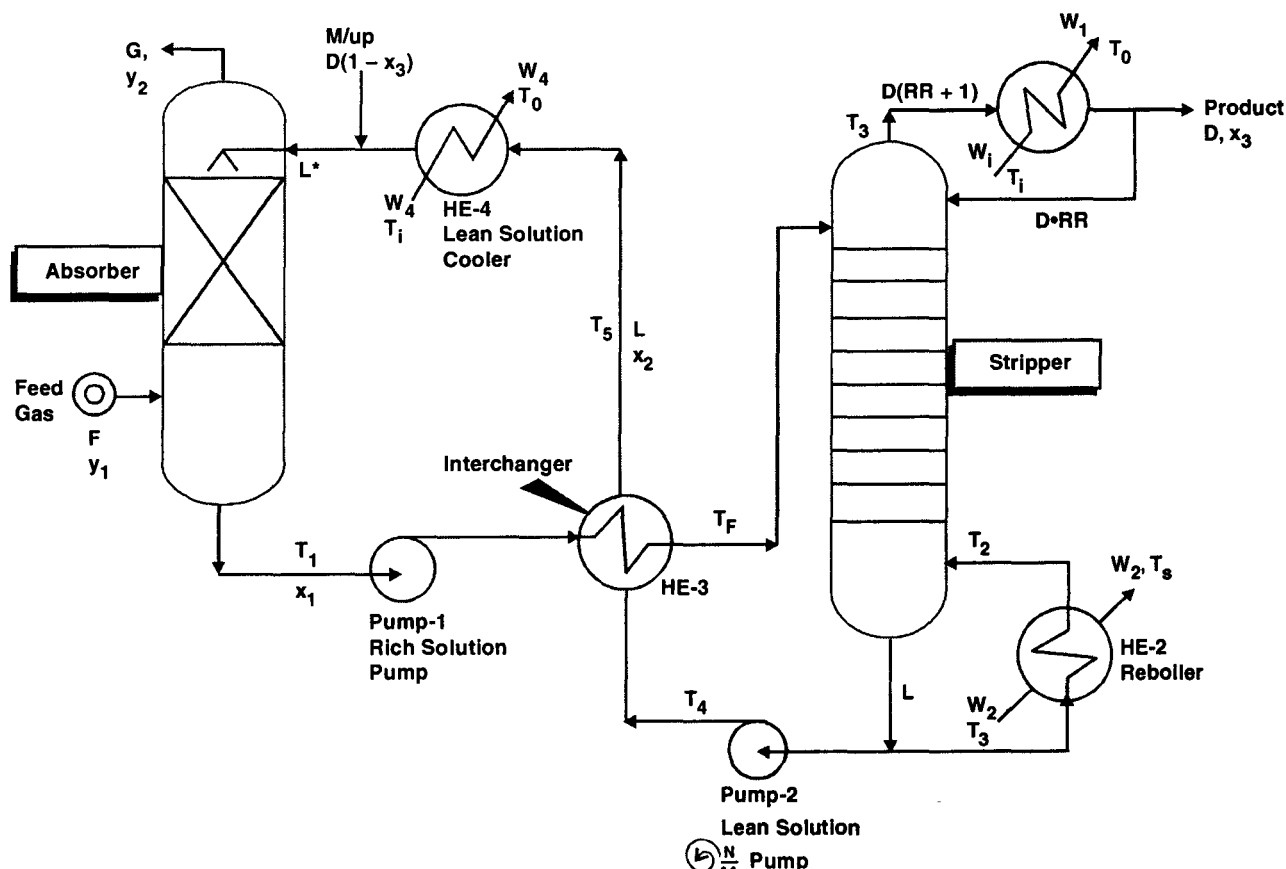
Fig. 8.10.1. *VOC Absorption and Solvent Regeneration in a continuous process.*

Fig. 8.10.1 shows the continuous and stready-state process involving the total system for VOC removal. It consists of a packed-bed absorber, a plate-tower stripper integrated with heat recovery system.

The gaseous feed stream F, kmol.h^{-1} with mole fraction of a VOC contaminant y_1 to be recovered or removed is fed to the absorber, where a solvent L, kmol.h^{-1} countercurrently streams down absorbing the **VOC** in the process.

The rich sol^n is stripped in a plate-tower and the solute (VOC component) in the OVHD (overhead) vapors is condensed in a total condenser, **HE-1** for recovery or further disposal. A part of the cooled solvent is recycled as reflux, another part goes up for M/up solvent fed to the absorber and remaining is stored as spent solvent laden with VOC.

Process Design Equations

ABSORBER

$$F = G + D.x_3 \qquad \qquad ...(8.10.1)$$

$$F.y_1 + L.x_2 = (L + D)x_1 + G.y_3 \qquad \qquad ...(8.10.2)$$

$$NTU_{o,G} = \frac{1}{1 - \left|\frac{\mathcal{H}}{P}\right|\frac{G}{L^*}} . \ln\left[\left(1 - \frac{\mathcal{H}}{P}.\frac{G}{L^*}\right)\left(\frac{y_1 - \frac{\mathcal{H}}{P}.x_2^*}{y_2 - \frac{\mathcal{H}}{P}.x_2^*}\right)\right] + \frac{\mathcal{H}}{P}.\frac{G}{L^*} \quad ...(8.10.3)$$

$$HTU_{o,G} = H_G + \frac{\mathcal{H}}{P}.\frac{G}{L^*}.H_L \qquad \qquad ...(8.10.4)$$

$$H_G = \alpha\left(\frac{F.M_G}{A_{ab}}\right)^\beta .\sqrt{Sc_G}.\left(\frac{(L+D)M_L}{A_{ab}}\right) \qquad \qquad ...(8.10.5)$$

$$H_L = \left(\frac{(L+D)M_L}{A_{ab}.\alpha_L}\right)^\delta .\varnothing\sqrt{Sc_L} \qquad \qquad ...(8.10.6)$$

$$Z = [HTU_{o,G}][NTU_{o,G}] \qquad \qquad ...(8.10.7)$$

$$A_{ab} = \frac{\pi}{4}.D_{ab}^2 \qquad \qquad ...(8.10.8)$$

The absorber dia, D_{ab}, is computed on the basis of vapor velocity equal to 75% of flooding velocity

$$D_{ab} = \left(\frac{4G.M_G}{0.75\pi G_{fl}.(3600)}\right)^{1/2} \qquad \qquad ...(8.10.9)$$

$$\log_{10}\left[G_{fl}.\left(\frac{a_P}{\epsilon^3}\right)\left(\frac{1}{g.\rho_G.\rho_L}\right)\left(\frac{\alpha_L}{\alpha_G}\right)^{0.2}\right] \qquad \qquad ...(8.10.10)$$

$$= 1.74 \left[\frac{L^*}{G} \cdot \frac{M_L}{M_G} \right]^{0.25} \cdot \left[\frac{\rho_G}{\rho_L} \right]^{0.125}$$

where,

F = VOC laden gas feedrate to absorber, $kmol.h^{-1}$

G = Gas/Vapor rate at the absorber exit (top), $kmol.h^{-1}$

Note : Gas & vapor are synoymous

L = Solvent effluent from stripper, $kmol.h^{-1}$. It is pumped to absorber top.

L^* = Solvent feedrate to absorber

$= L.x_2 + D(1 - x_3)$

y_1 = VOC component in feedgas stream, mol fraction

x_1 = VOC component in liquid effluent (rich solution) from absorber, mol fraction.

x_2 = VOC component in liquid feed to the absorber, mol fraction.

$NTU_{o,G}$ = Overall number of transfer units (gas phase)

$HTU_{o,G}$ = Overall height of a transfer unit (gas phase), m

$\mathcal{H}$ = Henry's law constant for the VOC component being absorbed

P = Absorber pressure, mm Hg

H_G = Height of a gas phase transfer unit, m

H_L = Height of a liq phase transfer unit, m

M_L = Mol. wt. of liq, $kg.kmol^{-1}$

M_G = Mol wt. of gas, $kg.kmol^{-1}$

Sc = Schmidt No., dimensionless

A_{ab} = Absorber area, m^2

D_{ab} = Absorber dia, m

$\alpha, \beta, \gamma, \delta, \varnothing$ are all H_G parameters.

$\alpha = 0.557$

$\beta = 0.32$

$\gamma = 0.51$

$\delta = 0.22$

$\varnothing = 0.00235$

STRIPPER

$$(L + D)x_1 = L.x_2 + D.x_3 \qquad \qquad ...(8.10.11)$$

Heat Balance :

$$(L + D).C_P.T_F + Q_2 = D.C_P.T_3 + L.C_P.T_4 + Q_1 \qquad \qquad ...(8.10.12)$$

Vapor Load :

$$V_{vap} = \frac{Q_2}{\lambda M_L} \cdot \frac{22.4 T_4}{273.2} \qquad \qquad ...(8.10.13)$$

Superficial Vapor Velocity

$$V_M = K_{G\text{-}L}\sqrt{\frac{\rho_L - \rho_G}{\rho_G}} \qquad \ldots(8.10.14)$$

STRIPPER DIAMETER

Estimate stripper dia, D_s, by dividing the vapor load by the superficial vapor velocity

$$\frac{\pi}{4}D_s^2 = \frac{22.4\,Q_2 T_4}{273.2 \times 3600\lambda M_L K_{G\text{-}L}\sqrt{(\rho_L - \rho_G)/\rho_G}} \qquad \ldots(8.10.15)$$

$$R_m = \frac{1}{a-1}\left[\frac{x_3}{x_1} - a\left(\frac{1-x_3}{1-x_1}\right)\right] \qquad \ldots(8.10.16)$$

$$N_m = \ln\left[\frac{x_3}{1-x_3}\cdot\left(\frac{1-x_2}{x_2}\right)\right]\Big/\ln a \qquad \ldots(8.10.17)$$

$$N = \frac{N_m + X}{1 - X} \qquad \ldots(8.10.18)$$

$$RR = \frac{R}{D} \qquad \ldots(8.10.19)$$

$$X = 0.75\left[1 - \left(\frac{R - R_m}{R+1}\right)^{0.5668}\right] \qquad \ldots(8.10.20)$$

$$Q_1 = W_1.C_{p,w}.(T_o - T_i) \qquad \ldots(8.10.21)$$
$$Q_1 = U_1.A_1.\Delta T_{lm,1} \qquad \ldots(8.10.22)$$

$$\Delta T_{lm,1} = \frac{(T_3 - T_o) - (T_3 - T_i)}{\ln\left(\dfrac{T_3 - T_o}{T_3 - T_i}\right)} \qquad \ldots(8.10.23)$$

$$Q_2 = W_2.\lambda_w \qquad \ldots(8.10.24)$$
$$Q_2 = U_2 A_2.\varnothing\Delta T_{lm,2} \qquad \ldots(8.10.25)$$
$$\Delta T_{lm,2} = T_s - T_4 \qquad \ldots(8.10.26)$$

$$P = x_2 \exp\left[A_1' - \frac{B_1'}{T_4 + T_{ref}}\right] + (1 - x_2)\exp\left[A_2' - \frac{B_2'}{T_4 + T_{ref}}\right] \qquad \ldots(8.10.27)$$

$$\frac{P.x_3}{\exp\left[A_1' - \dfrac{B_1'}{T_3 + T_{ref}}\right]} + \frac{P(1 - x_3)}{\exp\left[A_2' - \dfrac{B_2'}{T_3 + T_{ref}}\right]} = 1 \qquad \ldots(8.10.28)$$

Stripper Feed Liq Temperature

$$T_F = T_2 + (q - 1)\frac{\lambda}{C_p} \qquad \text{...(8.10.29)}$$

$$x_1 \cdot \exp\left[A_1' - \frac{B_1'}{T_2 + T_{ref}}\right] + (1 - x_1) \cdot \exp\left[A_2' - \frac{B_2'}{T_2 + T_{ref}}\right] = P \qquad \text{...(8.10.30)}$$

where,

L = Solvent effluent of stripper, kmol.h^{-1}

This is the lean sol^{n} which is pumped to the absorber top via two heat exchangers

D = Stripper OVHD product rate, kmol.h^{-1}

x_3 = Product (VOC) composition in OVHD liq, mol fraction

x_1 = VOC component in rich sol^{n} (absorber exit), mol fraction

x_2 = VOC component in lean sol^{n} (**HE-3** outlet), mol fraction

C_p = Sp. heat of liq stream (**HE-3 & HE-4**), kcal. kg^{-1}.k^{-1}

$C_{p,W}$ = Sp. heat of streams W_1 & W_2, kcal.kg^{-1}.K^{-1}

T_F = Feed stream stripper temperature, K

T_2 = Temp. of stripping stream (reboiler outlet), K

T_s = Saturation temp. of reboiler steam (condensing), K

T_4 = Stripper effluent temp., K

T_3 = OVHD vapor temp, K

T_{ref} = Reference temp, K

$\Delta T_{lm,1}$ = Log-mean-temp-difference over **HE-1**, K

$\Delta T_{lm,2}$ = Log-mean-temp-difference over **HE-2**, K

q = Fraction of stripping-steam that is vapor

λ = Latent heat of liq from stripper, kcal.kg^{-1}

Q_1 = Heat duty of OVHD condenser (**HE-1**), kcal.h^{-1}

Q_2 = Reboiler heat duty, kcal.h^{-1}

R_m = Minimum reflux

R = Operating reflux

RR = Reflux ratio

N = No. of trays of stripper column

N_m = Minimum No. of stripper trays

X = Mole ratio of solute (VOC component) in liq stream

a = Relative voltility

A_1', A_2', B_1', B_2' are the Antoine parameters

$\dfrac{a_p}{\epsilon^3}$ = Specific area of packings, m^2, m^{-1} of packed depth

K_{G-L} = Empirical constant of Souders-Brown Eq[n]
$\quad \simeq 0.10$

ρ_L = Density of liquid, $kg.m^{-3}$

ρ_G = Density of gas stream, $kg.m^{-3}$

M_L = Mol. wt. of liq stream, $kg.kmol^{-1}$

M_G = Mol. wt. of gas stream, $kg.kmol^{-1}$

$\mathcal{H}$ = Henry's law constant for the VOC component

U_1 = Overall htc of exchanger-1, $kcal.h^{-1}.m^{-2}.K^{-1}$

U_2 = Overall htc of exchanger-2, $kcal.h^{-1}.m^{-2}.K^{-1}$

A_1 = Heat exchange area of **HE-1**, m^2

A_2 = Heat exchange area of **HE-2**, m^2

D_s = Stripper dia, m

Heat Exchanger No. 3

It cools liq solvent **L** from T_4 to T_5 and heats up absorber BTMS from T_1 to T_F.

$$Q_3 = (L + D)C_P.(T_F - T_i) \qquad ...(8.10.31)$$

$$Q_3 = L.C_P.(T_4 - T_5) \qquad ...(8.10.32)$$

$$Q_3 = U_3 . A_3 . \Delta T_{lm,3} \qquad ...(8.10.33)$$

$$\Delta T_{lm,3} = \frac{(T_1 - T_5) - (T_F - T_4)}{\ln\left|\dfrac{T_1 - T_5}{T_F - T_4}\right|} \qquad ...(8.10.34)$$

where,

Q_3 = Heat duty of exchanger-3, $kcal.h^{-1}$

T_F = Rich sol[n] temp. at inlet to stripper, K

T_i = Cooling water temp. at inlet to **HE-1**, K

T_o = Cooling water temp. at outlet of **HE-1**, K

T_5 = Lean Sol[n] temp at **HE-3** outlet, K

U_3 = Overall htc of **HE-3**, $kcal.h^{-1}.m^{-2}.K^{-1}$

A_3 = Heat exchange area of **HE-3**, m^2

$\Delta T_{lm,3}$ = Log-mean-temp-difference over **HE-3**, K

Heat Exchanger No. 4

$$Q_4 = L.C_P.(T_5 - T_1) \qquad ...(8.10.35)$$

$$Q_4 = W_4.C_{P,w} (T_o - T_i) \qquad ...(8.10.36)$$

$$Q_4 = U_4 . A_4 . \Delta T_{lm,4} \qquad ...(8.10.37)$$

$$\Delta T_{lm,4} = \frac{(T_5 - T_o) - (T_1 - T_i)}{\ln \left| \frac{T_5 - T_o}{T_1 - T_i} \right|} \qquad \qquad ...(8.10.38)$$

PUMP NO. 1

$$HP_1 = K_{P,1} \cdot (L + D)N \qquad \qquad ...(8.10.39)$$

where,

HP_1 = Horse power of Pump No. 1

$K_{P,1}$ = Pump characteristics of Pump No. 1, $hp.h^{-1}. kmol^{-1}$ per unit tray

N = No. of trays in the stripper

L = Liquid rate, $kmol.h^{-1}$

D = OVHD rate, $kmol.h^{-1}$

PUMP NO. 2

$$HP_2 = K_{P,2} \cdot L \cdot Z \qquad \qquad ...(8.10.40)$$

where,

HP_2 = Horse power of Pump No. 2

$K_{P,2}$ = Characteristics of Pump No. 2, $hp.h^{-1}. kmol^{-1}$ per m of packed bed depth of absorber

L = Solvent (lean sol^n) circulation rate by Pump No.2, $kmol.h^{-1}$

Z = Absorber bed depth, m

MAKE-UP SOLVENT

$$L.x_2 = [L + D (1 - X_3)] \cdot x_2^* \qquad \qquad ...(8.10.41)$$

$$L^* = L + D (1 - X_3) \qquad \qquad ...(8.10.42)$$

where,

L = Lean sol^n rate, $kmol.h^{-1}$

$D(1 - X_3)$ = Make-up solvent feedrate, $kmol.h^{-1}$

L^* = Total solvent rate to the absorber, $kmol.h^{-1}$

x_3 = VOC composition in the OVHD (distillate of stripper), mol fraction

$(1 - x_3)$ = VOC-free solvent content in OVHD, mol fraction

x_2^* = VOC composition in the liq stream at absorber inlet, mol fraction

REFERENCE

Chemical Engineering, Jan.2001/P:94—98

□□

9

Revamping Absorbers and Strippers

Modern structured packings and high-performance random packings can considerably improve separation, increase thruput and reduce pressure losses in existing columns—normally a more cost-effective solution than installing a second column.

Plant designers are continually striving for upgrading existing columns with such design solutions that will give rise to lower fixed and operating costs and improved reliability and safety. Such goals can be achieved by an optimized design of the gas-liq contacting devices.

The gas-liq contacting devices most usually employed in absorption and stripping operations are countercurrent contacting columns, although some more exotic devices like static mixture, horizontal spray chamber, venturi scrubber, turbulent contact absorber do exist. The simplest gas-liq contactors are the bubble and spray columns, which are essentially empty vessels with dispersion devices such as spargers and nozzles.

A much more efficient apparatus known as staged plate tower permits the use of countercurrent flow of the gas and liq phases. A typical arrangement may consists of a vertical shell in which are mounted a number of equally spaced circular plates or trays. Such trays are available in different types :

bubblecap, sieve and valve

Differential or packed columns consist of a vertical shell which is filled with suitable packing material supported on a grid **(Fig. 9.1)**.

Random or dumped packings are available in various sizes and shapes. The most widely used among them are rings, saddles and slotted rings.

Bubblecap and spray columns are cheap but have a low efficiency and their use is only justified when columns present more interesting characteristics such as higher efficiency and lower pressure drop. In general, trays columns have good efficiency but a large pressure drop. Conventional packed columns are less efficient but have lower pressure drop.

The use of structured packing in revamping existing absorbers begets a number of important advantages :

1. **Lower Pressure Losses** : which mean small fans and compressors with more efficient intake stages.

Clean Gas

Lean Solvent

Distributor

Packing

Packing support grid

Untreated
gas

Rich Solvent
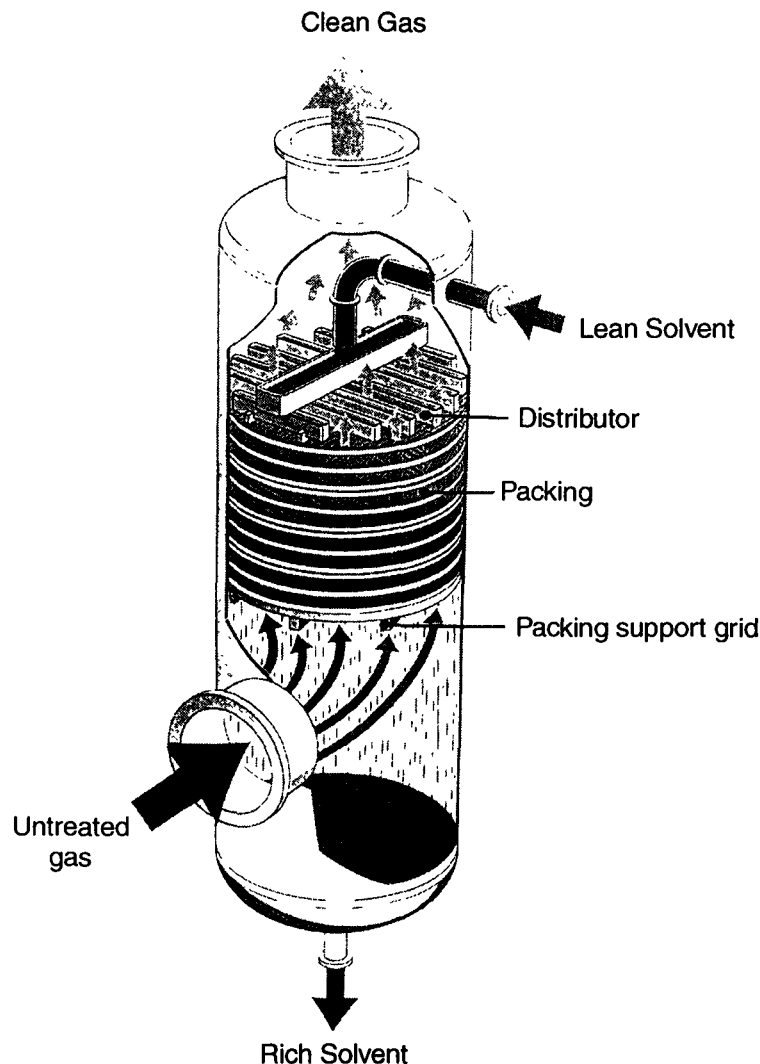
© **Sulzer Bros. LTD./Winterthur/Switzerland.**

Fig. 9.1. *Sectional arrangement of a countercurrent packed-bed absorption column.*

2. **Lower liquid loads :** saving pumping and processing costs.

3. **Compact Columns :** The structured packings permit high gas and liq loadings, resulting in smaller column dia – a favorable factor for pressurized columns or upgrading existing columns. Thanks to high separation capacities, columns heights are low, requiring much less headspace.

4. **Low Weight :** Lighter than comparable tray columns – a vital factor for offshore applications.

5. **Flexibility** permits extreme input fluctuations while performance remains virtually unaffected.

6. **Insensitive to Dirt and Foaming** allows the development of absorption process using solids suspensions. Structured packing are less sensitive to dirt or foaming than random packings or trays.

    The key to the outstanding performance of structured packing is the way in which gas and liq streams are handled by the packing.

The gas traffics thru the channels formed by the adjacent corrugated sheets and lie at a fixed angle w.r.t. the vertical. The cross-section of the channel has alternatingly the form of a diamond or a triangle and the gas flows thru it until the next element is reached. There it enters a new channel (rotated 90°) and subsequently flows thru the whole column following a three-dimensional zig-zag pattern.

The liq flows as a thin film down the individual sheets at a constant angle to the gasflow. The capillary wiremesh of gauze packing or special surface features on sheet packing contribute to uniform liq spreading. The regular flow pattern in the column insures an intimate contact between both phases and minimizes bypass.

The controlled way in which gas and liquid are brought into intimate contact enhances mass transfer, delays the onset of flooding and reduces gas-liq drag (that is press dr) thus allowing a significant increase in thruput and efficiency. This contrasts sharply with the chaotic flow (path of least resistance) in conventional random packing and their relatively poor spreading and liq distribution characteristics. Large openings coexist with small ones leading to a disordered flow pattern and ultimately to lower flooding limits.

Because of the following performance characteristics, modern structured packing have become the choice of first performance in upgrading existing absorbers and strippers :

I. High Capacity : The capacity of structured packings is higher than that of trays or dumped
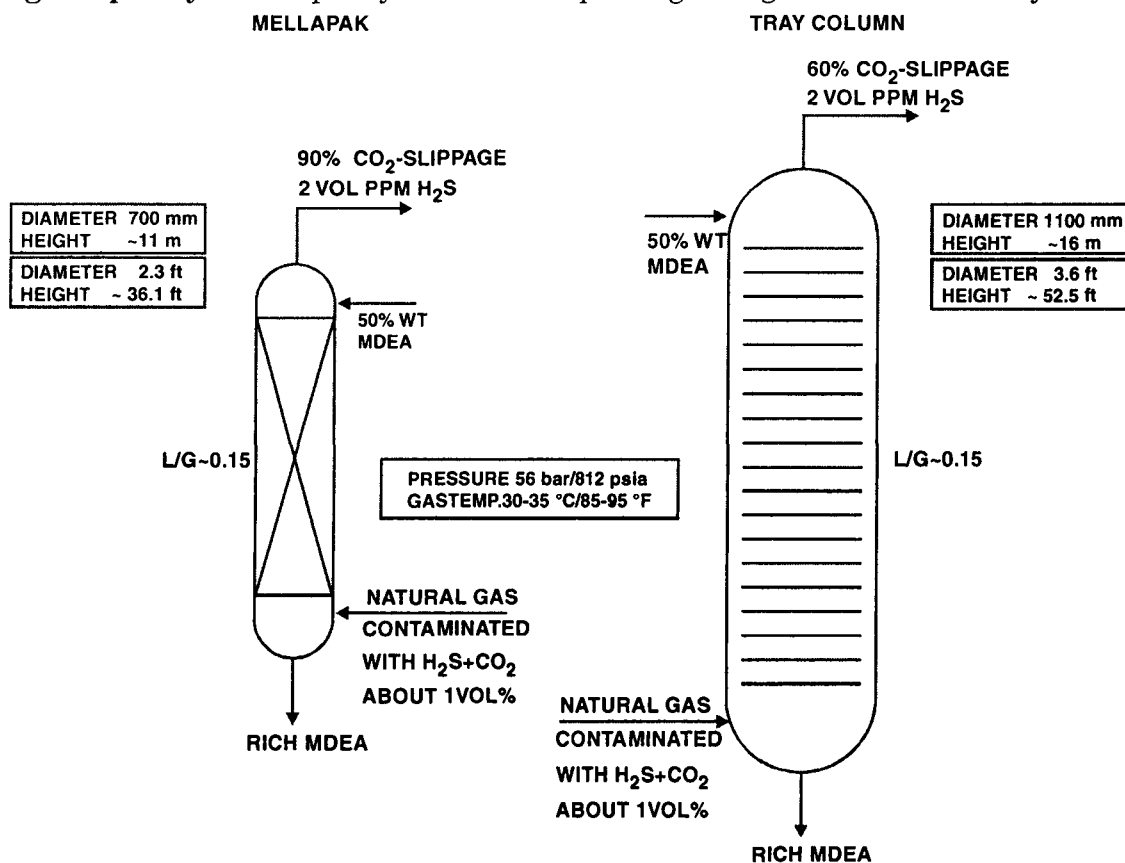
Source : *Experience with Structured Packings in High Pressure Gas Absorption* — Dr. Pietro Bomio *et.al.* © Sulzer Brothers Ltd/Winterthur/Switzerland.

Fig. 9.2. *Comparison between trays and Mellapak (to scale). Mellapak is the corrugated sheet packing of Sulzer. It is widely used in a large variety of unit operations such as distillation, absorption, stripping and scrubbing.*

packings for a given efficiency. Depending on physical properties and opening conditions the difference can be as much as 80% or more. This capacity boost-up is an attractive incentive for column revamps.

Examples : debottlenecking an existing amine absorption unit or when decreasing natural gas wellhead pressure compels the operator to process more gas volume in order to meet production schedule.

Fig. 9.2 illustrates the difference in column size between trays and structured packings.

Thanks to higher efficiency and capacity, column volume can be drastically reduced. Furthermore, since shell thickness and cost increases (and decreases) more than linearly with column dia, important saving of material can be achieved. For offshore applications, where weight is a main concern, this can be a decisive factor and a trayed column can be totally dispensed with a much compact and smaller volume tower filled with structured packing and yet giving higher separation efficiency.

II. High Efficiency : Structured packings beget a higher efficiency than conventional dumped packings (rings, saddles etc.,) That means, for a given number of theoretical trays, less packing height is required. This results again in savings of material, although not as dramatic as when the diameter can be reduced because the height occupied by the packing accounts for only 60–70% of total column height. A more important consequence of the higher efficiency of structured packing is that the equilibrium can be more closely approached, and thus allowing a sizeable cut in the circulation rate of the solvent (in absorbers) and a reduction of stripping gas or stream requirements or reboiler duty (in strippers).

Table 9.1 presents a case story for benzene scrubbing with toluene.

Table 9.1 Benzene Scrubber Revamps

	Trays	*Random Packing*	*Mellapak*
Column internals	13 trays	5 m Bed of Pall rings (50 mm)	5 m Packed depth of Mellapak
Column dia	1000 mm	1000 mm	1000 mm
Pressure	55 bar	55 bar	55 bar
Gas load	24 t.h^{-1}	30 t.h^{-1}	30 t.h^{-1}
Measured number of theoretical trays	8	4	12

Source : *Experience with Structured Packing in High Pressure Gas Absorption* – Dr. Pietro Bomio

III. Low Pressure Drop : For given efficiency and capacity, structured packings produce a very small gas pressure drop around an order of magnitude lower than trays and from 20 – 50% less than rings, depending on the operating conditions and physical properties. This feature is very important in units treating very large volume of gas (process absorbers with large gas recirculation such as ethylene oxide and acrylnitrile, fluegas desulfurization and so on), a reduction in pressure loss of just a few tenths of a bar can represent an important saving in compression power. **Table 9.2** illustrates the energy savings that can be obtained with **Mellapak** (structured packing of Sulzer Brothers).

Table 9.2 Energy Savings thru reduced Pressure Drop

Service   : **Quencher for SCOT Process**

Col. Dia   : **6 m**

Pressure   : **Atmospheric**

Gas Flowrate : **260 t.h⁻¹**

Trays	*Random*	*Packings*	*Mellapak*
Press. Dr (mbar)	70	25	9
Energy Savings (million kWh/yr)	–	2.8	3.9
Cost Reduction (kilo US $/yr)*	–	180	260

* 1 kilo US $ = 1000 US $

Source : *Improving Selectivity, Capacity and Efficiency of Hydrogen Sulfide/Carbon Dioxide removal Columns with Sulzer Structured Packing* – P Bomio *et.al.*

IV. Flexibility : *Another important advantage of structured packing with respect to conventional trays is their large turndown ratio (flexibility).* The correct operation of the trays relies on the right gas-liq interaction. This strong coupling between both flows makes them rather sensitive to load variations. Valve trays are efficient at design capacity but at low flowrates liq tends to weep that may produce unsatisfactory results. *Bubblecap trays are more flexible but less efficient. Random packings are less sensitive to changes in flowrates, but they're prone to gas-liq bypass* (channelling) at low loads. Structured packings, on the contrary, have an essentially unlimited turndown ratio, *i.e.*, the gas flowrate can be reduced to zero without affecting performance. As the liq flows down, it spreads over in thin film thruout the entire microsection of the structured packing in a very wide range of liq loads. For non-wetting system, special surface features and a microscopic finish have been developed to insure liquid spreading on the packing. Of course, this requires a good liquid distributor that will evenly distribute the liquid on the bed cross-section at the top.

EXAMPLES OF REVAMP

9.1. NATURAL GAS DEHYDRATION

Natural gas usually contains water in liquid and/or vapor form at source and/or as a result of sweetening with an aqueous solutions. Within certain temperature and pressure ranges, water can combine with various hydrocarbons to form hydrates which are precipitated in the form of a white floccular mass. Morever, in the presence of carbon dioxide and hydrogen sulfide, water vapor can cause very dangerous corrosion in pipelines and valves. It is, therefore, necessary to remove the water in order to prevent formation of hydrates in transmission lines, minimize corrosion and/or maximize the heating value of gas.

The best way of drying gases is generally absorption drying process using glycol, in which the gas stream, saturated with water vapors enters the absorption column at the bottom and comes into contact with triethylene glycol **(TEG)** either in countercurrent or cocurrent flow.

The majority of absorption towers operate as tray columns and historically **TEG** contactors were bubblecap trays. However, such columns can be revamped with high-performance structured packings to get higher capacities and much better separation performance.

The difference in capacity between tray columns and towers packed with structured packings for **TEG** is to the order of 80% and higher. Comparison between a bubblecap tower and a **Mellapak** tower is shown in **Fig. 9.1.1.**
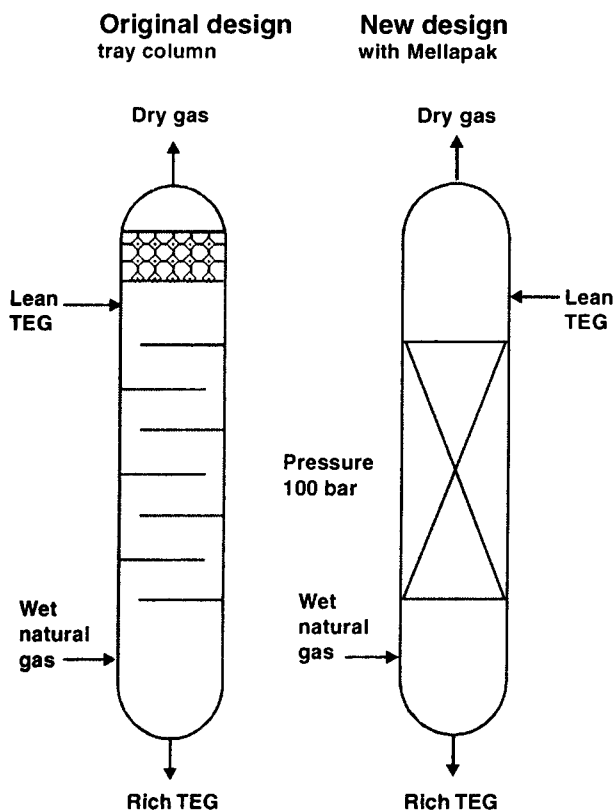
	New design with Mellapak same capacity		Revamp with Mellapak	
	Trays	Mellapak	Trays	Mellapak
Capacity	100	100	100	185
Column Φ mm	2,500	1,800	2,500	2,500
Φ ft	8.2	5.9	8.2	8.2
Turndown capability (Gas)	~ 1:5	>1:50	~1:5	>1:50
Weight (tons)	80	50		

© Sulzer Brothers LTD/Winterthur/Switzerland

Source : *Experience with Structured Packing in High Pressure Gas Absorption*–Dr. Pietro Bomio, *et.al.*

Fig. : 9.1.1. *Comparison between a bubblecap tower and a Mellapak tower.*

Structured packing performance remains unaffected at gas turndown of up to a factor of 50 (at gas flowrates of only several percent of design load). Liq turndown is given by the design of the liq distributor at the top of tower (Standard : 30 – 100%).

When the **TEG** trayed tower is revamped with structured packing, say **Mellapak, Flexipac,** the entrainment of liquid becomes negligible **(Fig. 9.1.2).**

This is due to the unique gas-liq contact mechanism in corrugated sheet packings – gas is brought into tangential contact with liquid, rather forced to flow thru it.

Because of the low liq holdup in structured packing, the operator can change gas thruput drastically with no problems whatsoever to his glycol level control system.

Absorber with structured packing is lucrative proposition. **Figure 9.2.1** illustrates repacking of a dumped packing tower of structured packing.
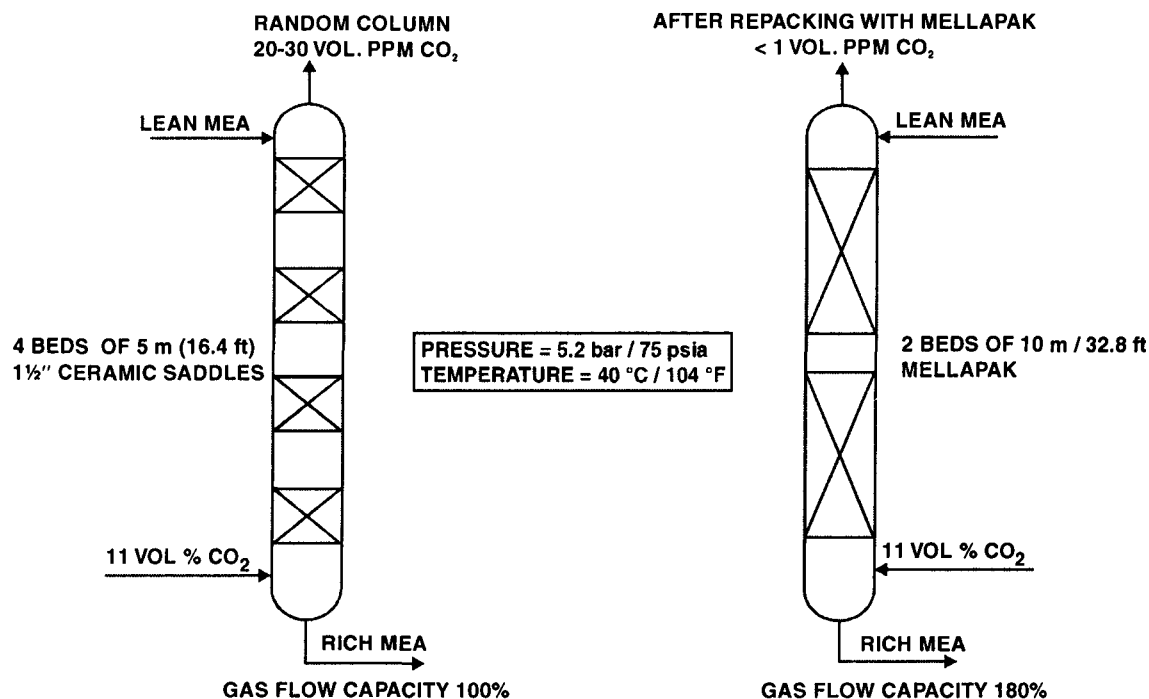
© Sulzer Brothers LTD/Winterthur/Switzerland.

Source : *Experience with Structured Packing in High Pressure Gas Absorption*–Dr. Pietro Bomio, *et.al.*

Fig. : **9.2.1.** *Repacking of a CO$_2$ absorber with monoethanolamine (MEA).*

Selective Absorption of Hydrogen Sulfide

An important problem with which gas processors are often confronted is the absorption of hydrogen sulfide from streams containing both hydrogen sulfide and carbon dioxide. This requires selective absorption of hydrogen sulfide from sour gas **(Fig. 9.2.2)**
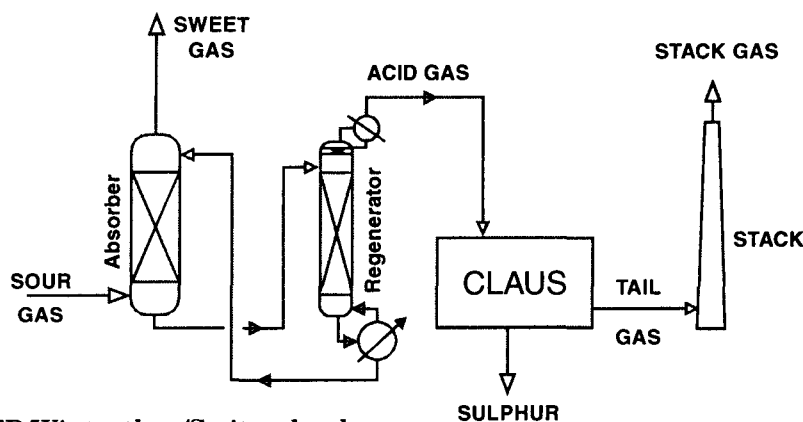
© Sulzer Brothers LTD/Winterthur/Switzerland

Source : **Improving selectivity, capacity and efficiency of Hydrogen Sulfide/Carbon Dioxide removal columns with Sulzer structured packing—Dr. P. Bomio,** *et.al.*

Fig. : **9.2.2.** *Selective absorption in Natural Gas sweetening.*
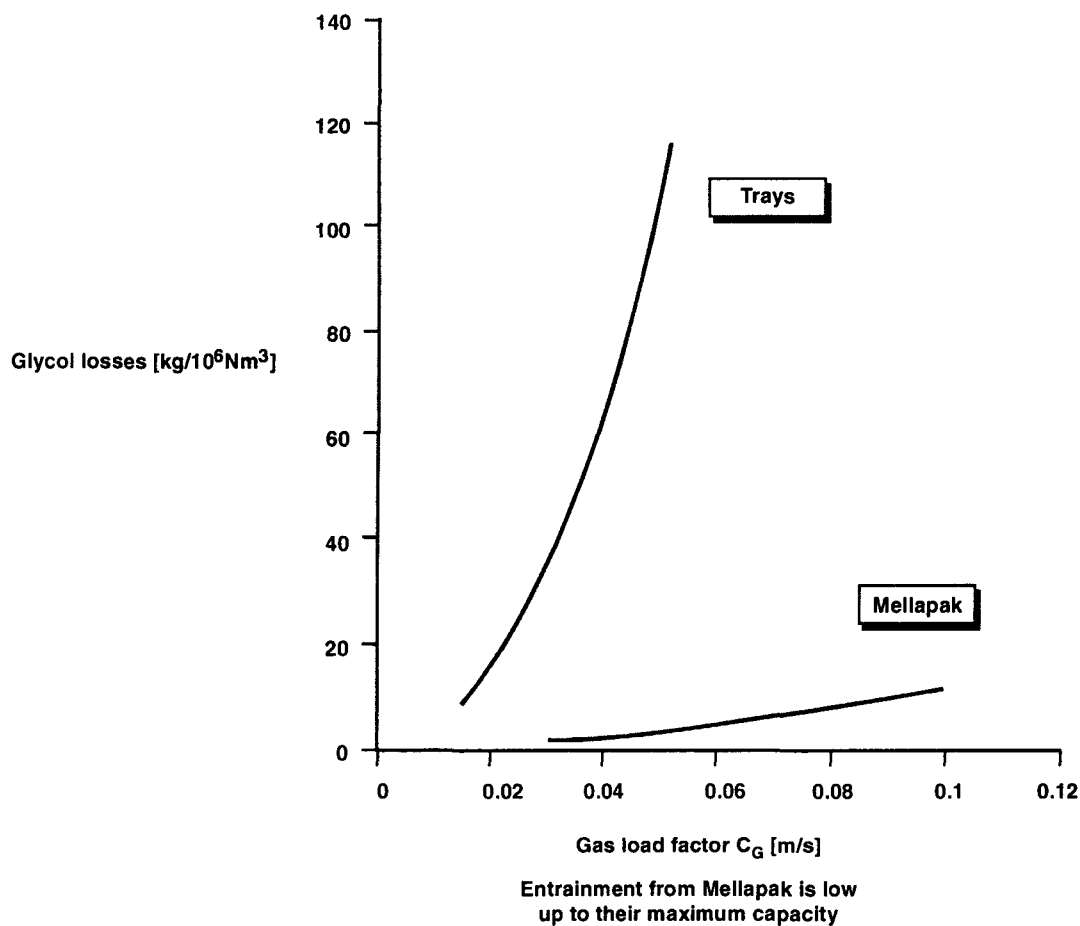
Entrainment from Mellapak is low
up to their maximum capacity

© Sulzer Brothers LTD/Winterthur/Switzerland.

Source : *Experience with Structured Packing in High Pressure Gas Absorption*–Dr. Pietro Bomio, *et.al.*

Fig. : 9.1.2. *Entrainment from Structured Packing (here it is Mellapak) is low upto their maximum capacity.*

9.2. ABSORPTION OF HYDROGEN SULFIDE AND CARBON DIOXIDE

Many synthetic gases, and other gases such as Natural Gas, refinery gas and coke oven gas contain hydrogen sulfide, and/or carbon dioxide. These components are normally removed by chemical and/or physical scrubbing processes :

— MEA, DEA, DIPA, MDEA, DGA, AMINE-GUARD, FLEXORB, UCARSOL, ACTIVATED, MDEA

— GIAMMARCO-VETROCOKE, BENFIELD, CATACARB

— RECTISOL, SELEXOL

— SULFINOL, AMISOL

Upgrading existing columns with structured packing can drastically improve capacity and separation efficiency. Modern structured packings such as **Mellapak, Flexipac, IMTP-T** stretch column capacity up to 80% than trays and random packings. These factors make revamp option of CO_2-

In selective absorption the aim is to remove hydrogen sulfide from a process gas but leave carbon dioxide in place. The selective reaction capability, *e.g.*, of methyl diethanolamine **(MDEA)** can be influenced by equipment choice and operating conditions.

Selective absorption begets certain positive benefits :
— smaller solvent rate
— compact regenerator
— lower energy consumption
— smaller Claus plant
— a richer feed to Claus plant

These advantages are depicted quantitatively in **Table 9.2.1.**

Table 9.2.1 Selective Absorption in Natural Gas Sweetening

	Non Selective Absorption			Selective Absorption		
	H_2S	CO_2	Nm^3/hr	H_2S	CO_2	Nm^3/hr
Sour Gas	7%	20%	5000	7%	20%	5000
Sweet gas	ppm	1%	3300	ppm	17%	4400
Acid gas	27%	73%	1320	58%	42%	600
Stack gas	–	47%	2030	–	19%	1300

As a side product, high purity carbon dioxide can be recovered from sour gas by a two stage absorption as shown in **Fig. 9.2.3**
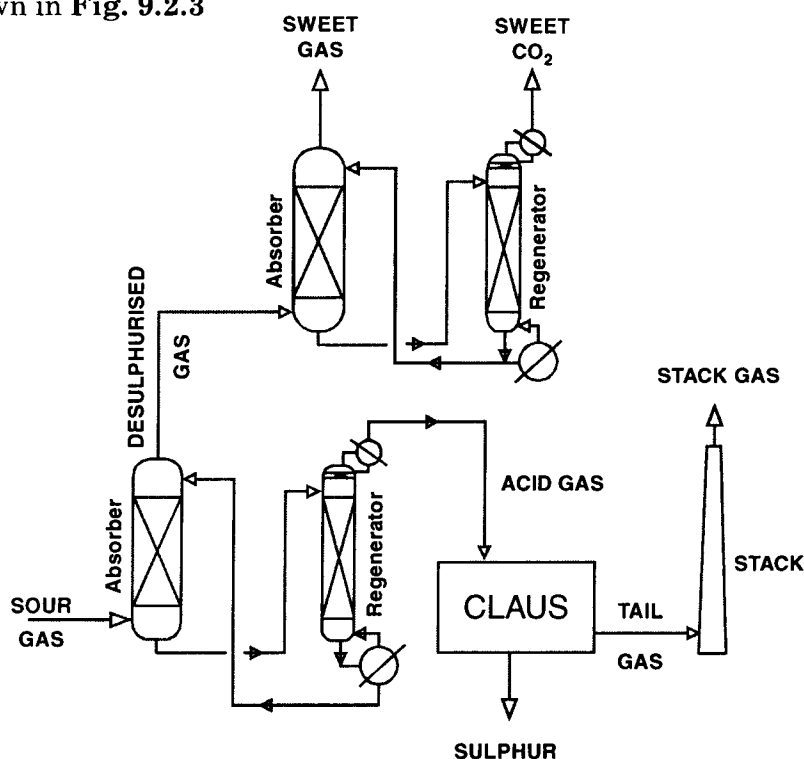
© **Sulzer Brothers LTD/Winterthur/Switzerland**

Source : *Improving selectivity, capacity and efficiency of Hydrogen Sulfide/Carbon Dioxide removal columns with Sulzer structured packing* — P. Bomio, *et.al.*

Fig. : 9.2.3. Carbon dioxide generation for Enhanced Oil Recovery.

This process is particularly attractive when carbon dioxide is required for Enhanced Oil Recovery (EOR). The sour gas is first selectively scrubbed to remove hydrogen sulfide down to ppm level, whereby carbon dioxide, to some extent, is also removed. Acid gas from the regenerator is treated in a Claus plant. The bulk of the carbon dioxide slips thru the selective absorber and is removed in a second, conventional absorber. This gas (practically free of H_2S) is regenerated and reinjected to EOR facility. The process can be harnessed to debottleneck a sulfur recovery unit.

Small slightly sour gas streams are often sweetened and the resulting acid gas is then incinerated directly without sulfur recovery. Sulfur dioxide release can be reduced by coupling a Claus plant to these installations. However, with relatively low H_2S concentration (approx. < 20%), additional energy input to Claus Unit goes up to preheat air or feedgas. Upgrading of the acid gas by selective absorption over a bed of structured packing results in a smaller, simpler and cheaper Claus plant **(Table 9.2.2)**. Structured packings subscribe to better selective absorption than trays.

Table 9.2.2 Selective Absorption of H_2S in Acid-gas Cleanup

	Direct Incineration			*Selective Absorption and Claus*		
	H_2S	*CO_2*	*Nm^3/hr*	*H_2S*	*CO_2*	*Nm^3/hr*
Acid Gas	10%	90%	3000	10%	90%	3000
Enriched Acid Gas	–	–	–	60%	40%	500
Sweet CO_2	–	–	–	ppm	100%	2500
Stack gas	–	75%	3600	–	18%	1100

Selective absorption of H_2S is a key factor in tailgas cleanup operation. For instance consider the SCOT (Shell Claus Off-gas Treating) process. It catalytically converts sulfur and sulfur components in the TG of a Claus Unit into hydrogen sulfide. After cooling (first in the LP Steam Generator and then in a quencher), the hydrogen sulfide is selectivity absorbed from the gas stream with an alkanolamine solution. Upon regeneration of the rich solution (loaded amine) the acid gas is recycled to the Claus unit. In this way the selective absorption reduces the total amount of gas recycled and increases its H_2S content. Increasing the selectivity in the absorber improves Claus plant operation and reduces the amount of circulating amine and therefore steam consumption in the regenerator. Structured packing shows better selectivity than tray **(Table 9.2.3)** and this gives rise to a reduction in the amine circulation flowrate of about 30% compared to conventional design with trays.

Table 9.2.3 Selective Absorption of Hydrogen Sulfide in Acid Gas Cleanup

	Trays			Mellapak		
	H_2S	CO_2	Nm^3/hr	H_2S	CO_2	Nm^3/hr
Enriched acid gas	34%	66%	880	56%	44%	540
Pressure drop (mbar)		60			10	
Amine flowrate (relative)		1.0			0.7	

When amine, whose reaction with hydrogen sulfide and carbon dioxide has favorable kinetics, is used the selectivity is based on the different velocities of reaction of hydrogen sulfide and carbon dioxide with amine. The rate of mass transfer is greatly affected by the mechanisms and kinetics of the chemical reaction taking place in the liquid. A selective solvent reacts readily with hydrogen sulfide but slowly (ideally infinitely slowly) with carbon dioxide. The different reaction rates cause a

shift in the mass transfer resistance to the gas for hydrogen sulfide (gas-side controlled) and to the liquid for carbon dioxide (liq-side controlled). Roughly speaking, liq-side mass transfer is related to interfacial area. Improving selectivity by using structured packing is due to the fact of lower liq holdup and higher capacity compared with trays and by about equal liq holdup and capacity but higher interfacial area (double the geometrical area) and ideal plug flow compared with dumped packing. To put it simply, a packing with good selectivity characteristics must have high interfacial area and efficiency (in order to absorb hydrogen sulfide) and low liq hold (in order **Not** to absorb carbon dioxide). Specially tailored structured packings, *viz.*, **Mellapak S** (developed by Sulzer Brothers, Switzerland) have logged very good performance for the selective absorption of hydrogen sulfide with tertiary amines from streams containing low to very high concentration of CO_2 both at low and at high pressures. **Figure 9.2.4** shows a comparison of the selectivities (expressed as **"slippage" of CO_2**) that can be reached with trays and with **Mellapak S**. The aim of selective absorption is to achieve as high a slippage as possible, ideally 100%.
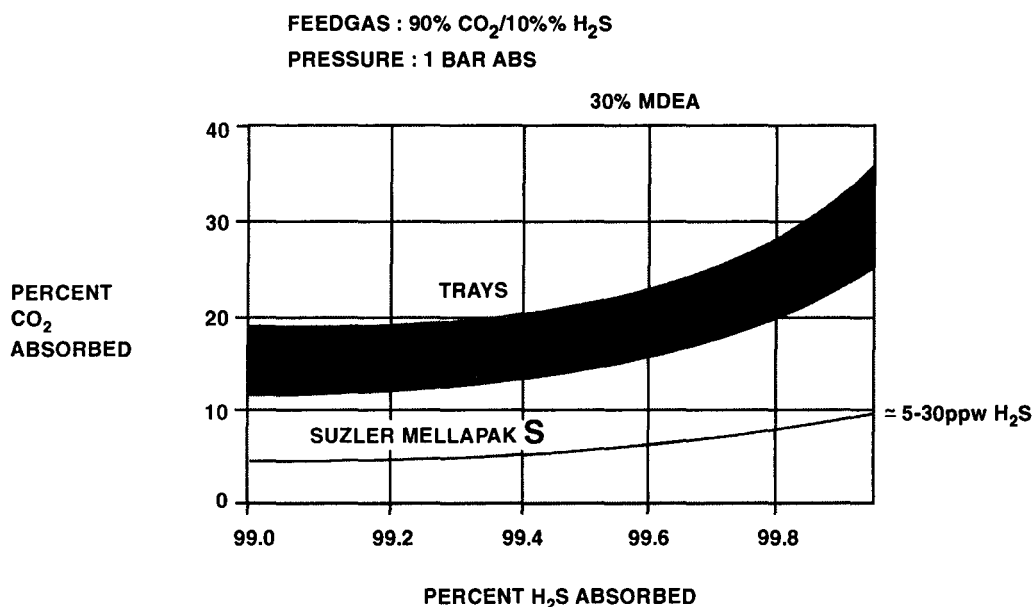
FEEDGAS : 90% CO_2/10%% H_2S
PRESSURE : 1 BAR ABS

Fig. 9.2.4. *Comparison of Selectivity : Mellapak vs. Trays.*

© Sulzer Brothers LTD/Winterthur/ Switzerland.

Source : *Improving selectivity, capacity and efficiency of Hydrogen Sulfide/Carbon Dioxide removal Columns with Sulzer Structured packing*—P Bomio, *et.al.*

9.3. REVAMPING ETHYLENE OXIDE ABSORBER

Ethylene oxide processes involve the direct vapor phase oxidation of ethylene over a catalyst containing silver.

Ethylene oxide is recovered from the reactor effluent gases by absorption at high pressure and then stripped out in the ethylene oxide stripper.

The top product of the ethylene oxide stripper is then purified by distillation. Byproduct is CO_2 which is subsequently removed by absorption in a hot potassium carbonate solution.

To achieve the same separation efficiency, the structured packings occupy much less column height than trays and beget much smaller pressuré drop **(Table 9.3-1)**. And therefore, less fan/blower power is required and that means less investment cost.

Table 9.3.1. Advantages of Structured Packing in EtO$_x$ Production

	Trays	*Mellapak*
Column Dia	6.6m	6m
Column Height	38m	34m
ΔP	370 mbar	50 mbar

By converting the existing tray column to Mellapak, with its high separation capacity, solvent water consumption gets considerably reduced. The ethylene oxide concentration at the absorber outlet remains changed **(Fig. 9.3-1)**.
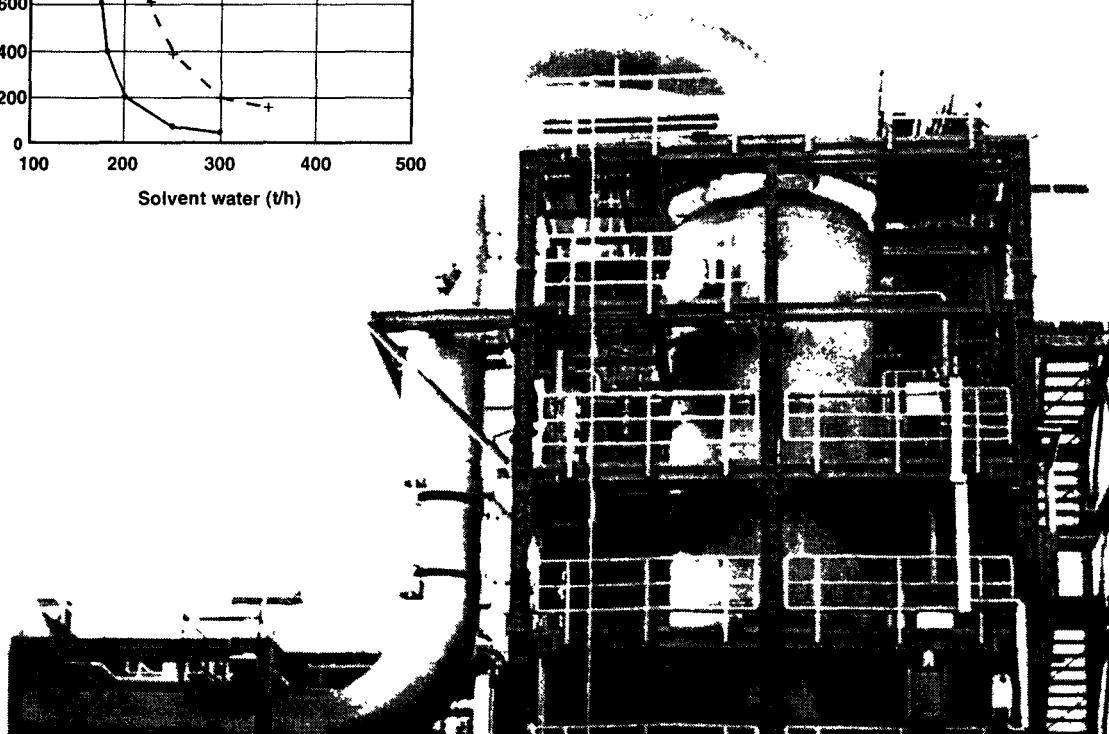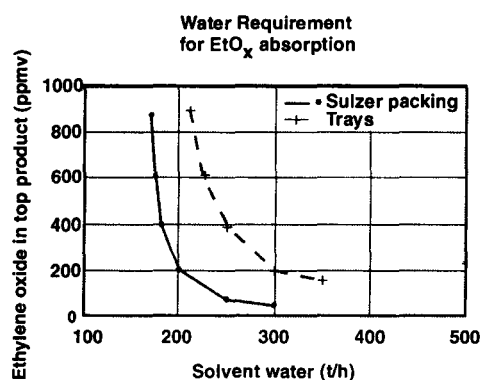
© Sulzer Brothers Ltd/Winterthur / Switzerland
Source : *Absorption Technology* — Sulzer Chemtech.

Fig. 9.3.1. *Water requirement for EtO$_x$ absorption.*

For column revamps from random packing or trays to structured packing, considerable energy savings can be achieved due to higher efficiency and lower pressure drop. **Fig. 9.3-2** illustrates the replacing trays by Mellapak in an ethylene oxide absorber.
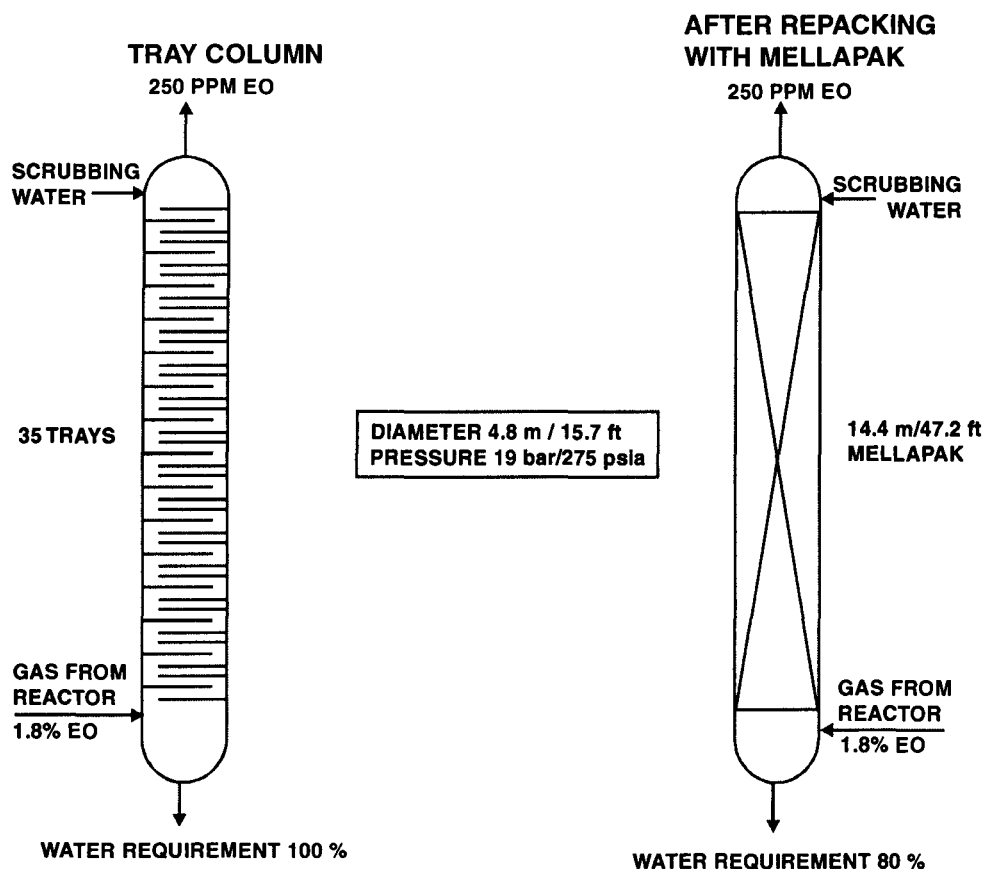
© Sulzer Brothers LTD / Winterthur / Switzerland

Source : *Experience with Structured Packings in High Pressure Gas Absorption* — Dr. P Bomio *et.al.*

Fig. 9.3.2. *Revamp from Trays to Mellapak of an Ethylene Oxide Absorber.*

The reason for converting this existing tray column to **Mellapak** was to optimize energy consumption. Due to the higher efficiency of structured packings, scrubbing liq could be reduced by about 20%. This change in scrubbing water resulted in a saving of approximately 7.5 tons of steam per hour for the regeneration stage. Over and above, the column pressure drop reduced by about 200 mbar, and for future capacity an increased capacity reserve of about 50% was established.

9.4. REVAMPING A PACKED-BED STEAM STRIPPER

Packings are a favorite choice for gas-liq contacting in stripping columns. Often, random packings are successfully applied in fouling applications. But tower operation remains satisfactory as long as the packings remain clean.

Feeds containing heavy organic tars can cause many process operating problems for separation columns. The organic tars plug the packed column. The fouled packing reduces the bed voidage and hence column's performance. As the tar accumulates and fills the packing's void volume, pressure drop across the column increases. These conditions compromise processing operations, limit product recovery and diminish service life of the packing and column.

By mid-nineties BASF **[Badische Aniline and Sodafabrik]** experienced operational problems with a stripping column at its Beaumont facility, Texas, USA due to organic tars present in the

feedstream. This column made use of three beds of ETFE random packing to process a liquid feed containing salts, acid and tar. While the desired product was recovered in the OVHD, the tar and salts accumulated in the column bottom. The packed tower's operation was satisfactory when the random packing was clean. But the tar in the feed combined the process fluid's aggressive tendency to break down ETFE packing, caused recurring plugging and packing degradation. With accumulation, these deposits grew into asphalt-like chunks on the packing. Not only did the tar fill the packing's void volume (and hence increased pressure drop across the column), the weight of the tar deposits reduced bed depth and lost interfacial contacting area significantly diminished separation and reduced capacity by 35% within a period of just 8 months. Mind please, the packed tower had started running at 90 % of its design capacity. Separation decreased and an increased level of desired product went into the bottoms **(Fig. 9.4-1).**
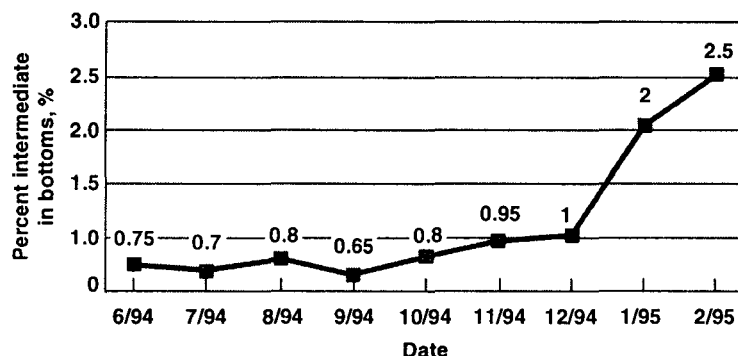
Fig. 9.4-1. *Percent of intermediates-slippage to the bottoms abruptly increased just after 6 months of operation as ETFE random packing got fouled heavily.*

After nine months of operation, performance declined to such an extent that the column was shutdown and the packing degraded and lumped into asphalt-chunks were removed.

Besides packing, the column's PTFE liner exhibited signs of wear.

To get rid of these recurring problems BASF ultimately decided to replace their plastic-lined column with a new zirconium vessel and got rid of 3 packed beds altogether and installed in their place **20 #s** of zirconium trays using new fixed valves shaped to prevent plugging.

Patented Fixed-Valve Trays come to the Rescue

The traditional fixed-valve trays feature a crude valve cover that is punched up from the traydeck. The physical stretching that occurs when punching the cover, makes the cover's shape similar to that of the punched orifice but actually smaller than the hole. Thus the punched valve design is expected to offer limited turndown or capacity. To compensate for this, the tray manufacturers seek to reduce the punched orifice size, which however renders the openings significantly more prone to fouling.

Additionally, the valve lift is another problem inherent with the punched fixed-valve design :

the valve lift is limited by the metal's ability to be stretched. Its maximum limit is 13 mm (reported).

However, the new patented fixed-valve cover design (Norton's fixed-valve tray constructed of **705 zirconium**) allows clearance up to **17 mm** (even on trays made of difficult-to-form or brittle materials such as zirconium and titanium). Therefore, the new fixed-valve cover provides an escape

area substantially greater than a punched valve of the same orific size. Thus the patented new fixed-valve tray affords little or no chance of plugging, begets lower pressure drops and improved capacity.

Why not Sieve Trays

Though sieve trays are also recommended for fouling services provided deck-holes are 13 mm or larger so that larger particles can pass thru the orifices without blocking or partially obstructing the openings. However, sieve tray capacity diminishes as orific size increases. Moreover, a high percentage of open area on the traydeck reduces the turndown capacity of a sieve tray.

However, the standard orifice size on the Norton's fixed-valve tray is **39 mm** — much larger than what is the practical size for the sieve trays — and that permits a high degree of open area. With such a design, a higher turndown is possible only by shielding the orifice and directing the liquid around the orifice. The cover's backleg is wider than the frontleg. As the liq flows across the traydeck, the backleg slows down the momentum of the liquid and prevents it from pouring into the orifice. The cover then deflects the vapor flow which then pushes the liquid forward and past the orifice. This shielding effect as enforced by the valve's backleg and cover provides the same trundown as conventional single-weight moving valves.

Why not Moving-Valve Trays

BASF could've opted for moving-valve trays. But they didn't. Because, materials contained in the feed could accumulate on the traydeck and cause valve-caps to stick when they came in contact with the traydeck.

Furthermore, moving valves deflect vapor horizontally. A part of the vapor escaping thru the opening between raised cap and orifice on the deck actually goes to push the liquid against the net direction of liquid flow, creating liquid backflow in local areas. Additionally, same kinetic energy is required to lift the cap up to keep the valve open. This increase the press. dr. across the tray.

In contrast to this, the valve covers of Norton's patented fixed-valve tray deflects the upflowing vapor horizontally and then directs it in the net flow direction of the liquid. This not only gives a forward push to the liquid flow, but also keeps the liq close to plugflow which helps reduce or eliminate dead areas on the tray, where solids can deposit. Thus the directional push produces a cleansing action that keeps materials from accumulating on the traydeck.

Conventional moving-valve tray gives rise to uneven aeration. Since a part of the vapor exits against the net direction of liq flow, vapor exits unevenly from the open valve inflicting uneven aeration and uneven spray heights. Whereas the fixed-valve cover directs vapor in the net flow direction of the liquid, whereupon vapor tends to leave more or less uniformly from the aerated froth. The total effect is a lower, more uniform spray height that more efficiently uses the tray spacing and adds capacity.

Results of Revamp

BASF carried out the revamp in August 1997. They replaced the three packed beds with 20 zirconium trays with the patented fixed-valve design into a new column (a new zirconium vessel) and resumed operations. Thirteen months of operation revealed :

1. Pressure Drop across the trays remained constant. That is, tars in the feed-stream were not plugging the trays.

2. Hydraulic Characteristics of the column were exposed thru gamma scanning. A series of

gamma scans was taken when the beds got badly fouled ; and then at the startup after revamp, and finally after 13 months of operation **(Fig. 9.4-2).**
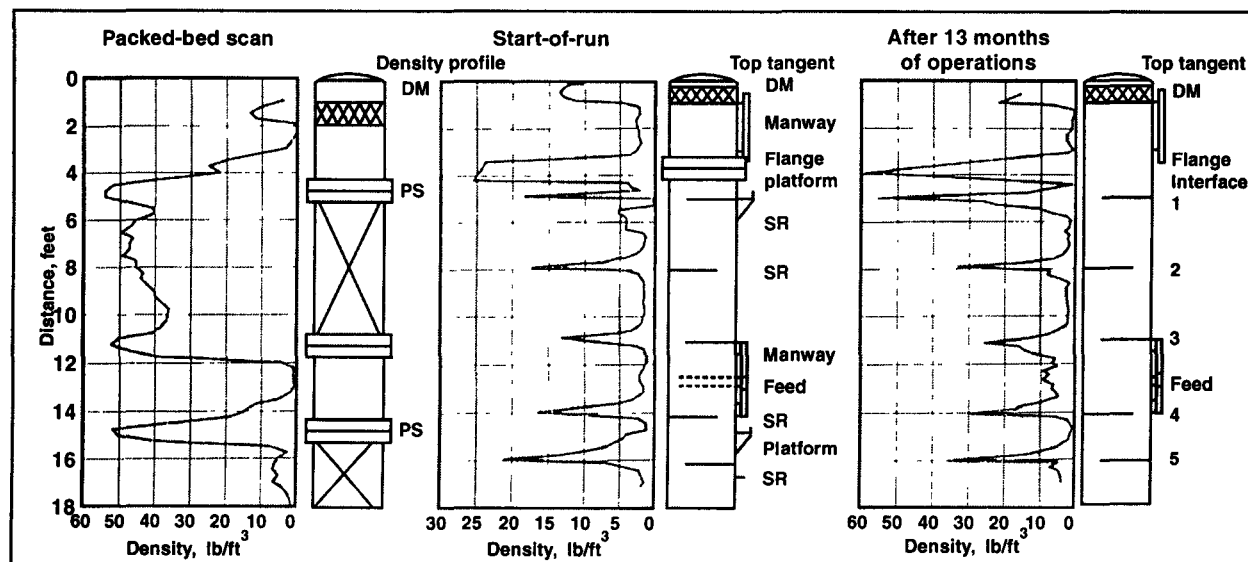
Fig. 9.4-2. *Series of Gamma Scans — the 1st in the series was packed-bed scan ; the 2nd revamped column scan after startup ; and the last one being column scan after 13 months of operation*

The first in the scanning series (packed-bed scan) shows heavy solids buildup in the top packed bed. The 2nd one, taken of newly trayed tower at the start-up, showed good hydraulic operation. The 3rd scan, taken after 13 months of operation, showed continued good hydraulic operation and no tar buildup.

3. Capacity Enhancement The packed column that was l/up with 90% of its designed load suffered from severe capacity limitation due to pluggage of ETFE random packings whereupon tower's capacity got reduced by 35% by the end of six months whereupon the column was taken shutdown.

After the column was revamped with patented fixed-valve trays, operation resumed at 90% capacity. Improved column performance polarized the BASF engineers to increase the load. And after 13 months, the tower was found operating at 100% of design capacity. This is also evident upon comparison of density profile at a given tray elevation in the 2nd and 3rd scans.

4. Product Loss was a cause of concern when the separation was carried out in packed beds. The intermediates that drained to BTMS shot up more than 3 times from 0.75% at startup to 2.50% at the end of six months, which led to unscheduled outage.

In sharp contrast trays demonstrated better performance. The product loss in the bottoms, after column was revamped with patented fixed-valve trays, remained essentially constant over 13 months though feedrate was increased by 20% forcing the stripper to run overloaded **(see Table 9.4-1)**

Table 9.4-1. *Summary of Column Operations Before and After Revamp.*

% of Capacity Utilization	Before revamp	After revamp
at startup	90	90
before shutdown	55	110
% of Product Loss (to BTMS)		
at startup	0.75	0.75
before shutdown	2.50	0.75

5. Salts Carryover was also a cause of concern as it led to corrosion of overhead system. This made the installation of a demister above the top packed bed mandatory. Though the same demister was retained even after the column was revamped with **20 #s** of zirconia trays, gamma scans showed little or no entrainment. Therefore, there was no post-revamp acid or salt carryover.

Column Inspection

After 13 months of operation, the plant was shutdown and the column was opened (after cleaning) for inspection :

Observations

(1) The cleanup time of the trayed column was far less than the packed column

(2) The trays were found clean and in good physical condition

(3) No plugging or tray damage

(4) No corrosion in the overhead system nullified salt or acid carryover

Economic Benefits

The column revamp rewarded BASF with a number of benefits

(1) Lower Maintenance Costs

due to the longer service life of the trays. The ETFE random packings had to be replaced after every 9 to 12 months due to degradation and mechanical damage.

(2) Longer Run Times

(3) Fewer Shutdowns

(4) Operational Profits increased

as fewer products were lost in the bottoms

Even after three years of service, the trays required no maintenance. The new trays eliminated the tower cleaning costs, cost of packing installation, removal and disposal, cost of packing replacement. The total direct cost savings that accrued from revamp are summarized in **Table 9.4-2.**

Table 9.4-2. Cost Savings Realized by Replacing Packing with Trays

Tower cleaning costs, $. y^{-1}	20000
Packing installation, removal and disposal, $. y^{-1}	20000
Cost of Replacement packing, $. y^{-1}	25000

9.5. REVAMPING A HYDROGEN CHLORIDE ABSORBER

Hydrogen chloride is highly soluble in water and hence readily absorbed in it. However, this chemisorption is accompanied by a large quantity of heat generation — about 1861 kJ per kg of HCl absorbed. If this heat is not adequately removed, the liberated heat will quickly push solution to its boiling point :

HCl gas initially at 300–302 K is allowed to get absorbed by water. The acid solution sets to boil when its strength reaches 14.5 wt% HCl.

Hence to produce hydrochloric acid of commercial strength (> 30 wt % and often greater than

35 Wt %) without excessive loss of HCl, heat must be removed which can be achieved either by evaporation of water from the acid itself or by sensible heat exchange, usually with C/W.

The two common techniques for absorbing HCl gas to manufacture hydrochloric acid are

1. Adiabatic absorption

2. Falling-film absorption

In the **adiabatic absorption**, rising HCl-loaded gas comes in contact with water stream moving countercurrently down in a packed bed and that heat of the reaction is taken care of by evaporation of water in the bed. In a falling-film absorption process, descending HCl-containing gas traffics cocurrently with water descending thru the tubes in a vertical heat exchanger and in that process HCl is absorbed by water-film adhering to the inner-wall of the tubes. The evolved heat is removed by C/W circulating in the shellside.

A **falling-film process** is able to produce hydrochloric acid of greater concentration (37 — 40 wt %) than an adiabatic process which ends up to an acid concentration of only 34% acid. **Another set of advantages of falling-film process being :**

— operation at a lower temperature

— lower ΔP

— higher turndown

The falling-film process being more economical, compared to adiabatic absorption of HCl, this route is generally more preferred. At the same time it is more troublesome to operate.

In the Calvert City, KY, USA is located one such falling-film unit owned by Pennwalt Corpn. This unit had been experiencing problems of large hydraulic instabilities and was unable to operate at design capacity.

CONFIGURATION

It's a packed unit in which pure HCl gas **(480 — 690 kPa. g/ 322K)** is absorbed in a falling-film absorber by dil. HCl solution coming from tails tower (a packed-bed absorber) via a **900mm seal-loop [Fig. 9.5-1].**

The unit is designed to produce 32 wt% aqueous solution of hydrochloric acid with an alternative design case of producing 35 wt% hydrochloric acid but at a slightly lower capacity.

Before the HCl gas is allowed to enter the absorber its pressure is let down to slight above the atmospheric pressure. The gas then enters the falling-film absorber, where it is absorbed by the dilute hydrochloric acid from the tails tower. Both the liq and gas streams descend down in the tubeside and are cooled by C/W circulating in the shellside. The product is cooled concentrated hydrochloric acid that flows out by gravity from the absorber bottom to the product tank via a **4.5 m seal-loop.** The unabsorbed HCl gas — called **by-gas** — leaves the absorber via a side-outlet at the bottom and returns to the tails tower thru a **by-gas line (100 mm ID).** The leftover hydrogen chloride is absorbed by water in countercurrent flow to form dilute acid. This dilute acid is returned to the absorber thru a 900mm seal loop and acts as absorbent of feed HCl-gas. Any HCl gas that is not absorbed in the tails tower flows to the vent scrubber where nearly all unreacted HCl gas is absorbed in a countercurrent stream of water producing a very dilute acid which is drained. The overhead from the scrubber is a mixture of unabsorbed inerts, which are vented.
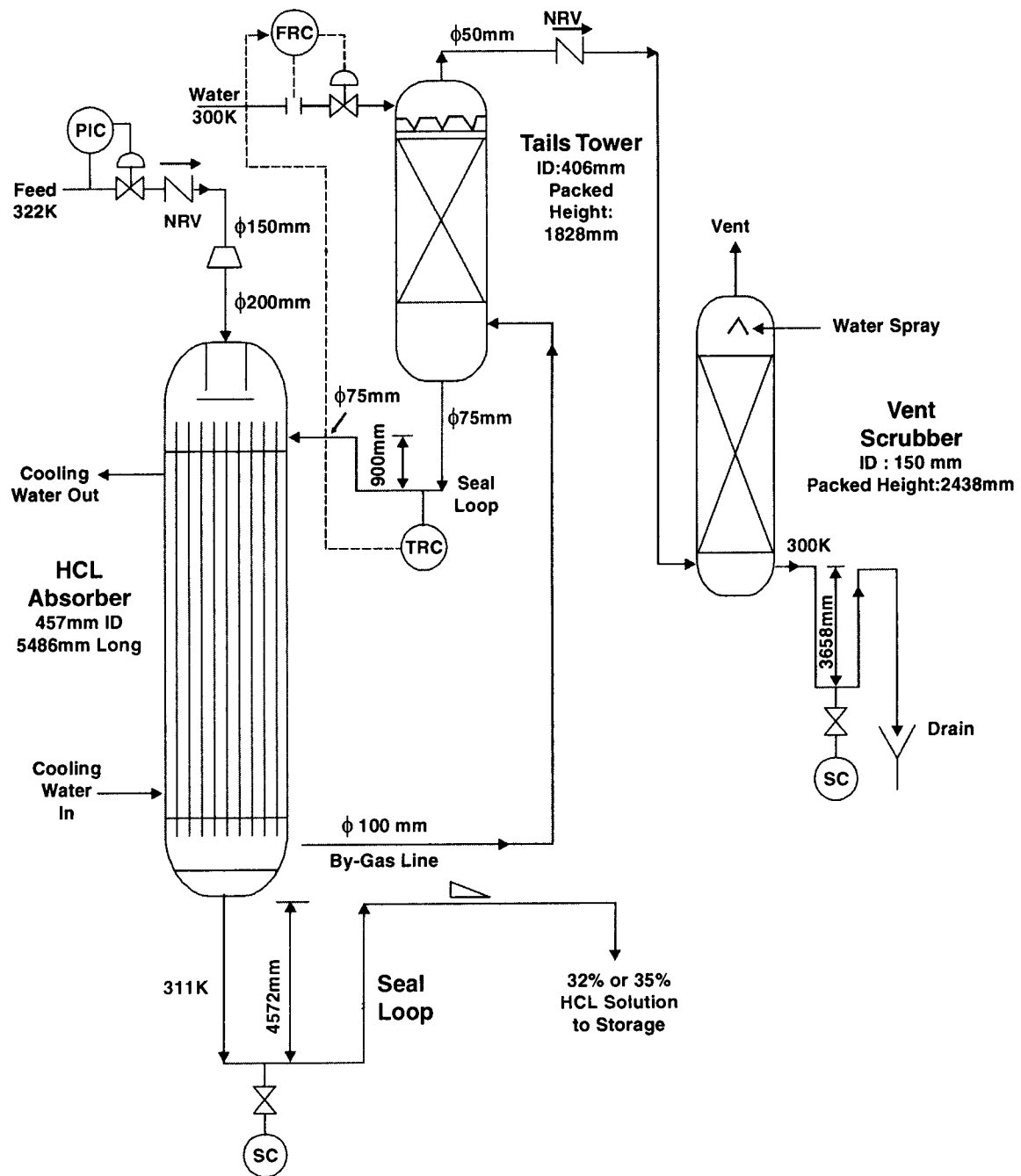
Fig. 9.5-1. *The falling-film HCl absorption unit at Pennwalt's Calvert City plant.*

The **absorber** is a shell-and-tube, vertical heat exchanger **[457mm ID × 5486mm Long]** with an inlet mixing and distribution chamber set at the top of the tubes.

The **distribution chamber** contains the gas and the liq distributors to tubes **(Fig. 9.5-2).**
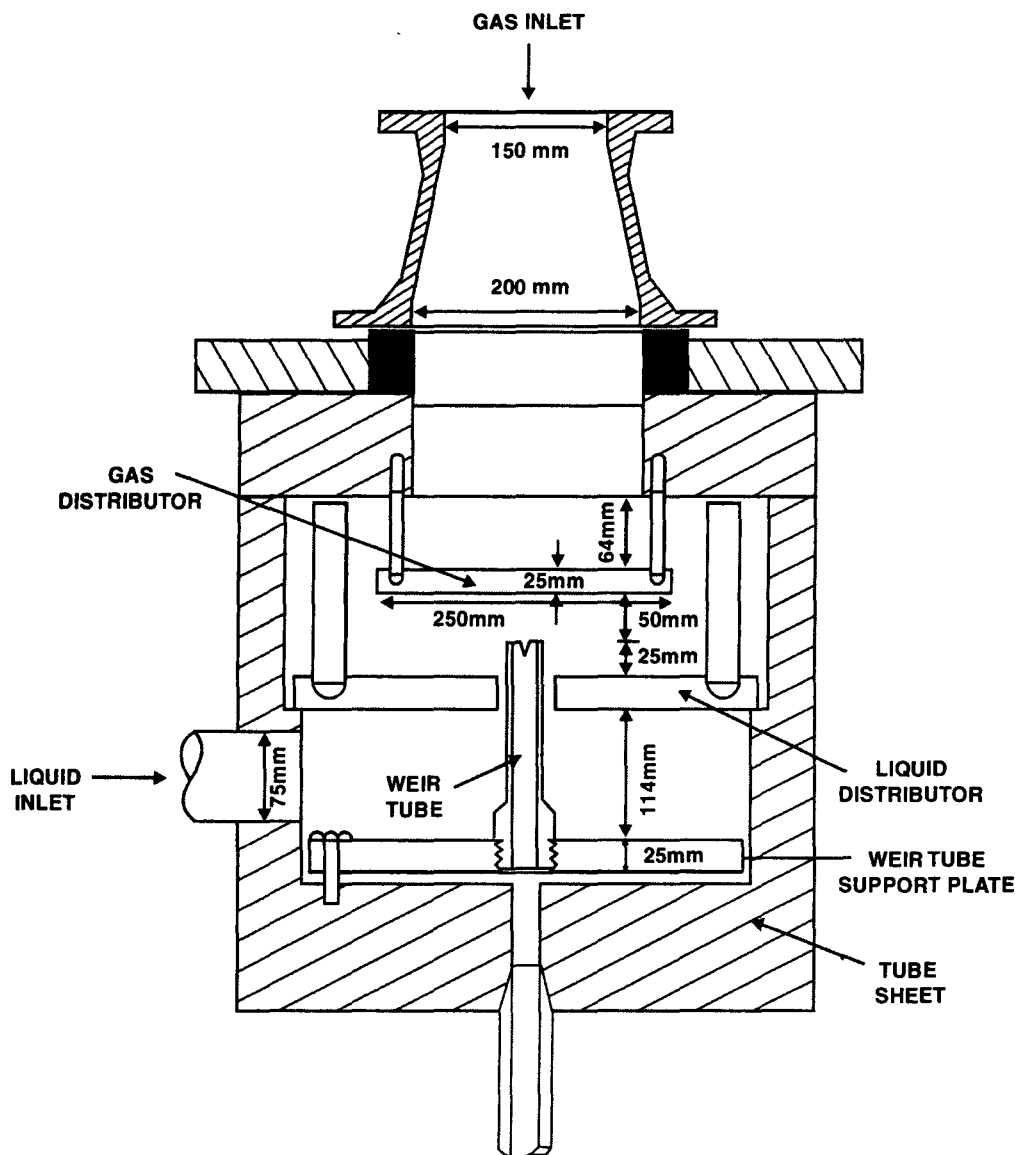
Fig. 9.5-2. *A typical distribution chamber which is fitted at the top of the absorber. It sports both gas and liquid distributors.*

The **liquid distributor** is a perforated plate with holes sufficiently large to sanction a clearance of ~ 3mm to the weir tubes. Liquid flows up thru these clearances. Each weirtube is provided with 4#s of **V-notches** cut at the top — each notch being **12mm deep**. After passing thru the liquid distributor, the liq overflows the weirs into the tubes.

The **gas distributor** is a flat, unperforated baffle located below the inlet gas nozzle. As the gas enters the inlet chamber it is deflected sideways by this baffle and it then enters the weir tubes and descends with the liquid. There is a total of **85 tubes (19mm ID)**.

The **tails tower** is a packed column **(406mm ID)** loaded with **25mm polypropylene saddles** to a bed depth of **1828 mm**. This bed is supported on a gas-injection type support plate.

The **vent scrubber** is a **150mm ID** column packed with a **2438mm bed of 15.87mm**

polypropylene Pall rings. The bed is supported on a grid type support plate while the liq is sprayed thru a single spray nozzle.

The Problem

Initially the highest thruput that could be reached was **50%** design capacity. Any attempt to run at higher thruput resulted in **blowing the liq seal between the absorber and the tails tower.** The seal breakage was haunted by collapse of the support plate with the effect that packings would dump into the tails tower bottom and sometimes would migrate further downstream and accumulate in the **by-gas** header.

When the absorber was lined up, the on-spec acid could not be produced at any flowrate. Leakage was detected from the inlet chamber into the space between the weirtube support plate and tubesheet. The leaks were so large that no water overflowed the weirs and its distribution profile was highly uneven.

The leaks were repaired by using silica cement and the system was returned to service. It produced on-spec acid for the first time.

However, *as the HCl-gas load and water flowrate were raised, the liquid seal between the absorber and the tails tower got blown.*

First Revamp

In an attempt to overcome this problem the seal depth was raised three times increasing the depth from **900mm** to **2700mm**. The control system was modified so that the temperature of liq in the seal leg was used to control the water to the tails tower. The C/W control valve was kept full open so that maximum cooling water was charged to the absorber. The feed control was put on manual to minimize fluctuations in flow.

During one shutdown, the top head of the absorber was removed and water was run thru the tails tower and the absorber to check the liq distribution. Severe maldistribution was noted. Air bubbles that got entrained with the water inflowing from tails tower to absorber enforced a lifting action — air lifting water preferentially into the tubes located near the water inlet nozzles. Since the liq distributor was observed to aggravate this gas lifting water, it was removed.

The original packing support plate of tails tower that got disintegrated due to frequent seal breakage was replaced by a grid-type support plate that held together better.

Result

The absorber was put back into service. However, the loss of seal frequented as efforts were made to increase gas loading beyond 50% of the design thruput.

Collapse of the new support plate in tails tower became a regular occurrence. And as a consequence fragments of packing found their way into almost all segments of the system piping.

Second Revamp

A perforated pipe, with perforations smaller than the packing, was installed at the **by-gas** inlet into the tails tower. This measure was adopted to avoid backflow of packings pieces into the **by-gas** header.

Another modification was the installation of a nitrogen purge in the absorber feed with the objective that a nitrogen purge of **3.5 – 8.5 Nm^3. h^{-1}** would help achieve smoother operation.

Result

Although the introduction of nitrogen purge somewhat improved stability, further increases of the purge achieved little. And, of course, *it did not solve the problem of blowing of seal.*

Third Revamp

The absorber inlet-gas distributor was temporarily removed, and the system was l/up. However, this didn't improve performance so it was reinstalled.

Another change was made :

> **the 25mm saddles in the tails tower were replaced by a mixture of 38-mm Pall rings and saddles**

Result

The repacking brought forth no difference in performance.

The system was, as usual, capable of processing approximately 50% of the design thruput. Any increases past this thruput caused the seal between the tails tower and the absorber to blow. Even at rates below 50% of design, the system was touchy and **upsets in the upstream units often caused the seal to blow.**

Hunt for the Clues

It was unclear whether the seal blowing problem originated in the tails tower (it might be due to flooding at the packing support plate) or in the absorber.

For the sake of investigation, the packed tails tower was converted to a spray tower by removing the packing and support plate and replacing the liq distributor by sprays. This also offered the additional benefits of eliminating pipeline blockage by bits of packing which could have been responsible for the problem.

During test run it was observed that when the water flowrate was less than 50% of design value, liq distribution appeared good, with a slight bias towards higher flows into tubes located near the water inlet nozzle. As soon as the water flowrate exceeded 50% of design, gas bubble were observed to enter the mixing chamber with the water from the seal loop. The amount of bubbling increased as the water flowrate was raised. The gas bubbles rising thru the seal loop distorted the liq distribution pattern and as a consequence, tubes closer to the inlet got larger quantities of water while those located further from the inlet nozzle were starving.

These observations led to the following conclusions :

1. There was gas entrainment in the seal liq.
2. The gas bubbles were born out of turbulence created when the tails tower water entered the seal loop.
3. This gas was entrained because liquid velocity in the seal loop was too large to allow the gas to vent back into the tails tower

Fourth Revamp

Packing was replaced by sprays as a means of gas-liq contact in the tails tower.

The diameter of the seal leg was doubled from **75mm** to **150mm.**

Result

The system was returned to service. However, the seal blew at exactly the same thruput as before, that is, at about 50% of the design thruput. No improvement was observed.

However, this trial proved beyond doubt that the tails tower was not responsible for blowing the seal.

It appeared, therefore, *that the most likely mechanism that could cause that seal to break would be the presence of liquid in the by-gas header.*

Fifth Revamp

So in order to eliminate the presence of water in the by-gas header the following modifications were implemented :

1. A boot with a manual drain was installed at the bottom of the vertical leg of the **by-gas header.**

2. To prevent any backflow of liq from the tails tower to the **by-gas header**, an inverted U-loop was inducted into the by-gas line just before it entered the tails tower **(Fig. 9.5-3**

The top of the inverted U-shaped inlet was about **900mm** above the by-gas inlet to tails tower.

Result

The system was returned to service. And for the first time it registered a 20% capacity enhancement. The seal blew at 60% of the design thruput instead of 50%.

The **by-gas header** boot was continuously monitored manually for liquid. It was observed that as the thruput at which seal blowing approached, the qty of liq drained shot up very rapidly. This confirmed that *the presence of liq in the by-gas header and its surge was responsible for seal blowing.*

So the problem area narrowed to the absorber or the bottom line (that drains 32% or 35% HCl sol$^{\underline{n}}$ to storage), as only these were the likely sources of liq in the by-gas line.

Liquid Distributor — the Suspected Culprit

Calculations showed that the bottoms line (of the absorber) was adequately sized. The line was thoroughly flushed and every bits of packing were removed. Trials with water *(no gas flow)* confirmed that this line was adequate to handle the design **BTMS** flow without liq backup.

Fig. 9.5-3. *A drain valve at the by-gas header vertical leg and an inverted U-shape entry of by-gas to tails tower are all set to minimize the presence of water in by-gas header.*

Material balance and heat transfer data indicated that material balance closed within 15% and measured heat transfer coefficients were low, of the order of **114 — 227 W. m^{-2}. K^{-1}**, compared to a design heat transfer coefficient of **625 W. m^{-2}. K^{-1}** of the absorber.

Poor liquid distribution could explain both the low **htc** and entrainment of liquid in the **by-gas header**, because a maldistributed liq flow may cause both poor apparent heat transfer as well as poor absorption. Poor absorption would, in turn cause an excessive flow of unabsorbed HCl into the **by-gas line**. This excessive flow could surge liq up the **by-gas header**.

Sixth Revamp

Since, tangential V-notched can beget better liq distribution than triangular **V-notches**, the top **12mm** of each tube inlet was cut and removed and tangential V-notches about 12mm deep were cut into the top of the tubes **(Fig.9.5-4)**.

Second, the liquid distributor, which had been previously removed (as gas bubbling action fed excessive quantities of liq into tubes located near the liq inlet) was reinstalled, as replacement of **75mm ID** seal leg with a **150 mm ID** one eliminated gas bubbles.

Third, it was discovered that the absorber was slightly leaning off the vertical. With the notched being only **12mm deep**, such a posture could well have contributed to some liq maldistribution. So the absorber was straightened to within ± **1.6mm**.

(a) Triangular
V-notch

(b) Tangential
V-notch
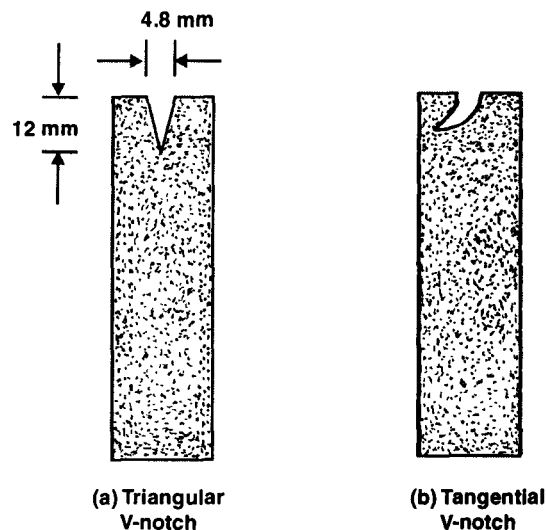
Fig. 9.5-4. *Triangular V-notches (a) were replaced by Tangential V-notches (b).*

Result

The system was returned to service only to discover that no improvement resulted. The seal blew again and at 60% of the design rate and the **htc** of the absorber was still low. At least some improvement was expected if liq distribution were to blame for poor hydraulic performance.

Trial after trial confirmed that seal breakage occurred at the same gas flowrate regardless of the liq flowrate. Seal was found to blow at 60% of the design gas rate, even though the ratio of liq flowrate to gas flowrate was doubled.

Thus seal blowing was primarily the function of the gas rate, not the liq rate. This means that gas maldistribution rather than liq maldistribution was the likely cause of seal-break. Because of gas maldistribution there occurred poor absorption and that manifested in lower **htcs**. Excessive unabsorbed HCl-gas would then reach the bottom of the absorber, causing high velocities and turbulence there and as it tended to escape via **by-gas line** it entrained liq from absorber bottom up thru the **by-gas header**.

The absorber was dismantled and its shell and tubes were inspected. Thin hard, white deposits of the silica cement that was previously used to seal the leaks were detected inside all the tubes, except for those located directly under the gas distributor baffle. The deposit-free tubes formed a clear circle corresponding to the diameter of the gas distributor baffle with an **accuracy of ± 6mm**. This observation lent further support to the gas maldistribution theory.

Seventh Revamp

Since the existing **gas distributor (mixing chamber)** was contributing to excessively high liquid flow in the area directly under the baffle it was replaced by a new **perforated-plate-type**

distributor which was installed to improve gas distribution. The new distributor was designed to prevent gas jets from impinging on the liq surface in the liq distributor.

In addition to this, a temporary bypass line from the tails tower top to the vent header was installed to improve **breathing** to prevent vent scrubber-packing from interfering with breathing.

Result

The system was returned to service. Full capacity was achieved for the very first time. On-spec HCl (32 wt%) was produced at 100% of design rate. Htc was measured to be ~ **625 W. m^{-2}. K^{-1}**, which was the design coefficient. The alternative design case, 35 wt % acid could also be produced but only at 85% of the design rate.

Overcoming the Last Hurdle

Though the main problem appeared to be solved, the system was still somewhat touchy. The seal blew when attempts were made to exceed 90% of the design gas rate while making 35 wt % acid. The seal also broke while making 32 wt % acid when the gas rate was increased suddenly by as little as 15%. This implied that some improvements were still required.

Whatever improvements observed were mainly due to the new gas distributor. Though the vent–scrubber **by-gas line** improved breathing realized thru reduced pressure fluctuations in the system, it didn't account for improved heat transfer and low liq entrainment in the **by-gas header**.

It was felt that the system stability could be further enhanced by installing

(1) a permanent drain on the by-gas line boot.

(2) a high-point vent in the BTMS line that transfers by gravity 32 wt% or, 35 wt % acid from the absorber bottom to the storage tank.

The drain would prevent liq entrainment from overfilling the **by-gas header boot** and flooding the **by-gas header**. The vent would eliminate intermittent siphoning in the BTMS line (Fig. 9.5-5)
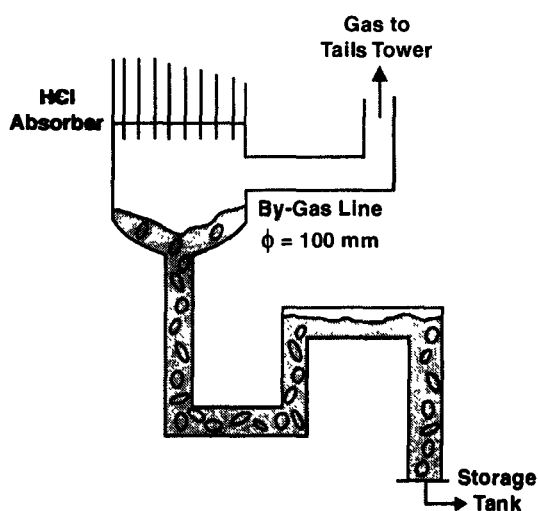
(a) Gas is entrained in bottom line and accumulated at high point. Static head decreases, backing up liquid.
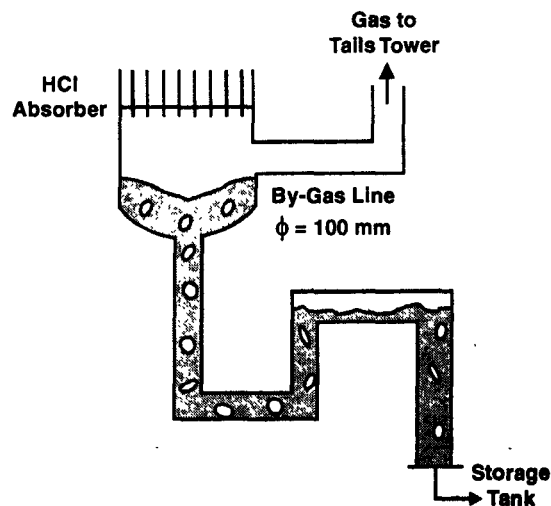
(b) Level rises, reducing gas entrainment. Gas bubble at high point is now larger, which backs off more liquid.
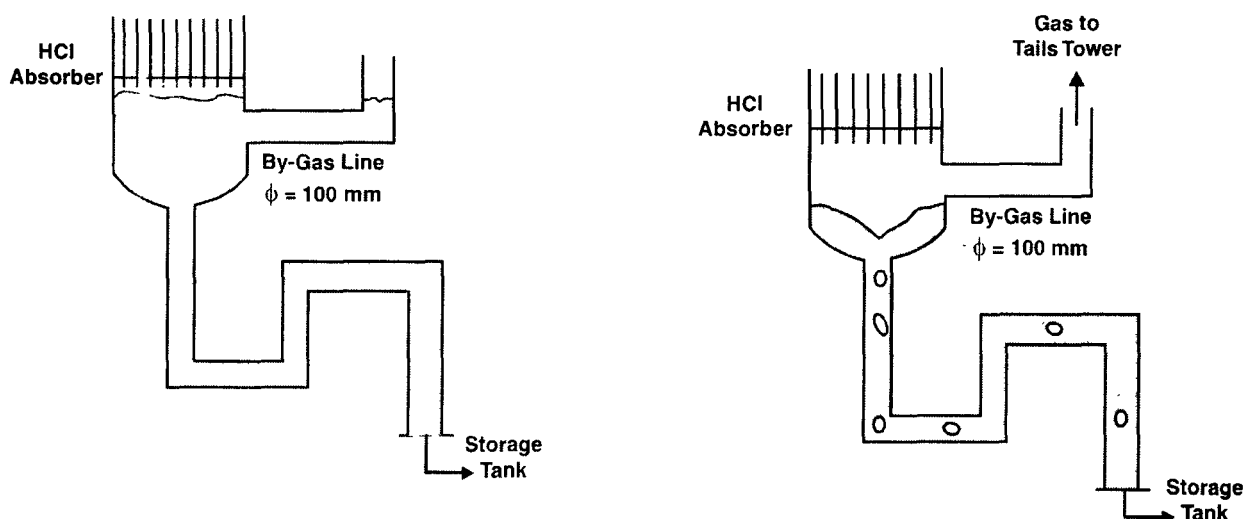
(c) Liquid level rises until bubble is pushed out. If level rises to the by-gas line elevation, it will stop gas flow in the by-gas line. This may cause the top seal (not shown) to blow.

(d) Once vapor is removed in part (c), a siphon is created, which quickly lowers liquid level, pulling a vacuum on the system and causing a further upset to the top seal.

Fig. 9.5-5. *Four stages of intermittent siphoning due to vapor accumulation at the high-point of BTMS drawline.*

The two objectives were implemented by installing a line connecting the bottom of the boot to the high-point in the BTMS line.

This single modification completely stabilized the system. Acid at a strength of 36.5 wt% (better than the alternative design case) was produced at 115% of the design capacity with no sign of instability.

REFERENCES

1. L Spiegel and W Meir — **Correlations of the Performance Characteristics of the various Mellapak types** [Institute of Chemical Engineers Symposium Series 104/1987 /A 203-215].

2. P Süess and L Spiegel — **Holdup of Mellapak Structured Packings** *[Chemical Engineering and Processes vol. 31/1992/2/P : 119-124].*

3. L Spiegel and W Meir — **A Generalized Pressure Drop Model for Structured Packings** [International Conference and Exhibition on Distillation and Absorption, Birmingham, England, Sep. 7–9/1992].

4. P Collins and K Breu — **Structured Packings for TEG Contactors – Design Methods and Operating Characteristics** [9th Continental Meeting of the European chapter of the Gas Processors Association, May 14, 1992].

5. J Kean, H Turner and B Price — **How Packing Works in Dehydrators** *[Hydrocarbon Processing, April 1991].*

6. M Souders and G G Brown, *Industrial Engineering Chemistry, vol.26/1934/P : 98–103].*

7. J L Bravo, J A Rocha and J R Fair — **Mass Transfer in Gauze Packings** [*Hydrocarbon Processing, Jan 1985./P : 91–95].*

8. P Bomio, M Laso, K Breu and N Wynn — **Improving Selectivity, Capacity and Efficiency of Hydrogen Sulfide / Carbon Dioxide removal columns with Sulzer structured packing** [SULFUR 88, Vienna, Nov. 1988].

9.   G Astarita, D W Savage and A Bisio — GAS TREATING WITH CHEMICAL SOLVENTS [John Wiley and Sons, New York, 1985].

10. L de Leye and G F Froment — **Rigorous Simulation and Design of Columns for Gas Absorption and Chemical Reaction.**

   I : Packed Columns

   II : Plate Columns

   [Computers and Chemical Engineering 10(5)/493–515]

11. W Meier — Sulzer Columns for Distillation and Absorption Processes *[Sulzer Technical Review, 61 (2)/P : 49–61].*

12. P M M Blauwhoff, B Kamphuis, W P M Van Swaaij and K R Westerterp — **Absorber Design in Sour Natural Gas Treatment Plants : Impact of Process Variables on Operation and Economics** *[Chemical Engineering Processes, vol.19/P : 1–26].*

13. Kurt Breu — **Gas Processing with Structured Packings for the Chemical Petrochemical and Gas Industry** [Sulzer Chemtech, TRK].

14. R Hauser and J Richardson, *Hydrocarbon Processing [Sept. 2000/P : 95–98].*

15. Henry Z Kister, **DISTILLATION OPERATION** [McGraw-Hill Publ., 1990].

16. Norton Chemical Process Products Corpn., **Bulletin PVT–1, 1997.**

17. H. Z. Kister *et. al* — **Absorber Troubleshooting : Systematic Investigation Pays Off** *[Chemical Engineering Progress, June 1992/P : 41–48].*

18. C E Hulswitt — **Adiabatic and Falling Film Absorption of Hydrogen Chloride** *[Chemical Engineering Progress, Feb. 1993/P : 50].*

19. J Coull *et. al.* — **Hydrochloric Acid Production in a Karbate Falling-Film-Type Absorber** *[Chemical Engineering Progress, August 1945/P : 525].*

20. W M Gaylord and M A Miranda — **The Falling-Film Hydrochloric Acid Absorber** *[Chemical Engineering Progress, Mar 1957/P : 139 M].*

□□

Cost Estimation of Absorption Tower

The cost of absorption towers can be estimated conveniently by using the following correlations with standard deviations < 10 %.

TRAY TOWERS

The total estimated cost of a tray tower (C_t) is calculated from

$$C_t = 50 \ [C_b \cdot F_M + N_T \cdot C_{bt} \cdot F_{TM} \cdot F_{TT} \cdot F_{NT} + C_{pl}] \qquad \text{...(10.1)}$$

where

C_b = base cost of tower in CS, Rs

F_M = cost factor for shell MOC = 1.0 for CS

N_T = total number of trays

C_{bt} = base cost for valve trays in CS, Rs

F_{TM} = cost factor for tray MOC = 1.0 for CS

F_{TT} = cost factor for tray type

F_{NT} = cost factor for number of trays

C_{pl} = cost of platforms and ladders, Rs

1. Base Cost of Tower (C_b)

For shell of carbon steel **(CS)**,

$$C_b = \exp \left[6.446 + 0.21887 \ln W_s + 0.02297 \left(\ln W_s \right)^2 \right] \qquad \text{...(10.2)}$$

valid for shell weight in the range

$$1930 \text{——} 445000 \text{ kg}$$

For shells made of materials other than CS, calculate shell cost by using the following correlation

$$C_s = C_b \cdot F_M \qquad \text{...(10.3)}$$

The shell cost data on which the above correlations are based include the cost of

• skirt

• a standard number and sizes of manholes

• a standard number and sizes of nozzles.

These are functions of tower dia, length and pressure rating.

Analysis of cost data for 200 absorption towers (and 200 distillation columns) revealed that shell cost (inclusive of skirt, nozzles and manholes) correlates equally well with both actual tower and shell weight. This shell weight is computed from

(1) tower dia (assuming 2 : 1 elliptical heads and ignoring the nozzles, manholes and skirt)

(2) tower length (tangent-to-tangent)

(3) design pressure (external or internal) by taking into account wind-load effects and varying shell thickness at the bottom and top of the tower.

2. Cost of Platforms and Ladders

The cost of platforms and ladders is correlated against tower dia and tangent–to–tangent length.

$$C_{pl} = 1017 \, D_i^{0.73960} \cdot L_t^{0.70684} \qquad \qquad ...(10.4)$$

i.e., the cost of platforms and ladders varies directly with tower dia & tower length

where

D_i = tower ID, m

L_t = tower length, m

This correlation is valid for

$$0.91 \, m \le D_i \le 6.40 \, m$$

$$8.23 \, m \le L_t \le 12.19 \, m$$

3. Cost of Tower Trays (C_{bt})

The base cost for tower trays is given by

$$C_{bt} = 278.38 \, \exp(0.5705 \, D) \qquad \qquad ...(10.5)$$

for carbon steel, where

C_{bt} = base cost per tray of CS

D = tray dia, m

$$0.6 \, m \le D \le 4.8 \, m$$

4. Cost Factor for Shell MOC (F_M)

Material	*Cost Factor, F_M*
SS304	1.7
SS316	2.1
Carpenter 20CB-3	3.2
Ni–200	5.4
Monel–400	3.6
Inconel–600	3.6
Incoloy–825	3.7
Titanium	7.7

5. Cost Factor for Tray MOC (F_M)

For **SS304** :	F_{TM}	$= 1.189 + 0.1894\ D$
For **SS316** :	F_{TM}	$= 1.401 + 0.2376\ D$
For **Carpenter 20CB-3** :	F_{TM}	$= 1.525 + 0.2585\ D$
For **Monel** :	F_{TM}	$= 2.306 + 0.3674\ D$

6. Cost Factor for Tray Types (F_{TT})

Tray Types	*Cost Factor (F_{TT})*
Valve	1.00
Grid	0.80
Bubblecap	1.59
Sieve with downcomer	0.85

7. Number of Trays Factor (F_{NT})

$$F_{NT} = \frac{2.25}{[1.0414]^{NT}} \qquad \qquad ...(10.6)$$

PACKED TOWERS

The total cost of a packed tower (C_t) is the sum of the shell cost, cost of packing, and the cost of platforms and ladders :

$$C_t = 50\left[C_b\, F_M + \frac{\pi}{4}\, D_i^2 \cdot Z \cdot C_p + C_{pl} \right] \qquad ...(10.7)$$

where

Z = height of the packed bed, m

C_p = cost of packing, Rs

Cost Of An Absorption Tower

Example 10.1. *Estimate the cost of a carbon steel absorption tower 0.9 m in dia and 17.5 m long (tangent-to-tangent) designed to withstand a pressure of 2240 kPa and containing 32 valve trays of 304SS.*

Give a corrosion allowance of 0.8 mm.

Solution : First to be calculated is the tower-shell weight (W_s). For this, we need to determine the shell thickness at top and bottom of the tower, beforehand.

Step – (I) Shell Thickness at Tower Top (Δ_{top})

$$\Delta_{top} = \frac{P_{dsgn}\,(D_i\,/\,2)}{S.\,E - 0.6\,P_{dsgn}}$$

where Δ = shell thickness, m

P_{dsgn} = design pressure, Pa

$\quad$ S = maximum allowable stress, Pa

$\quad$ E = joint efficiency = 85 %, usually

$\quad$ D_i = tower ID, m

$$\therefore \qquad \Delta_{top} = \frac{\left(2240 \times 10^3 \, \text{Pa}\right) \left(\frac{1}{2} \times 0.9 \, \text{m}\right)}{\left(9.45 \times 10^4 \times 10^3 \, \text{Pa}\right)(0.85) - 0.6\left(2240 \times 10^3 \, \text{Pa}\right)}$$

$$= 0.01276 \, \text{m}$$
$$= 12.76 \, \text{mm}$$

$\boxed{S = 9.45 \times 10^4 \text{ kPa for low alloy steel}}$

Add corrosion allowance of 0.8 mm

$\therefore \qquad\qquad\qquad\qquad \Delta_{top} = 13.56 \, \text{mm}$

Step – (II) Shell Thickness at Bottom (Δ_{bot})

$$\Delta_{bot} = \Delta_{WIND} + \Delta_{girth}$$

where,

Δ_{WIND} = thickness due to wind load

Δ_{girth} = thickness to withstand internal pressure when girth seam controls

Take,

$\qquad D_o = 900 \, \text{mm} + 25 \, \text{mm} \qquad = 925 \, \text{mm}$

$\qquad L_t = 17.5 \, \text{m}$

$$\Delta_{WIND} = \frac{1500\left(D_o + \frac{1}{2}D_i\right)}{S} \left|\frac{L_t}{D_o}\right|^2$$

$$= \frac{1500\,(0.925 + 0.45)}{9.45 \times 10^7} \left|\frac{17.5}{0.925}\right|^2$$

$$= 7.81 \times 10^{-3} \, \text{m}$$
$$= 7.81 \, \text{mm}$$

Step – (III) Shell Thickness to Withstand Internal Pressure When Girth Seam Controls (Δ_{GIRTH})

$$\Delta_{GIRTH} = \frac{P_{DSGN} \cdot \frac{1}{2} D_i}{2\,SE + 25\%\,P_{DSGN}}$$

$$= \frac{\left(2240 \times 10^3 \, \text{Pa}\right) \left(\frac{1}{2} \times 0.900 \, \text{m}\right)}{2\left(9.45 \times 10^4 \times 10^3 \, \text{Pa}\right)(0.85) + 0.25\left(2240 \times 10^3 \, \text{Pa}\right)}$$

$$= 0.006252 \text{ m}$$
$$= 6.25 \text{ mm}$$

Step – (IV) Bottom Thickness of Shell (Δ_{BOT})

$$\Delta_{BOT} = \Delta_{WIND} + \Delta_{GIRTH}$$
$$= 7.81 \text{ mm} + 6.25 \text{ mm}$$
$$= 14.06 \text{ mm}$$

Adding corrosion allowance

$$\Delta_{BOT} = 14.06 \text{ mm} + 0.8 \text{ mm} = 14.86 \text{ mm} \approx 15 \text{ mm}$$

Step – (V) Shell Weight (W_s)

$$W_s = \pi D_i [L_t + 0.8116 \, D_i] \, \Delta_{BOT} \cdot \rho_s$$

where ρ_s = density of shell material

$$= 7861 \text{ kg. m}^{-3} \text{ for CS}$$

$$\therefore \qquad W_s = \pi \, (0.9\text{m}) \, [17.5\text{m} + 0.8116 \, (0.9\text{m})] \, [15 \times 10^{-3}\text{m}] \, [7861 \text{ kg. m}^{-3}]$$
$$= 6078 \text{ kg}$$

Step – (VI) Base Cost of Tower (C_b)

$$C_b = \exp\left[6.446 + 0.21887 \ln W_s + 0.02297 (\ln W_s)^2\right]$$

$$= \exp\left[6.446 + 0.21887 \ln 6078 + 0.02297 \, (\ln 6078)^2\right]$$

$$= 24257$$

Step – (VII) Cost of Platforms and Ladders

$$C_{pl} = 1017 \, D_i^{0.7396} \cdot L_t^{0.70684}$$
$$= 1017 \, (\, 0.9)^{0.7396} \, (17.5)^{0.70684}$$
$$= 7113.899$$

Step – (VIII) Cost of Trays (C_{bt})

$$C_{bt} = 278.38 \exp (0.5705 \, D_i)$$
$$= 278.38 \exp (0.5705 \times 0.9)$$
$$= 465.185$$

(Step – (IX) Cost Factor For Tray Material (F_{TM})

$$F_{TM} = 1.189 + 0.1894 \, D_i$$
$$= 1.189 + 0.1894 \, (0.9)$$
$$= 1.35946$$

Step – (X) Cost Factor for Tray Types (F_{TT})

$$F_{TT} = 1.0 \text{ for valve trays}$$

Step – (XI) Number Tray Factor (F_{NT})

Since the number of **trays >20, F_{NT} = 1**

Step – (XII) Total Cost of Absorption Tower

$$C_t = 50 \, [C_b \, F_M + N_T \, C_{bt} \, F_{TM} \, F_{TT} \, F_{NT} + C_{pl}]$$
$$= 50 \, [24257 \, (1.0) + 32 \, (465.185) \, (1.3594) \, (1) \, (1) + 7114]$$
$$= \text{Rs. } 2580346$$

REFERENCES

1. ASME, *Pressure Vessel and Piping Design : Collected Papers*, 1960.
2. K M Guthrie, *Process Plant Estimation, Evaluation and Control* (Craftsman Book Co. of America, California, 1974).
3. A Pikulik and H E Diaz, *Chemical Engineering (Oct. 10, 1977)*.
4. A Mulet, *et. al., Chemical Engineering (Oct. 5, 1981/P–145)*.
5. A Mulet, *et. al., Chemical Engineering (Dec. 28, 1981/P–77)*.

Miscellaneous

11.1 HINDERED AMINES FOR EFFICIENT ACID-GAS REMOVAL

Hindered amines, a new breed of solvents, are potential gas conditioning agents that offer significant cost and energy savings. Three specific technologies were born to this family to handle gas treating applications commonly encountered in PCIs, CPIs, and refining industries:

1. **FLEXSORB SE** that specifically removes H_2S.
2. **FLEXSORB PS** that offers bulk removal of both CO_2 and H_2S.
3. **FLEXSORB HP**, which is meant for CO_2 removal, offers advantages over hot potassium carbonate.

Each system is adaptable to conventional absorber regenerator equipment or can be readily retrofitted to obtain energy savings or debottlenecking credits.

HINDERED AMINE DEVELOPMENT

Research into the acid gas reactions with amines led to improved technology for CO_2 removal, either alone or with H_2S. Side by side another new chemical concept emerged that led to selective H_2S removal from gases with high CO_2 loadings, e.g., greater than~1 mol CO_2 per mol of H_2S.

These concepts stem from a new strain of gas treating amines—the **hindered amines**. But before we get into hindered amines, we should look into the chemistry of amines as to how they remove acid-gases viz H_2S and CO_2.
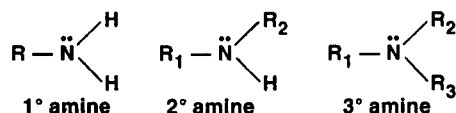
where R_1, R_2 and R_3 may be alkyl (CH_3, C_2H_5, n-Pr, n-Bu.....) or alkanol (—OMe,—OEt,—O—n-Bu......etc.) group.

Reaction with H_2S

It is a acid-base type and only one mode of reaction takes place

11.1
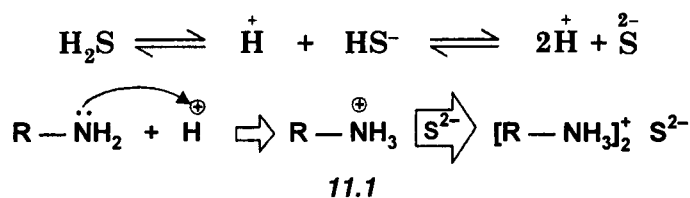
All types of amines — be it primary or secondary or tertiary — react in a similar way irrespective of whether aq. phase is present or not.

Reaction with CO_2

Two kinds of reaction are possible. One is acid base reaction

$$CO_2 + H_2O \rightleftharpoons HCO_3^- + \overset{+}{H}$$

$$HCO_3^- \rightleftharpoons \overset{+}{H} + CO_3^{2-}$$
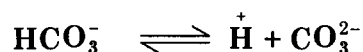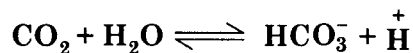
which is conventional neutralization reaction that follows via generation of bicarbonic and carbonic acids.
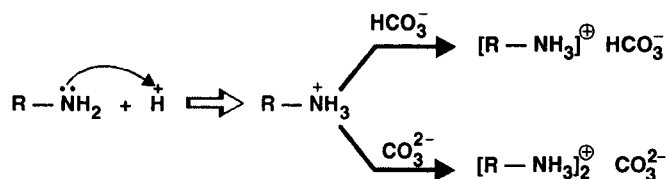
Water must obviously be present in the system so that bicarbonic and carbonic acids form prior to their removal by amines. All types of amines— primary, secondary and tertiary —subscribe to this neutralization reaction and in the same way : *the portion is abstracted by the lone pair of the N-atom explaining its basicity.*

The other type of reaction is carbamate formation which is unique to CO_2 as H_2S does not subscribe to this reaction.

Carbamic acid   Carbamate
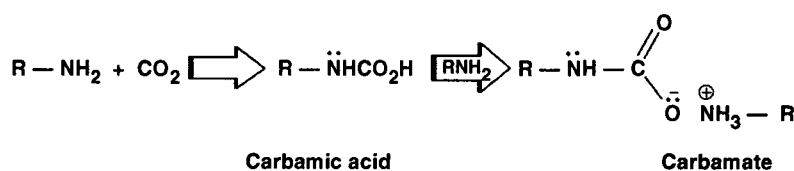
Only primary and secondary amines that have two and one replaceable H-atom-of the amine N do not give rise to this reaction which is based on thermodynamic stability of carbamate formed.

It is the high carbamate stability of linear primary and secondary amines that clamps thermodynamic limitation to the capacity of conventional amines for CO_2 removal about 0.5 mole CO_2 per mole of amine.

Overcoming this limitation would beget enhanced CO_2 capacity and much faster CO_2 mass transfer rates bringing about sizeable savings in terms of investment and energy for CO_2 removal and simultaneous CO_2/H_2S removal.

Theoretical analysis suggests that if this carbamate path is replaced by conventional acid-base reaction, CO_2 removal capacity can be enhanced to 1 mole CO_2 per mole of amine, *i.e.*, this reaction path leads to the formation of bicarbonate ion as the sink for CO_2.

Now the only way to make higher CO_2 loadings possible is to modify the amine structure so as to destabilize the carbamate structure. **Choosing the appropriate amine structure to achieve the desired carbamate stability is the key to hindered amine chemistry.**

Tertiary amines are a type of **sterically hindered** amines that are void of any N—H hydrogen

so that CO_2 gets no chance of forming carbamate leaving only the scope of acid base neutralization reaction to take place. However, if the feed gas contains both H_2S and CO_2, two competing acid-base reactions take place simultaneously.

3°-Amine + H₂S ⟶ **3°-Amine bisulfide + 3°-Amine sulfide**

3°-Amine + CO₂ + H₂O ⟶ **3°-Amine bicarbonate + 3°-Amine carbonate**
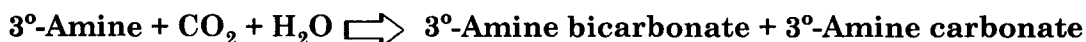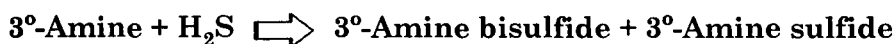
Hence for gases with high CO_2 loadings, selective H_2S removal by conventional tertiary amines is severely restricted. Entered the hindered amines—usually tertiary alkanolamines — that overcome this capacity limitation for selective H_2S removal. This has been made possible by their differential kinetics with H_2S and CO_2. Their reaction rate with CO_2 is very slow due to steric hindrance while their H_2S-absorption rate remains high since H_2S reaction involves a proton exchange with amine.

This is useful in selective H_2S removal from high CO_2-laden gases and endows the following advantages:

- **higher H₂S capacity**
- **lower solution circulation**
- **saving in investment**
- **saving in energy**

The rate of absorption in K_2CO_3 solution becomes significantly higher when the latter is promoted with amine. However, the conventional amine-promoted potassium carbonate processes do not improve the working capacity of the carbonate solution and the rate of CO_2-absorption is still well below the theoretical limit. The use of hindered amines overcomes these limitations and gives both higher working capacity and greater mass transfer rates than conventional amine-promoters.

Certain hindered amines offer considerable advantages in terms of capacity, rate of absorption, and chemical stability compared to the amines normally used in conventional hybrid scrubbing processes. Hindered amine, by virtue of its greater cyclic capacity possesses acid gas capacity advantages of up to 50%—the profitable outcome of steric hindrance which sets up a more favorable vapor/liquid equilibrium **(VLE)** curve. Besides, it is this very bulk effect that awards hindered amine system a mass transfer rate advantages of more than 100%.

Note : ⊘n means circulation

FLEXSORB SE

Developed in 1983, **Flexsorb SE** is a typical hindered amine that shows no corrosion problems, no fouling problems, yet exhibiting good operability under commercial conditions.

Applied to commercial scale, the advantages of **Flexsorb SE** over aq. **MDEA** is all too apparent as is evident in **Fig 11.1.1** that plots **H₂S slippage** against **relative solution circulation rate.**

Flexsorb SE exhibits a 40% capacity advantage relative to **MDEA** at the 300 vppm **H₂S** slippage. Since all data are based on constant ratio of regeneration steam to amine ⊘n rate, this 40% capacity gain translates to 40% energy savings, and significantly smaller equipment and reduced investment.

Flexsorb SE can also be used to sweeten (desulfurization) the low kilojoule gas produced in resid conversion process, FLEXICOKING, and also to clean up **TG** (tail gas). It can be used to desulfurize CO_2 used in enhanced oil recovery **(EOR)** operations. If the CO_2 is desulfurized prior to reinjection in the formation, recycle of high - pressure H_2S is avoided, reducing the potential of corrosion and concern of safety.
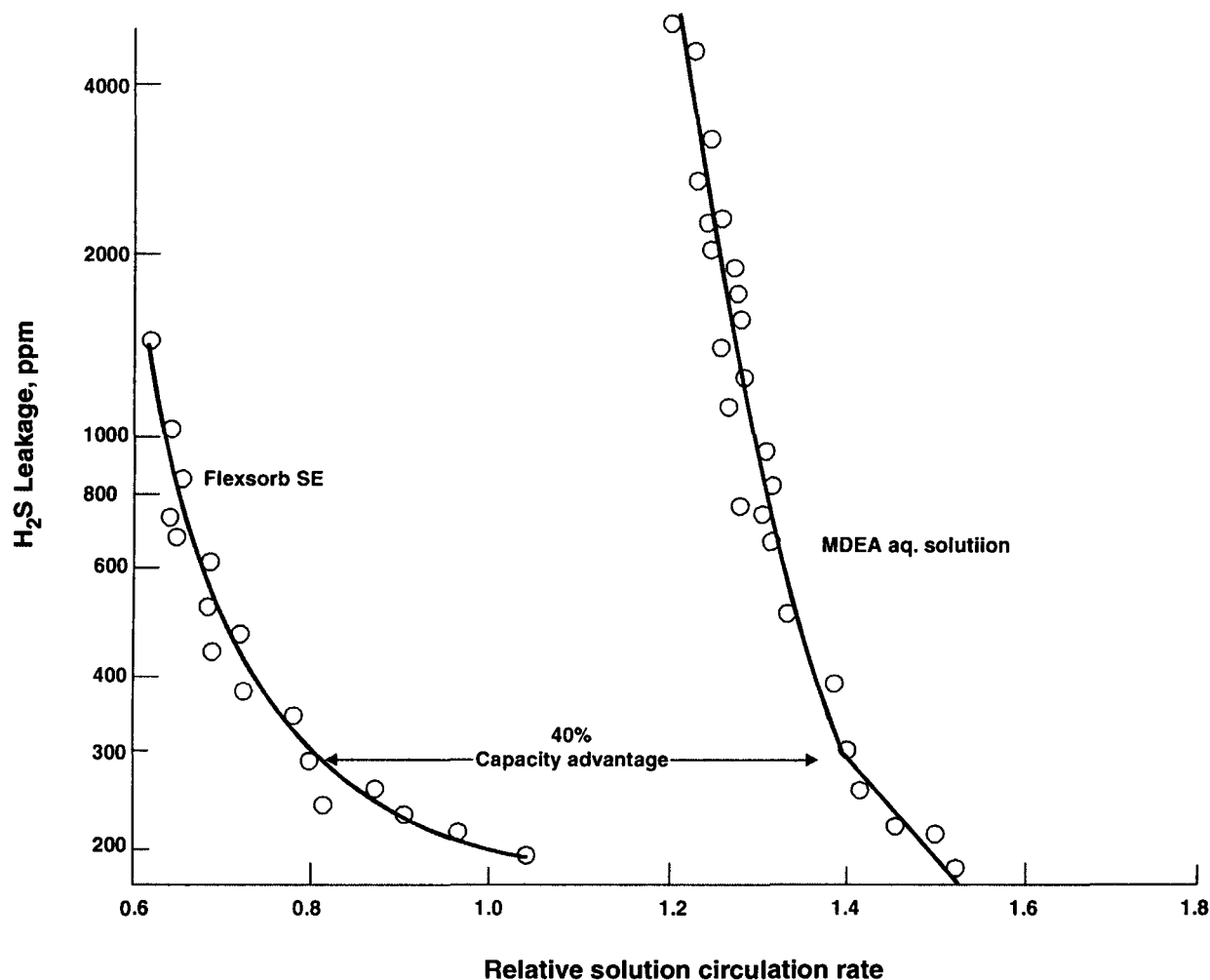
Fig. 11.1.1. *Flexsorb SE capacity advantage.*

In one typical desulfurization process, stoichiometric calculations revealed that by using **Flexsorb SE** 123 tons of sulfur could be removed per day from $8MMsm^3$/day low kilojoule gas and $1MMsm^3.day^{-1}$. **Claus Sulfur Plant TG**

[1MM $sm^3 = 1$ million standard m^3

$\angle$____(15°C/100 kPa.abs)]

Compared to aq. **MDEA, Flesorb SE** requires only 41% of amine $\textcircled{s}n$ rate and 51% of the steam rate in order to achieve a targetted clean-up level of about 115 vppm H_2S (Table 11.1.1)

TABLE 11.1.1 FLEXSORB SE vs. MDEA

BASIS **Desulfurization of 8 MMsm³.day⁻¹ of low kilojoule gas and 1MMsm³.day⁻¹ of Claus TG.**

Total sulfur removed 123 tpd

Solvents used:

1. FLEXSORB SE

2. MDEA (methyldiethanolamine)

	% of MDEA
FLEXSORB $\oslash$n rate, $m^3.h^{-1}$	41
Steam rate, $kg.h^{-1}$	51
Regenerator	
Dia, m	69
Height, m	87
Investment, $US (million)	74
Operating cost, $US (million)	57

Flexsorb SE requires a regenerator whose dia is 69% and height 87% of the regenerator used in **MDEA** system. And consequently investment cost is curtailed by 26% and operating cost by 43%.

BULK REMOVAL For bulk removal of H_2S + CO_2 from acid gases, **Flexsorb PS** is an improvement over conventional amine solvent processes.

Compared to conventional amine solvent processes, this technology rewards a 30% cut in amine $\oslash$n rate **(Fig. 11.1.2).**
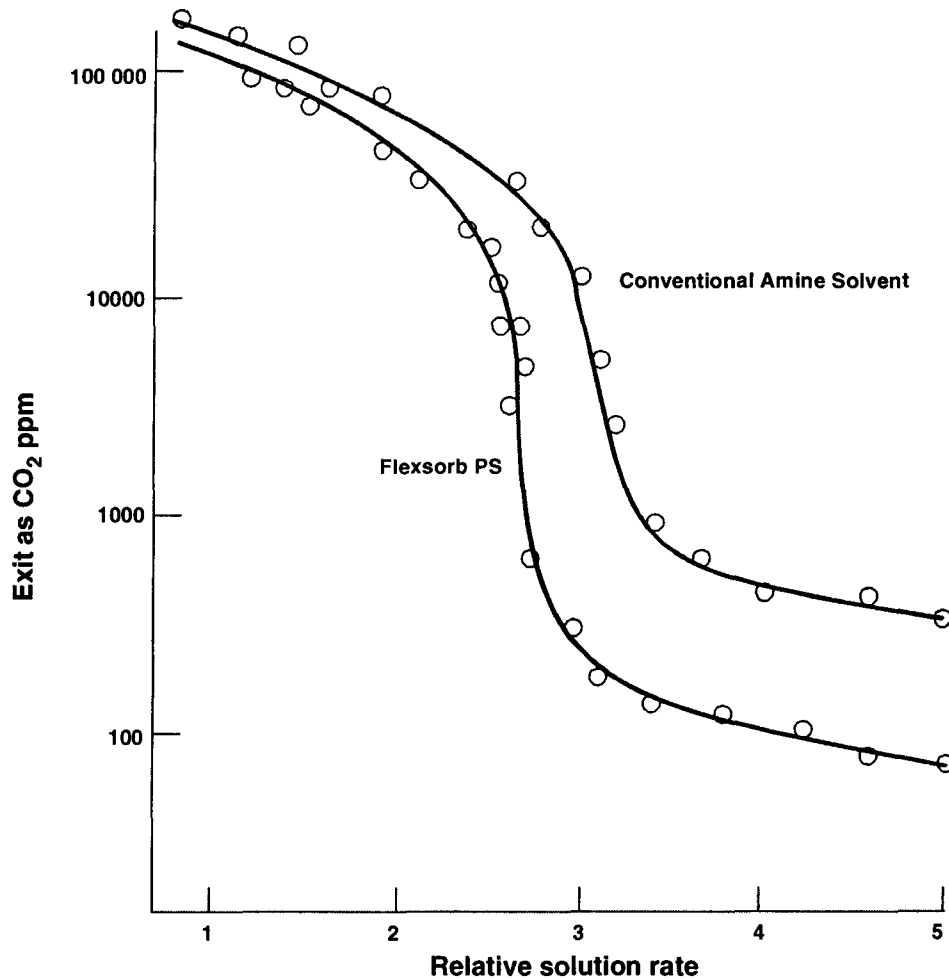
*Feed gas : 14% CO_2, 2% H_2S; pressure 200 psia

Fig. 11.1.2. *Flexsorb PS Capacity Advantage over conventional amine-solvent.*

This capacity enhancement begets improved performance which can be used to achieve significantly lower exit gas CO_2 and/or H_2S concentrations, when there are economic incentives to do so.

Significant economic credits can be realized when this technology is harnessed for treatment of large volume of gas viz. 48 MMsm³.day⁻¹ of **NG** at 5.5 MPa.g as encountered in liquefied natural gas **(LNG)** plant. Typically, the CO_2 concentration would be reduced from 18.5 mol% to 50 vpm and the H_2S concentration 0.1 mol% to 4 vppm.

Performance comparison is presented in **Table 11.1.2.**

TABLE 11.1.2 Performance Comparison of Flexsorb PS, Conventional Amine and Conventional Physical Solvent

BASIS **48MMsm³·day⁻¹ of NG**

Pressure : 5.85 MPa.g.

Composition : 18.5 mol% CO_2 + 0.1 mol % H_2S

Treated Gas Composition : 50 vppm CO_2 + 4vppm H_2S

Process ▷	*Flexsorb PS*	*Conventional Amine Solvent*	*Conventional Physical Solvent*
	← ————— *% of base* —————→		
Solution @n rate (m³h⁻¹)	base	124	198
Steam rate (kg.h⁻¹)	base	104	15
Power input (kWh)	base	120	290
Economics			
Investment (US$, million)	base	+34	+58
Operating costs (MMUS$.year⁻¹)	base	+6.3	+27.8

Flexsorb PS requires 24% lower @n rate than conventional amine-solvent system whereas the solution @n rate in conventional physical solvent is about twice that of **Flexsorb PS** system.

This lower @n rate translates into significantly smaller equipment requirements. And that begets equipment savings of MM$34 and MM$58 respectively.

[MM$ = million US$]

Also energy consumption is significantly reduced. Annual operating costs of **Flexsorb PS** were computed out to be MM$6.3 and MM$27.8 lower than the amine solvent technology and physical solvent technology respectively. These lower costs are the direct outcome of reduced solvent @n rate.

Over and above, **Flexsorb PS** has significantly higher stability than conventional amine-solvent combinations. Enhanced stability means lower amine degradation and that translates to lower amine make-up costs, and reduced reclaimer operation.

Additionally, **Flexsorb PS** solvent can be used in retrofit applications whereupon easy

debottlenecking or energy savings can be achieved in existing units. Of course, most or all of these credits are achievable in units where conventional processes are used to remove CO_2 in the absence of H_2S.

FLEXSORB HP Promoted hot potassium carbonate chemistry is the most commonly used technology to remove CO_2 downstream of steam reformer, and for CO_2 removal in ammonia plants. In this regard, **Flexsorb HP** rewards a 30% higher cyclic capacity than conventional hot pot. carb. technology (Fig.11.1.3).
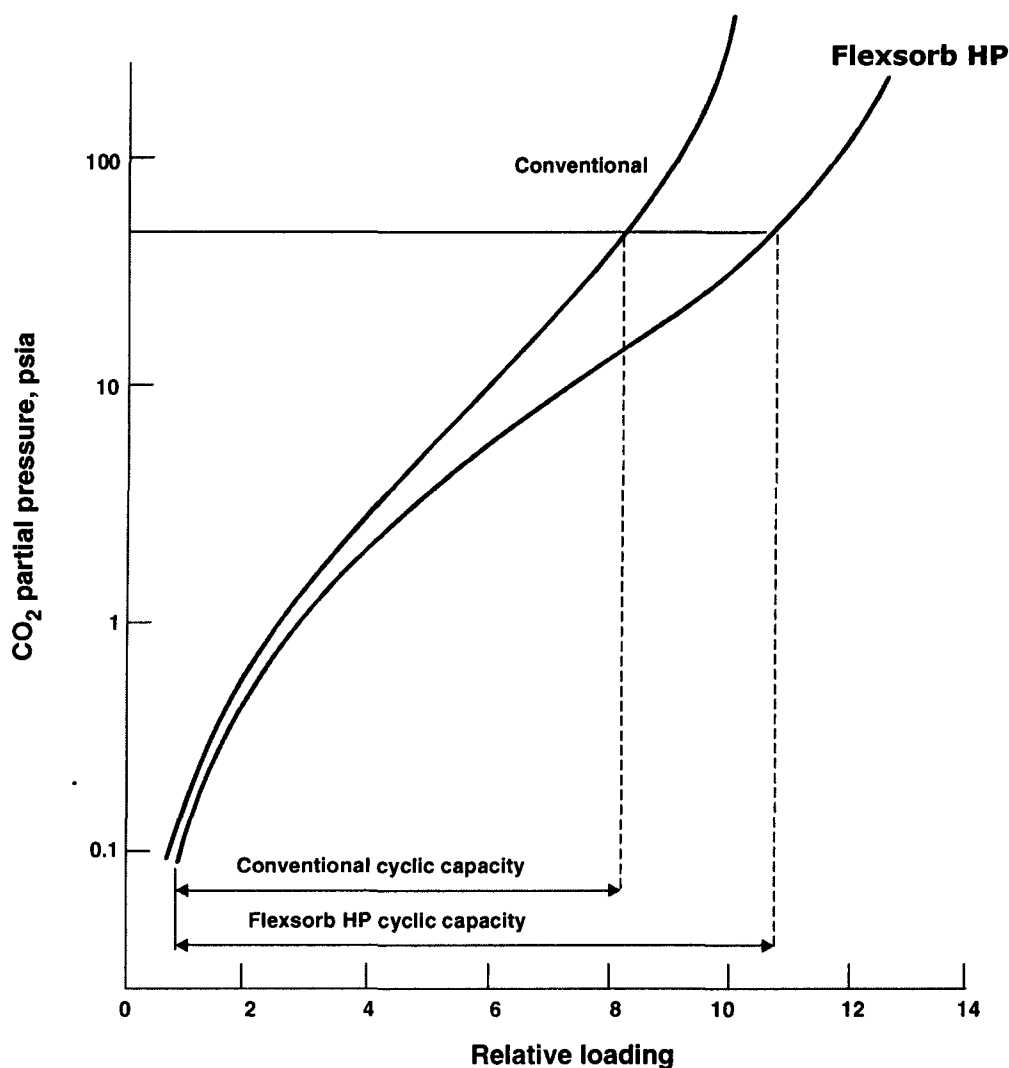
Fig. 11.1.3. *Flexsorb HP Capacity Advantage over Conventional Hot Potassium Carbonate solvent.*

Flexsorb HP offers significant credits in terms of lower operating cost and reduced investment. **Table 11.1.3** presents an economic comparison between **Flexsorb HE** & potassium carbonate chemistry for CO_2 removal in a typical steam reforming hydrogen plant.

TABLE 11.1.3 Economics of Flexsorb HP & Hot Potassium Carbonate in CO_2 Removal in a Steam Reforming Plant

BASIS **0.566 MMsm³.day⁻¹ HYDROGEN PLANT**
1.723 MPa.abs. ABSORBER
FEED : 19.9 mol% CO_2
TREATED GAS : 0.2 mol% CO_2

Process ▷	*Flexsorb* *HP*	*Conventional Hot* *Potassium Carbonate*
Solvent ⓢn rate, ($m^3.h^{-1}$)	base	1.19 times base
Reboiler duty	base	1.11 times base
Economies		
Investment (MM\$)	base	+1
Operating cost (MM\$.year⁻¹)	base	+0.4

In this typical example, about 19% lower solvent ⓢn and 11% lower reboiler heat duty is required than conventional promoted hot potassium carbonate technology. These process advantages reward an investment savings of ~MM\$1 for grassroot applications and an annual operating savings of MM\$0.4. In retrofit applications, the energy credits are distinctly greater.

11.2. PROS AND CONS OF DIFFERENT PROCESSES FOR SELECTIVE REMOVAL OF H_2S AND CO_2

NG, Shift Gas, Syn Gas [resulting from coal gasification as well as from partial oxidation of sulfur-contaminated FO] Steam Reformed gases contain H_2S and CO_2. And the onus of the task of removing H_2S from gases containing a heavy load of CO_2 is simply demanding because of the different characteristics of the two acids :

CO_2 is acidic in wet streams forming, bicarbonate and carbonate ions and liberating H^+ ions which are corrosive.

H_2S is acidic whether wet or dry and apart from being corrosive it is highly toxic and remains so even after combustion (as it leads to the formation of SO_2).

For this reason, specifications for pipeline gases delimit the CO_2 concentration to a maximum of 0.5 to 3 vol% but the H_2S to only 2 to 5 vpm.

There are three distinct processes for selective removal of CO_2 and H_2S from above gases :

• **Oxidative**

• **Solvent-based**

• **Tertiary amine (Hindered amine) based.**

Oxidative Processes

are based on aireal oxidation of H_2S to sulfur with the help of a compound which is easily oxidized by atmospheric O_2 and easily reduced by H_2S.

The best liquid oxidative processes can achieve H_2S removal efficiency as high as to leave treated gas with less than 1ppm of H_2S with complete selectivity towards CO_2. Of these, the best known are **Giammarco Vetrocoke** and **Stretford**. However, options for their acceptance are narrowed down due to their complexity and composition. Vetrocoke utilizes potassium arsenite/ arsenate mixture while Stretford makes use of vanadium compounds—both are of environmental concern as they cause ecological problems.

Besides, both these processes are fretted with side reactions yielding compounds with S at higher oxidation state. This sulfur must be eliminated and that involves extra step and loss of chemicals. And as a consequence investment costs are high and applications are restricted to small plants only.

Dry oxidation processes are based on aireal oxidation of H_2S to elemental S over iron oxide beds. Their capacity limitation restricts their application to small gas streams containing H_2S in the ppm range.

Solvent-based Processes

Certain polar organic solvents exhibit good selectivity for H_2S and CO_2 against **HCs** (hydrocarbons) and for H_2S against CO_2. **Rectisol, Purisol, Selexol, Cryofrac** are typical solvent-based processes that can be operated in either a selective or non-selective mode.

In a typical selective absorption scheme, the two acidic components of the feedgas are removed sequentially in two absorbers–H_2S first, and then CO_2. The solvent path is in the reverse direction, absorbing CO_2 first and then H_2S.

The remaining part of CO_2-rich solvent is regenerated by flashing at low pressure. The lean (regenerated) solvent is then introduced into the CO_2 absorber some trays below the top. And that's how solvent utilization and regeneration is integrated between two absorption systems, reducing the cost of H_2S removal.

However, this advantage is lost when only H_2S is to be removed. This situation is encountered with raw NG having an acceptable level of CO_2. Besides, the incentive for solvent based H_2S removal is lost if the H_2S content is low as low level H_2S means reduced partial pressure of H_2S the main driving force in this type of process. And, therefore, lower the H_2S-content in the raw gas the less efficient becomes the H_2S removal efficiency. Due to lower solvent loadings, the solvent ℗n rate is pressed high.

Tertiary Amines are called hindered amines. As the replaceable H atoms of NH_2 group of 1° amine (RNH_2) are gradually replaced by alkyl or aryl group

$$R - \overset{..}{N}H_2 \quad \boxed{RX} \quad R_2\overset{..}{N}H \quad \boxed{RX} \quad R_3\overset{..}{N}$$

1° amine   2° amine   3° amine
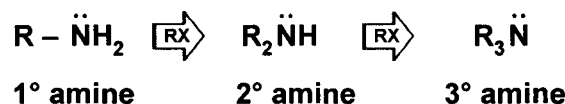
the accessibility of attacking electrophile to lone pair of electrons of N for electrophilic attack becomes progressively sterically hindered. Hence the difference in reactivity of primary, secondary and tertiary amines towards H_2S and CO_2.

The use of tertiary amines for selective H_2S removal is based on the difference in reaction rates for H_2S and CO_2 absorption. All amines, whether primary, secondary or tertiary, react with H_2S in the analogous way, *i.e.*, by neutralization to form bisulfides

$$R-\overset{\cdot\cdot}{N}H_2 \quad + \quad H_2S \quad \rightleftharpoons \quad R - \overset{+}{N}H_3 \big] H\bar{S}$$

$$R - \underset{R}{\overset{\cdot\cdot}{N}H} \quad + \quad H_2S \quad \rightleftharpoons \quad R_3\overset{+}{N}H_2 \big] H\bar{S}$$

$$R_3\overset{\cdot\cdot}{N} \quad + \quad H_2S \quad \rightleftharpoons \quad R_3\overset{+}{N}H \big] H\bar{S}$$
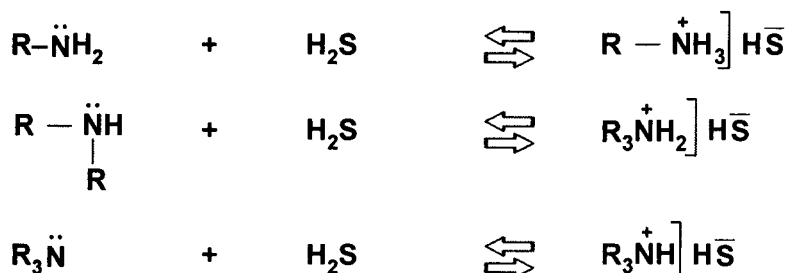
There are differences between individual amines within any of the three groups. Their intrinsic behavior towards CO_2 and H_2S reflects more the nature of the individual amine rather than whether they are 1°, 2° or 3° amine.

When CO_2 is present, two reactions are possible : *neutralization and carbamate formation.* [see **11.1.1**]

The reaction rate for H_2S absorption is very fast CO_2-absorption is somewhat slower in carbamate formation and much slower in bicarbonate formation. That's why, 1° and 2° amines that may form carbamate exhibit negligible selectivity for H_2S over CO_2, whereas 3° amines show a high selectivity.

In order to reap the advantage of the selectivity of tertiary amines in designing a plant, it is necessary to limit the absorption contact time and that means lowering of absorber height. Therefore, a selective plant usually has fewer trays in the absorber than a conventional plant.
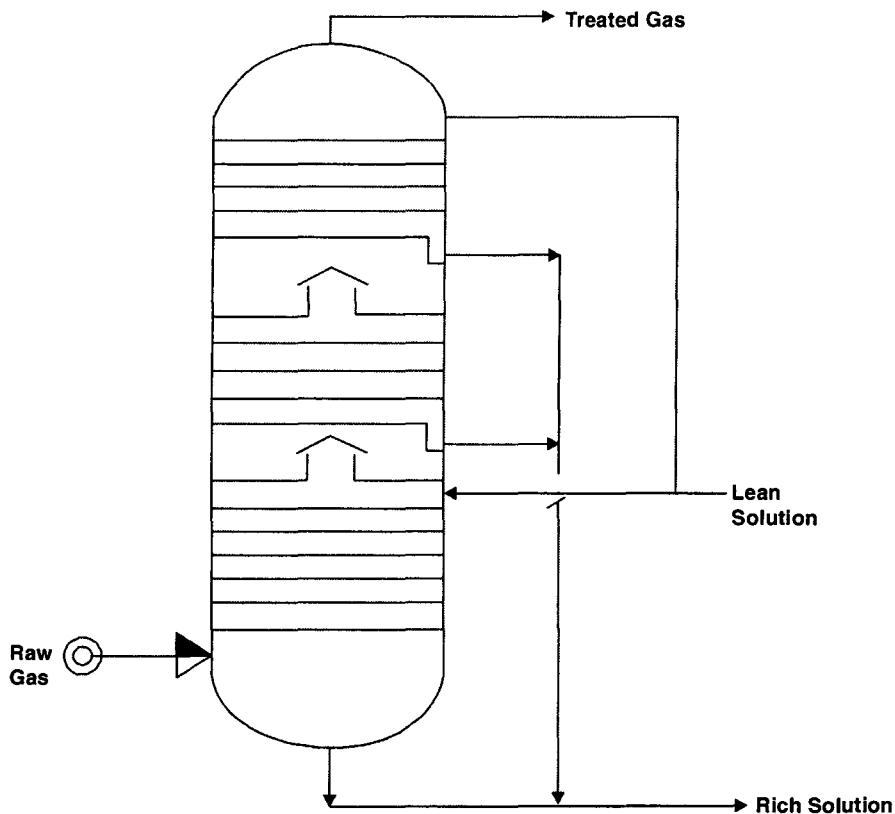
Fig. 11.2.1. *The absorber configuration that gives optimum selectivity.*

Inasmuch as the kinetic differences between H_2S and CO_2 absorption are not very great, it is usually impossible to obtain good selectivity and, at the same time, high purity. If contact time is kept low, a poor H_2S specification is obtained in the treated gas. On the other hand, if contact time is kept high, selectivity will suffer.

The most widely used tertiary amine is **MDEA** (methyldiethanolamine) which is a stronger base than **TEA** (triethanolamine). Subsequent efforts have enhanced the performance of the **MDEA** process.

Of course, the H_2S absorption rate is gas-phase controlled process and is favored by trays with gas-liq contact devices (valves, slots, etc.,) that promote turbulence with high gas velocities. Furthermore, the selectivity for H_2S is higher when the solution is lean due to obvious reason and it drops as the acid gas loading increases.

To enhance selectivity, the best configuration is that one which splits the absorber into several sections operating in series with respect to the gas path **(Fig. 11.2.1)**.

In such a configuration, the sections are fed in parallel. Lean solution is taken out from the bottom of each section before full loading is achieved. This system improves selectivity at the expense of solution loading.

Selefining Process

It is a novel process that operates on hindered amine philosophy. The solvent is a tertiary amine dissolved in organic solvent containing very little water. The near anhydrous operation denies CO_2 hydration down to a point that arrests carbonate or bicarbonate formation almost completely.

In contrast, H_2S, which is already an acid may combine with the amines in anhydrous medium by way of neutralization reaction. The selectivity of H_2S vs. CO_2 absorption depends on equilibrium properties rather than kinetic behavior.

Advantages

The use of an organic solvent instead of an aqueous solution has some other important consequences :

1. The absorber can be made as tall as necessary to pack up many trays as to achieve desired treated gas specifications without hampering selectivity. Fortunately, the mass transfer properties of the hindered amine solution in organic solvents are quite good and hence achieving treated gas of targetted specification does not require taller than normal absorbers.

2. The process requires lower solution rate, because the ʂng solution can be kept in contact with **RG** to full solution loading without kinetic restrictions.

3. The selectivity is, by and large, independent of absorption pressure. This rewards economies in pressure-vessel cost credits.

Of course, 100% selectivity is not achievable, not is it actually required in this type of plant. Some qty. of CO_2 gets *physically absorbed* by the ʂng solution. But inasmuch as the ʂng solution volume is low, it reduces the amount of CO_2 absorbed.

Most of the applications make it a mandatory to keep some water in the ʂng solution so as to produce stripping steam in the regenerator. This water hydrates some qty. of CO_2 permitting neutralization to take place in the aftermath and that tends to reduce selectivity to some extent.

Fortunately, from the commercial point of view of the overall CO_2 leakages due to these mechanisms are quite acceptable. Selectivity is higher than that of any industrial process other than the oxidative processes.

A great number of combinations of tertiary amines and organic solvents, with the optimum water content for each mixture have been tested for corrosiveness, thermal and chemical stability, as well as feasibility of operating the process. **Table 11.2.1** reports a typical pilot plant run.

Table 11.2.1 Typical Selefining Process : Pilot Plant Results

Stream ▶	*Raw Gas*	*Acid gases*	*Treated gas*
H_2S vol %	0.50	14.16	1.6 ppm wt.
$CO_2 : H_2S$ mol ratio	39.6	6.06	–
Operating Press. (bar absolute)	30	1.3	30
Operating Temp. (°C)	40	40	42

SOME IMPORTANT FEATURES

Shown in **Fig. 11.2.2** is a typical **Selefining** process scheme. This one is basically the same as that of any other amine unit with some minor variation and improvements. By virtue of high selectivity and low solution circulations, the system boasts following features :
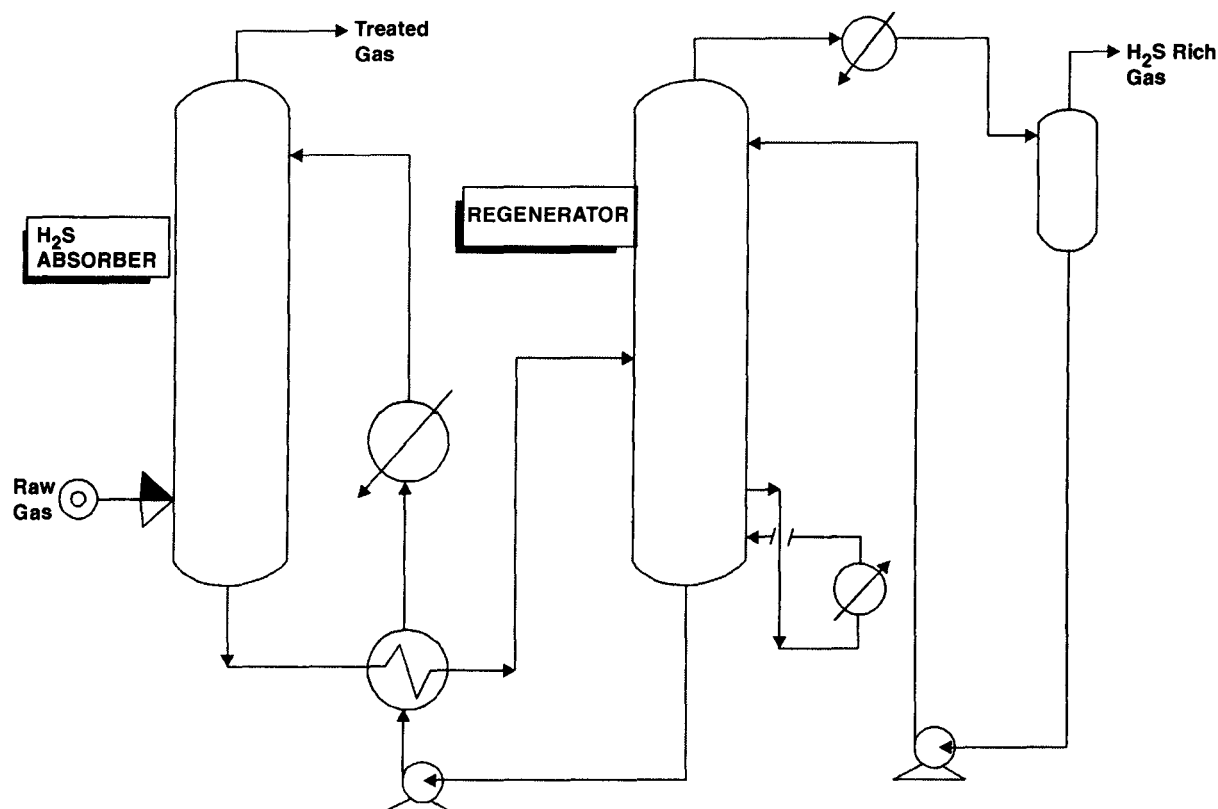
Fig. : 11.2.2. *A typical process flow diagram of Selefining Process.*

1. Less than **1 ppm** of **H₂S** can be obtained in treated gas without adversely affecting process economics.

2. The solution regeneration section as well as the ⊘n system are reduced in size.

3. Investment cost, operating cost, and the costs of utilities and chemicals are low.

Applications

The selefining process can be applied advantageously in treating NG, Syn gases, and Claus Tail Gases. Typical applications includes situations where :

- **RG** (raw gas) contains **H₂S** and little **CO₂**, so that all or most of the **CO₂** may be left in the treated gas to be sold.

- **RG** contains little **H₂S** in comparison with **CO₂**, and a concentrated **H₂S** stream is required as feed to a Claus unit.

- Pure **CO₂** must be produced, free of **H₂S** for injection into crude reservoirs for enhanced oil recovery or for chemical or industrial uses.

When **Selefining** process is applied to the purification of **Claus TG** after their reduction to H_2S, sulfur removal be as complete as desired. In some cases, these completely do away with the final incinerator.

Existing amine plants can be easily retrofitted by simply changing the absorbent solution.

REFERENCES

1. *Hydrocarbon Processing, May 1981/P:118—124.*
2. *Hydrocarbon Processing, August 1981/P:111—116.*
3. *Oil and Gas Journal, July 16, 1984/P:76—79.*

11.3. CORROSION PROBLEM IN GAS ABSORPTION COLUMN

Aqueous alkanolamine is the preferred solvent used in industries for acid-gas removal. However, this solvent entails the potential risk of corrosion which is a serious problem. The result may be catastrophic.

CASE HISTORY # 1

It was July 23. Year 1994. A refinery at Romeoville, Illinois, USA, owned and operated by the Union Oil Co. of California, experienced a disastrous explosion and fire as its **amine absorber**–a pressure vessel–ruptured and let out huge quantities of inflammable gases and vapors. It killed seventeen people, hospitalized another seventeen and inflicted a damage exceeding $ 100 million. **Loss of structural integrity due to uninhibited corrosion caused this catastrophic failure.**

The **NBS** (National Bureau of Standards) marshalled a detailed investigations that included chemical analyses, fracture mechanics analyses, stress corrosion cracking susceptibility tests and hydrogen cracking susceptibility tests. The test results confirmed the susceptibility of plate material (ASTM A516, Grade 70, CS) of the amine absorber to hydrogen-induced cracking was root of the problem. Besides, the repair welds that were done in the field, and had not been stress relieved, were particularly sensitive to amine attack, *i.e.,* **amine-induced corrosion and cracking.** It was found

that SCC propagated both parallel and perpendicular to the weld. This mode of propagation clearly distinguishes SCC and reflects the different stresses along the weld area.

Several case histories attest to stress-corrosion cracking as a serious problem, especially for amine absorbing columns. This process operates under elevated pressures and temperatures to remove acid gases–hydrogen sulfide (H_2S) and carbon dioxide–from process streams.

Industry Survey

NACE (National Association of Corrosion Engineers) conducted a survey of similar refinery vessels and associated equipment. The survey results indicated that about 60% of twenty four absorbers evaluated exhibited cracking. Erstwhile data indicated that 12 of 14 MEA (monoethanolamine) units and 3 of 5 DEA (diethanolamine) units exhibited cracking.

A similar survey by the Japan Petroleum Institute indicates that SCC has afflicted 72% of the amine gas treatment facilities.

Corrosion Problems

Eight types of corrosion have been identified :
— **general**
— **galvanic**
— **crevice**
— **pitting**
— **intergranular**
— **selective leaching**
— **erosion**
— **stress corrosion cracking**

General corrosion is characterized by more or less uniform corrosion over the entire surface area exposed to corrosive environment.

Galvanic corrosion occurs when two dissimilar metals are coupled together in presence of an electrolyte (*e.g.*, water with dissolved salts or CO_2) whereupon the anode (the more electropositive metal) corrodes away

$$M - ne \Rightarrow M^{n+}$$
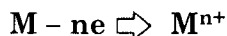
Oxidation takes place at anode.

For example, *when 316 SS trays of the absorber are bolted together with mild steel bolts, the latter act as anode and hence preferentially corrode away leaving stainless trays unaffected.* This is due to difference in electrode potential of the two metals. As a result the trays get loosened and may be dislodged during process upsets.

Crevice Corrosion is the outcome of a concentration cell formed in a crevice between two metal surfaces. This is mostly encountered where tubes are attached to tubesheets. Corrosion sometimes goes so severe that tubes appear to have been cut with a saw at tubesheet.

Pitting corrosion is characterized by highly localized in its nature that occurs at isolated spots resulting in pits or corrosion pockets. Sometimes this results in deep penetration. Presence of halide ions, particularly chlorides, and stagnant areas usually promote pitting. *Inhibitor concentration is critical with pitting*, if it fails to arrest the attack completely, pitting can be intensified.

Intergranular corrosion typifies itself as that type of corrosion that occurs at the grain boundaries. It is the result of improper heat treatment of steel. **Weld-decay** and **knife-line attack** are the outcrop of intergranular corrosion arising out of incorrect welding procedure.

Selective leaching manifests itself as selective dissolution of one element from a solid alloy. The most outstanding example is **Monel** metal used in amine systems; **copper is selectively leached out from Monel**–a copper-nickel alloy–by amine in the presence of oxygen.

Erosion corrosion is the chemical/electrochemical attack of the metal followed by mechanical wearing of the corroded surface–the latter arises from abrasion of moving fluids. It is aggravated by the presence of suspended solids or gas bubbles in the flowing liq stream and the most susceptible zones of attack are tube bends, elbows, tees, valves, pumps, flowers, impellers (damage due to cavitation) etc.

Stress Corrosion Cracking (SCC) is the corrosion augmented by residual tensile stress. The factors that affect SCC attack are :

1. temperature

2. solution composition and concentration

3. metal composition

4. residual stress in the metal

5. metal structure

Protecting the Plant

In all amine gas absorption columns, the most problematic and challenging task is protecting the heated surfaces. And there are two options available to battle this corrosion :

Option - II ▶ **Use of Inhibited Amine System (IAS)**

Option - II ▶ **Applying thermoplastic coatings to protect the vital equipment components.**

Inhibited Amine System (IAS)

makes use of a corrosion inhibitor dozed to the aq. alkanolamine solution to control corrosion.

Corrosion occurs in these systems due to greater amine strength, higher acid gas loadings, and increased temperature **[Fig. 11.3.1]**

Controlling corrosion is complicated by amine type and the nature of acid gas (H_2S, CO_2 or, H_2S-CO_2 mixes). Generally increasing ratio of H_2S/CO_2 results in more severe corrosion **(Fig. 11.3.2)**

First successful amine inhibiting was introduced in 1996 in a CO_2-absorber to control a severe corrosion problem. Both the loading and absorbent (MEA) concentration were increased as corrosion was brought to bay.

For successful introduction of IAS, the process engineer should make

1. In-Depth Study of the plant flowsheet, operating parameters to identify the corrosion types and correlate them with observed design and operating conditions.

2. Amine Solution Analysis to determine its quality and chemical corrosiveness. Such an analysis quite often points out design and operational problems that affect corrosion rates and energy costs.

3. Basic Design Considerations such as exchanger approach temperature, reflux ratio,
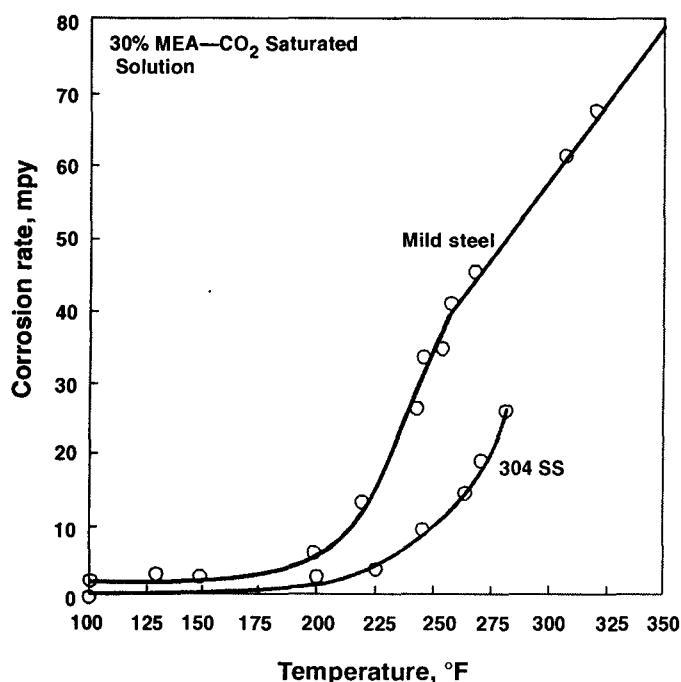
Fig. 11.3.1. *Corrosion increases with the increase of temperature in amine system and there is a very marked increase at ≥ 370 K.*
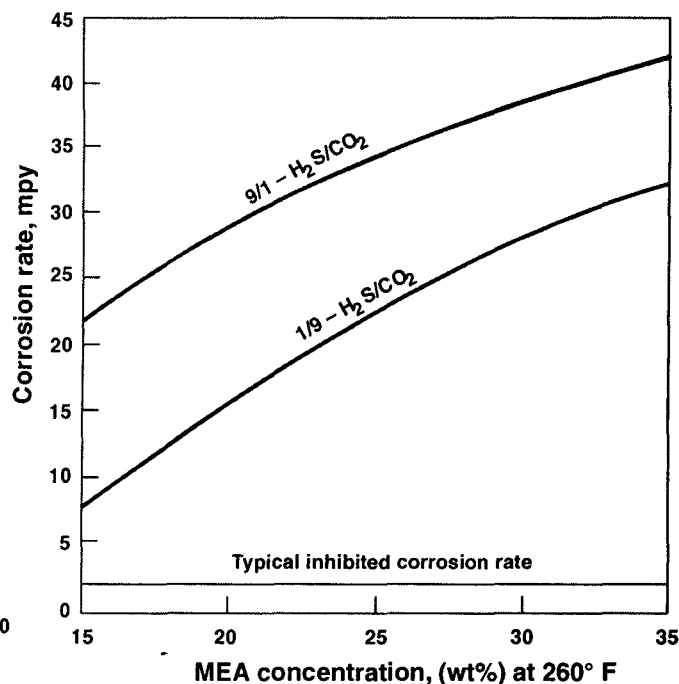
Fig. 11.3.2. *The rate of corrosion commensurates with amine concentration.*

flow velocities, reboiler surface area, condenser duty. These are to be evaluated according to an amine computer simulator program. Areas that may be troublesome are readily identified and checked in detail.

4. Plant visits on a regular basis after the performance test.

HOW GOOD IS IAS ?

Corrosion inhibition system injected to solvent amines not only eliminates corrosion as a design and operating constraint, but also saves capital and operating costs and enhances gas removal capacity.

One typical **IAS** is **Amine-Guard ST** of Union Carbide. The system involves two corrosion inhibitors that are initially added to the ⊘ng solution in ppm to passivate the unit. A minimal make-up is required, usually monthly to maintain a passive state. For example, a ~114 m³ **(30000 gallon)** solution inventory with a **113.5 m³.h⁻¹ (500 gpm)** ⊘n rate, inhibitor charge and total annual M/up requirement is **90–227 kg (220–500 lb)**. The inhibitor dozing equipment consists of a mixing vessel **(0.189—1.89 m³** size) with a mixer, an injection pump and a tap into the ⊘ng amine line.

This **Amine-Guard corrosion inhibition**-optimization has been field tested at a number of plants utilizing **MEA** and **DEA** for gas and liq sweetening.

Once inhibited, the absorber's amine concentration can be increased to **30 wt% MEA**, or **55 wt% DEA** coupled with higher acid gas loadings, and yet without incurring corrosion. Absence of corrosion eliminates the need of continuous reclaiming in **MEA** system.

CASE HISTORY # 2

In the **MEA** treating facility with

* design capacity **0.62 MMsm³ day⁻¹** of low pressure **(0.96 MPa) gas**

$$1 \text{ MM sm}^3 \text{ day}^{-1} = 1 \text{ Million standard m}^3 \text{ day}^{-1}$$

(15°C/100 kPa)

* solution flow rate **13.625 m³.h⁻¹**

* **1.5 m dia contactor**

* a diameter with mechanical and activated charcoal filters for treating a slip stream of lean solution.

found a minor corrosion problem (the entire unit was made of carbon steel, except **HE** tubes which were stainless) and adopted **Amine Guard ST** corrosion-inhibition program. After process optimization, the plant harvested the following benefits :

1. Amine concentration in the lng **MEA** was shot up from **13 wt%** to **22 wt% MEA.**

2. Solution flow rate was cut down to half, *i.e.,* from **8.62 m³.h⁻¹** to **4.31 m³.h⁻¹.**

3. Increased **MEA** concentration augmented *acid gas loading* from **0.24** to **0.28** moles acid gas per mole **MEA.**

4. Reclaimer being inoperative saved fuel, lowered **MEA** losses and maintenance costs.

5. *Overall energy consumption got reduced* by **27%** leading to a savings of **1.302 MMsm³ day⁻¹.**

6. **Corrosion became virtually nonexistent.** A very low and uniform rate of corrosion under 0.5 mil per year (0.0127 mm per year)* was recorded on 22 test coupons inserted in hot (344K), rich **MEA** solution for periods of 26 to 44 days.

CASE HISTORY # 3

In another **MEA** treating facility, reboiler fouling was a recurring problem, leading to poor heat transfer and inadequate **MEA** regeneration. After inhibitors were introduced into the lng solution, corrosion rate decreased 500-fold, from 0.0345 mm year⁻¹ to 6.5×10^{-4} mm year⁻¹.

CASE HISTORY # 4

In one liquid sweetening unit (Vada Plant of Warren Petroleum, Crane, Texas, USA) two 3mm packed sections of a column (DEA gas treater) had been plagued with two problems :

• **High Sulfur Level in the Condensate :** 0.90% H_2S, 360 ppm MeSH, 150 ppm EtSH, and 30 ppm **COS**

• **Poor Mass Transfer** characteristics in the packed bed.

These two problems were solved by

1. introducing **Amine Guard** as a result of which the plant attained the capability to increase DEA concentration to 55% raising the basicity and capacity for acid gas removal

---

```
* Note : 1 mil is one thousandth part of an inch.
```

2. incorporating two mixer-settler stages in series upstream of the packed column.

The liquid $\oslash$ṇ rate to the gas treater was gradually reduced from **27.25 m³.h⁻¹ to 20.43 m³.h⁻¹**. *A fuel saving of 1.12 MMsm³. day⁻¹ resulted.*

CASE HISTORY # 5

In another refinery at New Mexico, **DEA plant** runs at **60% capacity** treating **1.31 to 1.34 MMsm³.day⁻¹** of low pressure **(1.58 MPa.g)** gas containing **2.5% CO₂** and **0.8% H₂S**. Although the plant was operating relatively trouble free without excessive corrosion **Amine Guard ST** was introduced for energy savings and improved product purity.

After amine inhibition, the solvent concentration was increased from 22% to 55% DEA, and its $\oslash$ṇ **rate was curtailed from 113.54 m³.h⁻¹ to 72.66 m³.h⁻¹. The benefits accrued include :**

1. **Improved Operation :** H₂S in the sales gas droped from **2.76 mg.m⁻³** to **0.46 mg.m⁻³**.

2. **Energy Savings :** Reboiler heat duty dropped approximately **20%**.

3. **Equipment Savings :** A DEA absorber column used to sweeten regeneration gas from molecular sieve dehydration beds was put off from service, freeing a 2100 mm dia column.

4. **Corrosion Protection :** Corrosion rate dropped below **0.0127 mm per year [12.7 µm.y⁻¹]** in the hot (380 K) rich **DEA** downstream of **HE.**

Coatings put up a physical barrier between the corrosive species and the vessel wall. Epoxy resins have made a much headway in protective coatings field. These materials react in place whereupon it develops a protective coating that has good adhesion and acceptable resistance to corrosion.

During earlier applications the epoxies were amine cured. Subsequently, polyamide epoxy coatings were developed. These substance have increased adhesion property. Some flexibility, improved water and chalk resistance as compared to epoxies.

Thermoplastic coatings (lacquers) are applied by means of a solvent into which these are dissolved. The solution is applied on the surface and allowed to dry. As the solvent evaporates out, it leaves the non-volatile portion of the coatings that forms the film. The film-forming process is merely the physical evaporation of the solvent leaving the thermoplastic resin on the surface as a continuous film. Most coatings are made up of several different solvents with various evaporation rates. This procedure ensures a continuous final film. In case the solvent evaporates too quickly, it may cool the surface of the coatings to such an extent that water is condensed and get entrapped in the film. This water condensation renders the coating turn white. This is called **blushing**. The film that is blushed is generally porous and does not have same resistant characteristics as a smooth resin film properly formed over the vessel wall.

Conversion Coatings, as they dry out in series of steps, undergo a chemical and physical change in the process of film formation.

An important conversion reaction is **catalyst conversion** or **cross-linking** that takes place at ambient temperatures. The modified epoxy resin is mixed with an amine just before application. The drying process that follows is a chemical reaction of the amine and epoxy resin in such a way that cross-linkage takes place. Here, the amine actually takes part in the chemical reaction and becomes an integral part of the new polymer. The reaction is exothermic and can take place in absence of air.

In another conversion process, a polyamide resin reacts with a second resin, i.e., chemical

reaction takes place between two resins—one epoxy and the other polyamine—whereupon cross-linkages are formed during drying process creating a solid resin film. This film is somewhat more resilient and elastic than films produced during amine-epoxy reaction.

Amine-cured epoxy resin coating formulations develop room-temperature cured finishes that have many film properties normally associated with baked coatings. These properties are obtained as the active hydrogens ($-NH_2$) of alifatic amines react with the epoxy groups of the resin giving rise to a complex three-dimensional polymer structure.

Amine-cured epoxy resin coatings combine excellent resistance to most corrosive materials with outstanding resistance to mechanical shock and abrasion. Additionally, because of their extraordinary adhesion, a broad range of substrates may be protected by these coatings.

They have unmatched resistance to alkali-attack. Besides, they also offer excellent corrosion resistance to a number of solvents, dilute mineral acids and salt water.

The abrasion-resistance of composite amine-cured epoxy resin coatings is excellent.

Over and above, completely cured films of amine-cured epoxy resin formulations are completely non-toxic and odourless. And that explains why these high performance coatings are one of the most widely used industrial-maintenance finishes.

Costs of Coating

The cost factor of a coating is always a critical consideration; it is a serious factor. Under some circumstances, it may be the only factor. However, coatings cost should not be given higher priority over the coating properties that provide the basis for long-time effective coating protection. Frequently, wrong coatings are selected. This is due to the fact that the persons entrusted with coating selection are not knowledgeable in the field and may lack basic facts. So very often than not, a second-rate coating system is applied over less-than-the-best surface preparation and that inflicts the company with considerable losses due to recurring cost required to maintain the structure from corroding to the point of becoming a safety hazard.

Any repair program must take into account operating conditions. Nearly 70% of all coating failures have resulted from poor or inadequate surface preparation.

Coating Failure

Many coating failures occur due to improper coating selection. A coating that was designed to resist certain environments can fail if these limitations are exceeded.

Temperature is the prime limitation to the efficacy of modified epoxy-based coating materials. The effect of temperature on the adhesive strength of polymer coatings to metal substrates is obvious. As the temperature is raised, the loss of adhesion of the coating in contact with the solvent liquid increases. This is due to the fact that as the temp. is raised, the permeability of the solvent thru the coating increases whereupon the weight percent absorbed by the coating increases and the diffusion coefficient of solvent thru the coating increases.

Another factor that is responsible for coating failure is the difference in thermal expansion coefficient between the coating and the substrate. As a result compressive stresses develop in the coating whereupon **blisters** are born. Inasmuch as blisters are believed to be the precursor to substrate corrosion, any measure that could mitigate or eliminate blister formation would also delay the onset of substrate corrosion.

While protective coatings can be successfully used at moderate wet temperatures, diffusion thru coating readily occurs at temperatures exceeding 363K. This invites blistering and premature breakdown.

Recent Developments

Recent advances in the field of temperature resistant coating have led to the development of modified epoxy formulations that warrant unprecedented protection of process equipment in high-temperature service. They derive strength from densely cross-linkages in the resin system. This unique intermolecularly bonded polymer composite ensures erosion-corrosion protection against damage to equipment operating with water and other aq. solutions operating at high temperatures. Additionally, these totally noncorrodable formulations have extremely low water permeability, which together with their electrical insulation characteristics, deters bi-metallic corrosion of the underlying substrate.

REFERENCES

1. R.L Pearce and M.S DuPart, *Hydrocarbon Processing, May 1985/P: 70—72.*
2. C.H Samans, *Corrosion, vol 20/No. 8/1964/P: 256—262.*
3. E.N Skinner *et. al., Corrosion, vol. 16/No.12/1960/P:593—600.*
4. M.G Mogul, *Hydrocarbon Processing, Oct 1999/P: 47—56.*

11.4. MOC OF CO_2-ABSORBER (MEA SYSTEM)

One of the prime unit processes of the PCIs and CPIs is the hydrogen generation thru natural gas reforming and subsequent purification by MEA (monoethanolamine) absorption. The cost of downtime, which for larger plants can exceed US$ 25000 a day in gross profits, requires that selection of materials and fabrication procedures be engineered.

Corrosion

Corrosion plays a decisive role in the selection of materials. Corrosion the shellside of some of the stainless steel tubes has been reported in several of these plants.

Corrosion rates of the martensitic **Type 410SS** are, on the average, an order of magnitude greater than those of the aluminium-bearing ferritic **Type 405**. However, **Type 410SS** exhibits larger pitting in pitting-environments.

So far as pitting corrosion is concerned, it has been observed that

1. **Monel** is unattacked.
2. **Incoloy 800** shows better pitting & wear resistance than **Type 304SS**.
3. The **Carpenter 20-Cb3** alloy as well as **Type 316SS** suffer from less pitting, when compared to the nonmolybdenum bearing alloys.
4. The **Carpenter 20-Cb3** tubes show no better resistance to attack than the **Incoloy 800** tube in the baffle-support area.
5. **Type 317SS**, containing 3.5 Mo and the **60-30-5 Cu-Ni-Fe** alloy display pronounced resistance to pitting as well as increased wear resistance when compared with other materials.

SELECTION OF MOC

1. **All vessels and exchanger shells in the MEA scrubbing system can be constructed of carbon steel. Type A-516 Gr B** is recommended for the higher pressure components, otherwise **A-285 Gr C** is recommended.

2. **The piping, in general, can be made of A-53 Gr B seamless carbon steel.** However, 304SS is recommended for pipes containing gas condensates at temperature exceeding 325K & also for the piping-section downstream of the pressure-let down valve to the regenerator.

3. **Type 316SS is recommended for let-down valve, Type 304SS for trays in the regenerator and for the hot condensate pump.**

4. **It's wise to use 304SS in the construction of**
   - **the two hotter bundles of the lean/rich MEA exchanger**
   - **the absorber-feed cooler**
   - **the reclaimer**

5. **All other exchangers except the regenerator-reboiler can be provided with A-214 CS tubing.**

6. The regenerator-reboiler is subject to more severe corrosion than any other item of equipment in the **MEA** system. This exchanger handles semi-stripped **MEA** solution in the shellside and heating medium in the tube-side. In case the heating medium is a process gas containing CO_2, the tube-bundle must be stainless steel (inasmuch as CO_2 dissolved in hot condensate forms carbonic acid that rapidly attacks carbon steel). It has been found that **316SS** to be only marginally better or equal to **304SS**. On this basis **304SS tubes are recommended for reboiler bundles if operating temp. and solution strength are properly controlled.**

REFERENCES

1. E D Montrone and W P Long, CHEMICAL ENGINEERING (Jan. 25,1971).

11.5. QUANTUM LEAP TECHNOLOGY

— An Innovative Natural Gas Dehydration Technology

Natural Gas **(NG)** is often associated with water vapor as well as **VOCs** (volatile organic compounds). While triethylene glycol **(TEG)** is typically used to remove via absorption the water content, it also absorbs the **VOCs** which are removed via distillation. A large load of **VOCs** is condensable; they can be condensed and recovered. And the remaining **VOCs** constitute the non-condensable hydrocarbons **(NHCs)** whose amount is considerable. The 1996 US Environmental report projected USA alone generating 40000 tons of **NHCs** per year. These are vented to the atmosphere or are "free-floated" to a flare at atmospheric pressure or they end up in the combustion chambers where they're thermally oxidized and incinerated. This method entails the risk of incomplete combustion or explosion due to inadequate mixing of oxygen. So the onus of the industry lies in the disposal of NHCs either as a salable product or as a fuel used up in the regenerator.

Engineered Concepts, LLC, Farmington, New Mexico, USA has commercialized a natural gas dehydration system **QLT** (Quantum Leap Technology) that has been reported to eliminate more than 99.74% of hazardous air pollutants **(HAPs)** composed of **BTEX** (benzene, toluene, ethylbenzene and

---

Note : Monel tubes in this service have logged much extended life-time.
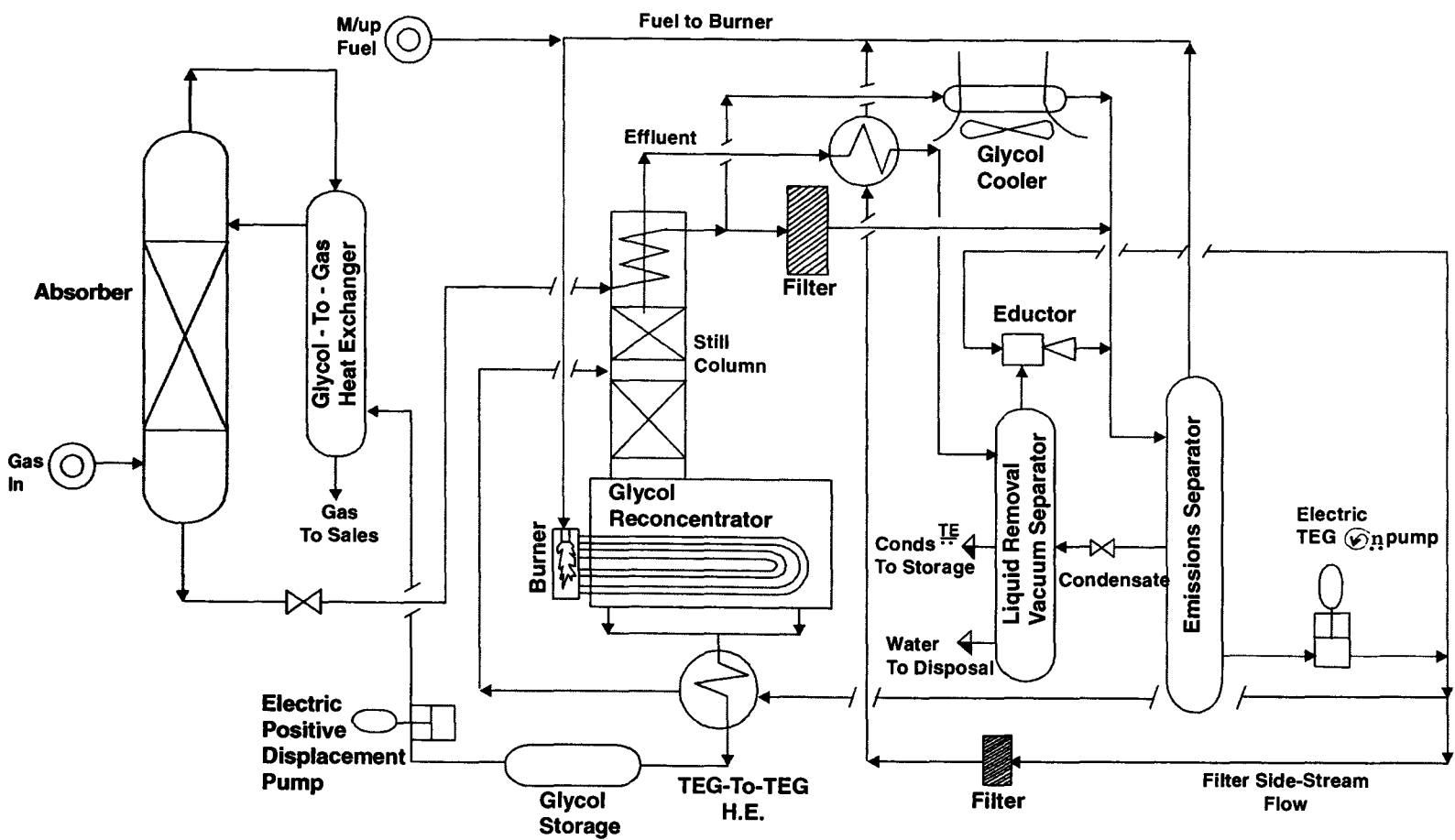
Fig. 11.5.1.

xylene) and emits insignificant quantities of **VOCs** with no detectable emissions of methane technology cuts short fuel consumption by 50% or more. Its application spans small remote wellhead units and retrofits to large plants and off-shore systems.

The **QLT process** consists of "**dry**" TEG (low-water content glycol) continuously injected to the absorber by a pump **(Fig. 11.5.1)**. The dry glycol absorbs the water load of **NG** which whereupon gets dry.

The now "**wet**" glycol is regenerated by distillation at atmospheric pressure at 433–477K, cooled by glycol-glycol heat exchange and recycled to the absorber via an electric pump. Many dehydrator units operate pressure-powered pumps to deliver dry glycol to the absorber; but these pumps require large volumes of **NG** and high pressure to operate. The use of electric-powered process permits lower gas flowrates to be used. This minimizes emissions, permits the dehydration unit to run at lower operating pressures with the immediate benefits of minimal risk of pipeline corrosion induced by water condensation plus input power requirements.

The **OVHDs**—mostly water vapor & hydrocarbons—are collected under a controlled vacuum and partially condensed at 322—327K. Vacuum separation recovers the condensed **HCs** and water. These are separated by gravity. The vacuum is generated by ⓥ̰n̰g̰ **TEG** thru an eductor. It removes the **NCHs**, compresses the stream to about 207 kPa.g & routes it to an emissions separator. The glycol condenses out and recirculated [re ⓥḛd̰] thru the **OVHD** condenser, glycol cooler, filters and the eductor, while the **NCHs** are fed to the regenerator fuel system or sold.

Notes :

1. The **QLT system** costs 25—50% more than conventional TEG-based dehydration systems, depending on how the process is applied (*i.e.,* retrofits cost more than building the **QLT system** into a new dehydrator). However, payback can be realized in less than 2 yr., ever for a small application.

2. The emissions of CO_2 can be reduced by more than 2000 tons. yr^{-1} by eliminating the thermal oxidizer.

3. The first commercial unit was installed at KERR McGEE's Fort Lupton, Co., facility to treat 30 million standard ft^3 per day of **NG** at 6.96 MPa.g/350K rewards a pay-back of k$150 per annum [based on $ 5/MMBtu gas] in recovered liquid products and reduced fuel consumption. At a capital cost of k$200 vs. k$275 for the conventional distillation skid and thermal oxidizer that it replaced, the system has paid the differential capital investment in just 6 months.

Note : ⓥ̰n̰g̰ means circulating

11.6. USE CHART TO ESTIMATE ACID GAS SOLUBILITY IN TEG

Process engineers can calculate absorption of H_2S and CO_2 in triethylene glycol to optimize sulfur recovery.

When sour **NG** or acid gas is subjected to dehydration by using triethylene glycol (**TEG**), a substantial quantity of H_2S and CO_2 is absorbed in the **TEG**. Upon regeneration, the rich **TEG** solution liberate these acid gas components. Obviously, the amounts of these compounds absorbed, and consequently liberated from the glycol, depends on their concentration in the gas being dehydrated and the absorber pressure & temperature.

Charts **(Fig. 11.6.1)** have been generated defining the solubility of H_2S and CO_2 in **TEG** vs the temperature at different partial pressure (appearing as the curve parameter) of H_2S and CO_2 enable the process engineer to determine the qty of acid gas absorbed per unit volume of **TEG** ⊘ng at any set operating pressure & temperature of the absorber.

Developed on the basis of experimental data, these charts are useful to quantify the amount of H_2S & CO_2 available via **TEG** dehydration of natural gas.
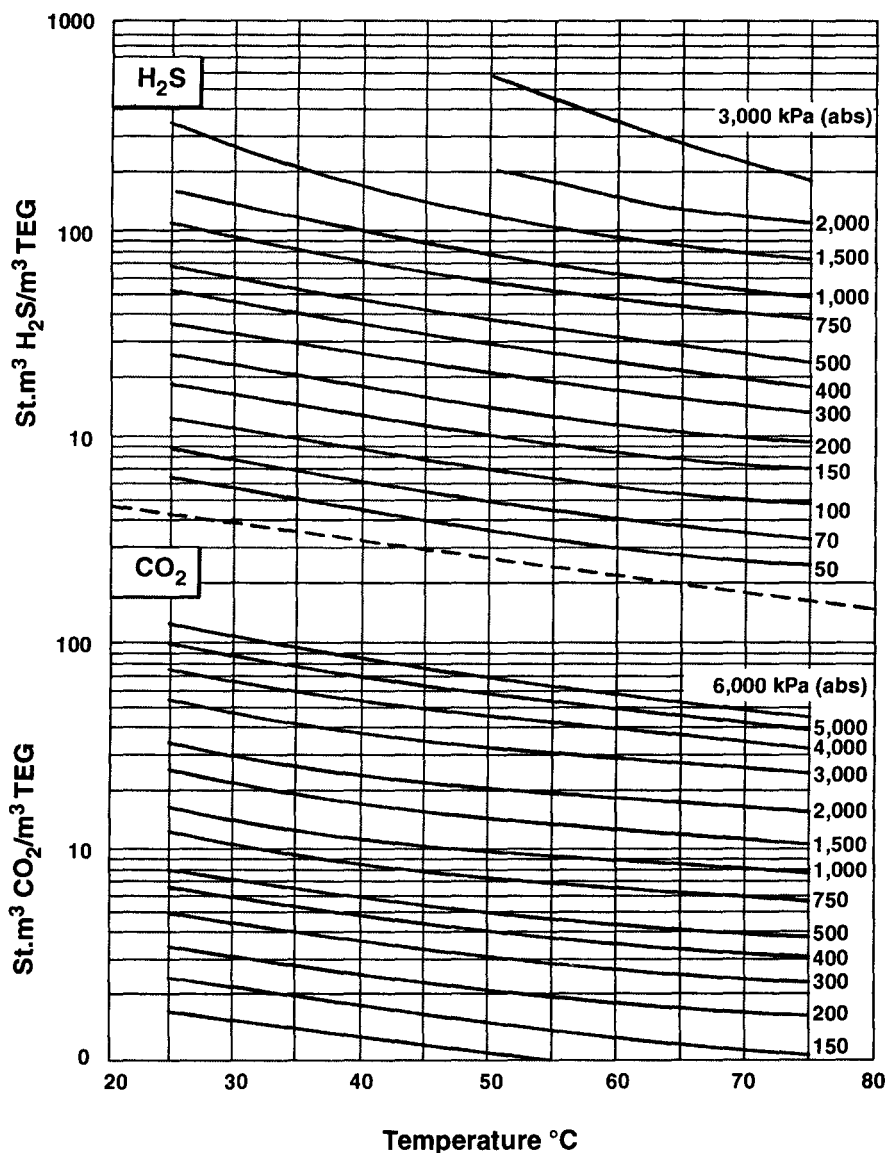
Source : Hydrocarbon Processing, January 2004

© : **GULF Publishing Co., Houston, TX, USA**

Fig. 11.6.1. *Solubility of H_2S and CO_2 in TEG vs. Temperature, while partial pressure appears as the Curve Parameter.*

H₂S Absorption

Example : Sour gas is treated in a TEG absorber operating at 6MPA. abs/303K.
Sour gas Contains 5 mol% H₂S

TEG Ⓥṇ rate : 8 lt. min⁻¹

Calculate the amount of H₂S absorbed per day.

Solution :

$$\text{System pressure, P} = 6 \text{ MPa.abs.} = 6000 \text{ kPa. abs.}$$

$$\text{H}_2\text{S content in SG} = 5 \text{ mol\%}$$

$$\text{Partial press of H}_2\text{S, } p_{\text{H}_2\text{S}} = \text{Mole fraction of H}_2\text{S} \times \text{P}$$

$$= \frac{5}{100} \times 6000 \text{ kPa. abs.}$$

$$= 300 \text{ kPa. abs.}$$

Amount of H₂S absorbed = 32 scm **[Fig. 11.6.1]**

at 300 kPa.bas./303K (30°C)per m³ of TEG Ⓥe̤d̤

$$\textbf{TEG Ⓥṇ rate} = 8 \text{ lt.min}^{-1}$$

$$= (8\text{lt.min}^{-1}) (60 \text{ min.h}^{-1}) (24 \text{ h.day}^{-1})$$

$$= 11520 \text{ lt}$$

$$= 11.52 \text{ m}^3$$

∴ **Qty of H₂S removed per day**

$$= 32 \frac{\text{scm}}{\text{m}^3 \text{ TEG}} \times 11.52 \text{ m}^3 \text{ TEG}$$

$$= 368.64 \text{ scm}$$

Note : This amount of H₂S tantamounts to 0.5 ton of sulfur.

Important : The experimental data, on the basis of which the above solubility curves were generated, were obtained with pure glycol. In an actual dehydration facility, the glycol is regenerated to about ≥ 99% purity. If the glycol is not regenerated to this purity, then the amount of H₂S or CO₂ absorbed per unit volume of lean glycol Ⓥe̤d̤ would be slightly less.

Note : Ⓥṇg̤ means circulating; Ⓥe̤d̤ is circulated; Ⓥṇ is circulation

REFERENCES

1. MG Eskaros, **Glycol Dehydration** *(Hydrocarbon Processing, July 2003/P : 80—81).*
2. E. Wichert & G.C. Wichert, **New Charts estimate Acid Gas Solubility in TEG** *(Hydrocarbon Processing, January 2004/P:47—48).*

□□

INDEX

□□

ABSORPTION AND STRIPPING

The primary objective of the book is to help readers gain sufficient insight into twin unit operations–**ABSORPTION AND STRIPPING**– and their application to industries.

Almost all major Chemical Process Industries (CPIs) and Petrochemical Industries (PCIs) are associated with these two unit operations which, very often than not, operate in tandem with distillation in many plants.

Starting from the very basics, the book has discussed, at length the necessary fundamentals and theoretical development of absorption and stripping, the mechanism of absorption and desorption, theoretical correlations to determine the efficiency of absorption & stripping, evaluation of number trays in trayed columns and estimation of packed bed height in packed towers. Nearly a hundred numerical examples will help the readers to get a good grip on the theories explained. More than six hundred colored, black & white illustrations will do justice to it.

Hydraulics of operation of all the three basic tray types– sieve, valve & bubble-cap trays– and that of packed bed have been explained to the minutest details. Discussed also are the factors and parameters that influence the hydraulics of packed towers. This is followed by the basic concepts of **design of Tray Towers** and **Packed Columns**. Since great emphasis has been laid on design, two chapters deal exclusively with **Design**. Amalgamated with them are adequate numbers of design examples of industrial columns. Design consideration, design guidelines & operation of important industrial absorption have been discussed at length.

Packings enjoy a special position in the book as they come almost inevitably with absorption & stripping operations. So one whole chapter has been devoted to packing. Equally important are **Packed Tower Internals** without which the packing's functions get seriously impaired. So little wonder why each & every such tower internals has been discussed in comprehensive details.

Since the book banks heavily on industries, the last three chapters have been devoted to **Absorption & Stripping of Industrial Importance, Revamping of Absorbers & Strippers, and Cost Estimation of Absorption Towers**. Professional chemical engineers may find them interesting.

The treatment of the book is simple and easy-going, such that anyone with a basic understanding of engineering and science is able to comprehend.

P. Chattopadhyay, Senior Lecturer in Mechanical Engineering of Techno India College of Technology, Salt Lake, Kolkata and formerly a Senior Process Engineer of HFC Haldia Division for 25 years backed up by more than two-decades of experience as part-time Lecturer of Advance Course in HFC Training Institute teaching such subjects as Engineering Thermodynamics, Fluid Mechanics, Engineering Mechanics, Heat Transfer and Unit Operations.

Chattopadhyay has authored nine books.
Besides he has co-authored the book CFB Technology. He also has to his credit eighteen Technical papers & Seminar Articles.